SDC - 92 - 276
June, 1992

Proceedings of the SDC Collaboration Meeting at KEK

May 26 - 29, 1992
KEK, Tsukuba, Japan

Editor:
H. Iwasaki (KEK)

Local organizers:
M. Chiba (Tokyo Metropolitan University)
H. Iwasaki (KEK)
T. Ohska (KEK)
K. Yasuoka (University of Tsukuba)

The SDC Collaboration Meeting

May 26-29, 1992
KEK, Tsukuba, Ibaraki 305, Japan

[1] Plenary Session

May 26 (Tuesday)

Status of SSC Project and the SSC Research Program	V. Luth	- 14
Report from Spokesperson	G. Trilling	- 51
Report from Project Manager	T. Kirk	- 65
Report on Superconducting Magnet	A. Yamamoto	- 95

May 29 (Friday)

Report from Tracking Group		
Scilicon	Y. Unno	- 184
Outer Tracker	T. Ohska	- 215
Report from Calorimeter Group	D. Green	-255
Report from Muon Group	S. Terada	-285
Report from Electronics Group		
Front-end electronics	H. Williams	- 306
Data acquisition	M. Nomachi	- 328
Report from Computing Group	L. Price	- 340

AND 5215

[2] Silicon Tracking

< Detector R&D >

Capacitance Measurement of DSSD	H. Miyata	- 367
Capacitances in Silicon Microstorip Detectors: Measurements and Simulations	H. Sadrozinski	- 389
Radiation Damage of the SSD	N. Tamura	- 409
Signal Simulations of the Silicon Syrip Detector	Y. Unno	- 424
Lorentz Force Effects Experimental Plans	H. Ziock	- 446
Double Sided Sensor (Barrel & Disk)	T. Ohsugi	- 455
Comments on Production of DSSD	K. Yamamoto	- 464
Silicon "Wedge" Detector R & D	P. Fisher	- 478
Quality Assurance	H. Sadrozinski	- 526

< Mechanical System >

Silicon CDR	A. Seiden	- 533
Mechanical Design Review	W. Miller	- 543
Mechanical Design Study at KEK	Y. Unno	- 571
Alignment: Placement Tolerances	H. Ziock	- 590
Detector Module Design	H. Spieler	- 603
Ladder Assembling at KEK	Y. Unno	- 623

< Cost & Schedule >

Silicon Tracker Cost & Schedule Review	A. Grillo	- 643

< Beam Test at KEK >

Beam Test of the SDC Double-sided Silicon Strip Detector	Y. Unno	- 653
KEK Beam Lines for the Beam Test	A. Murakami	- 672
Analog Readout ICs	H. Spieler	- 689
Testing of a 64-channel Bipolar Amplifier-comparator Chip	H. Sadrozinski	- 712
SDC Portable DAQ	M. Nomachi	- 719

[3] Tracking/Electronics Joint

< Straw Tracker R & D >

Activities in Japan	T. Ohska	- 728
Straw R & D at Duke	S. Oh	- 738
R & D Progress from Colorado	W. Ford	- 782

< Resolution >

Resolution Studies of 4 mm Straws	H. Ogren	- 795

< Readout Electronics >

Straw ASD	M. Newcomer	- 803
Conceptual Studies on FEB of the Straw Chamber	S. Odaka	- 819
Straw Electronics Layout	R. Berg	- 827
New TMC Design with Toshiba Gate Array	Y. Arai	- 840
Radiation Damage Test of Time Memory Cell	M. Chiba	- 851
A Plan of Cosmic-ray Test of Straw Readout at Tokyo Metropol. Univ.	K. Yamauchi	- 871
DCC Design for the SDC Straw Tube Tracker	P. Sinervo	- 875

< Trigger >

SDC Straw and Muon Triggers	J. Chapman	- 895

< Mechanical Study >

Mechanical Measurements on 4 m Prototype	D. Rust	- 932
Mechanical Considerations for a SDC Outer Straw Tracker for the SSCL	R. Swensrud	- 946

< HV System >

HV System for Straws	D. Rust	- 970

< Fiber Tracker >

Scintillating Fiber Tracker Future R & D	D. Koltick	- 976

[4] Tracking/Integration Joint

Tracking Utilities Update	J. Piles	- 1007
Mechanical Considerations for a SDC Outer Straw Tracker for the SSCL	R. Swnsrud	- 1012

[5] Calorimeter

< Overview >

SDC Calorimetry - Status and Near Future	D. Green	- 1035
TDR Mechanical Design	L. Bartoszek	- 1063

< Prototype >

Report from Prototype Task Force	G. Foster	- 1073
Update on Baseline Barrel EM - Mechanical and Optical	D. Underwood	- 1080
Barrel EM Calorimeter Options	G. Foster	- 1113
Pb Stack Options	L. Bartoszek	- 1136
Fabrication of Tiles and Fibers	K. Hara	- 1153
Aging Test of Bent Fibers	Y. Miyamoto	- 1184
Optics Design of Prototype EM Tile/Fiber	M. Okabe	- 1194
The Tile-Fiber System for SDC Calorimetry	V. Hagopian	- 1208
Development of Cockcroft-Walton PMT Base	K. Hara	- 1239
Quality Control for Prototype Tile/Fiber Production	I. Nakano	- 1252

< Radiation Damage >

Report of RADDAM 1992 Conference	V. Hagopian	- 1266
Radiation Damage of Tiles, Fibers, and Tile/Fiber Assemblies	K. Yasuoka	- 1315
Study of Dose-rate Effects on the Radiation Damage of SCSN23, ...	N. Giokaris	- 1345
SDC Calorimeter Rad-Hard Scinitillator	G. Foster	- 1362

< PMT Development >

Development of MA PMTs and Green Extended PMTs	S. Suzuki / Y. Yoshizawa	- 1385

< Readout >

Digital Photomultiplier Tube Readout	G. Foster	- 1402

< CDF Plug Upgrade >

Present Status of the CDF Plug Upgrade EM Calorimeter	S. Kim	- 1423

< Calibration >

Calorimeter Calibration - Recent Activity	A. White	- 1452

< Shower Maximum Detector >

Shower Maximum Detector	T. Muller	- 1463
Shower Max Photon Readout	P. Cushman	- 1486

< Forward Calorimeter >

Study of Total Reflection between Liquid Scintillator and Grass Resin	T. Masumaru	- 1526
Recent Results in High-Pressure Gas Calorimetry	N. Giokaris	- 1540
L* and GEM Calorimeter Transmutation Studies and Applicability to SDC	W. Wilson	- 1578

< Simulation >

Present Status of SDCSIM (Calorimeter Part)	M. Asai	- 1602

[6] Magnet/Calorimeter/Integration Joint

Tracking Utilities Update	J. Piles	- 1614
Calorimeter Support System	L. Bartoszek	- 1622

[7] Muon System

< Tube >

Mechanical Consequences of Tube Layer Ordering	C. Daly	- 1629
Cost Estimate of Barrel Muon Tubes	S. Mori	- 1650
Drift Tube Simulation Study	K. Norik	- 1652

< Intermediate System >

SDC Intermediate Muon System	D. Carlsmith	- 1669

< Forward System >

Forward System	A. Skuja	- 1679

< Labor Estimate >

Labor Estimate	C. Grinnell	- 1687

< Trigger >

RPC Solution for the SDC Muon Trigger Counters	S. Amendolia	- 1693
SDC Trigger Rates	W. Smith	- 1698

< Phi Cracks >

Physics Impact of Phi Cracks in the SDC Barrel Muon System	S. Errede / J. Wiss	- 1714
Study of Loss due to Missed Coverage in the Barrel Muon Detector	M. Daoudi / U. Nauenberg	- 1726

< Sparsification >

Sparsification Study I	S. Willis	- 1734
Sparsification Study II	Y. Asano	- 1741
Impact of Sparsification on Muon Trigger/Reconstruction Efficiency ...	N. Kanematsu	- 1752

< Background Study >

A Background computations for SDC Set-up at 40 TeV	Zholobov G. V.	- 1771
Neutron Rates in the SDC Forward Muon System - Design Optimization	A. Kulik	- 1813

[8] Muon/Electronics Joint

< Overview >

Muon Electronics Overview and Development Plan	S. Terada	- 1843

< Readout >

ASD Development	Y. Asano	- 1848
New TMC Design for Muon with TOSHIBA Gate Array	Y. Arai	- 1863
Status of TMC Modules	M. Ikeno	- 1871

< Trigger >

Muon Detector Trigger	J. Chapman	- 1883
Muon Trigger Electronics	H. Sakamoto	- 1898
Level-1 Muon Trigger Using Xilinx FPGA	T. Zhao	- 1924

[9] Muon/Integration Joint

SDC Intermediate Muon System Status	F. Feyzi	- 1932

[10] Electronics

< Organization >

Organization Plan	A. Lankford	- 1967

< Trigger >

SDC Trigger Rates	W. Smith	- 1973
Trigger Activities in Japan	H. Sakamoto	- 1997
SDC Trigger Emulation Module	W. Smith	- 2012
Distributed Processing for Straw Tube Trigger Simulation	K. Kondoh	- 2027

< Bus Swich>

R & D of MOBY - Multi-pass Organization on Bus Yard	E. Kanatani	- 2045
High Speed Switch System	O. Sasaki	-2055

< Data Acquisition >

Interests and Resources for DAQ Subsystem in Japan	H. Fujii	- 2078
Event Builder Subsystem	M. Nomachi	- 2085
Development of the SPARC-VME-CAMAC Data Acquisition System (Potable DAQ)	Y. Takeuchi	- 2089
Potable DAQ Standard Crate	M. Nomachi	- 2109
Readout Control for High Luminosity Accelerators	R. Belusevic	- 2113

[11] Computing

< Overview >

Strategy and Plan for SDC Computing	L. Price	- 2121

< Task Force>

Core Software Task Force	S. Frederiksen	- 2132
SDC Core Task Communications Services	G. Kubena	- 2147
Data Modelling Package Task Force Requirements	B. Scipioni	- 2170
Status of Software Development Task Force	A. White	- 2182

< Distibuted Computing System >

JSD Farm: Distibuted Computing Facility at KEK	Y. Morita	- 2218
Distibuted Computing System at Tokyo Metropolitan University	S. Kitamura	- 2230
Harnessing Modern Virtual-Memory Systems for Distibuted Computing of SSC	H. Yoshida	- 2245
Evolution of Computers to Massive Parallel Processors	K. Hasegawa	- 2274
Development of Simple Distibuted Batch Processing System	M. Kawaguchi	- 2294

< SDCSIM >

SDCSIM	S. Kunori	- 2307
Japanese Activities for SDCSIM	M. Asai	- 2326

The SDC Collaboration Meeting

May 26-29, 1992
KEK, Tsukuba, Ibaraki 305, Japan

[1] Plenary Session

May 26 (Tuesday)

Status of SSC Project and the SSC Research Program	V. Luth	-14
Report from Spokesperson	G. Trilling	-51
Report from Project Manager	T. Kirk	-65
Report on Superconducting Magnet	A. Yamamoto	-95

May 29 (Friday)

Report from Tracking Group		
Silicon	Y. Unno	-184
Outer Tracker	T. Ohska	-215
Report from Calorimeter Group	D. Green	-255
Report from Muon Group	S. Terada	-285
Report from Electronics Group		
Front-end electronics	H. Williams	-306
Data acquisition	M. Nomachi	-328
Report from Computing Group	L. Price	-340

The Superconducting Super Collider

STATUS OF THE SSC PROJECT AND THE SSC RESEARCH PROGRAM

Vera Lüth

SSC Physics Research Division

May 25, 1992
KEK, Tsukuba, Japan

The Superconducting Super Collider

THE SSC PROJECT AND RESEARCH PROGRAM

- INTRODUCTION
- THE STATUS OF THE SSC PROJECT
  - Completed Facilities and Acquisitions
  - Facilities under Construction
  - Facilities under Design
- PHYSICS RESEARCH FACILITIES
  - Experimental Halls and Facilities
  - External Beams and Calibration Hall
  - Off-line Computing
- THE PHYSICS RESEARCH PROGRAM
  - Particle Physics Theory
  - SDC
  - GEM
  - B Experiments
  - Other Experiments
- FUNDING AND SCHEDULE

The Superconducting Super Collider

THE MACHINE

- A giant step beyond existing facilities
  - 40 TeV - a factor 20 in c.m. energy
  - 10^{33} cm^{-2} s^{-1} - a factor of 100 in luminosity

THE PHYSICS POTENTIAL

- Probing measurements of many aspects of the Standard Model
  - top production and top mass
  - W and Z production
  - B physics - the origin of CP Violation
  - elastic and diffractive proton-proton scattering
  - high energy ν interactions and observation of ν_τ
- Exploration of the TeV scale to determine what lies beyond the Standard Model
  - Electro-weak symmetry breaking - Higgs single or multiple - elementary or composite
  - Supersymmetry
  - Technicolor
  - Compositeness of quarks and leptons
  - additional gauge bosons
  - .....

SSC Luminosity Potential

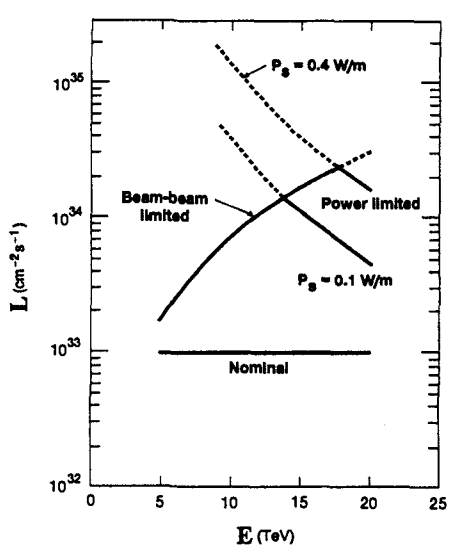

L ~ B • I

B = Brightness (N_B/ε_N)

I = Total current

TIP-02221

SEARCH FOR HIGGS PARTICLE

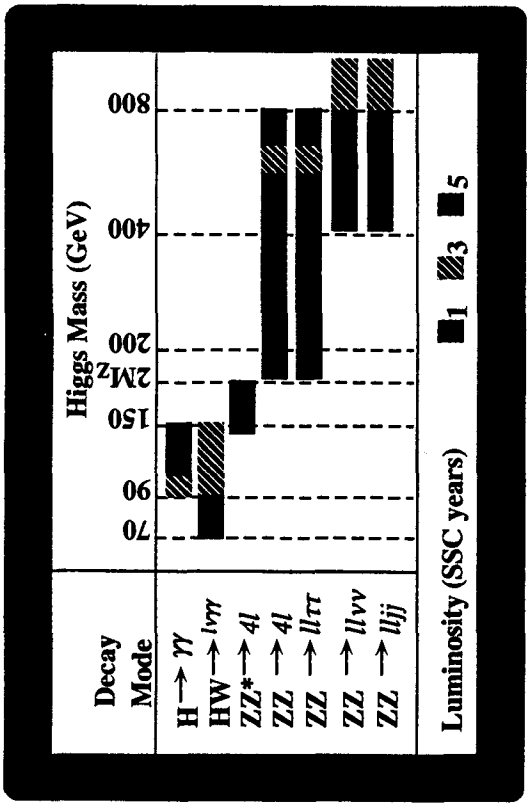

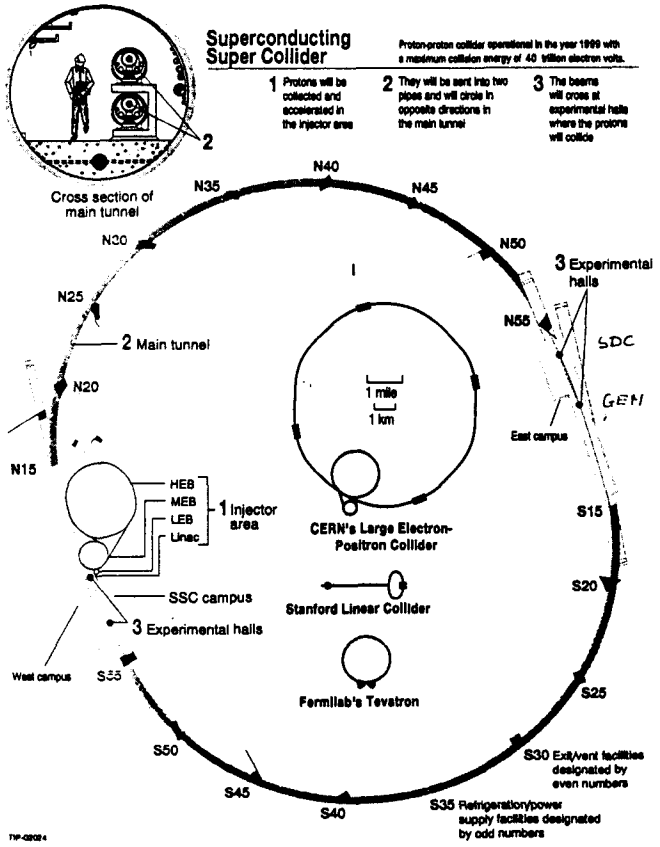

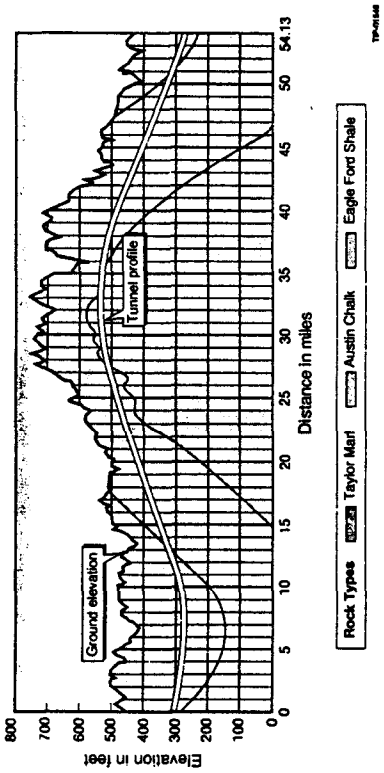

The Superconducting Super Collider

PROJECT STATUS:

Completed Facilities and Acquisitions

- Magnet Development Laboratory
- Accelerator Stystem String Test
- Cryogennics Duilding
- Exploratory Shaft
- 70 km² of Land
- Central Office and Laboratory Facilities at Waxahachie (5ha)
- Interim Office and Laboratory Facilities at De Soto

Facilities under Construction:

- Magnet Delivery Shaft at N15 site
- First Tunnel Sections N15-N20, N20-N25
- Magnet Test Laboratory
- Ion Source and Linear Accelerator

Facilities under Design

- Collider Tunnel
- Low Energy Booster
- Medium Energy Booster
- Extracted Beams and Test Facilities
- Experimental Halls and Facilities at IR-5 and IR-8

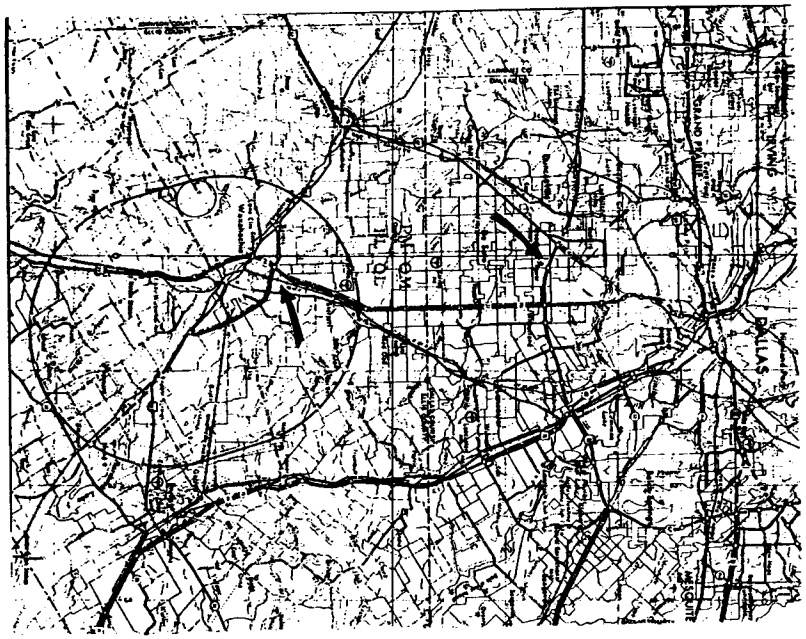

SSC Laboratory — Magnet Systems

Changes from 40mm to 50mm CDM

		40mm	50mm
Field Quality			Improved
Operating Margin		4-5%	8-10%
Wire Strand	I	6μ, 1.3:1	6μ, 1.5:1
	O	6μ, 1.8:1	6μ, 1.8:1
Cable	I	23 strand	30 strand
	O	30 strand	36 strand
Bore Tube		32mm	up to 45mm
Collar		15mm	17mm
Yoke		horizontal split	vertical split
		266.7mm OD	327.3mm OD
Skin		276.2mm OD	340mm OD
Cryostat		610mm OD	660mm OD
			(686mm)

SSC DIPOLE MAGNET

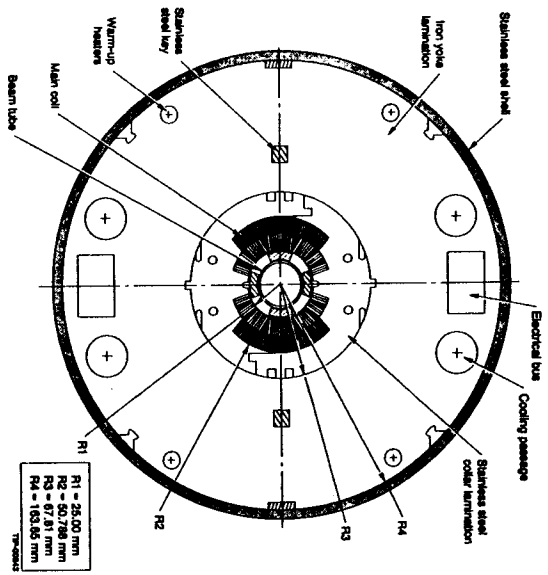

50 mm coil magnet cross section

DIPOLE TESTS

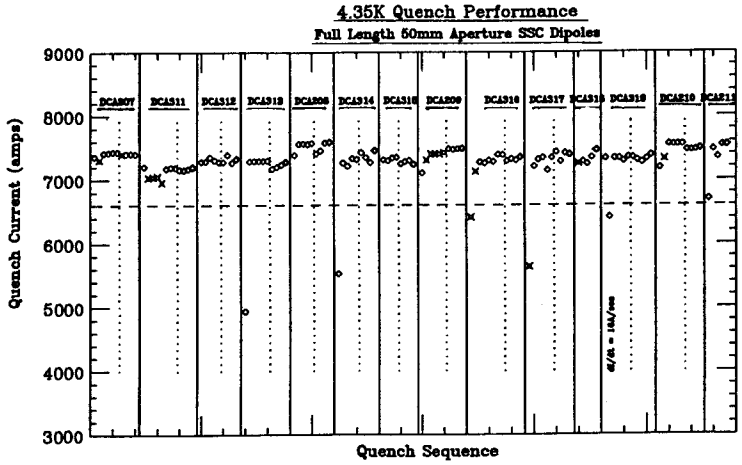

Notes:
(1) – DCA200 series magnets are BNL; DCA300–on BNL/WEC
– DCA300 series magnets are FNAL; DCA313–on FNAL/GDSS
(2) – dotted line indicates thermal cycle
(3) – after first two magnets (DCA207, DCA311), ramp to quench sequence was: 16A/sec to 8500A, wait 10min, 4A/sec to quench

Quench Origin:
+ – upper inner coil
× – lower inner coil

—— BNL - WESTINGHOUSE
—— FNAL - GENERAL DYNAMICS

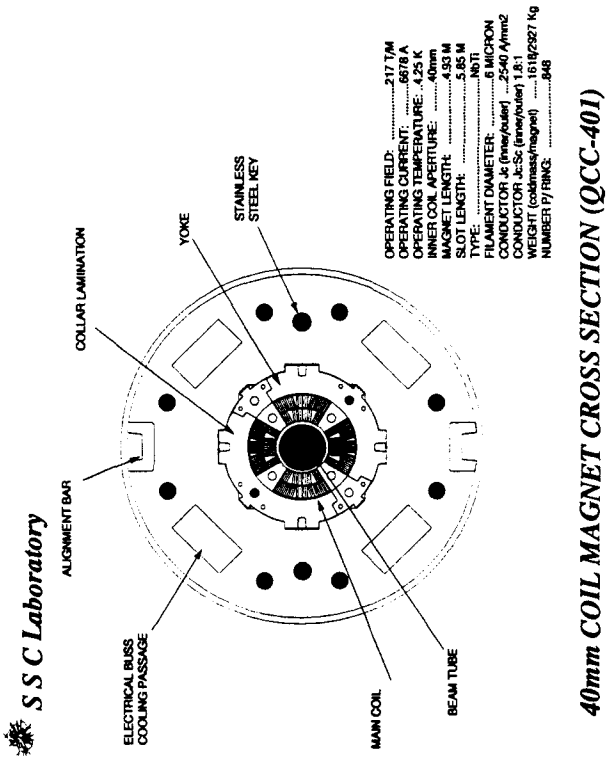

40mm COIL MAGNET CROSS SECTION (QCC-401)

The Superconducting Super Collider

THE SSC COMPUTING FACILITIES

- MISSION:
  - Design, Procure, Implements and Operate Off-line Computing Facilities in Support of Detector Design and Data Simulation and Analysis
- ACTIVITIES:
  - Design and Implement Physics and Detector Simulation Facility (PDSF)
  - Develop System Services and Ututilities for PDSF
  - Develop Mass Storage Capabilities
  - Develop Data Base Methodologies for HEP
  - Support Applications Programs - Libraries
  - Study Hardware/Software Architectures
- PDSF
  - Multi-Vendor RISC-Based Computing Facility to Exploit Parallelism in UNIX Environment
  - PDSF Performs as a Single Integrated System: March 1992: 3000 MIPS, 92 CPU'compared to 0.4 events/min per CRAY

The Superconducting Super Collider

THE EXPERIMENTAL PHYSICS RESEARCH PROGRAM

The Physics Research Program should match the potential of and the investment in the SSC Accelerator Project.

- Two major detectors with complementary as well as overlapping capabilities aimed at the phyics of the multi-TeV scale.
  - SDC (SOLENOIDAL DETECTOR COLLABORATION)
    - charged particle tracking in a 3.4 m diameter , 8.5 m long solenoidal magnet
    - vertex detection
    - hermetic calorimetry
    - lepton identification and energy measurement
  - GEM (GAMMA ELECTRON MUONS)
    - photon identification and energy measurement
    - lepton identification and energy measurement
    - muon momentum measurement in a solenoidal magnet of 30 m length and 18 m diameter
    - rubustness at higher luminosities
- Several smaller detectors adding diversity and coverage of phenomena at low transverse momentum.
- Future experiments making use of secondary and extracted beams from the collider or the booster accelerators.

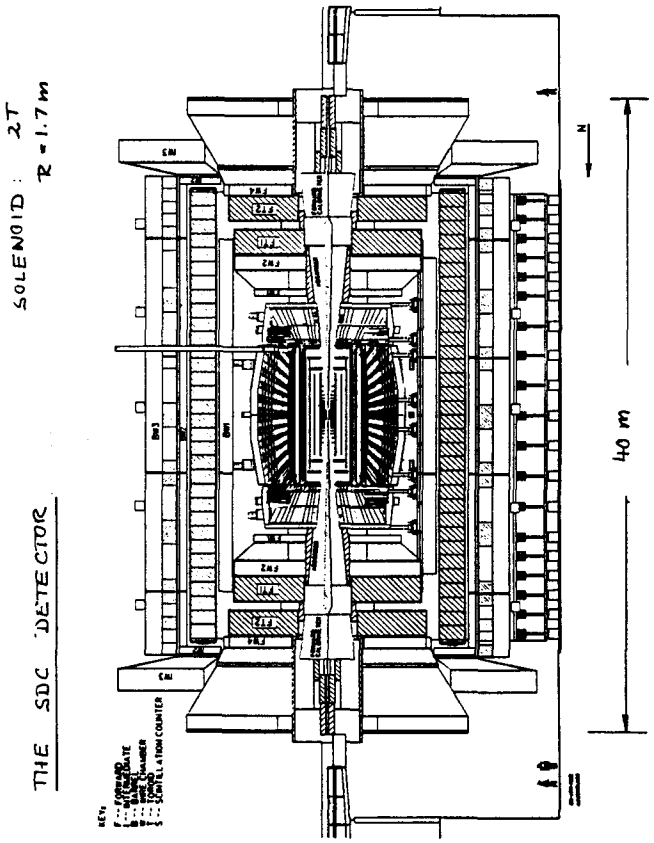

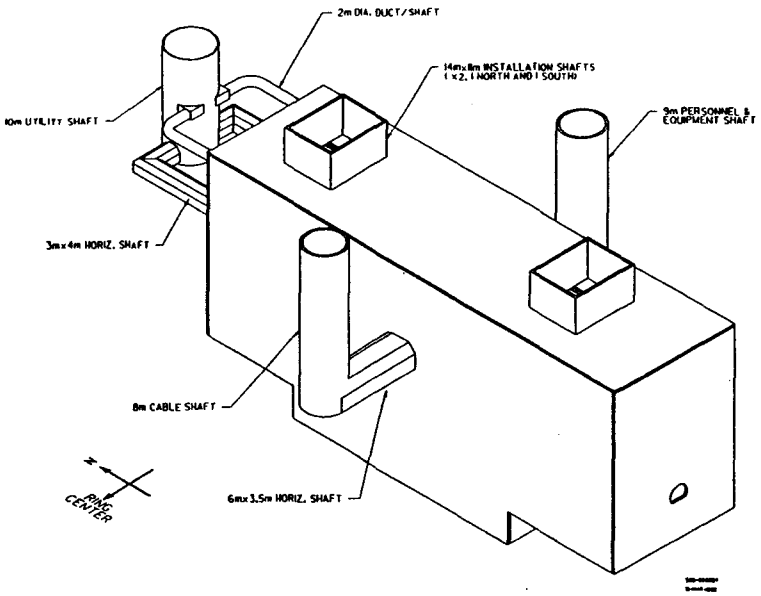
2m DIA. DUCT/SHAFT
14m x 8m INSTALLATION SHAFTS (×2, 1 NORTH AND 1 SOUTH)
10m UTILITY SHAFT
9m PERSONNEL & EQUIPMENT SHAFT
3m x 4m HORIZ. SHAFT
8m CABLE SHAFT
6m x 3.5m HORIZ. SHAFT
N
RING CENTER

32

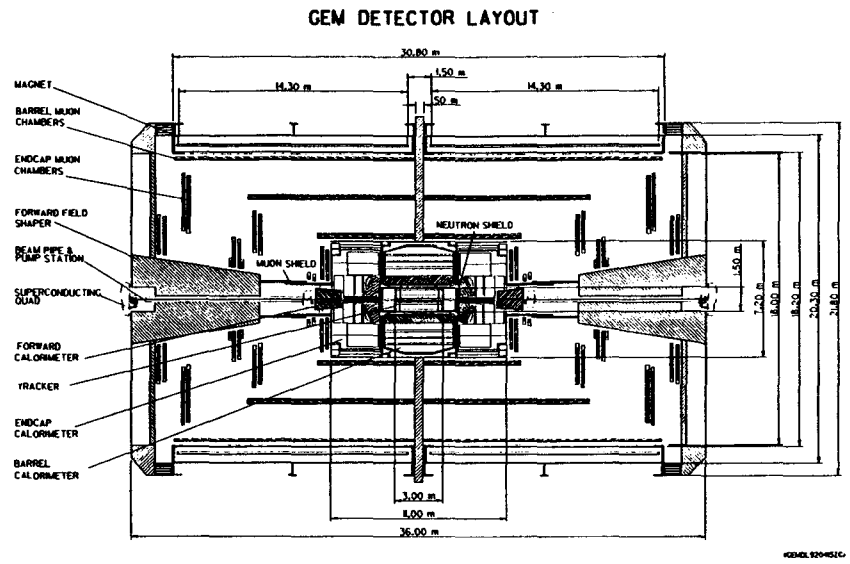
GEM DETECTOR LAYOUT
30.80 m
1.50 m
14.30 m
14.30 m
.50 m
MAGNET
BARREL MUON CHAMBERS
ENDCAP MUON CHAMBERS
FORWARD FIELD SHAPER
BEAM PIPE & PUMP STATION
SUPERCONDUCTING QUAD
FORWARD CALORIMETER
TRACKER
ENDCAP CALORIMETER
BARREL CALORIMETER
NEUTRON SHIELD
MUON SHIELD
1.50 m
7.20 m
18.00 m
18.30 m
20.30 m
21.80 m
3.00 m
11.00 m
36.00 m

30

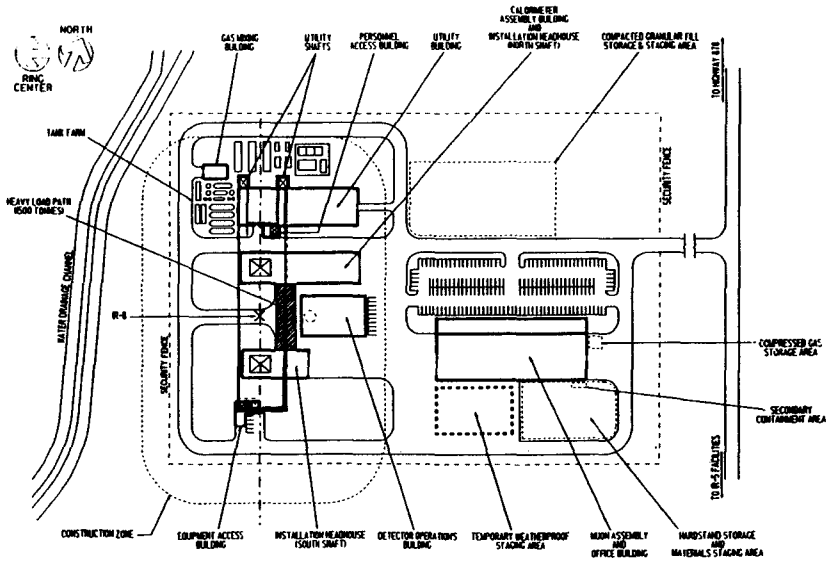
NORTH
RING CENTER
GAS MIXING BUILDING
UTILITY SHAFTS
PERSONNEL ACCESS BUILDING
UTILITY BUILDING
CALORIMETER ASSEMBLY BUILDING AND INSTALLATION HEADHOUSE (NORTH SHAFT)
COMPACTED GRANULAR FILL STORAGE & STAGING AREA
TO HIGHWAY 878
SECURITY FENCE
TANK FARM
HEAVY LOAD PATH (500 TONNES)
WATER DRAINAGE CHANNEL
IR-8
COMPRESSED GAS STORAGE AREA
SECONDARY CONTAINMENT AREA
TO IR-8 FACILITIES
CONSTRUCTION ZONE
EQUIPMENT ACCESS BUILDING
INSTALLATION HEADHOUSE (SOUTH SHAFT)
DETECTOR OPERATIONS BUILDING
TEMPORARY WEATHERPROOF STAGING AREA
MUON ASSEMBLY AND OFFICE BUILDING
HARDSTAND STORAGE AND MATERIALS STAGING AREA

33

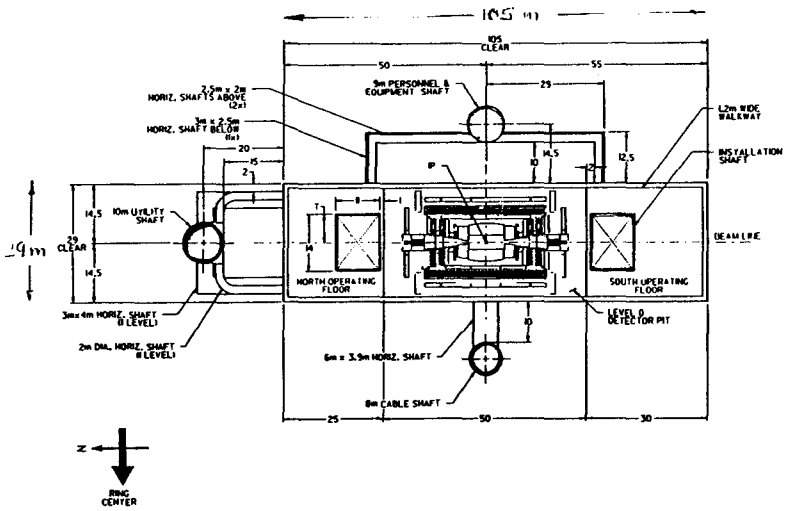
105 m
105 CLEAR
50
55
29
9m PERSONNEL & EQUIPMENT SHAFT
HORIZ. SHAFTS ABOVE (2x)
HORIZ. SHAFT BELOW (1x)
L2m WIDE WALKWAY
INSTALLATION SHAFT
10m UTILITY SHAFT
29 m CLEAR
BEAM LINE
NORTH OPERATING FLOOR
SOUTH OPERATING FLOOR
3m x 4m HORIZ. SHAFT (1 LEVEL)
2m DIA. HORIZ. SHAFT (1 LEVEL)
LEVEL D DETECTOR PIT
6m x 3.5m HORIZ. SHAFT
8m CABLE SHAFT
25
50
30
N
RING CENTER

31

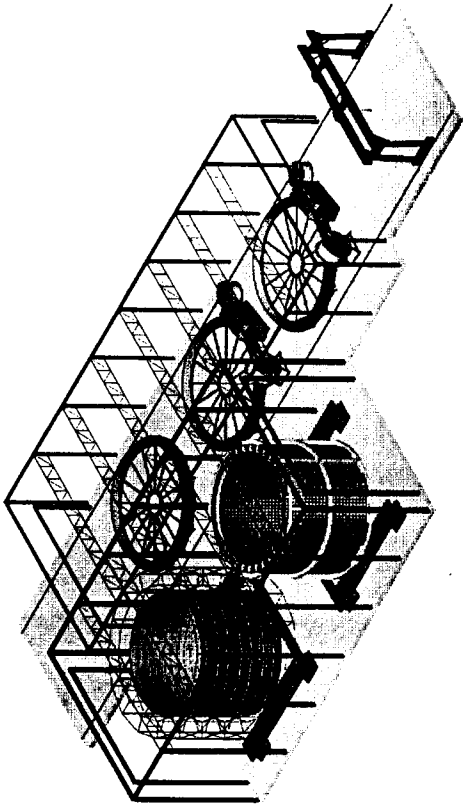

GEM COIL WINDING FACILITY

The Superconducting Super Collider

THE INITIAL PHYSICS RESEARCH PROGRAM

PROPOSALS:

- The Experimental Program is Proposal Driven
- International Advisory Panels:
  - Scientific Policy Committee
  - Program Advisory Committee
- SDC Milestones :
  - May 1990: Expression of Interest
  - Dec. 1990: Letters of Intent
  - Jan. 1991: Approved to proceed to Technical Design Report (TDR)
  - April 1992: Submission of TDR
  - May 1992: Review of TDR by Experts
  - July 1992: PAC Meeting Decision on Stage I Approval ?
  - Sept. 1992: DOE Review ?
  - Dec. 1992: Decision on Stage II Aproval ? Begin Construction ?

The Superconducting Super Collider

THE INITIAL PHYSICS RESEARCH PROGRAM

- GEM Milestones :
  - July 1991: Expression of Interest
  - Dec. 1991 Letters of Intent
  - Jan. 1992: Approved to proceed to Technical Design Report
  - July 1992: Review of Magnet Design ?
  - Oct. 1992: Submission of TDR ?
  - Nov. 1992: Review of TDR by Experts ?
  - Jan. 1993: PAC Meeting ? Decision on Stage I Approval ?
  - March 1993: DOE Review ?
  - April 1993 Decision on Stage II Aproval ? Begin Construction ?
- Milestones for Smaller Experiments:
  - July 1990: Expression of Interest
  - Spring 1993: Workshop on B Physic
  - Fall 1993: Letters of Intent ?

The Superconducting Super Collider

SMALLER EXPERIMENTS AT SSCL

OPTIONS
- Colliding Beams at 40 TeV
- Circulating Beams of 20 TeV, 2 TeV, 0.2 TeV
- Secondary Beams of n, γ, ν. . .
- Extracted Beams at 20 TeV, 2 TeV, 0.2 TeV

LOW PT PHYSICS

Eoi 02 Orear	Elastic Scattering
Eoi 19 Bjorken	A Full Acceptance Experiment
Eoi 14 Krisch	Polarized Beam Experiments

B PHYSICS

Eoi 08 Lockyer	A Solenoidal Collider Experiment
Eoi 13 Rosen	A Gas Jet Experiment
Eoi 14 Cox	An External Beam Experiment
Eoi 21 Schlein	A Forward Collider Experiment

OTHER

Eoi 15 Giacomelli	Search for Magnetic Monopoles
Eoi 04 Sobel	A Long Baseline Neutrino Experiment
Eoi 17 Bryant	Relativistic Atomic Physics

The Superconducting Super Collider

CP VIOLATION AND B DECAYS

COMPETING EFFORTS:

- LEP EXPERIMENTS
- $e^+ e^-$ B FACTORIES
- TEVATRON EXPERIMENTS
- SSC EXPERIMENTS

ADVANTAGES AT THE SSC:

- HIGHER $b\bar{b}$ PRODUCTION RATES - absolute and relative
- HIGHER B MOMENTA - Better Vertex Separation
- A DEDICATED FACLITIES

DISADVANTAGES AT THE SSC:

- HIGHER INTERACTION RATES
- HIGHER MULTIPLICITIES
- HIGH RADIATION LEVELS

V. Lüth May 17,1992

SSC STATUS

HADRO-PRODUCTION OF BEAUTY

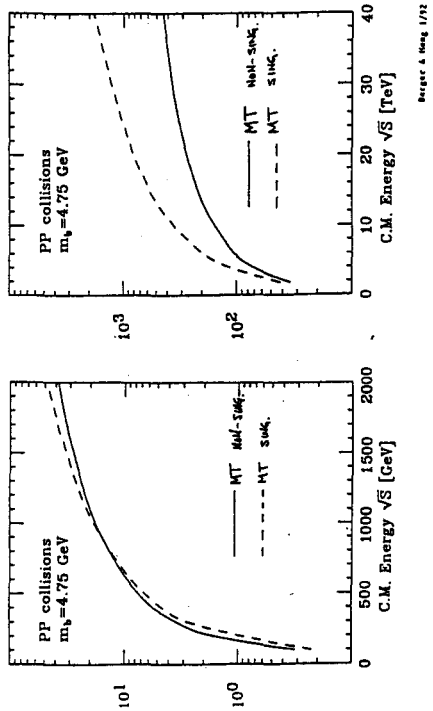

CP ASYMMETRY MEASUREMENTS AT THE SSC

	Fixed Target	Gas Jet	Collider	B Factory	Units
Energy E_{cm}	193	193	40,000	10.6	GeV
Lumminosity L	10^{33}	$2 \cdot 10^{33}$	$3 \cdot 10^{31}$	$3 \cdot 10^{33}$	$cm^{-2}s^{-1}$
Cross Section $\sigma_{b\bar{b}}$	1	1	500	0.0012	μb
Fraction f_o	0.75	0.75	0.75	1.0	
Efficiency ε	0.031	0.006	0.08-0.3	0.39	
Dilution D^2	0.31	0.14	0.16	0.22	
$\varepsilon D^2 f_o B$	$3 \cdot 10^{-7}$	$3 \cdot 10^{-8}$	$6 \cdot 10^{-8}$	$3.5 \cdot 10^{-6}$	
N prod/s	1000	2000	15000	4	
Error on CP Asmmetry	0.02	0.04	0.015	0.08	

SSC Project
$8,249 Million

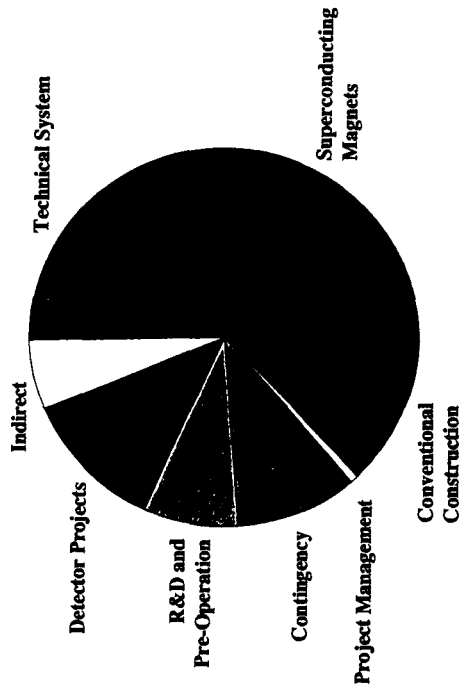

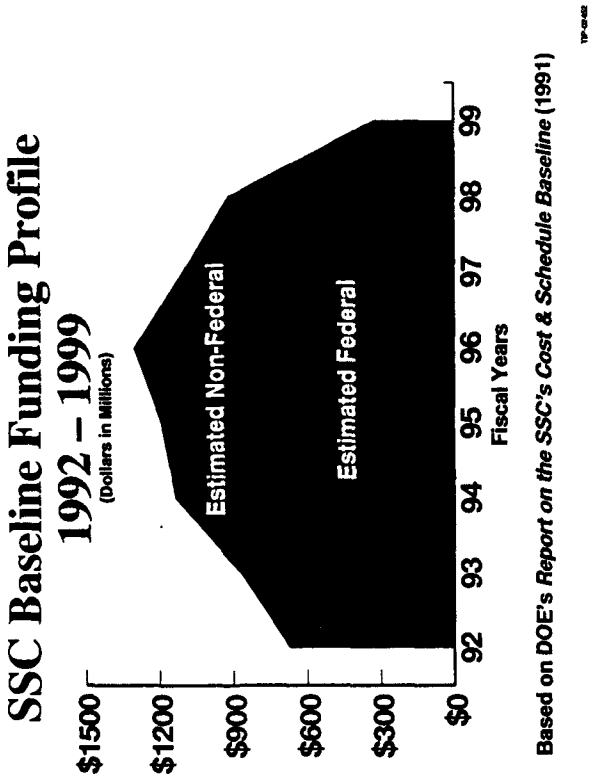

The Superconducting Super Collider

THE INITIAL PHYSICS RESEARCH PROGRAM

- SSC Resources:
  - Project Funds for Detectors FY90 $M 625
  - Project Funds Off-line Computing FY90 $M 87
  - Project Funds for Generic R&D FY90 $M 40

  Project Funds for Experiments FY90 $M 752

  - Project Funds for Halls, Experimental Facilities, and Infrastructure FY90 $M 179

- PAC Recommendation:
  - Two Large Detectors for High E_t Physics
  - Initial Alotment of FY92 $M 225 for Each of the Two Large Detectors, with $M 100 in Reserve.

- Other Resources
  - Non-SSC US Funds and Infrastructure
  - Non US Funds and Infrastructure

V. Lüth May 17,1992 SSC STATUS

REVIEW OF SDC May 4-9, 1992

- PANEL PAC and "Experts"
- EVALUATION:
  - I Scientific Merit
  - II Technical Feasibility
  - III Cost and Schedule
  - IV Management - Resources

  } BASELINE

- SUBPANEL:
  - A Solenoidal Magnet
  - B Tracking
  - C Calorimeters
  - D Muon Detector
  - E Electronics - DAQ - Computing
  - F Halls - Installation - ES&H
  - G Physics - Detector Integration
  - H Cost - Schedule
  - I Management - Resources
- REPORT

  Summary
  Subpanel Reports
  Comments - Questions

REVIEW OF SDC CONCERNS AND ISSUES

SOLENOIDAL MAGNET
- Coil thickness
- ratio of stored energy to cold mass
- very large compressive force
- lack of access for repairs

→ study failure modes

TRACKING SYSTEM
- effects of aging, crosstalk on straws
- no tests yet on Si mechanical structure or module mounting
- extremely agressive schedule

→ justify size, rapidity coverage and performance requirements

CALORIMETER
- detail and justify shower max. detector design; segmentation vs η
- photon detector details?

→ Cost reduction via improved fabrication and assembly methods

MUON SYSTEM
- Alignment (and placement) methods not credible
- Study trigger robustness vs η

→ Investigate staging options

REVIEW OF SDC

ELECTRONICS, DAQ, COMPUTING
- trigger level II, III still vague
- man power needs for software substantial
- schedule very tight

HALLS, FACILITIES, INSTALLATION, ESRH
- assembly and storage space very tight
- muon assembly - installation very complicated and sequential
- access to inner detector very time-consuming and disruptive
- radiation damage due to beam needs more study

DETECTOR - PHYSICS INTEGRATION
→ study detector performance as fct. of η, examine physics potential vs performance, explore staging scenarios.

COST - SCHEDULE
→ improve engineering for fabrication, assembly and installation of calorimeter and μ system
→ examine engineering manpower
→ improve readibility of cost estimate

SDC REVIEW

MANAGEMENT - RESOURCES
→ present more detail of subsystem management and planning, interaction with SSCL
→ present plan for cost reduction and deferral to match presently identifiable resources

REVIEW OF SDC May 4-9, 1992

SUMMARY:

I Detector well-conceived, well matched to potential of 40 TeV collider

II Detector of very challenging design and magnitude, based on solid, broad based R&D. At this stage, many concerns about unresolved problems, but no 'show stoppers'.

III Very tight schedule!
Methods and detail of cost estimation are variable. Improvements in engineering of fabrication and assembly required for calorimeter and muon system! Manpower estimates need review.

IV Management plan ok, project engineer needed! Subsystem management needs to be specified, coordinate activities. A very competent international collaboration.

PAC cannot recommend Stage I approval unless initial project costs are matched by available resources!

PAC MEETING JULY 10-15, 1992

Woodshole, MA Academy of Science

FRIDAY, 7.10.
1pm - 6pm SDC PRESENTATIONS

SATURDAY, 7.11.
9am - 12pm DISCUSSIONS : SDC
1pm - 6pm GEM PRESENTATIONS

SUNDAY, 7.12.
9am - 12pm DISCUSSIONS : GEM

MONDAY, 7.13. - WEDNESDAY, 7.15
CLOSED SESSIONS

GOAL: STAGE I APPROVAL FOR SDC!
→ FORMULATION OF PROJECT BASELINE!

The Superconducting Super Collider

PHYSICS RESEARCH DIVISION

FRED GILMAN, Associate Director
Vera Lüth
Harvey Lynch
+ 35 PHD
+ 25 Visitors. } + Project Staff

OBJECTIVES:
- Plan and Build a Research Program
  - Physics
  - Detectors
  - Test Beams
- Plan and Build a Research Infrastructure
  - Library, Offices, Laboratories
  - Computing, Electronics
  - Engineering
  - Experimental Halls, Facilities
  - Campus,
- Recruit staff and attract Visitors

Report to the SDC

KEK, May 26, 1992

George Trilling

51

Recent SDC Events

Appointment of SDC Project Manager.
Tom Kirk began May 4, 1992.

Modification of bylaws to handle new SDC management structure being voted on.

Modification of Executive Board Representation.
U.S./Canadian university representation goes from 6 to 8.
Two members from Former Soviet Union.

SDC presentations in Korea (April).

PAC Review (May 4-10).

SSC Symposium in Beijing (May 21-24).

SDC Muon Leadership Visit to Russia (May 18-23).

52

SDC NUMBERS IN EACH COUNTRY

COUNTRY OR REGION	NO. COLLABORATORS
U.S.	561
Brazil	5
Canada	26
France	21
Italy	27
Japan	101
U.K.	15
Israel	2
C.I.S. (former U.S.S.R.)	106
Eastern European countries	12
P.R.C.	35
Total Collaborators	911

53

Applications for Admission to the SDC

University of Alabama (Tuscaloosa)

University of South Alabama (Mobile)

Institute of Nuclear Physics (Krakow)

54

How Do We Solve the Shortfall?

BUILD A CHEAPER DETECTOR
Minimizing costs, while mainlaining capability, has been a constant theme of the SDC design efforts. It is the strong view of the SDC that further descoping will substantially reduce the detector capabilities. The issues of requirements and scope will be further addressed in the parallel sessions.

LOCATE MORE NON-U.S. COLLABORATORS
Given the existence of HEP programs all over the world which compete for resources, it may be difficult to find more contributions from abroad. Nevertheless we shall continue to seek additional resources both intellectual and financial from outside the U.S.

STAGE THE DETECTOR TO REDUCE PRESENT FUNDING NEEDS
Everyone wants a complete detector by the time that the SSC reaches design luminosity. If one postpones some of the funding until after turnon, detector completion will be many years delayed, hardly consistent with the expectation of top priority for the SSC program. The collaborators want to see important physics within their lifetimes.

GET MORE U.S. FUNDING
(See next transparency)

PAC Report

General Comments:

The panel was very impressed by the broad scientific and technical base of the SDC and by the high quality of the SDC Technical Design Report. The TDR is based on a strong R&D program that has been supported in part by SSCL, together with significant support from international SDC collaborators, and carried out by the collaboration to develop new technologies and study technological choices for SSC detector subsystems. Many of the difficult choices of technologies for the various subsystems have been made and the collaboration is clearly focused on the remaining issues. The appointment of a Project Manager and soon a Project Engineer are very positive steps toward the goal of creating the SDC detector. While some important technical questions remain open at this time, the panel is convinced that the collaboration is capable of building a powerful detector and doing world class physics at the SSC when the collider begins operations.

It is the panel's consensus that the design of the detector described in the TDR is well matched to the physics goals stated by the SDC.
However, we are seriously concerned about the lack of a credible funding plan for the project. We strongly urge SDC to examine its actual resources from the SSC project, under the previously stated guidelines, and from other institutions in the U.S. and abroad, and to address methods of reducing or delaying project costs.

Potential Further Resources from the U.S.

In its report, the Witherell Subpanel suggests that funding for small SSC experiments might be available in the latter part of the 1990's from the base program on a competitive basis, and recommends not committing the $80M(FY92) presently held in reserve for such experiments until funding for the large detectors is secure.

If the SSCL chooses to follow up on this possibility, and allows assignment of 1/2 of the $80M(FY92) to the SDC detector, the shortfall would be reduced by nearly a factor of 2.
The remaining shortfall of ~$50M would amount to about $6M/year. The SDC would hope to cover this amount through redirection of existing engineering/technical personnel, supported by base program funds, into SDC efforts. This is already happening at a modest level in the collaborating national laboratories.

If the SSCL does not allow consideration of the $80M(FY92) for the large detectors, the shortfall will go from $6M to $10M per year, a figure that we would still hope to cover via base program redirection, but with much greater difficulty.

These figures do not include potential TNRLC support. Present support for SDC work is at ~$2M/year. If continued, this would provide substantial help in completing the funding.

SDC DETECTOR FUNDING SUMMARY

(All amounts expressed in FY1992 dollars)

Estimated Detector Cost	$584M
Estimated Cost Offset (Non-U.S.)	~ $200M
Net U.S. Cost	~ $384M
Anticipated SSCL Funds ($275M in FY1990$)	$292M
Shortfall	~ $92M

Note: The "~" above reflects the substantial uncertainty in the cost offset from non-U.S. contributions.

PAC Report

Issues of Cost, Schedule, and Resources

.....
The panel strongly urges the collaboration to examine its actual U.S. resources and those that can be reasonably anticipated from foreign countries, and present in July a plan to construct a detector within the available funds and with adequate capability to execute a strong physics research program at the start of the SSC operation.

..... (concluding paragraph before the appendices):
If the SDC collaboration can provide a credible plan to design and build a detector for the initial stage of SSC operation that is consistent with the available resources, a positive recommendation by the PAC would be possible, and probable, in July. If such a plan is not provided, Stage I approval will likely be delayed until the entire experimental program with two major detectors can be examined. Such a delay would likely jeopardize the ability of the collaboration to be ready in 1999.

SDC Response on Funding Issues

Develop better information on "available resources":

1) From SSC Project, we can count only on $292M (FY92$).

2) We need to further refine our best estimate of non-U.S. resources. We have a preliminary International Funding Plan and estimate ~$200M in cost offsets.

3) We need to estimate more precisely the potential level of U.S. resources (engineering/technician) supportable by the base program, and we have started a survey of such resources.
Note: The single most important factor in determining whether base program resources can be made available to the SDC fabrication effort is each group's willingness to request and defend the necessary redirection of effort as representing its top scientific priority. The issue is NOT one of expansion but of redirection.

4) We need to work with the SSCL to see if commitment of part of the TNRLC detector support to the SDC fabrication can be secured.

Funding increments will probably not cover the full shortfall (~$90M).

Respond further to the PAC request:

1) Careful reexamination of subsystem costs to see where savings can be achieved. PAC report provides some suggestions.

2) Search for detector items, paid by U.S. funds, which could be delayed beyond startup date and satisfy the following conditions:
   a) Reduced detector at startup can do physics matched to the expected reduced startup luminosity.
   b) Missing capabilities can be added over the three years following the startup.
   c) The reduced detector must match resources that we can identify **now**.

Note: It will probably take 2 - 3 years for the SSC to reach design luminosity with increments of about an order of magnitude each year.

What items do we delay?

We must reduce U.S. costs and retain a detector which can do physics at reduced luminosity, and can be completed without excessive difficulty. Examples:

Tracking:
Defer silicon disk system.
Calorimetry:
Defer separate massless gap readout.
Defer readout of two longitudinal segments in endcap EM.
Muons:
Stage rapidity coverage of outer muon system (BW2/BW3, IW2/IW3,FW4/FW5) and scintillator.
Trigger/Electronics:
Defer level 1 tracking trigger.
Defer level 2 trigger.
Reduce level 3 processor farm.
Other Ideas??

We need to consider what physics we can do at 10^{30} - 10^{31}, and use that as guidance for evaluating the staging options.

How to finance the completion of the detector?

1) ***Funding before Turnon*** **(Roy Schwitters View)**
There is high probability that the needed monies will be found within the SSC Project over the next 7 years (very small on scale of $8B project). Possibility: $80M presently reserved for small experiments. However neither Lab management nor DOE wants to make this commitment now.

2) ***Funding after Turnon***
New monies from U.S. HEP operating and equipment funds, since SDC should have very high priority at that time, and hopefully additional support from at least some of non-U.S. collaborators.

We must emphasize to the PAC and the SSCL that it is essential to complete our detector by the time design luminosity is reached.

Concluding Remarks
(Some Tasks for this Meeting)

We need to begin preparing our July response to the SSCL/PAC and defining the detector which will satisfy the funding conditions laid down. The final decision on this will have to be at the Exec.Board/Tech.Board meeting in late June.

We need to proceed in the direction of improving our international funding plan and better defining responsibilities especially in the areas of electronics and muon systems.

We need to develop further the international responsibilities in the development of prototypes for the various subsystems.

We need to prepare further the processes for review and decision later this summer for the relevant subsystem Issues.

Report from Project Manager

Thomas B.W. Kirk
(Argonne National Laboratory)

KEY AREAS OF SDC EXPER. EFFORTS
1992 – 1999

SCIENTIFIC FOCUS:

- STANDARD MODEL & BEYOND SM PHYSICS INVESTIGATIONS
- RELATIONSHIPS TO OTHER PROGRAMS (STRUCTURE FNS, QCD, ETC.)
- BENCHMARK PHYSICS PROCESSES
- DATA PROCESSING & STORAGE FOR MAX. PHYSICS EXPLOITATION
- Further R&D FOR FUTURE UPGRADES OF DET. CAPABILITY

DETECTOR PROJECT FOCUS:

- BASELINE COST, SCHEDULE & TECH. PERFORMANCE SPECIFICATION
- ASSIGNMENT OF DETECTOR ELEMENTS FOR DESIGN & CONSTRUCTION
- CREATION OF THE PROJECT MGMT. & REPORTING SYSTEM
- IDENTIFICATION OF RESOURCES TO MEET THE NEEDS OF THE PROJECT

T. KIRK
MAY 1992

The Project Manager's Dilemma . . .

TECHNICAL PERFORMANCE
better!

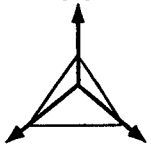

cheaper! COST PERFORMANCE

faster! SCHEDULE PERFORMANCE

Once the basic mission has been identified, its execution becomes a continuous struggle to stay within the sponsor's *triangle of acceptability.*

PROJECT TERMS (& TRANSLATION FOR PHYSICISTS)

BASELINE: THE CURRENT PLAN FOR THE SDC DETECTOR; MUST BE SELF-CONSISTENT AMONG THE TECH. PERF., COST & SCHEDULE ASPECTS

ALTERNATE: A PROPOSED ALTERNATIVE TO THE BASELINE THAT HAS TECHNICAL, COST OR SCHEDULE ADVANTAGES, BUT WHICH HAS NOT YET BEEN ADOPTED

QUALITY ASSURANCE: A SYSTEM OF ACCEPTANCE TESTS, QUALITY CONTROLS, TRACKING & DOCUMENTATION WHOSE PURPOSE IS TO ENSURE THAT THE CONTROLLED ITEMS MEET ALL THEIR TECH. PERFORMANCE SPECIFICATIONS

VALUE ENGINEERING: THE PROCESS BY WHICH A DEFINED TECHNICAL DEVICE OR SYSTEM IS REDUCED IN COST WITHOUT TECHNICAL COMPROMISE THROUGH THE APPLICATION OF OPTIMUM, COST-EFFECTIVE MFGR. TECHNOLOGIES

CONFIGURATION MANAGEMENT: A SYSTEM OF CHANGE-CONTROL, RECORD-KEEPING & PERSONNEL NOTIFICATION WHOSE PURPOSE IS TO LIMIT SIGNIFICANT CHANGES TO THE CONTROLLED ITEM TO THOSE THAT HAVE BEEN FORMALLY AGREED TO BY THE RELEVANT MANAGERS

RESOURCE-LOADED TRACKING: AN INTEGRATED SYSTEM OF COST & SCHEDULE TRACKING THAT RELATES THE RATE AT WHICH RESOURCES (MONEY & EFFORT) ARE APPLIED TO PROJECT ELEMENTS AND THE SCHEDULE THESE ITEMS WILL EXPECT TO REACH COMPLETION AS A RESULT (IE SCHEDULE DETERMINATION DRIVEN BY RESOURCE APPLICATION RATE)

Basic SDC Project Goals and Tools for their Realization

GOAL	TOOL
• The detector must meet its physics performance specs.	• Physicist oversight, insight and reviews
• The detector elements must work (technical performance)	• Engineering reviews, CM and Q/A Programs
• The detector must be ready on time (schedule performance)	• Management role, i.e. planning, tracking and resource allocation
• The costs cannot exceed the funding provided (cost performance)	• Value engineering, early procurement, and vigilant production oversight; vigorous sponsor solicitation

Strategy for Detector Work

- Offsite Design & Production to Max Extent
  - — U.S. Sources
  - — Non-U.S. Sources
- SSCL - Based Integration & Installation
  - — Installation at SSCL is intrinsic
  - — Integration has three key areas of application
    - detector subsystems
    - machine/detector interface
    - conventional facilities interface
- Beam Tests / R & D Activity
  - — FNAL in early years
  - — CERN/BNL/KEK/BEPC for special studies
  - — SSCL after 1996
- Management and Tracking
  - — SSCL - based for high level aspects
  - — Offsite - based for subsystem level aspects
  - — Coordination/liaison personnel as needed
- ESH Aspects
  - — Installed elements must meet SSCL standards
  - — Offsite activity must meet local standards

SDC Management

- Management is organized by major subsystems (WBS) with staff support functions.
- Subsystem managers are geographically dispersed *
- Major technical decisions are made by SDC Technical Board
- Reporting is through PRD for SDC Project and through SDC Executive Committee for Collaboration Issues
- Tracking, reporting, integration and change control are centered at SSCL
- Details of management tropical areas and methods in SDC Project Management Plan (Draft due to D&E, September 1991)

* heavy burden so far on "somebody"---

SOLENOIDAL DETECTOR COLLABORATION

DRAFT PROJECT MANAGEMENT PLAN

APRIL 1, 1992

Submitted by

M. Gilchriese
SDC Project Manager
Physics Research Division
Superconducting Super
Collider Laboratory

Approvals

F. Gilman
Associate Director
Physics Research Division
Superconducting Super
Collider Laboratory

J. Rees
Project Manager
Superconducting Super
Collider Laboratory

R. F. Schwitters
Director
Superconducting Super
Collider Laboratory

#2OT—000006

TABLE OF CONTENTS

1.0 INTRODUCTION....1
1.1 Scope....1
1.2 Participants....1
1.3 Applicability....1
1.4 Background....2
1.5 Reference Documents....3

2.0 OBJECTIVES....4
2.1 Program Objectives....4
2.2 Physics Objectives....4
2.3 Technical Objectives....4
2.4 Schedule Objectives....6
2.5 Cost Objectives....6

3.0 MANAGEMENT ORGANIZATION AND RESPONSIBILITIES....7
3.1 Overview....7
3.2 SSC Management and Oversight....7
3.3 SSCL Organization....9
3.4 Physics Research Division....11
3.5 Solenoidal Detector Collaboration....12
3.6 SDC Subsystem Management....14

4.0 NATIONAL AND INTERNATIONAL PARTICIPATION 16
4.1 SSCL Objectives....16
4.2 Government Coordination of International Programs....16
4.3 The SDC plan....17
4.4 Foreign Travel Needs....18

5.0 WORK PLAN....20
5.1 SSC Project Overview....20
5.2 The SDC Detector....20
5.3 Method of Performance....22
5.4 Responsibilities....23
5.5 Plans and Implementation....23
5.6 Project Compliance....24
5.7 Relationship to other SSCL Divisions....25

6.0 ENVIRONMENTAL, SAFETY & HEALTH PROTECTION....26
6.1 Overview....26
6.2 Environmental Protection....27
6.3 Safety and Health Protection....27
6.4 Emergency Preparedness....28
6.5 Compliance....28

7.0 CONFIGURATION MANAGEMENT, DOCUMENTATION AND CHANGE CONTROL....29
7.1 Documentation....29
7.2 Document Control....29
7.3 Organizational Responsibilities....30
7.4 Change Control....31
7.5 Configuration Status Accounting....32

7.6 Reviews and Audits....32
7.7 Change Control Authority....33

8.0 PROJECT WBS AND COST ESTIMATE....34
8.1 SDC Project Work Breakdown Structure....34
8.2 Cost Estimates....35
8.3 SDC Funding....36
8.4 Cost Management....37

9.0 SCHEDULES....39
9.1 Overview....39
9.2 Major SDC Milestones....39
9.3 Summary Schedule....40
9.4 Logic and Detailed Schedules....40
9.5 Schedule Baseline....41
9.6 Schedule Management....41

10.0 MEASUREMENT AND REPORTING....43
10.1 Performance Measurement....43
10.2 Reporting....44
10.3 Project Review Meetings....45
10.4 Formal Communications....45

11.0 SYSTEMS ENGINEERING AND INTEGRATION MANAGEMENT PLAN46
11.1 Overview....46
11.2 Detector Engineering....46
11.3 Conventional Facilities....48
11.4 Documentation....48
11.5 Configuration Management....50
11.6 Technical Reviews....50
11.7 Test, Evaluation, & Commissioning....50
11.8 Integration....51

12.0 QUALITY ASSURANCE PLAN....52
12.1 Overview....52
12.2 SDC Quality Objectives....52
12.3 QA Implementation....52
12.4 QA Compliance....54
12.5 Quality Awareness/Training....54

13.0 UTILITIES FOR THE SDC DETECTOR....55
13.1 General....55
13.2 Site Plan....55
13.3 Overall SDC Utility Requirements....55

14.0 ADVANCE ACQUISITION PLAN....59
14.1 Introduction....59
14.2 Major Procurement Policy Considerations....59
14.3 SDC Procurement Objectives....60
14.4 SDC Procurement Approach....60
14.5 Major Acquisitions From Industry....62

15.0 GLOSSARY....63
15.1 Acronyms....63
15.2 Terms....64

APPENDICES

APPENDIX A -- SDC COLLABORATION PARTICIPANTS....66
APPENDIX B -- SDC BY-LAWS....67
APPENDIX C -- REFERENCE DOCUMENTS....71
APPENDIX D -- PROJECT ORGANIZATION AND KEY PERSONNEL....72
APPENDIX E -- WORK BREAKDOWN STRUCTURE....75
APPENDIX F -- PROJECT SUMMARY COST ESTIMATE....76
APPENDIX G -- FUNDING PROFILE....77
APPENDIX H -- FUNDING PLAN....78
APPENDIX I -- PROJECT MILESTONE LIST....79
APPENDIX J -- KEY DOCUMENTS....80
APPENDIX K -- INSTITUTIONAL AGREEMENTS....81
APPENDIX L -- COST ESTIMATING PROCEDURES....82

LIST OF TABLES AND FIGURES

FIGURE 2-1 THE SDC DETECTOR....5
FIGURE 3-1 SSC MANAGEMENT AND OVERSITE....8
FIGURE 3-2 THE SSCL ORGANIZATION....10
FIGURE 3-3 PHYSICS RESEARCH DIVISION ORGANIZATION....11
FIGURE 8-1 SUMMARY WBS FOR THE SDC PROJECT....34
FIGURE 9-1 SDC SUMMARY SCHEDULE....40
FIGURE 13.1 IR8 SURFACE FACILITIES....56

TABLE 1.1 COLLABORATION INSTITUTIONAL MEMBERSHIP....2
TABLE 7.1 DETECTOR SPECIFICATION APPROVAL LEVELS....30
TABLE 8.1 SUMMARY SDC COST ESTIMATE....36
TABLE 9-1 MAJOR SDC MILESTONES....39

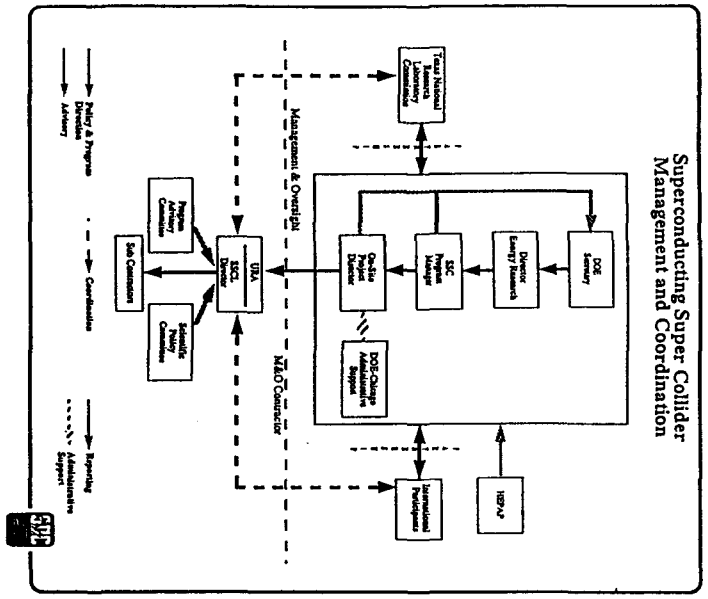

77

Physics Research Division Organization

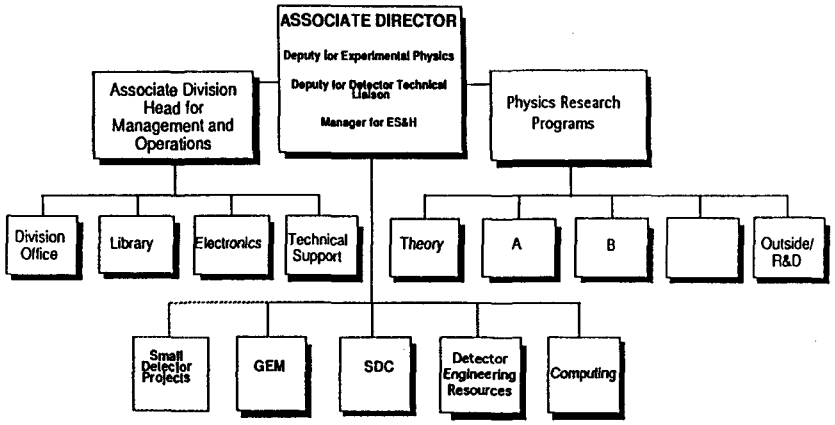

78

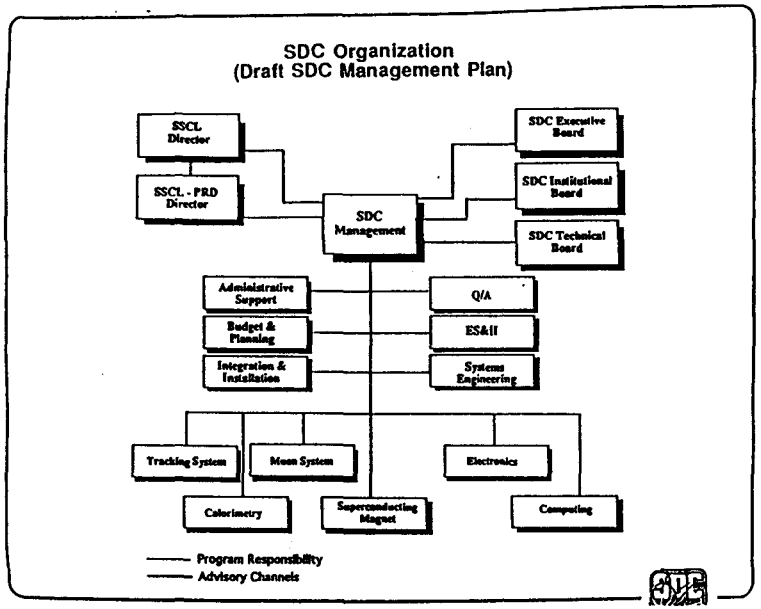

79

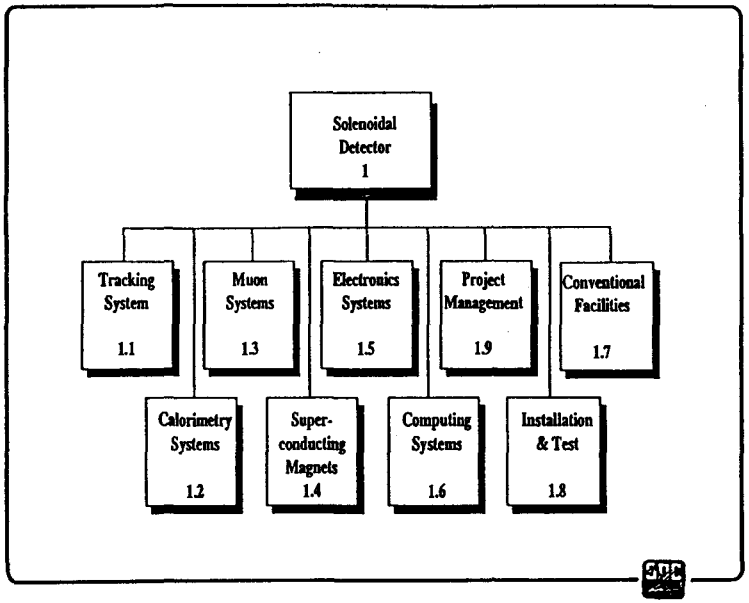

80

Detector Cost Considerations

- The cost estimation and tracking will follow methodology described in the SDC Project Management Plan (PMP)
- Resources to meet the approved cost elements will be provided through multiple U.S. and non-U.S. resources
  - — multiple accounting methods for foreign contributions
  - — resulting cost tracking will be evaluated using SSCL methodology (U.S. protocols)
- Reporting on project evolution will follow the prescriptions identified in the SDC PMP
- Oversight and review of the cost performance will be carried out as prescribed in SDC PMP

Summary of SDC Detector U.S. Cost Estimate by Subsystem

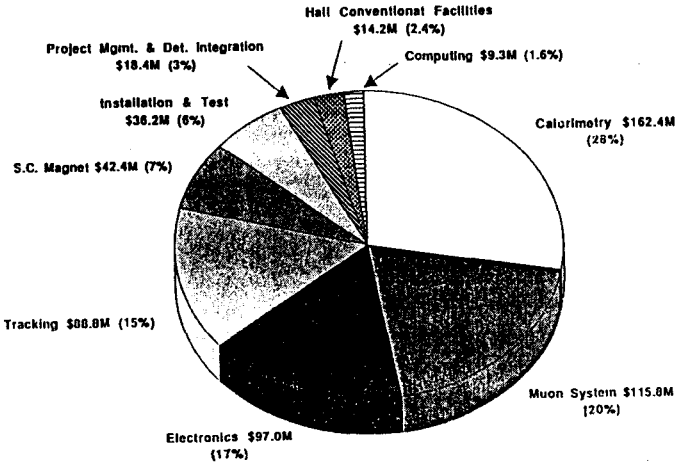

Total FY92 U.S. Cost Equivalent = $584M

Cost Summary

- Detailed "bottoms-up" estimate for all systems
- Based on Parameters Book Rev. D
- All costs (including R&D and prototypes) from U.S. FY93 - FY99.
- No physicists salaries
- U.S. estimating practices (to the best of our ability)
- Does not take account of existing infrastructure - calculate cost offsets later
- Non - U.S. contributions (cost offsets) will not be discussed here - presented in separate session
- Cost information documented at three levels of detail
  1) Cost and schedule summary
  2) Cost detail - rollup
  3) Cost backup

Cost History

- Previous estimates escalated to FY92
- Same accounting as present detailed estimate
- See graph

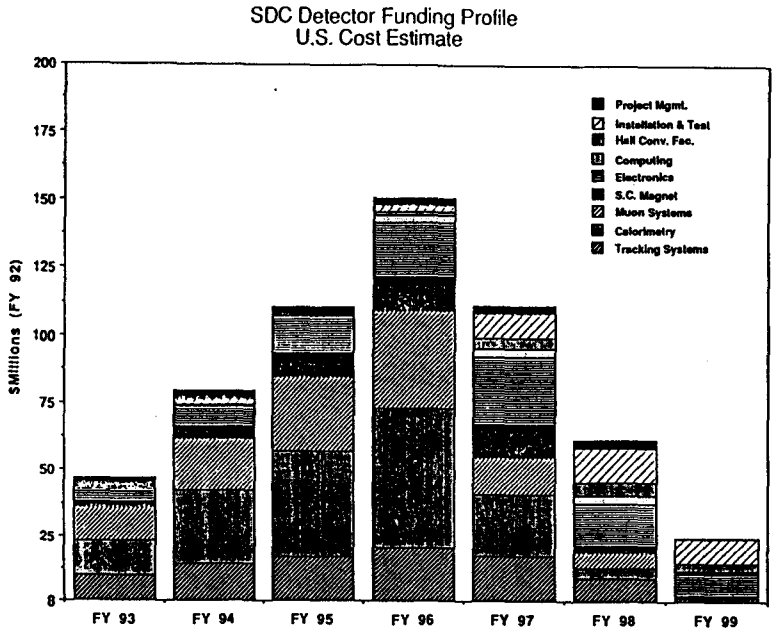

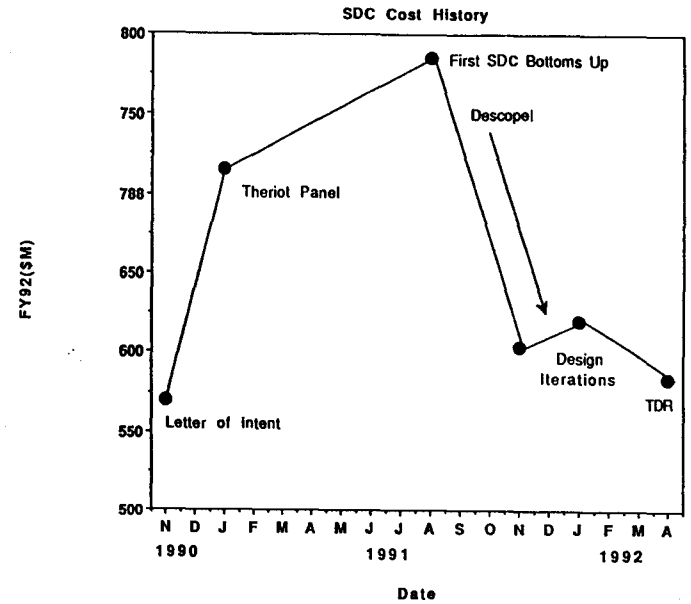

Funding Profile(FY93- FY99) and Previous Funding

- Integrated schedule does not yet exist => preliminary funding profile only
- Construction funding profile - U.S. equivalent - see Fig.
- Funding - from SSCL "detector pot"

FY91(post LoI approval in Jan. '91)	$2.4M
FY92(present)	$16.4M
FY93(request - start construction)	$35-40M

- In addition there is funding this year (FY92) from non - U.S. sources (≈ $3 - 5M), State of Texas (≈ $2 equivalent) and other SSCL and DHEP sources (≈$3M)

	LoI	TDR
Silicon	28 m^2 ---------->	17m^2
Straws	8 ---------->	5 superlayers
	188,000 ---------->	137,164 channels
Intermediate	straws ---------->	gas microstrip detectors
Central calor.	41,000 ---------->	20,352 tower channels
	25,000 ---------->	47,104 shower max. channels
	Pb ---------->	Fe hadronic absorber
Forward calor.	7000 ---------->	1056 channels
Muon system	108,400 ---------->	89,864 wire channels
	7,800 ---------->	4496 scintillation counters
	28 ---------->	22 layers - central region
	26 ---------->	24 layers - forward region
	4m ---------->	3m forward toroid thickness
Trigger	----decrease scope---->	
DAQ	----stage part of Level 3--->	

Schedule Summary

- Fully integrated schedules under development - first pass complete by Sept. 1 in time for DOE review
- Summary schedule - see Figs.
- What's on or close to the critical path?
  - Barrel toroid and its support
  - Central calorimeter
  - Underground hall
- See summary book for more details

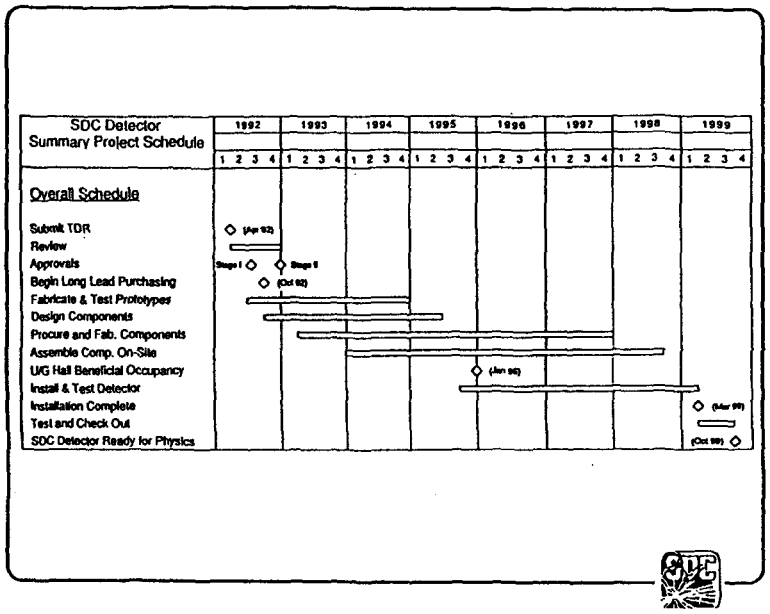

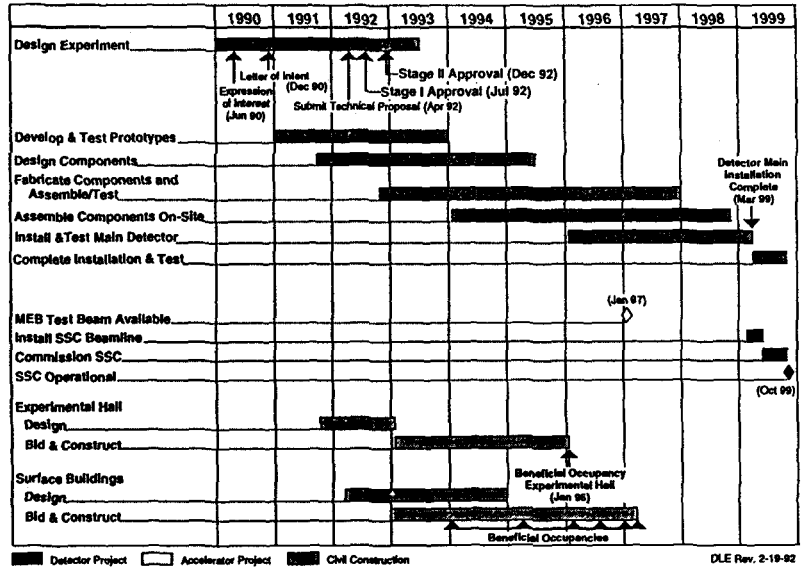

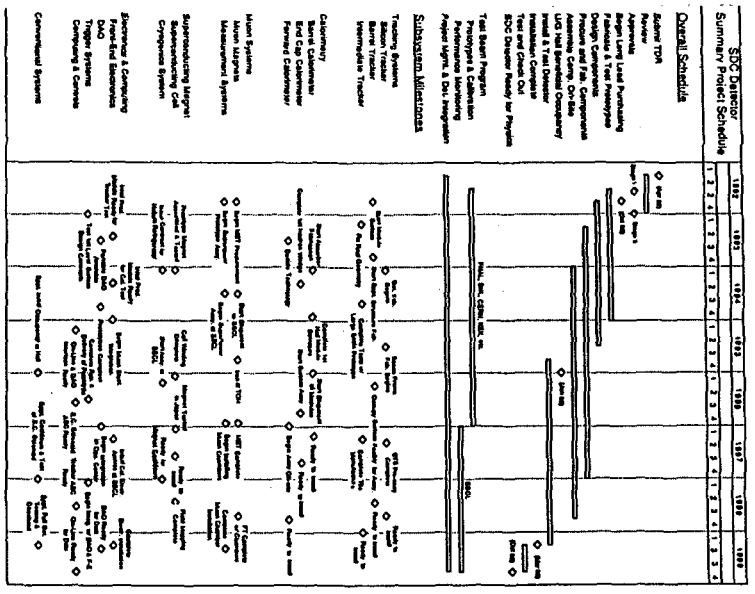

Measurement and Reporting Overview

An integrated cost/schedule/technical Performance Measurement System (PMS) will be utilized on the SDC Project, in order to support SDC project management and reporting. Based on the SDC WBS, and the baselines established following establishment of the approved SDC Technical Design, the SDC will establish monthly performance measurement reporting. For SDC activity performed at non-US institutions, or involving in-kind contributions, special procedures will be implemented to track schedule and technical progress. In most cases those special approaches will be spelled out in individual institutional agreements established by SDC management.

Future Plans

- **Level of detail needed for project of this magnitude greater than previous HEP experiments!**
- **Cost machinery in place and can track detector design changes**
- **Need to integrate schedules**
- **Detailed funding profiles and identify major procurements**
- **Survive DOE review in September!**
- **Establish baseline cost**

REPORT ON SUPERCONDUCTING MAGNET

Akira Yamamoto

KEK

Presented SDC Collaboration Meeting held at KEK on
May 26, 1992

CONTENTS

- Progress of Design Study
  - Boundary Condition Revised
  - Support System and Impact on Transparency
- Progress of Prototype R&D
  - Conductor
  - Coil Winding
  - Vacuum Vessel (Honeycomb / Isogrid)
- Summary

THIS IS A CO-OPERATIVE WORK

AMONG

FNAL
KEK
SSCL
P.S. ASSOCIATE.
TOSHIBA
FURUKAWA ELECTRIC.
IHI / SUMITOMO LIGHT METAL

Table 5-1
General requirements of SDC solenoid.

Magnet envelope		
Cryostat	Inner radius	1.70 m
	Outer radius	2.05 m
	Total half length	4.389 m
Nominal magnetic field		2 T
Transparency	(η=0)	1.2 X_0
		0.25 λ_I
Cool down time		< 14 days
Quench recovery time		< 4 hr

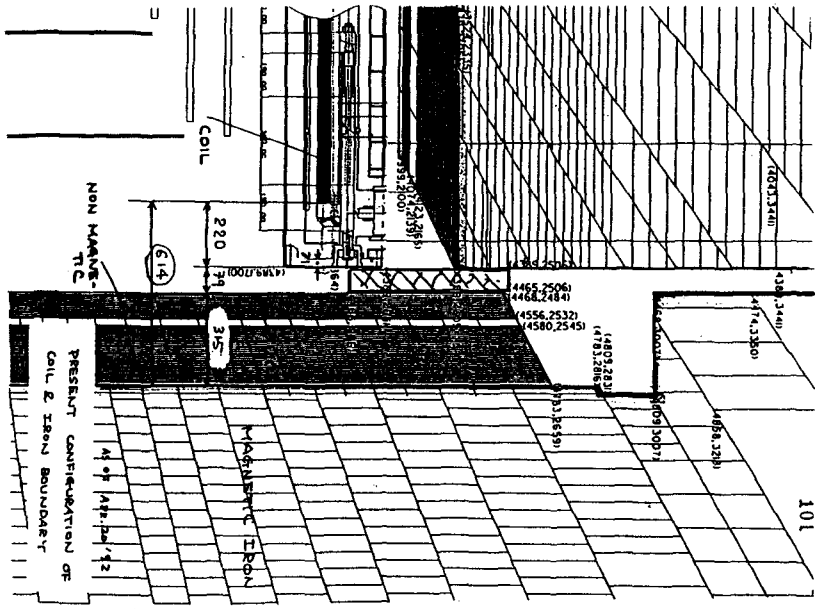

Superconducting Magnet

- Technical challenges : 1. material transparency $\sim 1.2X_0$
  2. compressive force (1700 tonf)

  in addition to predictable and stable operation
  safety against quenches

- Solutions :

[A] $\frac{E(\text{stored energy})}{M(\text{cold mass})} = 7.4$ kJoule/kg ($\Delta = 0.4X_0$)
~ 5 in past

→ development of high strength aluminum stabilized superconductor

→ increase of quench propagation velocity by pure aluminum strips

[B] lighter material for outer vacuum vessel ($\Delta = 0.2X_0$)

→ isogrid (grid-stiffened) shell or brazed aluminum honeycomb panel

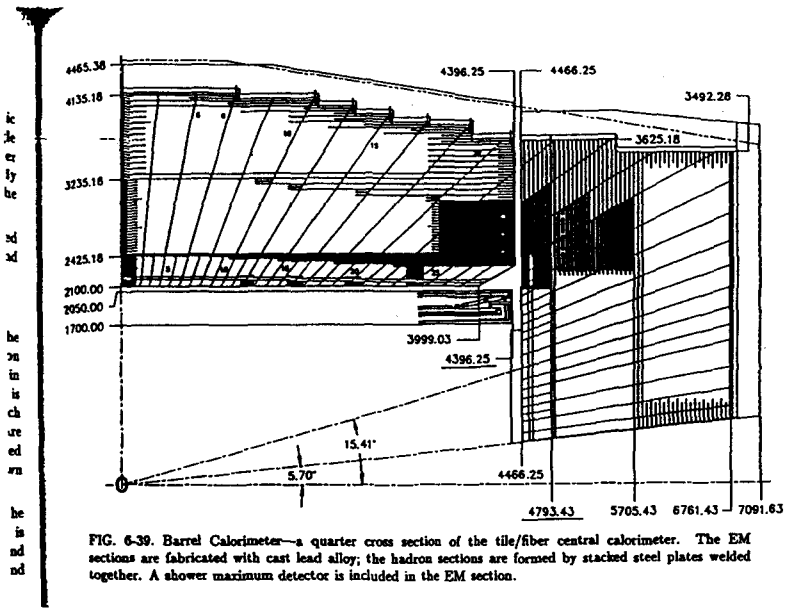

FIG. 6-39. Barrel Calorimeter—a quarter cross section of the tile/fiber central calorimeter. The EM sections are fabricated with cast lead alloy; the hadron sections are formed by stacked steel plates welded together. A shower maximum detector is included in the EM section.

PARAMETERS IN PHYSICS AND ENGINEERING

Requirements from Physics	Engineering Parameters important
	Coil
- Magnetic Field	- Mechanical Safety at 2 T
Bc = 2 T	Max. Stress (2 τ) < 60 MPa
Fz = 1300 tonnes	(@ Y.S.0.2% = 67 MPa)
	associated with outer support cylinder
- Tranparency	- Stability in Superconductivity
X = 1.2 Xo (@η = 0)	MQE = 0.27 J
< 3.0 Xo (@η = 1.5)	(same level as that in TOPAZ, CDF)
λI = 0.25 λI (@ = 0)	- Thermal Safety after QUENCH
	Tmax ≲ 100 K
	Δε < 0.05 % (elastic condition)
	Cryostat (Vacuum Wall)
	- Stability against Buckling
	Pbkl > 2 atm

According to recent technical decision for calorimeter to take feromagnetic iron abosorber option:

Axial Distance b/w Coil and Iron-end:	47 - 62 cm
Maximum Stress (2 τ) in the Coil :	52 - 54 MPa
Axial Compressive Force * :	1100- 1300 t
Axial Decentering Force :	20 - 15 t/cm

(* Axial Compressive Force in Air : 1,700 tonnes)

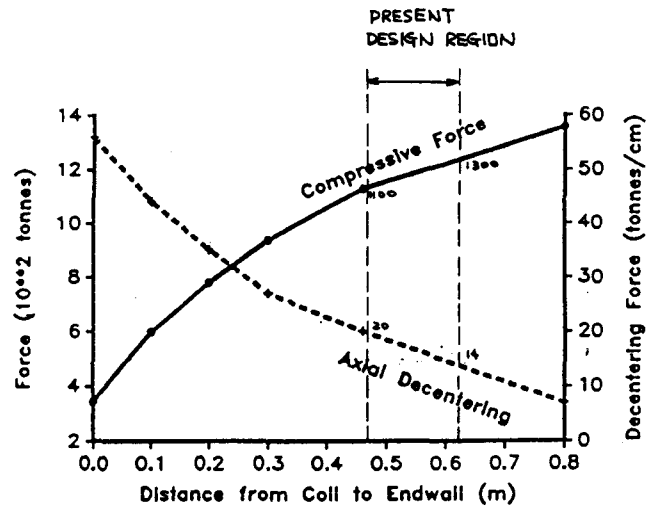

FIG. 5-1. Coil compressive force and axial decentering force as a function of the axial distance between the end of the coil and the iron endcap calorimeter.

Table 5-2
Baseline design parameters of SDC solenoid.

Dimensions:		
Cryostat	Inner radius	1.70 m
	Outer radius	2.05 m
	Half length	4.389 m
Coil	Effective radius	1.84 m
	Half length	4.12–4.18 m
Conductor	Thickness	44 mm
Outer support cylinder	Thickness	31 mm
Electrical parameters		
Central field		2.0 T
Nominal current		8,000 A
Inductance		4.6 H
Stored energy		146 MJ
Stored energy / cold mass		7.4 kJ/kg
Typical charging time		1 hour
Mechanical parameters		
Effective cold mass		20 tonnes
Total weight		25 tonnes
Radial magnetic pressure		1.6 MN/m²
Axial compressive force		11 MN (15)

Table 5-3
Transparency of the solenoid.

Element		Thickness [mm]	X_0	λ_0	Saving %
Outer vac. wall	(Isogrid)	11	0.138	0.0321	⇒ ~0.2%
	(Honeycomb)	(7.1)	(0.080)	(0.0180)	
Outer rad. shield		2.0	0.022	0.0051	
Outer sup. cylinder		31.0	0.348	0.0787	⇒ ~0.4%
Superconductor					E/m = 1.5 kJ/kg
(Al stab)		39.0	0.438	0.0990	
(Nb.Ti/Cu)		2.9	0.181	0.0167	
(GFRP)		3.1	0.016	0.0058	
(Al Strip)		2.0	0.022	0.0051	
Inner rad. shield		2.0	0.022	0.0051	
Inner vac. wall		6.0	0.067	0.0152	
Super-insulation		2.0	0.007	0.0023	
Total	(w/ isogrid)		1.261	0.2651	~ 0.6%
	(w/ honeycomb)		(1.203)	(0.2510)	

Table 5-5
Design parameters of the SDC superconductor.

Aluminum stabilized superconductor	
Superconductor material	Nb Ti/Cu
Stabilizer	Al (99.999% +200 ppm Zn)
Area ratio (Nb/Ti/Cu/Al)	1/1/29.8
Conductor size	43.8×4.37 mm^2
Superconductor strand	
Strand diameter	1.277 mm
Nb Ti filament diameter	20 μm
Number of filaments.	4100
Superconductor cable	
Overall size	6.4×2.5 mm^2
Number of cables	10 (2×5)
Cabling pitch	50–60 mm
J_c in Nb Ti (at 5 T, 4.2 K)	2500 A/mm^2
Critical current (at 5 T, 4.2 K)	16,000 A
Characteristics of stabilizer	
RRR (Cu)	100
RRR (Al)	500
Yield Strength of Al (at 77 K)	67 MPa
Shear strength b/w Cu / Al	20 MPa
Conductor welding joint	
Joint resistance (at 4.2 K)	$< 10^{-9}\ \Omega$

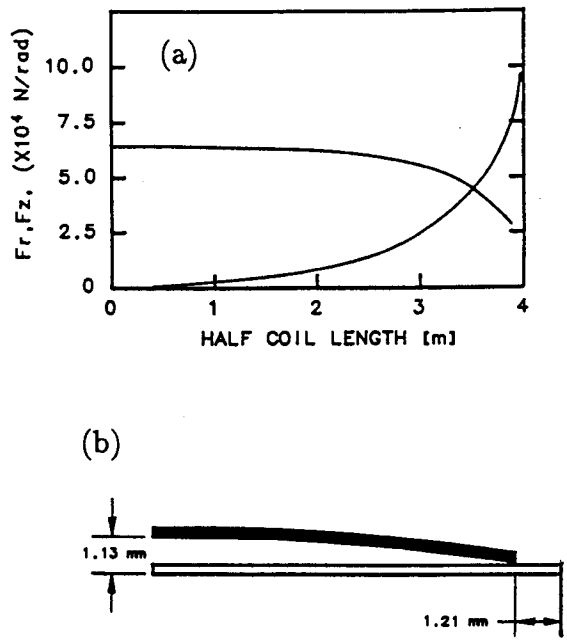

FIG. 5-8. (a) Radial and axial components of the force on the superconducting coil; (b) deformation of the coil under these forces.

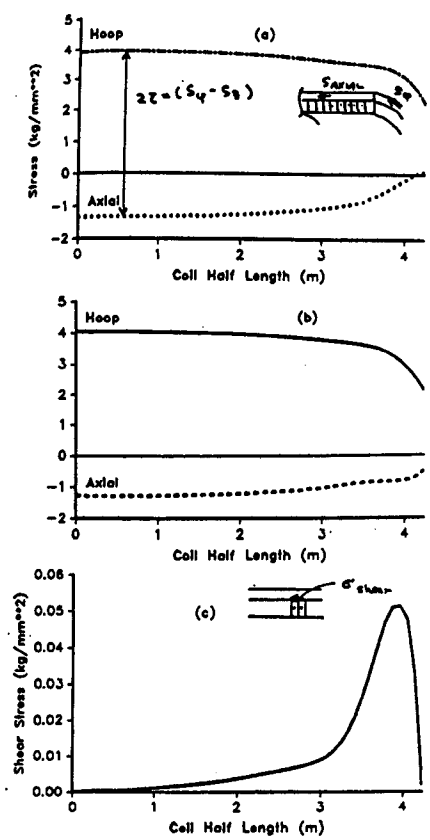

FIG. 5-9. Stresses as a function of axial position (a) on support cylinder, (b) on superconducting coil, and (c) on epoxy joint.

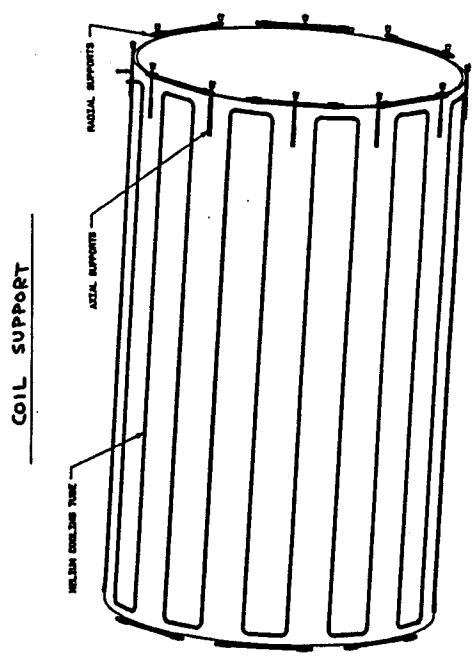

FIG. 5-7. Solenoid cold mass. Radial supports are on both ends, axial supports are on one end only.

COIL SUPPORT DESIGN

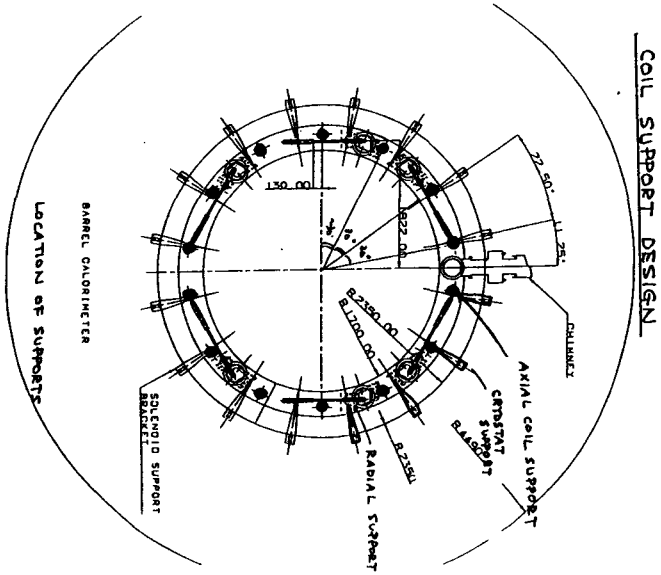

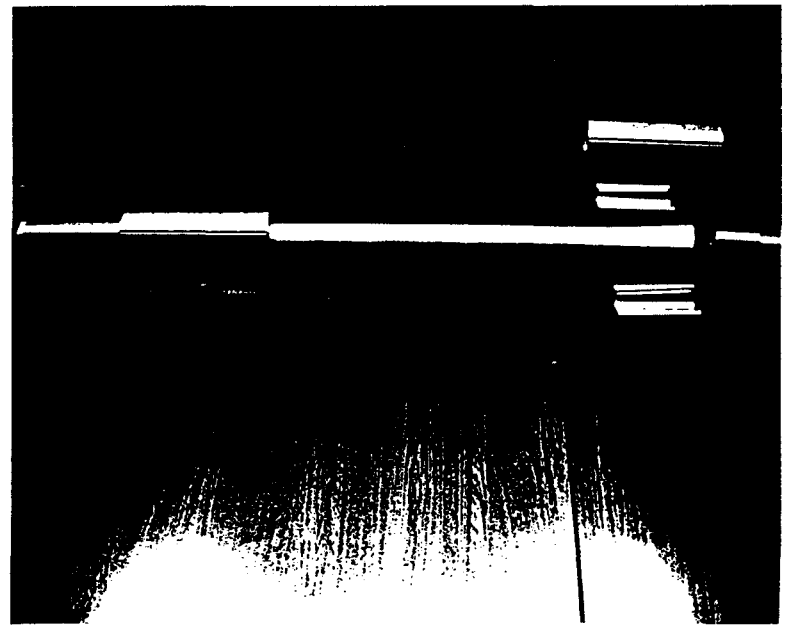

DESIGN OF AXIAL SUPPORTS OF THE COIL

	TDR	RE-REVISED (APRIL 28)
MATERIAL FOR SUP.	GFRP	GFRP
TYPE	SINGLE	SINGLE
DIA. OF SUPPORT	ϕ20mm	ϕ20mm (18)
EFFECTIVE LENGTH	300mm	300mm (240)
MATERIAL FOR BASE	Ti-Alloy	Al-Alloy(7075)
DIA. OF BASE	ϕ50mm	ϕ50mm
LENGTH OF BASE	~150mm	~150mm
# OF AXIAL SUPPORT	14	14
TENSILE FORCE/14RDS.	≥300tonnes	≥300tonnes
BUCKLING FORCE/14RDS.	100tonnes	100tonnes
THERMAL LOADS/14RDS.	~600mW	~600mW
BUMP IN TRANSPARENCY	3.7	1.4
(MAX) at η=1.4	at tR=60mm	(tR=60mm)

Table 5-8
Design load of the coil support system. (RADIAL SUPPORT)

Function		Upward	Downward	Left/right	F/B-ward
Global force					
Coil weight	(ton)	−20	20		
Applied load	(ton)	40	40	40	40
Design load	(ton)	20	60	40	40
Force constant	(t/mm)	2	2	2	2
Support stiffness	(t/mm)	>10	>10	>10	>10

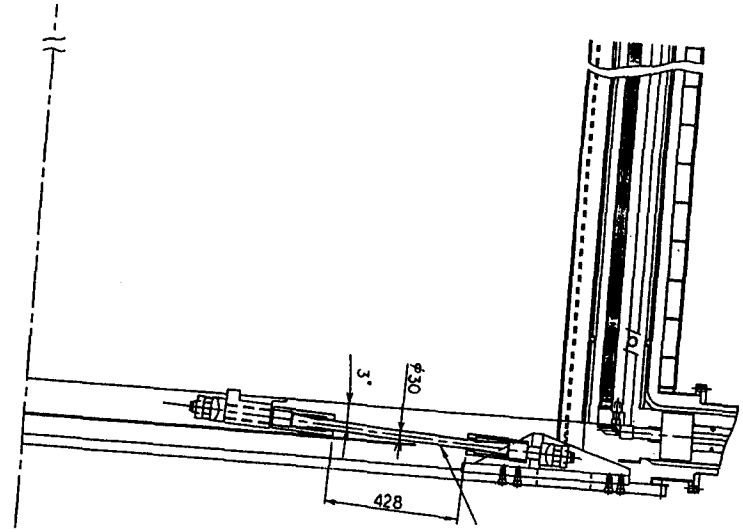

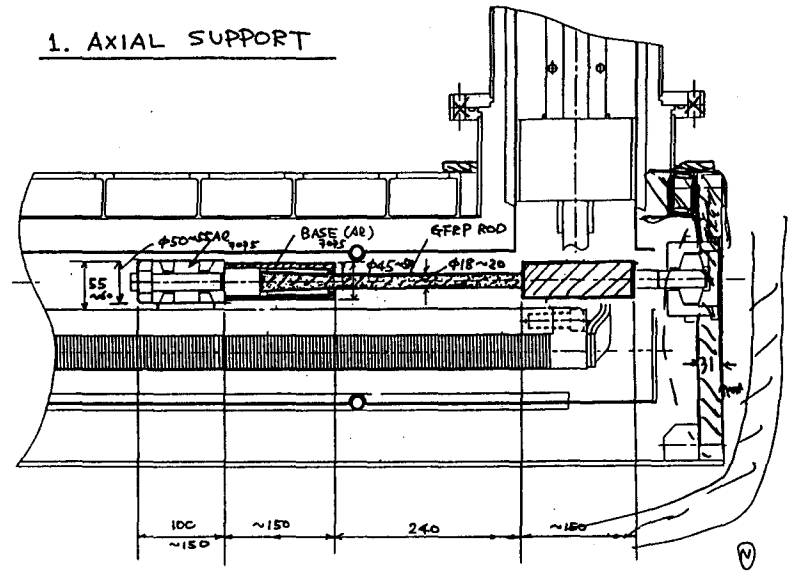

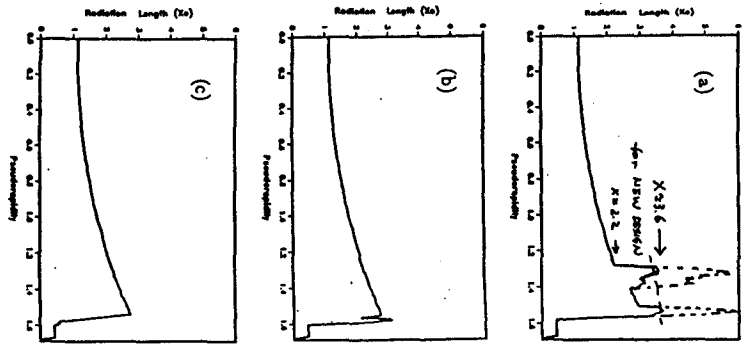

FIG. 5-5. Thickness of solenoid, in radiation lengths, as a function of pseudorapidity: (a) is a path through an axial support and is typical of 6% of the circumference, (b) is through the metallic end fitting of a radial support, 15% of the circumference, and (c) is through the GFRP section of a radial support, 21% of the circumference.

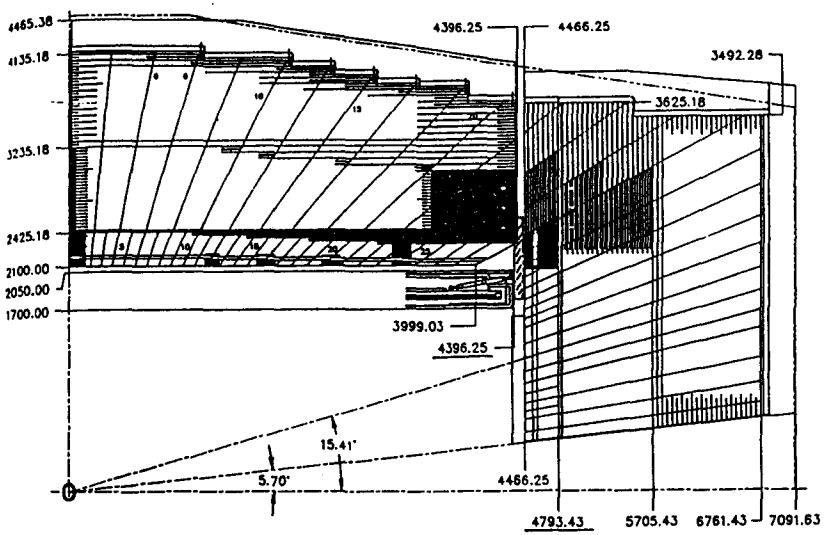

FIG. 6-39. Barrel Calorimeter—a quarter cross section of the tile/fiber central calorimeter. The EM sections are fabricated with cast lead alloy; the hadron sections are formed by stacked steel plates welded together. A shower maximum detector is included in the EM section.

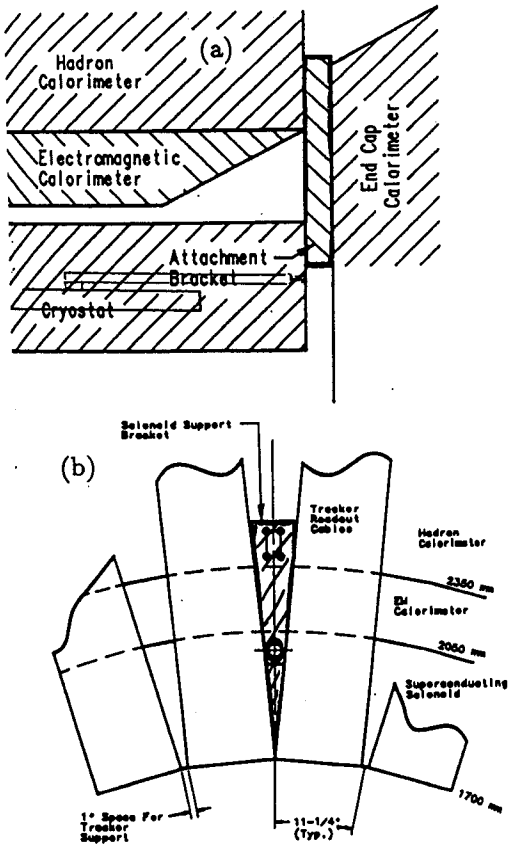

FIG. 5-13. Cryostat attachment to the barrel hadron calorimeter, (a) section view, (b) enlarged end view.

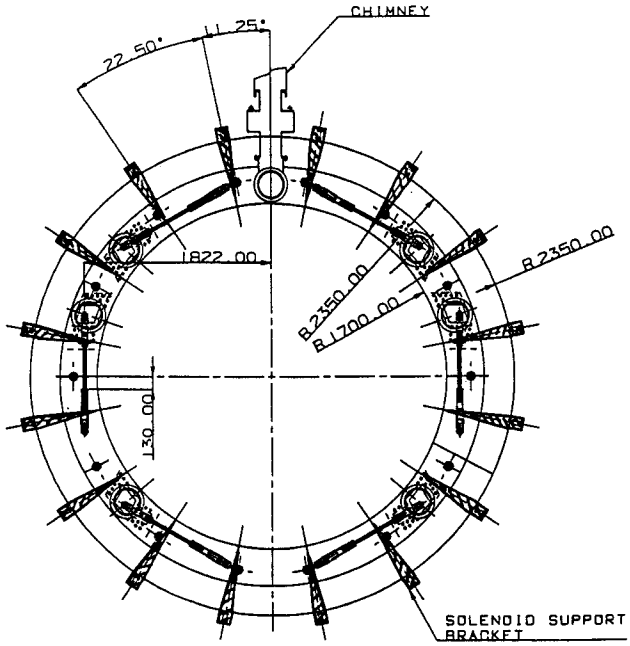

BARREL CALORIMETER

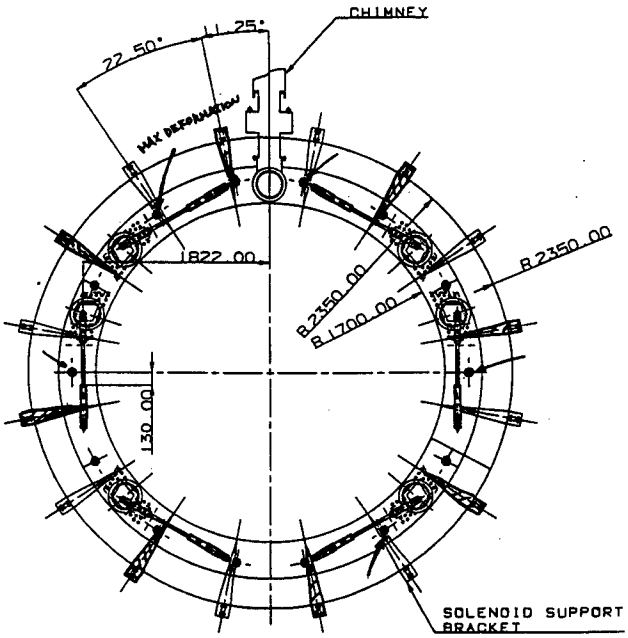

BARREL CALORIMETER

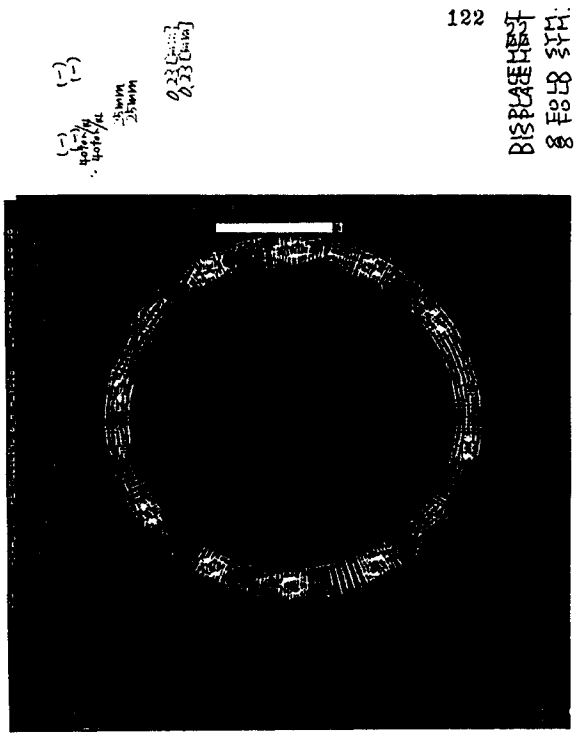

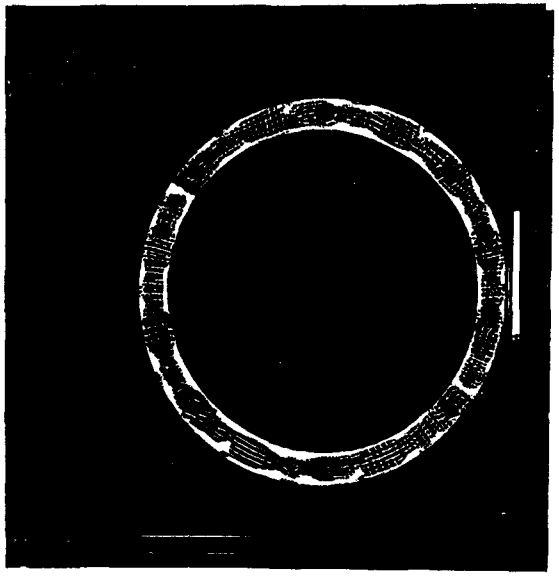

STRESS

8 FOLD SYM.

123

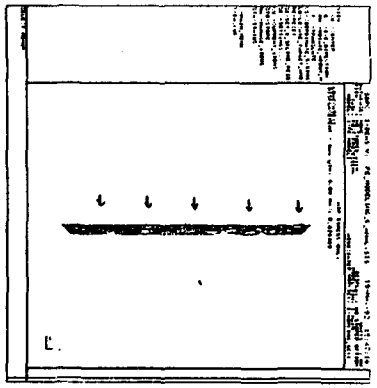

124

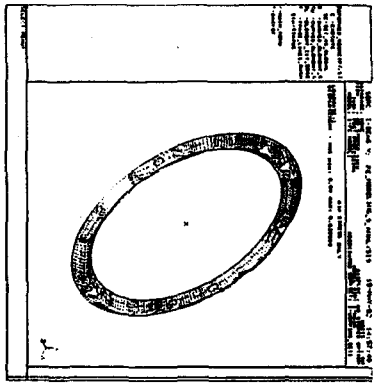

AIR ONLY

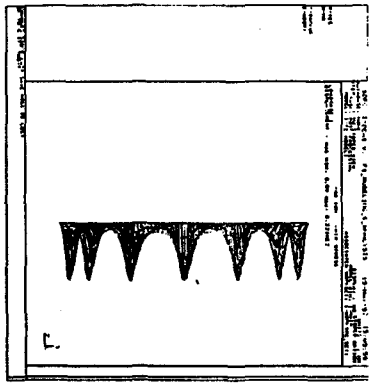

125

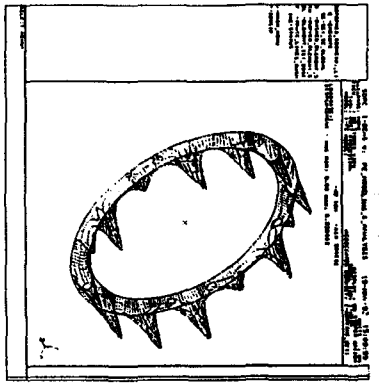

AIR & OFF

SUPPORT FOR CRYOSTAT &BULKHEAD STRESS ANALYSIS

	16 FOLD SYMMETRY		8 FOLD SYMMETRY	
	MAX STRESS	DISPLACE-MENT	MAX STRESS	DISPLACE-MENT
1 ATM. (-40T)	0.65 kgf/mm2 [6.5 MPa]	0.04 mm	0.78	0.04
1 ATM+Fz(40ton) ← →	3.1	0.16	3.1	0.16
1 ATM-Fz(-40T) ← →	4.4	0.23	5.1	0.23

126

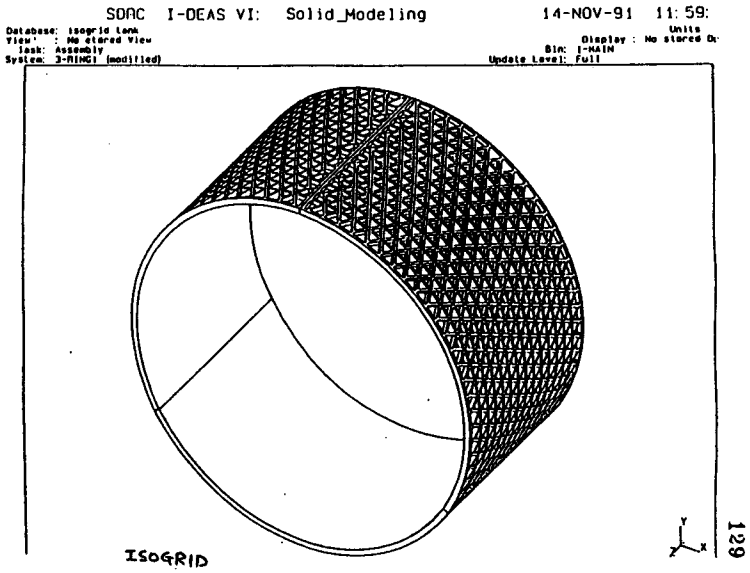

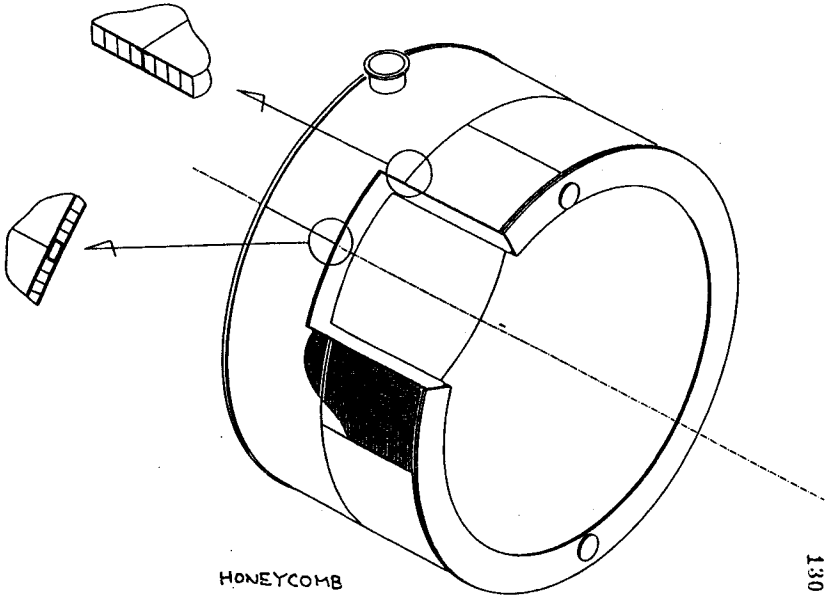

CRYOSTAT VACUUM WALL DESIGN

Table 5-6
Outer vacuum shell requirements.

Vacuum load	1 atm radial and axial
Design standard	
Radial collapse pressure	> 2 atm
Axial buckling load	> 2 atm
Allowable stress	Based on ASME press. vessel code
Material	Aluminum alloy
Construction	Welded joints

- HOW WE MAY SAVE MATERIAL?

  ⇒ HONEYCOMB / ISOGRID IN OUTER VESSEL

Table 5-7
Comparison of solid, isogrid, and honeycomb outer vacuum shells.

	Solid	Isogrid	Brz. honeycomb
Aluminum alloy	5083	5083-H32	6951/4045-T6
Total thickness (mm)	27	46	46
Skin thickness (mm)	—	4.0	3.0 + 3.0
Skin layers	—	single	double
Node configuration	—	triangle	hexagon
Effective thickness (mm)	27	11	7
Weight reduction ratio	1	1/2.5	1/3.9
Radiation thickness (X_0)	0.303	0.123	0.079
Maximum size of plate (m × m)	2 × 6.4	2.2 × 4.3	1.2 × 4
Units to be welded	8 (= 2 × 4)	12 (= 3 × 4)	21 (= 3 × 7)

THERMAL LOAD AND COOLING CHARACTERISTICS

Table 5-9
An estimate of steady state thermal loads for the SDC solenoid.

Component	300 to 77 K	77 to 4.2 K	300 to 4.2 K
Thermal radiation	300	30	—
Conduction			
Coil support rods ($n = 24$–36)	24	2.5	—
Shield support rods ($n = 12$)	3	—	—
Chimney and service port	36	4.5	—
Current leads (8 kA pair)	—	—	30
Total thermal load	363 W	37 W	30 L/hr

WITH CONTINGENCY OF 20%

Table 5-12
Cooling parameters in excitation and after quench.

Excitation of the coil		
Static heat-in-leakage		37 W
Eddy current loss in support cylinder	(@ 1 mT/s)	88 W
Quality of two phase helium	Inlet	0.8
	Outlet	0.5
He mass flow into cooling pass required		23 g/s
He mass flow into current leads	(2 × 8,000 A)	1 g/s
Quench recovery in coil		
Energy dumped into coil		88 MJ
Recovery time assumed		4 hr
Cooling power required		6.2 kW
Cooling efficiency assumed		0.8
Liquid (two phase) helium flow required		28 g/s (830 L/hr)
Total liquid helium for recovering		3,300 L

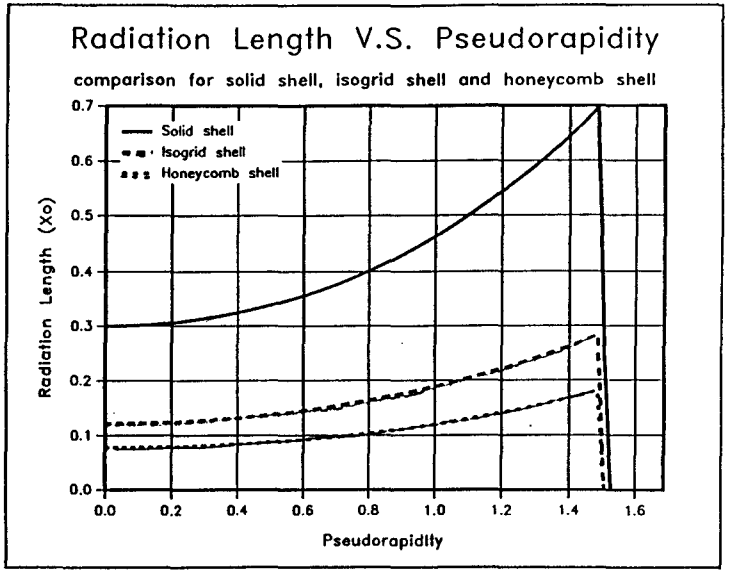

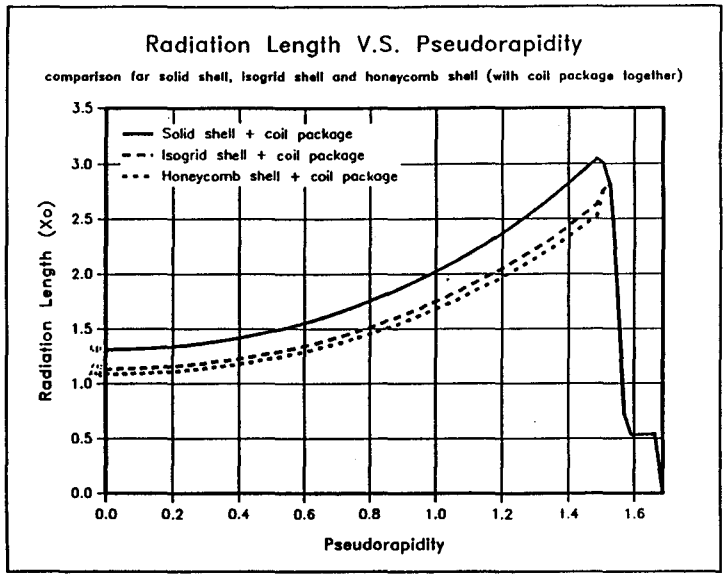

SDC CRYOGENIC SYSTEM

MINIMUM 4.35 K COOLING POWER REQUIREMENT FOR THE REFRIGERATOR/LIQUEFIER

1. STEADY STATE: 304 WATTS PLUS 1.2 G/S RETURNING AT 300 K -> 425 WATTS
2. CHARGING: (35 MINUTES) 88 + 425 = 513 WATTS
3. COOLDOWN: (14 DAYS) 700 WATTS
4. QUENCH RECOVERY: (4 HOURS) 2500 WATTS AT 4.5 K

Table 5-14
General requirements on the cryogenics for the SDC solenoid.

Typical refrigeration capacity	**1,500 W at 4.4 K**
Liquid helium transfer rate	**750 L/hr (after quench)**
Liquid helium storage capacity	**5,000–10,000 L**
Cold gas helium mass flow at 60 K	**12 g/s**

SDC CRYOGENIC SYSTEM

SOLENOID QUENCH RECOVERY

1. 3300 LITERS OF LIQUID HELIUM REQUIRED.
2. 10,000 LITER STORAGE DEWAR - ENOUGH LIQUID IS AVAILABLE TO RECOVER FROM 2 BACK-TO-BACK QUENCHES.
3. COMPRESS AND STORE THE GAS. RELIQUEFY DURING STEADY STATE OPERATION -> 12 HOURS/QUENCH WITH 1500 WATT REFRIGERATOR/LIQUEFIER.
4. A PRESSURE OF 0.31 MPa (45 PSIG) IS NEEDED IN THE LIQUID HELIUM SUPPLY DEWAR AT THE START OF QUENCH RECOVERY TO DELIVER THE REQUIRED FLOW RATE OF 28.5 GRAMS/SEC (3300 LITERS IN 4 HOURS). DEWAR NORMAL OPERATING PRESSURE IS 0.07 MPa (10 PSIG).

SDC CRYOGENIC SYSTEM

STEADY STATE 4.35 K LIQUID HELIUM REFRIGERATION LOADS

	ESTIMATED
1. SOLENOID SYSTEM	37 WATTS
2. CONTROL DEWAR	13
3. TRANSFER LINE	50
4. 10,000 LITER LHe DEWAR	4
5. VLPC SYSTEM - DISTRIBUTION	200 (BUDGET-?)
TOTAL	304 WATTS

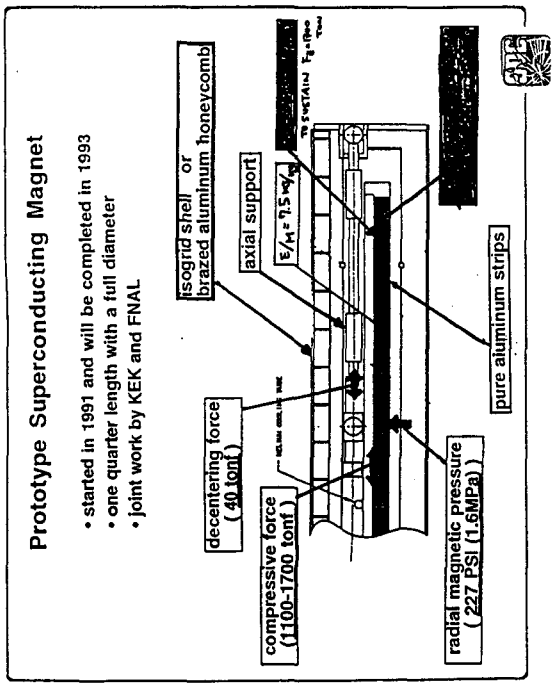

Table 5-16
Design parameters of the prototype R&D solenoid.

Dimensions		
Cryostat	Inner radius	1.70 m
	Outer radius	2.06 m
	Half length	1.17 m
Coil	Effective radius	1.85 m
	Half length	0.95 m
Conductor	Thickness	44 mm
Outer cylinder	Thickness	33 mm
Transparency	Radiation thickness	1.23 X_0
	Interaction length	0.26 λ_0
Electrical parameters		
Central field		1.54
Nominal current		11,250 A
Inductance		0.68 H
Stored energy		48 MJ
E/M		10 kJ/kg
Mechanical parameters		
Effective cold mass		4.5 tons
Total weight		8 tons
Radial mag. pressure (Θ_z =0)		1.73 MPa
Axial compressive force		16.7 MN
Maximum hoop stress		43 MPa
Maximum axial stress		−19 MPa
Maximum shear stress		62 MPa
Peak field in coil		3.8 T
Load line ratio		70%

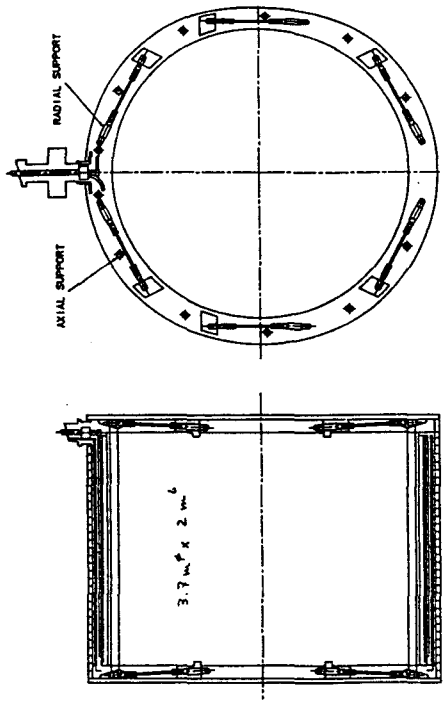

FIG. 5-16. SDC prototype solenoid. Dimensions are given in Table 5-16.

DEVELOPMENT OF HIGH STRENGTH AL STABILIZED SUPERCONDUCTOR

WHY IS IT NECESSARY?

- Present superconductors used in CDF, TOPAZ etc. are mechanically too weak to sustain electromagnetic force at B = 2 T.
- Mechanical design under elastice boundary condition is desired in the SDC thin solenoid to be loaded with combined stress in terms of hoop and axial components ($2\tau_{\cdot} = S_\phi - S_z$)

GOAL OF DEVELOPMENT

- Yield Strength (0.2%) at 4.2 K — > 60 MPa (min); > 70 MPa (desired)

HOW TO IMPROVE MECHANICAL STRENGTH?

- Specially Additional Impurity — Zn (200 ppm)
- Mechanical Cold Work — Drawing and/or Rolling (10 - 20 %)

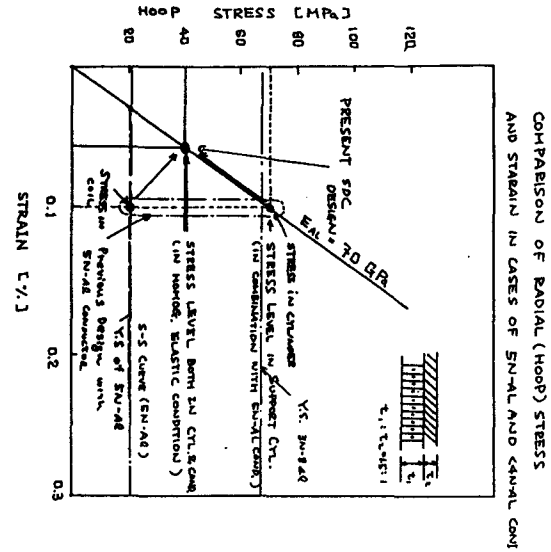

Table 3. Mechanical strength and RRR of aluminum matrix on production stages

Step	at RT (kgf/mm2)		at 77K (kgf/mm2)		RRR
	σB	σ0.2	σB	σ0.2	
1. 5N (based material)		2.3		~3	2,500
2. Alloyed (200ppmZn)			13.6~15.5	2.6~3.6	680
3. Extruded	5.2	2.3	15.7	2.9	630
4. Cold-worked(12%)	6.6	6.5	15.9~17	7.5~8.9	490
5. Curred	6.3~6.6	5.3~5.6	15.6~16.1	6.5~7.3	530
6. Aged at RT(after 6months)			same as above		

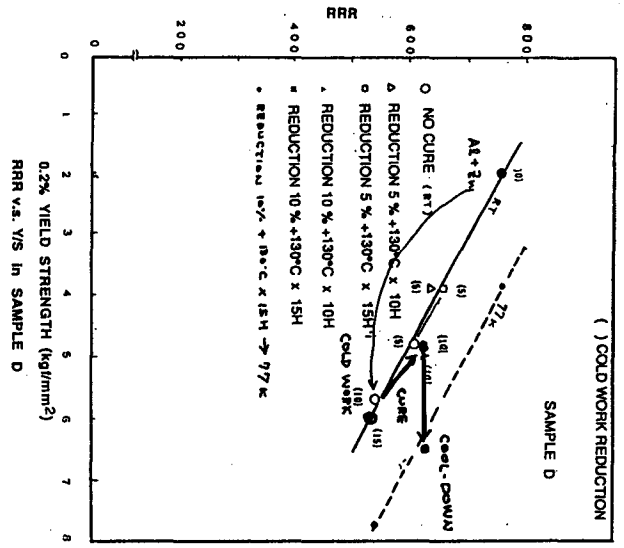

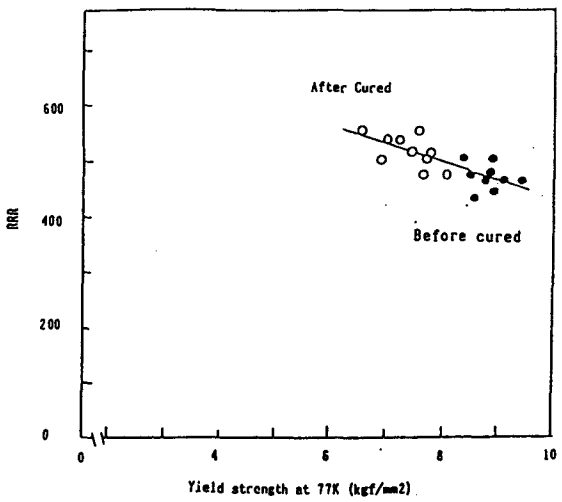

Figure 10. The relationship between the yield strength (77K) and RRR of aluminum matrix on the cold reduction ratio for the full-sized SDC conductor.

148

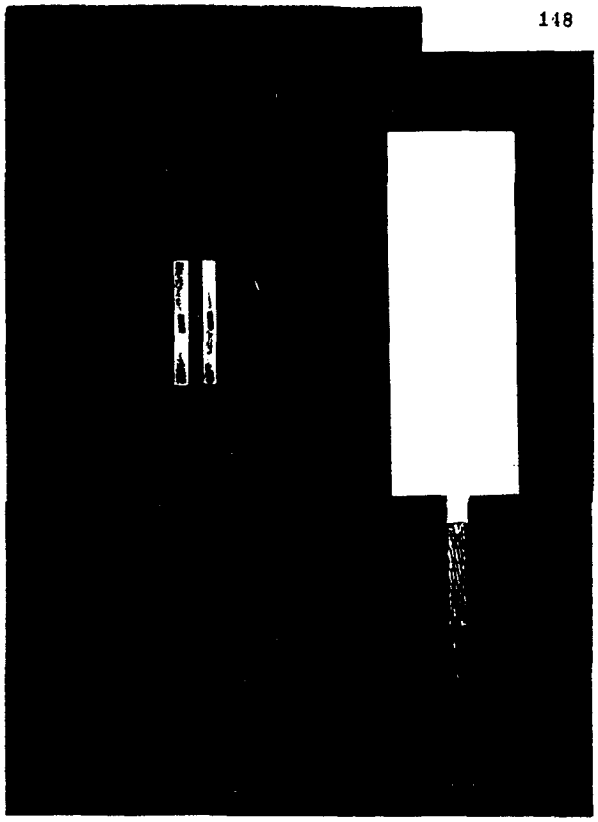

149

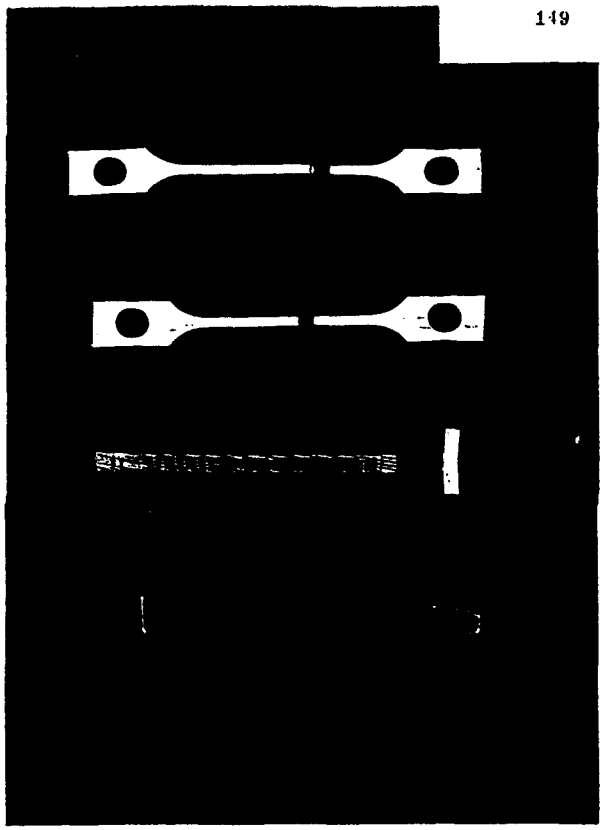

150

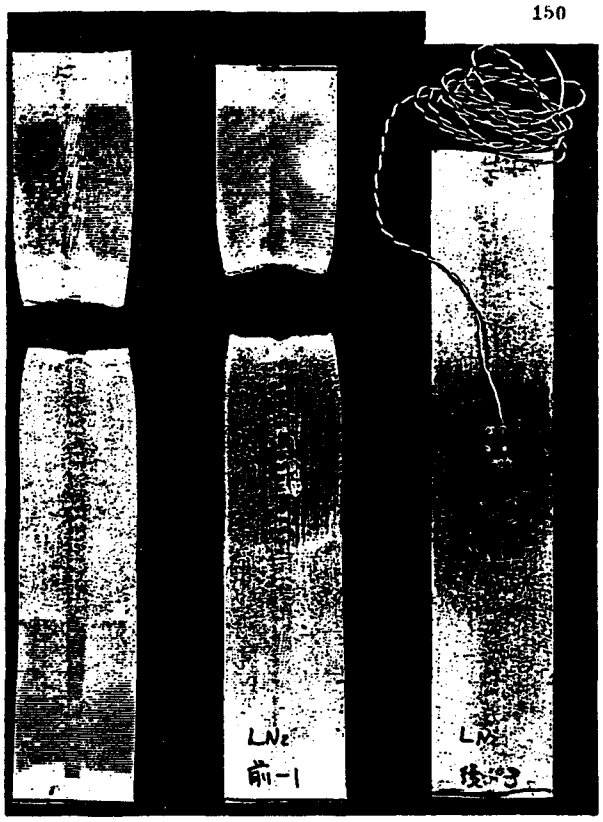

151

MECHANICAL CHARACTERISTICS OF SDC SUPERCONDUCTOR

ITEM	SPEC	TEST RESULT before Curing			TEST RESULT after Curing		
S C Strand		RT	77K	4.2K	RT	77K	4.2K
T.S. [kgf/mm²]		88.9 (88.7) (89.4) (88.6)	121.1 (121.0) (121.1) (121.1)	150.3 (155.7) (144.9)			
Y.S.(0.2%) [kgf/mm²]		40.2 (42.9) (38.6) (39.0)	47.4 (46.7) (45.0) (50.4)	76.9 (76.9) (76.8)			
Elogation [%]		3.0 (3.0) (3.0) (3.0)	1.5 (1.5) (1.5) (1.5)	1.6 (1.6) (1.6)			
Stabilizer (Al)		RT	77K	4.2K	RT	77K	4.2K
T.S. [kgf/mm²]		6.3 (6.2) (6.4)	14.7 (14.6) (14.7)	30.4 (30.6) (30.1)	6.0 (6.0) (6.0)	14.5 (14.4) (14.5)	30.2 (30.2) (30.2)
Y.S.(0.2%) [kgf/mm²]	6.0	6.0 (5.8) (6.2)	8.0 (8.0) (7.9)	9.7 (10.0) (9.3)	5.2 (5.4) (4.9)	6.7 (6.6) (6.7)	7.4 (7.0) (7.7)
Elogation [%]		22.4 (23.0) (21.8)	53.9 (55.4) (52.4)	55.0 (55.0)	33.4 (32.8) (34.0)	61.4 (64.2) (58.6)	54.7 (58.6) (52.7)
Overall		RT	77K	4.2K	RT	77K	4.2K
T.S. [kgf/mm²]		11.2 (11.2) (11.2)	17.9 (17.8) (17.9)	( ) ( )	10.7 (10.7) (10.7)	16.8 (16.7) (16.8)	30.2 ( ) ( )
Y.S.(0.2%) [kgf/mm²]		10.3 (10.2) (10.3)	11.2 (11.0) (11.4)	( ) ( )	7.9 (8.0) (7.8)	8.1 (7.7) (8.4)	( ) ( )
Elogation [%]		10.8 (11.0) (10.5)	15.6 (15.3) (15.8)	( ) ( )	11.9 (11.9) (11.9)	16.8 (16.8) (16.7)	( ) ( )
Shearing(Al/Cu)		RT	77K	4.2K	RT	77K	4.2K
[kgf/mm²]	2	3.9 (3.9)	5.8 (5.4)	4.5 (4.5)	3.7 (3.9)	5.7 (6.6)	8.7 (8.7)

CHARACTERISTICS OF SDC SUPERCONDUCTOR

ITEM	SPEC	before Curing	after Curing
Diamension(mm)			
Strand Dia.	1.277	1.273	
Cable			
thicness	~2.5	2.34	
width	~6.4	6.14	
Conductor			
thickness(L)	(4.42)	4.42	
(S)	(4.32	4.35	
width	43.8	43.8	
corner	≤0.5	0.4	
Al/Cu/NbTi Ratio	27.9/1/1	27.9/0.9/1	
Twist pitch(mm)		27	
IC(A)*1			
at 3.0T		23950	24580 *2
at 4.0 T		19750	20250
at 5.0 T	≥16000	16025	16475
at 6.0 T		12600	13075
at 7.0 T		9225	9500
at 8.0 T		5890	6120
4.2k, $10^{-11}\Omega$cm			
RRR	Al Cu	Al Cu	Al Cu
at 0 T	~600,100	497 95	506 97
at 1.0 T		215 79	243 81
at 2.0 T		162 66	198 67
at 3.0 T		140 55	184 56
at 4.0 T		127 47	178 48
at 5.0 T		118 41	176 42

CROSS SECTIONS OF SDC SUPERCONDUCTOR

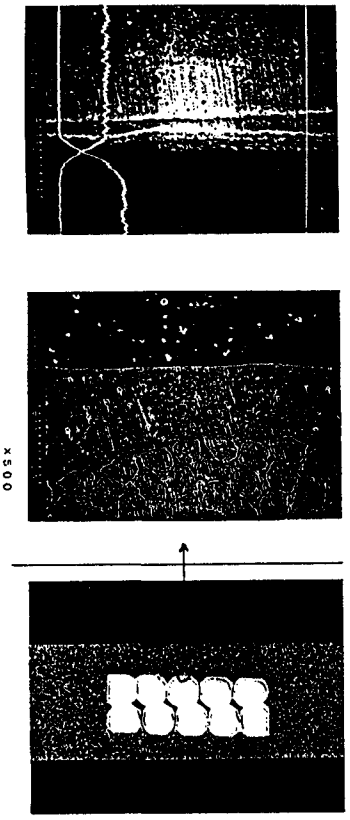

COIL WINDING

WHAT TO BE LEARNT?

- HOW DO WE WIND SUCH HIGH STRENGTH CONDUCTOR ($\sigma_{0.2}$ = 60 ~ 90 MPa)?
  ⇓
  - HIGH SPRING-BACK EFFECT CORRESPONDING $\sigma_{0.2}$
- HOW MAY WE APPLY INTERNAL PRESSURE DURING WINDING AND MAY KEEP IT AFTER COIL WINDING.

PLAN

1. STIFF GND INSULATION COMPLETED BEFORE WINDING
2. PRE-FORMING (WINDING) OF CONDUCTOR ON TEMPORAL MANDREL
3. INNER WINDING WITH HOOP COMPRESSION ON INNER SURFACE OF OSC / GND INS.
4. CURING WITH APROPRIATE FORCE

COIL WINDING

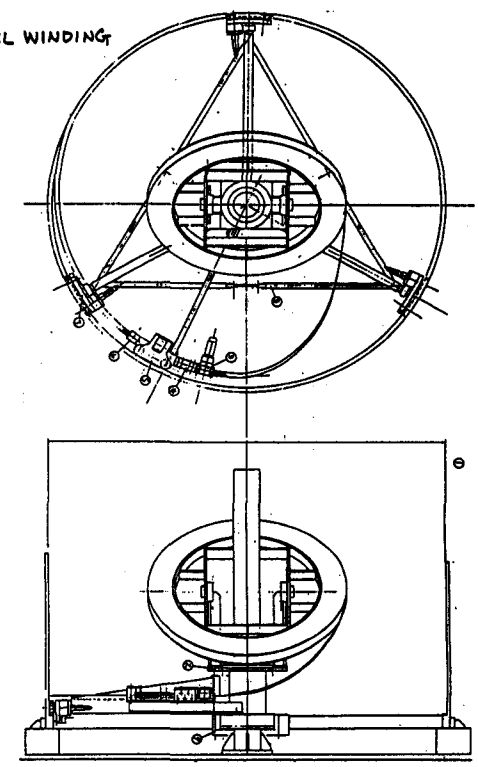

FIST WINDING TEST

FIG.10-1 SCHEMATIC VIEW OF THE PROTOTYPE COIL WINDING MACHINE

156

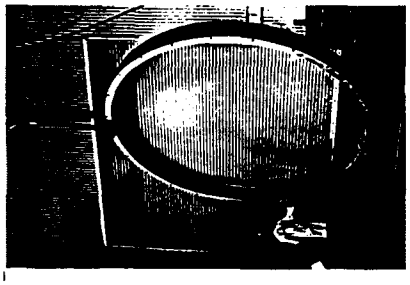

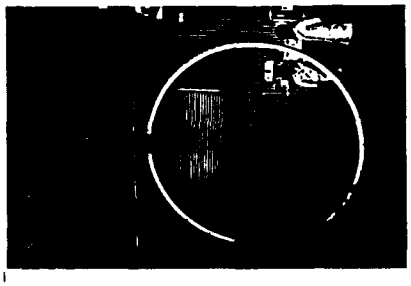

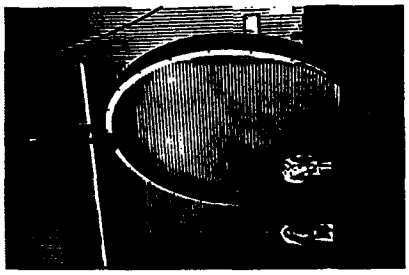

157

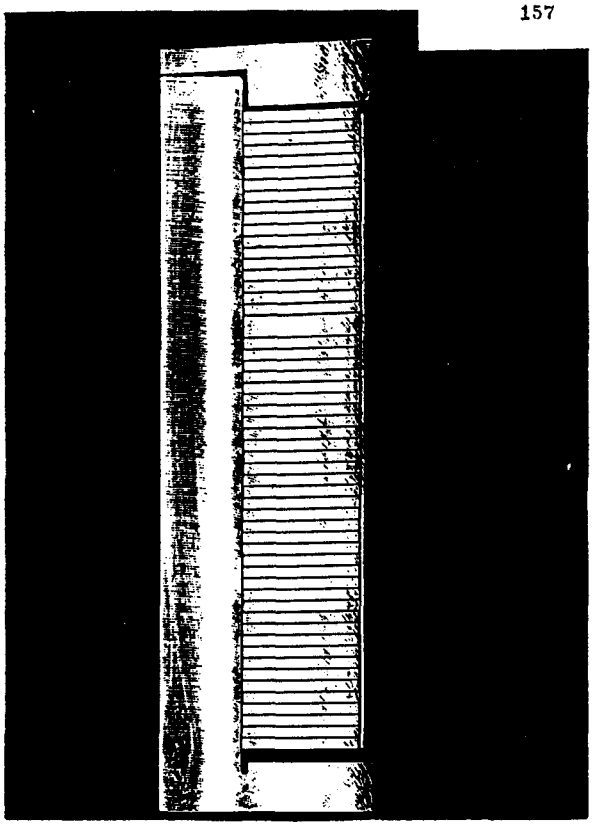

158

RESULTS OF EPOXY BONDING

STRENGTH TEST

σ_s > 5 MPa (measured)

at sample from 1st winding

(Calculated Shear Force

< 0.5 MPa)

159

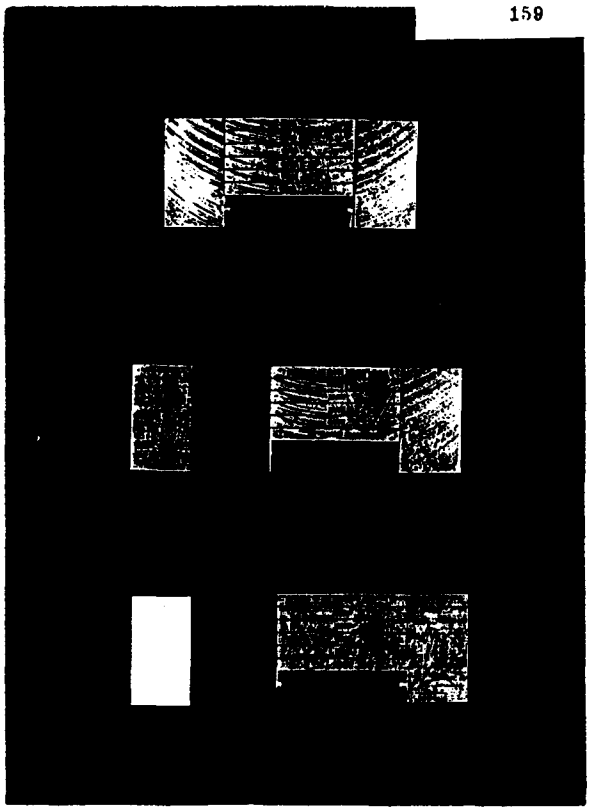

160

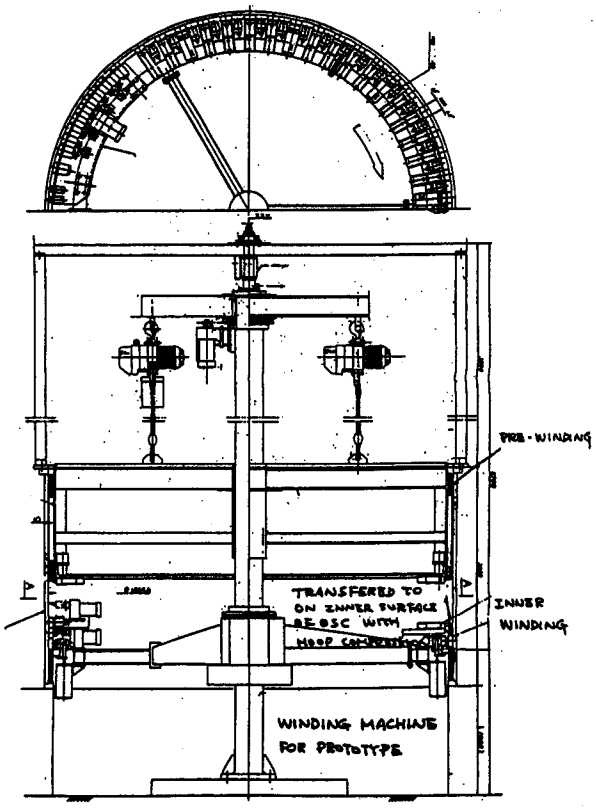

161

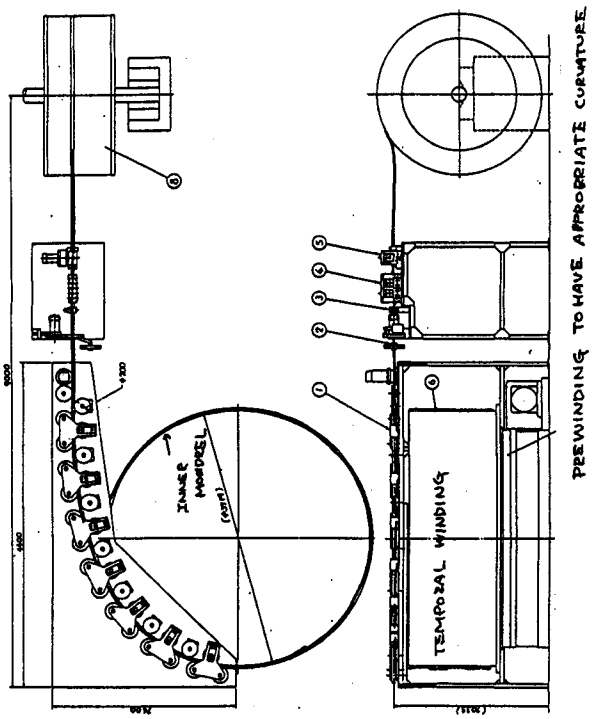

162

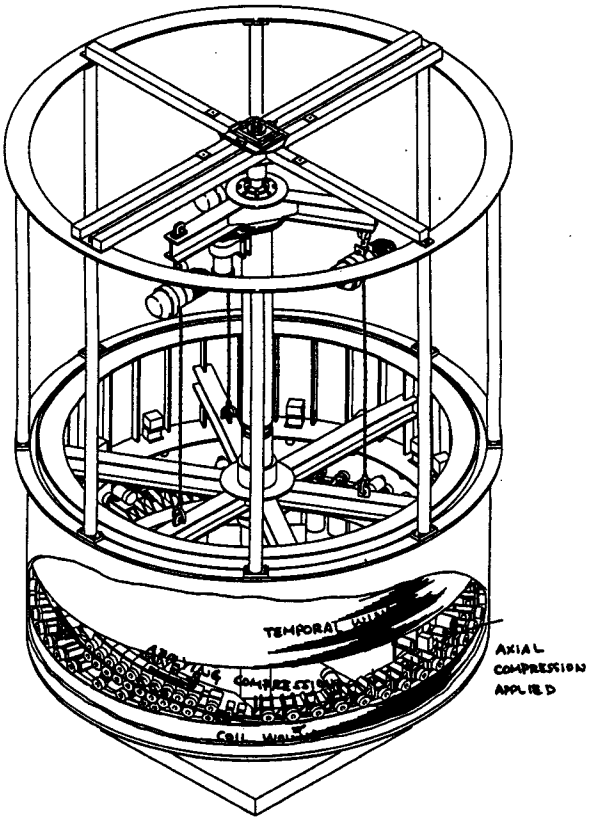

163

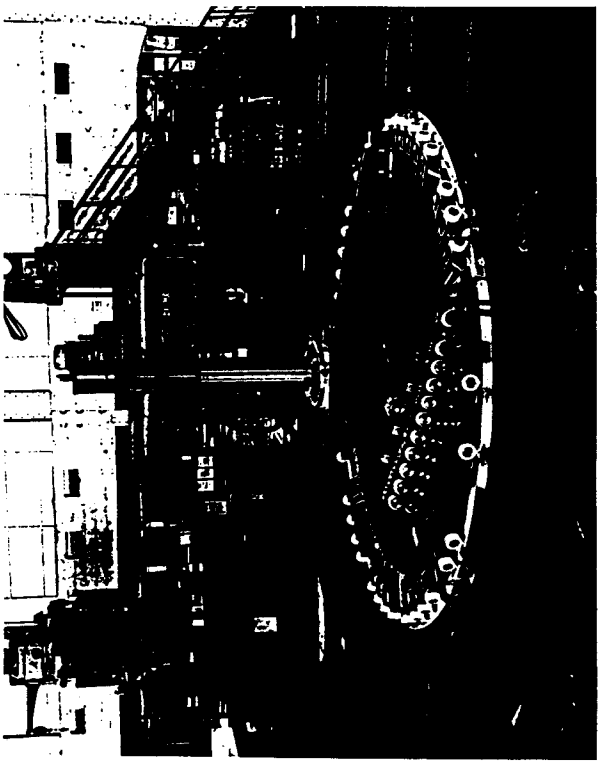

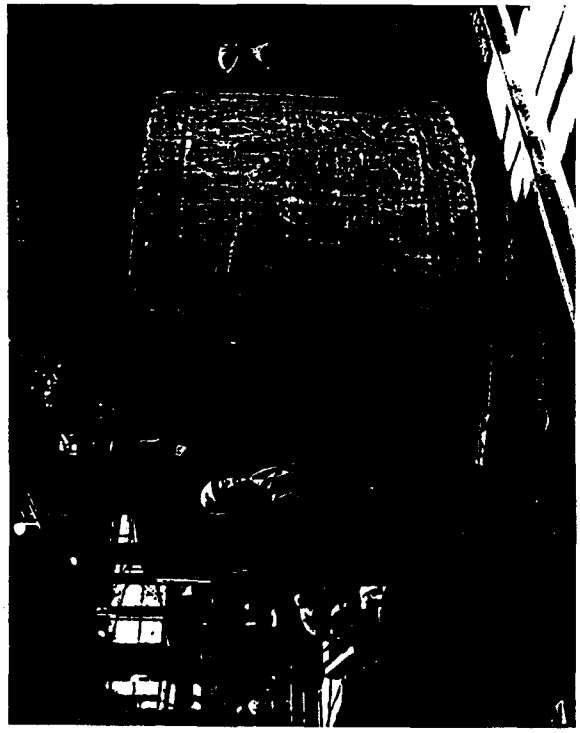

SDC Solenoid
Outer Vacuum Shell R&D

Purpose:

The SDC solenoid is required to be thin in terms of radiation lengths. If this shell were made with conventional techniques (e.g. Welded shell of solid aluminum) then it would be a major contributor to the overall thickness of the coil in terms of radiation lengths. (.3 λ_r) For this reason the SDC magnet group began a program to develop an improved technique to fabricate this shell.

Outer Vacuum Shell Specifications:

outer radius	2.05 m
total length	8.72 m
High Reliability	metallic - welded
Radiation tolerant	> 6 megarads (10 yrs @ 10^{34} cm^{-2} s^{-1})
Safe - predictable	built to ASME/CGA codes

Plan:

The outer vacuum shell thickness for a solid shell is determined by elastic stability criterion for a cylindrical shell under external pressure.

The SDC magnet group evaluated various fabrication techniques intended to achieve the equivalent stiffness of a solid plate but with much less material.

We chose to pursue R&D on two techniques that we judged most likely to lead to a practical shell that would meet the requirements of SDC:

1) Brazed Aluminum Honeycomb

2) Aluminum ISO grid

R&D is in progress at this time on both techniques. I will discuss our progress and plans:

Option 1) <u>Honeycomb</u>

Characteristics of Brazed Aluminum Honeycomb Panels

- Near optimal use of material for high stiffness
- High Thermal Resistance = => Weld able
- High Reliability (no epoxy adhesives)

Honeycomb Vacuum Shell Design Specifications

Honeycomb Outer Vacuum Shell

Aluminum alloy	A6951/A4045
Total thickness	45 mm
Skin thickness	3.0 mm + 3.0 mm
Skin layers	double
Node configuration	hexagon
Effective thickness	7.1 mm (Al)
Weight reduction ratio	1/3.83
Radiation thickness	0.08 Xo

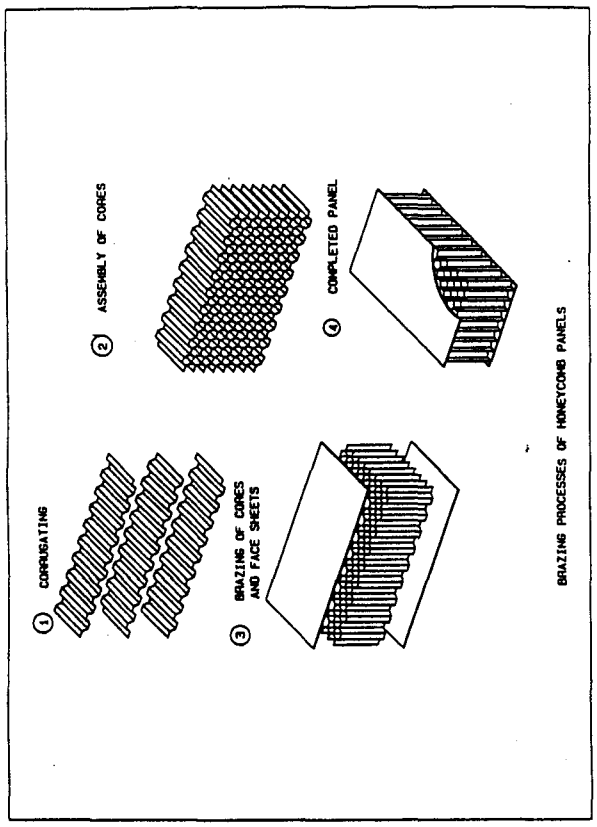

	3 POINT BENDING with Bending Roller	4 POINT BENDING
Concept		
Shearing Force Distribution	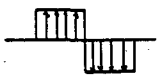	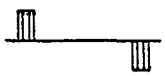
Bending Moment Distribution		
Possibility of Cores Collapsed	Expected	None
Possibility of Shearing Deformation	Expected	None
Bending Size	Long	Limited

HONEYCOMB VACUUM STRUCTURE

RESEARCH AND DEVELOPMENT

(3RD EFFORT)

4 POINT PNAEL BENDING WITH CONSTRAINT FIXTURES

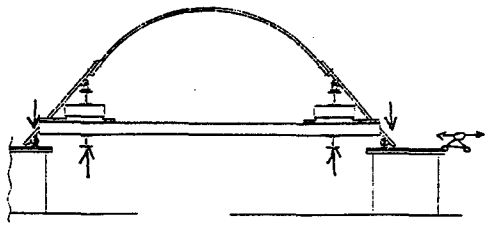

RESULTS

1. BENDING SUCESSFUL DOWN TO R/T RATIO OF 46 WITHOUT BUCKLING,
2. RADIAL SPRING BACK OF 10 % OBSERVED AFTER RELEASING,
3. ~~HORSE BACK~~ (SADDLE) SAGITA OF 15 MM , (IT COULD BE ELIMINATED WITH ANOTHER CONSTRAINT FIXTURE).

172

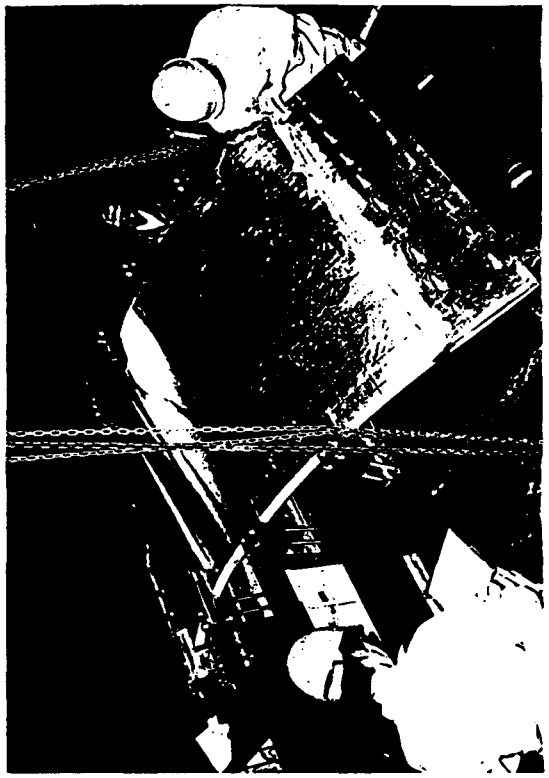

173

174

Option 2) <u>ISO grid Shell</u>

Characteristics of Aluminum ISO grid construction

- A lattice of intersecting ribs forming an array of equilateral triangles.
- Isotropic (no directions of instability or weakness)
- Efficient use of material for either compression and/or bending
  - Lightweight
  - Proven analysis techniques
  - Can be optimized for wide range of loading intensities
  - Readily reinforced for concentrated loads and cutouts
  - Regular pattern of nodes provides attach points for other structures
- Easily fabricated from solid Al plate with NC machine tools yielding a very reliable material of known costs.

175

- Large experience base :

  In use on major space programs, extensively investigated by NASA, military, and industry.

  Fermilab has received structural analysis and engineering design assistance from P.S. Associates

  Companies with ISO grid construction experience are available for R&D and for production of final shell. (e.g. machining, welding, bending)

R&D on Machining and Bending ISO grid Panels

Machining

Panel size -	0.63 m x 1.1 m	(two panels)
Panel thickness -	46 mm	
Sin thickness -	4 mm	

Bending RESULTS

Radius Formed To:		Thickness:
Plate 1	2.05 m	46 mm
Plate 2	2.05 m	46 mm

CONCLUSIONS

1. No significant problems in brake forming plates if skin is on outside radius. No buckling or web crippling observed.
2. Small deformations observed near edge nodes...understood and easily fixed ===> no problems

ISO grid Vacuum Shell Design Specifications

ISO grid Outer Vacuum Shell

Aluminum alloy	5083
Total thickness	46 mm
Skin thickness	4.0 mm
Skin layers	single
Node configuration	triangle
Effective thickness	11 mm (Al)
Weight reduction ratio	1/2.5
Radiation thickness	0.12 Xo

Conclusions of ISO grid R&D and Plans

- Technique is likely to be successful but somewhat less efficient than Aluminum honeycomb.
- SDC magnet group decided to fabricate prototype shell using this technique. (3 Al plates 2.5 m x 5 m are on order from Alcoa)
- We will fabricate a large test panel from 5083-H321. This will have exact circumferential and longitudinal weld configurations as Prototype shell. Test panel will be formed to 2.05 m radius.
- More weld joint tests will be done with 5083-H321
- Decision for final shell will depend on outcome of Honeycomb R&D effort.

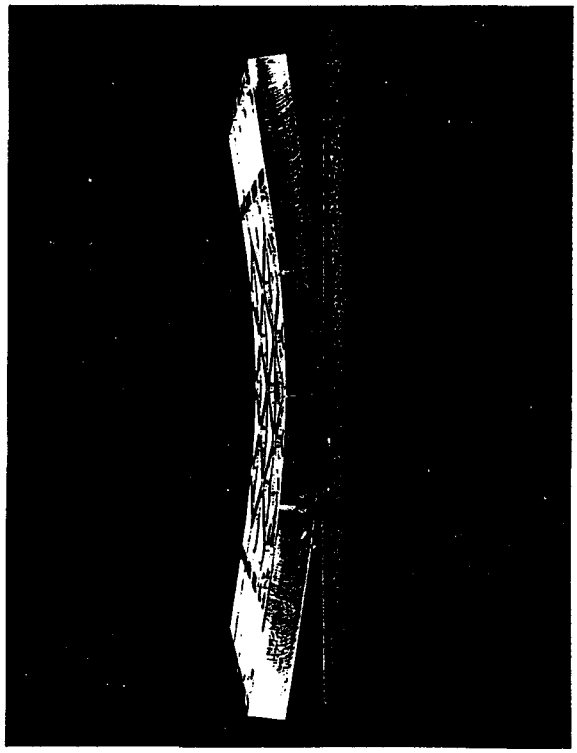

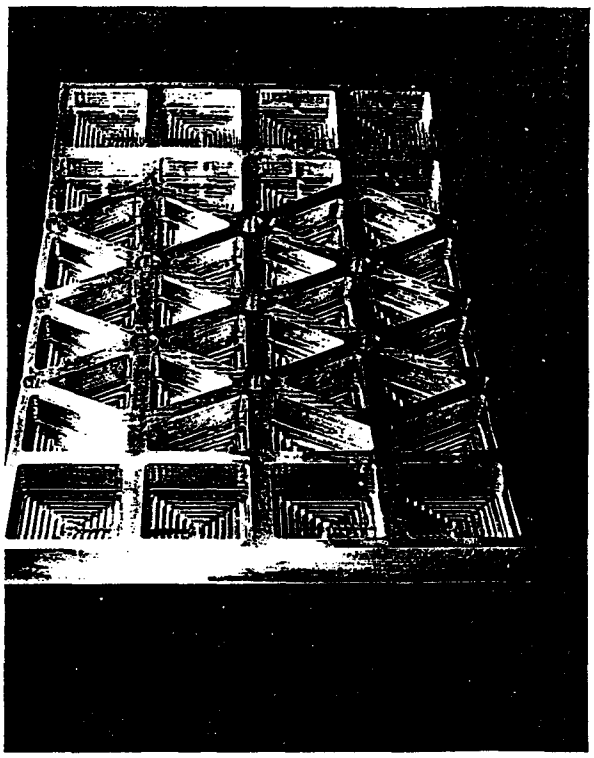

Table 5-17
Overall schedule for the prototype solenoid and the production solenoid. The Japanese fiscal year begins April 1 of the year indicated.

JFY1991	Prototype Magnet Development
	—Superconductor fabrication (by May) '92
	—Winding machine development (by July)
	—Outer support cylinder fabrication
	—Isogrid vacuum wall development
JFY1992	—Coil winding (Sept ~ Dec)
	—Cryostat element fabrication
JFY1993	—Assembly of the magnet
	—Cool-down and excitation in air
JFY1994	Production Magnet Fabrication
	—Superconductor fabrication
	—Cryostat element fabrication
JFY1995	—Coil winding
	—Magnet assembly
JFY1996	—Magnet assembly continued
	—Cool-down and excitation test in air
	—Transportation to SSCL
JFY1997	—Cool-down and excitation in iron
	—Field mapping

SUMMARY

DESIGN STUDY

- THE LATEST DESIGN BOUNDARY CONDITION OF B=2.0T AT X=1.2Xo WITH Z(Fe-END)=4.783 m , ΔZ(Fe-COIL)= 0.62m AND Fz(COIL)=1300 tonnes WITHIN ACCEPTABLE FORCE LEVEL.
- THE SUPERCONDUCTING COIL MAY BE SUPPORTED WITH 2 x 6-FOLD RADIAL SUPPORTS AT BOTH AXIAL ENDS AND WITH 14 (=12+2) AXIAL SUPPORTS AT THE CHIMNEY END. THE AXIAL SUPPORTS REQUIRE X_{max} =3.6Xo AROUND η=1.5 WITH IN A REGION OF 6% OF CIRCUMFERENCE.
- CRYOSTAT MAY BE SUPPORTED WITH 8-FOLD SUPPORT-BAR FROM THE BARREL CALORIMETER, ALTHOUGH 16 FOLD SUPPORT WAS PREFERRED. STIFFNESS OF THE SUPPORT-BAR AGAINST ΔFz = 40 tonnes AND ΔF/ΔZ=15 ton/cm SHOULD BE IMPORTANT.

PROGRESS ON PROTOTYPE R&D

- SUPERCONDUCTOR OF 6km HAS BEEN NEARY COMPLETED. IT MAY SATISFY TO HAVE σ0.2=67MPa AT 4.2K
- COIL WINDING MACHINE IS BEING DEVELOPED. THE PROTOTYPE COIL IS TO BE WOUND BY THE END OF THIS YEAR.
- EPOXY BOUNDING SHEAR-STRENGTH MEASURED USING SAMPLES TAKEN FROM THE FIRST WINDING TEST WAS ≥ 5MPa AND LARGER BY A FACTOR 10 THAN EXPECTING IN FEM ANALYSIS.
- VACUUM VESSEL WITH ISOGRID IS IN PROGRESS. BRAZED HONEYCOMB CYLINDER IS BEING DEVELOPED IN PARALLEL.
- PROTOTYPE MAGNET ASSEMBLY IS TO BE CARRIED OUT IN 1993.

Report from Tracking Group

I. Silicon

Y. Unno
Physics, KEK

Abstract

The Silicon Tracking group had the meeting focused on Detector R&D, Mechanical System, and Beam test at KEK. Capacitance measurements of p- and n-side structures assured the R&D direction and Full size prototype DSSS's were produced. A full signal simulation program was developed and basic characteristics of the Silicon tracking system was checked. Strong design progress were made for the wedge DSSS as well as the mechanical systems including the ladder assembling at KEK. A beam test is being planned to start in the fall of 1992.

Silicon subgroup meeting in the SDC meeting at KEK, May 26-29, 1992

==========

May 26 (Tue) Afternoon - Detector R&D	S. Amendolia(Chair)
Build#3-6F #625	
13:30 Opening address	A. Seiden
13:50 Capacitance Measurement I	M. Miyata
14:10 Capacitance Measurement II	H. Sadrozinski
14:30 Radiation damage	N. Tamura
14:50 Pulse simulation	Y. Unno
15:10 Break	
15:30 Plans for tests of mag. field effect	H. Ziock
15:50 Double sided sensor (Barrel&Disk)	T. Ohsugi
16:10 Comment on Production of DSSD	K. Yamamoto
16:30 Discussion on Quality assurance	H. Sadrozinski(Chair)
17:00 Adjourn	
17:30 Silicon group dinner - Susi restaurant "Naniwa"	

==========

May 27 (Wed) Morning - Mechanical System	A. Seiden(Chair)
Build#3-3F #325	
9:00 Mechanical design status	W. Miller
9:40 Mechanical design study at KEK	T. Kohriki/Y.Unno
10:00 Alignment requirements	H. Ziock
10:20 Discussion	A. Seiden(Chair)
10:50 Break	
11:10 Detector module design	N. Spieler
11:30 Ladder assembling at KEK	T. Kohriki/Y.Unno
11:50 Discussion on double-sided bonding	Y. Unno(Chair)
12:20 R&D and construction schedule	A. Grillo
12:40 Adjourn	

Afternoon - Tracking/Integration Joint session
Main Build. Lecture Hall

Evening - SDC group dinner

==========

May 28 (Thu) Morning - Beam test at KEK	T. Ohsugi(Chair)
Build#3-4F #425	
9:00 Plan for the beam test at KEK	Y. Unno
9:20 Beam line at KEK	A. Murakami
9:40 Amp-comparator for the beam test	N. Spieler
10:00 Update on Tek amplifier-comparator chip	H. Sadrozinski
10:20 VME-UNIX DAQ for the beam test	M. Momachi/Y. Yasu
10:40 Discussion	H. Sadrozinski(Chair)
11:20 Adjourn	

May 28 (Thu) Afternoon - Working hours
Build#3-3F #325
Les Alamos - KEK meeting, etc...

==========

Focuses of the Silicon Group Meeting

1) Detector R&D

Capacitance measurements
Radiation damage
Signal simulation
Double-sided sensor prototype production
Wedge detector development

2) Mechanical System

Mechanical design status
Mechanical design study at KEK
Alignment requirement
Detector electronics design
Ladder assembling at KEK

3) Beam Test at KEK

Plan for the beam test at KEK
Beam lines at KEK
Amp-comparators
Update on Tek amp-comparator
VME-UNIX DAQ for the beam test

Capacitance Measurements

- p- and n-side capacitance measurement samples are produced and measured

detail structure of both surfaces

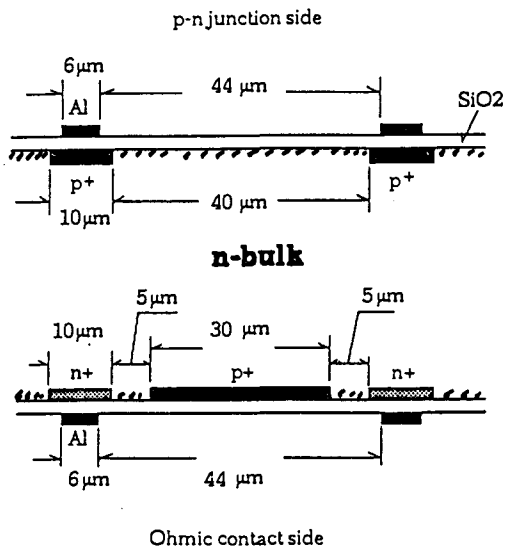

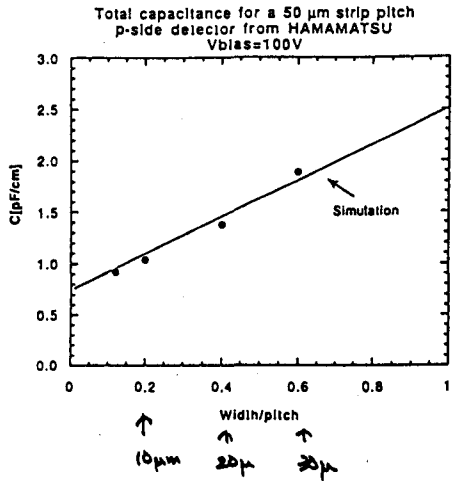

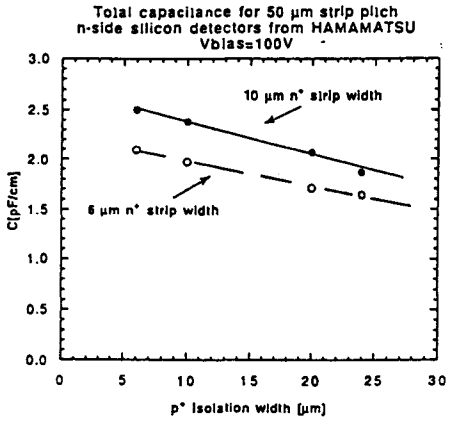

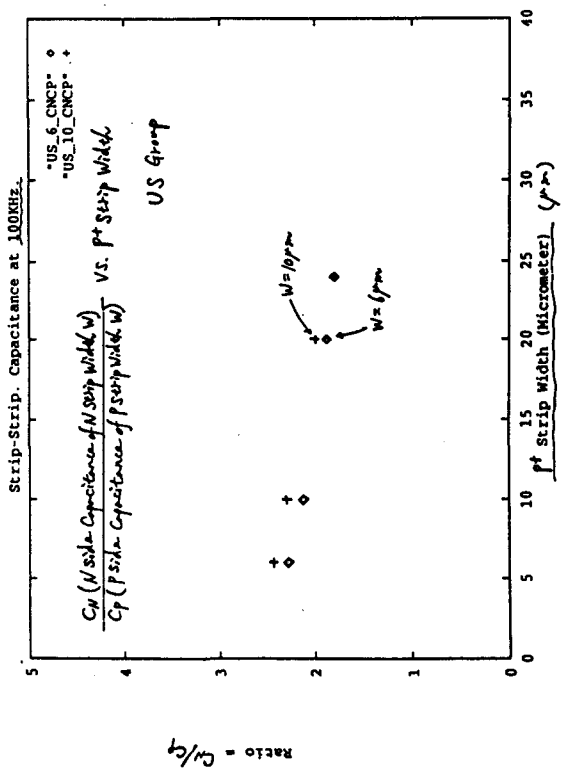

Figure 15: AC interstrip capacitance
5.88cm strip length

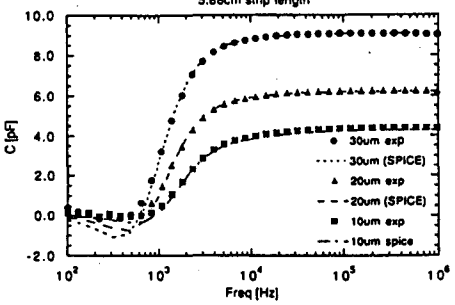

Signal Simulations of the Silicon Strip Detector

Y. Unno
Physics, KEK

J. Leslie, R. Sonnenblick
SCIPP, UC Santa Cruz

Abstract

Signals from the double-sided Silicon strip detector are simulated including the effect of 2 Tesla magnetic field. Induced currents of holes (p-side) and electrons (n-side) created by the charged particle are integrated, shaped, and discriminated with electronic noises, as expected for the SSC. Efficiencies, resolutions, and means are evaluated as a function of the threshold. A set of optimum is being searched.

Simulation steps

1) E- field calculation - Poisson eq. on meshed space

2) Particle trajectory

3) Energy deposition according to the Landau+Atomic binding exitation fluctuation in a step of 15 μm depth

4) Drift of electrons and holes in E & B and induced currents

5) Charge integration and CR-RC shaping

6) Discrimination with noise to get timing

Setup #3

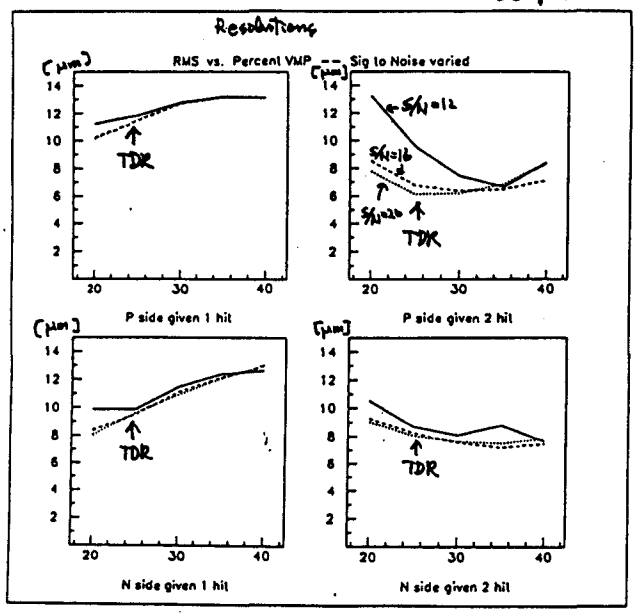

Conclusions

(The results presented are preliminary...)

- Evaluation of efficiency, resolution, and mean indicates ...
- S/N = 12 - 20 does not affect very much.
- Faster shaping is better to have the timing in the bucket. $\tau_p = 20ns$
- Threshold at 25% of the most probable charge is a good choice...
- Threshold variation (±10%) has very little effect.
- Resolutions:

  p-side 12 μm/single hit, 7 μm/double hits
  n-side 10 μm/single hit, 9 μm/double hits

(due to effective sensitive regions in the strip pitch?)

 H. Sadrozinski

Tek 64ch. Bipolar Amp-Comp.

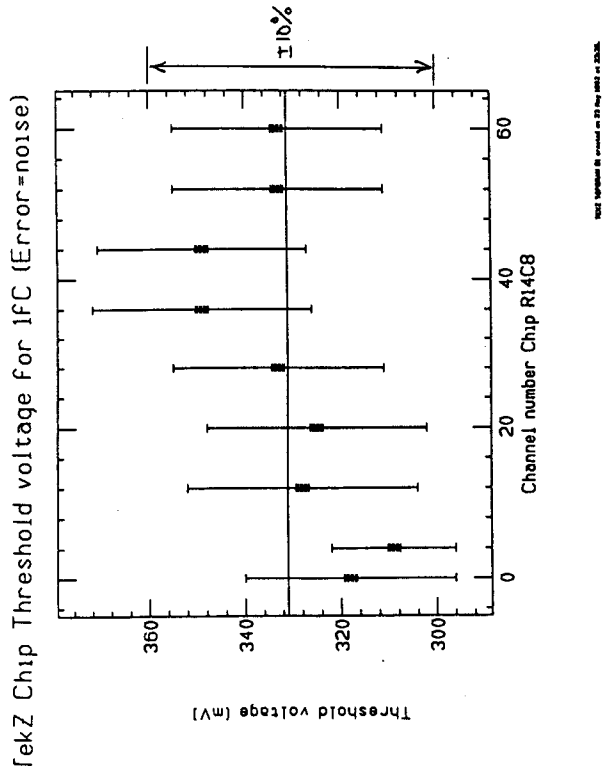

Production of Full-size Prototype Double-sided Silicon Strip Sensor for the SDC

- DSSS for the Barrel is produced!!

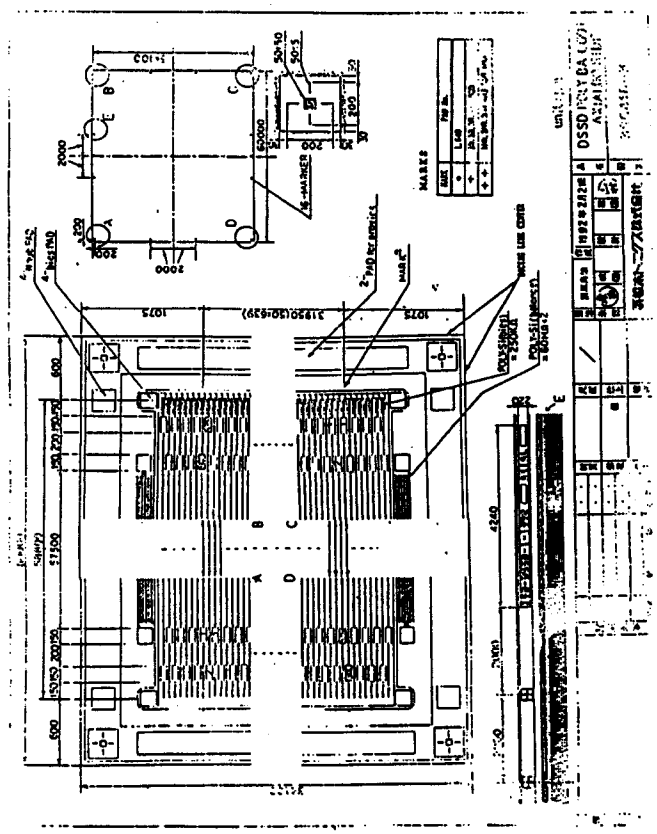

200

SILICON "WEDGE" DETECTOR R & D

BRUCE BARNETT
BARRY BLUMENFELD
PETER FISHER
AIHUD PEVSNER
JACK SPANGLER

JOHN KRIZMANIC
JOE ORENDORF
DAVE NEWMAN
JOHN SICARDA
JOHN SNIDER
KATE CRYSTAL
JOE CARLSON

[redacted]
27 MAY 1992

201 T. Ohsugi

Comment on Wedge Sensor

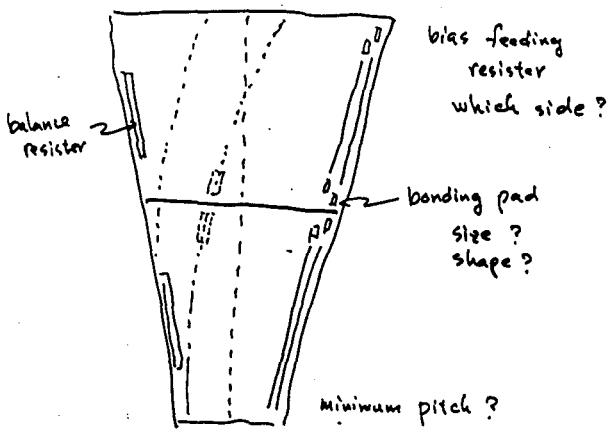

Stereo side
~~Ohmic Side~~

1) bonding pad ..... size, shape, direction ?

2) crossing angle ....dead area ...

Proposal :

[illegible]

202

Mechanical System

203 B. Miller

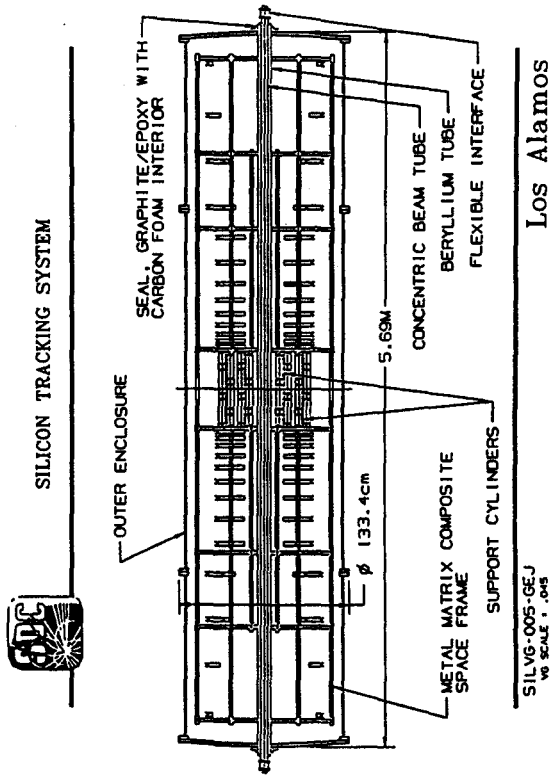

Ladder Assembling at KEK

T. Kohriki and Y. Unno
Physics, KEK

together with

Hamamatsu Photonics Co. Ltd

Abstract

Tools for assembling the Barrel ladder are being prepared. Using the tools, a ladder with mechanical detectors and Polycyanate-CFRP ribs is assembled. Wire-bondings are under investigation jointly with Hamamatsu Photonics Co. Ltd.

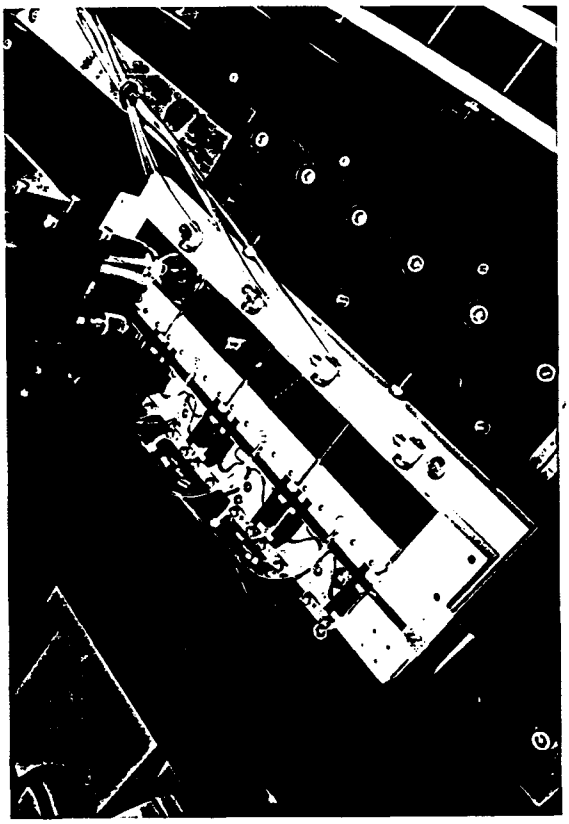

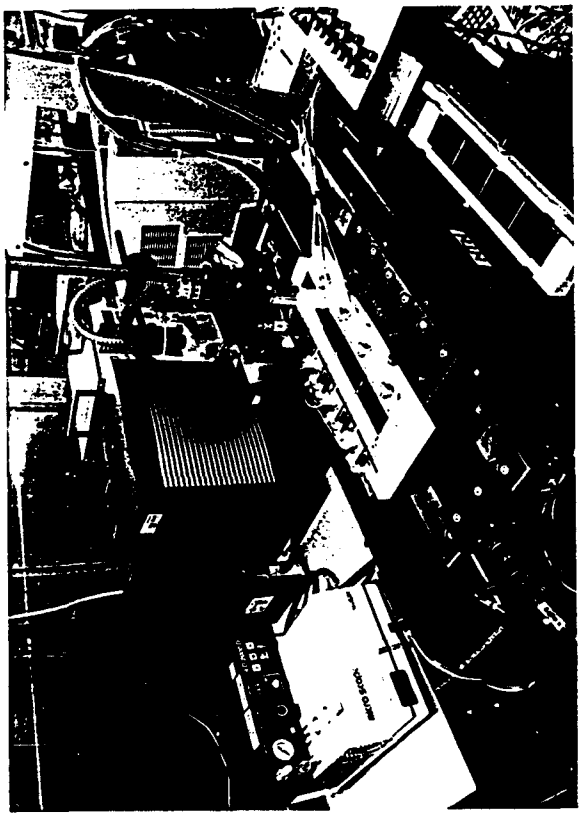

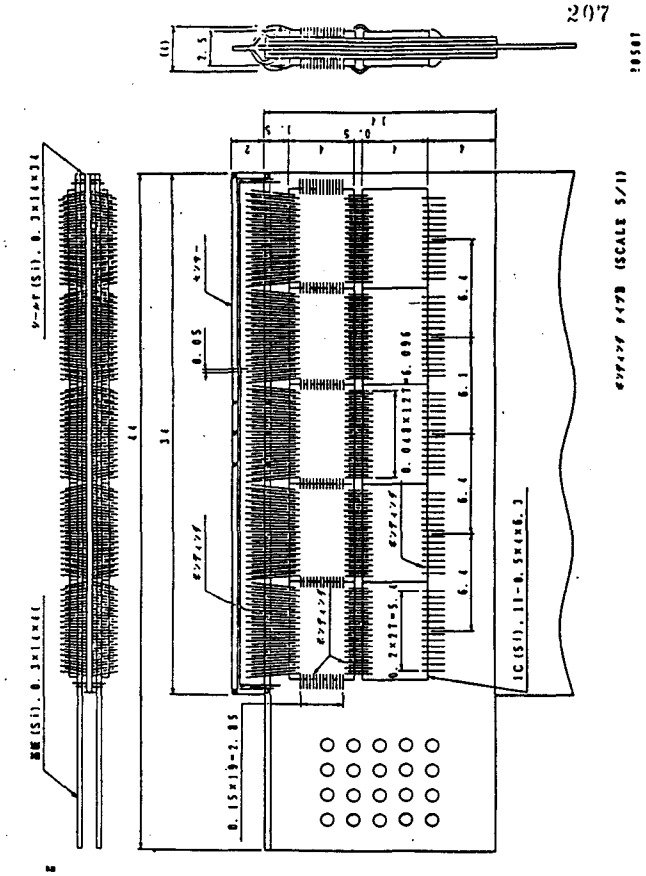

Beam Test at KEK

Beam Test of the SDC Double-sided Silicon Strip Detector

Y. Unno
Physics, KEK

for

The SDC Silicon Tracking Group

Abstract

The beam test of the DSSD for the SDC Silicon tracking system(STS) is being planned to check-out the prototype DSSD, and eventually at the end, the full signal stream from the sensor to the data acquisition provisioned in the SDC. The first beam test will be held in the fall of 1992 at a test beam line at KEK. A plan for the setup and job sharing is being discussed. New components, effect of magnetic field, etc. will be tested in the later stages utilizing the setup.

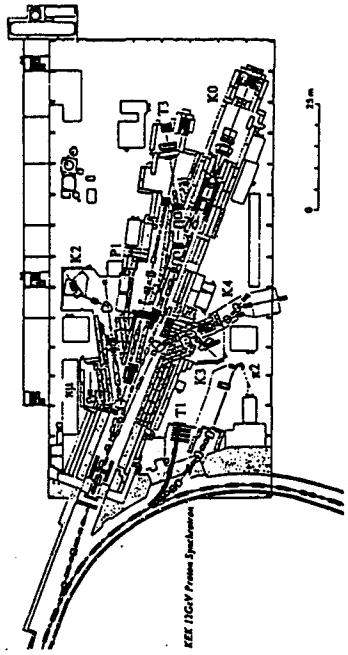

Fig. 56 Layout of the beam lines in the KEK-PS East Counter Hall.

Detector Module - PC board

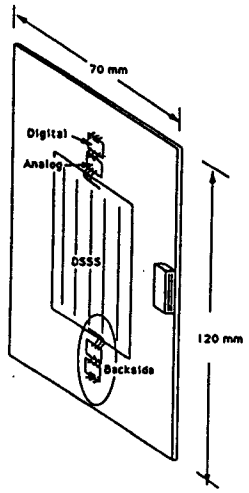

6 cm Detector Module/PC board

Setup

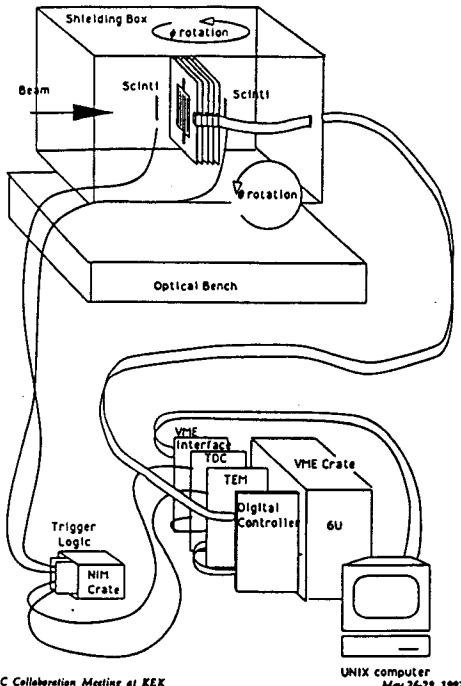

Milestones

• Place orders for AT&T and Tek chips	May-June
• Place order for Digital chip	May 29
• Receive AT&T and Tek chips	Sep 15
• Assemble & test one module	Sep 30
• TEM by W. Smith	Sep(?)
• Ship partial modules to Japan	Oct 15
• Complete the mechanical system	Oct 1
• All modules assembled and tested	Nov 1
• Complete the trigger counters, logic, DAQ and ready for the beam	Nov 15

• KEK PS operation

1992	Oct - Dec(T1)
1993	Feb - March(T1)
	May-July(π2)
	Oct - Dec(π2)

Summary

• Capacitance measurements

- p-side capacitance: C_p ~1.0 pF/cm @ w=10 μm
- n-side capacitance: p+ isolation method works and a wider p+ isolation width reduces the capacitance. C_n/C_p ~ 1.8 @ w=10 μm & w(p+)=24 μm
- Frequency dependences are reproduced with SPICE

• A Full signal simulation program is in hand
- S/N = 12 ~ 20 does not affect very much
- ±10% Threshold variation has little effect
- Tek Bipolar chip has shown ≤ ±10 % variation!

• Full-size Prototype DSSS's are produced!!

• Design progress for the Wedge DSSS.

• Mechanical design is detailing and strong progress is being made for the ladder assembling at KEK.

• Beam test of the DSSD is being planned to start in the fall of this year, 1992 (to be the first user of the SDC portable DAQ).

REPORT FROM TRACKING GROUP

OUTER TRACKER T.K.OHSKA

May 26

Afternoon session :

Overall Discussion on organization on electronics : A. Lankford

Straw plans for '93 : Straw group

May 27

Morning session :

Joint Tracking/Electronics Meeting : T.K. Ohska

Afternoon session:

Outer Tracking Meeting - Staging / Descoping : W. Ford

Outer Tracking Meeting - Integration : T. Thurnston

J. Piles , R. Swensrud

May 28

Morning session : H.H. Williams

Activities in Japan : T.K. Ohska
Chamber test setup at TMU : K. Yamauchi
Readout on Chamber Tests : S. Oh
4 m Module Tests : D.Rust
Colorado works for straw : W. Ford
Chamber Resolution Calculation : H. Ogren
Space Constraints for Electronics : R. Swensrud
Design of frontend board : S. Odaka
Electronics layout : R. Van Berg
Discussion

Afternoon session : Straw group workshop
Chamber test/Connectors/Frontend board....

HV system requirement for straws : D. Rust (Indiana)

Activities in Japan : T.K. Ohska (KEK)
Straw FEB/Heat

Chamber test setup at TMU : K. Yamauchi (TMU)
Chamber test status for straws

Readout on Chamber Tests : S. Oh (Duke)
Assembly/cosmic ray test/high rate on straws

4 m Module Tests : D.Rust (Indiana)
Test results on straws-attenuaton etc.

Colorado works for straw : W. Ford (Colorado)
Cosmic ray test on straws with Mark II chamer

Chamber Resolution Calculation : H. Ogren (Indiana)
Analysis on integrated charge on straws

Space Constraints for Electronics : R. Swensrud (Westinghouse)
Drawing/space availability

Design of frontend board : S. Odaka (KEK)
FEB design for straws - Microcrate/cooling

Electronics layout : R. Van Berg (Penn)
Placement of FEB for straws

Discussion

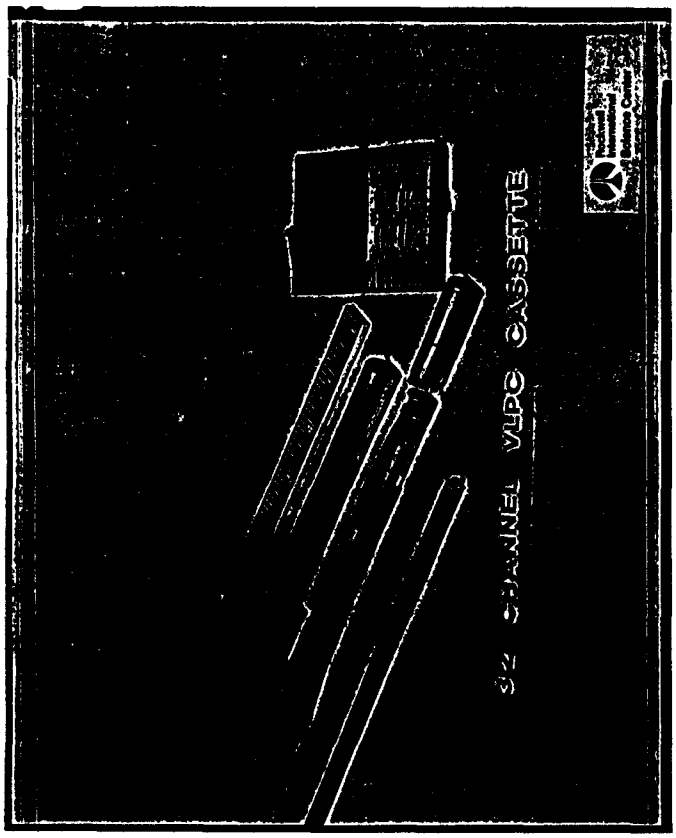

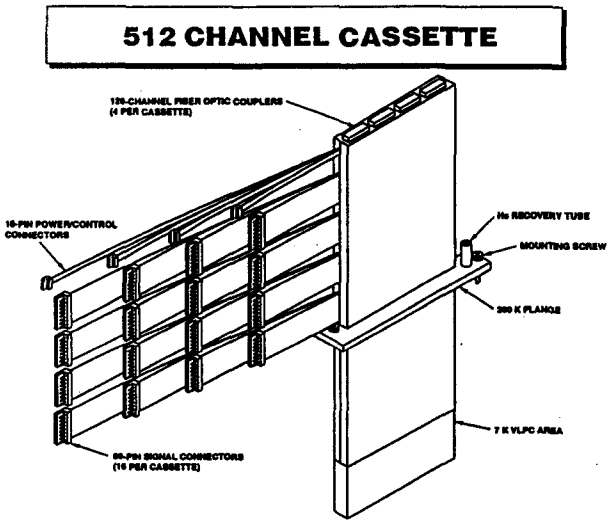

Fig. 4 Conceptual design of a 512 channel VLPC cassette. The funding request is aimed at building two of these cassettes and operating them by the end of 1992 or early 1993.

Science Center
Rockwell International Corporation
3370 Miraloma Avenue
P.O. Box 3105
Anaheim, California 92803-3105

Rockwell International

031-BC16

March 24, 1992

Prof. M. Atac
Department of Physics
University of California - Los Angeles
Los Angeles, California 90024

Dear Muzaffer:

The purpose of this letter is to update you on the status of Lot HISTE -III Visible Light Photon Counters (VLPCs).

VLPCs exhibiting very good performance have been obtained from lot HISTE-III. Wafer fabrication of this lot of devices was completed recently on the HISTE (High-Rate Scintillating Fiber Tracking Experiment) contract from UCLA.

The lot included three groups of wafers with different variations of material parameters; all three groups yielded operating VLPCs. Detailed evaluation of the best performing group has been carried out using dies of an 8-element line array from each of the three wafers in that group. Results to date are very positive and are summarized below.

Quantum efficiency in the visible and infrared spectral regione was measured on these devices and concurrently on a Solid State Photomultiplier (SSPM) fabricated earlier in lot HMC for checkout of a HISTE mask set. Table I summarizes the device quantum efficiencies estimated from these data. The estimated accuracy of these measurements is +5% to -15%.

TABLE I
Quantum Efficiency* (%)

Wavelength (μm)	HMC Device	HISTE-III Device
Visible - 0.55	85	80
Infrared -1.0 to 2.0	1	< 0.12
3.2	3	< 0.25
15	38	< 1.3
20	30	< 0.5

* These devices do not have the anti-reflection coating optimized for the visible spectrum.

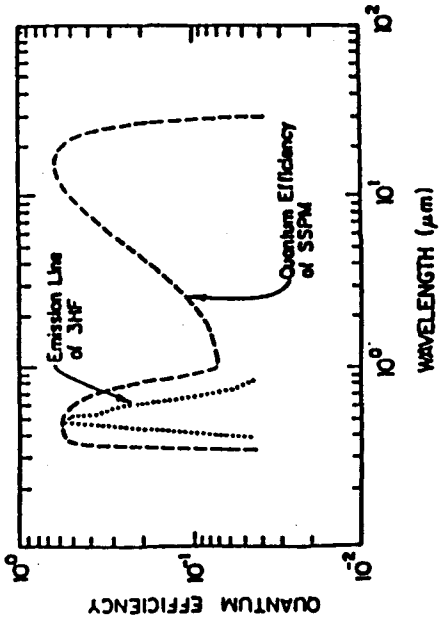

Goals of The BNL Beam Test.

Start May 1992

- Operation of 128 channel system.
- Produce: accurate Ribbons
  - Bicron
  - Kuraray
  - FTC
- Light yield from 4.3 meter fibre with SDC length wave guide.
- Measure resolution
  - checks fibre placement
- Stability of system for 1 month run.
- Self Trigger (3 superlayer trigger)

Special properties of straw modules which affect the design of the HV system:

1) Relatively high steady state currents.

≲ 1.5μa per wire at design $\mathcal{L}$

Apply safety factor & allow for operation in excess of design $\mathcal{L}$

∴ Plan for 5.5μa/wire

or ≲ 1 ma/module (l ≲ 2w)

2) Large number of independent isolated elements.

Design should include a way of isolating the faulty elements.

Could be in units of modules, sections of modules or ultimately individual straws

3) A module has a large capacitance

50 pf/straw → 10 nf/module

1. Prototype construction.

2.7 meter 64 channel
3.0 meter 100 channel
4.0 meter 159 channel

2. Resolution Measurement.

as a function of distance
as a function of high voltage
as a function of rate
as a function of amplifier

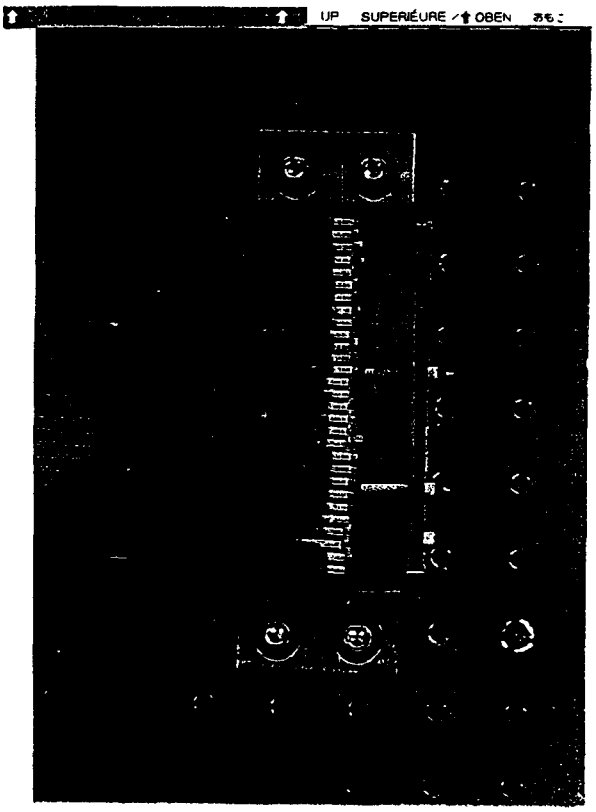

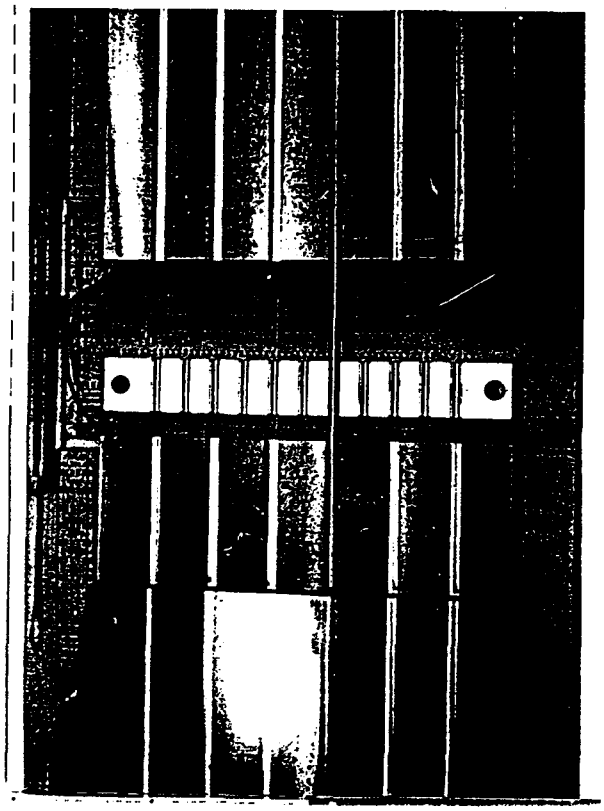

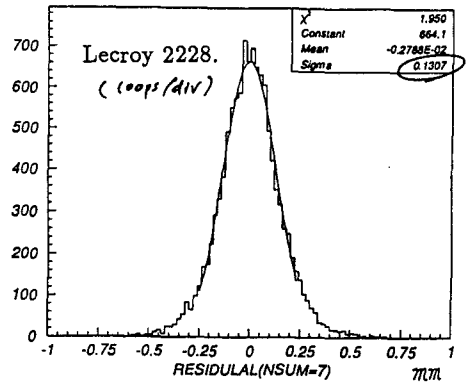

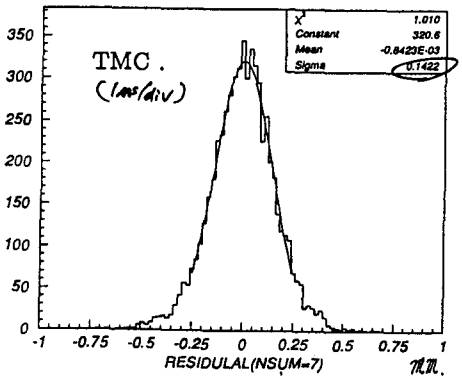

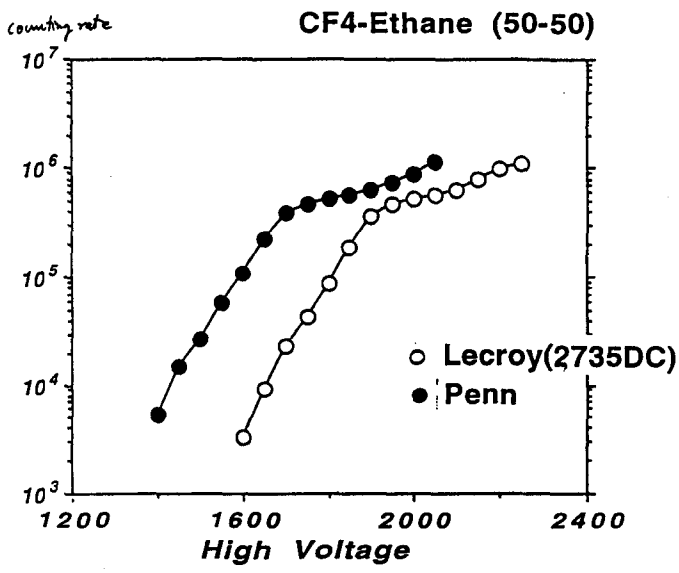

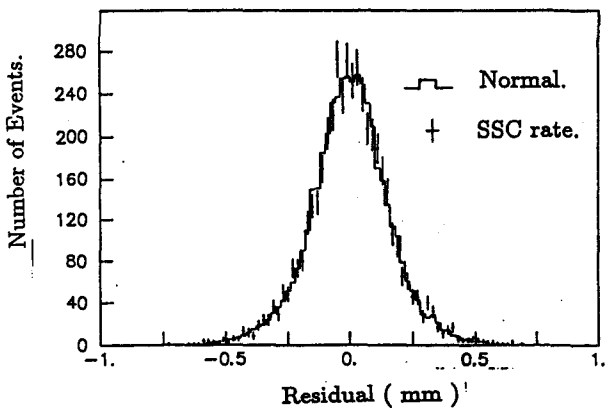

5 × 10 millicurie Sr90 sources.
Singles rate 1~2MHz
Current drawn 5μAmp / channel
(Gain ~10⁵)
Equivalent to 70cm from beam line at 10³³

Resolution of ≲ 120μm is not difficult obtain even under SSC condition.

Signal attenuation can be overcome by raising HV ~150V

Penn electronic (ASD) looks good

TMC performs as expected.

A Plan of Cosmic-ray Test of Straw Readout at Tokyo Metropolitan Univ.

Kazuo YAMAUCHI

1. Purposes :

* To test the newly fabricated TMC or ASD using the signals from the Straw Chamber.
* To measure the spatial resolution to compare with the previous results of the other experiments.

2. Straw Chamber :

Made by Indiana Univ. and has 64 straws.

3. Electronics :

* ASD
* TMC or
  TDC and ADC

4. Gas supplying system :

* CF_4 (80%) + Isobutane (20%)
* Ar (80%) + Isobutane (20%)

SDC
Program Advisory Committee Meeting
May 5, 1992

Signal Attenuation in a Straw Chamber

- 4 meter straw
- Copper coated Kapton (150 nm) 90 ohms.
- 37 μ diameter wire, Gold plated tungsten

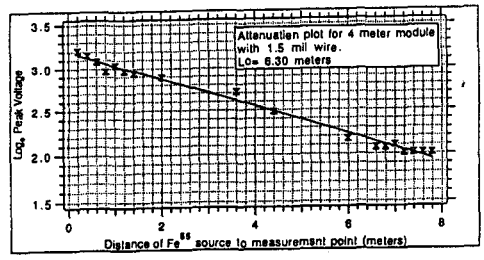

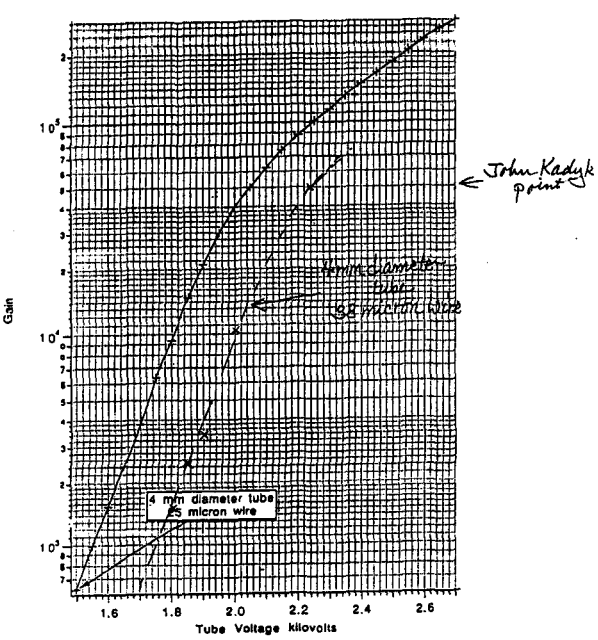

Fig. III.3. The gain curve of a 4 mm straw drift tube with CF4 -isobutane 80:20 gas. The absolute calibration of the curve is accurate to about 15% but the shape of the curve reflects the true dependence of the gain on voltage.

Tu 12" prototype
confidence level distributions vs input σ

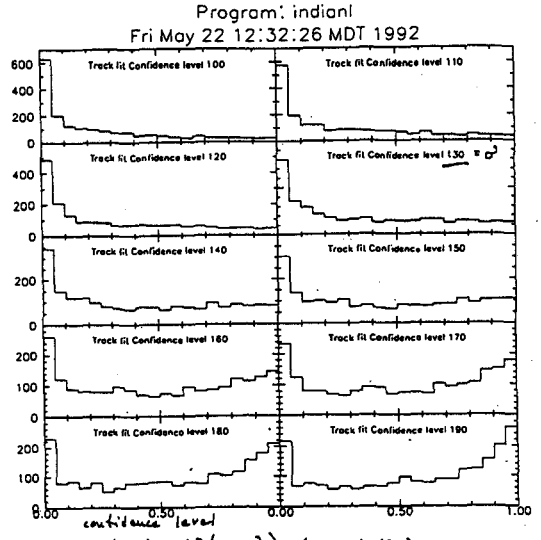

gas: Ar/C_4H_6 (?/100-?) (nom. 50/50)
HV: 1850V (↔ 2230V @ 1atm)
V_{th} = 1V (LeCroy 2735) ≃ 20 fC
with premixed 50/50, HV max ≃ 1800V, pulse height 1/4 that at 1850V
σ ≃ 200μm.
Non-linear drift velocity function ?

COLORADO

Run: 1195 Event: 7
Bubble Display

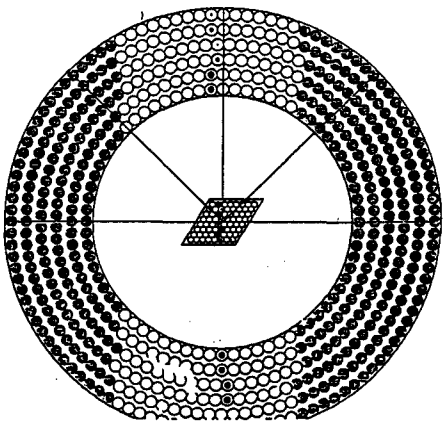

OGREN May 23

CHAMBER RESOLUTION CONTRIBUTIONS

WHAT ARE MAJOR CONTRIBUTIONS?

1) TDC RESOLUTION ($\Delta\sigma = v_0 \Delta\tau$)

2) PULSE HEIGHT SLEWING (TIME WALK)

3) NOISE (TIME JITTER)

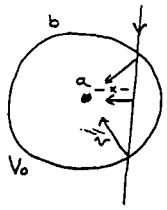

$v = 110\ \mu/ms \quad B=0$

$\cong 70\ \mu/ms \quad B=2T$

$\alpha \approx 180$ e/cm

$G \approx 2\times10^4$ gain

$$Q(\tau) = \frac{1}{2}\int_{x/D}^{\min(y_w,\tau)} \left(\frac{2\alpha G v^2 \tau'}{\sqrt{(v\tau')^2 - x^2}}\right) \underbrace{\frac{1}{2\ln(y_0)} \ln\left(1+\frac{(\tau-\tau')}{\tau_0}\right)}_{q_0} dx$$

TERMINATION

$$\tau_0 = q^2 \ln(y_a) / (2\mu + V_0)$$

$1.0 \frac{cm^2}{sec \cdot Volt}$

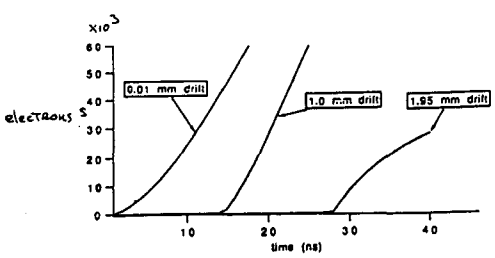

Fig. 1 The charge distribution as a fuction of time for three tracks.

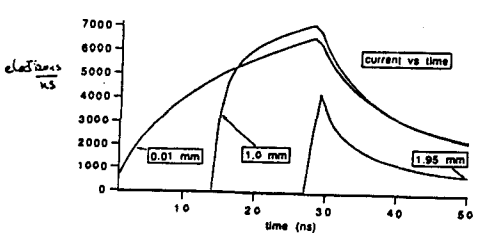

Fig. 2 The current distribution for three tracks.

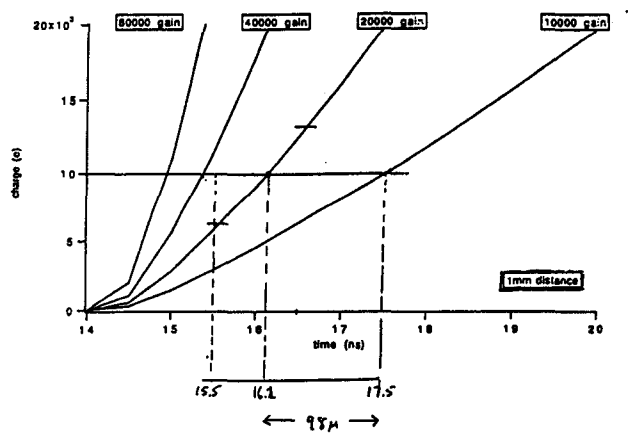

Fig. 3 . Charge distribtion for a track at 1mm for four different gains. Drift velocity as in B=2T field.

5) Conclusions:

It appears we may need run our chambers at a somewhat higher gain than 20000. A gain of 40000 with a threshold of about 15000e is shown in Fig. 5. It will give us the following contribution to the resolution for a 1 mm track:

$d\sigma =$ 35μ time resolution

$d\sigma =$ 52μ time slewing

$d\sigma =$ 22μ time jitter

$d\sigma =$ 100 μ intrinsic (difusion and clustering)

The total resolution is then about $d\sigma =$ 120 μ

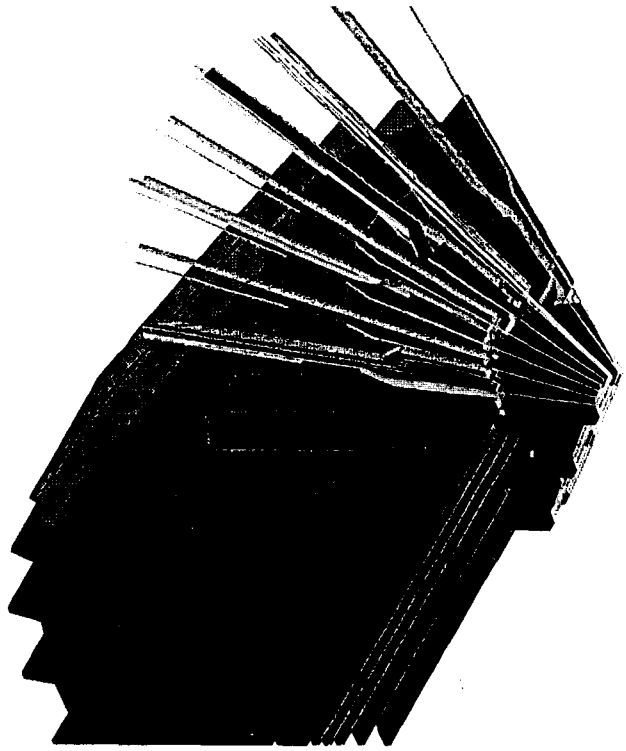

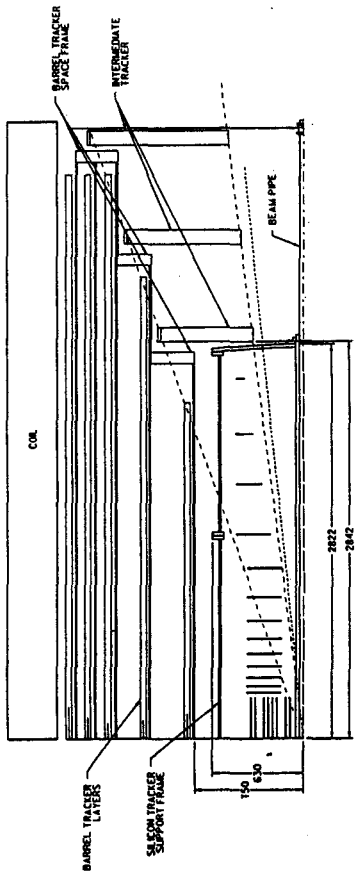

STRAW TRACKER LAYOUT

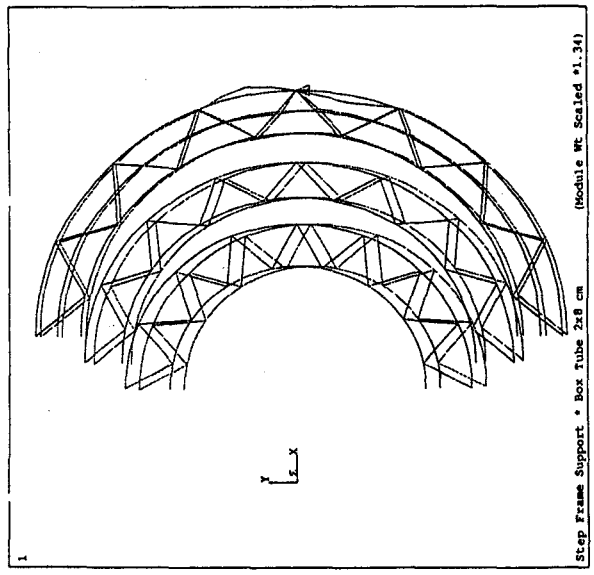

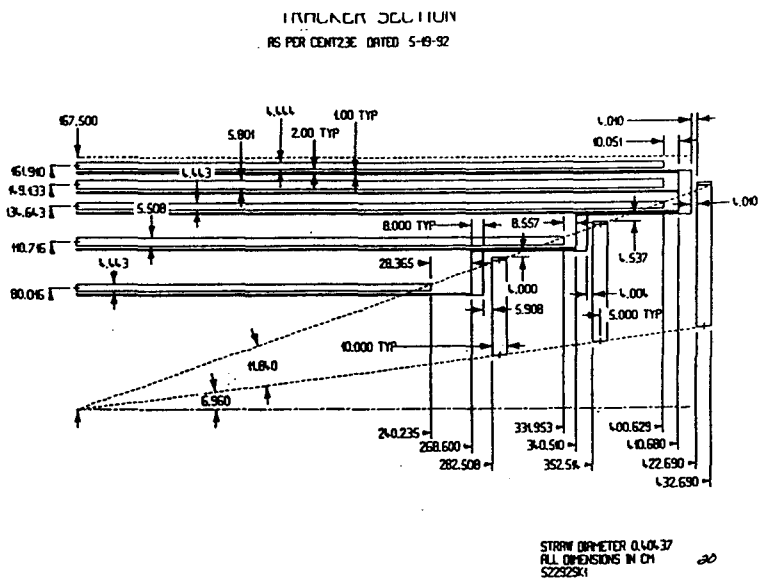

215

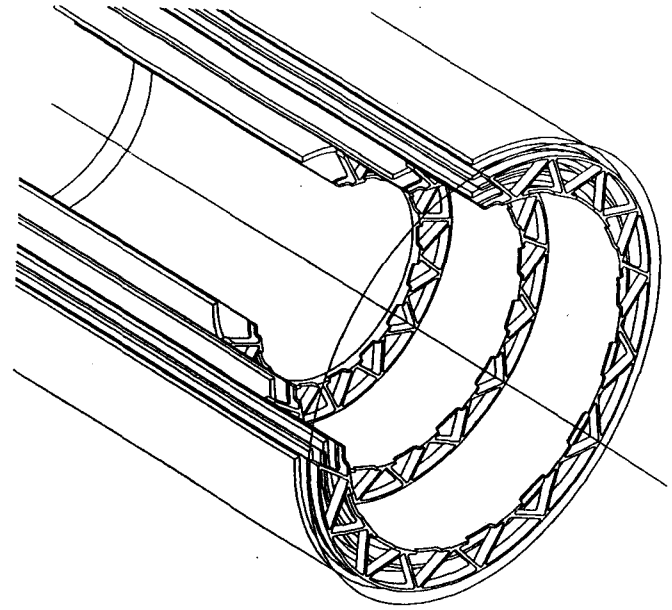

213

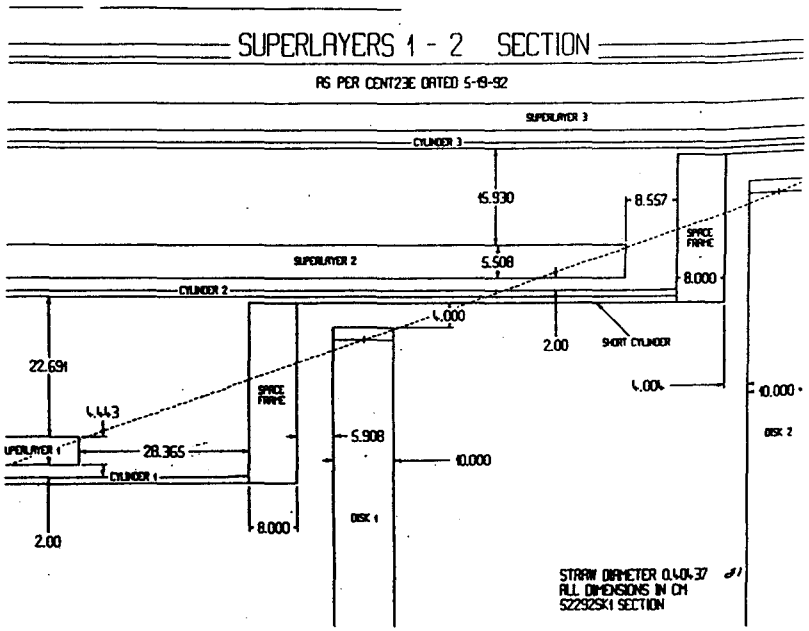

216

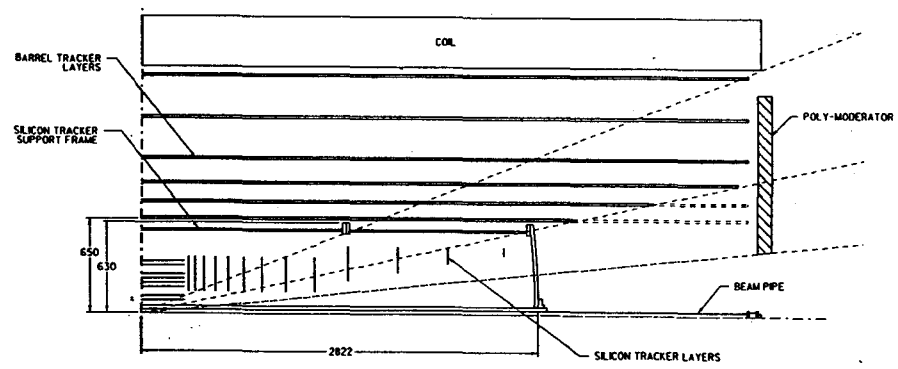

FIBER TRACKER LAYOUT

20-MAY-1992

SD000364

214

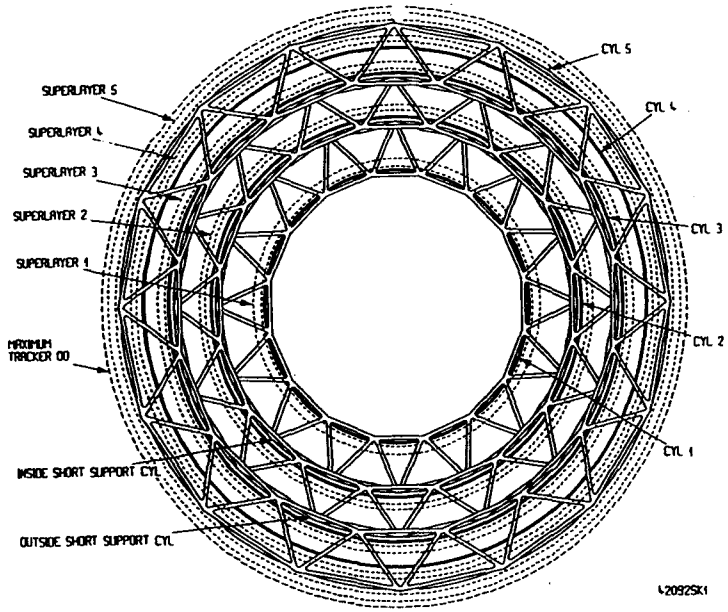

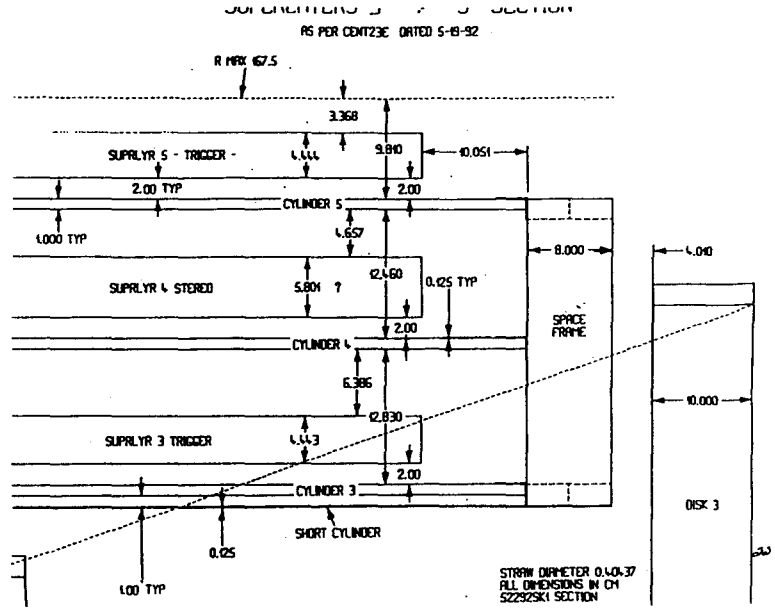

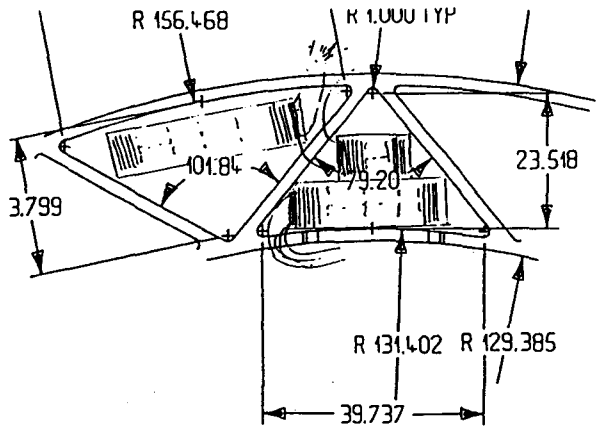

42892SPFR3
4-28-92 DM

ELECTRONICS VOLUME SUPERLAYER 2

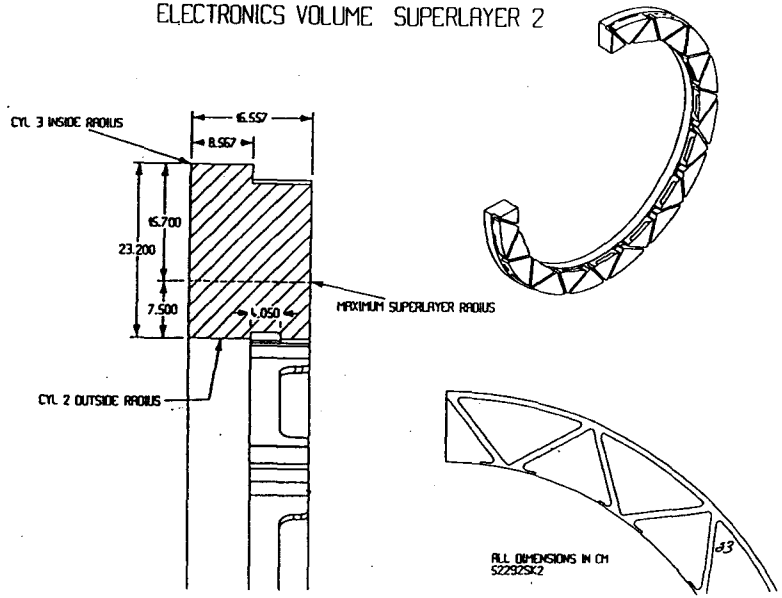

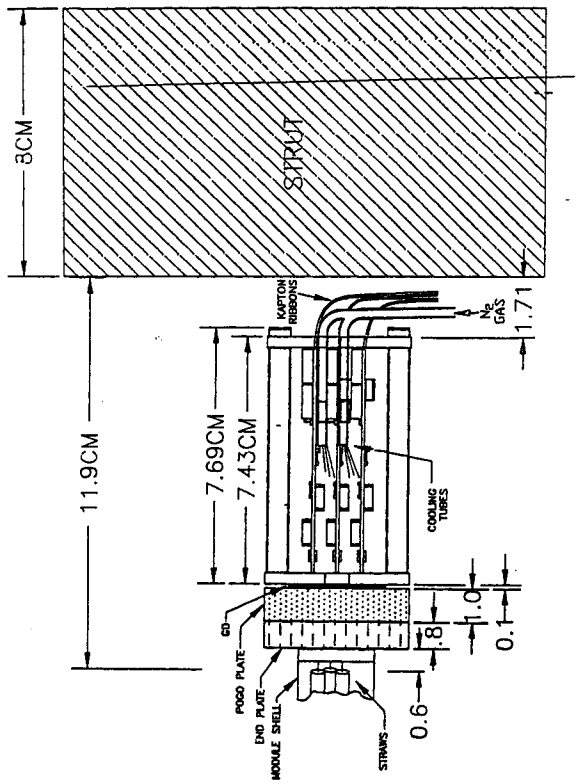

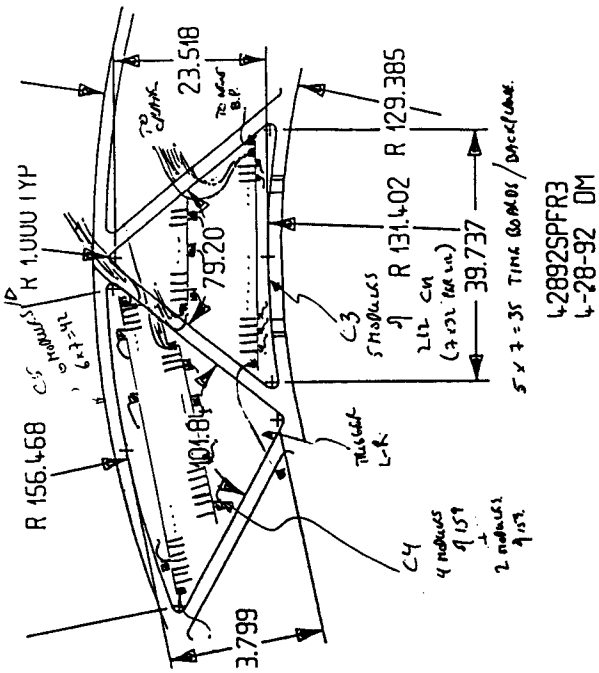

Tracking System Staging Options

	Total $	U.S. $
1. Stage 6 Si disks (each end) ($|\eta|<1.5$)		2 M ←
2. " 4 " " " " " 1.8		1.5 M
3. Stage straw, 9 GMD level 1 off-detector trigger circuitry		1.2 M
4. Stage straw level 2 " " " "		0.5 M
5. Stage straw inner superlayer:		
a. modules	1 M	1 M ←
b. electronics	1 M	0.2 M
. Remove (once & for all) layers 7,8 of each axial superlayer:		
a. mechanics	0.2 M	0.2 M
b. electronics	1.0 M	0.2 M
. Stage ITD: $16.1 M – (design, R&D, prep)		0 M
. Stage scifi level trigger circuitry and readout of 1st 3 superlayers	5.9 M	
. Stage readout of stereo layers	4.8 M	
. " " " 4th + 5th superlayers	4.5 M	
. " " " 2nd layer of outermost superlayer	4.3 M	
Total (baseline tracker, no electronics)		3.0 M

w Ford 5/28/92

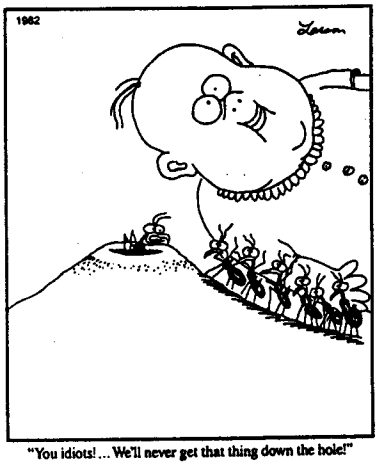

"You idiots!... We'll never get that thing down the hole!"

Do we have enough space for straw tube readout electronics?

Report from Calorimeter Group

Daniel P. Green
(Fermilab)

5/92
KEK

SDC CALORIMETER GROUP

- STAGE
- COST SAVINGS
- SECONDARY GOALS
  R+D
  PROTOTYPE

PAC

DRAFT - NOT FOR DISTRIBUTION 5/15/92 V5

The panel commends the proponents for building a prototype to test many of the design concepts and construction techniques.

Tracking

At the core of the tracking system is a silicon strip tracker that provides pattern recognition and b and τ vertexing. This inner tracking system is used in conjunction with an outer tracking system (straw tubes and gas microstrip detectors or scintillating fibers), which improves the momentum resolution and provides a Level-1 trigger selecting charged tracks with a minimum transverse momentum. The panel was impressed by the progress in the design of this system, but was concerned about the following issues:

- The forward-backward reach of the silicon tracker adds considerably to the complication and cost of the tracking system. It is not clear that the forward tracking system (i.e., silicon plus gas microstrip detector) has been optimized for cost and performance. The necessity for high-quality tracking in the forward region should be better justified.

- The calculated occupancies for the innermost layers of straw tubes are very high at design luminosity. The fiber system offers an attractive alternative that could, in principle, be more effective at high luminosity. Although considerable R&D must be performed before the fiber system can be considered viable, recent progress with fiber read-out has been impressive. The panel recommends that the R&D on scintillating fibers be continued.

Calorimeter (NO QUESTIONS, BUT ....)

The calorimeter, which has been considerably descoped since the submission of the LoI, has a segmentation, thickness and coverage that is appropriate for the proposed physics program. Further significant descoping would not be wise. The main concerns were:

- Some of the estimated costs of the calorimeter — such as ~ $10/kg for steel and $48 per scintillating tile — are high. A re-examination of the

ENDCAP: EM3/EM2 STAGING
BARREL/ENDCAP MG STAGING

+ COSTS ⇒ ABSORBER AND SCINTILLATOR

***** Agenda for the May SDC Meeting of the Calorimeter Group *****

May 26 (Tue) ORGANIZED BY K. TAKIKAWA

9:00 - 12:20	Plenary sessions	
12:20	Executive Board meeting	
2:00 - 6:00	Joint magnet/calorimeter/integration meeting	
	*Calorimeter/solenoid interface	
	Update on solenoid issues (15 min) - A. Yamamoto	
	Update on magnetic geometry (15 min) - Green/Bartoszek/???	
	Tracker utilities update (15 min) - J. Piles	
	Alignment lines of sight from muon system (15 min) - Piles/Grinnell	
	Discussion and action items (15 min)	
	*Calorimeter support/BWl interference (30 min) - Bartoszek/Piles/Muon group rep	
8:00	Resource Committee meeting	

May 27 (Wed)

9:00 - 12:30	Subgroup sessions	
	-- "General"	
9:00	Present and Near Future of the SDC Calorimeter	Dan Green
9:30	TDR Mechanical Design	Larry Bartoszek
	-- "Prototype"	
10:10	Report from Prototype Task Force	Bill Foster
10:30 - 11:00	Break	
11:00	Update to Baseline Design EM Calorimeter - Mechanical and Optical	Dave Underwood
11:40	High-Resolution and Stacked-Lead Barrel EM Options	Bill Foster
12:10	Pb Stack Option	Larry Bartoszek
12:30	Adjourn	
12:30	Executive Board meeting	
2:00 - 6:00	Subgroup sessions	
	-- "Prototype"	
2:00	Mass Fabrication of Tiles and Fibers	Kazuhiko Hara
2:40	Ageing Test of Bent Fibers	Yoshinori Miyamoto
3:00	Optics Design of Prototype EM Tile/Fiber	Masakazu Okabe
3:20	Optics for the Large HAD Prototype Tiles	Vasken Hagopian
3:50 - 4:20	Break	
4:20	Photomultiplier Cockcroft-Walton Bases	Kazuhiko Hara
4:40	Quality Control for Prototype Tiles, Fibers, and PMTs	Itsuo Nakano
	-- "Calibration"	
5:00	Status of the Calibration System and Specifications for the Prototype	Andy White
	-- "Forward Calorimeter"	
5:30	Study of Radiation Effect on Total Reflection between Liquid Scintillator and Glass for the SDC Forward Calorimeter	Taro Masumaru
	-- "Simulation"	
5:50	Present Status of SDC-SIM Calorimeter Part	Makoto Asai
6:20	Adjourn	

7:00 Collaboration dinner

May 28 (Thu)

9:00 - 12:30 Subgroup sessions
-- "Radiation Damage":
9:00 Report of Tallahassee Raddam 1992 Conference — Vasken Hagopian
9:40 Radiation damage of Tiles, Fibers, and Tile/Fiber Assemblies — Kiyoshi Yasuoka
10:20 Low Dose Rate RADDAM — Nikos Giokaris
10:50 - 11:20 Break
11:20 Rad-Hard Scintillator Development — Bill Foster
-- "PMT Development"
11:50 Development of MAPMT and Green-Extended PMT — Seiji Suzuki/ Yuji Yoshizawa *

12:20 Adjourn

1:30 - 3:00 Institutional Board meeting
3:00 - 6:00 Technical Board meeting

1:30 - 6:00 Subgroup sessions
-- "Shower Maximum Detector"
1:30 Present Status of Shower Maximum Detector and Prototype Design Progrses — Thomas Muller/ Prisca Cushman
-- "CDF Plug Upgrade"
2:30 Present Status of the CDF Plug Upgrade Tile/Fiber Calorimeter — Shinhong Kim
3:10 - 3:40 Break
-- "Readout"
3:40 Digital Calorimeter Readout — Bill Foster
-- "Forward Calorimeter"
4:20 FCAL High Pressure Gas Option — Nikos Giokaris
4:50 GEM Forward Calorimeter Transmutation Studies and Applicability to SDC — Bill Wilson
5:20 Adjourn

May 29 (Fri)

9:00 - 12:30 Plenary sessions

---

27 TALKS ⇒ APOLOGIES FOR FAILURE TO SUMMARIZE

MEGA-TILE DESIGN : (FOSTER)
- single piece of scintillator contains many tiles
- tiles optically separated by grooves filled with white epoxy.

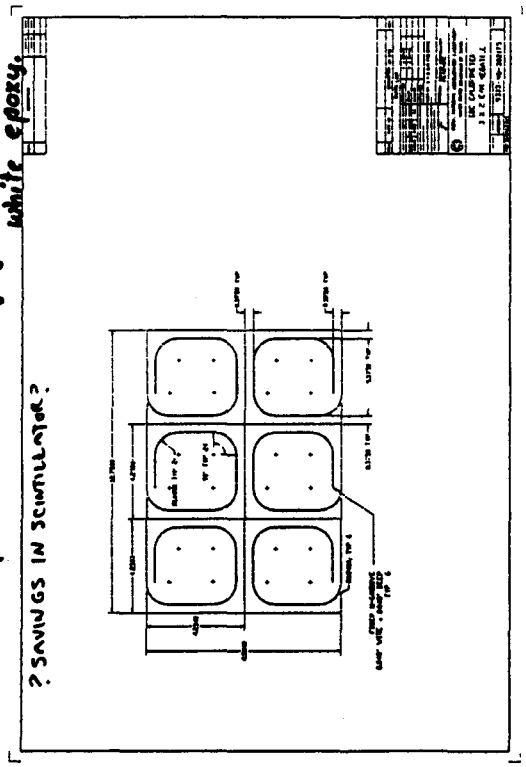

? SAVINGS IN SCINTILLATOR ?

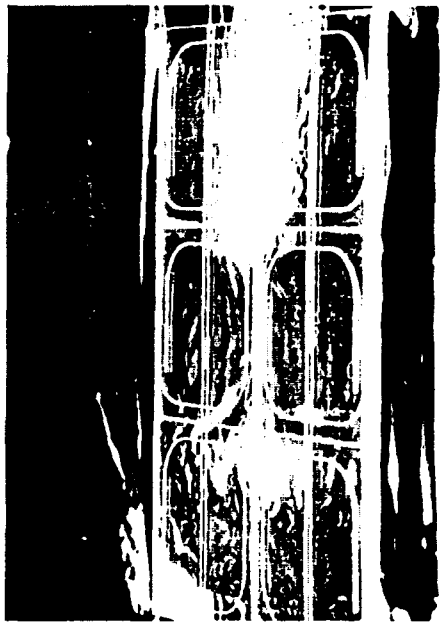

2x3 MEGATILE
SDC - BNL PHOTO
ALSO TSUKUBA, S. KIM MEGATILE

INDUSTRIALIZE OUR ~~COTTAGE~~ INDUSTRY !

Fabrication of Tiles and Fibers for the SDC Calorimeter

presented by K. Hara (University of Tsukuba)

CONTENTS :

1. Number of Scintillator Tiles and Groove Length
2. Grooving
   - Laser Milling
   - Injection Molding
   - CNC Machining
3. Tile Edge Cutting and Painting
4. Fiber Mirroring
   - Aluminum sputtering / evaporation
   - painting white
5. Waveshifting Fiber and Clear Fiber Splicing
   - heat splicing
   - splicing using glue
   - small connector
6. Summary

EXPLORE SPECS ON OPTICS

2. Light Loss Caused by Fiber Bending

1) Result

MIYAMOTO

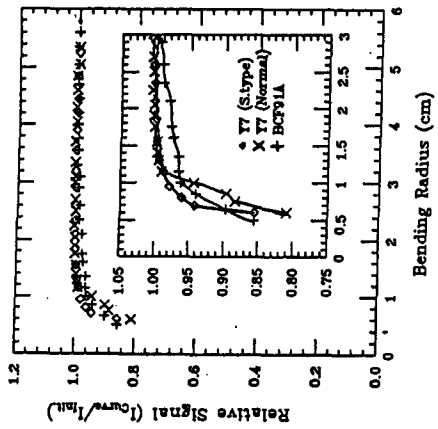

OKABE

TIGHTEN UP ON OPTICS UNIFORMITY

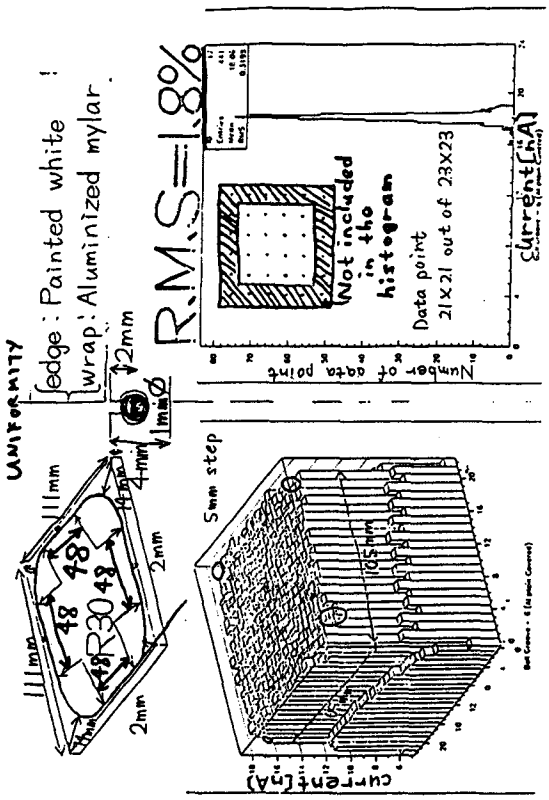

HAGOMAN

EXPLORE OPTICS OF LARGER TILES (HAO 2)

(25 X 25) CM. SIGMA PLATE DESIGN

PLATE SCALE: 2:1

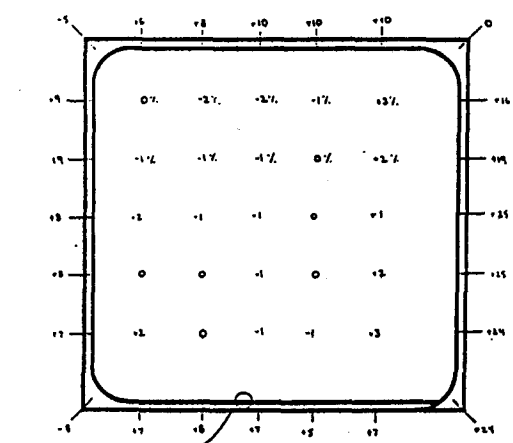

	Between fiber and edge	On fiber
Bottom side	-1%	7%
Left side	7%	8%
Top side	9%	10%
Right side	20%	25%

RADDAM, ⊥ NONUNIFORMITY

YASUOKA

10

Normalized Response Map TSUKUBA DATA, β SCANNER

The light yield at each point was normalized by the light yield at the tile center.

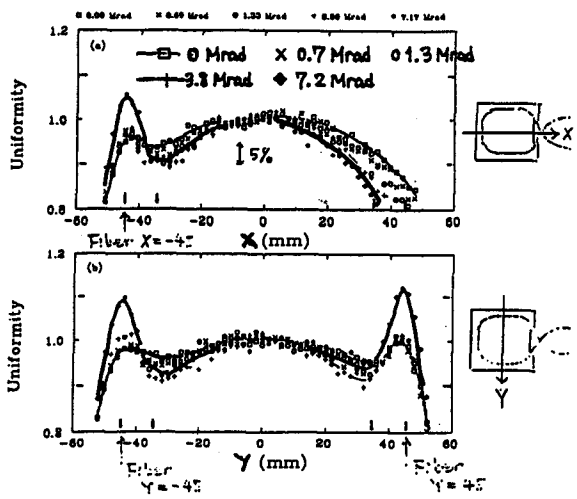

Degradation of response uniformity is small upto ~1 Mrad, and ≤ 5% at 3.8 Mrad.

NAKANO

Manufacturing Process

ESTABLISH QC PROCEDURES

- Tiles specs (423.808) — cutting specs (sample test T1) — grooving specs — painting specs → Tile/Fiber test TF1, sample test TF2
- WSFibers (423.808) specs — mirroring specs (sample test F1, test F3) → splicing specs (test F4) → Tile/Fiber
- C Fibers (423.808) specs → splicing (sample test F2)
- PMTs (20.352) specs → test PB1, sample test PB2
- Bases (20.352) specs → test B1

Barrel & Endcap

ABSORBERS

Fe:
- NEW GOS
- DIFFERENT MANUFACTURING
- 1/64 → 1/32 FEWER PIECES
- RELAXED SPECS
- BEIJING - SHIPYARD VISIT
- DUBNA - JINR SHOPS
- ⇒ EXPLORE CHINESE/RUSSIAN MANUFACTURE

Pb:
- EXPLORE CAST/STACKED OPTIONS
- ⇒ ALLOWS MECATILE APPLICATION (FEWER PIECES ⇒ REDUCED LABOR?)
- COMPARE COST/PERFORMANCE

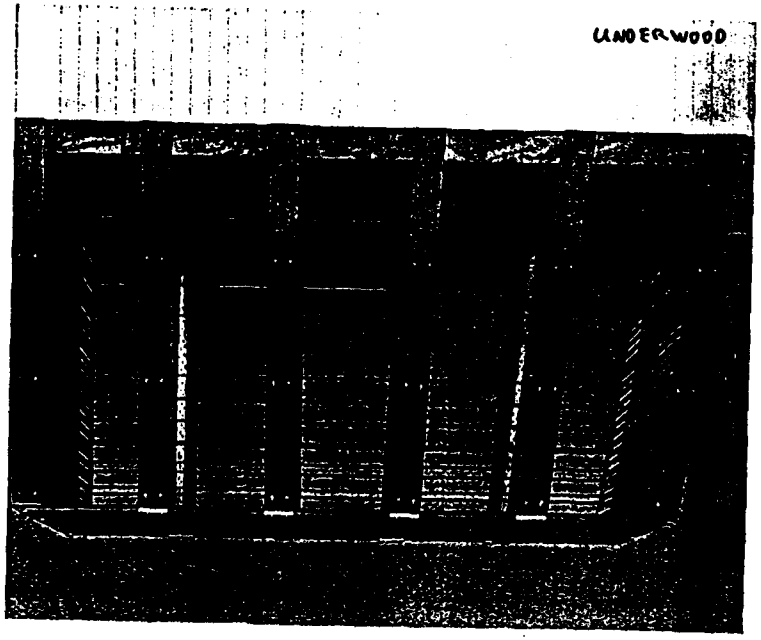

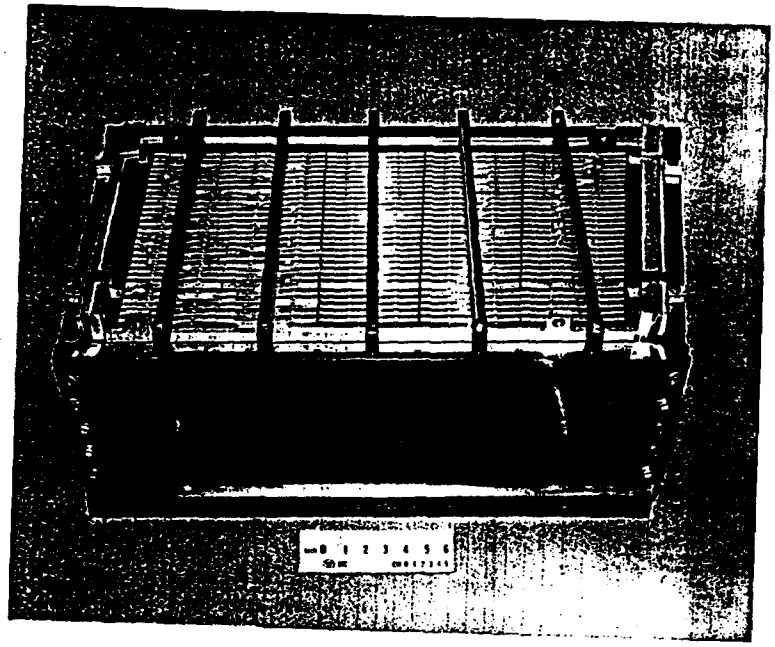

271

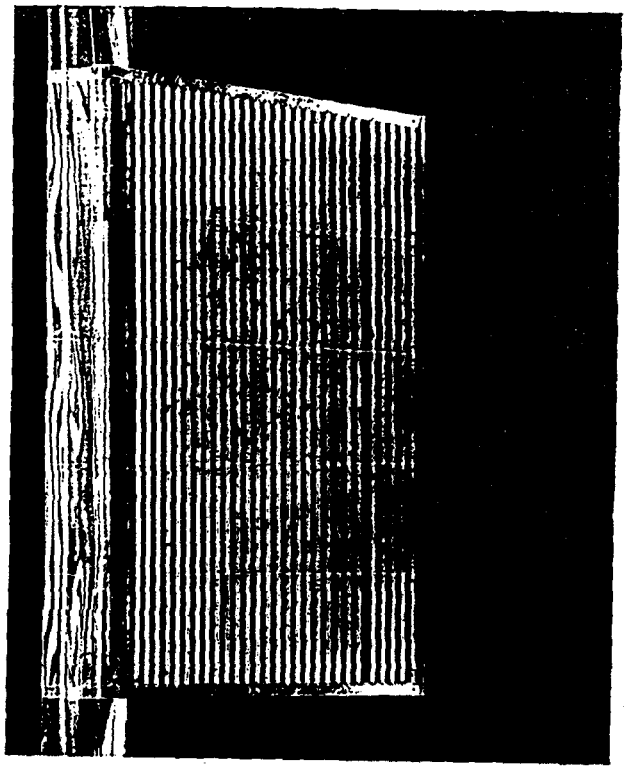

272

273

FOSTER

COMPRESSION STACK

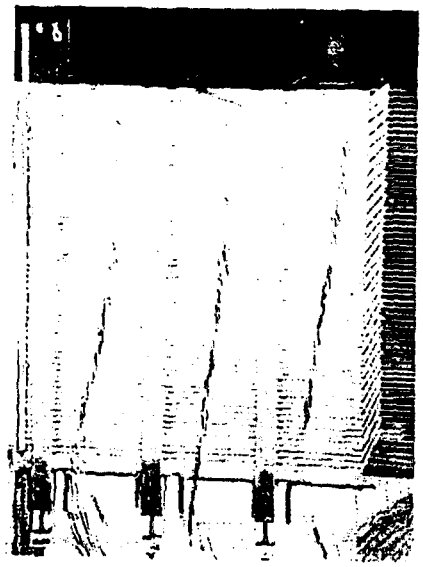

BANDS → PIANO WIRE

274

2x(2x3)

BNL TEST MODULE

COMPRESSION STACK

IN BNL TEST BEAM NOW

UNDERWOOD

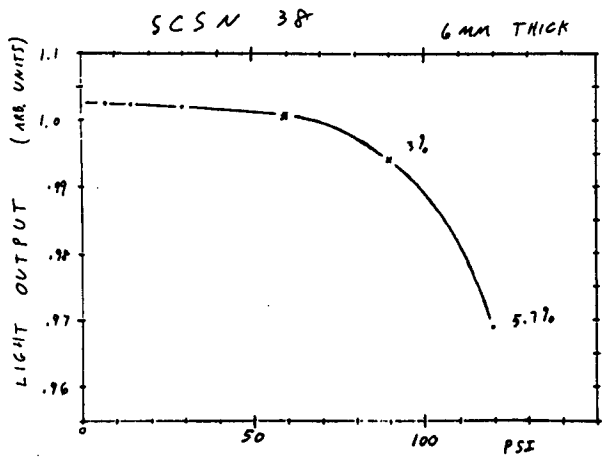

$$\text{LIGHT} = 1.05 - .0081\, e^{\frac{PSI}{50}}$$

TWICE AS BAD FOR 3 MM THICK

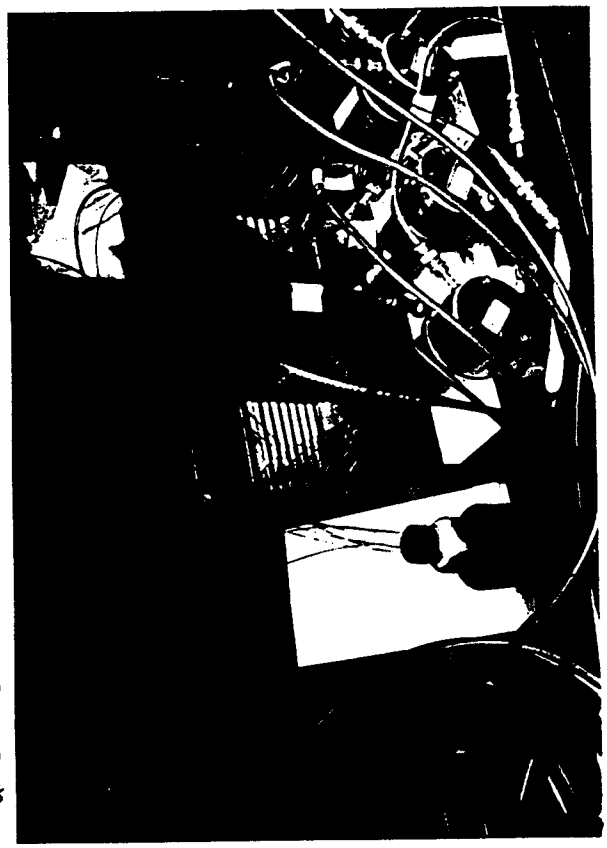

HAMA

PMT BASES

EXAMPLE: DYNAMIC RANGE 20X COF/0Ø
⇒ FIXED I_{max}, REDUCE "NOISE FLOOR"

9. PMT, COCKCROFT-WALTON BASE

A) Continue to develop a photomultiplier tube suitable for the SDC barrel calorimeter --- Hamamatsu

B) Cockcroft-Walton base of mold type --- Matsusada — ACHIEVED 1/10 NOISE OF ZEUS BASE

C) More compact Cockcroft-Walton base using surface mount technology --- Rin-ei seiki

---

So far the plan.

Data will be presented in the May SDC meeting at KEK.

HAMA

CW BASE

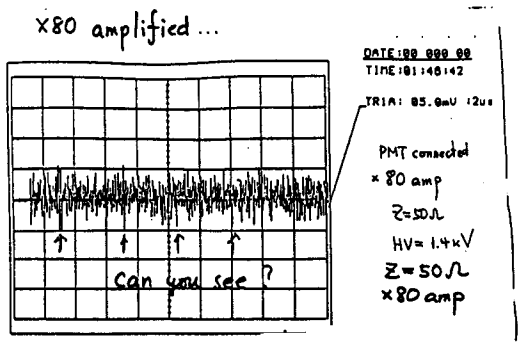

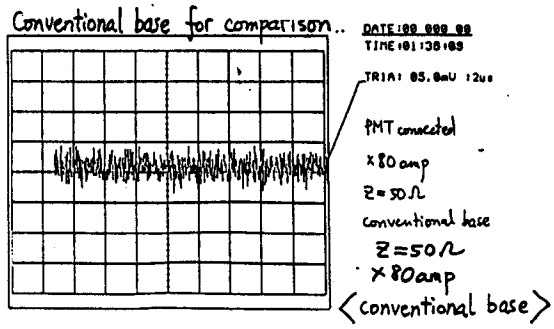

CUSHMAN/
MULLER

SM TRANSDUCER OPTIONS

MCPMT

Uniformity accross PMT

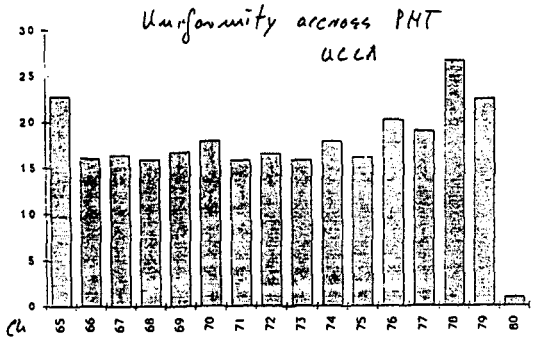

REDUCED CROSSTALK

HAMAMATSU

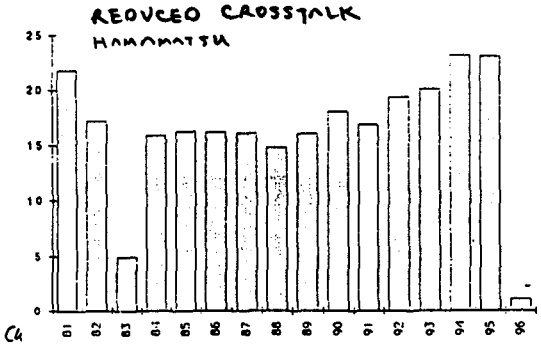

GIOKARIS

FCAL OPTIONS - HIGH PRESSURE GAS

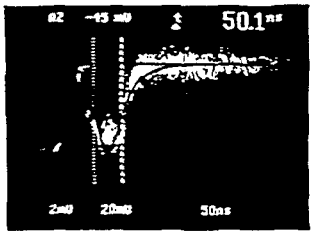

95% Ar + 5% CH4 at 100 Atm
E = 1.25 kV/mm
Am241 alpha source
Shuvalov preamplifier
(a)

2mm gas gap

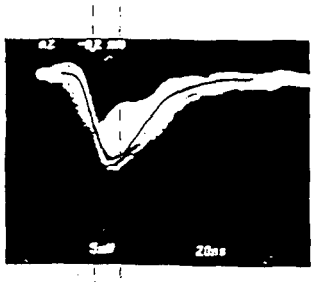

95% Ar + 5% CH4 at 100 Atm
E = 0.75 kV/mm
50 GeV electrons
Volkov preamplifier
(b)

~50 nsec base width
(~35 nsec for scintillator at present)

ASAI

PUT CALORIMETER INTO SDC SIM
⇒ EVALUATE PHYSICS IMPACT OF CHOICES

SDC Collaboration Meeting 27/May/1992 KEK

Calorimeter Packages:

CL -- Barrel and endcap Tile/Fiber calorimeter with Shower-Max calorimeter

CI -- Forward calorimeter

CF -- EM / Hadron shower shape and punchthrough parametrization

CP -- Detailed (tile level) description

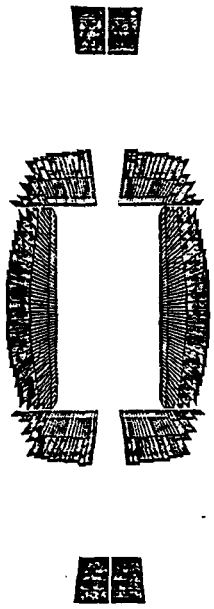

Solenoidal-Detector-Collaboration

M. Asai (Hiroshima U.) SDC SIM (Calorimeter) p.2

WHY? TEST MECHANICS - FULL SCALE
TEST CRACKS/HERMETICITY
TEST MANUFACTURING ⇒ CONSTANT TERM

PREPRODUCTION PROTOTYPE WEDGE

* TEST SDC COLLABORATION - THIS IS A PROTOTYPE OF SDC NOT JUST A CALORIMETER

CONTAINMENT

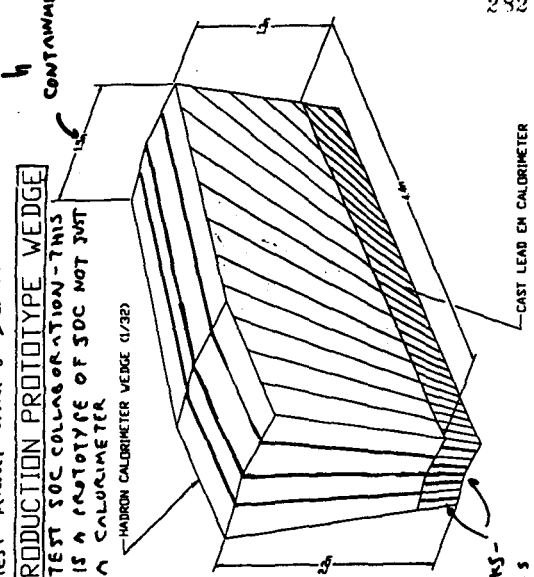

~70T (35+35)
2 FULL SIZED
1/32 WEDGES
TEST BEAM (1M$)
+ 5M$

SDC Preproduction Prototype

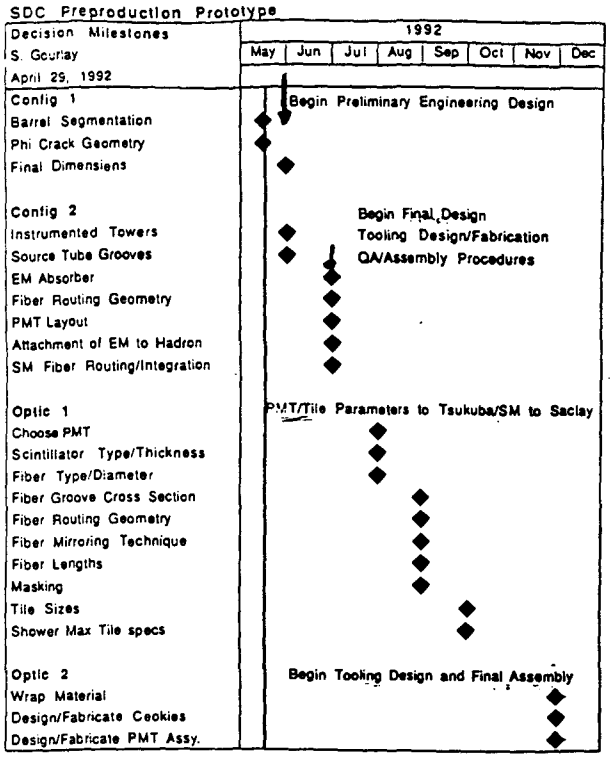

READY ~ JUNE 1993

LBL – MOVING FIXTURE ENGINEERING

STAGING: AS SUGGESTED BY PAC

COSTS:

SCINT – NEW TILE METHODS
INDUSTRIALIZATION
QC/QA

ABSORBERS – Fe
1/32 ⇒ COST SAVINGS
FOREIGN PARTICIPATION

ABSORBERS – Pb
CAST/STACKED
REVIEW ⊖
JUNE EB/TB

⇒ RETURN TO PAC IN JULY WITH A RESPONSE CONTAINING REDUCED COSTS

SDC Collaboration Meeting at
KEK, May 26-29, 1992
S. Terada; KEK

Muon Subgroup Summary
(Incl. Muon/Integ. Muon/Elec. Joint)

I. Discussions on Detector Arrangement:

1) Layer ordering of BW1 → Prefer 2φ4θ2φ
- Confusion volume (Muon I.D. performance); J. Wiss
- Mechanical rigidity; C. H. Dary

Recommend 4φ4θ with θ tubes at outer radius.

2) BW-IW interface
-Continuous θ coverage, Realizable support scheme for IWs'; F. Feyzi, D. Carlsmith

Recommend extension of BW3 with IW3 inside.

Need detailed engineering and evaluation to the access space between BW2 and BW3.

3) Place of barrel scintillator; in BW2 or BW3

Access, Performance, Cost

We Should start studies.

4) Interference between bottom BW1 octant and calorimeter support must be studied.

L. Bartoszek

C.H. Dary

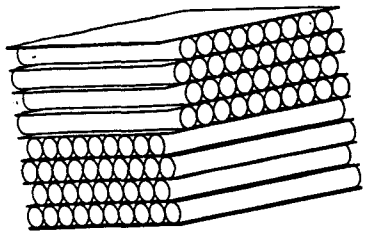

4θ, 4φ (or 4φ, 4θ) tube layout

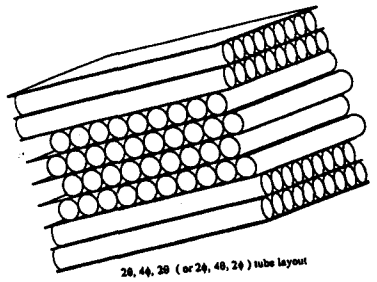

2θ, 4φ, 2θ (or 2φ, 4θ, 2φ) tube layout

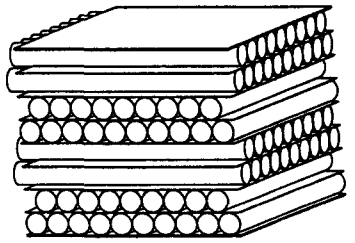

2θ, 2φ, 2θ, 2φ (or 2φ, 2θ, 2φ, 2θ) tube layout

C.H. Dary

Results for BW1

Deflections for Supports Moved in From Corners Effect of Tube Order Layout in BW1 Modules	
Tube Layout	Maximum Deflection (mm)
4 Theta, 4 Phi	0.797
→ 4 Phi, 4 Theta	0.797
2 Theta, 4 Phi, 2 Theta	0.963
→ 2 Phi, 4 Theta, 2 Phi	0.968
2 Theta, 2 Phi, 2 Theta, 2 Phi	1.066
2 Phi, 2 Theta, 2 Phi, 2 Theta	1.066

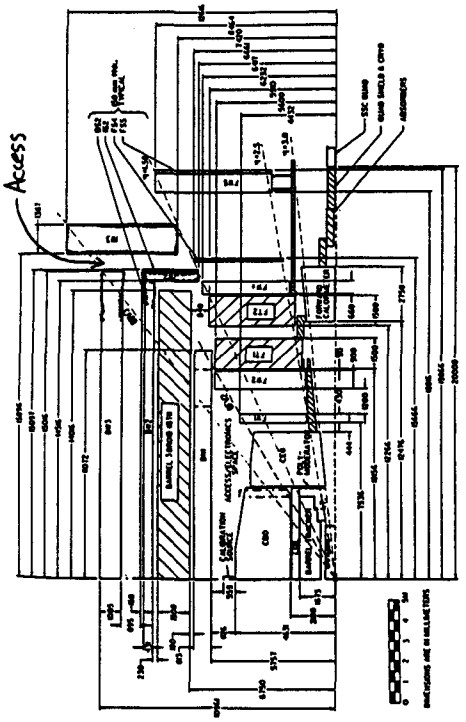

FIG. 2.7. Layout of the muon system.

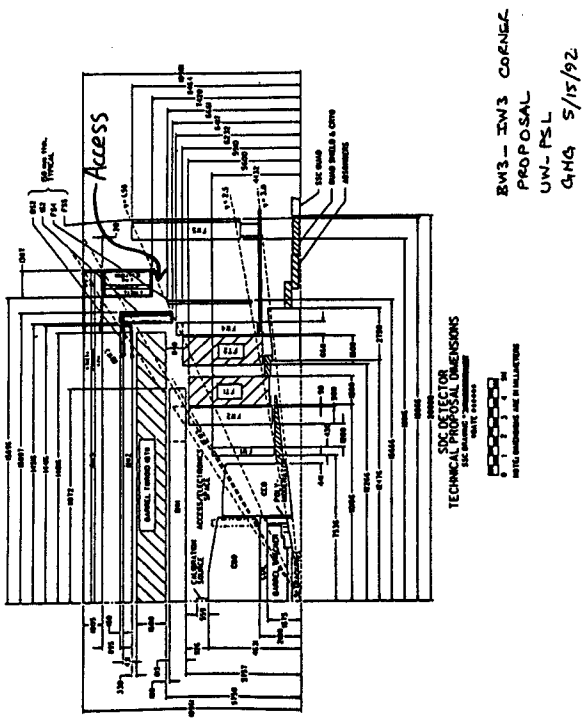

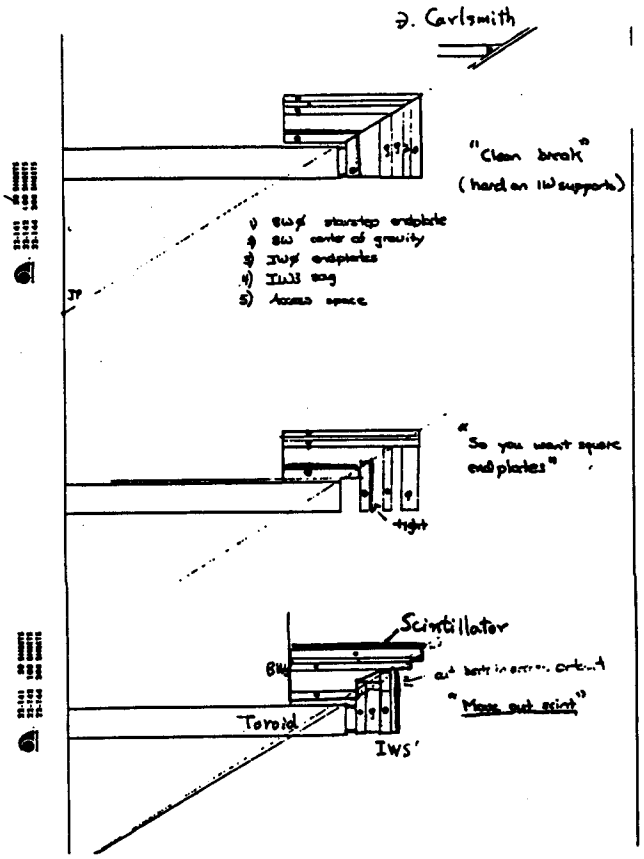

L. Bartoszek

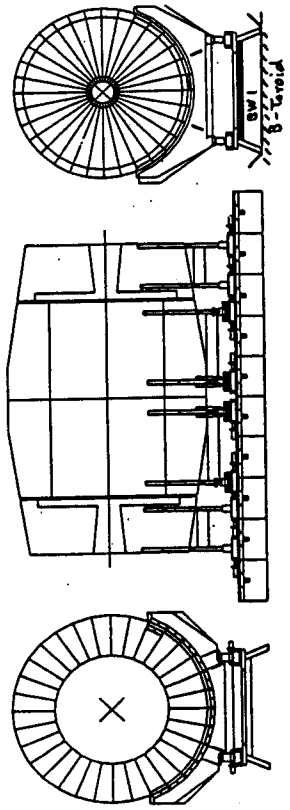

5) Tube sparsification issue

Save 22% of Barrel theta tube channel count

S. willis, V. Sirotenko,

N. Kanematsu

Y. Asano

- Trigger efficiency, Number of effective layers
- Effect of EM debris

Recommend that BW1 and BW3 remain sparsified according to the baseline design.

Recommend that BW2 be only partially sparsified to obtain $\langle n_{hit} \rangle \sim 5$ instead of 4. (BW2 has worst E.M. debris)

293

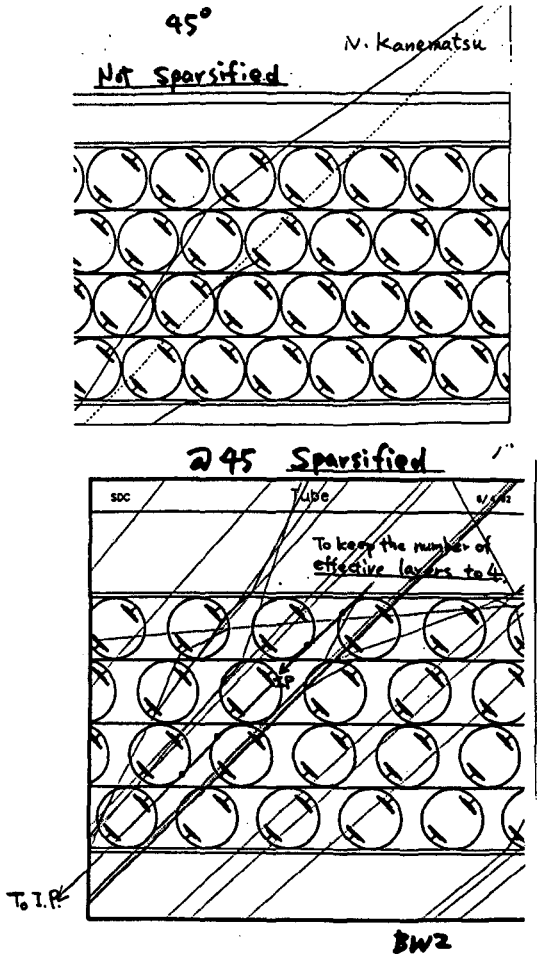

294

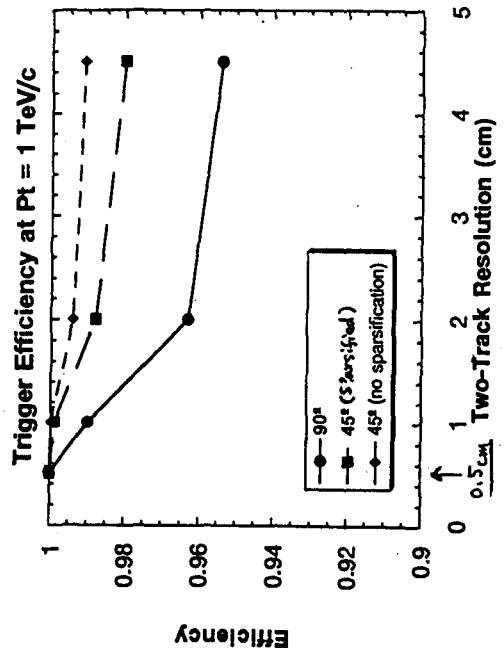

295

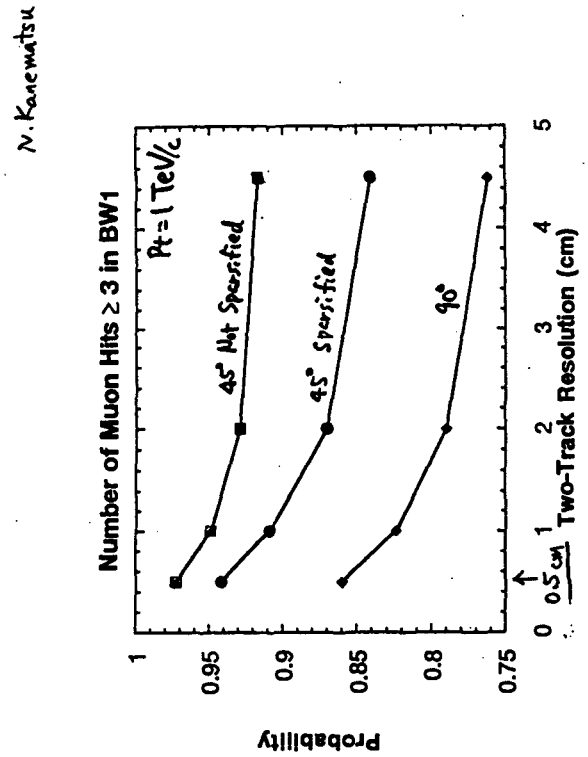

296

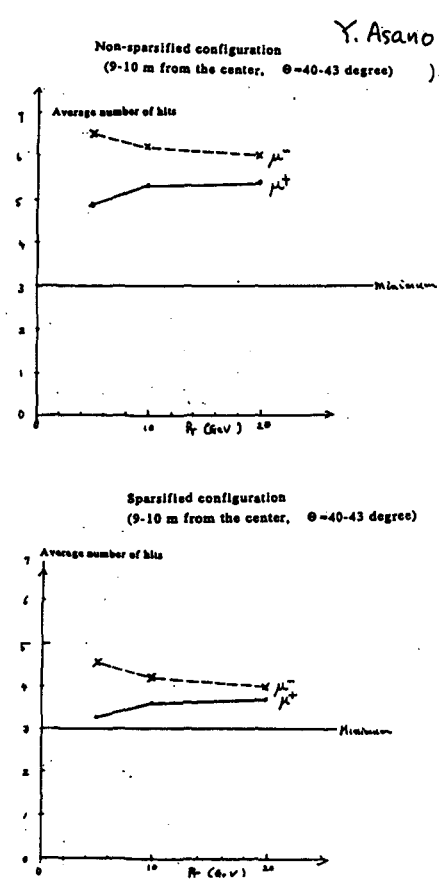

II. Discussions on Descope/Staging Options

1) Barrel;
- -Toroid thickness
- -Fewer chamber layers

Recommend to keep present design.

2) Intermediate;
Stageable except for octants trapped by cables (3/8 octants)
Saving; ~$3M

3) Forward;
Two possible scenarios;
a) Keep both ends but limit to one toroid and minimal tracking (no trigger).
b)Leave off one of the forward arms
Saving; ~$12M for either a) or b)
Majority of muon group felt b) was better than a).
Note, Russian group not present during discussion.

4) Miscellaneous;

Cheaper toroid Support	~$2M
Delay gas recirculation	~$2M
Optimize alignment system	~$1M
	~$5M Total

Saving; ~ $20M Grand Total

III. Presentations etc.

i) S. Amendoria; RPC solution for the SDC muon trigger counters

ii) W. H. Smith; Muon trigger rate

iii) A. Skuja; Forward system design by Russian group

iv) A. Kulik; Neutron Rate in the SDC Muon System

v) S. Mori; Tube production in Japan

vi) G. Feldman; Phi crack filler chamber

vii) C. Grinnel; WBS, Z-boundaries of BWs'

viii) S. Errede, J. Wiss; Physics Impact of Phi Crack in the Barrel Muon System

ix) Mourad Daoudi, Uriel Nauenberg, Victor Slonim; Study of Loss due to Missed Coverage in the Barrel Muon Detector

x) Zholobov G. V.; A background computations for SDC set-up at 40 TeV IHEP, Protvino, 19/05/1992 Meeting report

xi) Khalatyan Norik; Drift tube simulation study

S. Amendoria — SDC Muon Group, KEK, May 28, 1992

PRELIMINARY BASIC ISSUES ON THE RPC SOLUTION FOR THE SDC MUON TRIGGER COUNTERS

Presented by S.R. Amendolia on behalf of the SDC Italian Group.
Information comes from References on RPC's and from unreferenced test results from Italian Colleagues

RPC = RESISTIVE PLATE COUNTERS
(evolution of the Petrov counters)

REFERENCES

BASIC: "Development of RPC", R. Santonico et al., NIM 187 (1981) 377-380

PROGRESS: "Progress in RPC", R. Cardarelli et al., NIM A263 (1988) 20-25

"Performance of RPC at beam flux up to 140 Hz/cm²", M. Bertino et al., NIM A283 (1989) 654-657

READOUT: "RPC readout system", L. Antoniazzi et al., NIM A307 (1991) 312-315

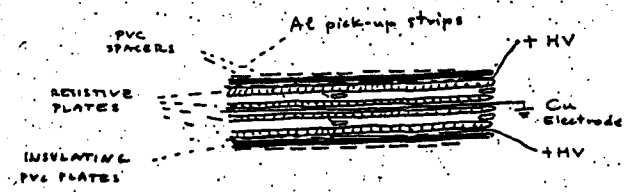

SKETCH OF DOUBLE LAYER RPC

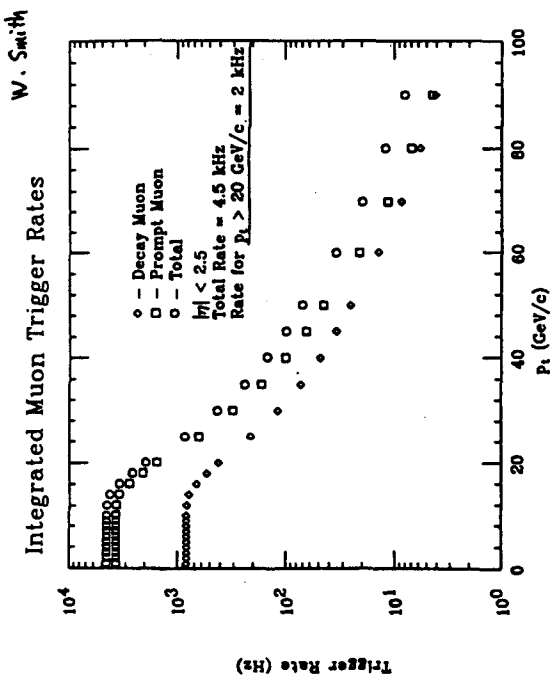

A. Skuja

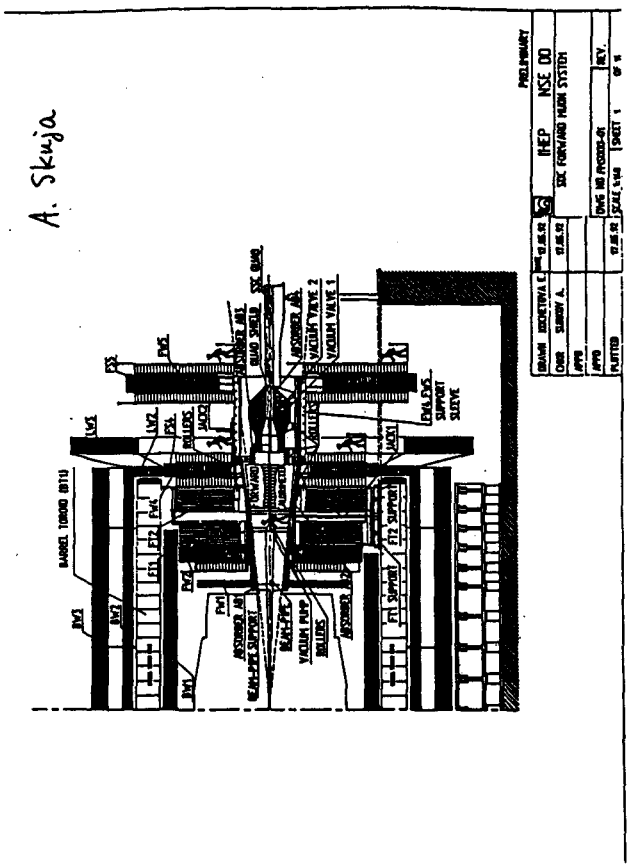

A. Kulik

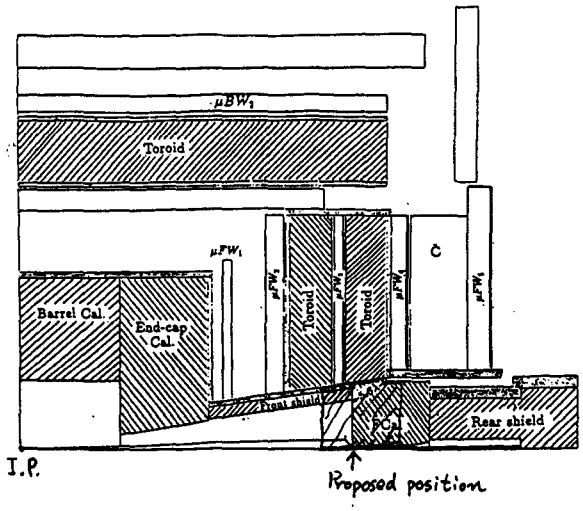

Fig.2 The base-line setup. The heavy absorbers (Iron and calorimeters) are shown in hatched and the Ployethylene shields are shown in green.

A. Kulik

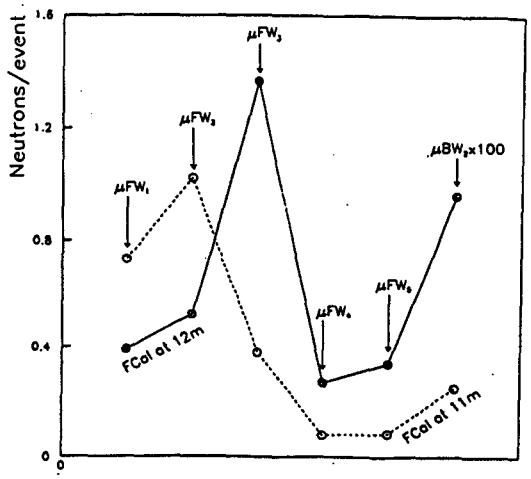

Fig.7 Total neutron rates for initial (12 m) and proposed (11 m) FCal positions. The data are normalized to one event in the IP.

IV. Presentations at Muon/Elec. Joint meeting

i) S. Terada; Muon Electronics Overview and Development Plan in Japan

ii) Y. Asano; ASD development

iii) Y. Arai; Design of TMC for muon readout

vi) H. Sakamoto; Muon trigger electronics

v) J. Chapman; Muon detector trigger

vi) M. Ikeno; Status of TMC module

vii) T. Zhao; Level-1 muon trigger using Xilinx FPGA

Minitower Project at KEK Test Beam

Purpose:

a) Provide test bench for the development of a chamber trigger electronics.

b) Provide a mini-station for testing an overall read-out scheme.

Chamber Setup: Two sets of 4 x 4 tube arrays (32 ch.) simulating BW2θ and BW3θ

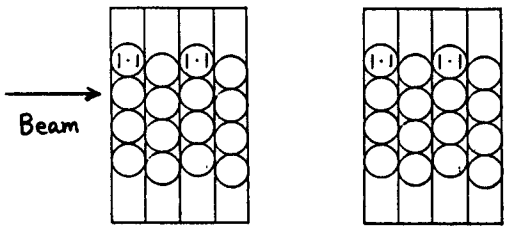

Test Beam at KEK PS:

a)T1 beam line; pion 0.5 ~ 2 GeV/c, 5 x 10^4 ppp at 1 GeV/c

b)π2 beam line; pion 1 ~ 4 GeV/c, 2 x 10^5 ppp at 3 GeV/c

Schedule: Beam Test at ~~Jan.~~ Feb. 1993

Report from Electronics Group
(Front-end Electronics)

Hugh Williams
(University of Pennsylvania)

Front End Electronics

Emphasis on:

Straw Tracking Readout

Muon Chamber Readout

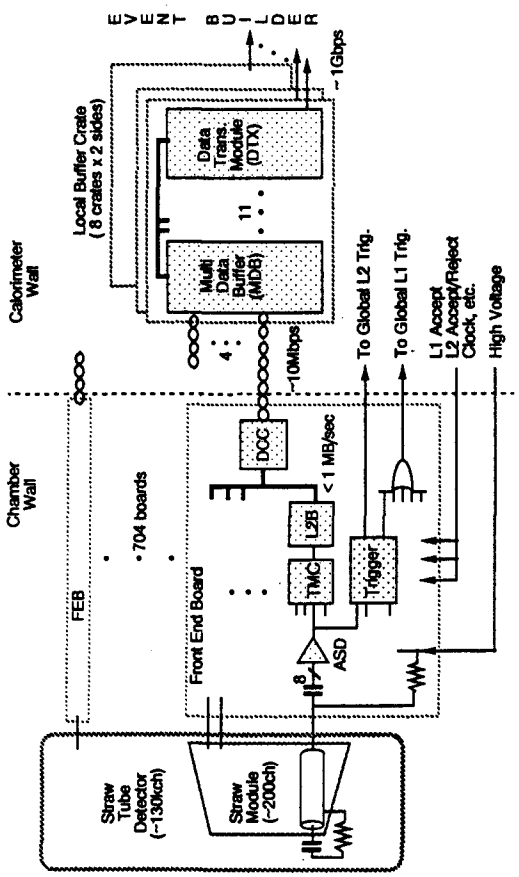

Straw Electronics Overview

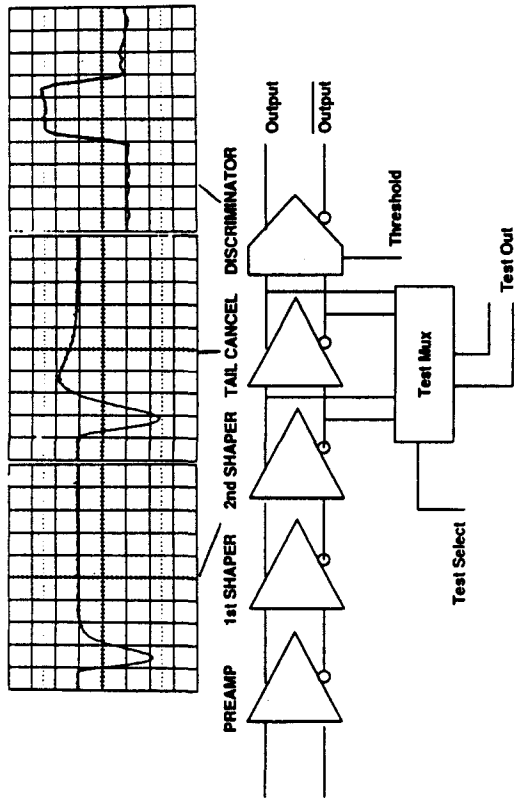

ASD - Summary of Measurements

* Gain	75% of expected value, uniform chip to chip, channel to ch. (few %)
* Peaking time	7ns observed, 6 ns expected
* Threshold Var.	< 0.5 fC ch. to ch. < 1 fC chip to chip
* Input impedance	125 +/- 10 ohms meas. 110 ohms expected
* Crosstalk	None observed for < 10fC with threshold at 0.5 fC
* Threshold Temp Var.	< 0.2 fC for 40 C
* Time Walk	4.5 ns for 1 - 15 fC (in agreement with SPICE)
* Yield	80% of chips

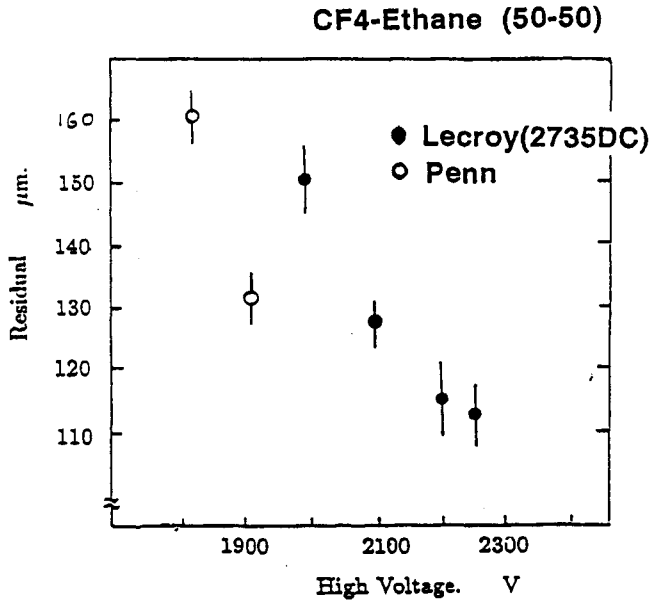

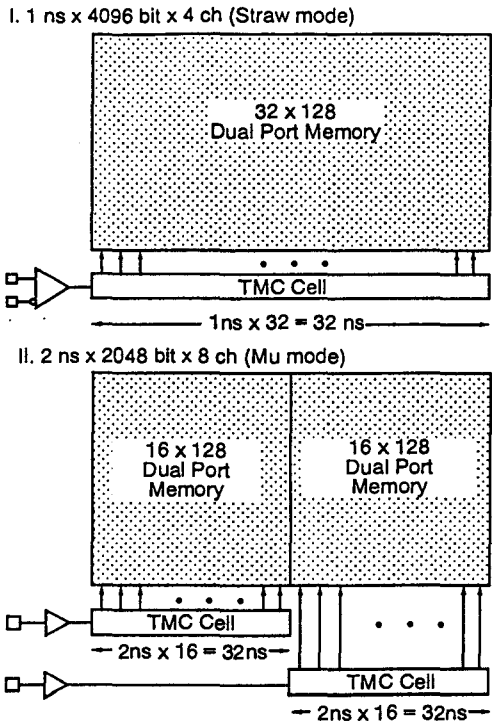

TMC4004/8 Memory Block

Features on Toshiba Rad-Hard Technology

Process

- 1 μm CMOS, Twin-Well Process.
- Radiation Hard up to 1 Mrad(Si).
- Low Temperature Process (< 900 °C).
- Thin Gate Oxide (150 Å), Epitaxial Wafer (5 μm).
- Guard Band Structured MOS FET.

Gate Array

- Sea-of-Gate (≤ 172 k gates. TMC1004 ~ 25 k gates).
- Compatible with Industry TC140G Series.
- Tpd = 0.4 ns.

Preliminary Design for Differential Receiver on TMC (using Toshiba gate array)

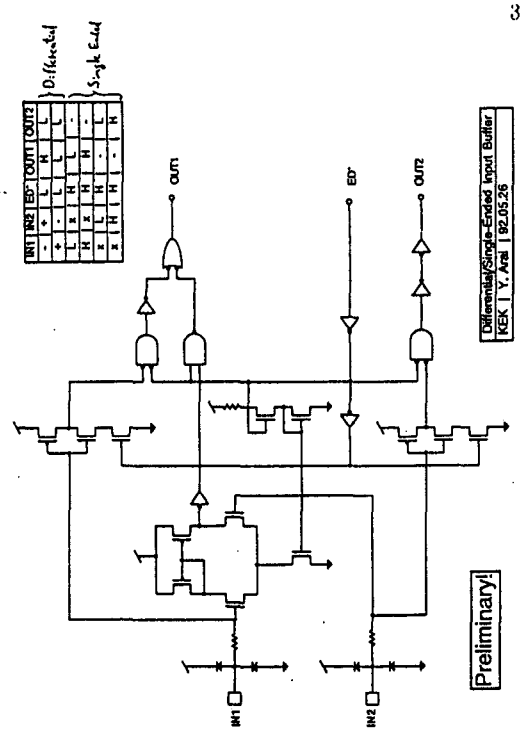

Level 2 Buffer

- Receive TMC output when L1 accept is asserted.
- Encode/Format Input Data.
- Buffer the data for L2 decision time (~ 50 μs).
- Transmit data to DCC.
- Combined with TMC if possible.

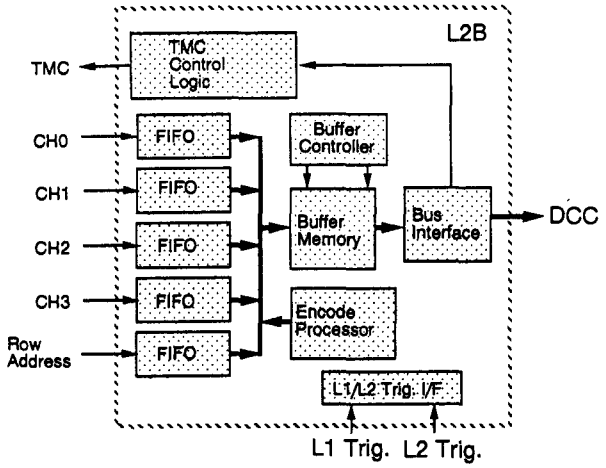

Introduction

The straw tube DCC design is constrained by

- Noise on analogue FE caused by digital activity
- Space and power considerations
- Rad-hard requirements

Several groups involved in DCC architectural design and simulation

- SSCL group has been working on
  - High-level simulations of buffering strategies
  - Noise issues on the Front End Board (FEB)
  - Data transmission technologies from FEB
- Toronto/McGill group has been studying
  - Detailed simulations of a "straw man" design
  - Buffering from L1 → Crate Interface Card (CIC)
  - Design of prototype ASIC's for DCC on FEB

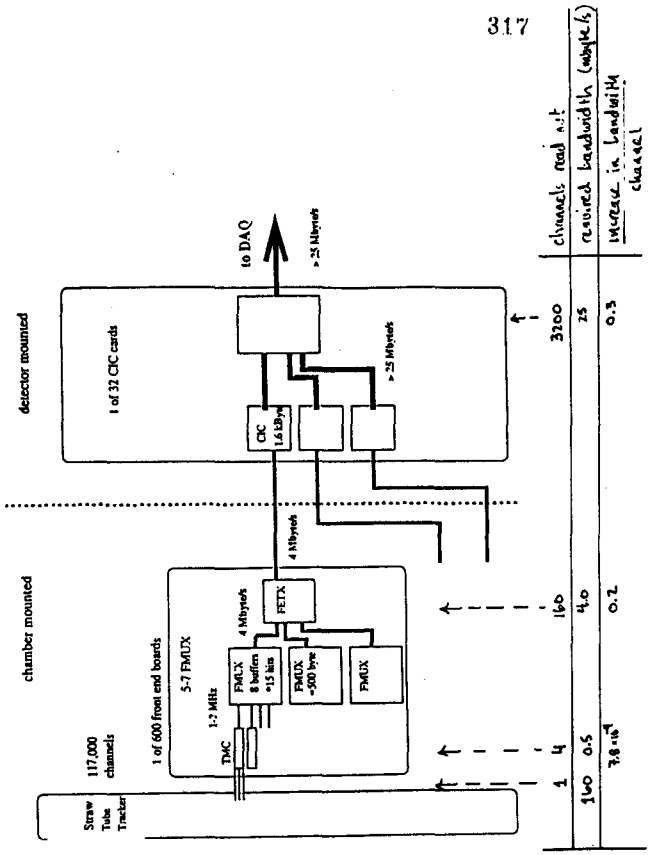

Alternatively, have TMC generate "end-of-trigger" hit

- This control information also has modest impact

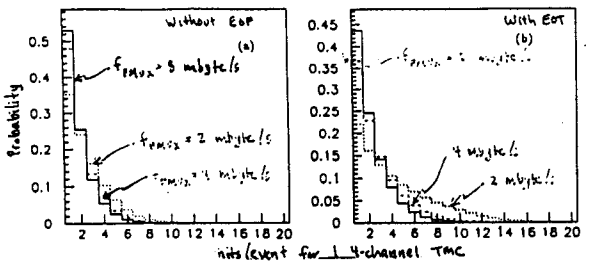

Figure 2: FMUX occupancy (in terms of hits) for one four-channel TVC/AMU without (a) or with (b) one empty hit for each event. The occupancy is shown for three different FMUX-FETX-CIC bandwidths of 2 (dotted), 4 (dashed) and 8 Mbyte/s (solid histogram).

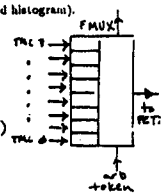

Prefer having control information

- Inherently more robust (error detection easier)
- More flexibility

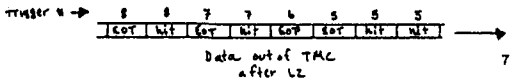

Water-cooled *Micro Crate*

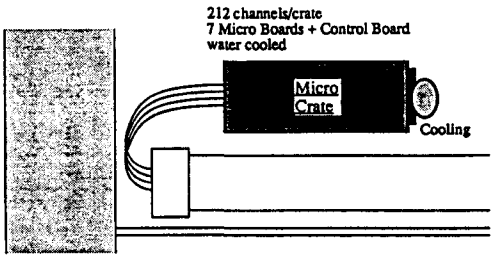

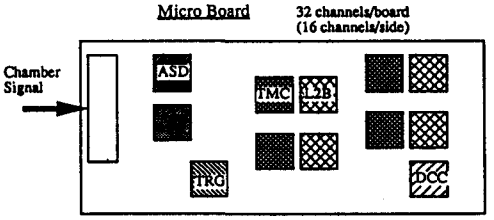

Summary

* Understand Straw Signals
* Amp/Shaper/Disc satisfies specifications
* TMC provides full capability for time meas.
* L2B chip under design
* DCC - block schematic & high level simul.
* Radiation Hardness not a problem
* Primary emphasis now on
  - full system test
  - substrate & mounting
  - cooling

SDC Collaboration Meeting at
KEK, May 26-29, 1992
S. Terada; KEK

Muon Electronics
Overview and Development plan

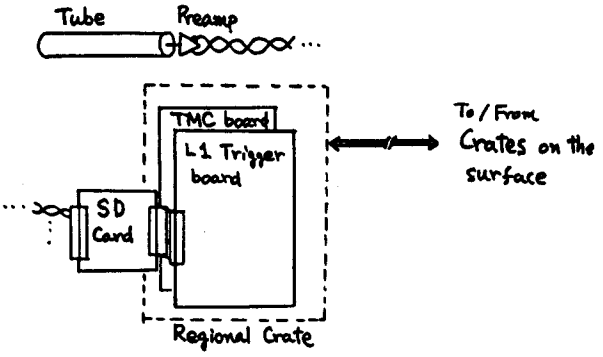

Development of Amp. Shaper Discri. (ASD)

Short term:

-For BNL Beam Test (June. 1992) ; ~4 ch.

a) Hybrid ASD used for the VENUS forward chamber

b) Penn. straw ASD chip

-For Minitower Chamber at KEK Beam Test (Feb. 1993); ~32 ch.

a) Penn. straw ASD chip?

Long term:

- For the Supertower prototype (May 1993); ~1,000 ch.
  - a) Muon ASD chip based on the straw ASD chip?
  - b) New preamp chip + New SD chip?
- For the Final Muon system (April 1994?); 100,000 ch.
  - a) Muon ASD chip based on the straw ASD chip?
  - b) New preamp chip + New SD chip?

Development of the TMC Board

-For the Minitower Chamber at KEK Beam Test (Feb. 1993); ~32 ch.

CAMAC-TMC module; 32 ch./board , 1μs Storage

- For the Supertower prototype (May 1993); ~500 ch.

VME (9U)-TMC module; 64ch./board, 1μs Storage

Development of the L1 Chamber Trigger Board

-For the Minitower Chamber at KEK Beam Test (Feb. 1993); ~32 ch.

First Prototype; 16 ch./board use FPGA's

- For the Supertower prototype (May 1993); ~500 ch.

Prototypes; 64 ch./board use FPGA's and/or Michigan wire trigger chips?

VME TMC MODULE

9U Single-width module

32-channel or 64-channel

129usec Full Scale

Common stop or Common start operation

DSP56001 for Data Formatting

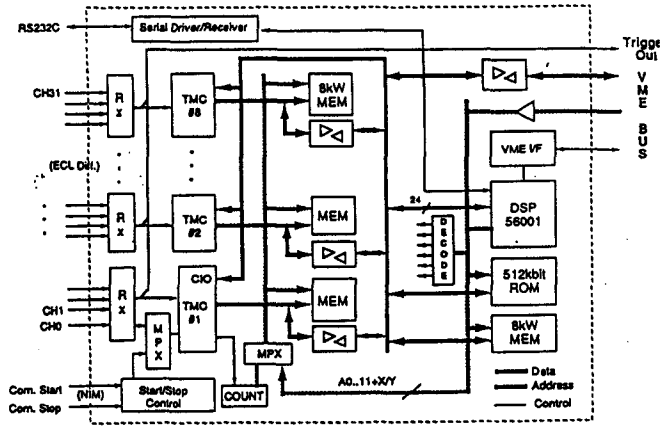

TMC-VME Module

JSD Working Group on Muon Chamber ASD

M. Abe	Graduate student, Univ. of Tsukuba
Y. Asano	Institute of Applied Physics, Univ. of Tsukuba
K. Mitsuhashi	Graduate student, Univ. of Tsukuba
H. Ikeda	KEK

Dependence on termination resistor

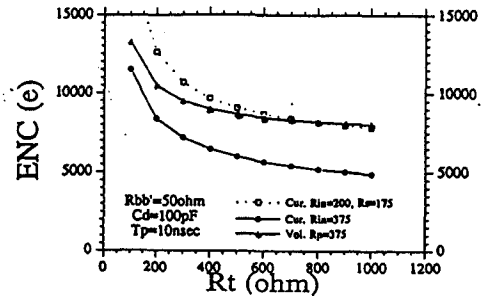

Dependence on Peaking time

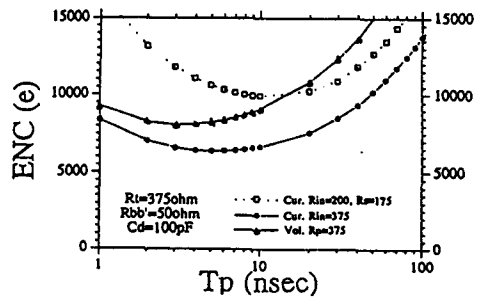

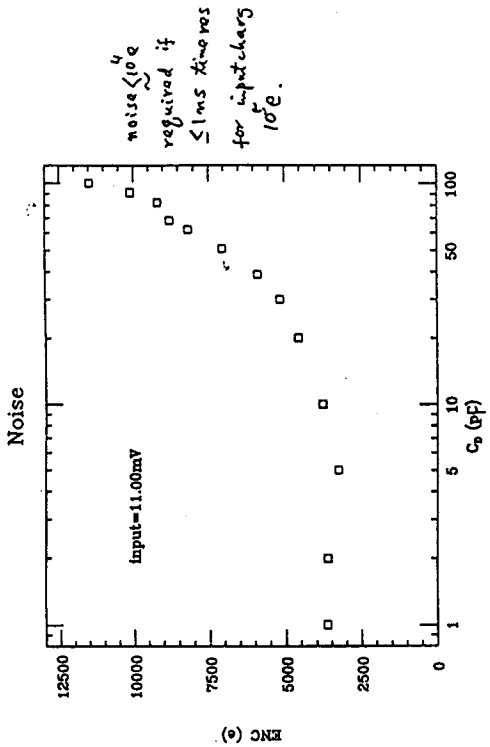

VENUS FC pre-amp.

Measurement

Summary

Straws

* All individual pieces of straw readout in good shape; emphasis on system test

Muon

* Progress on readout for muon supertower good.

  Production electronics can share TMC, L2B; possibly ASD, DCC.

+ Good collaboration between groups on various continents.
+ Reasonably detailed list of responsibilities

Where are we now ?

Trigger, DAQ group

Masa NOMACHI

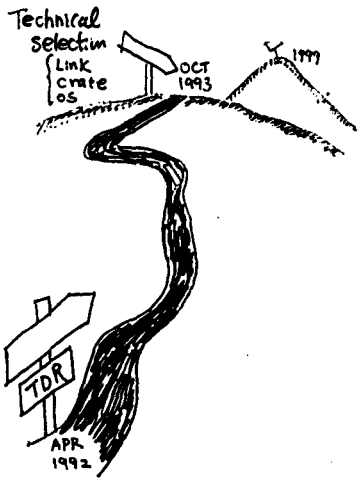

Where are we now ?

Trigger, DAQ group

Masa NOMACHI

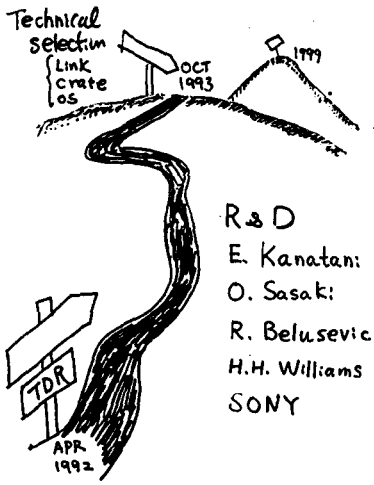

R&D

E. Kanatani:	Trigger processor
O. Sasaki:	Switch for Event builder
R. Belusevic	DSP, Transputer
H.H. Williams	Dec
SONY	Data storage.

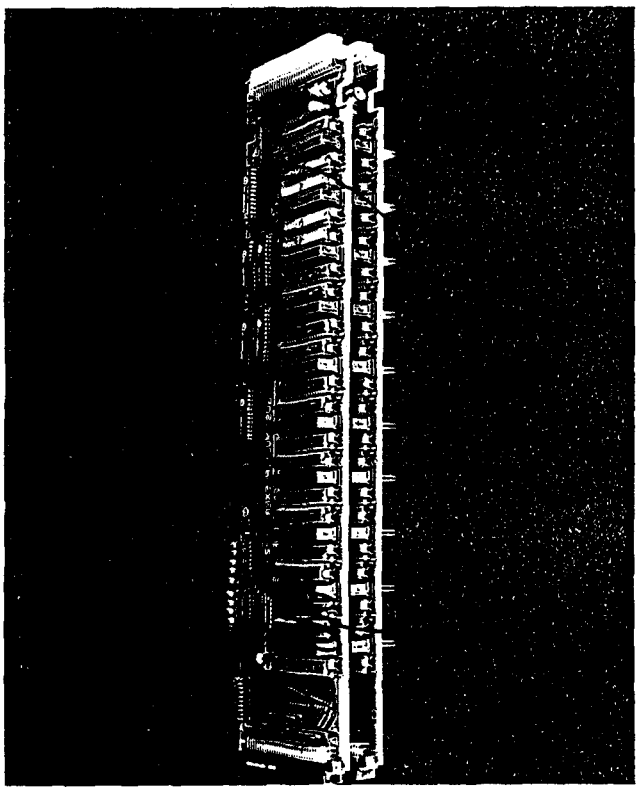

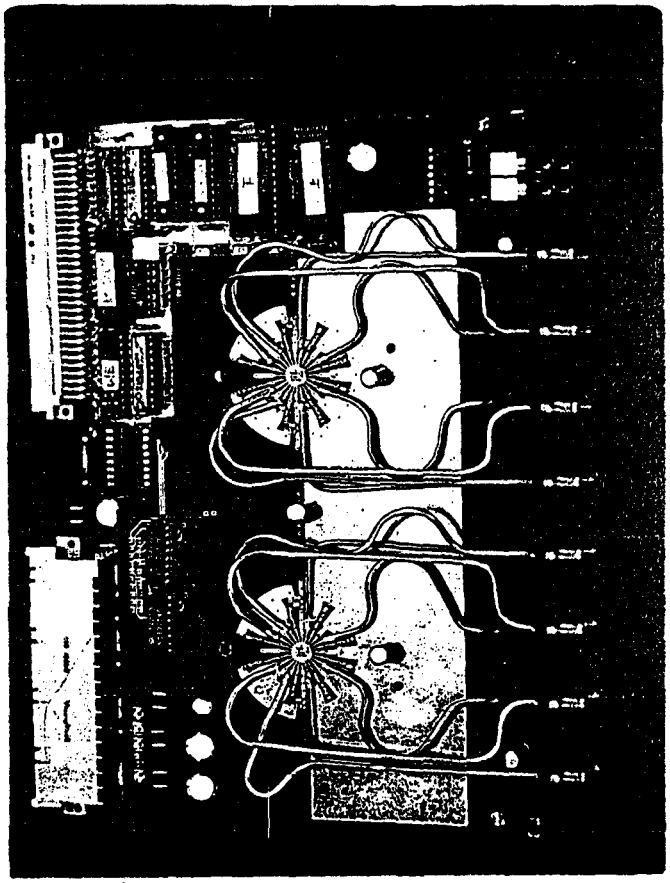

Where are we now ?

Trigger, DAQ group

Masa NOMACH

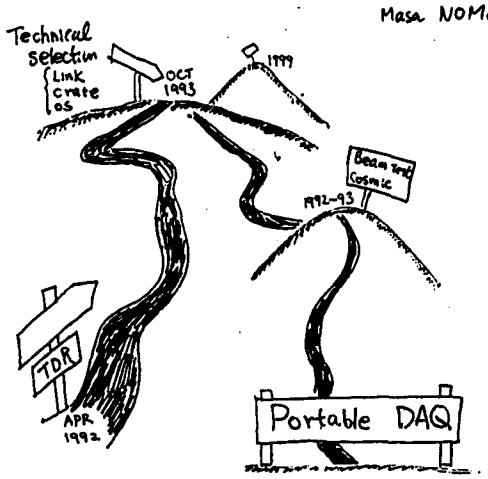

A. Fry	PDAQ software
M. Nomach	PDAQ Hardware
W. Smith	TEM
H. Fujii	Development in JAPAN
Y. Takeuchi	PDAQ performance

Joint meetings for the beam test, the bench test and the cosmic run.

Resource Sharing for Portable DAQ

Coordination & Advising

Botlo (GEM/SSCL)
* Fry (SDC/SSCL)
LeDu (LBL/SDC)
* Nomachi (KEK/SDC)
Michigan (SDC)

Goals:

IDENTIFY & RECOMMEND SUITABLE HARDWARE & SOFTWARE

DESIGN SOFTWARE INTERFACES FOR MAXIMUM RE-USABILITY

PARTITION THE TASKS IN PORTABLE DAQ throughout collaboration

FACILITATE UMBRELLA LICENSING IF POSSIBLE

Portable DAQ

SSCL, KEK, Michigan
LBL, Irvine

- Software Recommendations
- Soft ware Developments
- Hard ware Recommendations

<u>Support</u>

UNIX work stations with established VME interface cards
SUN, DEC ....
+ VxWorks MVME167

VME + CAMAC (via VME)

- Use J1+J2 monolithic Back plane "Commercial."
- No special signals on P2
- Full address decoding
- Release on acknowledge for the interrupt.

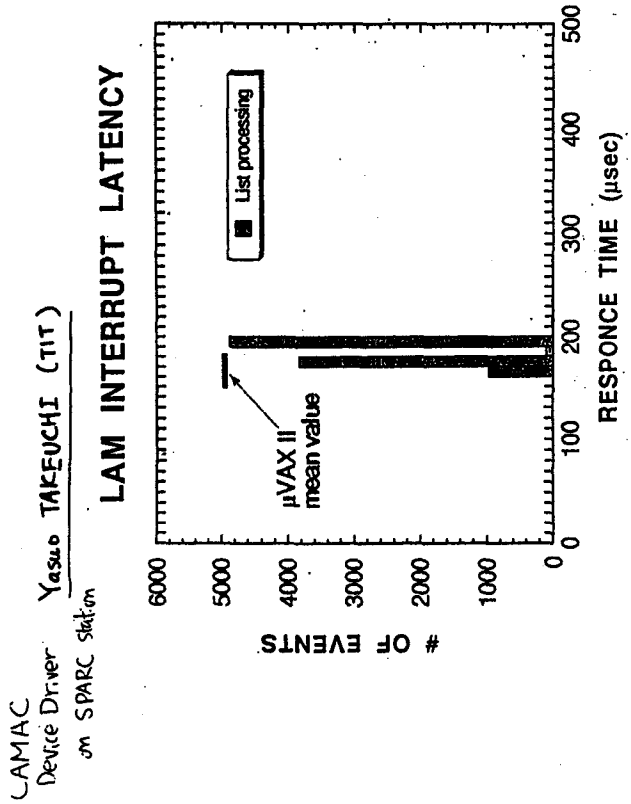

FRT SSCL

PARTITIONING

1) MICHIGAN
   RUN CONTROL
   ERROR HANDLING
   MONITORING

2) KEK
   BUFFER MANAGER
   HISTOGRAMMING &
   DISPLAY

3) LBL
   realtime readout, histogramming

4) Irvine
   assist LBL
   supply calorimeter codes

5) SSCL / GEM
   drivers for SPARC, VxWorks
   debugging tools
   user interface

6) SSCL / SDC
   INTEGRATION / SCHEDULE
   LIBRARY
   TEMPLATES

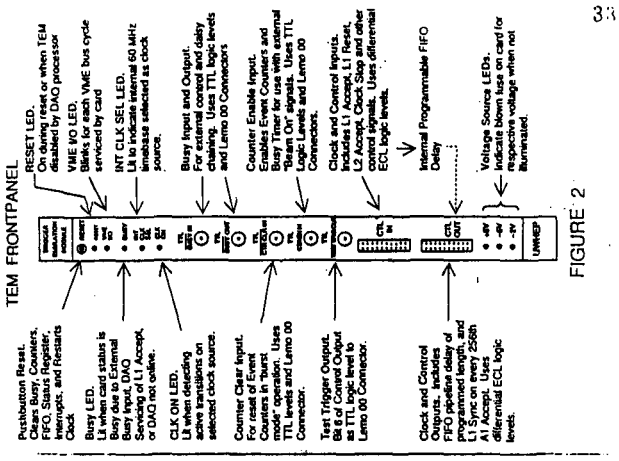

FIGURE 2

SDC Trigger Emulation Module (TEM)

Performance Specification

W. H. Smith, T. Gorski, S. Dasu, J. Lackey
University of Wisconsin

SDC Note SDC 92-00250
May 22, 1992

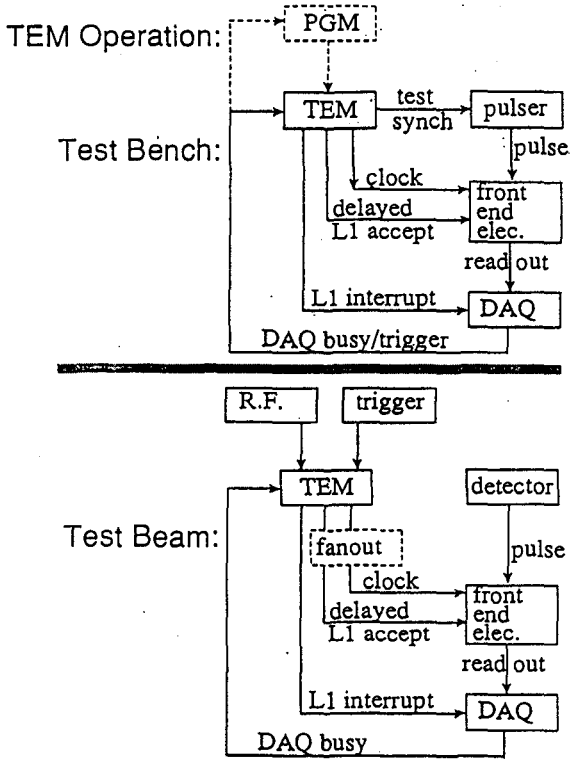

W. Smith 5/29/92

Trigger System Staging

① Stage US Part of L3 Farm
(3.9M → 1.2M)

Savings = 2.7 M

② Stage L1 Forward Muon Trigger

Savings = 0.5 M

⇒ Total Savings = 3.2 M

COMPUTING REPORT

Summary of PAC Presentation

KEK Collaboration Meeting

L. E. Price
May 29, 1992

EVENT SIZE AND PROCESSING

Assumptions

Trigger Rate	100 Hz
Event Size	1 MB
Processing for reconstruction	1000 SSCUPS sec/event
DST Event Size	100 KB
Processing for analysis/histo.	10 SSCUPS sec/event

Hardware Requirements

Data recording rate	100 MB/sec
Annual storage	2 PB
Production processing	10^5 SSCUPS
Master DST at SSCL	100 TB
Working DST	10M events, 1-10 TB
Analysis Processing (distrib.)	10^5 SSCUPS total 3 TB fast storage 30 TB med. sp. stor.

SDC COMPUTING ARCHITECTURE AT SSCL

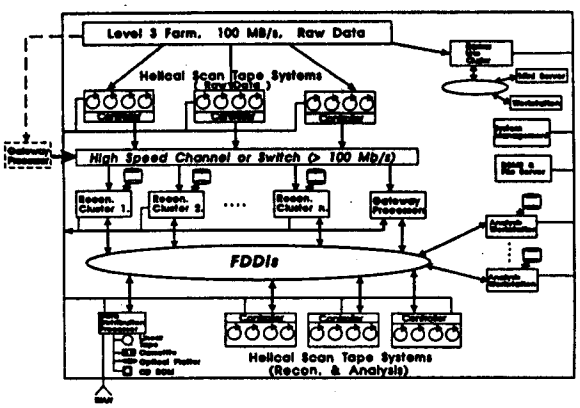

Production System Example

Data Reconstruction Ranch

Compute servers (20 x 200 SSCUPS)		25
Cabinet, bus, power supply	1	
CPU Boards (4 CPUs w. 512 MB/ board)	5	
Disk (5 GB)	4	
Network interface	2	
Basic software		
Control/management workstations	5	
Tape drives	5	
Raw data tape library		
Data servers	3	
Recorders	3	
Tape robot	1	
Control/management workstation	1	
Internal network		

Analysis Tape Library

Recorders	20
Tape robot	1
Control/management workstations	5
Internal Network	
Data Servers to analysis system	20

Simulation Facility

Compute servers	25
Disk Arrays	1.6 TB
Control/management workstation	1
Tape drive	1
Internal network	

Express-line cluster

Software Requirements

"Open" operating system: UNIX/POSIX

Portability

Modularity

Graphical User Interface

Analysis "without programming" largely

Programming languages

Fortran 90 (including Fortran 77)

C++ (including C)

~~Kernal~~ Core system with basic system provided by computing group

Detector-oriented software provided by subsystem groups

Hierarchy of engineering and documentation standards

Review and certification process for all production code

Database organization of data

Metadata: keys and index files widely accessible

Hierarchical storage

Ability to read selected portions of event

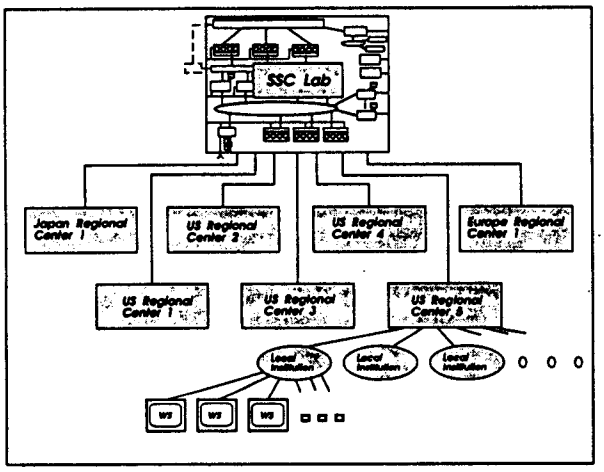

SDC Regional Computing Centers

OFFLINE COMPUTING SCHEDULE

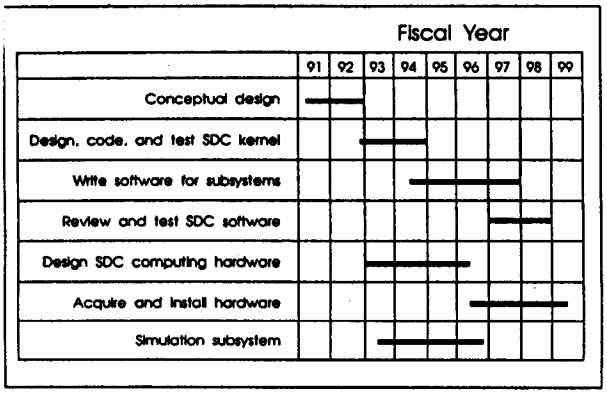

PAC comments

- Note that none of the offline computing costs are in the baseline budget
- The offline group has identified the correct set of issues and is attacking them in a reasonable way.
- The schedule for acquiring hardware and producing software is reasonable.
- The core software is to be written by professional programmers through the SSCL. the sub-committee applauds this approach. However, sufficient manpower resources are not yet available at SSCL but must be made so if the core software is to be written by the scheduled date of the end of 1994.
- The group is contemplating regional offline centers which will be funded outside of the SSC budget. The sub-committee supports regional center concept for foreign collaborators and notes that for this to work the associated networking will need strong DOE support.

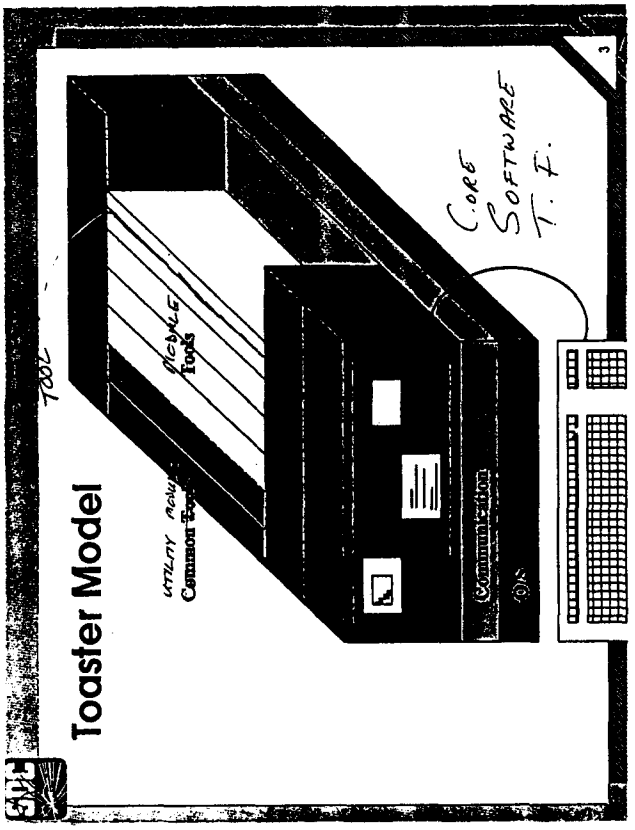

Urgent Computing Issues

Core software definition

Task Force: S. Frederiksen (chairman), B. Traversat, U. Nixdorf, J. Huang, S. Kunori, G. Kubena, C. Day, B. Hubbard, D. Adams, Y. Morita, K. Amako

Define software that will be centrally provided to support all aspects of SDC offline computing

Report: September, 1992

Data modeling and data structures

Task Force: B. Scipioni (Chairman), C. Day, R. Ennis, I. Gaines, E. May, U. Nixdorf, F. Rouse, Y. Takaiwa, S. Youssef

Design document: August, 1992

Prototype: June, 1993

Interaction with subsystems?

Data Modeling / Data Structures T.F.

Event-based Requirements

- **Analysis-time**

  Those data modelling activities which involve the logical definitions and associations among the data as is done in Entity Relationship modelling, for example.

- **Coding-time**

  Those data modelling activities which occur in direct support of, and during the time of, the physicist writing code.

- **Run-time**

  Those features of the data modelling package which execute while the physics application is running.

2.1 Implementation Independent Requirements

2.1.1 Analysis-time

2.1.1.1 User defined data types.
2.1.1.2 Plain data structures.
2.1.1.3 There should be user-defined lifetimes for types of data.
2.1.1.4 Certain classes should be built-in.
2.1.1.5 Event type and cross-event type are built-in types.
2.1.1.6 Data modelling operations on objects or collections of objects (classes).
2.1.1.7 Schema available to application at analysis-time
2.1.1.8 Edit or browse classes and dictionary interactively.
2.1.1.9 Schema evolution history/versioning accessible from repository.
2.1.1.10 Report generation capability for meta-data, e.g., schema, data dictionary from the browser.
2.1.1.11 Standard data modelling methodology.
2.1.1.12 The tool must support an object-oriented approach.
2.1.1.13 Cardinality between objects must be defined in relationships.

2.1.1.14 Error reporting during analysis.
2.1.1.15 Must have a Graphical User Interface (GUI) as well as text interface.
2.1.1.16 Same look and feel from the browser as from the rest of the tool. Must have the ability for multi-user presentations.
2.1.1.17 The modelling tool must have a generic levelling capability.
2.1.1.18 Direct manipulation of graphical objects.

2.1.2 Coding-time

2.1.2.1 Simple access to complex data types.
2.1.2.2 Must be able to refer to objects or types via relationships (pointers).
2.1.2.3 Access to data by name (not pointers) at coding-time.
2.1.2.4 Generate machine independent code for objects, templates, include files.
2.1.2.5 Package must include a make-like facility.
2.1.2.6 Accessible from 6 line FORTRAN program.
2.1.2.7 Full functionality from FORTRAN 90, C, and C++.
2.1.2.8 Error reporting during coding.

2.1.3 Run-time

2.1.3.1 Schema must be available to application at run time.
2.1.3.2 Error reporting during run-time.
2.1.3.3 Interactive data query language.
2.1.3.4 Report generation capability for physics data.
2.1.3.5 Interactive as well as programmatic interface to tool.
2.1.3.6 No significant performance penalty for using the tool, regardless of the amount of data.
2.1.3.7 The Data Repository should keep database of data access patterns to support future design and optimization efforts.
2.1.3.8 Data access method independent of media.
2.1.3.9 Data interface to OO-DBMS or R-DBMS.
2.1.3.10 Application and machine independent data structures.

SDC Software Process Document
Outline Draft

Version 4

May 22, 1992

Larry W. Roberts

IBM Federal Systems Company
3700 Bay Area Boulevard
Houston, Texas 77058

IBM

Software Development T.E.

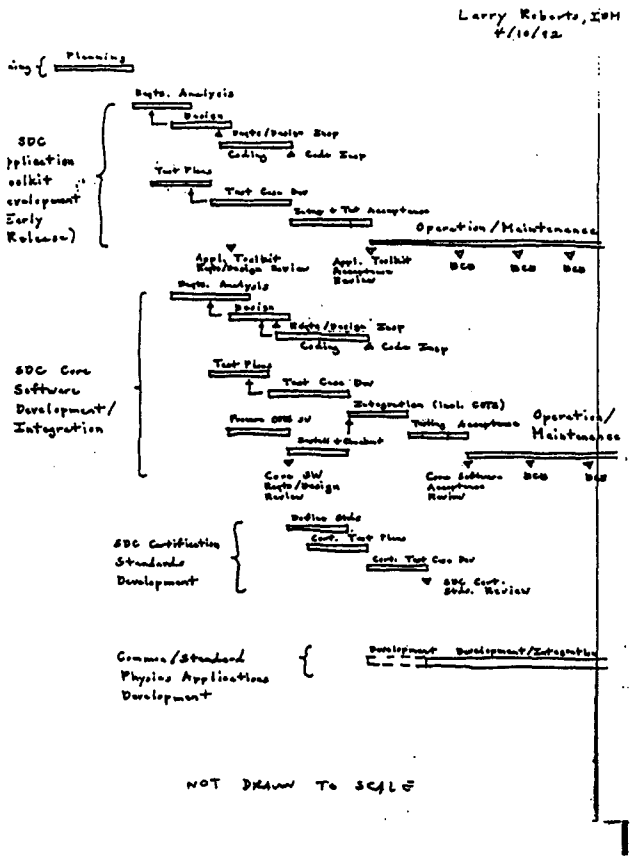

Urgent Computing Issues

Software development system

Task Force: A. White (Chairman), F. Abe, T. Watts, L. Roberts

Software development methodology

Choice of tools

Development manager environments ("Process enactment")

Report: October, 1992

Simulation requirements and transition

New Task Force: S. Kunori (Chairman)

Report: January, 1993

Urgent Computing Issues

Cost and Schedule

New Task Force

Report: September, 1992

Organization at SSCL

Relation to GEM and PR Computing group

Relation to HEPLIB

Collaboration with Japan

Monthly meeting

Task forces

Ongoing Japanese work on computing

Talks at this meeting:

Distributed computing sys. using shell script	Y. Morita
Application of MACH to SSC Computing	H. Yoshida
Massively parallel computing system	K. Hasegawa
Distributed computing system at Tokyo Metropolitan University	S. Kitamura
SDC SHELL in Japan	M. Asai

Computing reviews

Establish committee from SDC outside of computing group to comment on computing plans periodically.

Propose first review for August collaboration meeting

Simulation update

Action plan

Hire at least 5 people at SSCL

Define core software for design phase in fall

Define data modeling process and SDC data structures

Plan software development process and tools

Plan SDC simulation system

Detailed cost and schedule

Define computing organization, particularly at SSCL

Integrate software planning with subsystems

HARDWARE COSTS AT SSCL

Table 10-7
SDC computing costs.

Cost Element	FY92 M$	Potential L=10^33 % Savings
Production storage system:		
Tertiary storage system	3.70	2.5
Communications link to online	0.25	
Production computing farm (10^6 SSCUPS)	6.00	4.0
Production disk system(s)	1.50	1.0
Software	2.00	1.0
Data distribution system	1.00	
Express line system	1.00	0.5
Simulation system (10^6 SSCUPS)	6.00	4.0
Local analysis system	2.20	
External Networking	0.25	
Total	23.90	13.0

Scaling assumptions:
Cost of cpu ÷ 1.4 /year
Cost of storage ÷ 1.2 /year

EFFORT AT SSCL

Table 10-8
SSCL manpower required for SDC computing.

Task	FTE-yr.
SDC Computing Support group 4(1992) · 10(1999)	25
Hardware	
Requirement analysis	3
System design	6
System modeling	2
Procurement	2
Installation	5
Testing	5
Software	
Core system (production and analysis)	
Requirements analysis	5
Design	10
Coding	5
Testing	5
Reviews	2
Documentation	3
Physics/Detector Systems	20
(additional 80 FTE-yr provided by the SDC)	
Simulation software	10
(additional 40 FTE-yr provided by the SDC)	
	118

POTENTIAL STAGING OF OFFLINE COMPUTING SYSTEM

Quick Analysis shows potential staging of $13 M

BUT

- ~480 M for detector computing is in separate WBS line
- No allocation has been made at SSCL of this money between either
  - SDC, GEM, Other
  - Hardware vs Software/People
- Our budget for hardware is not in any sense approved or funded, so we cannot claim the fruits of potential staging

[2] Silicon Tracking

<Detector R&D>

Capacitance Measurement of DSSD	H. Miyata	- 367
Capacitances in Silicon Microstorip Detectors: Measurements and Simulations	H. Sadrozinski	- 389
Radiation Damage of the SSD	N. Tamura	- 409
Signal Simulations of the Silicon Syrip Detector	Y. Unno	- 424
Lorentz Force Effects Experimental Plans	H. Ziock	- 446
Double Sided Sensor (Barrel & Disk)	T. Ohsugi	- 455
Comments on Production of DSSD	K. Yamamoto	- 464
Silicon "Wedge" Detector R & D	P. Fisher	- 478
Quality Assurance	H. Sadrozinski	- 526

<Mechanical System>

Silicon CDR	A. Seiden	- 533
Mechanical Design Review	W. Miller	- 543
Mechanical Design Study at KEK	Y. Unno	- 571
Alignment: Placement Tolerances	H. Ziock	- 590
Detector Module Design	H. Spieler	- 603
Ladder Assembling at KEK	Y. Unno	- 623

<Cost & Schedule>

Silicon Tracker Cost & Schedule Review	A. Grillo	- 643

<Beam Test at KEK>

Beam Test of the SDC Double-sided Silicon Strip Detector	Y. Unno	- 653
KEK Beam Lines for the Beam Test	A. Murakami	- 672
Analog Readout ICs	H. Spieler	- 689
Testing of a 64-channel Bipolar Amplifier-comparator Chip	H. Sadrozinski	- 712
SDC Portable DAQ	M. Nomachi	- 719

Capacitance Measurement of DSSD I

H. Miyata, T. Aso : Niigata Univ.
T. Ohsugi, M. Okada : Hiroshima Univ.
Y. Unno : KEK

Contants

(1) Measurement Tools & Method
(2) P Side Measurement
(3) N Side Measurement
(4) Summary & Future Plan

(1) Measurement Tools & Method

We used

1) Probe Station ..... MICROMANIPULATOR co. MODEL 6620

2) Probe .....MICROMANIPULATOR co.
Tungsten
Probe point ~5μm φ

3) Capacitance METER...
YHP
Model 4277A
LCZ METER

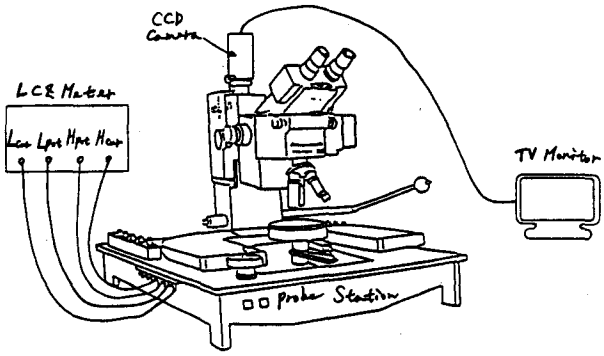

4) 2-point 4-probe Method

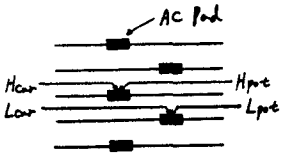

A small current from a current source is flowed between Lcur and Hcur probes and the voltage is measured between Lpot and Hpot probes.

5) Measurement Error

Usually the measurement error is less than 0.5 PF.

(2) P Side Measurement

Capacitance Measurement Sample (P Side)

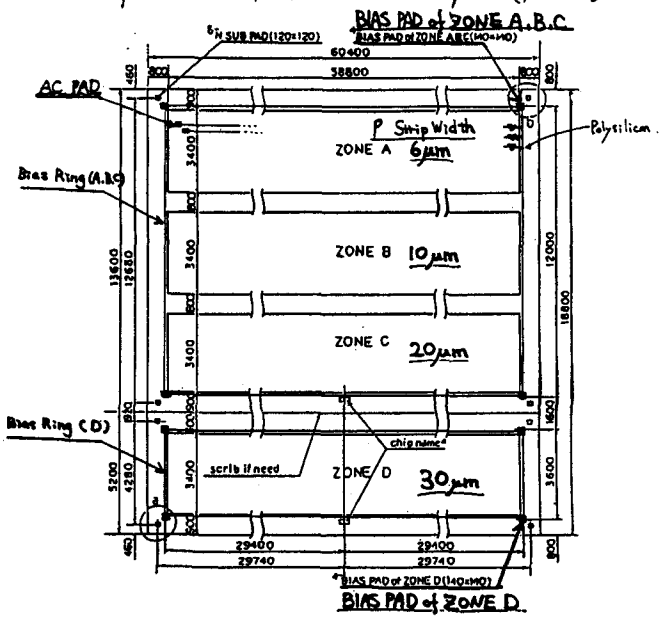

Chip Size	60.4mm×60.4mm
Effective Area Size	3.4mm×58.8mm
Strip Length	58.8mm
Strip Pitch	50μm
Number of Strips	64本
Wafer Thickness	300μm
Strip Width Zone A	6μm
〃 B	10μm
〃 C	20μm

371

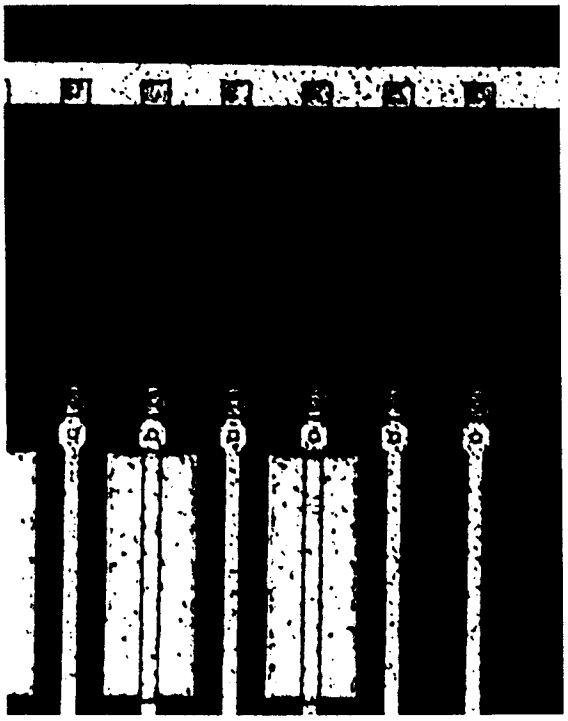

372

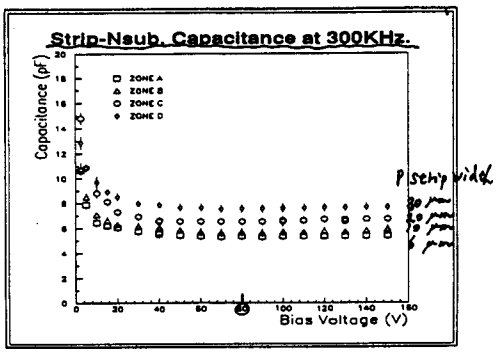

Fig 11: Bias Dependence of Strip-Nsub. Capacitance.

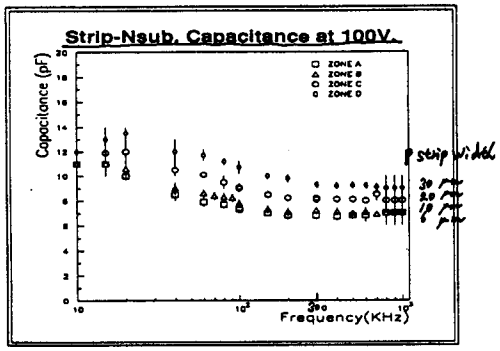

Fig 12: Frequency Dependence of Strip-Nsub. Capacitance.

373

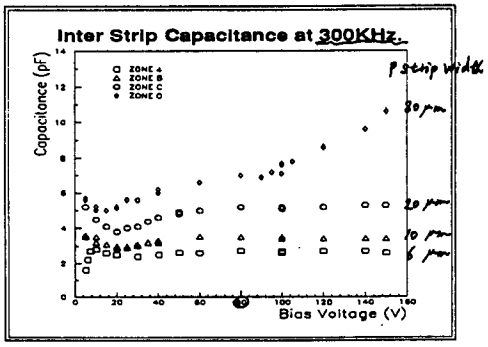

Fig 14: Bias Dependence of Inter Strip Capacitance.

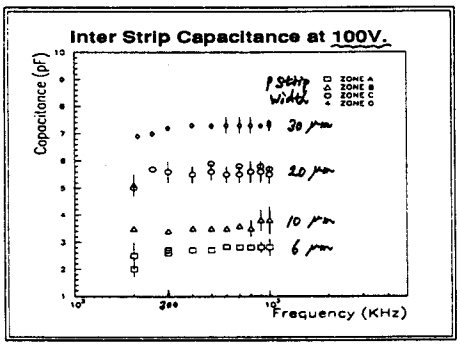

Fig 15: Frequency Dependence of Inter Strip Capacitance.

374

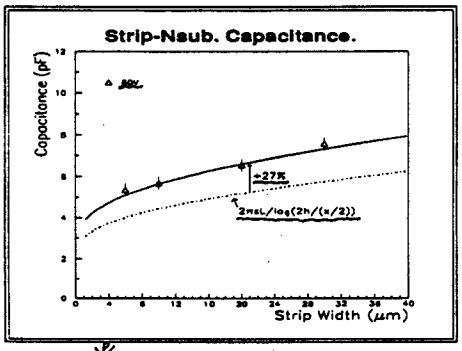

Fig 16: Strip Width Dependence of Strip-Nsub. Capacitance.

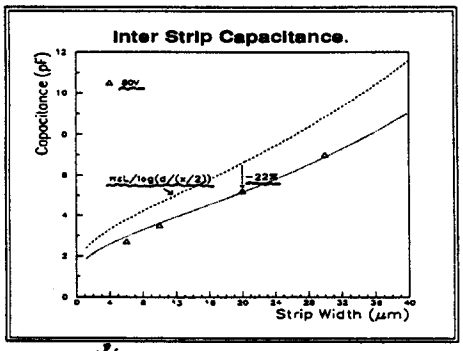

Fig 17: Strip Width Dependence of Inter Strip Capacitance.

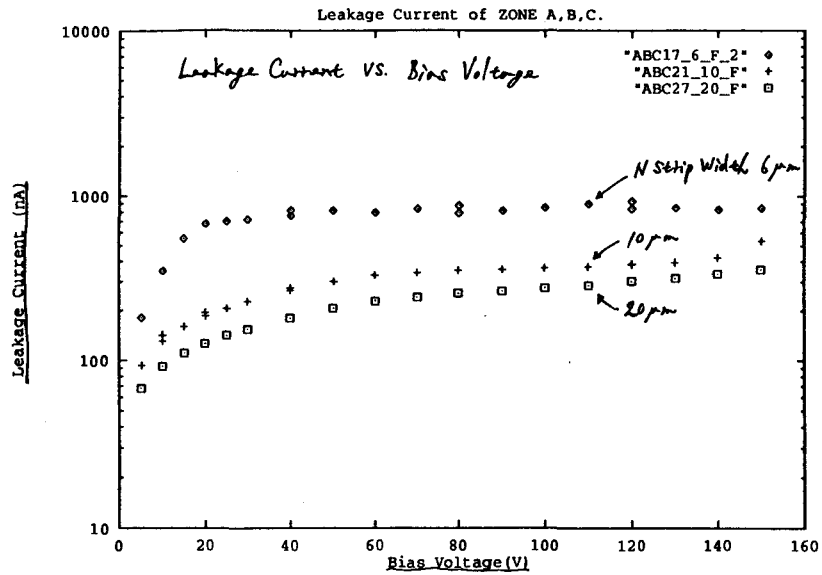

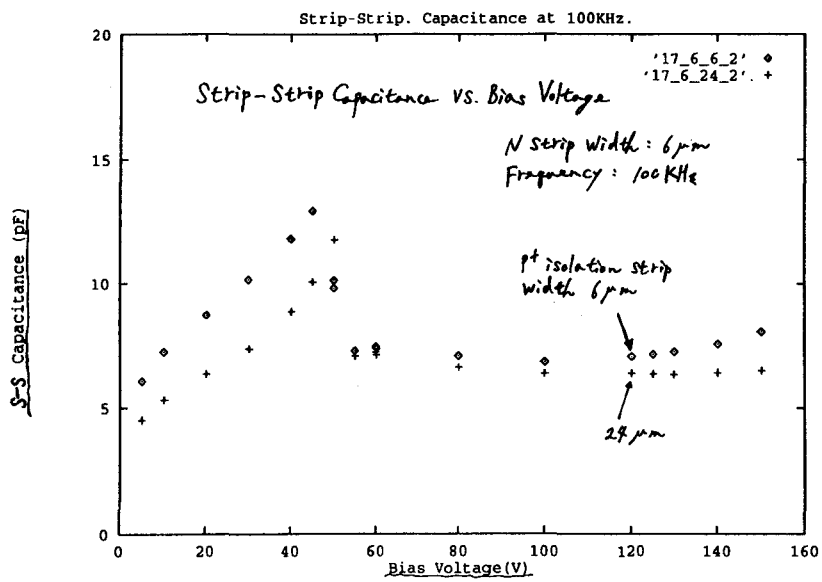

Simple Approximation Formula of SSD Capacitance

(1). Inter Strip Capacitance

2 parallel Conductive Wires of Radius a

$$C_{ss} = \frac{\pi \varepsilon L}{\log \frac{d}{a}}$$

SSD; a : strip width /2 (50μm)
d : strip pitch
L : strip Length (0.0588 m)

(2). Strip-Sub Capacitance

Conductive Wire and Infinite Conductive Plane

$$C_{sn} = \frac{2\pi \varepsilon L}{\log \frac{2h}{a}}$$

SSD; a : Strip Width /2
L : Strip Length
h : Thickness of SSD (300μm)

(3) N Side Measurement

Measured Sample SSD-N-CA 0230

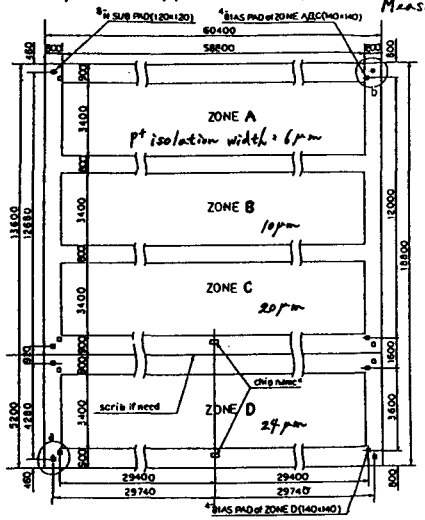

POLE-S: BIAS AC-SSD (x STRIP on x SUB.) for CAPACITANCE MEASUREMENT

CHIP SIZE ..... 60400 μm x 58800 μm
STRIP LENGTH ..... 58800 μm
STRIP WIDTH ..... DEPEND ON TYPE 1,2,3
STRIP PITCH ..... 50 μm
P ISOLATION WIDTH ... DEPEND ON ZONE A,B,C,D
THICKNESS ..... 300 μm

ZONE A
P ISOLATION WIDTH .. 6 μm
NO. OF STRIPS ..... 88 (STRIP:84 , GUARDSTRIP:4)
P SIDE ..... P COMMON(ZONE B~D) DIFFUSION

ZONE B
P ISOLATION WIDTH .. 10 μm
NO. OF STRIPS ..... 88 (STRIP:84 , GUARDSTRIP:4)
P SIDE ..... P COMMON(ZONE B~D) DIFFUSION

ZONE C
P ISOLATION WIDTH .. 20 μm
NO. OF STRIPS ..... 88 (STRIP:84 , GUARDSTRIP:4)
P SIDE ..... P COMMON(ZONE B~D) DIFFUSION

ZONE D
P ISOLATION WIDTH .. 24 μm
NO. OF STRIPS ..... 88 (STRIP:84 , GUARDSTRIP:4)
P SIDE ..... P COMMON DIFFUSION

THE CHIP NAME AND N OF THREE TYPES

TYPE NO.	chip name	STRIP WIDTH (P)
TYPE 1	06	6 μm
TYPE 2	10	10 μm
TYPE 3	20	20 μm

N SIDE DETAILS OF x & h ARE SHOWN IN DRAWING NO.350408-2

UNIT μm	SCALE /	NAME SSD-N-CA 0230	DATE '91.11.29
APPROVED: H.Aoki		DWG NO. 350408-1	REF UNIV. of HIROSHIMA
CHECKED:		HAMAMATSU PHOTONICS K.K	
DRAWN: K.Yamamura			

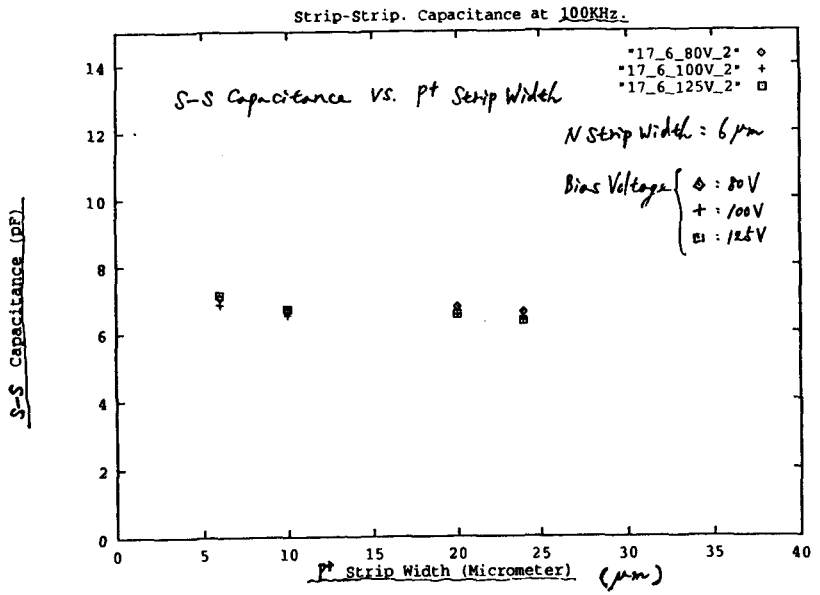
Strip-Strip. Capacitance at 100KHz.
"17_6_80V_2" ◇
"17_6_100V_2" +
"17_6_125V_2" ⊡
S-S Capacitance vs. p+ Strip Width
N Strip Width : 6 μm
Bias Voltage { ◇ : 80V
+ : 100V
⊡ : 125V
S-S Capacitance (pF)
p+ Strip Width (Micrometer) (μm)

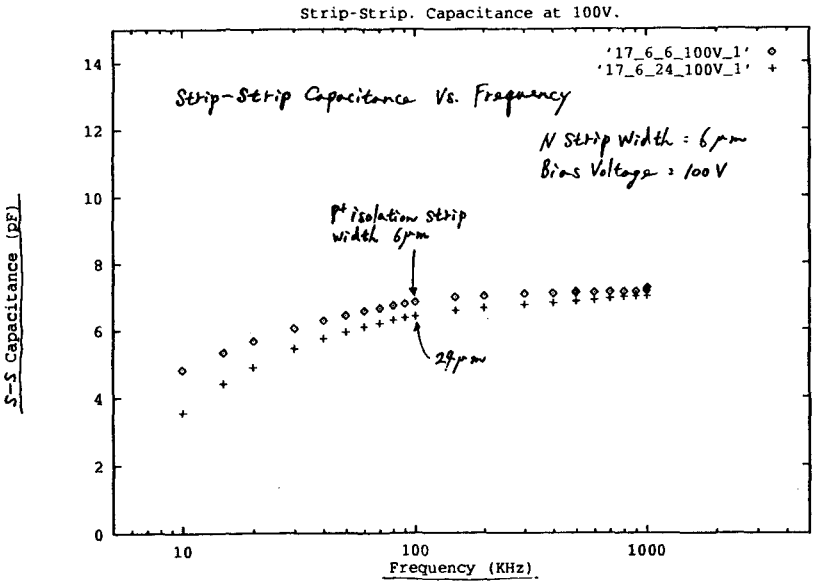
Strip-Strip. Capacitance at 100V.
'17_6_6_100V_1' ◇
'17_6_24_100V_1' +
Strip-Strip Capacitance Vs. Frequency
N Strip Width : 6 μm
Bias Voltage : 100 V
p+ isolation strip width 6 μm
24 μm
S-S Capacitance (pF)
Frequency (KHz)

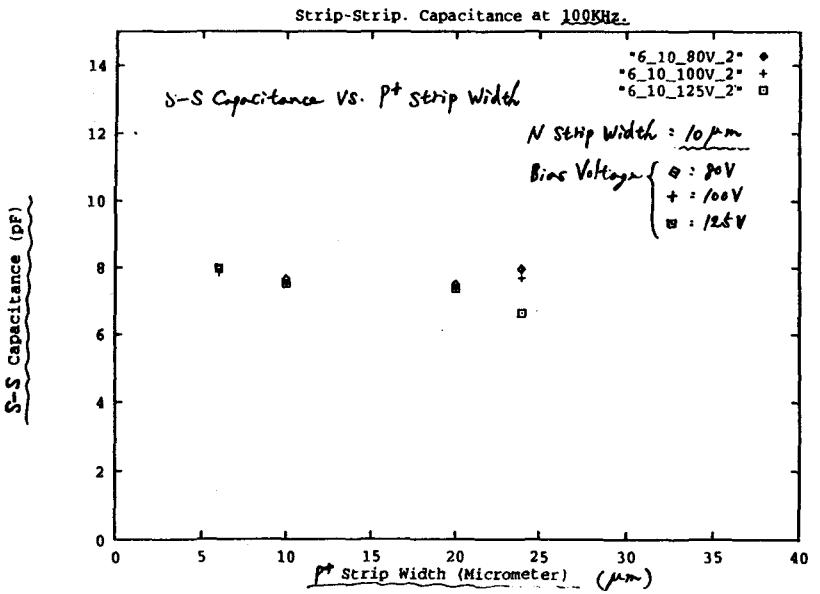
Strip-Strip. Capacitance at 100KHz.
"6_10_80V_2" ◆
"6_10_100V_2" +
"6_10_125V_2" ⊡
S-S Capacitance vs. p+ strip Width
N Strip Width : 10 μm
Bias Voltage { ◆ : 80V
+ : 100V
⊡ : 125V
S-S Capacitance (pF)
p+ Strip Width (Micrometer) (μm)

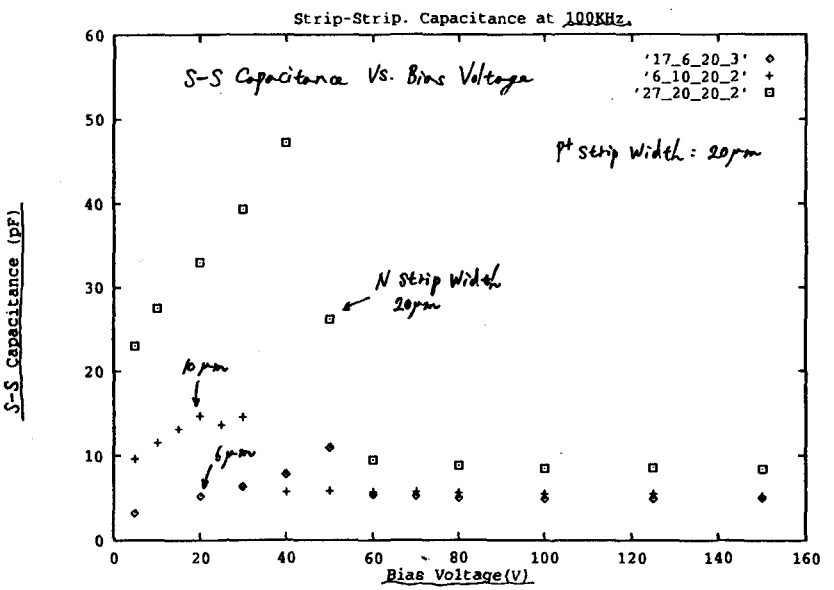
Strip-Strip. Capacitance at 100KHz.
'17_6_20_3' ◇
'6_10_20_2' +
'27_20_20_2' ⊡
S-S Capacitance Vs. Bias Voltage
p+ strip Width : 20 μm
N strip Width 20 μm
10 μm
6 μm
S-S Capacitance (pF)
Bias Voltage(V)

"US Group's Result"

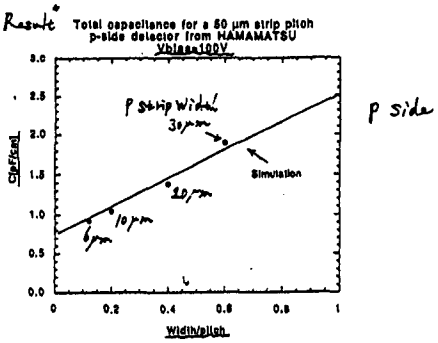

Fig. 1 The capacity/cm as function of strip width on the junction side.

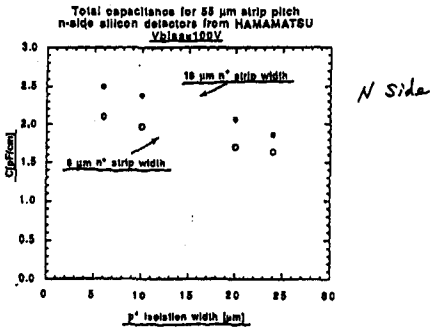

Fig. 2 The capacity/cm as function of blocking p-implant width on the ohmic side. The parameter is the strip width.

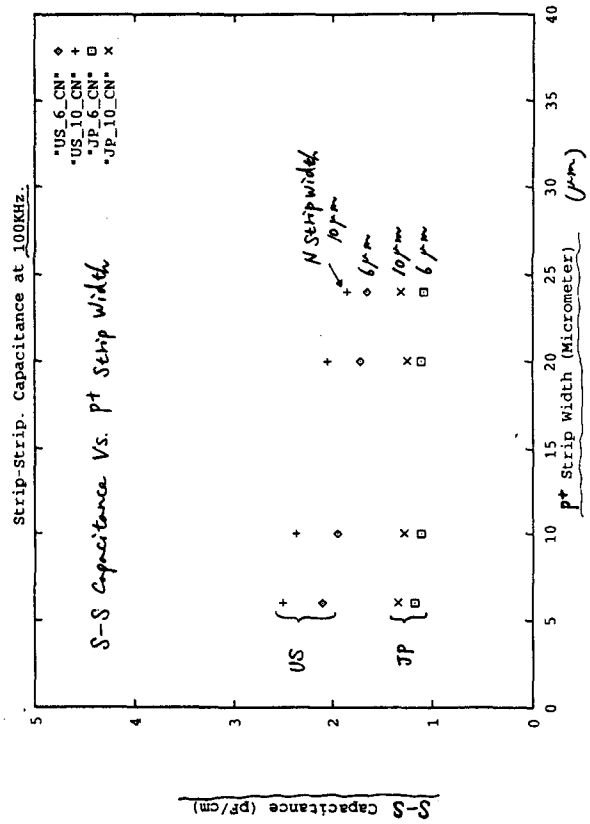

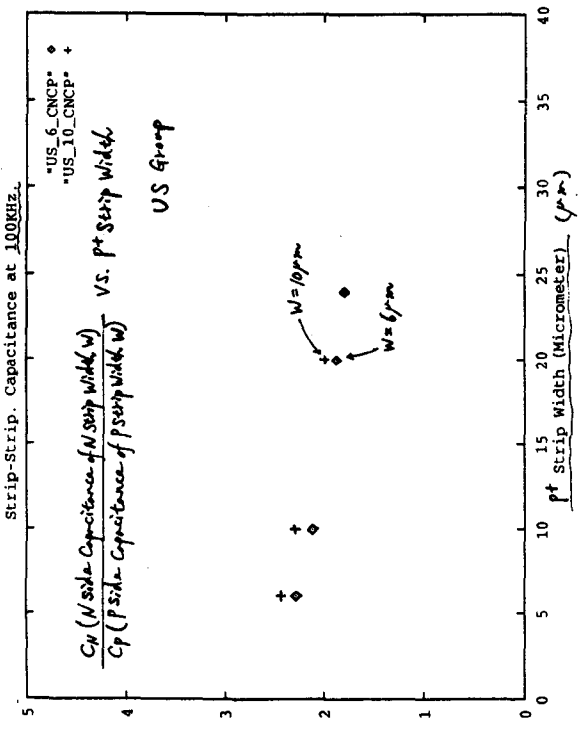

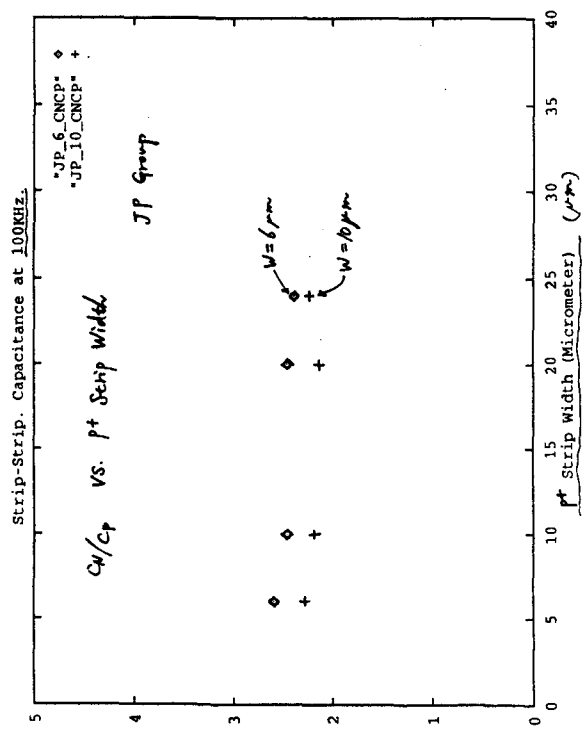

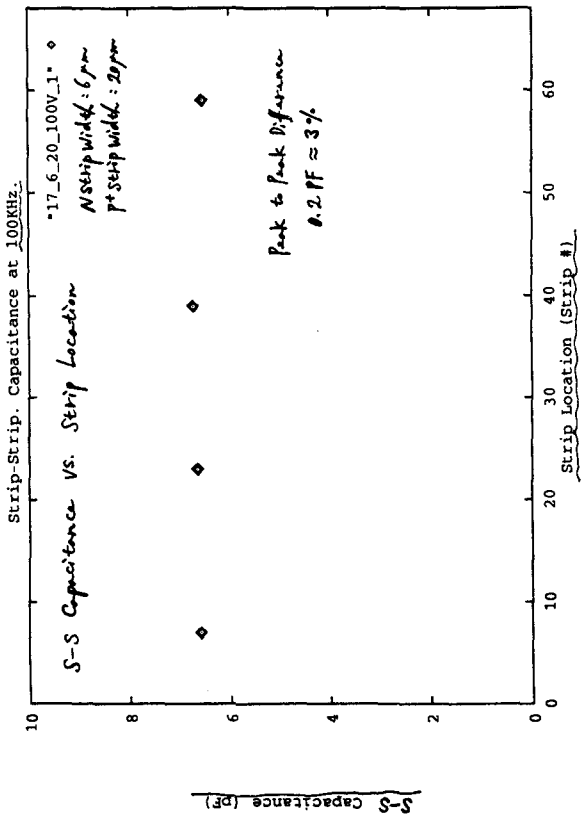

(4) Summary & Future Plan

1) N side strip-strip capacitance is about <u>2 times larger</u> than that of P side capacitance for the same strip width.

2) <u>Narrow N strip</u> (6μm) and <u>wide p+ isolation strip</u> (24μm) is best for minimizing S-S capacitance.

But we have to think about increase of
- × Resistance of Al electrode (35Ω/cm for 10μm width)
- × Leakage Current

3) Since our measurement is for the case of floating strips, we have to reproduce measured capacitance for both P & N side by analytic formula or MC simulation.

4) We need to make wire bonding, in order to measure capacitance for grounded strips.

CAPACITANCES IN SILICON MICROSTRIP DETECTORS: MEASUREMENTS AND SIMULATIONS

Emanuela Barberis
Nicolo Cartiglia
Craig LeVier
Hartmut F.-W. Sadrozinski

May 26, 1992
SDC Collaboration Meeting
KEK, Tsukuba, Japan

General Chairman
John W. Dawson
Argonne National Laboratory
Bldg. 362 - HEP
Argonne, IL 60439 USA
(708) 252-6541 • FAX (708) 252-5782

1 • 9 • 9 • 2
IEEE NUCLEAR SCIENCE SYMPOSIUM
October 27-31, 1992
Orlando, Florida

Program Chairman
Wesley H. Smith
University of Wisconsin
Department of Physics
Madison, WI 53706 USA
(608) 262-2281 • FAX (608) 263-0800

May 7, 1992

TO CORRESPONDING AUTHOR:
Hartmut F.-W. Sadrozinski
University of California
SCIPP, Nat. Sci. 2
Santa Cruz, CA 95064
USA

TITLE OF PAPER:
Maasurement of Intership and Coupling Capacitances of Silicon Microstrip Detectors

AUTHORS:
E. Barberis, N. Cartiglia, J. Leslie, C. LeVier, H.F.-W. Sadrozinski, K. Yamamoto, K. Yamamura, T. Ohsugi, Y. Unno, T. Aso, H. Miyata, and N. Tamura

Dear Corresponding Author:

This is to acknowledge the receipt of abstracts and summaries for the paper named above, which you have submitted to the Program Committee of the 1992 Nuclear Science Symposium.

The Program Committee will meet during the month of June. You will be notified of the decision of the committee with regard to your paper soon thereafter. At that time, authors of accepted papers will be given instructions on how to prepare manuscripts of their paper for publication in the proceedings of the Symposium.

We consider you, the "corresponding Author," to be the principal contact on all matters regarding this paper. If the address given above is incorrect, or if another person should receive correspondence instead of you, please let me know as soon as possible.

Please refer to your paper number, (236) in all correspondence.

On behalf of the program committee, thank you for your interest in the symposium.

Sincerely yours,
Wesley Smith
Wesley Smith

Please address correspondence to:
Prof. Wesley Smith
University of Wisconsin
Department of Physics
1150 University Ave
Madison, WI 53706 USA

detail structure of both surfaces

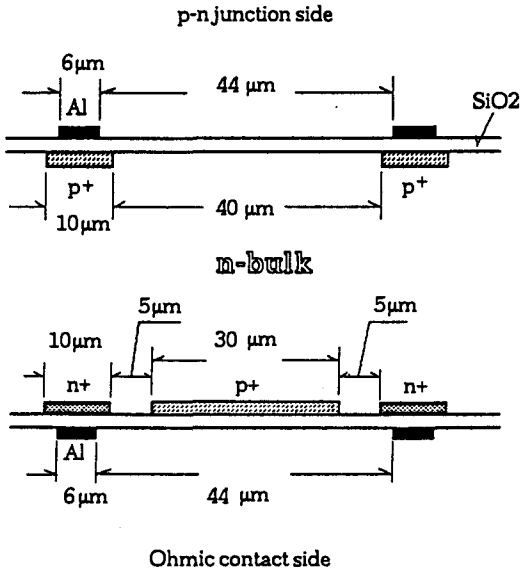

- Measurements of capacitance in silicon microstrip detectors show pronounced frequency dependence.
- We can explain these measurements as the effect of a network of distributed frequency independent resistors and capacitors.
- We simulate these networks with SPICE to extract the true distributed capacitances (pF/cm) and resistances (Ω/cm). Include grounds!
- The SPICE model of these network have to be included in the simulation of the frontend response to signals originating in the bulk.

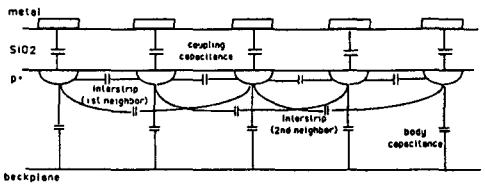

Figure 8: Hamamatsu detector cross-section & SPICE implemented capacitances

MEASUREMENTS: Use HP 4284 LCR meter 100 Hz–1 MHz.

Coupling capacitance (~ strip width) determines signal.

Body capacitance (~ strip pitch) gives depletion voltage, stores energy.

DC interstrip capacitance (~ width/pitch).

AC interstrip capacitance (~ width/pitch) determines noise

DC-to-AC interstrip capacitance determines crosstalk (5%).

Next:

Irradiations with ^{60}Co.

Figure 7: Convergence of SPICE deck (sample coupling capacitance circuit)

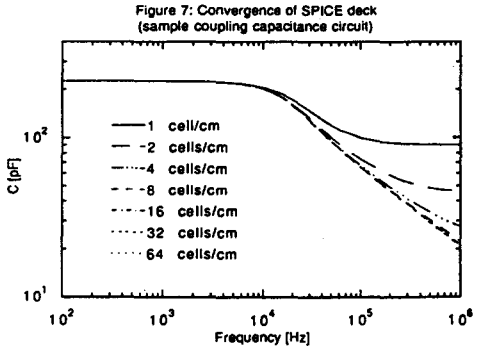

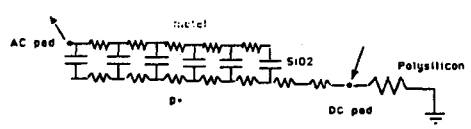

Figure 6: Simulated detector using discrete components (Coupling portion only)

We use the capacitance test chips manufactured by Hamamatsu Photonics.

Length=5.88cm, pitch=50μm, AC-coupled, both junction and ohmic side samples.

Junction side: p strip width 6,10,20,30 μm
Ohmic side: n strip width 6,10,20 μm and p isolation implant width 5,10,20,24 μm.

Figure 9: Coupling capacitance (SPICE & measured)
5.88cm strip length

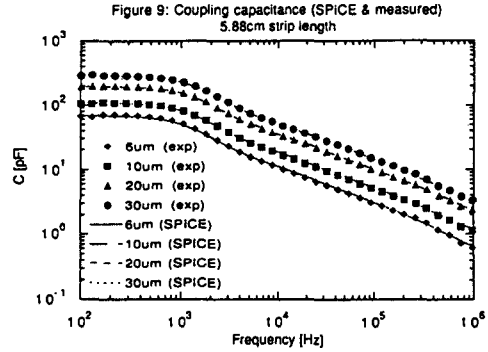

Given this data, we may infer the following values of resistance for the p+ implant and the uncoupled resistance adjacent to the bonding pad.

Table 1: p+ resistance

strip width	*p+ resistance*	*uncoupled resistance*
6μm	670KΩ/cm	42KΩ
10μm	400KΩ/cm	25KΩ
20μm	200KΩ/cm	10KΩ
30μm	140KΩ/cm	8.3KΩ

Table 1: p+ resistance

strip width	*p+ resistance*	*uncoupled resistance*	*C/cm (pF/cm)*
6μm	670KΩ/cm	42KΩ	11.9
10μm	400KΩ/cm	25KΩ	18.9
20μm	200KΩ/cm	10KΩ	34.1
30μm	140KΩ/cm	8.3KΩ	50.2

Figure 10: Body capacitance (SPICE)
5.88cm strip length

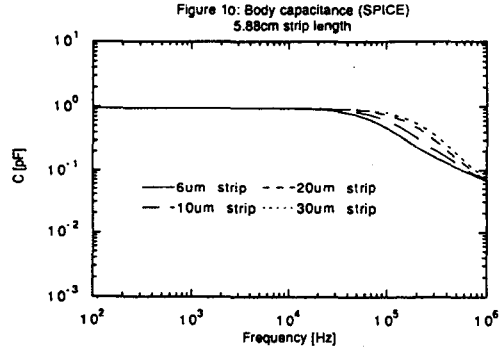

Table 2: 3dB frequencies for body capacitance measurements

strip	*R(kΩ)*	*C(pF)*	*F(3dB)*	C/cm (pF/cm)
6μm	2940	0.94	$4.3x10^4$	0.16
10μm	2352	0.94	$7.2x10^4$	0.16
20μm	1176	0.94	$1.4x10^5$	0.16
30μm	823	0.94	$2.1x10^5$	0.16

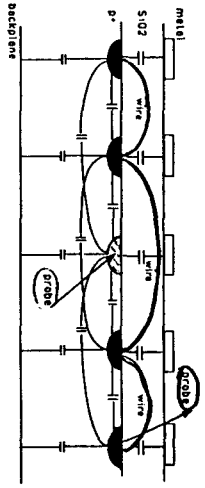

Figure 11: Probe placement for DC interstrip capacitance measurement

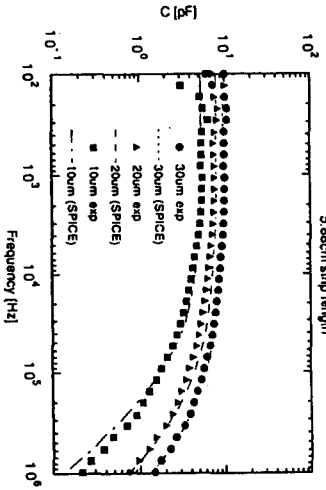

Figure 12: DC interstrip capacitance 5.88cm strip length

Table 3: Extra resistance suggested by DC interstrip capacitance measurements

Strip	*R(kΩ)*	*C/cm (pF/cm)*
10μm	270	0.94
20μm	60	1.36
30μm	33	1.62

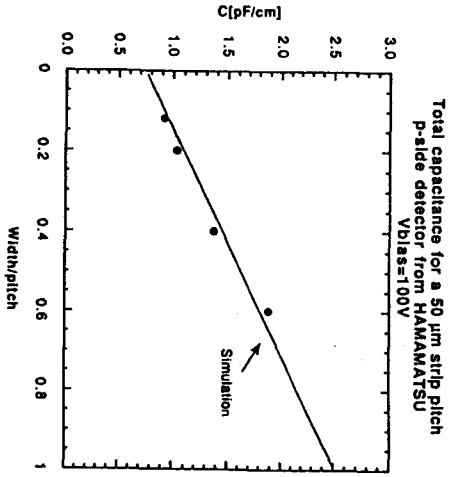

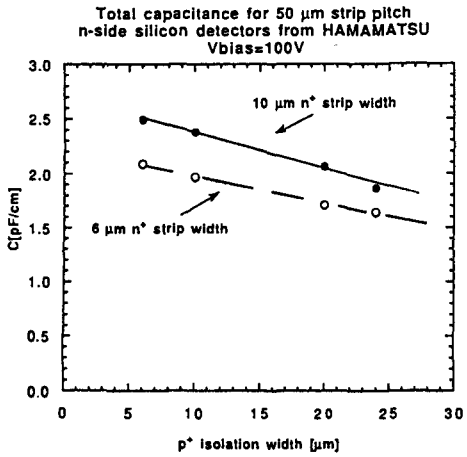

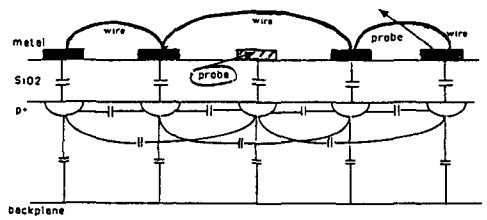

Figure 14: Probe placement for AC interstrip capacitance measurement

22

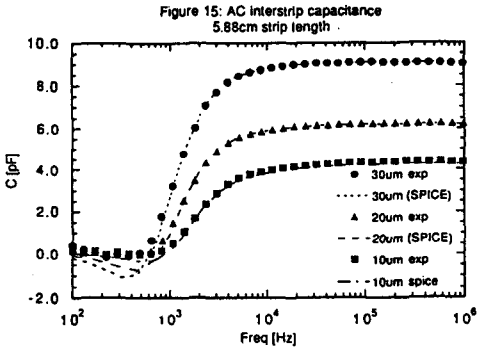

Table 4: Extra resistance suggested by AC interstrip capacitance measurements

Strip	*R(KΩ)*	*C/cm at 10^6 Hz (pF/cm)*
10μm	25	0.73
20μm	150	1.07
30μm	110	1.56

Radiation Damage of the SSD

Okayama Univ. N. Tamura

Irradiation of 65MeV protons on Photo-diodes and silicon strip detectors in March, 1992.

I Radiation test of Photodiode

Biasing during the irradiation
Cold/Warm detectors
Keeping detectors always biased

II Radiation test of Silicon Strip-detectors

Passivation
Polyimide, SiO_2, SiN
Isolation
Al(Electrode)/Poly-silicon/SiO2/Si(Substrate)
Al(Electrode)/SiN/SiO_2/Si(Substrate)

I Radiation test of Photodiode

1. Effects of biasing during the irradiation

V_{bias}(=30V) was applied during the irradiation.
⇓
Slightly steeper rise of I_{leak} at Semi-breakdown region.
No other significant effects, so far.

2. Cold/Warm detector ← Los Alamos

Kept 1/2 of detectors at 0 °C and another 1/2 at room temperature.
⇓
1) Decrease of Leakage Current (Annealing)
[redacted]
Cold : Slow
Warm : Fast

2) Depletion voltage ("Break-point" of Capacitance @10kHz)
[redacted]
Cold : Slow Change (Constant or small decrease)
Warm : Increase
Confirmed the effect ~~shown~~ @ LANL

3. Effects of keeping detectors biased

Some detectors were kept biased all the time between the successive measurements.
⇓
1) I_{leak} increases in Semi-breakdown region.
No change below the region !
2) I_{leak} decreases in both regions by annealing.

II Radiation test of Silicon Strip-detectors

Noises of a strip was measured for various cases.

1. Radiation effects of passivation
Polyimide, SiO_2, SiN

A sharp rise (x10) of noise in all cases
⇑
Surface effect / Charge-up ?

Rising point (Bias Voltage) ⇔ Leakage current
1: SiN 2: SiO_2 3: Polyimide (Low→High)

Noise decreases by characteristic time constant
τ < 10 hours
⇑
Rearragement of Ions ?

1: Polyimide 2: SiO_2 3: SiN (Fast→Slow)

Note:
Decrease of leakage current is much slower. ⇐ Photo Diode data
⇓
Two sources of the noise ?

2. Radiation effects of Inlsulator
Al(Electrode)/Poly-silicon/SiO2/Si(Substrate)
Al(Electrode)/SiN/SiO_2/Si(Substrate)

Almost same as for Passivation

Noise decreases by characteristic time constant

1: Poly-silicon 2: SiN (Fast→Slow)

Summary

1. Biasing causes an increase of Leakage-current in Semi-Breakdown region

2. By keeping detectors cold
⇓
Slow decrease of Leakage-current
~ No rise of Depletion-voltage

3. Irradiation causes sharp rise of Noise at high bias voltage
⇑
Strongly depens on Passivator/Insulator

Probably charge-up/discharge effects

1) SiN causes a large effect on the noise
easy increase & hard decrease
2) Time constant is < 10 hours even for SiN
⇓
Effects in the Real case will not be too large ?!

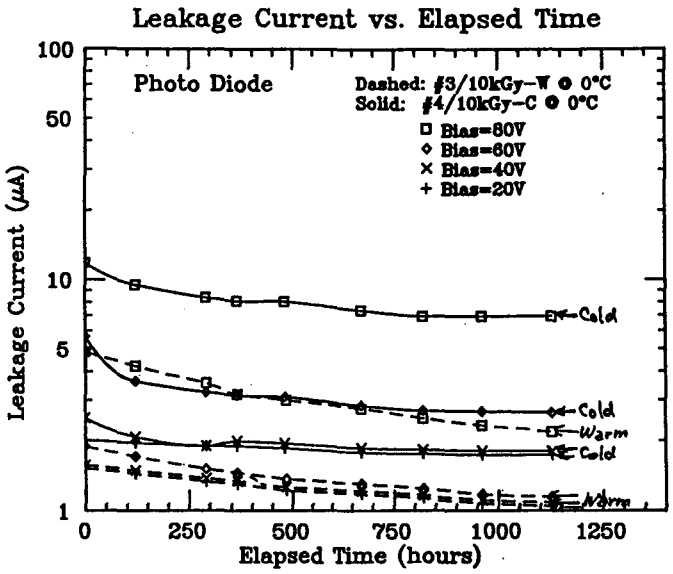
Leakage Current vs. Elapsed Time
Photo Diode
Dashed: #3/10kGy-W @ 0°C
Solid: #4/10kGy-C @ 0°C
Bias=80V
Bias=60V
Bias=40V
Bias=20V
Cold
Cold
Warm
Cold
Warm
Leakage Current (μA)
Elapsed Time (hours)

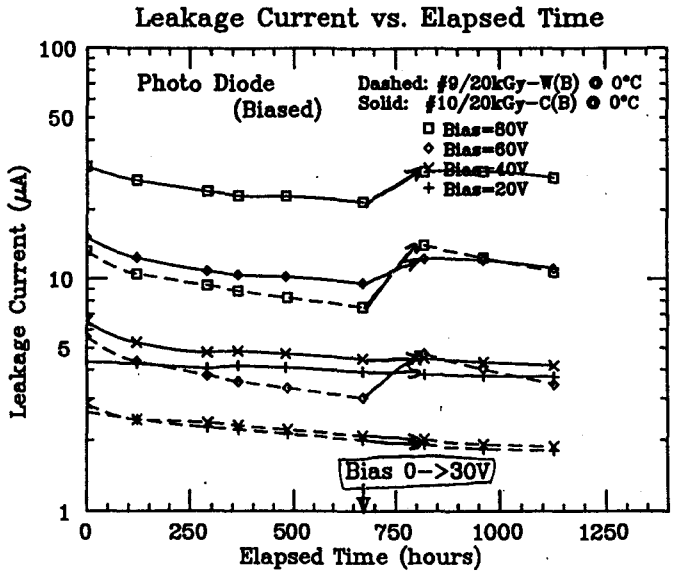
Leakage Current vs. Elapsed Time
Photo Diode
(Biased)
Dashed: #9/20kGy-W(B) @ 0°C
Solid: #10/20kGy-C(B) @ 0°C
Bias=80V
Bias=60V
Bias=40V
Bias=20V
Bias 0->30V
Leakage Current (μA)
Elapsed Time (hours)

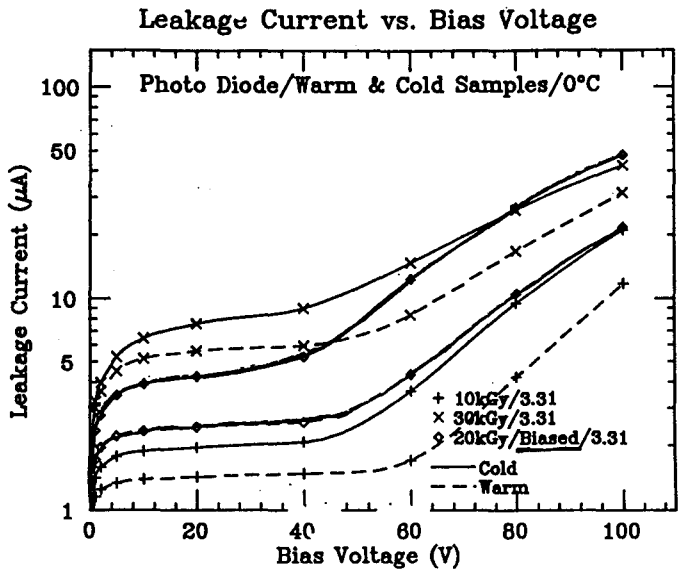
Leakage Current vs. Bias Voltage
Photo Diode/Warm & Cold Samples/0°C
10kGy/3.31
30kGy/3.31
20kGy/Biased/3.31
Cold
Warm
Leakage Current (μA)
Bias Voltage (V)

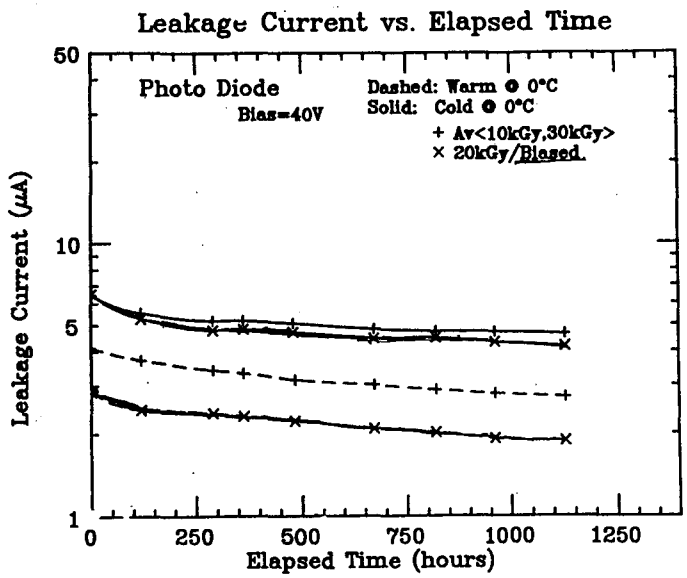
Leakage Current vs. Elapsed Time
Photo Diode
Bias=40V
Dashed: Warm @ 0°C
Solid: Cold @ 0°C
Av<10kGy,30kGy>
20kGy/Biased
Leakage Current (μA)
Elapsed Time (hours)

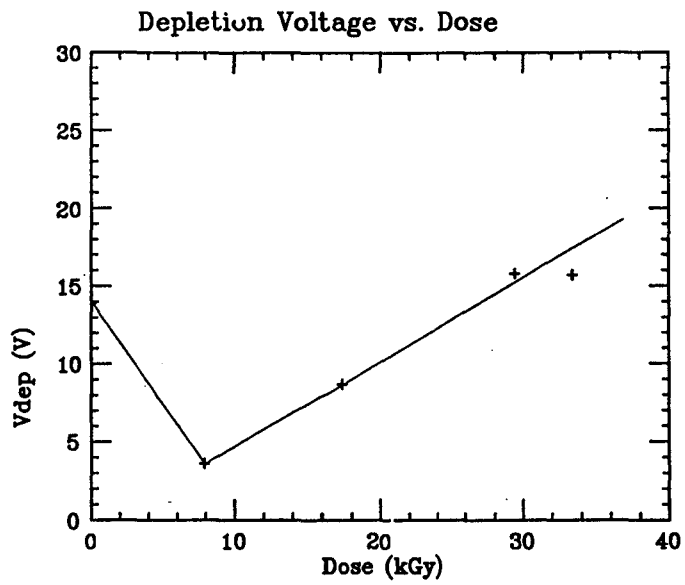
Depletion Voltage vs. Dose
Vdep (V)
Dose (kGy)

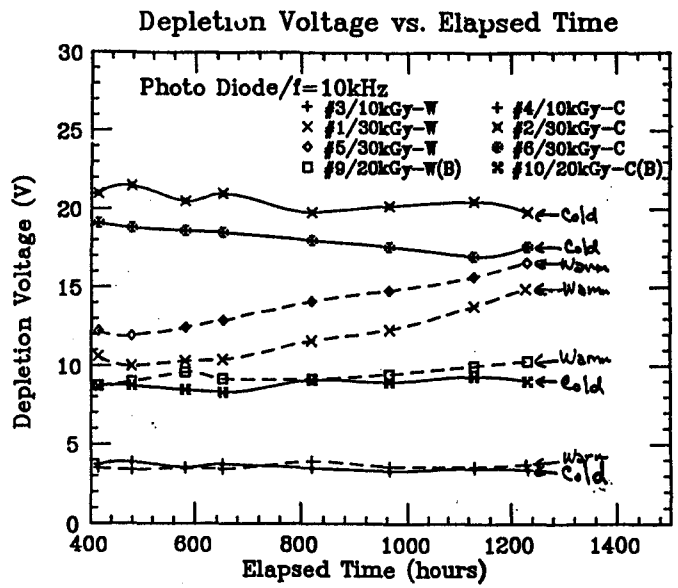
Depletion Voltage vs. Elapsed Time
Photo Diode/f=10kHz
+ #3/10kGy-W
+ #4/10kGy-C
× #1/30kGy-W
× #2/30kGy-C
◇ #5/30kGy-W
● #6/30kGy-C
□ #9/20kGy-W(B)
✱ #10/20kGy-C(B)
Cold
Cold
Warm
Warm
Warm
Cold
Warm
Cold
Depletion Voltage (V)
Elapsed Time (hours)

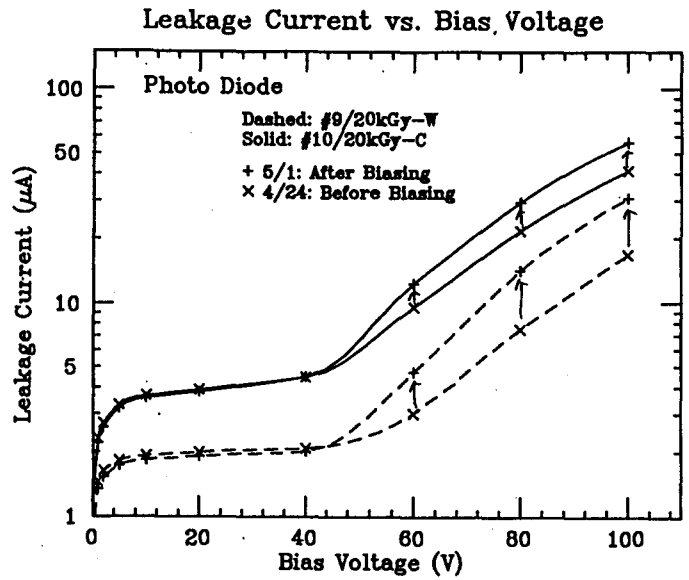
Leakage Current vs. Bias Voltage
Photo Diode
Dashed: #9/20kGy-W
Solid: #10/20kGy-C
+ 5/1: After Biasing
× 4/24: Before Biasing
Leakage Current (μA)
Bias Voltage (V)

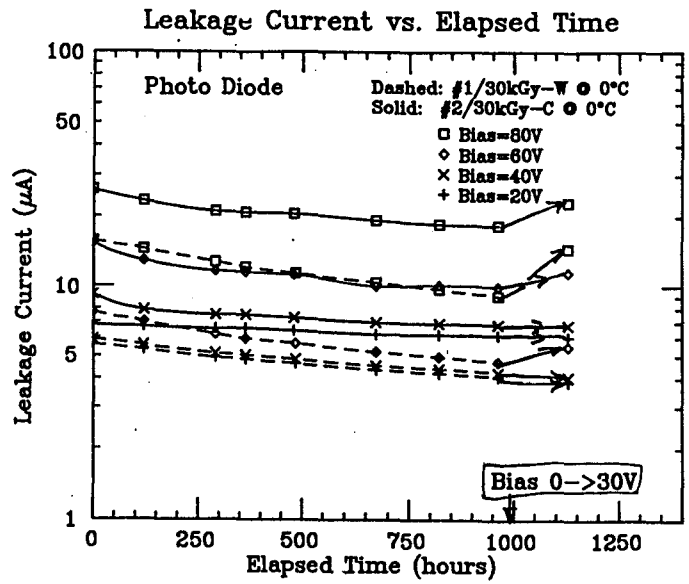
Leakage Current vs. Elapsed Time
Photo Diode
Dashed: #1/30kGy-W @ 0°C
Solid: #2/30kGy-C @ 0°C
□ Bias=80V
◇ Bias=60V
× Bias=40V
+ Bias=20V
Bias 0->30V
Leakage Current (μA)
Elapsed Time (hours)

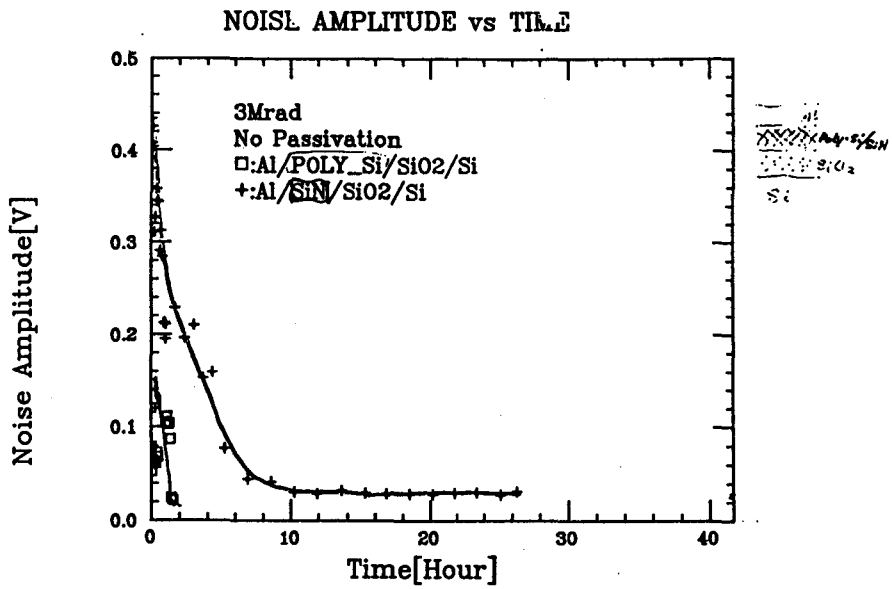
NOISE AMPLITUDE vs TIME
3Mrad
No Passivation
□:Al/POLY_Si/SiO2/Si
+:Al/SiN/SiO2/Si
Noise Amplitude[V]
Time[Hour]
0.0
0.1
0.2
0.3
0.4
0.5
0
10
20
30
40

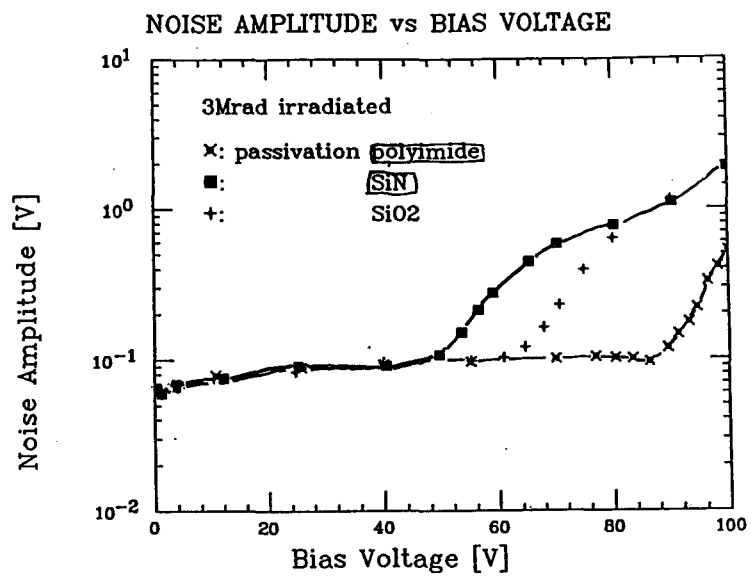
NOISE AMPLITUDE vs BIAS VOLTAGE
3Mrad irradiated
×: passivation polyimide
■: SiN
+: SiO2
Noise Amplitude [V]
Bias Voltage [V]
10^{-2}
10^{-1}
10^{0}
10^{1}
0
20
40
60
80
100

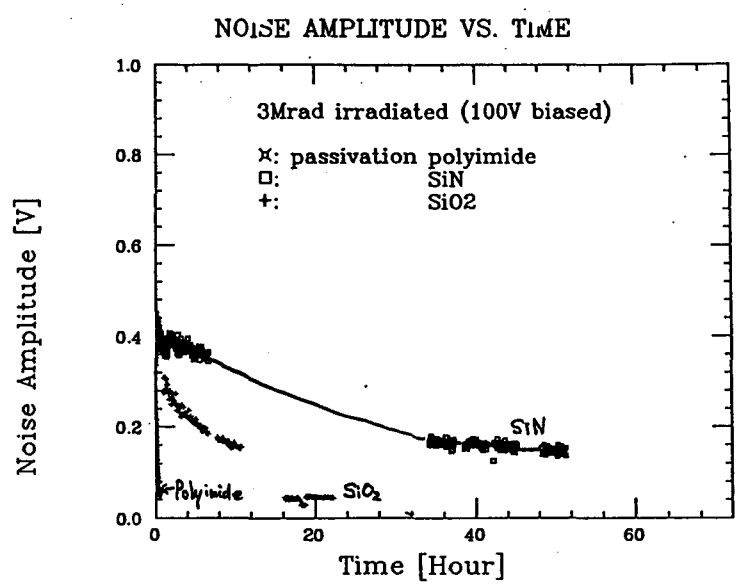
NOISE AMPLITUDE VS. TIME
3Mrad irradiated (100V biased)
×: passivation polyimide
□: SiN
+: SiO2
Noise Amplitude [V]
Time [Hour]
SiN
Polyimide
SiO_2
0.0
0.2
0.4
0.6
0.8
1.0
0
20
40
60

Signal Simulations of the Silicon Strip Detector

Y. Unno
Physics, KEK

J. Leslie, R. Sonnenblick
SCIPP, UC Santa Cruz

Abstract

Signals from the double-sided Silicon strip detector are simulated including the effect of 2 Tesla magnetic field. Induced currents of holes (p-side) and electrons (n-side) created by the charged particle are integrated, shaped, and discriminated with electronic noises, as expected for the SSC. Efficiencies, resolutions, and means are evaluated as a function of the threshold. A set of optimum is being searched.

Introduction

- Why signal simulations?

- better understanding on what we get ...
  through our particular readout scheme

- then, optimization of the scheme...
  specification of the frontend electronics

- What is the detector and the environment?

- Double-sided Silicon Strip Sensor
- 2 Tesla magnetic field

- What is the scheme?

- charge integrating preamplifier → S/N
- unipolar shaper → shaping time τ
- comparator → threshold V_T
- 16 ns beam crossing → bucket identification

Simulation steps

1) E- field calculation - Poisson eq. on meshed space

2) Particle trajectory

3) Energy deposition according to the Landau+Atomic binding exitation fluctuation in a step of 15 μm depth

4) Drift of electrons and holes in E & B
   and induced currents

5) Charge integration and CR-RC shaping

6) Discrimination with noise to get timing

SETUP:

* Double-sided Detector
* Pitch = 50μ
* Width = 10μ
* Tilted 6° about z-axis
* V(depletion) = 50V
* V(bias) = 90V
* $\vec{B} = 2T\,\hat{z}$

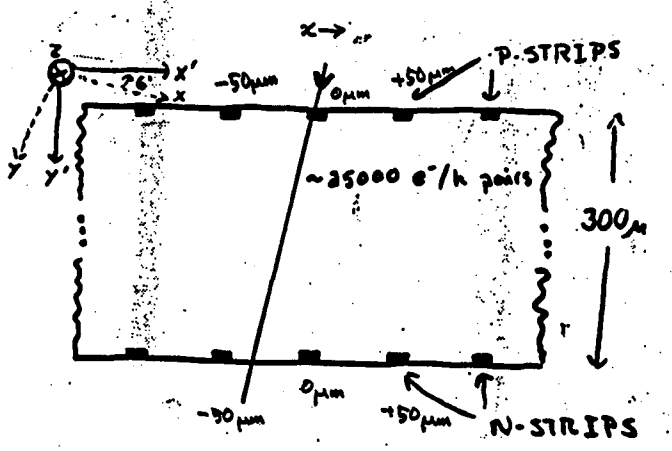

A little geometry. –

* In much of the detector $E_x \ll E_y$

$\Rightarrow$ $v_y \sim \mu E_y$

$v_x \sim \mu \mu_H E_y B$

$\frac{v_x}{v_y} = \frac{\Delta x}{\Delta y} \sim \mu_H B$ ($\equiv \theta_H$: Hallangle)

So $\Delta y = 300\mu$ implies:

$\Delta x_H = 20\mu$; $\Delta x_e = 80\mu$

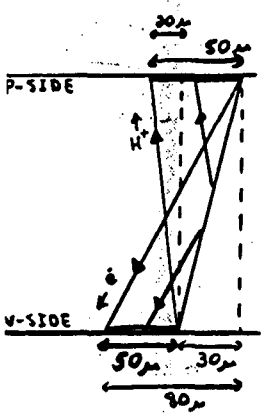

* BOTH electrons + holes are collected in a region spanning 50μ
* Given Pitch = 50μ, at most 2 strips will get significant signals.
* Near the strips, $E_x \gg E_y$ is possible, distorting this simple picture a little.

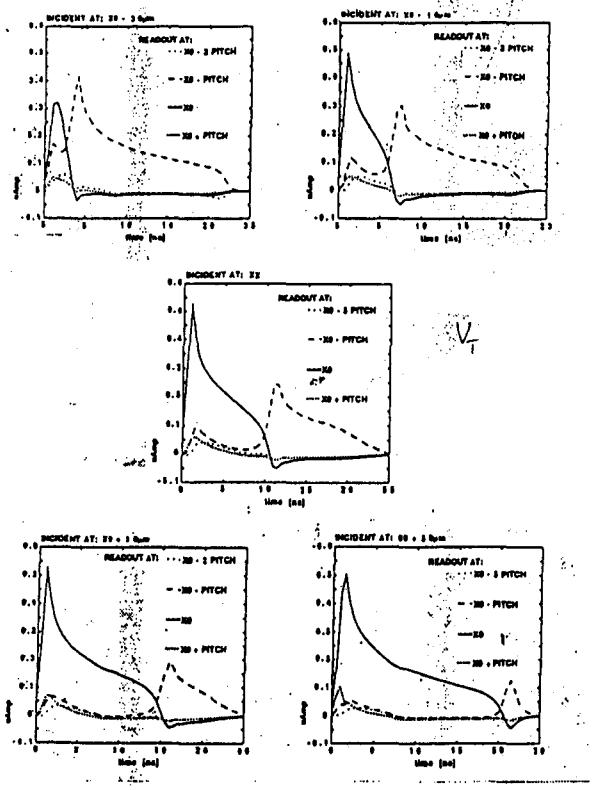

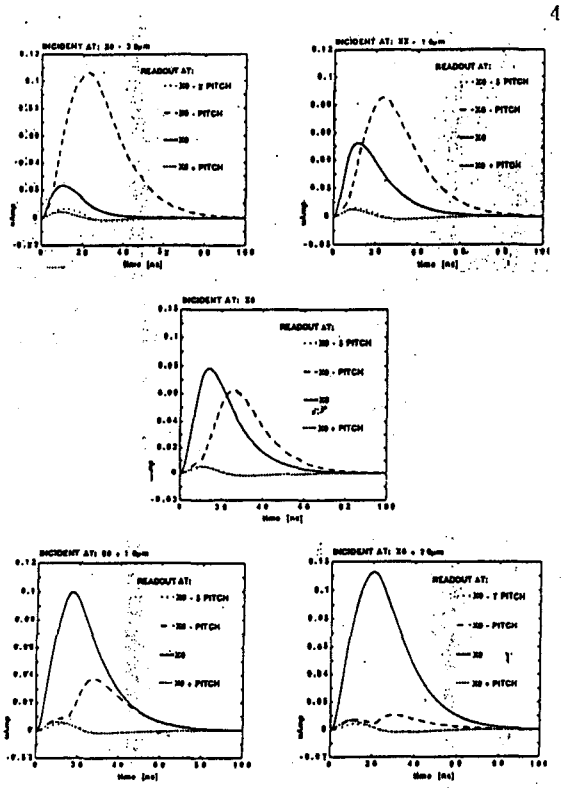

Y.Unno
April 22, 1992

Landau+ fluctuation simulation

Y.Unno
Physics, KEK
&
SCIPP, UCSC

Abstract

Energy deposition in a thin Silicon detector is simulated a la G. Hall including both the Landau distribution and the excitation of the atomic binding energy levels. The excitation of atomic levels is important to have correct width of the energy deposition. The method is applicable for the thickness of as thin as 15 microns which corresponds to 1-2 ns time bin.

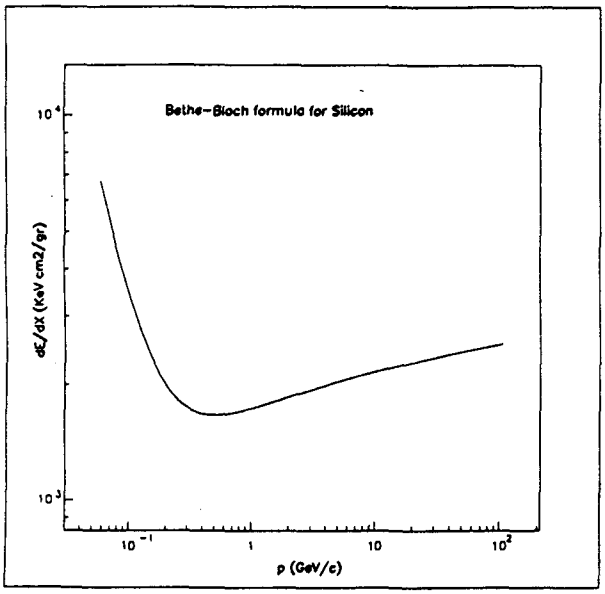

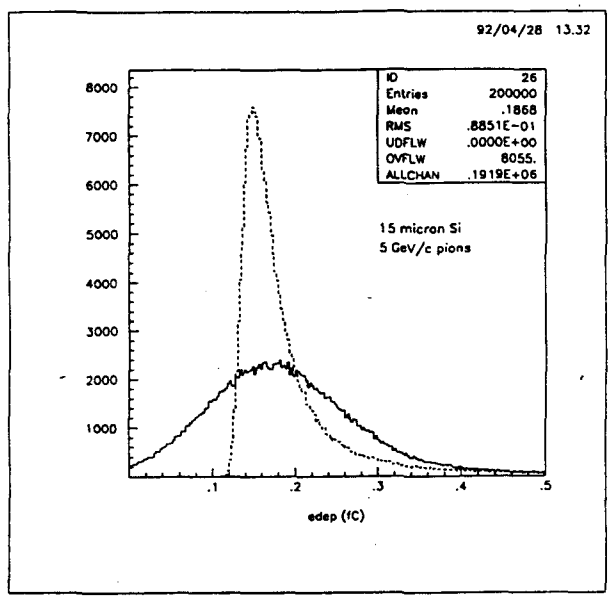

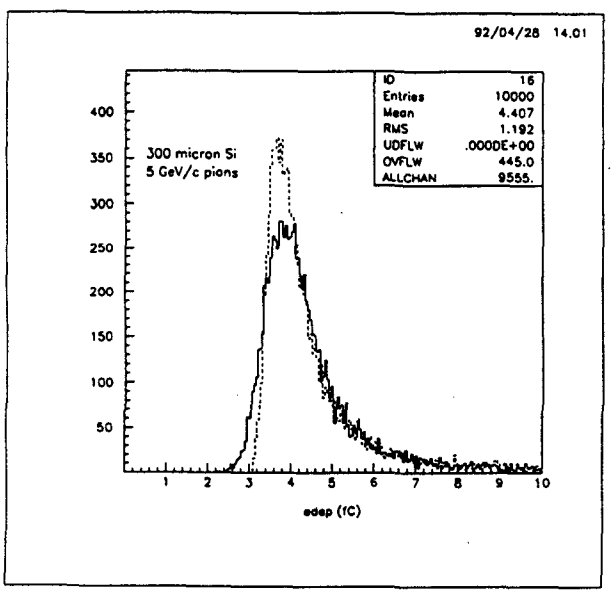

METHOD:

① Generate lots of "EVENTS"

Input : * $-25_\mu \le X_{inc} \le 25_\mu + 300_\mu \tan(6°)$
Chosen randomly (flat distribution)

* Energy deposited in each of the 20 bins (length 15_μ). Chosen randomly according to the (corrected) Landau distribution.

Output: Unconvoluted signal from:
$p(-100), p(-50), p(0), p(50)$
$n(-100), n(-50), n(0), n(50)$

② Analyse Events (Part 1) :

Input:

* V_{th} OR % VMP = (20, 25, 30, 35, 40)
* σ_{th} OR Sig. to Noise = (12, 16, 20)
* Amp. time constant τ = (15, 20, 25) ns

Output: $t_r = t_r(V_{th}, \sigma_{th}, \tau)$ of $p(-100), p(-50), \ldots$
= earliest time at which the absolute value of the convoluted signal > V_{th}

lote: Instead of adding noise to our signal
e jiggle V_{th} w/ a Gaussian distr. ($\sigma = \sigma_{TH}$)

TIME WALK

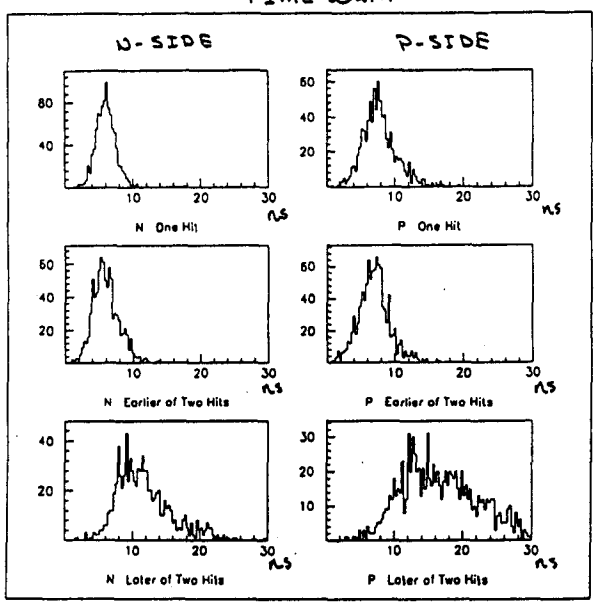

METHOD (cont'):

③ Analyse Events (Part 2):

Input: % VMP, Sig. to Noise, τ
AND Amp. time bucket $[t_0, t_0 + \Delta t]$

$t_0 = (0, 1, 2, 3, 4)$ ns

$\Delta t = (12, 14, 16, 100)$ ns

Output:

(p,n) side ⊗ { frac. of: ∅ hits (inefficiency)
1 hit
2 hits
>2 hits
(single, double) hits ⊗ { mean / RMS of $X_{inc} - X_r$

NOTE: X_{rec} = { center of hit strip (single hit)
Avg. of centers (double hit)

SETUP	Sig. to Noise	Tau	Window	Code for varied parameter
I	16	20ns	0-100ns 0-16 1-14	——— - - - - - · · · · · · ·
II	16	15 ns 20 25	0-16ns	——— - - - - - · · · · · · ·
III	12 16 20	20ns	0-16ns	——— - - - - · · · · · · ·

These three setups will be used in the following plots.

Setup #3

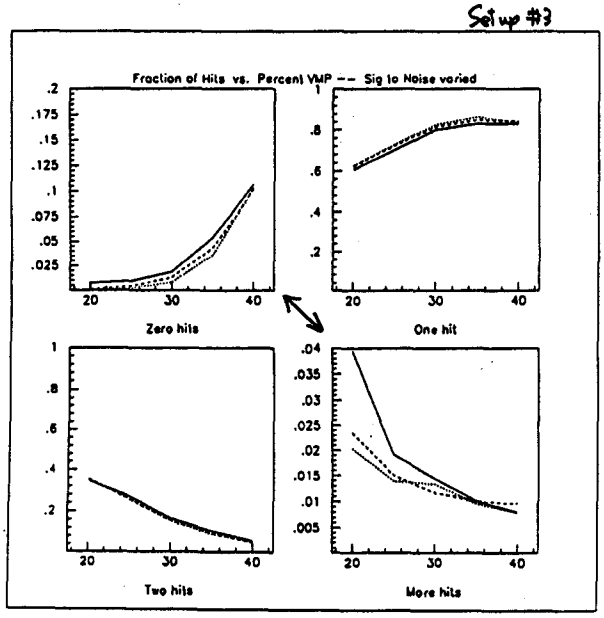

410

Setup #3

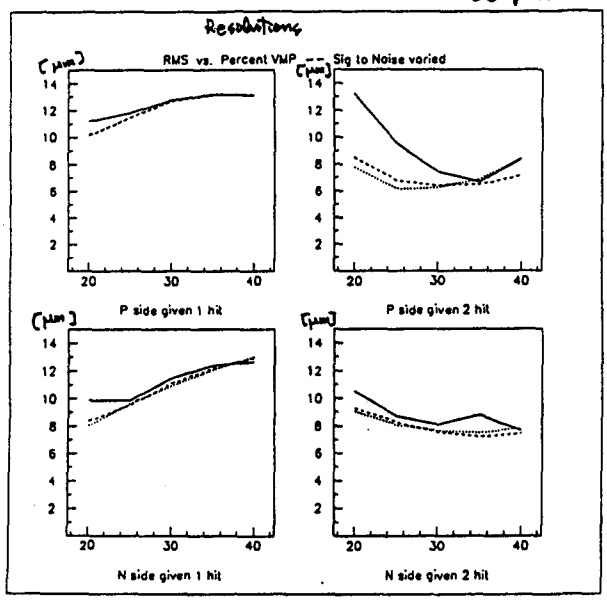

411

Setup #3

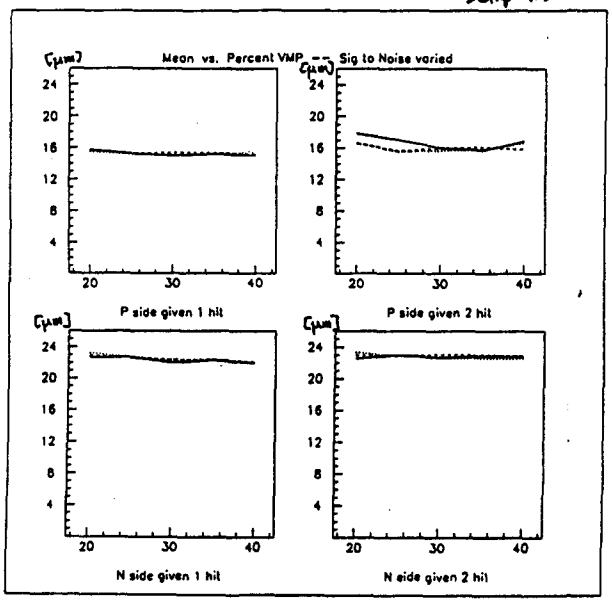

412

Setup #2

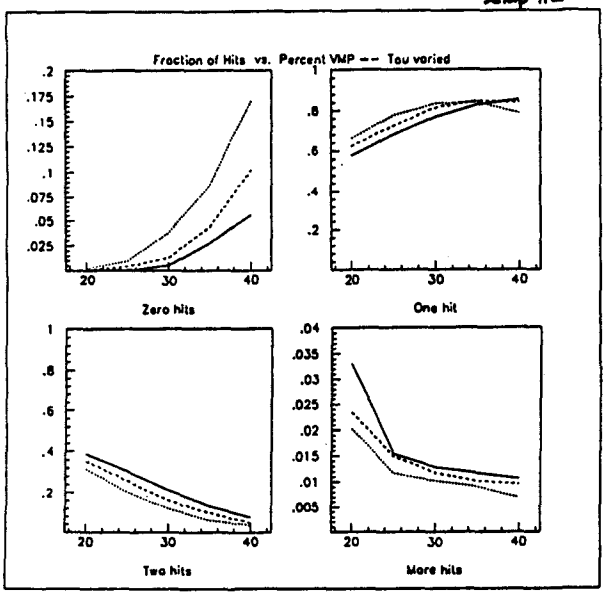

413

Setup #2

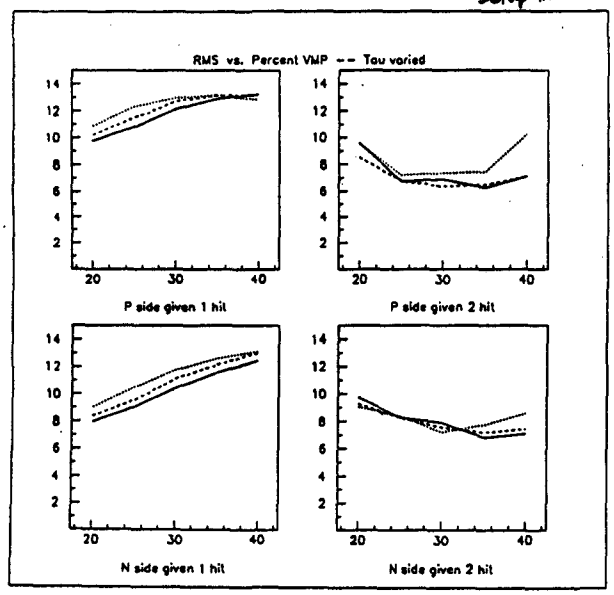

Setup #2

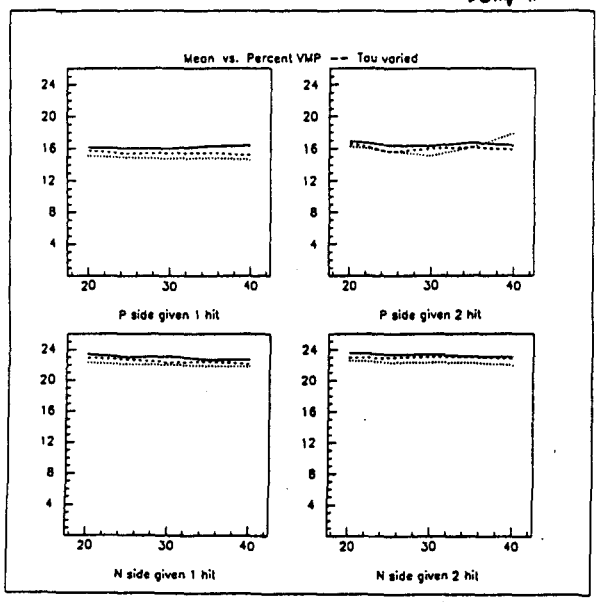

Conclusions

(The results presented are preliminary...)

- Evaluation of efficiency, resolution, and mean indicates ...
- S/N = 12 - 20 does not affect very much.
- Faster shaping is better to have the timing in the bucket. $\tau_p = 20$ns
- Threshold at 25% of the most probable charge is a good choice...
- Threshold variation (±10%) has very little effect.
- Resolutions:

  p-side 12 μm/single hit, 7 μm/double hits
  n-side 10 μm/single hit, 9 μm/double hits

(due to effective sensitive regions in the strip pitch?)

LORENTZ FORCE EFFECTS EXPERIMENTAL PLANS

Hans Ziock

KEK meeting
May 1992

LANL

CHARGE COLLECTION IN SILICON STRIP DETECTORS

E. BELAU, R. KLANNER, G. LUTZ, E. NEUGEBAUER, H.J. SEEBRUNNER and A. WYLIE
Max-Planck Institut für Physik und Astrophysik, Werner-Heisenberg-Institut, Munich, Fed. Rep. Germany

T. BÖHRINGER, L. HUBBELING and P. WEILHAMMER
CERN, Geneva, Switzerland

J. KEMMER
Technische Universität, Munich, Fed. Rep. Germany

U. KÖTZ *
DESY, Hamburg, Fed. Rep. Germany

M. RIEBESELL **
University of Hamburg, Fed. Rep. Germany

Nuclear Instruments and Methods 214 (1983) 253–260
North-Holland Publishing Company

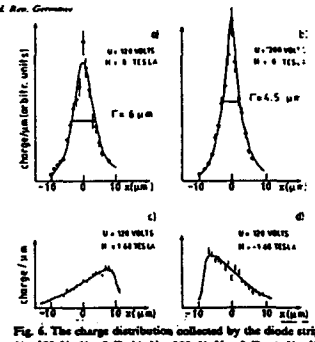

Fig. 6. The charge distribution collected by the diode strips: a) $U = 120$ V, $H = 0$ T; b) $U = 200$ V, $H = 0$ T; c) $U = 120$ V, $H = 1.68$ T; d) $U = 120$ V, $H = -1.68$ T.

Table 2
Lorentz angle and Hall mobility for holes in silicon versus magnetic field

Voltage (V)	Magnetic field (T)	$\tan\theta_L \times 10^3$ measured	$\tan\theta_L \times 10^3$ corrected *)	μ_H [cm²/Vs]
120	0	$+4.5 \pm 1.5$	-2 ± 3.5	–
200	0	$+0.5 \pm 1.5$	$+2 \pm 3.5$	–
120	1.68	$+58 \pm 2.5$	$+52 \pm 4.5$	310 ± 30
200	1.68	$+56 \pm 2.0$	$+50 \pm 4.0$	300 ± 25
120	1.32	$+51 \pm 2.0$	$+46 \pm 4.0$	350 ± 25
120	-1.68	-50 ± 2.0	-48 ± 4.0	290 ± 25

*) Corrected for the measured angle for zero magnetic field [$(-2.5 \pm 1) \times 10^{-3}$] and the deflection of the beam by the magnetic field at 1.68 T [$(4.0 \pm 1.0) \times 10^{-3}$].

1.2 Silicon (Si)

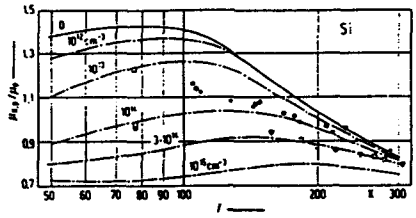

Fig. 96. Si. Hall scattering factor $\mu_{H,p}/\mu_p$ vs. temperature for p-type Si. Lines: theoretical results for different acceptor concentrations [78N1]. Experimental data: ▽: $n_a = 3.5 \cdot 10^{14}$ cm^{-3} [57L]; ●: $n_a = 2 \cdot 10^{13}$ cm^{-3} [63M]; ○: $n_a = 9 \cdot 10^{12}$ cm^{-3} [63M]; ▲: $n_a = 1 \cdot 10^{14}$ cm^{-3} [58B]; □: $n_a = 4 \cdot 10^{12}$ cm^{-3} [63R].

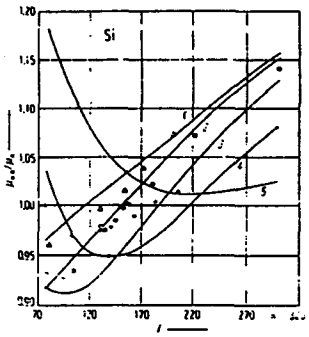

Fig. 97. Si. Hall scattering factor vs. temperature for n-type Si. Experimental data: triangles: $n_d = 2 \cdot 10^{13}$ cm^{-3}, open circles: $n_d = 1.5 \cdot 10^{14}$ cm^{-3}; full circles: $n_d = 4.6 \cdot 10^{15}$ cm^{-3}. Solid lines (1 ... 5): theory for $n_d = 1 \cdot 10^{13}$ cm^{-3}, $1 \cdot 10^{14}$ cm^{-3}, $1 \cdot 10^{15}$ cm^{-3}, $1 \cdot 10^{16}$ cm^{-3} and $1 \cdot 10^{17}$ cm^{-3} [74H1].

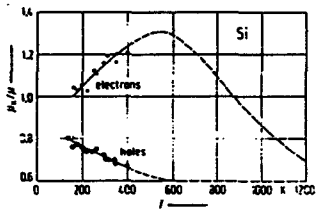

Fig. 95. Si. Hall scattering factor μ_H/μ vs. temperature. n-type samples have $n_d = 1.75 \cdot 10^{14}$ cm^{-3} or $2.1 \cdot 10^{15}$ cm^{-3}; p-type samples have $n_a = 3.1 \cdot 10^{14}$ cm^{-3} or $7.0 \cdot 10^{14}$ cm^{-3}. Curves theoretical [54M].

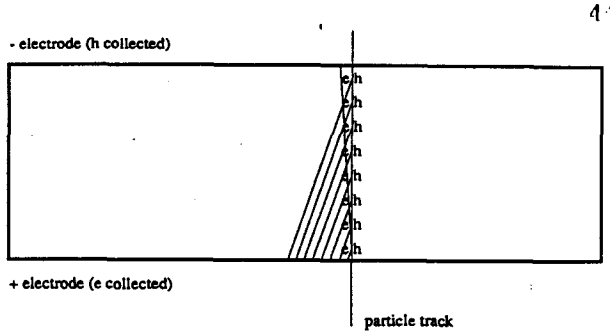

lorentz force: $F = q(v \times B)$

assume B is into the page, then
for holes (q=+e, v is along +y) and thus F is to the left,
for electrons (q=-e, v is along -y) and thus F is still to the left

The magnitude of the angle the electrons and holes make with respect to the direction of the electric field is given by $\tan\theta_L = \mu_H B$

μ_H is the Hall mobility (NOTE that it is not equal to the drift mobility)
$\mu_{He} \sim 0.1650$ m^2 / Vsec $\quad \mu_{De} \sim 0.1350$ m^2 / Vsec
$\mu_{Hh} \sim 0.0310$ m^2 / Vsec $\quad \mu_{Dh} \sim 0.0450$ m^2 / Vsec

thus for a 2 Tesla field, 300μm thick detector
$\tan\theta_{Le} = 0.33$ ==> $\theta_{Le} = 18.26°$ ==> max displacement = - 99.0μm
$\tan\theta_{Lh} = 0.062$ ==> $\theta_{Lh} = 3.55°$ ==> max displacement = - 18.6μm

μ_H is the Hall mobility (NOTE that it is not equal to the drift mobility)
μ_{He} = 0.1650 m^2/V
μ_{Hh} = 0.0310 m^2/V

thus for a 2 Tesla field, 300μm thick detector
$\tan\theta_{Le}$ = 0.33 ==> θ_{Le} = 18.26° ==> max displacement = - 99.0μm
$\tan\theta_{Lh}$ = 0.062 ==> θ_{Lh} = 3.55° ==> max displacement = - 18.6μm

Tip the detector by an angle θ_T so that the hole distribution is as wide as the electron distribution ==> $\tan\theta_T = (\tan\theta_{Le} - \tan\theta_{Lh}) / 2$ ==> θ_T = 7.6°

The holes cover the range 0 to $-D\tan\theta_T - D\tan\theta_{Lh}$ (0 μm -> -58.8μm)
and have a mean position of $(-D\tan\theta_T - D\tan\theta_{Lh}) / 2$ (-29.9 μm)
The electrons cover the range $-D\tan\theta_T$ to $-D\tan\theta_{Le}$ (-40.2 μm -> -99.0μm)
and have a mean position of $(-D\tan\theta_T - D\tan\theta_{Le}) / 2$ (-69.6 μm)

LANL

What to Measure

- μ_{He} and μ_{Hh}
- Time difference on adjacent strips (both sides)
- Pulse shape on adjacent strips (both sides)
- Position resolution as function (both sides)
  - of discrimination level
  - of angle of detector

Dependencies on:
- B field value
- Temperature
- Radiation damage

LANL

Equipment needed

- Lasers
  - 1064 nm, ~1nsec rise & fall, ~ 2mm absorption length UCSC
  - ~ 800 nm, ~1nsec rise & fall, ~ 20μm absorption length ????
- Fiber to guide laser light
  - small spot
  - small divergence
- Precision stage
  - preferably nonmagnetic
  - ~ 1 μm accuracy
  - hardware to mount it, the fiber, and get fiber close to detector

LANL

More Equipment needed

- LANL Magnet & power supply, Field uniform to ~ 1 part in 10^4
  - 3" gap, 6.3" diameter pole pieces ~ 19.0 kG
  - 2" gap, 8.0" diameter pole pieces ~ 21.5 kG
- Detectors
  - Both n strip & p strip ≤ 50 μm pitch
  - rad damaged detectors
  - side opposite strips should not be aluminized
  - bonded out strips
- Electronics
  - Tek 602 digitizing scope, at least 2 channels, preferably 4
  - fast low noise amplifiers
  - slower electronics, analog readout system
- Miscellaneous Hardware

LANL

Proposed Time Frame

- Begin real measurements ~ August
- Measurements will take several months
- Radiation damage run interference
- Magnet
  - setup ~ mid June
  - mapping end of June
- Begin procuring equipment ~ June -> August

LANL

Double Sided Sensor
(Barrel & Disk)

Takashi Ohsugi
(Hiroshima University)

1992.

Prototype
followed by this spec.

Specification of Double-Sided Silicon Sensor
(for Barrel Section)

1) Substrate
   - Type: n-type
   - Resistivity: 5~6 kΩ · cm
   - Thickness: 300 ± 10 μm
2) Size
   - Overall dimension: 60 mm x 34.1 mm
   - Effective Area: 58.8 mm x 32.0 mm
   - Dead Area: 600 μm from edge
3) Strip
   - Pitch: 50 μm on both surfaces
   - Strip Isolation of Ohmic Side: p+ blocking line method
   - Pattern Accuracy
     - Position: ± 1 μm
     - Size: ± 1 μm
     - Relative Position of both sides: ≤5 μm
4) Bias Resistor
   - Polycrystalline Silicon on both sides
   - Resistance Value: 250 ± 50 kΩ
5) Electric Properties
   - Initial Leakage Current: ≤ 1 μA (overall)
     ≤ 100 nA / channel
   - Bias Voltage Tolerance: ≤ 150 V
   - Decoupling Capacitance of Strip
     - Breakdown Voltage: ≥ 100 V
     - Capacitance: ≥20 pF / cm
   - Readout Capacitance: ≤1.2 pF/cm (junction side)
     ≤ 1.8 pF/cm (ohmic side)
6) Fiducial Mark for Integration
   (Patterns and position are defined by figure.)
   Position Accuracy Relative to Strips: ± 1 μm
7) Dicing
   Full Cutting by Diamond Saw.
   Cutting Zone: ± 30 μm

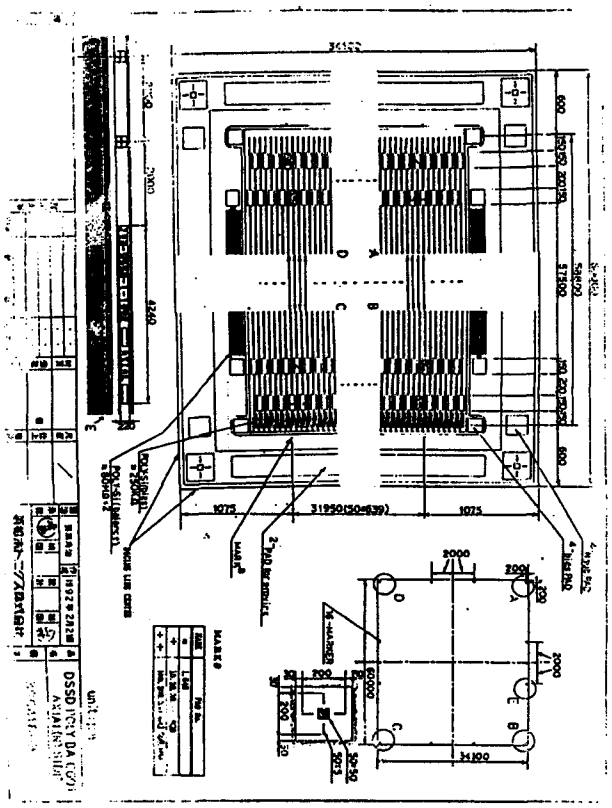

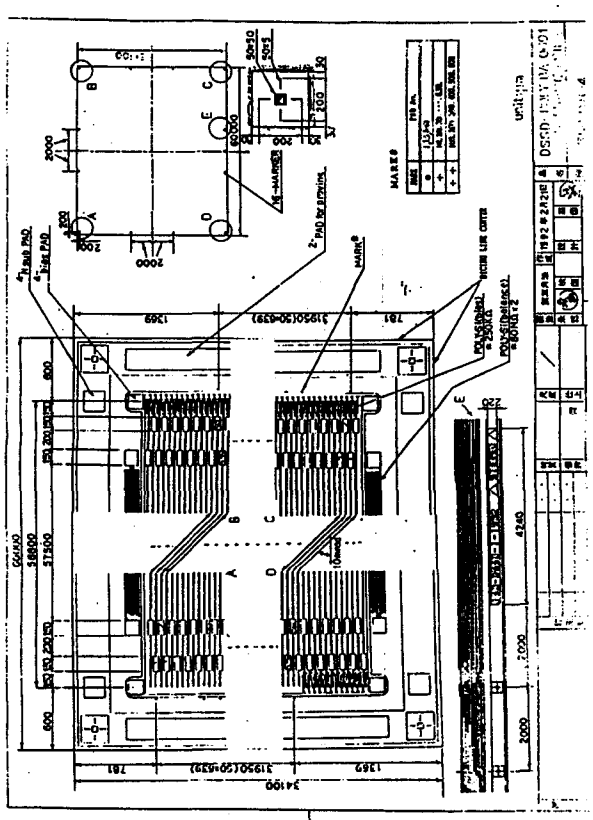

459

Ohmic Side

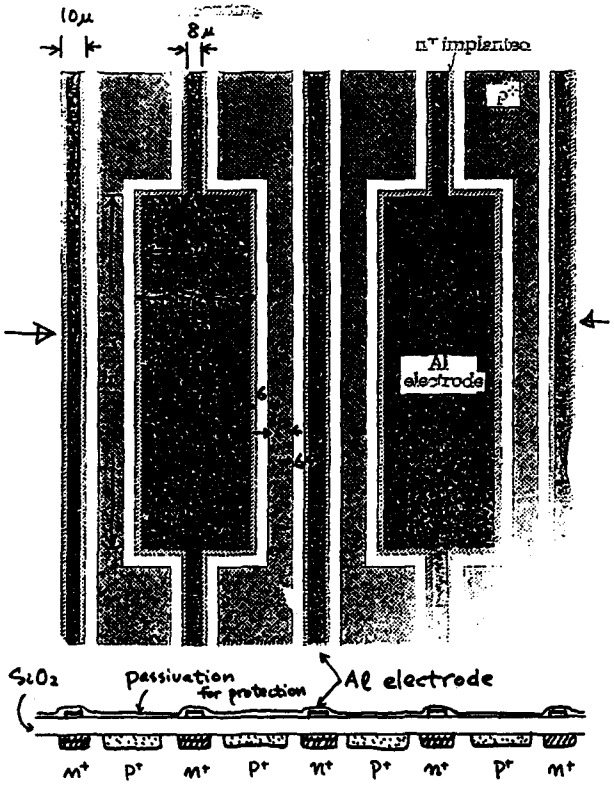

460

Nois Amplitude

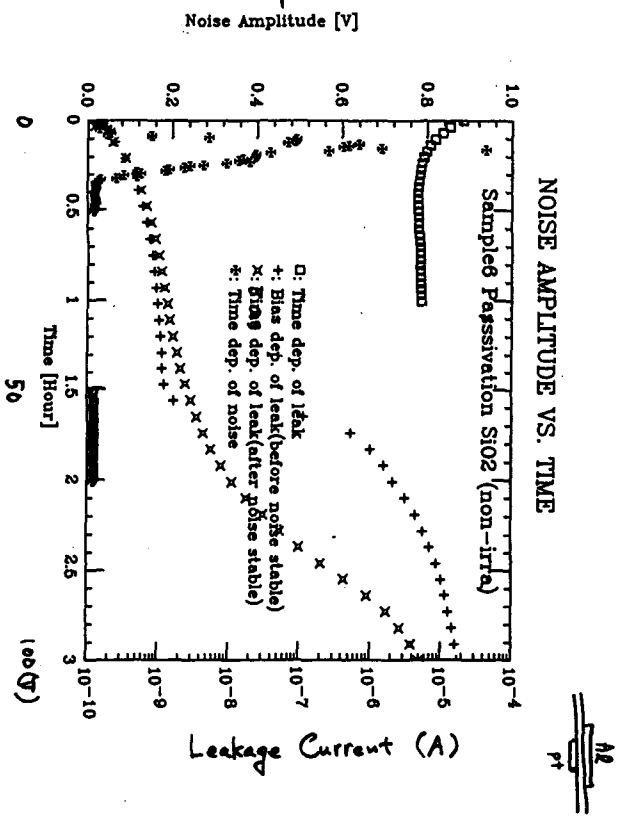

461

Comment on Wedge Sensor

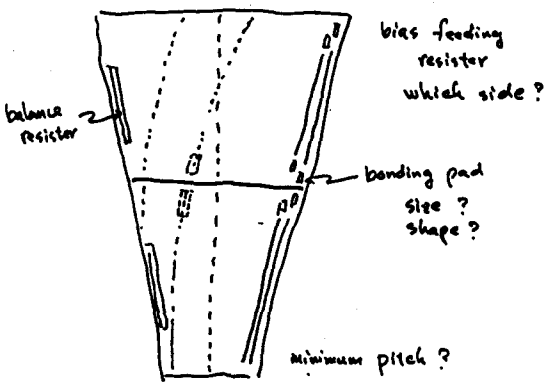

Stereo side
~~Ohmic Side~~

1) bonding pad ..... size, shape, direction ?

2) crossing angle ....dead area ...

Proposal:

let's start making with an ohmic side (single side) wedge sensor

462

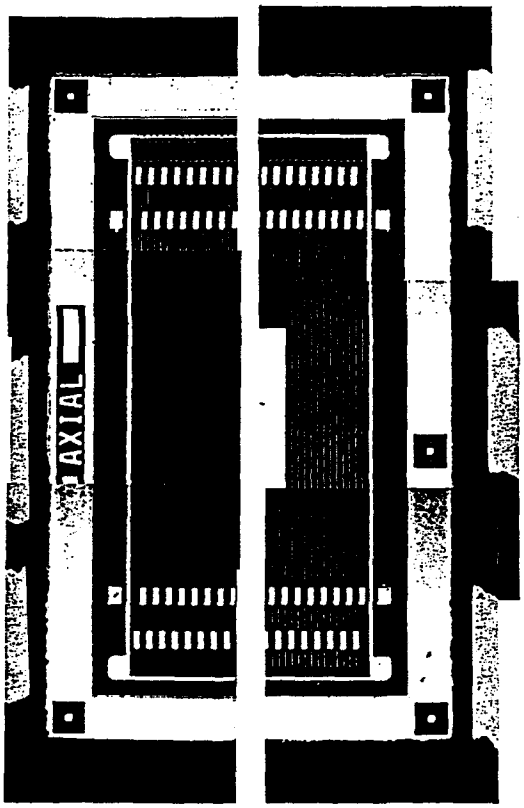

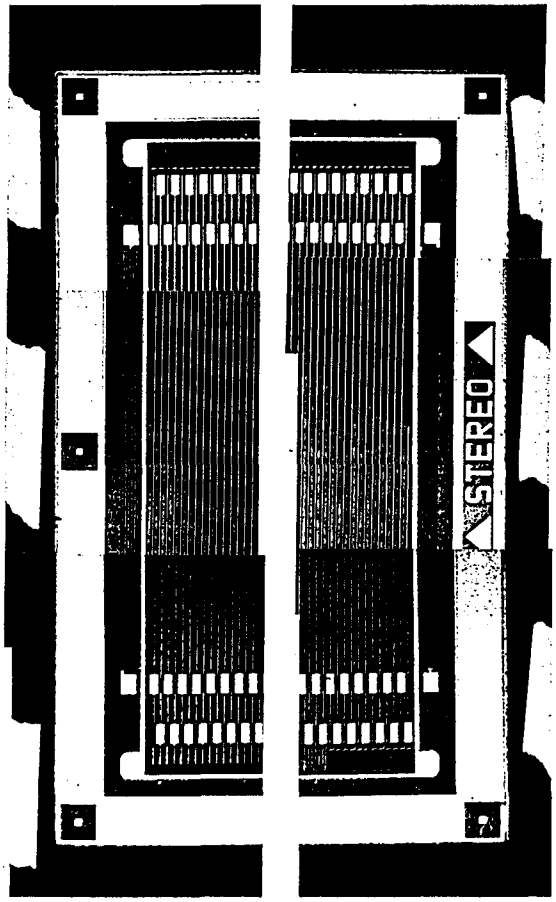
STEREO

464

465

Comments on Production of DSSD

K. Yamamoto
(Hamamatsu Photonics)

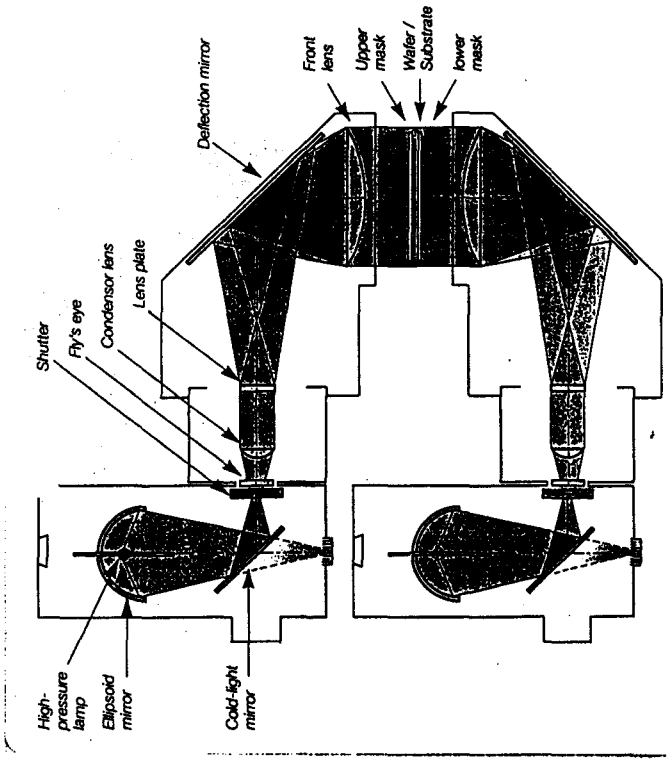

466

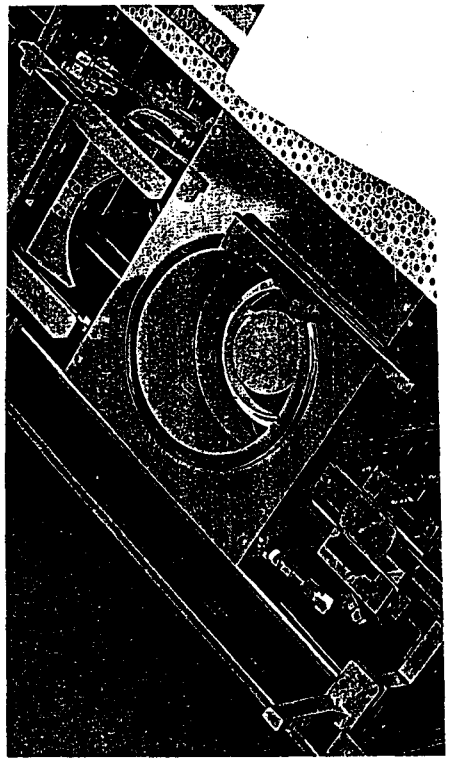

467

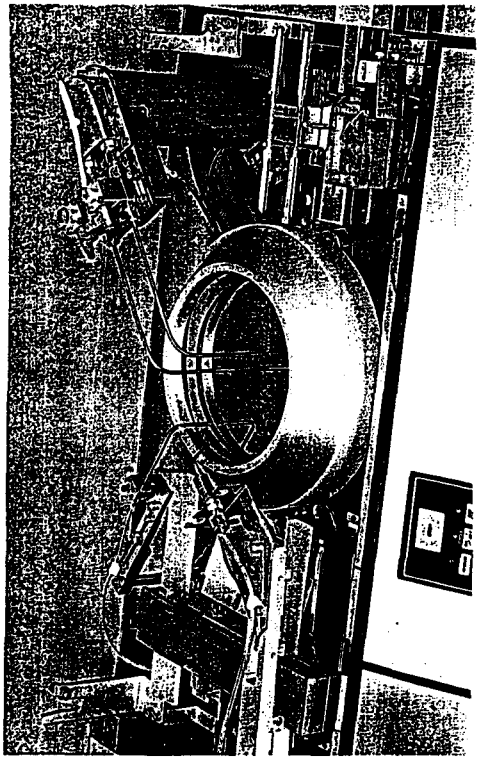

468

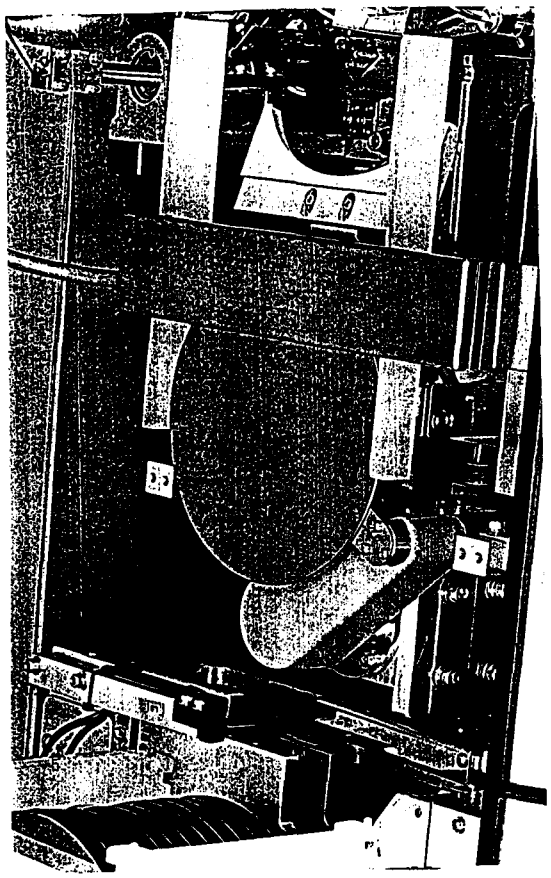

469

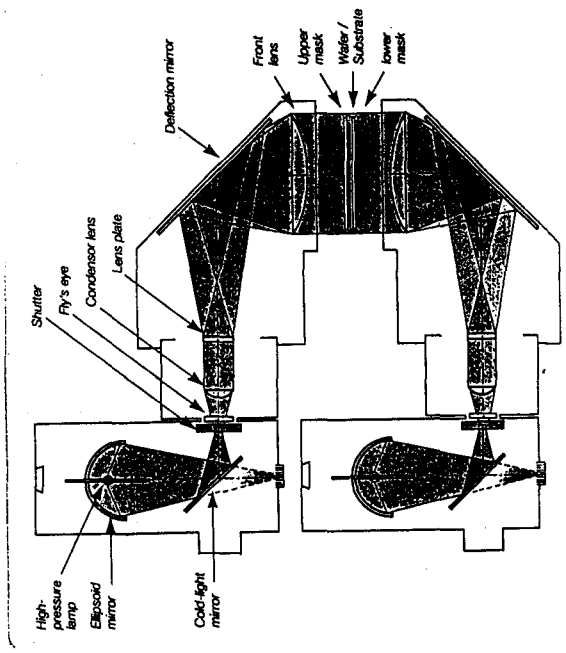

470

Proximity Mechanism

An option permits the precise definition of proximity or separation distances, preventing mask or wafer/substrate damage.

Functional Schematic of the SUSS MA 25 in Double-Side Exposure Mode

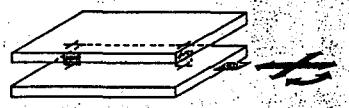

Wedge compensation between the two masks is achieved. Lower mask is aligned to the upper.

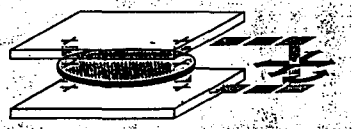

The masks are separated. The transport system holds the wafer in the alignment position. The lower mask (which is registered to the upper) is aligned to the wafer.

Wafer is placed on the lower mask. The transport moves away. The upper mask moves down to the selected proximity gap.

471

SUSS MA 25 – The Economical Solution

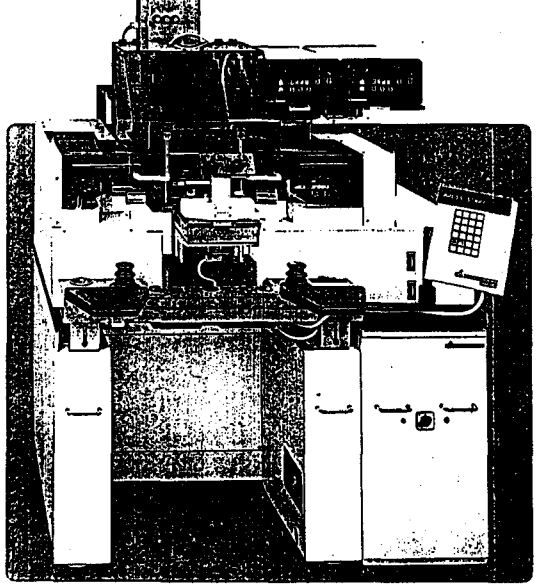

472

473

474

475

EQUIPMENT INVESTMENT LIST FOR DS-SSD

EQUIPMENT	USE
RESIST COATER & DEVELOPER SYSTEM	BOTHSIDE WAFER PROCESS WITH BACKSIDE PROTECTION
BOTH-SIDE MASK ALIGNER	BOTHSIDE WAFER PROCESS FOR ALIGNED PATTERN
ION IMPLANTER RECONSTRUCTION	DOPING PROCESS
SPUTTERING SYSTEM RECONSTRUCTION	ALUMINIUM DEPOSITION FOR FULL SIZE
PLASMA-CVD SYSTEM RECONSTRUCTION	PASSIVATION FILM DEPOSITION FOR BOTHSIDE PROCESS
SOG COATING SYSTEM	2 LAYER METALLIZATION
FLATNESS TESTING SYSTEM	CHIP WARPAGE EVALUATION
FTIR SPECTROMETER	PASSIVATION FILM EVALUATION
PROBING & MEASUREMENT SYSTEM	ELECTRICAL CHIP TEST
WIRE BONDING MACHINE	CHIP ASSEMBLY
TOTAL	

FILE 920525B.JSW

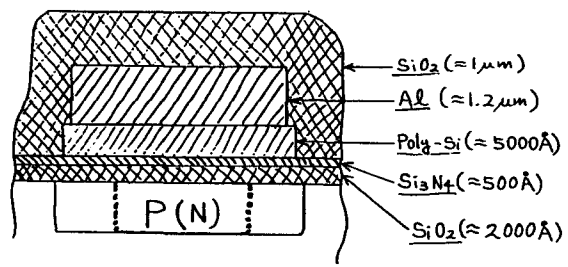

SiO_2 : Low-temp SOG

Al : Suputtering

Poly-Si : Low-pressure CVD

Si_3N_4 : Plasma CVD

SiO_2 : Thermal Oxidation

P(N) : Ion Implantation

SILICON "WEDGE" DETECTOR R & D

BRUCE BARNETT
BARRY BLUMENFELD
PETER FISHER
AIHUD PEVSNER
JACK SPANGLER
JOHN KRIZMANIC
JOE ORENDORF
DAVE NEWMAN
JOHN SICARDA
JOHN SNIDER
KATE CRYSTAL
JOE CARLSON

[redacted]
27 MAY 1992

MOTIVATION

- SOLENOID DETECTOR COLLABORATION (SDC) REQUIRES NOVEL TRACKING FOR $|\eta| > 1$

↓

"WEDGE" DETECTORS

- VARIABLE PITCH (~25 - 60 μ OVER 13cm)
- DOUBLE SIDED

↓

MANY QUESTIONS

SDC SILICON TRACKER SYSTEM

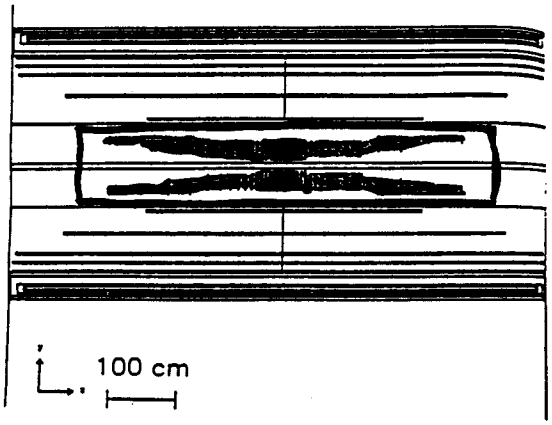

[redacted] BARREL

[redacted] DISKS

[redacted] VESSEL

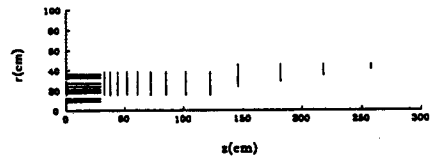

FIG. 4-2. Silicon tracker design.

Table 4-2.
Dimensions for tracker

Barrel	r	z	Silicon Area
(1)	9 cm	30 cm	
(2)	12 cm	30 cm	
(3)	18 cm	30 cm	[redacted]
(4)	21 cm	30 cm	
(5)	24 cm	30 cm	
(6)	27 cm	30 cm	
(7)	33 cm	30 cm	
(8)	36 cm	30 cm	

Disks	r_{in}	r_{out}	z	Silicon Area
(1)	15 cm	39 cm	33 cm	
(2)	15 cm	39 cm	38 cm	
(3)	15 cm	39 cm	44 cm	[redacted] (both sides)
(4)	15 cm	39 cm	52 cm	
(5)	15 cm	39 cm	61 cm	
(6)	15 cm	39 cm	72 cm	
(7)	15 cm	39 cm	85 cm	
(8)	15 cm	39 cm	102 cm	
(9)	15 cm	39 cm	122 cm	
(10)	22.5 cm	46.5 cm	146 cm	
(11)	28.5 cm	46.5 cm	182 cm	
(12)	34.5 cm	46.5 cm	218 cm	
(13)	40.5 cm	46.5 cm	258 cm	

Total Area = 16.94 m^2

Layout of discs 1 to 8 showing segmentation (10)

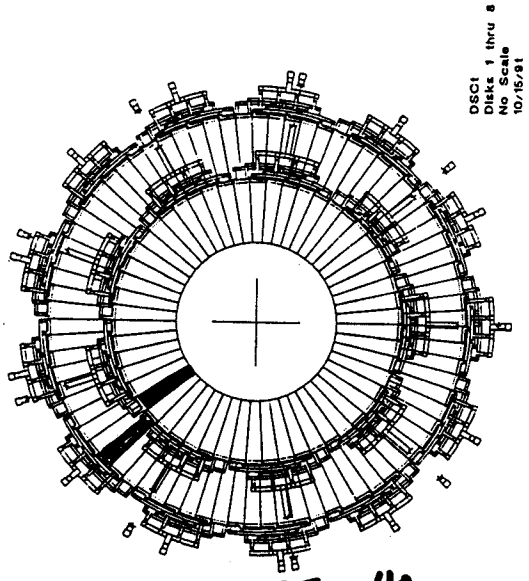

INNER 25μ - 40μ
OUTER 40μ - 55μ

How Si DETECTORS WORK:

- OVERVIEW
  - IONIZING PARTICLES LIBERATE e-h PAIRS
  - DRIFT IN INTERNAL FIELD
  - COLLECT CHARGE ON ANODE/CATHODE
- DETAILS
  - CONSIDER IONIZATION DETECTOR
  - SINGLE e-h PAIR

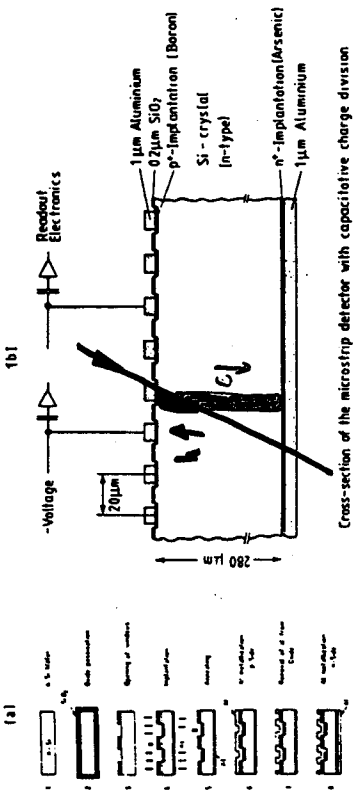

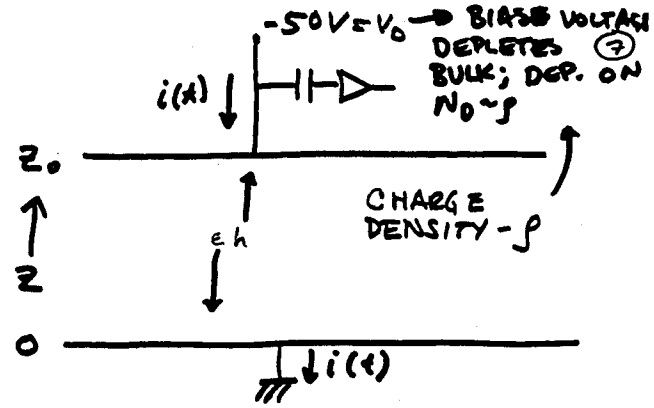

E. POTENTIAL: $\varphi(z) = az^2 + bz$

E. FIELD: $\vec{E}(z) = 2az\hat{z} + b\hat{z}$

VELOCITY: $\vec{v}(z) = \mu \vec{E}(z)$

WHERE

$a = \rho/2\epsilon$

$b = (\rho z_0/2\epsilon) + (V_0/z_0)$

EQUATION OF MOTION:

$$2a\mu t = \ln\left[\frac{(2az+b)}{(2az'+b)}\right]$$

$$z \rightarrow z'$$

THEN:

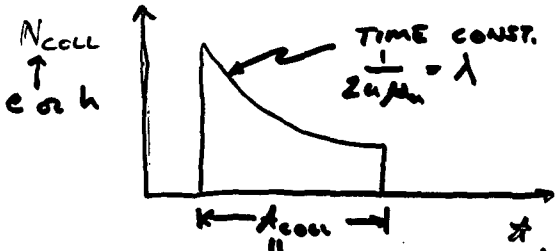

$$t_{coll} = \lambda \ln\left(\frac{2az_0+b}{b}\right) \quad h$$

$$\lambda \ln\left(\frac{b}{b+2az_0}\right) \quad e$$

SPECIFICALLY:

$N_D = 10^{12}/cm^3$

$V_D = -50\ V$

$z_0 = 300\mu$

$t^e_{coll} = 15\ ns$ $\quad t^h_{coll} = 41\ ns$

$\lambda_e = 55\ ns$ $\quad \lambda_h = 146\ ns$

INDUCED CHARGE

RAMO'S THM. (1939)

$$i(t) = e\,\vec{v}\,\vec{\nabla}\phi_w$$

CURRENT ON ELECTRODE

WIEGHT POTENTIAL
$\nabla^2\phi_w = 0$
$\phi_w(\text{ELECTRODE}) = 1$

INDUCED (CONT.)

FOR ANODE $\quad \phi_w(z) = z/z_0$

$$i(t) = \frac{e\mu}{z_0}\left[(2az_1+b)e^{2a\mu t} - b\right]$$

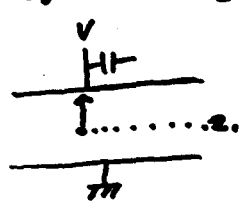

$$Q_{coll} = \sum_{e,h}\int_0^\infty i_e(t)\,dt$$

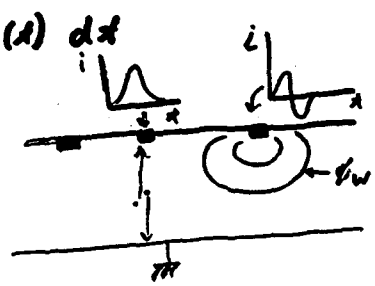

INDUCED (CONT.)

OBSERVATIONS

- MUST COLLECT <u>BOTH</u> e-h FOR $Q_{coll} = 1$
- DIFFUSION CONTRIBUTES TO CHARGE SHARING BETWEEN STRIPS
- PULSE SHAPE DEPENDS ON V_D, ρ & z_0

FOR MULTISTRIP DEVICE, THINGS GET MORE COMPLICATED

WEDGE DEVICES - QUESTIONS

FURTHER COMPLICATIONS

- DEPLETE ENTIRE DEVICE?

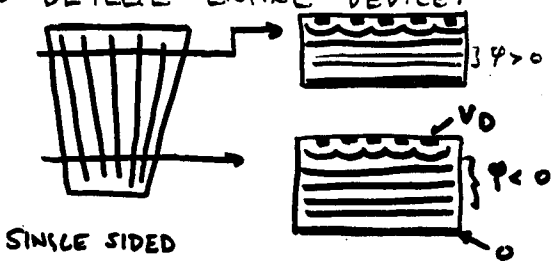

- TIMING -
  - HIT/NO HIT THRESHOLD CROSSING **LATER** AT LARGER PITCH?
  - MORE **TRAPPING** (⇒ LONGER DRIFT?)
  - **SIGNAL DISPERSION** → VARIABLE CAP. ALONG STRIP?

W.D. QUESTIONS (CONT.)

- RESOLUTION - VARY ALONG STRIP?
- "Z WALK" IN DOUBLE SIDED DEVICE
  → VARIABLE PITCH LEADS TO **RADIAL** DEP. IN Z-OFFSET

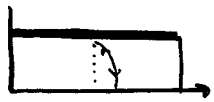

- B-FIELD **NORMAL** TO DETECTOR PLANE
  - HOW SENSITIVE TO VARIATION?
  - RESOLUTION EFFECTS?

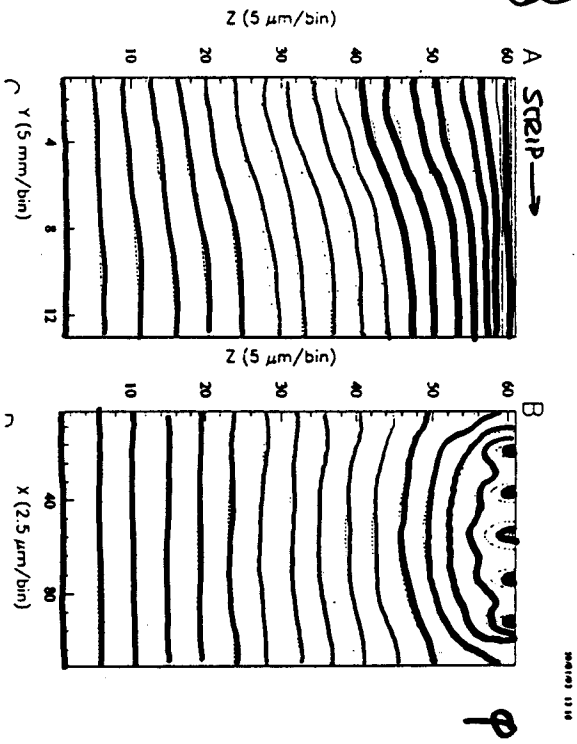

JHU ACTIVITIES

- PROTOTYPES
  - JHU #1 - SINGLE SIDED WEDGE - 3 TYPES (⇒ IN HAND)
  - JHU #2 - DOUBLE SIDED, WEDGE - BEING DESIGNED
- SIMULATION
  SINGLE PARTICLE MOVER (SPM)

  STUDY
  - PULSE SHAPE/TIMING
  - DEPLETION
  - "Z-WALK"
  - B-FIELD

PROTOTYPE (CONT.)

JHU PROTOTYPE #1:

- SINGLE SIDED
- 3 DEVICES / WAFER

384 ch	30-60 μ	A/C	COUPLED	FOXFET BIAS
384 ch	30-60 μ	D/C	COUPLED	
256 ch	60-100 μ	A/C	COUPLED	

- DESIGN FINALIZED W/ MICRON SEMICONDUCTOR

EXPECT DELIVERY IN FEB.

DELIVERED 28 FEB. 1992!

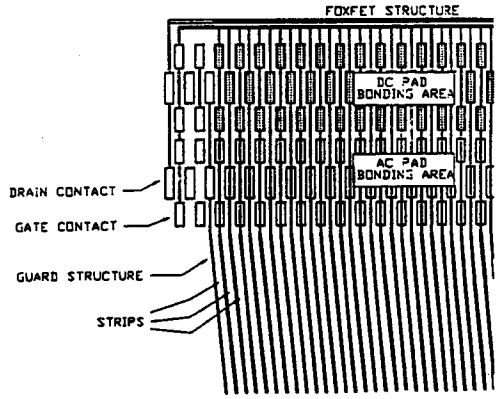

Figure 2: FOXFET AC readout design for MICRON Corp. order

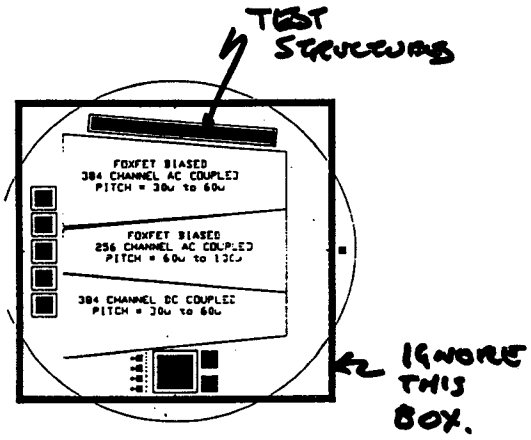

Figure 1: Silicon wafer design for MICRON Corp. order

JHU #1 TESTING

- STATIC TESTS
  - LEAKAGE CURRENT
  - C-V ⇒ DEPLETION
  - CONTINUITY / ISOLATION

RESULTS

- LEAKAGE CURRENTS VERY HIGH ⇒ >20% OF STRIPS ABOVE 1nA
  SPEC → NO MORE THAN 2 STRIPS ABOVE 1nA
- DEPLETION VOLTAGE VARIES 6 - 100 V
- CONCERNS ABOUT PROBING
  - HOW MANY TIMES?
  - AC PADS - BREAK THROUGH?

JHU #1 TESTING

- DYNAMIC TESTS

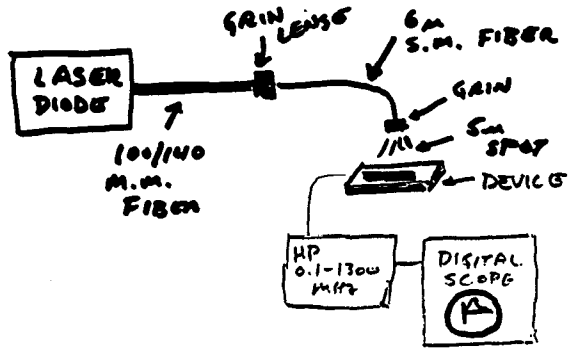

- AT 1064 nm 300μ Si ABSORBS 10% OF LIGHT ⇒ UNIFORM DEPOSITE OF CARRIERS
- 50μW ~ 10^5 e-h PAIRS/ns
- RISE/FALL < 1ns (???)

JHU #1 - DYNAMIC (CONT.)

- STUDY
  - CHARGE SHARING BETWEEN STRIPS

➡ RESOLUTION = (f(r))

WHAT IS SHAPE OF "DOUBLE HIT" REGION? → (CRUCIAL FOR SDC)

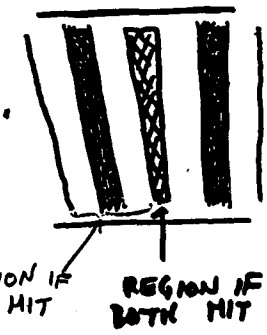

- PULSE SHAPE / Q_coll.

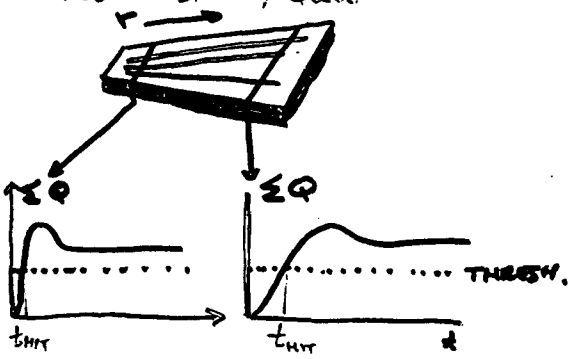

- HOW DOES t_{HIT} VARY WITH r?
- CAN STRIP SHAPE BE USED TO COMPENSATE?

JHU #1

- TEST BEAM / COSMIC / ^{90}Sr SOURCE
  - EVENTUALLY, COUPLE TO SVX - SRS/SDA SYSTEM
  - ~5 ELEMENT TELESCOPE UNDER DESIGN

⬇

- NEED HOLDER, ETC
- TRIGGER FOR TEST BEAM, FREE RUN FOR ^{90}Sr, COSMIC (~30% LIVE TIME)

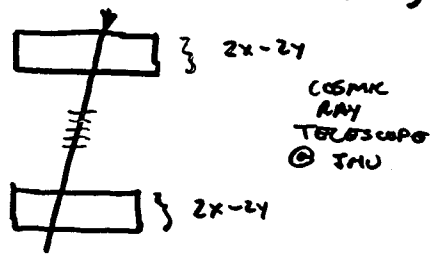

JHU #2

DOUBLE SIDED PROTOTYPE ➡
MANY MORE QUESTIONS

- WEDGE, 25-60 μ

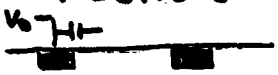

- BIAS OPTIONS FOR n-SIDE

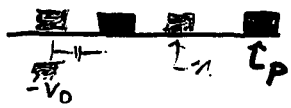

↳ PUNCH THROUGH - MICRON HAS DONE IT → WORKS, BUT NOT RAD. HARD

FORFET - NOT ATTEMPTED (?)
BUT RAD. HARD (?)

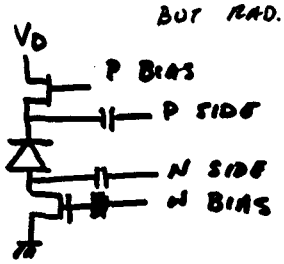

- CORRECT "φ BITE"?

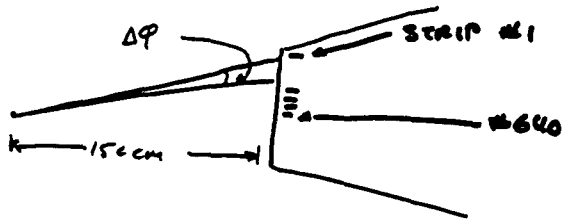

SDC WEDGE DEVICE TYPE A

→ FOR CONSTANT PITCH, Δφ NOT CONSTANT.

φ BITE (CONT.)

$\Delta\varphi(\#1) = 185$ μrad END
$\Delta\varphi(\#640) = 191$ μrad MIDDLE

⬇

NOT SIGNIFICANT

- n SIDE STRIPS

2 WAYS TO DO IT:

(1)

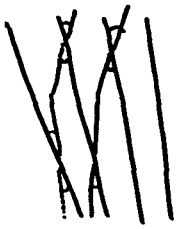

"CONSTANT STERED ANGLE"
~10 mrad

- CROSSING POINTS CURVE SLIGHTLY (~1/20)
- 50 μ PITCH
- NOT EVENLY SPACED

n-SIDE (CONT.)

(2)

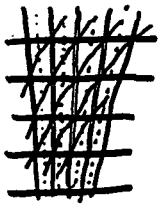

a. CHOOSE CROSSING POINTS
b. CONNECT

⬇

- CAN CHOOSE ANY CROSSING GEOMETRY SUBJECT TO BONDING
- OBVIOUS OPTIONS
  A. STRAIGHT
  B. CURVED ALONG CONT θ
  ↳ "RED HERRING"

⬇

NEW QUESTIONS
- WHAT SPACING? IN PARTICULAR

SPACING (CONT.)

$$P_T = \frac{KBL^2}{S}$$

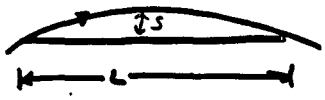

[illegible] CONTRAST TO [illegible] [illegible] MINIMIZE S WITH p-SIDE STRIPS AND L W/ n-SIDE

$$\frac{\delta P_T}{P_T} = \frac{\delta S}{S} = \frac{0.5\,cm \times 2}{12} = 8\%$$

$$= \frac{\delta s}{s} = \frac{10\mu}{1000\mu} = 1\%$$

- IS THIS THE ONLY ISSUE?
- CAN WE CHOOSE SPACINGS DIFFERENTLY ON DIFFERENT DISKS TO IMPROVE?

n-SIDE QUESTIONS (CONT)

- CAN 25μ PITCH W/ p+ IMPLANT BE MADE? μ SAYS YES!
- BONDING?

ACTION:

- [illegible] ON #2 DESIGN NOW - [illegible] APRIL.
- [illegible] FINAL DESIGN, #3.

SIMULATIONS

- [illegible] PULSE SHAPE [illegible] SIMULATION DRIFT IN DEVICE
- SPM V1.00 [illegible] RESULTS UNDERSTANDABLE, BUT SCARCEY (TIMING).

➡ MAKE SURE IT'S RIGHT!

DEVICE SIMULATIONS

- SIMULATE PULSE SHAPE IN A DETAILED WAY
- BASED ON SAILOR, ZIOCK, KINNISON & HOLZSHIEW (NIM, 1981)
- INCLUDE
  - DETAILED FIELD CALC. (BASED ON TEDM.)
  - INDUCTION EFFECTS (VIA RAMO'S THM.
  - DIFFUSION
  - TRAPPING / LEAKAGE
  - LANDAU FLUCTUATIONS, DELTA RAYS

METHOD

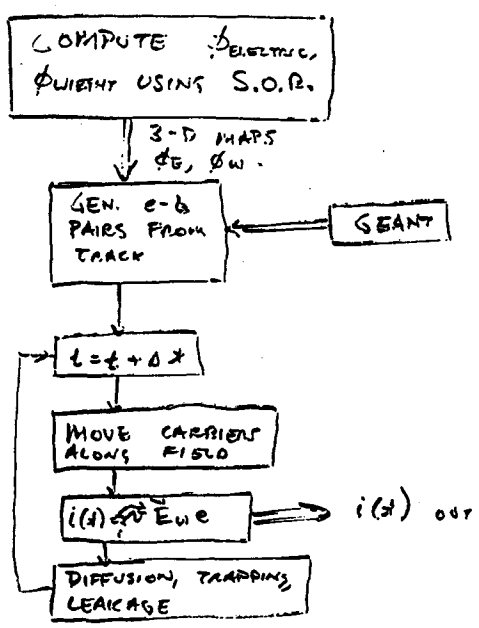

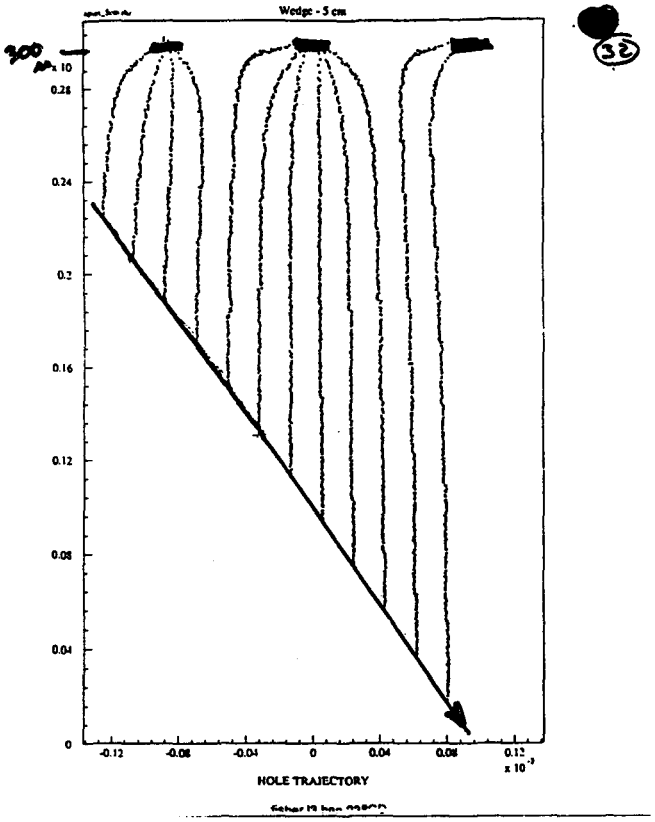

DEVICE SIMULATIONS

(32) (33)

- PECULIAR GEOMETRY → SEVERAL QUESTIONS:
  - HOW SERIOUS IS E_y?
    (STEREO RING PITCH ~400μm, PROBABLY NOT VERY.)
  - HOW DOES SIGNAL TIMING (WALK) VARY
    - ALONG R STRIP?
    - AS A FUNCTION OF (IMPACT POINT, STRIP)?
    - IMPACT ANGLE
    - B FIELD
  - HOW MANY STRIPS DOES A M.I.P. FIRE?
  - CAN THE SHAPE OF THE IMPLANT LAYER HELP?

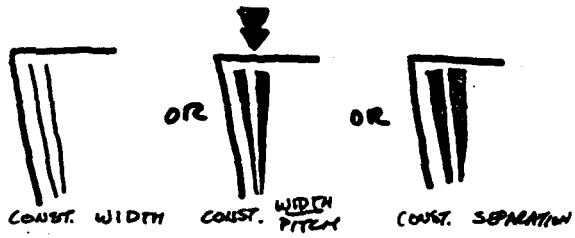

INITIAL STUDY

(34)

- 5 STRIP SINGLE SIDED DEVICE
- $N_D = 10^{12}/cm^3$
  $V_D = -50V$
  PITCH = 50μ
  STRIP WIDTH = 10μ
  PARALLEL DEVICE
- DIFFUSION
  NO TRAPPING
  " LEAKAGE
  " FLUCTUATIONS

INITIAL STUDY (CONT.)

(35)

RESULTS - SPM V1.01

- $Q_{coll}(X_0)$ LOOKS QUALITATIVELY CORRECT ⇒ AREAS UNDER STRIP ELECTRO-STATICALLY SEPARATED. $Q_{coll}(X_0 = 32\mu) = 1fC$
- TIME WALK ($= t_{cross} - t_{impact}$) < 11 ns FOR 1 fC BUT MUCH LONGER FOR 2, 3 fC
- PULSE SHAPES LOOK QUALITATIVELY CORRECT (???)
- INDUCTION CAUSES NEIGHBORING STRIP TO ALWAYS FIRE
  ⇒ 2 CLOSEST STRIPS FIRE

NEED SOME MEASUREMENTS

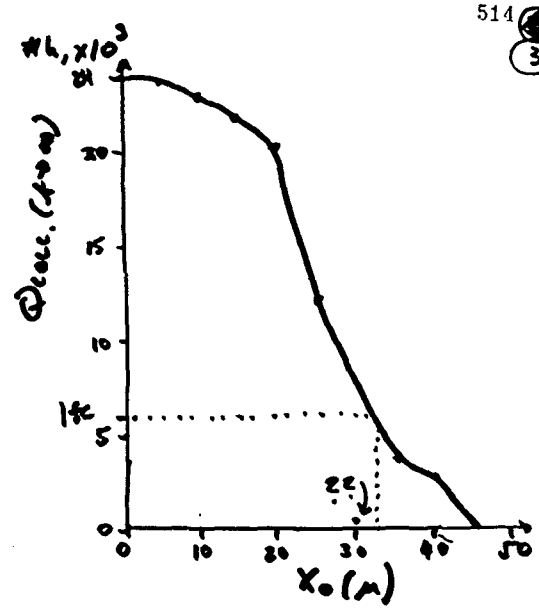

MANY THANKS TO KATE CRYSTAL AND JOE CARLSON!!

SIMULATIONS
CONCLUSIONS

- VERSION 1.00 → WORKING BUT PROBABLY NOT USEFUL (UNREALISTIC)
- VERSION 2.04 NOW READY AND BEING TESTED

NEED SOME DATA TO SEE IF WE ARE ON THE RIGHT TRACK!

CONCLUSIONS

- JHU #1 PROTOTYPE IN HAND → BEING TESTED (LEAKAGE CURRENTS HIGH)
- JHU #2 - IN FINAL DESIGN STAGE W/ MICRON → WAIT FOR RESULTS FROM JHU #1
- LASER PULSER BEING PUT TOGETHER
- SIMULATIONS BEING TESTED

PLENTY TO DO!

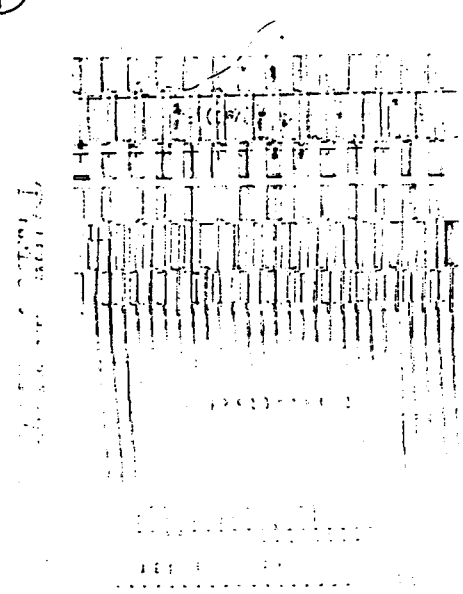

TOP_SILOX

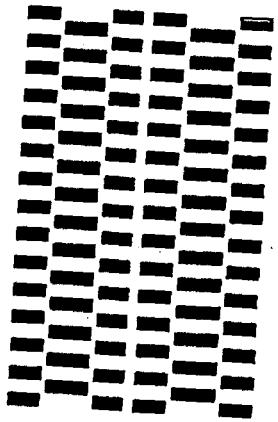

520

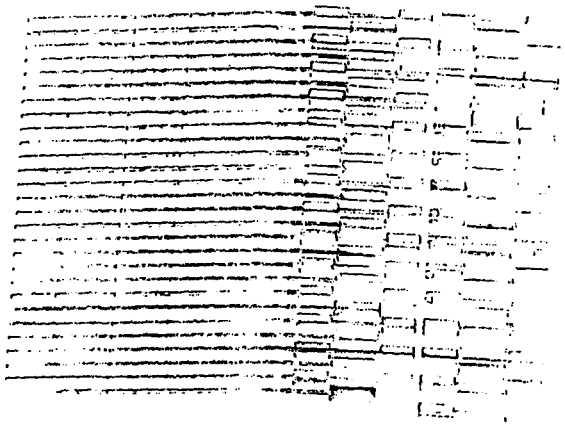

521

BOTTOM CONTACT

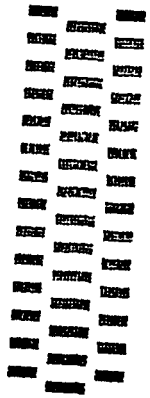

518

BOTTOM N+

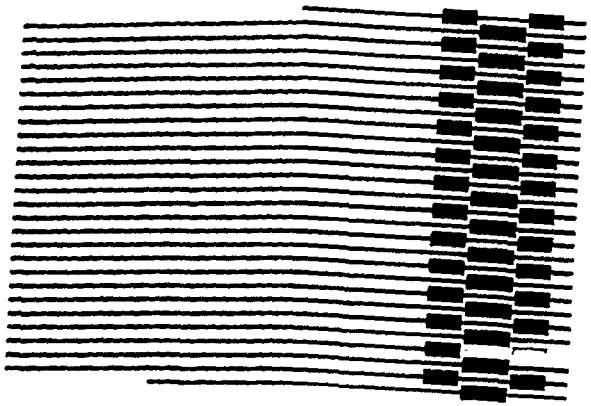

519

BOTTOM SILOX

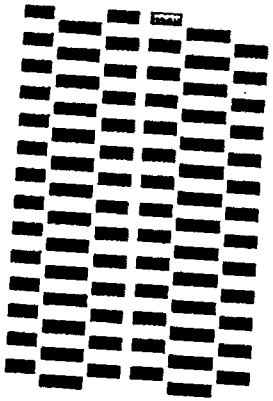

521

TOP_CONTACT

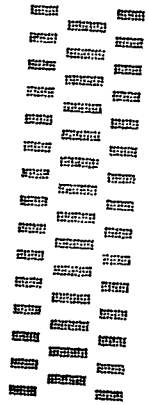

522

BOTTOM P+

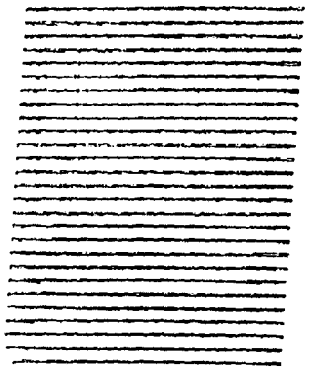

525

TOP_PPLUS

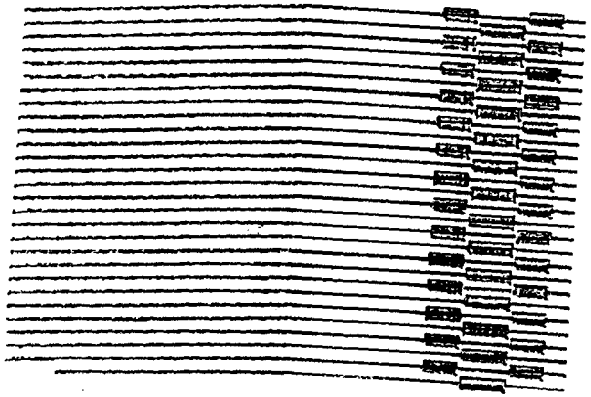

523

Quality Assurance

Hartmut F.-W. Sadrozinski
(Santa Cruz Institute for Particle Physics)

QUALITY ASSURANCE (QA)

- Design
- Thorough test of many parameters under many operational conditions.

  Prototypes before manufacturing.

  Samples during manufacturing (i.e., take $\frac{1}{N}$ sample of production – N = 100?)

QUALITY CONTROL (QC)

- Test of crucial parameters on every channel.

QA TESTS (Prototypes, samples)

QA Bipolar Chips (all channels on a die)

Threshold curves for 3 inputs (1,2,4 fC)

Temperature cycles

Butane

Irradiation (Gamma)

Input Protection

Power consumption

QA CMOS Chips (full functional chip)

Functionality

Voltage quantity

Irradiation

Butane

Thermal cycling

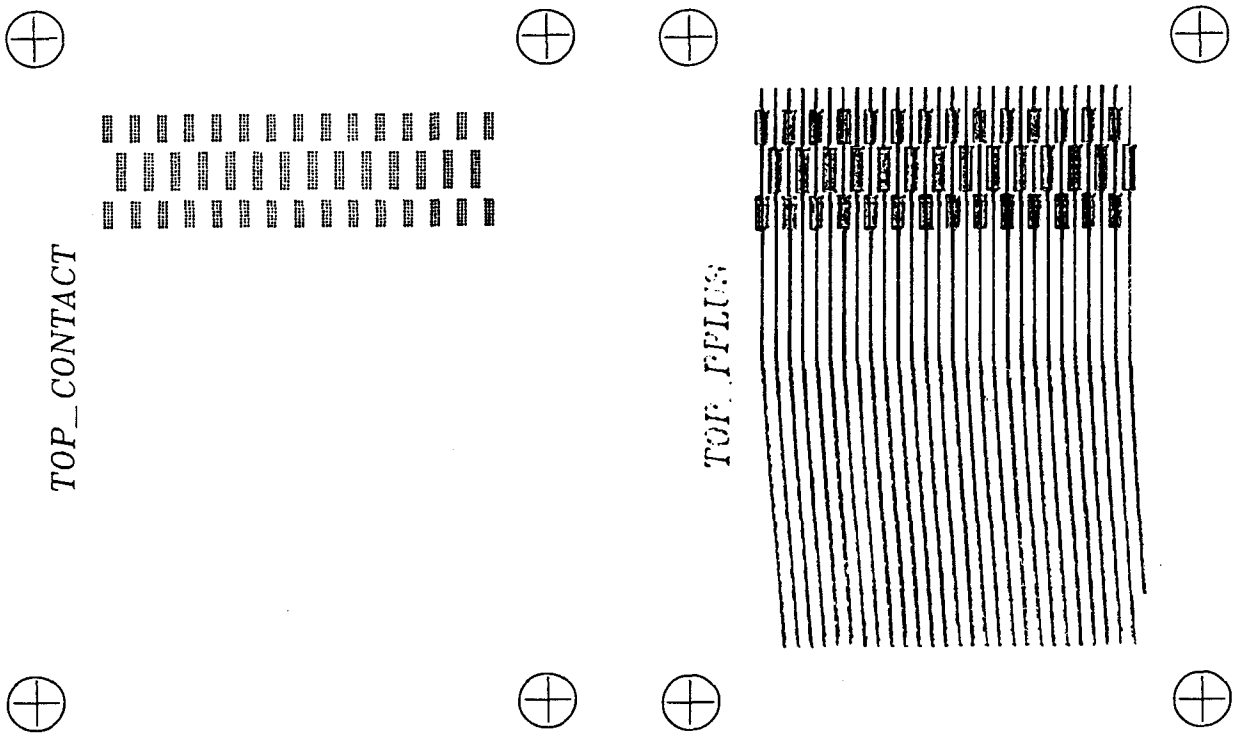

QC TESTS (All channels)

Bipolar Chips (every chip with probecard)

Power

Count rate at 1 fC input with 0.5 and 2 fC threshold

CMOS Chips (every chip with probecard at factory?)

Power.

Test vectors.

Detectors (every detector on probecard)

Leakage on guard, bias.

Leakage through every coupling cap.

Value of bias resistor.

Modules (every module)

Guard ring current.

Bias current.

Readout laser pulsar signal on every channel.

Silicon CDR

A. Seiden
UCSC

This past year have made major progress in a number of areas - hear in subsequent talks.

Decisions:

12 cm readout units.
2 Chip front-end; bipolar amplifier, shaper, discriminator plus digital storage chip.
Geometrical layout + simulations.
10 mrad stereo angle.

Hope in next few months to finalize conceptual design of fiber readout system.

Expect to test full detector modules around October. With successful completion of these tests will have design of basic units out of which we make detector.

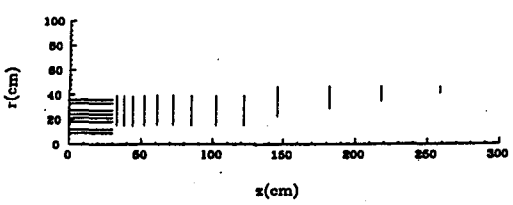

Fig. 1. Silicon tracker design.

Table 2. Dimensions for tracker

Barrel	r	z	
(1)	9 cm	30 cm	
(2)	12 cm	30 cm	
(3)	18 cm	30 cm	6.78 m² for Barrel.
(4)	21 cm	30 cm	
(5)	24 cm	30 cm	
(6)	27 cm	30 cm	
(7)	33 cm	30 cm	
(8)	36 cm	30 cm	
Disks	r_{in}	r_{out}	z
(1)	15 cm	39 cm	33 cm
(2)	15 cm	39 cm	38 cm
(3)	15 cm	39 cm	44 cm
(4)	15 cm	39 cm	52 cm
(5)	15 cm	39 cm	61 cm
(6)	15 cm	39 cm	72 cm
(7)	15 cm	39 cm	85 cm
(8)	15 cm	39 cm	102 cm
(9)	15 cm	39 cm	122 cm
(10)	22.5 cm	46.5 cm	146 cm
(11)	28.5 cm	46.5 cm	182 cm
(12)	34.5 cm	46.5 cm	218 cm
(13)	40.5 cm	46.5 cm	258 cm
		Total Area = 15.94 m²	

10.16 m² for Disks (both sides)

Barrel

8 layers
Inner radius = 9 cm
Outer radius = 36 cm
Half length = 30 cm
Number of detectors = 3,600

Forward and Backward System

13 disks on each side
On average about 7 layers hit for each track
Inner radius = 15 cm
Outer radius = 46.5 cm
Half length = 258 cm
Number of detectors = 3,112

Full System

Total area = 17 m²
Number of channels = 6.5 million (2 × 50,000 chips)
Power per channel = 1 mW

All detectors are double-sided.
ϕ measurement on one side,
10 mrad small angle stereo on other side.

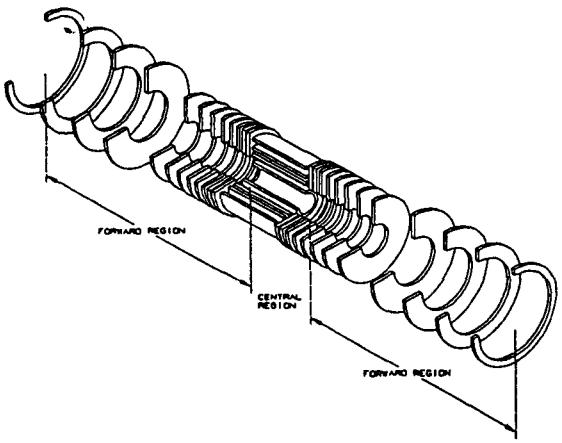

STS detector arrays (pictorial view).

Extrapolation of Tracks from Silicon

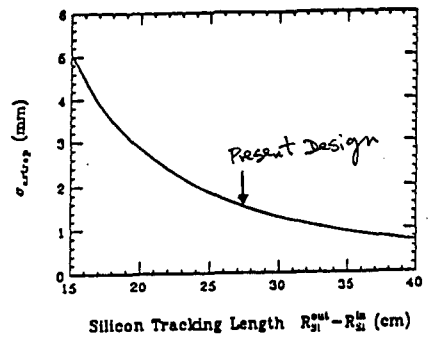

Fig. 6. Position error at 1.6 m radius vs. silicon tracking length.

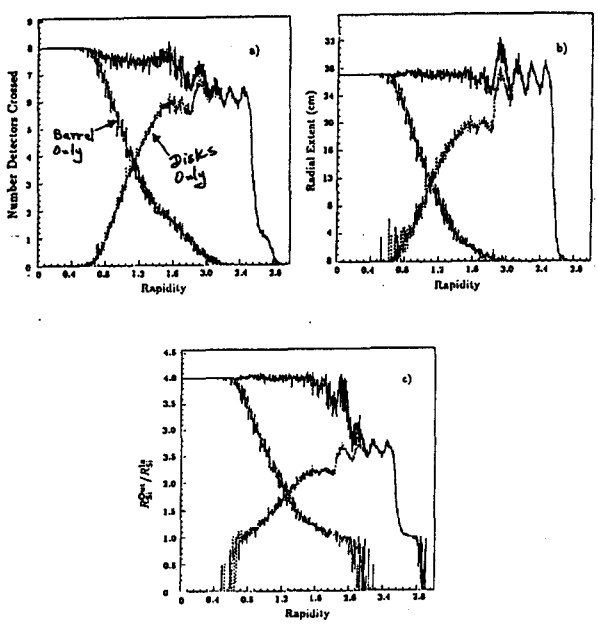

Geometrical Characteristics of Design, Averaged over Beam Spot Size.

300 GeV $H^0 \to e^+e^-\mu^+\mu^-$

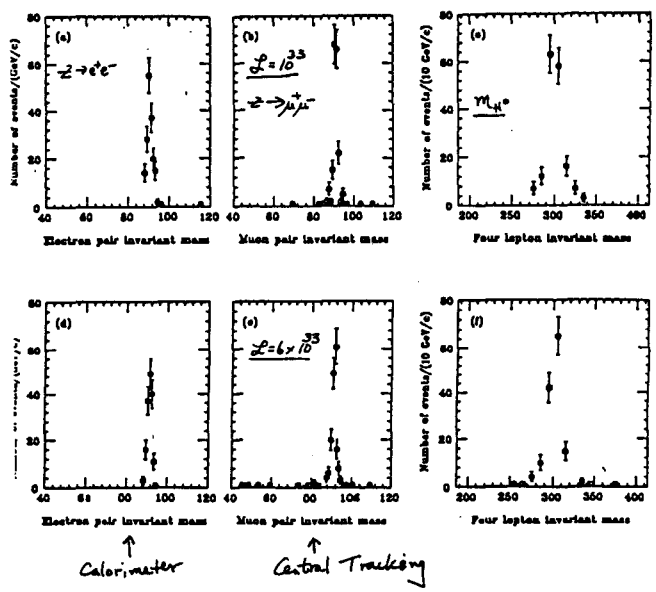

Summary of efficiencies and number of fake tracks for $H^0 \to e^+e^-\mu^+\mu^-$ events for various configurations

Luminosity	Fakes per event with p_t>5 GeV/c	Track efficiency p_t>10 GeV/c	Electron E/p efficiency 0.7<E/p<1.4	M_Z cut efficiency e	μ	Higgs reconstruction efficiency
1×10^{33}	0.03 ± 0.01	0.991	0.96 ± 0.01	0.99 ± 0.01	0.99 ± 0.01	0.84 ± 0.04
3×10^{33}	0.04 ± 0.02	0.989	0.96 ± 0.01	1.00 ± 0.01	0.97 ± 0.01	0.83 ± 0.04
6×10^{33}	0.18 ± 0.03	0.972	0.93 ± 0.01	1.00 ± 0.01	0.93 ± 0.02	0.75 ± 0.04

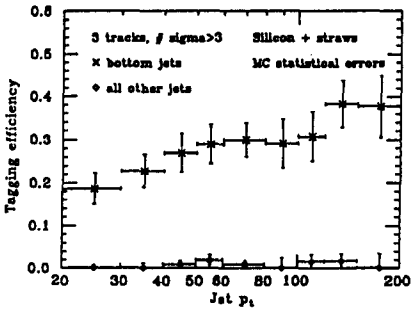

b tagging efficiency vs. jet p_t for the full tracking system.

Must complete R&D within about 2 years. Includes making final prototypes of everything. Have to concentrate very hard to get this done on time!

Silicon Tracking System (STS)

Mechanical Design Review

KEK Meeting
May 27, 1992

W. Miller
Los Alamos National Laboratory

STS Mechanical Design

Topics

- Design Requirements
- Construction Description
- Material Considerations
- R&D Accomplishments
- Future Work

STS Top Level Requirements

Characteristic	Requirement	Approach
Material radiation length	< 3% @ normal incidence	● Low-Z materials, ultralightweight structures, low mass electrical cables/connectors
Positional stability	R_ϕ, R, Z-5, 80, 250 μm respectively	● Ultrastable, ultra-stiff support structures and materials ● Kinematic mounting of subsystems ● System isothermality
Electronic cooling	13 kW @ 2 mW/channel heat dissipation	● Evaporative cooling system (phase change @ constant temp) ● Non-corrosive fluid compatibility with electronic circuits and strip detector
Detector sub-cooling	0°C silicon strip detector operation at near 1 atmosphere	● Hydrocarbon evaporative cooling fluid (Butane)
Radiation exposure	10 Mrad, throughout 10 years service life	● Select rad-hard materials
Maintainability	Accessibility and detector replacement	● Maintainable silicon module sub-structures

STS Top Level Requirements

Alignment

- Maximum local misalignment (resolution of alignment measuring equipment)

Silicon	5 μm	Circumferential
	250 μm	Z (barrels) or R (disks)
	80 μm	R (barrels) or Z (disks)
Global	10 μrad's	Azimuthal rotation of silicon vs straws or gas microstrips
	15 μm	Common centering silicon vs straw
	40 μm	Common centering silicon vs gas microstrips
	500 μm	Centering of tracker on beam

- Maximum placement error (complete STS)

Silicon	25 μm	Circumferential
	250 μm	Z (barrels) or R (disks)
	80 μm	R (barrels) or Z (disks)

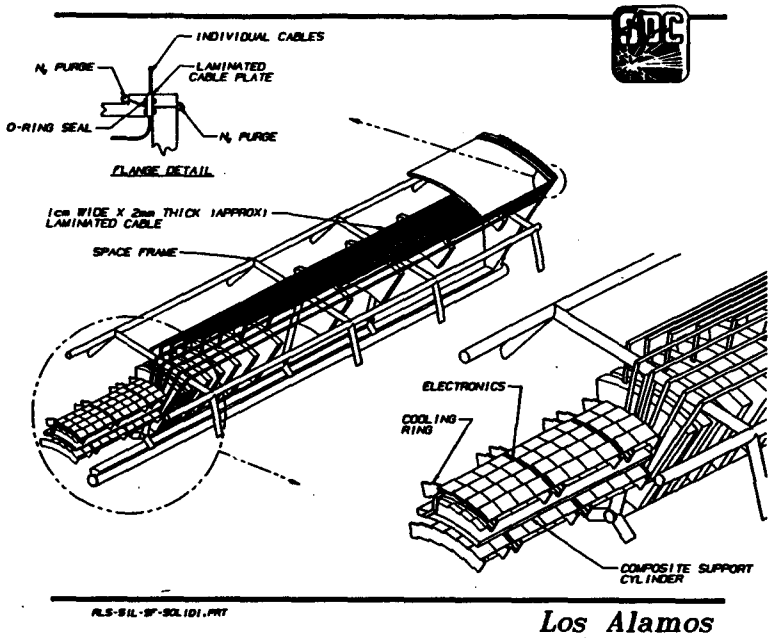

SILICON TRACKING SYSTEM

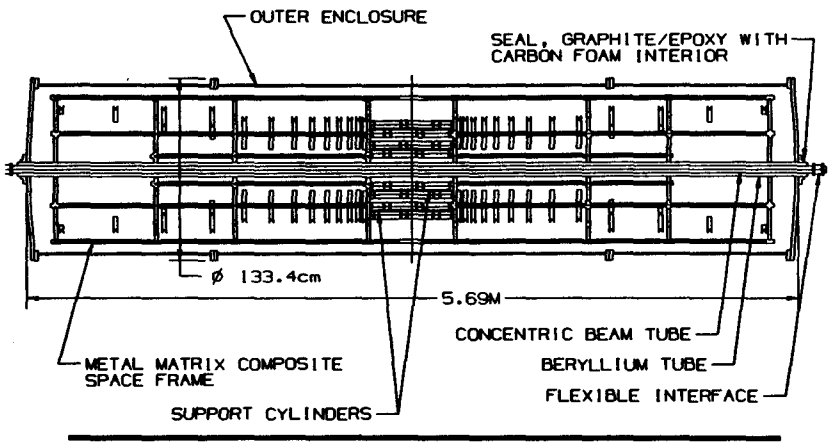

SILVG-005-GEJ
VG SCALE = .045

Los Alamos

FWD REGION (Section)

Silicon Tracking System

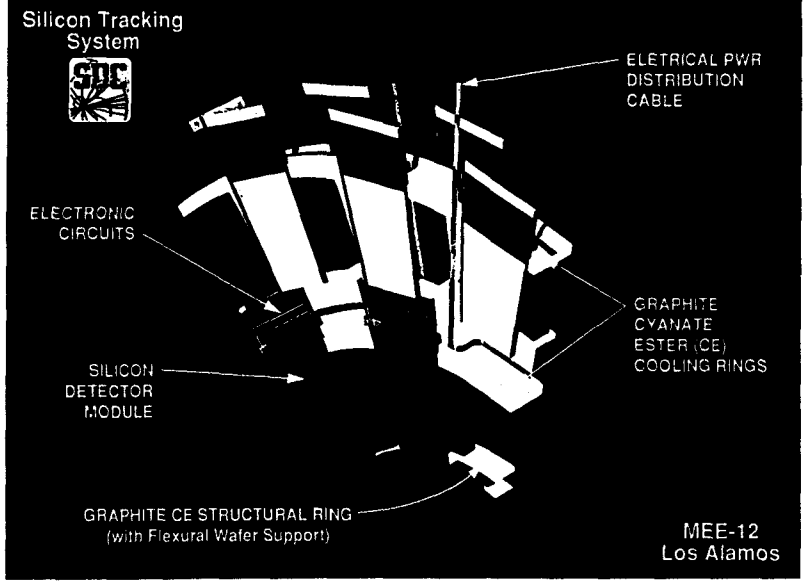

MEE-12
Los Alamos

SILICON DETECTOR WITH SPACE FRAME (Cut Away)

Silicon Tracking System

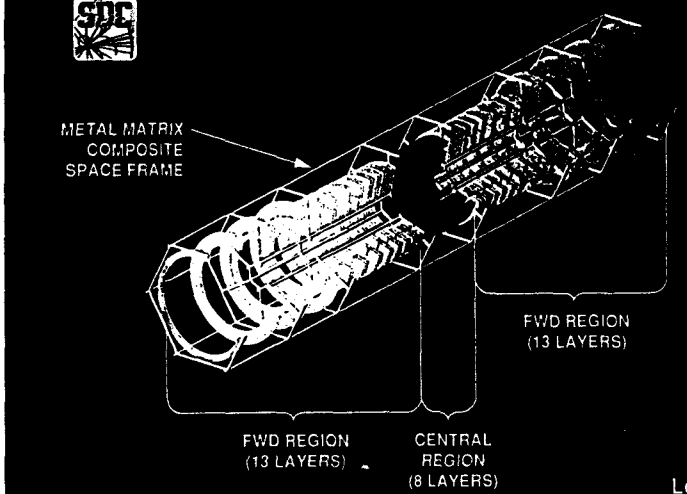

MEE-12
Los Alamos

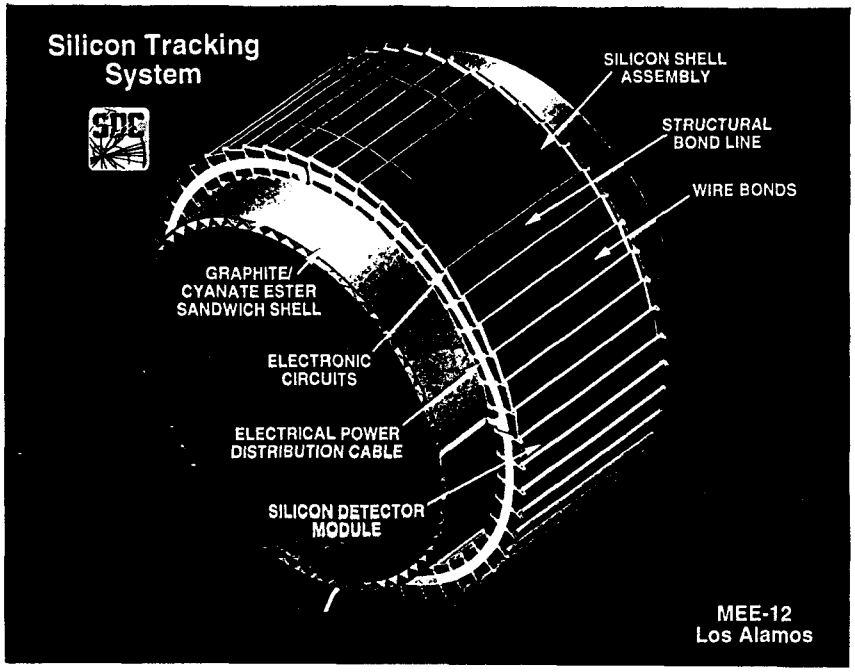

SHELL STRUCTURES

4-Point Bend Test Experiment Setup

Graphite/Epoxy Sandwich Panel Core Study

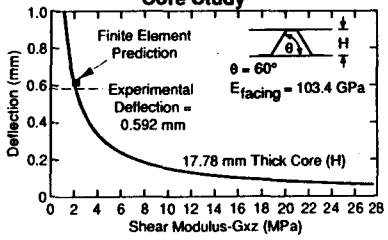

Graphite Epoxy Radiation Test Panel

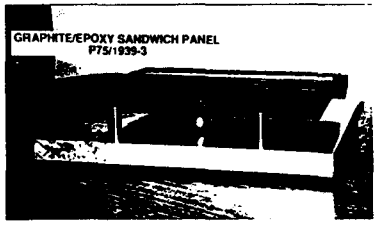

MEE-12/WM-c602

Los Alamos

MEE-12/WM-577

Silicon Detector Description and Quantities

Component	Central Region	Forward Region (total)
Silicon Wafers	3600	3112
Electronics Modules	1800	1632
50 μm Strips	2,304,000	4,177,920
Silicon Layers	8	26
Silicon Subassemblies	12	26
Silicon Detector Modules	1080*	1632

12-cm-long modules total, 1440 of which are structurally joined to form 720, 24-cm-long assemblies

Los Alamos

MEE-12/WM-578

Silicon Detector Module Specifications

	Central Region	Forward Region
Shape:	Rectangular	Trapezoidal
Active Detector Width:	3.2 cm	~6.4 cm
Number of Channels:	1280 (640 per side)	2560 (1280 per side)
Heat Dissipation:	1 mW per channel*	1 mW per channel*
Module Heat Load:	1.28 W	2.56 W
Thermal Conductive Area: (at cooling surface)	0.8 cm x 3.3 cm	~0.8 cm x 6.5 cm
Module Heat Flux: (at cooling ring surface)	0.5 W/cm^2	0.5 W/cm^2
Operational Temperature: (at silicon detector surface)	0°C	0°C
Cant angle:	~7.4°	0°

* Cooling system design point 2mW/channel

Los Alamos

Silicon Shell Support Results
(preliminary)

Gravity Effects - Cooling Ring/with Silicon Weight Included

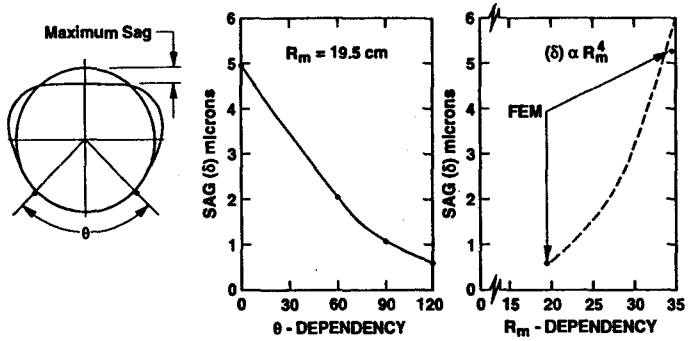

Ring Material - P75/1939 Quasi-Isotropic
E = 109.2 GPa

Los Alamos

STS Silicon Shell (Gravity Loading)

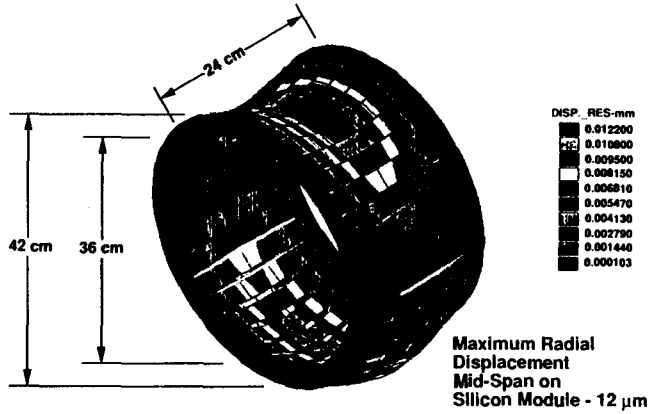

Maximum Radial Displacement Mid-Span on Silicon Module - 12 μm

MEE-12/WM-c625

Los Alamos

Silicon Tracking System

THERMAL STABILITY STUDIES

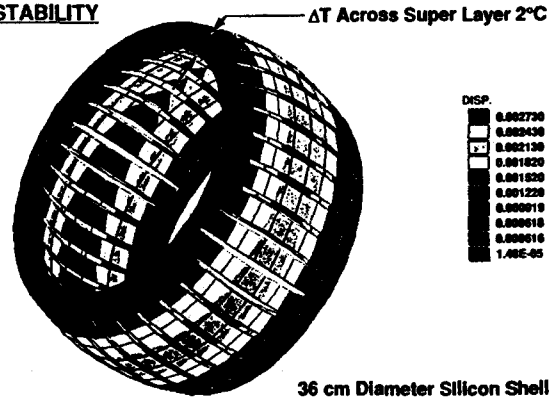

36 cm Diameter Silicon Shell

MEE-12/WM-c584

Los Alamos

Silicon Shell Support Results
(preliminary)

Gravity Effects - Silicon Detector Module/IM6 Graphite Strips

Simple Beam Module (FEM)

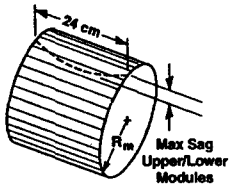

	Sag - Microns	Module Sag: Δ sag* micron
R_m - 19.5	12.40	11.59
R_m - 34.5	21.22	13.89

*Removing ring deflection

Module sag is virtually independent of cylinder radius

For L = 20 cm vs 24 cm Δ sag = 8.0 microns max @ R = 34.5 cm

Quasi-Isotropic IM6, E = 78.3 GPa

Los Alamos

Central Region Support Study

Interim Results

Module Sag - Localized effect, upper and lower modules

- **Contribution from module is virtually independent of shell radius, but dependent upon graphite strip geometry and material properties**
  - **For span between cooling < 24 cm sag contribution diminishes as L^3**
- **Ring contribution increases with shell radius to 4th power**
  - **Linearly dependent upon ring material properties**
  - **Analysis must be revised after cooling ring material investigation is complete**

Los Alamos

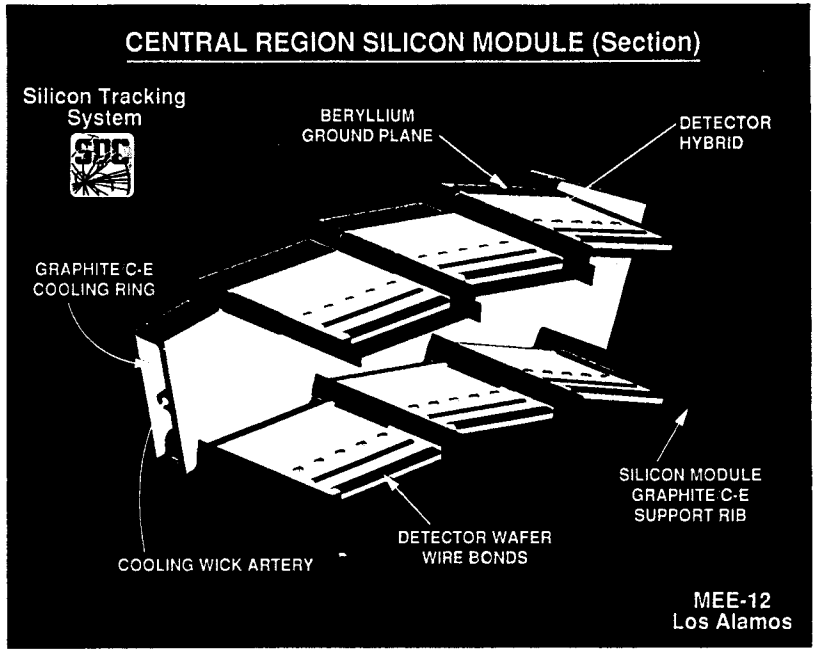

Silicon Tracking System

Cooling Ring NDT Evaluation (Ultrasonic)

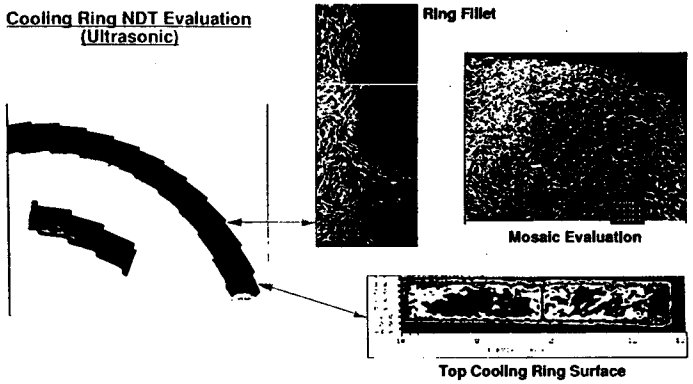

MEE-12/WM-c589

Los Alamos

Silicon Tracking System
COOLING RING k_T TEST SUMMARY

Vendor/Reports Data

- Chopped Fiber/Phenolic Resin (MX 4925 Molding Compound 43/57 V/O)
- Generic Laminate (SAMPE/1985)
- UHM Graphite/Epoxy 60/40 V/O

Experimental Data - STS Program

- Cooling Ring (30° Segment)/MX 4925 Phenolic Molding Compound
- Cooling Ring (30° Segment) P75/954-3 60/40 V/O (1)
- Cooling Ring (30° Segment) P75/954-3/AlN 43/45/12 V/O
- Cooling Ring (30° Segment) P75/954-3 60/40 V/O (2)

(1) 90 µm Fiber Length
(2) 400-600 µm Fiber Length

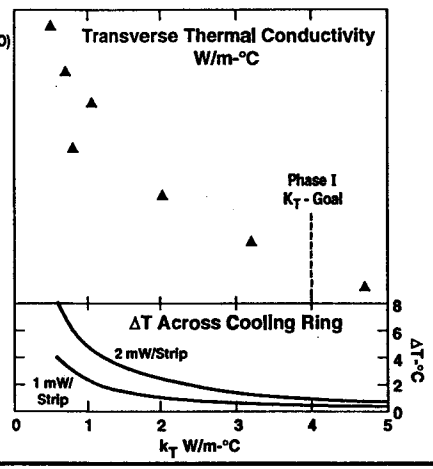

Los Alamos

Silicon Tracking System

TV HOLOGRAPHY INSPECTION TECHNIQUE

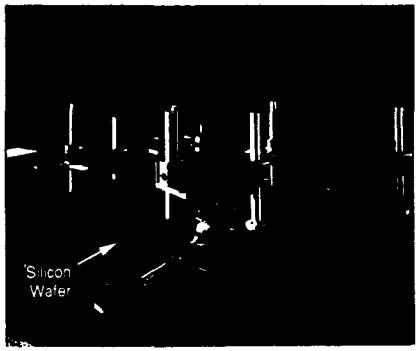

OPTICAL BEAM PATH

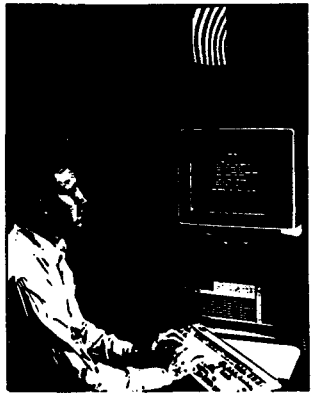

FRINGE PATTERN

MEE-12/WM-c591

Los Alamos

Silicon Tracking System

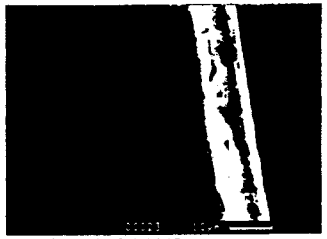

EDGE CONDITIONS FOLLOWING DIAMOND CUTTING

STRIPS/BONDING PAD AREA

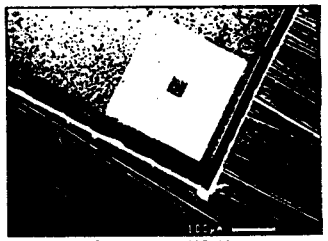

CORNER FIDUCIAL

MEE-12/WM-592

Los Alamos

Silicon Tracking System

Cooling Ring/Wick Test

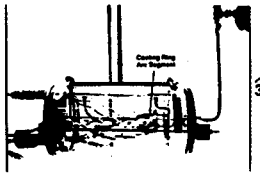

30° Segment Test

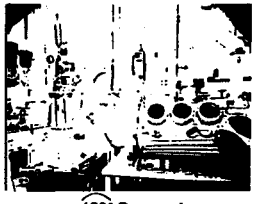

120° Segment

Wick Test

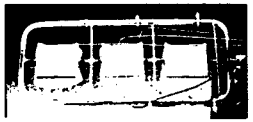

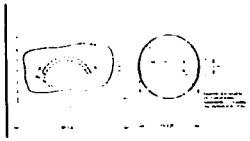

Cooling Ring Test Chamber

MEE-12/WM-c588

Los Alamos

Silicon Tracking System

Wick Development

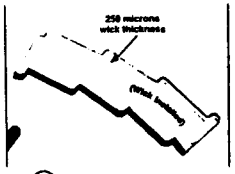

30° Segment Machined Polystyrene Wick

Molded Wick Specimen (~400 μm thick Polystyrene)

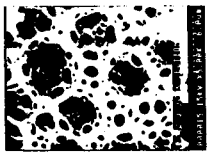

Wick Structure Photomicrograph

Delrin Mold

MEE-12/WM-c587

Los Alamos

STS Materials Summary

Component	Material	Key Criteria
Cooling and Structural Rings	P75 Chopped Graphite Fiber/Cyanate Ester resin	● Moldable material for fabricating complex ring geometry ● Low Coefficient of Thermal Expansion (CTE) ● Low Coefficient of Moisture Expansion (CME) ● Minimize structural distortions from thermal gradients ● Radiation resistant, zero creep structure ● High radiation length (25 cm)
Cooling Ring Wick	Polystyrene	● Moldable material for replicating complex geometry ● Microstructure tailorable (4 μm, pore radius) to achieve optimum wicking behavior ● High radiation length ● Radiation resistant
Support Cylinders (central region)	UHM Graphite Fiber/ Cyanate Ester resin 25 μm prepreg	● Ultra thin prepreg, less susceptible to fracture ● Sandwich shell construction with ultra low areal density, 1.2 kgm/m^2 ● Quasi-isotropic facing sheet construction for maximum stability

Los Alamos

STS Materials Summary (cont)

Component	Material	Key Criteria
Enclosure	UHM Graphite Fiber/ Cyanate Ester 25 μm prepreg	● Construction same as support cylinders ● Part of STS support concept requires maximum stiffness and stability
Cable	Laminated Beryllium	● Low voltage power transmission for electronics ● Require high radiation length (35 cm) ● Solderable
Space Frame	Metal Matrix Composite (Mg-graphite)	● Maximum stiffness and stability to limit potential distortion from 5 meter truss "metrology" frame ● Stiffness 50% > G/cyanate ester ● Near zero CTE and zero CME ● Zero creep ● Impervious to butane and radiation

Los Alamos

KEY STS MAJOR MILESTONES

- Conceptual STS design and preliminary structural studies completed
- Materials for all major components have been selected
- Butane evaporative cooling proof-of-principle tests, with machined polystyrene wick completed
- Demonstrated moldability of polystyrene wicks to desired microstructure
- Compression molded ultra-thin (450 μm) high thermal conductivity cooling ring segments (P75/cyanate ester - 30° arc segments)
- Developed mold process steps for graphite/polymeric composite cooling ring
- Demonstrated durability and fabricability of 24 cm long edge-bonded silicon detector module
- Established construction techniques for ultra-light weight (1.2 kg/m^2) graphite/ composite sandwich shell
- Demonstrated 5 μm stability of truss core panel after exposure to 1×10^{15} n/cm^2
- Verified butane and composite material compatibility in radiation environment
- Preliminary assessment of strip detector compatibility with butane, adhesives, and graphite composite materials complete
- Developed alignment methods for achieving 25 μm placement accuracy (Rϕ)

Los Alamos

KEY STS NEAR TERM GOALS

- Complete mold development process steps for full 360° cooling ring
  - Dimensional quality
  - Material property uniformity
  - High transverse thermal conductivity
- Successful performance demonstration of a fully integrated cooling ring/molded polystyrene wick
  - Artery feed integration
  - Performance boundaries
- Silicon shell (central region) stability demonstration test (0°C)
  - 5 μm stability
- Complete demonstration of assembly/alignment of large silicon shell structures
  - Reasonable construction
  - Maintainable
  - 25 μm placement
- Completion of material compatibility tests in radiation environment
  - Detector
  - Graphite/cyanate ester
  - Electronic chips
- Demonstrations of kinematic mount performance for silicon substructures

Los Alamos

Mechanical Design Study at KEK

T. Kohriki and Y.Unno
Physics, KEK

Abstract

Mechanical design of the Barrel section of the Silicon tracking system of the SDC is being studied at KEK. The design of support ring is approached from a different point of view to the CDR of the STS. One end-plate for 8 layers of ladders has advantages of precision machining and alignment. An epoxy-CFRP plate was machined and evaluated for mechanical stability against moisture. A structure with cyanate-CFRP skin and porous-Carbon core is being investigated to have much better stability. A wick which has higher permeability is also being investigated.

Introduction

• Barrel in the CDR

- Four Silicon ladder cylinders

- Two Silicon cylinders kinematically supported from one support cylinder
- Two support cylinders supported from the space frame

→

- Many split- joints
  to fix the position of a Silicon cylinder
- Independent Silicon cylinders
  has various advantages but...

- Other concerns:

- Molded cooling ring/thin-wall glue-joint to form box structure
  No trade-off for accuracy - strength ?
- Kinematical mounts to be glued on a ladder

A Different Approach

• One end-plate

- Precision press forming (sandwich, e.g.)
- Precision machining

• This has advantages of

- Easy machining, higher freedom in design
- High strength
- High precision with machining
- High mechanical stability
  due to no split-joint for layers
- High precision ladder placement
  by placing ladder on high precision surface
- Alignment markers on outer edge
  determines all the layers

• Disadvantages?
(Many of advantages of the CDR might become ...)

- Must insert the ladders and align middle ladder in case of fixing - might be solved by careful thought
- Integration of the wick
- Lateral motion stability near the center
  - plate is strong
  - Box structure of
  plate-8 layers of Silicon ladders - plate

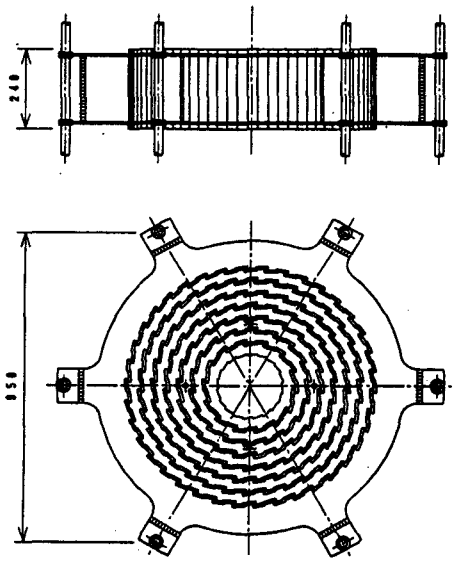

BARREL ASSEMBLY

Epoxy-CFRP endplate

- First try for machining

- Used in space programs but ...
  - Not a sandwich plate
  - Not a polycyanate resin

- Material specification

- Fiber:	M40 (PAN class)
- Resin:	Bisphenol A (Epoxy resin)
- Ply orientation:	0°/90°/±45°
- Plate thickness:	0.75 mm
- Ply:	8 plies
- V_f:	58%
- Elastic modulus:	79 GPa[1]
- CTE[2]:	1.12 ppm/°C
- Moisture absorption:	~1.2 wt%

- Process:

- Press forming
- Milling machine cutting

[1]Pa = N/m²: kgf/mm² = 9.8x10⁶ Pa
[2]CTE = Coefficient of Temperature Expansion

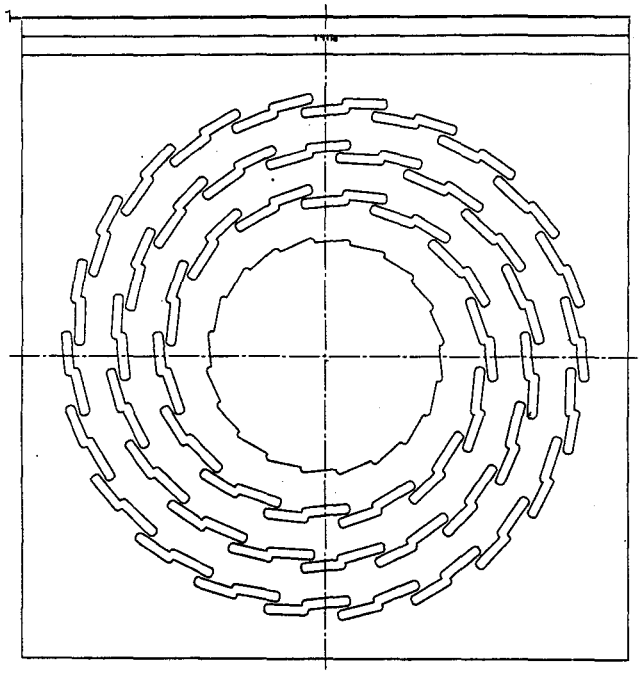

Moisture Absorption and Dimensional Stability

- Epoxy-CFRP

- Cycle:

- Initial state → Drying (Vac. & 80°C) → Moisture absorption (Water bath & 80°C) → Drying

- Distorted near 1 wt%
- Much smaller distortion with polycyanate resin

Note:
- No moisture distortion on Carbon fiber
- Only resin is affected by moisture

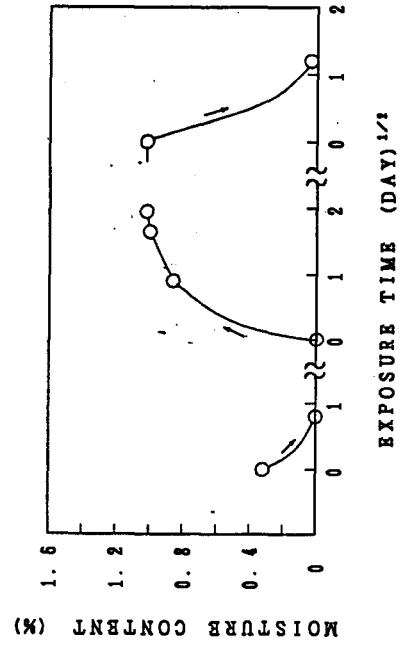

579

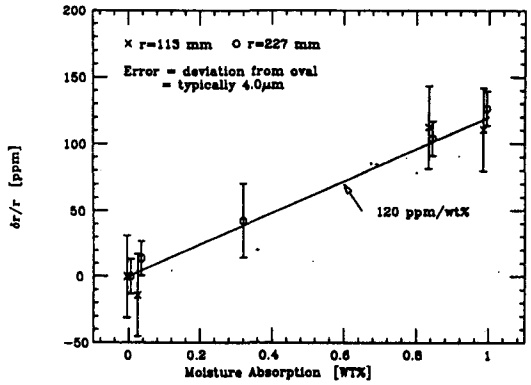

580

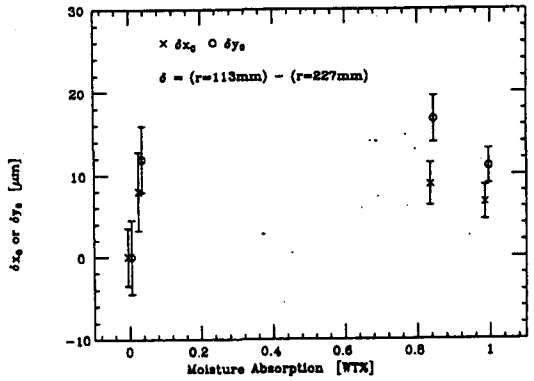

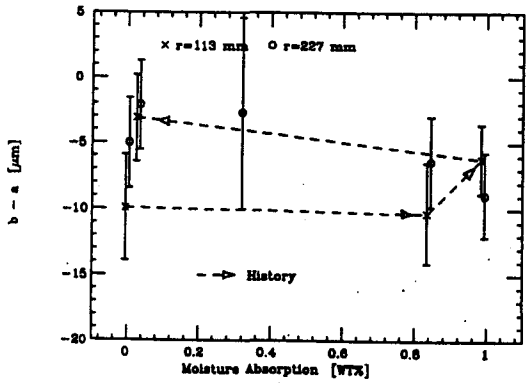

581

A New Sandwich Plate

- Thin skin & Porous core sandwich
- Skin:

- Granoc® XN50A/RS-3

- Manufacturer:	Nippon Petrochemicals Co. Ltd.
- Carbon fiber:	Granoc XN-50A
- Resin:	Polycyanate
- Ply orientation:	0/90/±45
- Number of plies:	8 plies
- Thickens:	0.22 mm
- V_f:	60%
- Elastic modulus:	101 GPa
- CTE:	-0.2 ppm/°C
- Moisture absorption:	0.49 wt%
- CME[3]:	28.8 ppm/wt%
(- Radiation length:	~28 cm)

582

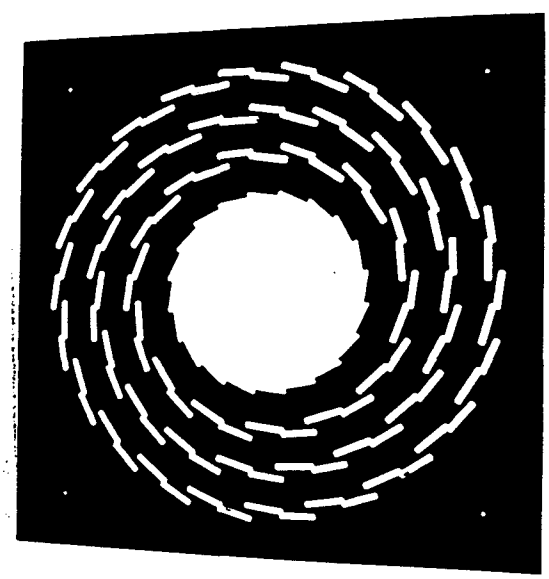

[3]CME = Coefficient of Moisture Expansion

• Porous Core:

- Porous Carbon PC5565

- Porous diameter:	55 μm(2~100 μm possible)
- Porosity:	65 % (~70% possible)
- Density:	0.45 g/cm^3
(- Radiation length:	94.6 cm)
- Bending modulus:	4 GPa
- Thickness:	2 mm (1~15mm possible)
- CTE:	0.6 ppm/°C

• A comparison ...

- CDR:
  2x (2 x 450 μm Graphite/Epoxy Cooling ring)
  + two G/E support cylinders (effective 670 μm)
  = ~ 0.72 + 0.27 %X_o= ~1.0 %X_o

- Polycyanate-CFRP/Porous carbon core sandwich:
  2 x (2 x 220 μm Skin + 2 mm Core, e.g.)
  = ~ 2 x (0.32% + 0.21%) X_o
  = ~ 1.1 %X_o

- Two-plate connecting frame adds some mass
- Same order; can be thinned more...

CFRP Study

• Polycyanate-CFRP (calculation@V_f=60%)

Designation	Layer Structure	Elastic Modulus GPa	CTE ppm/°C	Moisture Absorp. wt%	CME ppm/wt%
XN40/RS-3	Type1	118	+0.1	0.49	25.3
	Type2	78	+0.2	0.49	38.0
XN50A/RS-3	Type1	150	-0.2	0.49	19.2
	Type2	101	-0.2	0.49	28.8
XN70A/RS-3	Type1	216	-0.6	0.49	13.9
	Type2	144	-0.6	0.49	21.0
M40J/RS-3	Type1	117	0.9	0.46	28.0
	Type2	75	0.9	0.46	42.0

Type1: [0°/90°]ns, Type2: [0°/90°/+40°/-45°]ns
Moisture absorption: at a relative humidity 60% and the room temperature
CME: distortion from the moisture absorption to the absolute dryness
M40J: PAN-high elasticity cargon fiber

• Possible application areas:

- Support Ring/Plate:

CTE	~ 0 ppm/°C	XN40/RS-3/Type2
		XN50A/RS-3/Type2
	~ 1 ppm/°C	M40J/RS-3/Type2

- Ladder Rib:

CTE	~ 0 ppm/°C	XN40/RS-3/Type1
		XN50A/RS-3/Type1
	~ 1 ppm/°C	M40J/RS-3/Type1

- Space Frame:

CTE ~ -0.5 ppm/°C XN70A/RS-3

- When super-high elastic PAN-Carbon fiber orientation is used with Polycyanate resin RS-3, Polycyanate-CFRP has about the same (Radiation length x Elasticity) value as Mg-MMC.

- CFRP is much easier to process than MMC.

Wick Study

- A wick made by dissolving binders
  - very good control on the size of pores 0.1~10 μm
  - very good connection of neighboring pores
  - high permeability
  - has been used for various filter elements
- Samples:
  - Polyvinylalchole (PVA) r_p~5μm
  - Polysulfone r_p~0.1~1μm
  - Polystyrene will be possible after R&D
- Wick location - outer on the plate
  - easy maintenance

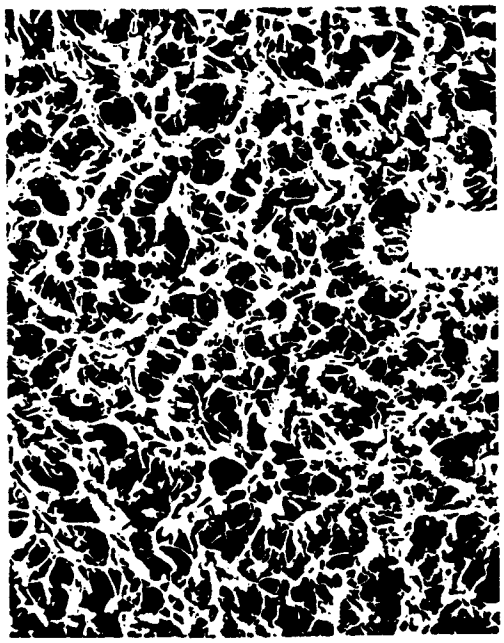

Summary

- KEK has been investigating the mechanical design of the Silicon Tracking System of the SDC, so far independently from Los Alamos.
- A different approach is taken to design the support of the barrel silicon cylinder, i.e. one end-plate for 8 layers, whose advantage is easily obtainable high precision and easy alignment of the whole set of cylinders.
- Study on mechanical stability has been started, machining an Epoxy-CFRP plate, against moisture absorption. This showed a CME of ~120 ppm/wt%.
- A CFRP based on Polycyanate resin has much better characteristics for moisture absorption, e.g. ~20 ppm/wt%, and a sandwich plate will be manufactured with Polycyanate-CFRP skin and a porous carbon core.
- A wick material study shows there is a good candidate using a manufacturing process of dissolving binders which has good control on diameter of pores and continuity.
- In future, we would like to go along with Los Alamos for the mechanical system realization.

ALIGNMENT : PLACEMENT TOLERANCES

Hans Ziock

KEK meeting
May 1992

LANL

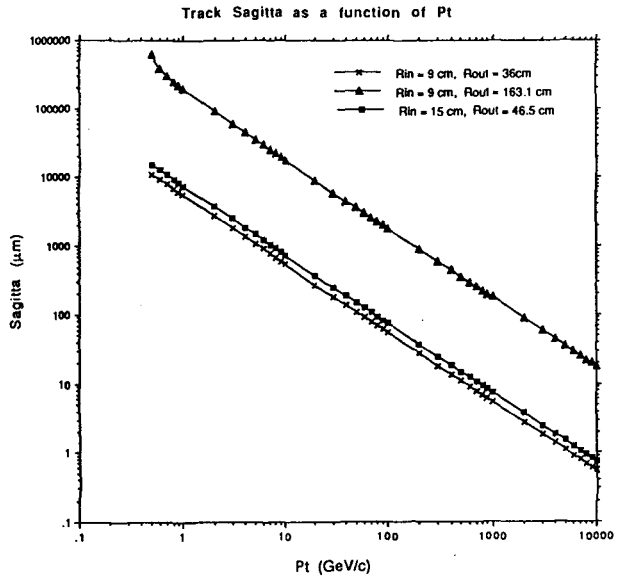

TWO QUESTIONS:

1) How accurately must the positions and orientations of the detectors be known at all times relative to some externally defined global reference system, and

2) How accurately must detector components be placed, regardless of how well their positions and orientations are later determined?

LANL

Concentrate on placement tolerances

Given the measured coordinates and orientations of the detectors one can **in principle** always translate from the local detector coordinate system to the global coordinate system

In practice

- Involves complicated math
- 6 constants/detector
- 3-D hit information

Questions

- Is there enough time for the calculations?
- Are all the constants known all the time?
- Is true 3-D information for a hit available?

LANL

PRECISION DESIRED

$\sigma_{r\phi} = 50\mu m/\sqrt{12} = 14.43\ \mu m$

Would like to be dominated by intrinsic detector resolution, not knowledge of detector locations

$\therefore$ Would like to know positions in $r\phi$ to 1/3 of that value ~ 5 μm

$\Rightarrow$ Total error = 15.3 μm

Similar considerations apply for other variables:

$\sigma_K = 2.81 \times 10^{-5}\ m^{-1}$ from inherent resolution of barrel Si - Straw system

$\therefore$ Would like other contributions to σ_K to be $\sim 10^{-5}\ m^{-1}$

LANL

LEVEL II TRIGGER CONSIDERATONS

- Level II $\sigma_{pt}/p_t^2 = 5\ (TeV/c)^{-1} \Rightarrow \sigma_{pt}/p_t = .005 p_t$ [p_t in (GeV/c)]
- $\sigma_{pt}/p_t^2 = 0.005\ (GeV/c)^{-1} = 2\sigma_K/.3B \Rightarrow \sigma_K = 0.0015 m^{-1}$ (B = 2 Tesla)
- Level II decision time ≤ 50 μsec
- All local ⇒ global transformations
  - Involve only *adds & multiplies* using constants
  - Will use *adds & multiplies*
- Detector does not measure 3-D point
  - Instead provides two independent 2-D measurements
  - Must correlate those to get 3-D point
  - Not always possible
- No reliance on stereo information to correct $r\phi$ information
- Level II resolution for forward region comes mainly from Si

LANL

Rotation of the strips about the x-axis by an angle β

Vertical height covered by a single strip becomes

$h = L\sin\beta + P\cos\beta$ where:

L is the detector length = 12 cm
P is the detector pitch = 50 μm
[Note that as $\beta \to 0$ the vertical height goes to P as it should.]

Averaging h^2 over the area covered by a single strip gives:

$$\sigma^2 = \frac{\int_{-P/2}^{P/2}\int_{-L/2}^{L/2} (z\sin\beta + y\cos\beta)^2\, dz\, dy}{\int_{-P/2}^{P/2}\int_{-L/2}^{L/2} dz\, dy}$$

$$\sigma^2 = \frac{\int_{-P/2}^{P/2} \left[\frac{z^3}{3}\sin^2\beta + zy^2\cos^2\beta + z^2 y\sin\beta\cos\beta\right]\Big|_{-L/2}^{L/2} dy}{PL}$$

$$\sigma^2 = \frac{\int_{-P/2}^{P/2} \left[\frac{L^3}{12}\sin^2\beta + y^2 L\cos^2\beta\right] dy}{PL}$$

$$\sigma^2 = \frac{\left[\frac{L^3}{12}y\sin^2\beta + \frac{y^3}{3}L\cos^2\beta\right]\Big|_{-P/2}^{P/2}}{PL}$$

$$\sigma^2 = \frac{L^2\sin^2\beta + P^2\cos^2\beta}{12}$$

$$12\sigma^2 - P^2 = (L^2 - P^2)\sin^2\beta$$

$$\sin\beta = \sqrt{\frac{12\sigma^2 - P^2}{L^2 - P^2}}$$

FOR L = 12 cm
P = 50 μm

desired σ (μm)	σ (comment)	Lsinβ (μm)
14.434	$P/\sqrt{12}$	0.00
15.000		14.14
15.275	$\sqrt{(P/\sqrt{12})^2 + 5^2}$	17.32
16.000		23.92
16.137		25.00
17.000		31.11
18.000		37.26
19.000		42.80
20.000		47.96

Lsinβ is the amount one end of a strip is raised relative to the other.

Assuming that in placing detectors in $r\phi$, one would introduce at most a comparable raising of one end of the detector relative to the other, one sees that a 25 μm value produces a total error 12% greater than the inherent resolution of the detector.

For a high momentum track from the origin

$$\phi = \phi_0 + Kr \qquad \text{where}$$

K is the curvature
ϕ_0 is the initial track azimuth
ϕ is the azimuth, and
r is the radius

Fitting a track corresponds to minimizing the squared deviations between the curve described by the preceding equation, and the measured circumferential distances d.

$$\chi^2 = \sum_{i=1}^{m} \frac{(r_i\phi_i - d_i)^2}{\sigma_i^2}$$

The sum is carried out over the m layers. Differentiating χ^2 with respect to ϕ_o or K and setting the result to 0 yields the following equations

$$\begin{pmatrix} \Sigma\frac{r_i^2}{\sigma_i^2} & \Sigma\frac{r_i^3}{\sigma_i^2} \\ \Sigma\frac{r_i^3}{\sigma_i^2} & \Sigma\frac{r_i^4}{\sigma_i^2} \end{pmatrix} \begin{pmatrix} \phi_o \\ K \end{pmatrix} = \begin{pmatrix} \Sigma\frac{r_i d_i}{\sigma_i^2} \\ \Sigma\frac{r_i^2 d_i}{\sigma_i^2} \end{pmatrix}$$

which have as solutions

$$\begin{pmatrix} \phi_o \\ K \end{pmatrix} = M \begin{pmatrix} \Sigma\frac{r_i d_i}{\sigma_i^2} \\ \Sigma\frac{r_i^2 d_i}{\sigma_i^2} \end{pmatrix}$$

where

$$M = \frac{1}{\Sigma\frac{r_i^2}{\sigma_i^2}\Sigma\frac{r_i^4}{\sigma_i^2} - \left(\Sigma\frac{r_i^3}{\sigma_i^2}\right)^2} \begin{pmatrix} \Sigma\frac{r_i^2}{\sigma_i^2} & \Sigma\frac{r_i^3}{\sigma_i^2} \\ \Sigma\frac{r_i^3}{\sigma_i^2} & \Sigma\frac{r_i^4}{\sigma_i^2} \end{pmatrix} \qquad (1)$$

Writing the matrix M as $\begin{pmatrix} A & -B \\ -B & C \end{pmatrix}$ we have (2)

$$K = C\,\Sigma\frac{r_i d_i}{\sigma_i^2} - B\,\Sigma\frac{r_i^2 d_i}{\sigma_i^2}$$

$$K = \sum_{i=1}^{m}\left(C\frac{r_i^2}{\sigma_i^2} - B\frac{r_i}{\sigma_i^2}\right) d_i = \sum_{i=1}^{m}\alpha_i d_i \qquad (3)$$

which will have an error

$$\delta K = \sum_{i=1}^{m}\alpha_i \delta d_i$$

For the statistical error in the curvature measurement due to the resolution of the individual $r\phi$ measurements (*i.e.* $d_i = P/\sqrt{12}$), from the above we have

$$\sigma_K^2 = \sum_{i=1}^{m}\alpha_i^2 \delta d_i^2 \qquad (4)$$

Using 25 μm for δd_i (the nominal placement error), 6 layers for m, and the values of r_i in the forward silicon system for a track with n = 2.5, we find using eq 1 -> 3

layer	Z (m)	r (m)	α (m^{-2})
1	1.0200	0.1686	-7.6298
2	1.2200	0.2016	-7.3376
3	1.4600	0.2413	-6.2131
4	1.8200	0.3008	-2.9434
5	2.1800	0.3603	2.2260
6	2.5800	0.4264	10.1976

and then from eq. 4) $\sigma_K = 4.0947 \times 10^{-4}\ m^{-1}$. Comparing this to the level II trigger requirement $\sigma_{pt}/p_t^2 = 5\ (TeV/c)^{-1}$ @ 1 TeV/c, or $\sigma_K = 1.5 \times 10^{-3}\ m^{-1}$, we see again that the 25 μm placement requirement accuracy in $r\phi$ leads to an error in σ_K which is approximately 1/3 the total resolution value we are trying to achieve (just as desired).

For the combined silicon - straw barrel system, the values of the coefficients α_i for the 13 layers are given below. I have assumed

σ = 12 μm for the silicon layers and
σ = 80 μm for the straw superlayers.

Silicon Layer #	Radius (cm)	α_i (m^{-2})	Straw Superlayer #	Radius (cm)	α_i (m^{-2})
1	9	-0.257	1	81.6	0.021
2	12	-0.323	2	110.3	0.067
3	18	-0.425	3	135.1	0.124
4	21	-0.461	4	148.8	0.161
5	24	-0.487	5	163.6	0.206
6	27	-0.504			
7	33	-0.507			
8	36	-0.494			

As before,

$$\delta K = \sum_{i=1}^{m}\alpha_i \delta d_i$$

The table indicates that:

a) All the silicon layers except the inner two make an approximately equal contribution to the curvature and therefore the momentum measurement. The inner two layers however contribute significantly to the impact paracter measurement, and would contribute more to the momentum measurement if one were not assuming vertex constraint.
b)The inner few straw superlayers are only important for pattern recognition, and
c) The outer few straw layers have a large impact on the momentum measurement.

Using the values given above for α_i and the σ values of the individual layers as the δd_i in the following equation

$$\sigma_K = \sum_{i=1}^{13}\alpha_i^2 \delta d_i^2$$

we find $\sigma_K = 2.81 \times 10^{-5}\ m^{-1}$, or

$$\frac{\sigma_{pt}}{p_t^2} = \frac{2\sigma_K}{0.3B} = 0.09\ (TeV/c)^{-1} \qquad @\ 1\ TeV/c,\ B = 2\ Tesla$$

Radial Displacement

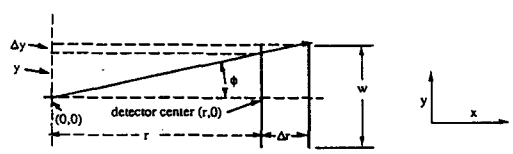

Consider a detector whose center is a radial distance r from the origin. Again assume that the detector center is at x=r, y=0, z=0, and that the strips are parallel to the z-axis. At a position y on the detector, the angle of a ray from the origin to that point is given by

$$\tan\phi = y/r. \qquad (5)$$

At a radial position r + Δr, the new y position is (r+Δr)tanφ and the error in y (Δy) is then Δrtanφ, or using (5)

$$\Delta y = \Delta r y/r$$

Averaging Δy^2 over the entire width (w) of the detector gives:

$$\sigma^2 = \frac{\int_{-w/2}^{w/2}\left(\frac{\Delta r y}{r}\right)^2 dy}{\int_{-w/2}^{w/2} dy}$$

$$\sigma^2 = \frac{\left(\frac{\Delta r}{r}\right)^2\left[\frac{y^3}{3}\right]_{-w/2}^{w/2}}{w} = \frac{(w\Delta r)^2}{12r^2}$$

$$\Delta r = \frac{\sigma r\sqrt{12}}{w}$$

Taking the worst case (r = 9 cm, w = 3.2 cm), and again assuming that the systematic error should be limited to ~5 μm, and one finds that

r (cm)	Δr (μm)	r (cm)	Δr (μm)
9	48.7	24	129.9
12	65.0	27	146.1
18	97.4	33	178.6
21	113.7	36	194.9

Conclusions

SILICON SYSTEM ALONE

- $r\phi$ placement tolerance of 25μm is well matched to system resolution
  - Rotation of strip
  - Level II trigger resolution requirements for forward section
- r placement tolerance of 80μm is well matched to system resolution
  - Could be slightly better for inner layers (50 μm)

SILICON / OUTER SYSTEM

LANL

Detector Module Design

Helmuth Spieler
LBL

SDC Silicon Tracker Meeting at KEK
May 27, 1992

Schematic of module assembly with cables

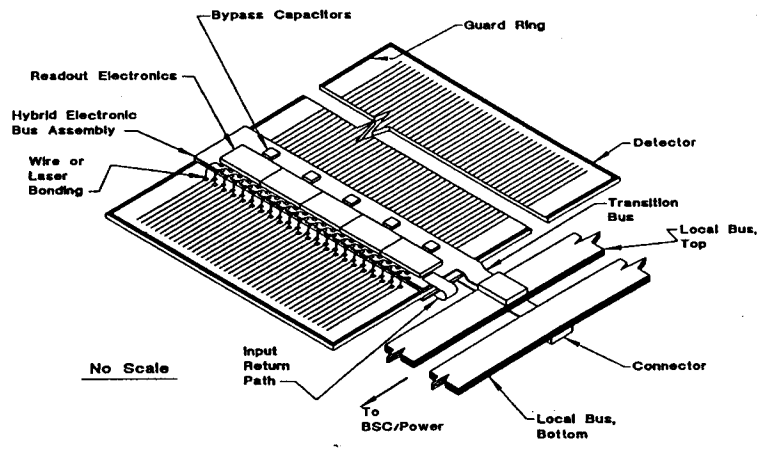

CROSS SECTION OF DETECTOR MODULE
(note difference in x and y scales)

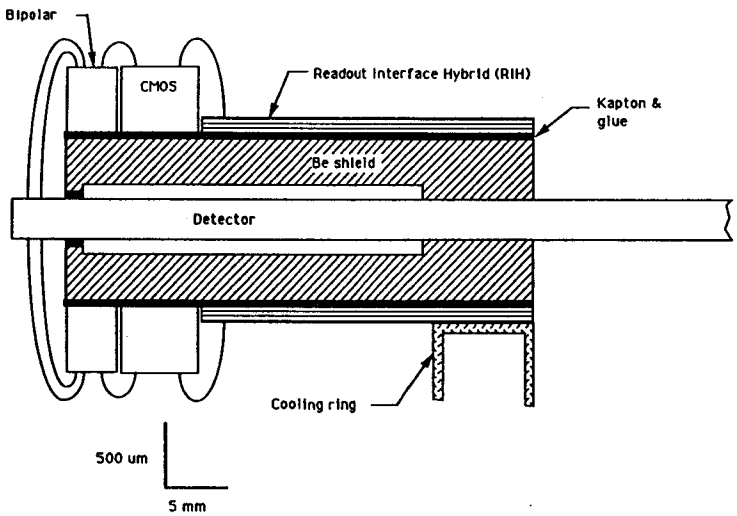

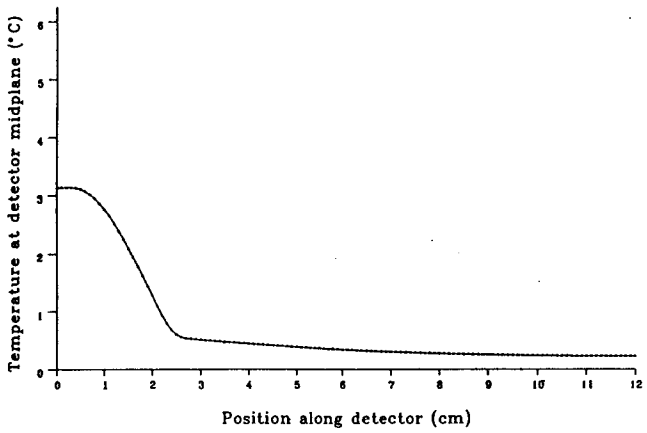

Detector temperatures for baseline configuration

Common Mode Coupling

Cross-coupling through shared signal paths

Typically addressed by

a) reducing common impedances
("copper braid syndrome")

b) decoupling networks
(series resistors/inductors, bypass capacitors, etc.)

Both incur excessive mass

Alternatives:

a) Break common paths through
proper signal and power routing
(Abolish "Ground Connections"!)
electronic design

b) Eliminate decoupling networks by
subdividing critical and "dirty" lines
electronic design
cable design

Helmuth Spieler
Nov. 1, 1991

IDEAL CONFIGURATON: ONLY LOCAL SIGNAL LOOPS

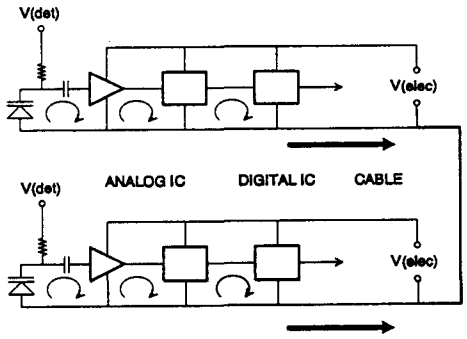

HELMUTH SPIELER
01-NOV-91

SINGLE-SIDED DETECTORS:
COMMON MODE COUPLING VIA DETECTOR BIAS LINE

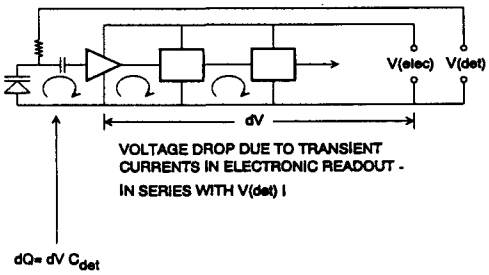

HELMUTH SPIELER
01-NOV-91

SINGLE-SIDED DETECTORS:
COMMON MODE COUPLING VIA DETECTOR BIAS LINE

ISOLATE DETECTOR BIAS LINE FROM ELECTRONICS

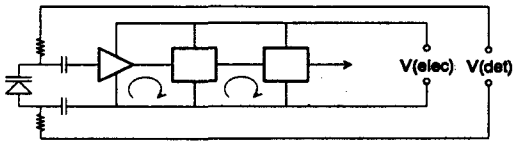

ADD RESISTIVE DIVIDER TO REFERENCE BIAS VOLTAGE
TO ELECTRONICS AND PREVENT CAPACITOR BREAKDOWN

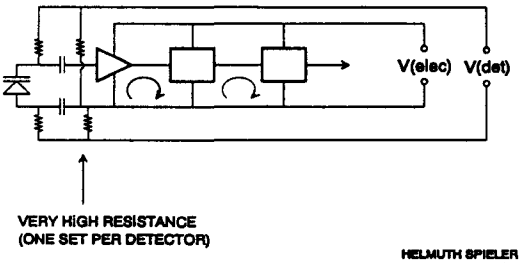

HELMUTH SPIELER
01-NOV-91

611

DETECTOR ARRAYS: SECONDARY LOOPS

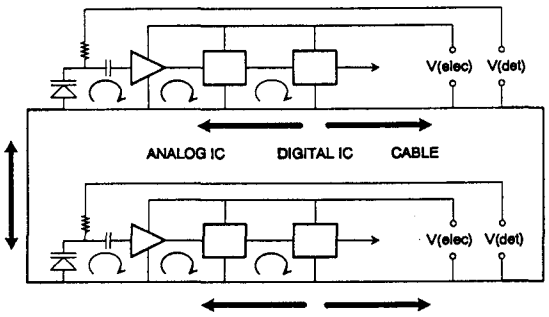

HELMUTH SPIELER
01-NOV-91

612

DETECTOR ARRAYS: BREAKING SECONDARY LOOPS

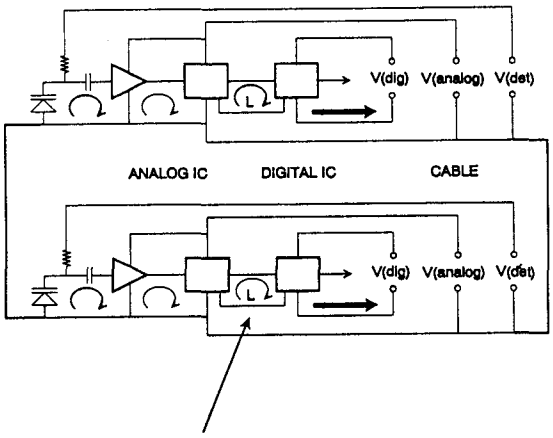

L: Local Signal Loop
One Connection per Channel,
but Only One Common Return per Chip.
Local Loop has High Impedance
to Digital Power Supply Lines.

HELMUTH SPIELER
01-NOV-91 rev.

613

INPUT CURRENT LOOP IN SIMPLISTIC DOUBLE-SIDED DETECTOR

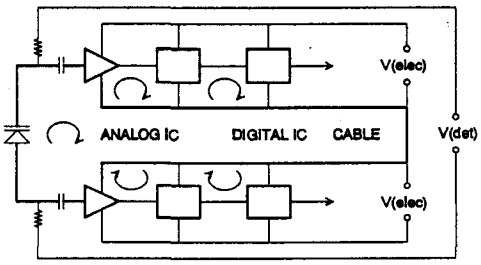

NDT RECOMMENDED

HELMUTH SPIELER
01-NOV-91

614

CONNECTION SCHEME FOR DOUBLE-SIDED DETECTORS

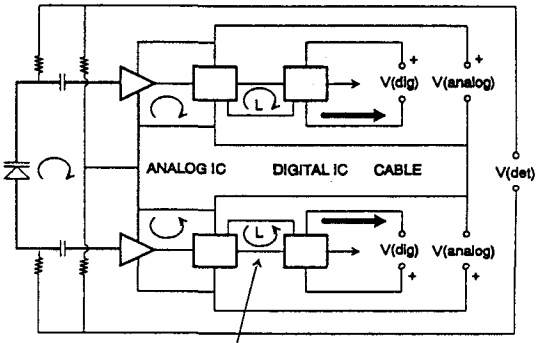

ON DETECTOR

L: Local Signal Loop
One Connection per Channel,
but only One Common Return per Chip.
Local Loop has High Impedance
to Digital Power Supply Lines.

HELMUTH SPIELER
01-NOV-91 rev.

Module Connections (Cable Traces)

I. DC voltages/currents

1. Detector bias	Positive Bias Negative Bias ground ref.	2 + 1
2. Analog Power V_{CC} = 3.5V Preampifier Current Set Analog ground		2 + 1
3. Comparator threshold (differential) use analog ground for reference		2
4. Calibration level (differential) (also 2 pulse lines, see below) use analog ground for reference		2
5. Digital Power V_{dd} = 5V Logic + Drivers Digital Ground		2 + 1
	Total DC Lines:	10 + 3

Pulsed Signals (all differential)

1. Calibration (off + 3 combinations)	2 x 2
2. Master Reset	1 x 2
3. Chip Control (send, receive + 2 other modes)	2 x 2
4. 60 MHz clock	1 x 2
5. I/O Bus	12 x 2
Total Data Lines:	18 x 2

SCHEMATIC CABLE LAYOUT

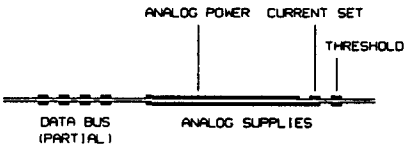

HELMUTH SPIELER
28-OCT-91

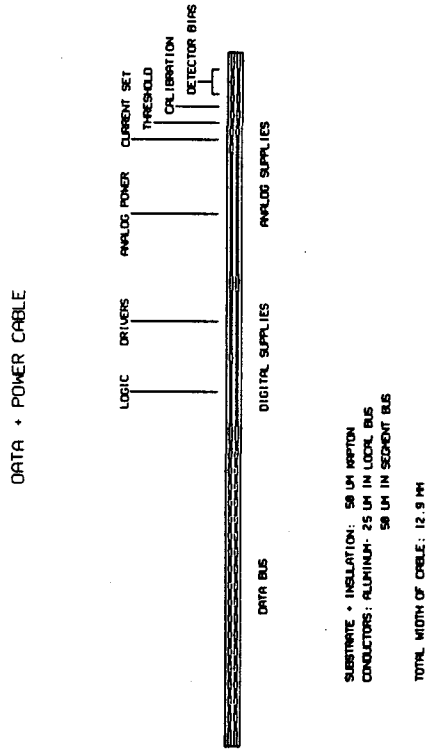

HELMUTH SPIELER
31-OCT-91

Status of Module Design

GOAL: Simplified module operational in Nov. 1992
to verify module design concept.
Settle design concept in early 1993

1. Analog IC (BJT)
   - circuit at AT&T (Issy Kipnis)
   - Layout complete
   - 1 chip with 64 complete channels
   - 1 test chip with 16 preamplifier array + circuit blocks
   - Run shared with Penn

   Submissions to Tektronix + Westinghouse this summer

2. Digital IC (CMOS)
   Three ICs in preparation:

   1. Test time stamping + buffering (UCSC) - beam test
      time stamping, data buffer,
      slow MUX for readout, differential outputs
   2. Fast readout (LBL) - to test fast readout of module
      time stamping, single stage buffer
      sparsification for fast readout, differential outputs
      (uses existing circuits + SVX2 sparsification)
   3. Final design (UCSC+RAL)
      time stamping, full buffering
      sparsification for fast readout, differential outputs

3. Prototype Cable
   - Multiconductor cable as shown in CDR
   - Copper cable received (trial run)
   - Aluminum cable in fabrication (w. connection pads)

ATT ANALOG IC (I. KIPHIS, UBL)

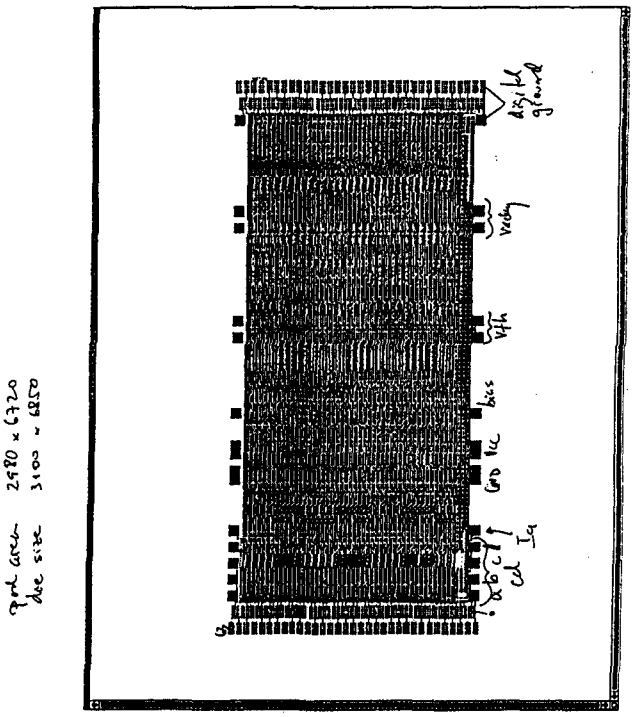

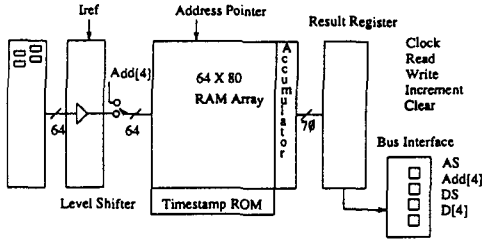

UCSC DIGITAL IC FOR TEST BEAM READOUT (J. DEWITT)

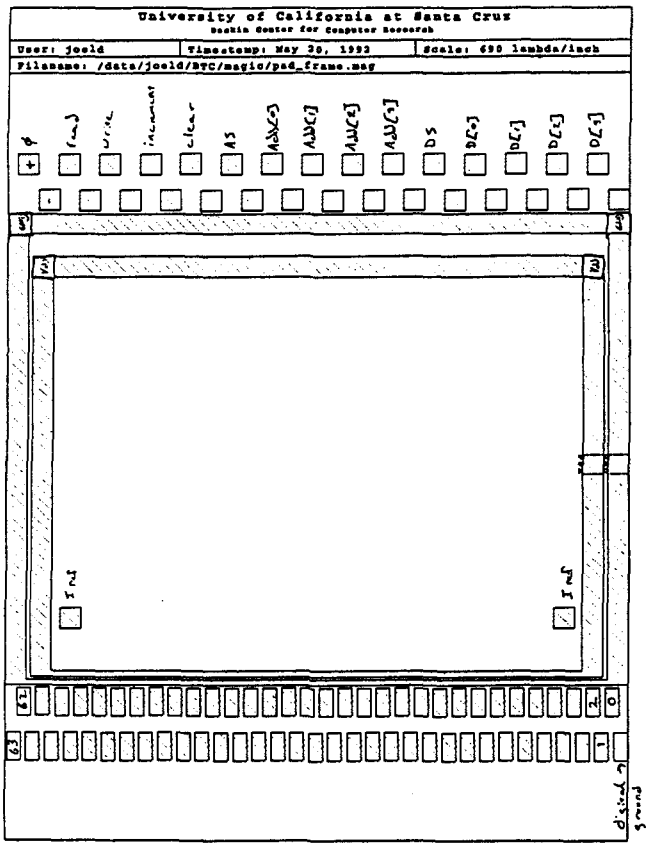

4. Cross-Talk Measurements

Bruce Schumm, Hiro Aihara

use existing strip detectors and hybrid preamps with external shaper + MCA

interference sources:

1. Dig. IC with 60 MHz counter
2. Cable (single-ended or differential)

Change spacing from detector and insert shielding materials of varying thickness

View oscilloscope traces, measure charge pick-up vs. shaping time, measure frequency spectrum

First Results: Thin shielding adequate (Be plate)

5. Substrate for test Readout Interface Hybrid

Minimal shielding, but careful differential layout required

Connecting lines from cable to 5 ICs

Radiation length of metal on substrate

'smeared' over 3.2 cm x 12 cm detector

Al: 0.04% (1.6% of silicon) 8 LAYERS

Cu: 0.25% (10% of silicon)

Proposal: use Cu for hybrid to allow standard technology ??

Al for local cables, Be for outer cables

Low mass connectors compatible with Cu and Al traces

Will draw up layout when I get back to LBL.

Ladder Assembling at KEK

T. Kohriki and Y. Unno
Physics, KEK

together with

Hamamatsu Photonics Co. Ltd

Abstract

Tools for assembling the Barrel ladder are being prepared. Using the tools, a ladder with mechanical detectors and Polycyanate-CFRP ribs is assembled. Wire-bondings are under investigation jointly with Hamamatsu Photonics Co. Ltd.

Introduction

• It is important to establish the technology of assembling the ladder of the Silicon Tracking System before the production starts.

• Major differences from the past experience are

- Double-sided sensor
- Frontend electronics on the sensor

• Many factors have to be addressed during the process ...

- assembly precision
- strength
- electro-mechanical interplay including bonding
- distortion against thermal cycle etc.
- Butane compatibility

...

Tools & Jigs

• Wafer aligner

• Ladder assembling jigs

• Precisions of the tools/jigs

- Parallelness, Flatness, ...

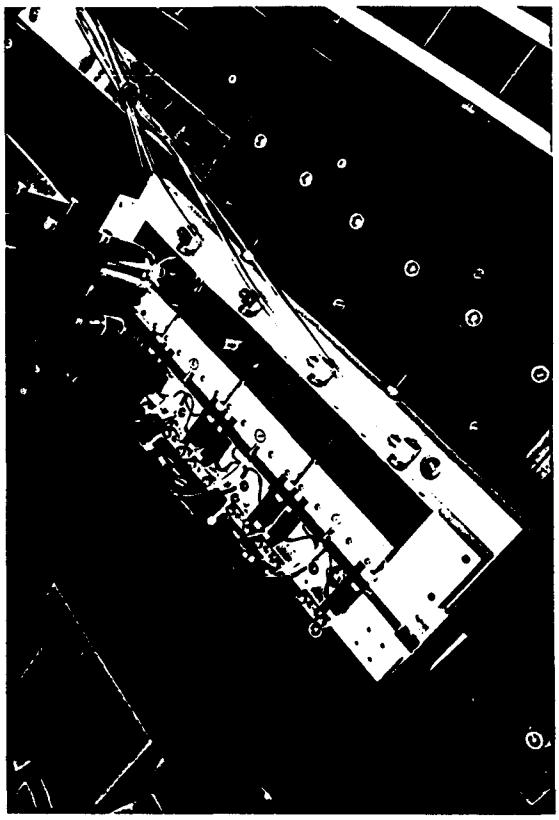

627

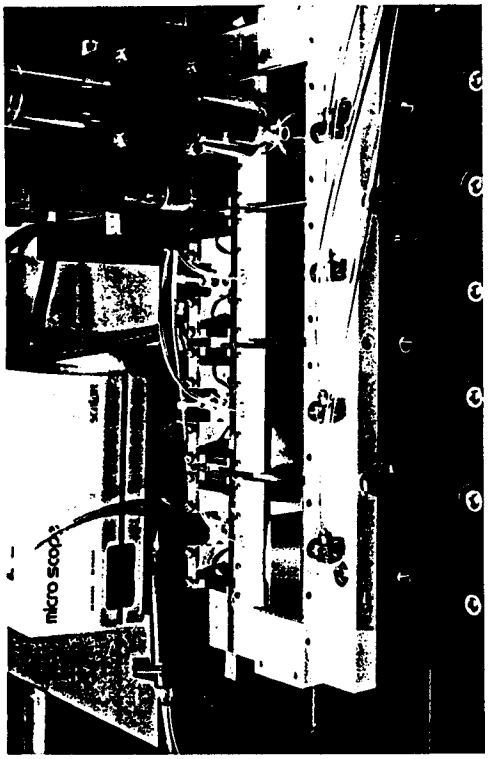

628

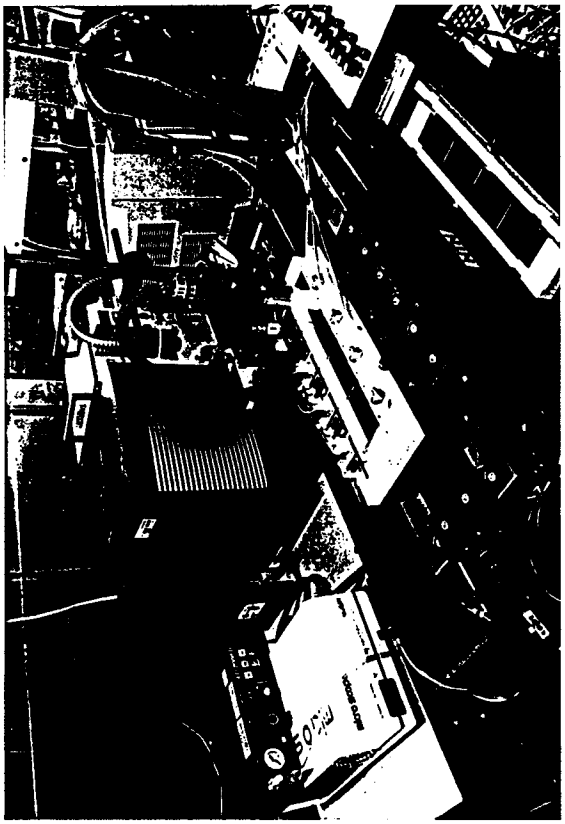

629

文部省 高エネルギー物理学研究所 殿

精機証－92－T035

1992年 4月13日
NTN株式会社
磐田製作所 精機工場
技術課 品質保証係

課長	担当
上都	清水

検査成績証

製番 1－SM

リニアモータ付エアスライド：
TASX30LD－4
ドライバ：
TASX30LD－1/200

測定項目		仕様	測定結果
空気消費流量		20 Nl/min以下	10 Nl/min
剛性		137 N/μm 以上	245 N/μm
真直度	上下方向	0.9μm以下/300mm	0.7μm以下/300mm
	左右方向	0.9μm以下/300mm	0.1μm以下/300mm
繰り返し位置決め精度		±0.3 μm以下	±0.05 μm

※ 測定時の空気供給圧力は0.39Mpa（G）である。

630

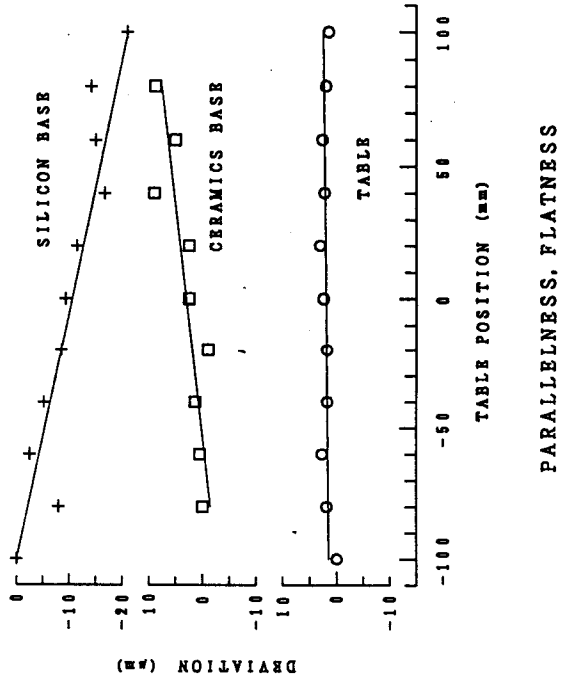

631

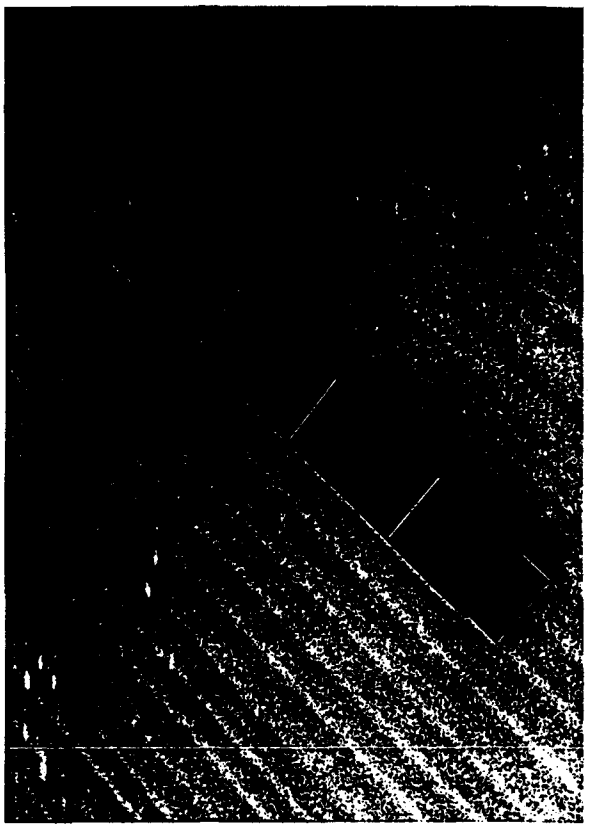

632

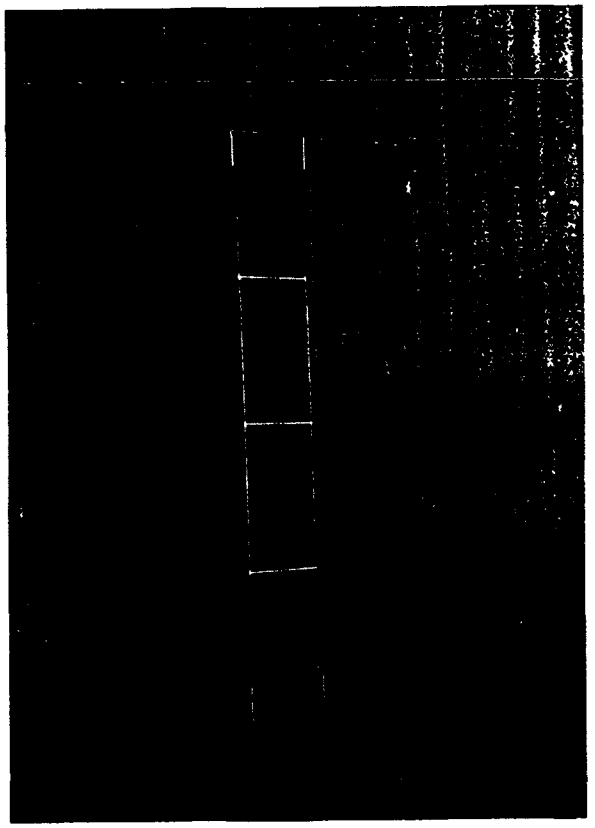

633

Ladder

- Rib:

- Polycyanate-CFRP
  XN50A/RS-3/[0°/90°]4s 0.22 mm

  - low CTE[1] -0.2 ppm/°C
    (Silicon CTE 2.6 ppm/°C)
  - low moisture absorption 0.5 wt%
  - low CME[2] 19 ppm/wt%

- Several types of glue are under investigation

- Room temperature cure Epoxy glue W/filler
- Heat cure Epoxy glue W/filler
- Room temperature curing UV cure glue WO/filler

- An assembled ladder W/UV cure glue

  - Precision

634

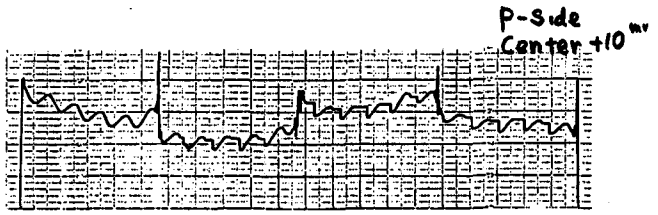

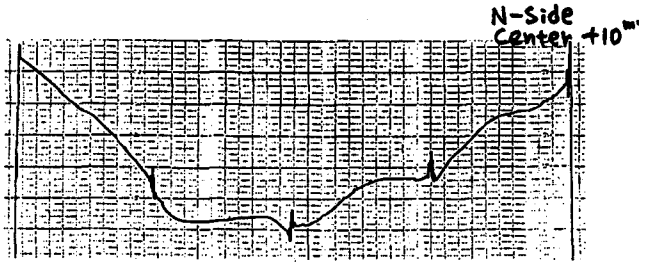

[1]CTE = Coefficient of Thermal Expansion
[2]CME = Coefficient of Moisture Expansion

920526 KEK

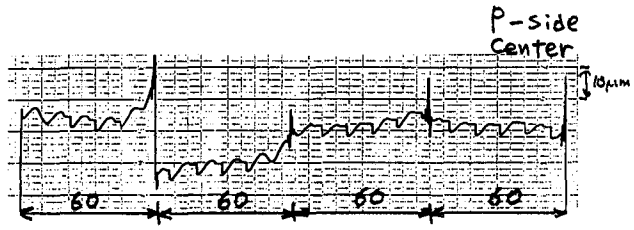

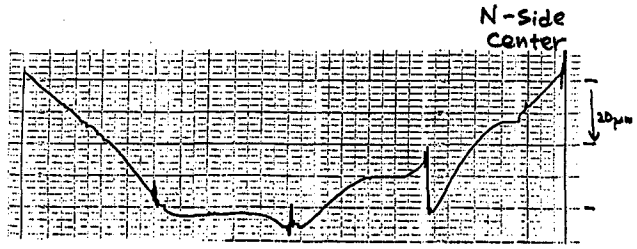

Assembling Process with Wire bonding

- Electro-mechanical system
  where we need help from Hamamatsu
- Proposed steps...
  need further improvement in situ

- Check the frontend carrier
- Check the detector itself
- Glue the carrier on a detector and wire-bond
- Check electrical continuity and short circuits
- Butt-glue another detector to form half of the ladder
- Wire-bond the detectors
- Check electrical continuity and short circuits
- Butt-glue two half-ladder to form full-ladder
- Glue the ribs on side

920526 KEK

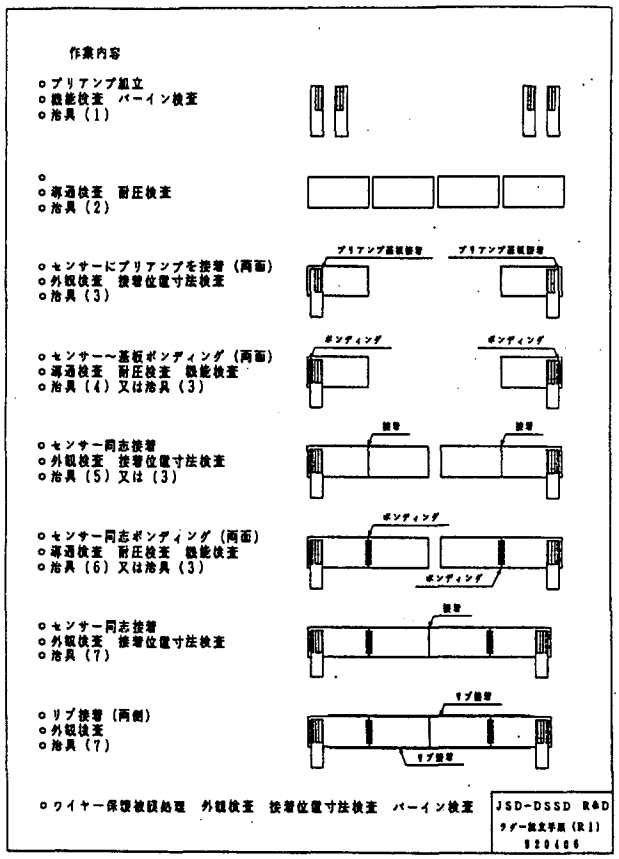

図. 3 ラダー組立手順

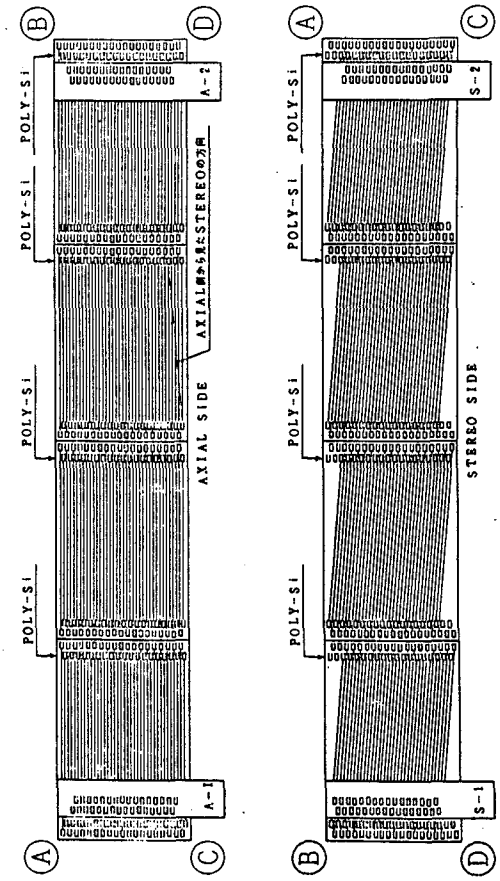

Wire Bonding

• Detector - Frontend Analog chip

- Elevation difference 1 mm
- Pad pitch difference
  - Detector 50.0 μm
  - Chip ~48 μm

  → non parallel wire-bonding
  Max. 6° (=(50 μm+60 μm)/1mm)?

- Bonding pads on chip carrier near the analog chip
  for the voltage reference
  for the power etc. of the chip

• Alternative method being looked into ...

- 50 μm pitch trace mountable carrier
- hopefully Be substrate (instead of Silicon)

→ very desirable because of

- parallel wire-bonding
- flip-chip mounting eliminating wire-bonding between analog and digital chips...

Any company who can make the carrier?

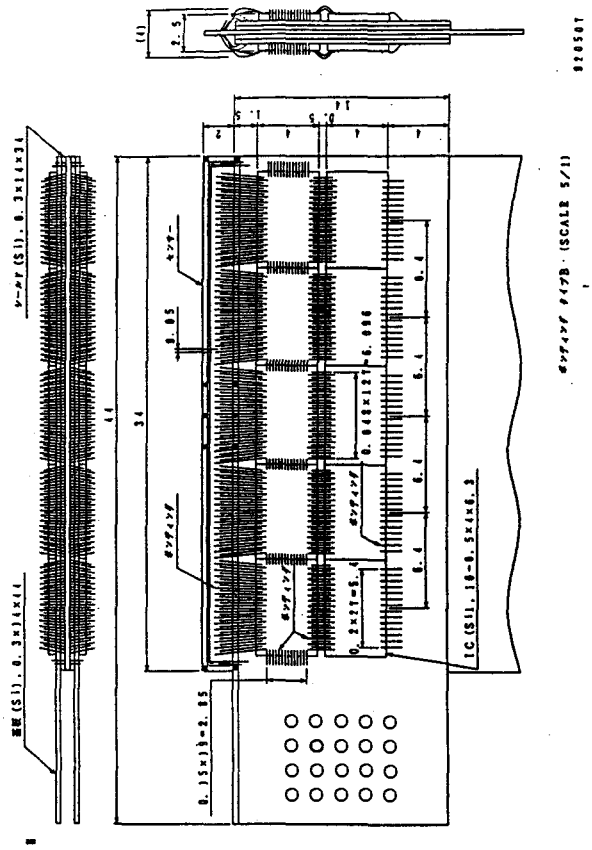

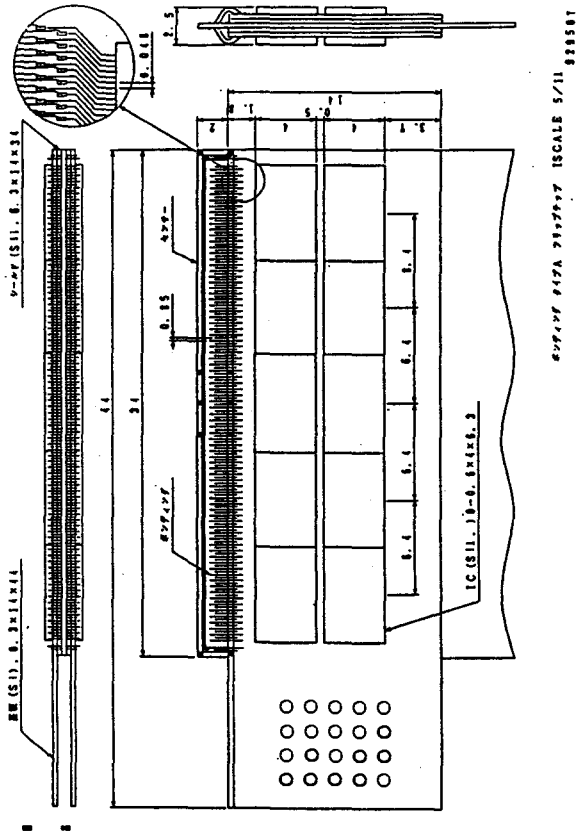

Summary

• We have been making progresses on the ladder assembling.

• Tools and jigs are prepared.

• A ladder is assembled and accuracy is evaluated.

• Wire-bonding is yet to come but work is underway.

• Be substrate, 50 mm trace mountable chip carrier is highly desirable.

Silicon Tracker
Cost & Schedule Review

Alex Grillo
UC Santa Cruz
SSCL PAC Review
7-May-1992

KEK Meeting
27-May-1992

Estimating Process

Principal Authors:

LANL:
William Miller
T. Thompson
C. Grastataro
R. Reid

LBL:
Roger Stone
Helmuth Spieler
Bob Barney

Project has been broken down to WBS level 5 elements

There are over 600 activities included in the project design

A cost and time estimate has been made for each activity

Engineering estimates
Vendor quotes
Based upon engineering drawings & specifications

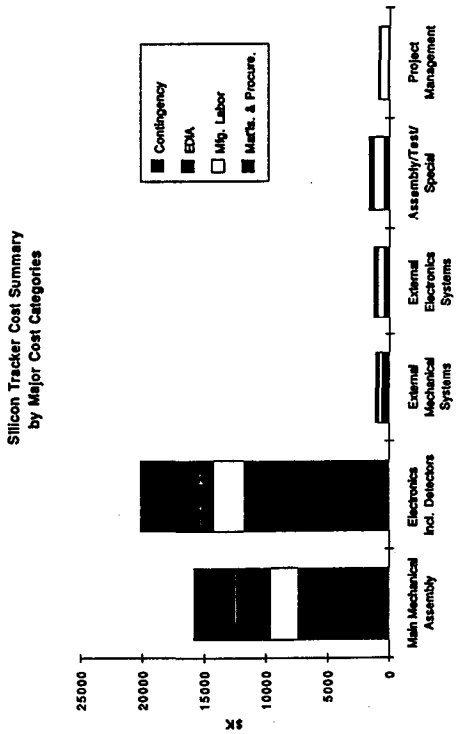

Major Cost Drivers

Item	Unit Cost, k	Unit	Number	Total, k
Barrel detector	$0.750	each	3600	$2,700
Frwd detector	$1.500	each	3112	$4,668
Barrel readout	$0.053	each	18000	$954
Frwd readout	$0.053	each	32640	$1,730
Optical trans/rec	$0.500	set	1236	$618
FEE Design/test Labor	$3,008	effort	1	$3,008
Enclosure/supports	$881.0	each	1	$881
Space frame/mounts	$501.0	each	1	$501
Disc cooling ring	$11.3	each	48	$542
Heat rejection sys	$516.0	each	1	$516
Trker assy/test	$879.0	each	1	$879
Mech Int/exp	$2,254.3	effort	1	$2,254
In-situ alignment	$511.3	sys	1	$511
Program Management	$848	effort	1	$848

Silicon Tracker Totals

Base Cost:	$32,472 K
Contingency:	26.9%
Total Cost:	$41,204 K

617

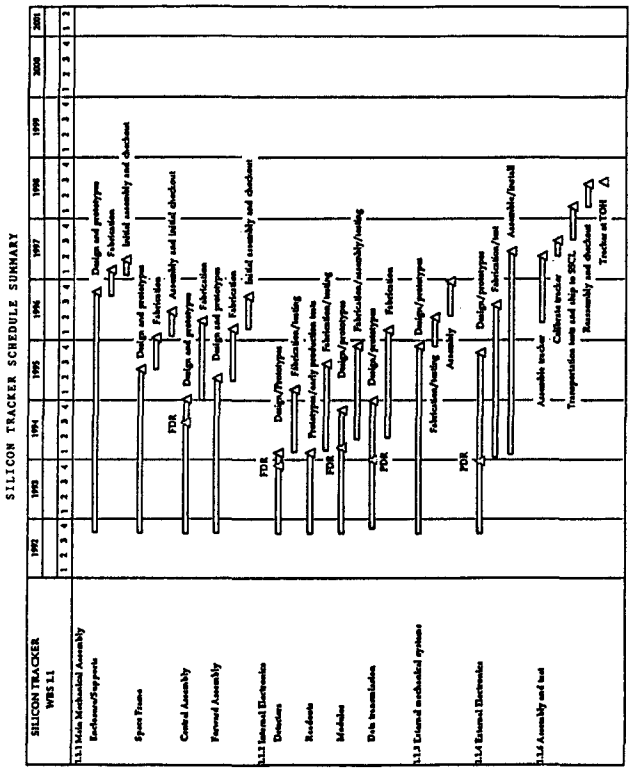

618

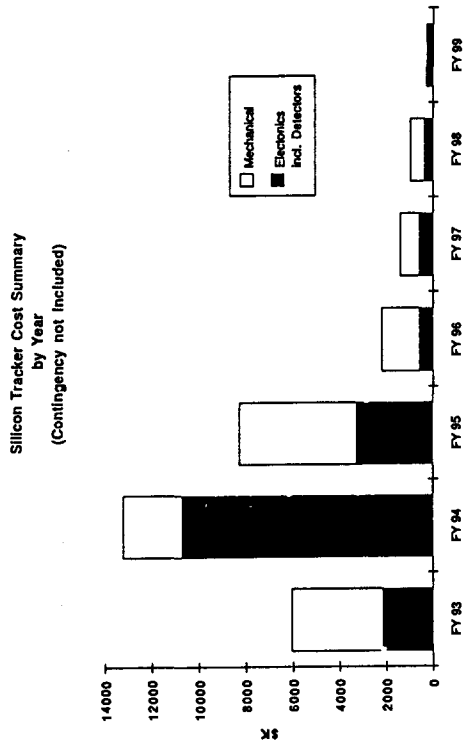

619

Where We Are with FEE

Bipolar Preamps:

Tek Chip Fully Functional in House
2 mW/channel but could be used with LANL's cooling margin

AT&T Chip on Order
Power usage corrected

Plans:
Run improved chip on Tek & Westinghouse
Compare performance & yield (cost)

CMOS Digital:

64 Channel Chip to be Received End of May
RAL designed and will test
Non-rad hard process
Want to improve output protocol

16 Channel Prototype to be Received End of May
Test speed and performance in UTMC Rad Hard technology

Plans:
Non-rad hard chip with improved protocol
- This year

Rad hard version early next year

650

Major Activities/Milestones for FY 93

Mechanical:

Build Central Region Prototype Cooling Ring	
Central Region Prototype (Stability) Tests	
Central Region PDR	Sep '93
Build Forward Region Prototype Cooling Ring	
Forward Prototype Ready for Test	Sep '93

Internal Electronics/Detectors:

Build Final Prototype Central Detectors	
Build Final Prototype Forward Detectors	
Build Final Prototype FEE	
Beam Tests at KEK	
Detector FDR	Sep '93
FEE FDR	Nov '93

DAT/DAQ:

Build Prototype DAT System	
DAT FDR	Jun '93

Big Job Ahead for Program Management

Revise Cost & Schedule to Reflect Current Plan
- More FEE prototype runs
- No BSC for DAT
- Clarify boundary between Silicon and Electronics budgets.

Add More Detail to Non-mechanical Schedule
For example:
Detail each prototype run
Include separate Wedge DET activities
Include KEK Beam Test and other tests

Incorporate Plans for Distributed Construction at All the Various Institutions as They Are Finalized.

Create System to Monitor Cost & Schedule Across All Institutions.
- LBL & LANL use different scheduling software
- SSCL uses yet another
- Need cost tracking system during construction

Some Immediate Deadlines

FY 93 Budget Proposal	June 10
Response to PAC	July 10
DOE Review	September

Beam Test of the SDC Double-sided Silicon Strip Detector

Y. Unno
Physics, KEK

for

The SDC Silicon Tracking Group

Abstract

The beam test of the DSSD for the SDC Silicon tracking system(STS) is being planned to check-out the prototype DSSD, and eventually at the end, the full signal stream from the sensor to the data acquisition provisioned in the SDC. The first beam test will be held in the fall of 1992 at a test beam line at KEK. A plan for the setup and job sharing is being discussed. New components, effect of magnetic field, etc. will be tested in the later stages utilizing the setup.

Introduction

• The Silicon tracking system (STS) of the SDC

- Position resolution — ≤ 12μm/side
- Beam crossing at 16 ns — Bucket ident.
- High radiation environment

- Tracks hits in angles
  - along the strip — $\theta \leq 60°$
  - perpendicular to the strip — $\phi \leq 14°$ (≥ 1 GeV/c)

- In the magnetic field of 2 Tesla
  - Barrel — along the strip
  - Disk — perpendicular to the strip

• Detector module - Readout scheme

- 50μm strip pitch
- 6cm+6cm = 12cm strip length
- 300μm thick (25,000 e MPC[1])
- Digital readout scheme:
  - Amp (ENC~1,500 e's)
  - Shaper(τ_p~20ns)
  - Comparator(V_T~1/4MPC)

[1]MPC=Most Probable Charge

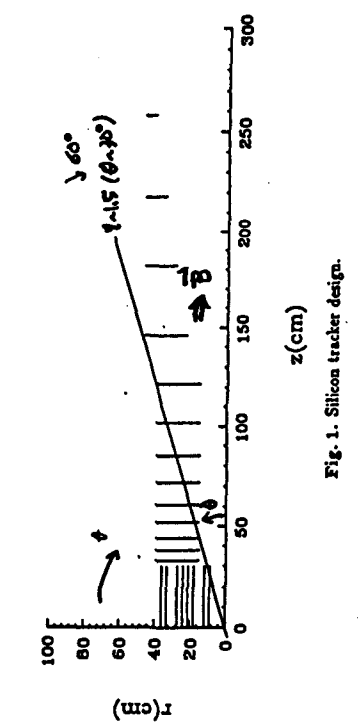

Fig. 1. Silicon tracker design.

•We will check-out...

- 6cm, and 12cm (bonded) detectors
- By moving the detector
  - θ and ϕ directions
  - 0 - 50 μm perpendicular to the beam (to check systematics relative to the defining DSSD's)
- With/Without magnetic field
- Irradiated detectors
- Final test ladders/Electronics on the detector

Measurements:
- Analog pulse shape (do we need this?)
- Pulse height distribution
- Time distribution
- Threshold variation
  - Hit multiplicity (0, 1, 2, ...)
  - Resolutions
  - Efficiency in the time window

• The beam test will span a year or more, to be done in stages when new components are available.

Beam line

• Two test beam lines at the KEK Proton Synchrotron

- T1:
  - Flexible scheduling
  - $\pi^{\pm}$
  - 0.5 ~ 2.0 GeV/c ← low momentum
  - $\delta p/p$ ~ 5%
  - $5 \times 10^{2-3}$ @ 1 GeV/c

- π2:
  - Rather crowded; advanced proposal required
  - $\pi^{\pm}$
  - 1.0 ~ 4.0 GeV/c ← higher momentum
  - $\delta p/p$ ~ 1%
  - $5 \times 10^{3-4}$ @ 3 GeV/c

- At the accumulating ring of the TRISTAN
- IT4:
  - Re-modeling, 4~5 GeV/c
  - electrons!, low intensity

• Obviously π2 is desirable but ...We can move to the line once we have completed the initial run and have confidence on the system. A magnet is in π2, too.

• Low momentum → multiple scattering

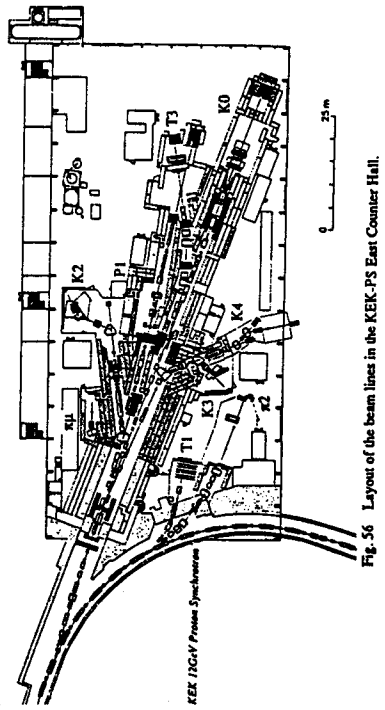

Fig. 56 Layout of the beam lines in the KEK-PS East Counter Hall.

Multiple Scattering

• Scattering angle:

$$\theta_M = \frac{13.6\,MeV}{\beta p} z \sqrt{\frac{x}{x_0}}\left[1 + 0.038\ ln\left(\frac{x}{x_0}\right)\right]$$

• Silicon:
- 1Xo = 21.82 g/cm^2 or 9.36 cm
- 300 μm Si = 0.32 %Xo
- $\sqrt{x/x_0}[1+0.038\ln(x/x_0)] = 0.04422$

• $\pi^{\pm}$:

p [GeV/c]	θ_M [mrad]	y [mm]@σ_x=5μm
0.5	1.25	4.0
1.0	0.607	8.2
2.0	0.301	16.6
4.0	0.151	33.1

• Butt the position defining detector telescope (PDD; downstream) with the device under test (DUT)

Setup

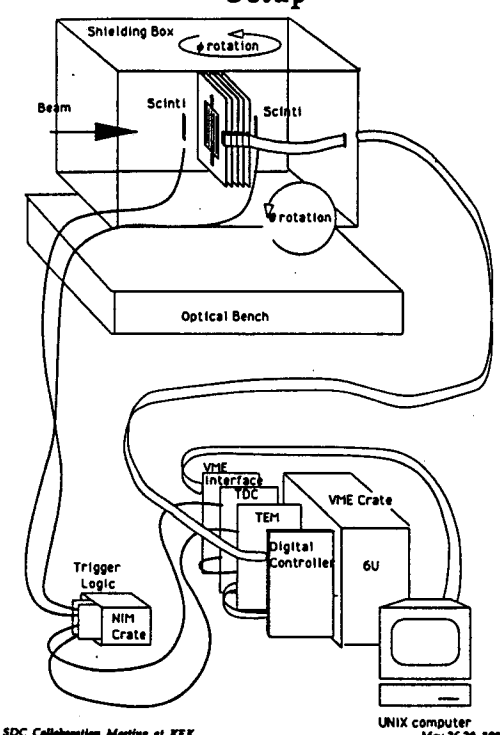

Double-sided Silicon Strip Sensor
Hiroshima/KEK/Hamamatsu

- 1st prototype under production...

- Specification:
  - Substrate: n-type, 4~8 kΩ, 300±10 μm
  - Size: 60.0 mm x 34.1 mm
    58.8 mm x 32.0 mm (active)
  - Strip: 50 μm pitch, double-sided
  - Stereo angle: 10 mrad.
  - Ohmic side isolation: p+ isolation strip
  - Bias resistor: 250±50 kΩ Poly-silicon

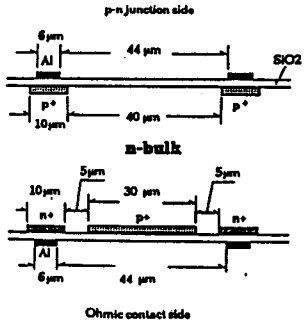

Frontend Analog and Digital
LBL/UCSC

- Analog:
  Bipolar transistor Amp⊗Shaper⊗Comparator

- AT&T chip H.Spieler/I.Kipnis@LBL
  - Baseline for the SDC
  - 64 channel/chip to have less fan-in/out angle

- Tek chip N.Spencer/W.Dabrowski@UCSC
  - Under development for ZEUS

- Both AT&T and Tek chips use common layout for input and output for inter-changeability

- Digital storage:

- MOSIS CMOS DTSC[2] chip J.DeWitt/UCSC
  - Variation of the chip for ZEUS

- This will not be test of final digital circuitry
- Clock at 62.5MHz
  to give time resolution and idea of clock noise

[2]DTSC = Digital Time Slice Chip

Detector module for the beam test
LBL/KEK

- Two kinds of detectors:

- Position defining detectors (PDD)
- Detector under test (DUT)

- Detector and chip carrier

- PDD's PC board, 6 cm DSSS
- DUT PC board, 6 cm & 2x6 cm DSSS
  ladder in a follow-up test

- PC board design and production LBL

- DSSS mounting and bonding
  - two at LBL
  - rest are at KEK/Hamamatsu

- DUT with "Frontend on detector with Kapton cable" should be developed to be tested in a follow-up test

- Frontend chip carrier with Kapton cable LBL

Detector Module - PC board

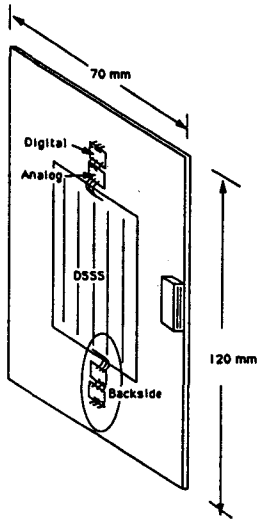

6 cm Detector Module/PC board

Mechanical System

KEK/Univ. of New Mexico

- Supports...
  - Two PDD's, one DUT, two PDD's
- Rotation mechanism for θ and ϕ directions
  - $\theta \leq 60° \rightarrow$ $300 \rightarrow 600\ \mu m$, $\theta_M \rightarrow \times 1.4$
  - $\phi \leq 14°$
- Linear motion of DUT by 0~50 μm relative to PDD
- Distance between DUT and PDD's to be ≤ 10 mm
  - 5 mm e.g. only for connector height
  - stack of 20 mm for five planes
- Vibration-free optical bench
- Light and electric shielding box
- A special container when 0°C cooling required
- Overall height < 40 cm
  to fit in an opening of a magnet:
  40 cm height x 100 cm width x 70 cm depth

"ASSEMBLED" STRUCTURE (WITHOUT ROT'N OR OVERALL TRANSLATION STAGES):

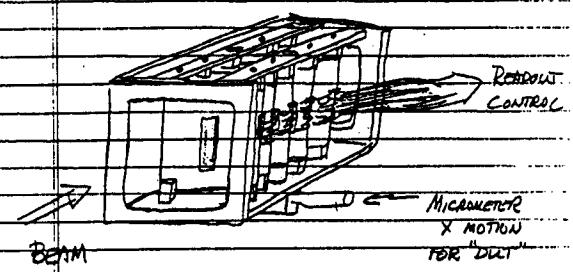

J.M. 6

"OVERALL" ROTATION & TRANSLATION:

- ROTATIONS ABOUT THE "X" & "Y" AXES:
- USE 2 ROTATION STAGES:

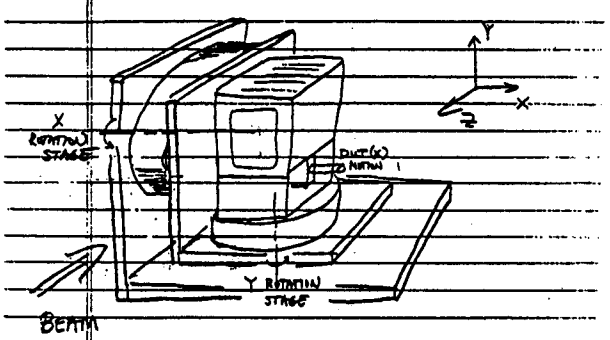

NOTE: ROT'N STAGES ~5" DIAMETER AND ~2" DEEP (ALONG AXIS OF ROT'N DIRECTION)

J.M. 7

WE NEED TO MAKE SURE THIS WILL FIT AND WORK IN THE MAGNET:

- STILL CHECKING ON ROT'N STAGE USE IN B FIELD (STANDARD STAGES INCLUDE BALL BEARINGS WHICH ARE A PROBLEM!?)
- APPROXIMATE SPACE BUDGET:
  - a) ~~MAGNET 40cm APERTURE~~
  - b) ~~DETECTOR SUPPORT STRUCTURE ≈ 16 cm~~
    - DUT MOTION MICROMETER SLIDE ≈ 4 cm
    - ~~Y ROT'N STAGE ≈ 5 cm~~
    - " " " SUPPORT/CLEARANCE ≈ 2 cm
    - X ROT'N STAGE SUPPORT ≈ 3 cm
    - 30 cm

THIS LEAVES SOME SPACE FOR OVERALL X MOTION OR FOR OVERALL Y MOTION.

J.M. 8

Cables and Digital Controller
UCSC

- Cables:
  - 5 detector modules - Daisy chained
  - Connection at the shielding box
  - Shielding box to the Digital Controller/VME
- Digital Controller in the VME crate
- 62.5 MHz clock generator

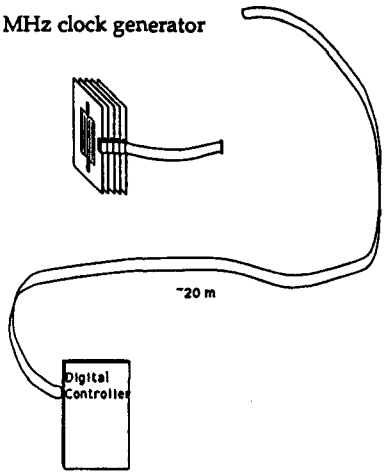

Trigger and DAQ
KEK

- Trigger - Scintillator planes
  - Timing into TDC-VME card
- DAQ
  - VME-UNIX: the portable DAQ of the SDC
  - Data transfer rate?
  - Interupt speed?

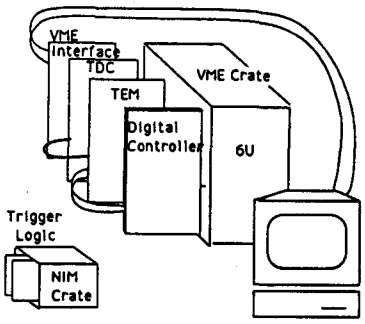

Milestones

• Place orders for AT&T and Tek chips	May-June
• Place order for Digital chip	May 29
• Receive AT&T and Tek chips	Sep 15
• Assemble & test one module	Sep 30
• TEM by W. Smith	Sep(?)
• Ship partial modules to Japan	Oct 15
• Complete the mechanical system	Oct 1
• All modules assembled and tested	Nov 1
• Complete the trigger counters, logic, DAQ and ready for the beam	Nov 15

- KEK PS operation

1992	Oct - Dec(T1)
1993	Feb - March(T1)
	May-July(π2)
	Oct - Dec(π2)

KEK BEAM LINES FOR THE BEAM TEST

SDC Collaboration Meeting
May 28, 1992, KEK

Akira Murakami, Saga University

I. Available beam lines at KEK

1. AR-IT4 (TRISTAN Accumulator Ring)
2. PS-π2 (12 GeV Proton Synchrotron)
3. PS-T1 (12 GeV Proton Synchrotron)

which is the best ?

Location of IT4, π2, T1 → Fig.

Contact person	PS-π2, PS-T1	T.Ohshima
	AR-IT4	F.Takasaki (?)

II. AR-IT4 beam line

1. Layout of the beam line

Layout of IT4 → Fig.

2. Beam parameters

particle	e^-
momentum range	2 ~ 5.5 GeV/c
momentum bite	~ ±5 %
spectrum	not measured, probably a peak at around 2 GeV/c
intensity	~ 20 cps / (2 cm x 2 cm) at 2 GeV/c (measured in March of 1991)
repetition cycle	1.3 μs
spill	0.06 ns
life time	200 ~ 350 min
beam size	1 cm x 1 cm (in FWHM)

3. Facilities

A movable table (~1m L x ~50 cm W) is available in the experimental area

moving range	~ ± 15 cm	horizontal direction
	~ ± 5 cm	vertical direction

4. Control of the beam

beam on/off	beam plug
beam momentum	bendig magnet
intensity	position of the internal target

** beam size is not changeable

5. Problems

The serious problems were found in the IT4-beam in May of 1991.
(by the B-factory group)

— the off-momentum background particles, i.e. the continuous lower momentum spectrum in the the beam spectrum.

— the very low (only 0.5 Hz or less per cm²) beam intensity.

may be due to bad shielding along the beam line,
misalignment of the beam line elements,
etc.

→ need to be fixed.

6. Replacement of the internal target and its driving system

The IT4 internal target and its driving system are scheduled to be replaced during the coming shutt down period of TRISTAN.

After this replacement, the internal target can be driven with a 10 μm step.

However, the life time of the AR beam will be decreased when the internal target is inserted deeply.

→ Therefore, we cann't expect to increase the beam intensity by controlling the position of the internal target.

At the same time,

realignment of the shield,
and
study of the beam properties

will be made by the B-factory group and us(?).

Manpower for this work is required.

7. Possible Users and the schedule

main users B-factory group

Users of the IT4 have to get an agreement with the SOR group about the position of the internal target.

III. PS-π2 Beam Line

1. Layout of the beam line

Layout of π2 → Fig.

2. Beam parameters

particle	π^+/π^- (unseparated)
momentum range	1 ~ 4 GeV/c
momentum bite	~ ±1 %
spectrum	a peak at around 2 GeV/c
	momentum spectrum → Fig.
intensity	π^+ 2.0 x 10^6 particles /pulse @ 10^{12} ppp
(at 3 Gev/c)	π^- 1.0 x 10^6
repetition cycle	2.6 sec (short pulse mode)
spill	0.5 sec (short pulse mode)
structure	flat top
beam size	1 cm x 1 cm (in FWHM)

π^+/p separation → TOF

beam profile → Fig.

at nominal operation of PS (3~4) x 10^{12} ppp

→ typical beam intensity (1~ 2) x 10^6 cps/cm²

3. Facilities

electronics hut, spectrometer magnet with B = 1.2 T

gap 50 cm

4. Control of the beam

beam momentum, intensity, beam size can be controlled.

5. Possible Users and the schedule

main users B-factory group is continuously using.
the other group will take 40 shifts (3 weeks).

6. Proposal and approval

A proposal has to be submitted at least a month before the PS-PAC meeting which is generally held in March, July and November. In the case of the test experiment which uses the test beam lines, e.g. π2 and T1 beam lines, the same procedure is required as the physics experiments.

However, when the test experiment requires the machine time less than 20 shifts, the approval of the "three members committee" of the PAC is enough to carry out the test experiment.

1 shift = 8 hours
~40 shifts/cycle, 1cycle = 3 weeks

Two ways to apply for the machine time for the beam test

1) Submitt a proposal in October to the PAC.

2) Get an approval of the "three members committee" of the PAC for the machine time less than 20 shifts and renew it if necessary at any time.

IV. PS-T1 Beam Line

1. Layout of the beam line

Layout of T1 → Fig.

2. Beam parameters

particle	π^+/π^- (unseparated)
momentum range	0.5 ~ 2 GeV/c
momentum bite	~ ±5 %
spectrum	a peak at around 7
intensity	π^+ 5.0 x 10^4 particles /pulse @ 10^{12} ppp
(at 3 Gev/c)	π^- 4.0 x 10^4
repetition cycle	2.8 sec (short pulse mode)
spill	0.5 sec (short pulse mode)
structure	flat top
beam size	1 cm x 0.5 cm (in FWHM)

at nominal operation of PS (3~4) x 10^{12} ppp

→ typical beam intensity (3~4) x 10^4 cps/cm²

3. Facilities

4. Control of the beam

beam momentum, intensity can be controlled.

5. Possible Users and the schedule

6. Proposal and approval

the same as the PS-π2 beam line

V. Summary

The PS-π2 beam line is the most suitable one.

This beam line satisfy the requirements

- beam intensity

  trigger rate ~ 50 Hz / strip · cm @ 10^4 cps / cm² 3 GeV/c

- multiple scattering

  $\sigma_x \simeq 11\ \mu m$ or $\simeq 22\ \mu m$ @ 3 GeV/c

  on the 2nd or 3rd SSD, respectively.

Requirements for the beam

- particle $\pi^{\pm}$ or e^{-}
- momentum range

π beam spread due to multiple scattering

E_π (GeV)	σ_x on "2" (μm)	σ_x on "3" (μm)
1	28	64
3	11	22
5	8	14

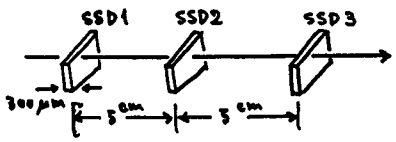

simulated with GEANT
by Iwata (Hiroshima Univ.)

$P_{\pi/e} \gtrsim 2$ GeV

Requirements (continued)

- intensity

  trigger rate $\gtrsim$ 1 Hz/strip·cm

- beam size $\gtrsim$ 1 cm × 1 cm
- spill
- structure

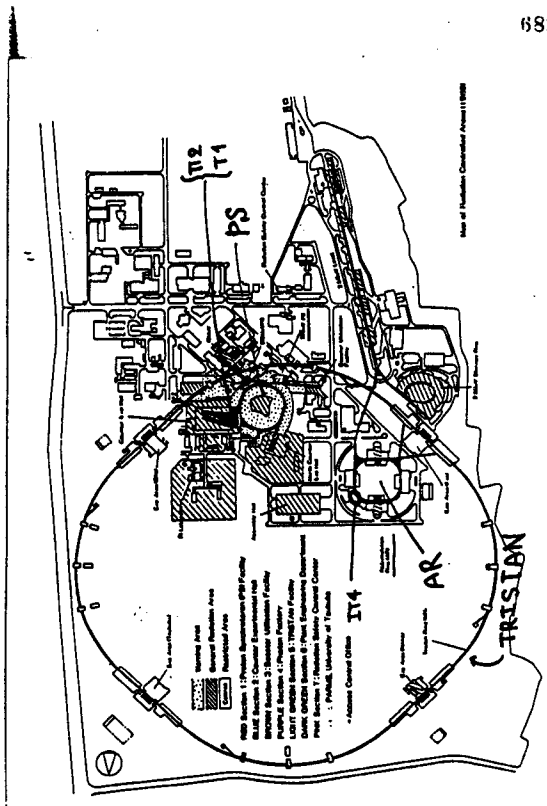

Location of IT4, π2 and T1

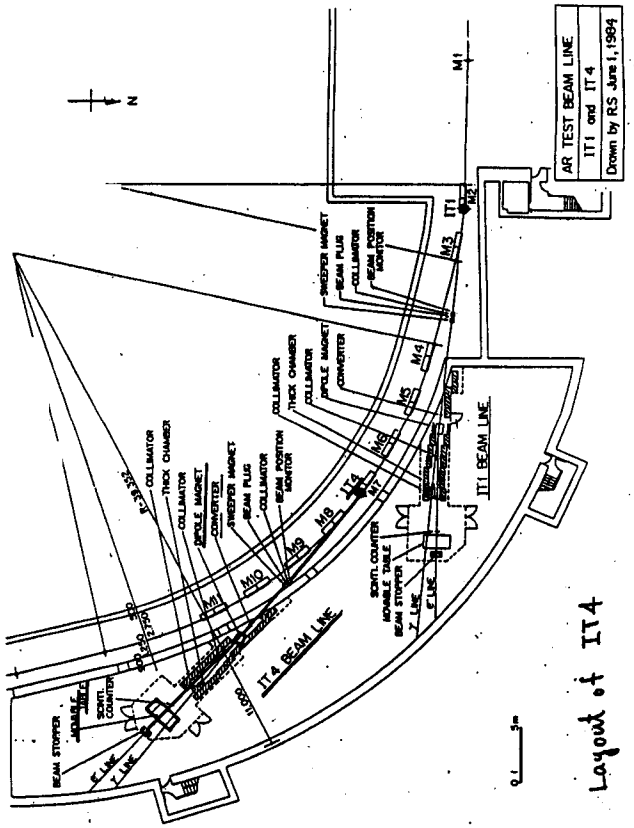

Layout of IT4

PS - π2 beam line

Figure 3.1: Layout of Beam Lines in the KEK-PS East Counter Hall (E-Hall).

Table 3.5 Parameters of the π 2 channel.

Momentum range	0.5 ~ 4.3 GeV/c
Production target	1 mm dia.x 10~15 mm Be
Central production angle	10°
Beam length	F1: 28 m, F2: 37 m
Solid-angle acceptance	0.6 msr; 9 mrad(H) x 21 mrad(V)
Momentum bite	±1% Δp/p
Beam character at intermediate focus	
Magnification	0.63(H), 3.8(V)
Dispersion	1.1 cm/% Δp/p
Beam character at final focus	
Magnification	F1: 1.3(H), 1.7(V) F2: 2.6(H), 4.7(V)
Dispersion	0.2 cm/% Δp/p
Particle yields	See Fig. 3.14

Momentum spectrum of π 2 beam

Figure 3.14: Beam intensities from the π2 line.

Layout of π2 and T1 beam lines.

separate P from π by TOF.

図2.3.7.4 π2 チャンネルのビーム強度(8 GeV)

Momentum Spectrum of the π2 beam

π 2. beam profile

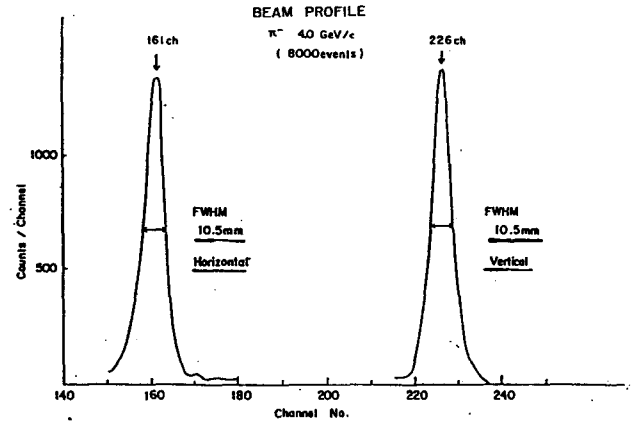

Observed beam profiles of π2 beam at the focal point F1 for 4.0 GeV/c. The spacing of wire (corresponding to channel) is 2 mm per channel.

図2.3.7.5 π2 ビームプロファイル

Analog Readout ICs

Helmuth Spieler
LBL

SDC Silicon Tracker Meeting at KEK
May 28, 1992

Requirements

Noise	$Q_n < 1200$ el (S/N>20)
Time Resolution	$\Delta t < 16$ ns for 1 fC$\leq Q_s \leq$8 fC
Power Dissipation	P ≈ 1 mW/channel for 12 cm strips
Dead Time	~50 ns goal (for operation at $\mathcal{L}=10^{34}$) (two successive 4 fC pulses)
Radiation resistance	$\Phi_c+\Phi_n \approx 10^{14}$ cm^{-2} (limited by type inversion in detector) Dose > 5 Mrad Demonstrated for both detectors and electronics (analog + digital).

Readout within 10 μs after receipt of level 1 trigger
(also for high-density jets)

Calibration inputs
Externally adjustable thresholds (differential inputs)
Chip disable

Vendor Selection for Analog IC:

Criteria:
1. Adequate speed
2. Radiation resistance
3. Circuit density (Circuit on pitch <45 μm)

3 vendors with suitable processes identified

1. AT&T
2. Tektronix
3. Westinghouse

Some technical issues:

1. AT&T
   - Well characterized (also radiation effects)
   - Currently available process (CBIC-U2)
     - relatively slow with large featurs size.
   - High-density process with improved speed
     - to be released in late summer
2. Tektronix
   - Well characterized (also radiation effects)
   - High speed and circuit density
   - Lateral PNP transistors
     - (low current gain after irradiation)
   - Vertical PNPs in preparation
3. Westinghouse
   - Need more data on radiation effects
     - (have obtained test devices)
   - Good speed and circuit density

Expect that all three vendors will have comparable processes (speed, density, radiation resistance) by end of 1992.

Note that for equivalent circuits (same functions for each) the currently available processes differ in power only by ~100 μW.

To allow valid comparison between vendors, specifically to assess

circuit trade-offs
radiation resistance of specific circuit
die size ($$$)
yield ($$$)

we need to fabricate test ICs through all three vendors.

Circuits to be designed to same specifications with same basic circuit, but details tailored to specific process.

Choice for first run: AT&T

Circuit and preliminary layout submitted (LBL)
PO issued (UCSC)
ICs expected in September

At least two different ICs:
1. Individual circuit blocks
2. Complete 64 channel front-end

+ perhaps
3. Array of preamplifiers

Goal is still to have 128 channels/IC in final design, but we selected 64 ch. for this run to obtain better yield data.

Extensive pre-qualification of multiple vendors is designed to reduce risk in final mass production run.

693

Silicon Tracker (SSC) Front-End Bipolar IC

TEKTRONIX

Preliminary Target Specifications

(SIMULATION RESULTS)

Detector		
Strip Length	12	cm
Strip Capacitance (1.2 pF/cm)	14.4	pF
Leakage Current (100 nA/cm)	1.2	μA
Bias Resistor	200	kΩ
Blocking Capacitance	144	pF
Integrator Peaking Time*	55	nsec
Output Noise Voltage	42	mV rms
Transfer Gain	215	mV/fC
Equivalent Input Noise Charge	1225	e rms
Peak Output Current	500	μA
Comparator Threshold (4σ)	165	mV
Time Walk (1fC-4fC)	14	nsec
Supply Voltage	3.5	V
Power Consumption	620	μW

* PROPAGATION DELAY + CHARGE COLLECTION
CR-RC SHAPER W. τ = 20 ns

Issy Kipnis
Lawrence Berkeley Laboratory
25 October 1991

694

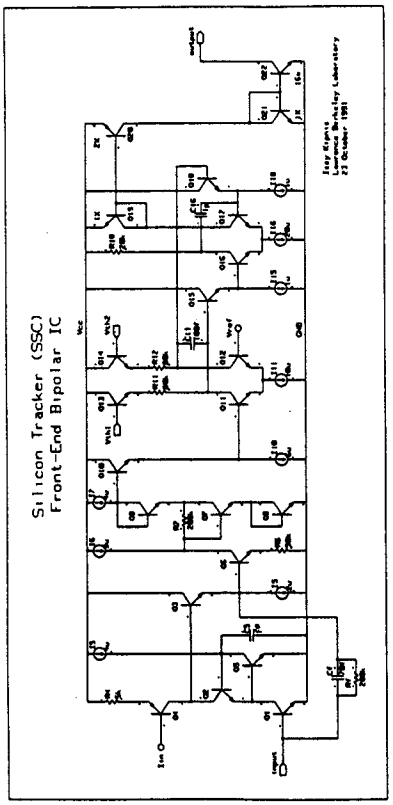

DIFFERENTIAL THRESHOLD INPUT
TIME CONSTANTS (DIFF. + INT.) SET BY RCs, NOT STRAYS

695

LIMITING AMPLIFIER!

Voltage at the input of the comparator

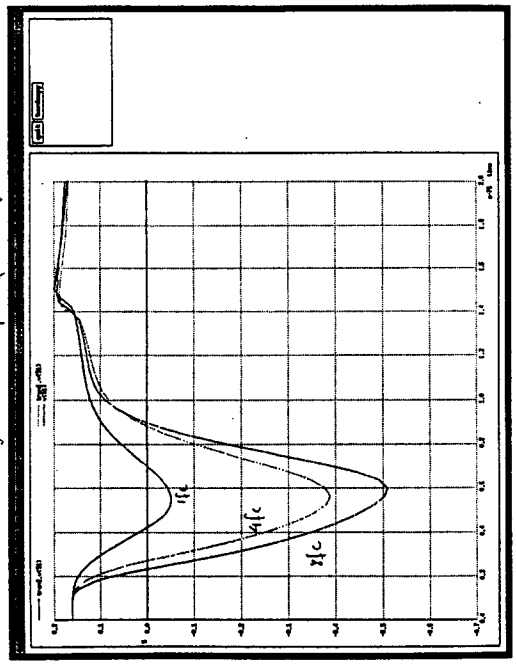

696

DIGITAL OUTPUT (COMPARATOR)
IS A CURRENT DRIVER

Output Current

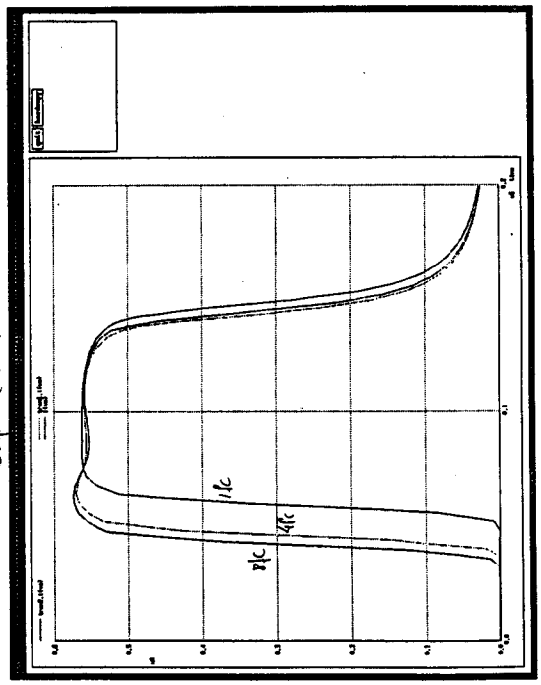

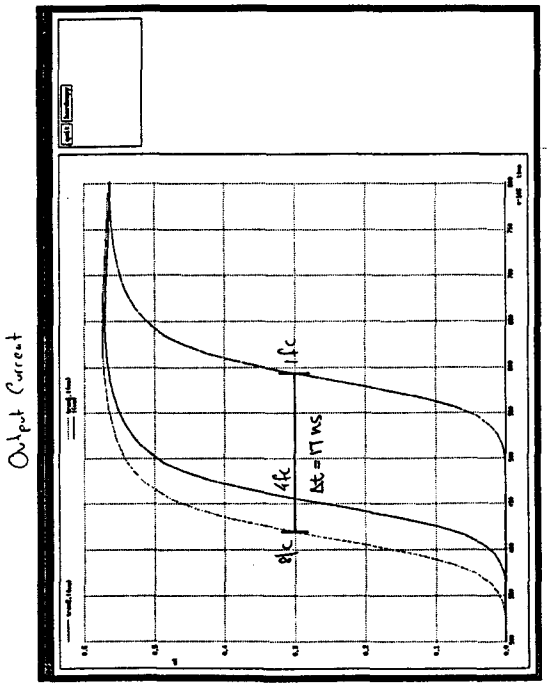

Silicon Tracker Bipolar Front-End (Tektronix)

Wladyslaw Dabrowski
INFN, Turin
(IPNT, Krakow)

Assumptions and goals

Strip capacitance	14.4 pF
Bias resistor	200 kΩ
Strip leakage current	1 μA
Judy's input current pulse	
Comparator threshold	4σ
Time walk (1fC - 8fC)	< 16 ns
Power comsumption	< 1 mW

Radiation effects on electronics
(no pnp transistors)

Other issus
- matching
- dead time
- area (money) budget

Compatibility with AT&T design
- high impedance output
- control and power lines structure

Some simulation results

gain	140 mV/fC
output noise	30 mV
equivalent input noise	1340 el
comparator threshold	120 mV
time walk (1fC - 8fC)	14.8 ns
(1.5fC - 8fC)	9.8 ns
power consumption	820 μW
+ digital receiver	60 μW
dead time (for two 4fC pulses)	100 ns

After 5Mrad and 10^{14} n cm^{-2}

gain	130 mV/fC
output noise	31.4 mV
equivalent input noise	1500 el
comparator threshold	117 mV
power consumption	860 μW

701

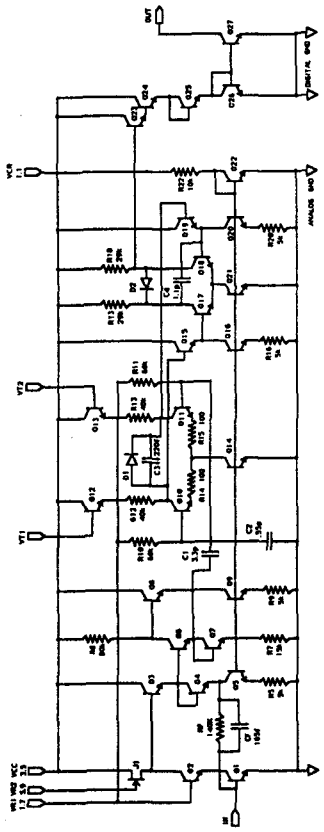

702

Silicon Tracker (SSC)
Front-End Bipolar IC (AT&T)

Detector

Strip Length	12	cm
Strip Capacitance (1.2 pF/cm)	14.4	pF
Leakage Current (100 nA/cm, $\Phi=10^{14}$ cm^{-2}, T=0 °C)	1.2	μA
Bias Resistor	200	kΩ
Blocking Capacitance	144	pF

Goals

Equivalent Input Noise Charge	1250	e rms
Differential Comparator Threshold	4σ	
Time Walk [1 fC - 8 fC]	16	nsec
Power Consumption	1	mW
High Impedance Output		

Preliminary Simulation Results (3-channels)

Output Noise Voltage	39	mV rms
Transfer Gain	180	mV/fC
Equivalent Input Noise Charge	1350	e rms
Peak Output Current	400	μA
Comparator Threshold (4σ)	155	mV
Time Walk [1 fC - 8 fC]	12	nsec
Supply Voltage	3.5	V
Power Consumption	950	μW

Issy Kipnis — Lawrence Berkeley Laboratory — 12 February 1992

703

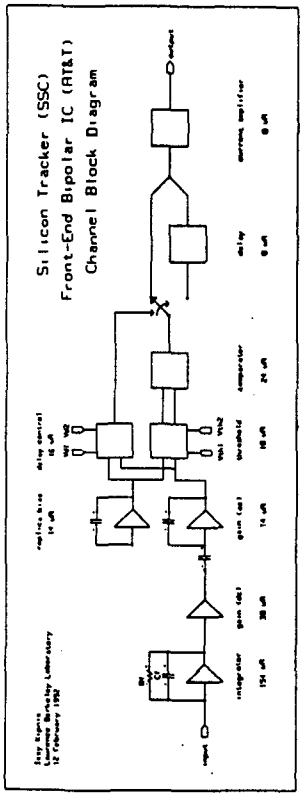

704

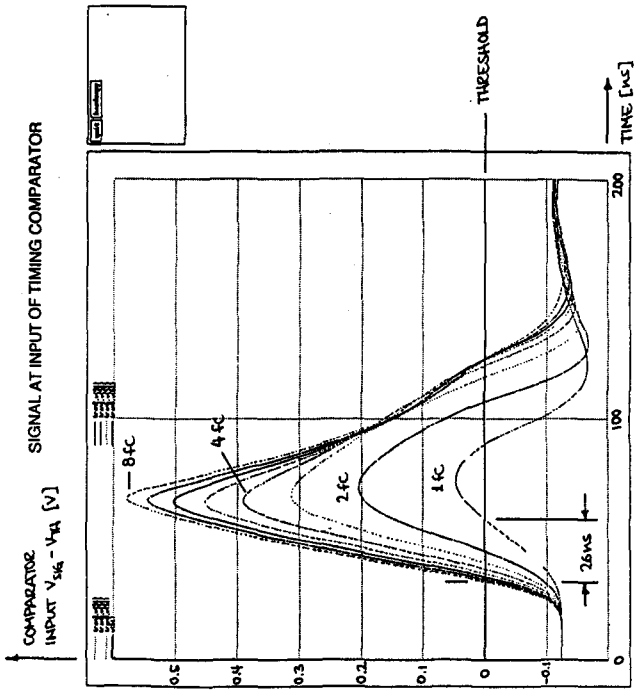

705

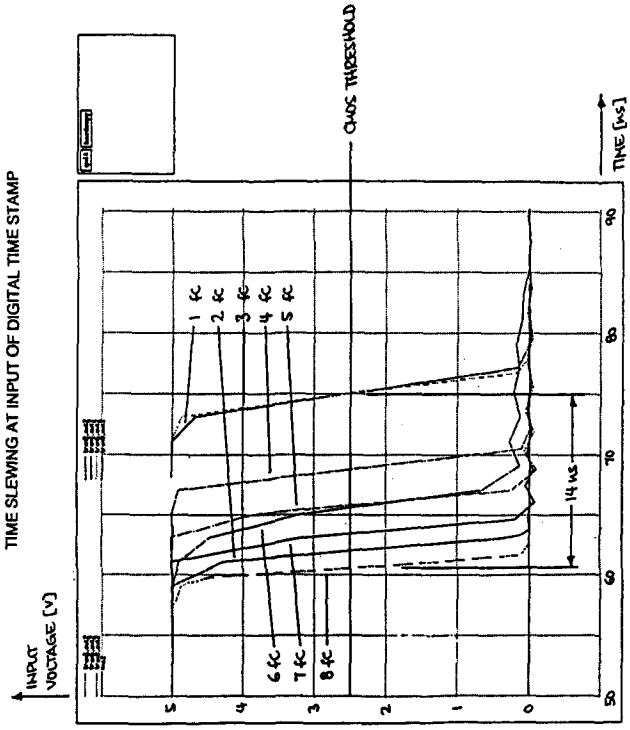

706

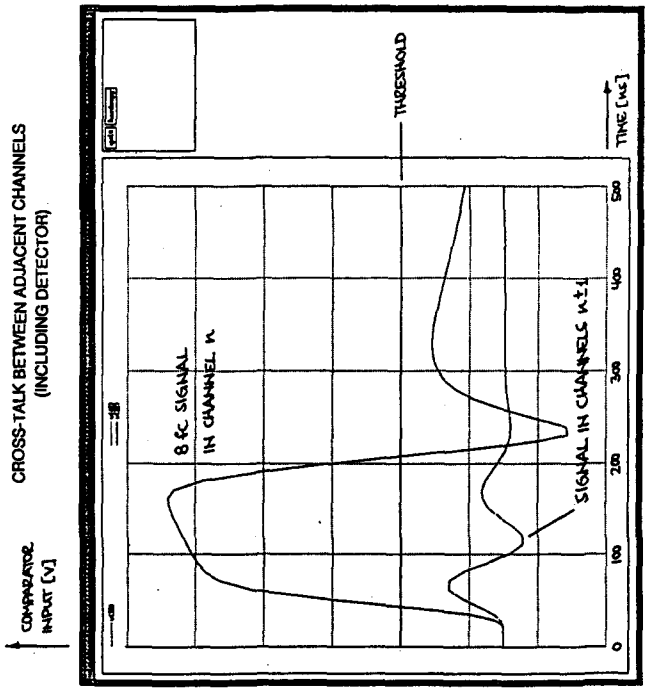

707

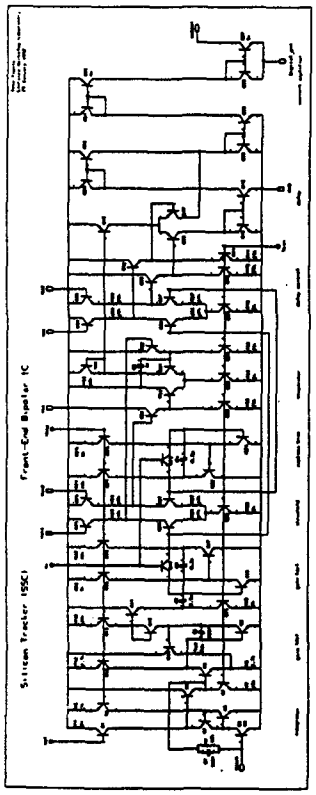

708

Silicon Tracker (SSC)
Front-End Bipolar IC (AT&T)

Noise Power Contributions

	$x10^{-6}$ [V^2]	%
Total	1533	100
Q_1	725	47.3
-Ic	-300	-19.6
-Ib	-300	-19.6
-rb	-125	-8.1
Detector Shot Noise	269	17.6
R_f	181	11.8
Q_1 of adjacent channel	93	6.1
Q_1 of adjacent channel	93	6.1
Detector Bias Resistor	58	3.8
R_4	21[1]	1.4
Other (< 1% each)	93	6.1

Notes.

- Adjacent channels contribute ~ 7% to the output noise voltage (increase the equivalent input noise charge by ~ 8%).

-Removing detector noise, Q_1 contributes 84% of the single channel output noise voltage.

Analog Readout Design Strategy

1. AT&T CBIC-U2 submission

Primary objective:
Proof of Principle to verify
1. electronic design concept
2. module design
3. demonstrate system operation
4. radiation resistance

Compromises:
1. die size (W= 3.1 mm, L= 6.85 mm)
2. 'slow' process
   - added gain stage and longer peaking time
3. dead time (due to longer peaking time)

Advantages:
1. earliest delivery date of the 3 candidate vendors
2. radiation resistance
3. simple layout changes for smaller device sizes (AT&T CBIC-V2, Westinghouse, Tek)

Circuit at AT&T (cell laid out by Issy Kipnis, W=40 μm)
Die layout complete (AT&T)
1 p-side chip with 64 complete channels
1 n-side chip with 64 complete channels
1 test chip with 16 preamplifier array + circuit blocks
Run shared with Penn

AT&T submission contains all elements of future designs
Note that walk compensation is an 'add on', *i.e.*
- it can be disabled by setting its threshold high
- it can be physically removed without changing the rest of the circuit.

2. Goals for subsequent designs

- reduce dead time
- minimize die size

Method:
reduce peaking time and
eliminate walk-compensation circuitry (if possible)

Comments:

Current data are for for p-side charge collection and n-side capacitance (= worst case).

Reduction of peaking time below 20 ns leads to significant ballistic deficit on p-side, but capacitance is lower so effective S/N can be preserved.

Capacitance on n-side is higher (current design value), but collection time about 1/2 of p-side, so shorter peaking time does not incur reduction of S/N.

Reduced peaking time improves timing (possibly allowing us to do without the walk compensation circuitry).

BUT: we will retain walk compensation circuitry in next round of designs until we have measured overall dispersion in system (incl. detector, dig. circuitry, *etc.*)

3. Next round of designs and fabrication runs

Same basic circuit with minor modifications tailored to vendor

1. Tektronix
   utilize JFET for preamp current mirror,
   lateral PNP loads where possible,
   resistors (especially high values) only when necessary

   Layout start (UCSC: Ned Spencer) soon

2. Westinghouse
   lateral NPNs and PNPs
   small devices
   smaller die (L= 5 mm)

   Layout start (LBL: Issy Kipnis): June 1

3. AT&T CBIC-V2
   similar to Westinghouse

   submit late 1992

TESTING OF A 64-CHANNEL BIPOLAR AMPLIFIER-COMPARATOR CHIP

David Dorfan
Ned Spencer
Max Wilder
Bill Rowe
Nicolo Cartiglia
David Hutchinson
Wladislaw Dabrowski
Hartmut F.-W. Sadrozinski

May 26, 1992
SDC Collaboration Meeting
KEK, Tsukuba, Japan

- The chip was produced in Tektronix SHPi. 64 Channels, 70 μm pitch, gain about 170mV/fC. Common threshold, calibration inputs common to every 4th channel.
- Simulations agree with measurements. Large resistors/capacitors result in large stray capacitances.
- Test philosophy: use threshold/discriminator output to find gain, noise, walk, risetime, propagation delay.
- With 10pF load, risetime is 30ns, noise is 1100e (expect 600 + 40 × C), propagation delay is 26ns power consumption is 133 mW = 2mW/channel, Walk (V_{th} = 1fC) is 11.5ns for 2-8fC input (min.ion. = 4fC)

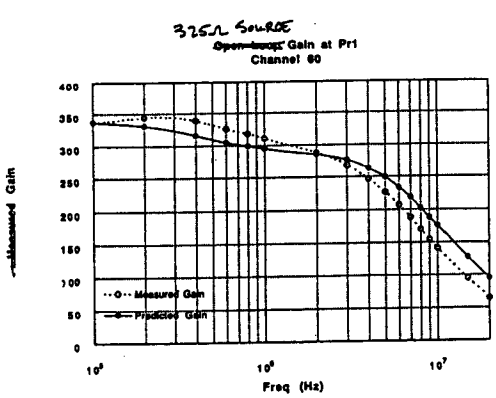

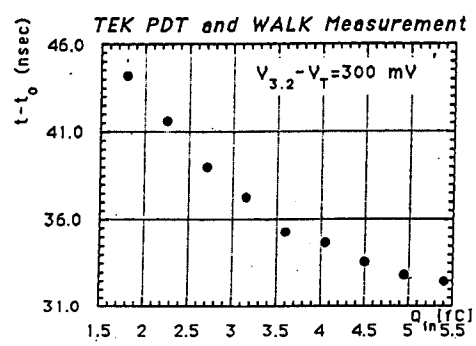

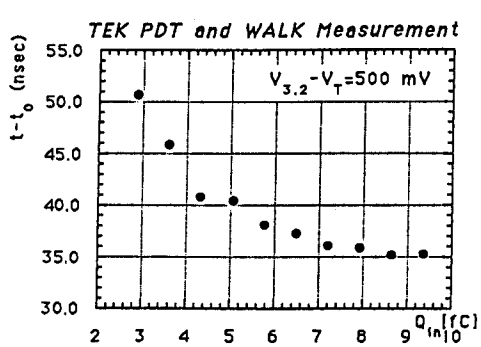

716

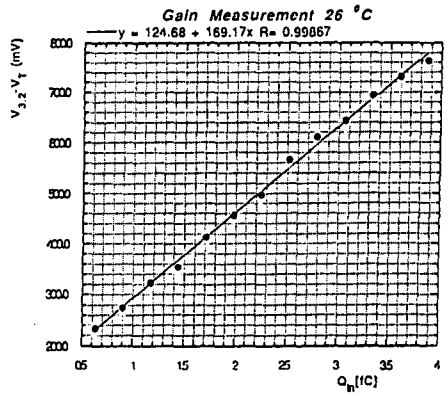

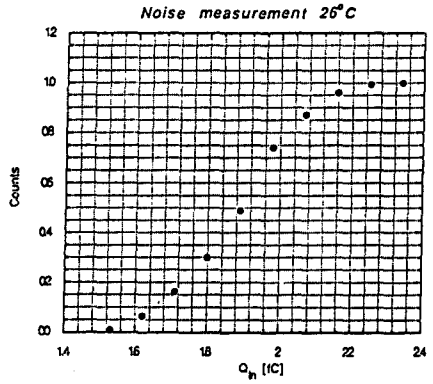

717

We can use a probe card to supply the power and input test pulses (through 25 fF calibration cap) and read the digital outputs. A hand-scan of 30 channels (5 chips) revealed good uniformity of gain and excellent yield.

The next step is the expansion of the probecard-based testing to a fully programmable system capable to do the SSC production testing.

718

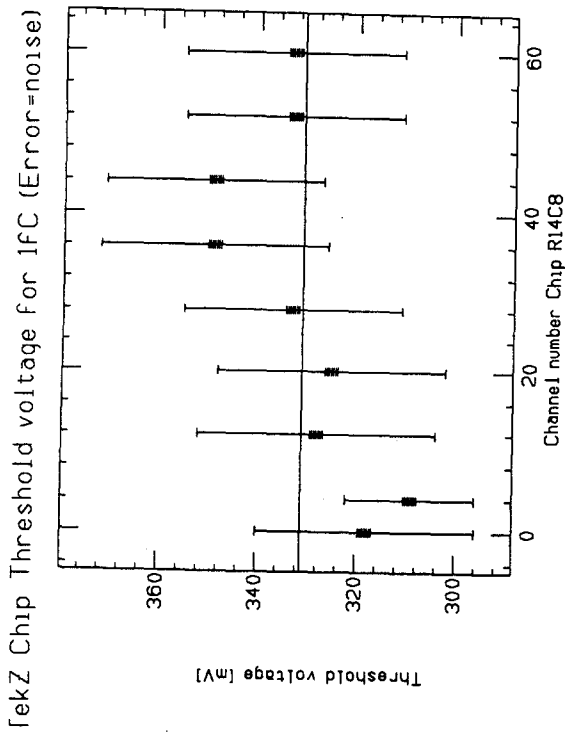

SDC portable DAQ

Masa NOMACHI (KEK)

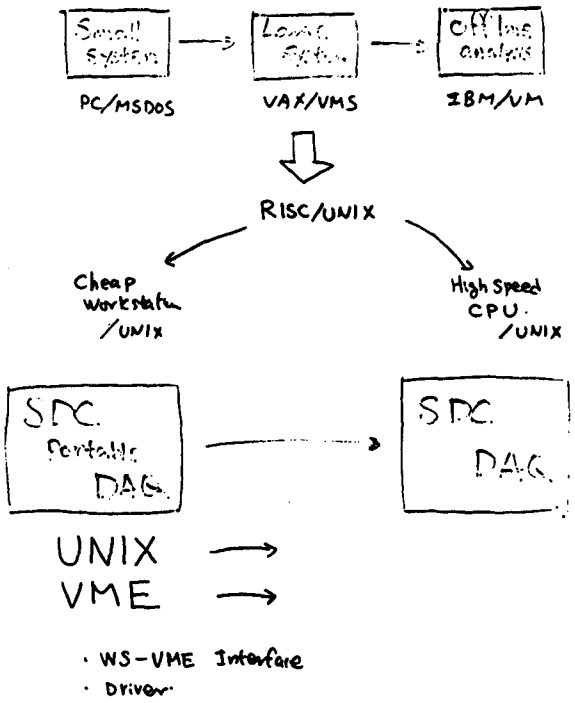

Interrupt Latency

DEC station 5000/200

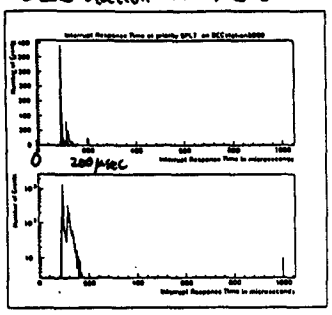

図13 DECS/ULTRIX上で解析データ表示プロセスPAWと3つのCPUバウンドプロセスを走らせた場合の割り込み応答時間のヒストグラム

μVAX II /VMS

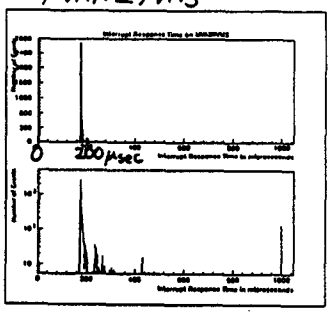

図14 μVAX/VMS上で解析データ表示プロセスPAWと3つのCPUバウンドプロセスを走らせた場合の割り込み応答時間のヒストグラム

みる必要がある。解析データ表示プロセスは若干通常より悪い使い方をした。DECS/ULTRIXの場合の結果は図13である。解析データ表示プロセスの他にCPUバウンドのプロセス2つを走らせている。解析データ表示プロセスの影響を受けてはいるがそれほどでもない。しかし、CPUバウンドのプロセスが入って、解析データ表示プロセスのみの場合より割り込み応答性が良くなっていることはかもしろい傾向である。VAX/VMSの場合は図14に示すが、あまり変化はない。

参考のためにVAX/VMSの場合について、デッドタイムを計算しシステムのデッドタイムの割合を割り出してみる。物理事象の頻度を100Hz、500Hz、1KHzでデータサイズが40バイト/400バイト/4000バイトの場合について試算した結果は表7である。実験によって割り込みの応答時間とデータ読みだし時間の割合はまちまちであるが、この表からわかるようにデータのサイズが大きくなるにつれ、割り込みの応答時間はシステムのデッドタイムの割合にきいてこなくなる。

結論及び計画

高エネルギー物理実験用データ収集システムに於けるVAX/VMSとDECS/ULTRIXとの「リアルタイム性」について、検証してきた。その結論として両者の差があまりなく、DECS/ULTRIXが使用に耐える可能性が十分にあることがわかった。従って、次のステップは実際のRISC/UNIXデータ収集システムを構築し検証することである。ただし、UNIXデータ収集システムはそこで走るプロセスの性質や数で大きく

Portable DAQ

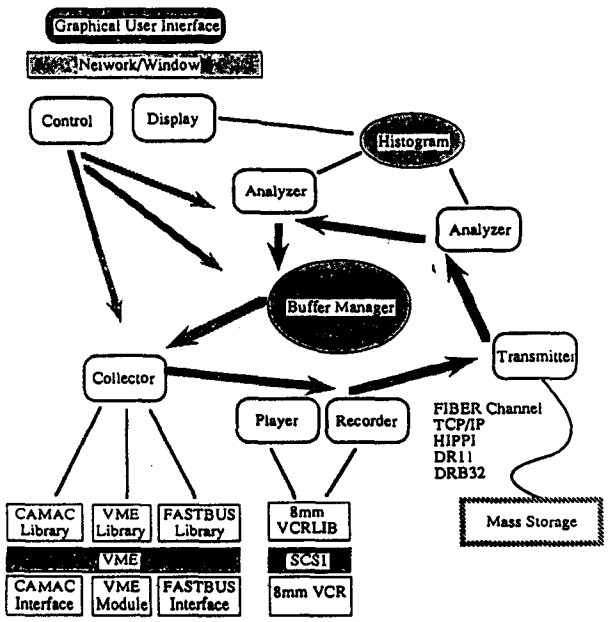

What DAQ provides

(by this workshop)

- Device Driver on UNIX
- Utility programs
  - · Buffer manager
  - · Histogramming (CERN Lib)
  - · GUI tool kit
  - · Run control tool kit
- TEM (Trigger Emulation Module)
  W. Smith (Wisc)

What DAQ define.

- Usage of the portable DAQ crate.

What each subgroup must provide.

- GUI
- Run control
- Read out crate

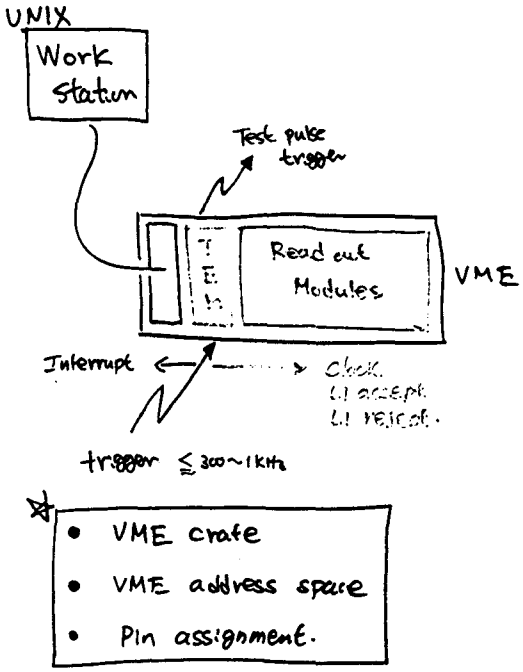
UNIX
Work Station
Test pulse trigger
Read out Modules
VME
Interrupt
Clock
L1 accept
L1 reject
trigger ≲ 300~1kHz
• VME crate
• VME address space
• Pin assignment.

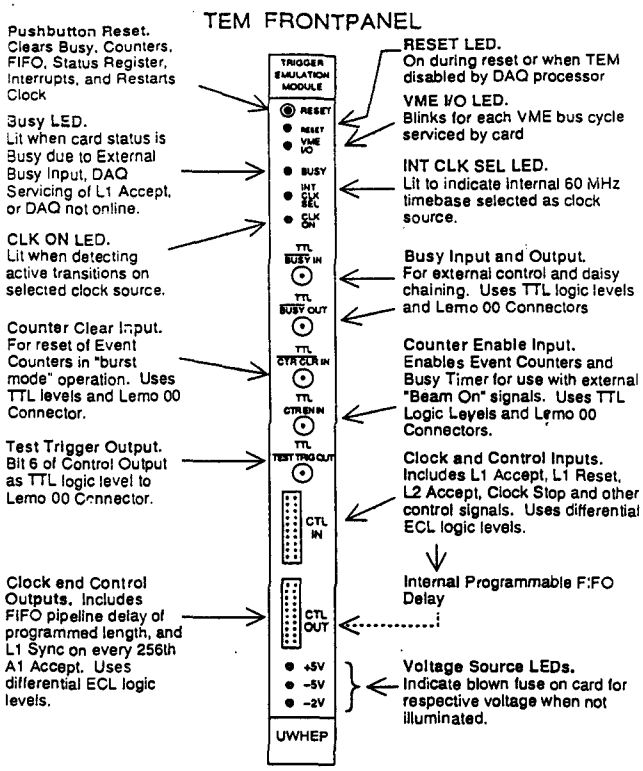
TEM FRONTPANEL
Pushbutton Reset. Clears Busy, Counters, FIFO, Status Register, Interrupts, and Restarts Clock
Busy LED. Lit when card status is Busy due to External Busy Input, DAQ Servicing of L1 Accept, or DAQ not online.
CLK ON LED. Lit when detecting active transitions on selected clock source.
Counter Clear Input. For reset of Event Counters in "burst mode" operation. Uses TTL levels and Lemo 00 Connector.
Test Trigger Output. Bit 6 of Control Output as TTL logic level to Lemo 00 Connector.
Clock and Control Outputs. Includes FIFO pipeline delay of programmed length, and L1 Sync on every 256th A1 Accept. Uses differential ECL logic levels.
TRIGGER EMULATION MODULE
RESET
RESET
VME I/O
BUSY
INT CLK SEL
CLK ON
TTL BUSY IN
TTL BUSY OUT
TTL CTR CLR IN
TTL CTR EN IN
TTL TEST TRG OUT
CTL IN
CTL OUT
+5V
-5V
-2V
UWHEP
RESET LED. On during reset or when TEM disabled by DAQ processor
VME I/O LED. Blinks for each VME bus cycle serviced by card
INT CLK SEL LED. Lit to indicate internal 60 MHz timebase selected as clock source.
Busy Input and Output. For external control and daisy chaining. Uses TTL logic levels and Lemo 00 Connectors
Counter Enable Input. Enables Event Counters and Busy Timer for use with external "Beam On" signals. Uses TTL Logic Levels and Lemo 00 Connectors.
Clock and Control Inputs. Includes L1 Accept, L1 Reset, L2 Accept, Clock Stop and other control signals. Uses differential ECL logic levels.
Internal Programmable FIFO Delay
Voltage Source LEDs. Indicate blown fuse on card for respective voltage when not illuminated.

FIGURE 2

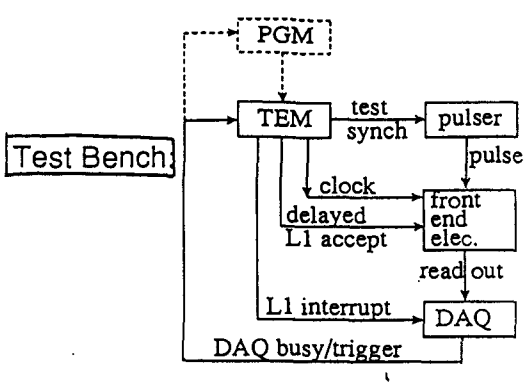
PGM
Test Bench
TEM
test synch
pulser
pulse
clock
delayed L1 accept
front end elec.
read out
L1 interrupt
DAQ
DAQ busy/trigger

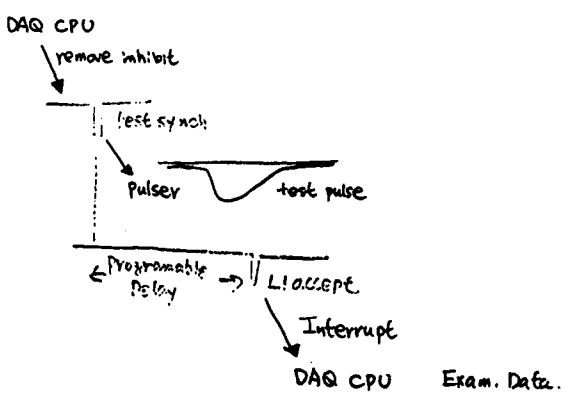
DAQ CPU
remove inhibit
test synch
Pulser
test pulse
Programmable Delay
L1 accept
Interrupt
DAQ CPU
Exam. Data.

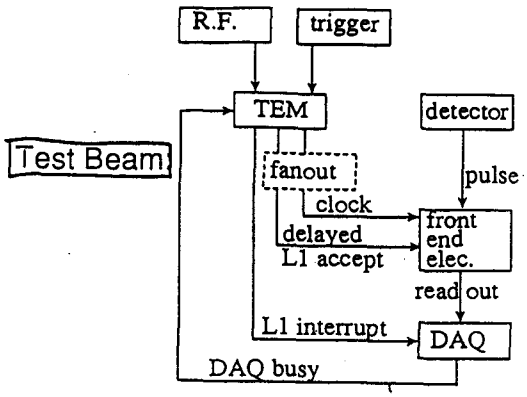
R.F.
trigger
TEM
detector
Test Beam
fanout
pulse
clock
delayed L1 accept
front end elec.
read out
L1 interrupt
DAQ
DAQ busy

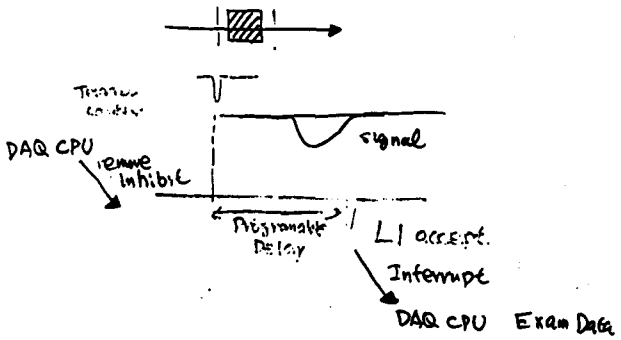
signal
DAQ CPU
remove inhibit
Programable Delay
L1 accept
Interrupt
DAQ CPU
Exam Data

[3] Tracking/Electronics Joint

< Straw Tracker R & D >

Activities in Japan	T. Ohska	- 728
Straw R & D at Duke	S. Oh	- 738
R & D Progress from Colorado	W. Ford	- 782

< Resolution >

Resolution Studies of 4 mm Straws	H. Ogren	- 795

< Readout Electronics >

Straw ASD	M. Newcomer	- 803
Conceptual Studies on FEB of the Straw Chamber	S. Odaka	- 819
Straw Electronics Layout	R. Berg	- 827
New TMC Design with Toshiba Gate Array	Y. Arai	- 840
Radiation Damage Test of Time Memory Cell	M. Chiba	- 851
A Plan of Cosmic-ray Test of Straw Readout at Tokyo Metropol. Univ.	K. Yamauchi	- 871
DCC Design for the SDC Straw Tube Tracker	P. Sinervo	- 875

< Trigger >

SDC Straw and Muon Triggers	J. Chapman	- 895

< Mechanical Study >

Mechanical Measurements on 4 m Prototype	D. Rust	- 932
Mechanical Considerations for a SDC Outer Straw Tracker for the SSCL	R. Swensrud	- 946

< HV System >

HV System for Straws	D. Rust	- 970

< Fiber Tracker >

Scintillating Fiber Tracker Future R & D	D. Koltick	- 976

Activities in Japan

Tokio K. Ohska
(KEK)

JSD Straw-Tube Readout Group (total 12) as of April 1, 1992

@KEK

Tokio K. OHSKA : co-Coordinator/electronics in general
Yasuo ARAI : Rad-hard process, Next generation TMC design, Electronics design
Shigeru ODAKA : Electronics fablication, coupling to tubes, structural design
Masahiro IKENO : Circuit design, High density Packaging , PC layout
Yoshiyuki WATASE ; electronics in general

@Tokyo University of Agriculture and Technology,
Main responsibility : L2B Circuit design

Tsuneo EMURA
Fumio SUDO

@Tokyo Metropolitan University, Fuculty of Science,
Main responsibility : Chamber test of electronics, Radiation test

Masami CHIBA
Tatsushige HIROSE
Ryosuke HAMATSU
Kouji KONDO
Kazuo YAMAUCHI

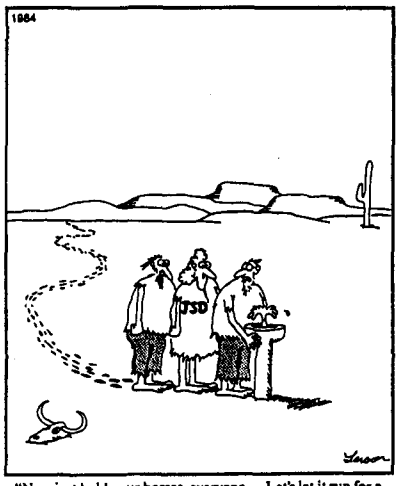

"Now just hold your horses, everyone.... Let's let it run for a minute or so and see if it gets any colder."

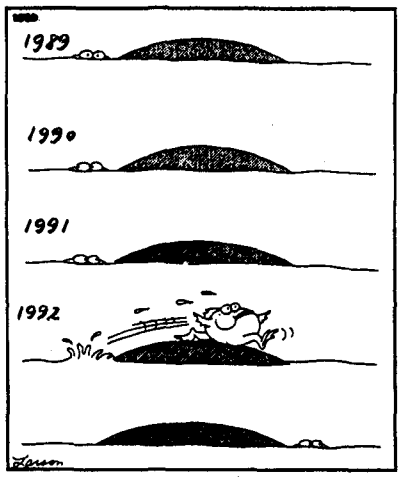

Another great moment in evolution

1. Rad-hard CMOS gate array

Started to work with Toshiba.
Schedule looks OK.
Need to workout on budget/cost.
------Y. Arai will give a talk later on this subject

2. Electronics packaging

Making mock-ups to get the feeling of available space.
Cooling study : Production of test set-up with heat modules.
Ordering thermperature sensors, softwares.
Collecting information.
Connectors : Daiichi Denshi Corp. (former OEM supplier to Amphenol) is working with us.
We may custom make the connectors.
------S. Odaka will give a talk later on this subject

3. Designing Level 2 Buffer

In a stage to learn to run the Toshiba program on work stations.

4. Chamber test, radiation test of electronics

Preparing the chamber test set-up at the TMU.
Radiation test facility is also available from the TMU.
-----K.Yamauchi will report on this.

5. Produce electronics using TMC so that other people can get themselves familialized with the TMC chips.

CAMAC TMC module version 1: 10 modules are available.
CAMAC/VME TMC module with intelligence : designing stage

We plan to provide VME units for muon test.
------M.Ikeno will give a talk later on this subject

Straw Tube Readout : Front-End-Board Heat Consideration Basics

April 20,1992 KEK T.K.OHSKA

Basic Facts (for 8-layer units)

(1) Assume that the available cross-sectional area for the electronics is the trapezoidal area defined by the 4 outermost straw tube centers. According to the conceptual design report, this trapezoid has dimentions of 9.024cm and 11.713cm for top and bottom sides. 2.443cm hight for an 8-layer unit.

This area is 25.33 sq.cm.

(2) According to the drawing presented at the Indiana Meeting on 8th of April '92, total available depth for the readout front-end-board is 12cm including space for straw tube end cap, connectors, HV resistors/capacitors, clearance for installation/removal.
To reduce unwanted stress to be applied to the straw tubes during FEB installation/removal work, I consider flexible joint mechanism to be essential between the endcap and FEB or between the endcap (with HV distribution part) and the rest of the FEB. This will easily take up 3 to 6 cm depth out of the available 12cm. If the flexible joint is not included here, we would need 2 to 4 cm clearance for installation/removal of board (mainly for repair work) in addition to depth needed for the endcap.

Depth available for the heat generating electronics would be 6cm out of the available 12cm total depth.

This brings the total volume for heat generating section of the FEB to be;
25.33 x 6 = 152 cubic centimeters.

(3) Assume the power consumption per channel is 45mW as mentioned by someone at the April meeting at Fermilab.

45mW x 212channels = 9.54 watts.

Hence the power density for that section is;
9.54 / 152 = 63mW/cc

(4) To get some idea, let me compare this number with a high power FASTBUS. According to the FASTBUS specification, inside of the FASTBUS crate is;
43.09cm wide x 36.7cm high x 42.6 cm depth.
Removing the depth for the rear-end connector (0.9cm) from the 426cm depth, total volume inside the fastbus crate is;

43.09 x 36.7 x 41.7 = 65945 cubic cm.

A rather high power FASTBUS crate produces 2kW, hence its power density is;

2000 W / 65945 cc = 0.0303 W/cc = 30mW/cc

Therefore, te power density for the straw FEB power generating section will be twice as much as that of the high power FASTBUS crate.

(5) Assuming the thickness of the FEB to be 1.6mm(1/16") and the average component height per side to be 1.5mm. One may argue that the thickness of a IC wafer is far less than 1.5mm and also there will be areas where only patterns on the FEB. However, I consider this 1.5mm to be reasonable for such boards from various considereations.
4.6mm per FEB and 4 layers = 18.4mm thickness out of 24.43mm height. This leaves 6mm gap for airflow (1.5mm space per gap.).
Average width ,(9.024+11.713)/2=10.37 cm, times 0.6cm gap = 6.2sq.cm. This is the openning for the air to flow through.

Density of air at 20 deg.C = 0.0012 g/cc
Specific Heat of air (20 to 440 deg.C) = 0.237 cal/(g.deg.C)
= 0.28 mcal/(cc.deg.C)
=1.19mJ/(cc.deg.C)
Since V (cm/sec) x 11.9mJ x 6.2 sq.cm = 9.54W, (for 1deg.C rise), the cooling air velocity, V must be1293cm/sec if only 1 deg.C air temperature rise is alowed.

At this point, we do not know how many degrees centigrade the air temperature rise is acceptable. (Local gain change in straw tubes).

If 10 deg.C rise is acceptable, 129cm/sec air flow is needed. This translates to 4.6km/hr or 2.9 mph air velocity.

This is about a slow walking speed so that one might think it is not very fast. However, in such a clamped area, where air flow path is not a simple one, I expect it very hard to provide such air flow speed.

(6) Should we add heat exchangers between FEBs in a radial way so that we can flow the cooling air in a circular fashion, we must provide enclosed air duct so that the cooing air does not go away from the FEB gaps to the support frame area. This will not be easy either. We must also provide approx imatelyIcm gap between FEBs for the heat exchanger.

(7) At this point, I would say that conduction cooling through the FEB boards to a cooled supporting frame section will be a better choice. (This justifies thick PC boards). One could add water pipe along the supporting frame structure to bring the heat to outside world.
45mW per channel x 129,744 total number of channels =5.8kW can be brought outside via water pipe.

(8) If we can bring the power per channel down to 30mW, it would help. But it would not significantly change the situation.

SUGGESTIONS:

(1) We will need heat exchangers.
(2) We should consider conduction cooling.
(3) This requires that PC boards for FEBs can not be ultra-thin.
(4) We should require more space for the FEBs. 12cm does not look sufficient to me. Another 4 to 6 cm will provide space for the cooling fixtures. We should not have built-in impossibles.
(5) Reducing the mass of FEB will not be the top priority.

Front-end Electronics Volume : 10cm x 2.5cm x 8cm = 200 cc

Considering air space, average density would be approximately 1.
Specific heat would average about 0.3 cal/g deg.C = 1.3 J/gdeg.C

Even at 6w power consumption total per unit,

6/(1.3 x 200) = 0.02 deg.C/sec

1 deg.C/50 seconds

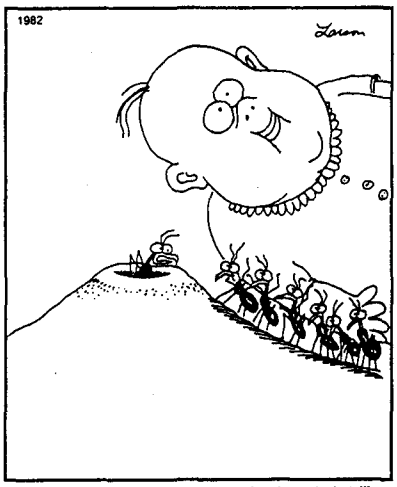

"You idiots!... We'll never get that thing down the hole!"

Do we have enough space for straw tube readout electronics?

Straw R&D at Duke

1. Prototype construction.
2.7 meter 64 channel
3.0 meter 100 channel
4.0 meter 159 channel

2. Resolution Measurement.
as a function of distance
as a function of high voltage
as a function of rate
as a function of amplifier

Seog Oh.

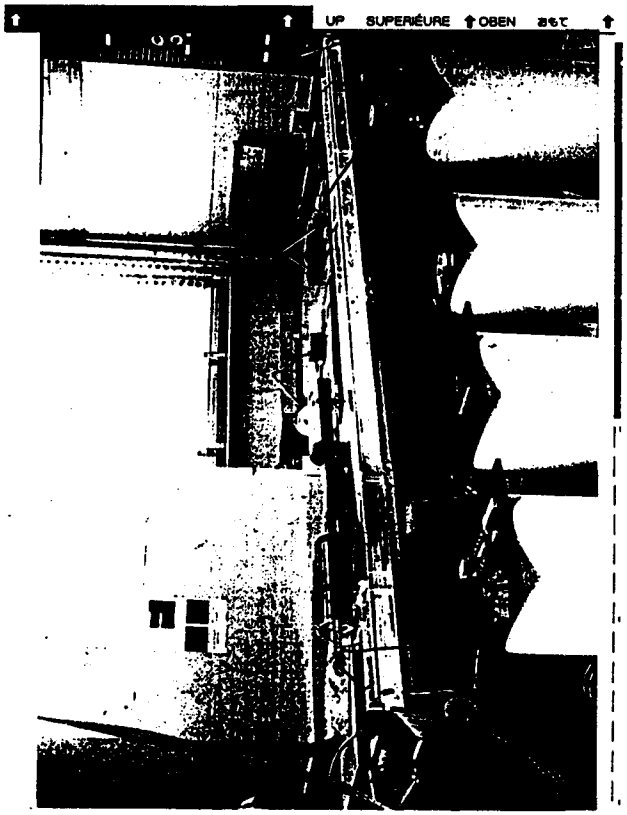

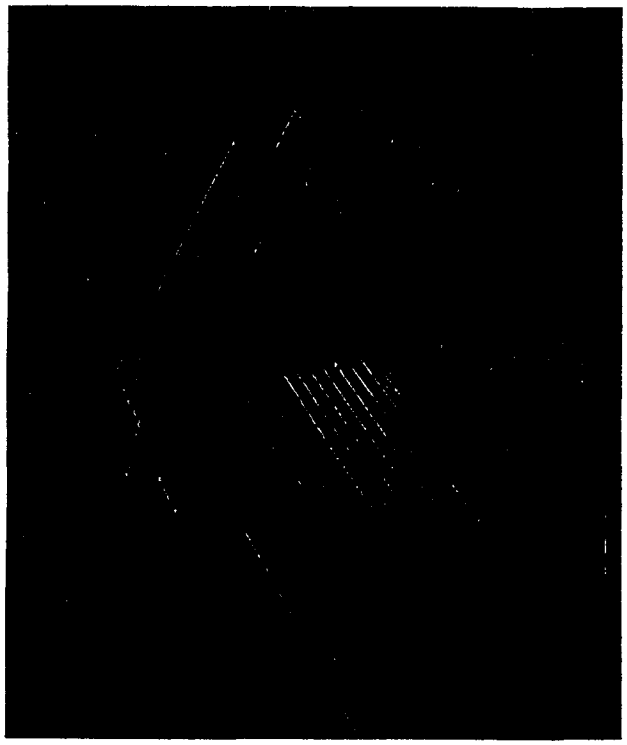

742

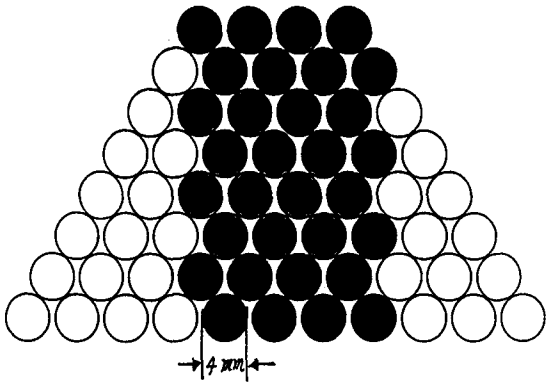

743

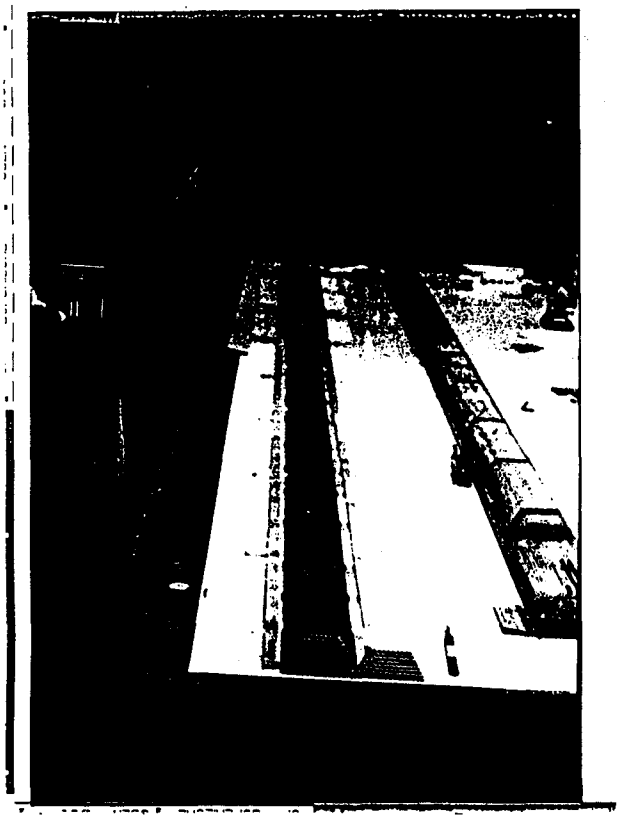

744

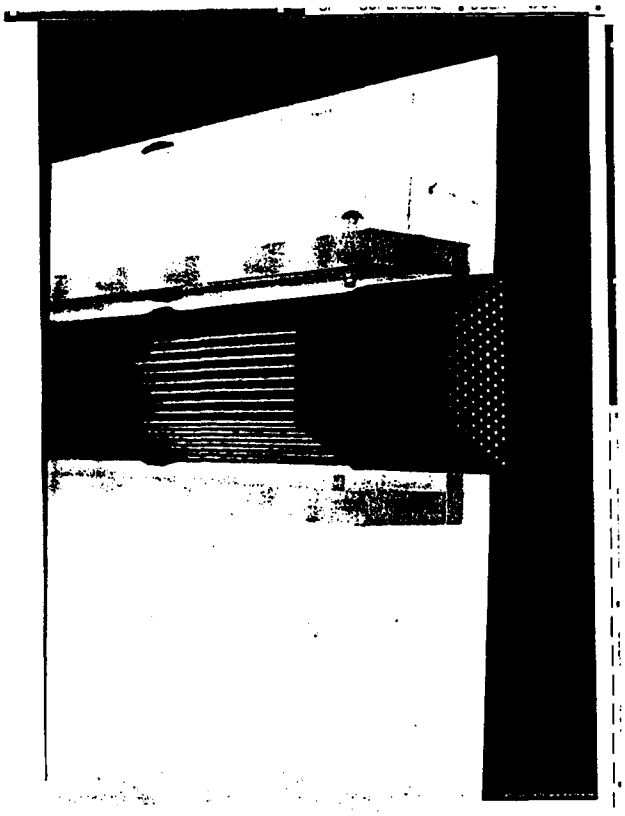

745

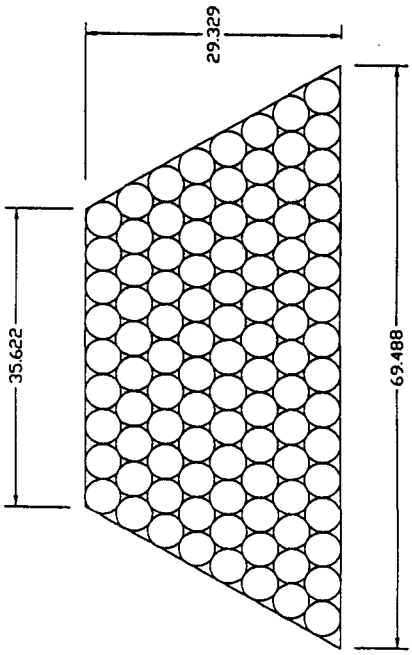

716

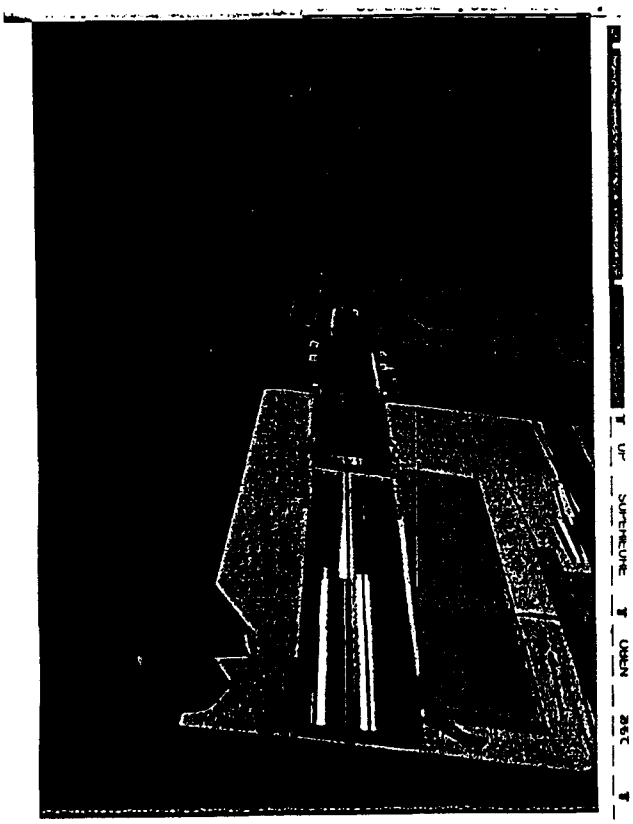

717

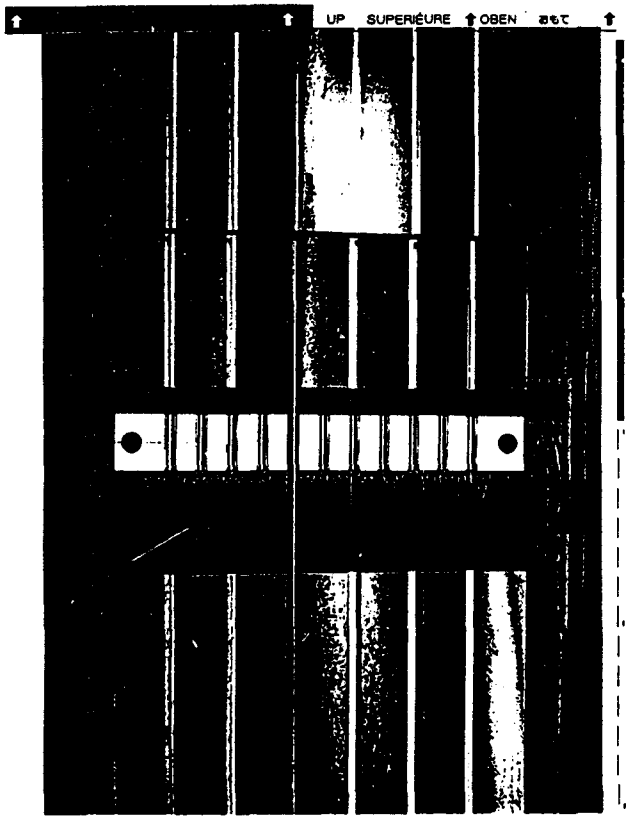

718

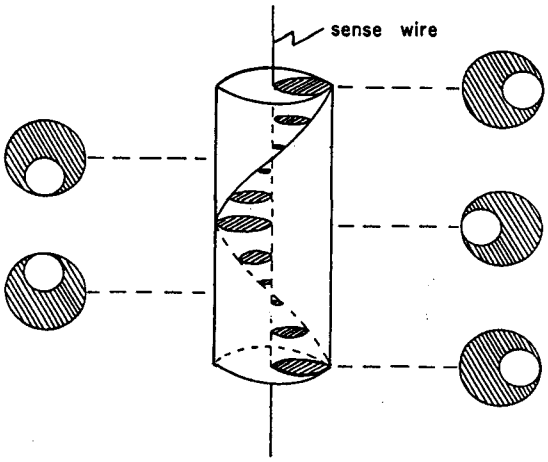

FIGURE 11

719

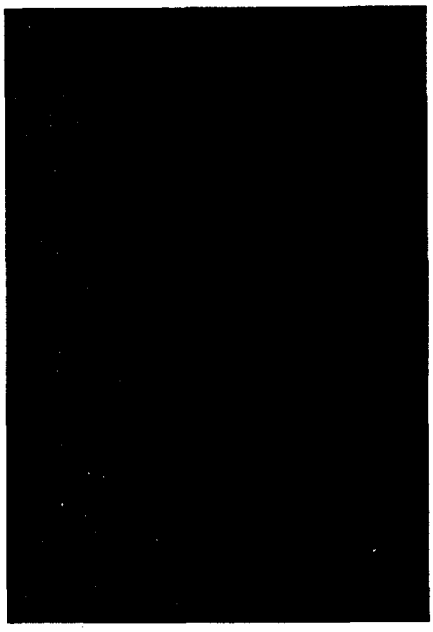

750

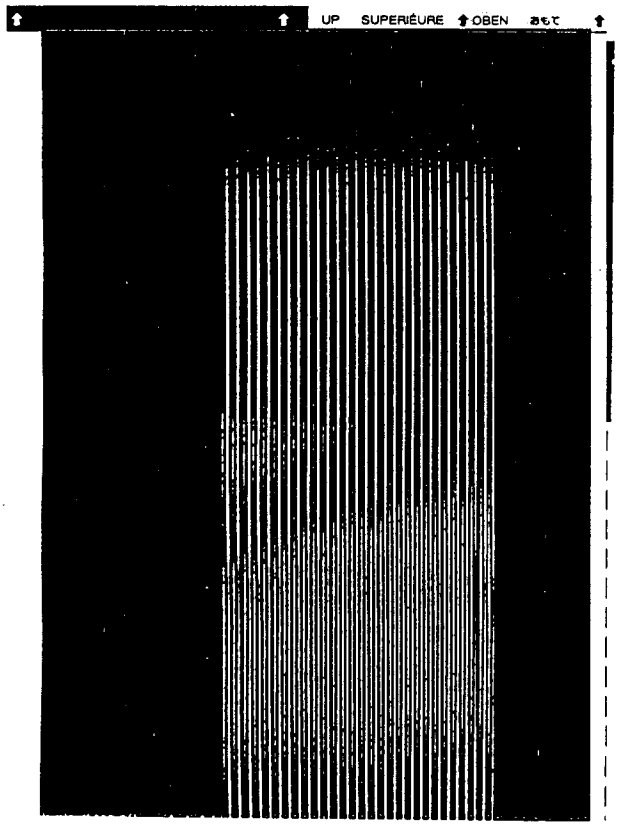

751

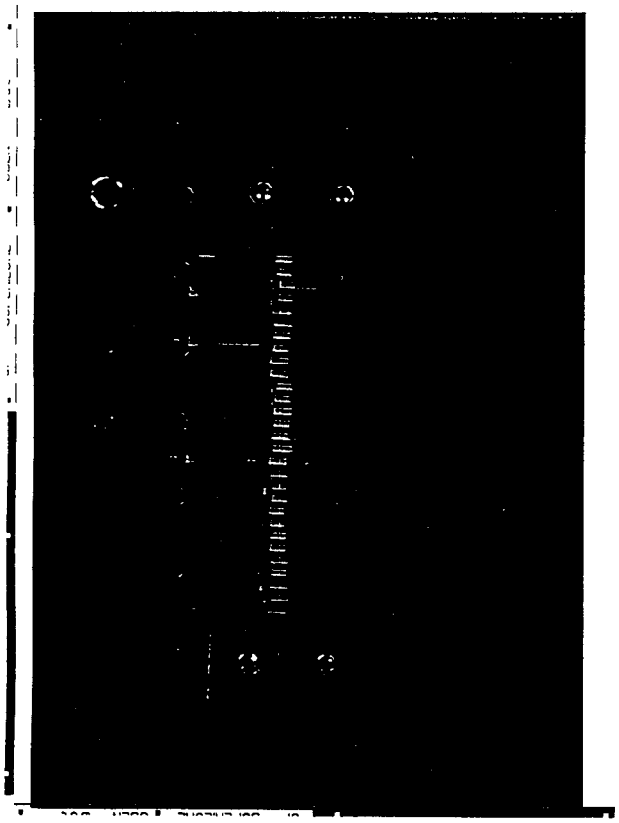

752

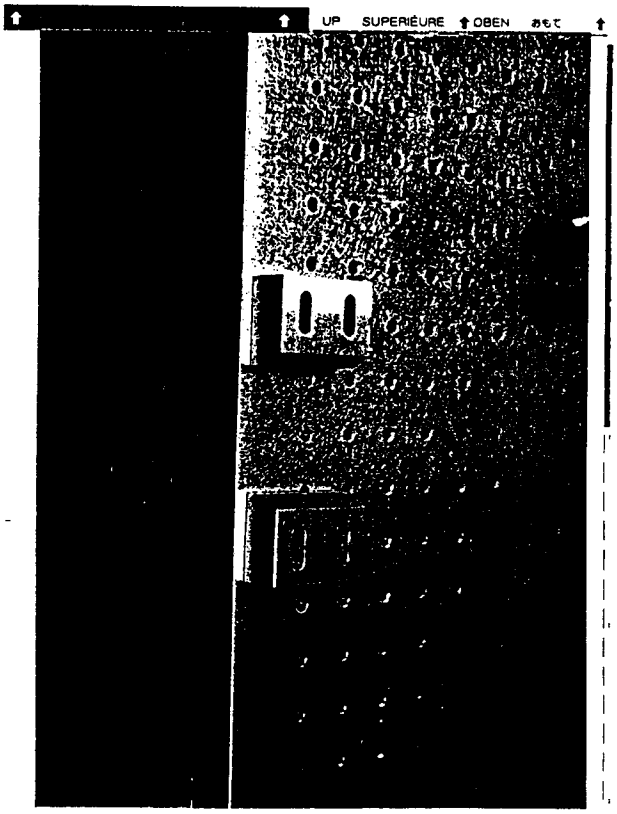

753

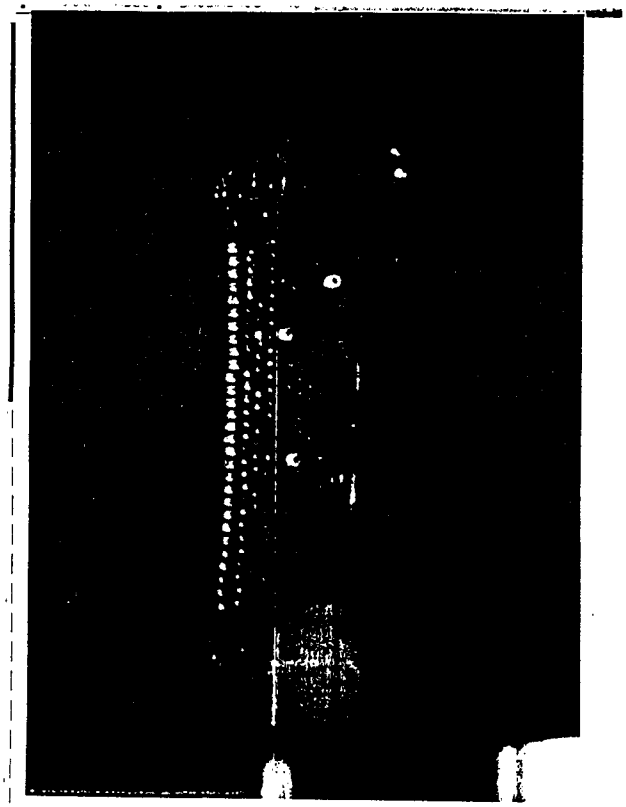

754

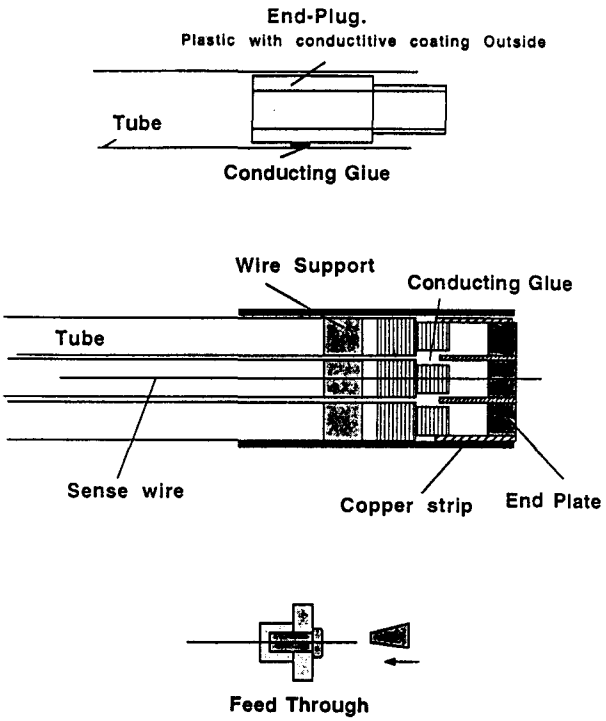

755

We have accumulated a great deal of experience from prototypes. The success of the prototypes shows that the chamber is stable, rugged and not difficult to construct.

756

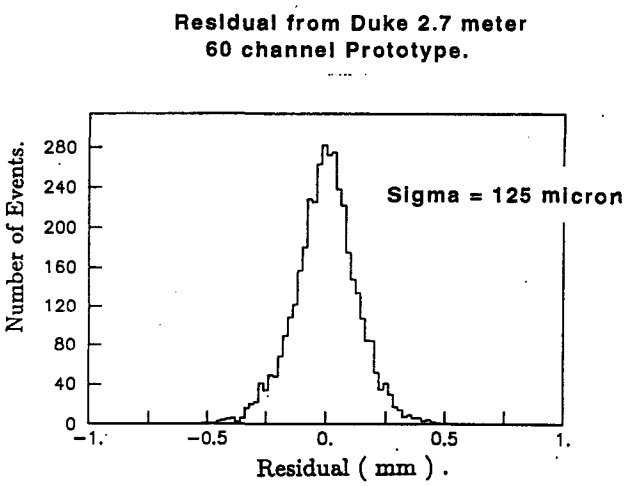

757

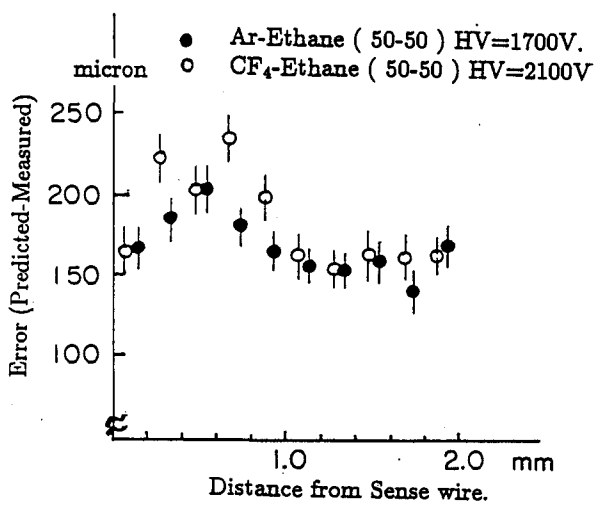

758

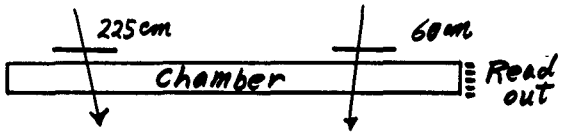

759

Cathod: 1500Å thick Cu
(20Ω/meter of straw)

Sense wire: 100Ω/meter

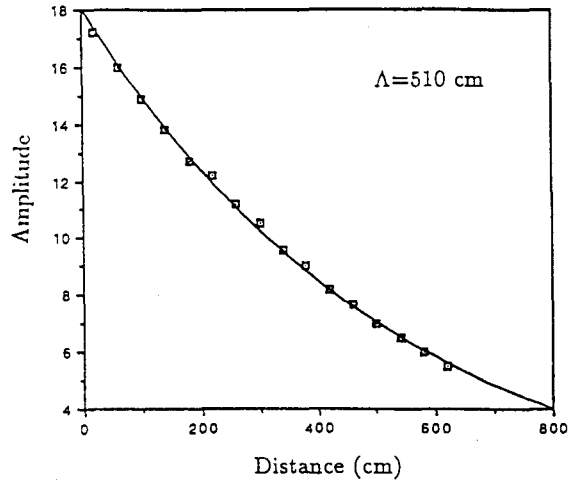

Fig. 1.14 Straw tube attenuation length measurement (7 m straw tubes).

760

HV= 2100 L= 60±10 cm

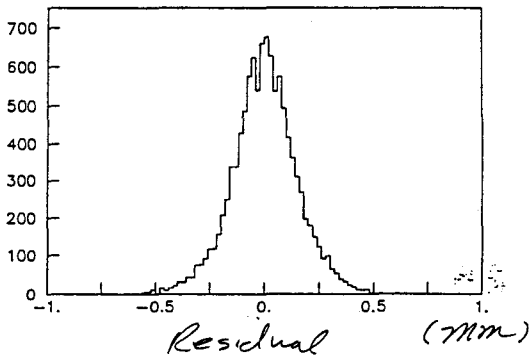

761

HV=2200 L= 225±10 cm

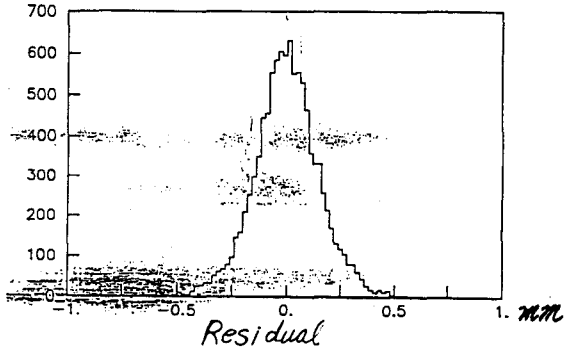

762

HV= 2100 L= 225±10cm

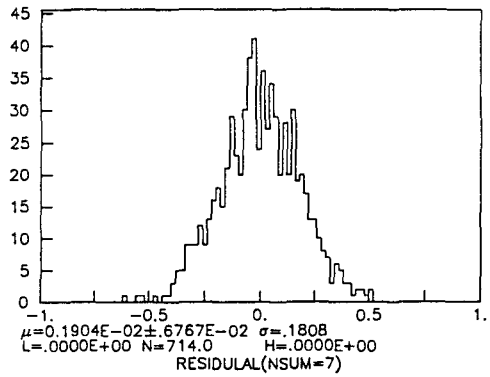

763

HV= 2200 L= 60±10 cm

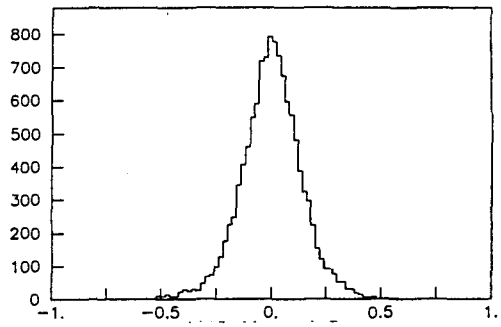

764

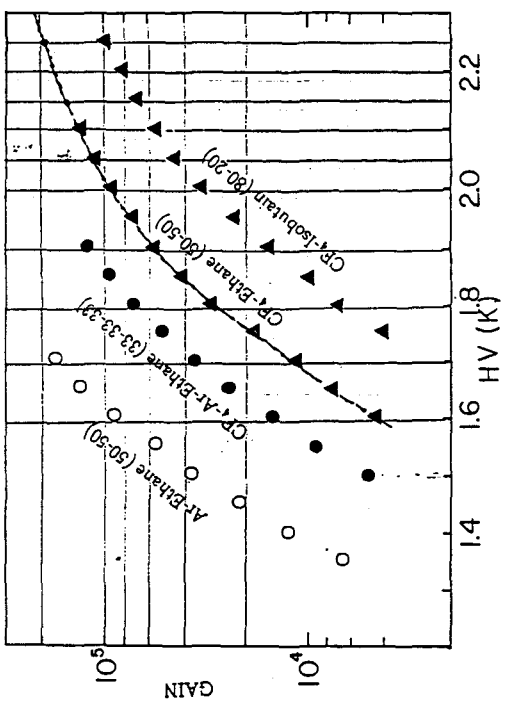

Figure 12

765

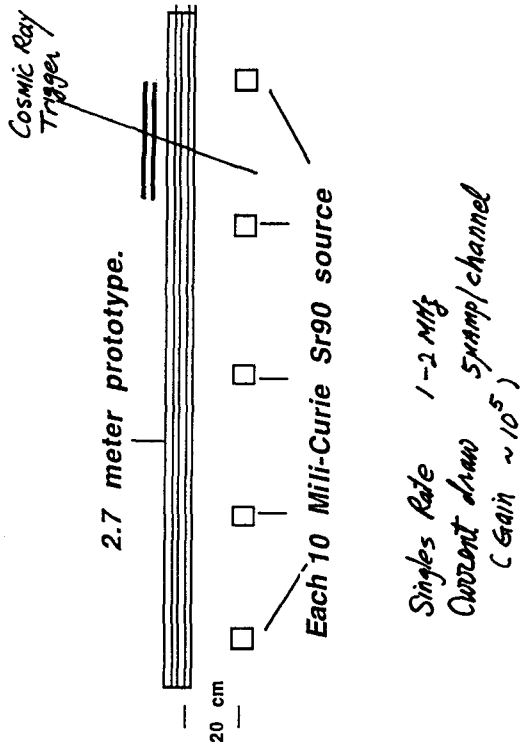

766

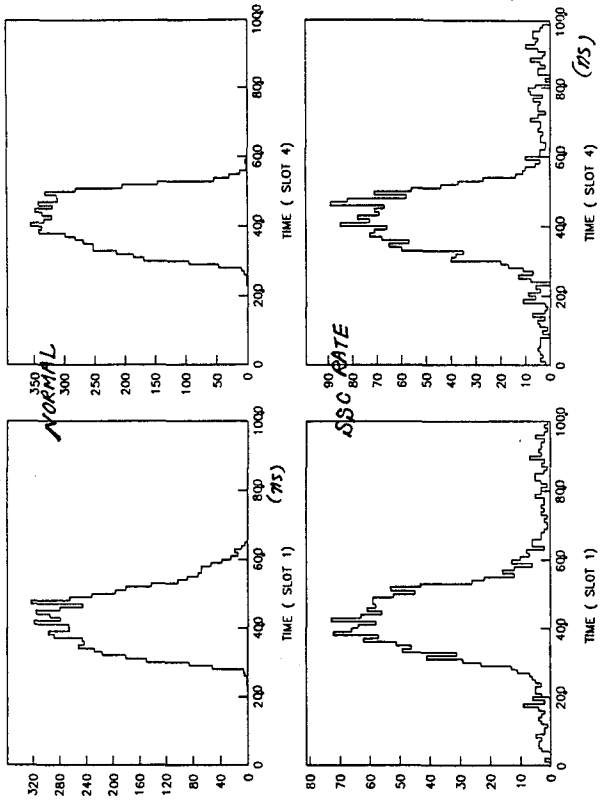

767

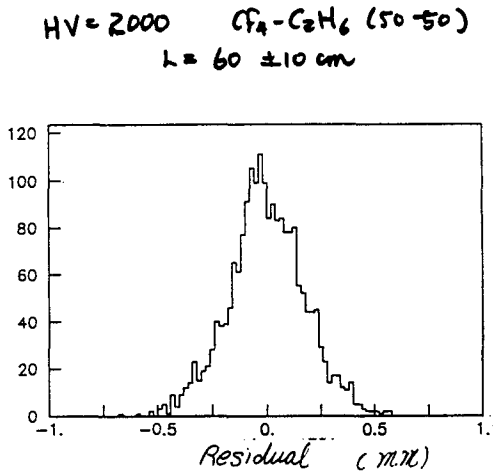

768

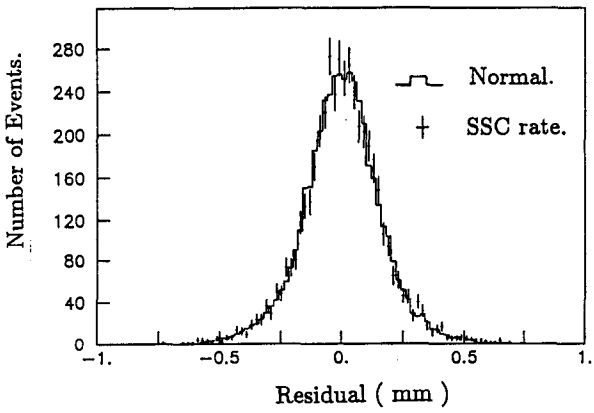

769

TMI

TMC1004 32-Channel CAMAC Multi-Hit

TDC Module Manual

Rev.1.0 Mar. 19, 1991

Prepared by Y. Arai
KEK, National Laboratory for High Energy Physics
1-1 Oho, Tsukuba, Ibaraki, Japan
Tel : 0298-64-1171 ex.6212
Fax : 0298-64-2580
Bitnet : ARAIY@JPNKEKVX

770

Gas : CF_4-C_2H_6 (50-50)

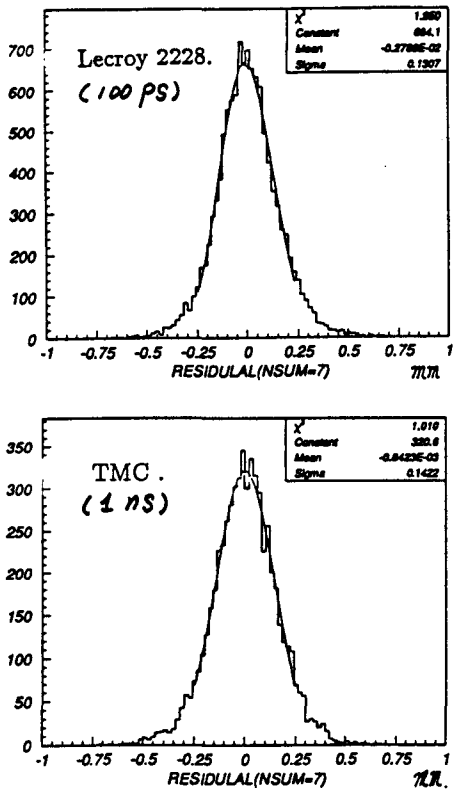

771

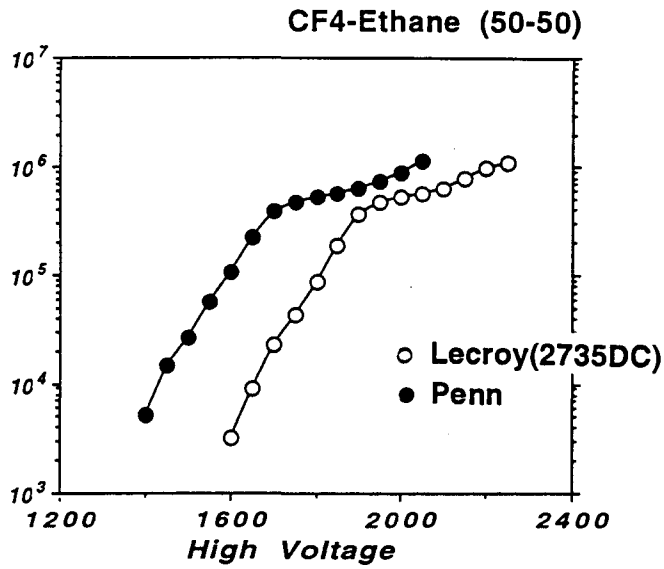

772

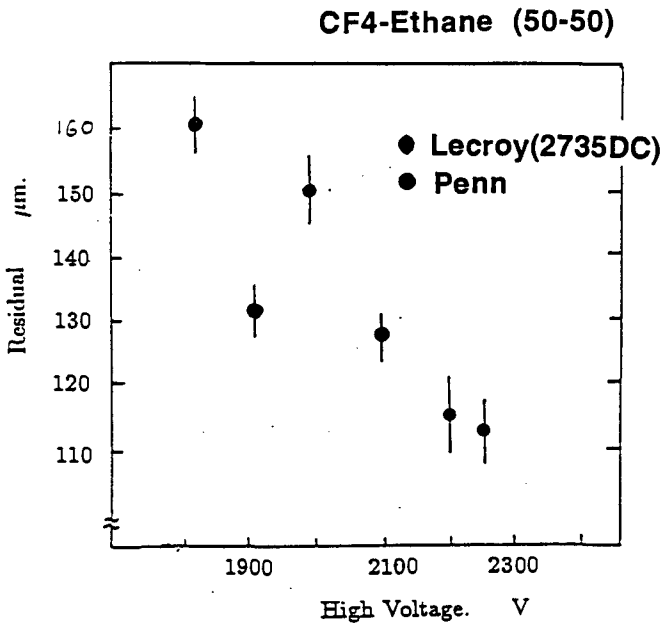

773

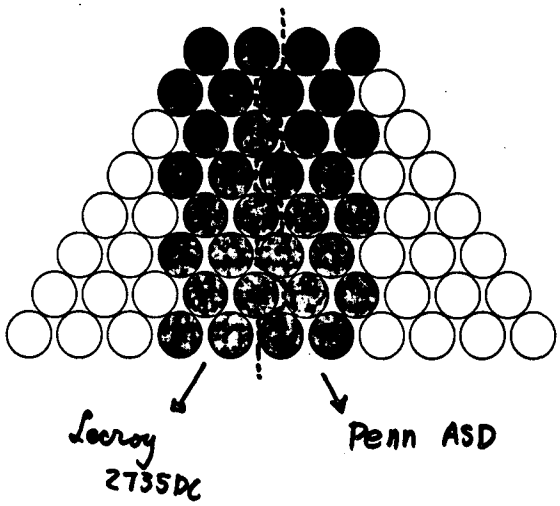

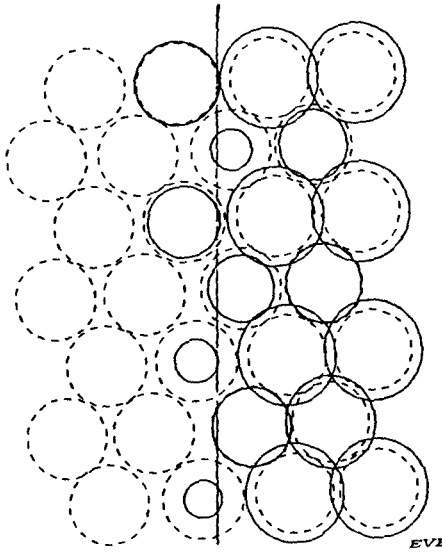

EVENT NUMBER 9

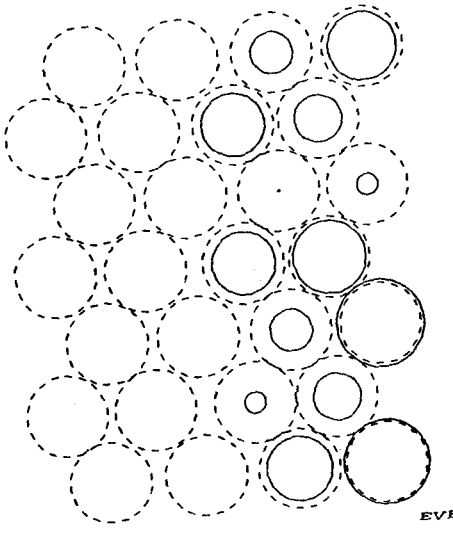

EVENT NUMBER 19

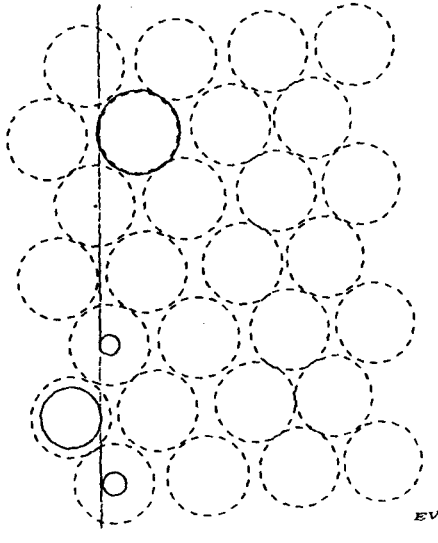

EVENT NUMBER 5

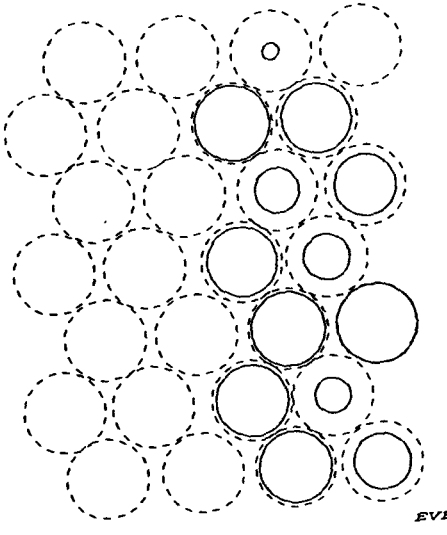

EVENT NUMBER 6

778

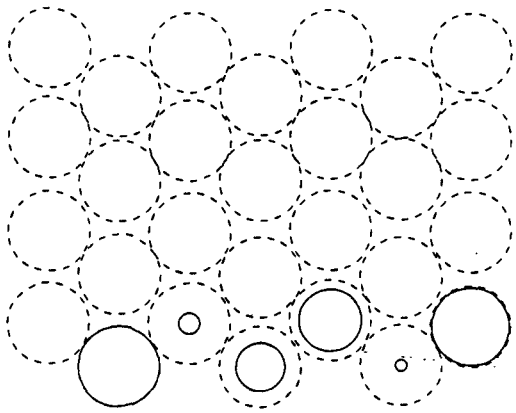

779

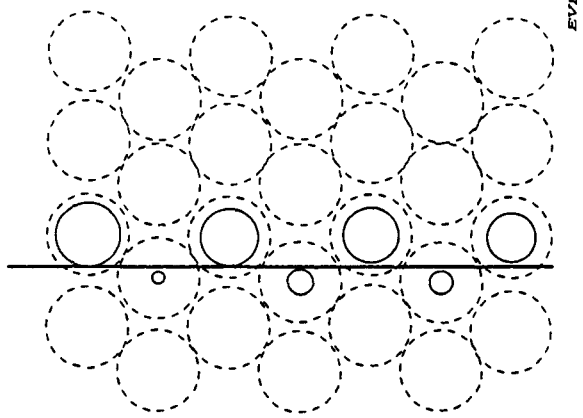

780

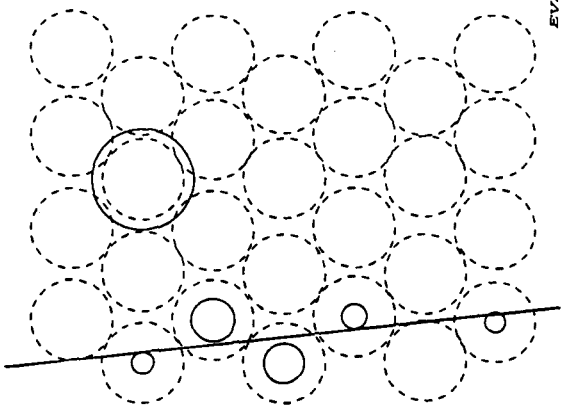

781

Resolution of $\lesssim 120\mu m$ is not difficult obtain even under SSC condition.

Signal attenuation can be overcome by raising HV ~150V

Penn electronic (ASD) looks good

TMC peforms as expected.

782

R&D Progress from Colorado

w Ford 5/28/92

1. A concept for a high density A-S-D board (and proposal for next step)
2. Status of (A-S) + D ("big" boards)
3. " " packaged (A-S-D)×8 boards, ECL drin
4. " " wire supports
5. cosmic ray tests - resolutions as function of gas mixture

783

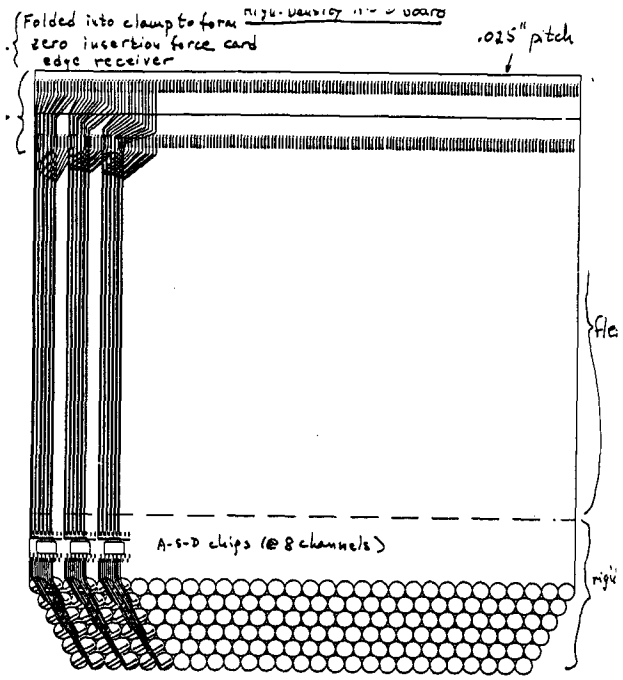

781

zero insertion force card edge connector (opens to release)

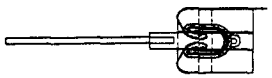

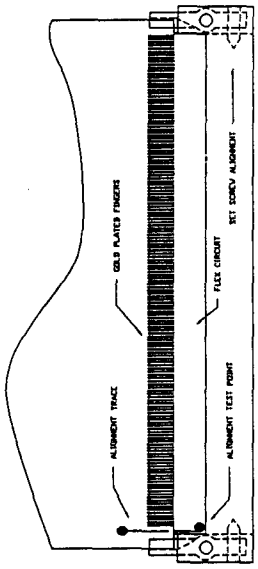

785

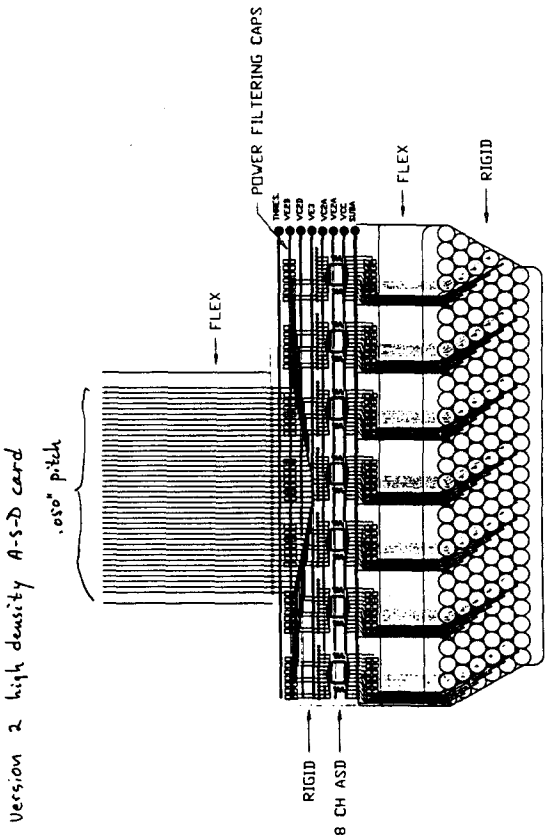

Version 2 high density A-S-D card

786

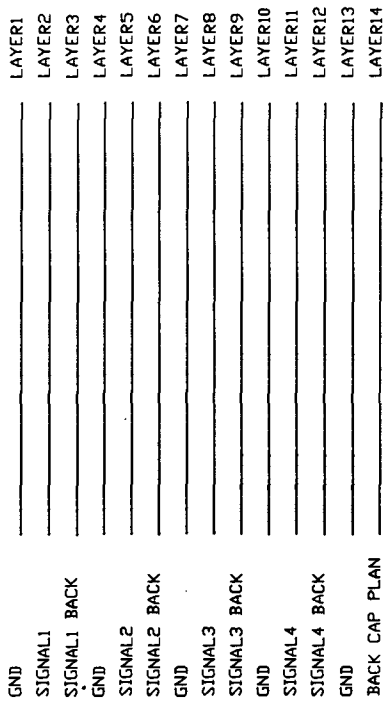

787

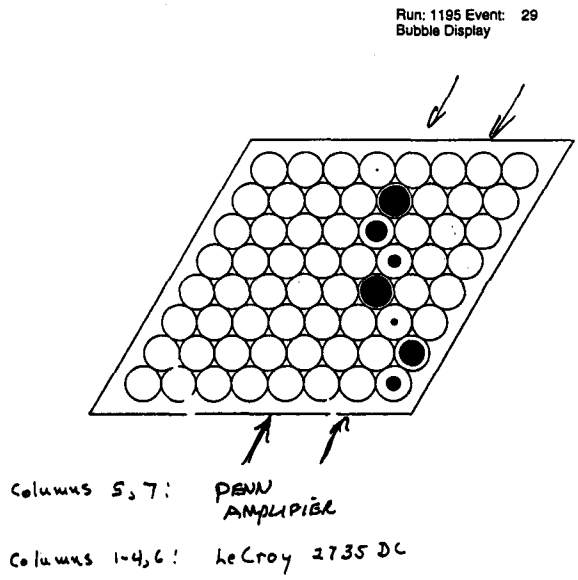

788

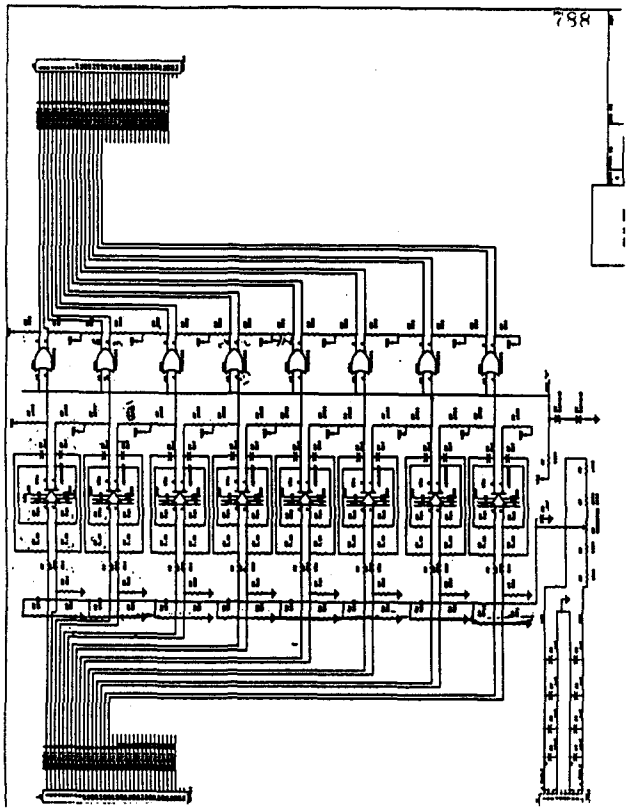

789

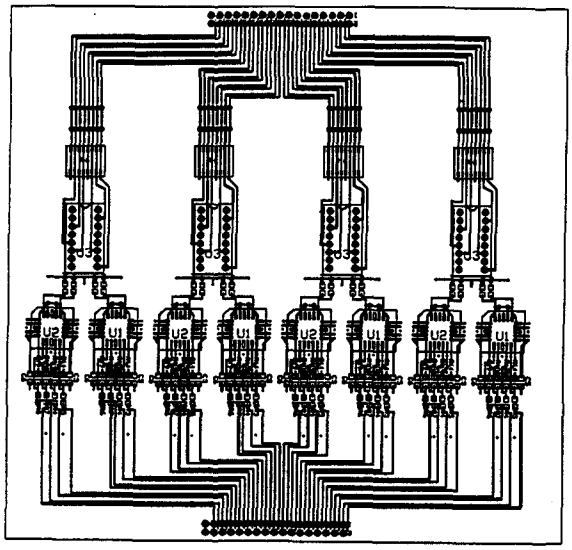

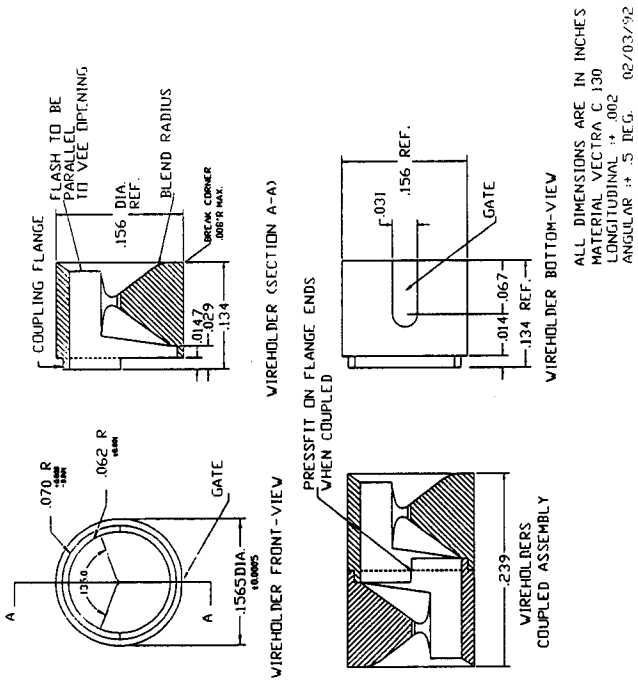

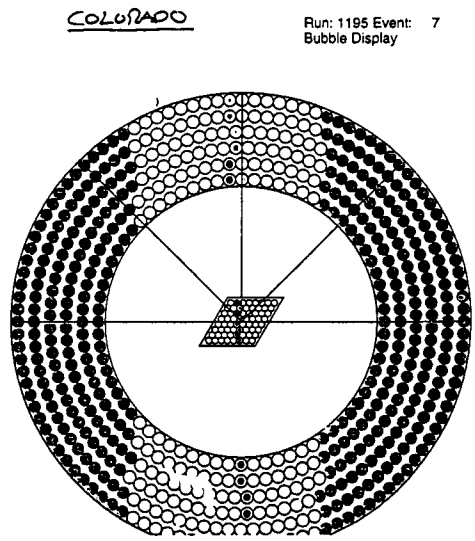

Iu 12" prototype
confidence level distributions vs input σ

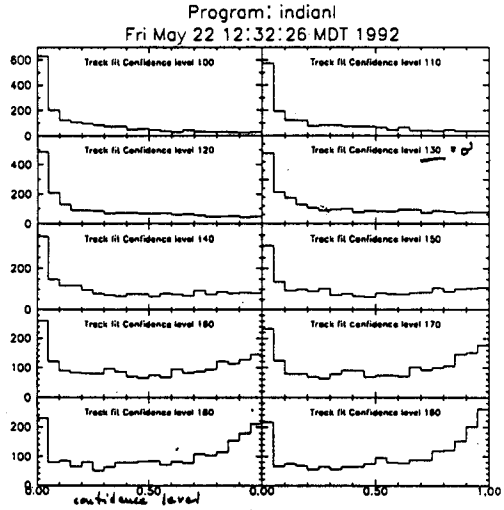

gas: Ar/C_2H_6 (?/100-?) (nom. 50/50)
HV: 1850V (↔ 2230V @ 1atm)
V_{th} = 1V (LeCroy 2735) ≈ 20 fC
with premixed 50/50, HV max ≈ 1500V, pulse height (pre-ampl.) 1/4 that at 1850V
σ ≈ 200 μm.
Non-linear drift velocity function?

Mark II Straw chamber
Segment confidence level

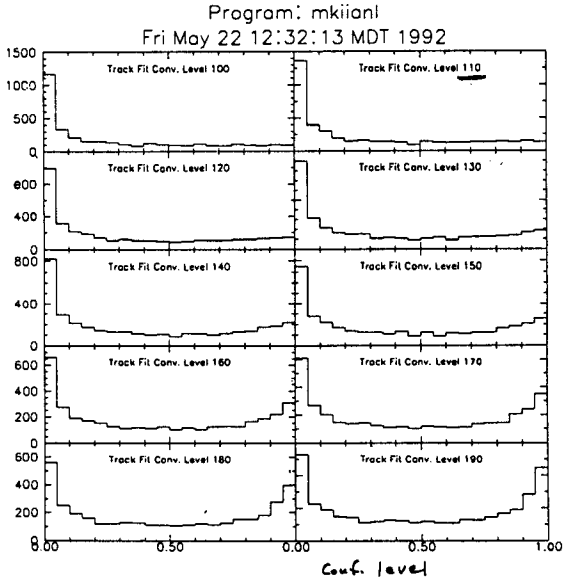

gas: Ar/C_2H_6 (50/50)

Mark II Chamber 2-segment tracks

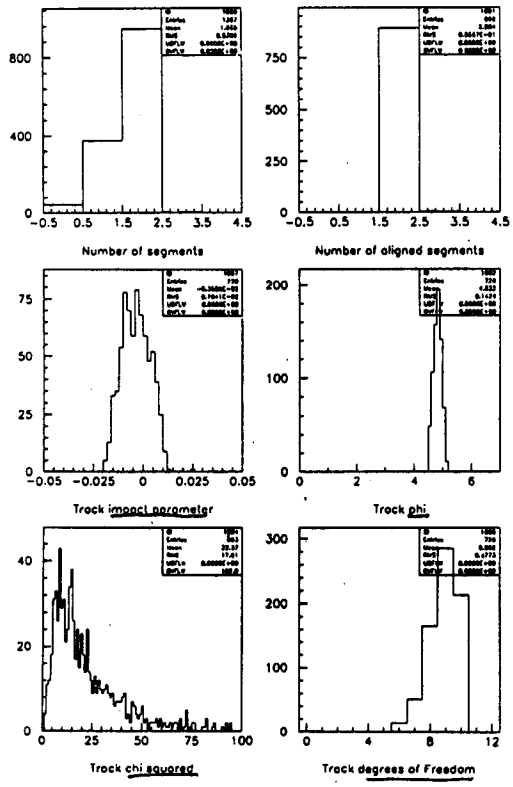

H. Ogren
SDC Collaboration Meeting
KEK
May 26, 1992

Resolution studies of 4 mm straws

This is a recalculation of the resolution studies of Iwasaki (KEK 89-158). These were carried out in order to understand what the limitations of the spatial resolution measurements are with a fast gas and 4mm straws.

1) TDC Resolution

The most straight forward limitation to the spatial resolution is the time resolution of the TDC. The TMC will have an effective time resolution of dt= 0.5 ns. The effective drift velocity of CF_4- isobutane in a 2T field is about 70 microns/ns. So the resulting spatial resolution is

$d\sigma$= 35 microns.

2) Time walk

At any fixed triggering threshold, there will be a time walk due to the statistical variation of the pulse height. The amount of time walk will depend on the slope of the charge vs time distribution. This slope is also a function of the distance of the track from the wire and the dirft veloclity. Fig. 1 shows the charge vs time curves for three tracks, one passing 0.01 mm from the wire, a second at 1.0 mm , and the third a 1.95 mm (just 50 microns inside the wall). The signal assumed a gain of $2*10^4$, an ionization of 100 electrons/ cm, a wire size of 19 microns, a straw radius of 2mm, and a voltage of 2150 V. The drift velocity was taken to be 70 microns/ns as in Section 1 , which would correspond to B=2 T.).

The current versus time is plotted in Fig.2. It is the slope of the total charge curve and for each of these tracks. I have not considered the effects of electronics shaping , since the front edge triggering is insensitive to the shaping for low thresholds.

A direct determination of the slewing requires a realistic value for the ionization fluctuations. Iwasaki has used Q_{low}= 0.5 $Q_{nominal}$, and Q_{high}= 1.6 $Q_{nominal}$. This was determined from an extrapolation of pulse height variation seen on the Topaz chamber. The fact that we will try to trigger on the first arriving cluster complicates this determination, however, previous measurements have indicated that there are 2-3 electrons for each cluster, so the poisson statistics for such clusters would give about the same number. This needs to be measured in our chamber.

Fig. 3 shows the charge distribution for a track passing at a distance of I mm from the wire, for several different gains. This plot can be directly used to estimate the slewing (time walk) as well as the time jitter due to electronic noise. Assuming the threshold setting is 10,000e and the nominal gain is 20000, the Q_{low} fluctuation corresponds to the 10000 gain curve and the Q_{high} fluctuation corresponds to a gain of 32000. Once the intercepts are found the time variation can turned into a distance variation by using the drift velocity.

3) Time Jitter

For this note I will use the number from Iwasaki's paper for the serial noise on a 4 meter straw:

ENC= 3000 electrons.

This effects the threshold directly , the effective time jitter is just the intersection on the +- 3000 e band about the threshold with the nominal gain curve. The effect can be seen in Fig. 3.

4) Comparison with zero magnetic field, cosmic ray tests.

The charge versus time distribution were generated using a nominal velocity of 110 microns. This is shown in Fig. 4. The present threshold setting are about 30000 electrons or 4.8 fC. As can be seen the time walk is expected to dominate the measurements at a gain of 40000.

5) Conclusions:

It appears we may need run our chambers at a somewhat higher gain than 20000. A gain of 40000 with a threshold of about 15000e is shown in Fig. 5. It will give us the following contribution to the resolution for a 1 mm track:

$d\sigma$= 35μ time resolution

$d\sigma$ = 52μ time slewing

$d\sigma$= 22μ time jitter

$d\sigma$= 100 μ intrinsic (difusion and clustering)

The total resolution is then about $d\sigma$= 120 μ

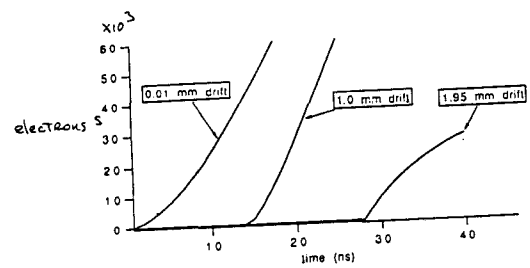

Fig. 1 The charge distribution as a fuction of time for three tracks.

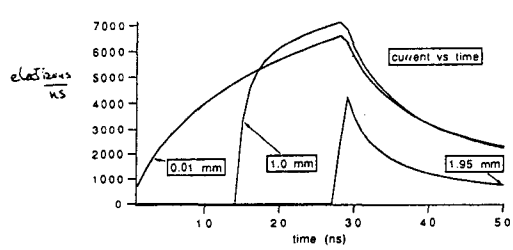

Fig. 2 The current distribution for three tracks.

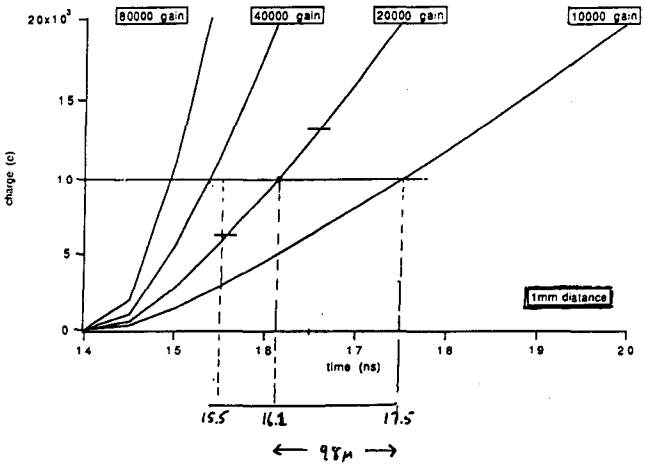

Fig. 3 . Charge distribtion for a track at 1mm for four different gains. Drift velocity as in B=2T field.

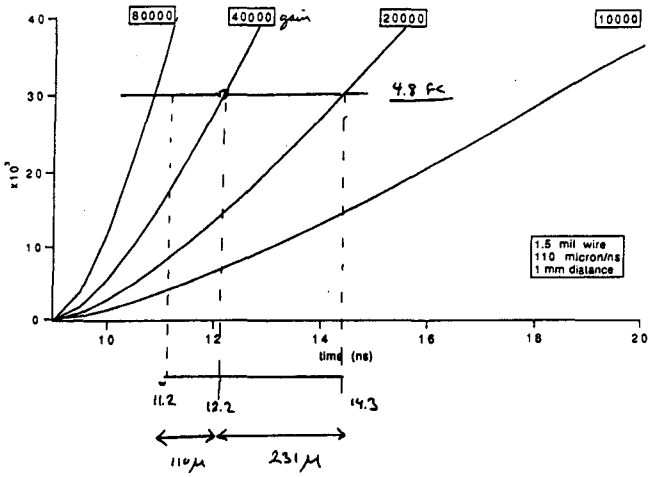

Fig. 4. Charge distributions for drifts with no magnetic field.

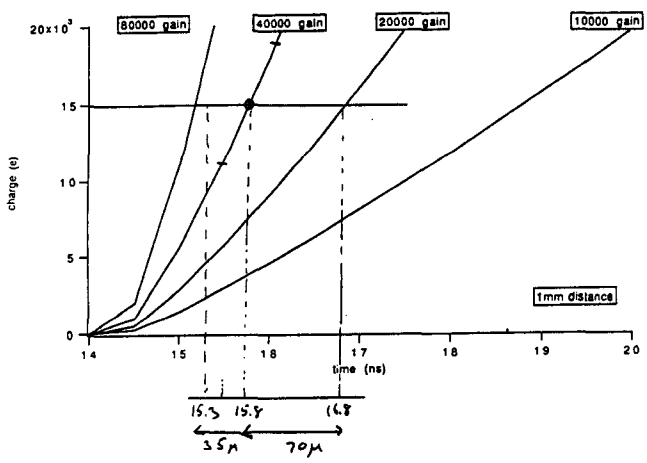

Fig. 5. Charge distribution for B=2 T. Showing the effect of using 15000e threshold and a gain of 40000.

OCREN May 27

CHAMBER RESOLUTION CONTRIBUTIONS

WHAT ARE MAJOR CONTRIBUTIONS?

1) TDC RESOLUTION ($\Delta\sigma = v_0 \Delta\tau$)

2) PULSE HEIGHT SLEWING (TIME WALK)

3) NOISE (TIME JITTER)

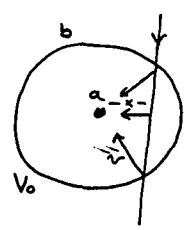

$v = 110\ \mu/ms \quad B=0$

$\simeq 70\ \mu/ms \quad B=2T$

$\alpha \approx 180\ e/cm$

$G \approx 2\times10^4$ gain

$$Q(\tau) = \frac{1}{2}\int_{x/D}^{\min(y_0,\tau)} \left(\frac{2\alpha G v^2 \tau'}{\sqrt{(v\tau')^2 - x^2}}\right) \underbrace{\frac{1}{2\ln(y_0)} \ln\left(1+\frac{(\tau-\tau')}{\tau_0}\right)}_{q_0} d\tau'$$

Terminating

$$\tau_0 = a^2 \ln(y_0) / (2\mu + V_0)$$

$1.0 \frac{cm^2}{sec \cdot Volt}$

Straw ASD

Mitchell Newcomer
(University of Pennsylvania)

STRAW ASD

Amplifier/Shaper/Discriminator - 8ch

Dual inputs (prototyping version)

Differential Outputs Programmable i_{out}
Disc, Analog (on prototype)

Detector Tail Cancellation t_0 = 1ns

Threshold 0 - 10 fC / Disable

Technology Tektronix SHPi(Quicktile)

Die Size 4.7 x 2.8 mm

Supplies +/- 3V (+/- 20%)

Power

Preamp/Shaper	7mW
Discriminator	8mW
Drivers	3mW (min)

Design Goals
Signal Processing Electronics

SENSOR/SYSTEM DRIVEN

Measurement Time	- 5-6ns
Double Pulse Res.	- < 25ns
Inherent Noise	- < 2000e
Timing Resolution	- < 1ns
Power	- < 20mW/ch (ASD)
Threshold	- 0 - 10fC minimum
Size	- At least 8ch/chip .5" sq. 8 ch.chip is OK

Goals are driven by both sensor characteristics and Technology tradeoffs.

IMPLEMENTATION

Differential Design where Possible

Low Level outputs 250mV

Good separation of Analog and Digital Functions

Technology

Tektronix SHPi process

NPN Transistors

Unity gain bandwidth, f_t	8GHz @$I_c = 1mA$
f_t	3GHz @$I_c = 100\mu A$
Current gain, β	100
Base resistance, r_b	250Ω
Collector base cap., C_{cb}	39fF
Collector sub. cap., C_{cs}	24fF
Base emitter matching	1mV

807

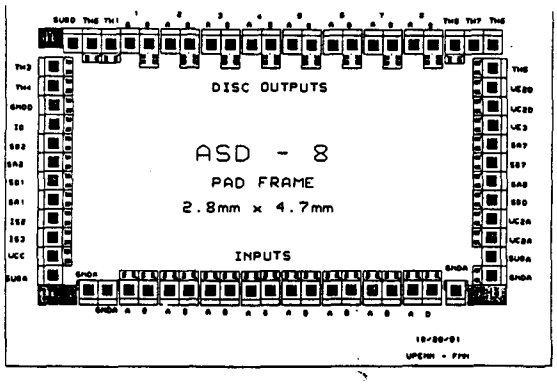

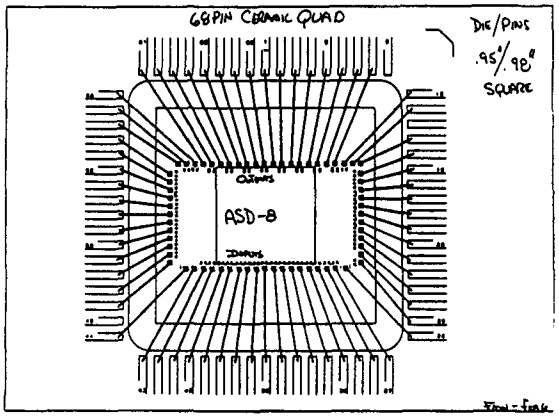

808

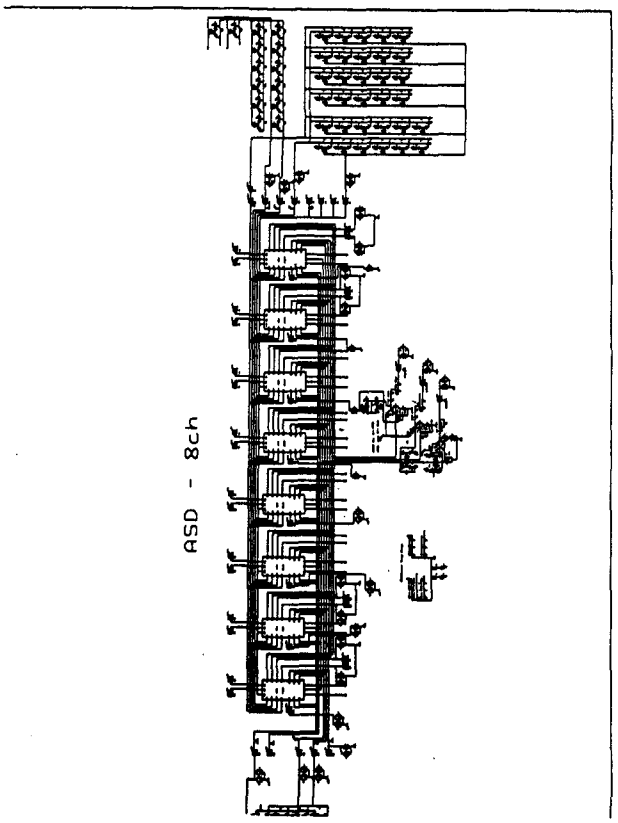

809

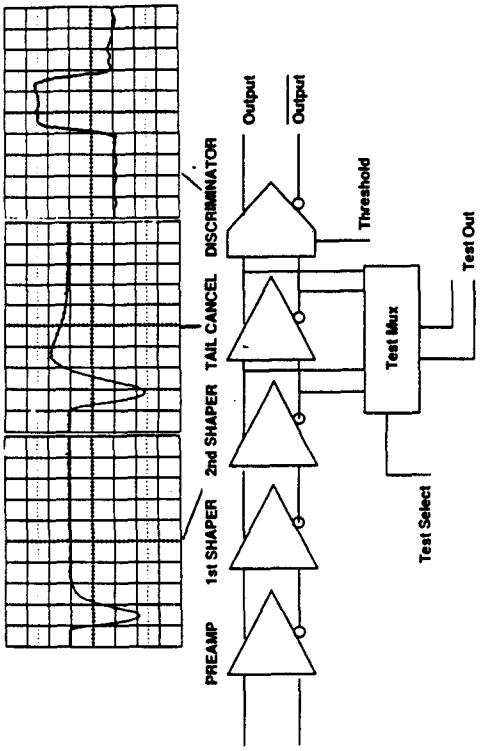

810

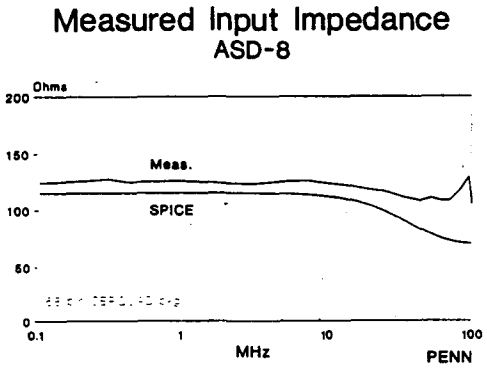

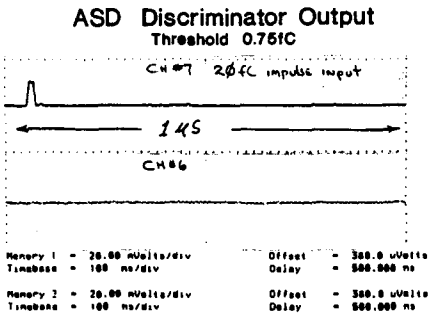

ASD-8
Impulse Response at Disc Input
SPICE..vs..Measured

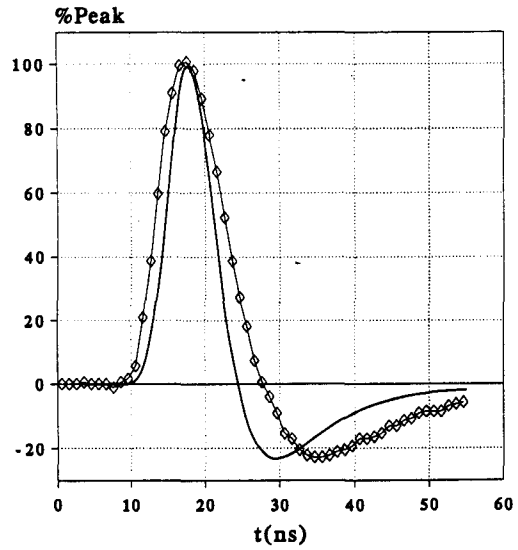

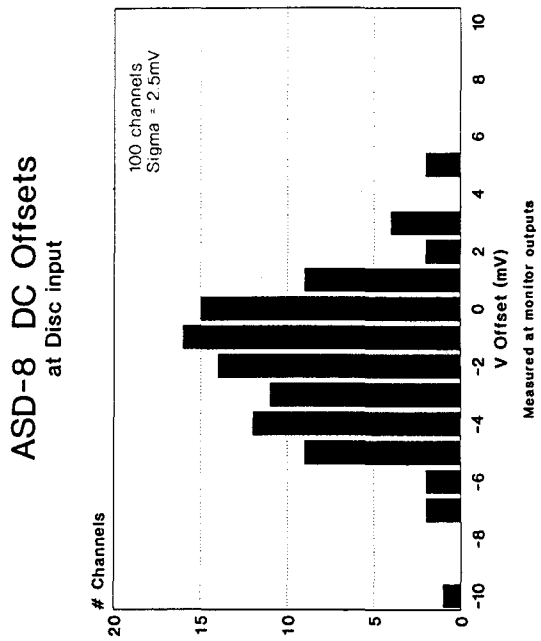

Input Protection test
(ZAP TEST)

Ideal - 2kV Spark Gap
150pF Cap, 10ohms series
Energy = 1/2CV = 0.3mJ
Test Damage .vs. # discharges

Available -
300V Avalanche Discharge
Good Selection of Caps

ZAP TEST-
100Hz x 60sec = 6000 discharges
Charge Cap - Avalanche Discharge
Ramp Cap value until damage is observed.

RESULT -
DC offset increased 10mV at 2000pF
AC rise time increased, Gain OK
Similar results with 2 channels

Energy = .1mJ

CLOSE

ASD-8
Preliminary Measurement Summary

- Yield 80% 33 packaged chips tested

  1 - no discriminators
  3 - one channel bad
  2 - two channels bad

  6 - Total bad chips

- Overall Performance

  Gain - 75% of expected SPICE value (preliminary)
  Uniform (5%) channel to channel

  Meas. Time - 7ns (SPICE prediction 6ns)

  Threshold Variation - 0.5fC channel to channel
  Chip to Chip 1fC (worst case)

  Input Impedance - 125ohms+/-10% (115ohms SPICE)

  Cross Talk - No cross talk observed for
  impulse inputs up to 10fC

  Threshold Temp Dependence - < .01fC/C^{o}

  Time Slew - 1 to 15fC (impulse input) 4.5ns
  maps pulse shape well

ASD BOARD

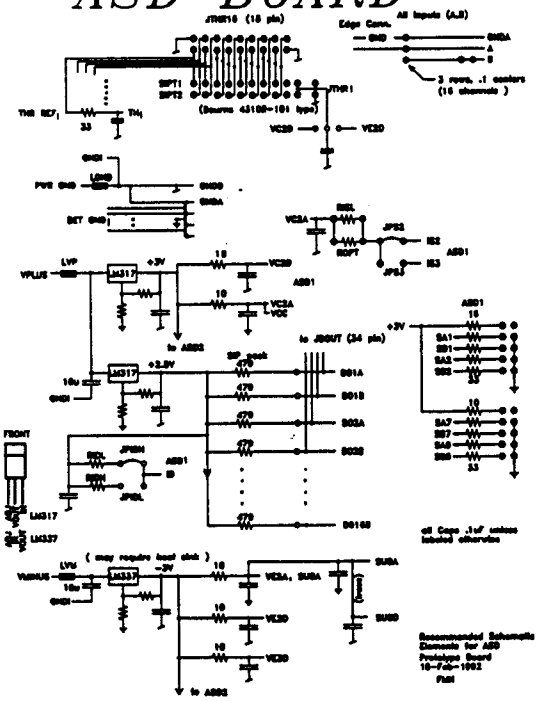

ASD STATUS

- ASD-8 continued testing (now)
  - Noise Measurements
  - Fault investigation
  - Refined gain measurements
- Board Tests-
  - Colorado ASD Board (~2 weeks)
    - Prototype module readout board
    - 2 ASD-8 chips (68pin PLCC)
    - ready for board manufacture
  - ORNL full density board (summer)
    - Straw interface and ASD chips
    - Chip on Board or Mini Package
- Cross Talk Measurements (Spring and Summer)
  - Straws, Connectors, ASD boards..
  - Then Ensemble
- ATT (CBIC-U) version of ASD-8 chip (fall)
  - Probable Enhancements-
    - Mask Programmable Shaping Time
    - Programmable Gain
    - Capacitive Coupling to Disc.

Radiation Tests Tektronix SHPi Process NPN TYPE, Neutron Radiation

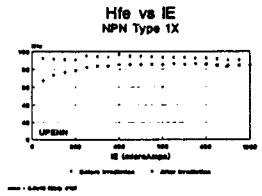

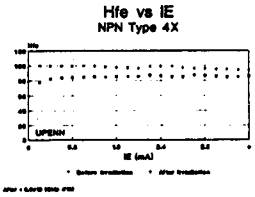

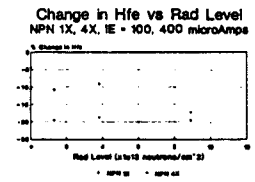

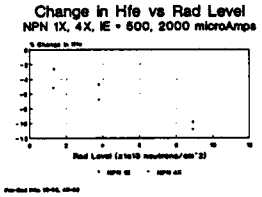

Low current anomalies are due to measurement set-up.

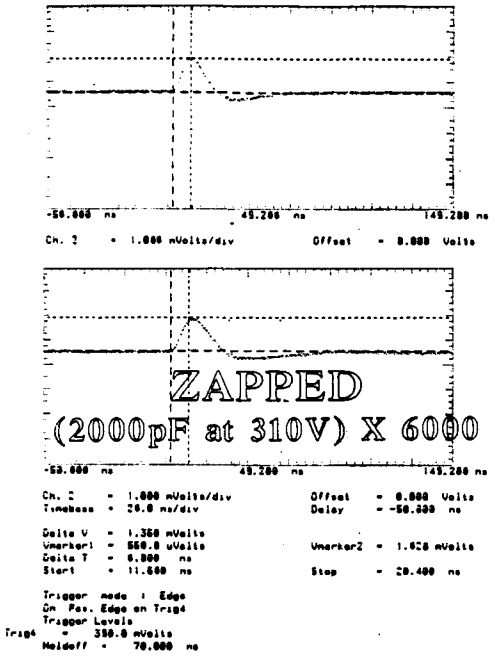

S. Odaka
SDC Collab. Meeting at KEK, May 1992

Conceptual Studies on FEB of the straw chamber

Spacing of the signal lines

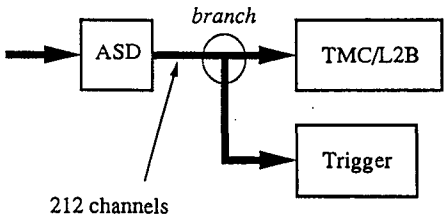

212 channels
× 2 lines/channel

straw module width ≈ 10 cm

→ ~ 250 μm spacing if drawn on a single plane

What is more:
a branch to TMC and Trigger-chip;
thru-holes are necessary there.

⇒ Need more space or *width* !
> several × 10 cm

Cooling

Air-cooling is not efficient
in a widely distributed system.

↓

water (liquid) cooling

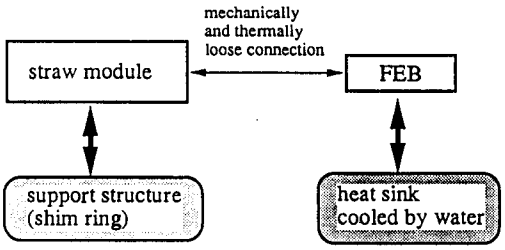

→ a flexible connection between the straw module and the FEB

Water-cooled *Micro Crate*

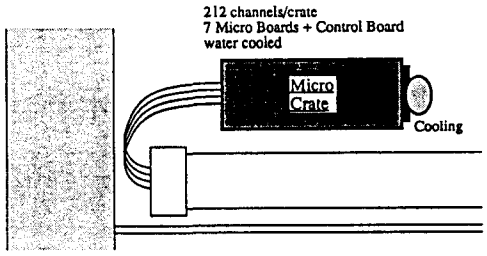

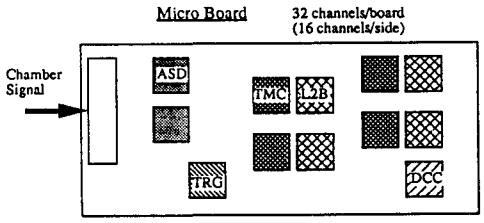

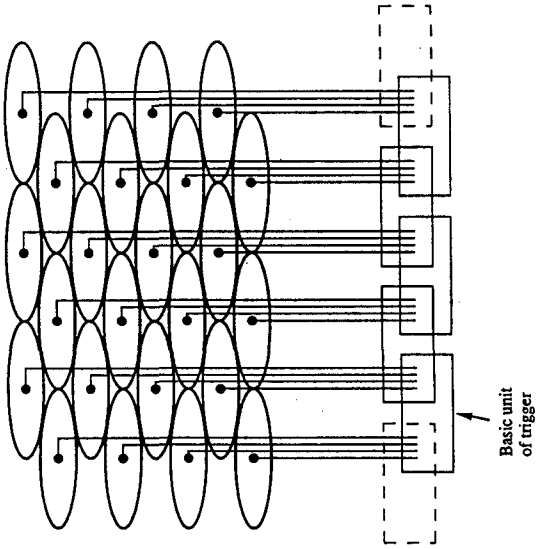

823

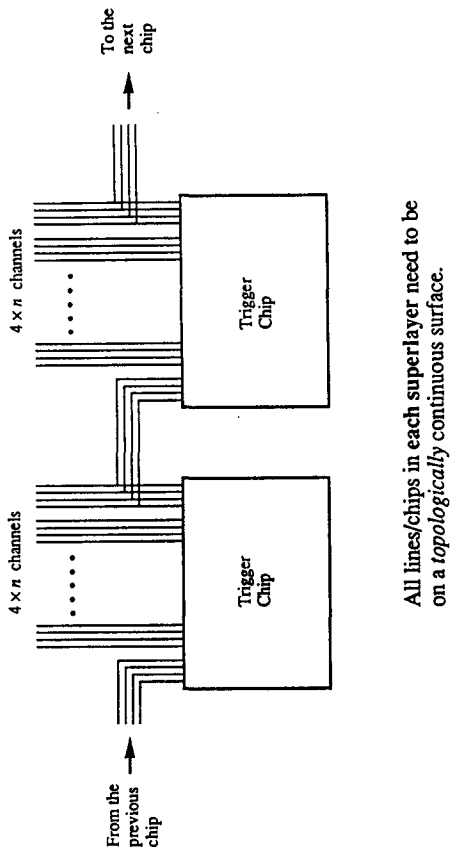

824

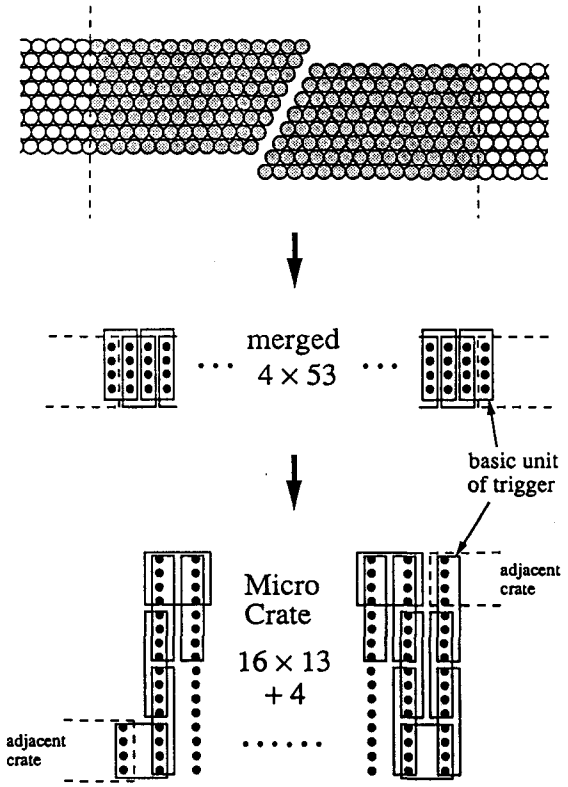

825

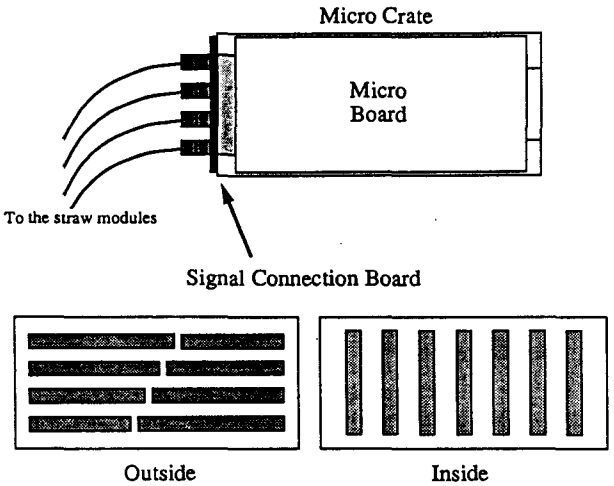

Surface-mount fine pitch connectors
Multi-layer PC board

826

What we are going to do:

look for suitable connectors;

specify the feasibility of using a multi-layer board for the signal connection;

build a mock-up of Micro Crate to test the cooling efficiency.

R. VAN BERG
5/27/92

STRAW ELECTRONICS LAYOUT

IDEAL:

NO MECHANICAL CONNECTION TO STRAWS

ZERO LENGTH CONNECTION TO ANODE/CATHODE

ZERO POWER DENSITY

ZERO VOLUME

- MODERATE REALITY:

ASD @ MODULE

INTEGRATED WITH HV COMPONENTS

FLEXIBLE CONNECTION TO TMC

QUESTIONS:

DISCONNECT FROM MODULE

SPACE FOR HV/ASD

SPACE FOR TMC

RELIABILITY

COOLING

CABLING

NUMBER of VARIATIONS

ACCESS - REPAIRABILITY

ALIGNMENT

SPACE FOR ASD -

CRNL SCHEME

CELEBRA SCHEME

OTHERS ...

SPACE FOR TIME MEASUREMENT -

WITHIN SPACE FRAME (SAFETY)

TRAPEZOIDAL OR RECTANGULAR

REPLACEABLE TMC + L2B + (TRIGGER)

SMALL BOARDS

REPAIRABILITY

YIELD

VARIATIONS

ALIGNMENT ?

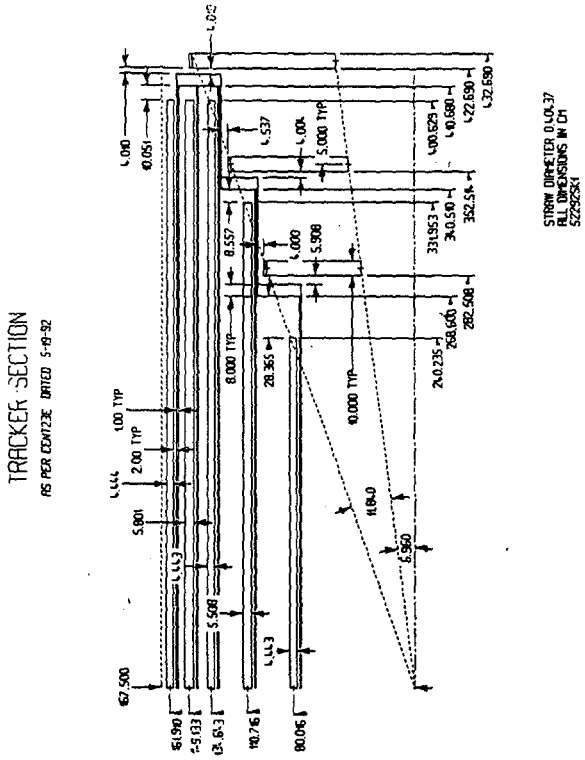

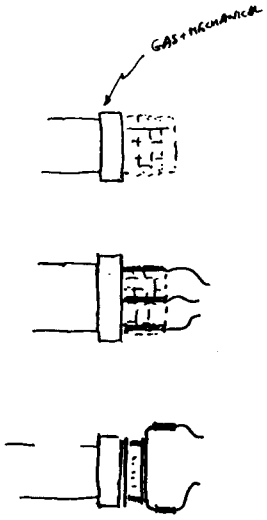
GAS + MECHANICAL

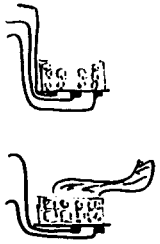

833

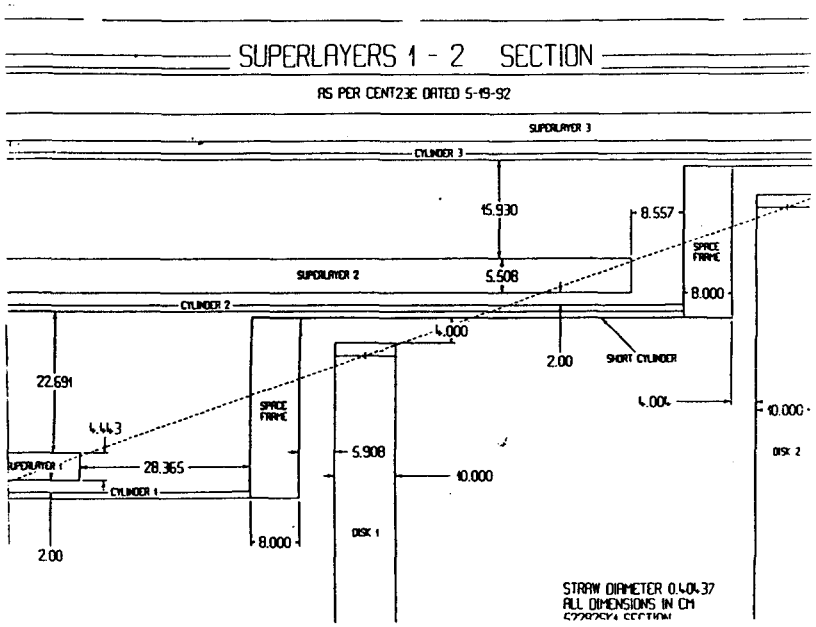
SUPERLAYERS 1 - 2 SECTION
AS PER CENT23E DATED 5-19-92
SUPERLAYER 3
CYLINDER 3
15.930
8.557
SUPERLAYER 2
5.508
CYLINDER 2
SPACE FRAME
8.000
4.000
2.00
SHORT CYLINDER
22.691
4.443
SPACE FRAME
4.00
10.000
DISK 2
5.908
28.365
10.000
CYLINDER 1
DISK 1
8.000
2.00
STRAW DIAMETER 0.40437
ALL DIMENSIONS IN CM

83

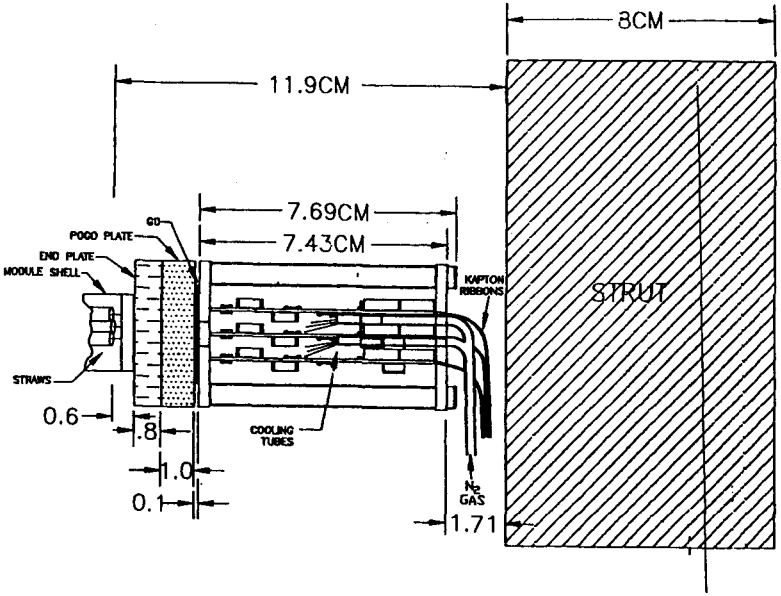
8CM
11.9CM
7.69CM
7.43CM
GD
POGO PLATE
END PLATE
MODULE SHELL
KAPTON RIBBONS
STRUT
STRAWS
0.6
.8
1.0
0.1
COOLING TUBES
N2 GAS
1.71

832

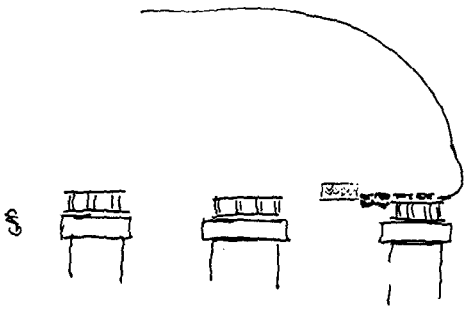

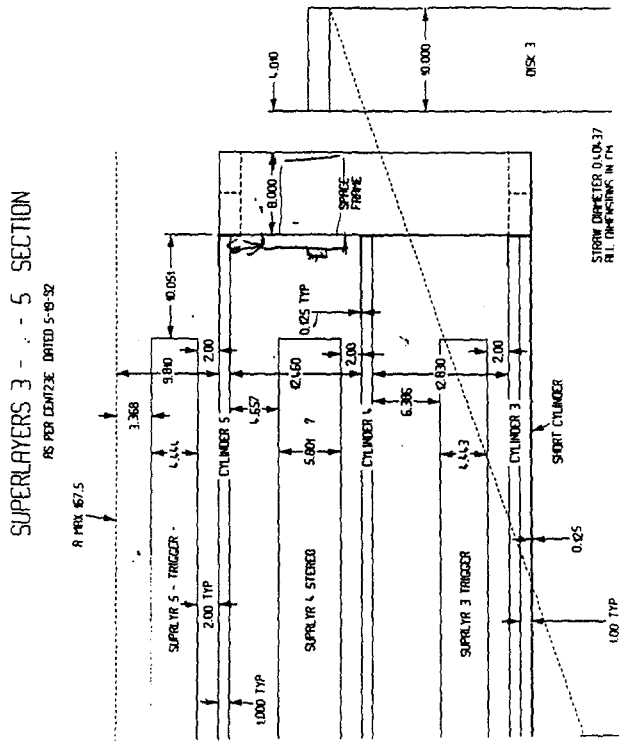

TIME BOARD

CHIP	CHAN/CHIP	8CH	16CH	32CH
TMC	4	2	4	8
L2B	4	2	4	8
TRIG	16+(1)	1	1	1-2
DCC (FGAC)	MANY	1	1	1-2
TOTAL		6	10	~20

($\sim 1\ cm^2$/chip)

PINS

INPUTS

DATA×N×2	16	32	64
CLK+L1+L2	15-20	15-20	15-20
POWER/GND	6-8	6-8	6-8

OUTPUTS

	~40	~50	~70
TOTAL	~84	~110	~160

FOR 1mm×1mm AN/SOCKET (2 AN)

NEED 4.2cm 5.5cm 8.0cm

⇒ MINIMUM (SINGLE SIDED) DIMENSION ~

5×2cm 6×2cm 8×3cm.

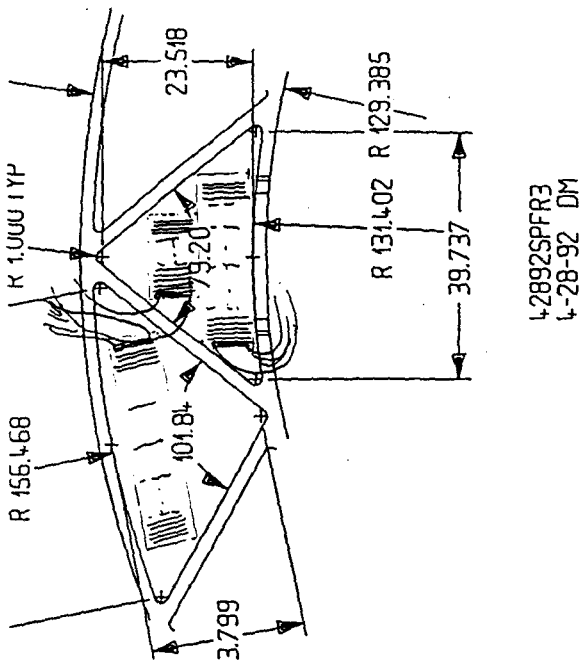

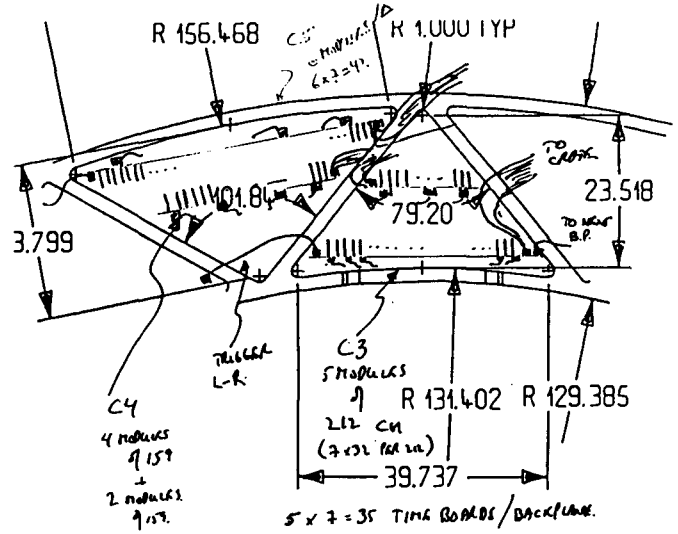

42892SPFR3
4-28-92 DM

New TMC Design with Toshiba Gate Array

SDC Collab. Meet. @KEK
1992.5.27 Y. Arai

- Toshiba Gate Array (TC140G), Library
- Toshiba CAD Software (VLCAD)
- New Cell Design (Differential Input Buffer)
- Rambus Channel

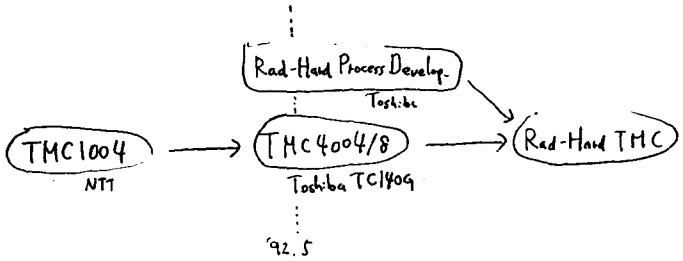

TC140G Series Gate Array

- 1.0 μm HC^{2}MOS Single Poly, Double Metal.
- 2.3 k ~ 172 k Gates (14 Sizes).
- Delay = 0.4 ns (2 input NAND, FO=2, L=2 mm).
- Sea-of-Gate Technology.
- Macro Cell/Function, Mega Cell/Function (RAM, ROM, ALU, Multiplier ...).

Toshiba Mega Cell Library

*RAM-I : Dual Port Memory
- 15.5 k Gates needed for 32 b x 128 w (4k bits) Memory.
  (4 k x 4 ch = 62 k gates)
- Address Access Time :
  Read = 7.1 ns (5V) [~12 ns (3V)]
  Write = 11.8 ns (5V) [~20 ns (3V)]

*FIFO :
- 2 k Gates needed for 8 b x 32 w FIFO.
- Cycle Time :
  Read = 12.8 ns (5V) [~21.6 ns (3V)]
  Write = 21.8 ns (5V) [~36.8 ns (3V)]
  (we may need circuit modification.)

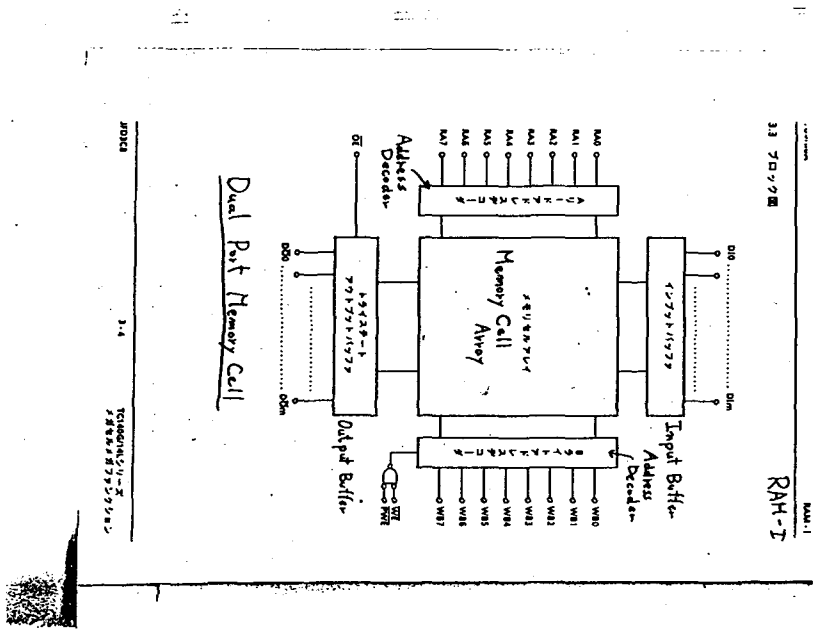

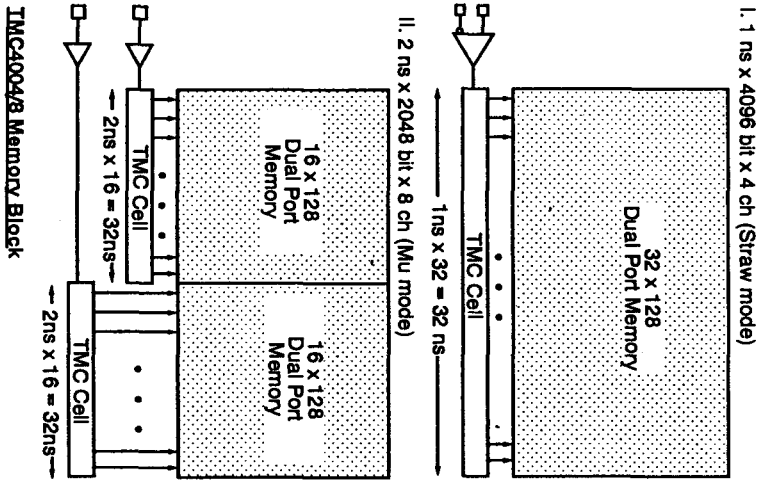

TMC4004/8 Memory Block

FIFO (XFIxxyy)

ドィッタ動作及び2つ
るRAM-Iを使用し、
。このため一般のメ
ロアプランはメガセ

10.3 ブロック図

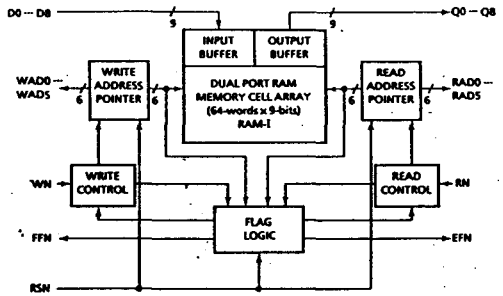

Figure 1. FIFO (64-words x 9-bits) Block Diagram

FIFO Cell

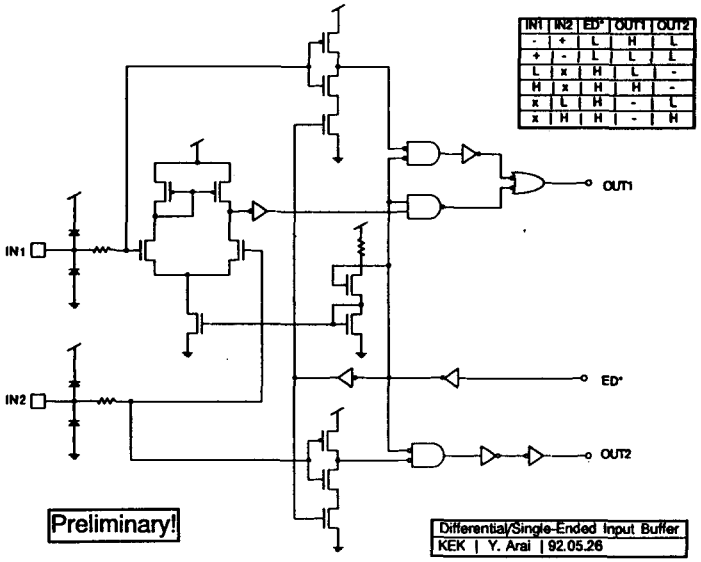

IN1	IN2	ED*	OUT1	OUT2
-	+	L	H	L
+	-	L	L	L
L	x	H	L	-
H	x	H	H	-
x	L	H	-	L
x	H	H	-	H

Preliminary!

Differential/Single-Ended Input Buffer		
KEK	Y. Arai	92.05.26

Toshiba CAD Softwares

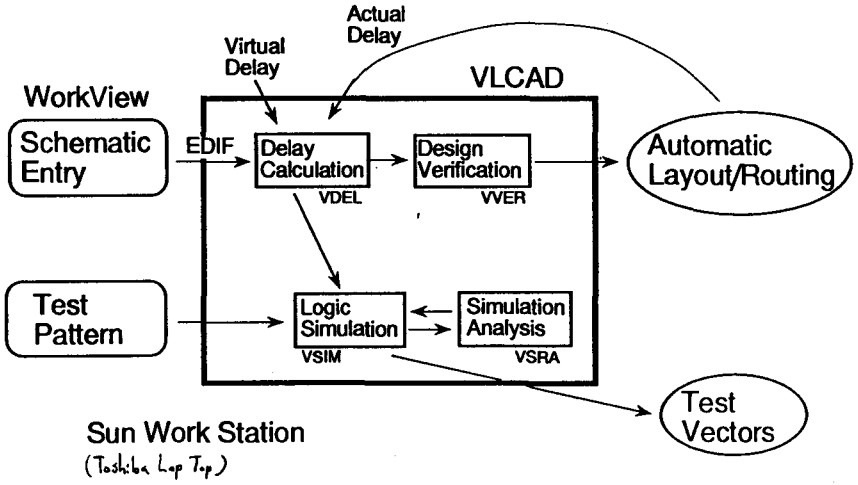

Sun Work Station
(Toshiba Lap Top)

Rambus Channel

- High-Speed Data Transfer Standard between High Performance CPU and Dynamic RAM.
- Rambus Inc.(USA) + Toshiba, NEC, Fujitsu.
- 9 bit bus + 250 MHz clock (both edges) ⇒ 500 MB/sec
- Vref = 2.2 V, ΔV = 600 mV.
- 64 pins, Vertical Surface Mount Package.

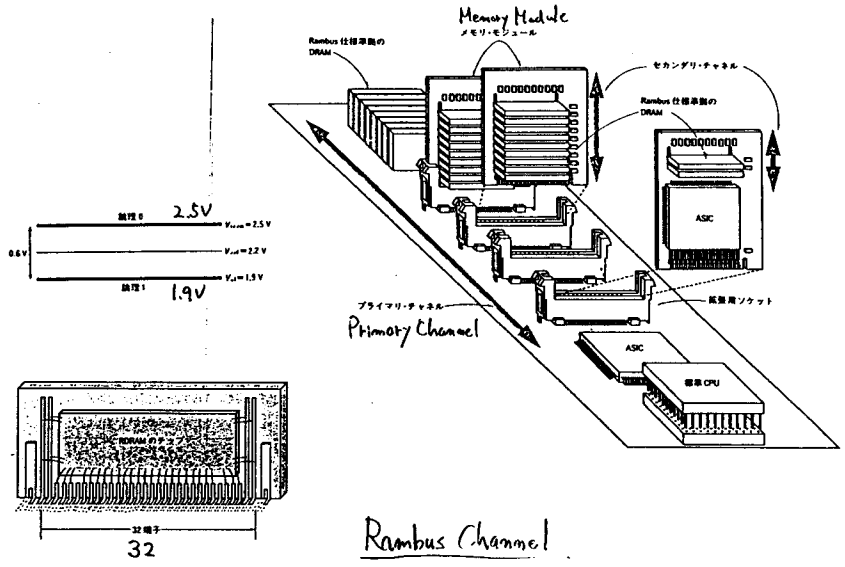

Plan

Test Chip ..... Input Buffers, THC Cells, Feedback, ...
(End of July)

THC4004/8
(End of this year)

Radiation Damage Test of Time Memory Cell

Masami Chiba and Katsuji Nakamura

Tokyo Metropolitan University

Yasuo Arai

KEK

May26-29, 1992
SDC Collaboration Meeting at KEK

Time Memory Cell (TMC) is considered to be the best chip for readout of the straw chamber. It will be set at 70-170 cm from the beam line and subjected several 10krad/year so that the radiation resistance is crucial for the application.

The TMC 1004 includes over10^5 MOS FETs which is made at NTT ~~without~~ non radiation hard process and the specifications are:

TMC1004

Process	:0.8μm N-well C-MOS
Gate oxide	:11nm
Clock	:31.25MHz
Channel	:4ch
Power consumption	:7mW/ch
Chip size	:5.0mm x 5.6mm.

For the sake of the radiation-damage test we used a special chip named TMC-PG1 which is made by the same process of TMC1004. It includes NMOS FET 2 ch, PMOS FET 2ch, ring oscillators with and without feedback circuits. We report here the test results of the two types of MOS FET which is the building block of TMC.

γ-ray irradiation was done at the ^{60}Co γ-ray irradiation facility at Tokyo Metropolitan University. It has 12,000Ci ^{60}Co in total. The radioactive isotope rods surround an irradiation cavity and irradiate about 1Mrad/h. We used a field flattener made of a lead cylinder to make uniform irradiation field and the irradiation rate reduced to a half. This system has a access tube

from outside to introduce cables from upper part of the irradiation chamber which enablas to test TMC in active.

[Fig. 1]

Illustration of the irradiation in the NMOS FET in saturation is shown in fig.2.

[Fig. 2]

The irradiation conditions of the TMCPG1 are as follows.

1. TMCPG1 power-off, all the pins are in short circuit
2. TMCPG1 power-on

MOS FET

Saturation:P1, N1

Cut-off :P2, N2

The saturation and cut-off states in the irradiation are explained in fig.3.

[Fig. 3]

In these conditions, threshold voltages and mutual conductance are measured. The definitions are shown in fig.4.

[Fig. 4]

Results of the measurements are shown in fig. 5.

[Fig. 5]

The threshold-voltage change against the dose is shown in fig.6.

[Fig. 6]

The results of "power-off" irradiated at Tohoku University (91.1) is consistent with those at TMU (91.7). The maximum change was ΔVt=-0.16V (27%) for 1Mrad. There was not large change in GM.

For "power-on", PMOS FET shows the same tendency as "power-off" with saturation of ΔVt=-0.074V and cut-off of ΔVt=-0.118V for 1Mrad.

On the other hand, NMOS saturation shows large threshold-voltage change from the dose of 50krad. In addition GM curve has two peaks from the dose of 200krad. It seems that NMOS cut-off is not so different from "power-off" in the threshold-voltage change ΔVt=-0.119V for 1Mrad but the GM curves show two peaks as NMOS saturation.

In fig. 7 Id-Vg curve of NMOS saturation is shown. From the irradiation dose of 50krad, Id increased at the low Vg. On the other hand NMOS cut-off and PMOS do not show such behavior.

[Fig. 7]

Annealing on the threshold voltage and the leak current Id at Vg=Vsub=0 is shown in fig 8. The large threshold-voltage change at NMOS saturation is seen. The annealing in a room temperature is also shown in the threshold and the leakage current.

[Fig. 8]

The cause of the irradiation effect on MOS FET is divided into interfacetrap and trapped-oxide charge with a method of P.S.McWhorter and P.S.Winokur [1] as in fig.2. They influence different behavior on Id-Vg curve as shown in fig. 9.

[Fig. 9]

The threshold-voltage shift ΔV_{th} is splitted into a contribution due to interface traps ΔV_{Nit} and a contribution due to trapped-oxide charge ΔV_{Not} as $\Delta V_{th}=\Delta V_{Nit}+\Delta V_{Not}$. The analyzed data is shown in fig.10.

[Fig. 10]

In conclusion there were differences in the irradiation effects between power-on and -off during the irradiation. It showed that power-on was needed for the test. The threshold change was -

0.1V in PMOS at 1Mrad but it was -0.07V even at 50krad and increased -0.17V at 200krad in NMOS. Although annealing was observed, it is needed to improve the radiation resistance for use in the straw readout.

We would like to thank Prof. T.Hirose and members of the high-energy physics laboratory (TMU) for extending their hospitality in the radiation-damage test. At the irradiation we were indebted to Prof. M.Katada and Dr. K.Yamauchi at the RI-research facility at TMU for use the irradiation facility.

References

[1]P.J.McWhorter and P.S.Winokur, "Simple Technique for separating the effect of interface traps and trapped-oxide charge in metal-oxide-semiconductor transistors", Appl. Phys. Lett. 48(2), 133(1986).

856

857

858

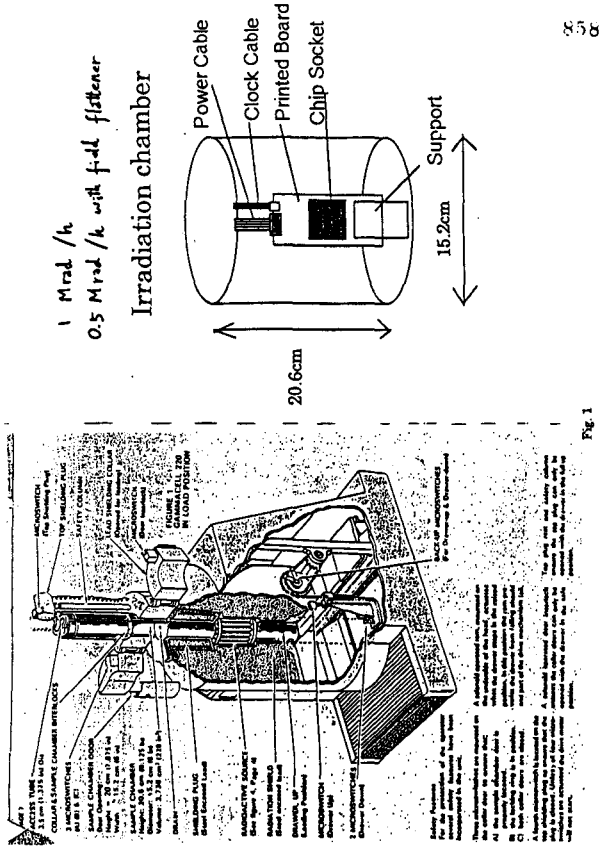

Fig.1

γ–ray irradiation

N-MOS FET(saturation)

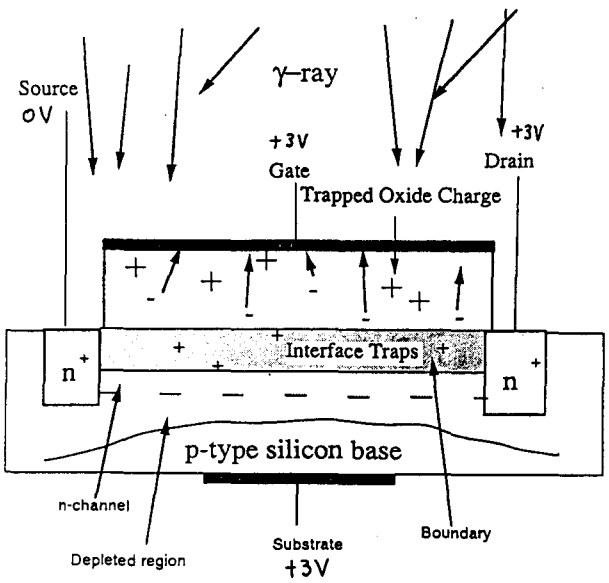

Fig. 2

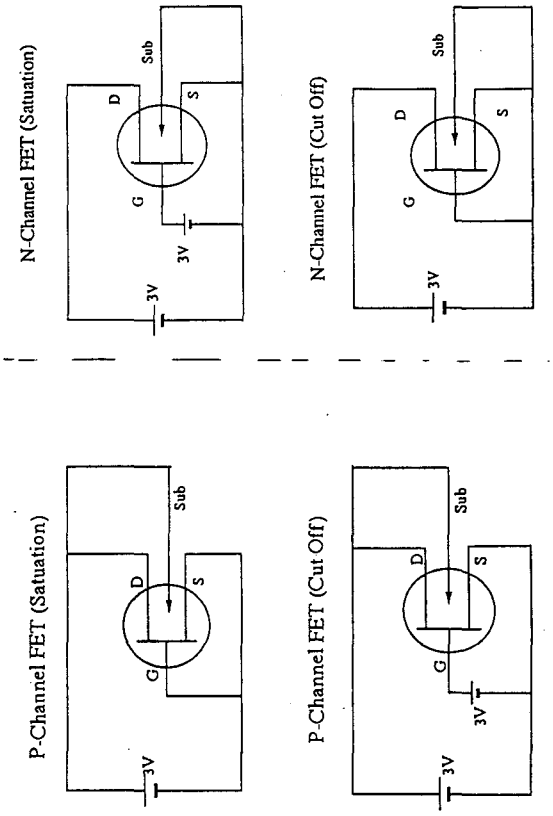

Fig. 3

Power-on

Idrain-Vgate curve

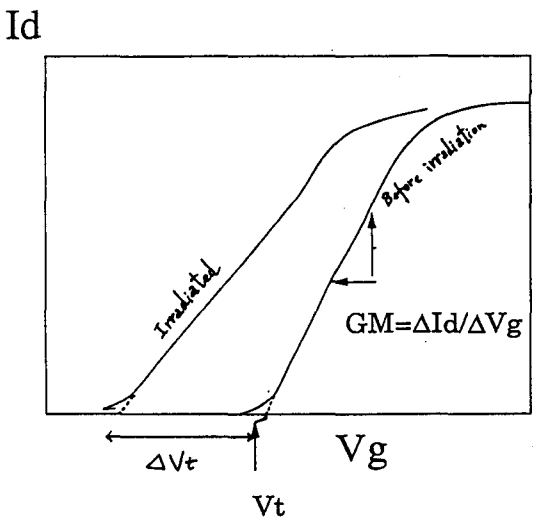

1.Threshold voltage:
Vt=Vg at Id starts to flow

2.Mutual Conductance:
GM=ΔId/ΔVg (VDS:Const.)

Fig. 4

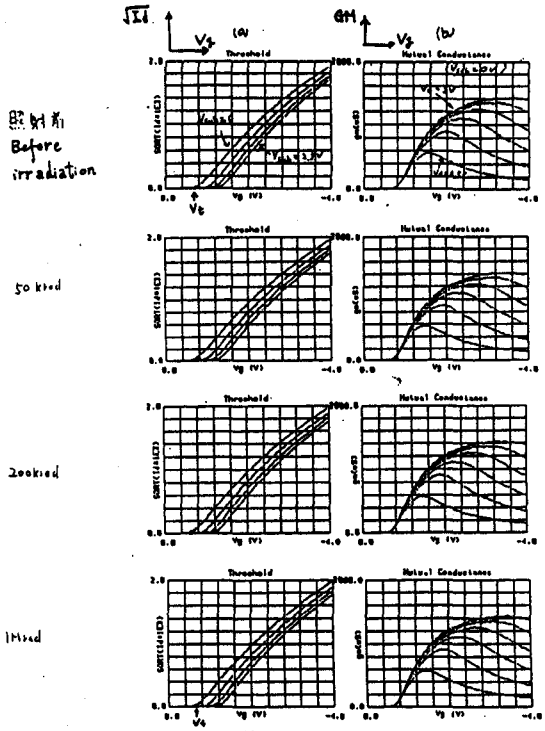

PMOS cut-off

Fig. 5(a) P2トランジスターの特性曲線. (a) しきい値, (b) 相互コンダクタンス, (c) チャンネルコンダクタンス, (d) Id-Vd 曲線

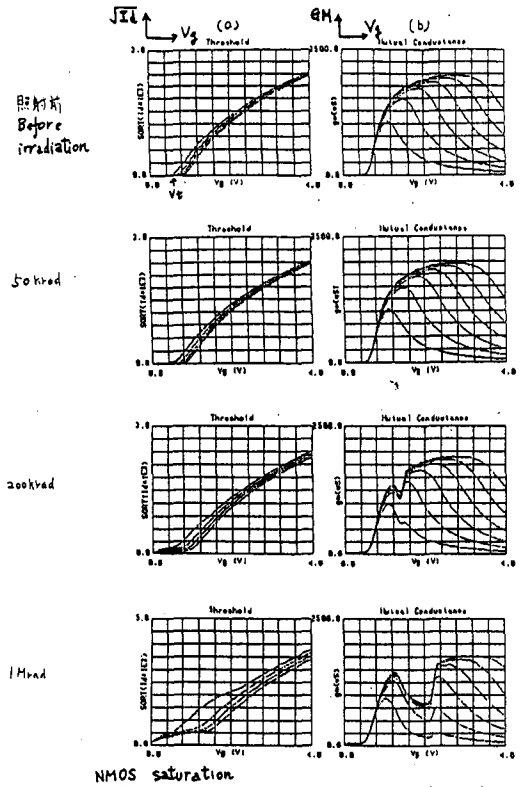

Fig. 5(b) N1トランジスターの特性曲線。(a) しきい値, (b) 相互コンダクタンス (c) チャンネルコンダクタンス (d) I_d-V_d 曲線。

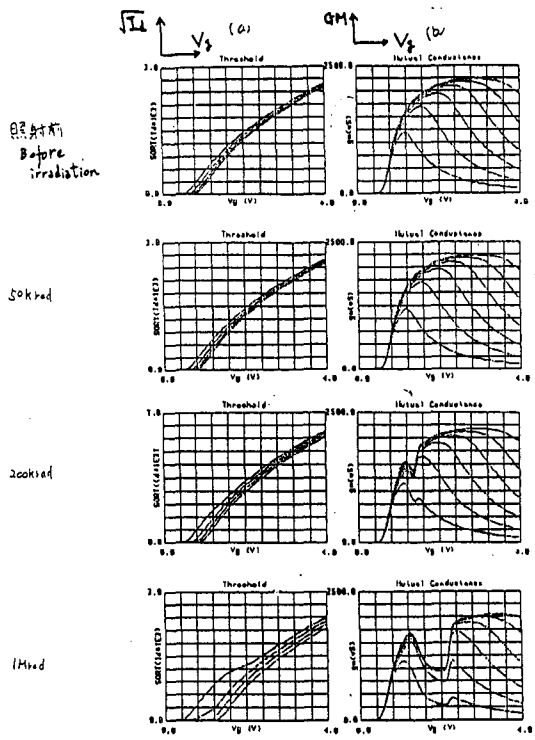

Fig. 5(c) N2トランジスターの特性曲線。(a) しきい値, (b) 相互コンダクタンス (c) チャンネルコンダクタンス (d) I_d-V_d 曲線。

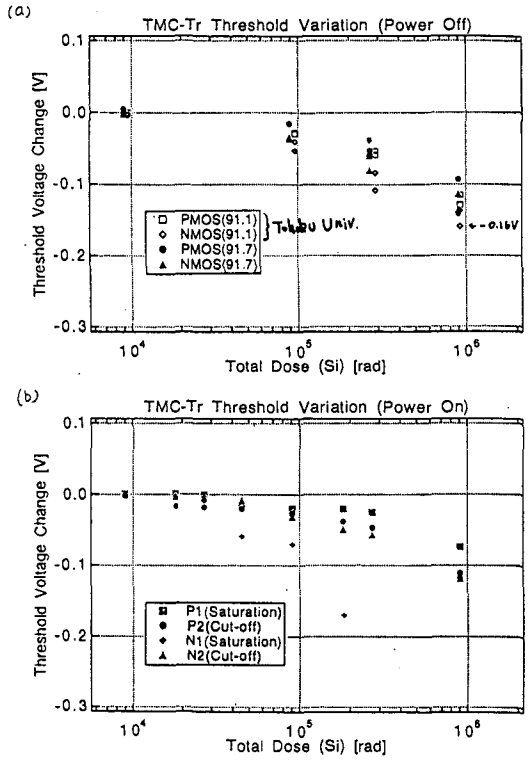

図6. しきい値の放射線照射による変化。(a) 電源切状態, (b) 電源ON時。

Fig. 6

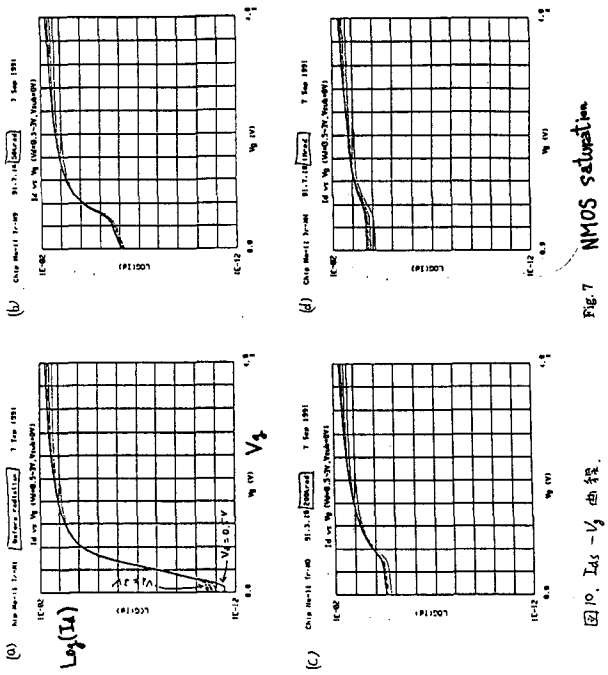

図10. I_{DS} - V_d 曲線。

Fig. 7

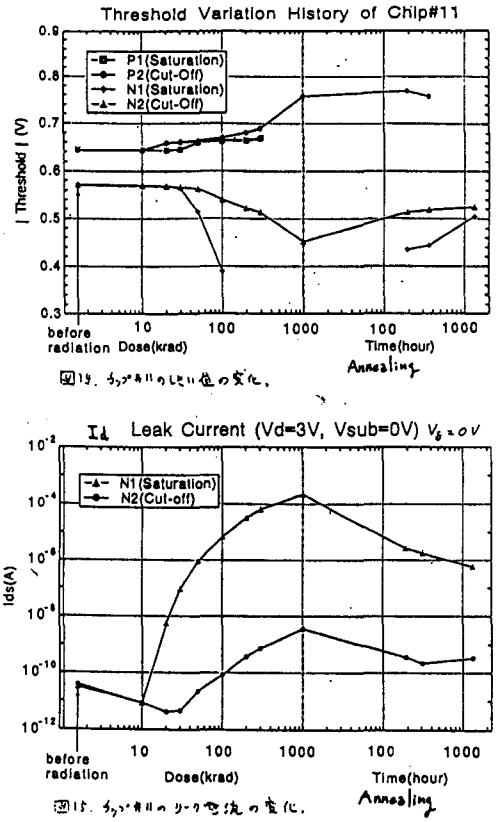

Fig. 8

Idrain-Vgate curve change by irradiation

2 method of McWhorter and Winokur: $\Delta V_{th} = \Delta V_{Nit} + \Delta V_{Not}$

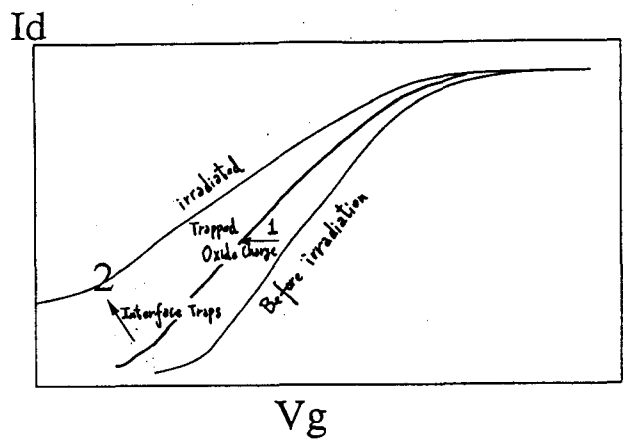

1,Trapped Oxide Charge
2,Interface Traps

Fig. 9

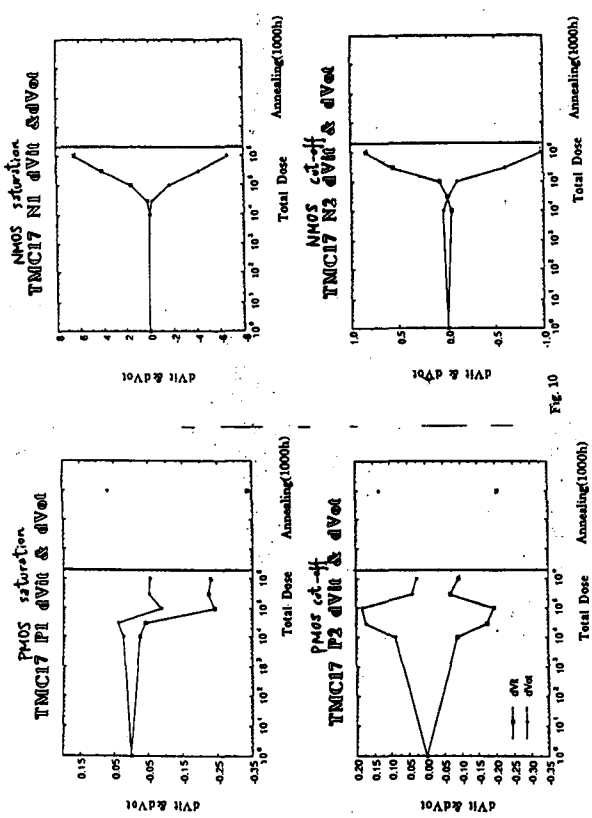

Fig. 10

Summary

1. Power-off

Max. $\Delta V_{th} = -0.16V$ 1 Mrad

no change in GM and Id

2. Power-on

	ΔV_{th}	Dip at GMcurve	Id
PMOS saturation	●	○	○
cut-off	○	○	○
NMOS saturation	×	×	×
cut-off	△	×	△

3. Interface traps and Trapped Oxide Charges are separated

4. Need to improve radiation resistance of TMC for straw read-out

A Plan of Cosmic-ray Test of Straw Readout at Tokyo Metropolitan Univ.

Kazuo YAMAUCHI

1. Purposes :

* To test the newly fabricated TMC or ASD using the signals from the Straw Chamber.
* To measure the spatial resolution to compare with the previous results of the other experiments.

2. Straw Chamber :

Made by Indiana Univ. and has 64 straws.

3. Electronics :

* ASD
* TMC or
  TDC and ADC

4. Gas supplying system :

* CF_4 (80%) + Isobutane (20%)
* Ar (80%) + Isobutane (20%)

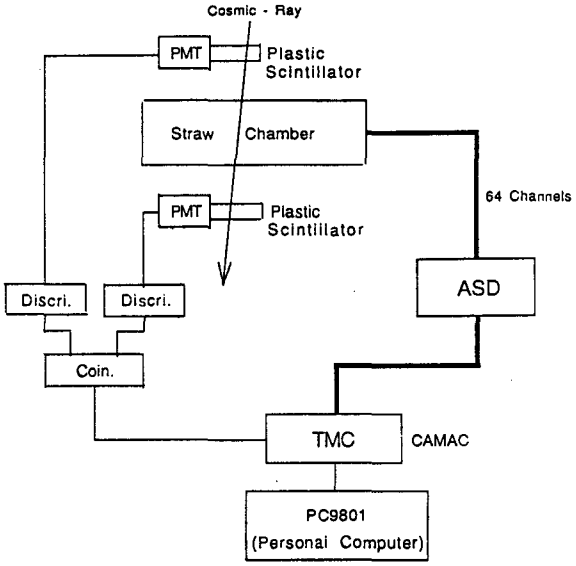

The Set-Up of Cosmic-ray Test

The Gas supplying system

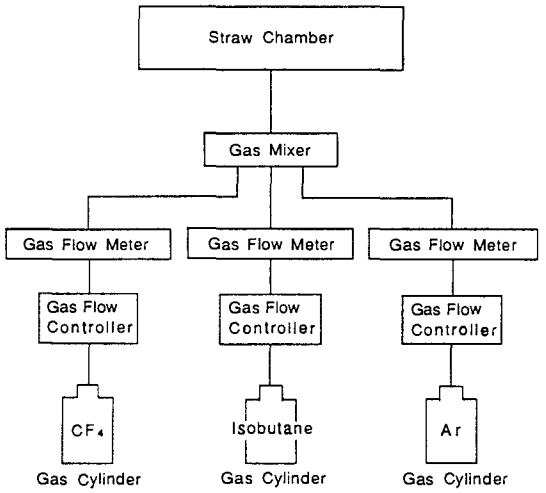

CF_4 (80%) + Isobutane(20%)
Ar (80%) + Isobutane(20%)
Precision of flow rate : ± 1%

KEK SDC Meeting
May 26, 1992
P.K. Sinervo

DCC Design for the SDC Straw Tube Tracker

- Introduction
- Models and Simulation Results
- Preliminary ASIC Development
- Goals and Schedule

IPP Group: A. Wölscher, G. Stairs, P. Sinervo — Toronto
K. Ragan — McGill

Introduction

The straw tube DCC design is constrained by

- Noise on analogue FE caused by digital activity
- Space and power considerations
- Rad-hard requirements

Several groups involved in DCC architectural design and simulation

- SSCL group has been working on
  - High-level simulations of buffering strategies
  - Noise issues on the Front End Board (FEB)
  - Data transmission technologies from FEB
- Toronto/McGill group has been studying
  - Detailed simulations of a "straw man" design
  - Buffering from L1 → Crate Interface Card (CIC)
  - Design of prototype ASIC's for DCC on FEB

Straw DCC Architectural Studies

Design of the DCC system has assumed

- Each FEB will instrument ~ 160 channels
- TMC will read out either 4 or 8 channels
- Crate Interface Card will handle 16-32 FEB

System Level Assumptions

- L1 accept rate $\leq 10^{-3}$
- L2 trigger rate $\leq$ 10 kHz
- occupancy/crossing/channel $\leq$ 0.05
- $\leq$ 3 crossings read out per trigger

DCC design avoids microprocessor on FEB

- Minimizes digital activity on FEB
- Consists of multiplexor (FMUX) and transmitter (FETX)
- Buffers and processors located on CIC

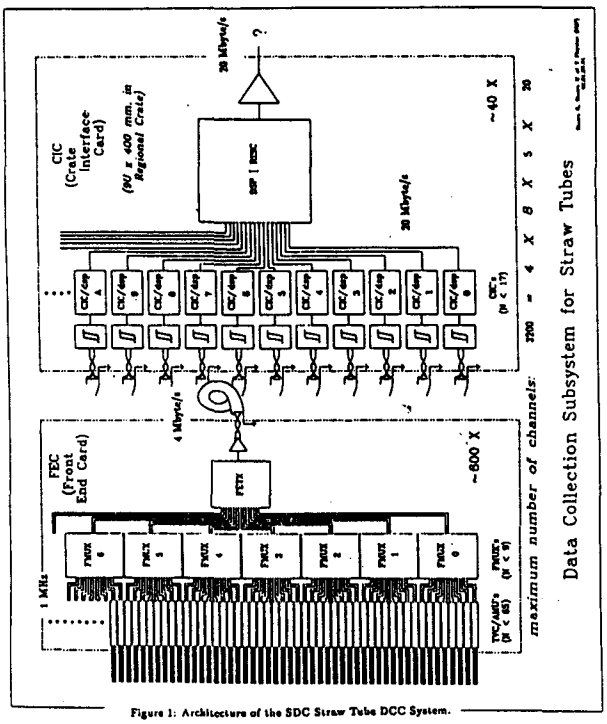

Figure 1: Architecture of the SDC Straw Tube DCC System.

Simulation Studies

VERILOG simulation studies have been performed

- Evaluate FE chip buffer requirements
- Buffer and bandwidth requirements on FMUX/FETX
- Requirements on CIC

Simulations have considered various issues

- Considered "event overlap"
- Physics correlations (min-bias and high p_t collisions)
- Ordering of data by channel and trigger ID
- Latencies in L1 and L2 trigger

Overlap and Data Correlations

Probability of 2 L2 triggers sharing hits is small

L1	L2	Prob(n<=5)	Prob-hit(straw)	Prob(n<=60)	Prob-hit(μ)
0.001	0.02	$4.9*10^{-3}$	$2*10^{-3}$	$5.7*10^{-2}$	$2.8*10^{-2}$
0.001	0.01	$4.9*10^{-3}$	$2*10^{-3}$	$5.7*10^{-2}$	$2.8*10^{-2}$
0.005	0.05	$2.4*10^{-2}$	$0.5*10^{-3}$	0.25	0.13
0.002	0.02	$0.8*10^{-3}$	$3.9*10^{-3}$	0.11	$5.6*10^{-2}$

2 L2 accepts within 5 crossings — hit shared with 2 L1 accepts — 2 L2 accepts within 60 crossings — hit shared with 2 L1 accepts

Considered effects of regional data correlations

- Estimated using hits from full SDCSIM (Carleton U.)
- Considered different physical layout

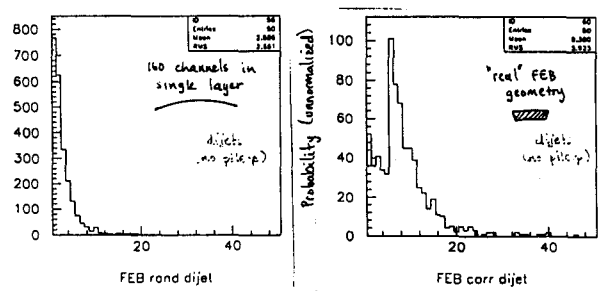

Data Correlations (with pileup)

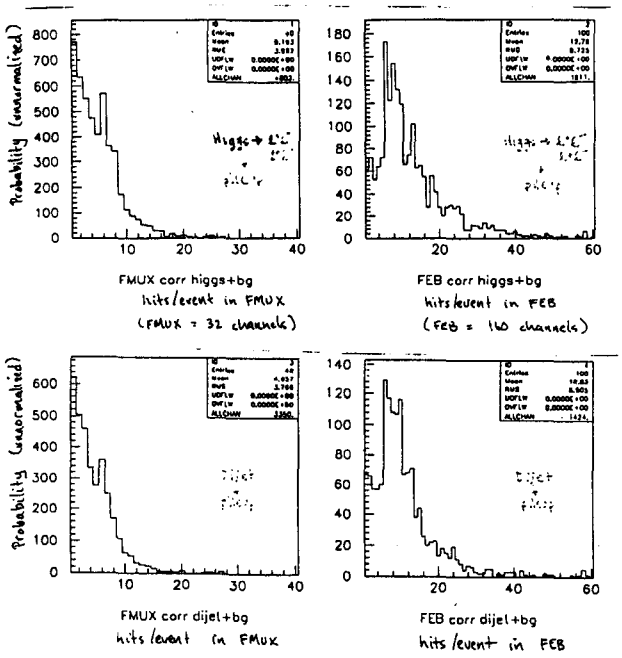

Data Ordering and L2 Latencies

Data moves off FEB in channel and event order

- Considered several strategies
  - Spacing L2 accepts to ensure readout completes
  - FE chip provides control information
- L2 accept spacing as large as 50 μs tolerable

"L2 Latency" has modest impact on buffering

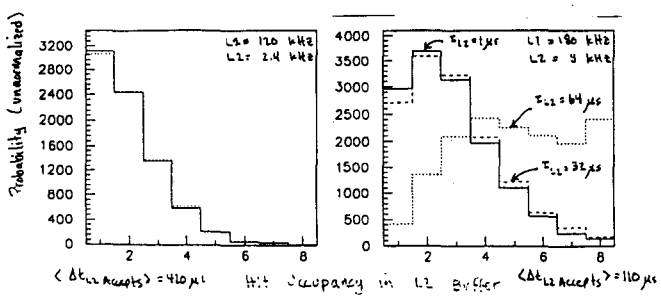

Figure 3: L2 buffer occupancy for a) L1=0.002 and L2 =0.02 and b) L1=0.003 and L2=0.05. The three cases τ = 1, 32, 64μs are superimposed on each other.

Alternatively, have TMC generate "end-of-trigger" hit

- This control information also has modest impact

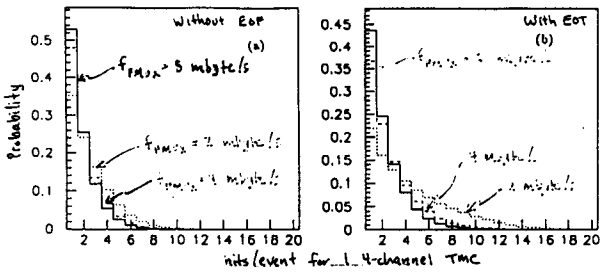

Figure 2: FMUX occupancy (in terms of hits) for one four-channel TVC/AMU without (a) or with (b) one empty hit for each event. The occupancy is shown for three different FMUX-FETX-CIC bandwidths of 2 (dotted), 4 (dashed) and 8 Mbyte/s (solid histogram).

Prefer having control information

- Inherently more robust (error detection easier)
- More flexibility

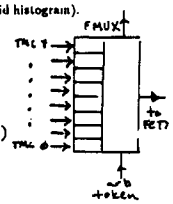

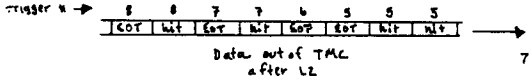

CIC Buffering Studies

Have performed preliminary buffering studies on CIC

- Data from each FEB is pushed to CIC
- FEB→CIC bandwidth ≤ 4 Mbytes/s
- CIC coalesces event data into a single packet

CIC Input Buffer Occupancies

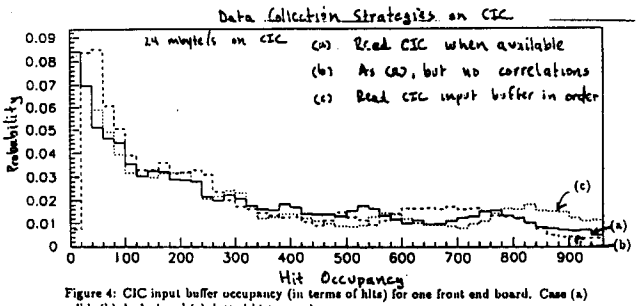

Figure 4: CIC input buffer occupancy (in terms of hits) for one front end board. Case (a) solid, (b) dashed and (c) dotted histogram).

For 1000 hit buffer:
fraction lost = .6 % (a), .05 % (b), 1.6 % (c)

CIC Input buffer requirements is affected by

- CIC latency
- Bandwidth of CIC → DAQ system

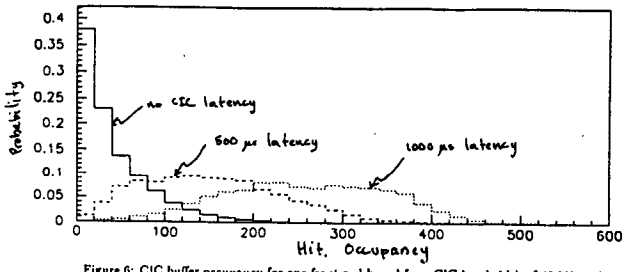

Figure 6: CIC buffer occupancy for one front end board for a CIC bandwidth of 48 Mbyte/s for three different CIC minimal stay times of 0 (solid), 500 (dashed) and 1000 μs (dotted histogram).

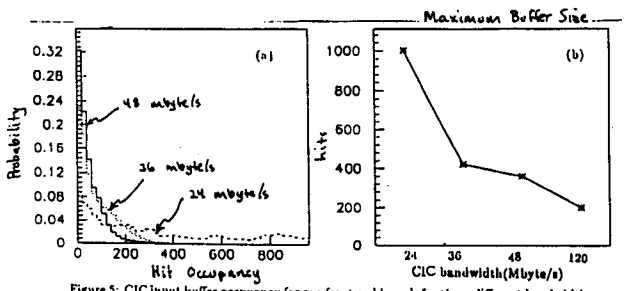

Figure 5: CIC input buffer occupancy for one front end board, for three different bandwidths on the CIC: 24 (dashed), 36 (dotted) and 48 Mbyte/s (solid histogram). The histogram in (b) shows the maximal (99.9%) occupancy.

Summary of Simulation Results

Results of simulation studies

Data buffering prior to L1 trigger	≤ 18 hits
Data buffering prior to L2 trigger	8 hits
TMC readout rate	4 Mbit/s
FMUX Buffer size (4 channel TMC)	15 hits
FMUX→CIC bandwidth	4 Mbyte/s
CIC Input buffer size	400 hits
CIC Output buffer size	1000 hits
CIC Output bandwidth	40 Mbyte/s

Other Observations

- Data correlations have modest impact
- L2 Accept latency can be 30 – 50 μs

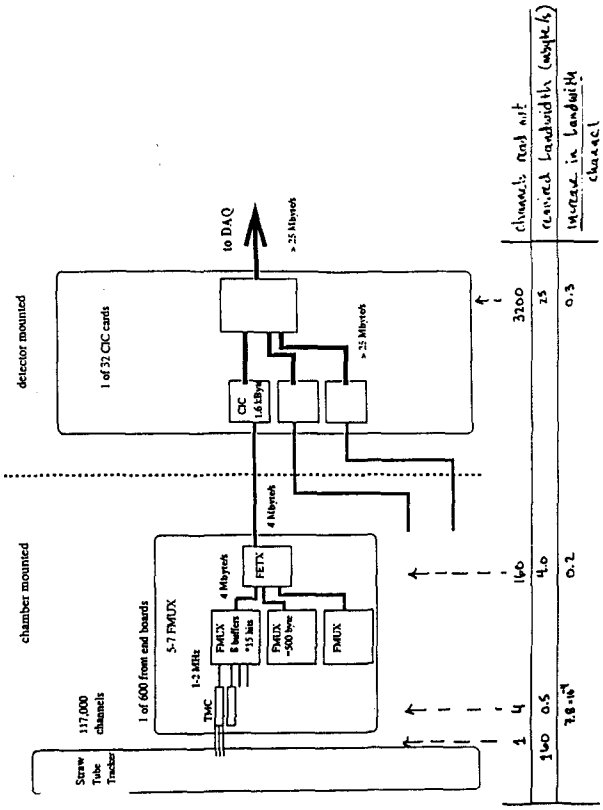

FMUX Prototype Development

Noise on FEB is significant technical risk

- Minimize digital activity on FEB
- Avoid high speed digital transmission
- Controlled risetime of signals
- Employ low-level differential signals ($\pm 100mV$?)
- Decouple analogue and digital components

Develop DCC design with minimal functionality on FEB

- Designing low-level differential receivers and drivers
- Simulated circuit designed by J. Van Der Spiegel

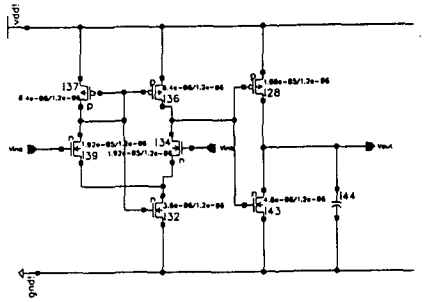

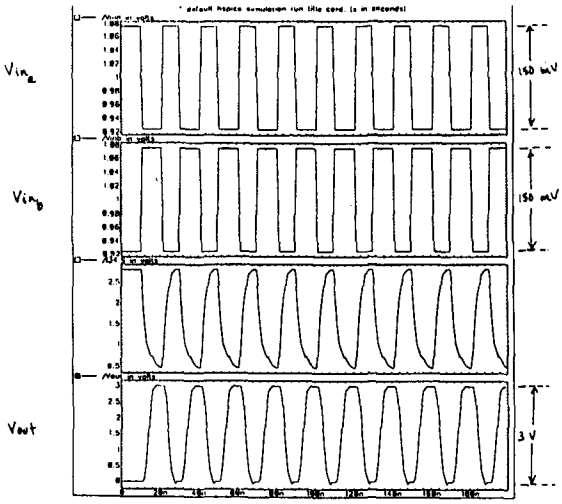

Receiver @ 50 MHz

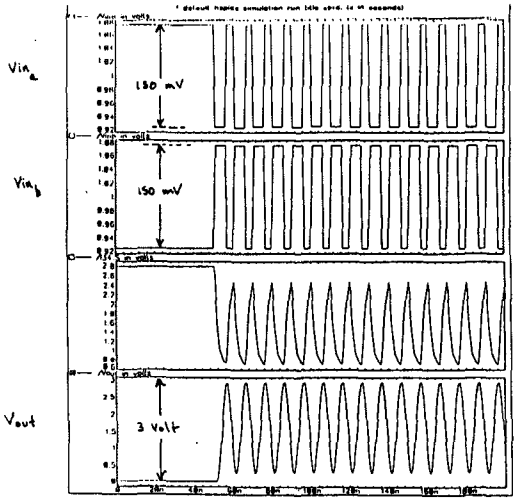

HSPICE Run with 100 MHz input

ASIC Development Schedule

First fabrication run of receiver will take place in July

- Use Northern Telecom 1.2 μ double-poly process
- Expect to use FPGA's to implement prototype FMUX
- More complete FMUX prototype ASIC by end of the year

Also designing test board for prototype FMUX

- Employ Trigger Emulation Module for trigger, clock signals
- Mezzanine architecture to allow tests of several circuits
- Confronting issues of clock distribution, slow control
- Expect to have design complete by end of summer

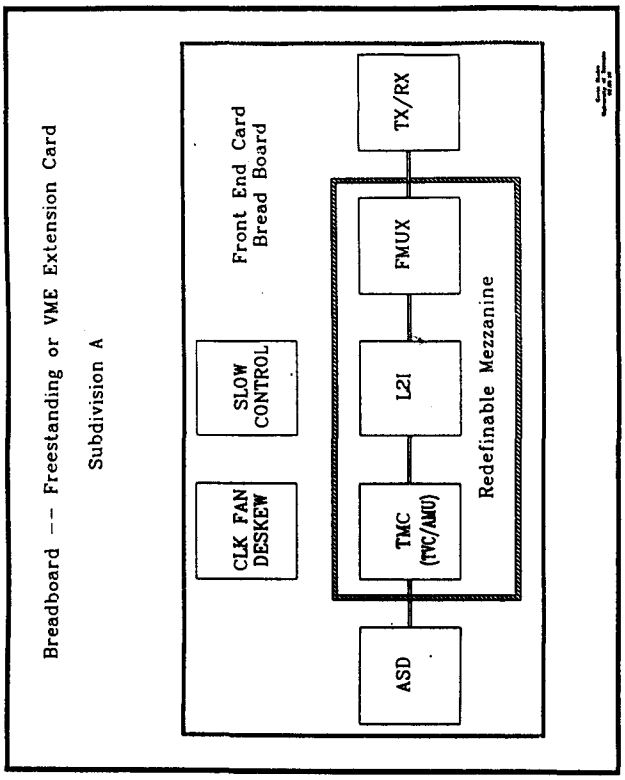

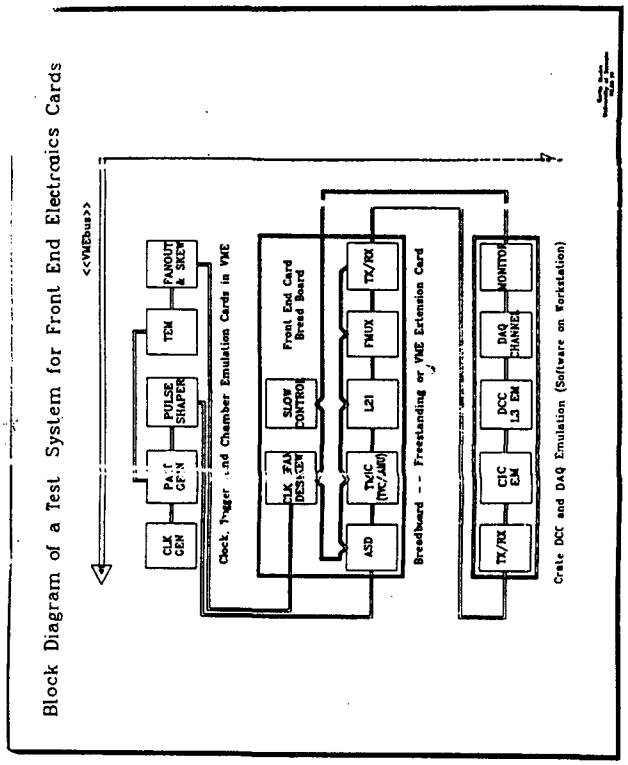

Summary

- Preliminary simulation work on FEB now complete
- Design of prototype ASIC's in initial phase
- Prototype receivers / drivers September 92
- Prototype FMUX available by November 92

SDC Straw and Muon Triggers

J. Chapman
University of Michigan
5 May 92

for the SDC Collaboration Review

Straw Tracker Trigger

Requirements
- Electron ID
- Muon P_t resolution

Design features

Options

Simulation studies

Circuit development

Test results

Future tasks
- Packaging - storage,trigger,DAQ
- Radiation hard implementation
- Integrated testing - noise

Requirements

Requirement	Motivation
Identify "stiff" track	High P_t physics
Determine crossing	Assemble event
Match with calorimeter/showermax	Electron ID
Match with muon	Improve P_t
Associate with silicon	Reject conversions

Basic Plan has all of the above.

Options:
- **Early vrs Late in the Level 1 ↔ Level 2 tradeoff**
- Precision/granularity

Background Rejection

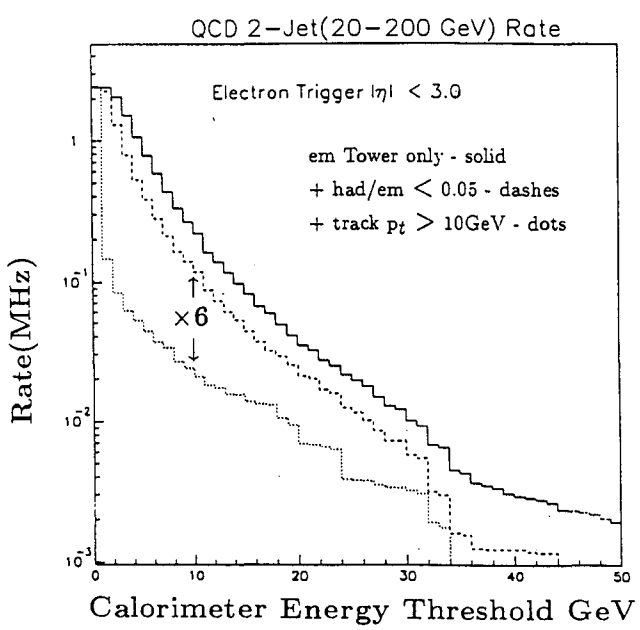

899

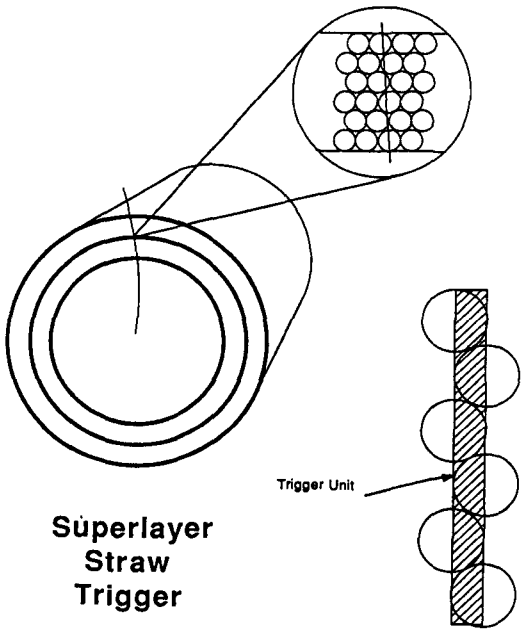

900

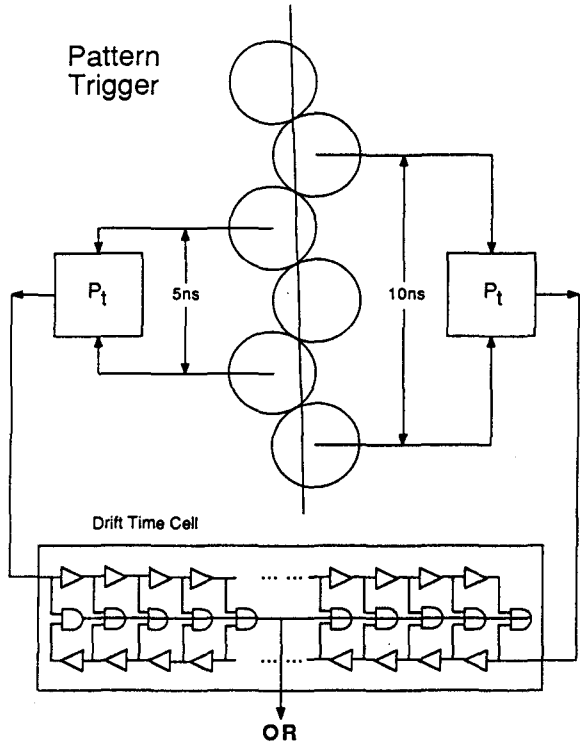

901

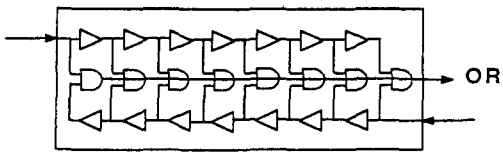

902

Straw Trigger Simulation

- Simulation work: (SDCSIM)
  - 450 H → WW events
  - 450 e and μ alone
  - 450 e and μ with min-bias
  - 450 min-bias at 1, 2, 3 × 10^{33}
- Trigger Options: (2 of 3 coincidence)
  - 64 overlapping wedges
  - ±3 straws (10GeV)
- Summary:
  - Efficient trigger with low "false" rate
  - CMOS ASIC implementation

903

Crossing Determination

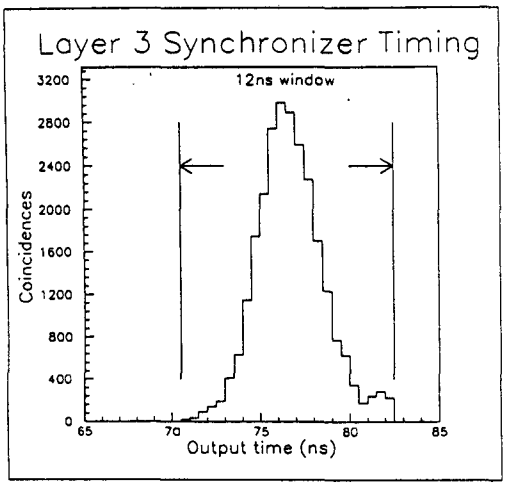

904

Single Layer Trigger

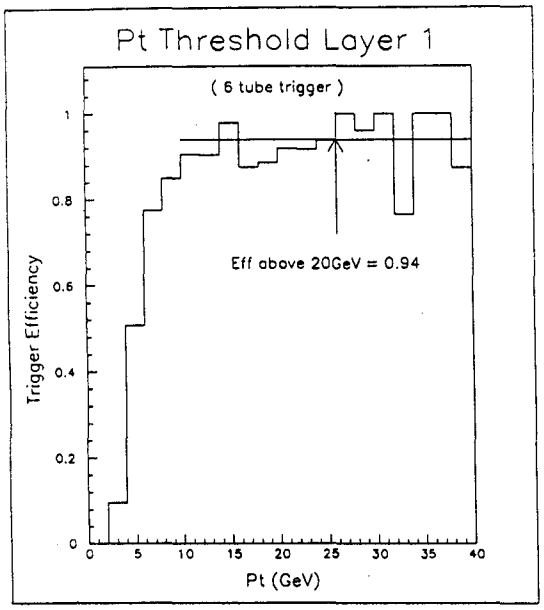

905

Single Layer Trigger

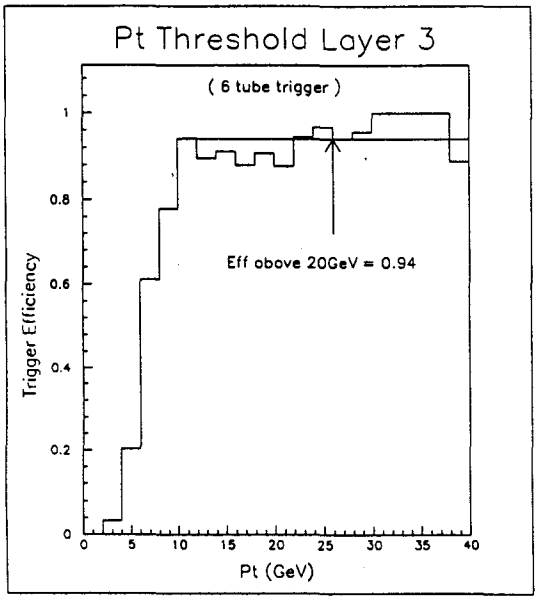

906

Single Layer Trigger

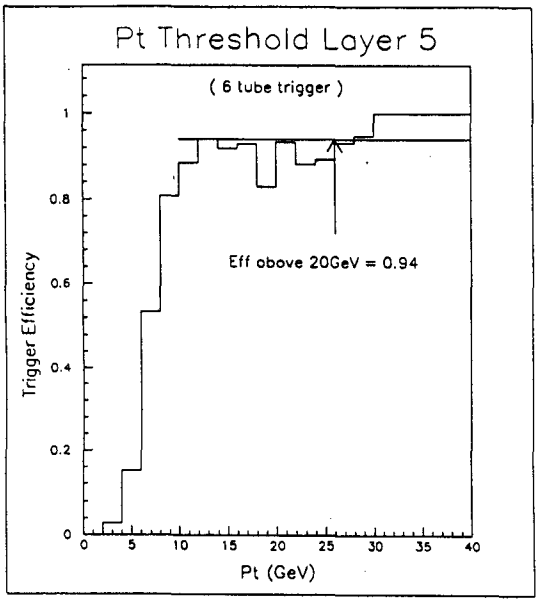

907

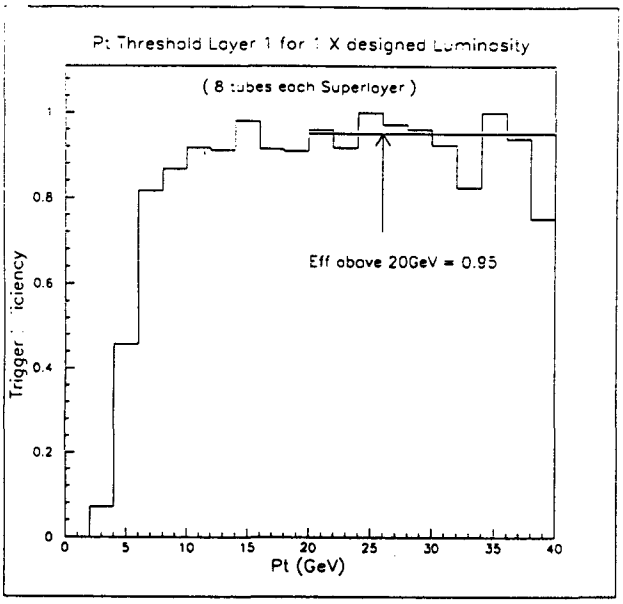

908

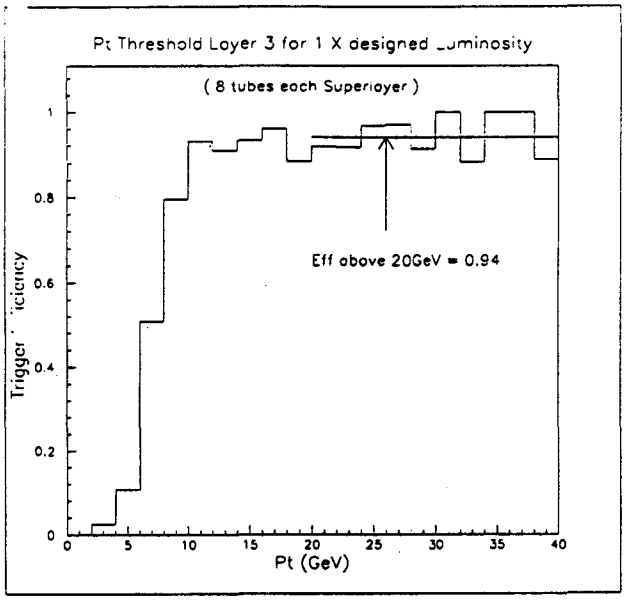

6

909

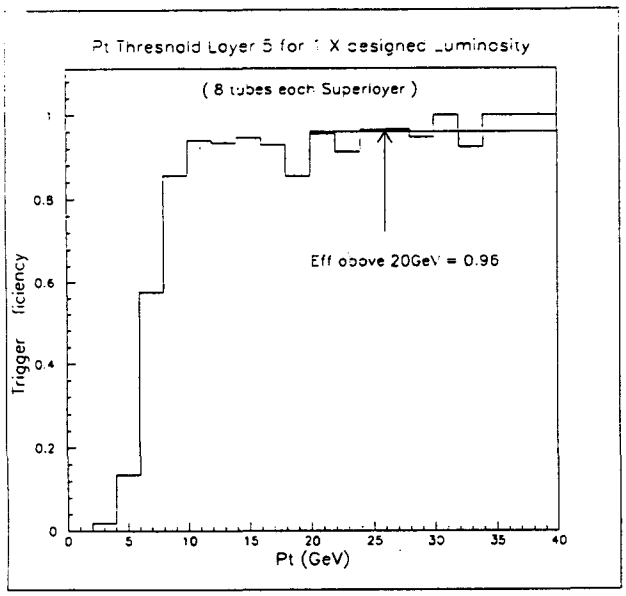

910

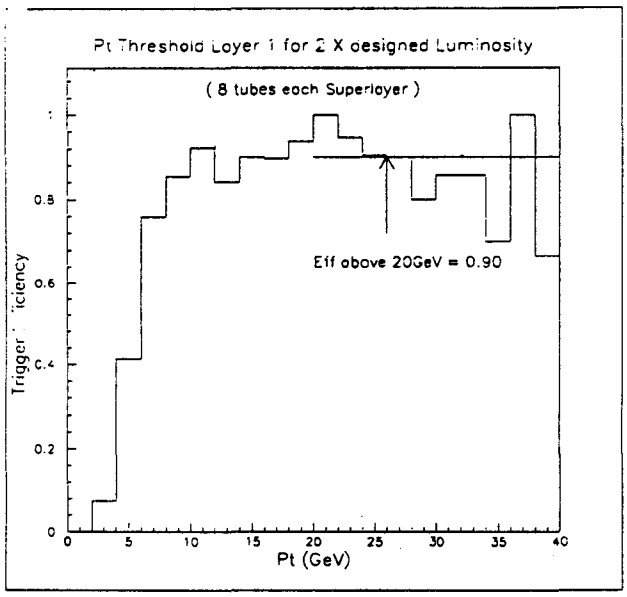

911

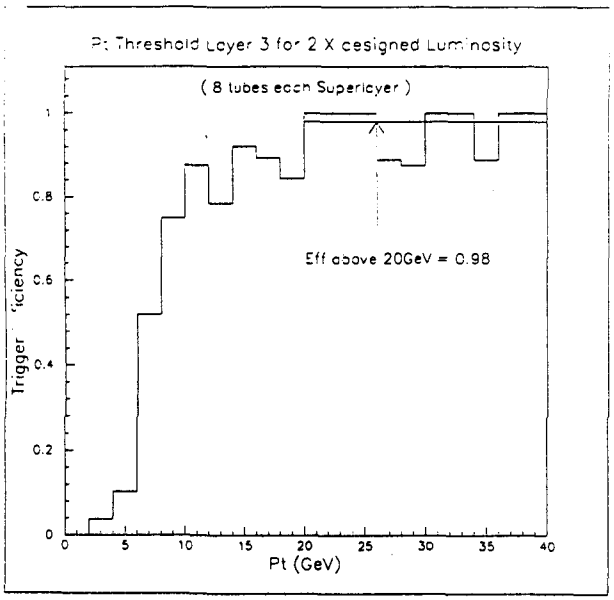

912

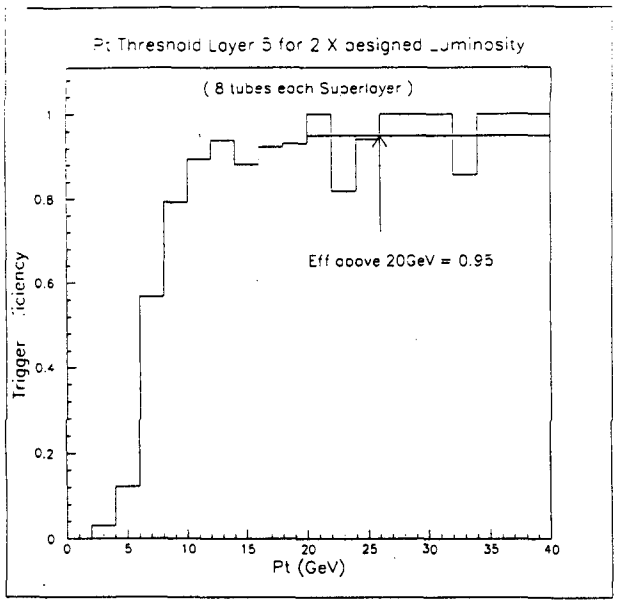

913

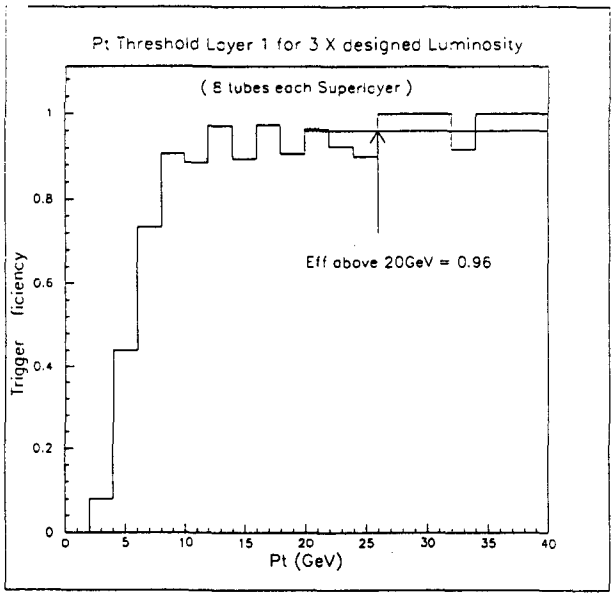

914

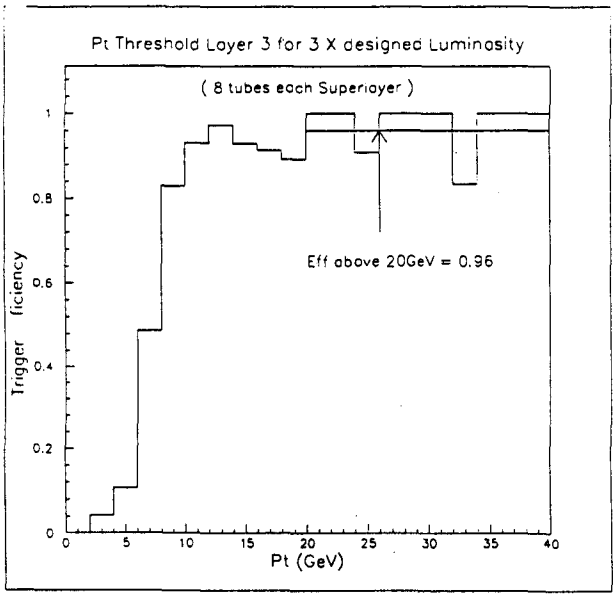

915

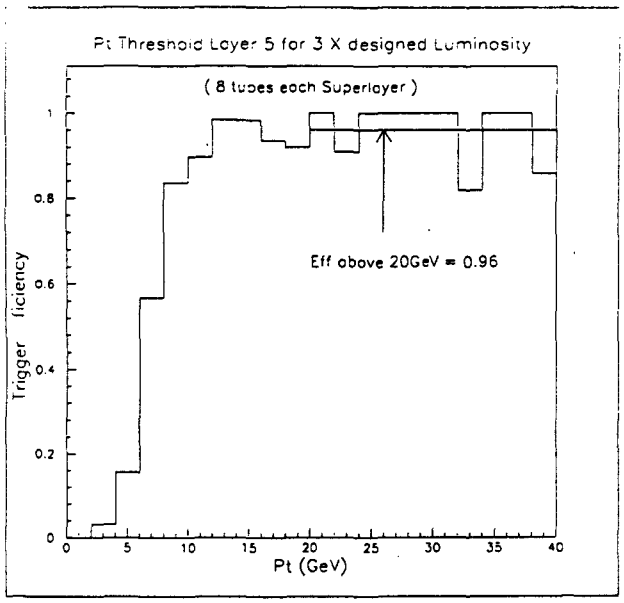

916

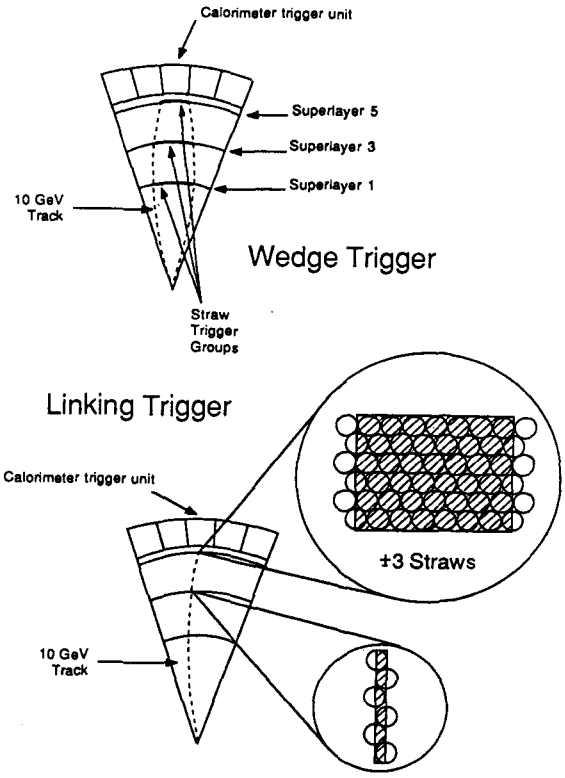

917

Wedge Trigger Option

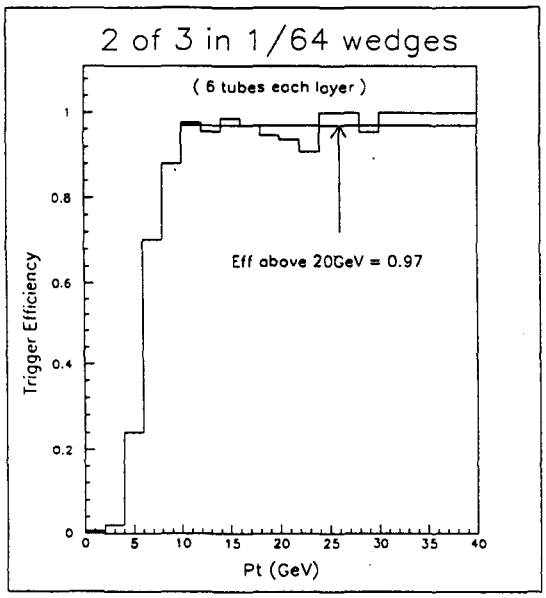

918

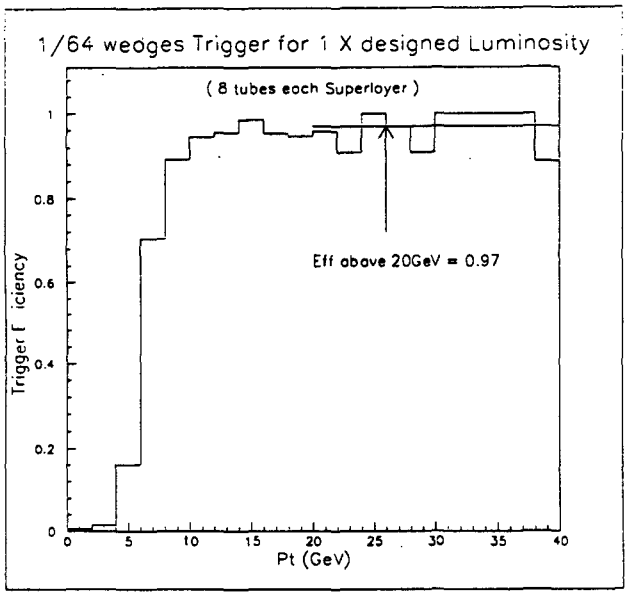

919

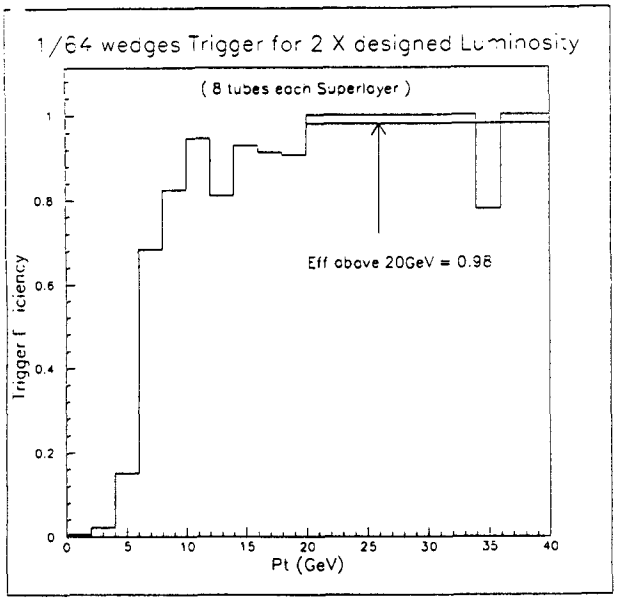

920

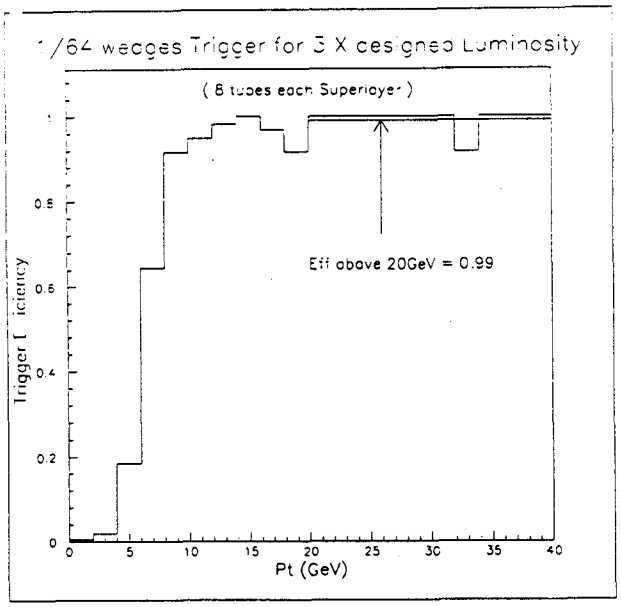

921

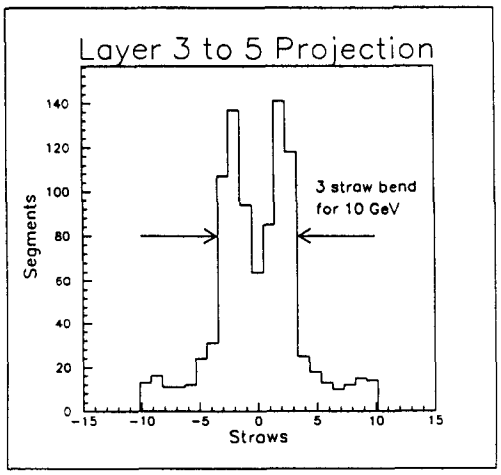

922

Interlayer Linking Option

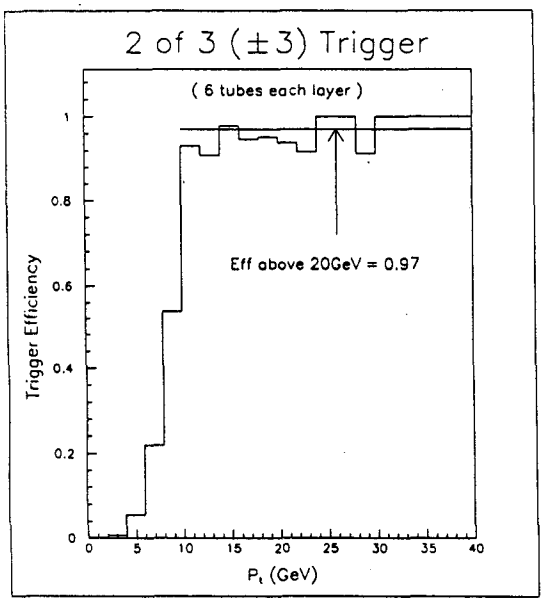

923

2 × Design Luminosity

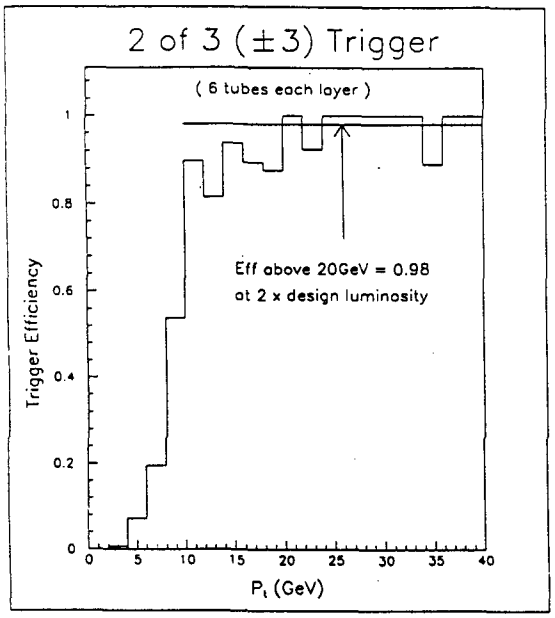

921

3 × Design Luminosity

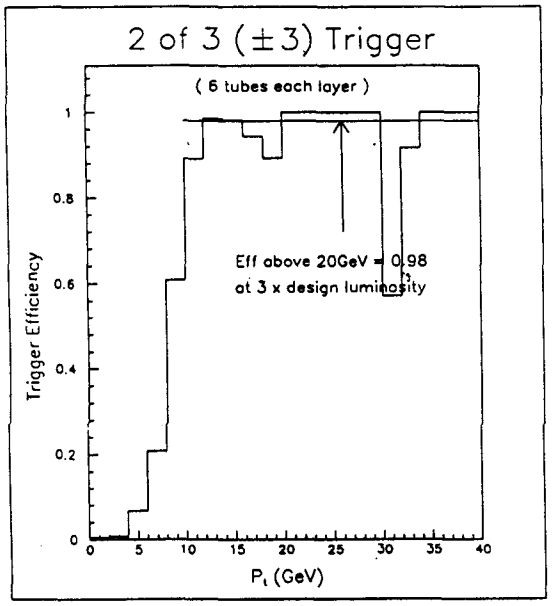

925

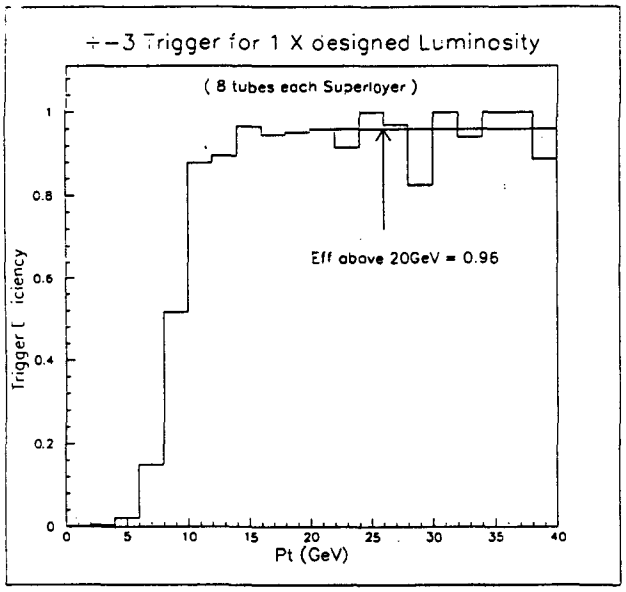

926

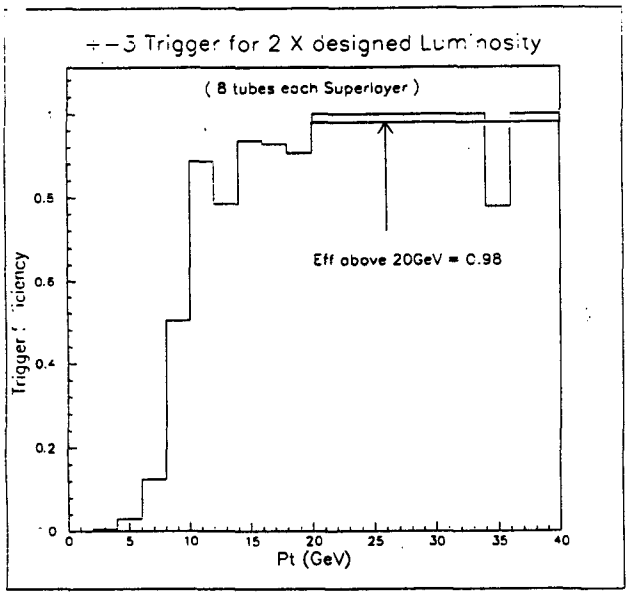

927

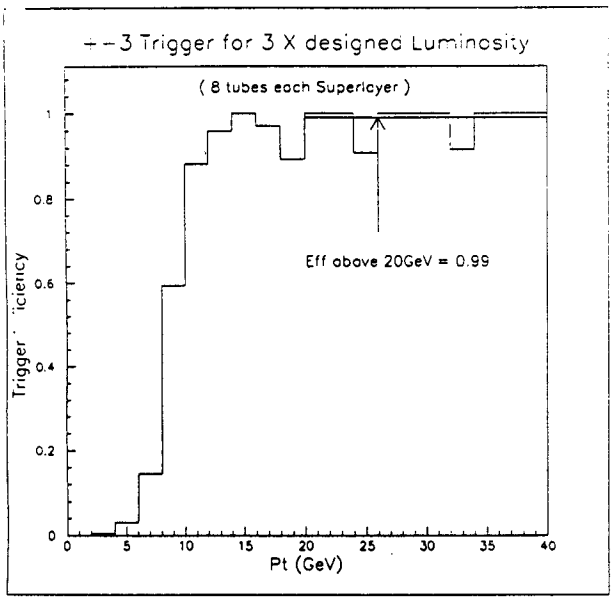

928

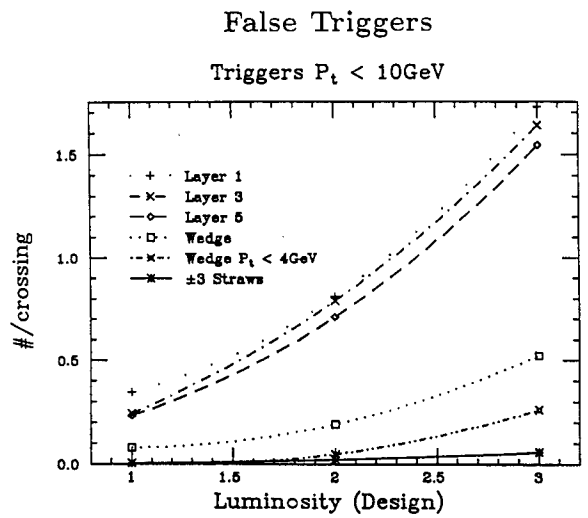

929

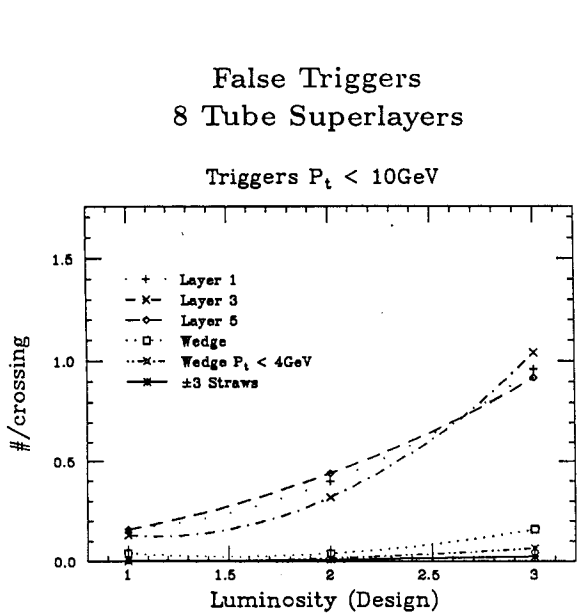

930

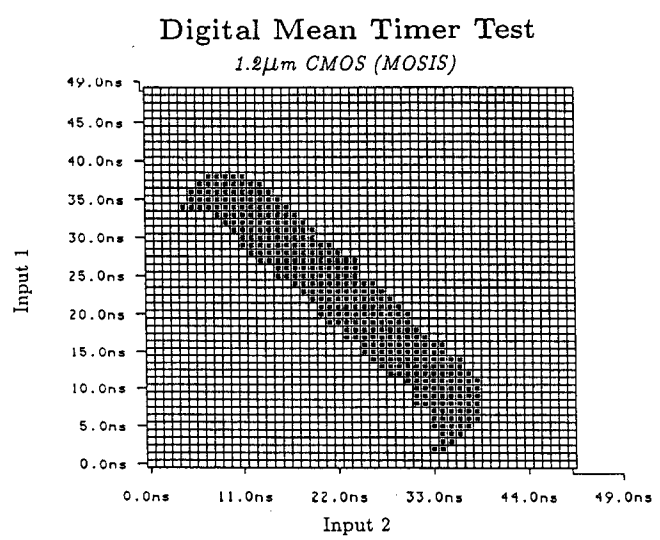

Note : Dots indicate presence of output at fixed time. Circuit test was done with a Tektronix LV511.

SDC Central Tracker Trigger

Performance Summary

- Level 1
  - Single Layer $P_t > 6$ GeV
    False rate $\approx 1/5$csx at 10^{33}
  - 2 of 3 superlayers $\pm$ 3 straws $P_t > 10$GeV
    False rate 1/225csx from minimum bias $P_t < 10$GeV
  - 2 of 3 superlayers, wedge ORs
    False rate 1/12csx mostly 5GeV $< P_t <$ 10GeV
- Level 2
  - "stiff" track "hits"
    500μm - 2000μm bins

Data Summary

- Level 1
  - 2 of 3 ($\pm$3 straws) 3-bits P_t/track
  - 2 of 3 wedge ORs (calorimeter wedges) 1-bit/wedge
- Level 2
  - Layer/module/trigger unit "hit" address

Some measurements on the 4 m Module at Ill

D. Rust 25 May 1992

Attenuation Picture:

38 μm: 51.4 Ω/m measured

Skin effect raises effective resistance to 62 Ω

Copper coated cathode 1500 Å: 25 Ω/m

$\frac{2Z_0}{R} = 6.4$ m 6.3 m is measured

Gain Measurement 38 μm wire CF_4-isobutane:

Use Fe^{55}. Compare with earlier measurement with 25.4 μm wire. Also Kadyk value.

Result: Gain curve shifts 200V to higher voltage changing from 25.4 μm to 38 μm.

[A little bigger than I expected; gas property]

Gas mixing ratio:

Obtained new more accurate flow meters (4%)

Made measurements using Gas Chromatograph

Discovered our standard mix of past year and ½ is 28% rather than 20%

D. Rust

SDC
Program Advisory Committee Meeting
May 5, 1992

Mechanical Measurements on 4 meter Prototype

- Measurements of deviation from straight line for the completed module
- The module was unconstrained in "phi".
- Meaurement with an "optical micrometer"

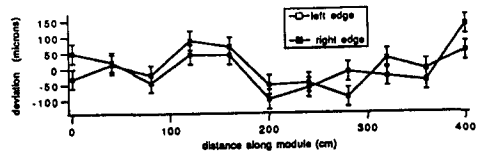

$\sigma \sim 65\mu$ → goal $< 40\mu$ (CONSTRAINED)

- On the detector the module is constrained by hold down attachments.

Signals from Fe^{55} source 2300V on wire

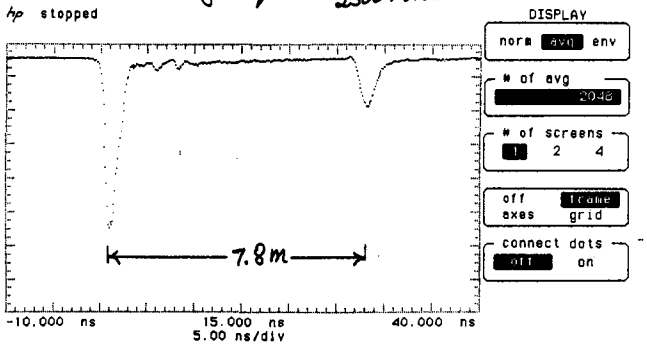

	Sensitivity	Offset	Probe	Coupling
Channel 2	2.00 mV/div	-7.500 mV	1.000 :1	dc (50 ohm)

Trigger mode : Edge
On Negative Edge Of Chan2
Trigger Level
Chan2 = -2.750 mV (noise reject OFF)
Holdoff = 40.000 ns

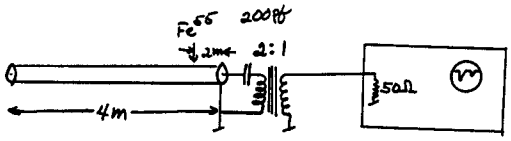

SDC
Program Advisory Committee Meeting
May 5, 1992

Signal Attenuation in a Straw Chamber

- 4 meter straw
- Copper coated Kapton (150 nm) 90 ohms.
- 37 μ diameter wire, Gold plated tungsten

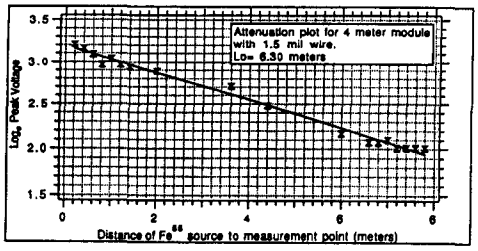

936

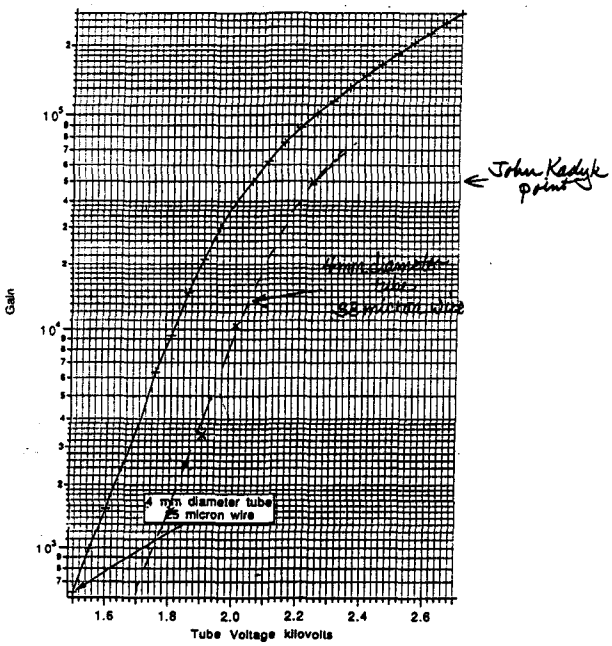

Fig. III.3. The gain curve of a 4 mm straw drift tube with CF_4 -isobutane 80:20 gas. The absolute calibration of the curve is accurate to about 15% but the shape of the curve reflects the true dependence of the gain on voltage.

937

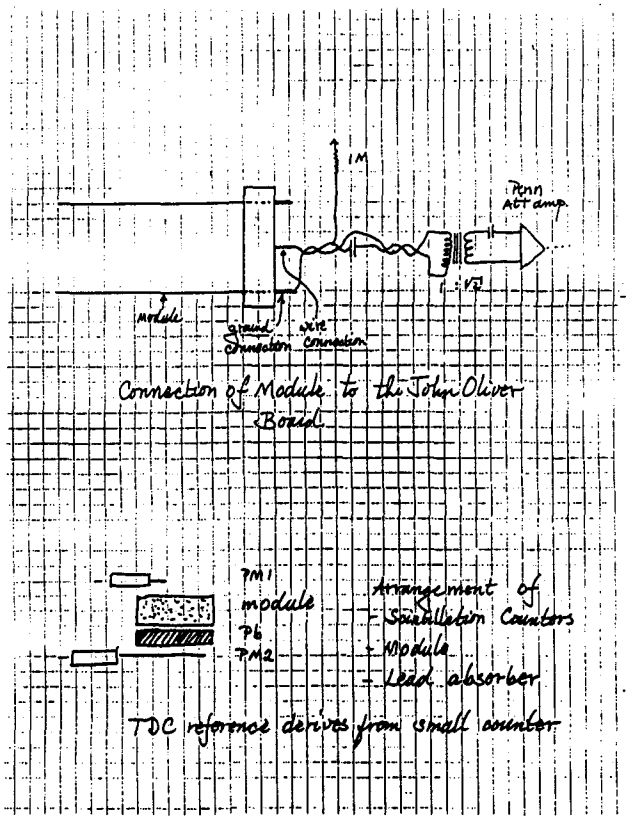

938

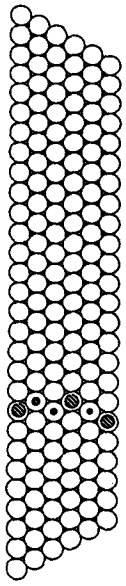

939

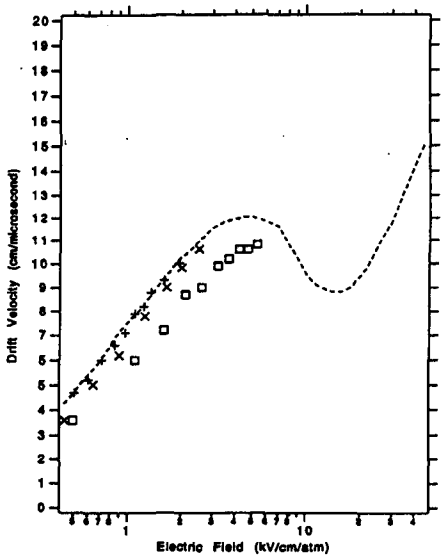

Fig. III.4. Measurements of the drift velocity in CF_4-isobutane 80:20 as a function of electric field strength. The squares are from R. Openshaw, *et al.*, the + are from T. Yamashita, *et al.* and the × are from J. Va'vra, *et al.* See the references. The curve is drawn through the points of Va'vra and continued according to the shape of the pure CF_4 and CF_4 - CH_4 mixture curves.

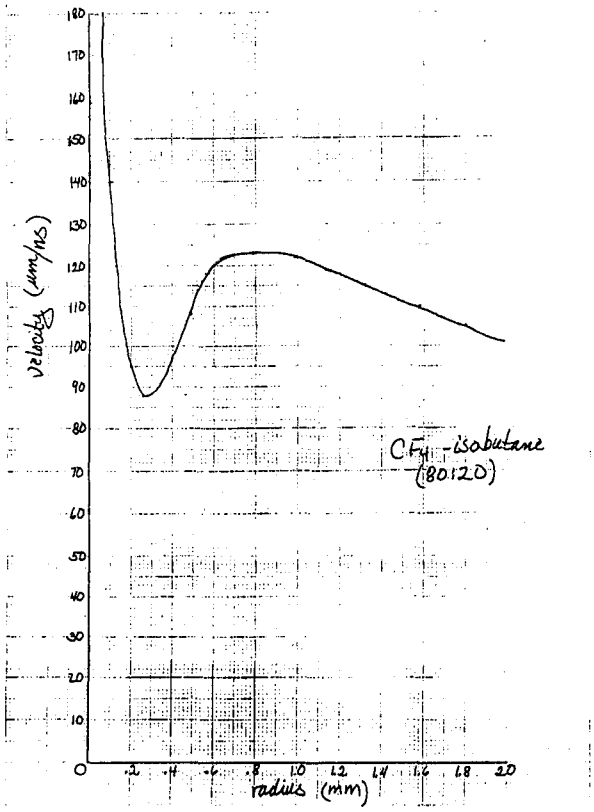

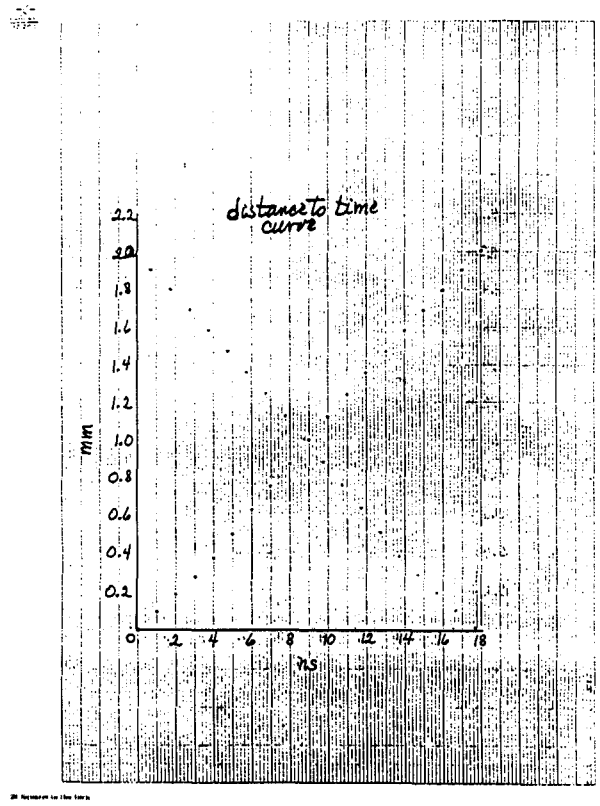

Velocity in the CF_4-isobutane mixture varies with electric field and hence radius but variation is limited.

Time to distance relationship nearly linear but with significant deviations from linearity.

Fitting program - parameter adjustment: Automatic
Offsets, displacements. 6 layers only.
16 channels total (so far).
Doesn't work at edges of pattern.

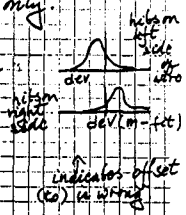

Evaluate the fit by leaving one layer out of the fit. Residual plots; χ^2 plot.

1 m module 6×10^4 gain/12 fC thresh 120 μm

4 m module 4×10^4 gain/5 fC thresh 130-140 μm

counters at far end

Still more to do

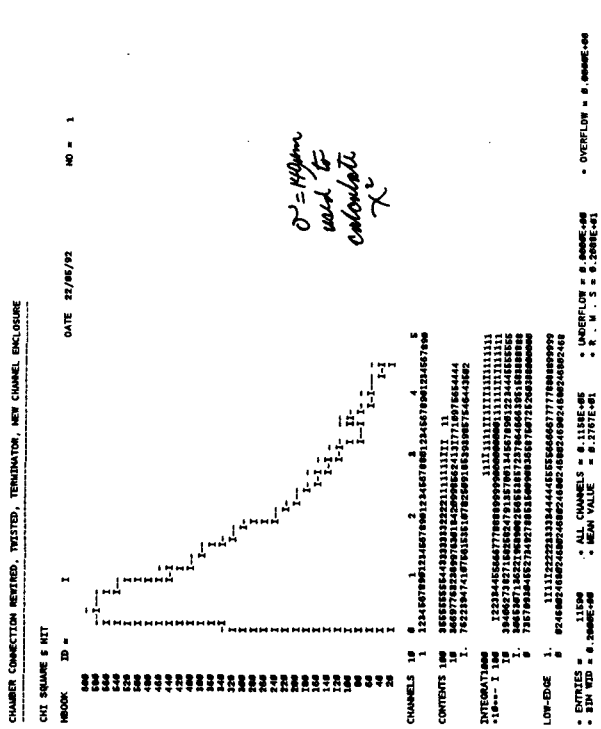

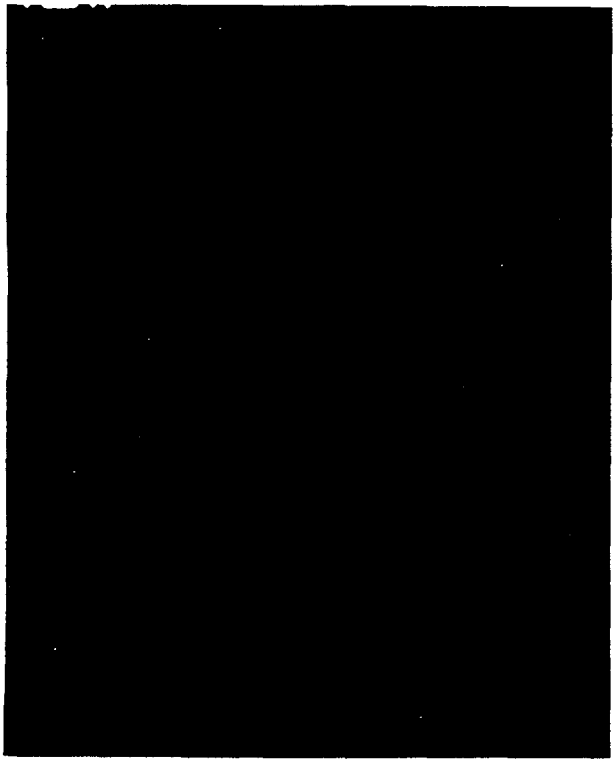

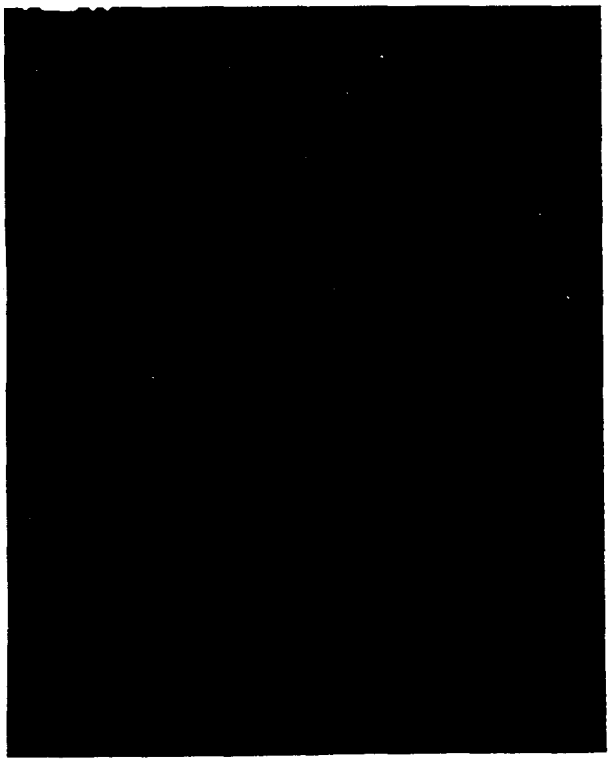

MECHANICAL CONSIDERATIONS FOR A SDC OUTER STRAW TRACKER FOR THE SSCL

SDC COLLABORATION MEETING
AT KEK JAPAN
MAY 25 1992

WESTINGHOUSE ELECTRIC CORPORATION
(W)STC
PITTSBURGH, PA

R. L. SWENSRUD (ROGER)

SDC OUTER TRACKER CYLINDER SPACEFRAME ENGINEERING GROUP

TABLE OF CONTENTS

1. Introduction
2. Overview of Outer Tracker
3. Mechanical Engineering
   - 3.1 Common Straw and Sifi Tracker Support Requirements
   - 3.2 Testing & Prototype Program
     - 3.2.1 Goals and Issues
     - 3.2.2 Requirements and Resolution
   - 3.3 Straw Tube System
     - 3.3.1 Detail Definition of Geometry
       - o Modules
       - o Support Structure
     - 3.3.2 Analysis
   - 3.4 Scintillating Fiber System
     - 3.4.1 Detail Definition of Geometry
     - 3.4.2 Analysis

SDC OUTER TRACKER CYLINDER SPACEFRAME ENGINEERING GROUP

3. MECHANICAL ENGINEERING

3.3 Straw Tube System

3.3.1 Detail Definition of Module Geometry

- o Module Superlayer Geometry Defined for All Trigger & C2 Stereo Layer
- o Stereo Superlayer C4 is Near Completion

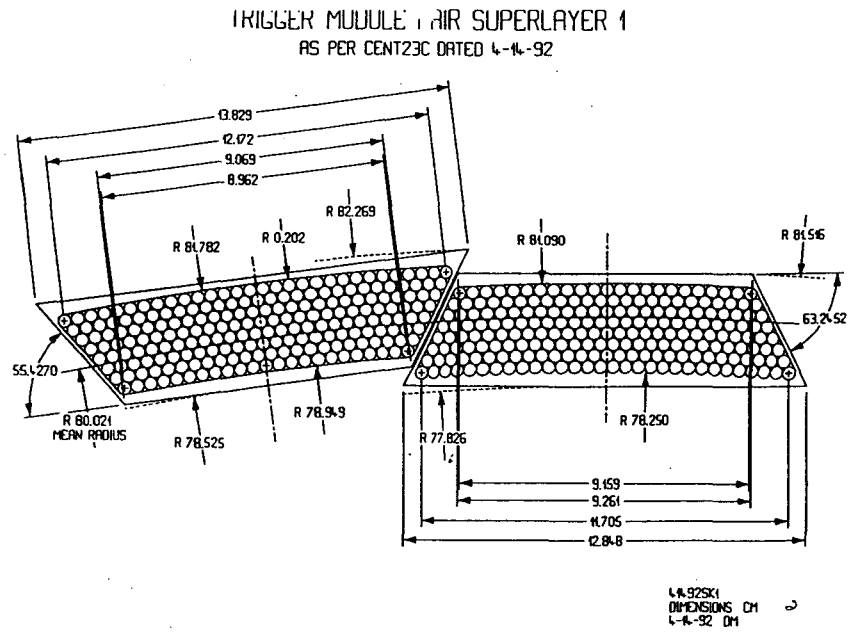

STEREO MODULES SUPERLAYER 2 AFTER ROTATION

AS PER CENT23E DATED 5-19-92

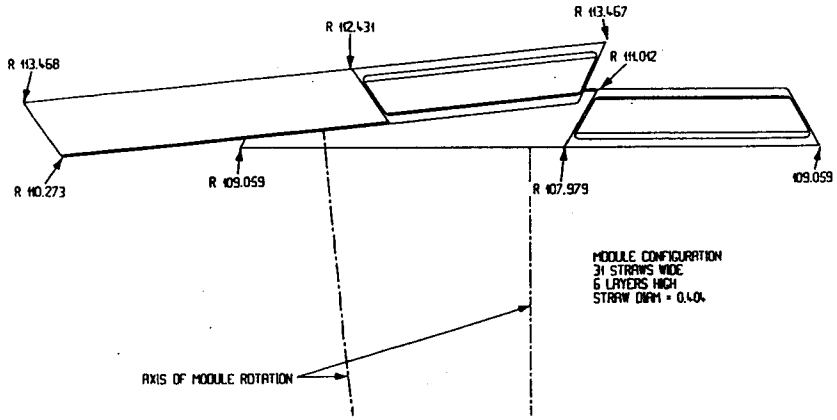

ALL DIMENSION IN CM
52192SK1

7

952

STEREO MODULES SUPERLAYER 2

AS PER CENT23B DATED 4-1-92

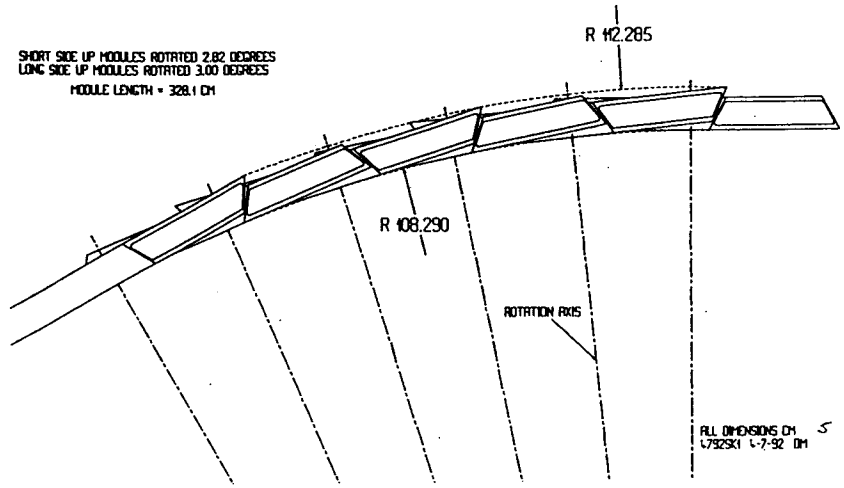

ALL DIMENSIONS CM
47192SK1 4-7-92 DM

5

950

STEREO MODULE SECTIONS - SUPERLAYER 2

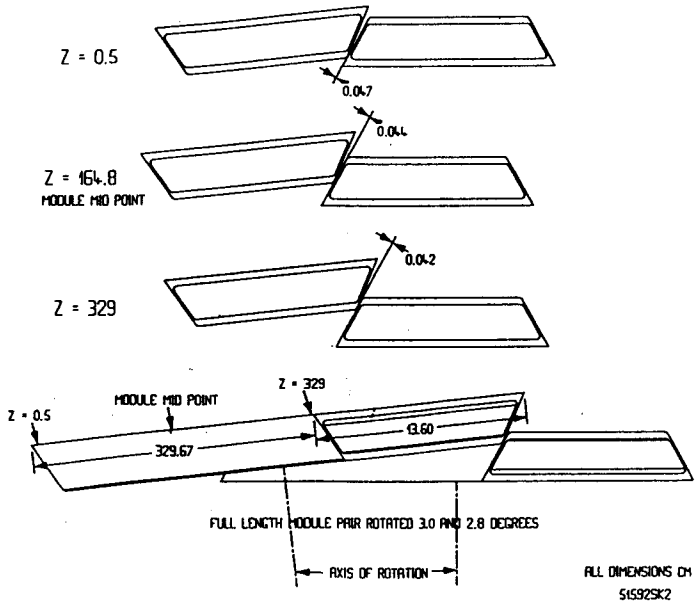

ALL DIMENSIONS CM
51592SK2

953

SUPERLAYER 2 STEREO MODULES BEFORE AND AFTER ROTATION

DOTTED LINES AND LARGE DIMENSION TEXT SIZE REPRESENT MODULES BEFORE ROTATION, SOLID LINES AND SMALL TEXT REPRESENT MODULES AFTER ROTATION

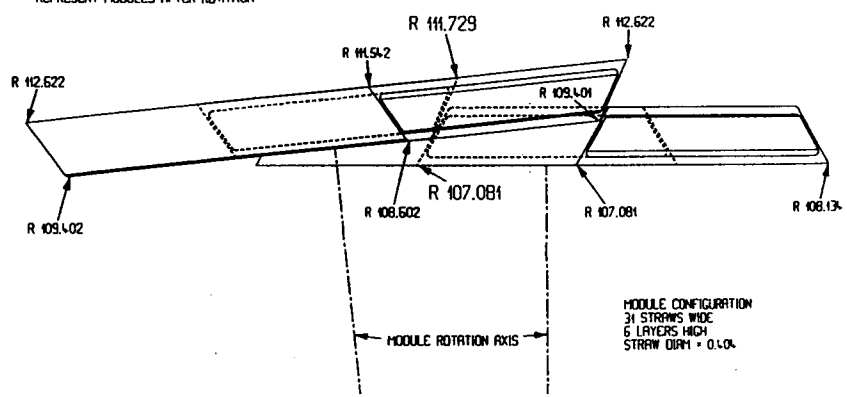

ALL DIMENSIONS IN CM
51692SK1 DM

6

951

SDC OUTER TRACKER CYLINDER SPACEFRAME ENGINEERING GROUP

3. MECHANICAL ENGINEERING

3.3 Straw Tube System

3.3.1 Detailed Definition of Geometry Continued

Support Structure

- o Support Structure Geometry is Being Developed
- o Outer & Intermediate Appear Compatible ~~Except for Cables~~

Viewgraph 12
RLS
<05-26-92>

Westinghouse
Science & Technology Center

12

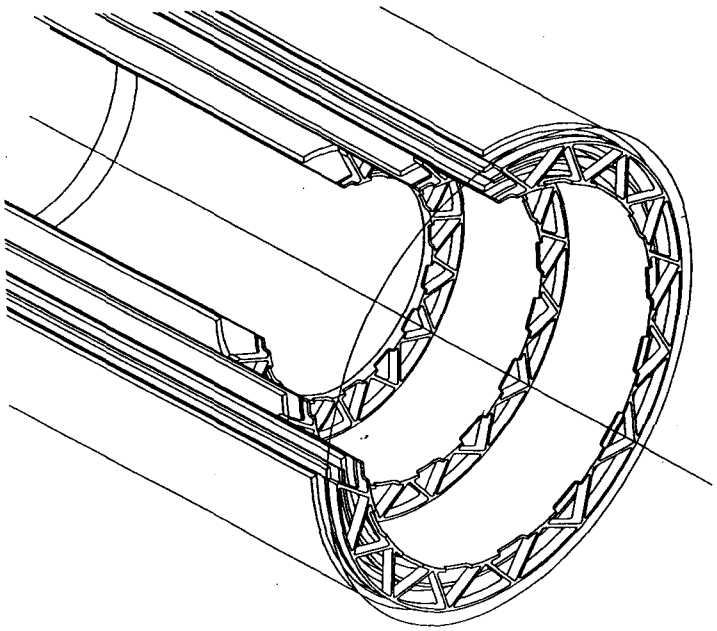

13

STEREO MODULE SECTIONS - SUPERLAYER 2

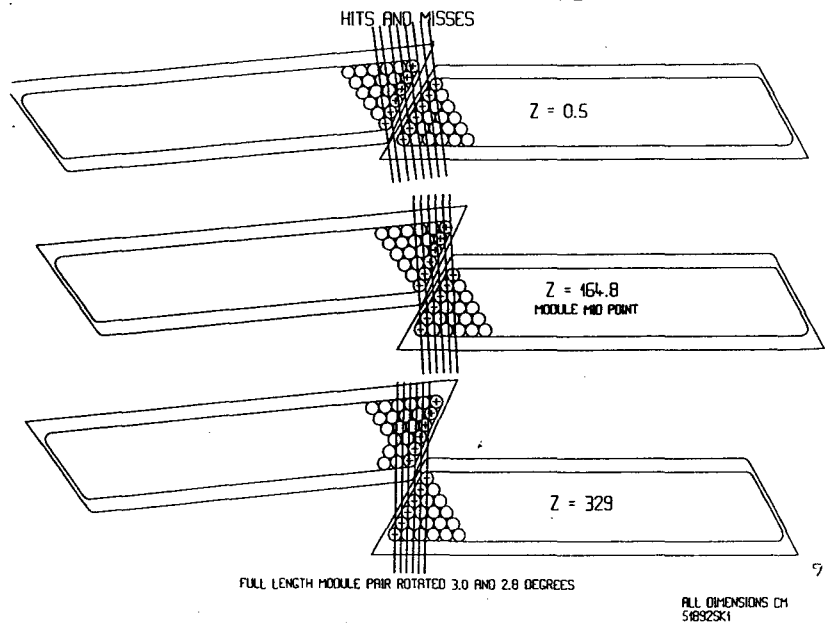

9

STEREO MODULES SUPERLAYER 2 BEFORE ROTATION

AS PER CENT23E DATED 5-19-92

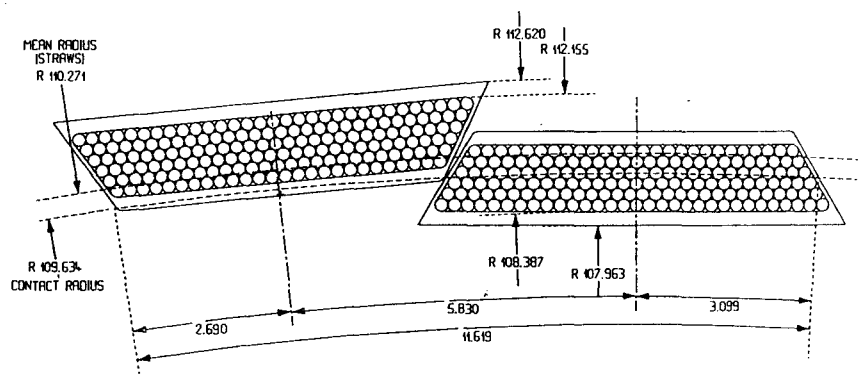

51992SK1

10

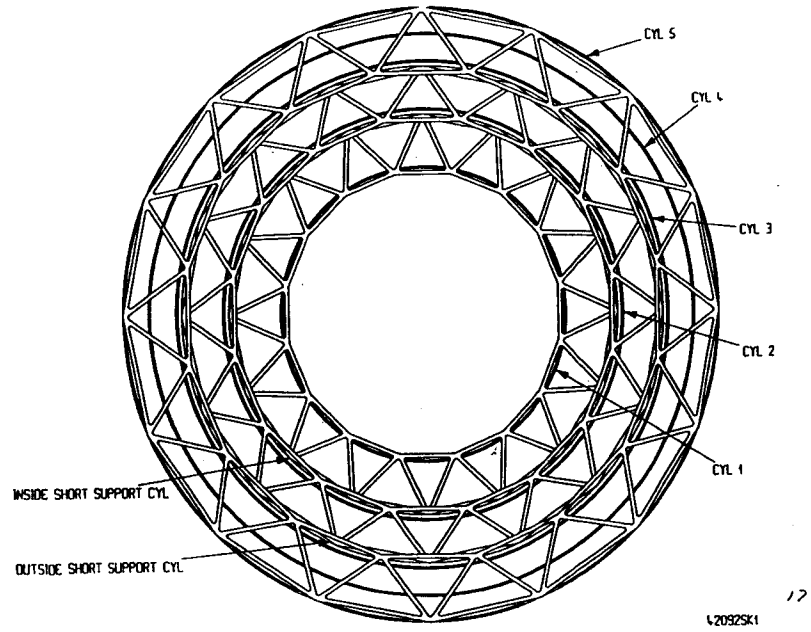
CYL 5
CYL 4
CYL 3
CYL 2
CYL 1
INSIDE SHORT SUPPORT CYL
OUTSIDE SHORT SUPPORT CYL
L2092SK1

17

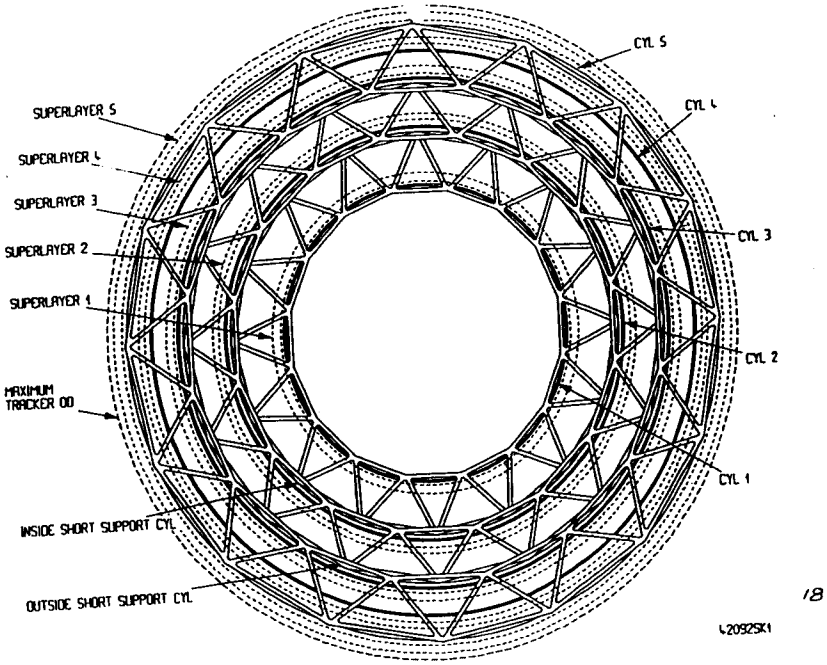
CYL 5
CYL 4
CYL 3
CYL 2
CYL 1
SUPERLAYER 5
SUPERLAYER 4
SUPERLAYER 3
SUPERLAYER 2
SUPERLAYER 1
MAXIMUM TRACKER OD
INSIDE SHORT SUPPORT CYL
OUTSIDE SHORT SUPPORT CYL
L2092SK1

18

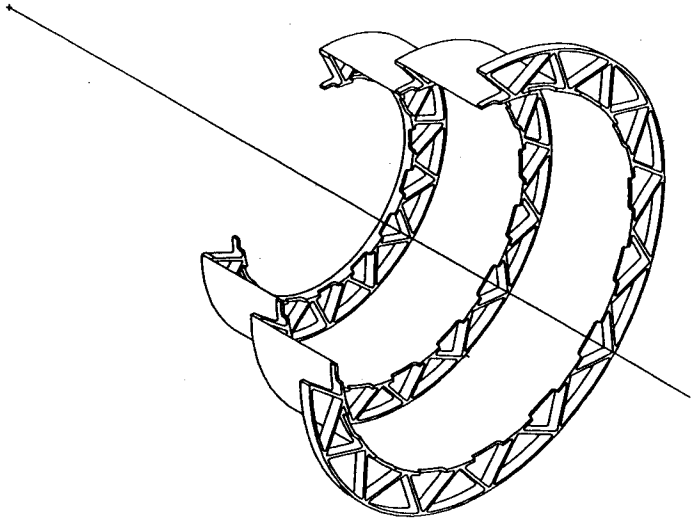

14

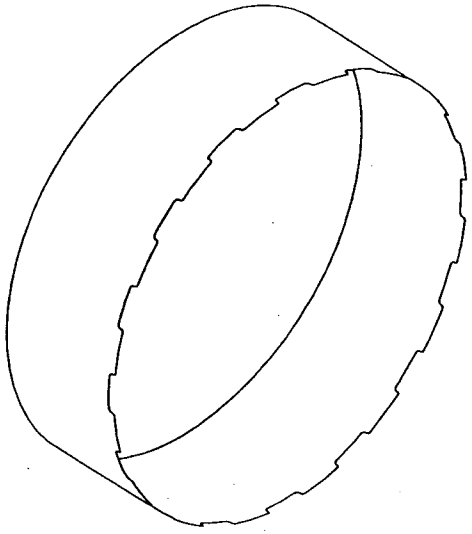

15

SUPERLAYERS 1 - 2 SECTION

AS PER CENT23E DATED 5-19-92

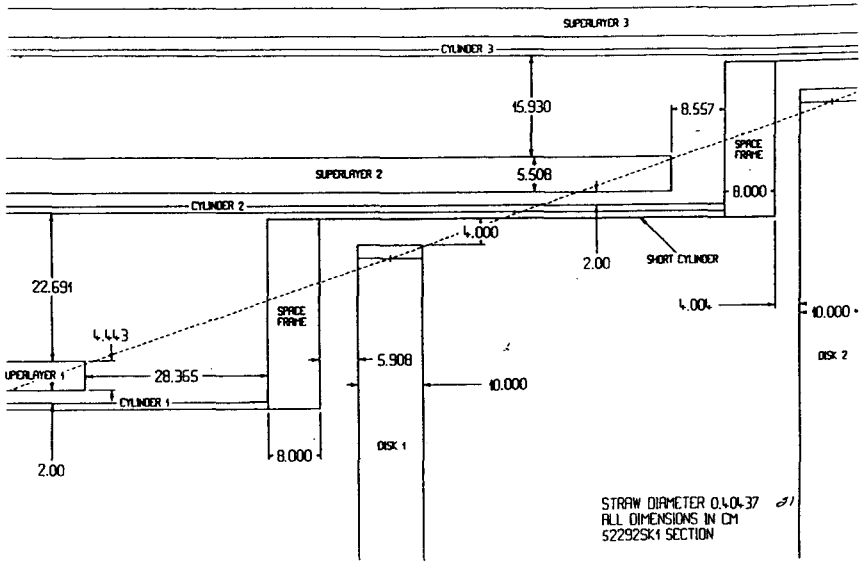

TRACKER SECTION

AS PER CENT23E DATED 5-19-92

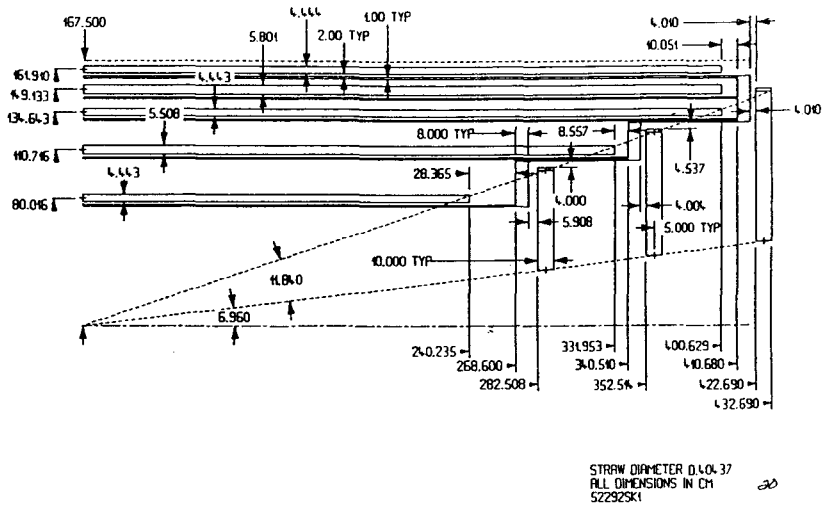

ELECTRONICS VOLUME SUPERLAYER 2

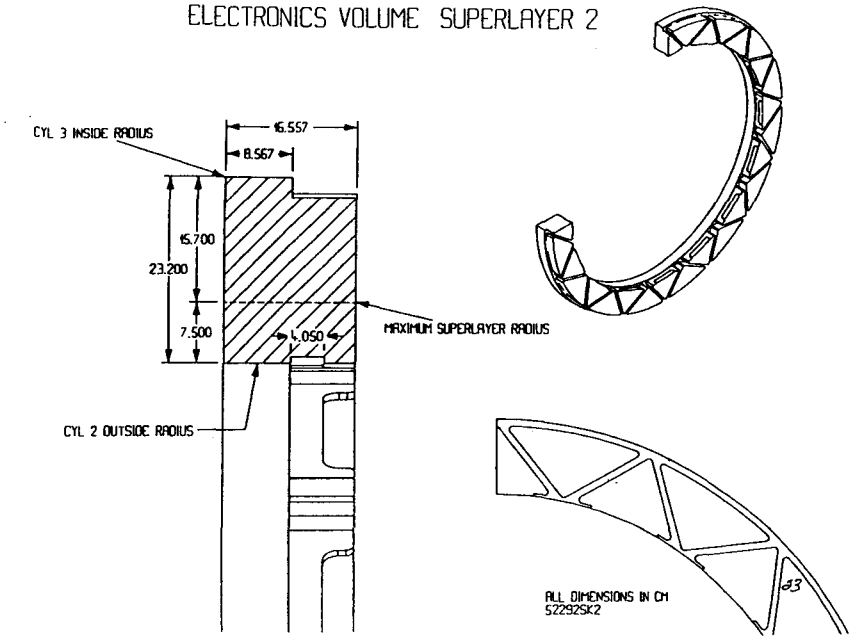

SUPERLAYERS 3 - 4 - 5 SECTION

AS PER CENT23E DATED 5-19-92

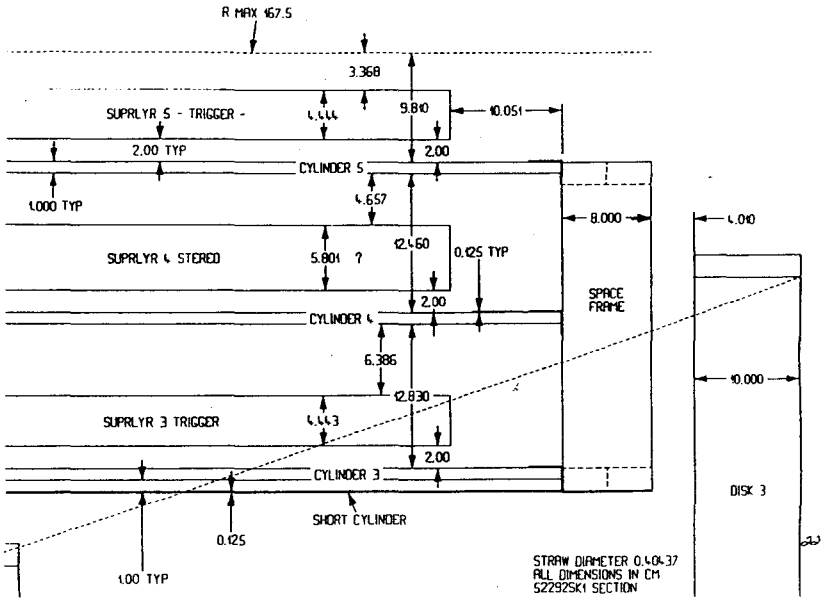

SPACE FRAME 2

MAX RADIUS = 129.237
MIN RADIUS = 104.762
16 SECTIONS - 32 WINDOWS
CUTOUTS 4 X 22 16 PLCS
TUBE SECTION 2 X 8

ALL DIMENSIONS IN CM

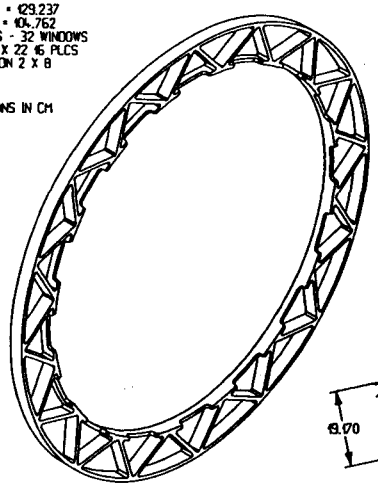

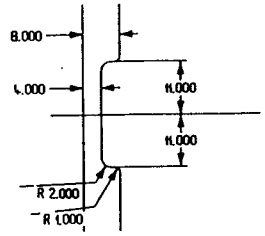

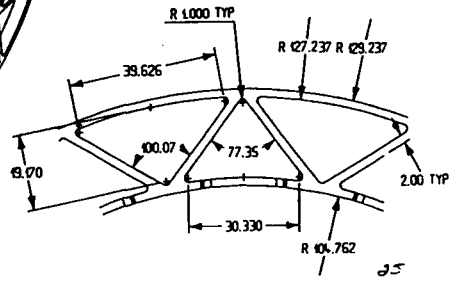

42992SK1
4-29-92 DM

958

MODULE LOCATION POINTS

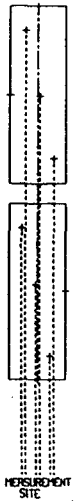

IF A PATTERN OF POINTS IS DISPLACED OFF CENTER ON A MODULE WHEN A LIKE MODULE IS ROTATED ABOUT Z = 0, ALL POINTS OR MEASUREMENT BALLS ARE VISIBLE FOR MEASUREMENT.

42392SK2
4-23-92 DM

956

SPACE FRAME 3

MAX RADIUS = 158.474
MIN RADIUS = 129.387
6 SECTIONS - 32 WINDOWS
UTILITIY CUTOUTS 4 X 24 16 PLCS
TUBE SECTION 2 X 8
LENGTH = 8.00

ALL DIMENSIONS IN CM

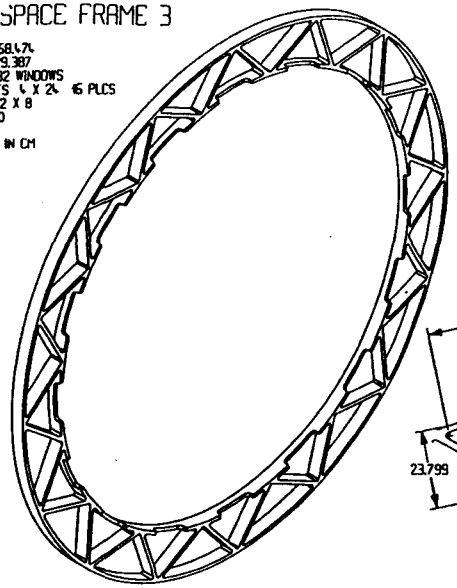

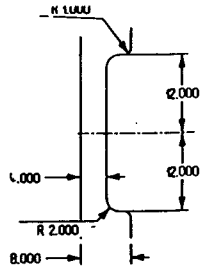

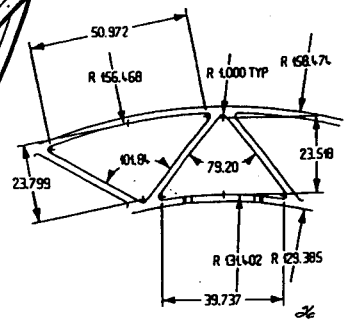

42892SPFR3
4-28-92 DM

959

SPACE FRAME 1

MAX RADIUS = 104.612
MIN RADIUS = 75.462
16 SECTIONS - 32 WINDOWS
CUTOUTS 4 X 16 16 PLCS
TUBE SECTION 2 X 8

ALL DIMENSIONS IN CM

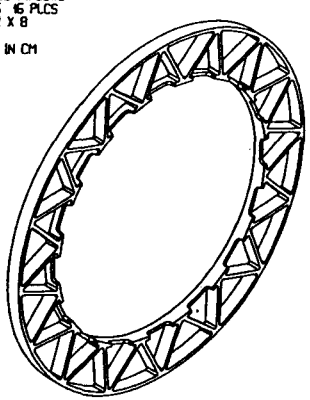

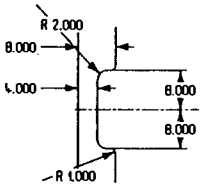

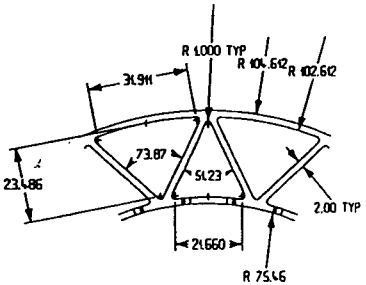

43092SK1
4-30-92 DM

957

HV System for Straws

D. Rust

25-May-1992

HV on module

HV cabling

HV power supply

HV monitoring

Special properties of straw modules which affect the design of the HV system:

1) Relatively high steady state currents.

$\lesssim 1.5\,\mu a$ per wire at design $\mathcal{L}$

Apply safety factor & allow for operation in excess of design $\mathcal{L}$.

$\therefore$ Plan for $\lesssim 5\,\mu a$/wire

or $\lesssim 1$ ma/module ($\lesssim 2$ w)

2) Large number of independent isolated elements.

Design should include a way of isolating the faulty elements.

Could be in units of modules, sections of modules or ultimately individual straws.

3) A module has a large capacitance

50 pf/straw $\rightarrow$ 10 nf/module

HV on module.

1) isolation of straw capacitance so that the module capacitance doesn't dump into one wire with high current when one wire discharges.

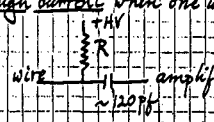

R could be small (~1K) if this were a small capacitance & fast trip on +HV. Since capacitance is large, R is made large. Using 5 μa/wire and a 10V max change, 2 MΩ is correct value. 1 ma discharge current. 20 ms time const.

5% gain change

R not so high that a trip on one wire is not easily sensed. 2 MΩ OK; adds 1 ma to already present steady state ≲ ma.

— R cannot be too high or too low but here is a compromise value ≲ 2M

2) Wire faults for which it should be possible to isolate and remove HV.

Broken wire

Loose wire - keeps tripping supply

Noisy wire - Spreads noise

The Aleph ECAL has fusing to disconnect broken wires.

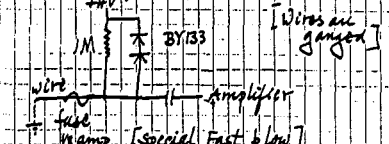

Pulse high current negative voltage on +HV line. The high current blows the fuse. [extra components - size]

Other possibilities:

A fusible resistor - Can it break reliably?

A special fuse blowing I.C.

would take a lot of power

~~Other?~~ Bring out several HV lines from each module.

Other?

FROM RAL 0235 44 6733 02.26.1998 12:44 NO. 1 P. 2

capacitances were measured to be 1.0 nF for the first and middle sections, but 1.2 nF for the third section. The difference between the calculated and measured values is assumed to be due to end effects. Each third of the layer receives its high voltage via a 1 MΩ resistor in parallel with a diode chain, and is connected to the anode output lead via a 10 nF capacitor in series with an 82 Ω resistor. Each pair of wires receives high voltage via a fuse. In the event of a wire breaking, the fuse can be blown by a high-current, low-voltage pulse applied to the high-voltage input. In this way the loss is reduced from a whole plane to two wires. The circuit diagram is shown in Fig. IV.12.

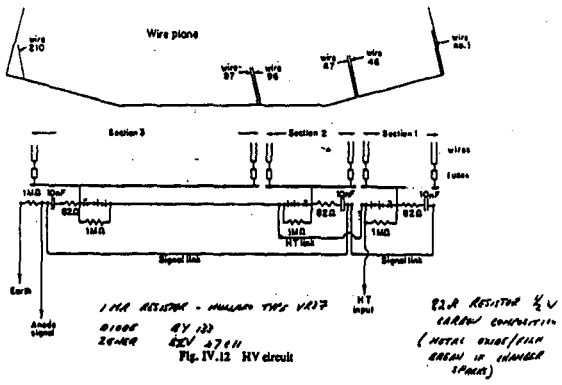

Fig. IV.12 HV circuit

The position of the ends of the wires is controlled by 1 mm wide Noryl wire supports running parallel to and 3 mm inside the end of the Al extrusion. The wire position in the channel is maintained by 3 mm wide Noryl wire supports running orthogonal to the wires. There is a wire support every 350 mm, but the position of the first support varies so as to average out their effects over the area of the petal. Every fifth layer has the same start position for the wire supports.

3.2.3 Lead layers

Each Pb layer is a laminate of 2 or 4 mm Pb, plastic sheets, graphite, and 1.6 mm PCB, with the pad pattern on one side and tracks on the reverse. The Pb is 2 mm ± 50 μm thick for layers 2 to 33 inclusive, and 4 mm ± 50 μm for layers 34 to 45 inclusive. For layer 1, as previously stated, the Pb is replaced by 2 mm Al. The plastics are two 125 μm sheets of Mylar plus four layers of 80 μm thick adhesive. The copper thickness on the PCB is 35 μm, including electroplating, plus 8 μm of tin/lead plating. A cross-section through a Pb layer is shown in Fig. IV.13. A detailed list, including the [illegible] shown in Table IV.12, in subsection 6.3.

HV Cabling
Small, low capacitance cable. (multi conductor?)
Probably strip cable in the detector changing to bundled wires; shielded cables.
Ground at module. Semi-ground at supply
Probably cable HV all the way to the surface because added capacitance ~ module capacitance.
500 ft × 20 pf/ft = 10 nf ~ chamber (module) capacitance.

HV racks allocated provisionally.

HV Power Supply
720 supplies in fairly dense package, ~ 1 kWatts
Similar to Le Croy system (2 bins required)
Trip on overcurrent; rate of rise trip not necessary
Computer controlled rampup & down

HV Monitoring
Voltages, Currents
Occupancy of straws

Scintillating Fiber Tracker Future R&D

D. Koltick May 6, 1992 SSCL

I. Status of VLPC's

- HISTE III
- Review of Project
- Prototype Cassette

II. BNL Beam Test

- Fibers
- Super Layers
- Trigger
- System photo-electron yield

III. Mechanical

- Flat Panels
- Small Cylinders
- Fiber Ribbon production
- Super Layer Production

IV. Status of Scintillating Fibers.

- 3HF Baseline.
- New Improved Types

V. Beam Test/Rad Damage studies.

- T-851 and beyond
- Environmental Effects
- Future Beam tests

VLPC - Visible Light Photon Counter

- A solid-state Photomultiplier
  - gain $\gtrsim 10^4$
  - Q.E. $\gtrsim 70\%$
    (devices have achieved 85%)
  - Rise time < 8 nsec
  - Cryogenic Operation ~7°K

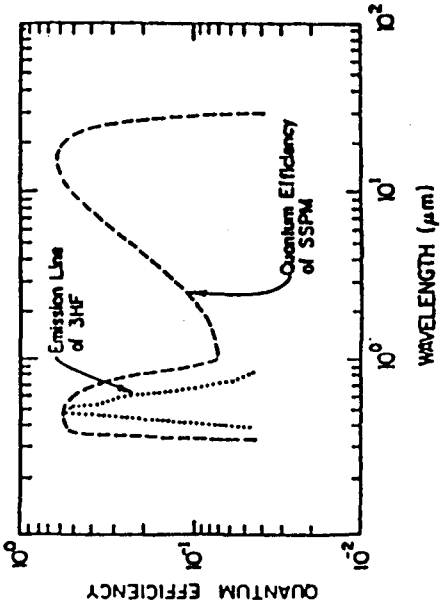

Science Center
Rockwell International Corporation
3370 Miraloma Avenue
P.O. Box 3105
Anaheim, California 92803-3105

Rockwell International

031-BC16

March 24, 1992

Prof. M. Atac
Department of Physics
University of California - Los Angeles
Los Angeles, California 90024

Dear Muzaffer:

The purpose of this letter is to update you on the status of Lot HISTE -III Visible Light Photon Counters (VLPCs).

VLPCs exhibiting very good performance have been obtained from lot HISTE-III. Wafer fabrication of this lot of devices was completed recently on the HISTE (High-Rate Scintillating Fiber Tracking Experiment) contract from UCLA.

The lot included three groups of wafers with different variations of material parameters; all three groups yielded operating VLPCs. Detailed evaluation of the best performing group has been carried out using dies of an 8-element line array from each of the three wafers in that group. Results to date are very positive and are summarized below.

Quantum efficiency in the visible and infrared spectral regions was measured on these devices and concurrently on a Solid State Photomultiplier (SSPM) fabricated earlier in lot NMC for checkout of a HISTE mask set. Table I summarizes the device quantum efficiencies estimated from these data. The estimated accuracy of these measurements is +5% to -15%.

TABLE I
Quantum Efficiency* (%)

Wavelength (μm)	NMC Device	HISTE-III Device
Visible - 0.55	85	80
Infrared -1.0 to 2.0	1	< 0.12
3.2	3	< 0.25
15	38	< 1.3
20	30	< 0.5

* These devices do not have the anti-reflection coating optimized for the visible spectrum.

Prof. M. Atac
March 24, 1992
Page 2

Rockwell International

It is clear that these HISTE-III devices combine high quantum efficiency in the visible spectrum with negligible quantum efficiency in the infrared. It should also be noted that these HISTE-III devices demonstrate a substantial performance improvement over the HISTE-II devices released for beam tests in December 1991 which had a visible spectrum quantum efficiency approaching 40%. The HISTE-III devices are Visible Light Photon Counters that could be made available for beam tests and other evaluations without the restrictions associated with SSPMs.

The dark count rate and biasing current of these HISTE-III devices are higher (factor of 2 to 4) than that of the best NMC devices. These can be reduced, if necessary, by tailoring the material parameters. Gain and gain dispersion have been observed qualitatively to be excellent, equivalent to or better than lot NMC devices. Quantitative data needs to be gathered.

HISTE-III VLPCs operate over a fairly wide temperature range (5 to 8.5K) with bias between 8.0 and 8.6V. Optimum performance is obtained at a temperature between 6.5 and 7K and at a bias of 8.2V, which is very comfortably below the breakdown voltage of 9.0 to 10.0V.

We plan to take data on additional devices. From past experience on impurity band conduction devices, we do not expect the variations from device to device on a wafer to be significant.

The VLPC refinement effort proposed for FY'92 funding will address adjustments between the various device performance characteristics (quantum efficiency, dark count, latchup, etc.) and material/process parameters (doping concentrations, layer thicknesses, AR coating) to provide optimization of the device performance and stability range for SSC requirements.

ROCKWELL INTERNATIONAL CORPORATION
SCIENCE CENTER - ANAHEIM

Paul Besser

F. J. Besser
Manager
Silicon Programs

FJB:bc

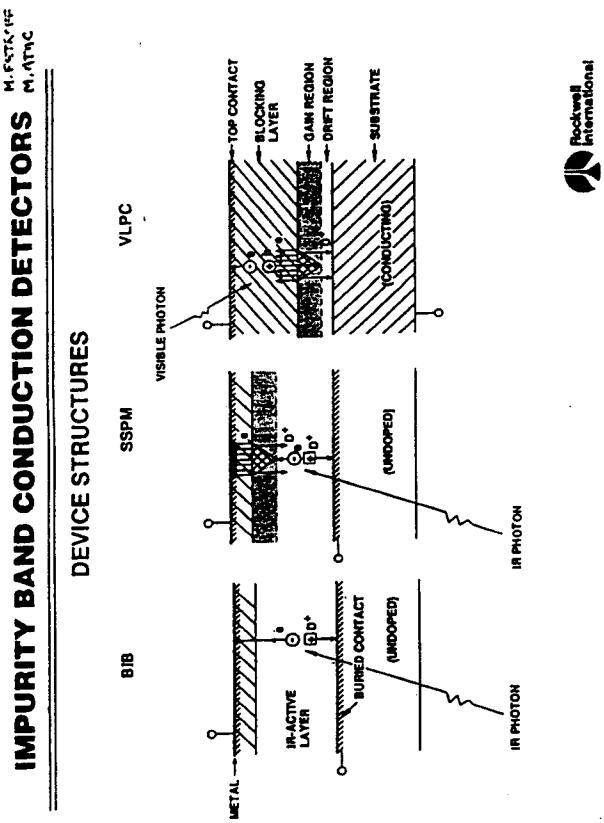

Level 1

The production and operation of 8-channel arrays of VLPCs with accurate dimensions and uniform operating conditions within each element of the array. This step has been accomplished. See Figure 1.

Level 2

The production and operation of working sub-assemblies consisting of 4 arrays (32 channels) with high density packing and uniform operating characteristics for each of the VLPC channels. This step has been accomplished. See Figure 2.

Level 3

The production of integrated sub-assemblies into a high density 128-channel unit which can serve as a sub-module for a fully integrated cassette. A design now exists and is shown in Figure 3.

Level 4

The production and operation of a fully integrated 512-channel cassette containing sensitive high speed pre-amplifiers and low voltage digital line drivers. This cryogenics module will accept the light output from a group of scintillating fibers and output a digital signal to both a fast trigger system and a simple latch for storage to be read by the data acquisition system. A preliminary design of the cassette now exists and is shown in Figure 4.

Level 5

The production and operation of a 16 cassette system (~8,000 channels) as is shown in Figure 5. This is the highest level of integration that is necessary for the SSC. This is the element that will be replicated to form the operating system.

984

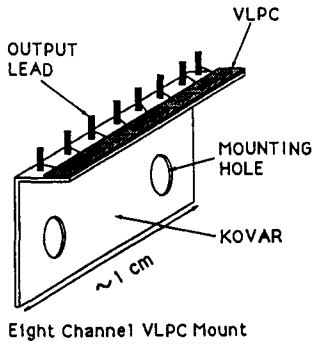

Fig. 1 An 8 channel VLPC array, wire bounded and placed unto a Kovar Mount. New mounts will be made of invar. The new pixels will be 1 mm in diameter, round to eliminate cross coupling. These have been successfully operated.

985

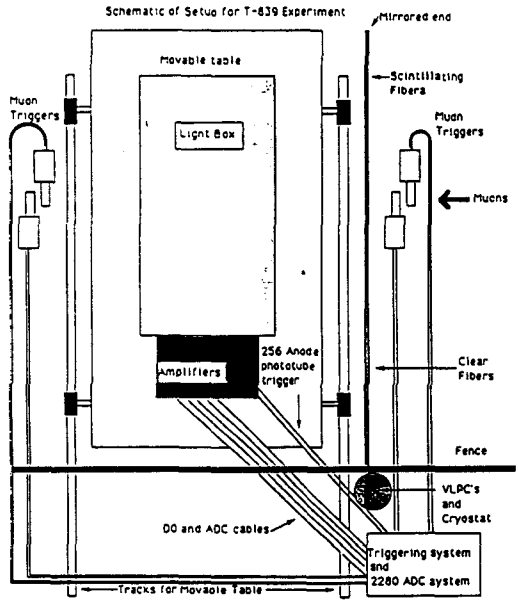

986

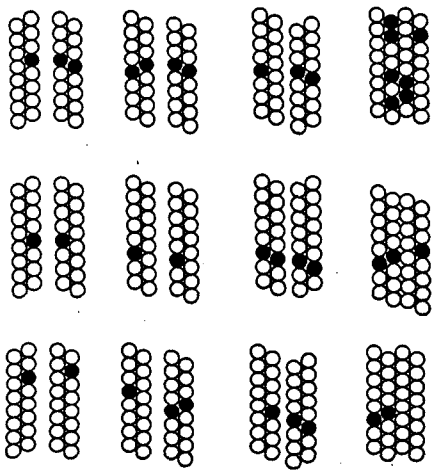

Schematic of T-839 Experiment

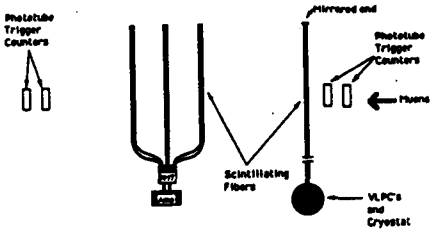

987

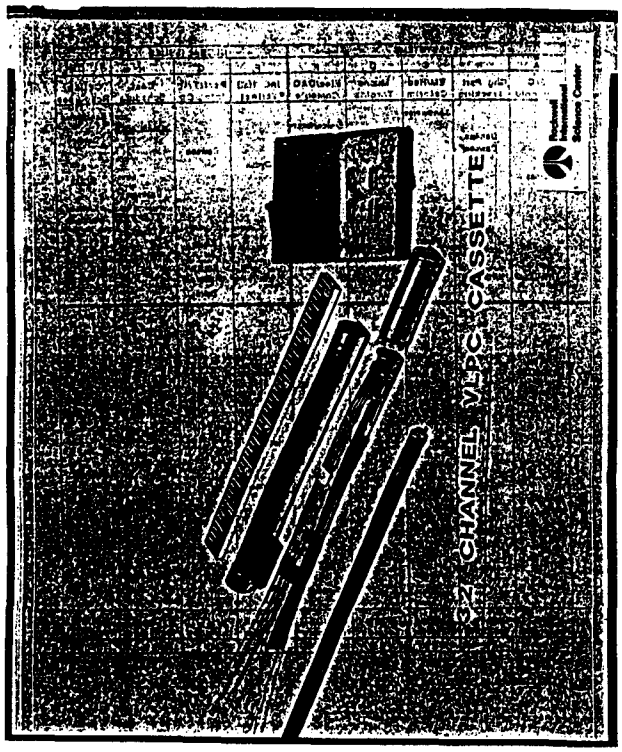

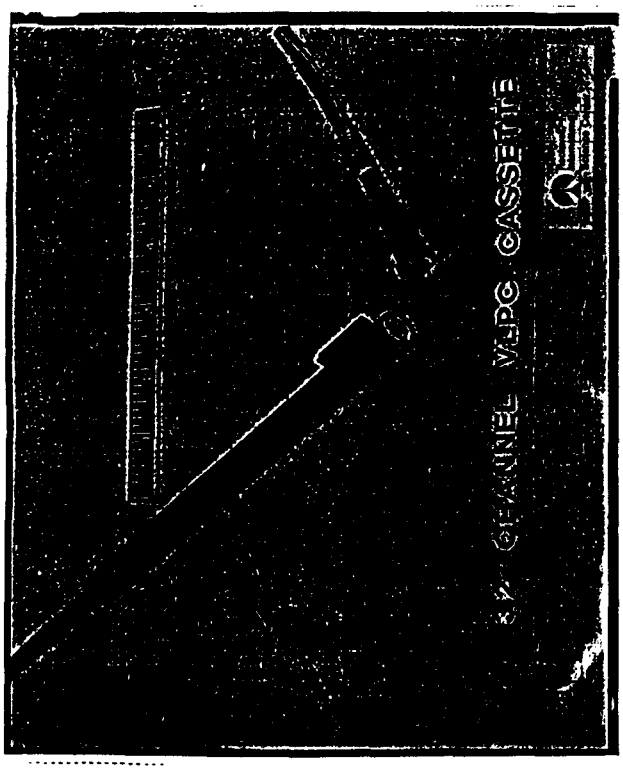

128 CHANNEL VLPC MODULE

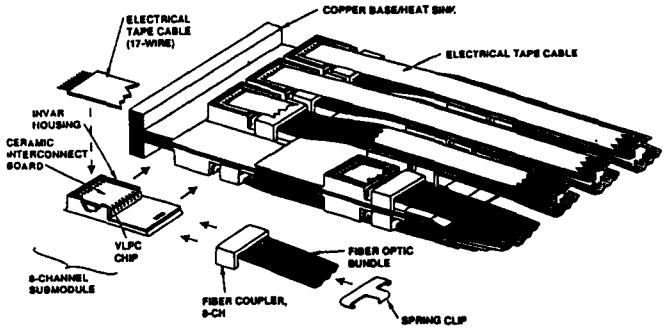

Fig. 3 Present preliminary design of a 128 channel VLPC module. There are many aspects of this design that need detailed analysis and critical review before prototype production can proceed.

512 CHANNEL CASSETTE

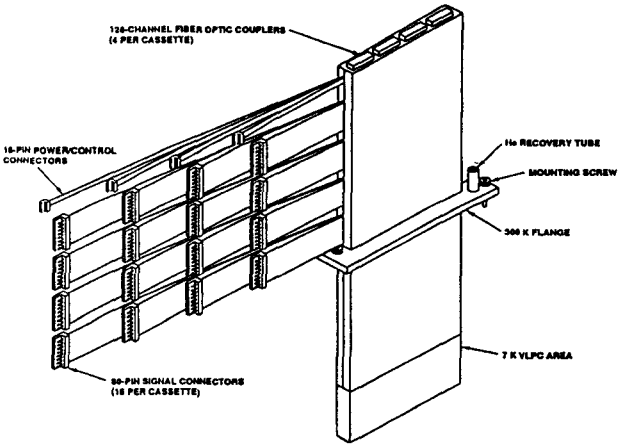

Fig. 4 Conceptual design of a 512 channel VLPC cassette. The funding request is aimed at building two of these cassettes and operating them by the end of 1992 or early 1993.

8192 CHANNEL CRYOSTAT BASELINE DESIGN

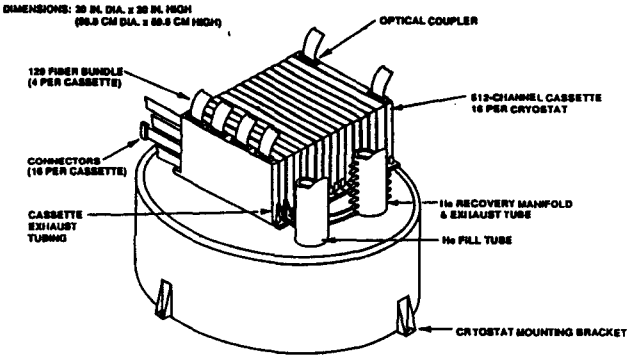

Fig. 5 Conceptual design of a 16 cassette cryostat. The funding request proposes only to build a cryostat capable of holding two cassettes. This will be adequate for verifying the design.

VLPC - Cryogenics

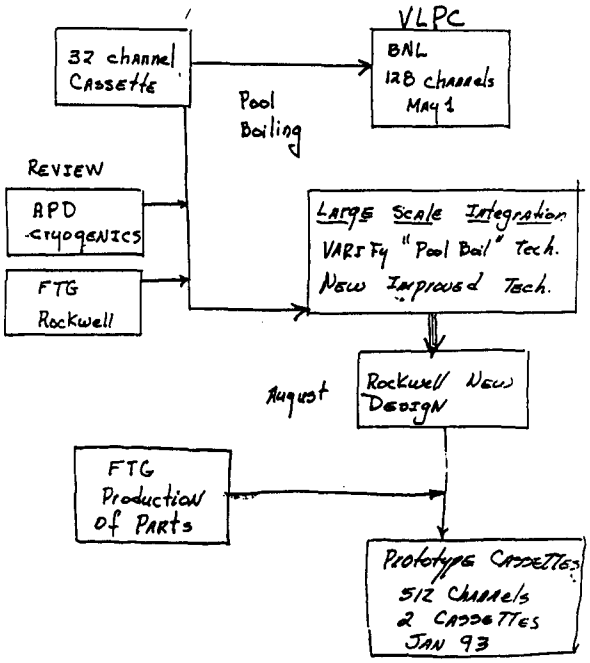

VLPC- Development

- HISTE - III excellent.
- November 1 HIST-III'
  - Anti- Reflective Coating Si_3N_4.
  - New Mask Set 1mm

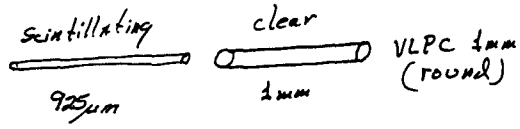

- Characterize one lot of Hist IV Range of Materials

Novem 1 1992 (Start)

Finish VLPC design optimization of SSC.

- Contact Resistance
- Latch-up suppression
- Fully optimized Q.E.

July 1993 - (Start)
Production of 10,000 channel lot of VLPC's.

Beam Test at BNL

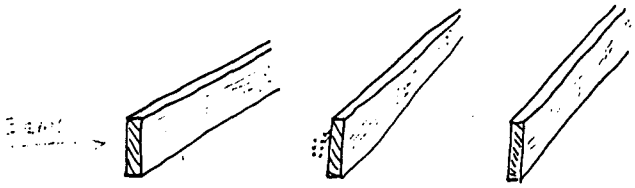

- Ribbons - Alternately placed on Eight 4.3 m x 1.6 cm Bundles.
- Readout with Histe III VLPC.
- Custom made Cryostat (design by Rockwell)
  - 128 VLPC channels (Max)
  - 3 double sided Super Layers
  - 830 μm SMF Ribbons (Accepted) (Beam Center has been placed)
  - 3 x 16 Doubled Ribbons

Goals of The BNL Beam Test.

Start May 1992

- Operation of 128 channel system.
- Producing accurate Ribbons
  - Bicron
  - Kuraray
  - ETC.
- Light yield from 4.3 meter fiber with 50 cm length wave guides.
- Measure resolution
  - checks fiber placement
- Stability of system for 1 month run.
- Self-Trigger (3 superlayer trigger)

Scintillating Fiber Front End Electronics

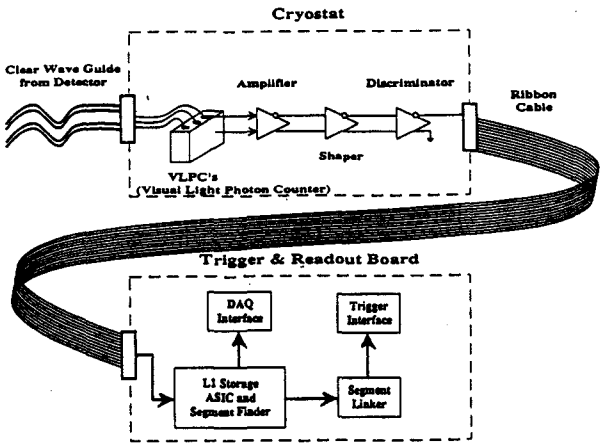

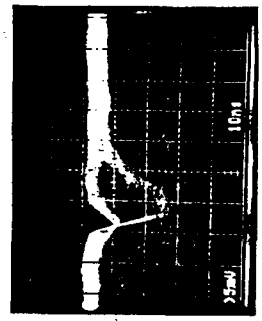

Single photoelectron pulses in VLPC.
The noise band is also clearly visible.

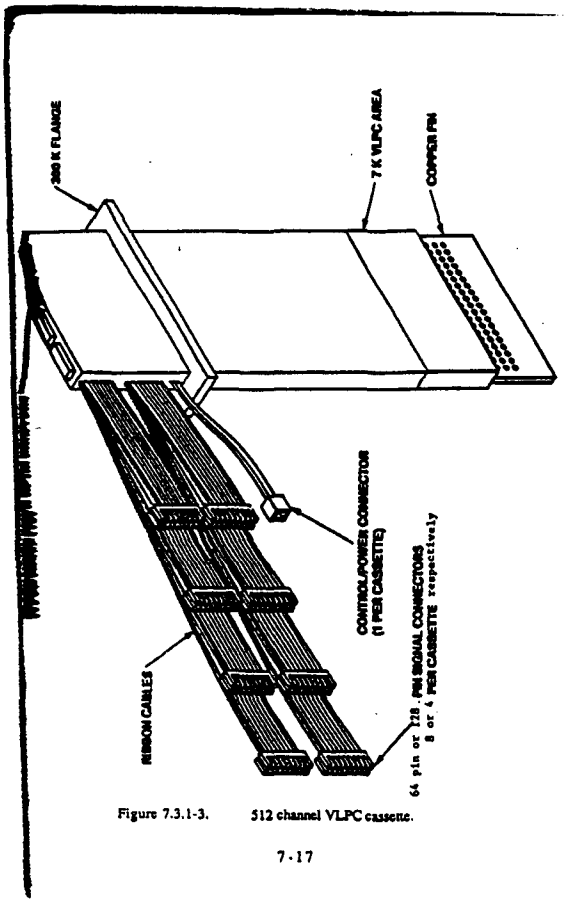

Figure 7.3.1-3. 512 channel VLPC cassette.

1000

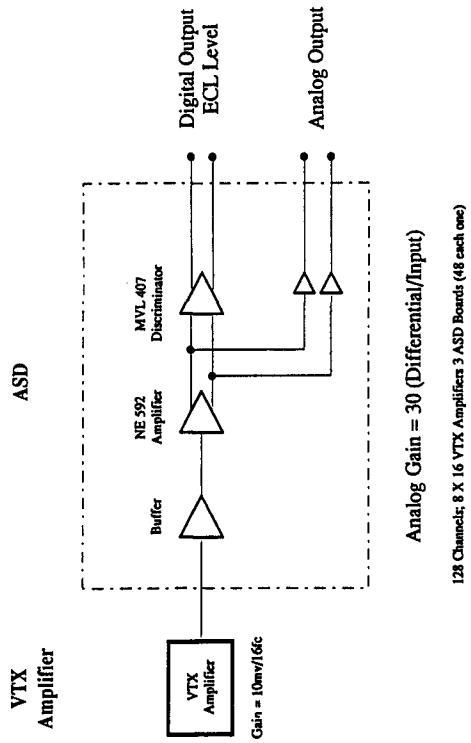

1001

PRE-PRODUCTION PROTOTYPE ELECTRONICS

GOALS
- ROOM TEMPERATURE OPERATION
- HIGH DENSITY
  - 512 PIXEL CASSETT
  - (16 CASSETTS IN ONE HELIUM THERMOS BOTTLE)
- PRE-PRODUCTION ASD ASIC's

PLAN
- SPICE to establish parameters
- PACKAGING & LAYOUT
  - cooling and high density interconnects
- FABRICATE 1024 channels

MEANS
- JOINT PROJECT
- SDC ELECTRONICS GROUP, FTG, ROCKWELL

SCHEDULE
- December '92 first cooldown

1002

Cryostat ASD Performance Characteristics:

Single Photon Counting Efficiency > 60%

Background counting rate < 5kHz

Cross talk < 2% for from 1 to 30 photons input

Time skewing < 5 ns for from 1 to 30 photons input

Output :

- Single ended 53 Ohms to ground
- Pulse width 14ns
- Bit rate 62.5 Mbs

Note:
Work is in progress on the final ASD which will reside inside the VLPC cryostat, but at the room temperature end, and on the definitions of the logic levels to be transmitted. The final decisions must wait for the determination of where the readout crates reside in relation to the cryostats as this determines the cable length and driver characteristics.

1003

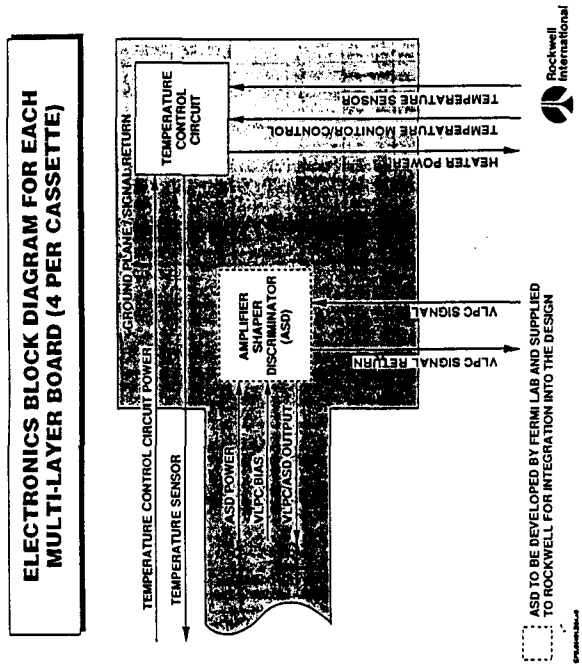

TYPICAL PRINTED CIRCUIT BOARD LAYOUT (PCB 2)

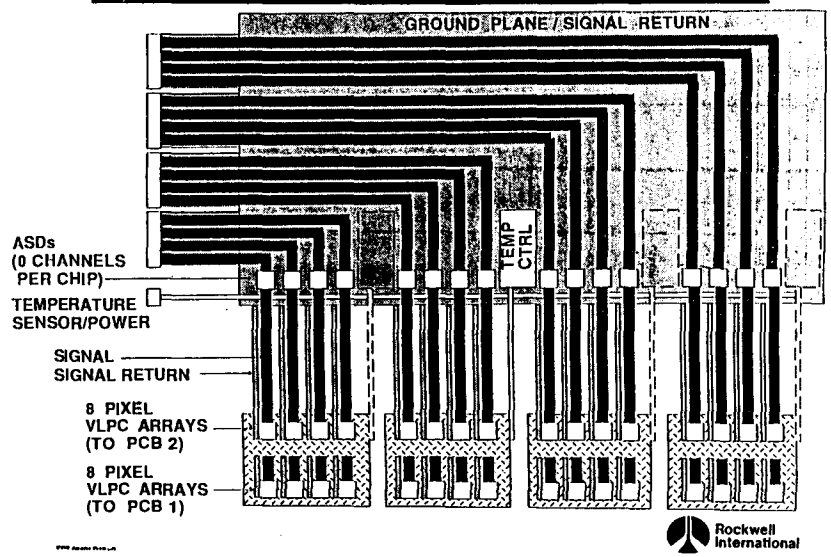

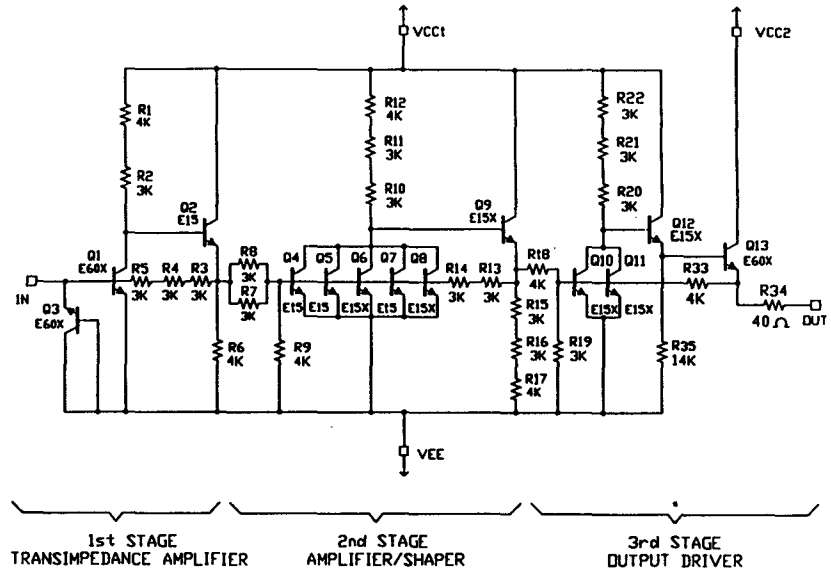

1001

1005

[4] Tracking/Integration Joint

Tracking Utilities Update	J. Piles	- 1007
Mechanical Considerations for a SDC Outer Straw Tracker for the SSCL	R. Swnsrud	- 1012

1007

Tracking Utilities Update

Jonathan A. Piles
(SSCL)

1008

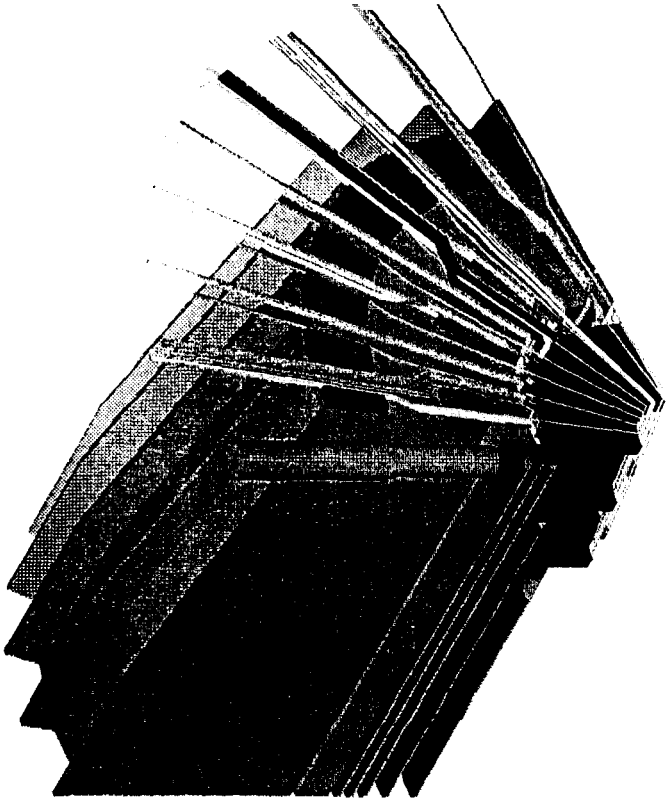

1009

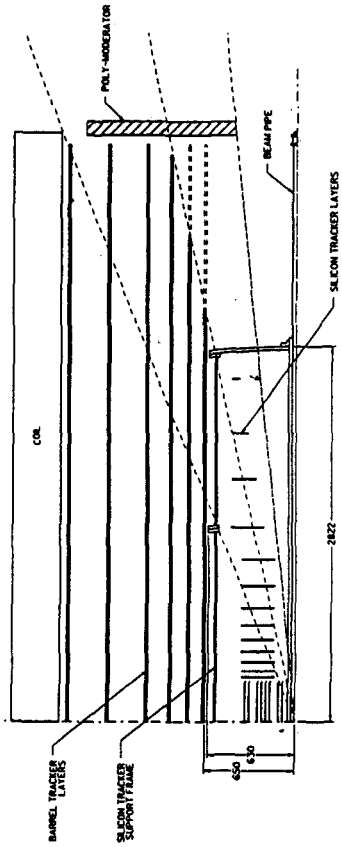

FIBER TRACKER LAYOUT

SD000364

20-MAY-1992

1010

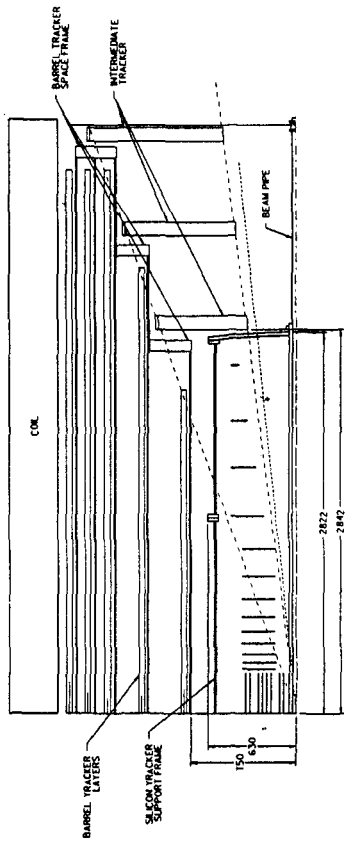

STRAW TRACKER LAYOUT

SD000363

20-MAY-1992

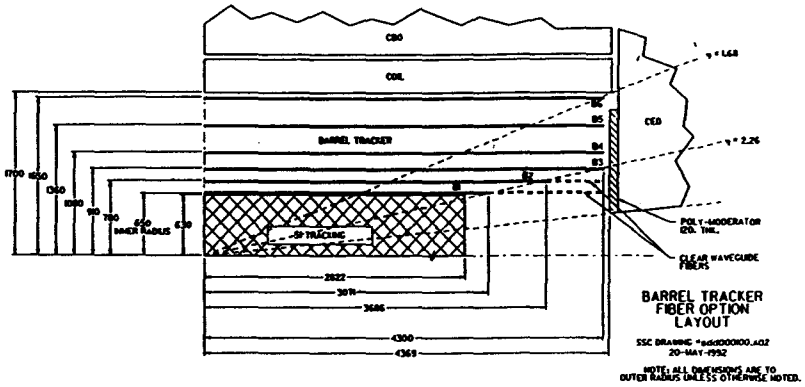
CBO
COIL
BARREL TRACKER
CED
η = 1.68
η = 2.26
B6
B5
B4
B3
B2
B1
1700
1550
1350
1150
950
750
650
INNER RADIUS
630
SP TRACKING
POLY-MODERATOR
CED. THK.
CLEAR WAVEGUIDE
FIBERS
2622
3078
3686
4300
4369
BARREL TRACKER
FIBER OPTION
LAYOUT
SSC DRAWING
20-MAY-1992
NOTE: ALL DIMENSIONS ARE TO
OUTER RADIUS UNLESS OTHERWISE NOTED.

SDC OUTER TRACKER CYLINDER SPACEFRAME ENGINEERING GROUP

3. MECHANICAL ENGINEERING

3.3 Straw Tube System

3.3.1 Detail Definition of Module Geometry

- o **Module Superlayer Geometry Defined for All Trigger & C2 Stereo Layer**
- o **Stereo Superlayer C4 Is Near Completion**

Viewgraph 11
RLS
<05-25-92>

Westinghouse Science & Technology Center

1

1011

TRIGGER MODULE , AIR SUPERLAYER 1
AS PER CENT23C DATED 4-14-92

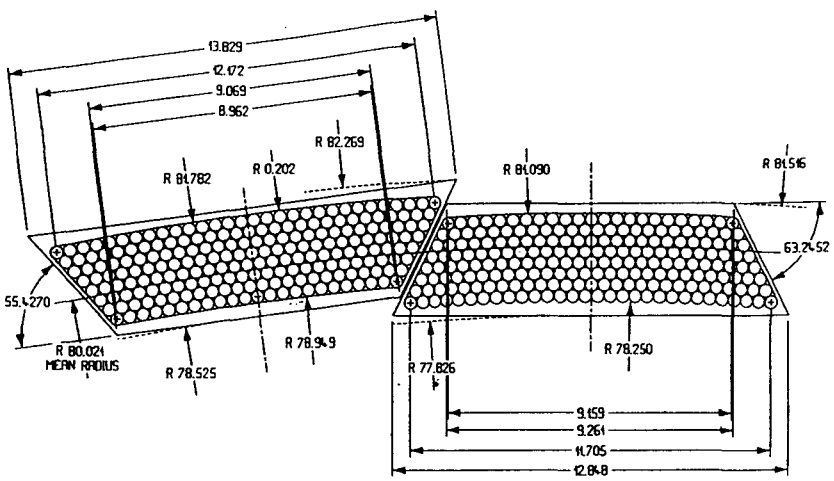

4-92SK1
DIMENSIONS CM
4-14-92 DM

2

1015

MECHANICAL CONSIDERATIONS FOR A SDC OUTER STRAW TRACKER FOR THE SSCL

SDC COLLABORATION MEETING
AT KEK JAPAN
MAY 25 1992

WESTINGHOUSE ELECTRIC CORPORATION
(W)STC
PITTSBURGH, PA

R. L. SWENSRUD (ROGER)

Viewgraph 1
RLS
<05-25-92>

Westinghouse Science & Technology Center

1012

SDC OUTER TRACKER CYLINDER SPACEFRAME ENGINEERING GROUP

TABLE OF CONTENTS

1. Introduction
2. Overview of Outer Tracker
3. Mechanical Engineering
   - 3.1 Common Straw and Sifi Tracker Support Requirements
   - 3.2 Testing & Prototype Program
     - 3.2.1 Goals and Issues
     - 3.2.2 Requirements and Resolution
   - 3.3 Straw Tube System
     - 3.3.1 Detail Definition of Geometry
       - o Modules
       - o Support Structure
     - 3.3.2 Analysis
   - 3.4 Scintillating Fiber System
     - 3.4.1 Detail Definition of Geometry
     - 3.4.2 Analysis

Viewgraph 2
RLS
<05-25-92>

Westinghouse Science & Technology Center

1013

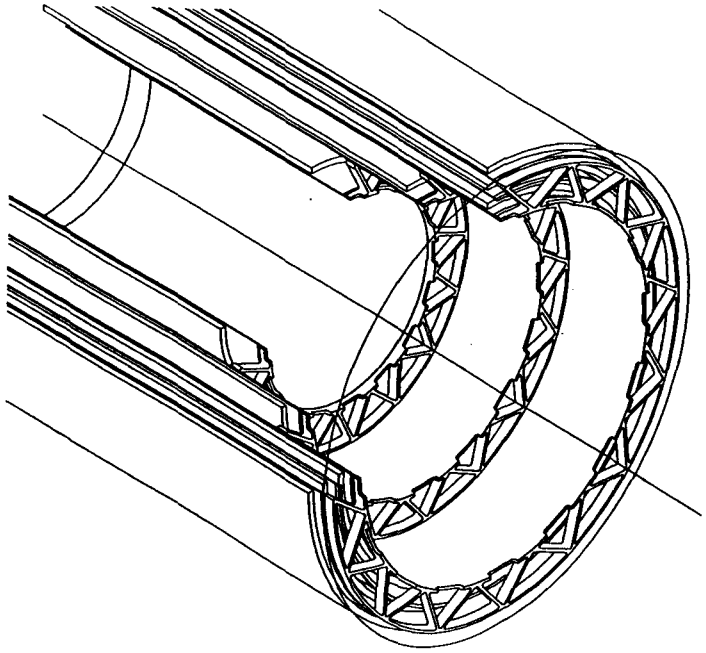

13

1018

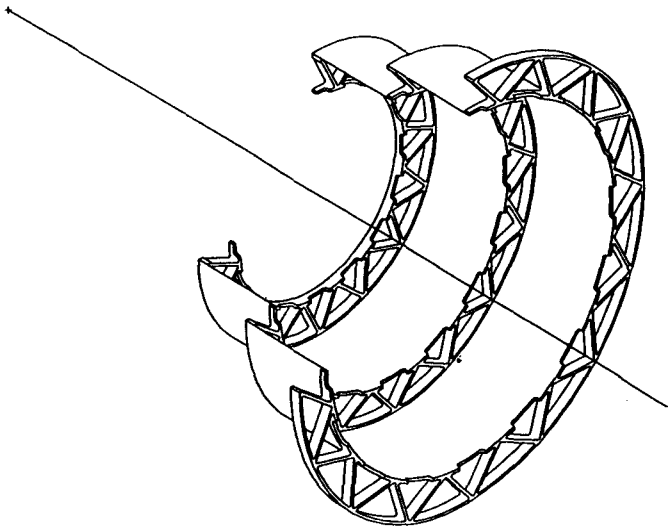

14

1019

STEREO MODULES SUPERLAYER 2

AS PER CENT238 DATED 4-1-92

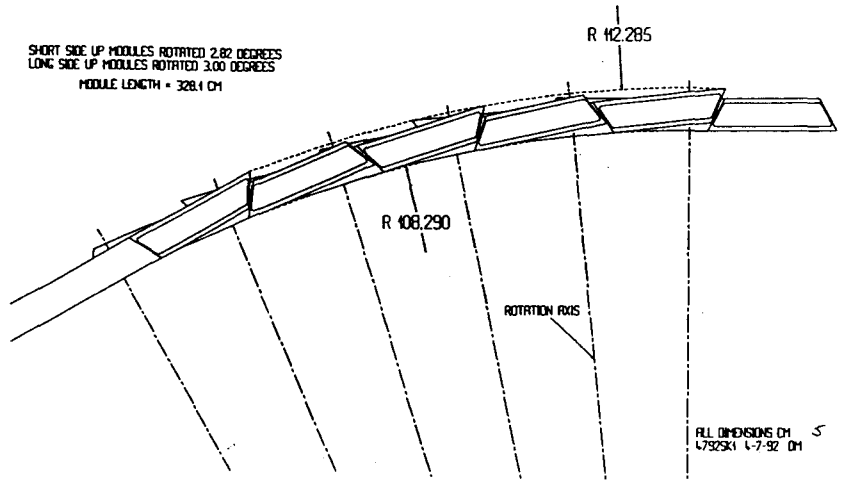

5

1016

SDC OUTER TRACKER CYLINDER SPACEFRAME ENGINEERING GROUP

3. MECHANICAL ENGINEERING

3.3 Straw Tube System

3.3.1 Detailed Definition of Geometry Continued

Support Structure

- **Support Structure Geometry is Being Developed**
- **Outer & Intermediate Appear Compatible ~~Except for Cables~~**

Westinghouse
Science & Technology Center

3

1017

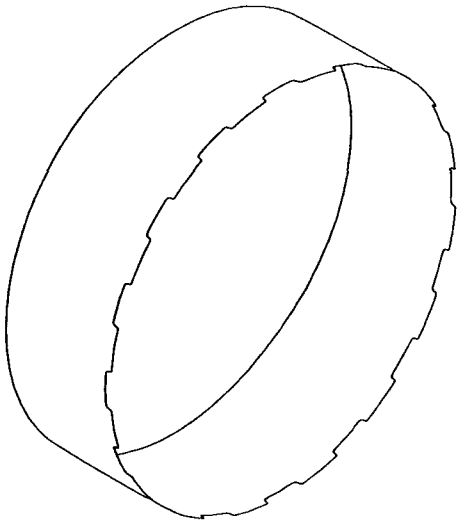

15

SPACE FRAME 1

MAX RADIUS = 104.612
MIN RADIUS = 75.462
16 SECTIONS - 32 WINDOWS
CUTOUTS 4 X 16 16 PLCS
TUBE SECTION 2 X 8

ALL DIMENSIONS IN CM

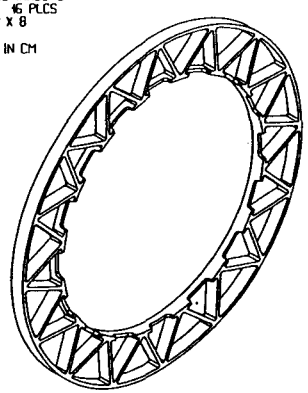

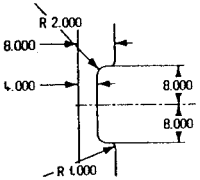

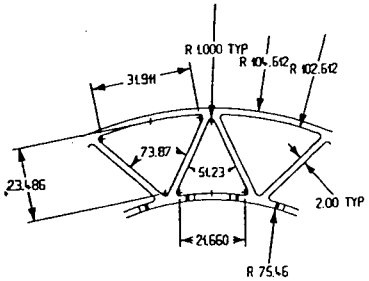

15

4 30 92 SK1
4-30-92 DM

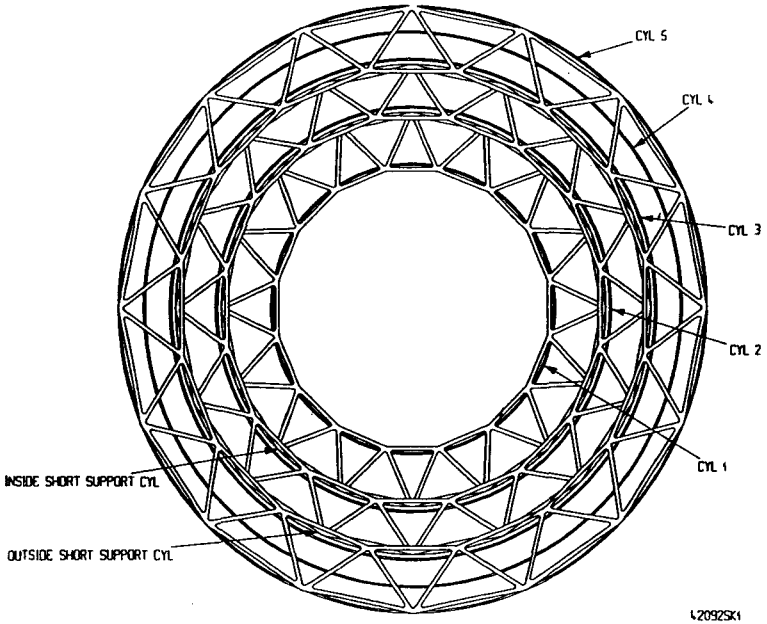

17

4 20 92 SK1

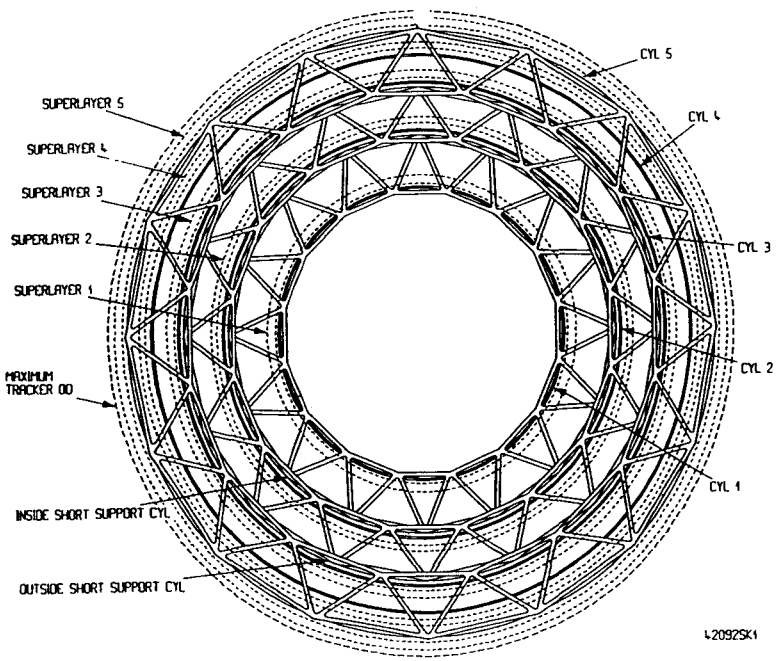

18

4 20 92 SK1

SDC OUTER TRACKER CYLINDER SPACEFRAME ENGINEERING GROUP

3. MECHANICAL ENGINEERING

3.3 Straw Tube System

3.3.2 Analysis of the System

ANALYSIS OVERVIEW:

- o The Finite Element Model
- o Material Variation Sensitivity
- o Analysis Results

Viewgraph 13
RLS
<05-25-92>

Westinghouse
Science & Technology Center

1

MODULE LOCATION POINTS

IF A PATTERN OF POINTS IS DISPLACED OFF CENTER ON A MODULE WHEN A LIKE MODULE IS ROTATED ABOUT Z = 0, ALL POINTS OR MEASUREMENT BALLS ARE VISIBLE FOR MEASUREMENT.

19

52292SX2
6-23-92 DM

COMPOSITE TABLES

STRUCTURAL COMPOSITE PROPERTIES, [0 +/-60]SYM

MATERIAL: (P75/ERL 1939-3) ASSUMPTION: LOW STRAIN APPLICATION

Wrap Angles:	[0 +/-60]	
Moisture	0%	0.2%
Column No.	9	10
EX, MSI	14.700	14.600
EY, MSI	14.700	14.600
EZ, MSI	0.982	0.957
GXY, MSI	5.570	5.530
GYZ, MSI	0.498	0.498
GXZ, MSI	0.499	0.499
MUXY	0.318	0.318
MUYX	0.318	0.318
MUYZ	0.232	0.231
MUZY	0.016	0.015
MUXZ	0.232	0.231
MUZX	0.016	0.015
ALPHA-X*	-0.155	-0.164
ALPHA-Y	-0.155	-0.164
ALPHA-Z	20.500	20.600

* CTE, microstrain/°F

Viewgraph 4
DAH
05.21.92

Westinghouse
Science & Technology Center

13

TRACKER SECTION

AS PER CENT23E DATED 5-19-92

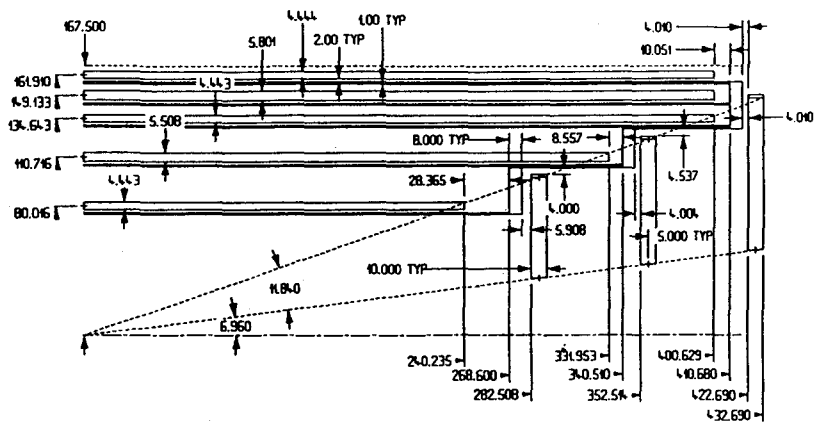

STRAW DIAMETER 0.404.37
ALL DIMENSIONS IN CM
52292SX1

20

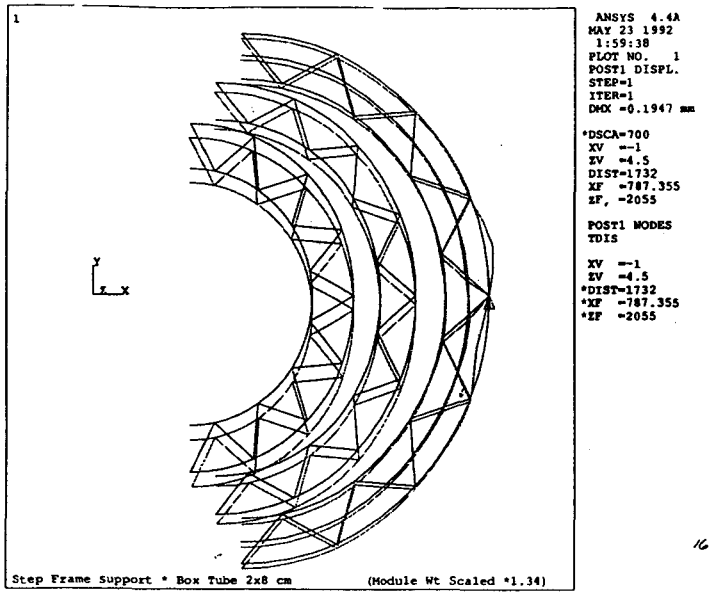

16

SDC OUTER TRACKER CYLINDER SPACEFRAME ENGINEERING GROUP

3. MECHANICAL ENGINEERING

Finite Element Model Properties

Step Frame Support * Box Tube 2x8 cm (Module Wt Scaled *1.34)
12.2170 MAY 22, 1992 CP= 2773.330

***** CENTROID, MASS, AND MASS MOMENTS OF INERTIA *****

CALCULATIONS ASSUME ELEMENT MASS AT ELEMENT CENTROID

CENTROID	MOM. OF INERTIA ABOUT ORIGIN	MOM. OF INERTIA ABOUT CENTROID
XC = 806.04	IXX = 0.3864E+10	IXX = 0.1201E+10
YC = 0.25891E-03	IYY = 0.3864E+10	IYY = 0.8902E+09
ZC = 2357.6	IZZ = 0.8037E+09	IZZ = 0.4925E+09
	IXY = -0.3585E-00	IXY = 99.96
	IYZ = -509.8	IYZ = -217.4
	IZX = -0.9186E+09	IZX = -0.8463E+07

*** MASS SUMMARY BY ELEMENT TYPE ***

TYPE	MASS (Kg)	
1	29.2720	struts (2x8)
2	6.31315	angle rings
3	212.536	shim rings w/ module wt.
5	17.4530	cable wt.
8	80.6313	endcaps etc.
9	79.6313	support cylinders
10	13.1245	endframe cylinders
12	40.0000	silicon
TOTAL	470.96	Quarter-model

Viewgraph 19
RLS
<05-25-92>

Westinghouse
Science & Technology Center

14

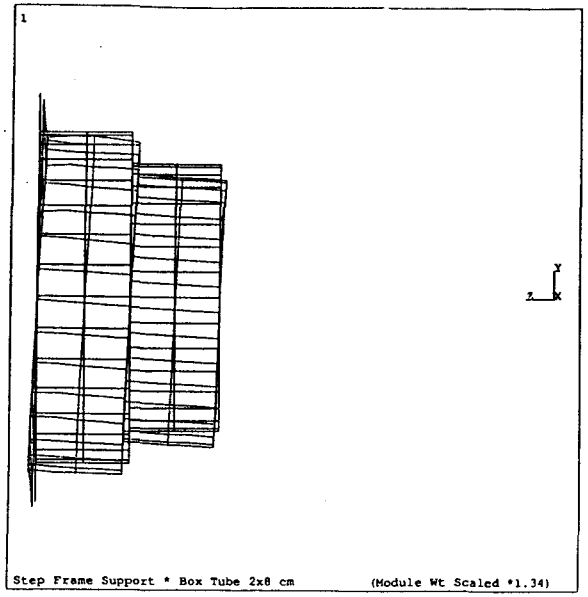

17

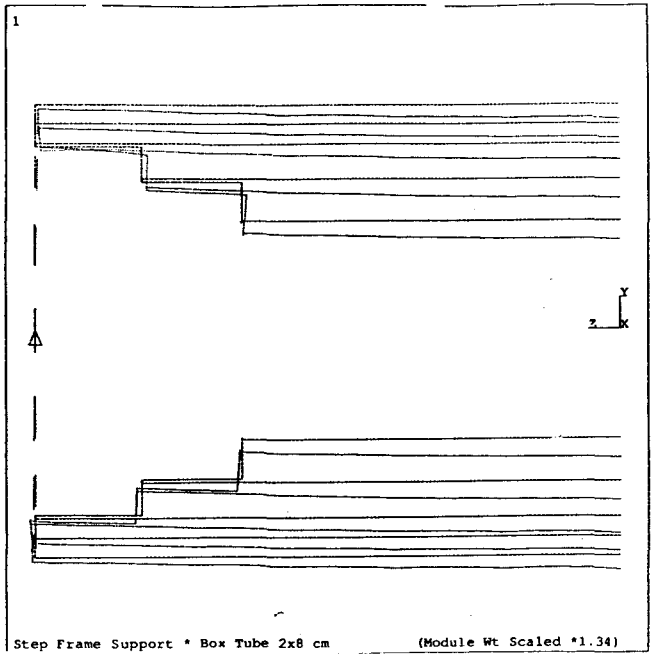

15

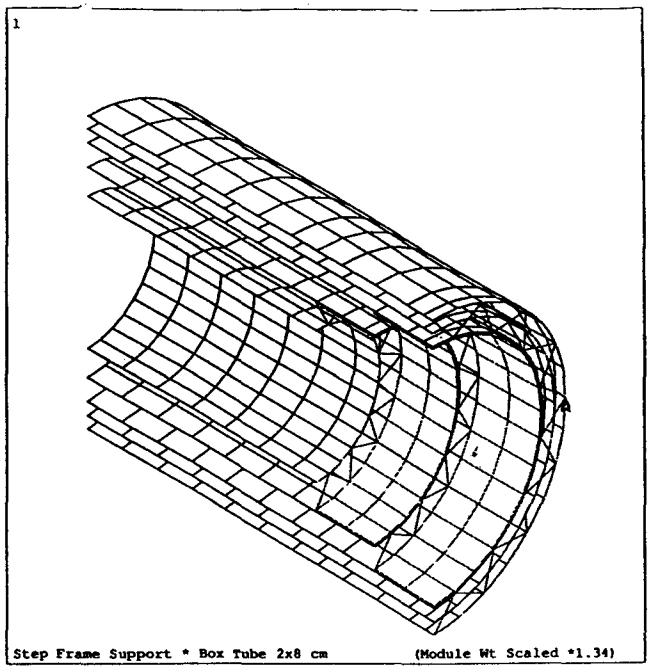

ANSYS 4.4A
MAY 23 1992
4:12:29
PLOT NO. 1
PREP7 ELEMENTS
TYPE NUM

XV =-1
YV =1
ZV =1
DIST=2691
XF =787.355
ZF =2055
PRECISE HIDDEN

PREP7 NODES
TDIS

XV =-1
YV =1
ZV =1
*DIST=2691
*XF =787.355
*ZF =2055
PRECISE HIDDEN

[5] Calorimeter

<Overview>

SDC Calorimetry - Status and Near Future	D. Green	- 1035
TDR Mechanical Design	L. Bartoszek	- 1063

<Prototype>

Report from Prototype Task Force	G. Foster	- 1073
Update on Baseline Barrel EM - Mechanical and Optical	D. Underwood	- 1080
Barrel EM Calorimeter Options	G. Foster	- 1113
Pb Stack Options	L. Bartoszek	- 1136
Fabrication of Tiles and Fibers	K. Hara	- 1153
Aging Test of Bent Fibers	Y. Miyamoto	- 1184
Optics Design of Prototype EM Tile/Fiber	M. Okabe	- 1194
The Tile-Fiber System for SDC Calorimetry	V. Hagopian	- 1208
Development of Cockcroft-Walton PMT Base	K. Hara	- 1239
Quality Control for Prototype Tile/Fiber Production	I. Nakano	- 1252

<Radiation Damage>

Report of RADDAM 1992 Conference	V. Hagopian	- 1266
Radiation Damage of Tiles, Fibers, and Tile/Fiber Assemblies	K. Yasuoka	- 1315
Study of Dose-rate Effects on the Radiation Damage of SCSN23, ...	N. Giokaris	- 1345
SDC Calorimeter Rad-Hard Scinitillator	G. Foster	- 1362

<PMT Development>

Development of MA PMTs and Green Extended PMTs	S. Suzuki / Y. Yoshizawa	- 1385

<Readout>

Digital Photomultiplier Tube Readout	G. Foster	- 1402

< CDF Plug Upgrade >

Present Status of the CDF Plug Upgrade EM Calorimeter	S. Kim	- 1423

<Calibration>

Calorimeter Calibration – Beam Activity — A. White — [illegible]

<Shower Measurement Detector>

Shower Measurement Detector — [illegible] — [illegible]

Shower Max Detector Research — [illegible] — [illegible]

<Forward Calorimeter>

Study of [illegible]

Liquid [illegible] Research — [illegible] — [illegible]

Remote Control [illegible]

High Pressure Gas Calorimetry — [illegible] — [illegible]

L* and GEM Calorimeter [illegible]

Studies and Applications [illegible] — [illegible] — [illegible]

<Simulation>

Present Status of GEANT [illegible] — [illegible] — [illegible]

SDC Calorimetry - Status and Near Future

Daniel P. Green
(Fermilab)

DRG
5/92

SDC CALORIMETRY -

STATUS AND NEAR FUTURE

CDR-CAL	9/91
TEST BEAM	FNAL 91, ... 3/92 (EM, SM, HAD, HF)
Pb/Fe	8/92
TDR	4/92
PAC	5/92
⋮	⋮
Pb/Pb	6/92
PAC	7/92
DoE	9/92

• PROTOTYPE ... 6/93

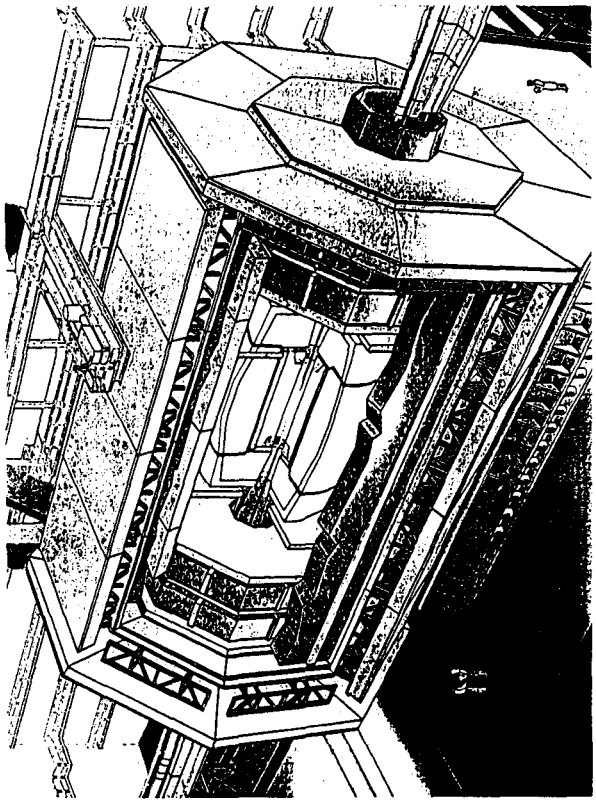

CERN COURIER

PAC - 5/92

SDC CALORIMETER SYSTEM REQUIREMENTS

1. Measure the energy, interaction time and direction of quarks (jets), electrons, neutrinos and photons. Provide triggers based on these properties.

2. Provide identification capabilities for electrons (EM/HAD compartments) and photons. Tag muons as noninteracting particles deep in the system. Provide hermetic coverage to allow for neutrino identification. Provide for tau identification with sufficient EM and HAD granularity.

3. Granularity must be sufficient to avoid pileup errors. Depth in EM must be sufficient to preserve precision of the energy measurement. Depth of HAD must be sufficient to contain 10 TeV dijet masses. Transverse scales are set by EM and hadronic shower sizes.

4. Angular coverage must be sufficient to avoid spurious missing Et generation. Precise electron energy measurement must extend over a sufficient angular range to be efficient for 2 gauge boson final states decaying into leptons. ($|\eta| < 6$, $|\eta| < 3$)

CENTRAL CALORIMETER GEOMETRY

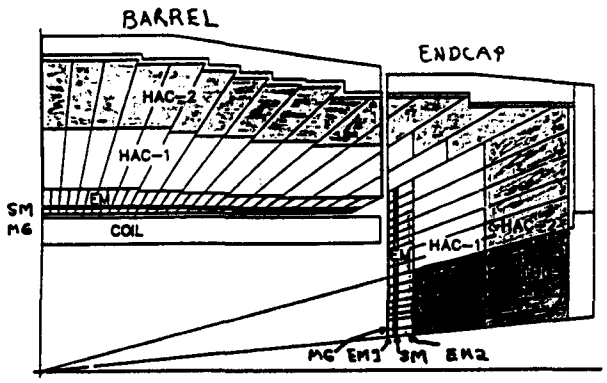

Longitudinal quarter section of the central calorimeter.

SOLENOID MATERIAL

SDC HAS A SMALL MARGIN OF SAFETY - EVENT AT $\theta = 30°$ IF 2mm IS NOT USED

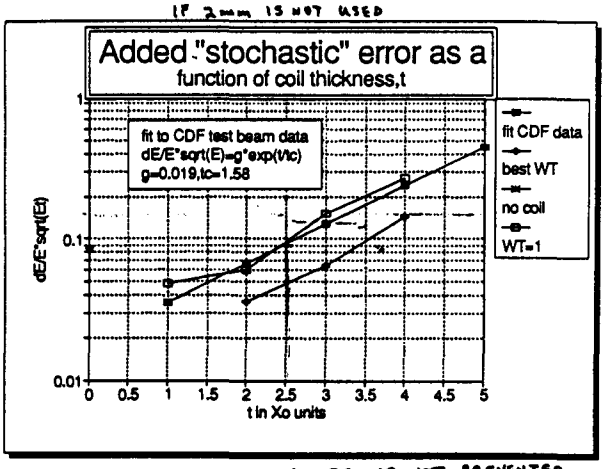

CONVERSELY - SDC IS NOT PREVENTED FROM DOING EM CALORIMETRY WITH $\sim 1\%$ STOCHASTIC COEFFICIENT BY THE SOLENOID

CONTRIBUTIONS TO THE EM RESOLUTION

- "CONSTANT" TERM -

EM calorimeter constant term budget.

Source of constant term	Contribution
Calibration tower to tower	0.2%
• Leakage	0.3%
• Transverse uniformity	0.5%
Tile-to-tile variations incl. thickness variations and longitudinal masking	0.5%
Absorber thickness variations	0.2%
• Radiation damage	0.5%
Total (added in quadrature)	< 1.0%

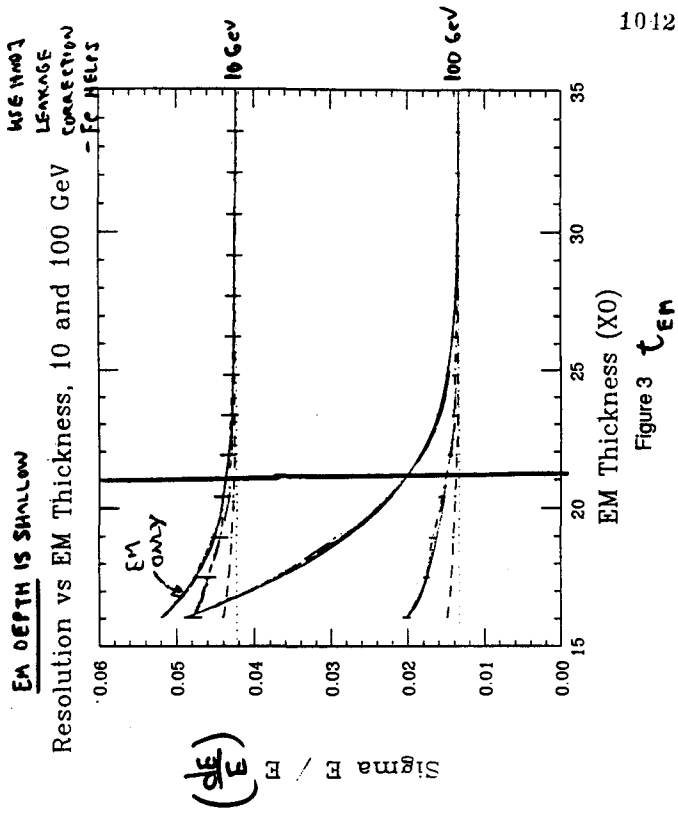

Figure 3 t_{EM}

1013

JJ LOSSES VS

$J \to Q\bar{Q} \to q\ell\nu$

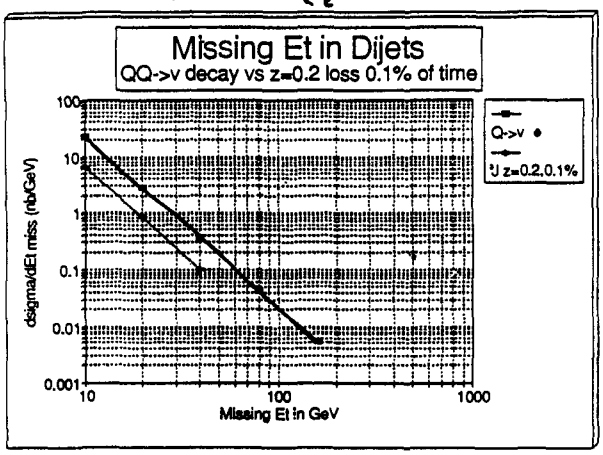

⇒ MUST REQUIRE THAT $\vec{E}_T$ NOT IN J DIRECTION IF 0.1% HERMITICITY IS NOT ACHIEVED

1014

HERMITICITY

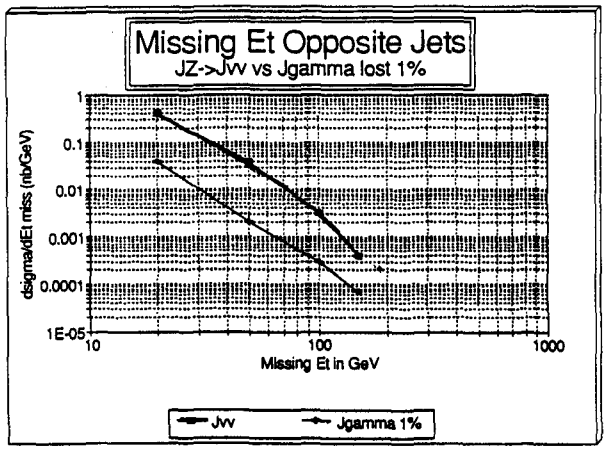

⇒ WITH 1% HERMITICITY REAL PHYSICS $\not{E}_T$ DOMINATES LEAKAGE AND/OR LOSSES

1015

FCAL: COVERAGE

What η coverage is required by E_T^{miss}?

$m(\tilde{g}) = 300$ GeV 3 jets with $E_T > 70$ GeV

$\phi(\text{jet}) - \phi(E_T^{miss}) > 40^\circ$ } NO JET LEAKAGE

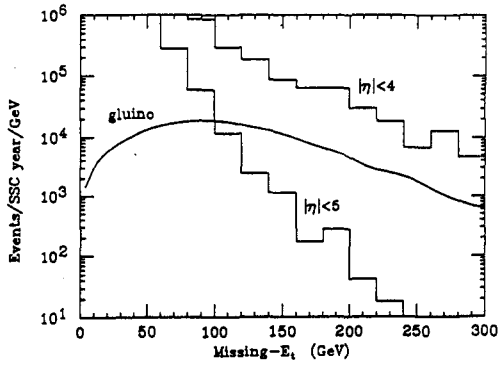

Fiducial region must reach $|\eta| = 5$.

$|\eta| < 6$

FOR FCAL COVERAGE

($|\eta| < 5$ FIDUCIAL)

1016

TILE/FIBER TRANSVERSE UNIFORMITY

"σ" TILE

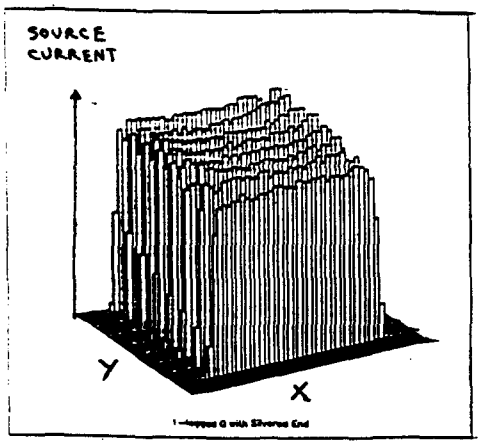

Figure 6.11 Transverse response map for a "Sigma" tile.

1017

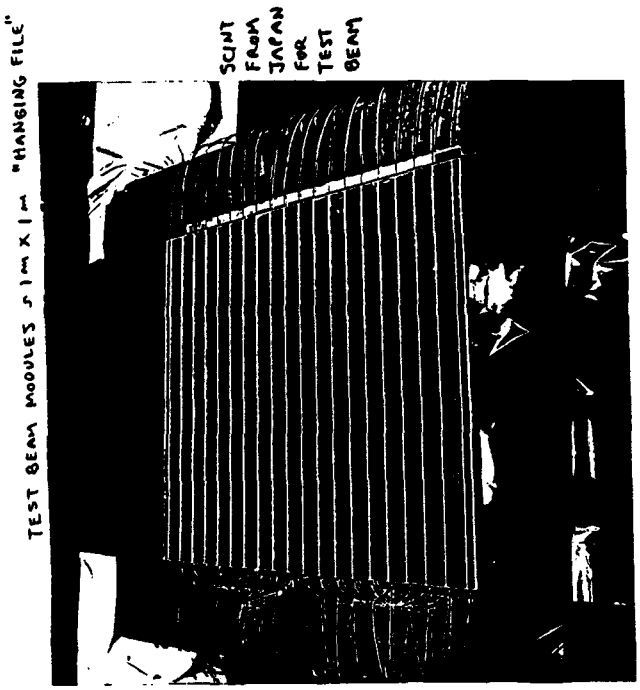

1018

SDC TEST BEAM CALORIMETRY

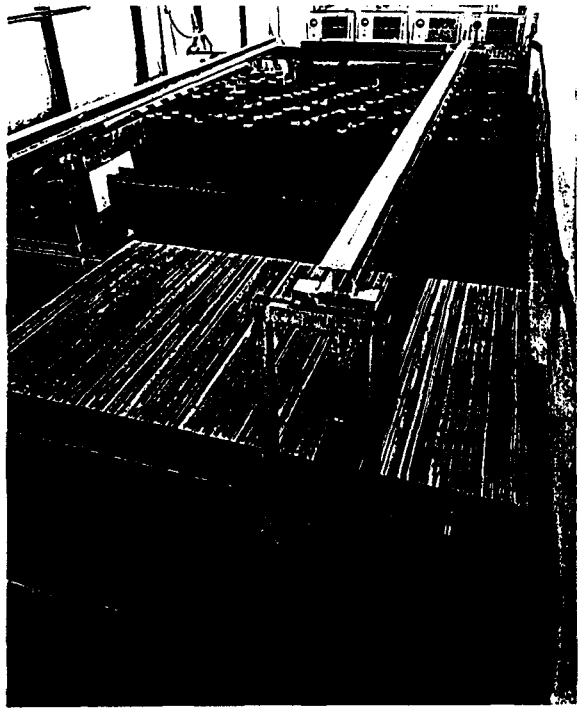

1019

"HANGING FILE" SDC
TEST BEAM DATA
Fe / Pb

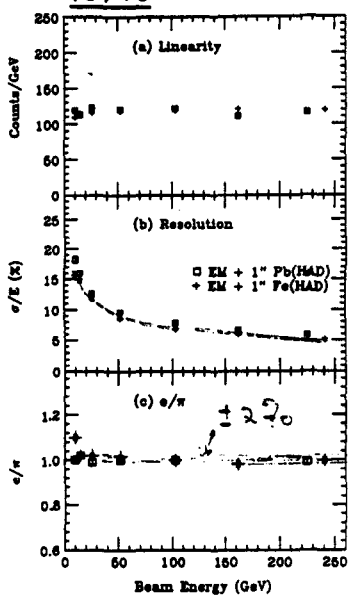

RELATIVE EM AND HAD CALIBRATION SET - NOT A HOMOGENEOUS MEDIUM

$\frac{dE}{E}$

$\frac{e}{\pi}$

E

1050

SAMPLING OPTIMIZATION - TDR

1/8" Pb EM
1" Fe HAC1
10 λ TOTAL DEPTH

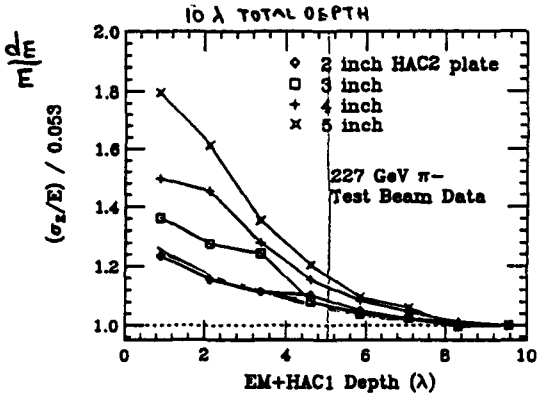

$\frac{dE}{E}$

TOTAL = 10 λ
2", 3", 4", 5" HAC2 SAMPLING

EM TEST MODULE - Pb CASTING 2x (5x2)

dE/E, ⊥ SCAN, SM

EM- HERMITICITY

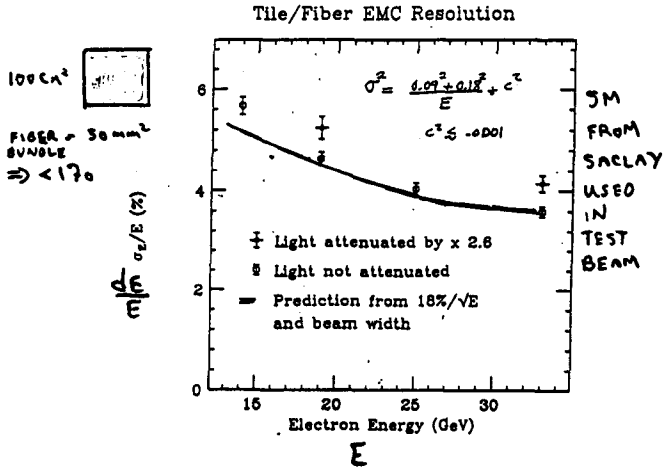

EM CONSTRUCTION IS HERMETIC

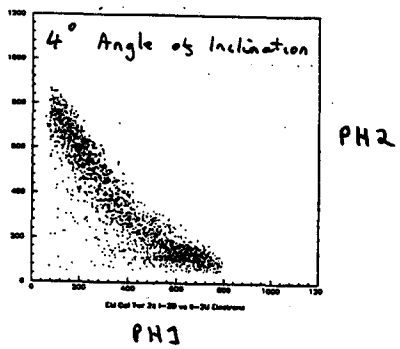

π^0 / γ REJECTION

SM STRIP WIDTH

Moliere Radius : Pb / Scint ≈ 3 cm

Strip Width : 0.05 / 8 ≈ 1.3 cm

Use narrow core for improved π^0 rejection ?

(γ-γ OPENING ANGLE VS SHOWER SIZE)

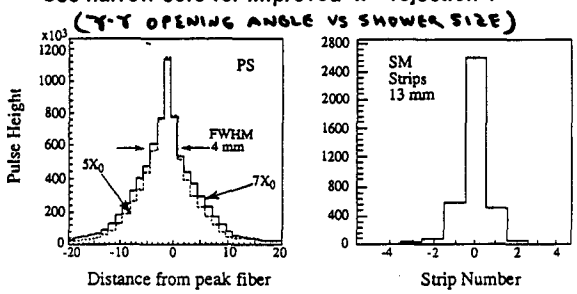

π^0 rejection factor for 80 % electron efficiency :

E_{π^0}	$\varepsilon_\gamma / \varepsilon_{\pi^0}$ (0.05/8)	$\varepsilon_\gamma / \varepsilon_{\pi^0}$ (0.05/16)
25 GeV	6.7	8.9
50 GeV	1.5	2.6
75 GeV	1.3	1.5

Trade-off : Readout fibers x 2

⇒ π^0 background x 2/3.

+ $H \to \gamma\gamma$ θ_γ

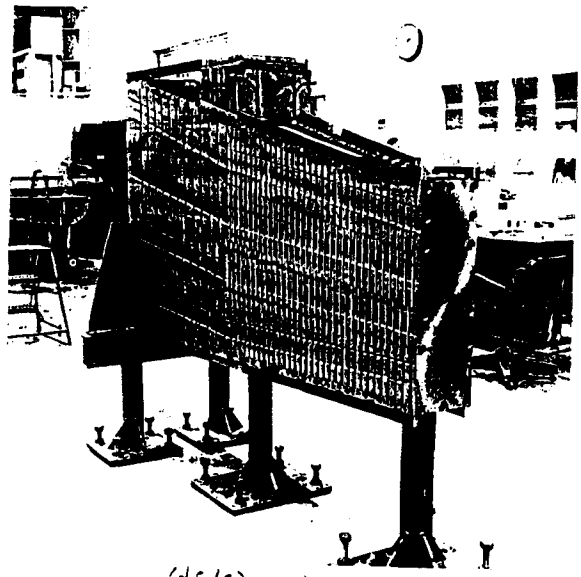

$(dE/E)_z$, ⊥ SCAN

HAD - HERMITICITY

1055

EMAND HAD CRACKS ARE NOT CONGRUENT

N

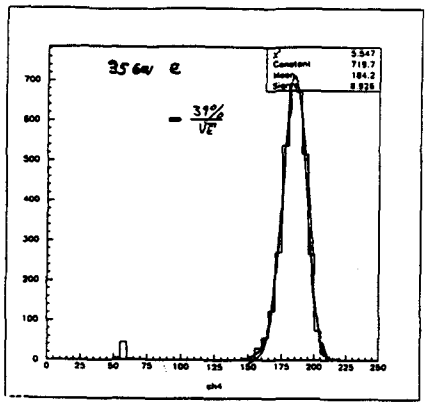

E

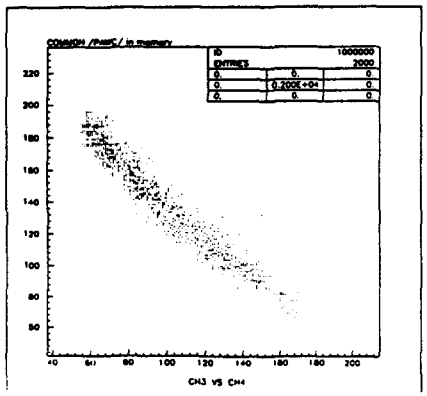

PH2

PH1

1056

Cs^{137} SOURCE TUBE CALIBRATIONS

±0.67% STABILITY, ABSOLUTE 2.37% SCALE SET

R&D ON SOURCE LOCATION CONTROL AND PMT SPACE CHARGE CORRECTIONS

1057

RADDAM

INDUCED LONGITUDINAL NONUNIFORMITY

$D_0 \sim 3.4$ MRAD

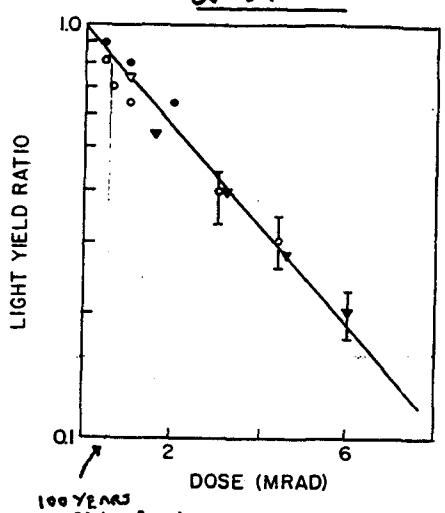

@ SM

100 YEARS @ $10^{33}/(cm^2 \cdot sec)$ IN BARREL

Figure 7. Summary plot of light yield ratio at shower maximum for Saclay data •, o Tsukuba data, ▼ Beijing data. The line is of the form $1-[d(z)]_{max} = \exp(-D/D_0)$.

1058

RADDAM, ⊥ NONUNIFORMITY

10

Normalised Response Map TSUKUBA DATA, β SCANNER

The light yield at each point was normalised by the light yield at the tile center.

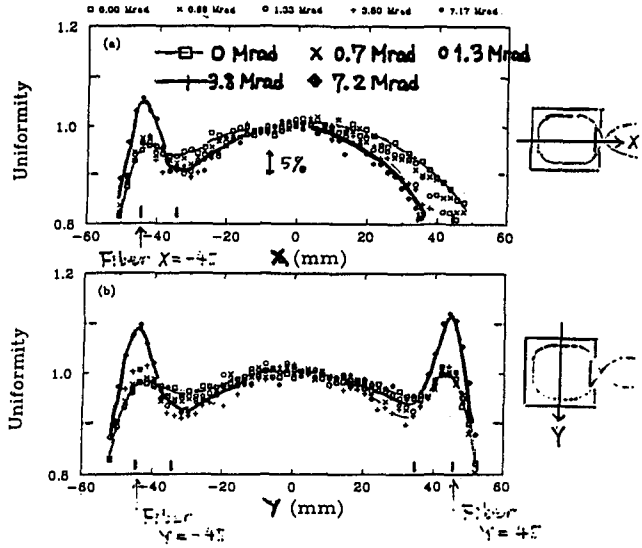

Degradation of response uniformity is small up to ~ 1 Mrad, and ≤ 5% at 3.8 Mrad.

IMPROVED RADDAM FOR ENDCAP?

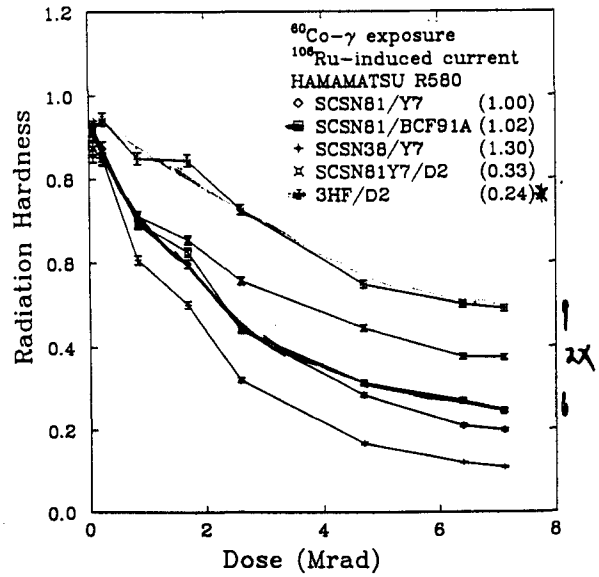

+ REDUCE OPTICAL PATH LENGTH
+ SILICA WLS (?)

Figure 17: Comparison of radiation hardness of scintillating tiles with waveshifting fibers; SCSN81/Y7, SCSN81/BCF91A, SCSN38/Y7, SCSN81Y7/O2, and 3HF/O2. These samples were exposed to ^{60}Co γ-rays and evaluated by measuring ^{106}Ru-induced currents. The number in parentheses indicates a relative light yield of each tile/fiber sample measured by using Hamamatsu R580. Data is joined together by a solid curve for convenience.

EXAMPLE: DYNAMIC RANGE 20X COF/OØ
⇒ FIXED I_{max}, REDUCE "NOISE FLOOR"

9. PMT, COCKCROFT-WALTON BASE

A) Continue to develop a photomultiplier tube suitable for the SDC barrel calorimeter --- Hamamatsu

● B) Cockcroft-Walton base of mold type --- Matsusada

ACHIEVED 1/10 NOISE OF ZEUS BASE

C) More compact Cockcroft-Walton base using surface mount technology --- Rin-ei seiki

---

So far the plan.

Data will be presented in the May SDC meeting at KEK.

WHY? TEST MECHANICS - FULL SCALE
TEST CRACKS/HERMITICITY
TEST MANUFACTURING ⇒ CONSTANT TERM
★ TEST SDC COLLABORATION - THIS IS A PROTOTYPE OF SDC NOT JUST A CALORIMETER

PREPRODUCTION PROTOTYPE WEDGE

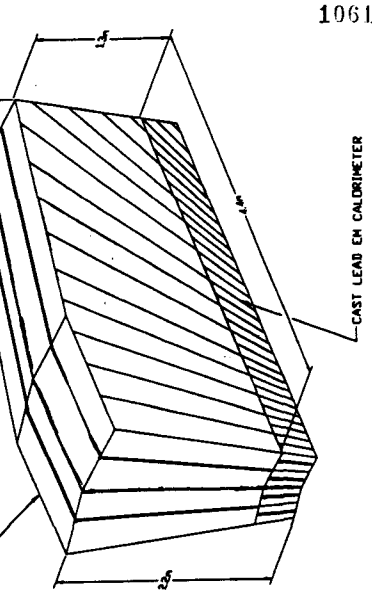

U70T (35+35)
2 FULL SIZED 1/32 WEDGES
TEST BEAM

SDC CALORIMETER SYSTEM SUMMARY

1. SDC Calorimetry is defined by "SDC Calorimeter Conceptual Design Report" and the TDR. Details will appear in the parallel sessions.
2. ● The calorimetry for SDC has been optimized for the Physics using both Monte Carlo simulations and an extensive program of beam testing. Tests of EM, SM, and HAD test modules were performed at FNAL in 1991.
3. In general, SDC has evolved to emphasize EM resolution, which has precise scales such as Z width/mass rather than HAD resolution where the basic quarks require a less accurate energy measurement due to inherent difficulties in jet definition.
4. Steel absorber and scintillator sampling are chosen on the basis of data. The resulting need for radiation damage studies and extensive calibration systems is being addressed. An existence proof for the barrel has been made. R&D for the endcap is in progress. Replacement plans exist.
5. ● The next step for the calorimeter group of SDC is to build and test a full size "preproduction prototype" of a barrel wedge. This must be done in 1993 if the SSCL schedule for SDC is to be met.
6. The forward calorimeter options have been reduced to 2 and the geometry has been chosen (backstop). Final technology choice is in progress.

1063

1064

TDR Mechanical Design

Larry M. Bartoszek
(Fermilab)

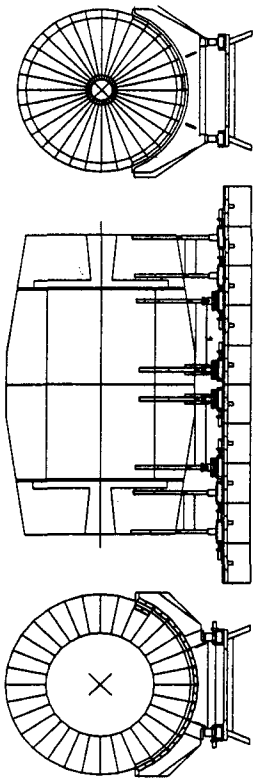

1065

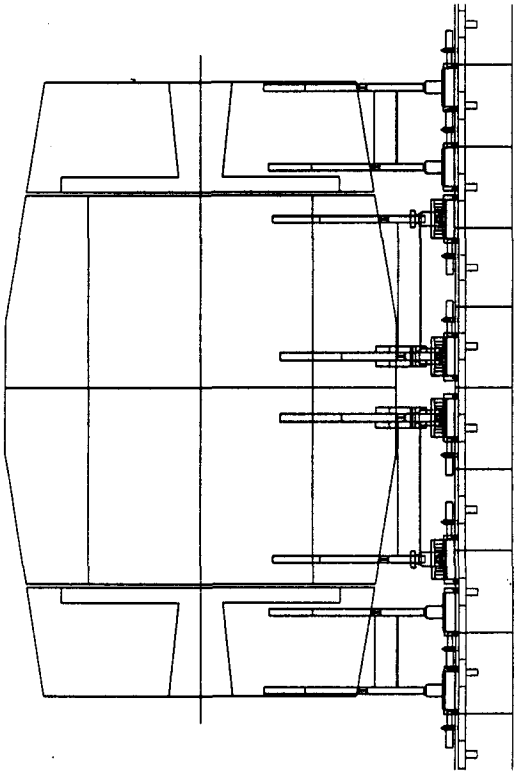

1066

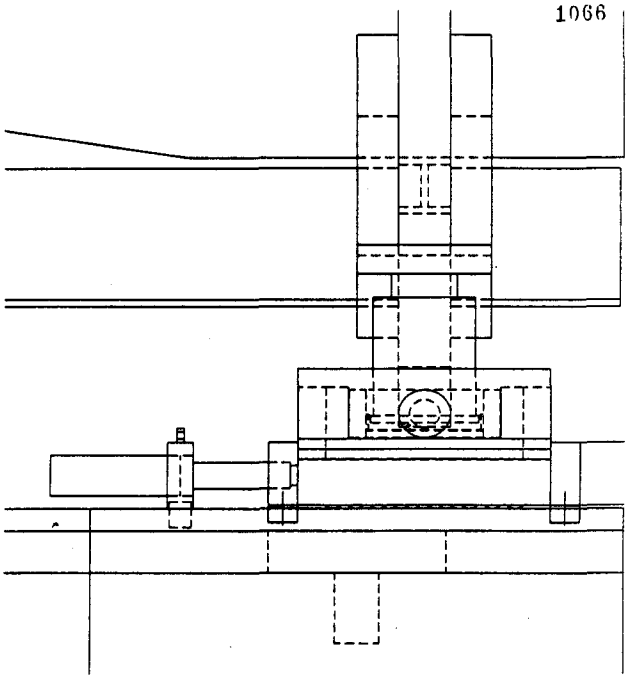

1067

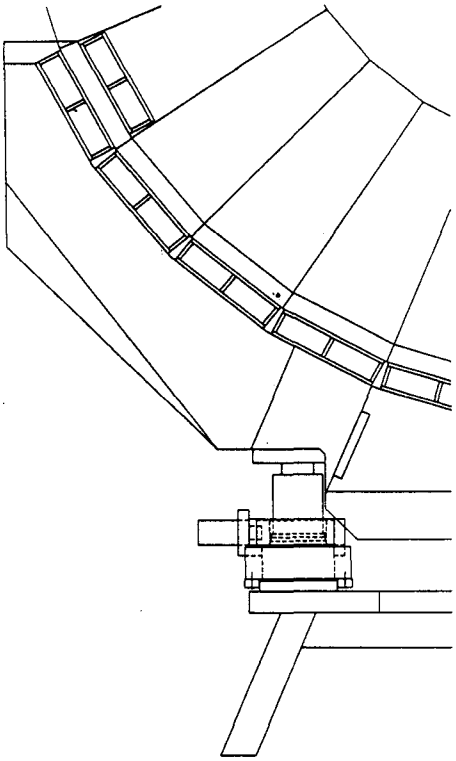

1068

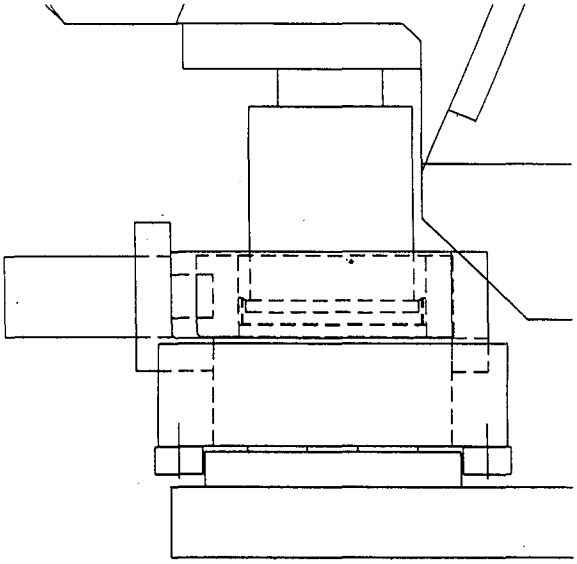

1069

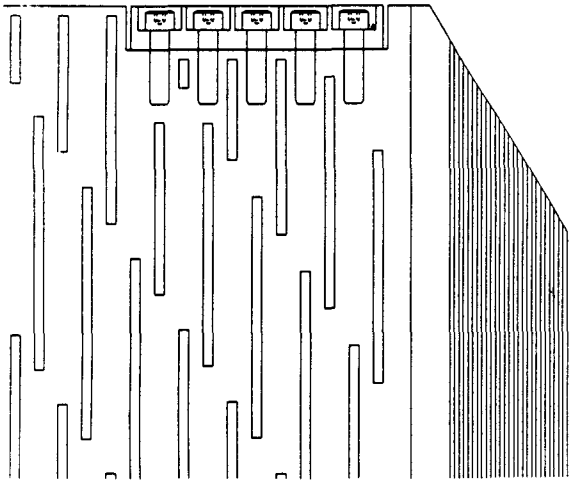

1070

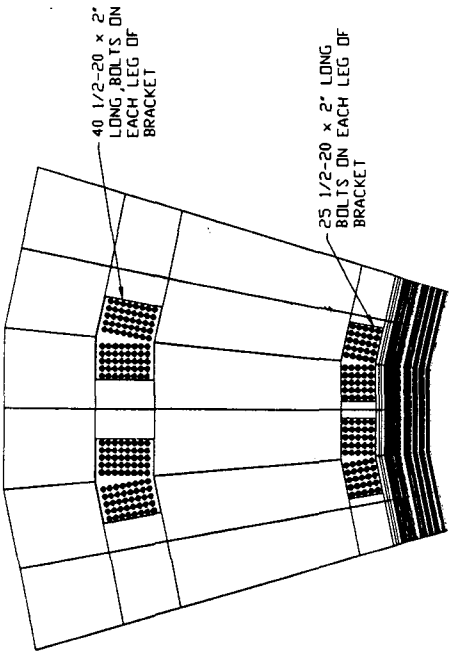

DRAWING OF BRACKETS ATTACHING BARREL WEDGES TO EACH OTHER

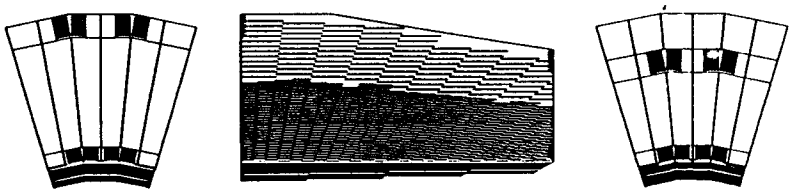

BEAM AXIS

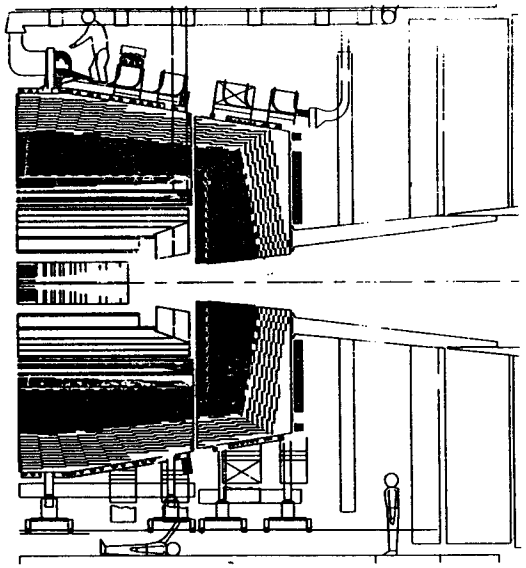

1073

Report from Prototype Task Force

G. William Foster
(Fermilab)

1074

PROTOTYPE WORKING GROUP

(J. FREEMAN, GW FOSTER CONVENERS)

- TUESDAY 5 PM CST TELECONFERENCE (ALTERNATE TUESDAYS WITH ENGR. TELEC.)
- OFTEN THE DISCUSSION MERGES W/ENGR. DISCUSSIONS
- SOME GROUPS (LBL, FNAL) STILL MAINLY INVOLVED WITH CURRENT PROTOTYPES.
- WE DON'T KNOW OUR BUDGET
- WE DON'T KNOW THE TIME AT WHICH THE PROTOTYPE SHOULD BE READY FOR BEAM
- WE DON'T EVEN KNOW THE BEAMLINE.

... BUT WE HAVE GONE AHEAD ANYWAY & ACTUALLY MADE SOME DECISIONS...

1075

WEDGE MOVING FIXTURE

POSSIBILITIES:

① Recycle existing fixture to get something in the beam ASAP.

② MAKE THE FINAL DEVICE
- more ###
- more delay
- more paperwork (Safety Reviews, etc.)

Decision: MAKE THE FINAL DEVICE

- 2 Full Wedges
- Provision for ENDCAP SECTION (eventually)
- Engineering from LBL likely

1076

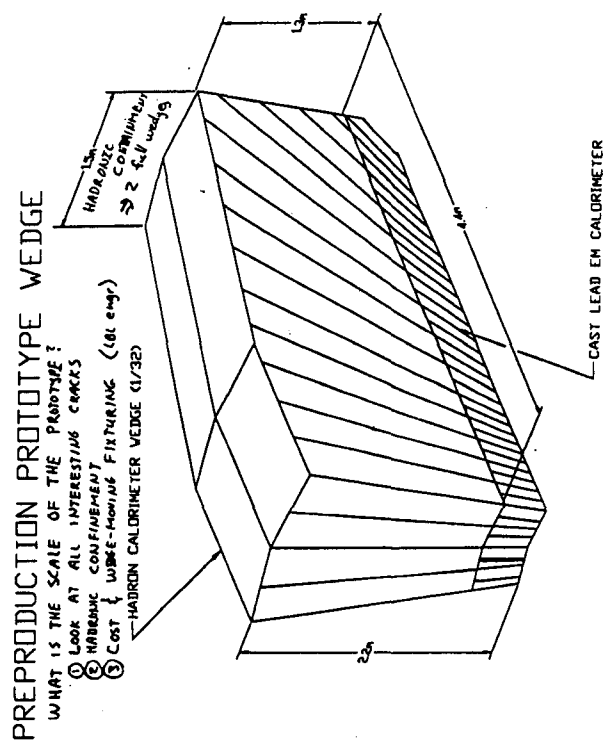

WHICH REGIONS TO INSTRUMENT?

Instrumented Sections of SDC Barrel Prototype

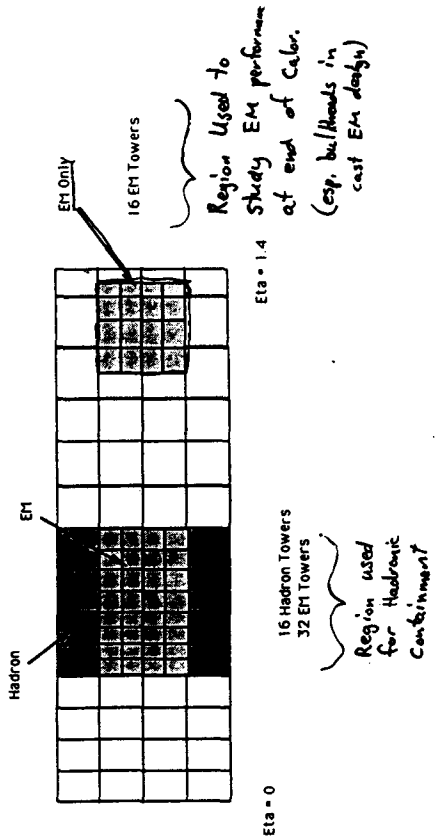

SDC Preproduction Prototype

Decision Milestones S. Gourlay April 29, 1992	1992 May	Jun	Jul	Aug	Sep	Oct	Nov	Dec
Config 1	Begin Preliminary Engineering Design							
Barrel Segmentation	◆							
Phi Crack Geometry	◆							
Final Dimensions		◆						
Config 2			Begin Final Design					
Instrumented Towers		◆	Tooling Design/Fabrication					
Source Tube Grooves		◆	QA/Assembly Procedures					
EM Absorber			◆					
Fiber Routing Geometry			◆					
PMT Layout			◆					
Attachment of EM to Hadron			◆					
SM Fiber Routing/Integration			◆					
Optic 1	PMT/Tile Parameters to Tsukuba/SM to Saclay							
Choose PMT				◆				
Scintillator Type/Thickness				◆				
Fiber Type/Diameter				◆				
Fiber Groove Cross Section					◆			
Fiber Routing Geometry					◆			
Fiber Mirroring Technique					◆			
Fiber Lengths					◆			
Masking					◆			
Tile Sizes						◆		
Shower Max Tile specs						◆		
Optic 2	Begin Tooling Design and Final Assembly							
Wrap Material							◆	
Design/Fabricate Cookies							◆	
Design/Fabricate PMT Assy.							◆	

Tue, May 19, 1992
to Bibbs!
Lib 166 Cons 44

Additional cost to produce two full 1/32 modules and instrument 4 X 4 towers in EM section at eta =1.4

Additional absorber cost (steel)	$263k
16 towers of additional EM readout	$47k
	$310k

365

1080

Update on Baseline Barrel EM
- Mechanical and Optical

David Underwood
(Argonne National Laboratory)

1081

UPDATE ON BASELINE
BARREL EM,
ETC.

1) MECHANICAL
   REVIEW DESIGN AND NEW η BOUNDARIES
   ARGONNE TESTS AND PLAN FOR PROTOTYPE
   REVIEW OF CASTINGS
   STRESSES IN INSTALLATION AND CASTING
2) REVIEW OF BEAM TESTS
   CRACKS AND BOUNDARIES
3) OPTICAL
   LARGE η TILE CONSIDERATIONS
4) OTHER TOPICS
   DENSITY
   GREEN PMTs
   LEAD ACTIVATION
   PRESSURE ON SCINTILLATOR

D. U.

1082

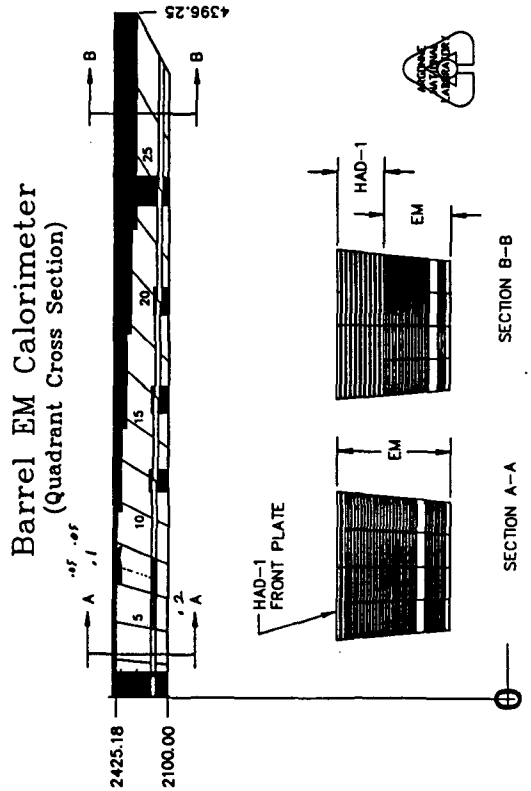

1083

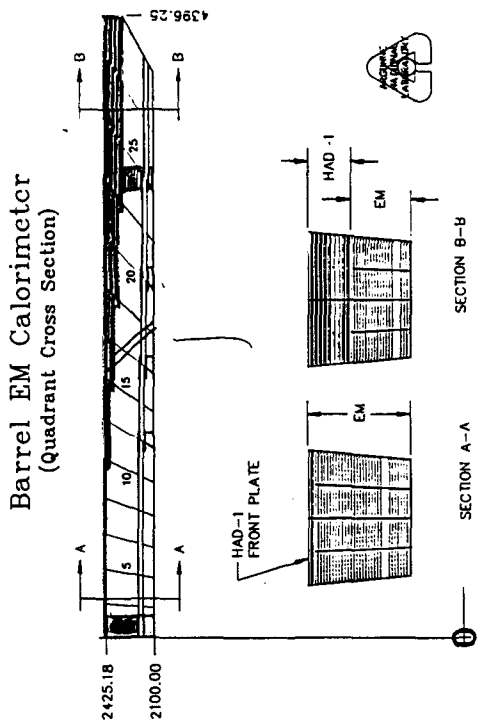

Argonne HEP Design Group Development Plan for Full Size Barrel EM Prototype

Tasks:

1. **18 cell test castings**
   - Mold rework
   - Casting with .5 Sn - .065 Ca alloy
   - Casting with 1.2 Sn - .065 Ca alloy
2. **Absorber Plate End & Bulkhead Connections**
   - Design Mold/Fixture
   - Fabricate Mold/Fixture
   - Castings
     Pure Lead
     .5 Sn - .06 Ca
     1.2 Sn - .06 Ca
     4.0% Sb
     6.0% Sb
     .05% Te
     End Connection Options
3. **10 Tower Casting**
   - Mold Rework
   - Frame Fabrication
   - Casting with preferred alloy
4. **Mechanical Tests**
   - Design & Fabricate Test Fixture
   - Instrument Module
   - Test for Stress & Deflection at 12 o'clock & 3 o'clock positions
5. **Full Scale Barrel EM Prototype**
   - Final EM Module Design
   - Mold Design
   - Mold Fabrication
   - Support Frame Fabrication
   - Mold Testing
   - Casting Full Size EM Prototype

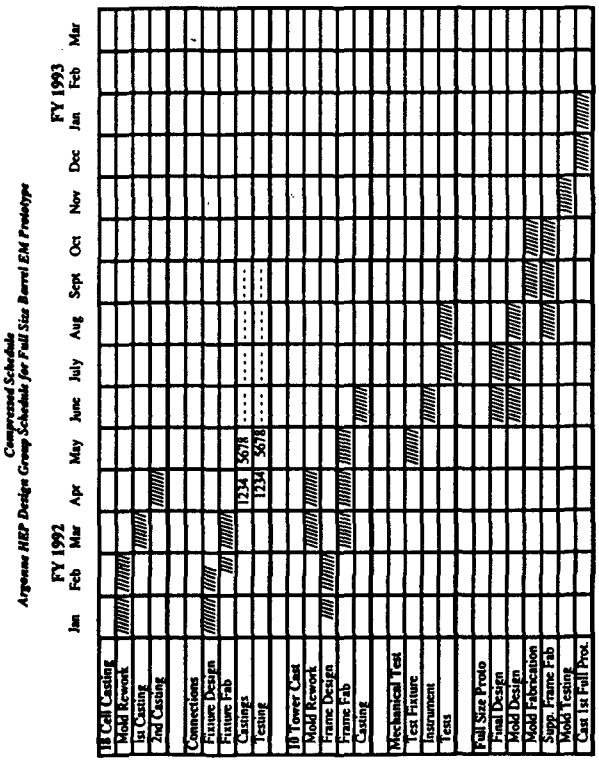

Maximum Stresses in EM Module

DURING TRANSPORT ONLY

	Maximum Frame Stress (psi)	Maximum Bulkhead Stress (psi)	Maximum Lead Stress (psi)
12 o'clock Position	22,605	3,552	1,116
3 o'clock Position	565	3,567	20.3

Deflections of EM Module

DURING TRANSPORT ONLY

	Z = 0			Z = 2000 mm			Z = 3999 mm		
	Beam Direction Deflection (mm)	Radial Deflection (mm)	Tangential Deflection (mm)	Beam Direction Deflection (mm)	Radial Deflection (mm)	Tangential Deflection (mm)	Beam Direction Deflection (mm)	Radial Deflection (mm)	Tangential Deflection (mm)
12 o'clock Position	2.67	.001	0.0	2.67	2.48	0.0	2.69	5.12	0.0
3 o'clock Position	.006	.002	.006	.001	.023	.058	.007	.005	.015

Update on Baseline Barrel EM - Mechanical and Optical

David Underwood
(Argonne National Laboratory)

UPDATE ON BASELINE
BARREL EM,
ETC.

1) MECHANICAL
   REVIEW DESIGN AND NEW η BOUNDARIES
   ARGONNE TESTS AND PLAN FOR PROTOTYPE
   REVIEW OF CASTINGS
   STRESSES IN INSTALLATION AND CASTING
2) REVIEW OF BEAM TESTS
   CRACKS AND BOUNDARIES
3) OPTICAL
   LARGE η TILE CONSIDERATIONS
4) OTHER TOPICS
   DENSITY
   GREEN PMTs
   LEAD ACTIVATION
   PRESSURE ON SCINTILLATOR

D. U.

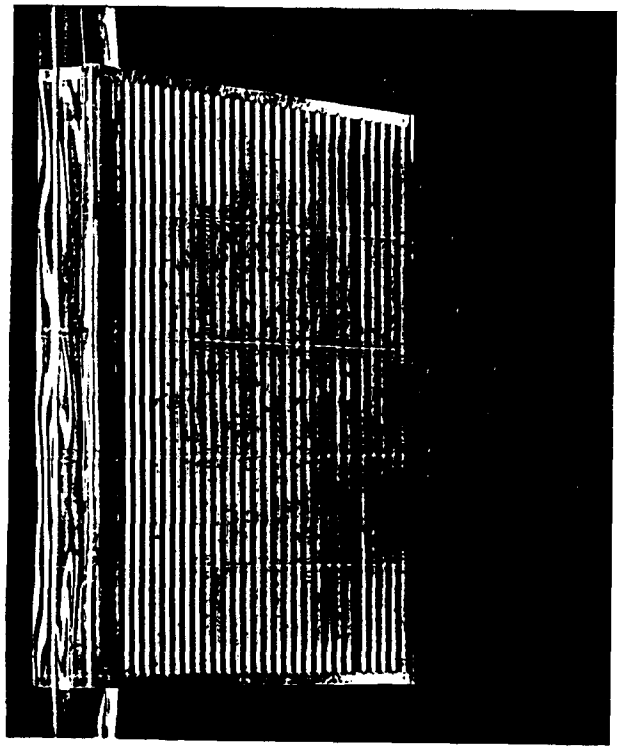

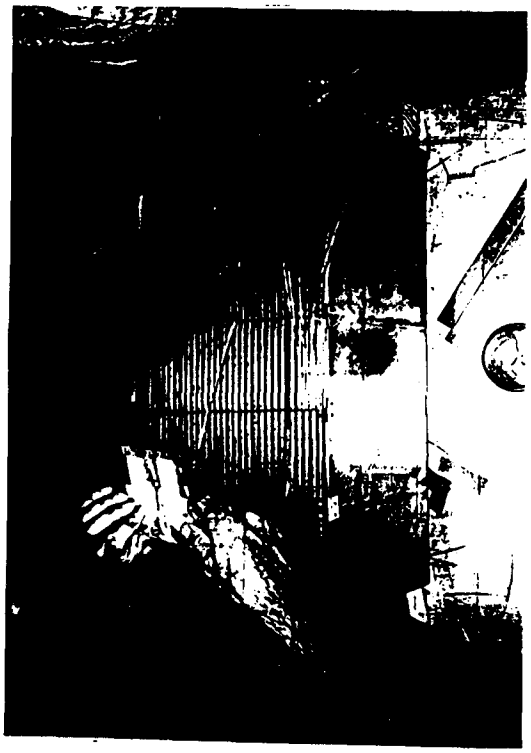

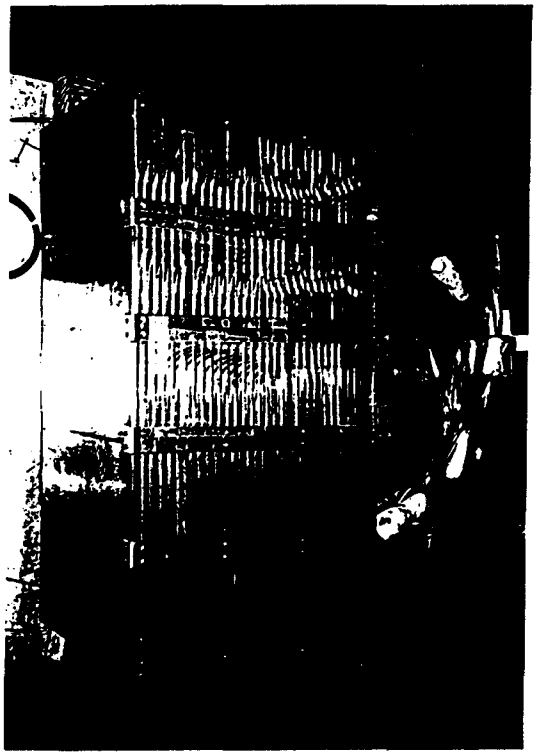

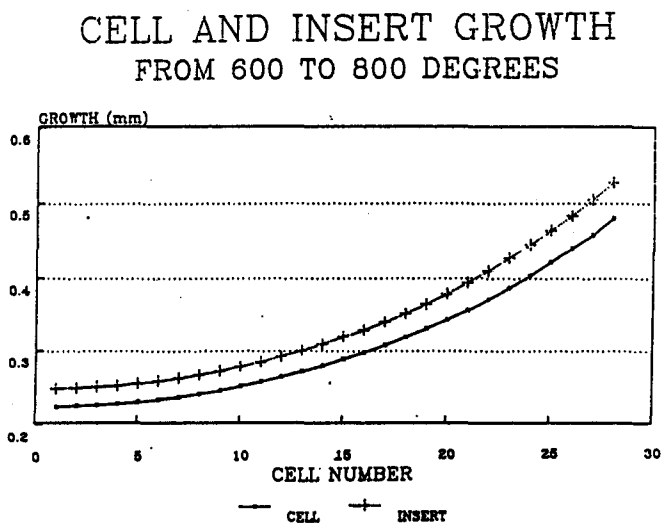

HERMITICITY

3 KINDS OF CRACKS

1) TOLERANCE AIR GAP + WRAPPING ∅

2) TOLERANCE AIR GAP + STEEL BULKHEAD ↑

3) FIBERS + SKINS + TOLERANCE ∅

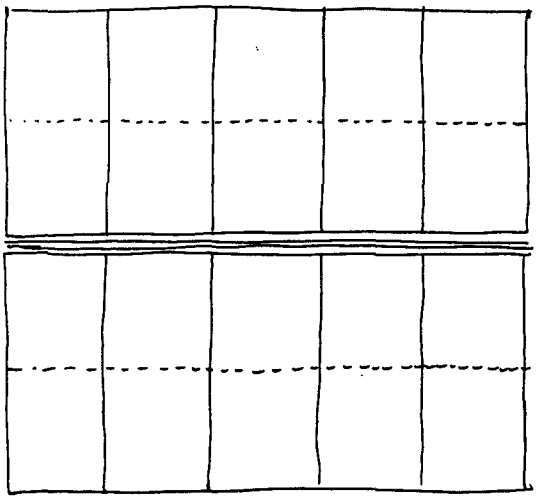

CRACK SCAN ACROSS "SIMPLE" TOWERS (Air gap only)

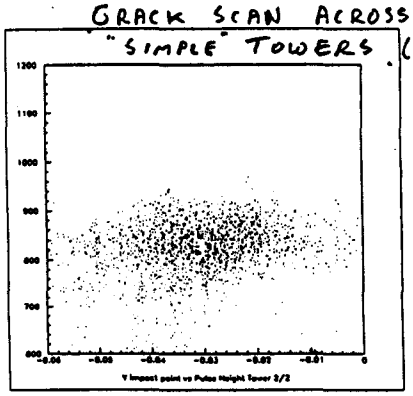

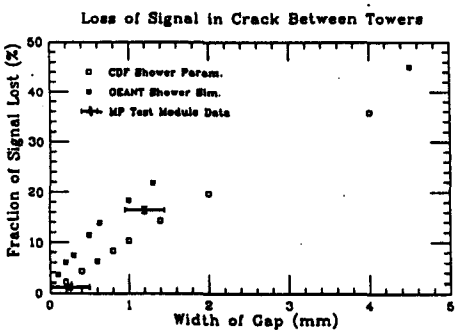

1096

Bulkhead area

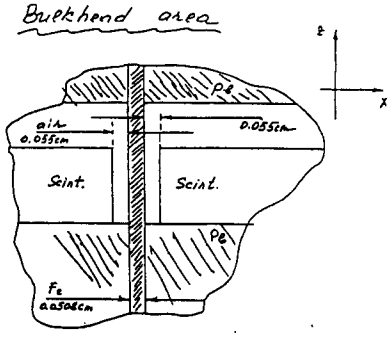

Scan Across Towers Separated by 0.5mm Stainless Steel Bulkhead

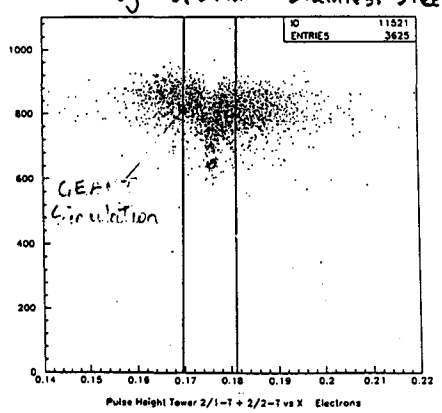

1097

InterModule Gap

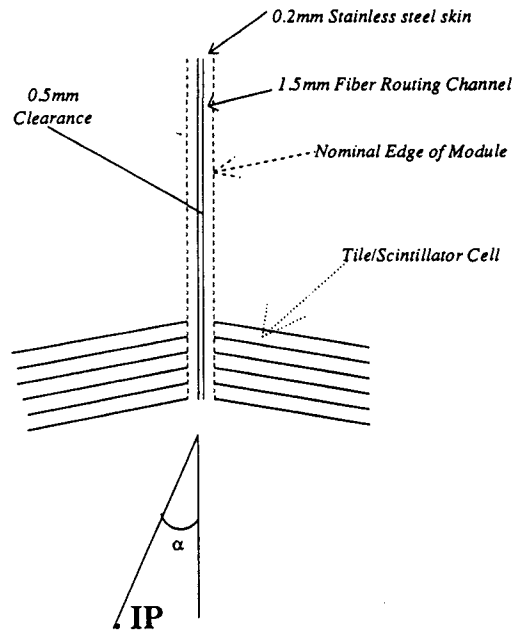

Inter-Module ϕ Crack Scan.

1098

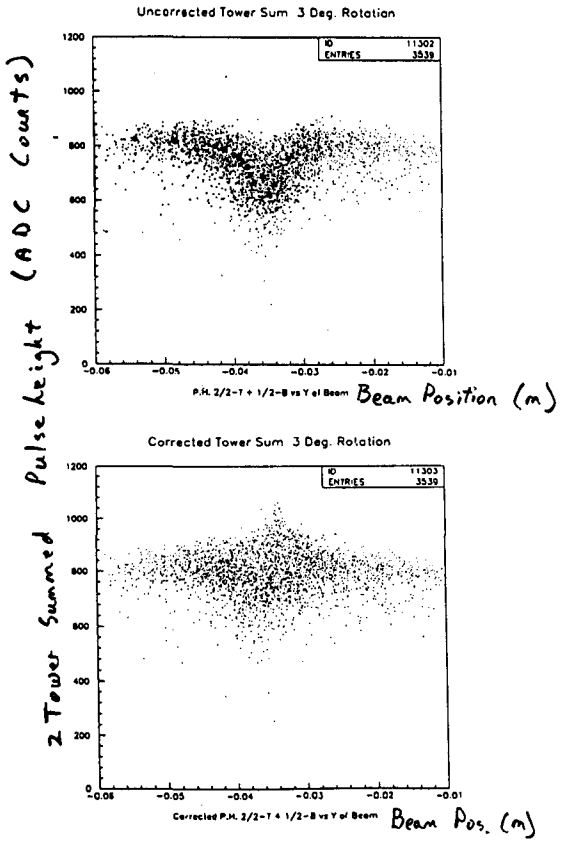

1099

GEANT Simulation: Energy Correction from Parameterisation

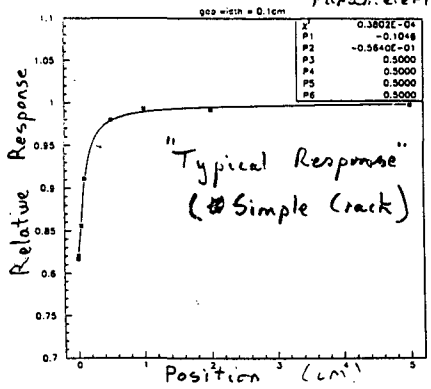

Uncorrected Energy

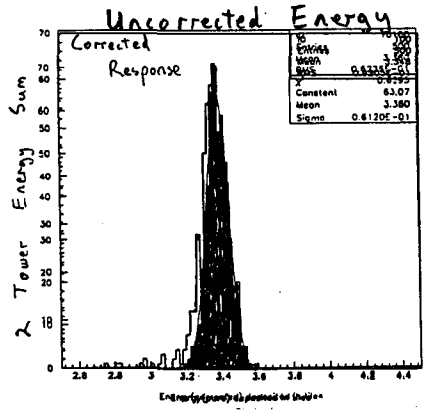

1100

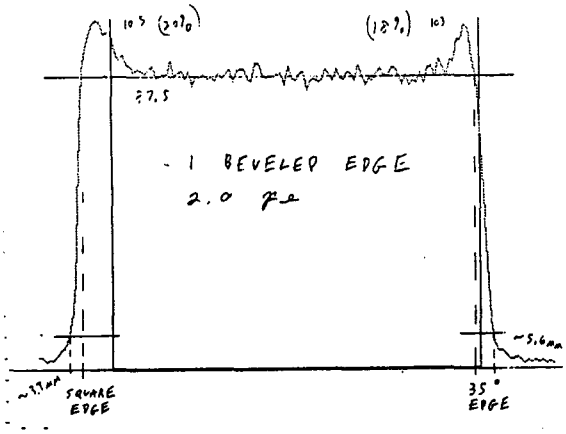

1101

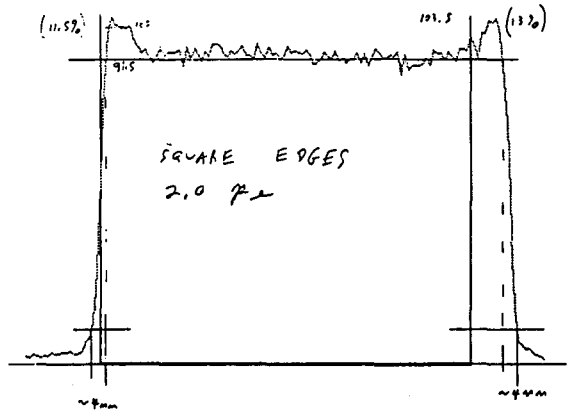

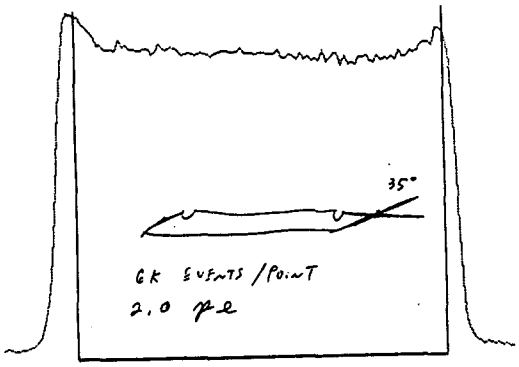

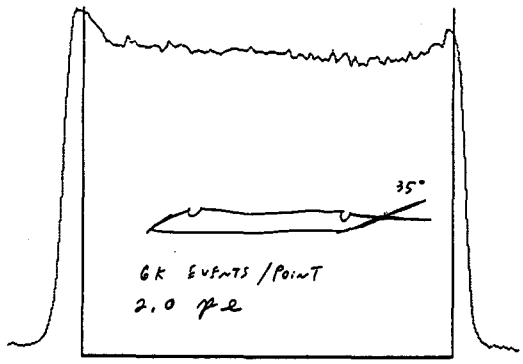

1102

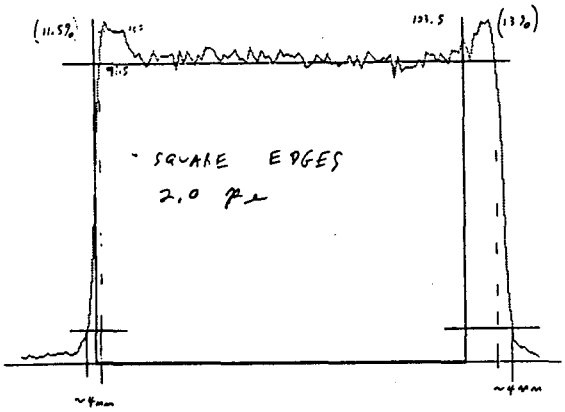

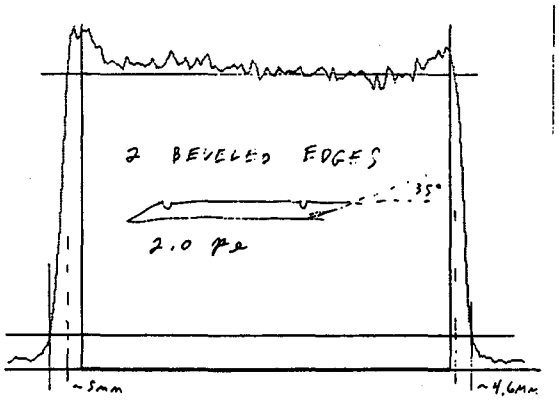

1103

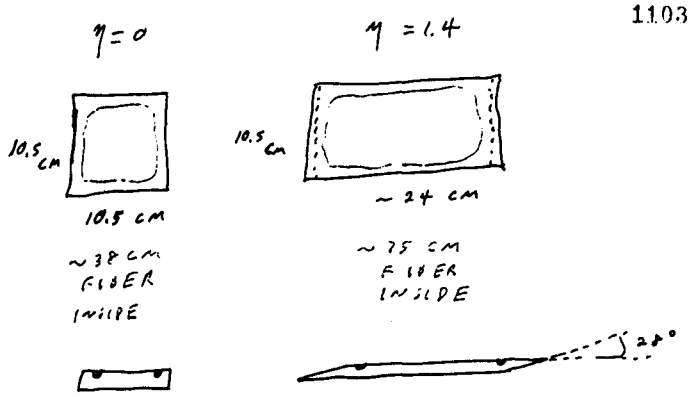

1104

POSSIBLE PROBLEMS WITH SINGLE FIBER / TILE (ALUMINIZED)

LARGE η EM TILES ARE > TWICE AS LARGE AS LOW η ONES.

LENGTH OF FIBER IN TILE ~ 75 cm

λ_{ATTEN} ~ 1.3 m IN FIBER

$\lambda_{EFFECTIVE}$ FOR ALUM. FIBER ~ $\frac{1+R}{1-R}\lambda$

R IS REFLECTIVITY

R	λ_{EFF}	$e^{-\frac{.75m}{\lambda_{EFF}}}$	DIFF.	$(1+R)e^{-\frac{.75}{\lambda_{EFF}}}$
.8	9. m	.92	8%	1.656
.7	5.6 m	.876	12%	1.489

FOR FIBER LOOP WITH 2 ENDS:

ENDS	MIDDLE	DIFF.
$1+e^{-\frac{.75m}{\lambda}}$	$2\times e^{-\frac{.37}{\lambda}}$	
1.56	1.50	4%

GEOMETRICAL FACTORS –
DO THEY FLATTEN LOOP RESPONSE TO < 4%
DO THEY NOT FLATTEN σ RESPONSE MUCH ?

1105

STUDY IN PROGRESS
(BARRY WICKLUND)

FOR OPTIMUM γ DETECTION:
BETTER ENERGY RESOLUTION,
BETTER SPACE RESOLUTION
FOR π^0 REJECTION

HOWEVER:
THE DENSITY OF A STACK WITH 2 MM Pb IS LOWER

SHOWER SIZE IS ~ 60% LARGER

PROBLEMS WITH SHOWER MAX.

1106

GREEN EXTENDED PMT

COMPARE PHILIPS XP2081
HAMMAMATSU R580-17

TO R580-15

BOTH SHOW 20% BETTER PHOTOCATHODE EFFICIENCY FOR A GREEN LED. } NOT FACTOR 2

$N_{\mu\mu} = \left(\frac{M}{\sigma}\right)^2$

1107

Table I
Neutronic Properties of Lead Additives

Element	Isotopic Composititon	Neutron Abs. cross section	Half life (days)
52 Tellurium	130 (35%)	small	stable
	128 (32%)	small	stable
	126 (19%)	small	stable
	125 (7%)	21 b	58 d
	124 (4.8%)	small	stable
	123 (0%)	420 b	119.7d
	122 (2.6%)	80 b	stable
51 Antimony	124 (0%)	small	60 d
	123 (43%)	100-500 b	stable
	122 (0%)	small	2.8 d
	121 (57%)	100-500 b	stable
50 Tin	124 (6%)	small	stable
	122 (5%)	small	stable
	120 (33%)	small	stable
	119 (8.6%)	small	293 d
	118 (24%)	small	stable
	117 (8%)	15 b	13.6 d
	116 (14%)	11.5 b	stable
20 Calcium	40 (97%)	small	stable
	44 (2%)	small	stable

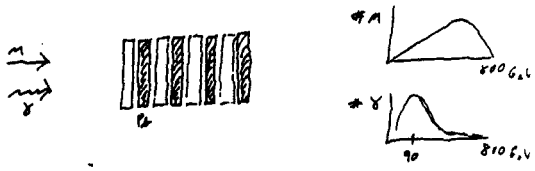

20 MEG. RAD IN ~ 5 DAYS

3000 MILLI REM/HR

"HALF LIFE". < 3 DAYS (NOT EXPONENTIAL)

ANALYSIS OF γ ENERGIES (200 LINES)

$^{51}Sb^{124}$	ANTIMONY	46 SEC	20 MIN	60 DAY
$^{51}Sb^{122}$			4.1 MIN	2.7 DAY
$^{81}Te^{200}$				26 HOUR
$^{82}Pb^{203}$		6.2 SEC		52 HOUR

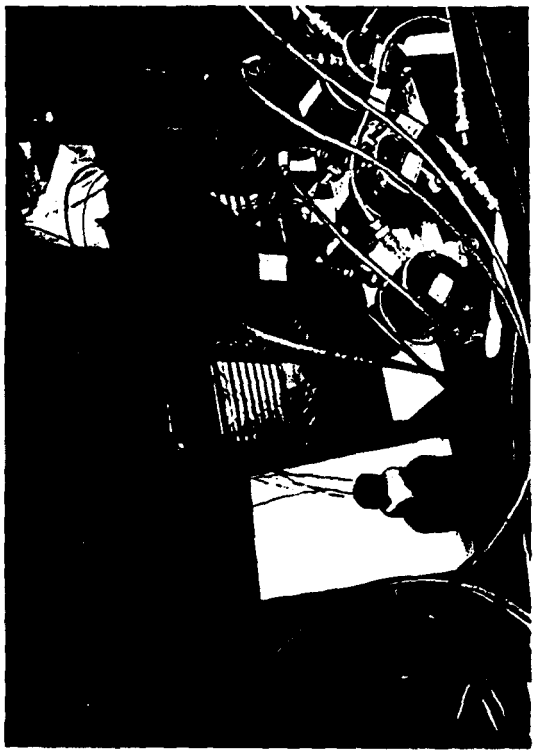

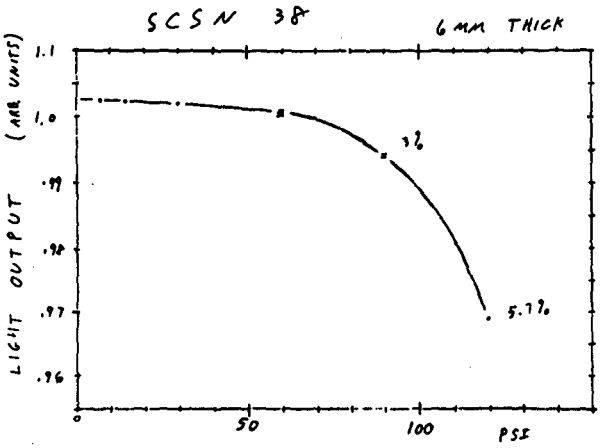

$$\text{LIGHT} = 1.05 - .0081\, e^{\frac{PSI}{50}}$$

TWICE AS BAD FOR 3 MM THICK

EFFECTS OF PRESSURE ON SCINTILLATOR LIGHT OUTPUT.

ATTEMPT AT LONG TERM TEST.
(2 THICKNESSES OF SCINTILLATOR)

SCSN 38	6 MM THICK	
DATE	PRESSURE FOUND	LIGHT 0 PSI / LIGHT PRESSURE
NOV 8	120 PSI	5.7 %
NOV 13	120	5.8
NOV 19	108	5.2

RH5	3 MM	
NOV 19	120	9.%
NOV 28	114	7.5

CONST. LONG TERM PRESSURE
CHANGED TUBE BASES
CHANGED TRIGGER DISC. LEVEL

JAN 10	105	11 %

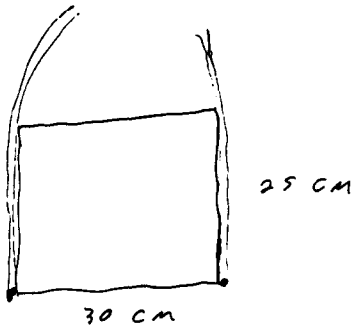
25 CM
30 CM

UPDATE ON...

BARREL EM CALORIMETER OPTIONS

GW Foster ~~April~~ MAY '92

The current baseline EM calorimeter is a Cast Lead + Stainless structure with 4mm Lead Plates.

We are investigating two significant design variations:

I. A "High Resolution Option" using 2mm Lead Plates, and → THIS TALK

II. A "Compression Stack" - an alternate assembly technique which minimizes the cracks between towers and provides greater flexibiliy for Shower-Max detectors. → L. BARTOSZEK TALK

I. HIGH RESOLUTION OPTION

WHY? (PAC doesn't think it's necessary, but...)

1) Equals the GEM accordion design $\lesssim 10\%/\sqrt{E}$
   ⇒ STOPS TALK OF "COMPLEMENTARY" DETECTOR CAPABILITIE
2) Smaller Constant Term:
   - Longitudinal sampling fluctuations diluted by SQRT(# Samples) 60 vs. 30
   - Transverse nonuniformities diluted due to increased shower spreading
3) Higher Plastic:Pb Ratio
   ==> more PE's
   ==> more margin on rad-damage
4) Plastic:Pb of up to 2:1 in EM does not compromise Hadronic Resolution (hanging-file).

OVERALL, THIS DESIGN IS MUCH LESS MARGINAL ON ACHIEVING PHYSICS GOALS. EM CALORIMETER IS NOT THE PLACE TO COMPROMISE PERFORMANCE

WHAT ARE WE DOING ABOUT IT?

Module for BNL Test Beam

- Two modules of 3x2 towers each
- Rectangular Geometry
- Compression Stack - 2mm Pb, 4mm Scint
- Mega-Tiles - TILE CRACK ≈ 0.020" (gap between tiles)
- Sigma Tile Design - single readout fiber
- Mirrored Fiber, inserted into tiles after stacking.
- Realistic Fiber Routing
  ==> Phi Crack Scan
- SM Detector? X no time
- Ready by end of ~~April~~ MAY. Shipped to BNL LAST FRIDAY

MEGA-TILE DESIGN:
- single piece of scintillator contains many tiles
- tiles optically separated by grooves filled with white epoxy.

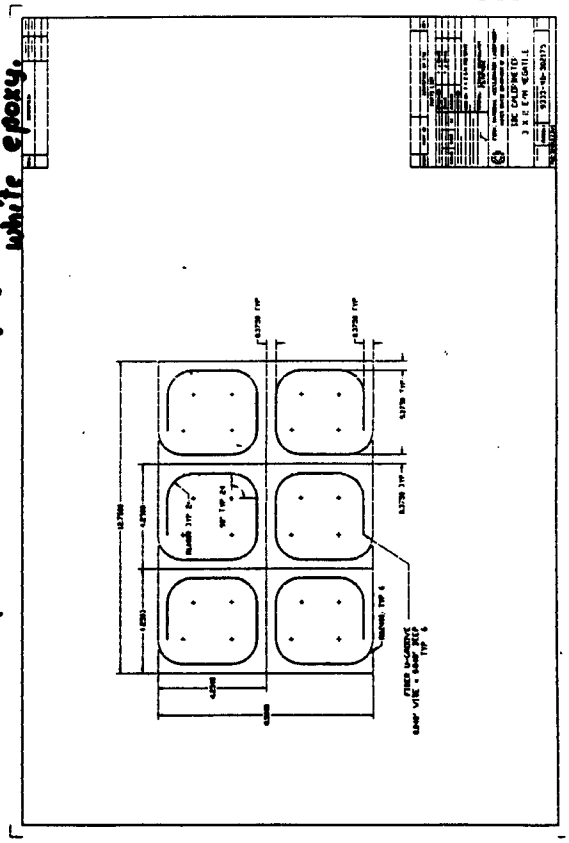

1117

1118

1119

II. COMPRESSION STACK DESIGN

WHY?

1. Minimize Cracks Between Towers in Eta & Phi

Why? "Piano Wires" represent less projective material than support bulkheads: (tensile structures are more efficient use of material than structures in torsion)

2. Cracks do not get worse towards end of barrel.

3. Mega-Tile Cost Savings

4. Freedom to segment Shower-Max detector arbitrarily inside ~4x8 array of towers.

1120

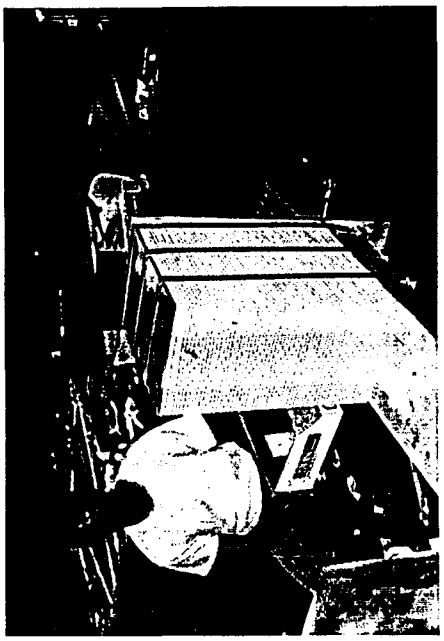

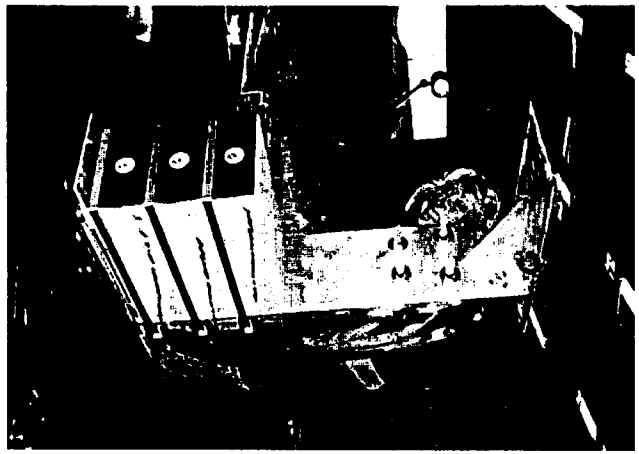

1121

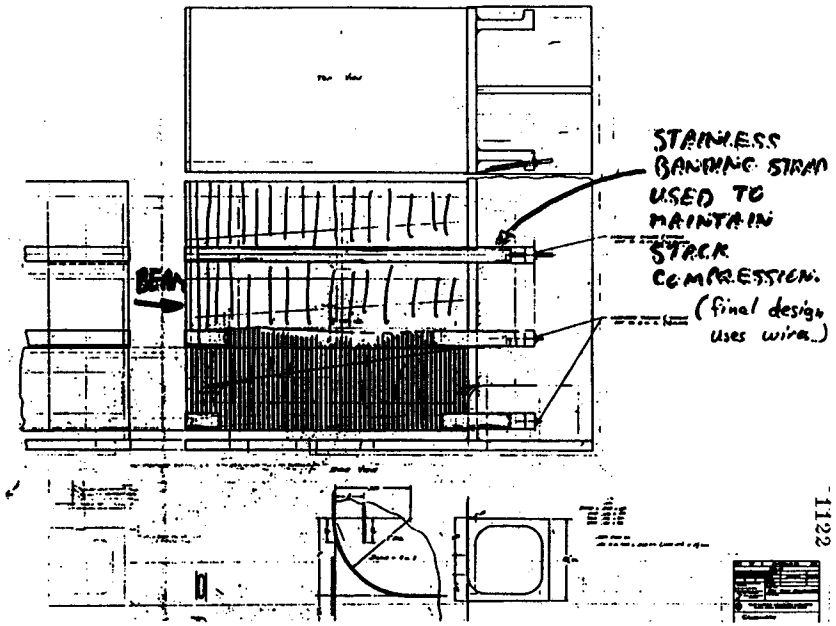

1122

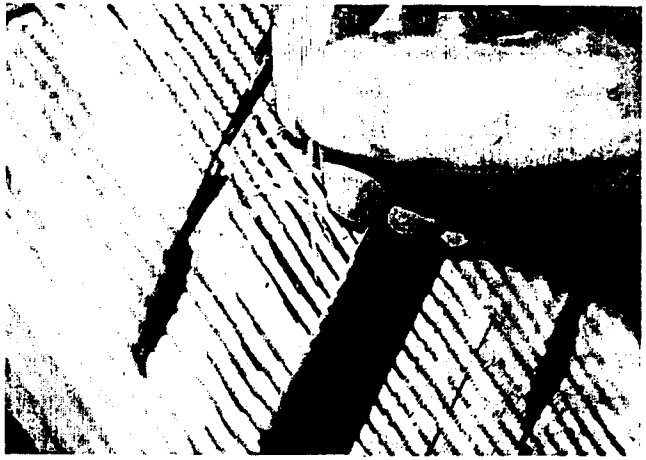

1123

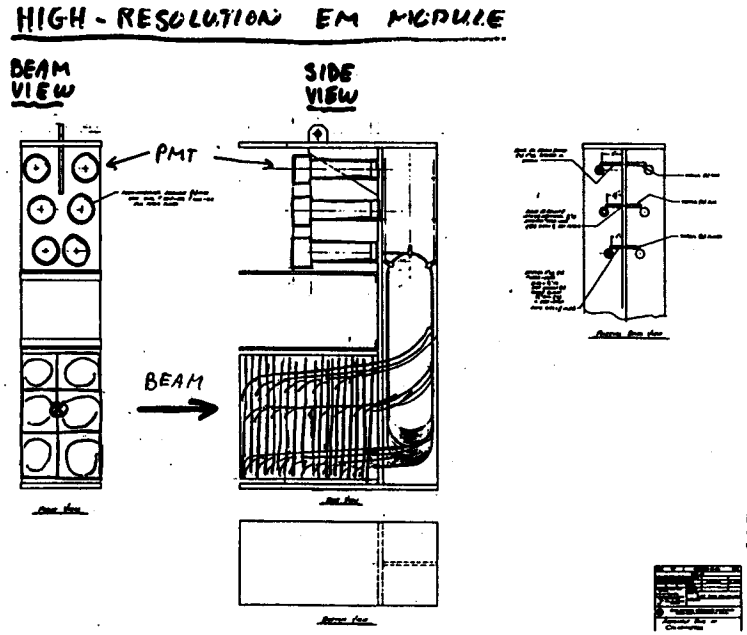

1124

1125

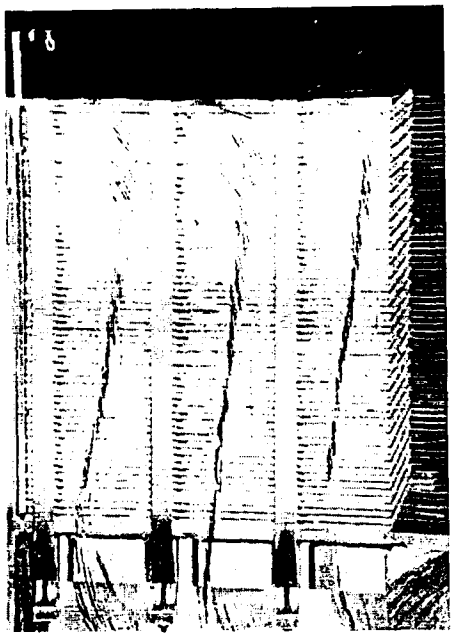

1126

WHAT HAVE WE LEARNED?

1. MEGA-TILE ASSEMBLY WORKS VERY WELL.

- STACK GOES TOGETHER QUICKLY AND ACCURATELY
- FIBERS INSERT EASILY INTO TILES AFTER STACKIN
- NO PROBLEM WITH DAMAGED FIBERS OR MIRROR.

⇒ WE WILL HAVE UPDATES TO LABOR COST/TILE, AND WE EXPECT THE PRICE/TILE TO GO DOWN.

2. WHITE EPOXY BETWEEN TILES CAN BE REDUCED TO ~250μ THICKNESS

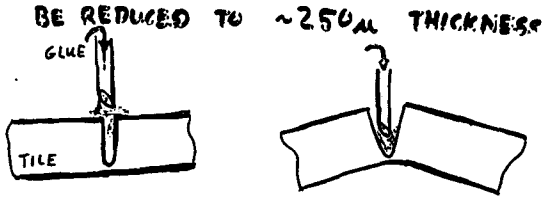

PHYSICIST'S CONCEPT
⇒ BIG MESS

TECHNICIAN'S CONCEPT:
⇒ WORKS FINE
⇒ NO MESS
⇒ SMALLER GROOVE POSSIBLE

* WITH 250μ EPOXY GAP, THE DROP IN RESPONSE AT TOWER BOUNDARY IS ≈ ZERO.

1127

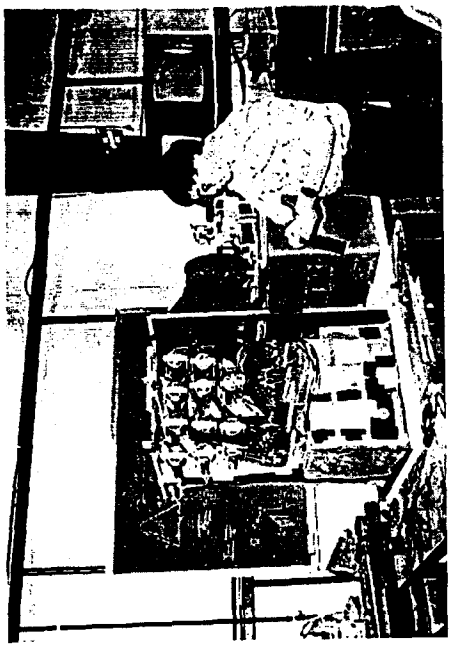

1128

1129

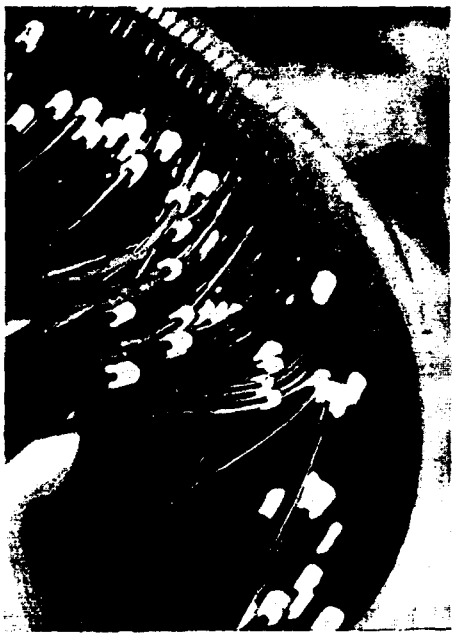

1130

3. TRANSVERSE UNIFORMITY:

- PRIMITIVE MASK (SIMPLE PATTERN ON XEROX PAPER) ACHIEVES $\sigma < 2\%$ ACROSS ALL TILES ON A MEGA-TILE

⇒ A MEGA-TILE CAN BE MEGA-MASKED

4. LONGITUDINAL UNIFORMITY [illegible] WITHOUT MASK [illegible] COOKIE.

- Q/C ON FIBER SPLICES IMPORTANT
- AT PRESENT WE STILL NEED LONGITUDINAL MASK TO BRING CONSTANT TERM $\lesssim 0.5\%$, but WE ARE GETTING CLOSER.

5. COMPRESSION STACK CAUSES NO PROBLEMS, MODULE SUPPORTS ITSELF WELL UNDER NOMINAL STRAIP TENSION.

1131

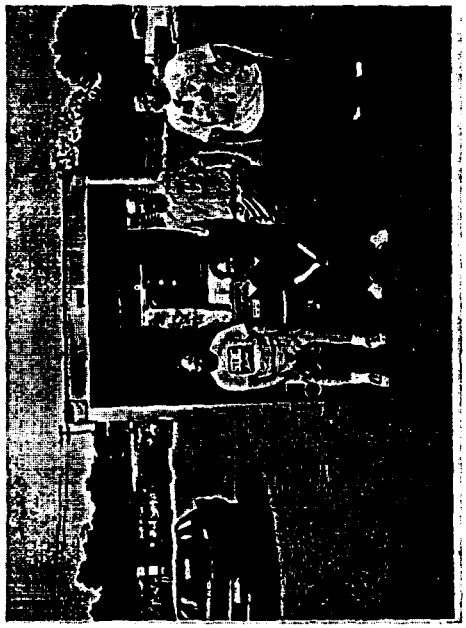

1132

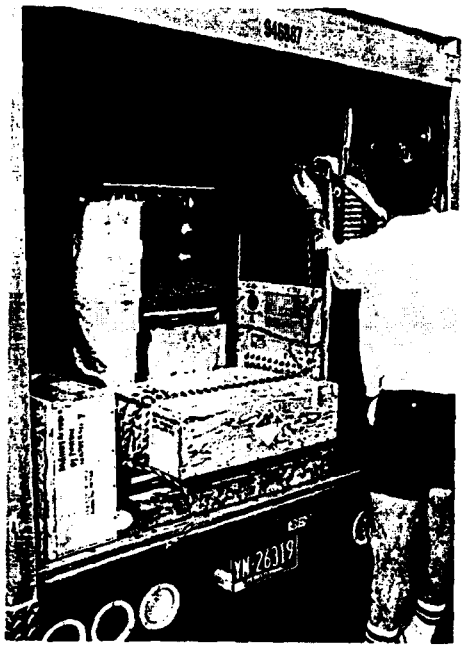

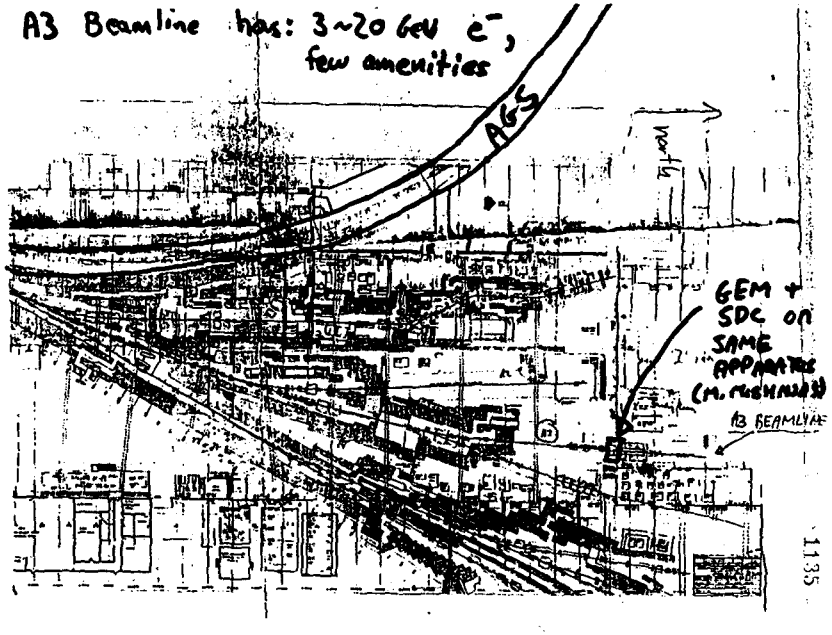
A3 Beamline has: 3~20 GeV e⁻,
few amenities
AGS
North
GEM +
SDC on
SAME
APPARATUS
(M. Rushinski)
A3 BEAMLINE

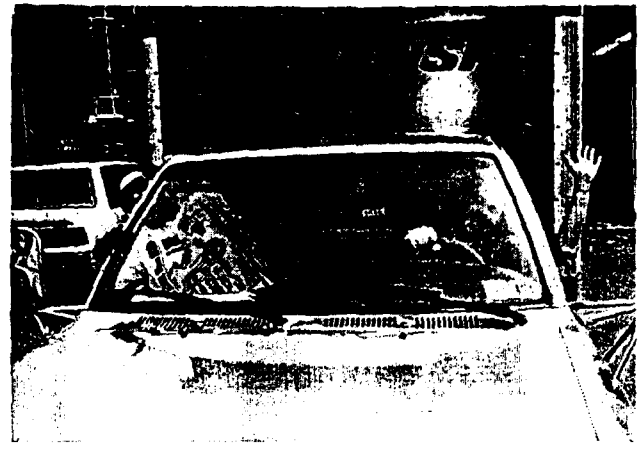

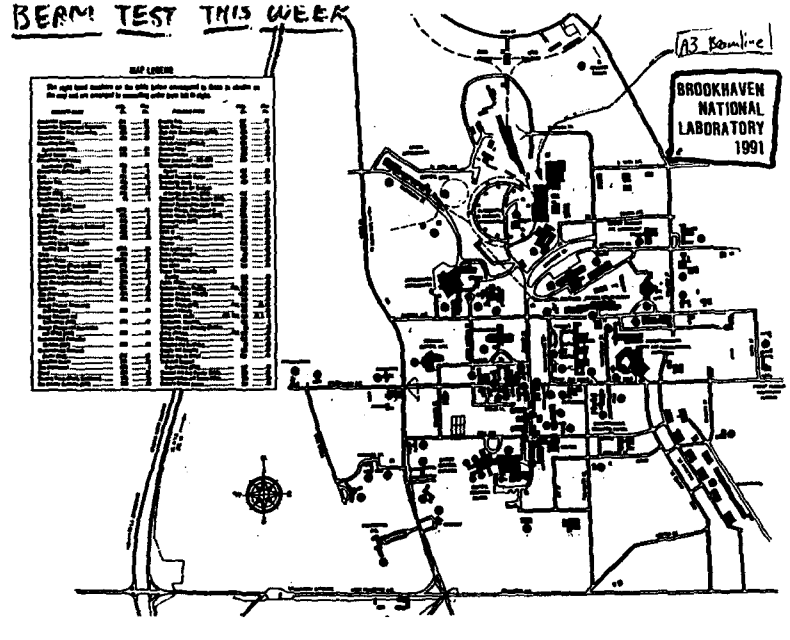
BEAM TEST THIS WEEK
A3 Beamline
BROOKHAVEN
NATIONAL
LABORATORY
1991

Calculation of tensioner parameters revisited
L. Bartosek 5/13/92

- I have been able to place 160 wires along the length of the EII module. From previous calculations, if $\mu = .1$, then the wires on one side must exert a total force equal to 5x the weight of the stack.

$$\frac{(5 \times 6000 \text{ lbs})}{160 \text{ wires}} = 187.5 \text{ lbs/wire}$$

This number has no factor of safety if $\mu = .1$. If we want a factor of safety of 2, the load/wire should be doubled.

This means the load/wire should be 375 lbs

- If we were to use Elgiloy wire, and tension the wire at this maximum load to 80% of yield strength,

$$\frac{375 \text{ lbs}}{\pi r^2} = .8(150 \text{ kci})$$

$$r = \sqrt{\frac{375 \text{ lbs}}{.8(150 \times 10^3 \text{ psi})\pi}}$$

$r = .032''$, $d = .063''$

- We will use 7x19 strand core Stainless 302 cable, 1/16" Diameter, McMaster-Carr # 3458T750, which has a breaking strength of 480 lbs

480 lbs ≥ 375 lbs, so we are safe.

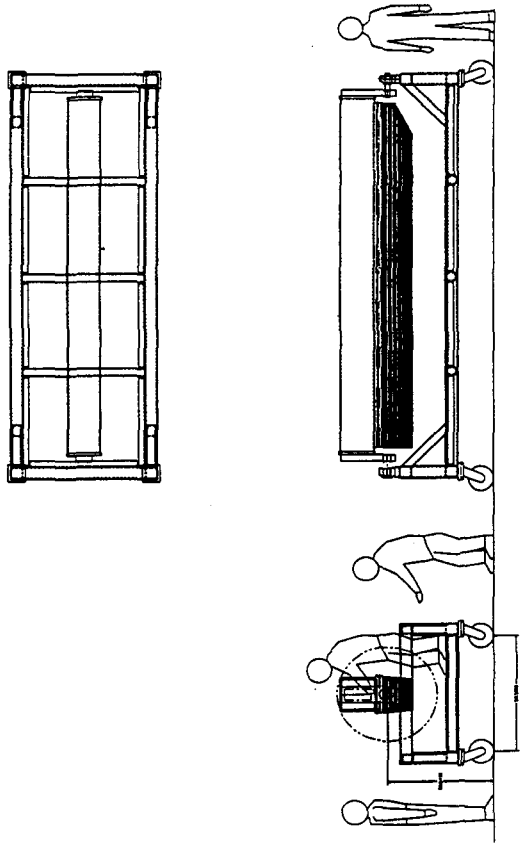

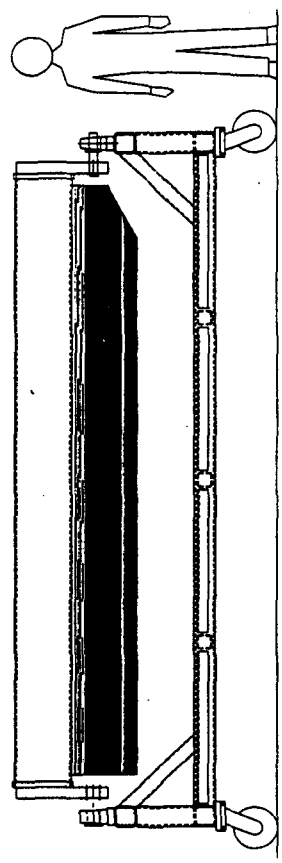

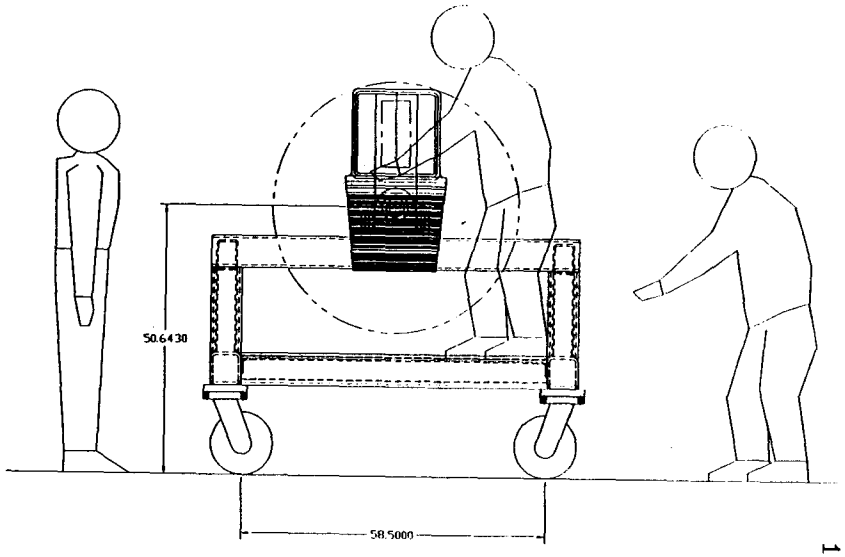

1110

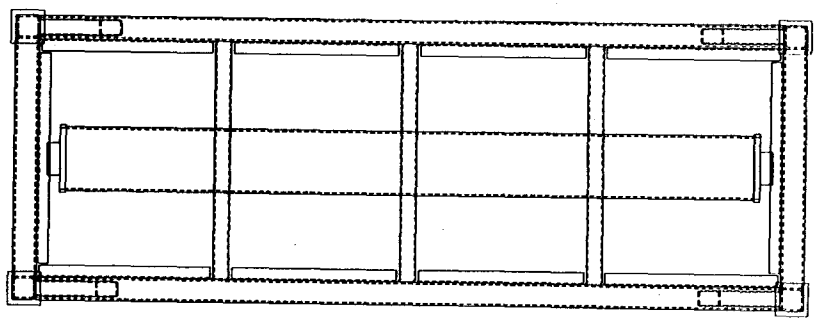

1141

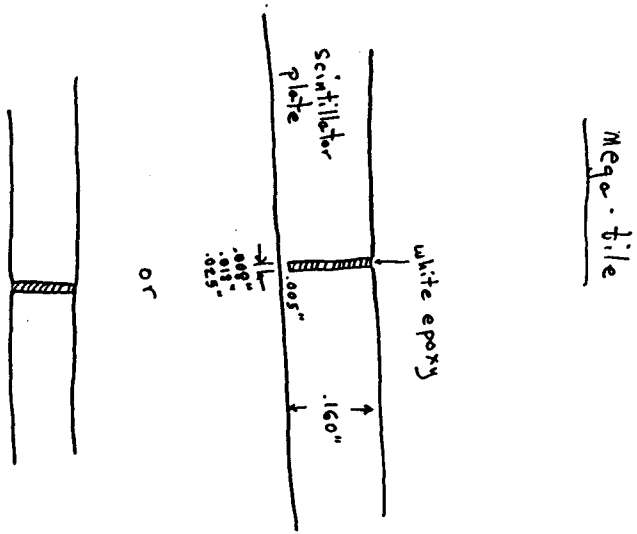

1112

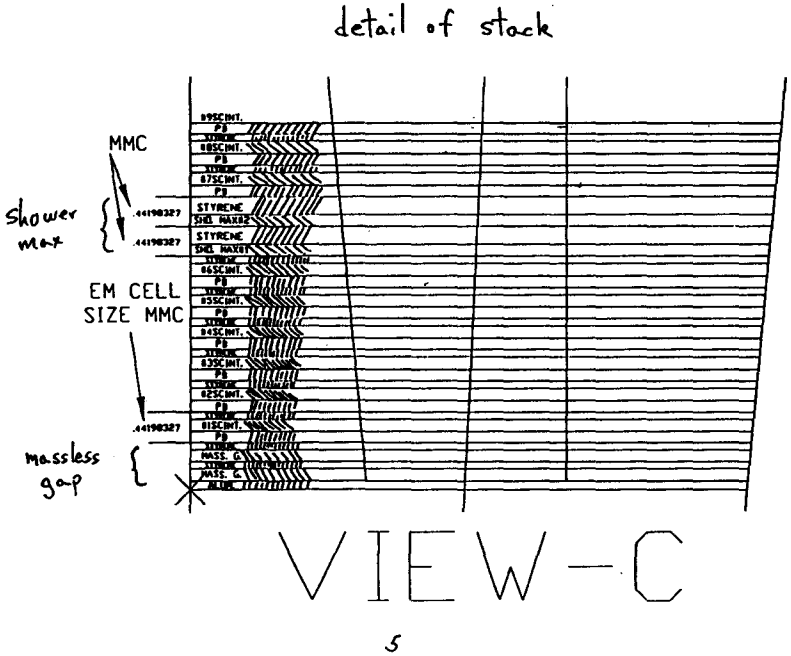

1113

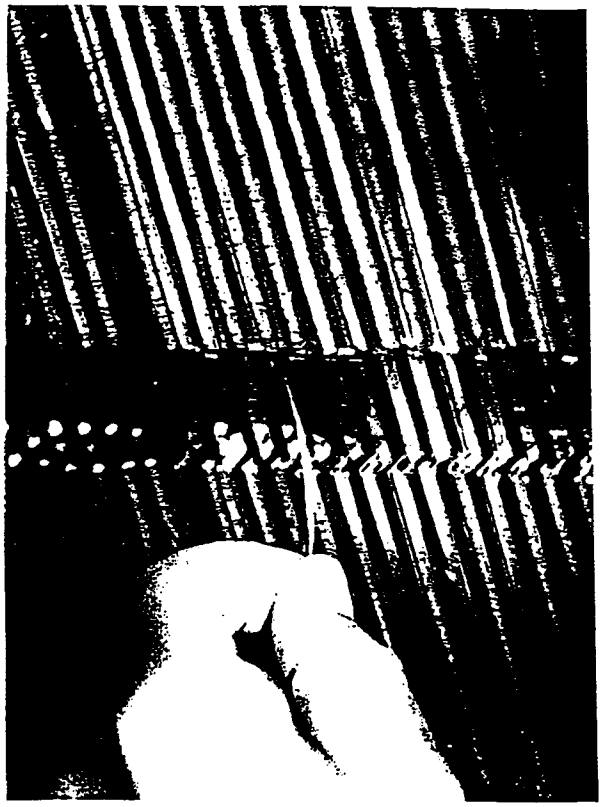

6

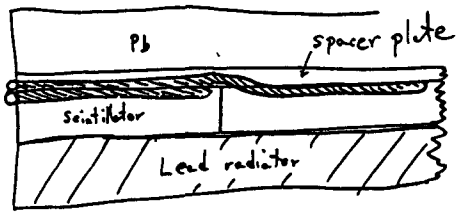

scheme for inserting fibers into inner tiles after assembly.

7

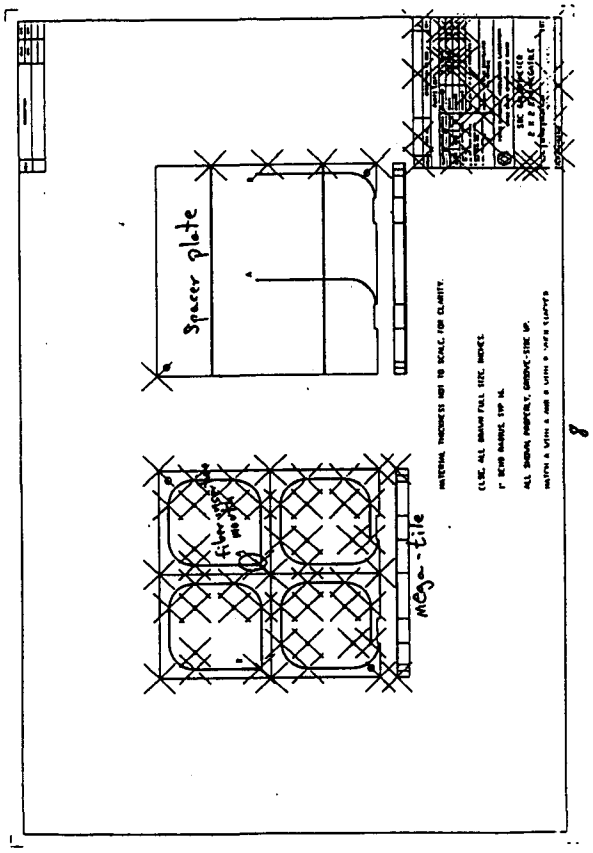

8

EXPERIMENT DATA

L(1)	L(2)	L(3)	μ
LEAD ON AL-MYLAR			
12.525	14.562	3.6675	0.23213664
12.525	14.562	3.5625	0.22030013
12.525	14.562	3.9666	0.25841365
12.525	14.562	3.7500	0.2360131
12.525	14.562	3.7500	0.2360131
		average =	0.23737536
		LOW=	0.22030013
L(1)	L(2)	L(3)	μ
LEAD ON SCINTILLATOR			
12.525	14.562	6.1250	0.45988536
12.625	14.562	5.0000	0.35344811
12.625	14.562	4.6750	0.34169763
12.525	14.562	4.5625	0.31312635
12.625	14.562	5.2500	0.37666663
12.625	14.562	5.5000	0.40008965
		average =	0.37418599
		LOW=	0.31312835
L(1)	L(2)	L(3)	μ
SCINTILLATOR ON MYLAR			
12.625	14.562	4.9880	0.35215277
12.525	14.562	4.8800	0.34051366
12.525	14.562	5.5120	0.40122024
12.525	14.562	5.7930	0.42787368
12.525	14.562	5.6470	0.40452068
12.525	14.562	5.0220	0.35548457
		average =	0.3802943
		LOW=	0.34051366
L(1)	L(2)	L(3)	μ
SCINTILLATOR ON SCINTILLATOR			
12.525	14.562	5.5650	0.40822008
12.525	14.562	6.7000	0.51697569
12.525	14.562	5.8840	0.44621473
12.525	14.562	6.2800	0.47505311
		average =	0.4611159
		LOW=	0.40822008

1118

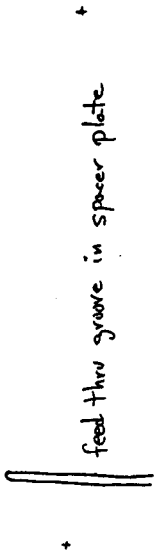

10

1119

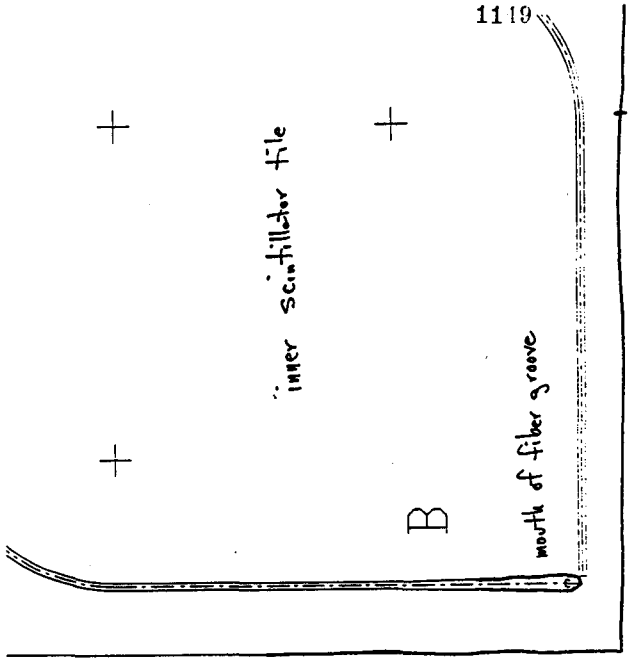

11

1150

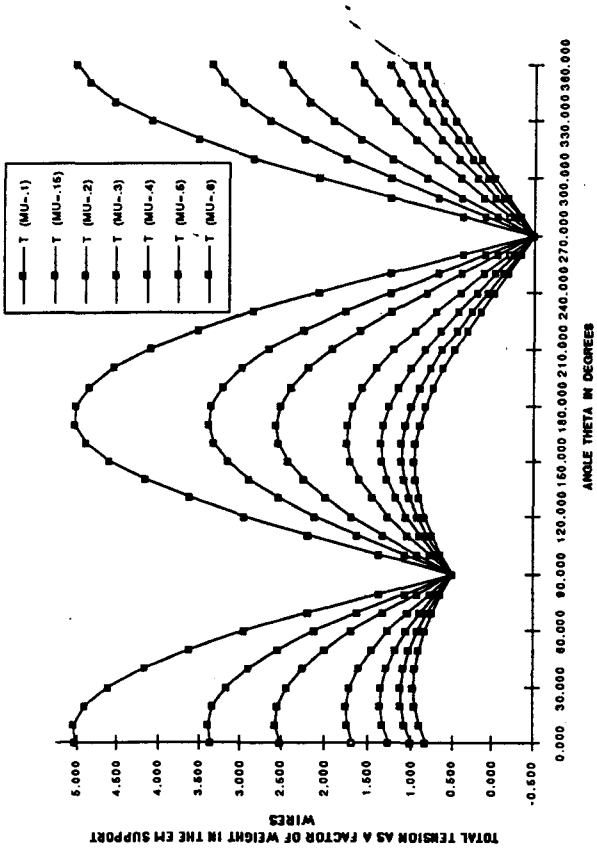

1151

Prototyping Schedule

- calorimeter in test beam at BNL
  May 21

  2 modules 2X3 towers, realistic cracks

  2mm pb, 4mm scint. (180 mega-tiles)

  $\sim 9\%/\sqrt{E}$ target resolution

  measure uniformity, light yield
- full length mechanical prototype in mid-June
  study assembly strategy, fiber routing
- engineering, costing studies

SDC BARREL EM PROTOTYPE MODULE
(FNAL)

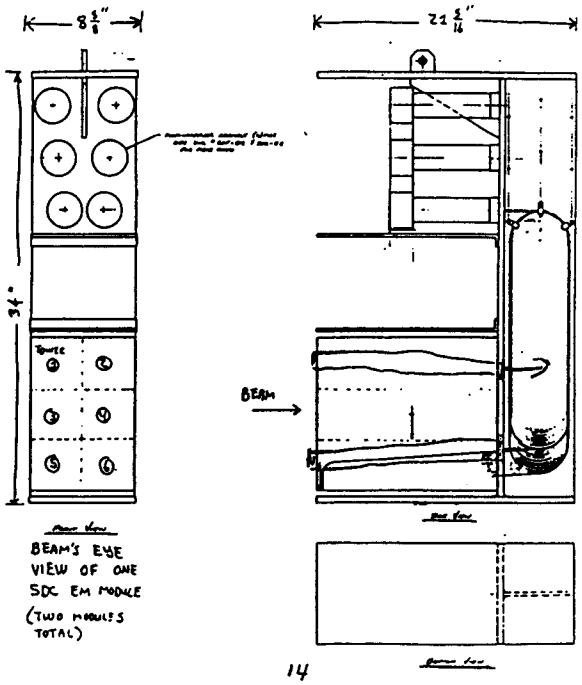

BEAM'S EYE VIEW OF ONE SDC EM MODULE (TWO MODULES TOTAL)

Fabrication of Tiles and Fibers for the SDC Calorimeter

presented by K. Hara (University of Tsukuba)

CONTENTS :

1. Number of Scintillator Tiles and Groove Length
2. Grooving
   - Laser Milling
   - Injection Molding
   - CNC Machining
3. Tile Edge Cutting and Painting
4. Fiber Mirroring
   - Aluminum sputtering / evaporation
   - painting white
5. Waveshifting Fiber and Clear Fiber Splicing
   - heat splicing
   - splicing using glue
   - small connector
6. Summary

1. NUMBER OF TILES (ave. tile size) AND GROOVE LENGTH

	Barrel	Endcap
EM	184、000 (12 cm sq) 70 km	83、000 (11 cm sq) 27 km
HACs	59、000 (33 cm sq) 60 km	18、000 (32 cm sq) 17 km

All tiles are 4 mm thick ==> 48 tons 344,000 pieces 174 km

Scintillators could be produced in 6 months.

Small quantity for the prototype modules can be made within a month.

2. GROOVING

Methods for Cutting Grooves:

(1) Laser Milling method
..... Not as fast as we expected

(2) Injection Molding method
..... Response is NOT uniform

(3) Conventional Maching method
..... Most Promising

Laser milling

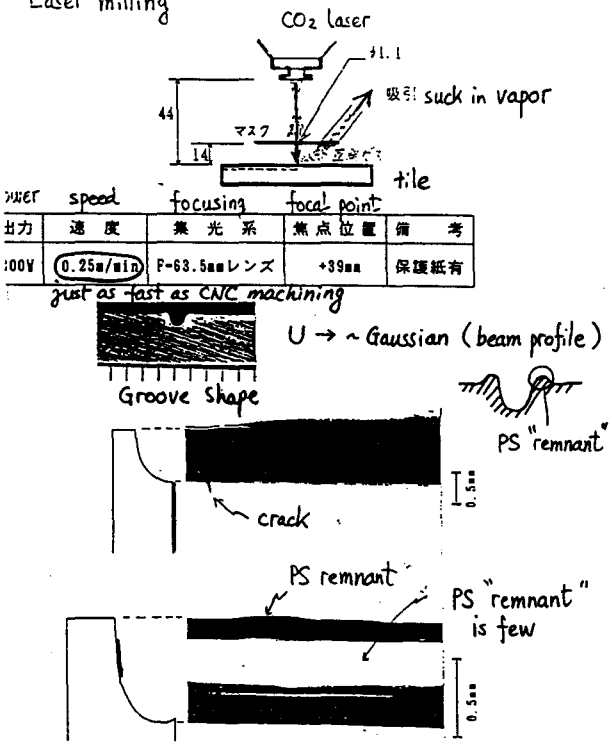

Response uniformity was measured by ^{106}Ru scan for the three grooving methods ....

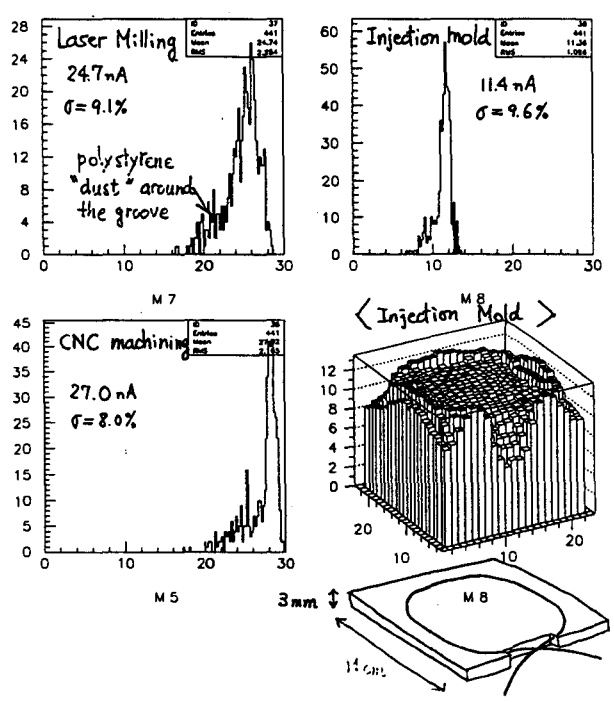

○ Laser Milling using CO_2 Laser

We adjusted the laser power and scanning speed,
At the best conditions,

- laser power : 300 W
- scanning speed : 25 cm/min
- sucking in polystyrene vapor instead of blowing off,

though,

- groove is gaussian reflecting the distribution of beam
- some polystyrene remainds around the groove
  => light yield is about 20% smaller
- scanning speed could be raised to ~100 cm/min, but not more
- laser equippment is not cheap

○ Injection Molding the Tiles with Groove

light yield is about 50%
response is not uniform (response is high near groove)

The groove is made smooth.
=> most of lights are reflected at the groove surface and not absorbed by the fiber.

Lights emitted near the groove are "selectively" absorbed.

○ CNC Machining : A history in Japan

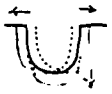

(A) U shaped grooves were used to be machined by scanning with the endmill 4 times => tiles for Raddam tests
(B) U or square shaped grooves of 1 mm deep can be made by single scanning at 300 mm/min (7000 rpm)
Ball groove can be made by additional pass at 700 mm/min
(C) Using a Thermwood machine, 1 mm deep square groove can be made at 1700 mm/min (16000 rpm)
2 mm deep groove (for ball groove) needs to be machined by 2 scanning

1 mm deep 2 mm deep + ball head

To machine 180 km of U/square (ball) groove, it takes

option (A) : 40,000 hrs (80,000 hrs*) = 4.6 years (9.1 years*)
option (B) : 10,000 hrs (14,000 hrs*) = 1.2 years (1.6 years*)
option (C) : 1,800 hrs (5,300 hrs*) = 0.2 year (0.6 year*)
* loss time for exchanging endmill/ballhead mill not included.

Realistically option (B) using 5 (7 for ball groove) machines or
option (C) using 1 (2-3 for ball groove) machines
can be adopted to finish in 2 years (1 day = 8 hrs)

⇨ Need to investigate the most efficient procedure for (automatic) setting of tiles on the stage, exchanging the mills, etc.

Groove Shape / Milling Speed and Light Yield

questions: Can we increase the milling speed without losing the "performance" ?
How precise should the groove shape be ?
"performance" :-light yield, uniformity, any mechanical damage

For 0.83mmφ fiber

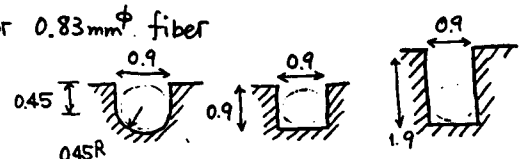

groove shape :	U	0.9x0.9	0.9x0.9	0.9x1.9
speed(mm/min)	300	300	1700	1700+1700 (2 passes)

○ light yield at the center of tiles (5 samples, each)

average #PEs	4.53	4.46	4.21	4.25
(ratio	1 :	0.98 :	0.93* :	0.94)
r.m.s #PEs	0.13	0.17	0.08	0.08
(rms/average	3% ≲ 6%	4% ≲ 9%	2%	2%)

*Light yield of single-pass U is lower by 10% than 4-pass U

○ Response uniformity around the groove compared to that around F300 (mm/sec) square groove,
Response on U-shaped groove is the smae within 2%
Response on F1700 square groove is the same within 1%
Response on 1.9 mm deep groove is about 40% lower

< square >
F300

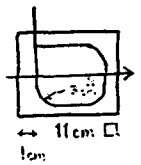

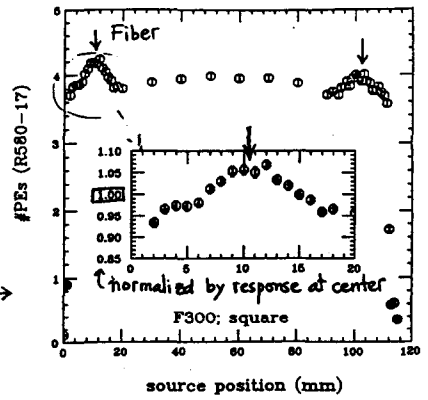

< U shaped >
F300

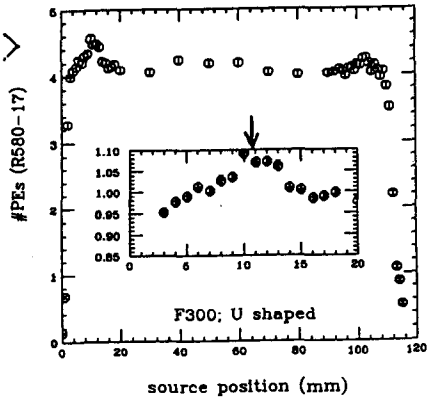

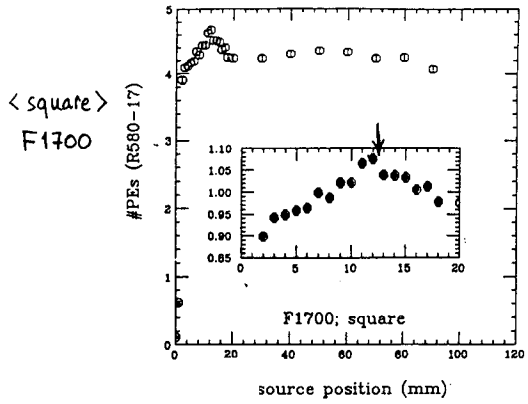

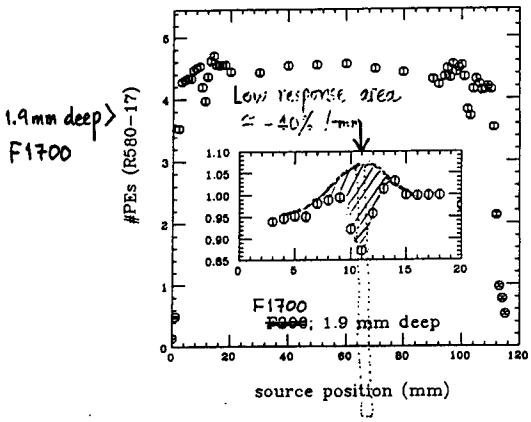

L.Y. could be different by 6% between ∪ in ⊔

In order to achieve response uniformity better than 2% . . . .

- "R" of the endmill head be precise to < 0.1 mm (light yield) by 9% between
- speed (roughness of groove surface) < "300" mm/min (L.Y.) F300/1700

-> The roughness may depend on durability of the mill.
Need to machine many tiles and measure light yield.

- groove depth be precise to < 60 μm (uniformity)

<-- Response on the groove is approximately proportional to the scintillator thickness ~~groove depth~~ $3.1^{t}_{mm} : 2.1^{t}_{mm} = 1 : 0.68 \simeq 1 : 0.6$

★ The requirement could be relaxed because of wider shower spread. May be possible to groove several paths at once on a motherboard using a multi-axis milling machine. (tile thickness can vary 200 μm at maximum...) Need a simulation.

○ Residual strain is not recognized even for the grooves machined at the highest speed.

may assist in craze developing

Strain measured with an apparatus using Babinet's compensator: Desired optical path difference is generated by changing the path lengths in quartz wedges with specific n. Measure displacement to get non-shifted/distorted interference fringes

$$F = \frac{\Delta_{(nm)}}{C\sqcup_{(cm)}}$$

with $C_{PS} = 55\ (kg/cm^2)^{-1}$

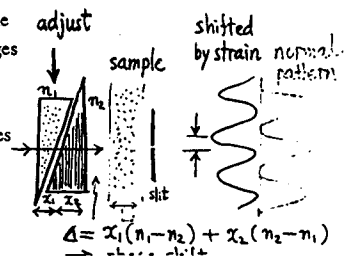

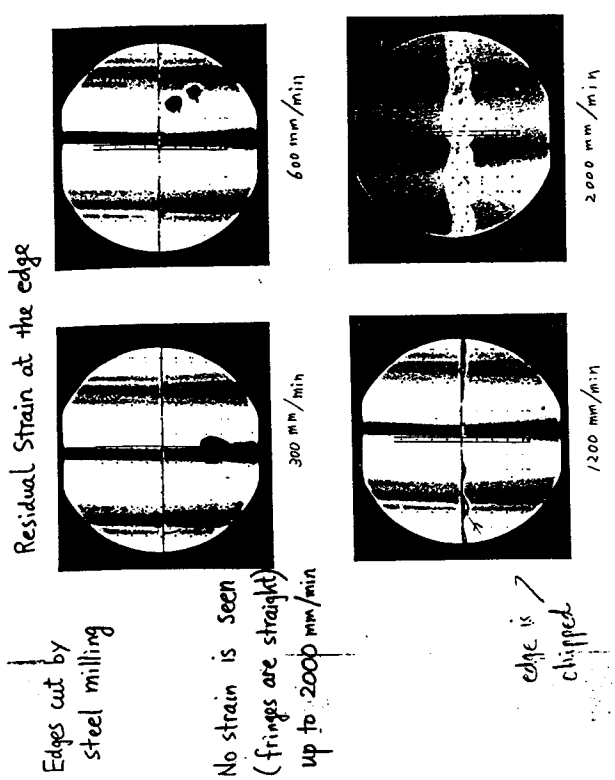

3. TILE EDGE CUTTING and PAINTING

Tile edge could be cut at 1700 mm/min using Thermwood (we havn't tried yet)

- It would take 2,300 hrs (0.8 year at 8 hrs/day).

Using a steel endmill, tile edge can be cut at 600 mm/min and 8-10 tiles at once (7000 rpm). At a higher speed, tile edge is chiped.

- It would take 820 hrs (0.3 year at 8 hrs/day). Loss time in machining procedure is not included.

questions: Can we increase the cutting speed without losing the performance ?
Can we make "Mega-tile"? -> no answer yet

○ Response uniformity near the edge

(a) edge cut by steel mill at 600 mm/min + painted white
(b) edge cut by steel mill at 300 mm/min + painted white
(c) edge cut and polished (diamond) + painted white
(d) edge cut and polished + white paper
Tile wrapped in white paper

-> (a) = (b) within 3%, (a) = (c) = (d) within 2%

Response uniformity is barely sensitive to edge surface, polished or painted white.

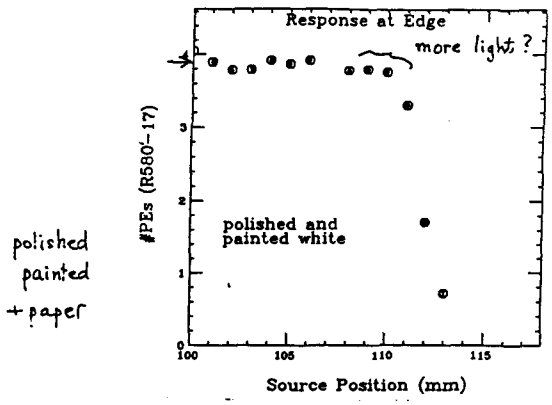

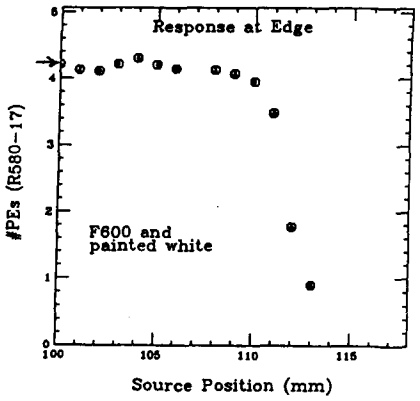

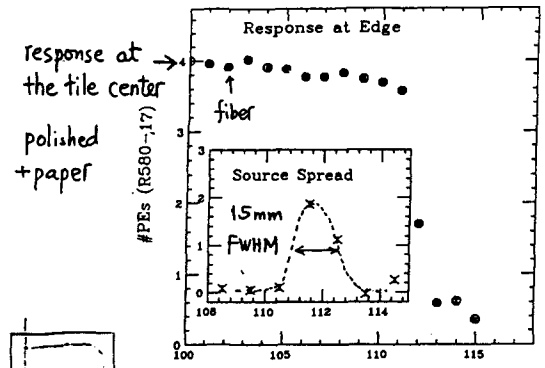

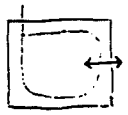

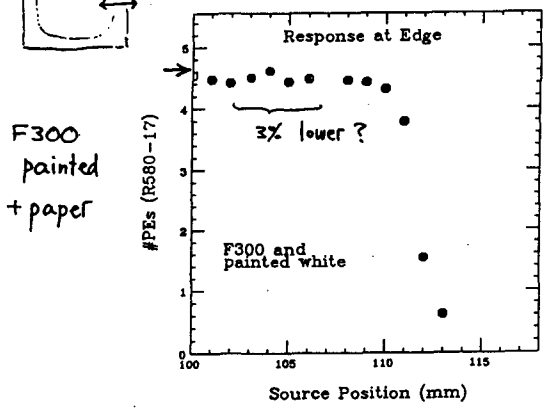

○ Redisual strain at the edge is not seen.
Residual

→ Need to measure for F1700 ones: Probably no strain

○ Adhesive strength/Radiation hardness of the white paint
white paint : BC-620 & NE560

- Adhesive strength after 1000 hrs at 60°C will be measured next month. (test under way)
- NE560 was radiation tested up to 7 Mrad and was OK. BC-620 was also measured by Fermilab/FSU and was OK.

Painting procedure is under consideration.
(Robot, or Man with a brush/roller)

Mega-tile is under consideration

4. Fiber Mirroring

The necessary quanitity of waveshifting and clear fibers could be produced in 10 months.

Mirroring the fiber end:
(A) Aluminum sputtering for 75 cm Y7 (1 mmϕ, 250 ppm)
(B) Aluminum evaporation + topcoat (acrylic paint), and
(C) Paint* white for 65 cm Y7 (0.83 mmϕ, 180 ppm)
*Surface is expected to be stable (against oxidation) compared to aluminum.

We measured (1) Increase of light when illuminated near end
(2) Attenuation curve
(3) Light yield when embedded in a tile

(1) In aluminum sputtering the reflectivity depends on surface flatness. Best result (89% more light with a variation of 3.2% compared to typical fibers with blacked end) was obtained when the ends are polished "chemically"

By aluminum evaporation or painting white, the light yield increases by 82% (4.2% rms variation).

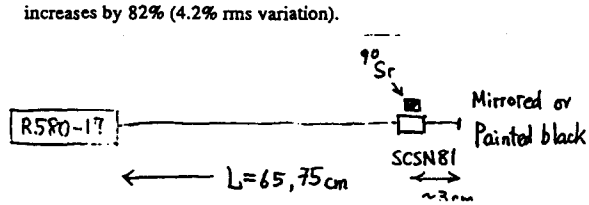

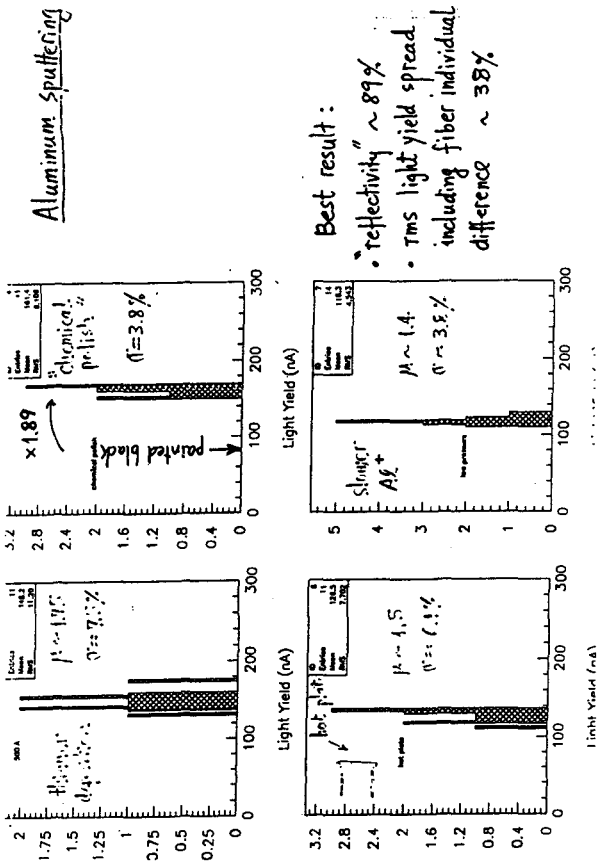

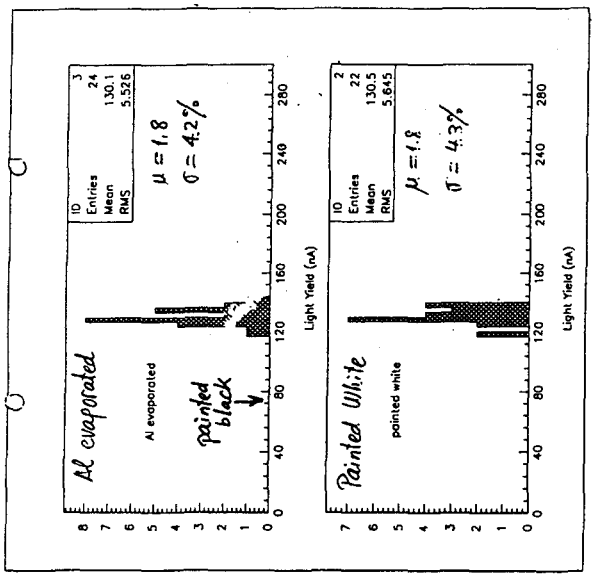

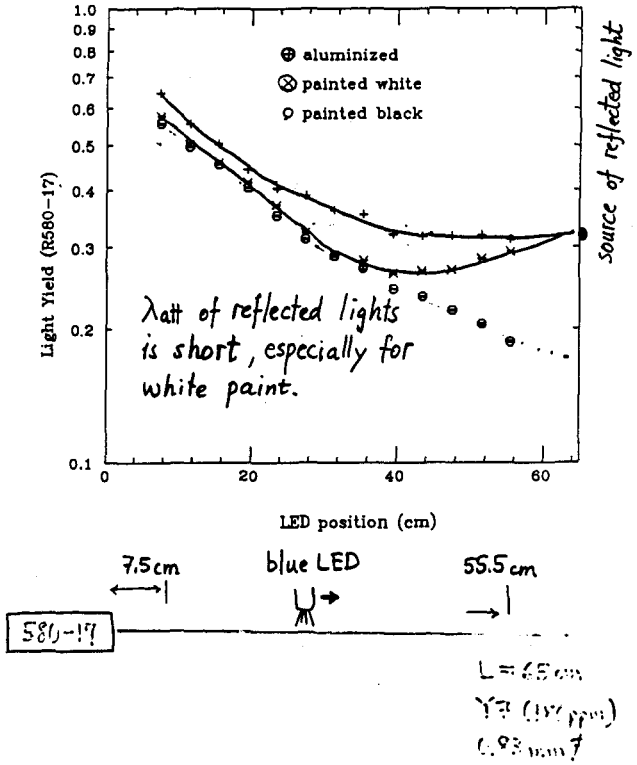

○ Attenuation curve

The attenuation curve of 65 cm long Y7 fibers (180 ppm) was measured by scanning with a blue (λ=470nm) LED.

Light yield increases certainly for mirrored fiber.
Light reflected by white paint shows short attenuation length and "disappears" after 30 cm.

○ Light yield

Mirrored fiber was embedded in the tile without damaging the end. The light yield was compared with the case the end was cut.

Al evaporation : 40% increase*
painted white : 22% increase*

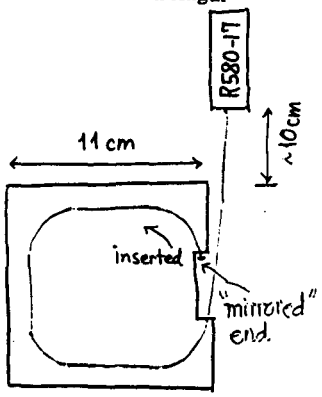

Al sputtered, top coated+Al evaporated, painted white can be damaged during insertion.

* Actual value is dependent on fiber length, dye concentration (= attenuation length)

5. Waveshifting Fiber and Clear Fiber Splicing

(A) heat splicing, as established for CDF plug upgrade
(B) splicing using glue for better mechanical rigidity
(C) connector for mechanical rigidity and easy calibration

(A) Heat splicing -

We have an experience of splicing about 200 fibers for the Raddam modules, using a glass tube and a Nichrome wire.

-> The light transmission was 90% with 5% rms variation.
-> Mechanically the joint is fragile

We started to investigate a method using a teflon* tube that
- adjusts the fiber axes,
- conducts heat to the joint,
- supports the joint mechanically

*material be selected, since teflon becomes breakable due to radiation

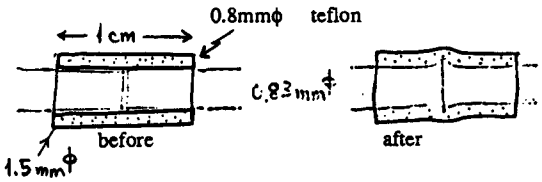

The first 3 samples showed 91.7%, 95.9%, 93.5% light transmission and mechanical strength increased "substantially"

*** Automatic splicer is under consideration. ***

(B) Splicing using glue

1 mmϕ fibers were glued together in teflon/stainless tubes. The glue (epoxy) was not used on the fiber end surface.

transmission : 68 - 76% for teflon tubes
73 - 80 % for stainless tubes

- stainless one is mechanically strong enough (up to 5 kgw) but teflon one is not (below 1 kgw).

- We worry about deterioration of glue due to radiation :

< Only specific glue is warrantable to use for long time. >

The samples were irradiated to ^{60}Co γ rays.

-> The glue (EP330) after 5 Mrad gets colored.
-> Mechanical strength is OK after 9 Mrad.

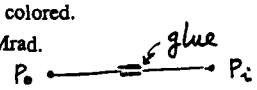

Clear fiber light loss due to radiation after 5 Mrad :

	1 m fiber		3 m fiber	
no glue	75.1%	3.8%	65.5%	0.1%
2 cm along	71.3%	2.7%	65.4%	1.1%
20 cm along	66.4%		63.4%	

Effect by glue 2 cm along the clear fiber is 4% for 1 m fiber and lifetime is shortened by 13%. Effect is larger for shorter fibers. Effect for 30 cm Y7 fiber is estimated to be about the same, since the lifetime of Y7 fiber is shorter than clear fiber.

→ Has to be confirmed

(C) Small size connectors

- Fiber-to-fiber connector is extremely useful in system integration (e.g. in endcaps), and quality control of tile/fibers is made possible using the components as they will be.
- Splicing with a connector is mechanically strong.

○ For 1 mmϕ fibers
(a) 8 ch disconnectable connector
(b) single ch disconnectable connector: by-product of (b)
(c) single ch Splicer

	(a) 8-ch connector	(b) 1-ch connector	(c) Splicer
size	5 x 21 x 26 mm³	5 x 7 x 26 mm³	3 x 5 x 10 mm³
T(%)*	83.5 (2.0)	84.0 (3.3)	88.9 (2.6)
durability	5% max	< 1%	2.5% max
cross talk	0.1% max	-	-

* Matching oil (silicon grease) was used, which increases the transmission by about 7%. Matching oil was radiation tested.

[3 clear fibers w/o M.O. -> T = 55.2% after 9 Mrad
3 clear fibers w/ M.O. -> T = 41.1% after 9 Mrad
M.O. loses 14% of initial light after 9 Mrad. Probably a few% at 1 Mrad, which is much smaller than the damage of tile/fiber.
-> wavelength dependence?]

Problems:
o Worse durability (reproducibility) of 8-ch one compared to 1-ch one is due to too thin latch thickness.
o Found weakness against heat
o Seems difficult to find space for Splicers
- > change material (ABS resin) to 3-3PA(nylon)
- > slightly thicker latchs for 8-ch connector
- > smaller size Splicer

○ For 0.83 mmϕ fibers.

- fibers in the same axis
- bare fibers be polished

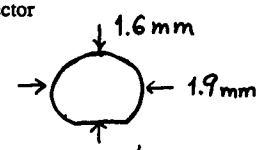

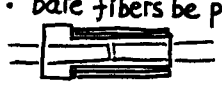

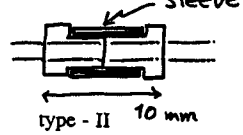

	type - I	type - II
T(%)	94.5 (1.8) *	94.6(2.2)

*matching oil used

New 8-ch connector shows T = 79.3% (4.4) w/o M.O. and T = 89.2% (3.4) with M.O. and latching works (too) fine. Transmission changes by 2% at 60°C and by 5% at 75°C.

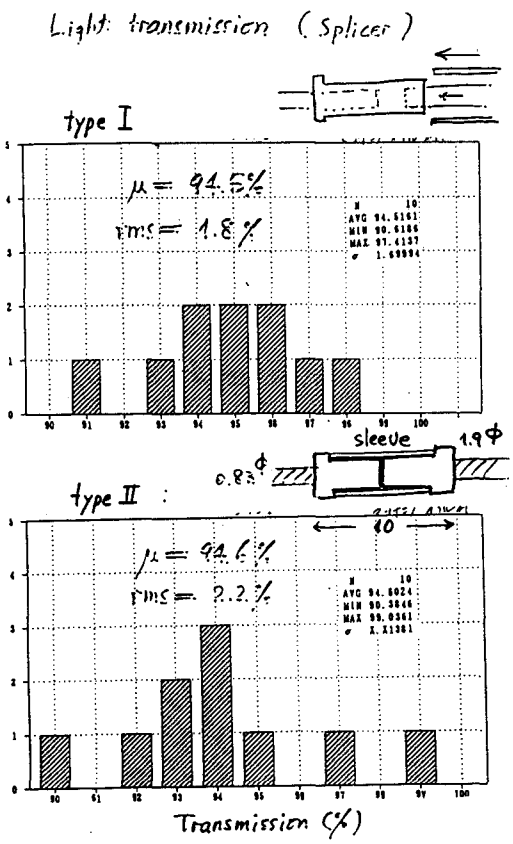

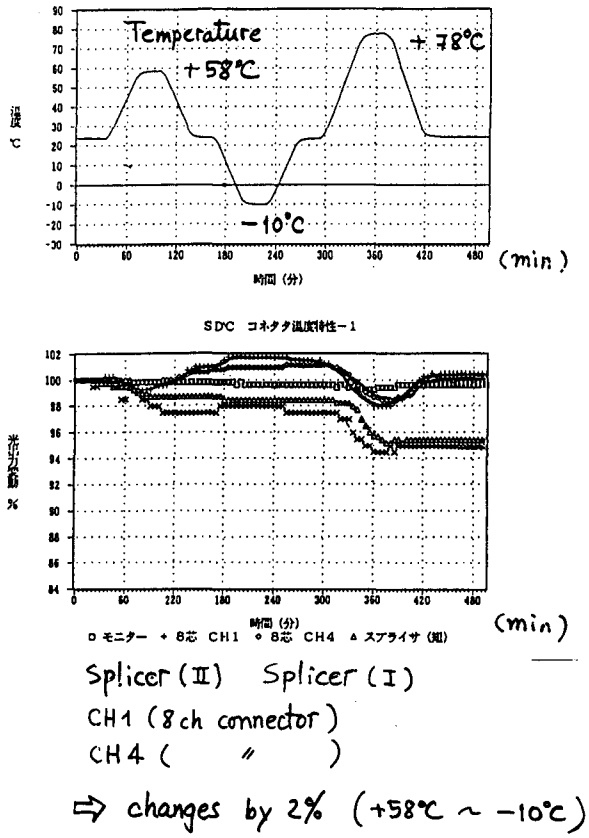

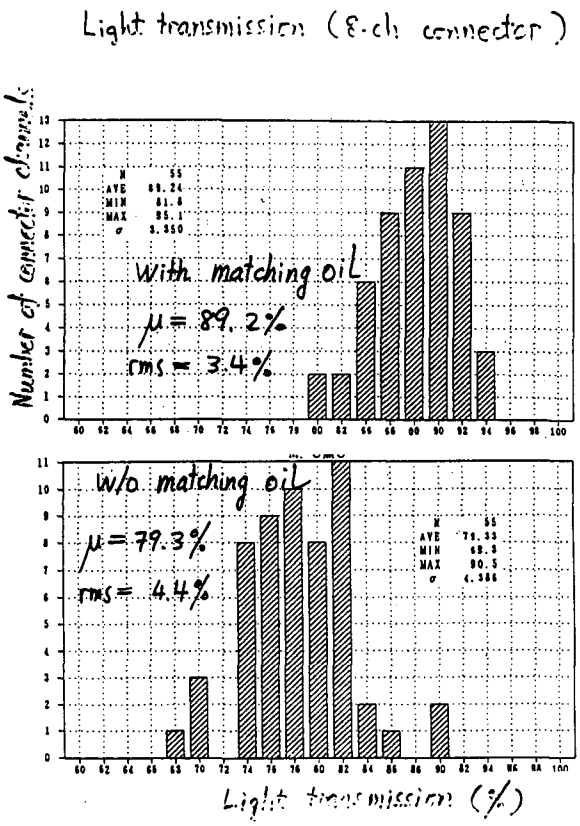

6. SUMMARY

1) Tile grooves can be made optically best by CNC machining. In order to finish all grooving in 2 years, 5(7) conventional CNC machines, or 1(3) high revolution/ speed Thermwood machines are needed for U/square (ball) shaped grooves. Groove depth be precise to 60 μm (?)
Groove roughness be controlled -> need to investigate how much light yield changes when the same cutter is used.

2) Tile edge could be cut in reasonably short time (4-10 months) either by a conventional machine or by a Thermwood. The surface roughness is not much important when painted white. (Tests using Thermwood need to be done)

3) Fiber mirroring

The light yield increases by 80-90% by aluminizing/painting white the fiber end. Light yield increases by about 40% when the aluminized fiber is embedded in the tile, but increases by about 22% for the painted fiber. Evaporated aluminum with topcoat and sputtered aluminum are damaged during insertion.

Light yield variation of 3.8% (rms) was obtained for the best sample including mirroring and fiber individual difference.

4) Splicing

Heat splicing seems to work through a (flexible) tube, which helps align the fiber axes and support the joint afterwards. More investigation and apparatus development are under way.

Small amount of glue seems possible to use at the joint without deteriorate much the transmission up to 5 Mrad. More detailed tests are required.

Small connector (1.9 mmϕ 10 mm long) provides light transmission of [redacted] 94.6% and an rms spread of 1.8%.

5) Tiles and Fibers can be fabricated.

Procedure (including calibration) for making tile/fiber assemblies (or Mega tiles) has to be established.

Our Raddam tile/fiber sample showed an rms light yield variation of 5.7% (max. deviation 13%), although fiber end polishing may have been premature.....

○ Ultrasonic welding for fixing fiber in the groove

UV curing epoxy is considered to fix the fiber in the groove.

If this epoxy turns out to be radiation soft,
we need alternative method or ball groove, or insert fibers in the tiles that are already positioned in the "structure".

-> A ultrsonic welder can cramp plastics, but not the tile itself which is cross-linked. (Cross-linked one becomes flaky)

-> Prepare pieces of non-cross-linked plastics (e.g. fiber) and be positioned through a kind of masking sheet

"Mega tile" .... ?

Two versions of Mega tile were produced for CDF plug upgrade .....

① Cut into pieces and glue them together
... mechanically not strong enough

② milled through and the gaps filled with white paint
... mechanical strength is ~OK.
X-talk ≲ 1%

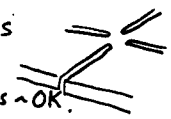

Test on

③ similar to ② but the gaps filled with white PS plate (with glue on both sides). PS plate is ultrasonic welded..

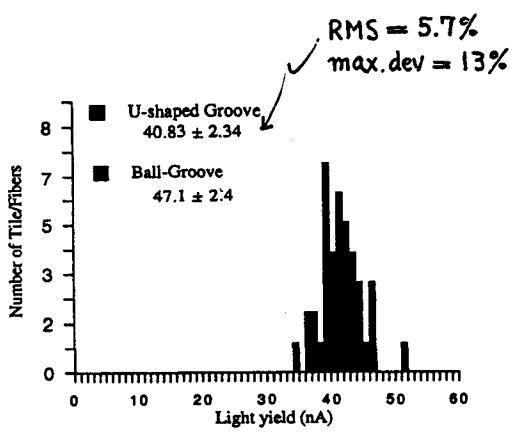

May 27,1992
Y.Miyamoto

Ageing Test of Bent Fibers

Plastic fibers in the SDC Tile/Fiber calorimeter are used in some curves. In this case the "Bending Loss" and the "Static Fatigue" are expected to be caused.

This time we measured the light loss of bent fibers and performed a few ageing tests : in normal condition and after heat cycle.

We also followed up the signals from Tile/Fibers after assembly.

List of Contents

1.Light Loss Caused by Fiber Bending
2.Signal Variation with Time of Curved Fibers
3.Heat Cycle Test of Curved fibers
4.Signal Variation with Time of Tile/Fibers
5.Summary & Future Plan

1 Light Loss Caused by Fiber Bending
a) Setup

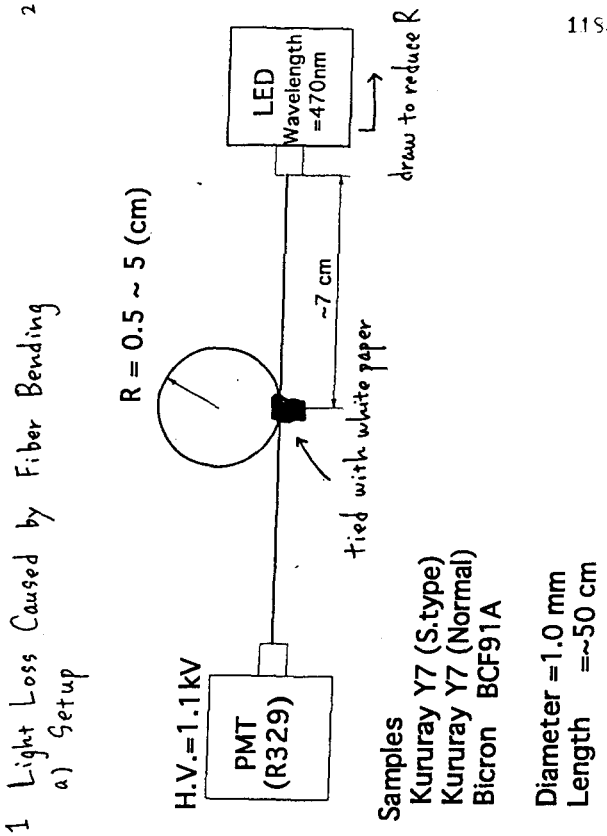

2 Light Loss Caused by Fiber Bending
b) Result

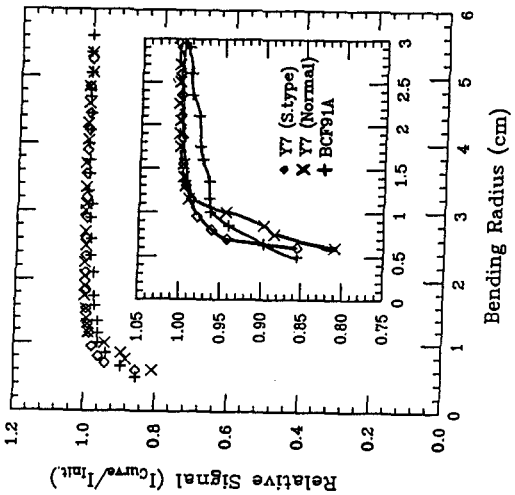

2 Signal Variation with Time of Curved Fiber
a) Setup

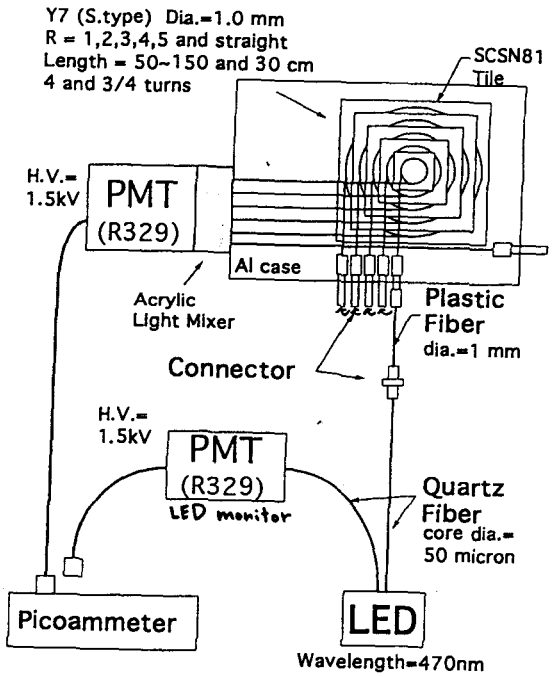

3. Heat Cycle Test of Curved Fiber

a) Setup

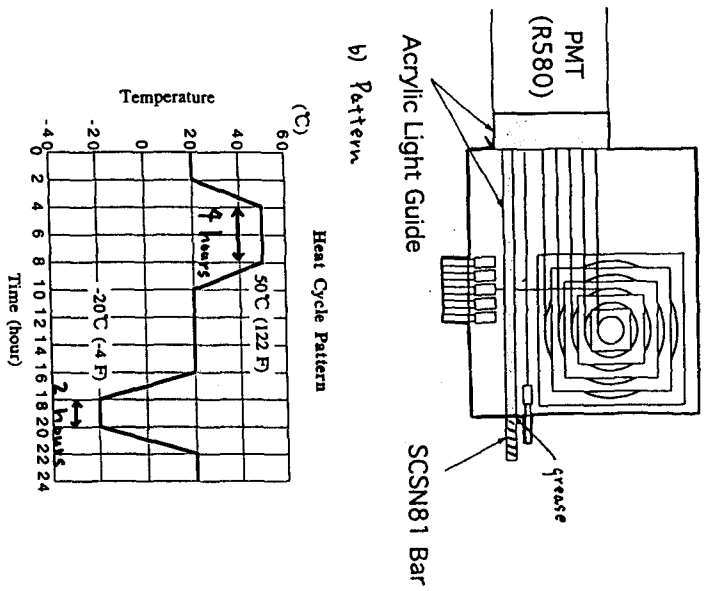

b) Pattern

2. Signal variation with time of Curved Fiber

b) Result

note: Light yield depends mainly on
- fiber length
- contacts at both ends (C1, C2)

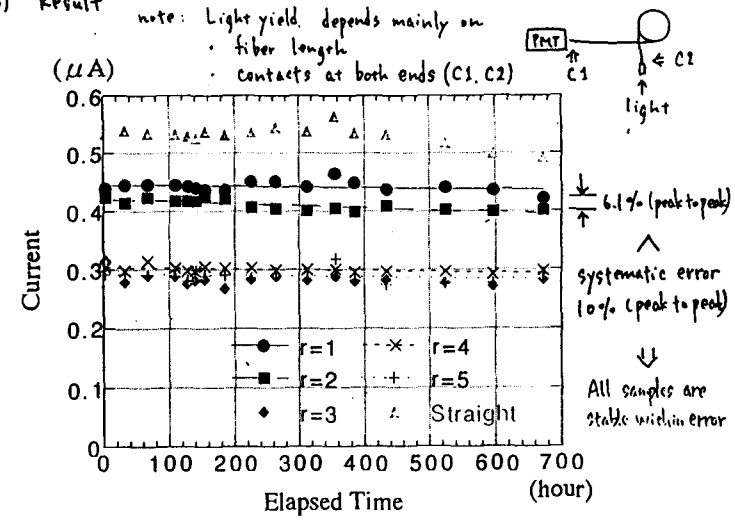

3. Heat Cycle Test of Curved Fiber

c) Result

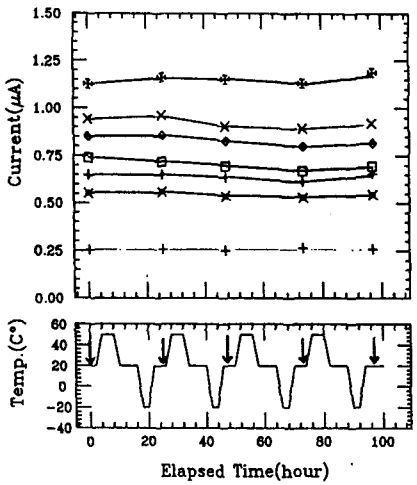

	fiber length	signal variance (peak to peak)
● Straight	26 cm	5.4%
× R=1 (cm)	57 cm	7.8%
◆ R=2 (cm)	95 cm	9.1%
■ R=3 (cm)	99 cm	10.3%
+ R=4 (cm)	122 cm	6.6%
× R=5 (cm)	146 cm	5.8%
+ BAR (Reference)		3.2%

Max variance 10.3%

⇕

systematic error ~10%

a) Setup

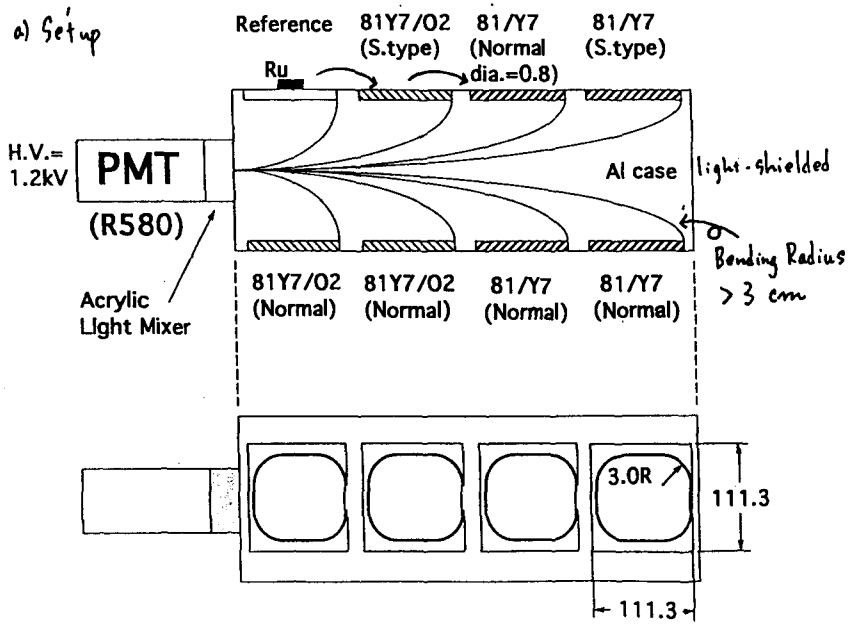

4 Signal Variation with time of Tile/Fiber

b) Result

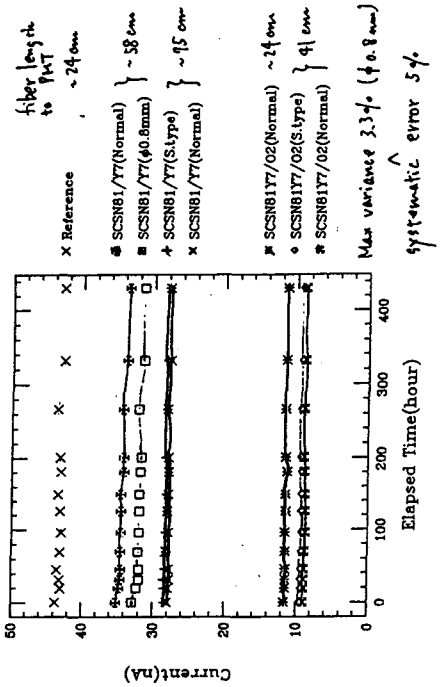

Summary

1. Bending loss was found at
   R < 1.5 cm for Y7 (Normal, S.type)
   R < 3.0 cm for BCF91A
2. & 3. signal variation with time of bent fiber
   In the range of R = 1 ~ 5 (cm)
   Y7 S.type fibers are stable within the error
   · during first 700 hours in normal condition.
   · after 4 times of heat cycle.
4. signal variation with time of Tile/Fiber
   For the Tile/Fiber with a fiber path radius of 3 cm, no decrease of signal was recognized during first 400 hours in normal condition.

Future Plan

1. More accurate measurement
2. Test of some other fibers ex. φ0.83mm, φ0.75mm
3. Heat cycle test of Tile/Fibers

1992 / 5 / 27

Optics Design of Prototype EM Tile / Fiber

Masakazu Okabe

We have been investigating the groove path and shape to achieve good transverse uniformity and high light yield.

CONTENTS

1. Samples
2. Setup for Measurement
3. Groove Path
4. Groove Shape
5. Conclusions

1. Samples

Tiles are 111 mm by 111 mm and 4 mm thick SCSN81 with edges polished. (Some tiles are painted white.)
Tiles are wrapped in white paper, or aluminized mylar.
Fibers are 150 ppm Y7 with a diameter of 1 mm.
Fiber end is not mirrored.

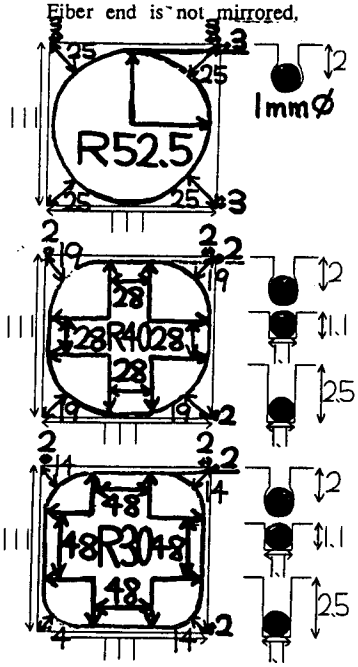

2. Setup for Measurement

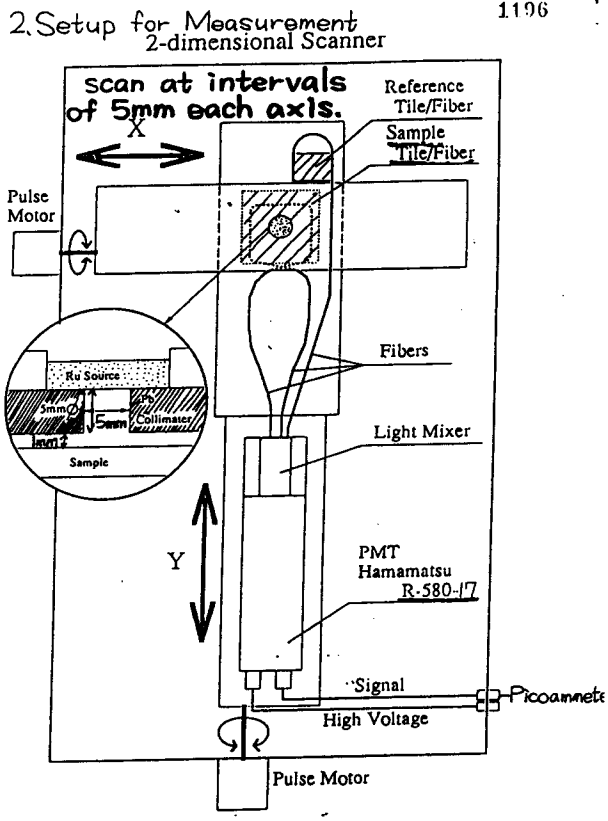

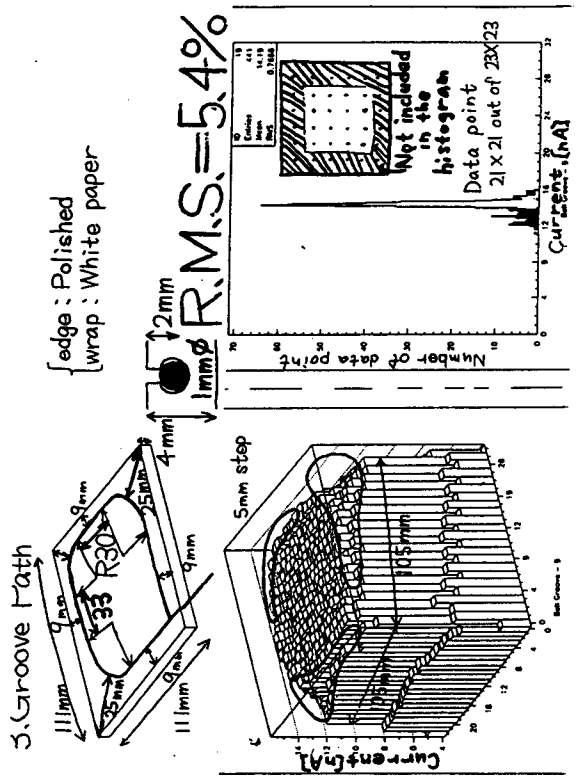

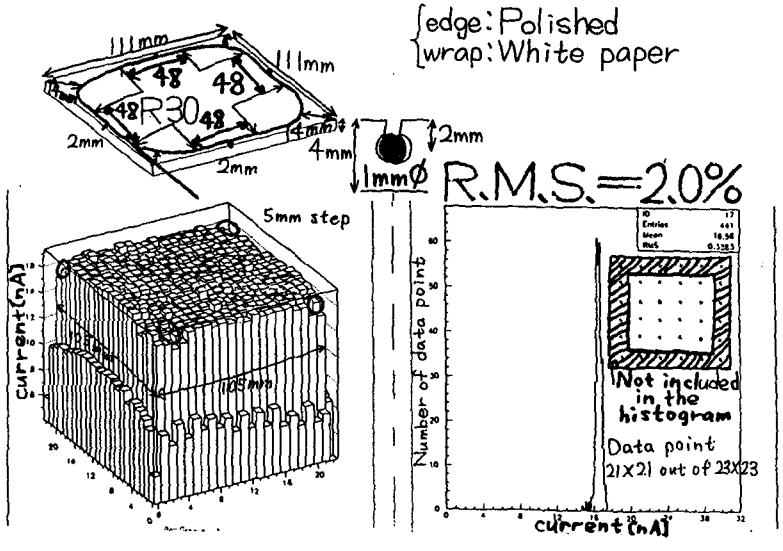
edge: Polished
wrap: White paper
111mm
111mm
48
48
R30
48
48
2mm
2mm
4mm
4mm
2mm
1mmØ
R.M.S.=2.0%
5mm step
current [nA]
105mm
Number of data point
Not included in the histogram
Data point
21X21 out of 23X23
current [nA]

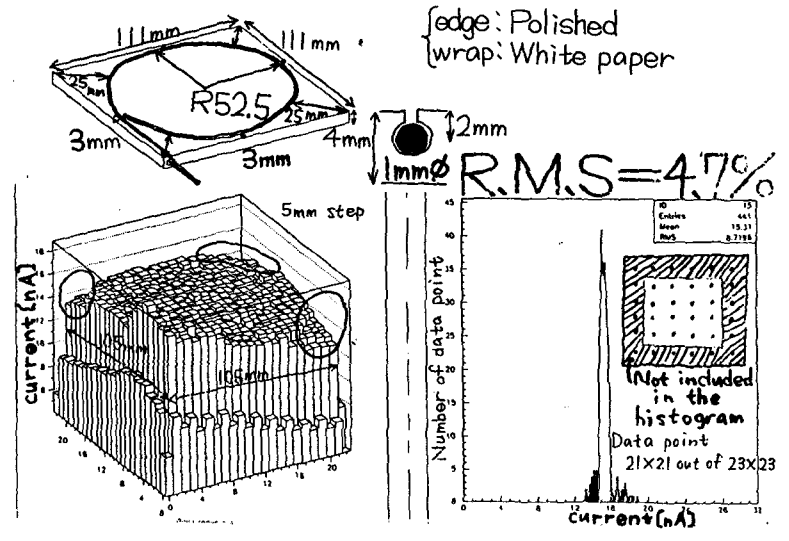
edge: Polished
wrap: White paper
111mm
111mm
25mm
R52.5
25mm
3mm
3mm
4mm
2mm
1mmØ
R.M.S=4.7%
5mm step
current [nA]
105mm
Number of data point
Not included in the histogram
Data point
21X21 out of 23X23
current [nA]

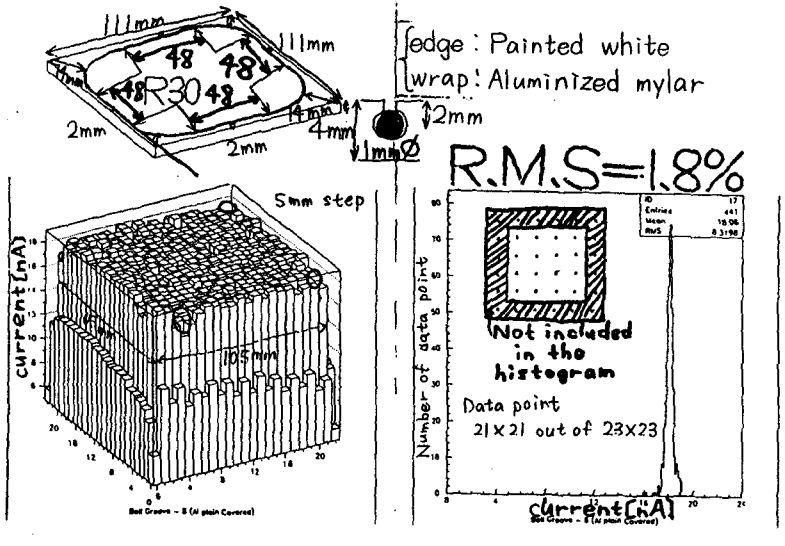
edge: Painted white
wrap: Aluminized mylar
111mm
111mm
48
48
R30
48
48
2mm
2mm
4mm
4mm
2mm
1mmØ
R.M.S=1.8%
5mm step
current [nA]
105mm
Number of data point
Not included in the histogram
Data point
21X21 out of 23X23
current [nA]

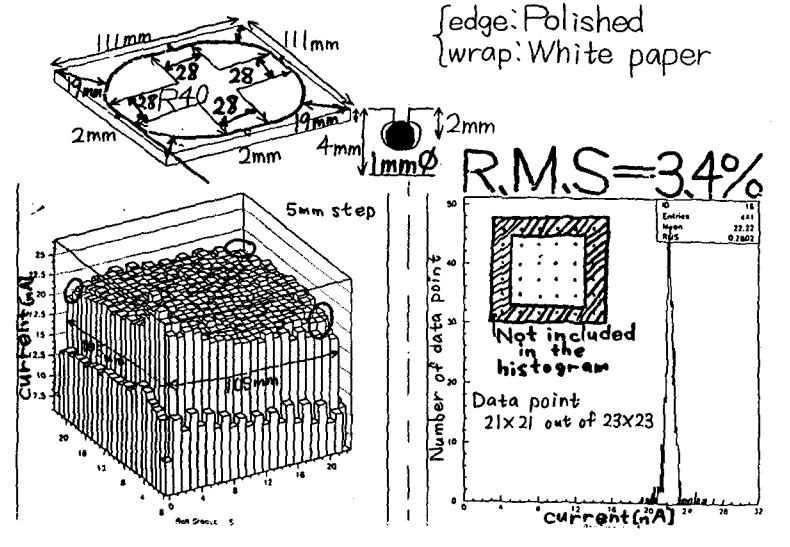
edge: Polished
wrap: White paper
111mm
111mm
28
28
R40
28
28
19mm
19mm
2mm
2mm
4mm
2mm
1mmØ
R.M.S=3.4%
5mm step
current [nA]
105mm
Number of data point
Not included in the histogram
Data point
21X21 out of 23X23
current [nA]

4. Groove Shape

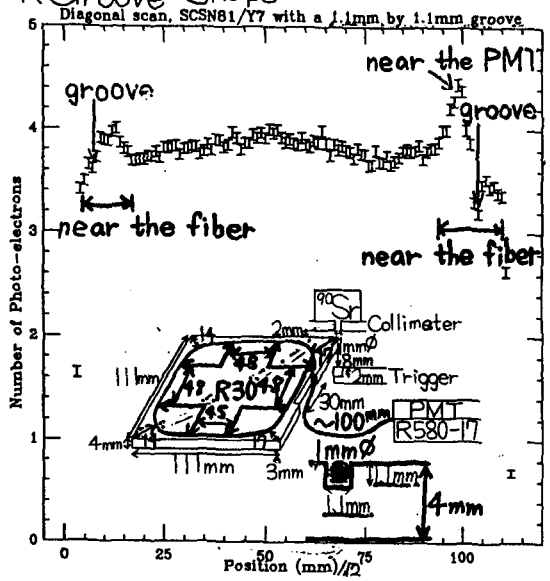

1201

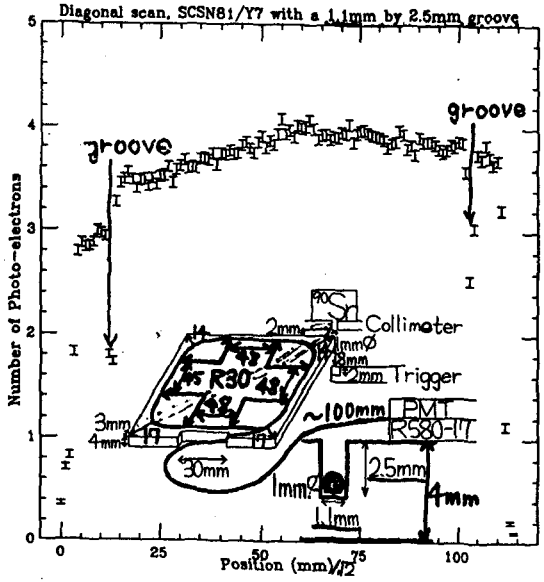

1205

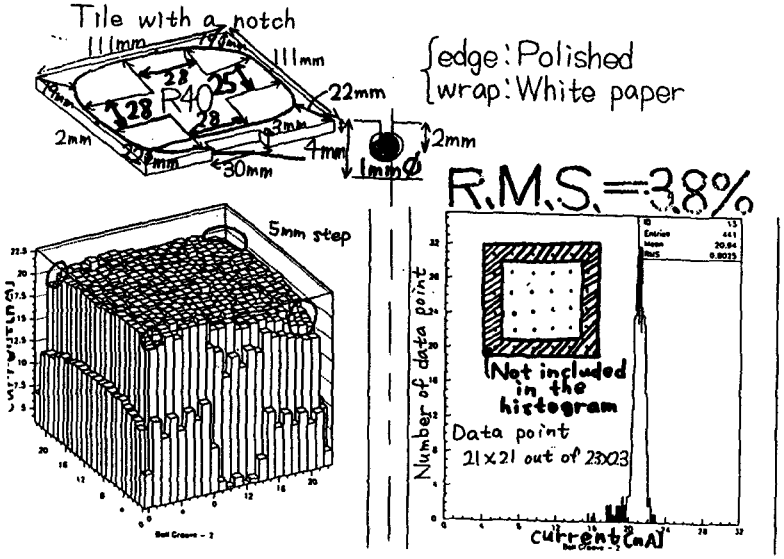

1202

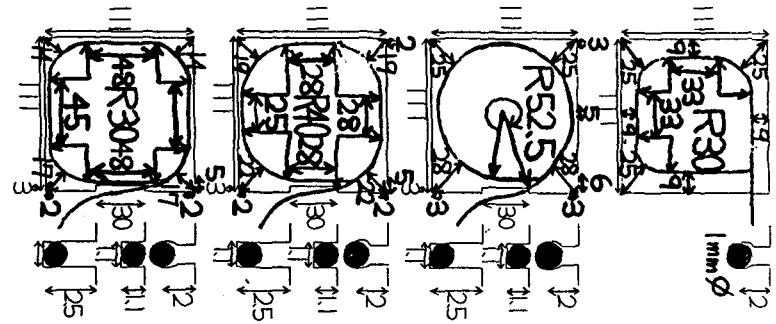

1203

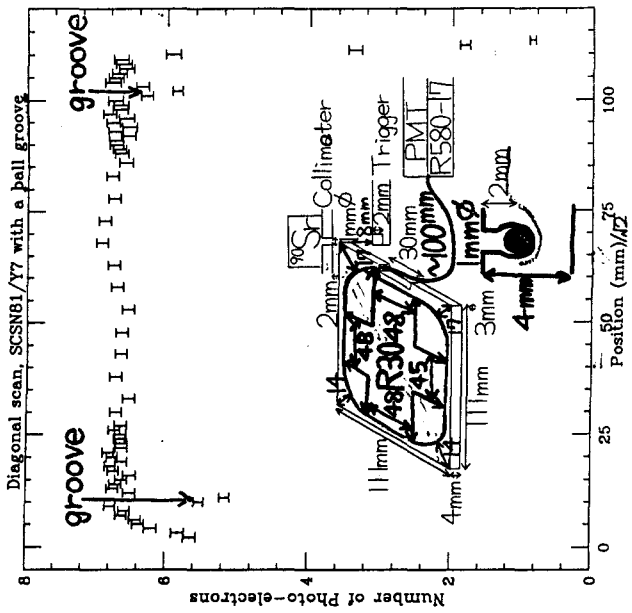

Conclusions

0) We have started optimizing EM Tile optics.

So far, the data shows that

1) Uniformity becomes better as the groove path is brought closer to the corner and to the edge.

2) For a 1.1mm square groove, the response near the groove is high by about 5% to 15%.

For a deep groove (1.1mm by 2.5mm), the response is observed to drop sharply on the fiber by approximately 40%.

For a ball groove, the response on the fiber drops by about 15%.

Of the three groove, the ball groove is the best in terms of uniformity.

3) We will study

1> Masking near the groove for 1.1mm square groove

2> Effect of mirrored fiber end

3> Effect of white painting of edge

4> Effect of aluminized mylar wrapping

5> Uniformity of mega - tile

The Tile - Fiber System For SDC Calrimetry

Vasken Hagopian
Florida State University

New Information:

1. "Sigma" shaped tile-fiber
   10 cm x 10 cm and 25 cm x 25 cm
2. K27 fluor concentrations in WLS fibers
3. Fiber diameters
4. Kuraray Y11 versus Bicron BCF91A

RADIATION DAMAGE STUDIES OF SCINTILLATORS

FLORIDS STATE UNIVERSITY

E. Bartosz	Undergraduate Student
M. Bertoldi	Engineer
E. Hernandez	Graduate Student
V. Hagopian	Physicist
K. Hu	Engineer
K. Immer	Undergraduate Student
K. Johnson	Physicist
C. Shafer	Graduate Student
J. Thomaston	Engineer
H. Wahl	Physicist
H. Whitaker	Undergraduate Student

Past Collaborators: M. Goforth, P. Rulon, J. Xu, A. Young

Excitation by:

1) 30 KeV X-rays - Similar to Charged Particles

2) Blue Light - Produced by small scintilator

Measured by:

1) Bi-alkalai phototube - Hamamatsu R-329

2) Extended Phototube - Eprom III RCA 8852

Radiation damage by:

3 MeV electrons
2 cm Diameter
200 Hz horizontal Sweep of 25 cm
2 namp to 1 mamp current

Recovery: Less than 10 days

SCSN81, Y7, and 3HF Comparison

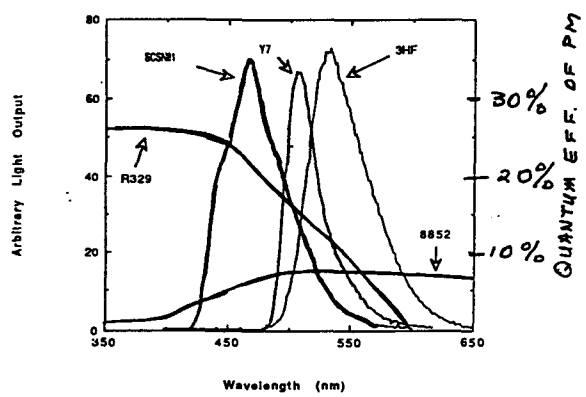

1212

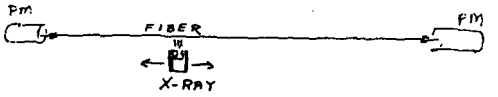

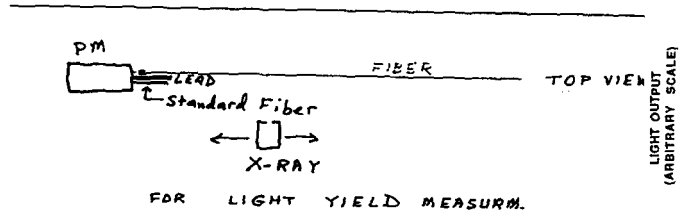

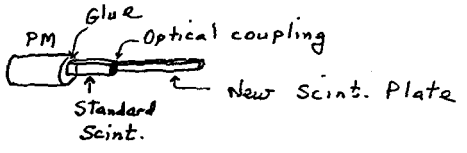

1213

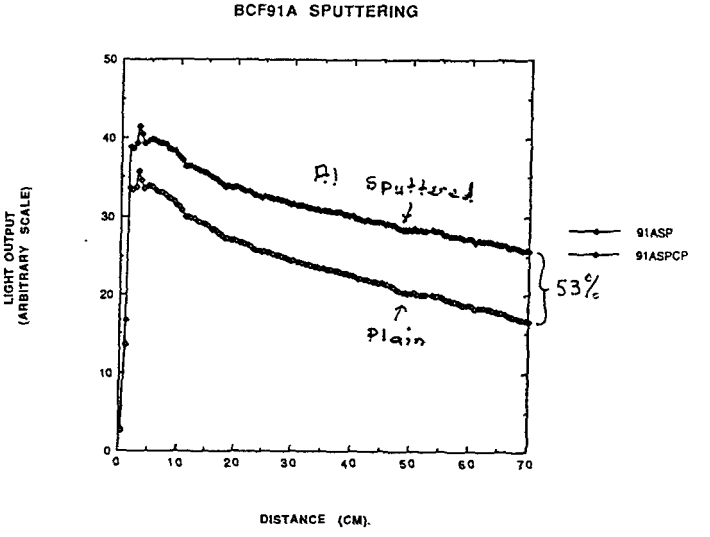

1214

Light output of scintillators scan is by 30 KeV X-rays

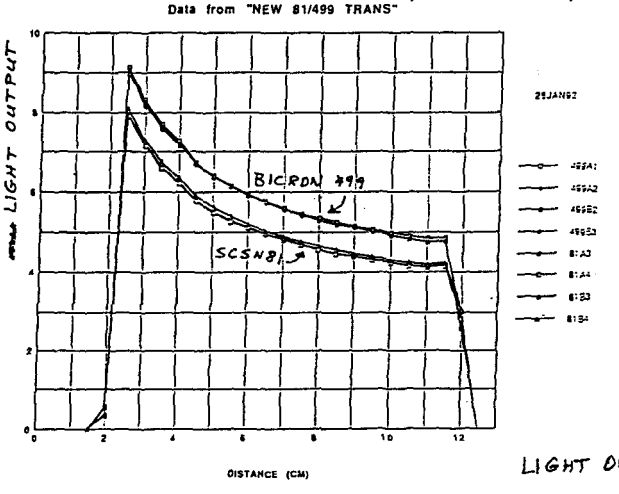

LIGHT OUTPUT

$\frac{BC\ 499}{SCSN81} = 1.16$

2cm x 10cm x 0.25 cm scintillators

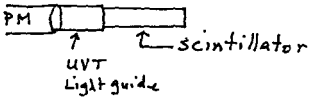

1215

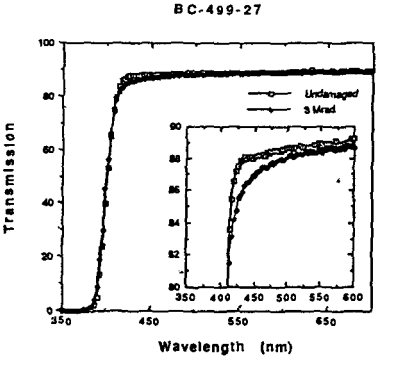

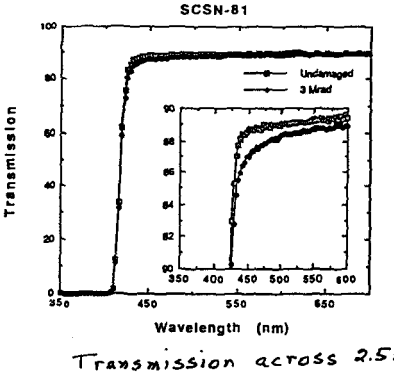

Transmission across 2.5mm plate.
3 Mrad data after recovery.

1216

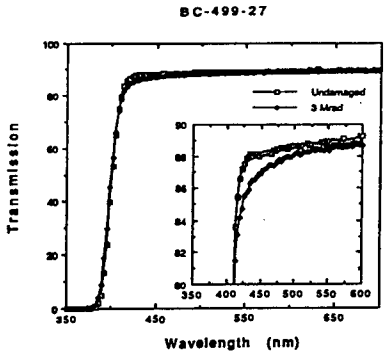

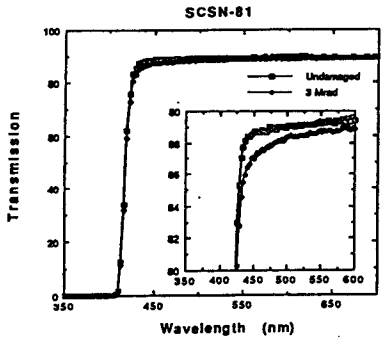

1217

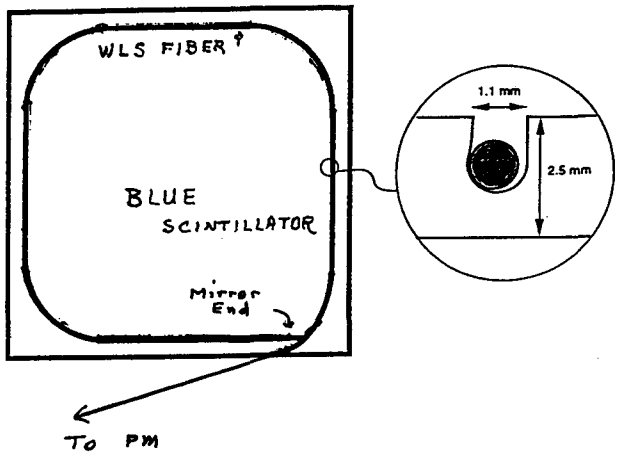

1218

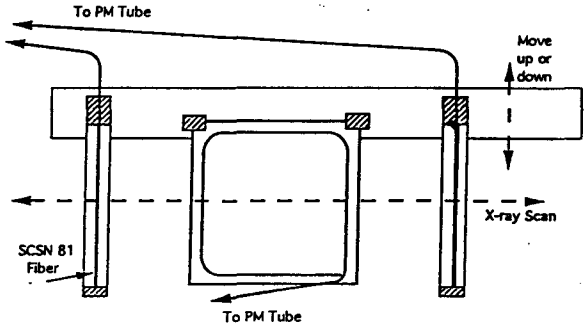

1219

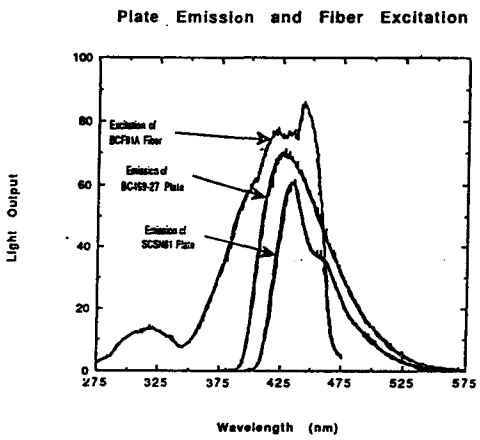

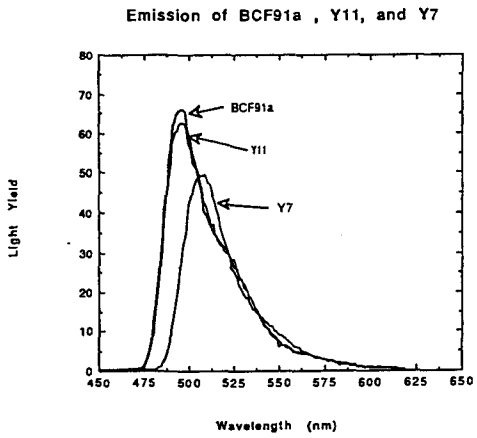

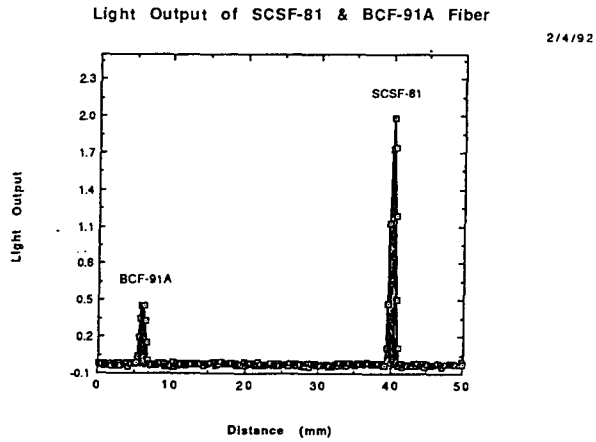

30 KeV X-Ray scan across two fibers
Fibers are 1mm.

Light output $\frac{BCF91A}{SCSF81} = 0.22$

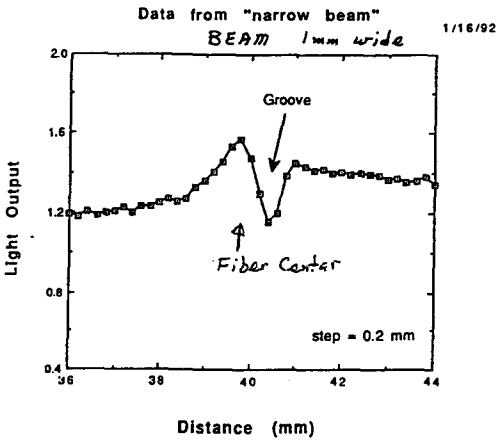

X-ray scan across groove with fiber

RELATIVE LIGHT OUTPUT

10 cm x 10 cm x 0.25 cm
Sigma shape groove
Bicron 499-27 + BCF91A

		FIBER END		
		Plain	TiO_2 paint	Sputtered
PLATE EDGE	Diamond cut	33±1	42±1	47±1
	Machine cut + TiO_2 paint	40	50	55
	Diamond cut + TiO_2 paint	41	52	58

(10X10) CM. SIGMA PLATE DESIGN

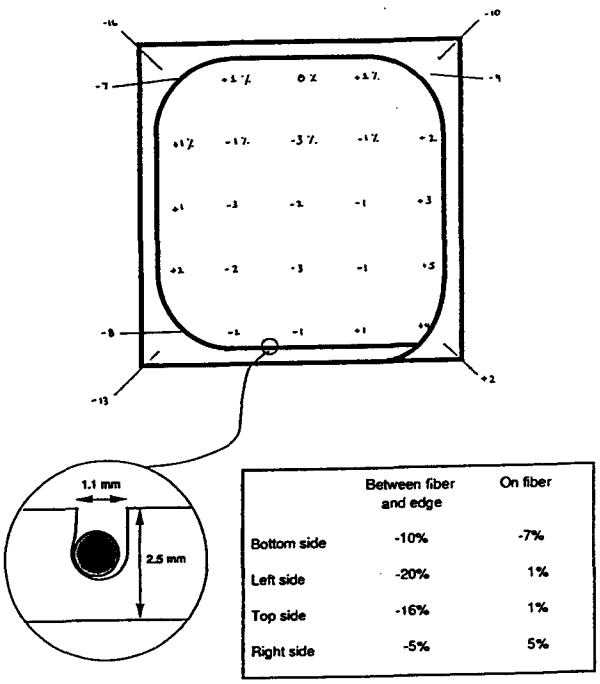

	Between fiber and edge	On fiber
Bottom side	-10%	-7%
Left side	-20%	1%
Top side	-16%	1%
Right side	-5%	5%

(10X10) CM. SIGMA PLATE DESIGN

PLATE AND FIBER IRRADIATED TO 2.65 Mrad.

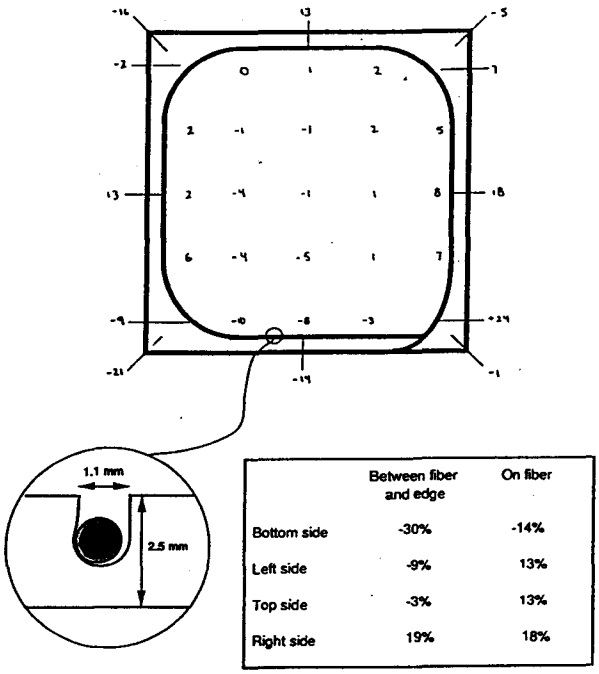

	Between fiber and edge	On fiber
Bottom side	-30%	-14%
Left side	-9%	13%
Top side	-3%	13%
Right side	19%	18%

(25 X 25) CM. SIGMA PLATE DESIGN

PLATE SCALE: 2:1

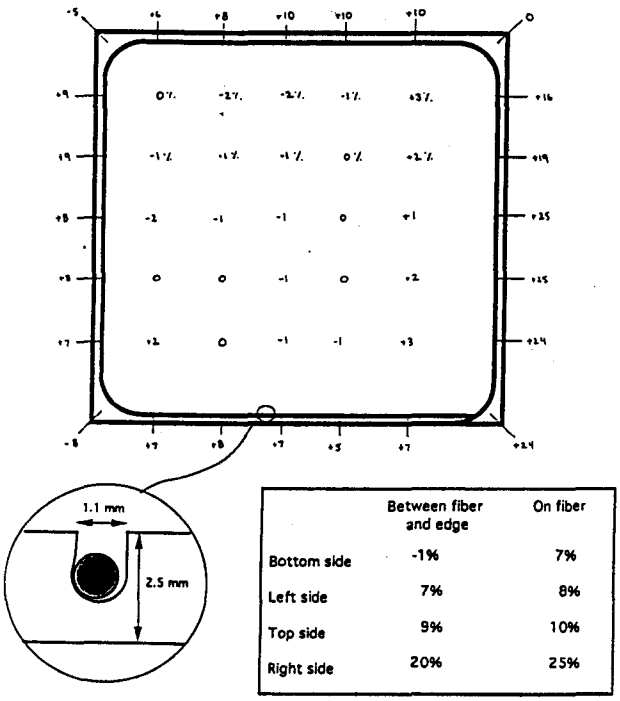

	Between fiber and edge	On fiber
Bottom side	-1%	7%
Left side	7%	8%
Top side	9%	10%
Right side	20%	25%

SCSN-81 & BCF-91A

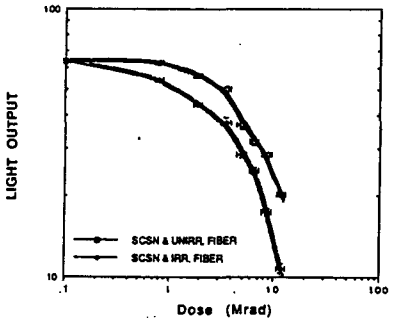

BC-499 & BCF-91A

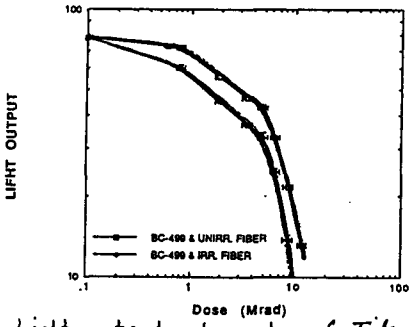

Light output at center of Tile-Fiber
Source 30KeV X-rays. Data after recovery

1228

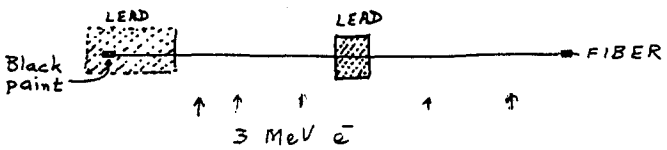

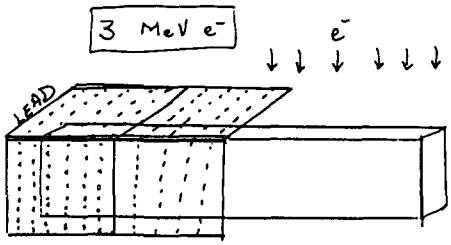

1229

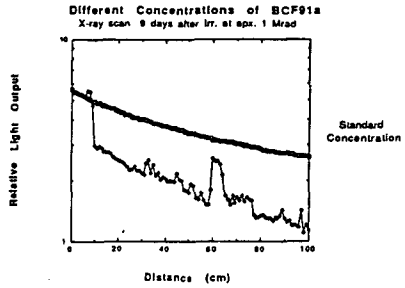

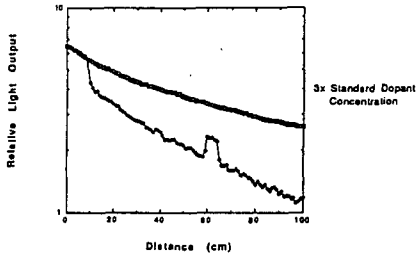

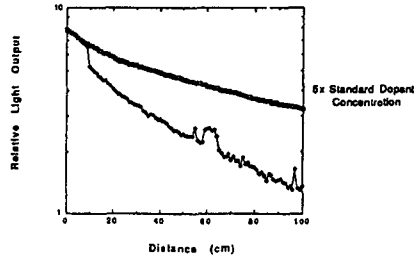

1230

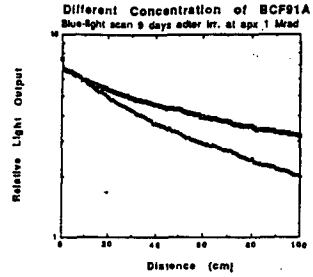

Blue light SCAN

1 MRAD

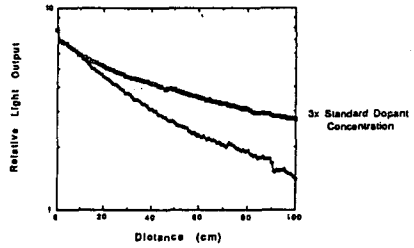

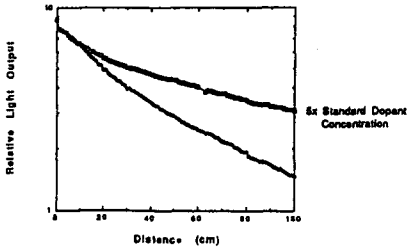

1231

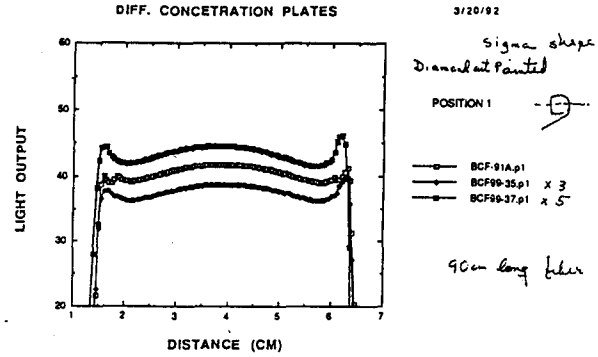

Increase K27 WSF by x3 and x5
Light output change by 10% only

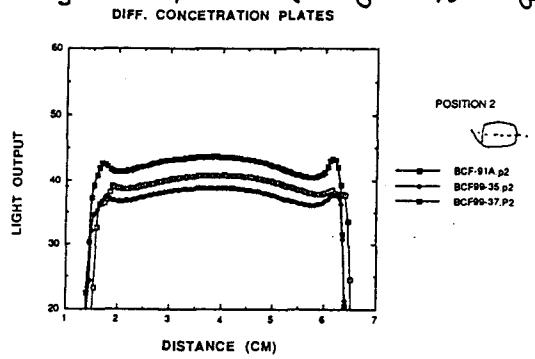

1232

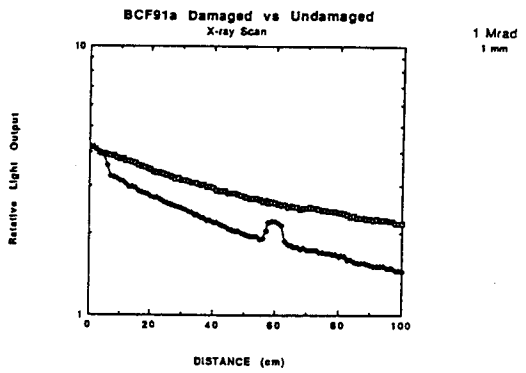

1233

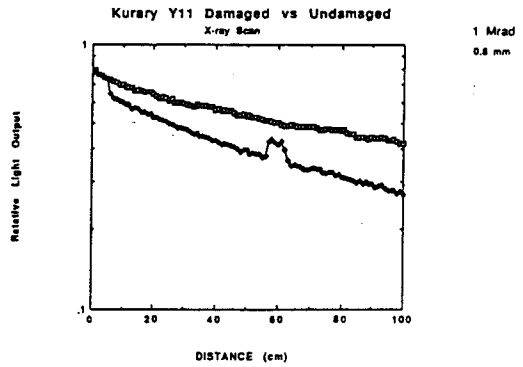

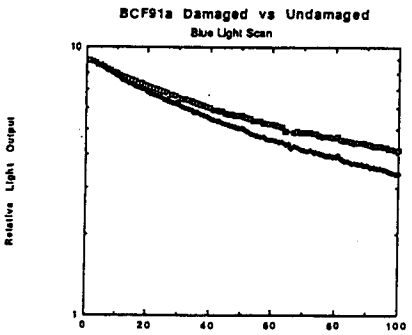

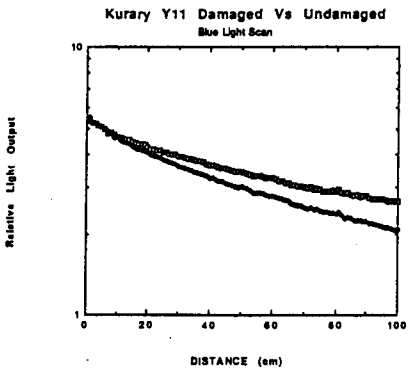

1234

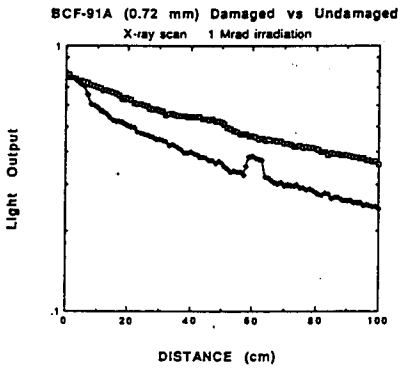

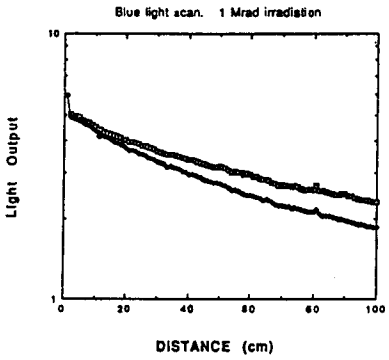

1235

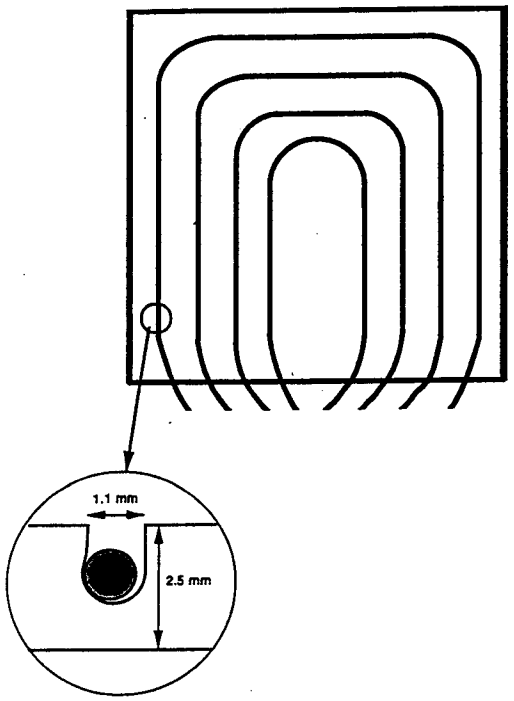

Fig. 7 .- Scintillating plate (10 cm. X 10 cm. X 0.25 cm) and four groove fiber assembly.

SCSN-81

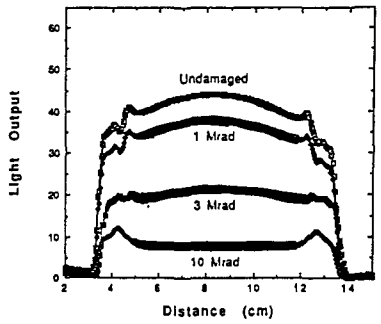

1-GROOVE

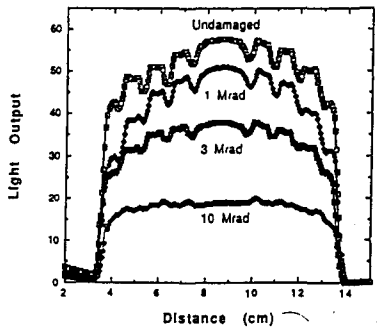

4-Groove

Irradiation Damage
10 cm x 10 cm x 0.25 cm

SCSN81 Scintillator--Irradiated
BCF91 Fiber--Irradiated

Light Output

	1 Groove	4 Grooves
0 Mrad	1.00	1.00
1 Mrad	0.84 ± 0.02	0.90
3 Mrad	0.48	0.67
10 Mrad	0.18	0.33

Conclusions

1. Plate Scintillators
   - No big variation in radiation hardness
   - SCSN81 is better by 10%
   - Light output variation of about 20%
   - Kuraray SCSN81 is 80% of Bicron 499-27

2. Fiber (WLS)
   - K27 Better than Y7
     - BCF91A is 20% brighter than Y11
     - Light output $\propto$ (Diameter)$^{1.2}$ from 0.7 mm to 1 mm
   - K27 Concentration
     - BCF91A is best, x3, x5 more radiation soft
     - Light output - independents of concentration

3. Multigroove vs. Single Groove
   - Reduce rad-damage by a factor of 2.

Development of Cockcroft-Walton PMT Base for the SDC Calorimeter

presented by K. Hara (University of Tsukuba)

CONTENTS :

1. Specifications for PMTand PMT Base
2. Tests of Low Noise C-W Base
3. Plan for Small Size C-W Base

Table 6-9
Draft PMT specification for SDC calorimetry.

Parameter	Requirement
Mechanical	
Diameter	19 mm (3/4") to 40 mm (1.25")
Length	~75 mm
End window	Flat face
Leads	Bare pins, solder leads, or socket type
Photocathode	
Useful Area	1 cm^2 minimum good area
Quantum efficiency	(Integral QE for distribution centered ~520 nm) 12% for EM section and 7.5% for the Hadronic section
Pulsed photocurrent	Maintain ~5% linearity for 10^4 p.e. in a 10 ns pulse
Average photocurrent	0.5 nA (uniform illumination 13 mm circle)
Lifetime photocurrent	1 mC for 50% gain loss
Uniformity	±15% over 13 mm diameter circle, silvered mesh on photocathode OK
Multiplier	
Gain	6×10^5 nominal → 1 p.e. = 1 fC
Linear Pulsed Current	25 mA for 10 ns with <2% nonlinearity, 100 mA for 10 ns with <5% nonlinearity
Rise time (20%-80%)	<4 ns (10 mA into 50-ohm load)
Fall time (80%-20%)	<6 ns
Pulse width (FWHM)	<8 ns
Width at baseline (5%)	<12 ns
Pulse shape at high currents	Pulse width (FWHM) changes less than 20% for output pulses between 1 mA and 50 mA
Average anode current	1 μA
Lifetime anode current	100 C for 50% gain loss
Anode capacitance	<10 pF to all other electrodes combined
Inductance of anode and last dynode	<4 nH
Voltage divider	Simple integer ratios of voltages allow Cockroft-Walton "charge-pump" type base. Typical example: 0 200 400 500 600 700 1000 V for Anode, D6, D5, D4, D3, D2, D1, K.
A 2:2:1:1:1:3 K	
Noise	
"Single-photoelectron"	<100 KHz at 0.5 of 1 p.e. peak → 0.5 fC
Afterpulsing	< 0.1%/ p.e.for afterpulses >10 p.e.
Pre-pulsing	Arrival < 5 ns early amplitude < 0.5% of signal from photocathode
Stability	
Long term	< 1%/month
Pulse recovery (target)	< 1% gain loss 100 ns after pulse of 10 mA × 10 ns

Taken from TDR

* 3/4" version R4125 available

1

HAMAMATSU
TENTATIVE DATA
May 1991

PHOTOMULTIPLIER TUBE
R4598 *

For High Energy Physics
1-1/8 Inch Diameter, Bialkali Photocathode
6-stage, Head-on Type

GENERAL

Parameters		Ratings	Units
Spectral Response		185 to 650	nm
Wavelength of Maximum Response		420	nm
Photocathode	Material	Bialkali	—
	Minimum Effective Area	25 (10 mm)	mm dia.
Window	Material	UV glass	—
Dynode	Structure	Linear focused	—
	Number of Stages	6	—
Suitable Socket		E678-14C (supplied)	—

QE : 20% @ 500 nm (12%)
16% @ 520 nm (@520 nm)

MAXIMUM RATINGS (Absolute Maximum Values)

Parameters		Ratings	Units
Supply Voltage	Between Anode and Cathode	2000	Vdc
	Between Anode and Last Dynode	250	Vdc
Average Anode Current		0.2	mA
Ambient Temperature		−80 to +50	°C

nonlinearity ≤ 2% (@ 0.15 mA)

CHARACTERISTICS (at 25°C)

Parameters		Min.	Typ.	Max.	Units
Cathode Sensitivity	Luminous (2856K)	60	80	–	μA/lm
	Blue (CS No.5-58 filter)	–	10.5	–	μA/lm
Anode Sensitivity	Luminous (2856K)	–	0.4	–	A/lm
Current Amplification		–	6×10^5	–	–
Anode Dark Current (after 30min. storage in darkness)		–	1	5	nA
Time Response	Anode Pulse Rise Time	–	2.0	(≤ 4) (≤ 2.5)	ns
Pulse Linearity (at 2% Deviation)		–	100		mA

TDR requires...

VOLTAGE DISTRIBUTION RATIO AND SUPPLY VOLTAGE 3 : 1 : 1 : 1 : 1 : 2 : 2

Electrode	K	Dy1	Dy2	Dy3	Dy4	Dy5	Dy6	F
Ratio	6	1	1.5	2.2	3.3	3.9	3.6	

Supply Voltage : 1500Vdc. K : Cathode. Dy : Dynode. F : Anode

Adopted ratio
5 : 1 : 1 : 2 : 3 : 3 : 3

AMP ≲ 6000 @ 2 kV !!

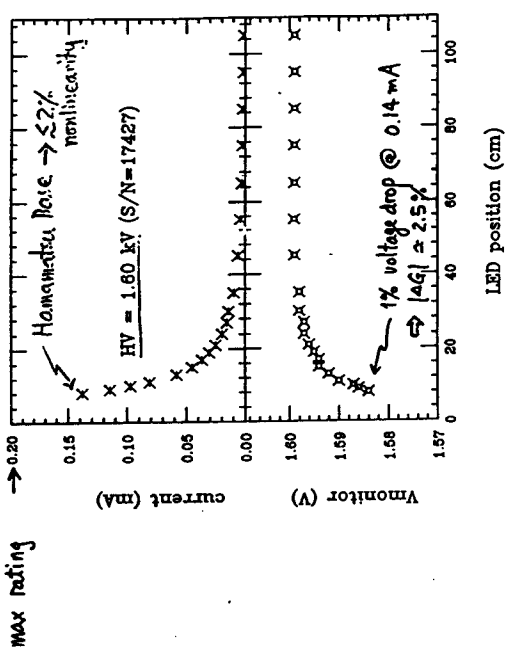

CW base works to ⟨I⟩ ≃ 0.15 mA

- Properties for pulsed signals have to be measured ..... linearity, pulse shape ...

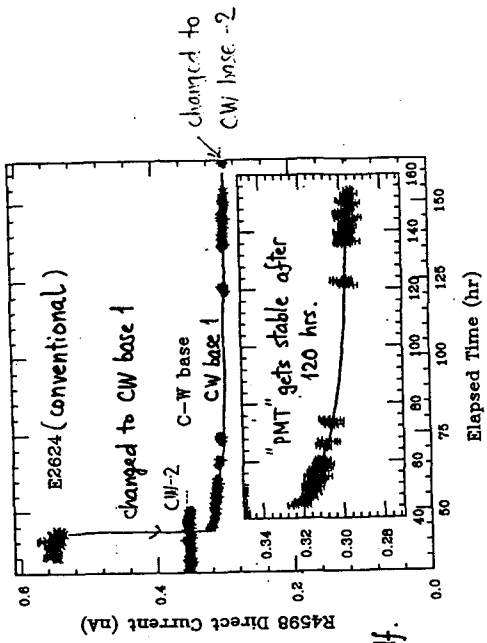

Stability

a scintillator block + ^{90}Sr was attached all the time

- CW base gets stable earlier than PMT itself.

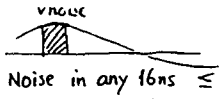

Noise in any 16ns $\leq 0.5\,fC$: $V_{noise} \leq 0.5\times10^{-15}\cdot 50/16\,ns = 1.6\,\mu V$ (@ 50Ω)

Specification of HPMC-1.8N-Tku3

(Cockcroft-Walton type Base for 9/8" 6-stage PMT)

1.	output voltage	-1800V (max)
		= 75 x input voltage (0 to 24V)
2.	monitor voltage	1 : 1000
3.	monitor accuracy	0.2% on cathode voltage
	reproducibility	0.05% (under constant temperature)
4.	dynode voltage ratio	Cathode 5:1:1:2:3:3:3 Anode
	voltage accuracy	100V+/-2V @ 1800V
5.	ripple	0.2V peak-to-peak @ 1800V
6.	anode ripple (no PMT connected)	0.5 mV p-p (@1400V into 1MΩ)
7.	stability	0.04%/hr @1800V after 4hr warming up (under constant temperature and input voltage)
8.	stability against magnetic field	0.1% typ @ 100 gauss
9.	protection	against ~~access~~ reverse connection and short at input line
10.	protection resistor	10 MΩ
11.	power consumption	12 mA (max) x 24V, 10 mA (typ) x 24V
12.	size	30ø x 65 L (mm)
13.	weight	110g (approx)
14.	cables	input : brown
		ground : red
		monitor : orange
		case ground : black
		signal : 50Ω coax

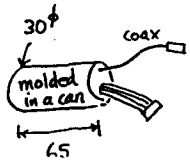

Noise Measurement

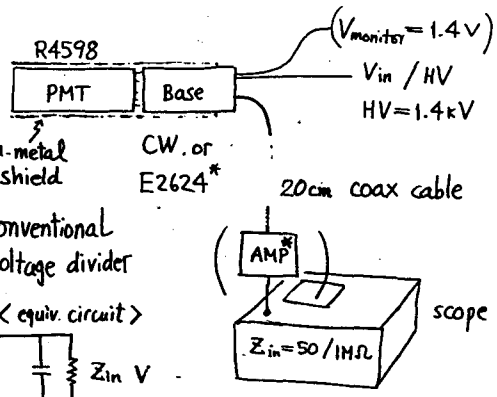

* conventional voltage divider

i_o <equiv. circuit>

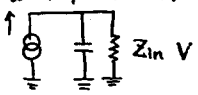

$$V = \frac{i_o}{\sqrt{(1/Z_{in})^2+(\omega C)^2}}\ ;\quad C = \underset{\text{PMT}}{\leq 8} + \underset{\text{cable}}{20} + \underset{\text{scope}}{20} = 48\,pF$$

$\omega = 2\pi \times 230\,kHz$

$$\frac{V(Z_{in}=1M\Omega)}{V(Z_{in}=50\Omega)} = 290 \text{ for } 230\,kHz \text{ noises}$$

< 290 for noises faster than 230kHz

* Hamamatsu C4543

$Z_{in}/Z_{out} = 50\Omega$

x 80 amplifier

50k – 700MHz

CW base for 10 stage. $\frac{3}{2}$" PMTs (eg R580)

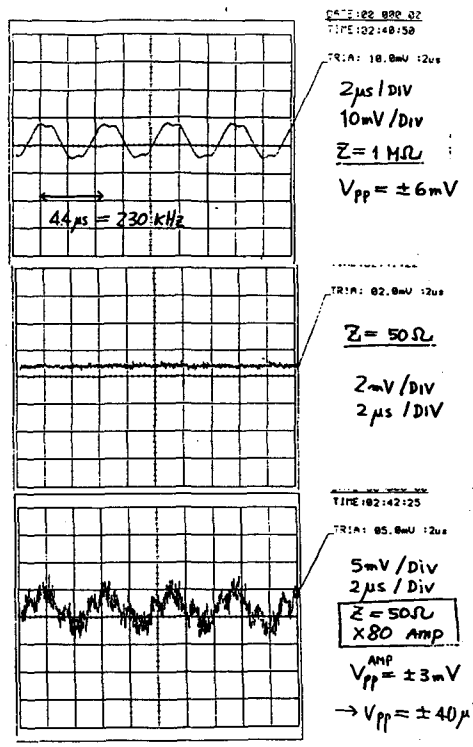

1217

CW base for $\frac{9}{8}$" 6-stage PMTs (e.g. R4598)

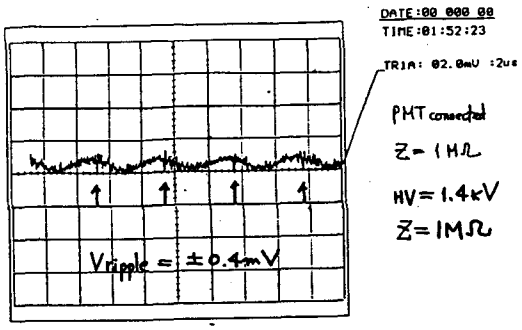

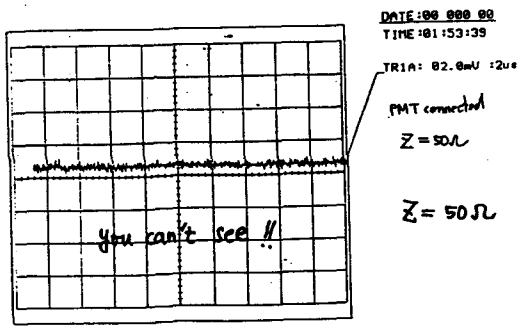

1218

x80 amplified ...

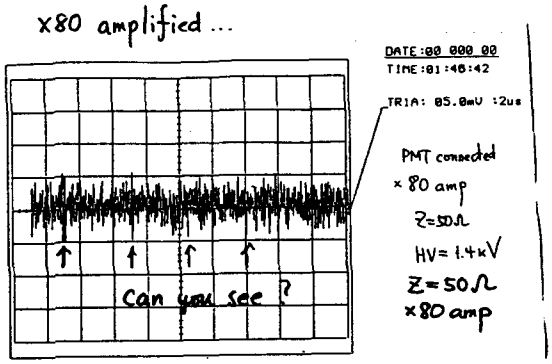

Conventional base for comparison..

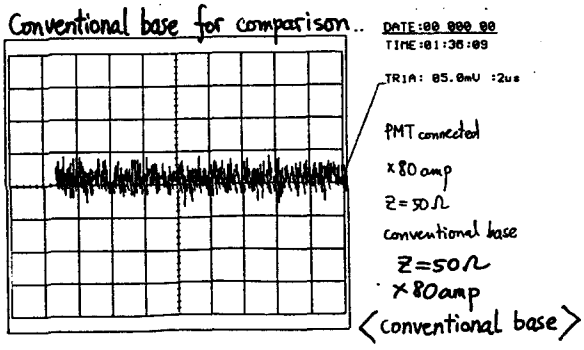

1219

another CW base ....

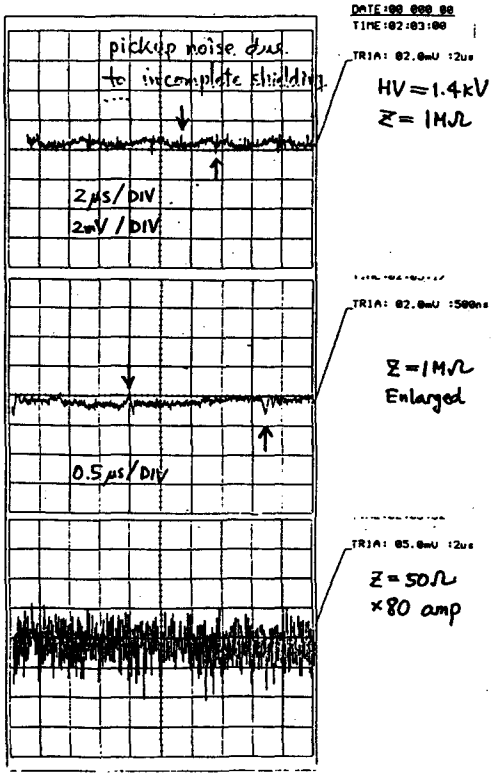

1220

— More samples ...

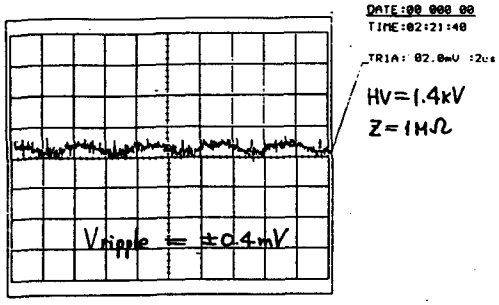

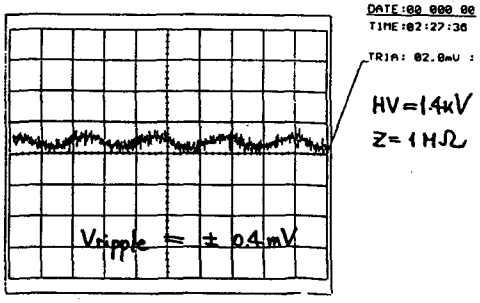

Plan for a small (and inexpensive) CW base

Put PC boards with CW base components inside PMT shielding case....

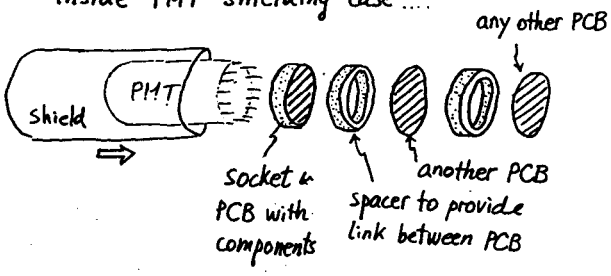

- More complete feedback circuit
- Noise filter (transformer, dynodes)
- Higher gain: optimum voltage ratio
- Fits to $\frac{3}{4}$" PMT
- Adopt surface mount method and reduce production time & cost
- 1st version (probably too big) will appear next month

Quality Control for Prototype Tile/Fiber Production

5/27/92

U. of Tsukuba
I. Nakano

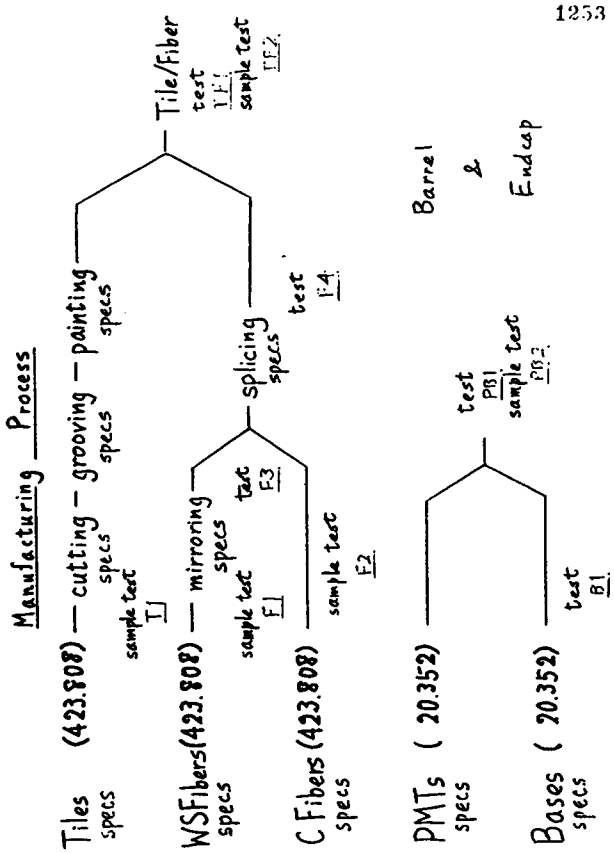

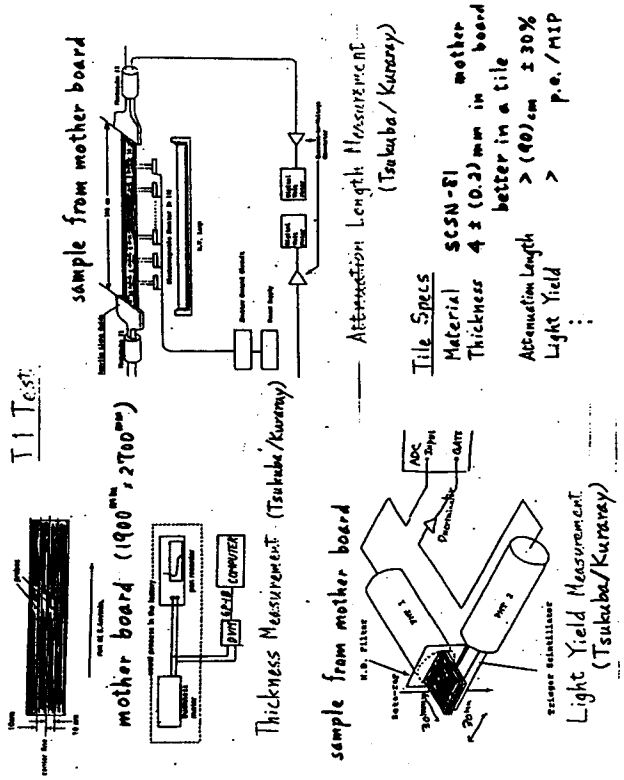

SPECS

Cutting

- Size — < 0.1% @ (24 ± 2)°
- Edge Surface — cutting speed 175-200 in/min @ 17,000 rpm
- ...

Grooving

- Surface — speed 75 in/min @ 18000 rpm
- Width — 0.8 mm ± 0.1 mm
- Depth — 3 mm ± 0.3 mm
- ...

Painting

- Material
- Thickness — ≤ 100 μm
- Adhesion Strength
- ...

SPECS

WS Fiber / C Fiber

Diameter	0.83 ± 0.02 mm	
Ellipticity	2(a-b)/(a+b)	≤ 0.02
Core	Polystyrene	n = 1.59
Cladding	PMMA	n = 1.49
Cladding Thickness	3% of diameter	

⋮

Dye YT (for WS Fiber)

⋮

Mirroring

Reflectivity > 0.84 ± 0.03

⋮

Splicing

Light Loss

Sample Test F1 Full Sample Test F3 F4

- Attenuation Length
- Light Yield

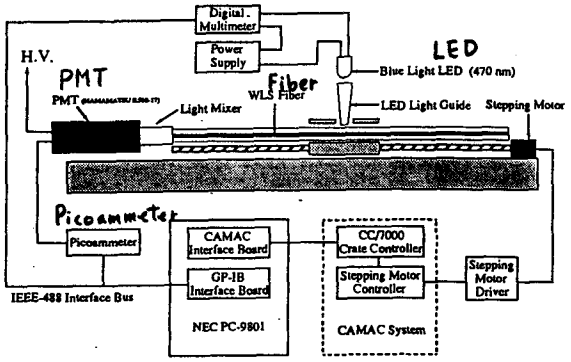

One Dimension Scanner (Tsukuba)

- Reflection Effect (Mirroring)
- Light Loss by Splicing (Splicing)

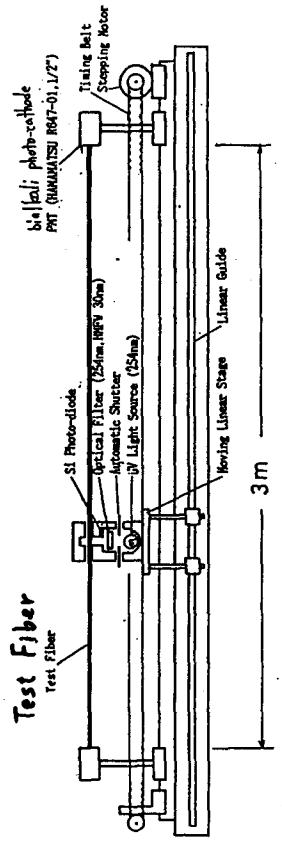

Attenuation Length Measurment System (Kuraray)

Sample Test F2

SPECTRUM ANALYZER (Kuraray)

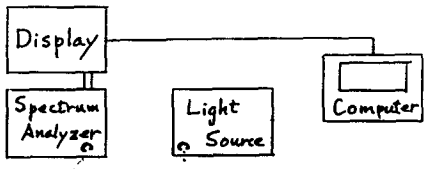

1m cut back

Ex.

15m

1m cut back

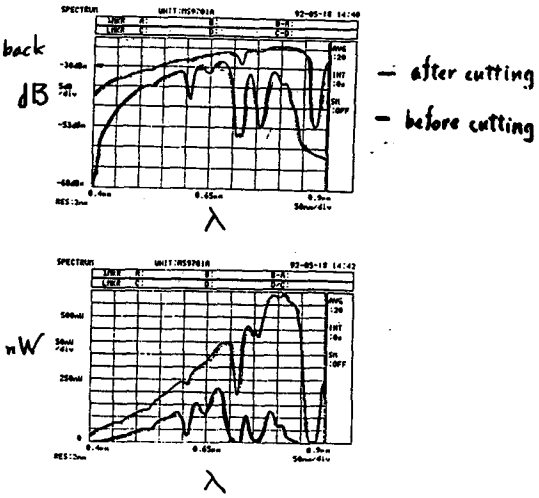

Full Sample Test TF1 Sample Test TF2

· Light Yield at a few points (TF1)

nA / # p.e.

2-dimensional Scanner (Tsukuba)

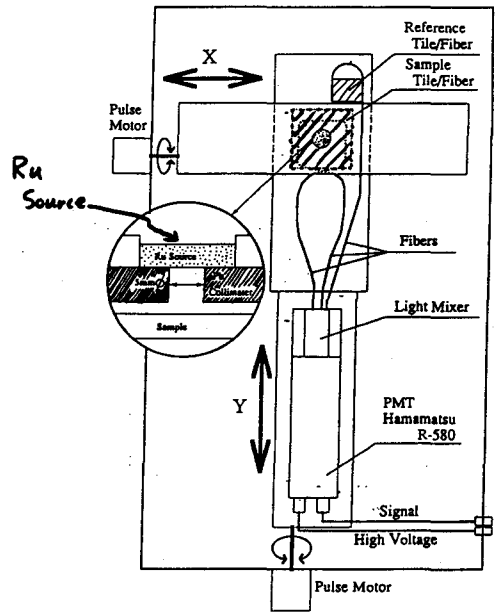

· Uniformity (TF2)

nA / #p.e.

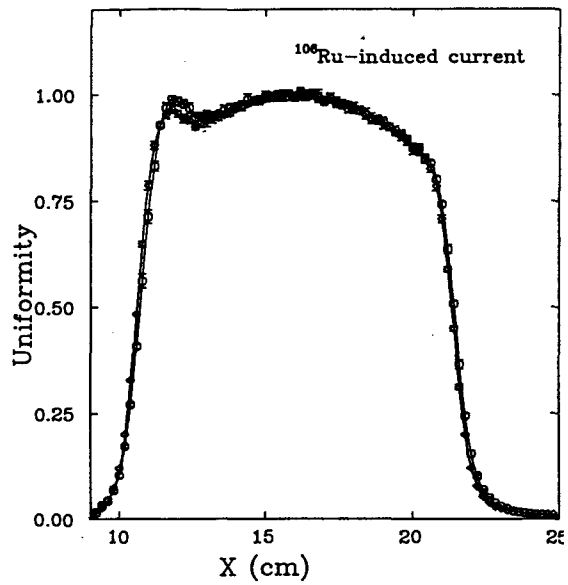

Specification of HPMC-1.8N-Tku3

(Cockcroft-Walton type Base for 9/8" 6-stage PMT)

1.	output voltage	-1800V (max)
		= 75 x input voltage (0 to 24V)
2.	monitor voltage	1 : 1000
3	monitor accuracy	0.2% on cathode voltage
	reproducibility	0.05% (under constant temperature)
4.	dynode voltage ratio	Cathode 5:1:1:2:3:3:3 Anode
	voltage accuracy	100V+/-2V @ 1800V
5.	ripple	0.2V peak-to-peak @ 1800V
6.	anode ripple (no PMT connected)	0.5 mV p-p (@1400V into 1MΩ)
7	stability	0.04%/hr @1800V after 4hr warming up (under constant temperature and input voltage)
8.	stability against magnetic field	0.1% typ @ 100 gauss
9.	protection	against reserve connection and short at input line
10.	protection resistor	10 MΩ
11.	power consumption	12 mA (max) x 24V, 10 mA (typ) x 24V
12.	size	30ø x 65 L (mm)
13.	weight	110g (approx)
14.	cables	input : brown
		ground : red
		monitor : orange
		case ground : black
		signal : 50Ω coax

Fig. 2. Specifications of CW bases made by Matsusada that fits to R4598 PMT.

Cockcroft-Walton type PMT base

Test 5!

Heat Cycle Tes

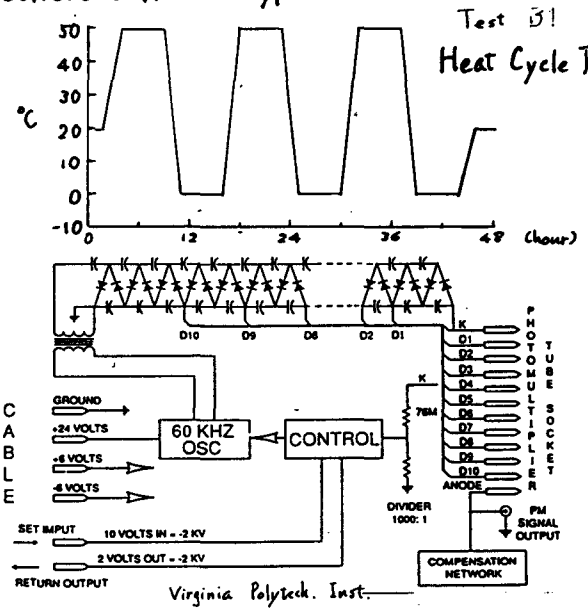

· Monitor Voltage vs Time

· Shock Test

early failure

· Temperature dependence

Table 6-9
Draft PMT specification for SDC calorimetry. (TDR)

Parameter	Requirement
Mechanical	
Diameter	19 mm (3/4") to 40 mm (1.25")
Length	~75 mm
End window	Flat face
Leads	Bare pins, solder leads, or socket type
Photocathode	
Useful Area	1 cm^2 minimum good area
Quantum efficiency	(Integral QE for distribution centered ~520 nm) 12% for EM-section and 7.5% for the Hadronic section
Pulsed photocurrent	Maintain ~5% linearity for 10^6 p.e. in a 10 ns pulse
Average photocurrent	0.5 nA (uniform illumination 13 mm circle)
Lifetime photocurrent	1 mC for 50% gain loss
Uniformity	±15% over 13 mm diameter circle, silvered mesh on photocathode OK
Multiplier	
○ Gain	6×10^3 nominal
Linear Pulsed Current	25 mA for 10 ns with <2% nonlinearity, 100 mA for 10 ns with <5% nonlinearity
Rise time (20%-80%)	<4 ns (10 mA into 50-ohm load)
Fall time (80%-20%)	<6 ns
Pulse width (FWHM)	<8 ns
Width at baseline (5%)	<12 ns
Pulse shape at high currents	Pulse width (FWHM) changes less than 20% for output pulses between 1 mA and 50 mA
Average anode current	1 μA
Lifetime anode current	100 C for 50% gain loss
Anode capacitance	<10 pF to all other electrodes combined
Inductance of anode and last dynode	<4 nH
Voltage divider	Simple integer ratios of voltages allow Cockroft-Walton "charge-pump" type base. Typical example: 0 200 400 500 600 700 1000 V for Anode, D6, D5, D4, D2, D1, K.
Noise	
"Single-photoelectron"	<100 KHz at 0.5 of 1 p.e. peak
Afterpulsing	< 0.1%/ p.e.for afterpulses >10 p.e.
Pre-pulsing	Arrival < 5 ns early amplitude < 0.5% of signal from photocathode
Stability	
○ Long term	< 1%/month
○ Pulse recovery (target)	< 1% gain loss 100 ns after pulse of 10 mA × 10 ns

Full Sample Test PB1 Sample Test PB2

- Dependence on time, temperature and anode current
- Short-term stability
- Current gain
- Rate effect

CDF

CEM

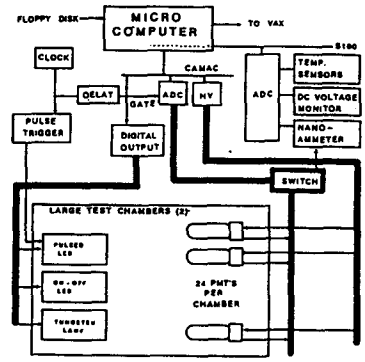

- Linearity
- Pulse recovery
- Long term stability

REPORT OF RADDAM 1992 CONFERENCE

AT

FLORIDA STATE UNIVERSITY

TALLAHASSEE, FLORIOA, USA

INTERNATIONAL CONFERENCE ON RADIATION

TOLERANT SCINTILLATORS and DETECTORS

BY

VASKEN HAGOPIAN

Florida State University

---- RADDAM '92 ----

INTERNATIONAL CONFERENCE ON RADIATION-TOLERANT SCINTILLATORS AND DETECTORS

FLORIDA STATE UNIVERSITY
TALLAHASSEE, FLORIDA
APRIL 28 TO MAY 2ND, 1992

CONFERENCE ORGANIZERS:

ROGER CLOUGH
SANDIA NATIONAL LABORATORIES
ORGANIZATION 1811
ALBUQUERQUE,NM
USA 87185
PH:(505)844-3492
FAX:(505)844-9624

KURTIS F. JOHNSON
FLORIDA STATE UNIVERSITY
DEPT. OF PHYSICS
TALLAHASSEE,FL
USA 32306
PH:(904)644-3893
FAX:(904)644-6735
E-MAIL:
FSUHEP::RADDAM92

PETER SONDEREGGER
CERN
CH-1211,GENEVA
SWITZERLAND
PH:(22)767-4670
FAX:(22)782-4897
E-MAIL:
RADDAM92@CERNVM

THIS SYMPOSIUM IS INTENDED TO BRING TOGETHER MAJOR RESEARCH WORKERS INVOLVED IN THE DEVELOPMENT OF ADVANCED, RADIATION RESIS-TANT SCINTILLATORS OR PARTICLE PHYSICS DETECTORS. PRESENTATIONS OF RESEARCH RESULTS WILL BE MADE IN THE AREAS LISTED BELOW, AND DISCUSSION SESSIONS WILL BE SCHEDULED ON KEY ISSUES WHICH REMAIN TO BE RESOLVED. SINCE AN IMPORTANT CONCERN IS COMMUNICATION BETWEEN RADIATION CHEMISTS AND DETECTOR DESIGNERS, TUTORIAL SESSIONS WILL BE ORGANIZED FOR BOTH PHYSICISTS AND CHEMISTS.

THE PROCEEDINGS OF THIS CONFERENCE WILL BE PUBLISHED AS A SPECIAL ISSUE OF THE JOURNAL: RADIATION PHYSICS AND CHEMISTRY.

* MATERIALS REQUIREMENTS FOR SCINTILLATOR-BASED DETECTORS
* RADIATION DAMAGE MECHANISMS IN POLYMERIC SCINTILLATORS
* STRATEGIES FOR DEVELOPING MORE RADIATION TOLERANT SYSTEMS
* PREDICTIVE AGING TESTS FOR SCINTILLATOR LIFETIMES
* SURVEY OF RADIATION RESISTANCE OF OPTICAL PROPERTIES IN DIFFERENT POLYMERS
* NATURE AND STRUCTURE OF RADIATION-INDUCED COLOR CENTERS
* THE ROLE OF OXYGEN
* KINETICS AND MECHANISMS OF COLOR CENTER ANNEALING
* RADIATION EFFECTS ON SCINTILLATOR DYES; SYNTHESIS OF ADVANCED DYES
* RADIATION DAMAGE TO OTHER ORGANIC MATERIALS CRUCIAL TO SCINTILLATION DETECTORS (ADHESIVES, COATINGS, ETC.)
* OPERATING EXPERIENCE AND LONG-TERM RADIATION RESULTS
* OTHER ADVANCES IN SCINTILLATOR PROPERTIES (SPEED, EFFICIENCY)

ADVISORY COMMITTEE:

NIKOS GIOKARIS, ROCKEFELLER UNIV.
DAN GREEN, FNAL / SDC
MICHAEL KASHA, FSU
AMELIA MAO, LIP, LISBON
STAN MAJEWSKI, CEBAF
ADAM PARA, FNAL
JIMMY PROUDFOOT, ANL
STEVE REUCROFT, BOSTON UNIV.

LOCAL ORGANIZING COMMITTEE:

VASKEN HAGOPIAN, FSU
KURTIS F. JOHNSON, FSU
JOSEPH SCHLENOFF, FSU

INTERESTED PARTIES SHOULD CONTACT ONE OF THE CONFERENCE ORGANIZERS BY E-MAIL, MAIL, TELEPHONE OR FAX TO OBTAIN FURTHER INFORMATION OR TO REGISTER.

RADDAM '92

April 28 - May 2, 1992
Florida State University
Tallahassee, FL 32306

This program is preliminary as to exact times. The first day is set. Grouping reflects both subject matter and requests by speakers as to preferred times due to travel restrictions.

Tuesday, April 28, 1992

9:00am	Registration in UPL 101
10:00	Words of Welcome - Robert M. Johnson, Vice President for Research (FSU)
10:20	Tutorial on Calorimetry - Dan Green (FNAL/SDC)
11:10	Tracking Tutorial - Steve Reucrofi (Northeastern University)
12:00pm	Lunch in Keen building, 7th floor
1:40	Briefing on the Research and Education Programs of the Texas National Research Laboratory Commission - Dr. Lynne Jordan Bowers (TNRLC)
2:10	Principles and Practice of Plastic Scintillator Design - Wayne Moser (Bicron Corporation)
2:50	Coffee Break
3:10	Users View of Radiation Damage to Plastic Scintillator - Carl Zorn (CEBAF)
4:00	Polymer Radiation Chemistry - Roger Clough (Sandia National Laboratory)
5:00	Reception

Wednesday, April 29, 1992

Scintillating Fibers

9:00am	Results from Fibre Irradiation Under Air, N_2, O_2, Ar and Vacuum - Agostinho Gomez (LIP)
9:30	Neutron/Proton Damage Assessment of Commercial Plastic Scintillating Fibers - William Dunn (Quantum Research Services, Inc.)
9:50	Measurement of Decay Times of Fast Scintillating Fibers - John Flournoy (EG&G)
10:20	Coffee Break

10:40	Scintillation Decay Times in Various Scintillators Before and After Irradiation - Agostinho Gomez (LIP)
10:50	Intrinsic Speed of Tile/Fiber calorimetry: The Need for a Fast Green WLS - G. W. Foster (FNAL)
11:00	Fiber Composition and Structure in Relation to Radiation Resistance - Alan Richardson (Nanoptics, Inc.)
11:30	Effects of Radiation on the Transmission Spectra of Stressed Fluorescent Fibers - Justin Gaynor (University of Florida)
12:00pm	Lunch in Keen building, 7th floor
1:00	Fluorescence Claddings on Silica Fibers for Rad-Hard Waveshifting Readout of Calorimeters - G.W.Foster (FNAL)
1:30	Radiation Effects on Wavelength Shifting Fibers Used with Liquid Scintillators - Kathy Young (Oak Ridge National Laboratory)
1:50	Radiation Hardness of Liquid Scintillating Fibers - James White (Texas A&M University)
2:10	Low Dose Rate Irradiations of Scintillating Fibers - Carl Zorn (CEBAF)
2:30	Structure and Dose Rate Effects on Optical Radiation Hardness in Scintillator Polymers - Anne Taylor (University of Florida)
3:00	Approaches to Optimizing Scintillator Polymers for Optical Radiation Hardness - Julie Harmon (University of Florida)
3:45	Leave for Wakulla Springs and Banquet

Thursday, April 30, 1992

8:30am	"Results from a Low Dose-Rate Irradiation Study on SCSN23, SCSN81, SCSN81+Y7, SCSN81+Y8 and 3HF Scintillators" - Nikos Giokaris (Rockefeller University)
8:55	"Ambient and Above Ambient Temper Bleaching of Polystyrene in Vacuum and Air Environment" - Shield Wallace (Professional Analysis Inc.)
9:20	"Effect of Dose Rate on Radiation-Induced Optical Absorbance of Polystyrene" - Ken Gillen, (Sandia)
9:45	"Problems in Application of Plastic Scintillators in Intense Radiation Fields" - Sergei Chemy (SSCL)
10:10	"Detector Simulation Studies Relating to Radiation Damage Studies" - Tony Gabriel (ORNL)
10:35	Coffee Break
10:55	"Dosimetry: New Approaches" - Bill McLaughlin (NIST)
11:30	"Optical Scintillator Properties of Compositions with Large Stokes Shift Dyes" - Jakob Tymianski (University of Florida)
12:00pm	Lunch in Keen building, 7th floor
1:00	"Preliminary Irradiation Tests of E.M. Fibre-Pb Calorimeter Modules at LURE" - Bernardo Tome' (LIP)
1:25	"Effects of Radiation Damage on Scintillating Fibre Calorimetry" - Ana Henriques - (CERN) -
1:50	"Radiation Damage Measurement in Lead/Scintillating Fiber Calorimeters" - Riccardo Desalvo (CERN)
2:40	"SILICAL: A Very Radiation Hard and Very Fast Calorimter" - Philippe Gorodetzky - (Center for Nuclear Research, France)
3:05	"Radiation Damage of Tile-Fiber Systems" - Vasken Hagopian (FSU)
3:20	"Radiation Damage Studies for SDC Barrel Calorimeter" - Ali Fazely (Southern University)
3:45	Coffee Break
4:05	"Radiation Damage of Tile/Fiber Scintillator Modules for the SDC Calorimeter" - Huishun Mao (IHEP-Beijing)
4:30	"Summary of Radiation Hardness Test Programs for SDC Calorimeter" - Aesook Byon-Wagner (FNAL)
5:00	"Changes of End Cap Calorimeter's Parameters After Irradiation" - Vitaliy Semenov (IHEP, Protvino)
5:15	APD's B. Johnson (Litton Industries)
5:30	End of Session

Friday, May 1, 1992

8:30am	"Influence of UV Absorbants on Radiation Stability of Wave-Length Shifters" and "Fluorescence Quenching of Plastic Scintillators in Oxygen" - Uwe Holm (University of Hamburg)
9:20	"Radiation Damage to 2-2'-Hydroxyphenylbenzothiazoles" - Anna Pla (FNAL)
9:45	"Radiation Damage on Silicon Micro Strip from High Energy Protons" - Arthur McManus (University of Virginia)
10:10	Coffee Break
10:30	"A New Polymer- Bound 3 HF-Based Scintillator" - Joseph Schlenoff (FSU)
10:55	"Red Emitting dyes" - Paul Cahill (Sandia)
11:20	"Spectroscopic Criteria for Wavelength Shifting, Fast, and Red, Infrared Scintillators" - Michael Kasha (FSU)
12:00pm	Lunch in Keen building, 7th floor
1:00	"Preliminary Results of the Development of Radiation Resistant Scintillator Based on Polycarbonate, Polysulfone and Epoxypolymer" - Nikolai Barashkov (Karpov Inst of Physical Chemistry)
1:25	"Development of Radiation Hard Scintillators" - Finley Markley (FNAL)
1:50	"Recovery of Radiation Damaged Light Pipe Materials" - Shah Jahan (Memphis State University)
2:15	"Temperature Dependence on the Recovery of Radiation - Induced Color Centers in Poly (Vinyl Toluene) - Tim Herod (FSU)
2:40	"UV-Vis Characterization of Radiation-induced Color Centers in Polyvinyltoluene" - Philip Trimmer (FSU)
3:05	Coffee Break
3:30	"Pre-Irradiation Environmental Effects on Radiation Damage of Plastic Scintillator Bases" - Heather Whitaker (FSU)
4:15	"Early Events in Hydrocarbon Radiolysis" - David Werst (Argonne National Laboratory)
4:40	"Optical Transducers for Scintillating Fiber Readout" - Howard Fenker (SSCL)
5:05	"Fiber Sputtering and Painting" - Erick Hernandez (FSU)
5:20	"Machining of Scintillator Tile for the SDC Calorimeter" - Maurizio Bertoldi (FSU)
5:30	"Conference Summary" - James Proudfoot (ANL)
7:45	End of Session

Tile/Fiber Central Calorimeter
(Quadrant Cross Section)

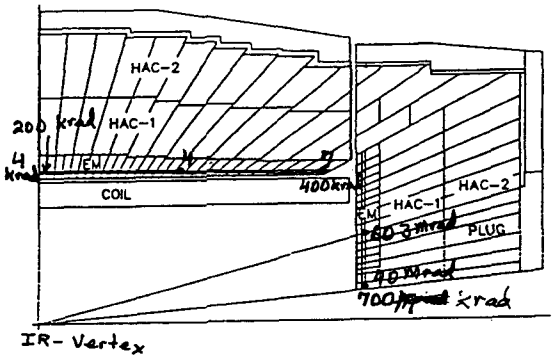

— 1 yr at 10^{33} /cm²sec

— 5 yrs at 10^{33} + 5 yrs at 10^{34}

IRRADIATION DAMAGE
TO

1. Light production (short λ UV) by polymer
2. Primary fluor
3. Secondary fluor
4. Light Transmission
   Longer λ has less loss

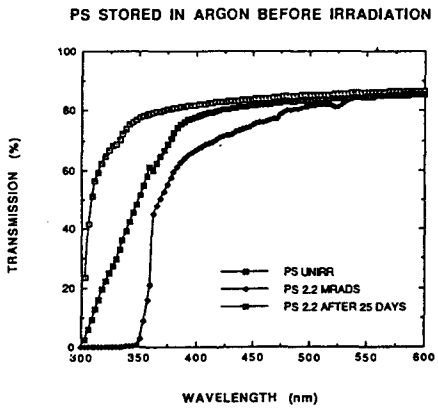

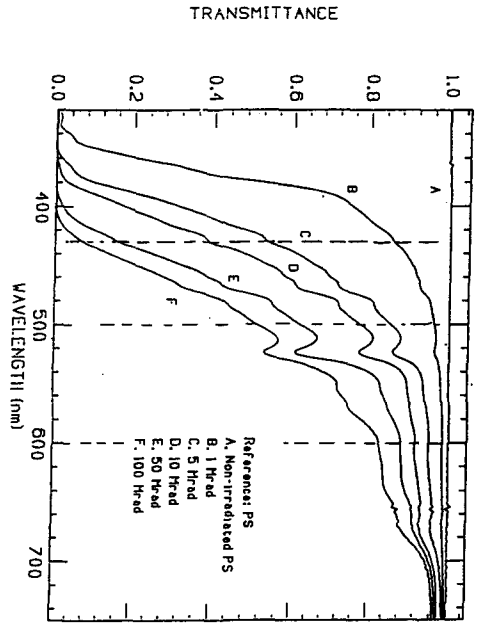

FIGURE 1

A. Brost et. al.

A. Pia

V. Hagopian

6/28/91

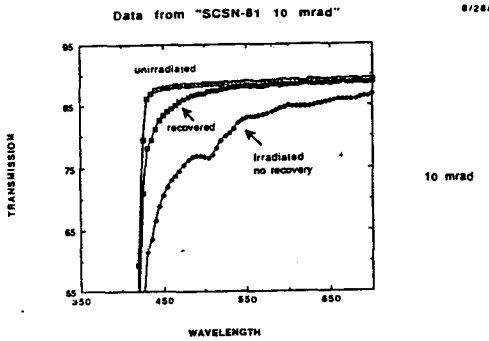

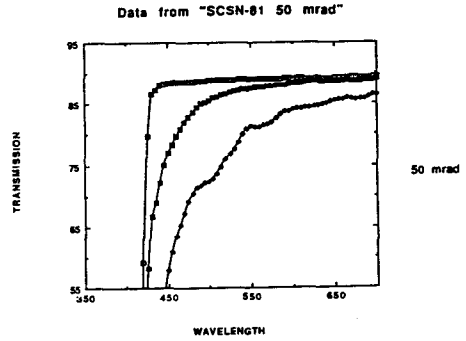

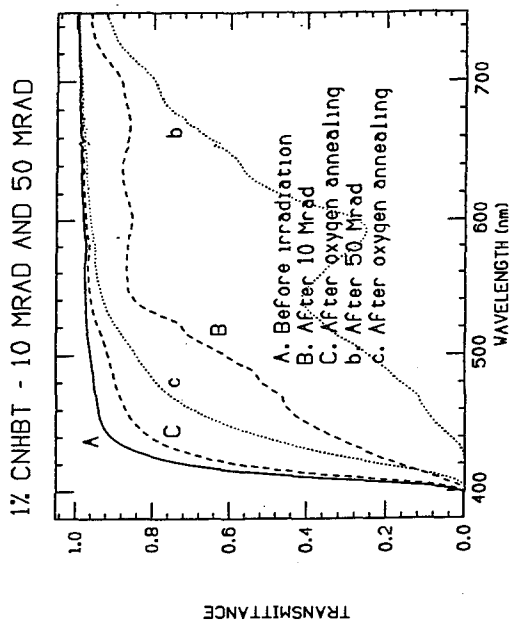

TRANS-KETO HBT ISOMERS

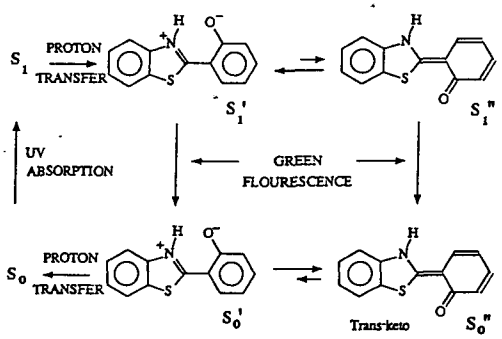

SCSF81 [redacted]. Excitation\Emission 5/19/92

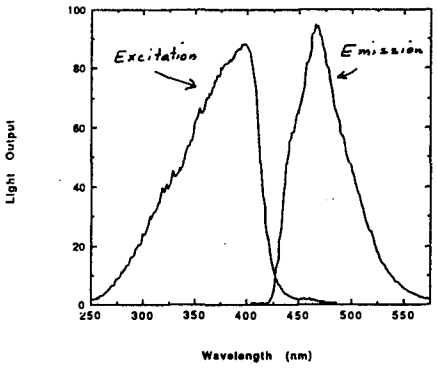

BCF91A Excitation\Emission 5/19/92

K 27

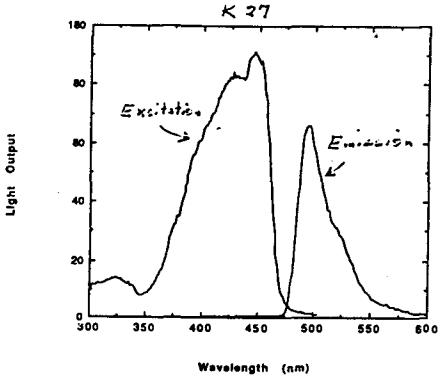

3HF Excitation/Emission 5/21/92

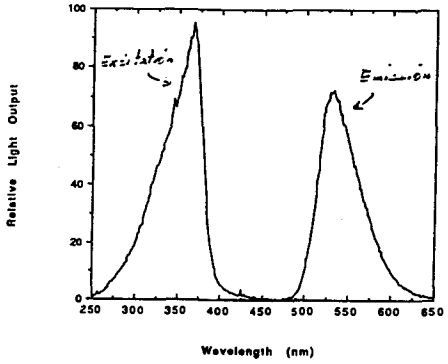

CHEMISTRY

NEW POLYMERS – should be (?) more radiation hard

V. Karasikov (Karpov Inst.)

J. Schlenov (Florida State University)

Adding Benzene Rings to shift emission to higher wavelengths

Make Fluor Polymerisable Vinyl-3HF

520 nm → 540 nm

M. Kasha (FSU)

By careful tuning of molecules one can adjust relative position of singlet and triplet states

Thereby tuning emission frequency and quatum yields

J. Harmon (U. of Florida)

Color centers form radicals

Associated Products

O_2 Diffusion & Quenching

Radical Ion Mobility

⇓

Recombination to form non colored molecules

Reduce Tg Permeability ∝ Ion mobility

Several approaches

Add Plasticisers

Use Copolymer

F. Marklay "Italian Dressing"

Add Oil to scintillator

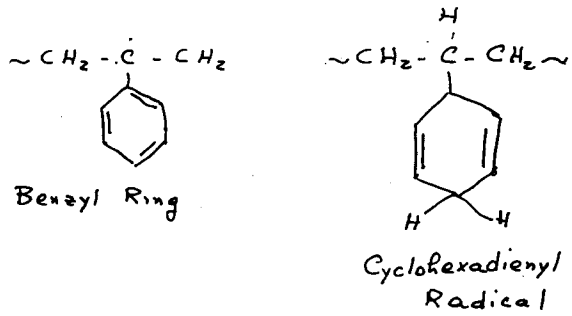

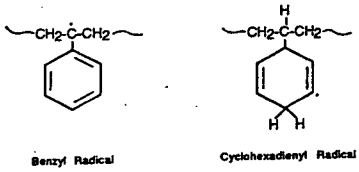

Absorption Bands (nm)

Benzyl	Cyclohexadienyl
258	308
293	314
304	512
316	554
422	
436	
452	

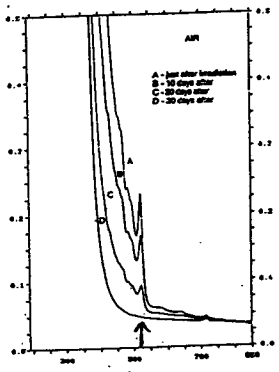

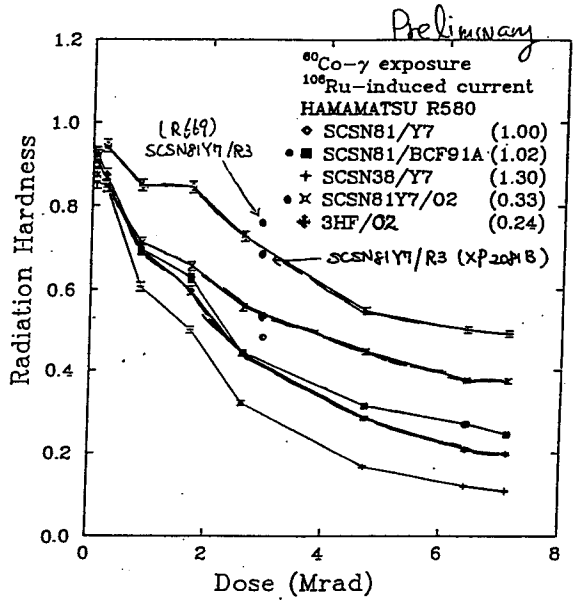

Figure 15: Comparison of radiation hardness of scintillating tiles with waveshifting fibers; SCSN81/Y7, SCSN81/BCF91A, SCSN38/Y7, SCSN81Y7/O2, and 3HF/O2. These samples were exposed to ^{60}Co γ-rays and evaluated by measuring ^{106}Ru-induced currents. The number in parentheses indicates a relative light yield of each tile/fiber sample measured by using Hamamatsu R580. Data is joined together by a solid curve for convenience.

1286

B. Sohm

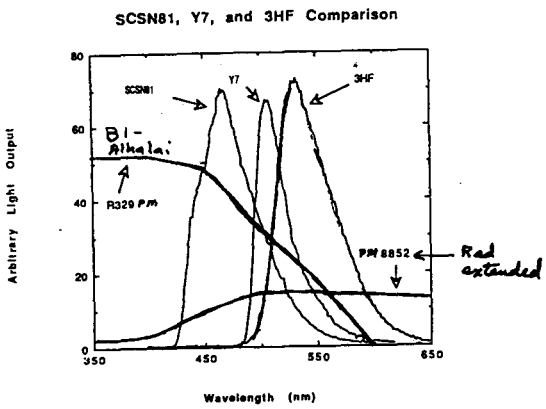

1287

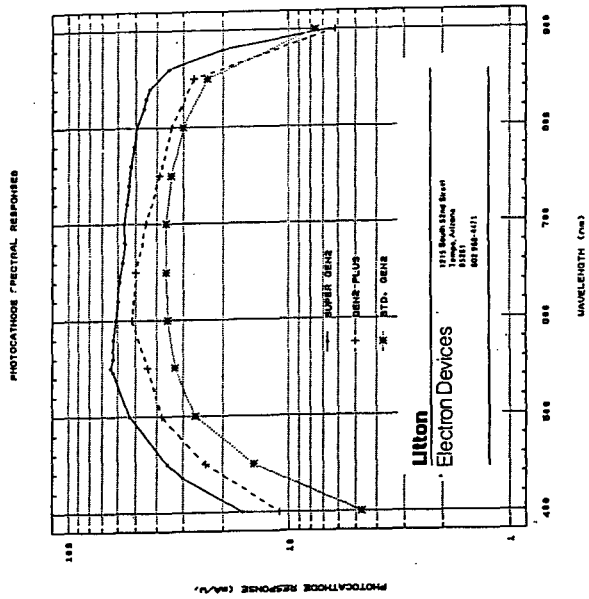

1288

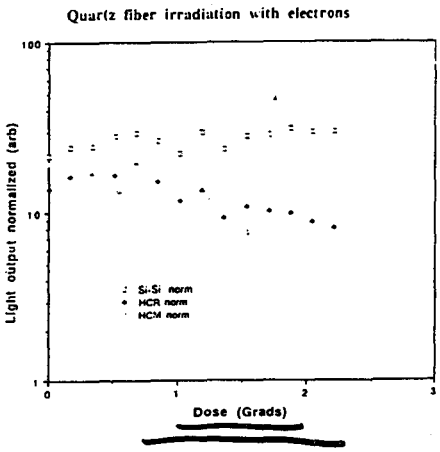

Can we turn this to advantage?

1289

NEUTRON IRRAD.

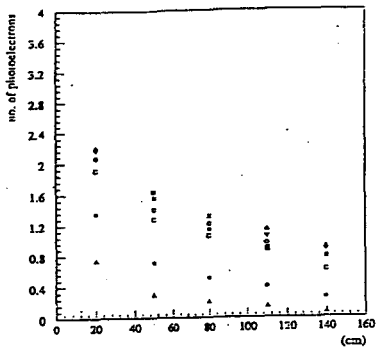

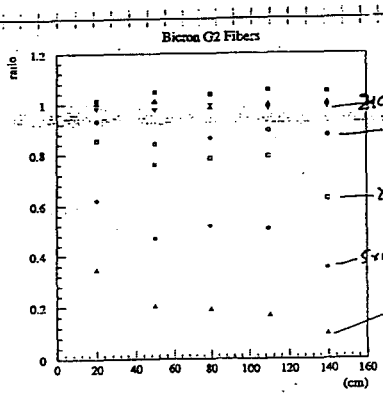

1290

DAMAGE TO SCINTILLATOR LIQUID

LIQUIDS: 0 vs 100 Mega Rads.

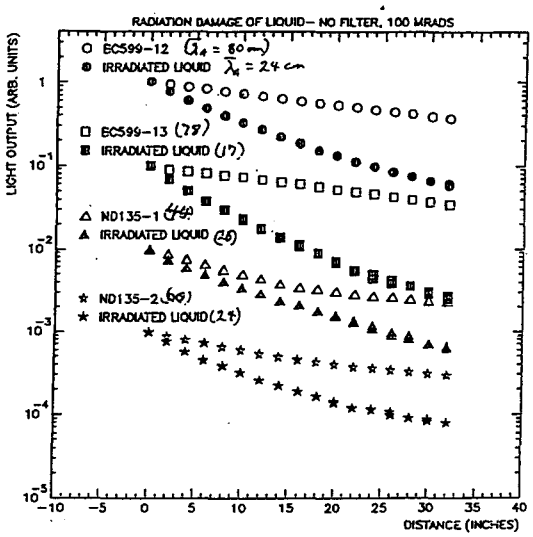

1291

DAMAGE TO GLASS TUBE

2mm Pyrex: 0 vs 100 megarads

** (IN AIR) **

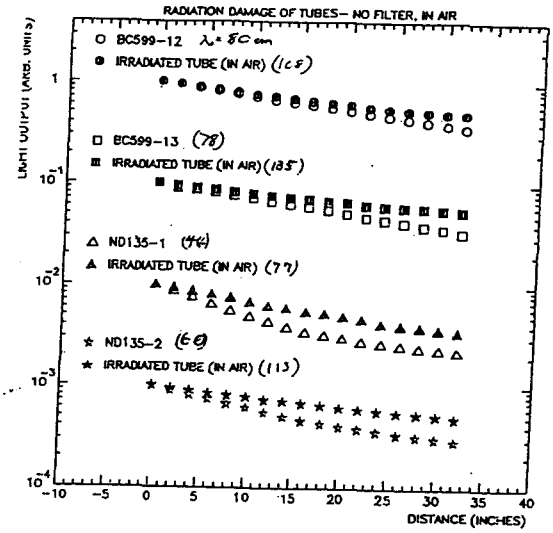

POSSIBLE CAUSES?

- Scattering of light in air-glass interface?
- short wavelengths killed?
- thick wall effect? {light produced in glass / other}
- or spiralling light?
- ?

1292

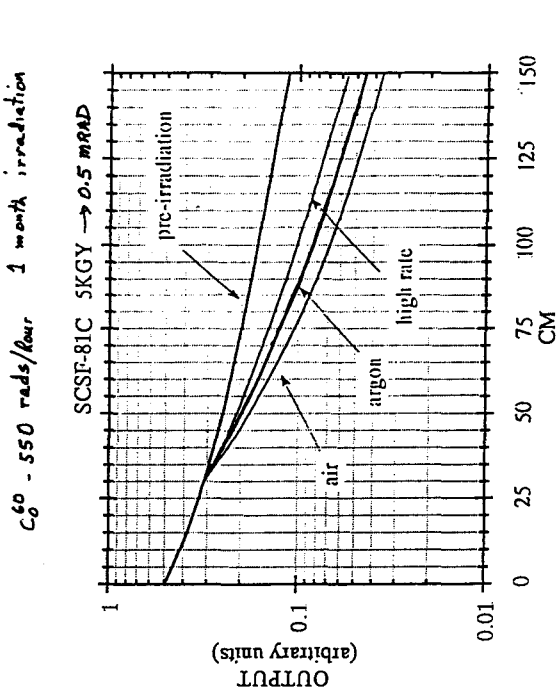

1293

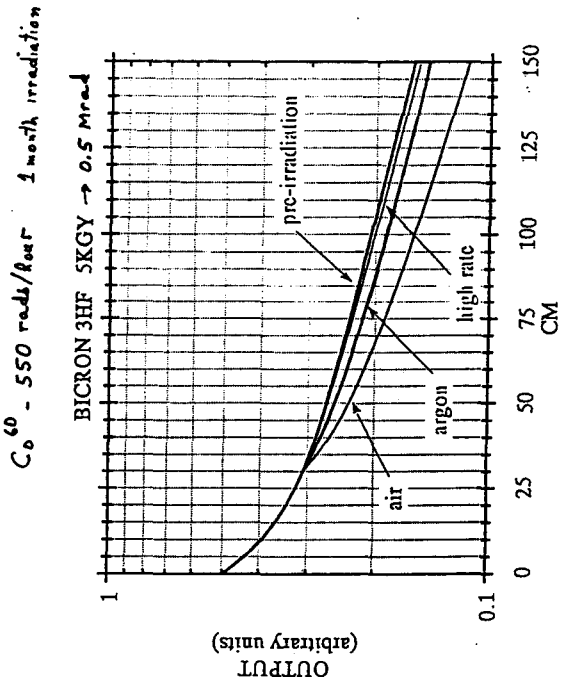

REALISTIC LOW DOSE RATE IRRADIATIONS OF PMMA MATERIALS

Initial damages after irradiation (air/argon)

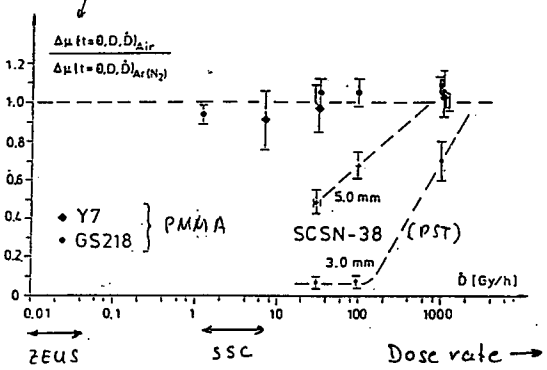

PMMA based materials:

- Build-up effect
- Long recovery times (in air, 10 kGy, 2mm, ~1 year)

Hope : PMMA recovers during low dose rate irradiation to permanent damage

But : at least down to dose rate 1 Gy/h there is <u>no recovery</u> during irradiation!

3.- LOW DOSE (250 Rad/hour) RESULTS

	Scint. Type		Attenuation Length Ratios $\Lambda_{after}/\Lambda_{before}$ @ 0.7 MRad	@ 1.6 MRad
1cm × 1cm × 20cm	SCSN23	Blue	0.81 ± 0.06	0.72 ± 0.05
	SCSN 81	Blue	0.76 ± 0.05	0.62 ± 0.04
	SCSN 81+Y7	Blue	0.93 ± 0.07	0.91 ± 0.06
	SCSN 81+Y8	Green	0.93 ± 0.07	0.95 ± 0.07
	3HF	Green	0.95 ± 0.07	0.91 ± 0.06
0.5cm × 1cm × 20cm	SCSN23	Blue	0.79 ± 0.05	0.76 ± 0.05
	SCSN 81	Blue	0.81 ± 0.06	0.71 ± 0.05
	SCSN 81+Y7	Blue	0.93 ± 0.07	0.94 ± 0.07
	SCSN 81+Y8	Green	0.96 ± 0.07	0.92 ± 0.06
	3HF	Green	0.93 ± 0.07	0.93 ± 0.07

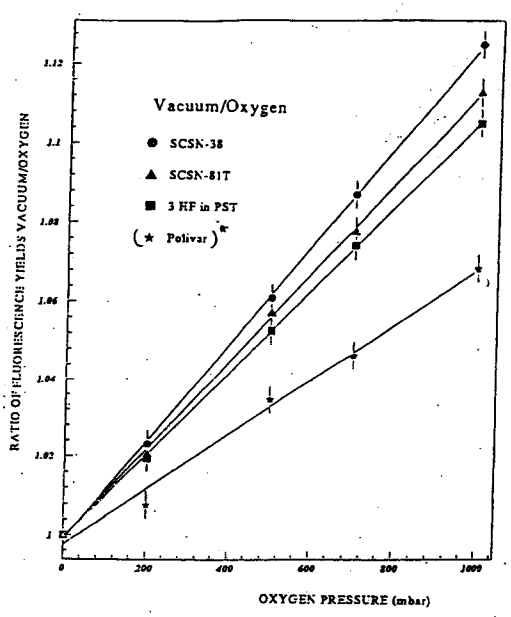

* these values are too low because we have not waited long enough! (PMMA, long diffusion time!)

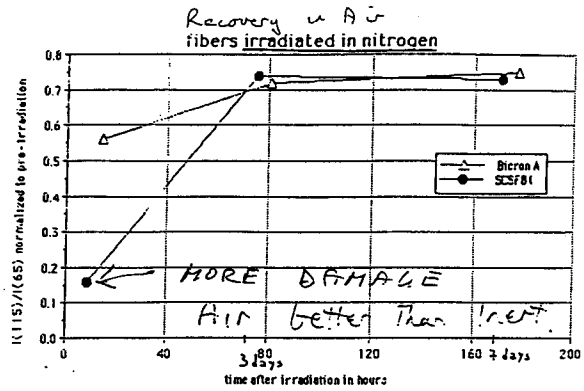

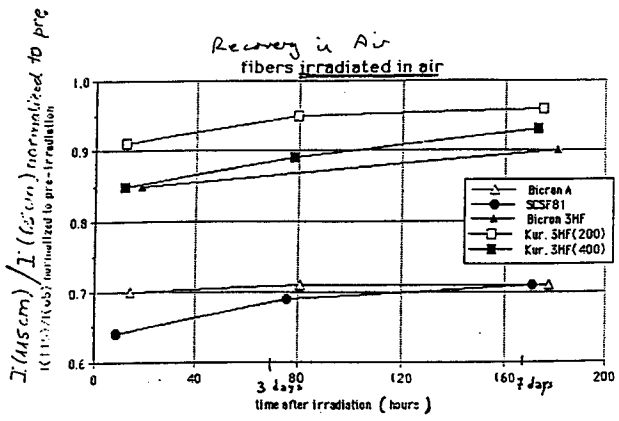

(LINES ONLY TO GUIDE THE EYE)

ATMOSPHERE & DOSE RATE

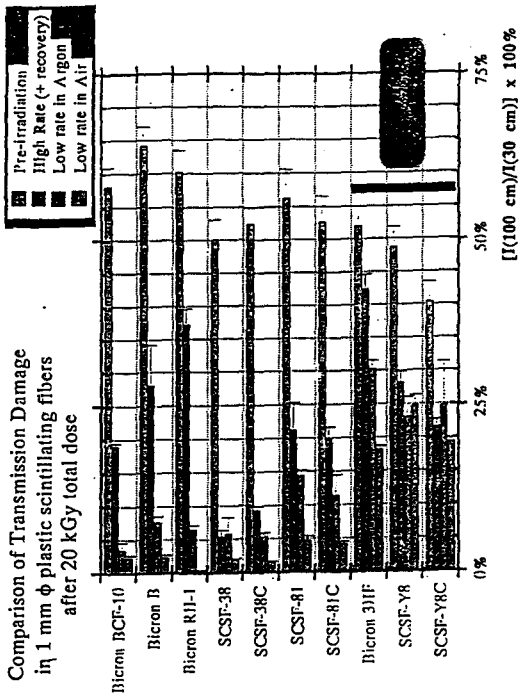

ATMOSPHERE

(11)

RESULTS AFTER IRRADIATION

(7 TO 14 HOURS RECOVERY TIME IN AIR)

Air Worse Than Inert.

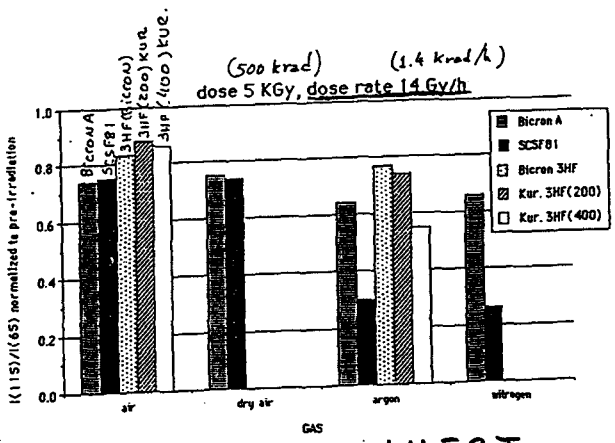

AIR Better Than INERT

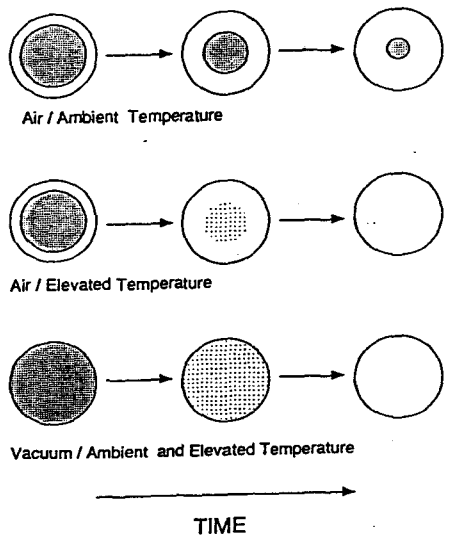

Radical - Radical Recombination. ⟷ O_2 Diffusion + Oxidation

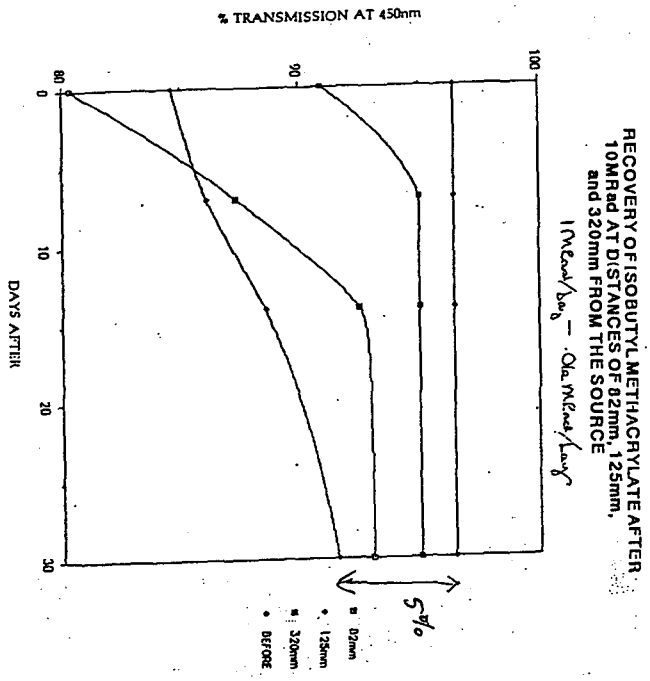

1302

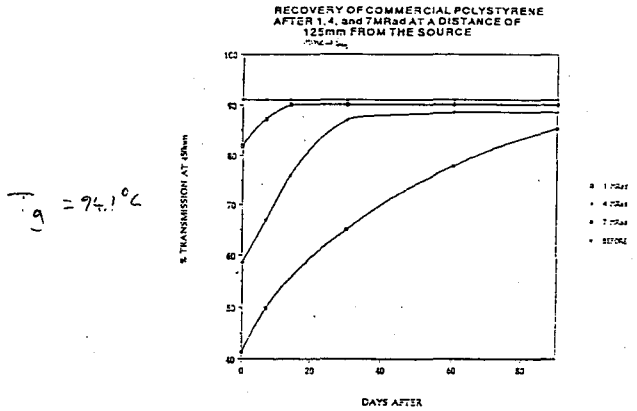

1303

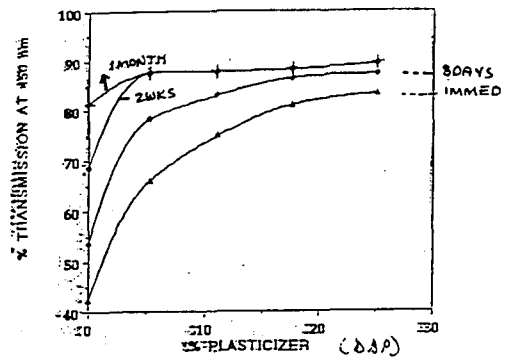

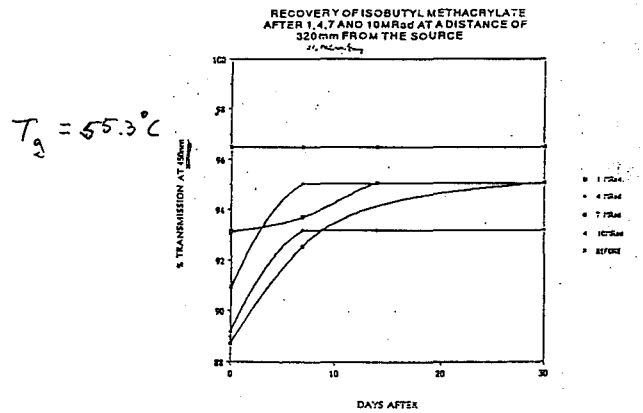

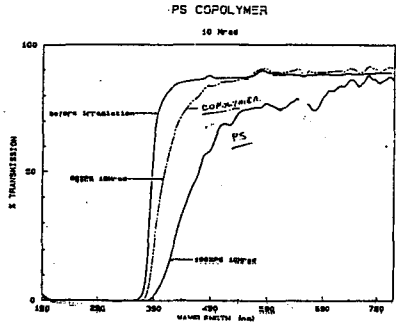

1301

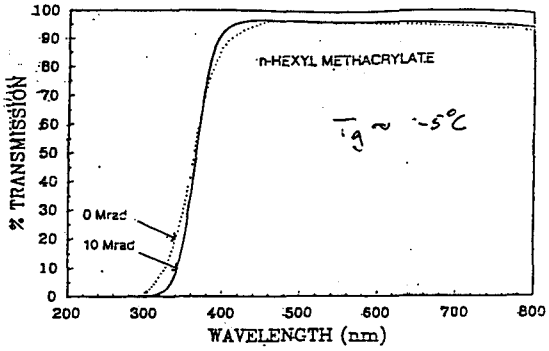

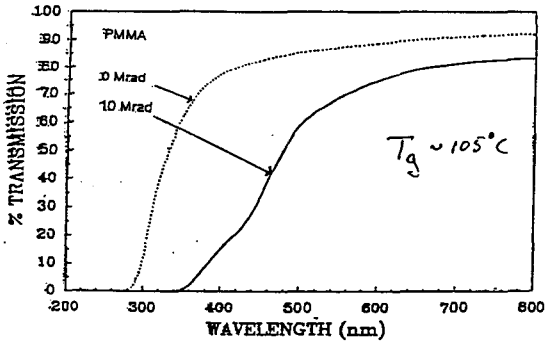

n-HEXYL METHACRYLATE BEFORE AND AFTER EXPOSURE TO 10 MRad IN ARGON AS COMPARED TO PMMA. BOTH SAMPLES ARE 1CM THICK.

1305

(11)

KURARAY 3HF + PTP

One of the few characteristics which is NOT affected τ_{decay}.

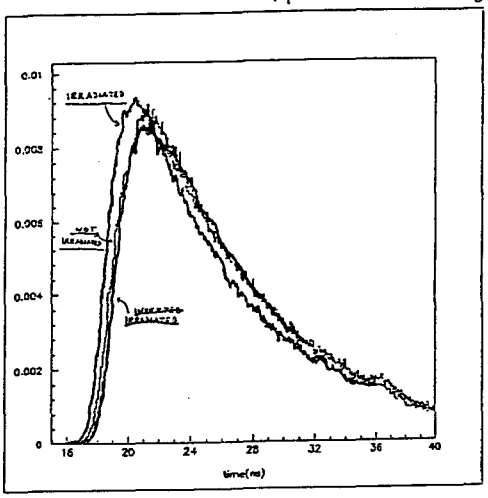

	NOT IRR.	IRR.	IRR. INVERTED
τ (ns)	7.9	7.4	7.9

1306

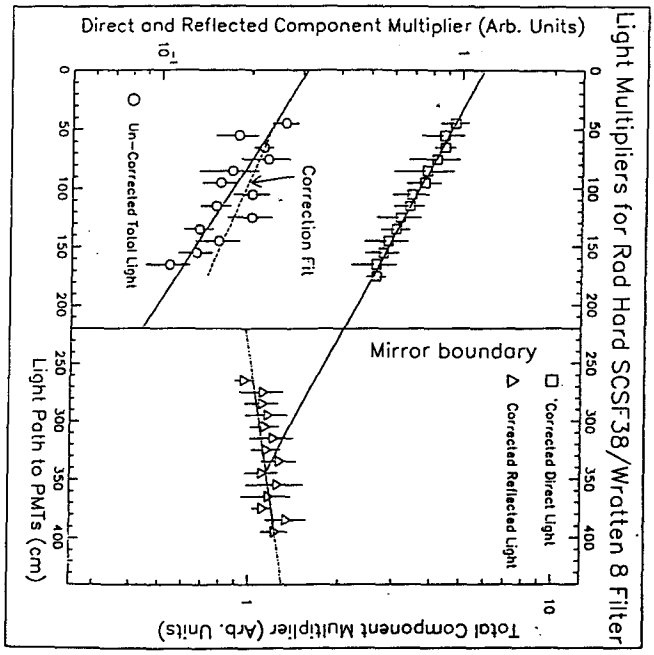

1307

Fiber SCSF38 (RHC)

SPACAL (Test)

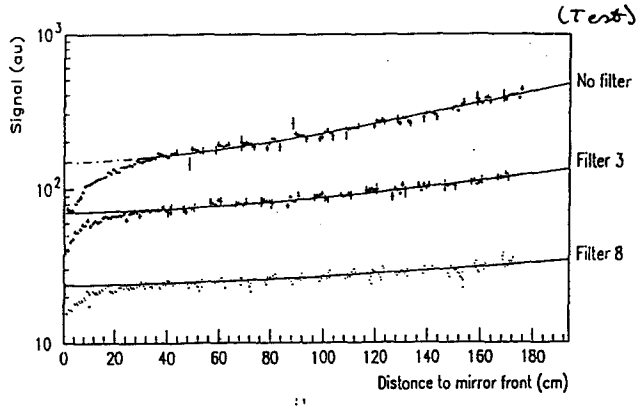

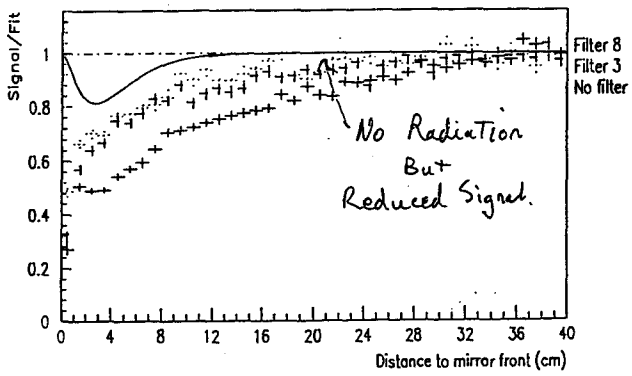

1308

SDC

Tile + Fiber

DUE DEPTH READOUT

CORRECTED USING TWO DEPTH READOUTS

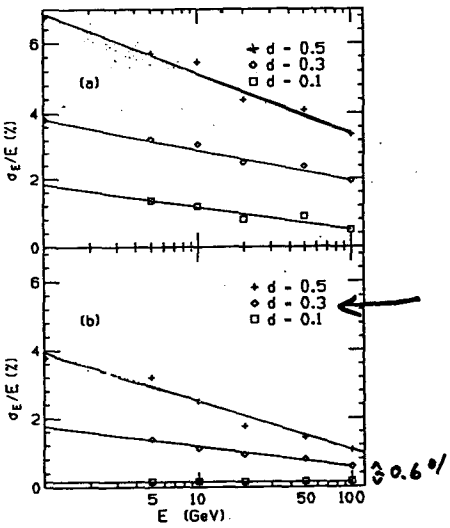

1309

Radiation Hardness = $\frac{\text{Light Yield after recovery}}{\text{Light Yield before exposure}}$

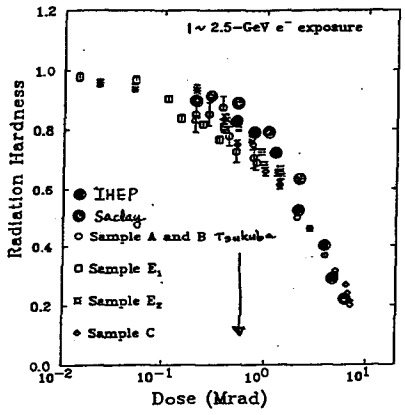

Transverse uniformity still < 2%.

Data from 3 site in good agreement.

different type PMT's used, slightly different calibration method, response to e⁻ beam, Ru or Co source

1310

Liquid Scint. + Fiber (CERN HAC)

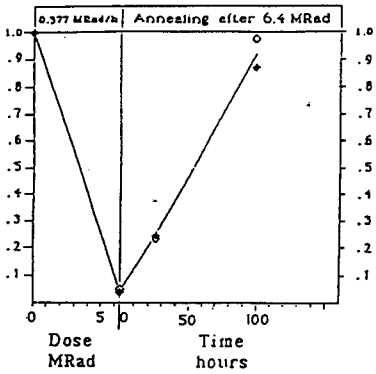

○ WLSF BCF - 91

✦ WLSF BCF - 91 + LS (BC-517P)

measured with green LED (550 nm) and Si photodiode (relative to reference nonirradiated fiber)

Fig. 6 Transmission of 1 mm diameter 1 m long fibers vs irradiation dose (6.4 Mrad max) and annealing time relative to reference nonirradiated fiber.

induced Constant Term ~ 2%

1311

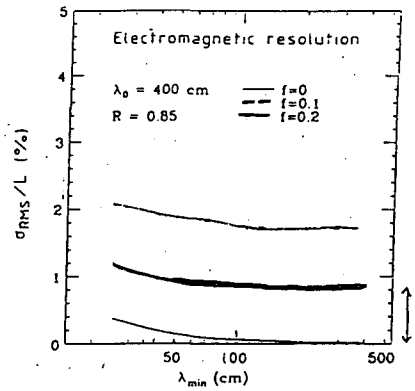

Erad = 1 GeV
E = 10 GeV

EAGLE

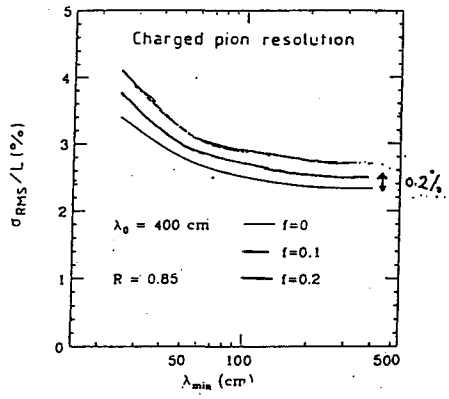

1312

Fit radiation hardness measurements to parametrization of:

A. Henriques

- light emission loss

$$\boxed{I(D) = I_0 e^{-D(z)/\gamma}} \qquad \gamma >>$$

$D(z)$ = Dose profile of ^{60}Co irradiation
γ = light emission reduction parameter

- light transmission loss

$$\boxed{1/\lambda_{att}(D) = 1/\lambda_0 + \alpha D(z)} \qquad \alpha <<$$

α = light transmission reduction parameter

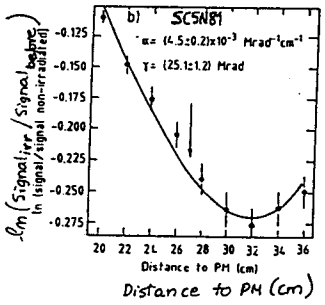

Distance to PM (cm)

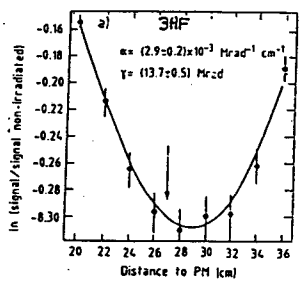

1313

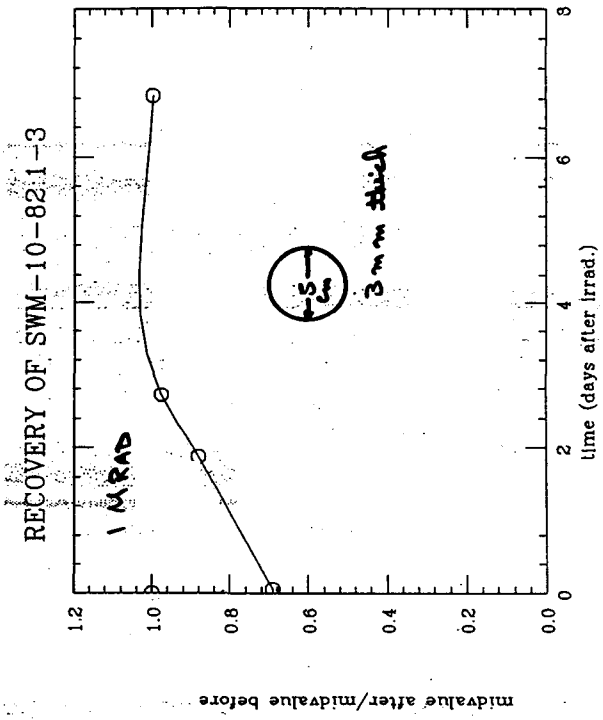

Proceedings to be published in the journal Radiation Physics and Chemistry

MEASUREMENT OF DECAY TIMES OF FAST SCINTILLATING FIBERS

J. M. Flournoy

EG&G Energy Measurements, Inc., 130 Robin Hill Road
Goleta, California 93117

ABSTRACT

A method is described for the determination of the decay times of scintillating fibers subjected to ionizing radiation. Excitation is by beta radiation from a custom-made $^{90}Sr/^{90}Y$ source. Pulse shapes are determined using time correlated single photon counting (TCPC) techniques.

KEYWORDS

Scintillators; scintillating fibers; decay time; photon counting; laser fluorescence.

INTRODUCTION

When a scintillator is excited by a pulse of ionizing radiation, the decay time of the emitted pulse of light usually appears to be longer than the fluorescence lifetime of the light-emitting solute. This is because, in most organic scintillators, excitation of the solute under the influence of ionizing radiation is by resonant energy transfer from excited solvent molecules, rather than by the direct absorption of a photon, as is the case with fluorescence. In cases where the fluorescence lifetime of the solute is only a few nanoseconds, the rate of this energy transfer often has a strong effect on the overall scintillation pulse shape. An example of this phenomenon appears in Fig. 1, which shows pulse shapes for the plastic scintillator BC-422, excited by fast 300-nm laser pulses (the narrower pulse shape) and by ^{60}Co gamma rays. These data were obtained in this laboratory.

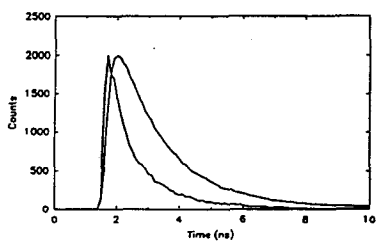

Fig. 1. Fluorescence and scintillation pulse shapes for BC-422.

SDC Meeting at KEK
May 26-29, 1992
Kiyoshi Yasuoka
Univ. of Tsukuba

Radiation damage of Tiles, Fibers, and Tile/Fiber Assemblies

1. Radiation field in the SDC calorimeter
2. Radiation damage of tile/fiber assemblies
   ANNEALING, $\dot{D}$, GAS, CONT./DISCONT., UNIFORMITY
3. Radiation damage of optical components; tiles and fibers
   OPTICAL SPECTRUM ANALYSIS
4. Effects of radiation damage to energy resulution
5. Conclusions

RADIATION FIELD IN THE SDC CALORIMETER

◎ THE SDC CALORIMETERS ARE REQUIRED TO BE SURVIVABLE FOR 10 YEARS AT 10^{34}

MAX. IONIZING DOSE:

$$\frac{A}{r^2 \sin^{2+\alpha}\theta}$$

	A (Gy m²)	α	⟨P_T⟩
PHOTONS	12% Gy yr⁻¹	0.93	0.3 GeV/c
HADRONS	2.9 Gy yr⁻¹	0.87	0.4 GeV/c

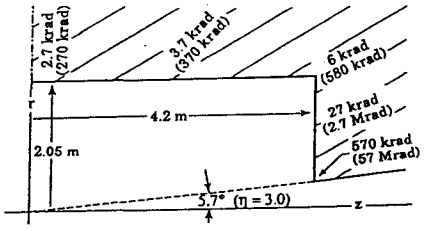

for 10 years of operation
@the design luminosity of 10^{33} cm^{-2}sec^{-1}

η	Dose (krad)	Dose Rate (rad/h)
0	27	1
1.5	58	2
3.0	5700	200

TILE/FIBER SAMPLES

TILE: 11.1 cm × 11.1 cm × 0.3 cm^t
FIBER: 1 m × 1 mm$^\phi$ (PS BASE, PMMA CLAD)
WRAPPING: WHITE PAPER

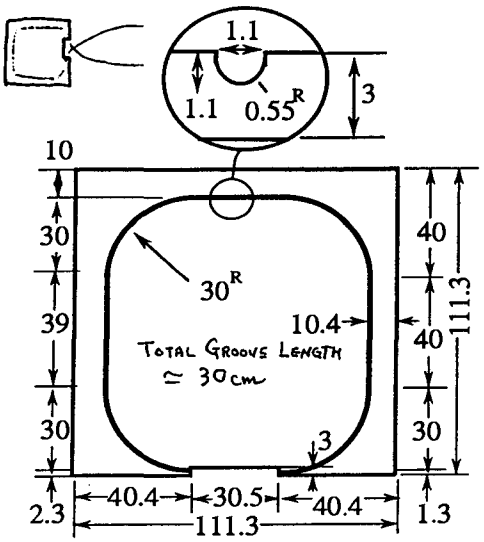

SCSN 81/Y7
SCSN 81/BCF91A
SCSN 38/Y7
SCSN81Y7/02
3HF /02

MEASUREMENTS OF ANNEALING EFFECTS OF RADIATION DAMAGE FOR T/F

(@ JAPAN ATOMIC ENERGY RESEARCH INSTITUTE)

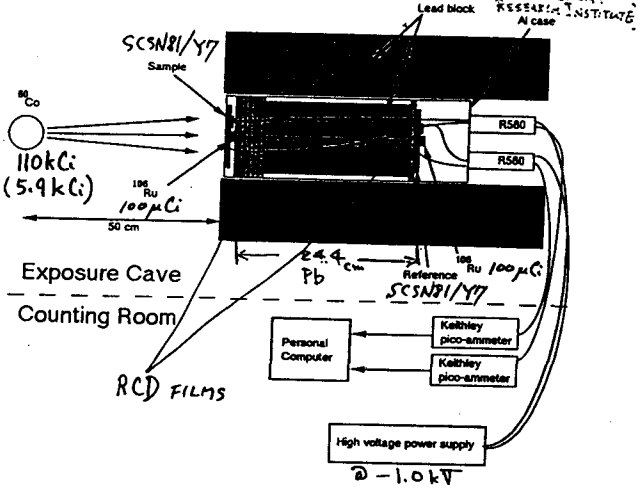

- PMT HV'S WERE TURNED OFF DURING THE IRRADIATION.
- AFTER STOPPING EACH IRRADIATION, THE CURRENT MEASUREMENT WAS IMMEDIATELY STARTED AT THE NORMAL OPERATION VOLTAGE.
- NO ACCESS TO THE T/F'S DURING THIS MEASUREMENT.

ANNEALING EFFECTS OF RAD. DAMAGE FOR TILE/FIBER ASSEMBLIES (5)

"HIGH" $\dot{D}$

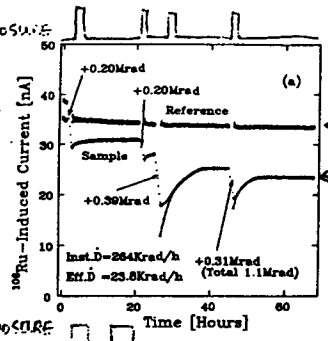

TOTAL 1.1 MRAD AT INST. $\dot{D}$ ≃ 264 KRAD/H

← REFERENCE

← SAMPLE (SCSN81/Y7)

"LOW" $\dot{D}$

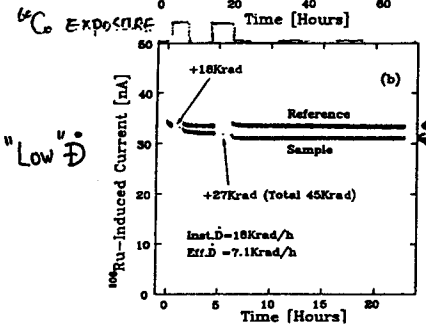

TOTAL 45 KRAD AT INST. $\dot{D}$ ≃ 18 KRAD/H

← REFERENCE

← SAMPLE (SCSN81/Y7)

EXPOSURE/ANNEALING ~ AIR/AIR

ANNEALING EFFECTS OF RAD. DAMAGE FOR TILE/FIBER ASSEMBLIES (CONT'D) (6)

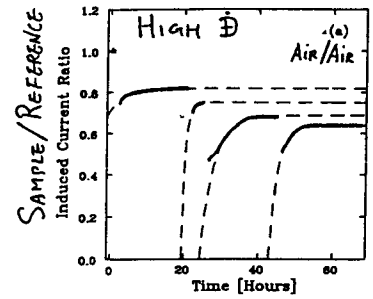

$R = R_0 (1 - e^{-t/\tau})$

$\tau \simeq 1 \sim 4$ [illegible]

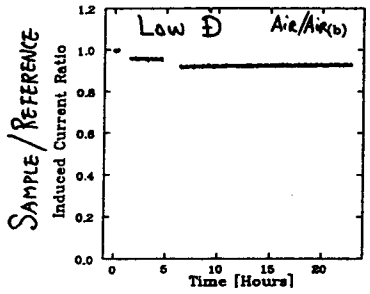

NO LARGE DROPS RIGHT AFTER IRRAD.

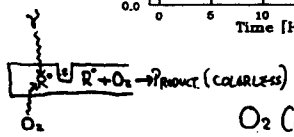

O_2 CONSUMPTION ⟺ O_2 SUPPLY

NOTE: Case (b) TAKES PLACE AT SSC

LIGHT YIELD MEASUREMENT (7)

X-Y SCANNER

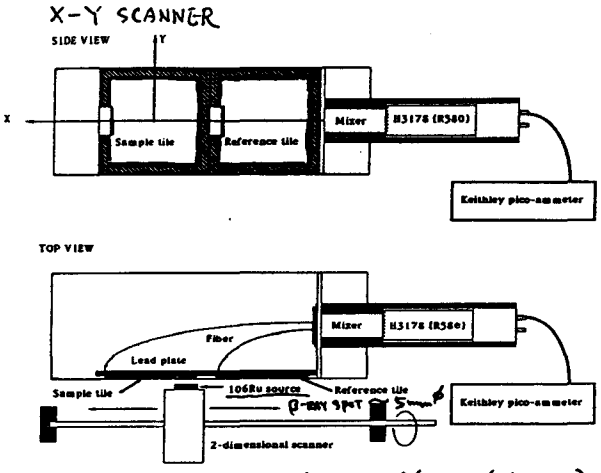

$$\text{"RADIATION HARDNESS"} \equiv \frac{\text{LIGHT YIELD (AFTER)}}{\text{LIGHT YIELD (BEFORE)}} = 1 - \text{RAD. DAMAGE}$$

WHERE

$$\text{LIGHT YIELD} = \frac{^{106}\text{Ru-INDUCED CURRENT (SAMPLE)}}{\text{" (REF.)}}$$

MEASURED AT THE CENTER OF TILE.

DOSE RATE DEPENDENCE (8)

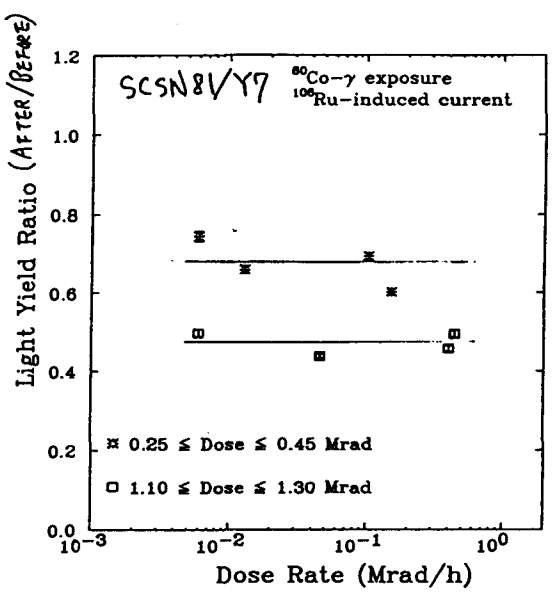

NO SIGNIFICANT $\dot{D}$-DEPENDENCE IS OBSERVED IN THE RANGE $6 \leq \dot{D}_{INIT} \leq 360$ KRAD/H

$\dot{D}_{INIT} = 0.2$ KRAD/H at $\eta = 3.0$ at [illegible] $\mathcal{L}$.

1323 (9)

EFFECTS OF GAS ENVIRONMENTS ON RADIATION DAMAGE.

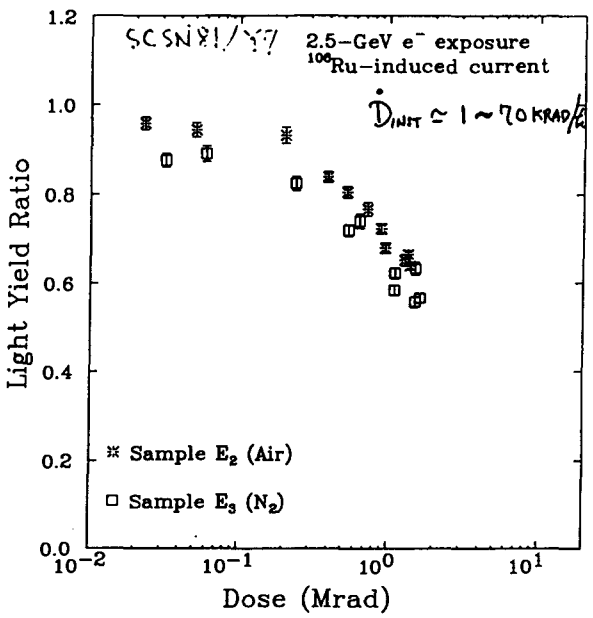

NO SIGNIFICANT IMPROVEMENT IN RADIATION HARDNESS WAS OBSERVED IN THE SAMPLES EXPOSED IN N_2.

1321 (10)

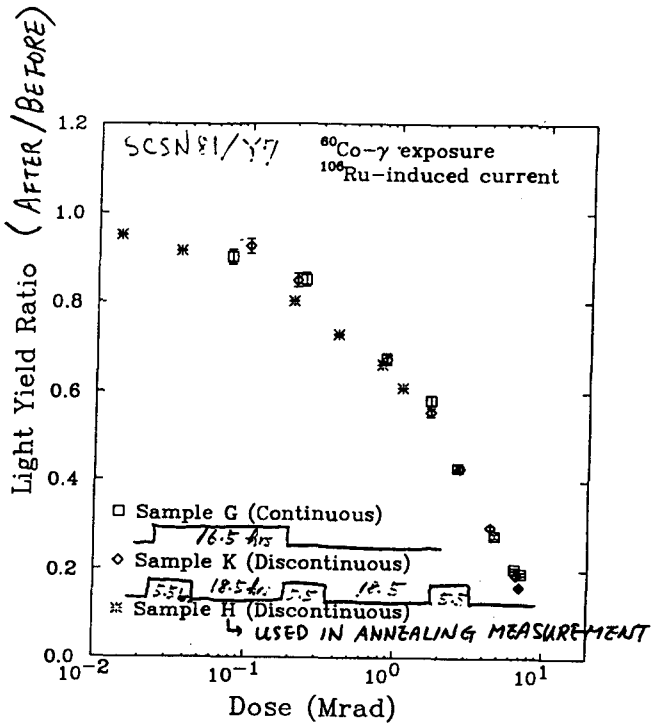

NO DIFFERENCE WAS OBSERVED BETWEEN THE CONTINUOUS & DISCONTINUOUS IRRADIATIONS.

1325 (11)

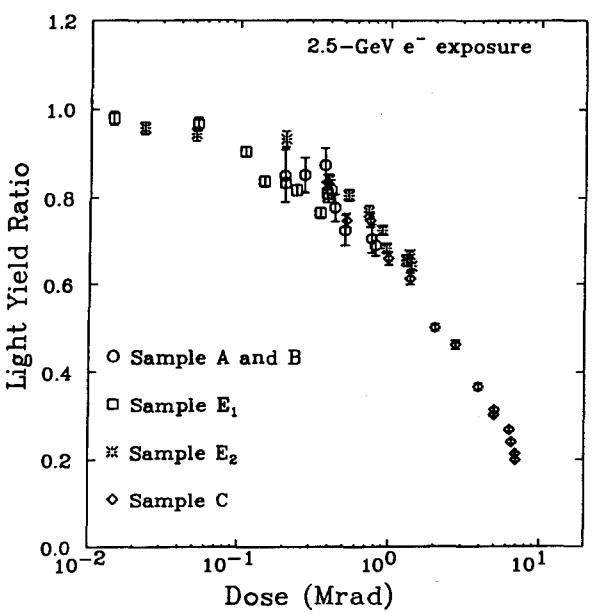

1326 (12)

RESPONSE UNIFORMITY BEFORE & AFTER IRRADIATION

SCSN81/Y7

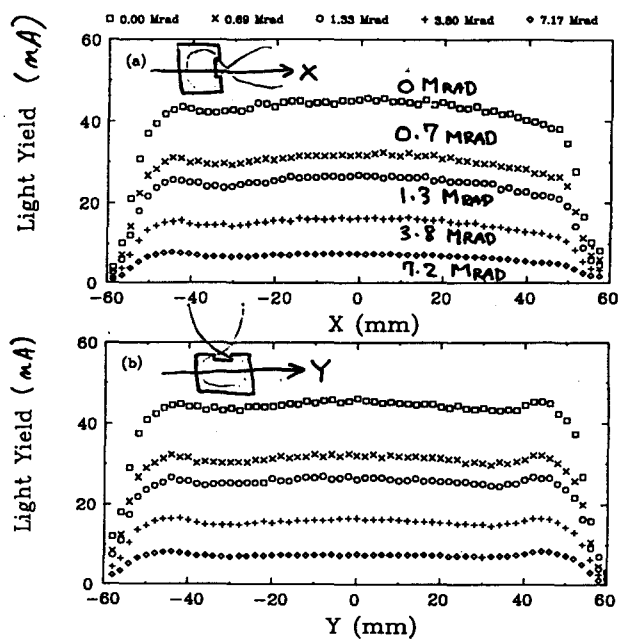

NORMALIZED RESPONSE UNIFORMITY

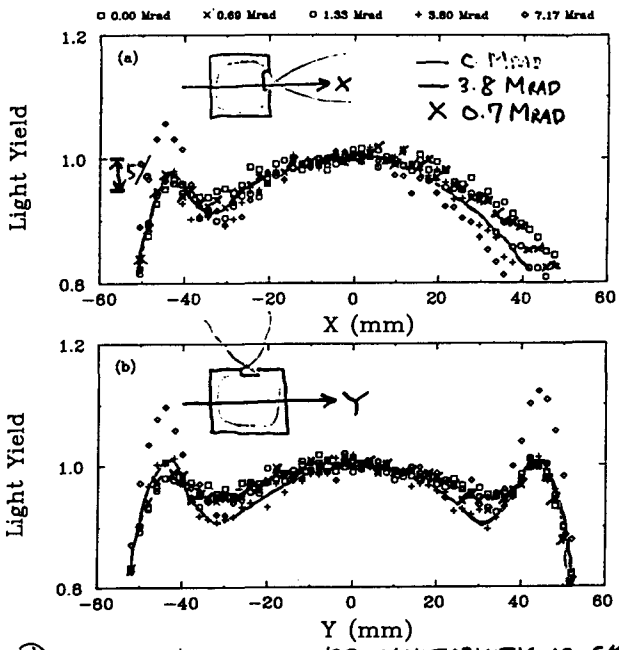

DEGRADATION OF RESPONSE UNIFORMITY IS SMALL UP TO 1 MRAD. AND ≲ 5% AT 3.8 MRAD.

DOSE IMBALANCE IN A TILE

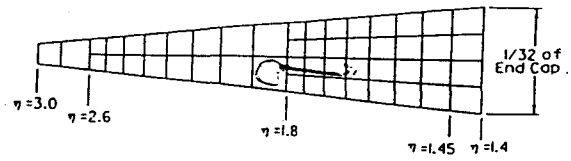

END CAP SEGMENTATION (EM)
ETA - PHI MAP
SSC DWG # SD0000096

η	Δη	ΔD/D (*)
0-1.4	0.05	0-12 %
1.4-1.8	0.05	13 %
1.8-2.6	0.1	25 %
2.6-3.0	0.2	44 %

(*) Dose imbalance in a tile at peak-to-peak

"NON UNIFORM IRRADIATION TEST w/ ^{60}Co"

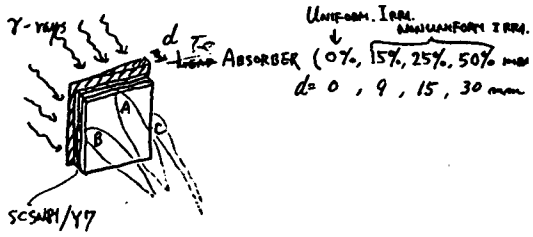

RESPONSE UNIFORMITY OBTAINED BEFORE & AFTER 4.2 MRAD IRRADIATION w/ 25% DOSE IMBALANCE IN A TILE.

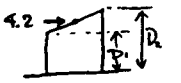

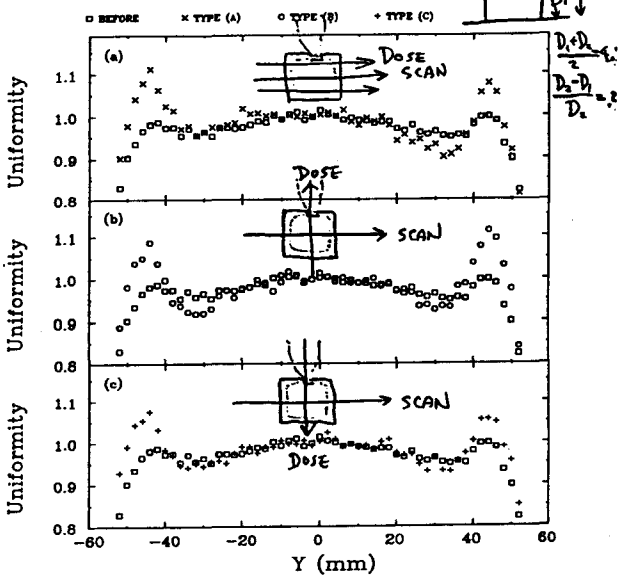

RESPONSE UNIFORMITY DOES NOT DEPEND STRONGLY ON HOW THE T/F IS PLACED WITH RESPECT TO THE DIRECTION OF DOSE IMBALANCE.

UNIFORMITY DEGRADATION AT Y = ±3.5, ±8.5 cm w/ NONUNIFORM IRRADIATION

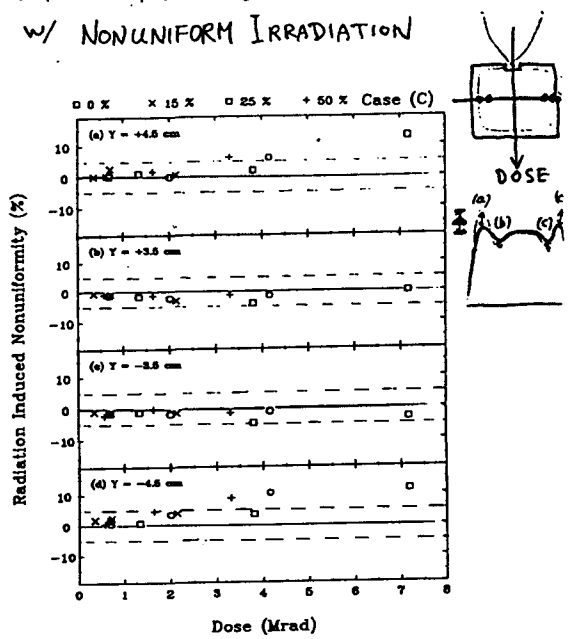

RADIATION-INDUCED NONUNIFORMITY DOES NOT DEPEND STRONGLY ON THE DOSE IMBALANCE BETWEEN 0 ~ 50% UP TO 3~4 MRAD.

$\Delta \leq 5\%$ for $D \leq 3.5$ MRAD

Radiation-Induced Nonuniformity

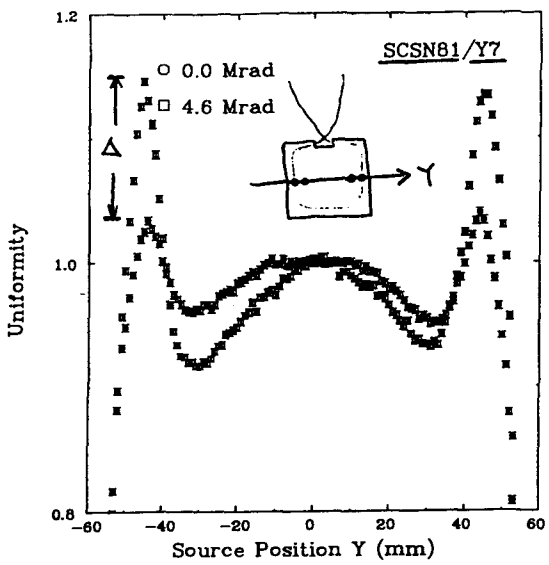

$\Delta(\pm 4.5\,cm) \sim 10\%$

$\Delta(\pm 3.5\,cm) \sim 5\%$

Radiation-Induced Nonuniformity (cont'd)

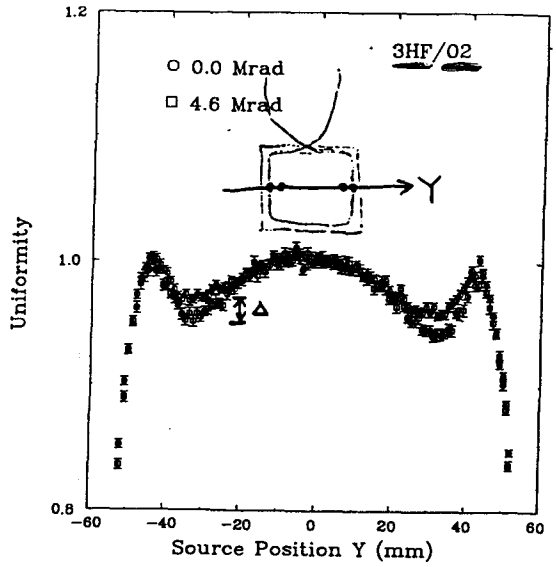

$\Delta(\pm 4.5\,cm) < 1\%$

$\Delta(\pm 3.5\,cm) \lesssim 2\%$

Good News!

Radiation Damage of Optical Components

(Tile → Bar, Fiber)

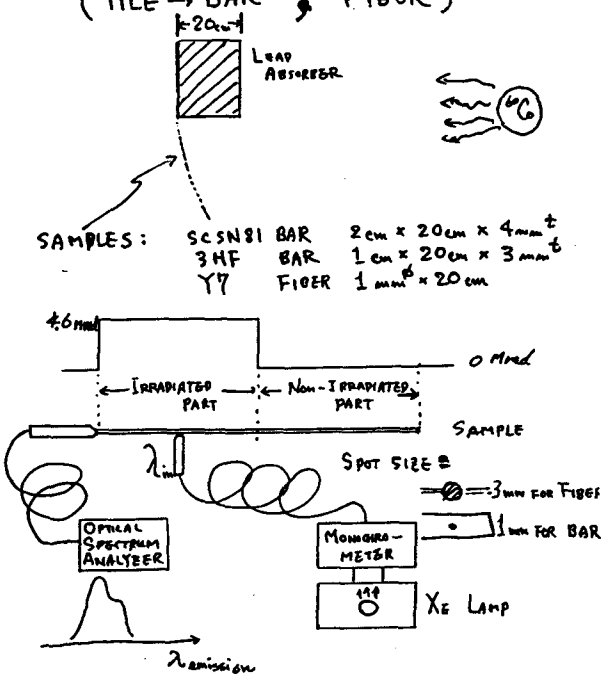

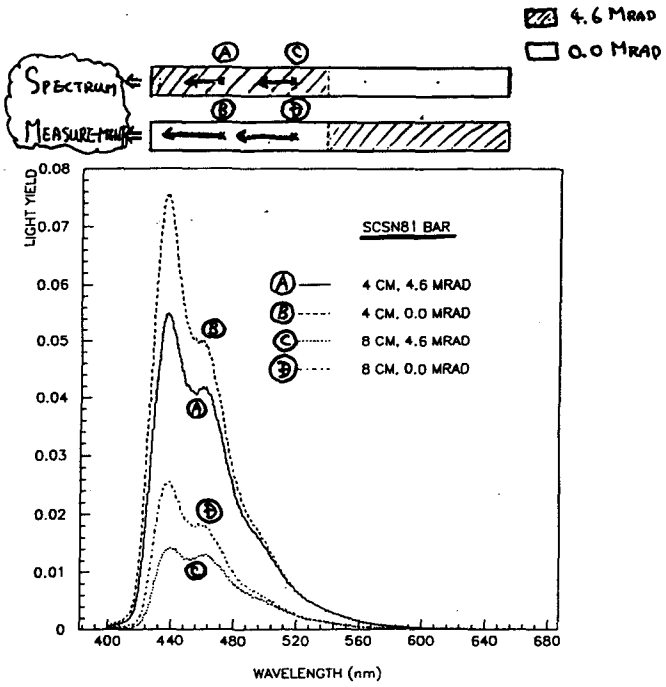

1335 (21)

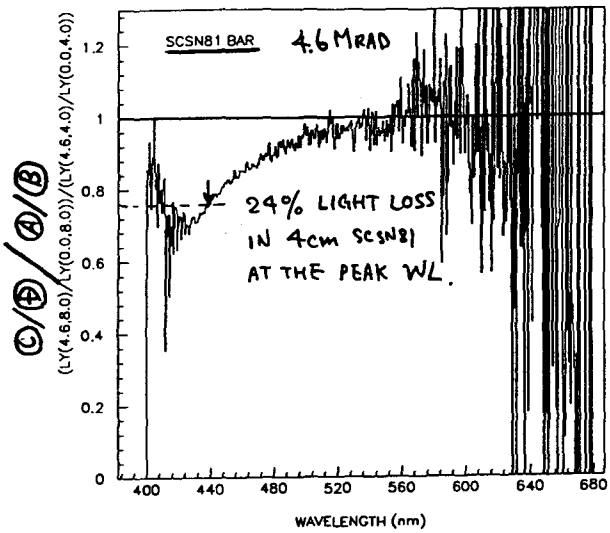

1336 (22)

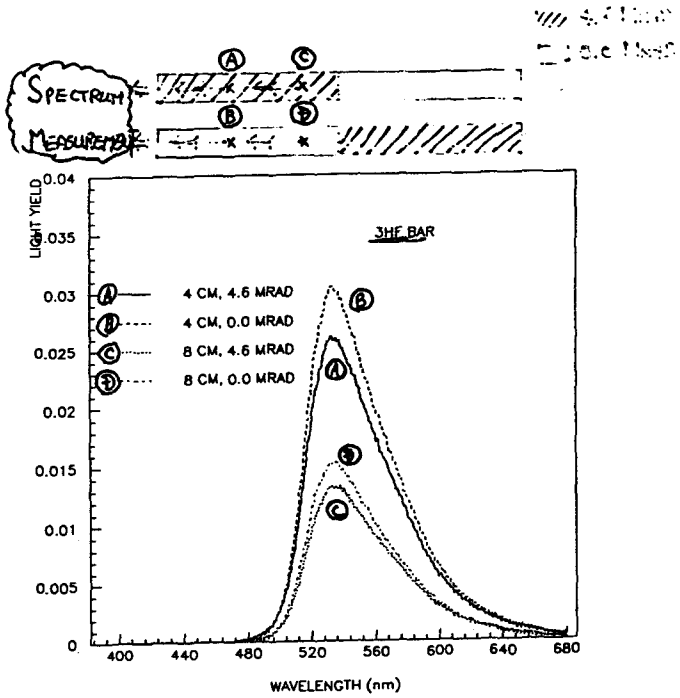

1337 (23)

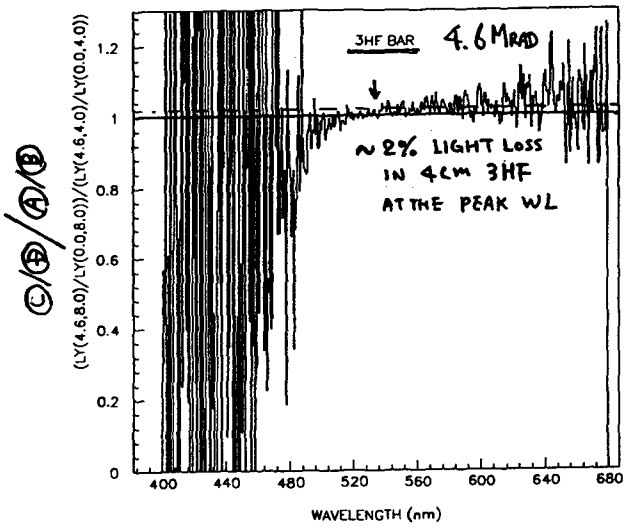

1338

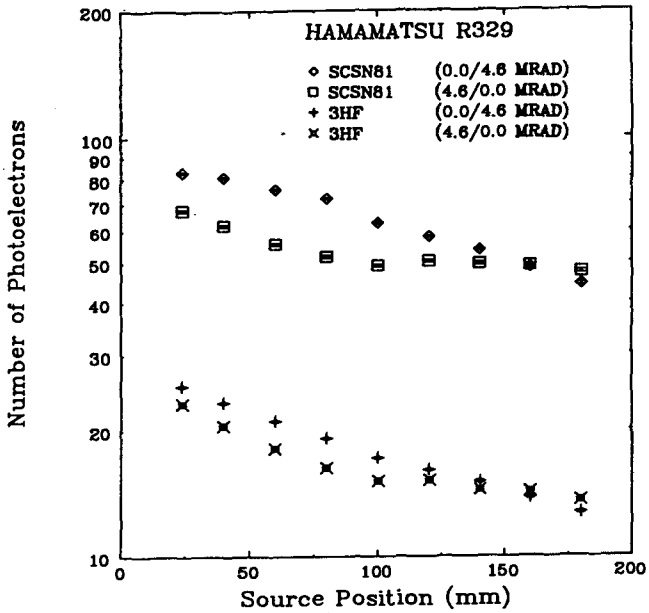

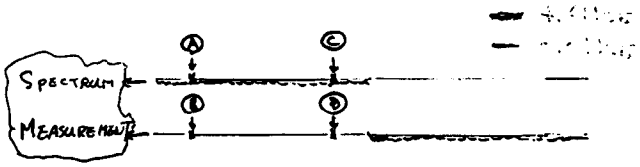

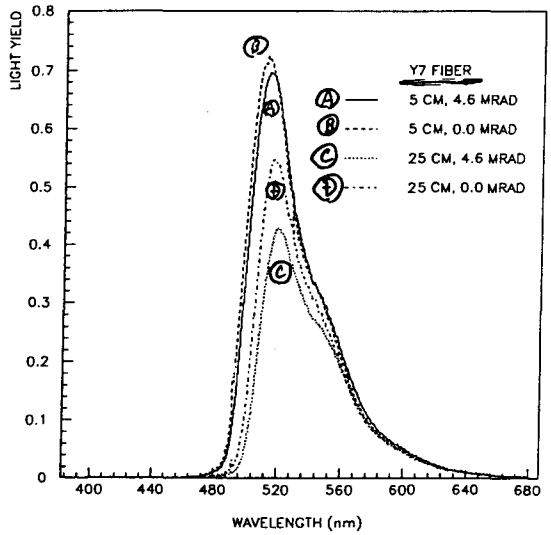

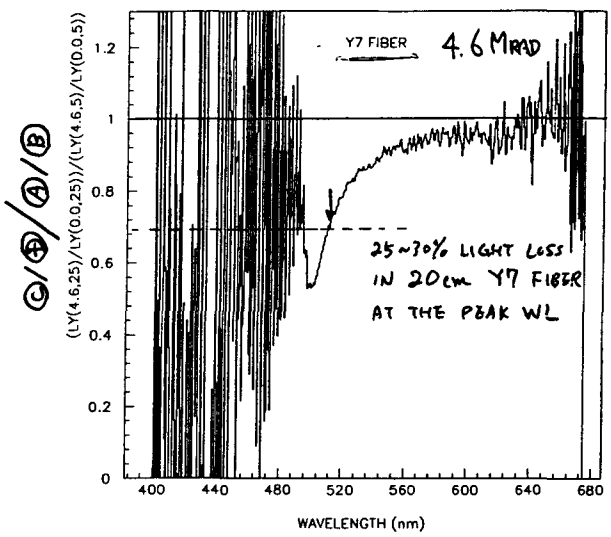

RADIATION DAMAGE OF T/F ASSEMBLIES FOR DIFFERENT COMBINATIONS

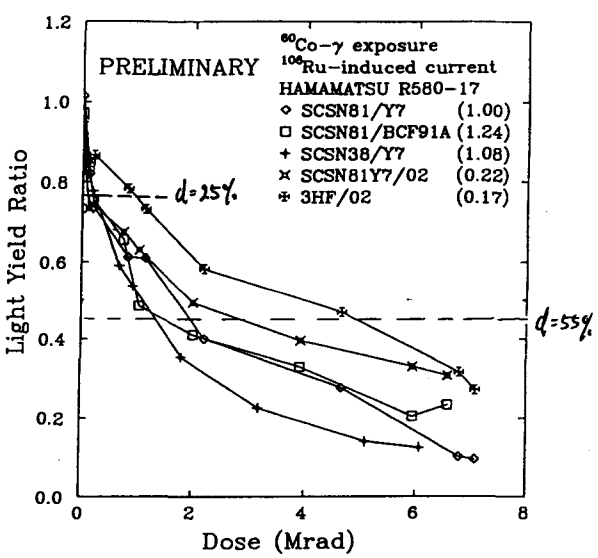

- 3HF/02 IS SIGNIFICANTLY RADIATION-RESISTANT.
- RED SENSITIVE PMT (EX. R669) WOULD SOLVE THE LIGHT YIELD PROBLEM FOR 3HF/02.

EFFECTS OF RADIATION DAMAGE TO ENERGY RESOLUTION

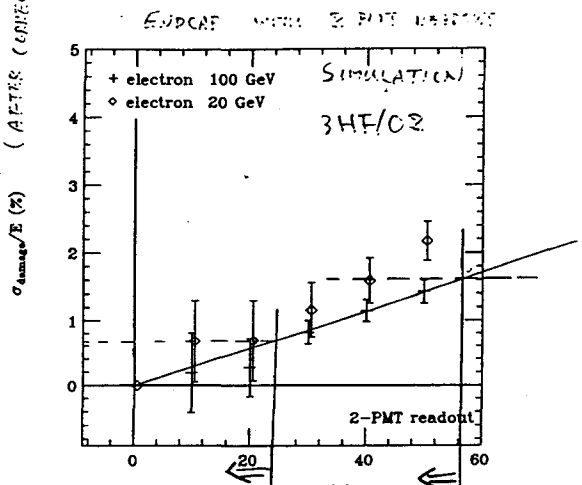

$$\frac{14.7\%}{\sqrt{E}} \oplus \frac{7.1\%}{\sqrt{E}} \oplus \left(\frac{\sigma}{E}\right)_{DAMAGE} < \frac{15\% \times 1.5}{\sqrt{E}} \oplus 1.0\%$$

Sampling — Photo statistics (20 p.e/GeV) — Requirement at $\eta = 1.4$

FOR 100 GeV e^-, $\left(\frac{\sigma}{E}\right)_{DAMAGE} < 1.6\% \oplus 1.0\%$ for 20 p.e/GeV

3HF/02 (Endcap w/ 2 PMT readout)

	200 p.e./GeV	40 p.e./GeV
PMT	Red sensitive (ex. R669)	Green extended (ex. R580-17, XP2081B)
$\left(\frac{\sigma}{\sqrt{100\,\mathrm{GeV}}}\right)_{\mathrm{Damage}}$	< 1.6% ⊕ 1.0% (stochastic)	< 0.64% ⊕ 1.0% (stochastic)
α	< 55%	< 25%
Dose	< 4.5 Mrad	< 0.7 Mrad

CONCLUSIONS

1. THE BARREL CALORIMETER USING SCSN 81/Y7 WILL SURVIVE FOR 10 YEARS OF RUNNING AT 10^{34}. (DOSE ~ 0.62 MRAD).

   DEGRADATION OF ENERGY RESOLUTION & RESPONSE UNIFORMITY → OK.

2. THE ENDCAP CALORIMETER USING 3HF/02 WILL SURVIVE UPTO A LIFETIME DOSE OF < 4.5 MRAD.

   THE RADIATION-INDUCED NON UNIFORMITY FOR 3HF/02 IS VERY SMALL (< 2%) UP TO 4.6 MRAD.

3. WE NEED STILL DEVELOPMENT OF RADIATION-RESISTANT T/F'S FOR THE END CAP CALORIMETER.

STUDY OF DOSE-RATE EFFECTS ON THE RADIATION DAMAGE OF SCSN23, SCSN81, SCSN81+Y7, SCSN81+Y8 & 3HF SCINTILLATORS

N. Giokaris – The Rockefeller Univ.
M. Contreras – Univ. of Chicago
A. Pla, J. Zimmerman – Fermilab
K. Johnson – Florida State Univ.

OUTLINE

1. MOTIVATION
2. EXPERIMENTAL PROCEDURE
3. RESULTS
4. CONCLUSIONS

Giokaris RAD-DAM WORKSHOP – FSU: 1990

1. MOTIVATION

SCSN23 SCINTILLATOR, USED FOR CDF BEAM-BEAM COUNTERS (BBC) EXPERIENCED SERIOUS RADIATION DAMAGE DURING THE 1988-89 RUN:

~ x 7 DECREASE IN ATTENUATION LENGTH
~ 40% DECREASE IN LIGHT YIELD
ESTIMATED DOSE: NO MORE THAN 10 KRad

N. Giokaris
RAD-DAM WORKSHOP
FSU : 1990

DOSE RATE : ~ 1 Rad/hour

Table II. BBC Lightpipe Dimensions

Counter #	Lightpipe Length (in)	Counter end Width (in)	Tube end Width (in)	Physical type
0	9/16	1.23	19/32	flat
1	3/4	2.39	1 3/4	flat
2	6	4.63	1 3/4	Double taper
3	12	8.94	1 3/4	Double taper

3. Measurements-Results

The measurements, mentioned in this paper, were perfomed after almost seven months after the end of the 1988-89 collider run at Fermilab. The BBC were removed from the collision hall after the end of that run. Although we did measure counters of all types i.e # 0, 1, 2 and 3 from both the forward and the backward planes [5] we will focus here on the comparison of a type # 1 BBC scintillator and of type # 1 scintillator from the same batch that was not exposed to radiation. These two scintillators were measured with the same photomultipliers at the same high voltage and with the same light guides. The current of photomultiplier A versus the ^{90}Sr source distance from light pipe A is shown in fig. 2. The difference in current between the two scintillators at zero

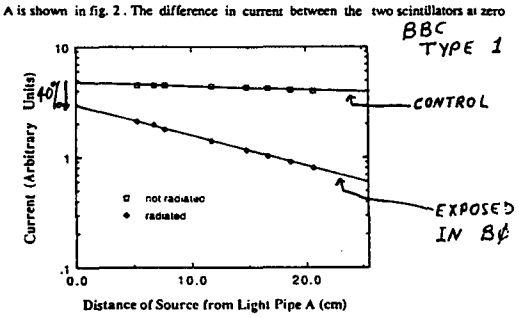

Fig. 2. Current of photomultiplier A versus the source distance from light pipe A.

been measured with a ^{90}Sr source and with cosmic rays after being exposed to 2 -> 4 Krad (lower limit) radiation. It was found that its attenuation length is 5 times shorter and its light yield 40% less than a control scintillator sample of exactly the same type and size. This damage could have been caused by a total beam loss close to the CDF detector. If this is not the case, we are forced to conclude that the damage was caused by a relatively small dose of radiation, delivered at a very small rate over a long period of time.

References

[1] KURARAY CO., LTD., Shuwa Higashi-Yaesu Building, 9-1, 2-Chome, Hatchobori, Chuo-Ku, Tokyo, 104 JAPAN.
[2] H. J. Frisch et al., CDF note # 250.
[3] T. M. Liss et al., CDF note # 552.
[4] F. Abe et al., Nucl. Instr. and Meth. A271 (1988) 387-403.
[5] N. Giokaris, CDF note # 1214.
[6] R. J. Yarema, Fermilab TM-1610.
[7] C. S. Lindsey et al., Nucl. Instr. and Meth. A254 (1987) 212-214.
[8] R. L. Clough et al., "Radiation Effect on Scintillating Fiber Optics for SSC", These Proceedings.

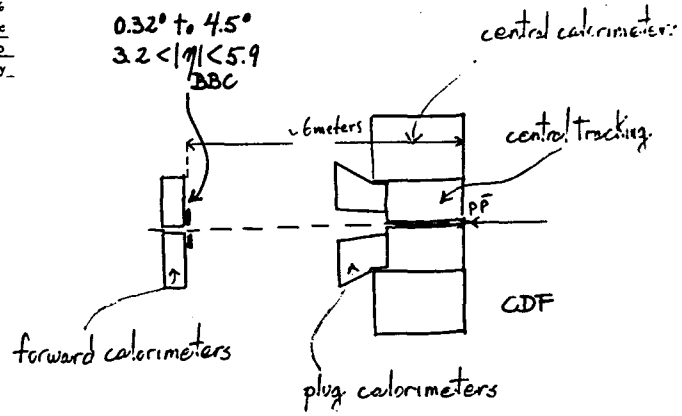

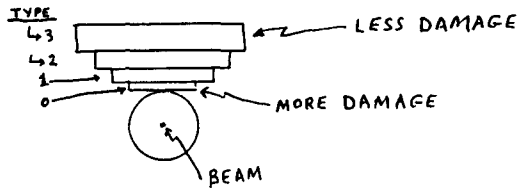

- DECIDED TO DO CONTROLLED RAD-DAM TESTS

(FIRST SET OF MEASUREMENTS PERFOMED IN SUMMER OF 1990)

SAMPLES : SCSN23, SCSN81, SCSN81+Y7 } SUPPLIED BY KURARAY
1x1x10 cm³

DOSES (^{60}Co source) : 10 Krad, 100 Krad, 1 Mrad

DOSE RATES : 1.2 Mrad/hour , 10.5 Krad/hour

WE FOUND: } M. Contreras, N. Giokaris CDF note #1341

- 10 to 40% DECREASE IN ATTENUATION LENGTH
- NO DROP IN LIGHT YIELD
- NO SIGNIFICANT DIFFERENCE BETWEEN THE TWO RATES

- COULD NOT EXPLAIN DAMAGE TO BBC

HOWEVER «LOW RATE», i.e 10.5 Krad/hour, WAS STILL HIGH

- DECIDED TO DO NEW TEST AT MUCH LOWER RATE

NEW TEST STARTED IN MAY 1991

- EXPOSURE TO RADIATION:

- ^{60}Co SOURCE - PHOENIX LAB, UNIV. OF MICHIGAN-ANN ARBOR } THE HELP OF ROBERT BLACKBURN HAS BEEN INVALUABLE

- EXPOSURE, RECOVERY AND MEASUREMENT WERE DONE IN AIR
- FIRST MEASUREMENT @ DOSE = 0.0 DONE ON APRIL 11, 91
- FIRST EXPOSURE : MAY 23, 91 → Sept. 3, 91 / DOSE : 0.7 Mrads
- SECOND MEASUREMENT @ DOSE = 0.7 Mrads : SEPTEMBER 7, 91
- SECOND EXPOSURE : OCTOBER 10, 91 → FEB. 10, 92 / DOSE : 0.9 Mrads
- SECOND MEASUREMENT @ DOSE = 1.6 Mrads : FEBRUARY 15, 92
- THIRD EXPOSURE : MARCH 20, 92 → ....

- SOURCE IS ON ~ 85% OF THE TIME
- DOSE RATE : ~ 250 Rads/hour
- DOSE MEASURED WITH FWT-00-60 FILMS MADE BY FAR WEST TECHNOLOGIES

2. EXPERIMENTAL PROCEDURE

- SETUP:

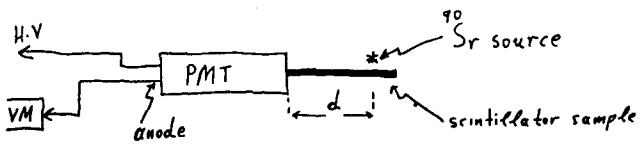

MEASURE: DC Voltage vs d

- SCINTILLATOR SAMPLES:

Bars: $1 \times 1 \times 20$ cm^3, $0.5 \times 1 \times 20$ cm^3

SCSN23, 81, 81+Y7, 81+Y8, 3HF } Supplied by KURARAY

- PMT

- Hamamatsu R1828-01; H1949 Assembly
- Bialkali Photocathode
- Response peaks at blue

TYPICAL "ATTENUATION LENGTH" AND LIGHT YIELD FOR 1cm × 1cm × 20cm BARS

CONTROL SCINT. TYPE	ATT. LENGTH λ [cm]	LIGHT YIELD V_0 [Volts]	
SCSN23	40	8.4	Blue emission
SCSN81	45	6.6	Blue emission
SCSN81+Y7	40	3.8	Green emission
SCSN81+Y8	35	2.7	Green emission
3HF	50	2.5	Green emission

NOTE: PMT response peaks at blue

REPRODUCIBILITY OF CONTROL ATTEN. LENGTH: MEASUREMENT: $\sim \pm 5\%$ $\approx$ MEASUREMENT ERROR

Reproducibility of control samples (λ) is $\sim \pm 5\%$.

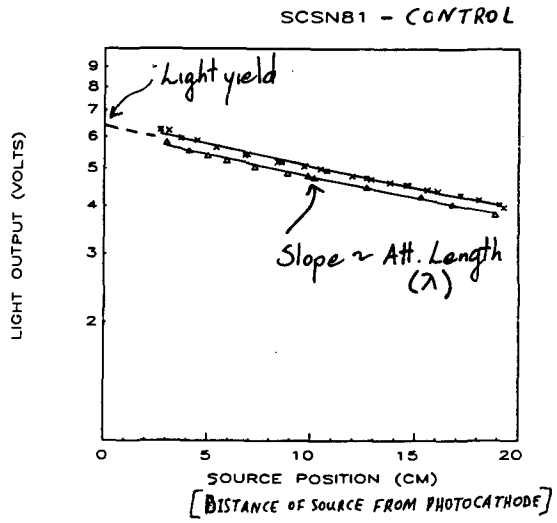

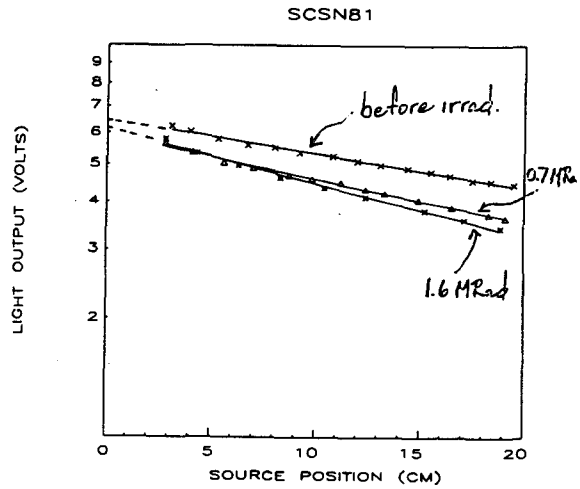

Measurement Performed by: A. PLA

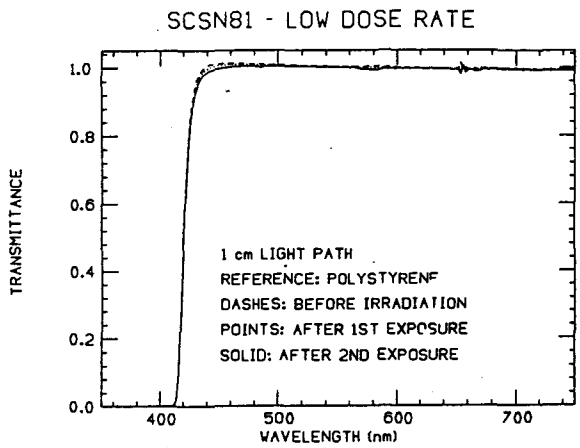

3.- LOW DOSE (250 Rad/hour) RESULTS

	Scint. Type		Attenuation Length Ratios $\Lambda_{AFTER}/\Lambda_{BEFORE}$ @ 0.7 MRad	@ 1.6 MRad
1cm × 1cm × 20 cm	SCSN23	Blue	0.81 ± 0.06	0.72 ± 0.05
	SCSN 81	Blue	0.76 ± 0.05	0.62 ± 0.04
	SCSN 81+Y7	Blue	0.93 ± 0.07	0.91 ± 0.06
	SCSN 81+Y8	Green	0.93 ± 0.07	0.95 ± 0.07
	3HF	Green	0.95 ± 0.07	0.91 ± 0.06
0.5 cm × 1cm × 20cm	SCSN23	Blue	0.79 ± 0.05	0.76 ± 0.05
	SCSN 81	Blue	0.81 ± 0.06	0.71 ± 0.05
	SCSN 81+Y7	Blue	0.93 ± 0.07	0.94 ± 0.07
	SCSN 81+Y8	Green	0.96 ± 0.07	0.92 ± 0.06
	3HF	Green	0.93 ± 0.07	0.93 ± 0.07

4. CONCLUSIONS

A. ATTENUATION LENGTH

A1. AT 250 Rads/hour (0.7 & 1.6 Mrads) SMALL DECREASE (~10 to 40 %) OBSERVED.

A2. NO SIGNIFICANT DIFFERENCE IN THE DAMAGE BETWEEN 250 Rads/hour, 10.5 Krads/hour & 1 Mrad/hour (FOR SAME TOTAL DOSE) OBSERVED.
IN CONTRAST WITH FIBER RESULT! (CARL ZORN)

A3. NO SIGNIFICANT DIFFERENCE IN THE DAMAGE BETWEEN THE 1 cm & 0.5 cm THICK SAMPLES OBSERVED.

A4. DECREASE IN ATTEN. LENGTH FOR GREEN SCINTS (SCSN81+Y7, +Y8 & 3HF) IS LESS THAN BLUE ONES (SCSN23 & SCSN81).

B. LIGHT YIELD

At 250 Rads/hour & 1.6 Mrads:
A SMALL (~ 8%) DROP OBSERVED

C. Zorn et al
HCTC meeting, Oak Ridge, 7-91

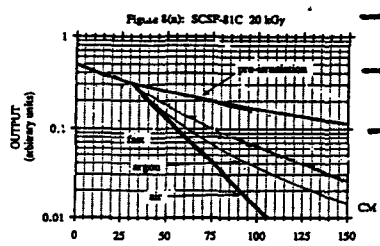

— Before irradiation
— 2 MRad 'fast' ~1 MRad/hour
— 2 MRad 'slow' @ 550 Rad/hour

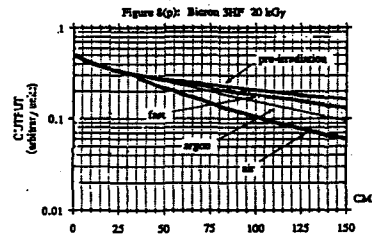

TEST A TILE-FIBER UNIT AT LOW RATE!!

WHAT NEXT?

1. FINISH PRESENT (i.e $\dot{D}$ = 250 Rads/hour) TEST
   i.e GO TO D ≈ 2.2 Mrads

2. DO A TEST AT : $\dot{D}$ = 5 Rads/hour
   D = 50 Krads

3. DO A NEUTRON EXPOSURE : $\sim 10^{13}$ n's/cm^2

[BBC DAMAGE IS STILL UNEXPLAINED
BUT!
2 or 3 ABOVE MAY SHED SOME LIGHT!]

SDC Calorimeter Rad-Hard Scintillator R&D

SCINTILLATOR TILES

Requirements Under Radiation

- Maintain Adequate Light Yield
- Maintain Adequate Uniformity
- Maintain Mechanical Integrity

The Direct Radiation-Induced Drop in the Scintillation Light Yield Is Small

- <~ 20% for a 50-MRad Dose (for most fluors)
- Major Effects are Due to Light Attenuation in Base Plastic

GW Foster 5/5/92

SDC Calorimeter Rad-Hard Scintillator R&D

Radiation Hardness and the SDC Calorimeter

The SDC Calorimeter is Specified to Survive "100 years" at Design Luminosity.

- Realistically, 10 years at 10^{33}, then 10 years at 10^{34}.
- Standard scintillators and fibers are adequate for the Barrel, which sees a lifetime dose of < 0.6 MRad.

The Baseline Design allows for periodic replacement of the scintillator assemblies in the Endcap EM, which see lifetime doses of up to 60 MRad.

If Economically Justified, it would be Tremendously Convenient if Rad-hard Materials could be found which avoid this Periodic Replacement.

GW Foster 5/5/92

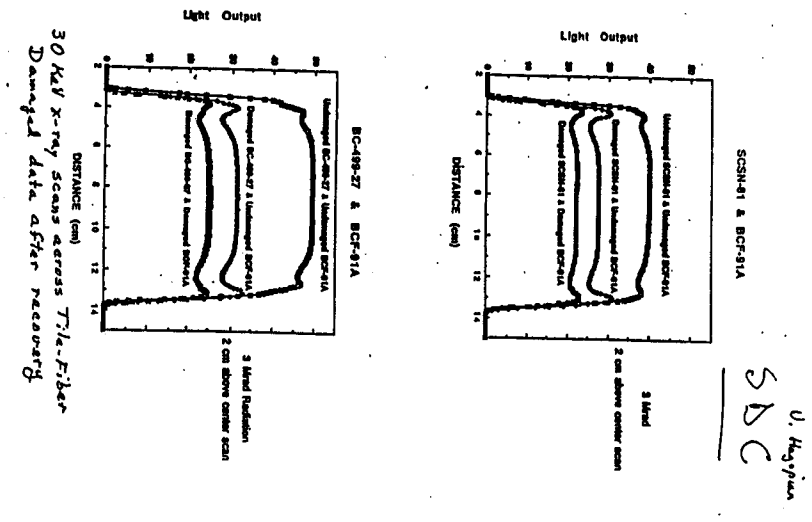

SDC Calorimeter Rad-Hard Scintillator R&D

PROPERTIES OF TILE/FIBER CALORIMETRY

Separated Function of Optical Components:

- Scintillator Plate
- Waveshifting Fiber
- Clear Readout Fiber

Each Component Sees Different Stress from Radiation Damage at Different Regions of Eta.

Separation of Function allows each component to be optimized to handle Radiation Damage.

GW Foster 5/5/92

SDC Calorimeter Rad-Hard Scintillator R&D

LIGHT YIELD & PHOTOSTATISTICS

SDC Baseline Design Maintains E_T Resolution

- ~400 PE/GeV In Barrel.....Safety Factor ~4
- ~4000 PE/Gev E_T at Eta=3.....Safety Factor ~40

Photostatistics Will Not Limit E_T Resolution In Region of Highest Radiation Damage

- Optical Masking at PMT will ensure Uniformity in Depth
- Rad-Damage Limit will come from Transverse Uniformity

GW Foster 5/5/92

SDC Calorimeter Rad-Hard Scintillator R&D

Strategies to Prevent light Drop from Scintillator Tiles

1.Reduce Optical Pathlengths

- 10cm in the Barrel
- 1-2cm (if necessary) near Eta = 3

2. Change Optical Wavelengths to Region of less Absorbtion

- Green Plate/Yellow Fiber
- Requires Fast, Efficient.new Fluors & PMT

GW Foster 5/5/92

SDC Calorimeter Rad-Hard Scintillator R&D

Strategies to Prevent light Drop from Scintillator Tiles (cont'd)

3.Keep The Plastic From Turning Brown

- Understand the Chemical Pathways... recent progress
- Obstruct them, or React Away the Radiolysis Products

4. Switch to a New Plastic Base Material

- Many Aromatic Polymers commercially available.
- Most of these will Scintillate.
- Light Yield and Optical Quality are Negotiable for the small region of high radiation damage.

GW Foster 5/5/92

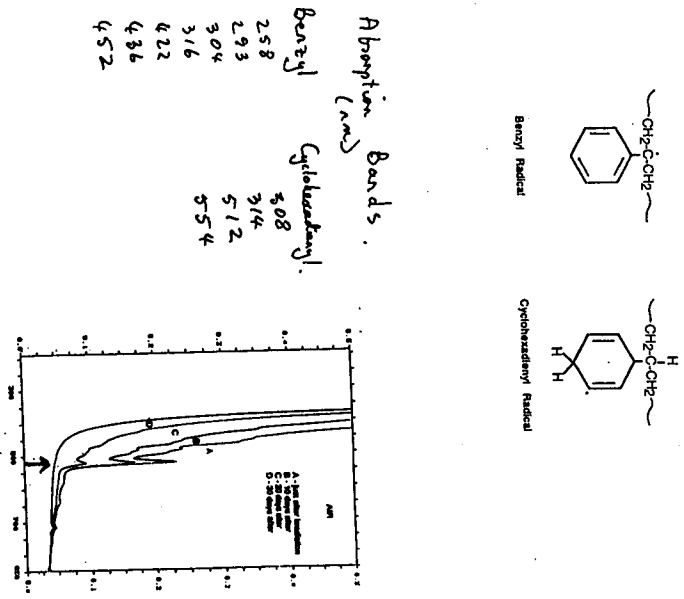

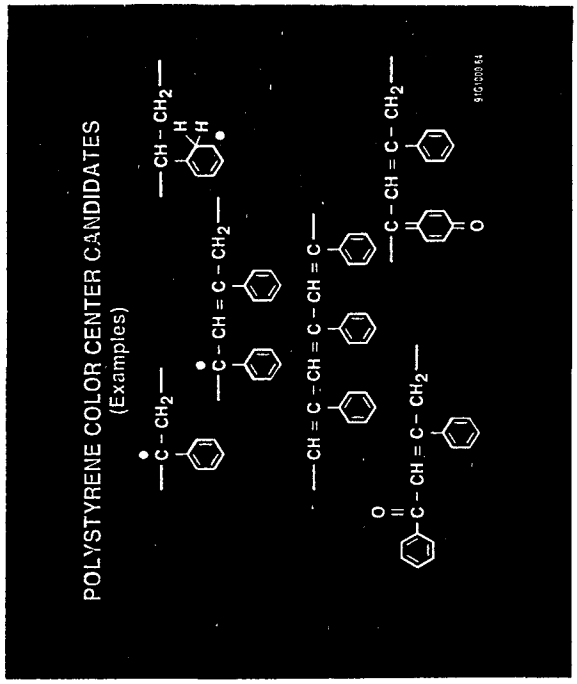

... Thousands of Anti RADS (Radical Scavengers) Commercially available...

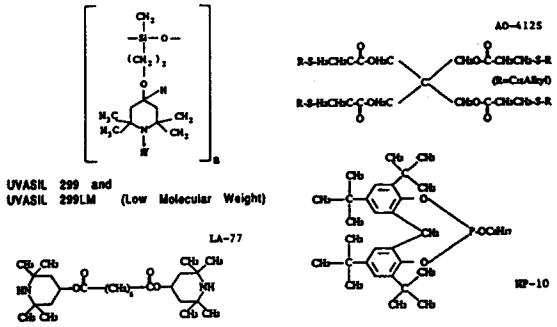

Fig. 9. Chemical structure of antirads

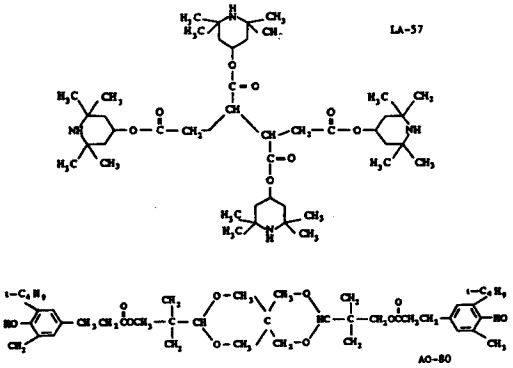

Some Success With Additives

SUMMARY AND CONCLUSIONS

Figure 31 summarizes the data for several of the most promising systems. D18UV is the sample discussed in the abstract. All samples (except the BC408 control from Bicron) are 70 pbw of Dow polystyrene, 30 pbw of DC705, 2 pbw para-terphenyl, .2 pbw of secondary shifter, and .5 pbw of antirad when present. It has been demonstrated that DC705 oil is effective in increasing the anneal rate of polystyrene scintillators. It has also been shown to be effective in activating antirad agents. Is theorized that major reason for the improvements is the increased mobility of reactive species. The DC705 used alone increases the permanent radiation damage, but that is negated by the antirads. Useful plates of scintillator have been made and are being tested with shifter fibers before and after radiation. Good scintillators have been made from polymers and it has been proven that they can be injection molded. A scintillator that decreases it's light output by only 4% after 10 megarads has been made.

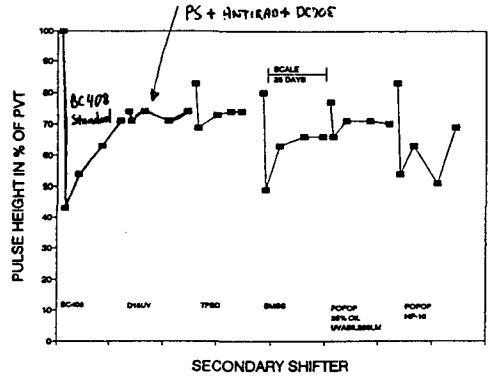

Fig. 31. Anneal rates for "best" samples 3-12-92 (30% oil except as noted)

Plates w/various Anti-RADS being tested @BICRON, MUCH etc..

MANY NEW PLASTICS INVESTIGATED

- Polyalphamethylstyrene
- Polyarylate
- Polyarylsulfone
- Polycarbonate
- epoxy
- Polyethyleneglycoldiallylcarbonate (CR-39)
- Polyethylenemethacrylicacid
- Polyethylenevinylacetate
- Polyethyleneterephthalate
- Polymethylmethacrylate
- Polyphenylsulfone
- Polystyrene
- Polystyrenesacrylonitrile
- Polystyrenemethacrylate
- Polysulfone
- Polyvinyltoluene
- Cellulosesacetateproprionate
- Polyetherimid
- Fluorinatedethylenepropylene
- Polystyreneacrylicacid
- Polymethylpentene
- Polyvinylbutaral
- Polyvinylidenefluoride
- Polyvinylpyrolidone
- POLY ISODECYL METACRYLATE

Fig. 27. Plastics investigated

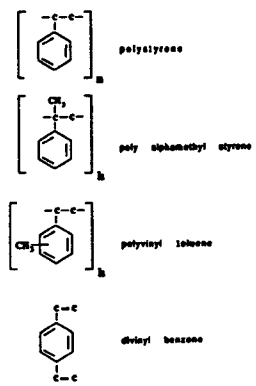

SDC Calorimeter Rad-Hard Scintillator R&D

WAVESHIFTING END OF SILICA FIBER

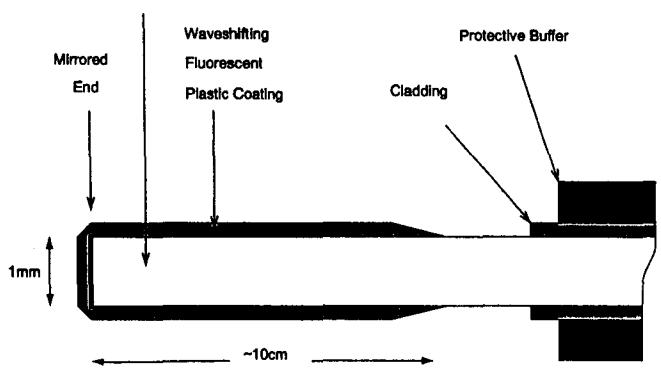

GW Foster 5/5/92

SDC Calorimeter Rad-Hard Scintillator R&D

FAST GREEN WAVESHIFTERS

PULSEWIDTH OF EM CALORIMETER

IS LIMITED BY FALL TIME OF WLS FLUOR

- Back to Baseline in 3 Crossings (no shaping)
- Back to Baseline in 2 Crossings (Clipline Shaping)
- Tests indicate we can achieve 6-8ns FWHM with fast dye

Evaluation & Test of Faster, Green Shifter Fluors

- Candidates from NE Technology, Bicron, & laser dyes
- Dye must have Established Track Record of Stability by '94

GW Foster 5/5/92

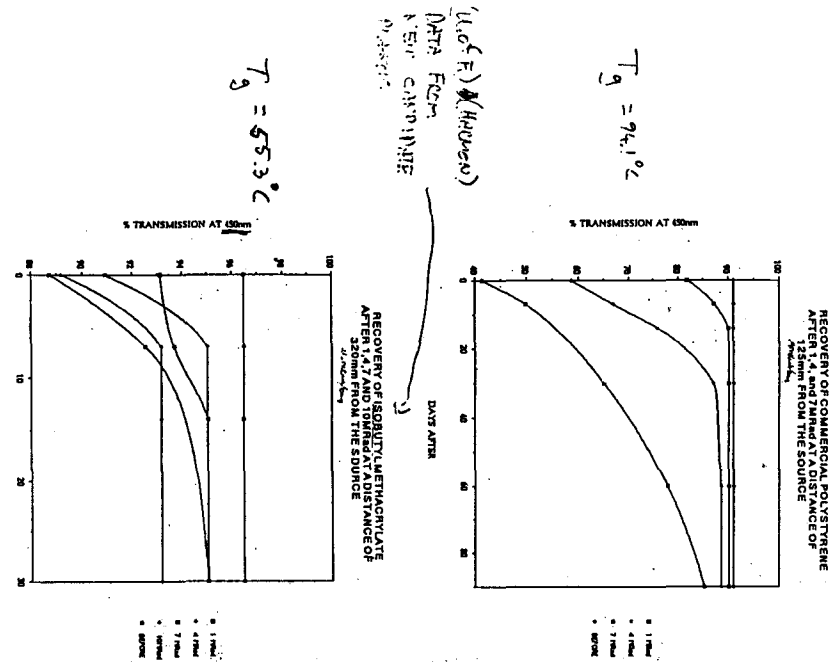

SDC Calorimeter Rad-Hard Scintillator R&D

WAVESHIFTER READOUT

SHORT OPTICAL PATH

- ~30cm in Barrel EM
- ~10cm (if necessary) in End Plug
- High-quality Optical Fiber *Not Required*

Does Not Have To Scintillate

- Non-Aromatic Vinyl Polymers & Siloxanes OK
- Does not have to carry Primary & Secondary Shifter Fluors
- Fluorescent Coating on Silica Fiber Candidate at High Eta

GW Foster 5/5/92

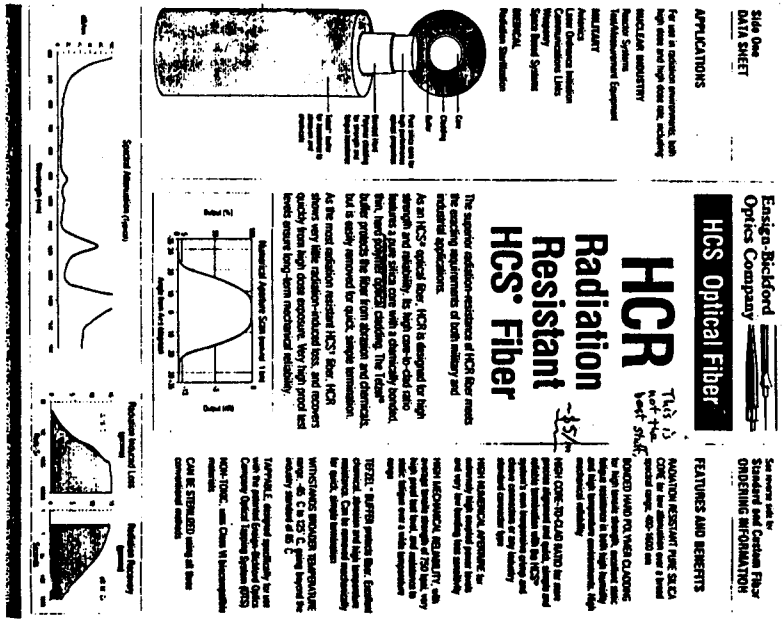

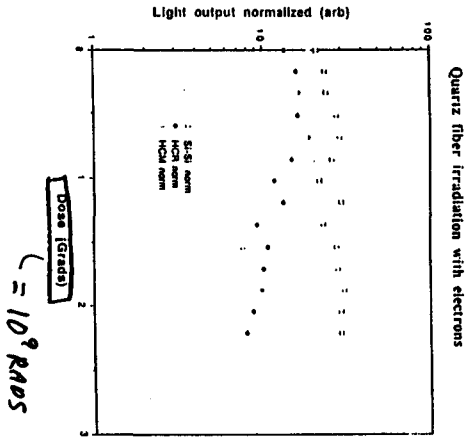

SDC Calorimeter Rad-Hard Scintillator R&D

RADIATION HARDNESS OF CLEAR READOUT FIBER

Longest Optical Path

- 2m in Barrel Tower, 30cm in radiation field
- 3-5m in Endwall, 0.1m-2.0m in radiation field

Large Variation in Total Dose Along Fiber

- 0.1 MRad-Meters worst case 100-yr dose in barrel
- 27 MRad-Meters integrated dose for readout fiber from Eta=3.0 in "pizza-pie" geometry at EM shower-max

Aging of Readout Fibers *Can* be Corrected at PMT

GW Foster 5/5/92

SDC Calorimeter Rad-Hard Scintillator R&D

RADIATION HARDNESS OF CLEAR READOUT FIBER (cont'd)

PS core/PMMA clad Fiber OK in Barrel

- Useable to total doses of ~1MRad-meter
- Useful for majority of channels in Endcap

Silica Fiber Probably Necessary Near Eta=3

- Useable to total doses of GigaRad
- Total Cost for using Silica on *Entire* ECEM ~~$300k

In between, maybe room for new candidates...

- e.g. polyisobutylmethacrylate (modified acrylic) cored fiber

GW Foster 5/5/92

NEGATIVE DOSE RATE EFFECTS (SANDIA GROUP)

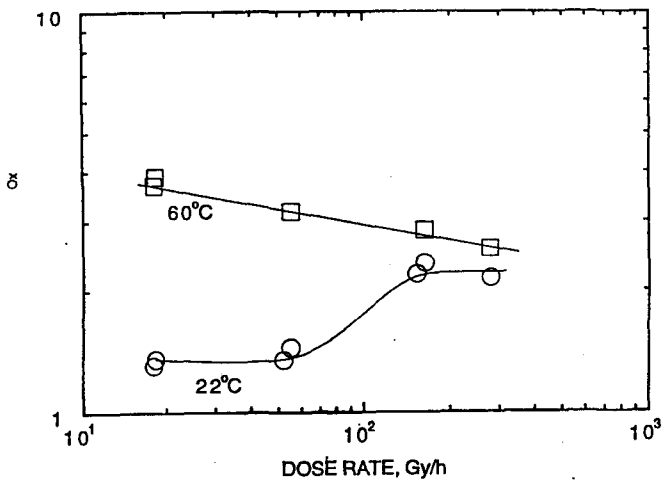

LESS DAMAGE AT LOW DOSE RATES

SUMMARY

J. Proudfoot
May 15, 1992

— RADDAM '92 —

INTERNATIONAL CONFERENCE ON RADIATION-TOLERANT SCINTILLATORS AND DETECTORS

FLORIDA STATE UNIVERSITY
TALLAHASSEE, FLORIDA
APRIL 28 TO MAY 2ND, 1992

CONFERENCE ORGANIZERS:

ROGER CLOUGH SANDIA NATIONAL LABORATORIES ORGANIZATION 1811 ALBUQUERQUE, NM USA 87185 PH:(505)844-3492 FAX:(505)844-9624	KURTIS F. JOHNSON FLORIDA STATE UNIVERSITY DEPT. OF PHYSICS TALLAHASSEE, FL USA 32306 PH:(904)644-3693 FAX:(904)644-6735 E-MAIL: FSUHEP::RADDAM92	PETER SONDEREGGER CERN CH-1211 GENEVA SWITZERLAND PH:(22)767-4870 FAX:(22)782-4897 E-MAIL: RADDAM92@CERNVM

THIS SYMPOSIUM IS INTENDED TO BRING TOGETHER MAJOR RESEARCH WORKERS INVOLVED IN THE DEVELOPMENT OF ADVANCED, RADIATION RESISTANT SCINTILLATORS OR PARTICLE PHYSICS DETECTORS. PRESENTATIONS OF RESEARCH RESULTS WILL BE MADE IN THE AREAS LISTED BELOW, AND DISCUSSION SESSIONS WILL BE SCHEDULED ON KEY ISSUES WHICH REMAIN TO BE RESOLVED. SINCE AN IMPORTANT CONCERN IS COMMUNICATION BETWEEN RADIATION CHEMISTS AND DETECTOR DESIGNERS, TUTORIAL SESSIONS WILL BE ORGANIZED FOR BOTH PHYSICISTS AND CHEMISTS.

THE PROCEEDINGS OF THIS CONFERENCE WILL BE PUBLISHED AS A SPECIAL ISSUE OF THE JOURNAL: RADIATION PHYSICS AND CHEMISTRY.

- MATERIALS REQUIREMENTS FOR SCINTILLATOR-BASED DETECTORS
- RADIATION DAMAGE MECHANISMS IN POLYMERIC SCINTILLATORS
- STRATEGIES FOR DEVELOPING MORE RADIATION TOLERANT SYSTEMS
- PREDICTIVE AGING TESTS FOR SCINTILLATOR LIFETIMES
- SURVEY OF RADIATION RESISTANCE OF OPTICAL PROPERTIES IN DIFFERENT POLYMERS
- NATURE AND STRUCTURE OF RADIATION-INDUCED COLOR CENTERS
- THE ROLE OF OXYGEN
- KINETICS AND MECHANISMS OF COLOR CENTER ANNEALING
- RADIATION EFFECTS ON SCINTILLATOR DYES; SYNTHESIS OF ADVANCED DYES
- RADIATION DAMAGE TO OTHER ORGANIC MATERIALS CRITICAL TO SCINTILLATION

ATMOSPHERE & DOSE RATE (BOW)

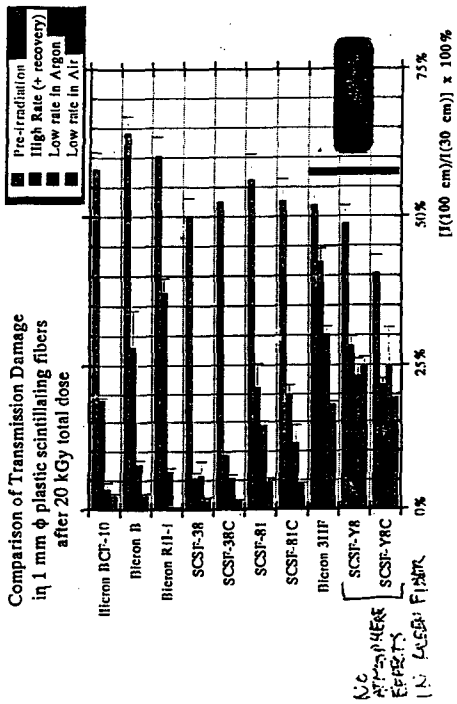

NO ATMOSPHERE EFFECTS IN LOCAL FIBER

Air Worse Than Vacuo

DEVELOPMENT OF MA PMTS AND GREEN EXTENDED PMTS

HAMAMATSU PHOTONICS K.K.
ELECTRON TUBE CENTER

SEIJI SUZUKI
YUJI YOSHIZAWA

1. LOW CROSS- TALK MULTI- ANODE PMTS FOR SHOWER MAXIMUM DETECTOR
2. DEVELOPMENT STATUS OF PMTS FOR SCINTILLATION TILE CALORIMETER

HAMAMATSU PHOTONICS K.K
1992.5.25

LOW CROSS-TALK MULTI-ANODE PMTS FOR SHOWER MAXIMUM DETECTOR

1) SPECIFICATIONS & DEVELOPMENT STATUS FOR SDC SHOWER MAX. DETECTOR
2) BASIC CONFIGURATION OF MULTI- ANODE PHOTOMULTIPLIER TUBE
3) CROSS-TALK CHARACTERISTICS OF CONVENTIONAL & DEVELOPED VERSION
4) NEW PHASE MULTI-ANODE PMT

HAMAMATSU PHOTONICS K.K
1992.5.25

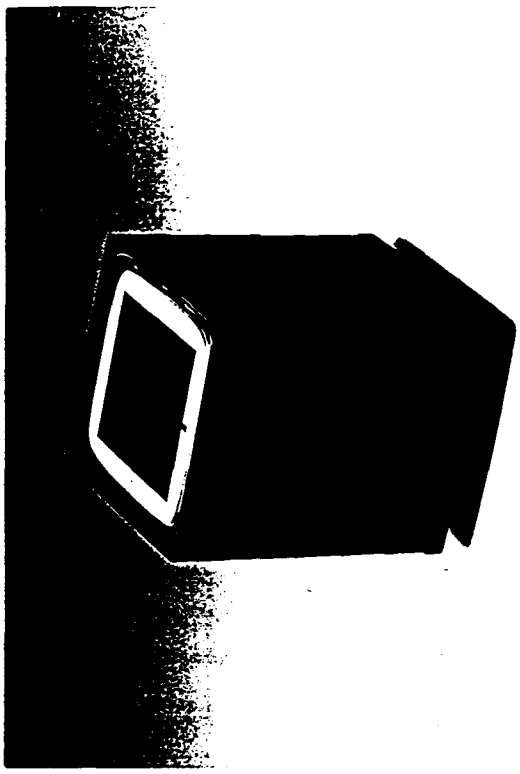

3 inch Square Position Sensitive PMT with Fine Mesh Dynode and 256(16×16) Matrix Anode.

SDC
SHOWER MAXIMUM DETECTOR

	SPECIFICATIONS	HAMAMATSU 8×8 MA PMT
CHANNEL No.	64	○ (64+16)
CROSS-TALK	< 2%	○
DYNAMIC RANGE	4,000	○ (>6000)
GAIN ADJUSTMENT	1:5	○
CATHODE GREEN SENS.	HIGH at 520 nm	△ DEVELOPMENT

CROSS-TALK : OPTICAL & ELECTRON TRAJECTRY
↓ PIXEL SIZE & SPL ELECTRODE

DYNAMIC RANGE : 15 fC – 80 pC
→PMT PULSE LINEARITY : 3 μA – 12 mA

HAMAMATSU PHOTONICS K.K 1992 5/21

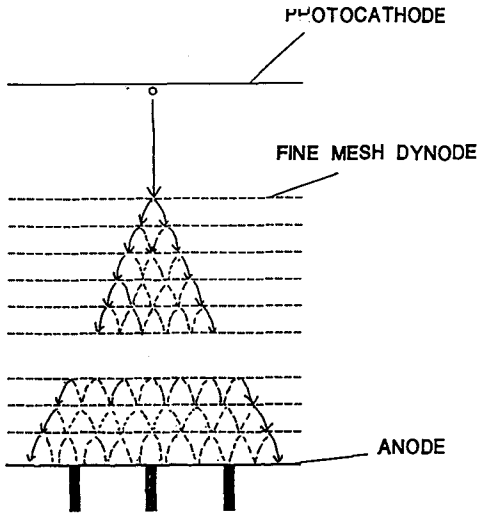

ELECTRON TRAJECTORY OF
CONVENTIONAL TYPE

H4140-01

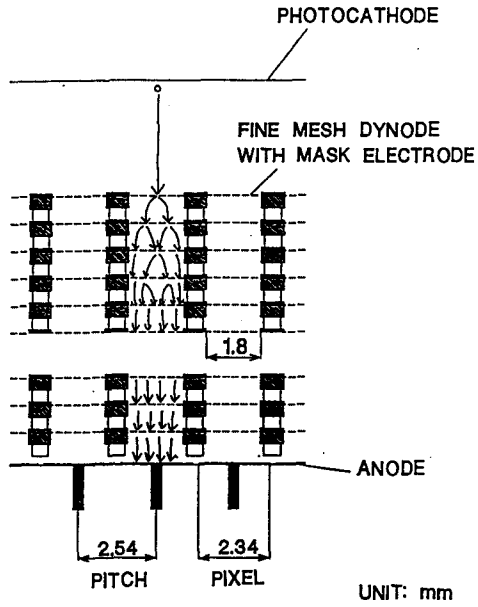

Fig. 2

ELECTRON TRAJECTORY OF
DEVELOPMENT TYPE

H4140-01MOD

Fig. 4

SPATIAL RESOLUTION OF H4140MOD (MASK)

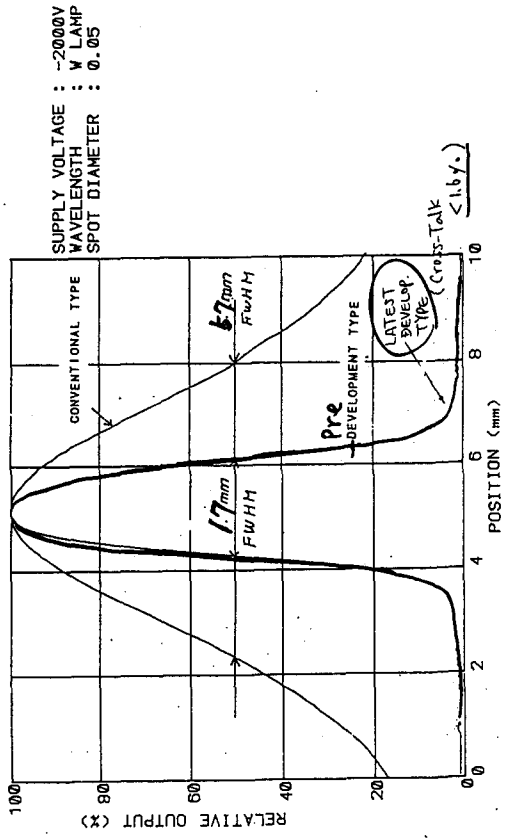

92. 3. 26

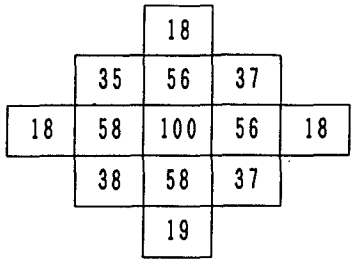

CONVENTIONAL TYPE

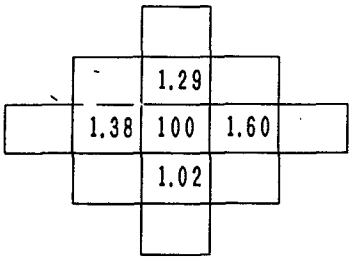

DEVELOPMENT TYPE

UNIT: %

CROSS-TALK CHARACTERISTICS
WITH INCIDENT LIGHT OF 1mmφ SPOT
ON ONE PIXEL.

H4140-01

OPTICAL CROSS-TALK
THROUGH PMT WINDOW

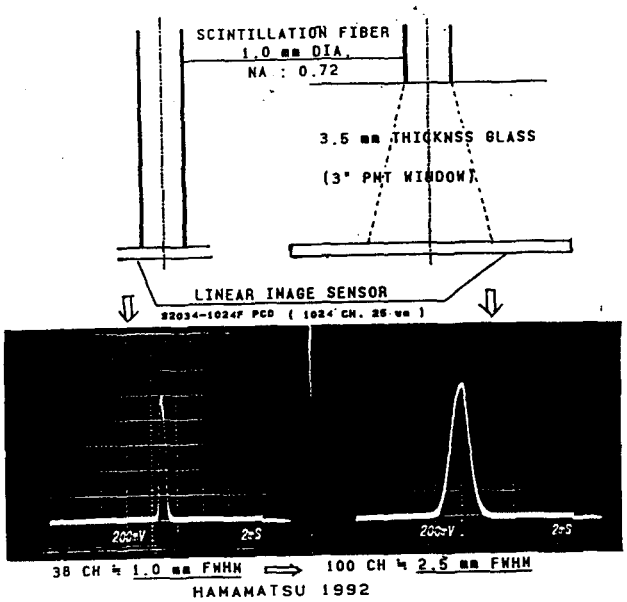

8x8(64) MULTI-ANODE PMT

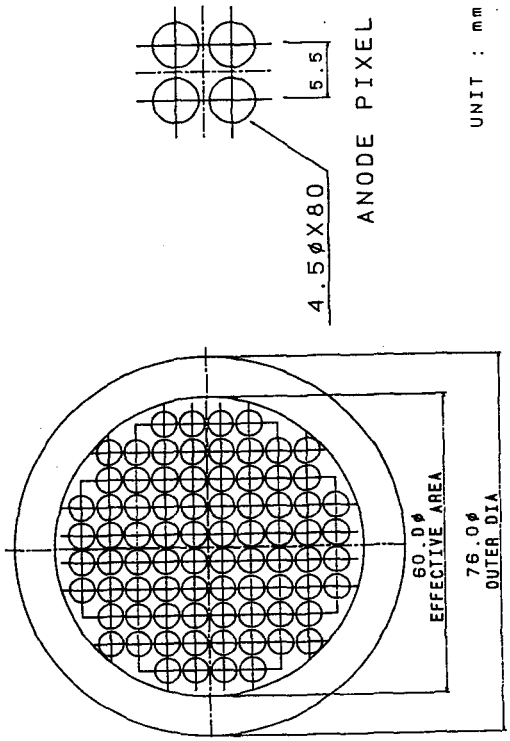

UNIT : mm

HAMAMATSU PHOTONICS K.K. 1992 5/20

Development Status of PMTs for Scintillating Tile Calorimeter

1. PMT Specification
2. Extended Green Photocathode
3. Explanation of Resolution
4. Conclusion

Hamamatsu Photonics

Electron Tube Center

PMT Specification List (Mechanical)

Specification for SDC Scintillating Tile Calorimeter	HPK Products			
	3/4" R5325	1" R5380	1·1/8" R5329	1·1/2" R5340 → Original Model ⇒ R580
Diameter = 19mm~40mm	18.6±0.7	25.4±0.5	28.5±0.5	38±1
Tube Length < 75mm	50±2	48±1.5	73±2	76±2
PMT Base	Glass Base Type			
Useful Area > 1cm²	15φmin.	21φmin.	25φmin.	34φmin.

Mechanical Samples of these PMTs are available on the display desk in building #3.

PMT Specification List (Electrical)

Electrical Specification	3/4" R5325	1" R5380	1·1/8" R5329	1·1/2" R5340
Uniformity < ±15% / ·13mmφ	△	○	○	○
Gain 6x10⁴ nominal	○	○	○	○
Linearity Pulsed Current 25mA < 2%, 100mA < 5%	○	○	◎	◎
Time Response Rise<4ns, Fall<6ns etc.	◎	○	○	○
Single Photoelectron Noise < 100KHz at 0.5 of 1 p.e.	○	○	○	○
Long Term Stability < 1% / month and Lifetime 100C for 50% gain loss	○	○	○	○
Voltage Divider with Simple Integer Ratio	△	△	△	○

△: under development

Typical Spectral Response

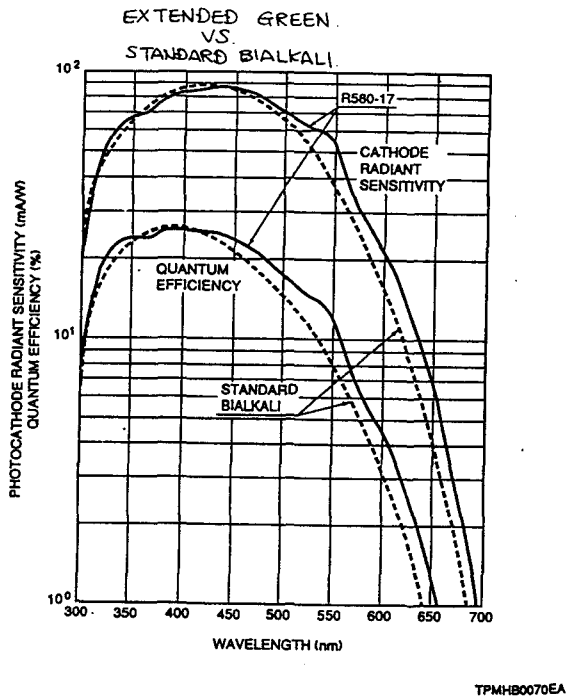

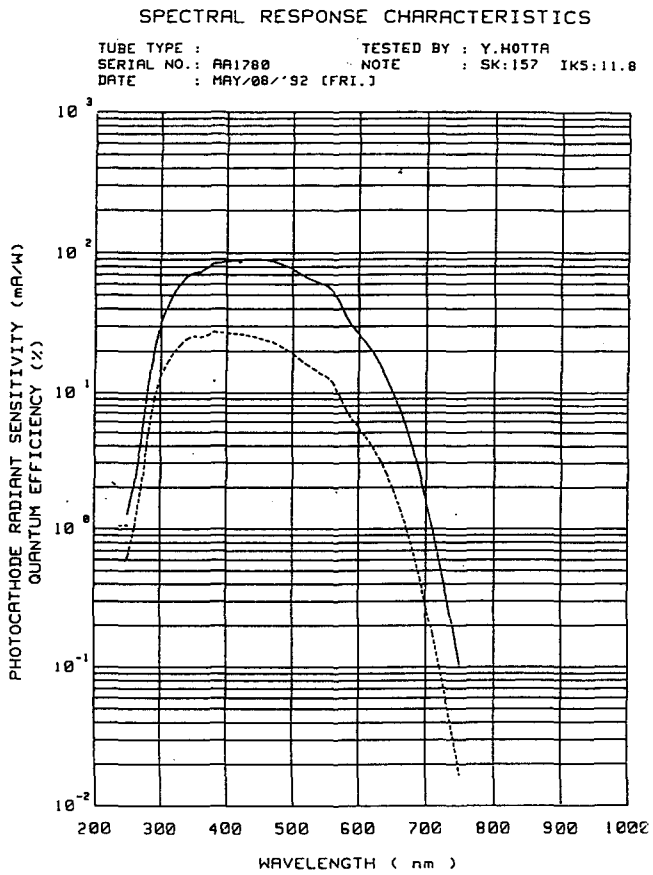

Explanation of Resolution

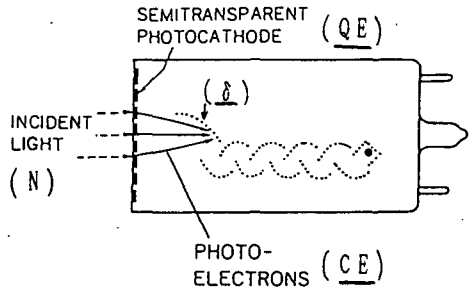

PMT Resolution (Rp)

$$Rp = 2.35 \left(\frac{1}{(N \cdot QE \cdot CE)} \times \frac{\delta}{\delta - 1} \right)^{1/2}$$

N : Number of Photons

QE: Quantum Efficiency

CE: Collection Efficiency

δ : Secondary Emission Yeild

Conclusion

HPK will continuously
make every effort to
achieve following items;

1. Extended Green Photocathode

2. Good Pulse Linearity

3. Good Stability

4. Low Cost

5. Stable Supply

BASELINE IMPLEMENTATION
OF THE DIGITAL PHOTOTUBE READOUT SYSTEM
FOR THE SDC CALORIMETER

September 3, 1991

Al Baumbaugh, G. William Foster, Sten Hansen, Jim Hoff,
Mark Larwill, Catherine Newman-Holmes,
Claudio Rivetta, Raymond Yarema, Tom Zimmerman
Fermi National Accelerator Laboratory

Digital Photomultiplier Tube Readout

G. William Foster
(Fermilab)

DIGITAL PMT

ADVANTAGES OF IMMEDIATE DIGITIZATION

- No External Analog Signal Transmission
- Fewer Crosstalk Problems
- Simpler System Integration: Well-Defined Interface
- Small Anode Capacitance (no Cable from PMT)
- FINITE IMPULSE RESPONSE
- AFTER DIGITIZATION, THE ENTIRE TRIGGER/DAQ SYSTEM IS 100% TESTABLE IN BEAM-OFF CONDITIONS.

FNAL / SDC

DIGITAL PMT

DIGITAL PHOTOMULTIPLIER TUBE READOUT

- Immediate Digitization at Base of Photomultiplier Tube
- Floating Point Digital Output - 20-bit Dynamic Range
- Gated Integrator Front End
- DC coupled for High Rate Operation
- Single Package Contains Base/HV and Digitizer
- Single Flat Cable Connection to PMT Base
- Same Digitized Output used for Trigger and DAQ
- Built-in Cockroft-Walton Base - No Exposed HV
- Upgrade Capabilities of Digital Trigger/Daq

FNAL / SDC

DIGITAL PHOTOTUBE READOUT - BLOCK DIAGRAM

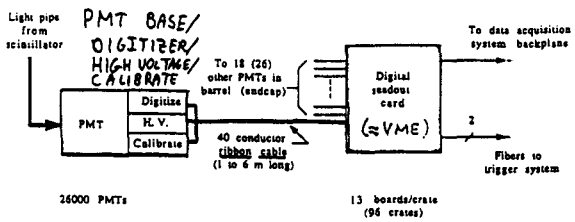

→ TWO COMPONENTS ⇒ Small engineering $

→ Flexible Mechanics ⇒ Simple mounting on Calor.

→ SINGLE FLAT CABLE TO EACH PMT
⇒ no ground loops, etc.

ALL ANALOG PROCESSING TAKES PLACE IN THE INTERIOR OF A LITTLE METAL CAN!

Fig. 8.3.3.1 - DIGITAL PMT READOUT SYSTEM BLOCK DIAGRAM. There are two components in the system. The first component is the PMT Base/Digitizer assembly which contains the Phototube HV, Digitization, Current Monitoring and Calibration circuitry. These are connected via flat cables to the second component, a card which contains the digital ASICs which perform DAQ, Trigger, and calibration/monitoring functions. In the baseline trigger design [3] this card accepts flat cables from 8 towers of calorimetry and transmits energy sums for two "trigger towers" onto optical fibers to the trigger.

PMT BASE/DIGITIZER CIRCUIT DIAGRAM

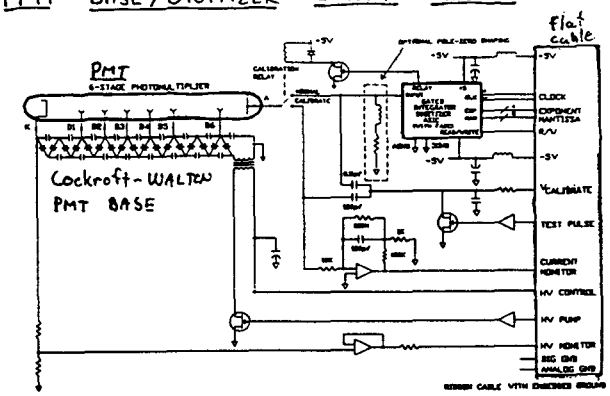

Fig. 8.3.3.3 - PMT BASE/DIGITIZER MODULE circuit diagram. It contains the Phototube, Cockroft-Walton "charge pump" HV supply, current monitor, charge injection circuit, and PMT digitizer ASIC. This diagram assumes the FADC has been integrated into the digitizer ASIC. In out initial design a commercial 8-bit FADC will be used.

Table 1: Digital Readout Specifications for Calorimeter and Shower-Max

	Digital Calorimetry Readout	Digital Shower-Max
Channel Count	~26,000	~47,000
Channels/Module	1 (single PMT Assy)	64 (Multi-anode PMT)
Location of Digitizer	PMT base	PMT Base
Location of L1/L2 Storage	Readout Crate (on Detector)	PMT Base
Dynamic Range	20 bits	13 bits
Least Count	10 MeV (1fC)	40 Mev (4 fC)
Full Scale	10 TeV (1nC)	160 GeV (160pc)
Accuracy	$\sigma < 0.2\%$ of Reading, (or 1 Least Count)	$\sigma < 1.5\%$ of Reading, (or 1 Least Count)
Crosstalk	$< 10^{-6}$	$< 10^{-3}$
Peak PMT Current	100ma	10ma
Signal Rise Time	~5-8ns (3-5?)	~5-8ns
Gate Timing Adjustment	+/- 0.5ns Programmable Individually Per Tube	+/- 0.5ns Programmable Individually Per Strip
Power/channel	~1W	~100mW
Flash ADC	Commercial 8-10 bit	5-bit; internal to ASIC
Output to L1 Trigger	12-bit Floating Point digital flat cable	Single Bit/Channel digital flat cable
Output Format to DAQ	12-bit parallel Digital Floating Point (8+1)bit mantissa, 4 bit exponent.	Serial Data Digital Floating Point (5+1)bit mantissa, 4 bit exponent.
High Voltage Supply	Cockroft-Walton on Base	Cockroft-Walton on Base
Current Monitor	1/PMT (on Base)	1/PMT (on Base)

DIGITIZATION ACCURACY vs. ENERGY

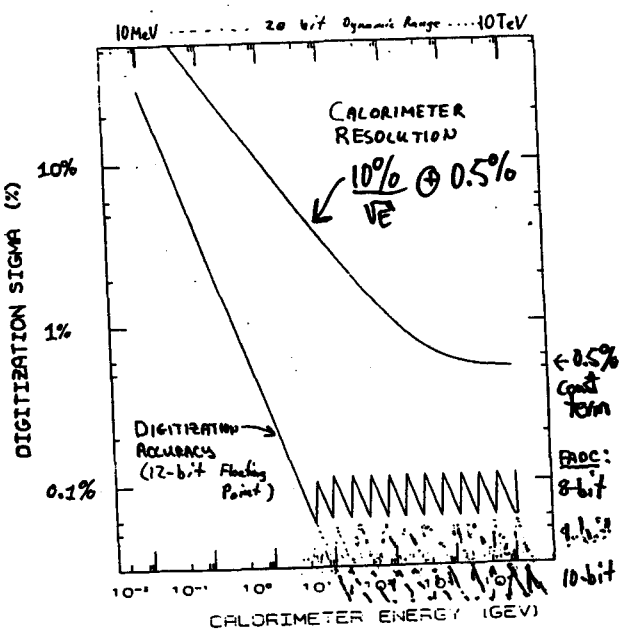

Fig.3.4 DIGITIZATION ERROR and ENERGY RESOLUTION OF CALORIMETER as a function of energy. The bottom curve gives the digitization σ (= least count)/$\sqrt{12}$) for the floating-point output of the digitizer. Except at the low end of the scale, a signal is digitized to a least-count accuracy which varies between 1/256 and 1/512 of itself. Also shown is a (rather optimistic) calorimeter energy resolution of $10\%/\sqrt{E} \oplus 0.5\%$.

CIRCUIT-PER-CHANNEL ON DIGITAL READOUT CARD

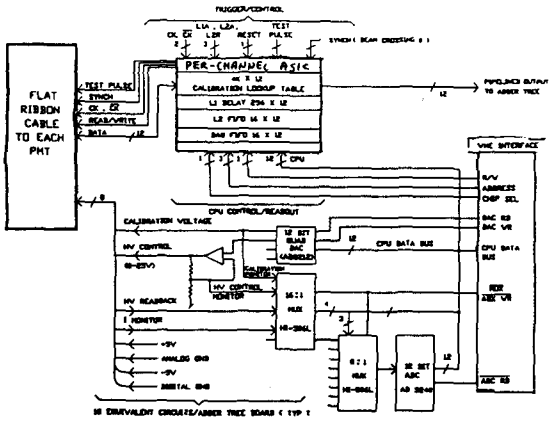

Fig. 8.3.3.4 - CIRCUIT-PER-CHANNEL ON READOUT BOARD for Digital PMT System. A single flat cable carries clock, data, and control signals to each PMT. The L1/L2/Calibration ASIC on the Readout Board recieves the digitised data from a channel, then passes it through a pipelined calibration RAM. The calibrated data is pipelined out to the trigger energy sum adders, and is also stored locally for ~256 crossings in the L1 delay memory. Upon reciept of a L1 accept, the output of the L1 delay is loaded into the Level2 FIFO, where it is stored pending a level 2 decision. The output of the L2 fifo is either discarded, or loaded into a DAQ FIFO for subsequent readout by the local processor in each crate. This ASIC also provides programmable timing for the ADC gate and test pulses. Also shown are the circuits for providing DC power and HV monitor/control voltages, which are constructed using standard DACs, multiplexors, and ADCs.

PHOTOTUBE DIGITIZER ASIC BLOCK DIAGRAM

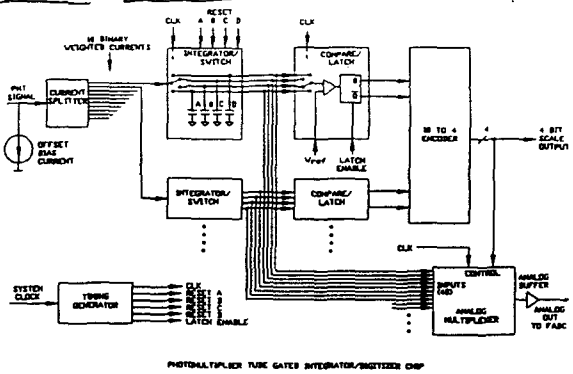

1. RESET CAPACITOR (16ns)
2. INTEGRATE PMT CHARGE (16ns)
3. DETERMINE RANGE/SCALE (16ns)
4. OUTPUT TO FADC (16ns)

} 4-phase 16ns Round Robin

Fig 8.3.3.5 - PMT DIGITIZER BLOCK DIAGRAM. Main circuit elements are: (i) Current Splitter, which splits the Phototube current into ~10 binary weighted scales; (ii) Integrator/Switch, which integrates the charge from each scale on one of four capacitors in a pipelined "round-robin" manner; (iii) Comparator/Latch, which determines if the capacitor contains an "interesting" voltage (between 1/2 and full scale), (iv) Encoder, which uses the comparator outputs to generate the 4-bit scale code ("mantissa"), and (v) Analog Multiplexor/Buffer, which selects the "interesting" capacitor voltage and outputs it the FADC on each cycle.

... more detailed PMT digitizer block diagram...

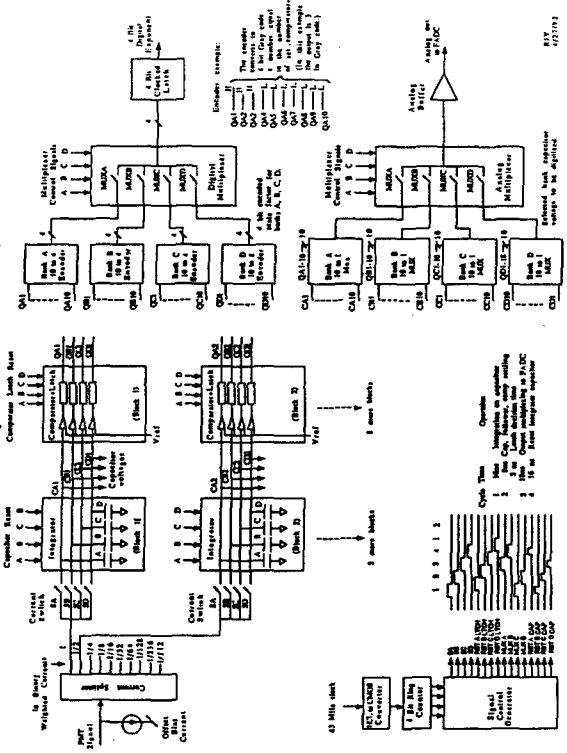

Detailed strategy for testing splitter/integrator chip, including milestones for ASIC development.

Version 1 - October '91 → testing complete, Writeup Jan 14

- Splitter Design (10 Output)
  - rise time OK
  - stability OK
  - DC Accuracy OK
  - Noise OK
  - Dynamic Range OK
  - Temp Drift OK
  - Run-Run reproduc. OK
- Gated Integrator (2-way) Works
- Integrator Reset Works
- Analog Output Mux Works
- Analog Output Buffer Works

Version 1a Feb '92 → testing complete, Mar 31 writeup

- More Sensitive Integrator
  Measure Noise floor <2000 e? } ≤ 1mV on 1 pC all scales
- Measure Linearity of Integrator → coming up
- Test of current amp to extend low range of splitter -->20 bits } WORKS FINE

VERSION 1a GATED Integrator/Current Splitter test chip.

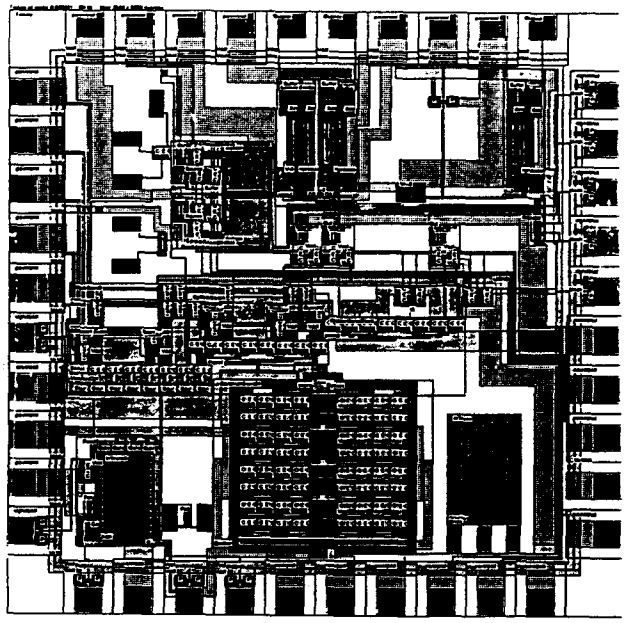

LINEARITY MEASUREMENT OF VERSION 1a

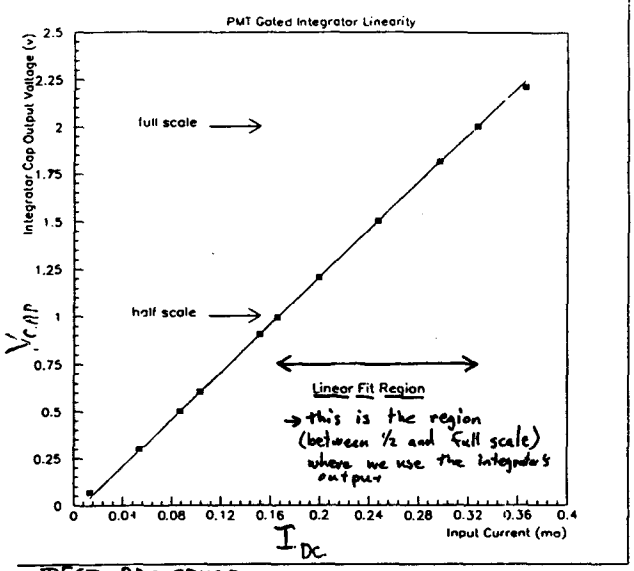

TEST PROCEDURE:

1) INJECT DC CURRENT
2) 16 ns gate time
3) Repetitive Clocking Waveform, Cap Reset
4) PLOT FINAL CAPACITOR VOLTAGE vs. DC INPUT CURRENT

GATED INTEGRATOR NON LINEARITY (cont'd)

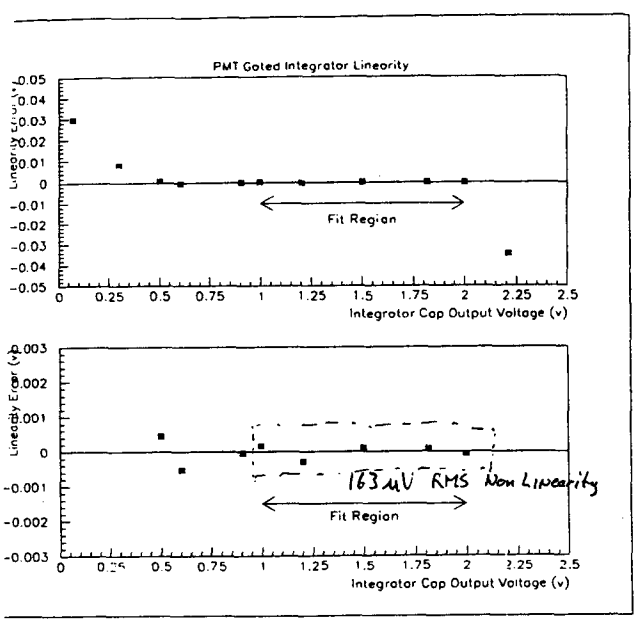

$$\text{NON LINEARITY} = \frac{163\,\mu v \text{ RMS}}{2V \text{ full scale}} = \underline{82 \text{ PPM}}$$

...good enough to justify a 16 bit FADC...

Table 3: Digital PMT Readout: Gated Integrator/Digitizer Performance Summary

	Specification	Measurement
Least Count (~noise level)	10 MeV (1 fc) = 0.1μA x 10ns current pulse from PMT	< 0.6 fc pedestal RMS for gate times <50ns on 1st version of Current Splitter/Gated Integrator Test Chip
Full Scale	= 10 TeV (1 nC) = 100ma x 10ns pulse = 10^6 least counts (20 bits)	Current Splitter measured linear for pulses up to 100ma
Accuracy	1-2% before calibration	Current Splitting Accuracy Measured < 0.7% on multiple ranges up to 100ma
Rise Time	~5-8ns (faster than scint rise time)	<4ns over entire dynamic range 0→100ma
Time Slewing vs. Pulseheight	<< 16ns PMT Gate Width	~1ns difference in splitter propagation delay for pulses of ~0 → 100ma
Gated Integrator		Functional
Capacitor Reset		Functional
Output Multiplexor and Buffer		Functional
Settling Time of Analog Output	<16ns to accuracy required by FADC	9ns settling to ~8 bit accuracy
Temperature Stability	<0.25% over 10 degrees CC operating temperature range	<0.5% change in Current Splitter Accuracy for 30 degrees C change.
Immunity to Run-to-Run Process Variation	< 1% before calibration	Current Splitting Absolute Accuracy Measured < 0.7% for test chips from two sepatate ORBIT runs
System Noise	$\sigma \leq$ 1 least count 6,000e^- RMS	$\sigma \sim 5000e^-$ (0.8fC) mesured on 60 MHz test board including FADC noise, discrete amplifier noise, digital noise from clock & line drivers, etc.

Version 2 April '92 → Back From Fab Testing Starting Now ~5/5/92

- Design complete
- layout ~3/4 complete
- 4 stage timing/control logic
- Takes data synchronously with FADC
- Low-Level Differential Clock
- No Auto-ranging logic: can switch low-->hi scales via changing jumpers
- This version should be usable for 1st pass PMT digitizer.

Version 3 ~July '92

- Automatic Ranging → Submitted ~10 APRIL 92, Back ~20 may
- "Final Splitter" for ~20-bit dynamic range.
- This version should be fully functional for PMT Dig Assy.

VERSION X
- FADC TEST CHIP
- BASED ON COMPARATOR DESIGN FOR V3.
- 5-bit, 30mw FADC for shower max
- 10-bit, 2-stage pipelined, 80mw FADC for calorimeter readout.

DIGITAL READOUT BOARD .... QUITE BORING, ACTUALLY...

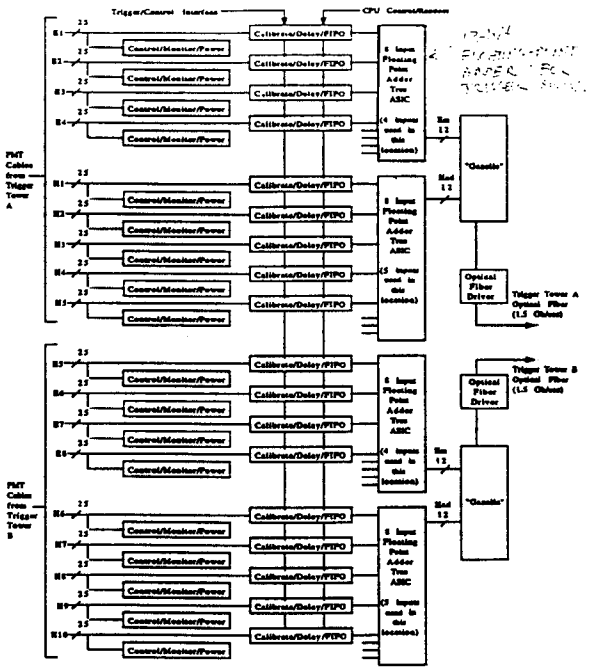

Fig. 8.3.3.3 - DIGITAL PMT READOUT BOARD BLOCK DIAGRAM. (Barrel Calorimeter Version). Each board has connects to eight calorimeter towers (18 Phototubes). HV Control, Monitor, Power, Calibration and DAQ functions are performed on a per-channel basis identically for all PM tubes. Trigger signals from 4 towers of calorimetry are summed into EM and HAC sums for two trigger towers. Trigger sums are formed digitally using the floating-point adder described in Section 12, and transmitted to the trigger by optical fibers on front panel.

2. FLOATING POINT ADDER FOR TRIGGER SUM OUTPUTS.

Two versions have been produced in 1.2u CMOS.

1st version (Sept 91) was fully functional in fall-through mode at 66MHz.

2nd version (Jan '92) contained:

- improvements in the clocking structure,
- logic changes due to a redefinition of our floating-point format,

--> Functions in synchronous pipelined mode at ~100MHz.

Design is essentially complete.

Seven copies of this subcircuit will be laid out and fabricated on a single die to form the 8:1 adder tree required for Trigger Tower Energy sums in the Baseline Trigger design.

Should have a working VME test board by this fall.

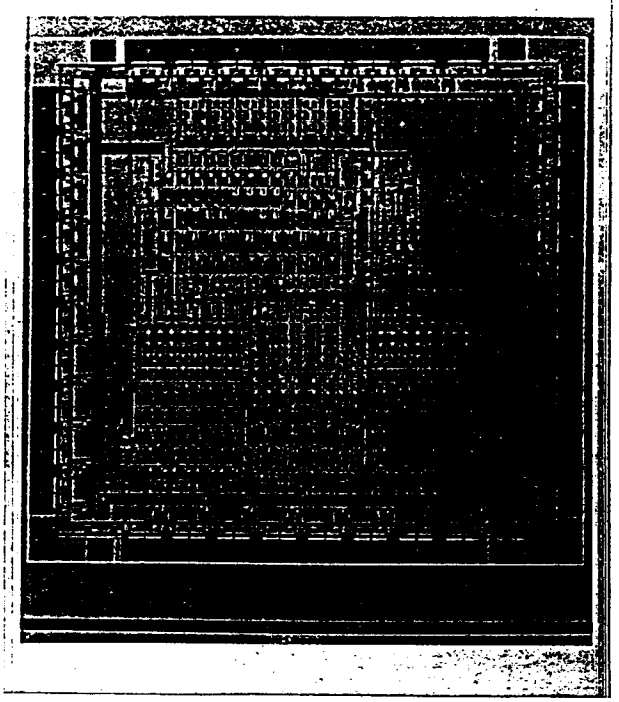

SUMMARY

- SUCCESSFUL TEST CHIPS FOR KEY ANALOG COMPONENTS:
  - current splitter
  - gated integrator
- CIRCUITS UNDER FABRICATION FOR REST OF DIGITIZATION ASIC
  - AUTO-RANGING
  - OUTPUT MULTIPLEXING
- SHOULD HAVE FULLY FUNCTIONAL PROTOTYPE BY END OF SUMMER
  - 18+ bits dynamic range
  - Commercial FADC
- INCORPORATION OF FADC ON CHIP PROCEEDING
- VME BOARDS, etc. READY FOR SYSTEM TEST
- LOTS OF NEW COLLABORATORS

Present Status of the CDF Plug Upgrade EM Calorimeter

presented by S.Kim (University of Tsukuba)
at SDC collaboration meeting
on May 28, 1992

Contents

1. Design Criteria

2. R & D status
   (a) Comparison of Scintillating Plates
   (b) Comparison of WLS fibers
   (c) Light Yields vs. Fiber Diameter
   (d) Mega-tile

3. Production of Tile/Fiber Sub-assembly
   (a) Structure of Tile/Fiber Sub-assembly (Pizza-pan)
   (b) Quality Control of tiles, fibers and tile/fiber

4. Collaborators and Time Schedule

May 20, 1992
Draft V3.2

Plug Upgrade EM calorimeter

1 Introduction

The design plan of the plug upgrade EM calorimeter is reported. The design criteria is described in Section 2. The specifications and the quality control procedures for tile, fiber and tile/fiber subassembly are described in Section 3, 4 and 5, respectively. In Section 6, energy calibration of the calorimeter is described. Time schedule is outlined in Section 7. Cost estimate is shown in Section 8. Section 9 shows a list of the collaborators working on the plug upgrade EM calorimeter.

2 Design criteria

The plug upgrade EM calorimeters is required to have the energy resolution of $\leq 17\% /\sqrt{E} + \leq 1\%$ as described in Physics Chapter.

The first term comes from the sampling fluctuation and the photostatistics. The sampling fluctuation with 5 mm lead plate is 14%/$\sqrt{E}$. If the number of photoelectrons per tile per MIP is 2 (1), the contribution of photostatistics is 7.4%/$\sqrt{E}$ (10.4%/$\sqrt{E}$) since the calorimeter response for electron is 4.0 MIP/GeV. This degrades the resolution down to 16%/$\sqrt{E}$ (17.5%/$\sqrt{E}$). Thus 2pe/MIP/tile is enough to satisfy the energy resolution criteria.

The second term comes from the non-uniform response over the surface of the tower. Such a non-uniformity can be attributed to the non-uniform response at different depths in a tower, the non-uniform response in different towers and the non-uniform respouse in a tile. The non-uniform response of the calorimeter due to tile gain non-uniformity was estimated using CDFSIM shower simulation. The tile gain was assumed not to have any systematic non-uniformity depending on the transverse position. 2% rms non-uniformity of the tile gain in different towers gives a 0.5% non-uniformity of the calorimeter response. 2% rms non-uniformity in a tile gives a 0.5% non-uniformity of the calorimeter response as well. 20% rms non-uniformity of the tile gain at different depth in a tower gives a 0.5% non-uniformity of the calorimeter response. Since the tower-to-tower gain variation can be reduced by setting adequate photomultiplier high voltages, we control the tower-to-tower gain variation down to 2.5% which corresponds to 10% rms tile-to-tile gain variation. Thus 2% rms non-uniform response in a tile and 10% tile-to-tile gain variation are enough to satisfy the energy resolution criteria.

Another requirement on the plug upgrade EM calorimeter is non-linearity smaller than 1% in the energy range between 10 GeV and 400 GeV. The non-uniformity of the tile gain in a tower causes the non-linearity. The non-linearity of the calorimeter due to the tile gain

Design Criteria of the CDF Plug Upgrade EM calorimeter

1. Energy Resolution:
   $<17\%/\sqrt{E}(\text{GeV}) \oplus <1\%$
2. Non-Linearity:
   $< 1\%$ (10GeV < E < 400 GeV)

Light Yield Requirement

Energy Resolution Stochastic Term

(1)Sampling Fluctuation with 5 mm Lead = $14\%/\sqrt{E}$
(2)Photostatistics
the number of photoelectrons per tile per MIP = 2 (1)
↓
contribution of photostatistics = $7.4\%/\sqrt{E}$ ($10.4\%/\sqrt{E}$)

Energy Resolution $= \sqrt{(1)^2 + (2)^2}$
$= 16.0\%/\sqrt{E}$ ($17.5\%/\sqrt{E}$)

2 photoelectrons per tile per MIP is enough for $17\%/\sqrt{E}$.

Plug EM upgrade
23 layers , 22.5 r.l.
1 layer = 4.0 mm Scintillator (0.010 r.l.)
+ 5.0 mm Lead (0.893 r.l.)
(ref. CDF1172)

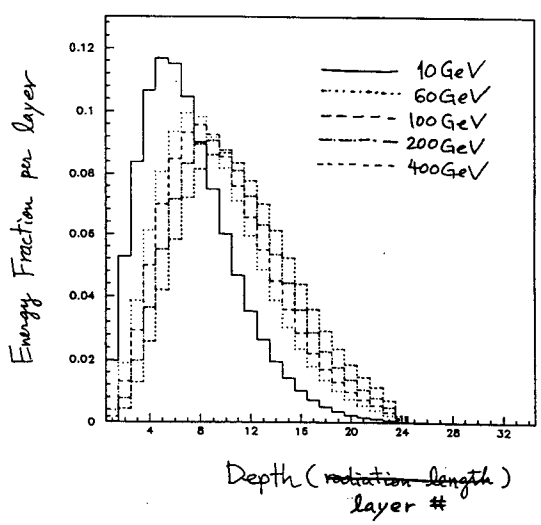

Uniformity Requirement

Transverse Uniformity

Shower longitudinal development is obtained by a CDF standard shower simulation which was tuned so as to reproduce 1985 testbeam data.

$F(t) = E\, t^{\alpha} e^{-\beta t}$,

t : depth in a unit of radiation length

$\alpha = 1.91 + 0.484\, \mathrm{Log}_e(E)$ E in GeV

$\beta = 0.582 - 0.014\, \mathrm{Log}_e(E)$ E in GeV

(ref . CDF892)

Shower fluctuation is simulated with fluctuations of α and β taking into account their correlation:

$\alpha' = \alpha \cos\theta - \beta \sin\theta$

$\beta' = \alpha \sin\theta + \beta \cos\theta$

α' and β' are uncorrelated.

At $\theta = 20°$, by giving the gain fluctuation of 2% around the average gain at each depth artificially, we obtained the following energy resolution degradation at the five energy points:

electron energy	energy resolution degradation
10 GeV	0.61 ± 0.01%
60 GeV	0.54 ± 0.01%
100 GeV	0.53 ± 0.01%
200 GeV	0.52 ± 0.01%
400 GeV	0.48 ± 0.01%

From this, 2% non-uniformity of tile/fiber gain is enough to achieve the energy resolution offset less than 1%. Transverse uniformity in a tile should be controlled to be less than 2%.

Longitudinal Uniformity

At $\theta = 20°$, by giving the gain difference of 10% between layers artificially, 1000 showers are generated and the non-linearity and the energy resolutioin are obtained. 100 gain sets of 1000 events are tested.

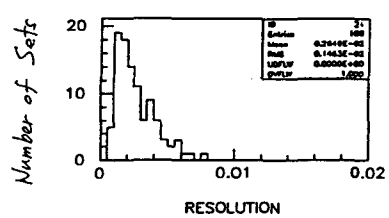

10GeV e⁻

We obtained the following energy resolution degradation at the five energy points:

electron energy	energy resolution degradation
10 GeV	0.26 ± 0.02%
60 GeV	0.22 ± 0.01%
100 GeV	0.22 ± 0.01%
200 GeV	0.23 ± 0.01%
400 GeV	0.24 ± 0.01%

Thus 10% longitudinal non-uniformity does not cause any significant resolution degradation.

Non-linearity was estimated as follows: As we calibrate the calorimeter with 100 GeV electron beam, we calculate the ratio of E/P at a certain energy to E/P at 100 GeV. This deviation from 1 was defined as non-linearity. The non-linearity has a maximum at either 10 GeV or 400 GeV. The maximum non-linearity is plotted for 100 gain sets.

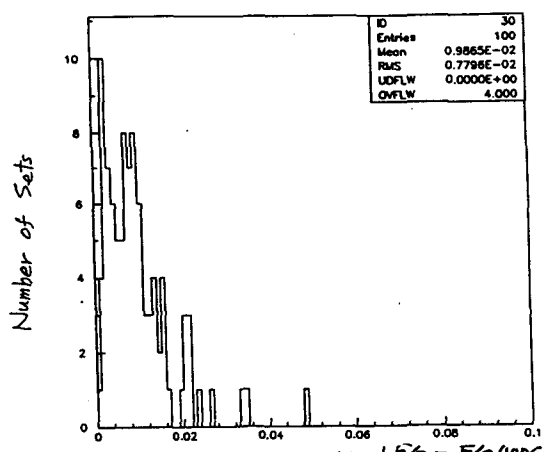

Non-linearity $\equiv \mathrm{Max} \left| \frac{E/p - E/p(100\,GeV)}{E/p(100\,GeV)} \right|$

Thus 10% longitudinal non-uniformity causes 1% non-linearity (0.99± 0.08%). This gives the limit to the tile-to-tile gain variation.

< 10% tile-to-tile gain variation

for γ,

photon energy	energy resolution degradation
10 GeV	0.56 ± 0.05%
60 GeV	0.45 ± 0.03%
100 GeV	0.40 ± 0.03%
200 GeV	0.39 ± 0.03%
400 GeV	0.37 ± 0.02%

Thus 10% longitudinal non-uniformity causes 1% (1.05 ± 0.10%) non-linearity. This give the limit to the tile-to-tile gain variation.

Setup for Light Yield and Attenuation Length Measurement for Scintillating Plates

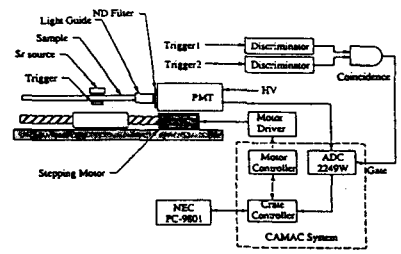

Figure 23: シンチレーター測定装置。トリガーには浜松ホトニクス R580 光電子増倍管を用いた。シンチレーターとライトガイドの接面にはオプチカルグリスをつけた。

Scintillator Sample

200 mm long × 20 mm wide × 4 mm thick

SCSN81
38C
38D

Number of Photoelectron : $N_{p.e.}$

(1) With ND filter, we set $\langle N_{p.e.} \rangle$ to ~0.05. Take data and fit it to a gaussian to get a single photoelectron peak.

(2) Take data with 10% ND filter.

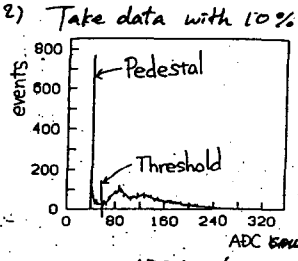

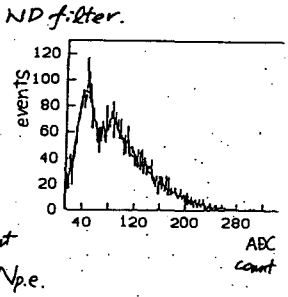

$$x \equiv \frac{\text{ADC count}}{\text{Single P.E. Peak}} \longrightarrow N_{p.e.}$$

$$\langle N_{p.e.} \rangle \equiv \mu$$

(a) Fitting Function $= A \sum \frac{e^{-\mu}\mu^n}{n!} \frac{1}{\sqrt{2\pi}\sqrt{n}\sigma} \exp\left\{-\frac{(x-n}{2\sqrt{n}\sigma}\right.$

or

(b) $\langle N_{p.e.} \rangle = \frac{1}{N} \sum_{i=1}^{N} x_i$ including pedestal

Radiation Damage Test of Scintillating Plates

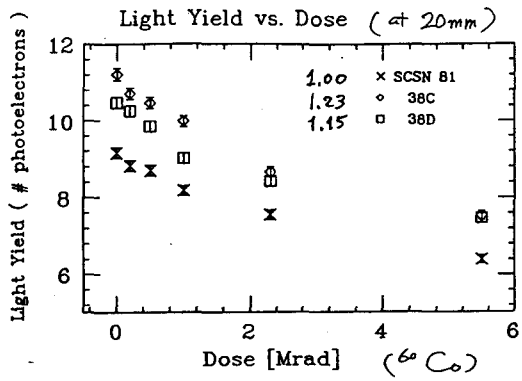

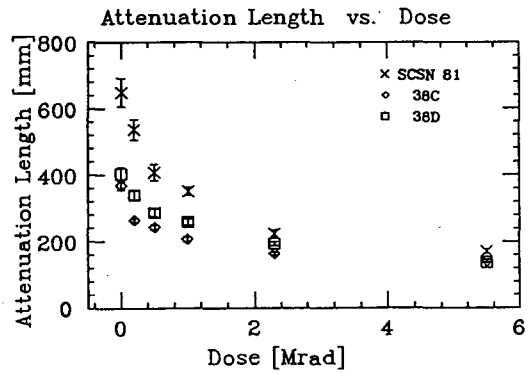

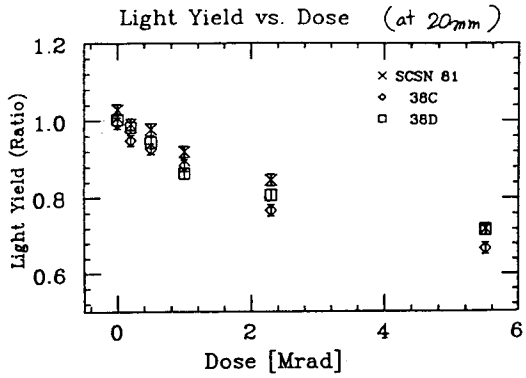

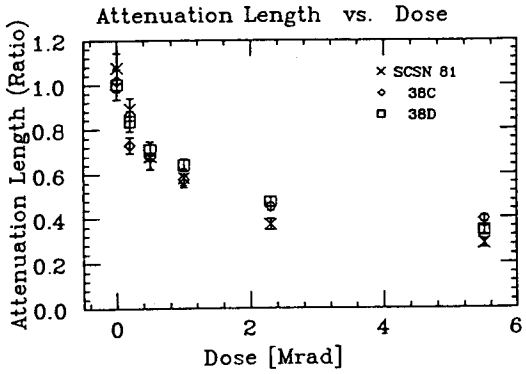

Setup for Light Yield Measurement for Tile/Fiber

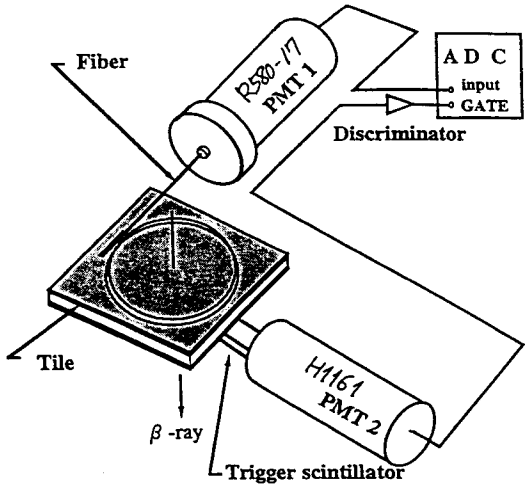

- 12cm × 12cm × 4mm thick Tile
- Two turn fibers in groove with a radius of 57.6 mm

R580_17

Serial Number	Number of Photoelectrons	Error	Ca.Luminous Sensitiviiy	#.ofP.E. Ca.L.Sensitivity
WB1985	3.80	0.14	129.0	0.0295
WB1999	3.78	0.14	135.0	0.0280
Average	3.79	0.10		0.0287

R329(H1161)

RC3947	2.79	0.10	95.8	0.0291

XP2081B

014316	4.32	0.16	180	0.0240
014330	3.60	0.13	169	0.0213
014388	3.00	0.11	116	0.0259
Average	3.49	0.07		0.0237

		Cathode Luminous Sensitivity		Number of Photoelectrons
R580_17	(16 tubes)			
	Average =	131.1	→	3.76 (1.30)
	R.M.S =	3.5	→	0.10 (2.7%)
R329	(25 tubes)			
	Average =	99.7	→	2.90 (1.00)
	R.M.S =	11.9	→	0.35 (12%)
XP2081B	(10 tubes)			
	Average =	156.8	→	3.72 (1.28)
	R.M.S =	17.0	→	0.40 (11%)

R580-17

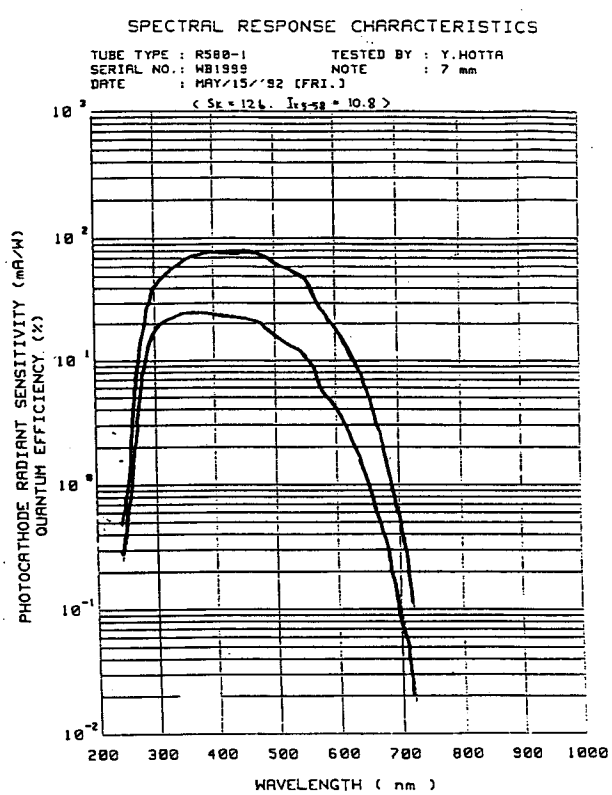

1139 (1/1)

XP2081B

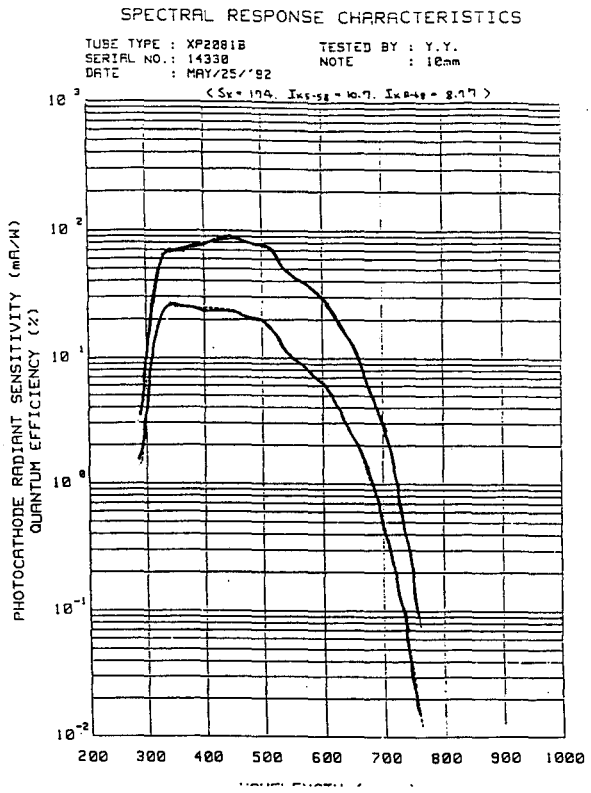

1110

R329

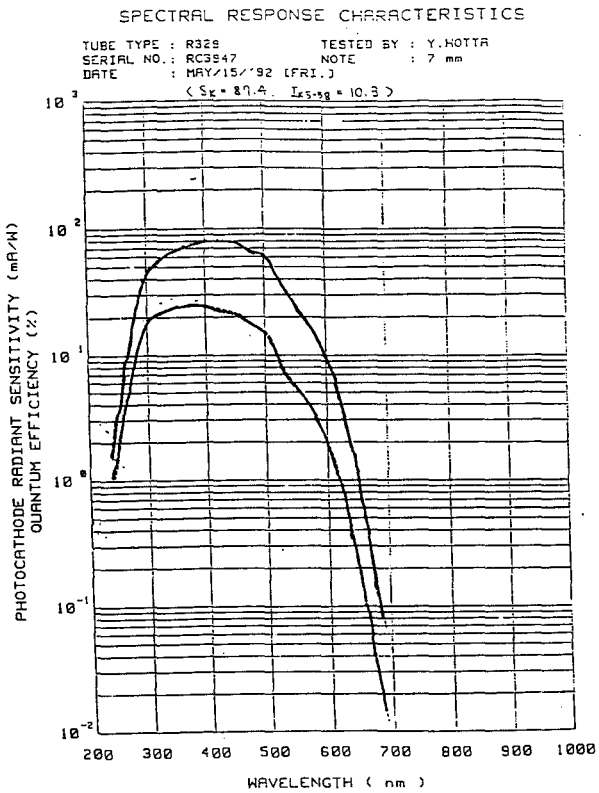

1111

Light Yield of Tile/Fiber

Fiber :	0.70 mm φ	Y7 150ppm
Tile 12cm×12cm ×4mm thick	81	PMT = R580-17
	38C	
	38D	

		Light Yield (# of p.e.)	
38C		7.33 ± 0.04	
		7.00 ± 0.04	
	Ave	7.17 ± 0.03	(1.27)
38D		6.78 ± 0.03	
		7.13 ± 0.04	
	Ave	6.96 ± 0.03	(1.23)
81		5.63 ± 0.03	(1.00)

1112

2-b Comparison of WLS fibers

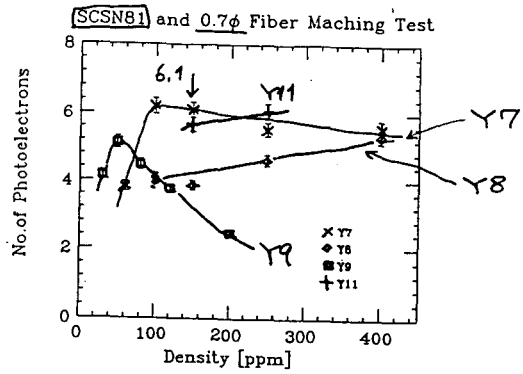

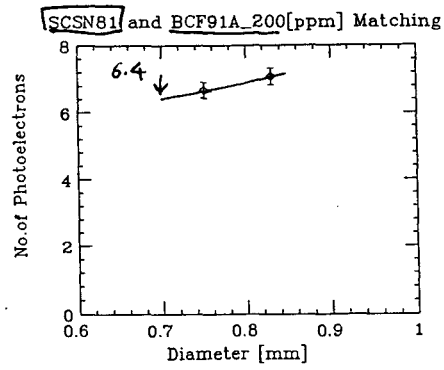

2-c Light Yield vs. Fiber Diameter

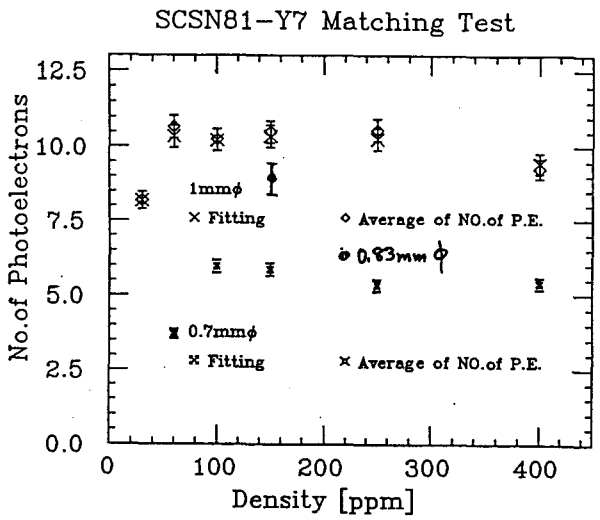

2-d Mega-Tile

1	2	3
4	5	6
7	8	9

Point Value / Center Value (%)

← 0.5 mm wide slit

← 0.5 mm wide 2 mm deep groove

↑ white sheet glued inside

1.24 ± 0.15	1.39 ± 0.16	0.053 ± 0.034
1.48 ± 0.18	Center	1.23 ± 0.16
0.43 ± 0.11	0.87 ± 0.13	0.22 ± 0.0087

Mean of 1,3,7,9 : 0.15 ± 0.03(%)

Mean of 2,4,6,8 : 1.20 ± 0.08(%)

3-a Structure of a Tile/Fiber subassembly ($\Delta\phi = 15°$)

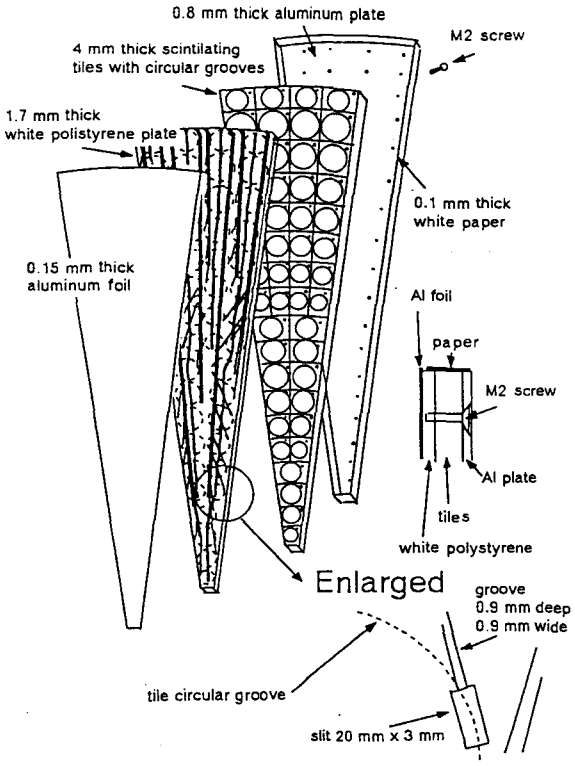

Lateral Segmentation

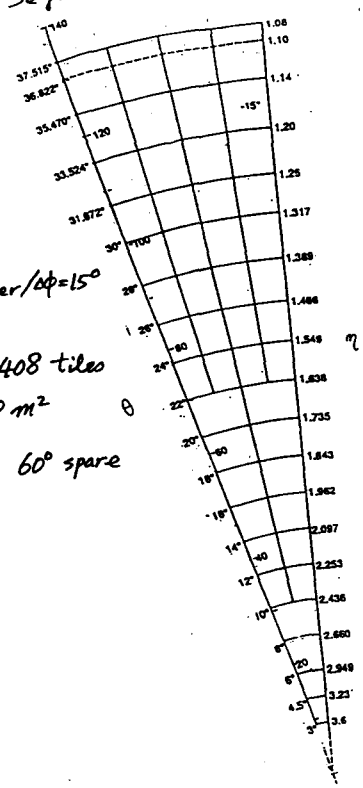

48 tiles/layer/$\Delta\phi$=15°

Total 57,408 tiles

340 m^2

including 60° spare

Fiber Routing

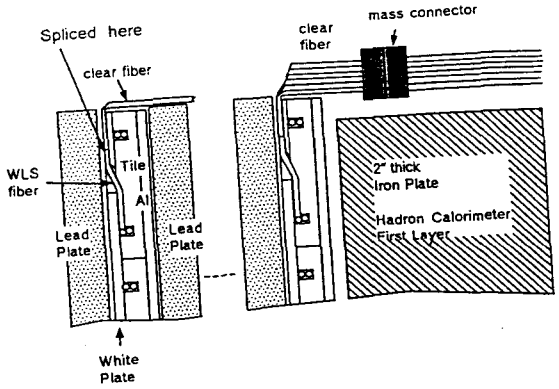

3-b Quality Control of tiles, fibers and tile/fiber

Optics

	Light Yields	Attenuation Length	Measurement Sampling
tiles	120 p.e. ± 2%	90 cm ± 15%	
fibers			
WLS fiber	6 p.e. ± 2%	1.5 m ± 15%	"
Clear fiber		10 m ± 15%	"
Splicing	Light Loss 10 ± 2%		"
tile/fiber	2 p.e. ± 2%		All

Radiation Damage for 500 krad dose (CDF 10 years dose at 3 degrees)

	Light Yields	Attenuation Length
tiles	> 80%	> 70%
fibers		
WLS fiber		> 70%
Clear fiber		> 70%

Size Tolerance

Tile thickness	4 mm ± 0.2 mm	All
Aluminum Plate thickness	0.8 mm ± 0.1 mm	"
White Polystirene thickness	1.7 mm ± 0.1 mm	"
Fiber Diameter	0.83 mm ± 0.02 mm	"
Hole Position	± 0.05 mm	
Accuracy for Grooving and Cutting	± 0.1 mm	

We know how good the gain uniformity of SCSN81 tile can be controlled from the experience of producing CEM scintillator SCSN38.

< SCSN38 plate>

	Mean Value	Variation in R.M.S.
Chemical material		1.0%
Thickness	4.95 mm	0.09 mm (2.0%)
Attenuation length	92 cm	13 cm (14%)

We summarise the above non-uniformities in the following tables:

< Single Plate >

	Gain variation at a tile center	Gain non-uniformity in a tile
Chemical material of tile	1.0%	0.5%
Thickness of tile	2.0%	1.5%
Attenuation length for 10cm long tiles	0.5%	0.5%
Attenuation length for 100cm long Y7 fibers	5.0 %	none
Attenuation length for 350cm long clear fibers	5.0 %	none
Overall	7.4%	1.7%

10 Collaborators

University of Tsukuba/KEK/Fermilab

Overall design and plan of sub-assembly	K.Kondo*
Quality Control of tile/fiber production and cosmic ray test of sub-assembly	S.Kim*, Y.Seiya*, K.Kondo, K.Takikawa, S.Miyashita, I.Nakano, K.Yasuoka, K.Hara, S.Ogawa, four graduate students
EM calorimeter assembly and mechanical design	M.Mishina*, Y.Fukui*, one engineer and three technicians
Calibration	M.Mishina*, Y.Fukui*, S.Kim*, K.Kondo, K.Takikawa, S.Miyashita, I.Nakano, K.Yasuoka, K.Hara, two graduate students, one engineer and three technicians
Physics	S.Miyashita*, S.Ogawa, M.Takano, Y.Seiya, two graduate students
Contact with Hadron calorimeter	K.Kondo*, S.Kim*, M.Mishina*
Contact with shower max. position detector	K.Kondo*, S.Kim*, M.Mishina*

* shows persons in charge.

8 Time schedule

1992	May	Complete a prototype of pizza pan.
	September	Start mass production of tile, fiber and pizza pan.
	October	Start assembling of pizza pan.
	November	Start cosmic ray test for quality control of sub-assembly units at University of Tsukuba.
1993	January	Start shipping of sub-assembly units to Fermilab.
	April	Complete shipping of sub-assembly units for a quadrant.
	May	Start installation of sub-assembly units into the lead structure.
	July	Complete all sub-assembly units of tile/fiber. Complete shipping of all sub-assembly units to Fermilab.
1994	February	Start cosmic ray test of the plug EM calorimeters.
	March	Start the electron beam calibration of the first plug EM calorimeter.
	July	Complete the electron beam calibration of the first plug EM calorimeter. Start the electron beam calibration of the second plug EM calorimeter.
	October	Complete the electron beam calibration of the second plug EM calorimeter.

CALORIMETER CALIBRATION

RECENT ACTIVITY:

A. WHITE
U. TEXAS AT ARLINGTON

- INFORMAL MEETING AT SSCL
  DURING SDC COLLAB MTG.

— SERIES OF MEETINGS AT SSCL
(AS PART OF "LOCAL" SDC CALORIMETER MEETINGS)

REQUIREMENTS DOCUMENT
(REPORT BY CRAIG BLOCKER AT FNAL (SDC MTG.)
↓
CIRCULATE / SDC_NEWS
↓
FEEDBACK

CALIBRATION QUESTION / TASK LIST
↓
WORK / INFORMATION

↓
CONCEPTUAL DESIGN

FINAL — PROTOTYPE

CALIBRATION REQUIREMENTS

GENERAL

- ALLOW CALIBRATION TO ACHIEVE DESIGNED PERFORMANCE GOALS
- SUPPLY MONITORING / DIAGNOSTICS

PHYSICS

A. ENERGY SCALE
GOAL ≤ 1% FROM MASSES OF KNOWN OBJECTS (Z, ψ, Υ, π^0)

B. ENERGY RESOLUTION
1. STOCHASTIC TERM (SMALL CALIB. EFFECT)
e.m. ≤ 1% INCREASE, had. ≤ 5% INCREASE
2. CONSTANT TERM
e.m. Σ CALIB. CONTRIBUTIONS < 1%
had. " " < 2%
a. TILE-TO-TILE VARIATIONS
LIGHT PRODUCTION, THICKNESS, LIGHT TRANSPORT
b. TOWER-TO-TOWER VARIATIONS
TILE VARIATIONS, PMT GAINS, ELECTRONIC GAINS.
c. SPATIAL NON-UNIFORMITY.
→ NEED RESPONSE MAP
d. TIME STABILITY
MONITOR SHORT / LONG TERM DRIFTS.
e. TIMING
VARIATION IN PULSE / GATE
f. RADIATION DAMAGE
$= f(t, \eta, \int \mathcal{L}$, TILE TYPE

C. LINEARITY / DYNAMIC RANGE

GOAL: CORRECTED LINEARITY < 1% (> 10 GeV)
< 100 MeV (< 10 GeV)
FOR ENTIRE DYNAMIC RANGE.

D. TIMING RESOLUTION
GOAL: BUCKET TAG $\sigma \sim 5$ nsec.

CALIBRATION SUBSYSTEMS (FUNCTIONAL REQS.)

A. IN SITU — "FINAL" CALIBRATION
— VERIFICATION OF WALL CALIBRATION
B. PEDESTALS — MEASURE ONCE / DAY (?) AND [illegible]
C. CHARGE INJECTION — VERIFICATION OF CURRENT SPLITTER AND DYN. RANGE
D. LASER — PMT GAIN MONITORING / LINEARITY
E. TILE EXCITATION (SOURCE [AND LASER?])
— MONITOR RADIATION DAMAGE
— DIAGNOSE TILE / FIBER PROBLEMS.
F. PRODUCTION TESTING
G. CALIBRATION TEST BEAM
— RELATION OF SOURCE / PARTICLE END
— VERIFICATION OF MODULE PERFORMANCE
H. OFFLINE CORRECTIONS

PROTOTYPE — CALIBRATION ISSUES

— TASK LIST — PROTOTYPE ITEMS?

→ WHICH ASPECTS OF CALIBRATION WILL BE <u>TESTED</u> ON PROTOTYPE?

→ WHICH CALIBRATION ELEMENTS SHOULD BE <u>PROVIDED</u> FOR PROTOTYPE.

→ WHAT DO WE HOPE TO <u>LEARN</u> FROM PROTOTYPE RELEVANT TO CALIBRATION?

CONCERNS:

- LOW LEVEL OF INTERACTION BETWEEN UTA / SSCL AND FNAL
- NEED TO ESTABLISH SCHEDULE FOR CALIBRATION / PROTOTYPE
- WHO WILL DO THE WORK!? (DAN'S LIST ETC!)

I. SOURCES

A. Position sensitivity — NEW IDEAS (SURGICAL BALLOON!...) — REQ. FOR POSITION ACCURACY ACROSS TILE?

B. Relative calibration of multiple sources

C. How many source tubes and where (which layers, which towers, phi and eta coverages) PROTOTYPE → ALL

D. Type of source to use

E. How long does it take to do a source calibration

F. Current monitoring circuit

G. D.C. current vs pulse gain of PMT

H. How well does the source response predict the shower response (for example, what is the effect of variations in absorber thickness)

I. Magnitude of current for the gain we will run the PMT's at.

PROTOTYPE : – TEST FULL IMPLEMENTATION.
– SCAN ALL TILES
– >CHEDULE : ISSUES TO BE SETTLED NOW (GROOVE SIZE...)
— COORDINATION OF SOURCE DRIVER DEVELOPMENT. (CSCL WUTA MC. PURDUE/FNAL)

II. PEDESTALS

The question here is how sensitive is the physics to abnormality in the pedestals or other low energy problems. This includes questions of pedestal widths, rate dependence, coherent effects. Physics processes to consider are missing Et, jets, and electron transverse profiles.

STUDIES NEEDED!

→ SOME ANSWERS FROM PROTOTYPE

III. PRODUCTION TESTING

A. How well do we have to do on tile-to-tile uniformity

B. What problems should we be looking for (broken fibers, light leaks, ?)

C. Do we determine tower-to-tower relative calibration here?

D. How long will it take or can it take? (COST / SCHEDULE, 10^6 TILES!)

PROTOTYPE : [illegible]

IV. OFFLINE CORRECTIONS

A. longitudinal leakage

B. Response maps, cracks, and edges

C. Massles gap correction

D. Optimal method of determining energy from multiple bucket information.

PROTOTYPE : [illegible]

V. TIMING VARIATIONS

A. What is the pulse shape? SSCL STUDIES
B. Effect of straight integration (digital scheme) vs integration + shaping (SCA scheme).
C. What are some reasonable methods for extracting energy from multiple bucket information?
D. What is effect of timing jitter within a single channel for various methods in C?
E. What is the effect of channel-to-channel timing variations?
F. What are possible global effects (such as eta dependence)?
G. How can be get channel-to-channel relative timing correct without beam?
H. How can we get a channel's timing correct with beam?
I. How stable will the timing signals to the electronics be?

PROTOTYPE : - CHANNEL-TO-CHANNEL TIMING DETERMINATION?

1460

1461

Charge Injection
==========

1. Relation of design(s) to choice of front end electronics. DESIGN FOR DIGITAL F.E. ONLY SO FAR.
2. Dynamic range requirements.
3. Expectations for channel to channel and time variations of front and electronics.
4. Precision requirements.
5. Required flexibility for calibration sequences: same charge repetition vs. patterns and scans.
6. How often to run charge injection calibration - how much data/number of patterns/time taken?
7. Number of channels to instrument? Single channel systems vs. central distribution of pulses.
8. Verification of charge injection performance.
9. Requirements for recording of bad channels/ bad codes/ ambiguities.
10. Front end integration issues.

PROTOTYPE : - WHICH ELECTRONICS?
↓
- DECISION vs. SCHEDULE
  - WHAT TO AIM FOR?
- COVER ALL CHANNELS?
  TRY DISTRIBUTED vs. ALL.
↓
- DETERMINE NATURE OF FINAL SYSTEM.

1462

Light Flasher
==========

1. Do we illuminate tiles and/or fibers?
2. If we illuminate tiles: how do we route fibers, where/how do we connect to the tiles, and which tiles do we illuminate?
3. Fraction of PMTs to monitor vs. variation of initial PMT characteristics and changes with time.
4. How to illuminate the photocathode - transverse variations/ fiber placement /relation to fibers from depth segment.
5. Laser stability requirements vs. intensity monitoring.
6. Dynamic range coverage.
7. Specification of accuracy, ranges for the optical attenuation system.
8. Laser pulse characteristics vs. calorimeter pulses (pulse shape).
9. Required frequency and duration of laser calibrations?
10. Rate dependence of PMT gains - relation to laser calibration measurements
11. Distribution of laser light over multiple fibers - tolerable variations vs. dynamic range coverage.
12. How many PMTs illuminated by a single laser; how many independent lasers; system control of multiple lasers
13. Timing requirements for flasher pulse: Global reference to crossing, channel-to-channel time consistency within a single laser system and across lasers, time jitter.
14. Frequency of light to be used

PROTOTYPE : - IF ILLUMINATE TILES
→ DESIGN ISSUES?
- AIM TO MONITOR ALL PMTS
- COOKIE DESIGN / CALIB. FIBER
+ DISCONNECT?
- SCHEDULE?

Shower Maximum Detector

Thomas Muller
(UCLA)

SHOWER MAXIMUM DETECTOR

Institutions :

Northeastern, Rockefeller, Saclay, Tel Aviv, UCLA, Yale + Italy, Japan

Responsabilities :

Mechanics :	France + Japan
Photodetectors :	U.S. + Italy
Electronics :	France + Italy + LBL.

Outline of talk :

- Electron / Gamma Identification
- Shower Max Requirements
- Shower Max and Massless Gap Detectors
- Photodetectors
- Test Results
- Shower Max Detector in Trigger

e / γ DETECTORS

PS	Preshower Detector between coil &EMC $\Delta\eta \times \Delta\Phi = 1.4 \times 0.05 / 160$ + stereo Rejected in favor of Shower Max.	Scint. Fibers
MG	Massless Gap First EMC tile $\Delta\eta \times \Delta\Phi = 0.05 \times 0.05$	Tile / Fiber
EMC	Electromagnetic Calorimeter $\Delta\eta \times \Delta\Phi = 0.05 \times 0.05$	Pb / Scint
SMD	Shower Maximum Detector within EMC η strips : $\Delta\eta \times \Delta\Phi = 0.05/8 \times 0.20$ Φ strips : $\Delta\eta \times \Delta\Phi = 0.20 \times 0.05/8$	Tile / Fiber
HAC	Hadronic Calorimeter $\Delta\eta \times \Delta\Phi = 0.10 \times 0.10$	Fe / Scint

e / γ IDENTIFICATION

	e Identification	Background	Detectors
	EM / HAD	$\pi^{\pm}$	EMC + HAC
	Isolation	jets	EMC + HAC
	E = p	$\pi^{\pm}\ \pi^{o}$	Trk + EMC
→	Track-Shower match	$\pi^{\pm}\ \pi^{o}$	Trk + SM
→	Shower Shape	$\pi^{\pm}$	SM
→	Shower Depth	$\pi^{\pm}$	MG
	Vertex Position	$\gamma \to e^{+}e^{-}$	Silicon Trk

	γ Identification	Background	Detectors
	EM / HAD	jets	EMC + HAC
	Isolation	jets	EMC + HAC
→	Shower Shape	π^{o}, $\pi^{o}\ \pi^{o}$	SM
→	Statistical Separation	π^{o}	MG

P_T spectrum of Photons in $W\gamma$ events, and of jets in Wjet events

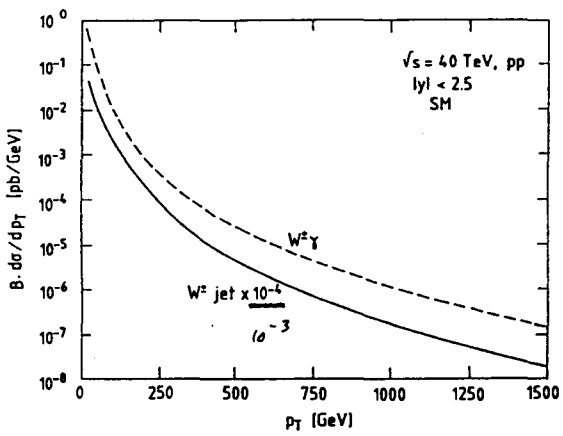

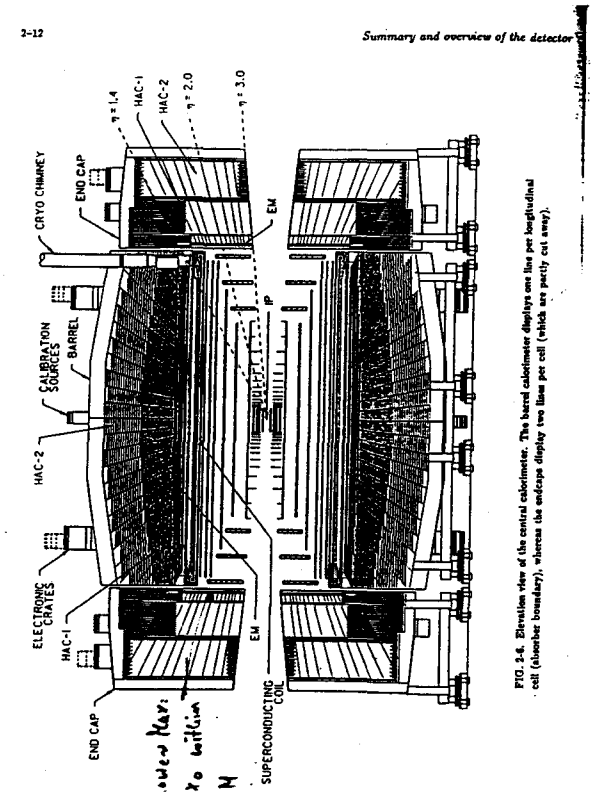

SHOWER MAXIMUM GRANULARITY IN BARREL

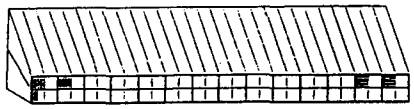

η strips — Physical SM strips — Φ strips

0.05/8 x 0.05 — Δη x ΔΦ — 0.05 x 0.05/8

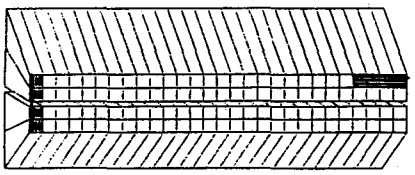

0.05/8 x 0.20 — Electronic channels — 0.20 x 0.05/8

- Gang 4 physical SM strips ⇒ 1 electronic channel

  Occupation @ $L = 10^{33}$: ≈ 0.3 %

- Upgrade path : Gang 2 strips ⇒ 1 channel

  0.05/8 x 0.10 — Electronic channels — 0.10 x 0.05/8

SHOWER MAXIMUM SEGMENTATION IN ENDCAPS

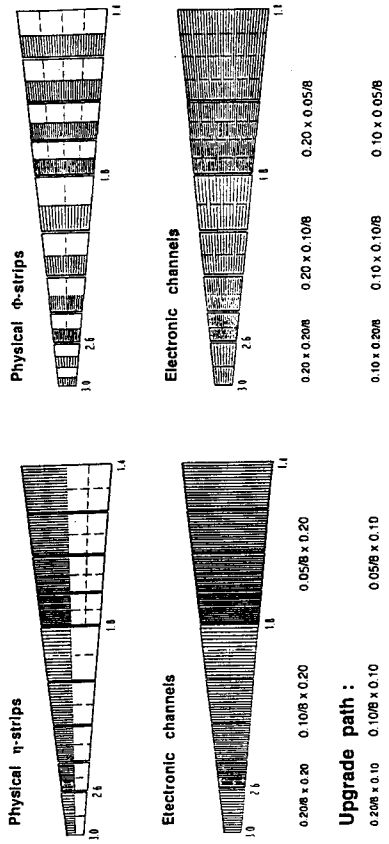

FIBER ROUTING

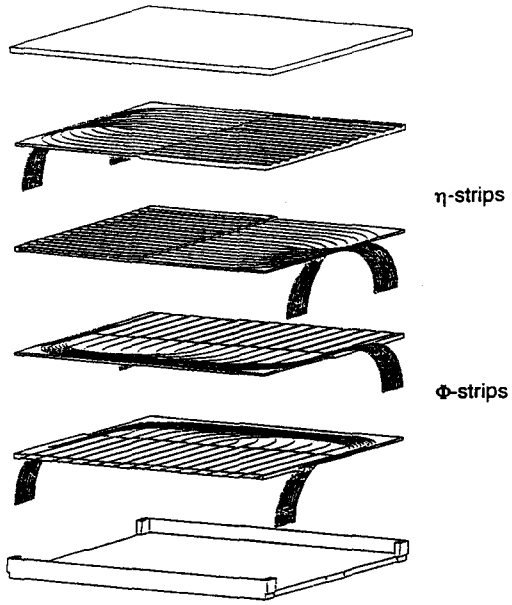

64 strips per 4-tower slot

! 5/26 : New ideas, covering 0.1 * 0.1, not bended

TRANSMISSION vs BENDING RADIUS

Clear polystyrene fiber
Diameter 1 mm, length 2 m
Light signal after 360° turn

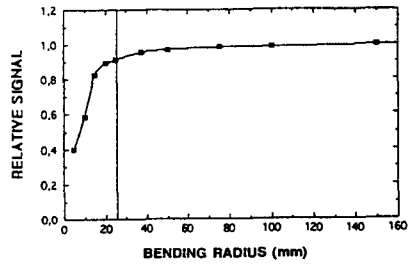

Conclusion : Minimum radius ≈ 1 inch

Fiber routing is difficult !
Easier with 0.7 mm fibers.

π^o / γ REJECTION

Moliere Radius : Pb / Scint ≈ 3 cm
Strip Width : 0.05 / 8 ≈ 1.3 cm

Use narrow core for improved π^o rejection ?

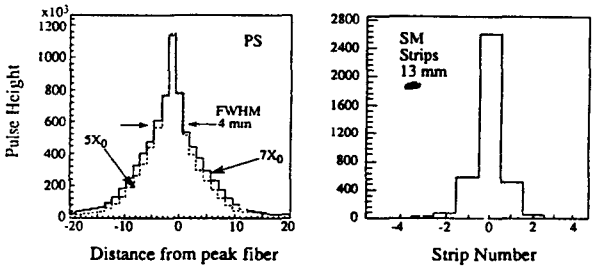

π^o rejection factor for 80 % electron efficiency :

E_{π^o}	$\varepsilon_\gamma / \varepsilon_{\pi^o}$ (0.05/8)	$\varepsilon_\gamma / \varepsilon_{\pi^o}$ (0.05/16)
25 GeV	6.7	8.9
50 GeV	1.5	2.6
75 GeV	1.3	1.5

Trade-off : Readout fibers x 2
⇒ π^0 background x 2/3.

RADIATION DAMAGE

Co^{60} irradiation of SM strips + WLS fiber

1.3 Mrad ---> 40% loss

SM Detector at shower maximum for E = 10 GeV

Barrel SM Detector @ 7 X_o @ eta = ~~3~~ 1.4

25% loss in 100 SSC years

Endcap SM Detector @ 7 X_o @ eta = 3

Quartz fiber readout

50% loss in 4 SSC years

Move to 10 X_o (shower max for 10 GeV)

50% loss in 7 SSC years

Retreat to eta = 2.6 ?

50% loss in 20 SSC years

Factor 4 loss probably O.K. at eta = 3

SHOWER MAX DYNAMIC RANGE

What can we get with 12 bits ?

Goal : EM shower position $\sigma \leq \Delta / 5$ = O(mm)
10 GeV < E_T < 1 TeV

Dynamic Range :

Energy 10 GeV - 1 TeV	33	@ 6 X_0
High tail @ 1 TeV	x 1.5	
Low tail @ 10 GeV	x 2	
Center of gravity	x 10	
Pedestal separation	x 4	minimal !
MCPMT gain variation	x 1	adjusted
Dynamic range	4000 ⇒ 12 bits	

η dependance x 2 barrel
x 5 ends

⇒ Limit η range covered by one MCPMT
Adjust overall gain (MCPMT anode voltage)

Photon readout : need ~ $4 10^3$

PHOTODETECTORS

Shower Max and Massless Gap Detectors

Baseline

Philips 64-channel PMT
Used in Fermilab beam test
QE = 12% @ 520 nm; crosstalk 5-10%

MCPMT Development

✓ Philips 64- and 96-channel PMT's
✓ Hamamatsu 256-channel PMT
Green-enhanced photocathodes QE = 16%
→ Ham. 64 large pixel PMT

Avalanche Photodiodes

EG&G APD with ball lens in beam test
QE = 60% @ 520 nm; no crosstalk
Arrays @ EG&G, Hughes, Advanced Photonix

APD-PMT

APD array in proximity-focussed image tube
Gain 5 x 10^5 and large dynamic range
64-channel prototypes for 1993 prototype
GaAs photocathode with QE = 34% @ 540 nm
Hughes Aircraft and Litton Electron Devices

SHOWER MAX DETECTOR IN TRIGGER

Level 1 : Decision time 4 μs
1 bit per 16 SM Φ strips
Protection against noisy EMC PMT's

Level 2 : Decision time 50 μs
8 bits per SM Φ strip
Track - shower match in Φ (1024 bins)
Shower shape in Φ

Level 3 : Decision time 100 MIPS-sec
12 bits per SM η- and Φ-strip
Track - shower match in η, Φ (σ ≈ 2 mm)
Shower shape in η, Φ
Mini - isolation cuts
Bremstrahlung cluster at same η, different Φ
Massless gap
$\pi^{\pm}$ rejection
π^0 / γ statistical separation

SUMMARY

Massless Gap EM energy correction
$\pi^{\pm}$ rejection
π^0 / γ statistical separation

10368 channels ⇒ 192 MCPMT's

Shower Max Track-shower match
Shower shape
Trigger Level 1, 2, 3

159 744 physical SM strips
47 104 electronic channels ⇒ 768 MCPMT's
Upgrade to match trigger segmentation
94 208 channels ⇒ 1472 MCPMT's

WHICH REGIONS TO INSTRUMENT?

Instrumented Sections of SDC Barrel Prototype

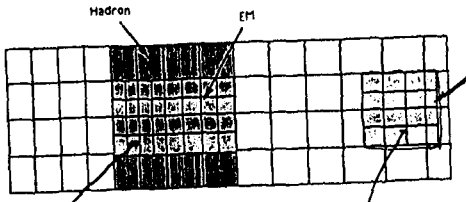

Region Used to study EM performance at end of Calor. (esp. bulkheads in cast EM design)

Region used for Hadronic Containment

SM
512 strips:
"Baseline": 128 el. channels
"Upgrade": 256 el. channels

MG
32 tiles 32 channels

SM
256 strips
64 channels per 128 ch.

MG
16 tiles 16 ch

$\boxed{\Sigma = 240 / 932 \text{ channels}}$

Candidates of Photon Detector for 1993

Existing:
Philips XP 1722 64 ch.
Hamam. H4140 Mod 256 ch.

In development:
APD - PMT 64 ch.
Ham. wide pixel PMT 64 ch.

1993 SMD Full scale Prototype test

System component issue
test implementation & compatibility of components

- **Test photodetctors** (64 Ch minimum per device)
- **First 16 channels signal processing ASIC ===>** Charge integrator --> 256 channels = 16 chips
- **Connectivity & cable** (Driver, output/input buffer, crosstalk...)
- **Simple read out ===> 32 channels VME digitizer card= 8 modules** *(as simple as possible) --> no sparcification & data reduction)*
  - Receiver
  - Shaper
  - Gain adjustment
  - Comparator/trigger
  - SCA pipeline
  - Digitizer chip

SDC ShowerMax - 5/22/92

PREPRODUCTION PROTOTYPE WEDGE

WHAT IS THE SCALE OF THE PROTOTYPE?
1. LOOK AT ALL INTERESTING CRACKS
2. HADRONIC CONFINEMENT
3. COST & WEDGE-MOVING FIXTURING (LBL engr)

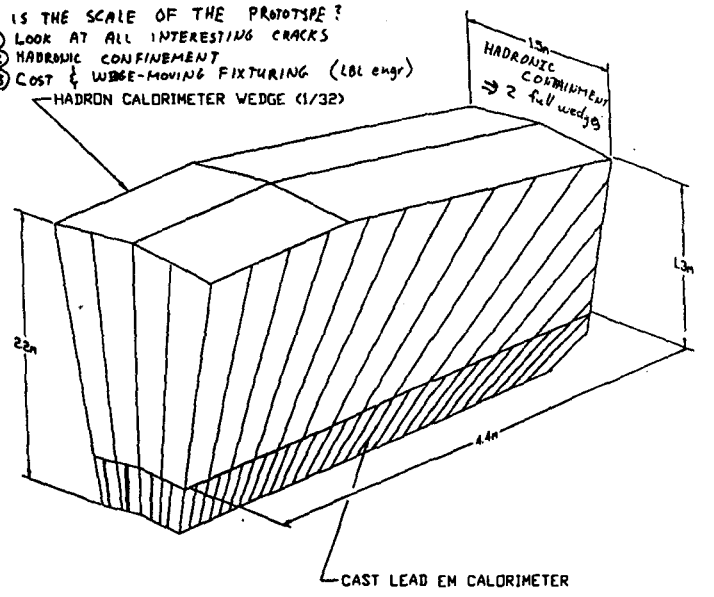

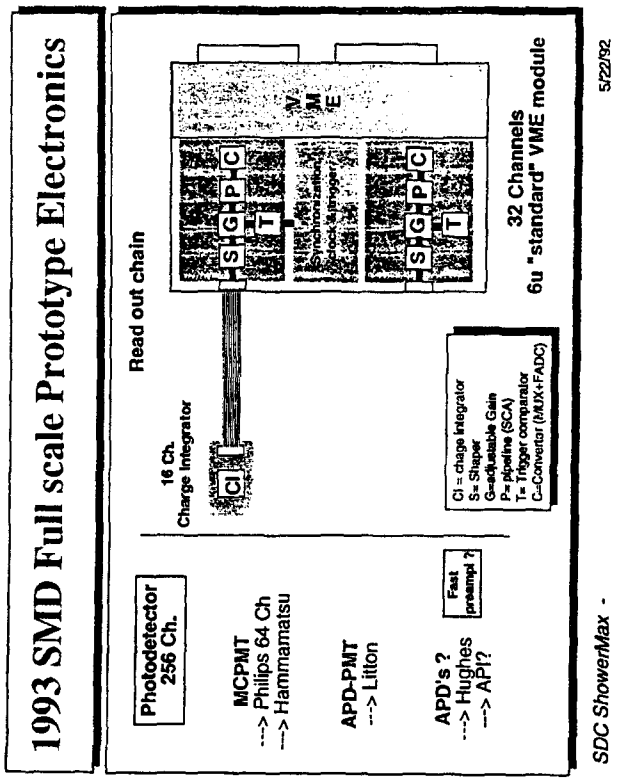

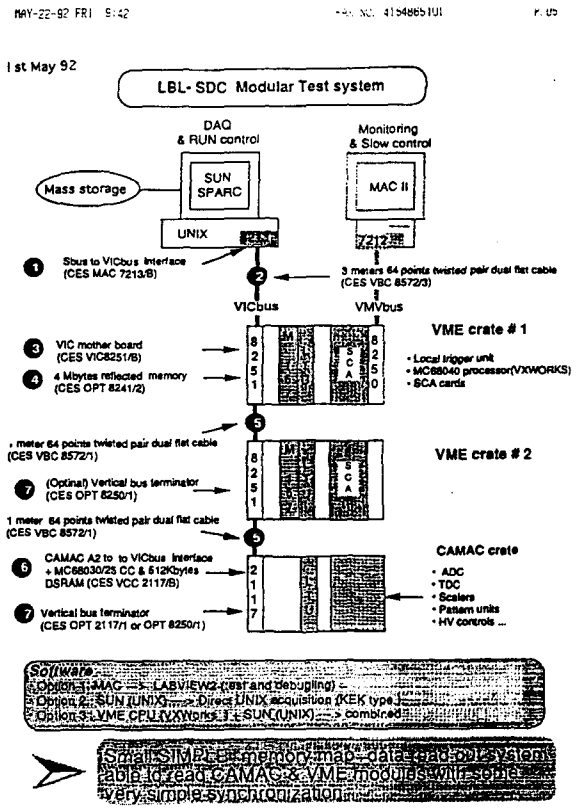

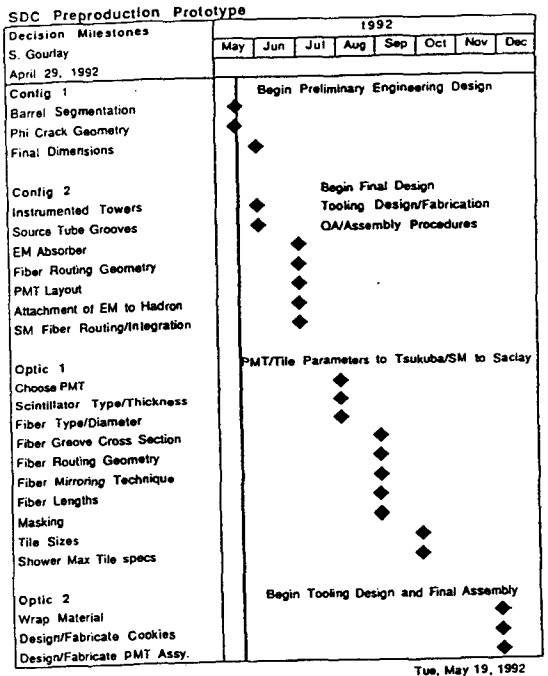

Next SMD group meeting to discuss proto '93 design June 18, FNAL

3

Shower Max Photon Readout

Priscilla B. Cushman
(Yale University)

WORK IN PROGRESS

* Monte Carlo Studies
  Ongoing work on π^0/γ separation
  (size of strips, depth of detector)
* Beam Test results ✓ π^0/γ, e/π, Energy Resolution
  (T841 at FNAL)
* Photodetector Testing ✓
  ⇒ Decision must be made by Jan '93 to be ready for '93 prototype
* Fiber routing, engineering, construction
  (Saclay)
* Tile-fiber testing in lab
  → what is best tile design
  → can we cheat - fiber leaving surface
  → fusing studies (1mm vs 750μ fibers)
  → # p.e.'s etc etc etc.
* Trigger + Front end electronics

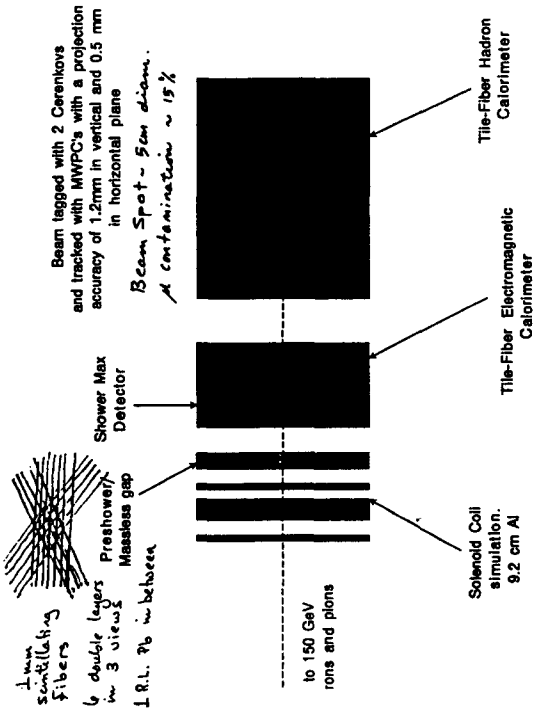

Schematic of the detector elements in the Fermilab Test beam T841.

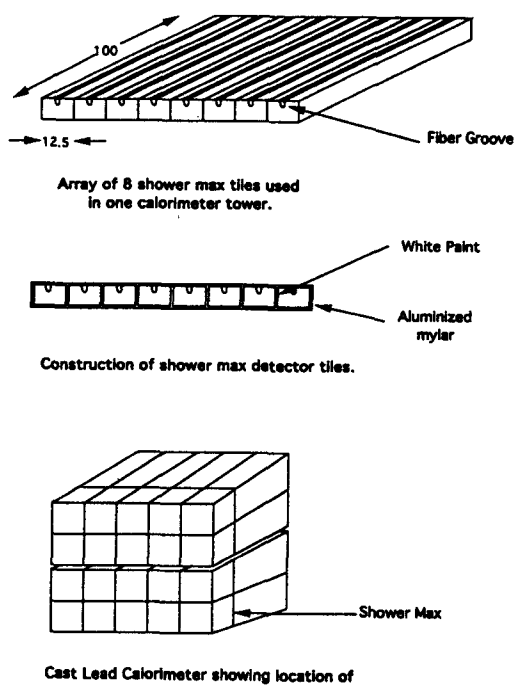

1490

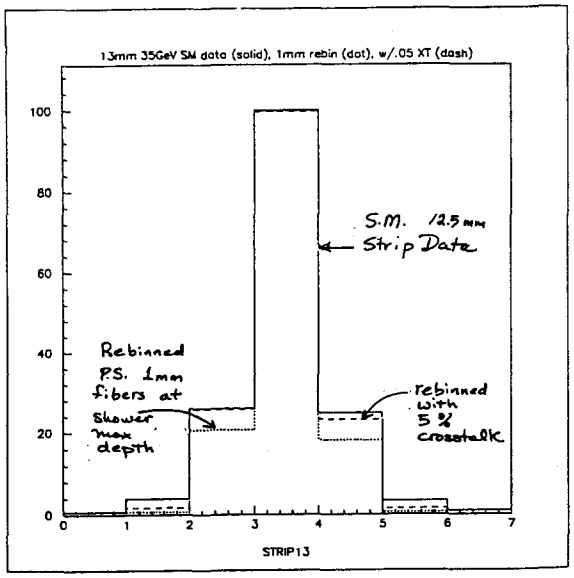

1491

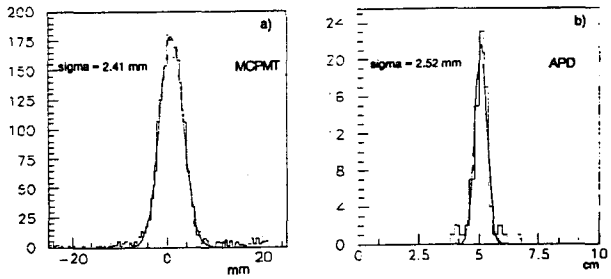

Shower Maximum Position Resolution at 35 GeV. Measured with MCPMT and APD readout.

Monte Carlo gives $\sigma = 2.4$ mm

1492

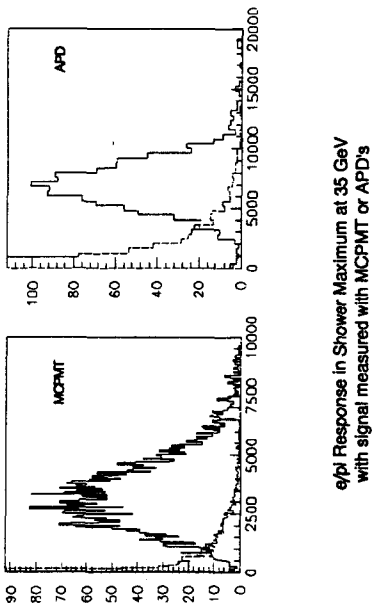

e/pi Response in Shower Maximum at 35 GeV with signal measured with MCPMT or APD's

π/e response at 35 GeV.

1493

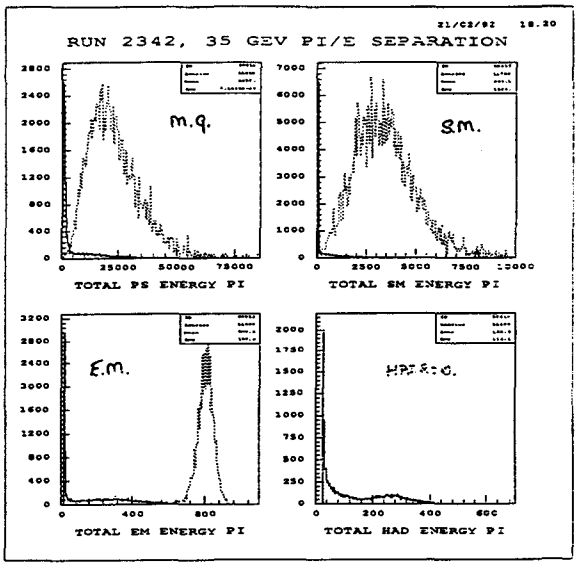

1194

35 GeV

Pions Remaining After Cuts on the Massless Gap, Shower-Max, the EM and Hadronic Calorimeter. Cuts applied Separately.

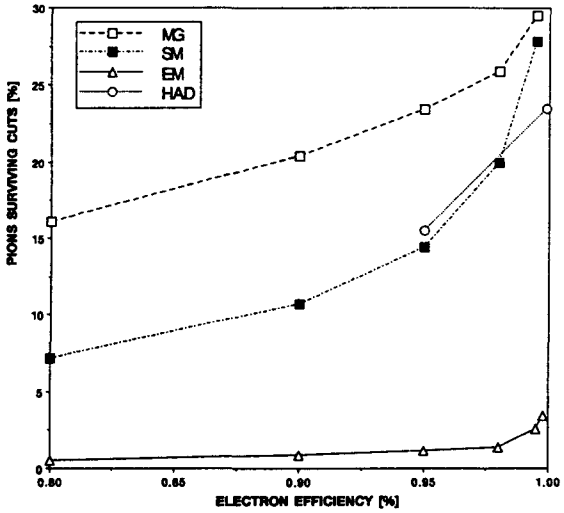

1195

Pions Remaining Versus Electron Efficiency Cutting on EM and Hadron Calorimeters, Adding Massless Gap or SM Cuts for 15, 35, and 50 GeV.

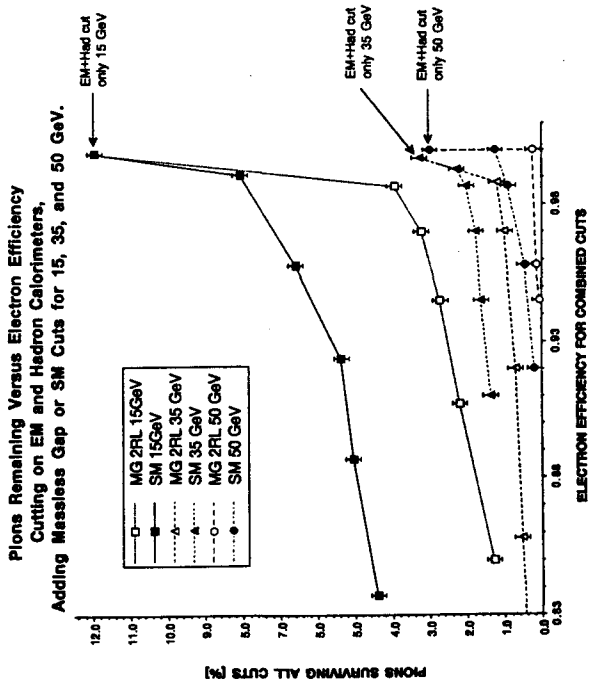

1196

Pions Remaining v Electron Efficiency after Cutting on EM and Hadron signals, Effect of Cuts on Massless Gap signal at 1 and 2 RL Depth for 15 and 35 GeV.

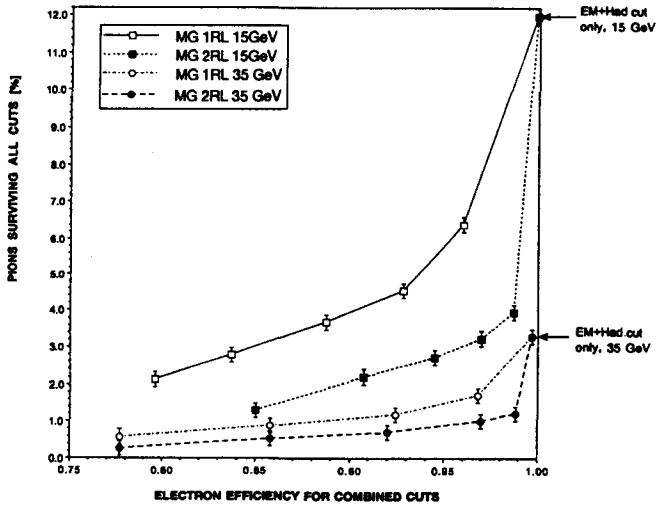

1197

EM Resolution Versus Beam Energy
Effect Of Material (1-2RL AL,Pb) In Front Of Calorimeter

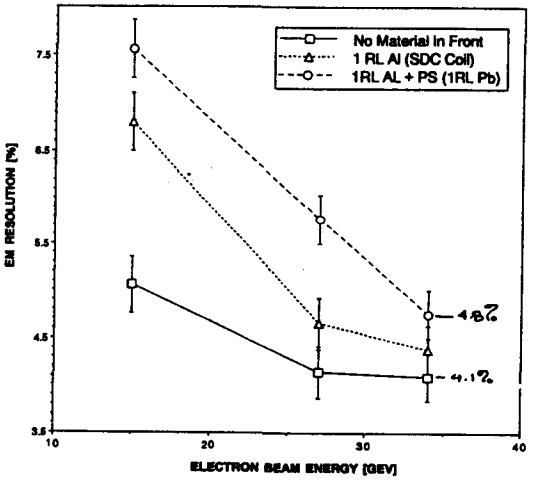

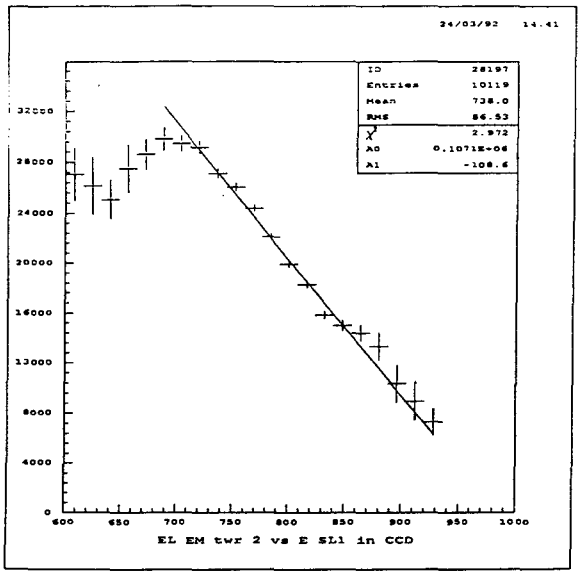

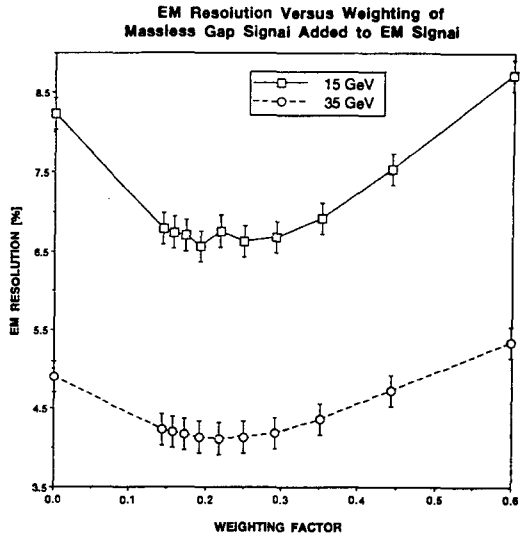

CONCLUSIONS

We have evaluated in a test beam at Fermilab the performance of our strip SM detector and the massless gap. This was done in conjunction with the prototype tile fiber EM and hadron calorimeters

We have measured the position resolution of the shower max detector to be 2.5mm.

We have shown that the shower shape does not change significantly between 5 and 7 radiation lengths.

The degradation to the EM resolution caused by the magnet coil is improved when the weighted signal from the massless gap is added to the EM signal.

We have measured the combined EM, Hadron, Masless Gap and Shower Maximum signals and shown how they provide a powerful method to separate electrons from charged pions.

Shower Maximum Photodetector Requirements.

* Dynamic Range ~ 4000
* High Quantum Efficiency in green
* Channel-to-channel gain uniformity
* < 1% crosstalk
* Cost effective [<$40 /channel ??]
* Fast timing characteristics

SHOWER MAX DYNAMIC RANGE

What can we get with 12 bits ?

Goal : EM shower position $\sigma \leq \Delta / 5$
10 GeV < E_T < 1 TeV

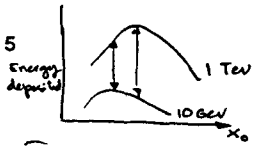

Dynamic Range :

Energy 10 GeV - 1 TeV	33	@ 6 X_0
High tail @ 1 TeV	x 1.5	
Low tail @ 10 GeV	x 2	
Center of gravity	x 10	
Pedestal separation	x 4	minimal !
MCPMT gain variation	x 1	adjusted
Dynamic range	4000 ⇒ 12 bits	

η dependance x 2 barrel
x 5 ends

⇒ Limit η range covered by one MCPMT
Adjust overall gain (MCPMT anode voltage)

PHOTODETECTORS

Shower Max and Massless Gap Detectors

Baseline

Philips 64-channel PMT
Used in Fermilab beam test
QE = 12% @ 520 nm; crosstalk 5-10%

Push on Existing Technologies

MCPMT Development

Philips 64- and 96-channel PMT's
Hamamatsu 256-channel PMT
Green-enhanced photocathodes QE = 16%

Avalanche Photodiodes

EG&G APD with ball lens in beam test
QE = 60% @ 520 nm; no crosstalk
Arrays @ EG&G, Hughes, Advanced Photonix

Develop new Technologies

APD-PMT

APD array in proximity-focussed image tube
Gain 5 x 10^5 and large dynamic range
64-channel prototypes for 1993 prototype
GaAs photocathode with QE = 34% @ 540 nm
Hughes Aircraft and Litton Electron Devices

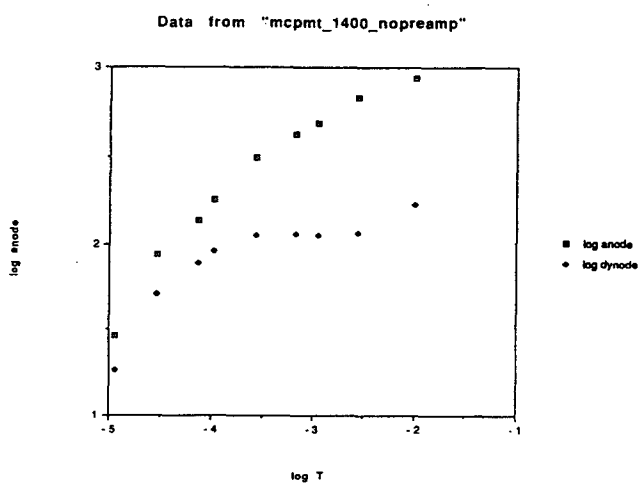

Tube at 1400 V. Saturation at 100 pC.

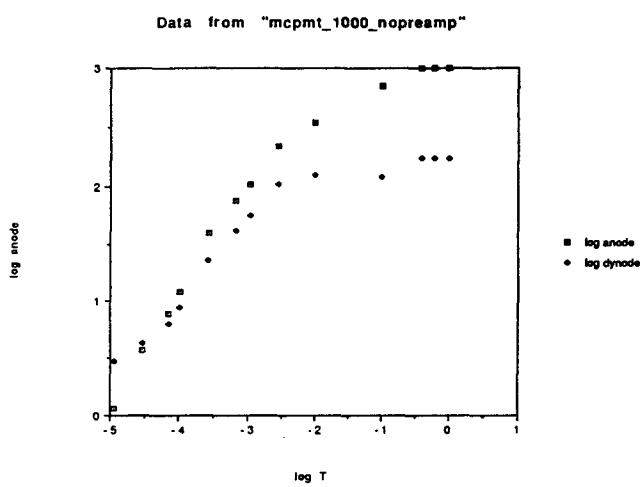

TUBE AT 1000 V. GAIN is 7×10^4
SATURATION AT 100 pC. in the dynode output.
SINGLE P.E. - 0.0112 PC. (NOT SEEN).
∴ from 10 pc. (0.1 pC) to 100 pC is x1000 dynamic range

1506

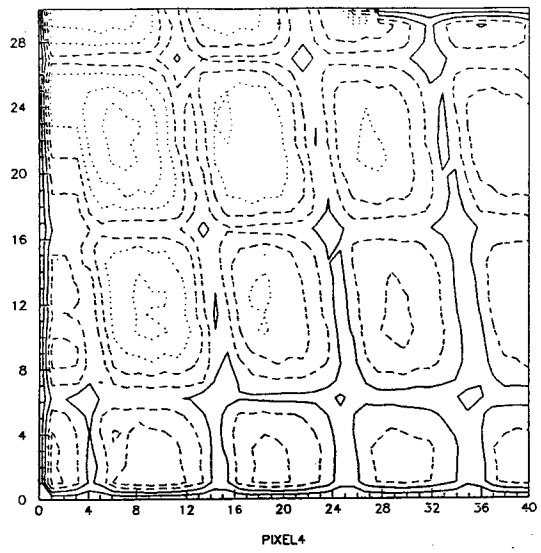

Map of Anode response using automated mapper : 500μ fiber moves by .01" steps (10/pixel pitch)

1507

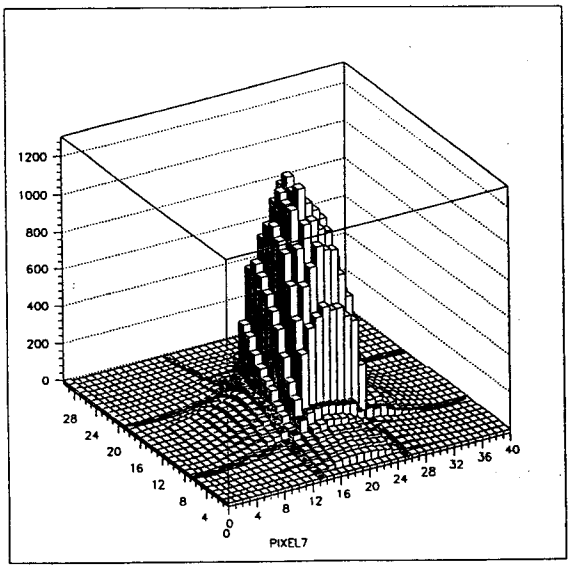

1508

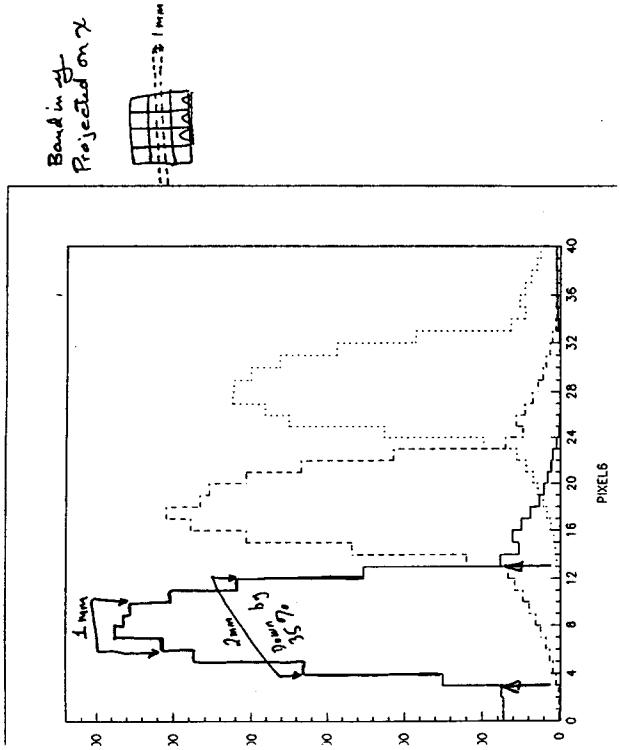

1509

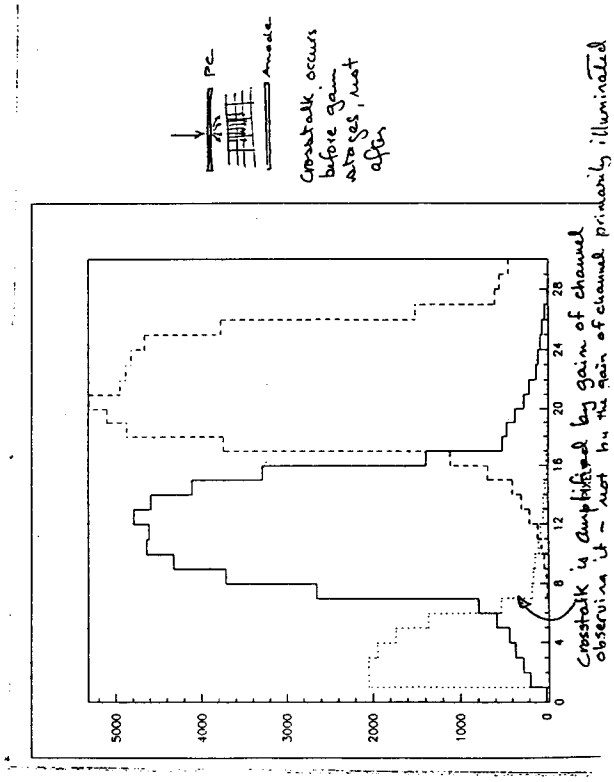

H20052 A01 b/w xlc

1510

cross talk profile

H4140 M01 Joyce, UCLA

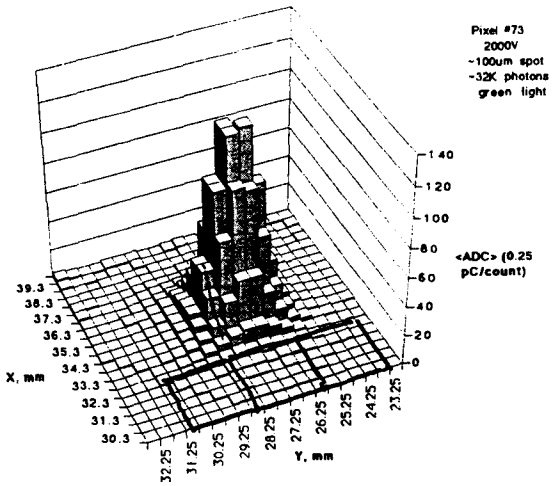

Page 1

1511

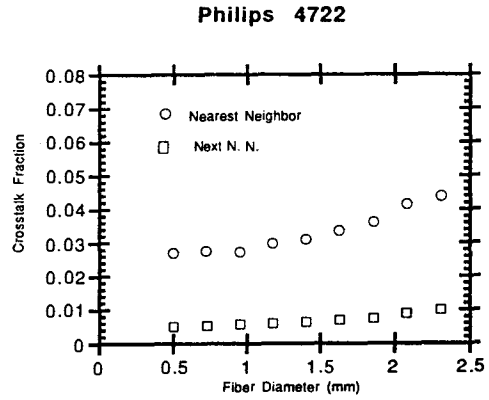

statistical uncertainty ~ ±.003

Systematic uncertainty ~ +.015 −.005
(centering errors)

⇒ Not exactly centered ⇒ much larger apparent crosstalk

1512

purple circles are bad electronic channels - since fixed

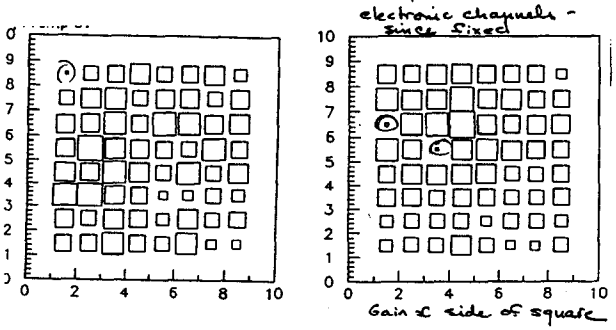

Gain Maps of 2 different XP4722's

Non-uniformity as large as 10:1
(But generally 3:1)

Must correct for in front end electronics

1513

Unformity accross PMT
UCLA

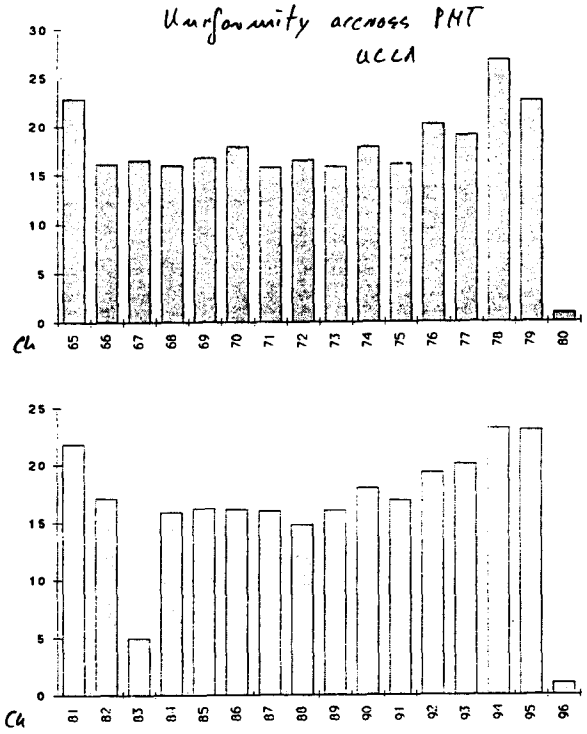

Uniformity accross PMT H4140 Mod

Hamamatsu

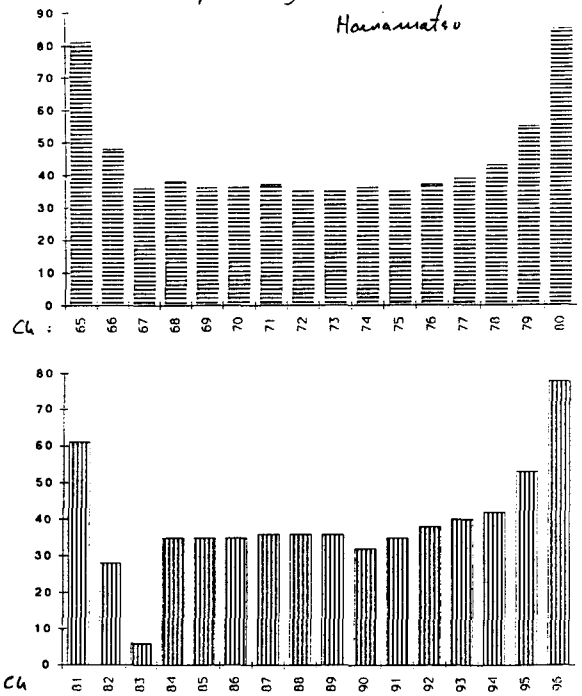

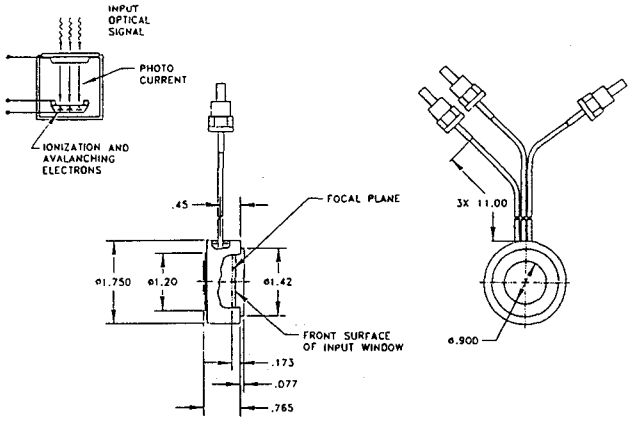

FIGURE 1
SCHEMATIC CROSS SECTION AND INTERFACE DIAGRAM FOR THE APDPMT

SK-11-7-91

PROPERTIES OF APD PMT

- APD in a tube [e-bombardment mode 8-12 kV]
  - (1) APD noise less of a problem due to ×2000 gain for photo electrons
  - (2) Low noise factor
  - (3) 50-1000 gain from APD (silicon p-n and pin junctions have unity gain) (less susceptible to amplifier noise)
- Large dynamic range
  - (1) Sensitive to single photoelectrons ($G \sim 5\times10^5$) Em. cal. Preshower, tracking
  - (2) Linear over 5-6 orders of magnitude (stable operation with 4 Amps output current observed.) Hadronic Calorimetry
- No base required - simple storage capacitor
  - (1) Draws current only when active
  - (2) No heat dissipation required as in powered divider chain
  - (3) Temperature dependence is easy to regulate (40% change in gain over 20°C)
- Proximity Focussed
  - (1) Insensitive to axial magnetic fields Operation inside Solenoid
  - (2) Good cross talk characteristics for multi-anode version
  - (3) Uniformity across surface to 5%
- Reasonable Cost
  - (1) \$500/tube and \$500/APD
  - (2) For 64 channel version ⇒ \$16/channel fiber readout
- Timing characteristics
  - (1) Excellent time jitter (~ 100ps) Time-of-flight applications
  - (2) rise Time ~ 10-20 ns better (2ns) for multi-channel versio

Gain as a function of photocathode voltage

(APD at 2000 volts)

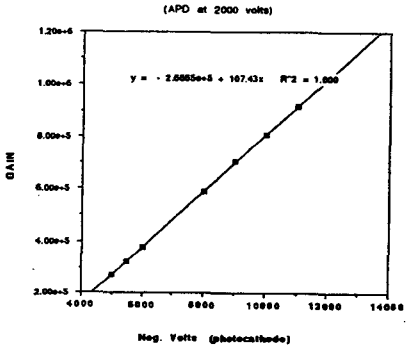

Tests at Litton

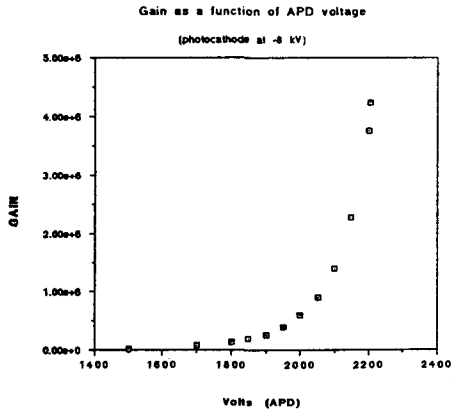

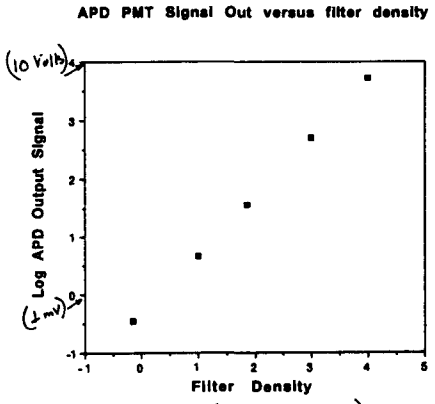

Log (Transmission)
Arbitrary scale

Solid State Laser (670 nm)

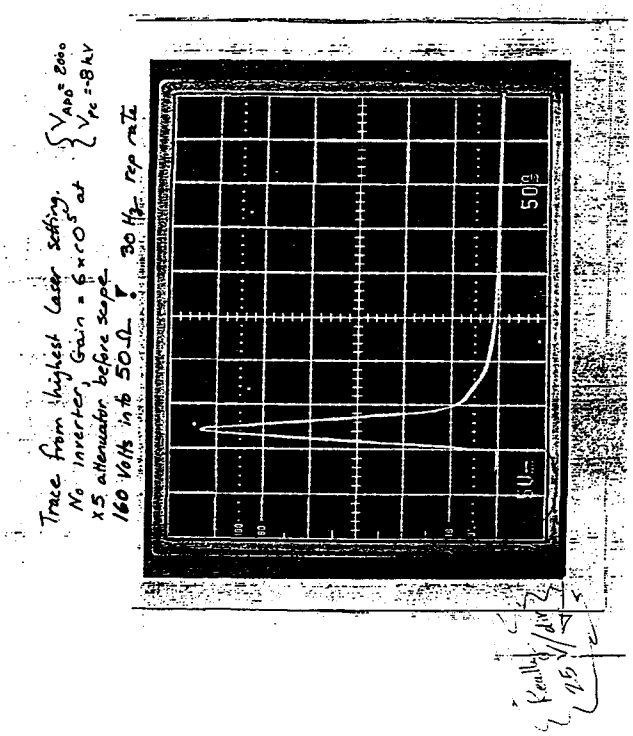

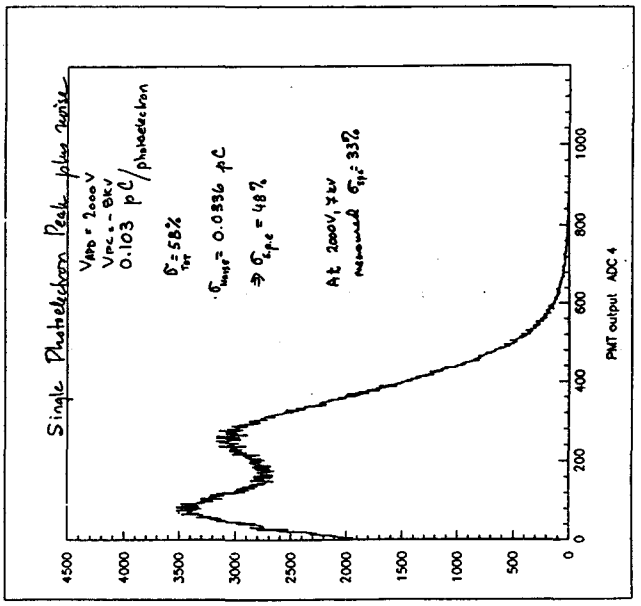

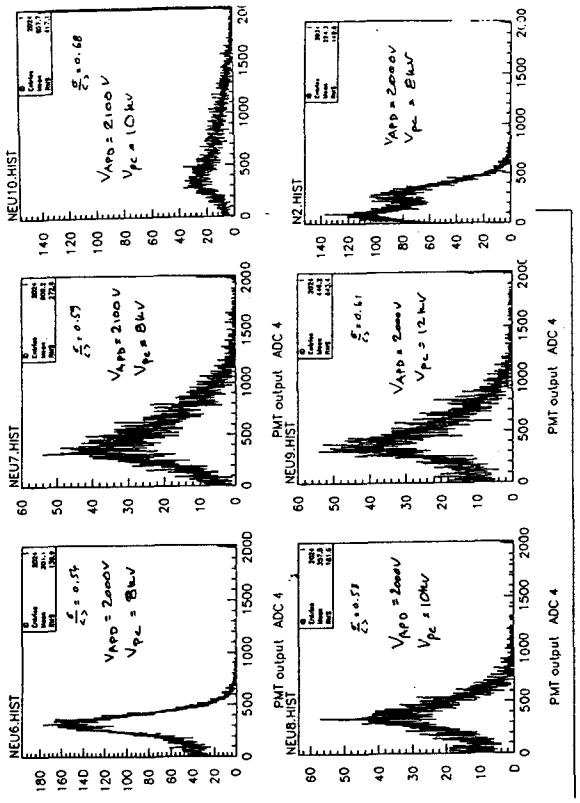

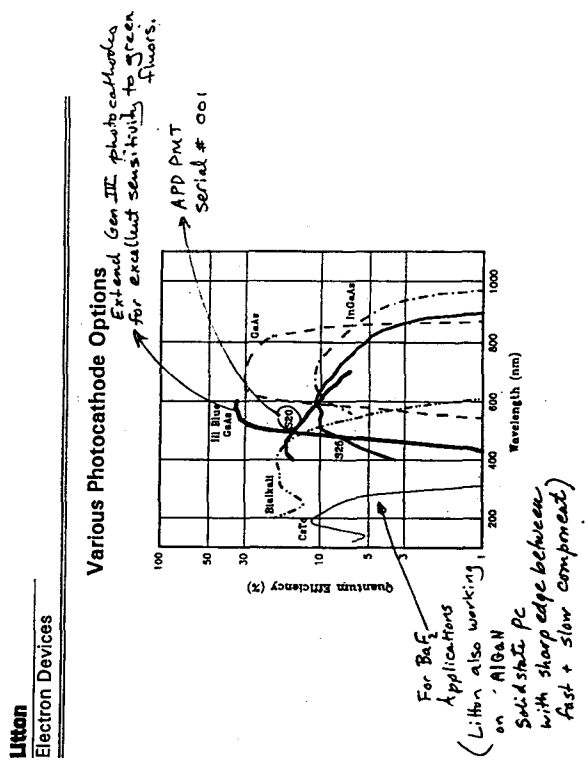

Hughes Aircraft

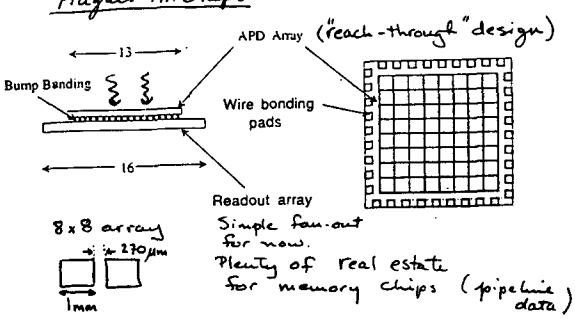

Advanced Photonics

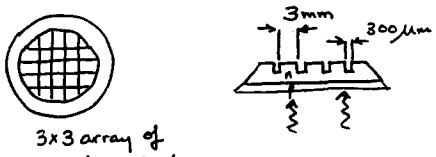

3x3 array of usable pixels
laser cut from large area "beveled edge" APD

Advantages of APD-PMT for Fiber Readout of Shower Max

* Large Dynamic Range (6-7 decades)
* Negative electron Affinity Photocathode (QE = 34% @ 540 nm)
* Virtually zero crosstalk
* Channel-to-Channel gain uniform to 5%
* Cost effective ($20/ch)
* Gain ≈ 5×10^5

MCPMT: 3-4 decades linearity
QE ~ 16%
1-5% X-talk
5:1 uniformity
$50-100 /channel
Gain – 10^6

APD: decades linearity
QE ~ 60%
< 1% crosstalk
95% uniformity
Gain ~ 200
Liquid Nitrogen Temp.

Rethink bare APD arrays at LN_2 temperature for tracking

Study of Total Reflection between Liquid Scintillator and Glass Resin for SDC Forward Calorimeter

Tue. 26th - Fri. 29th May 1992 , SDC collaboration meeting at KEK

Taro Masumaru Masami Chiba
Tokyo Metropolitan University
Norio Tamura
Okayama University
Akira Maki
National Laboratory for High Energy Physics (KEK)
Hideyuki Kawai
Chiba University

Abstract

1. position of F-CAL.

2. requirments of F-CAL. and
   spaghetti type cal. using liq. scinti.

3. surface state of material and total reflection.

4. total reflection test result.
   (SUS plate and SUS tube)

1. position of F-CAL

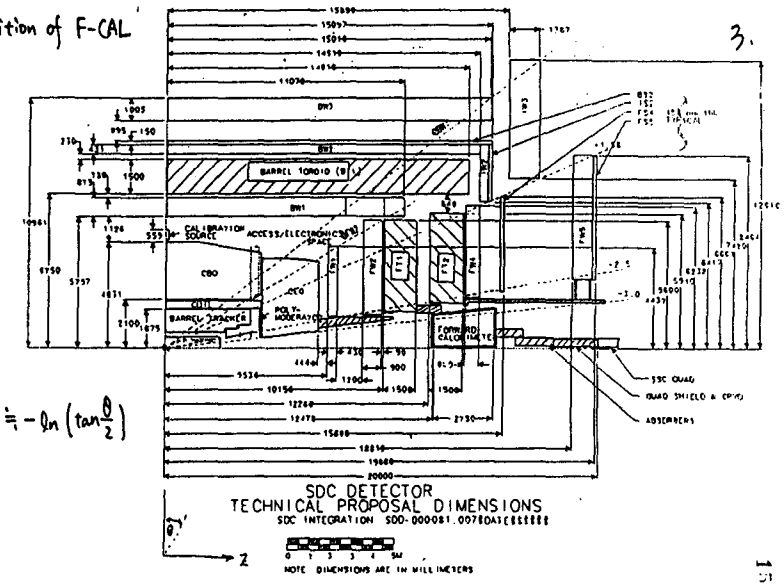

$\eta \fallingdotseq -\ln\left(\tan\frac{\theta}{2}\right)$

2. requirements of F-CAL

Requirements for the forward calorimeter in SDC

1. High radiation resistance.
   (Radiation dose is about 10 Mrad / year)

2. Fine granularity.

3. Fast time responce.

4. total reflection test result.

7.

1. Test of the total reflection by SUS plate coated with Glass Resin under ^{60}Co γ -ray radiation.
   ↳ By Irradiator "Gammacell 220" at RI facility in Tokyo Metropolitan Univ.
2. Test of the total reflection by SUS tube coated with Glass Resin.

2. spaghetti type cal. using liq. scinti.

5

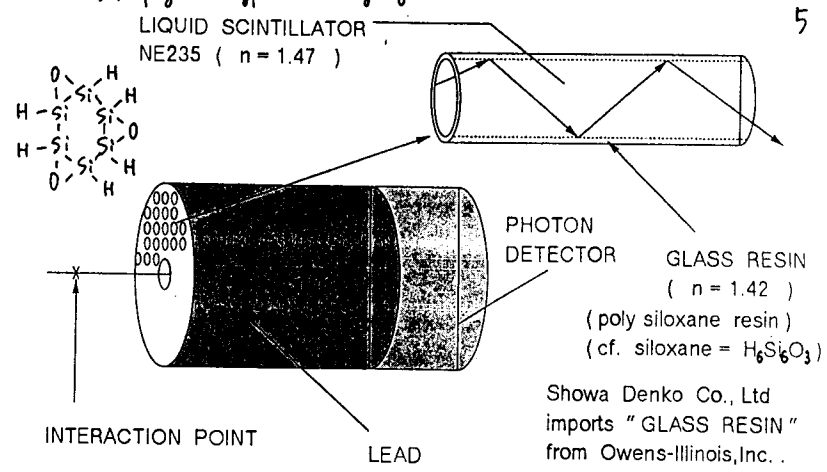

Showa Denko Co., Ltd imports "GLASS RESIN" from Owens-Illinois, Inc..

FIG. 1

Owens-Illinois, Inc. is in One SeaGate Teledo, OH 43666 U.S.A.

3. surface state of material and total reflection.

6.

MATERIAL	Surface of plate	TOTAL REFLECTION
LEAD plate	not smooth (non-polishing)	×
Aluminum plate	not smooth (little polishing)	×
SUS plate standard : 304	not smooth (non-polishing)	△
SUS plate standard : 304	smooth (polishing near mirror)	○
SUS tube standard 304	not smooth (little polishing)	△

8.

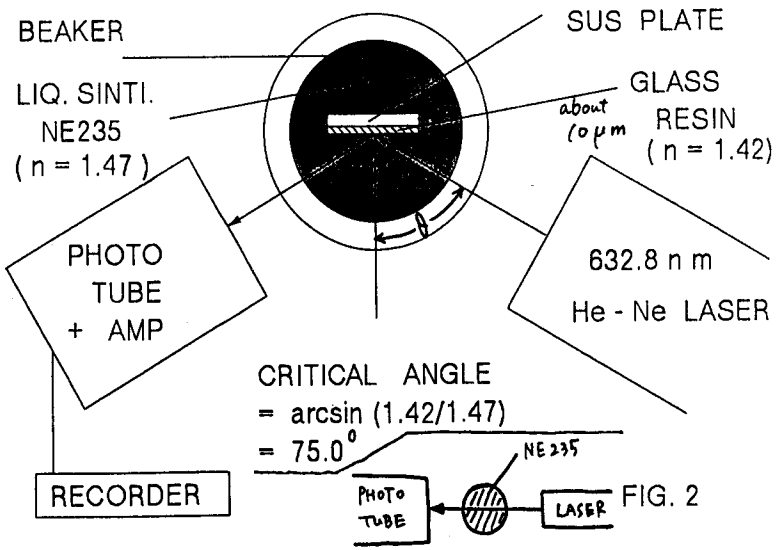

FIG. 2

11.

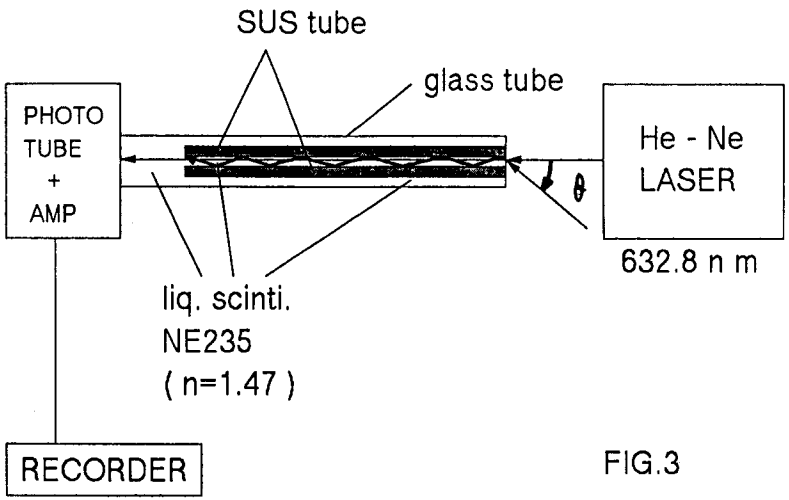

FIG.3

1536

9.

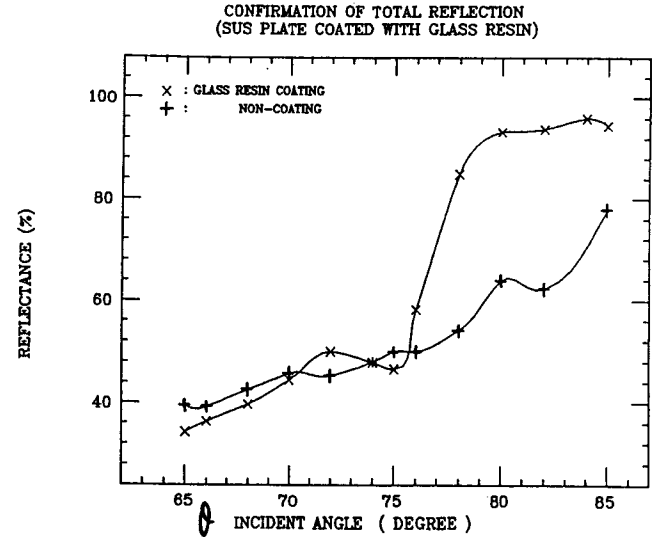

reflect.top

critical angle $= \sin^{-1}\left(\frac{1.42}{1.49}\right) = 75.0^{\circ}$

1531

12.

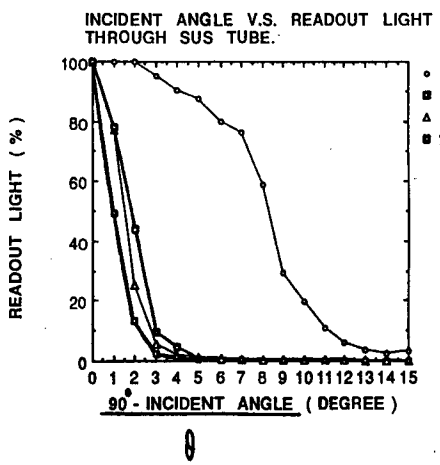

{ core poly-styrene $n = 1.59$
{ clad acrylic $n = 1.49$

NE 235
{ liquid scintillator $n = 1.47$
{ GLASS RESIN $n = 1.42$

$\theta_c = \sin^{-1}\left(\frac{1.49}{1.59}\right) \sim 70^{\circ}$

$\theta_c = \sin^{-1}\left(\frac{1.42}{1.49}\right) \sim 75^{\circ}$

1537

10.

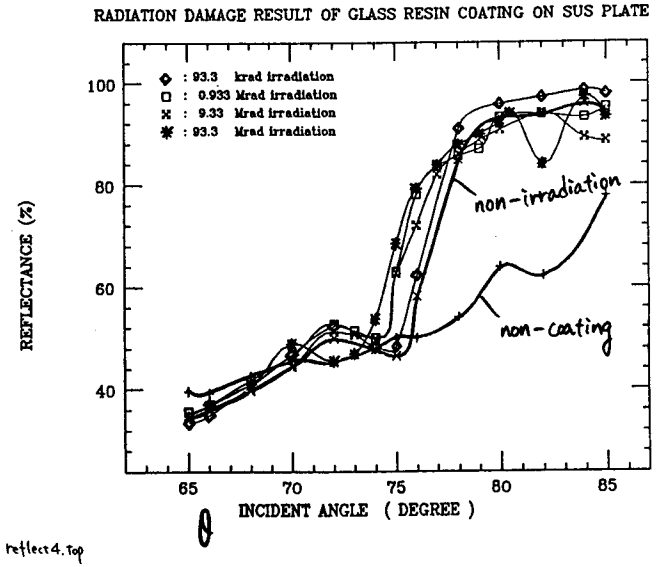

reflect4.top

1538

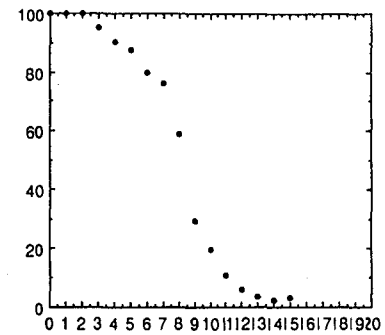

summary.

1 We found the total reflection by SUS plate coated with Glass Resin.

2 Glass Resin has very good radiation resistance up to 100 Mrad.

3 We did not find the total reflection by SUS tube coated with Glass Resin this time. This may be due to the tube surface. We are studying this point.

N. GIOKARIS
ROCKEFELLER UNIV.
MAY 26, 1992

RECENT RESULTS IN HIGH-PRESSURE GAS CALORIMETRY

L. Demortier, N.D. Giokaris, K. Goulianos, D.M. Khazins**
Experimental Physics Department
The Rockefeller University
New York, NY 10021

D. F. Anderson, S. Cihangir, A. Para, J. Zimmerman
Fermi National Accelerator Laboratory
Batavia, IL / 60510

I. Budagov***, G.A. Ivanov, A.I. Kalinin, A. A. Kurichin, N.O. Prokofiev & Yakov.
Joint Institute for Nuclear Research (Dubna)
P.O. Box 79, 101 000 Moscow

G. Fanourakis, F. Lobkowicz
Department of Physics and Astronomy
University of Rochester
Rochester, NY 14627

D. Carlsmith
Physics Department
University of Wisconsin
Madison, WI 53706

H.R. Gustafson
University of Michigan
Ann Arbor, MI 48109-1120

M. Morgan
Ability Engineering Technology, Inc.
South Holland, IL 60473

* Research supported in part by the Texas National Research Laboratory Commission under grant No. RGFY9160.
** Also JINR, Dubna.
*** Also INFN, Pisa, I-56010 Pisa.

TALK OUTLINE

I. RESULTS FROM TESTS WITH A HIGH PRESSURE TEST VESSEL

II. RESULTS FROM A BEAM TEST OF A PARALLEL PLATE PROTOTYPE EM CALORIMETER

III. RESULTS FROM RADIATION DAMAGE STUDIES ON HIGH PRESSURE GASSES

IV. DESIGN OF A HIGH PRESSURE GAS IONIZATION TUBE CALORIMETER FOR FCAL

V. 1992 R&D

VI. CONCLUSIONS

II, III AND IV : AVAILABLE AS PAPERS TO BECOME SDC NOTES
I & OTHERS : AVAILABLE AS SUPPORTING DOCUMENTATION

HIGH PRESSURE GAS CALORIMETRY

DEFINITION

USE AS SAMPLING MEDIUM HIGH PRESSURE GAS (~ 100 ATM)
DENSITY OF 100 ATM ARGON = 0.178 gr/cm^3 = 1/8 DENSITY OF LIQUID ARGON

MOTIVATION

UNITY GAIN

VERY RADIATION HARD

VERY FAST

GOOD ENERGY RESOLUTION

VERY EASY TO RECYCLE GAS (IF YOU EVER NEED)

NO TEXAS TOWERS PROBLEM (ENERGY SAMPLING FRACTION IS ~ 1%)

NO GLOW MODE PROBLEM (NO CHARGE AMPLIFICATION ON THE ANODE)

NO SPACE CHARGE PROBLEM

NO CRYOSTAT

NO IMPURITIES PROBLEM (ppb AT TMP)

NO GAS CHEMISTRY

AND VERY COST EFFECTIVE

II. PROTOTYPE PARALLEL PLATE ELECTROMAGNETIC HIGH PRESSURE GAS CALORIMETER
[1991 ÷ SUPPORT BY TNRLC] {FERMILAB T848}
10 HIGH PRESSURE VESSELS

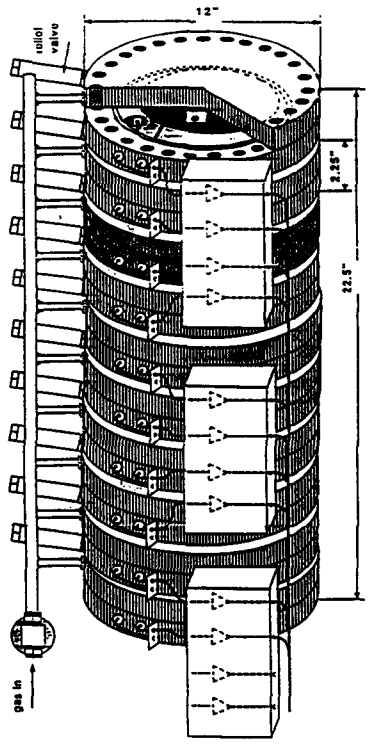

1514

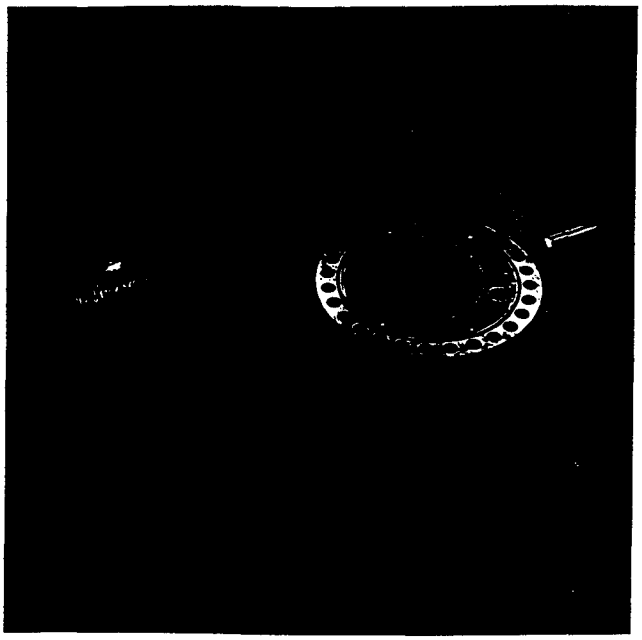

91-1632-1

1515

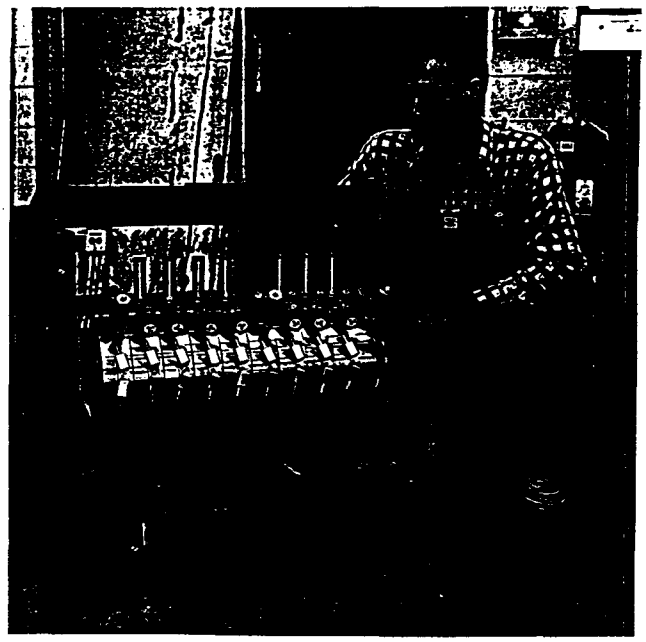

632-12

1516

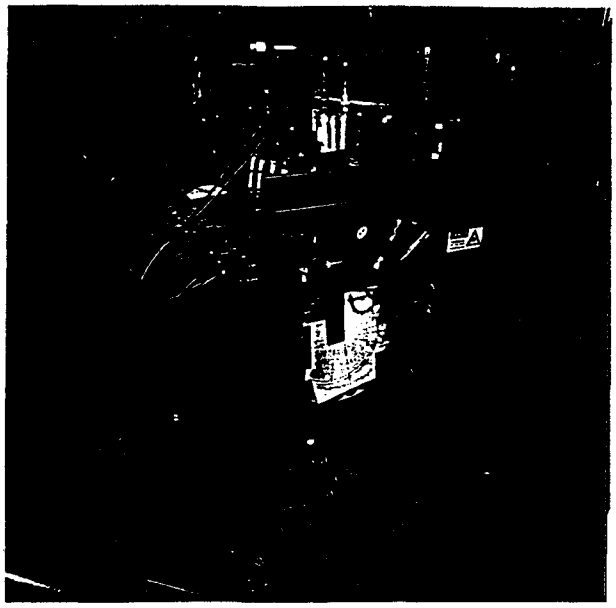

92-90-12

1517

RESULTS FROM THE BEAM TEST OF THE PARALLEL PLATE PROTOTYPE EM CALORIMETER

1518

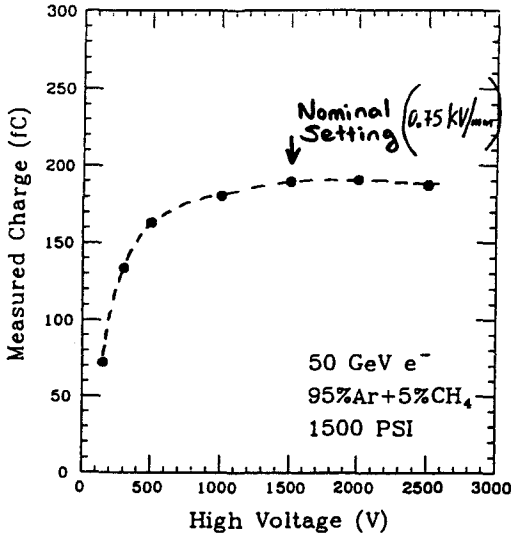

1519

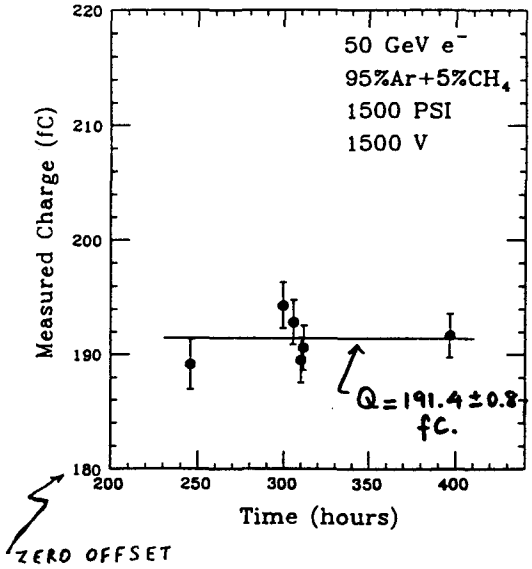

1550

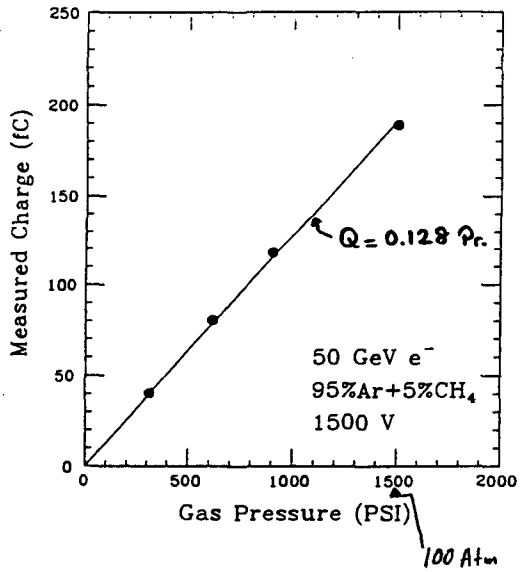

1551

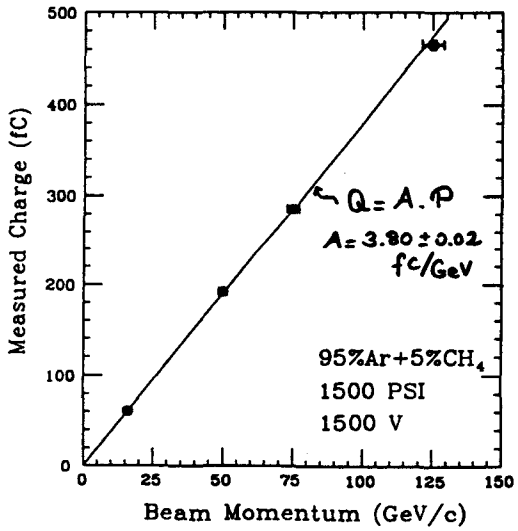

1552

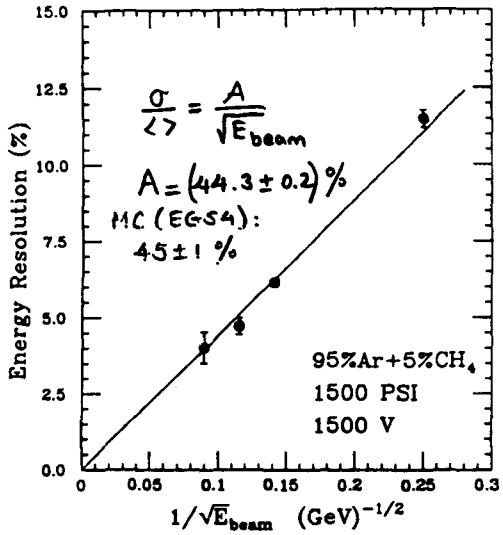

1553

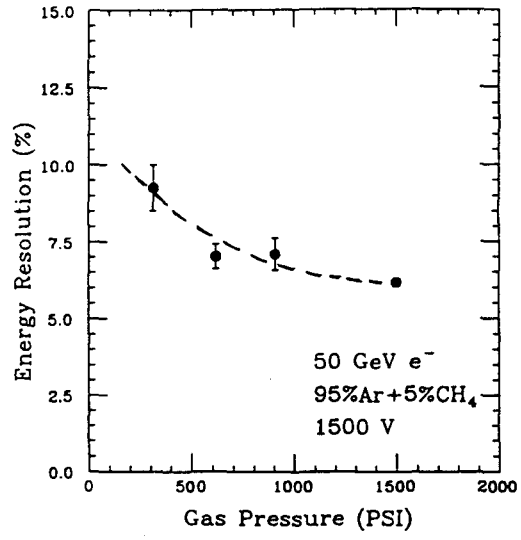

1554

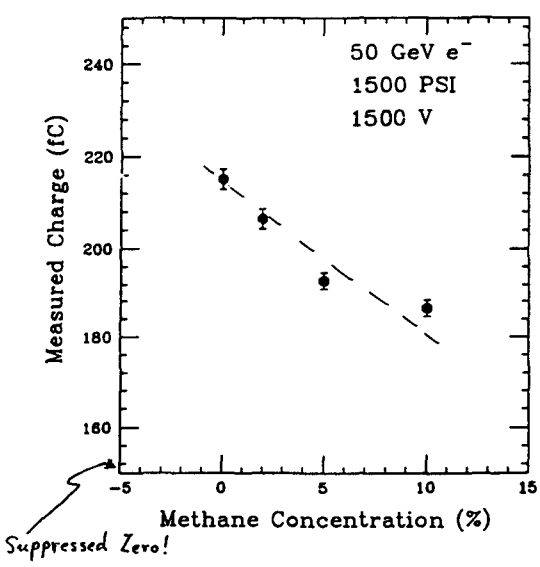

1555

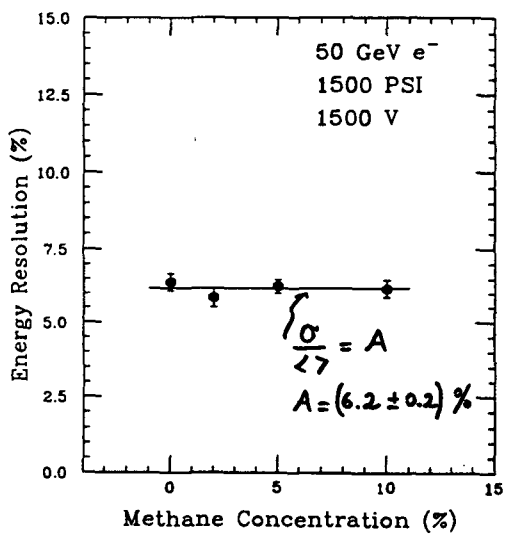

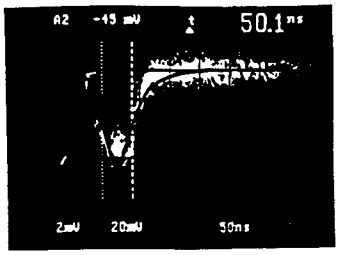

95% Ar + 5% CH4 at 100 Atm

E = 1.25 kV/mm

Am241 alpha source

Shuvalov preamplifier

(a)

2mm gas gap

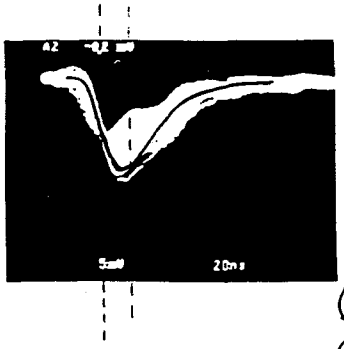

95% Ar + 5% CH4 at 100 Atm

E = 0.75 kV/mm

50 GeV electrons

Valkov preamplifier

(b)

~50 nsec base width
(~35 nsec for scintillator present)

CONCLUSIONS

PARALLEL PLATE PROTOTYPE EM TEST

(GAS MIXTURE: 95% Ar + 5% CH_4)

1. SIGNAL SATURATES FOR AN ELECTRIC FIELD E = 0.75kV/mm
2. SIGNAL VERSUS PRESSURE IS LINEAR IN THE TESTED RANGE 20—100 atm
3. SIGNAL VERSUS ENERGY IS LINEAR IN THE TESTED RANGE 20—125 GeV
4. ENERGY RESOLUTION AGREES WITH EGS4 MONTE CARLO PREDICTION
5. MEASURED ELECTRON DRIFT VELOCITY = 20 nsec/mm
6. FAST PREAMPLIFIER OUTPUT SIGNAL: RISE TIME IS LESS THAN 10 ns, BASE WIDTH IS ABOUT 50 ns
7. CHARGE COLLECTED IS 3.8 ± 0.4 fC/GeV, OR 85% OF THE EXPECTED CHARGE IF $e/\mu = 0.92$

PROTOTYPE EM PROVED TO BE VERY EASY TO OPERATE.

EM CALORIMETRY AT 100 atm WORKS!

III. RADIATION DAMAGE TESTS

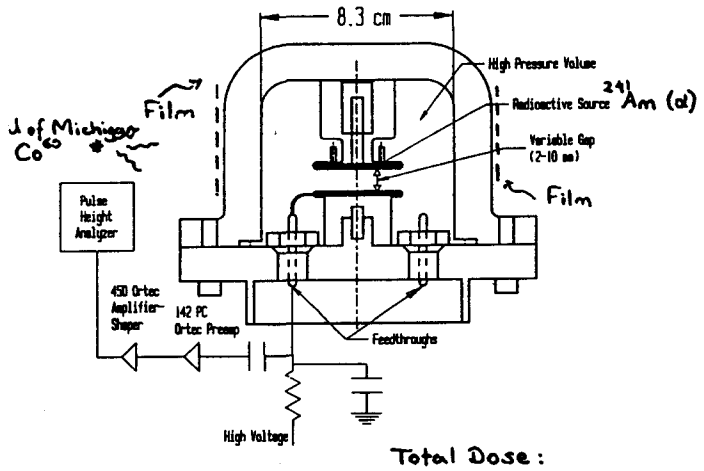

Total Dose:
~16 Mrad (Ion Chamber)
~50 Mrad (Film)

1560

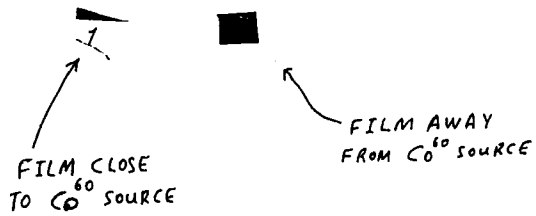

1561

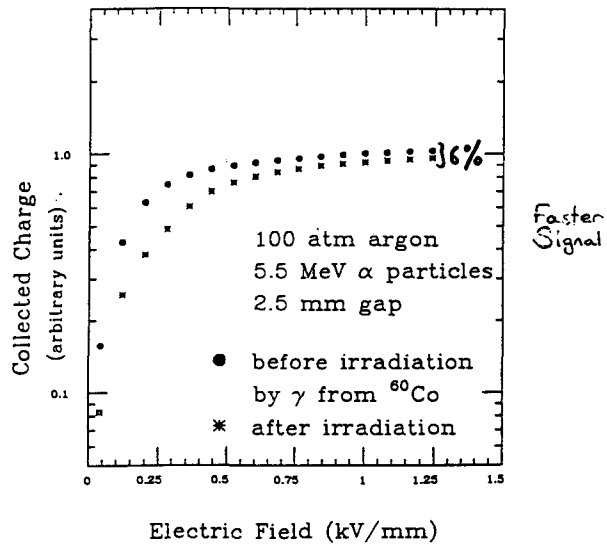

1562

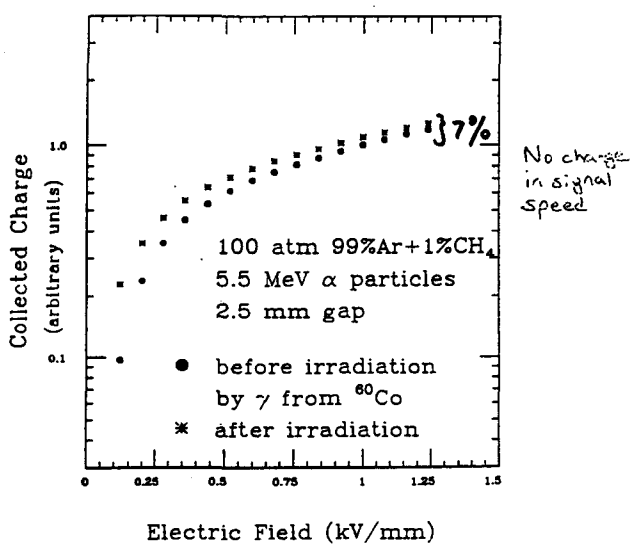

1563

Conclusions From Radiation Damage Tests:

- **Pure Argon (Ar) gas and 99% Ar + 1% CH_4 gas mixture at 100 Atm were exposed to 16 Mrad (maybe as high as 50 Mrad) of ^{60}Co gammas,**
- **No significant pulse height (from alpha source) reduction observed,**
- **No need to renew the gas for at least one year of SSC operation at nominal luminosity.**

Next Radiation Damage Tests:

Expose 95% Ar + 5% CH_4 and 90% Ar + 10% CH_4 to ≈ 1000Mrad of ^{60}Co gammas and neutrons with anode [redacted] connected to high voltage.

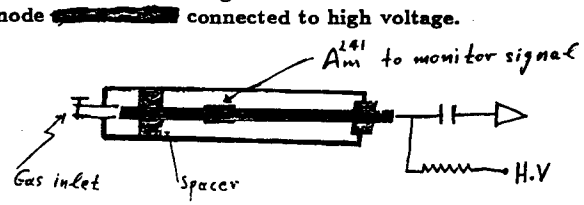

TUBE & ROD WITH Am^{241} SOURCE ARE UNDER CONSTRUCTION

1564

1565

IV. HIGH PRESSURE GAS TUBE CALORIMETER

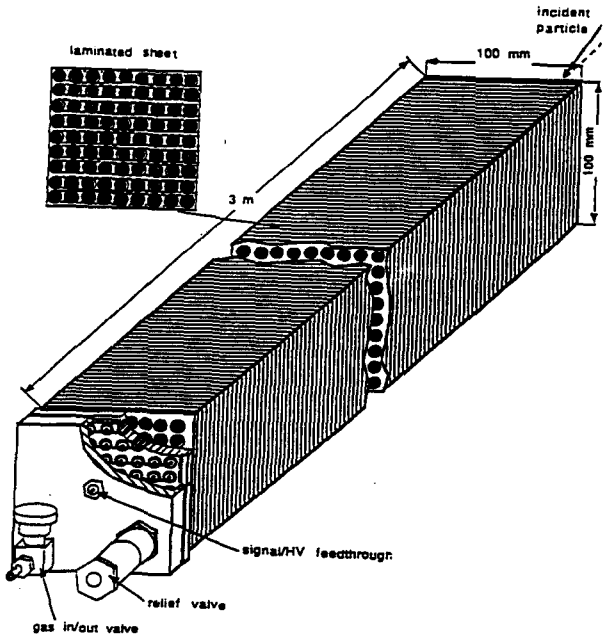

1566

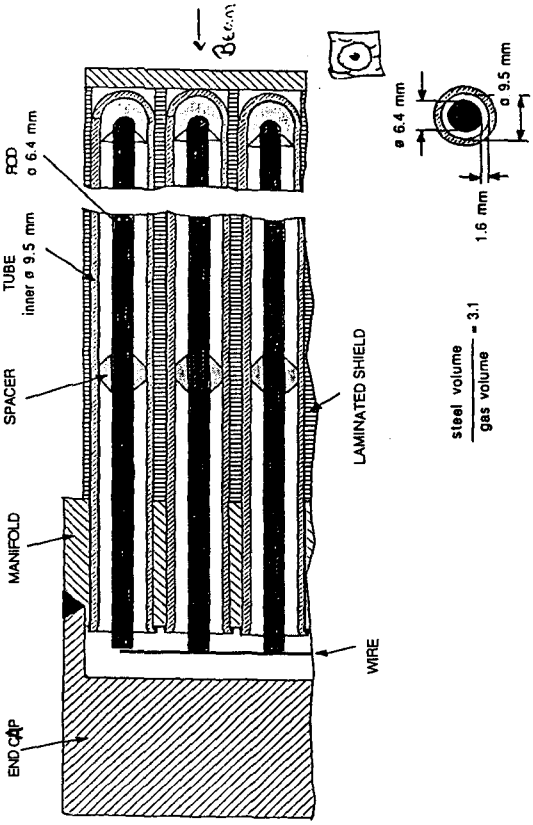

1567

- END PLATE WELDING TESTED HYDRAULICALLY
- WELDING FAILED AT 9,600 PSI
- OPERATING PRESSURE ~ 1,500 PSI

- A 2.1 x 2.1 x 3.6 m^3 PROTOTYPE MODULE HAS BEEN CONSTRUCTED

Ability Engineering Technology,

Area Code 312 331-0025
331-0036

16140 Vincennes Avenue, South Holland, Illinois 60473
(Rt. 6 & Vincennes)

October 21, 1991

Dr. Nikos Giokaris M/S 223
Fermilab
P. O. Box 500
Batavia, IL 60510

REF: Quote #1472
Hadronic Detector Cell
Rockefeller University

Large quantity budgetary cost estimate of Hadronic Detector Cell - full production:

STAINLESS STEEL TUBE SHEET AND TUBES

Tube Sheet	$ 629
Caps (End plates)	144
Wires (Rods)	310
Insulators (spacers)	126
Punch Set	25
Laminations	634
Relief Valve	28
Valve	40
Stack Lam.	90
Install Lam. Packs	140
Welding	416
Assy	342
Press Test	105
Weld Closed	90
Final Tests	125
Charging	240
	$3484

Price includes labor and material, but does not include final stacking and installation at site, or transportation costs to the site.

Very truly yours,
Ability Engineering Technology

Michael W. Morgan
President

MWM:jb

Price per module
Module = 0.1x0.1x 3 m³
↳ 64 tubes

SDC DETECTOR

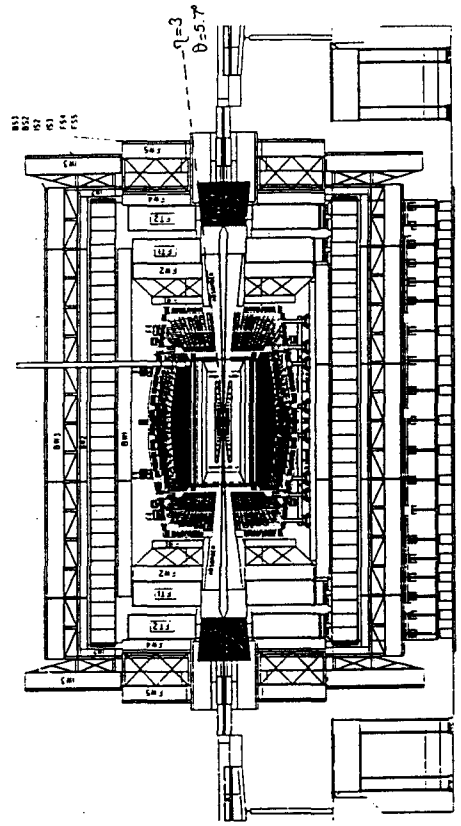

~800 modules per side
1600 modules total
$3,500/module
Total price: $5.6 M

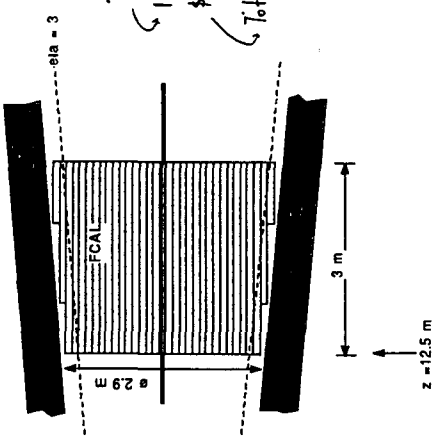

GEANT MONTE CARLO

$$\frac{\sigma}{E} = \frac{A}{\sqrt{E}} \oplus B$$

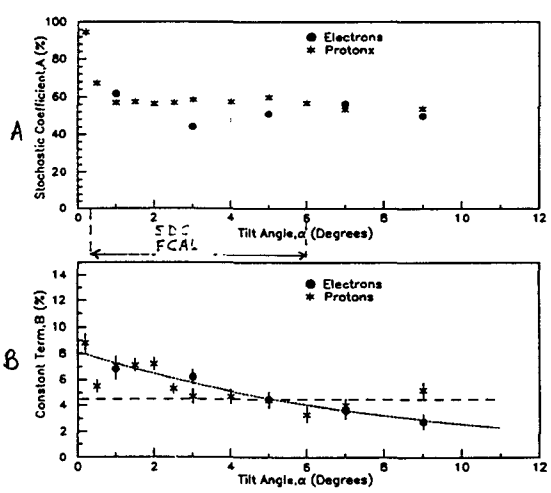

With 6 Radiation lengths of Preshower

NOT INSTRUMENTED!
JUST DUMMY PLATE

GEANT MUONS

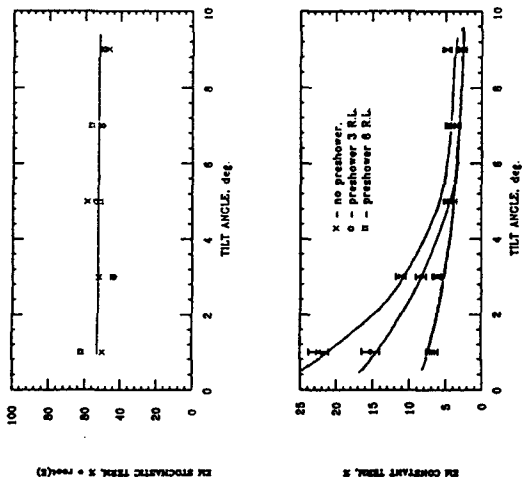

→ ANOTHER APPROACH UNDER CONSIDERATION:
MAKE EACH TUBE ITS OWN PRESSURE VESSEL
→ ACTUALLY ADOPTED (MAY 15, '92) BECAUSE OF ELECTRONICS CONSIDERATIONS.

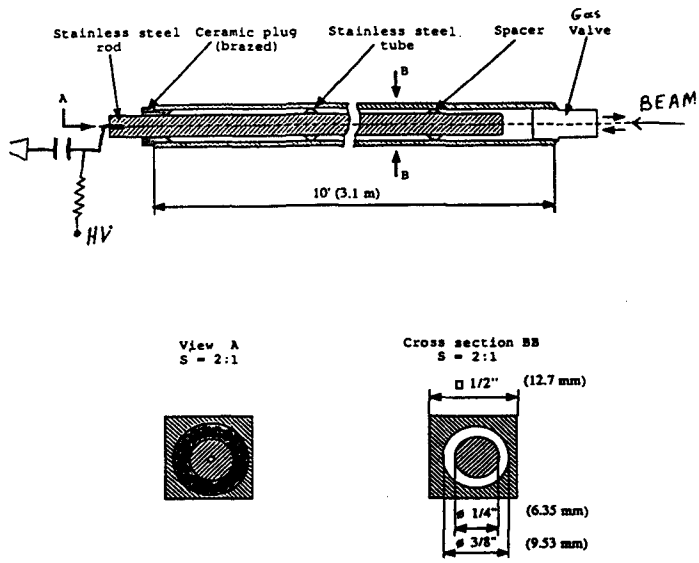

WELD TOGETHER 64 TUBES
TO MAKE ONE $0.1 \times 0.1 \times 3\ m^3$ MODULE

PRICE/MODULE $\approx \$3,500$ (see next page)

Ability Engineering Technology, Inc.

Area Code 708-331-0925
FAX 708-331-3000
16140 Vincennes Avenue, South Holland, Illinois 60473
(Rt. 6 & Vincennes)

May 4, 1992

Dr. Nikos Giokaris M/S 223 ✓ 4390
Fermilab
P. O. Box 500
Batavia, IL 60510

REF: Quote 81645
Hadronic Detector Cell
Rockefeller University

Large quantity budgetary cost estimate of Hadronic Detector Cell - full production: 64 tubes per cell, individual detector tubes.

STAINLESS STEEL TUBES

Tube	$ 9.82
Cap (for gas inlet)	2.25
Electrodes (rod)	4.85
Insulators (spacers)	1.96
Extrude (cylindrical-square)	9.90
Isolation & Relief	3.41
Cell Assembly (labor)	2.18
Welding-Brazing H.V side	6.50
Tube Assy	5.35
Press Test	1.65
Weld Closed	1.41
Final Tests	1.95
Charging	3.75
	$ 54.98
	x 64
	$3518.72

Price includes labor and material, but does not include final stacking and installation at site, or transportation costs to the site.

Very truly yours,
Ability Engineering Technology

Michael W. Morgan
President

MWM:jb

COMPARISON OF TILE-FIBER vs HIGH-PRESSURE GAS HADRONIC CALORIMETER

	TILE-FIBER*	HIGH-PRESSURE GAS
ENERGY RESOLUTION (single $\pi^\pm$)		
stochastic term	70%	60%
constant term	6%	5%
Noise term (0.2x0.2 tower)	~20 MeV (?)	~1 GeV
SIGNAL SPEED (pulse base width)	~40 nsec	~40 nsec
MINIMUM IONIZING DETECTION	YES	NO
RADIATION HARD	? (END CAP)	YES
CALIBRATION & MONITORING	HARD	EASY
COST ($/m³)	?	~140k**

* SDC TDR
** MUCH SMALLER FOR LARGE VOLUMES

V. 1992 R&D EFFORT

- DESIGN AND BUILD NECESSARY ELECTRONICS (PROTOTYPE UNDER CONSTRUCTION AT UNIV. OF ROCHESTER)
- BUILD AND BEAM-TEST HADRONIC TUBE PROTOTYPE $\equiv 0.4 \times 1.4 \times 3\,m^3$ (i.e. 11 MODULES)
- DEVELOP DETAILED SDC FCAL ENGINEERING DESIGN

NEED ~1,000 TUBES FOR PROTOTYPE

VI. CONCLUSIONS

- HAVE SHOWN THAT HIGH PRESSURE GAS CALORIMETRY WORKS
- A HADRONIC HP TUBE CALORIMETER WILL BE:

  RAD - HARD
  FAST (~35 nsec)
  SAFE
  VERY COST EFFECTIVE (~$140k/m³)
  +
  EXCELLENT HADRONIC ENERGY RESOLUTION!

L* and GEM Calorimeter Transmutation Studies and Applicability to SDC

W. B. Wilson,
T. R. England
D. M. Lee
A. P. Palounek
R. E. Prael
L. S. Waters
H.-J. Ziock
A. Gauron
G. Sanders

Los Alamos National Laboratory
Los Alamos, New Mexico USA 87545

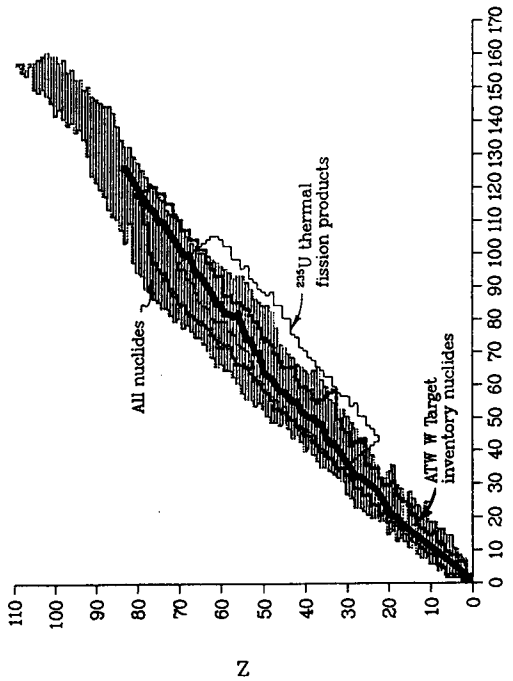

ATW nuclides and ^{235}U fission products

L*

Hadron Calorimeter Activation

Simulation by Dave Lee & W. Kinnison

LA-UR 90-2954 Lee+

LA-UR 90-3449 Lee+

Activation by Bill Wilson & Tal England

LA-UR 91-999 Wilson+

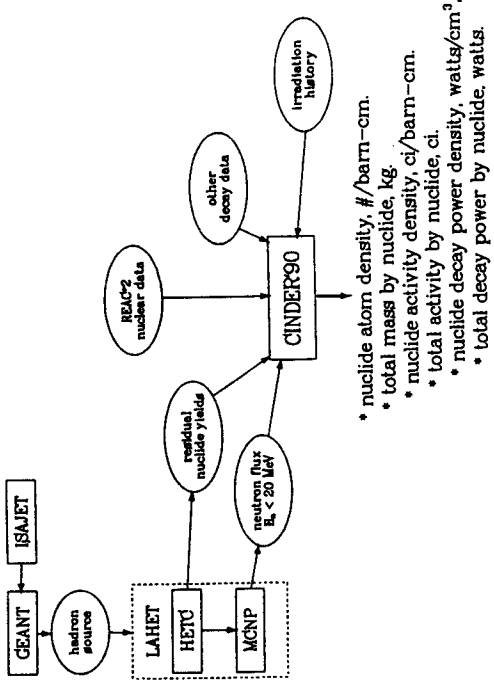

Fig. 1. Flow of L* hadron calorimeter activation calculations.

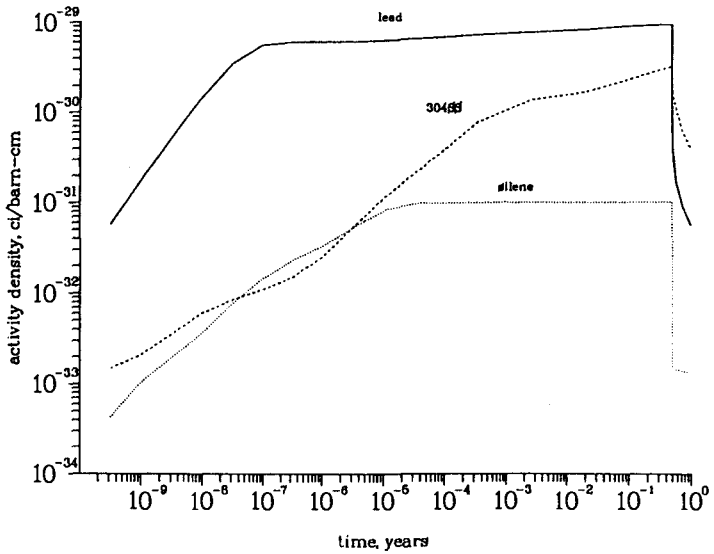

Fig. 6. Calculated activity density in L* hadron calorimeter materials during a 0.5-year irradiation and 0.5-year down period.

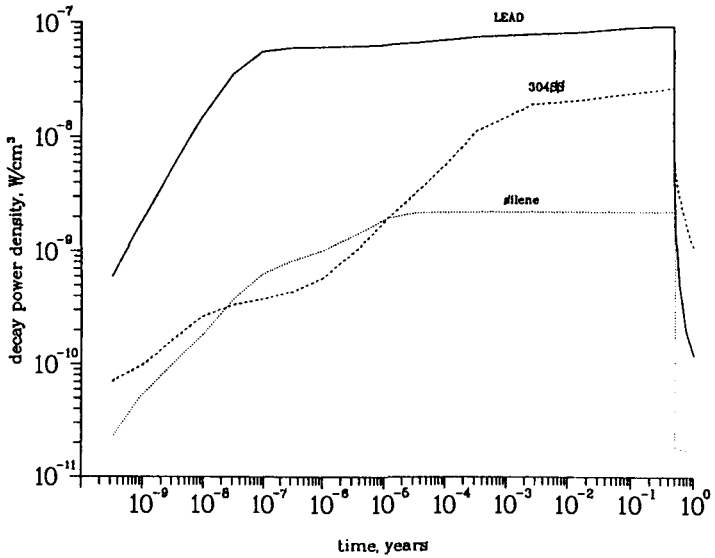

Fig. 7. Calculated decay power density in L* hadron calorimeter materials during a 0.5-year irradiation and 0.5-year down period.

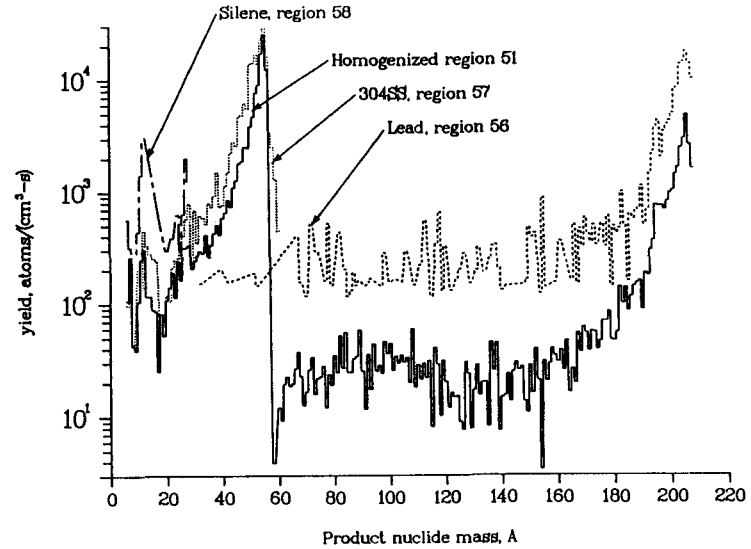

Fig. 2 Yield of product nuclides from spallation and fission from LAHET calculations.

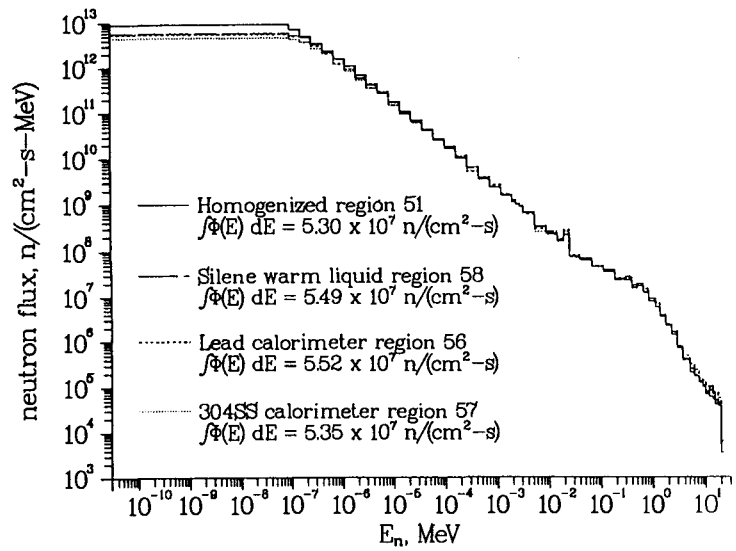

Fig. 3: Neutron flux for $E_n < 20$ MeV calculated with LAHET and MCNP Monte-Carlo codes.

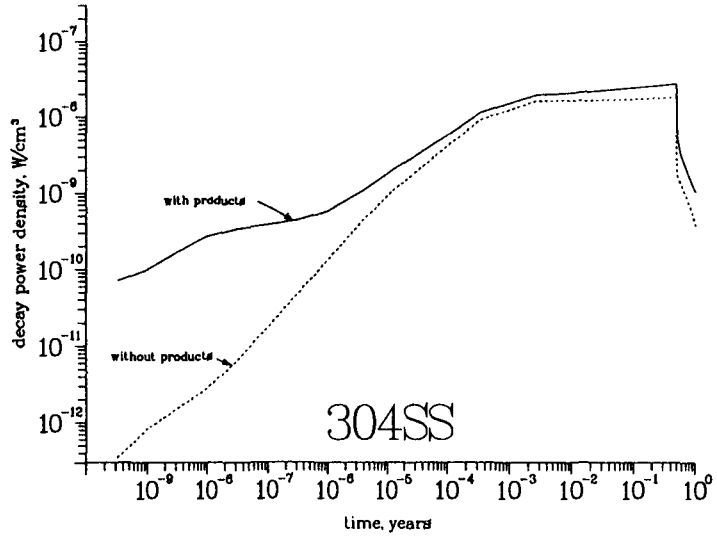

Fig. 9. Decay power density in the 304SS of the L* hadron calorimeter during a 0.5-year irradiation and 0.5-year down period calculated with and without LAHET spallation- and fission-products and their subsequent transmutation.

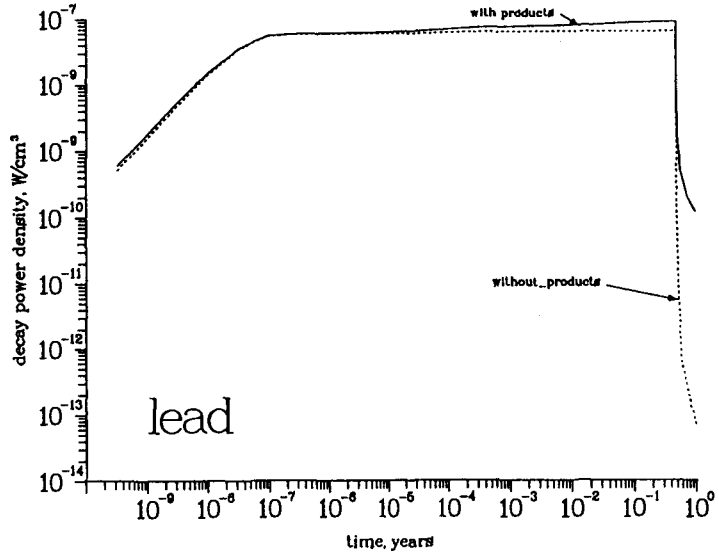

Fig. 8. Decay power density in the lead of the L* hadron calorimeter during a 0.5-year irradiation and 0.5-year down period calculated with and without LAHET spallation- and fission-products and their subsequent transmutation.

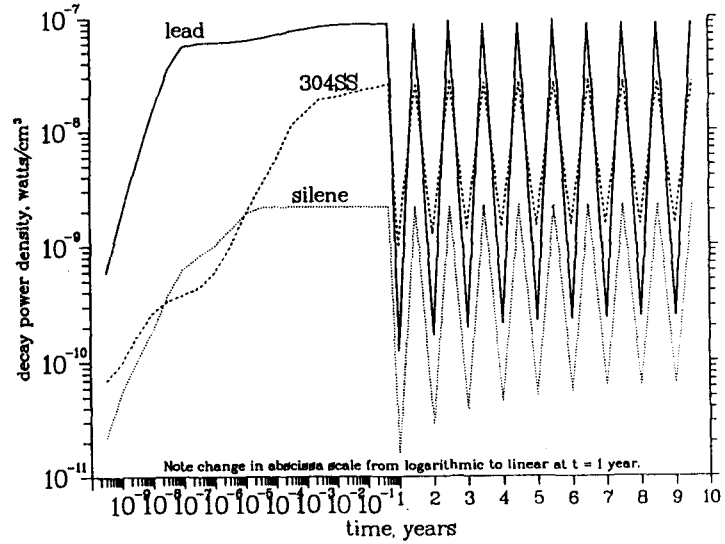

Fig. 4 Decay power densities due to the decay of activation products in the lead, 304SS, and silene regions of the hadron calorimeter of the L* detector for the SSC

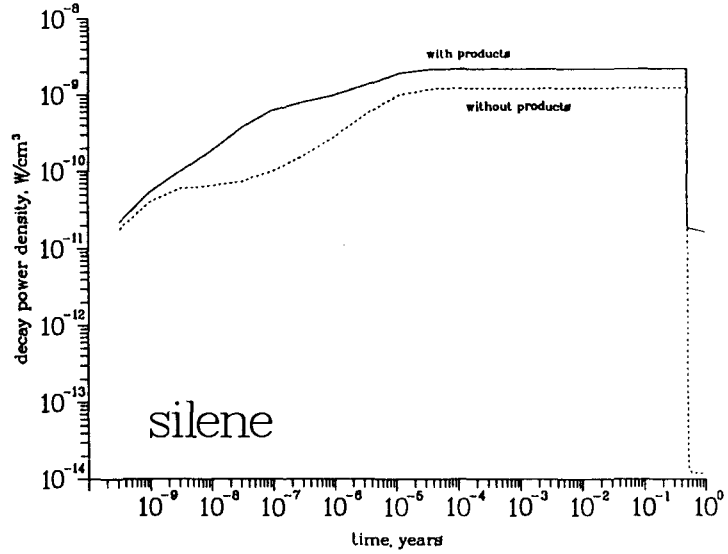

Fig. 10. Decay power density in the silene of the L* hadron calorimeter during a 0.5-year irradiation and 0.5-year down period calculated with and without LAHET spallation- and fission-products and their subsequent transmutation.

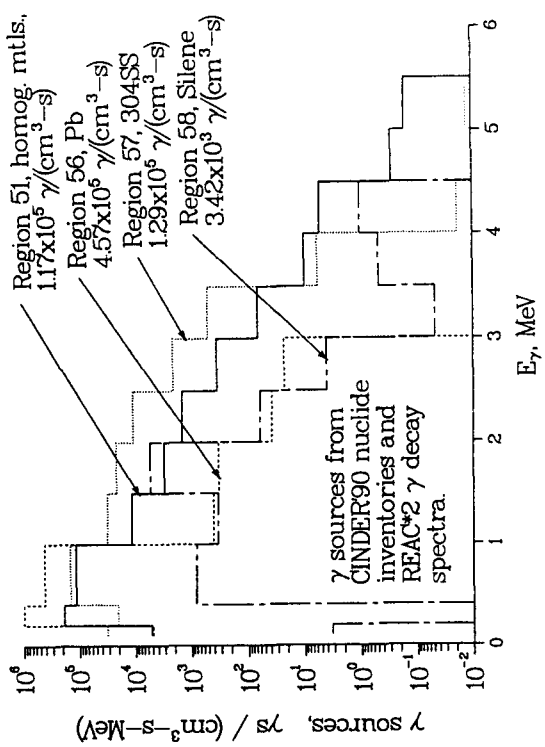

Fig. 5. Calculated decay γ sources in detector materials following six months operation.

GEM

Forward Calorimeter

Activation

Simulation by Laurie Waters

LA-UR incompl. Waters+

Activation by Bill Wilson & Tal England

LA-UR incompl. Wilson+ (>400p)

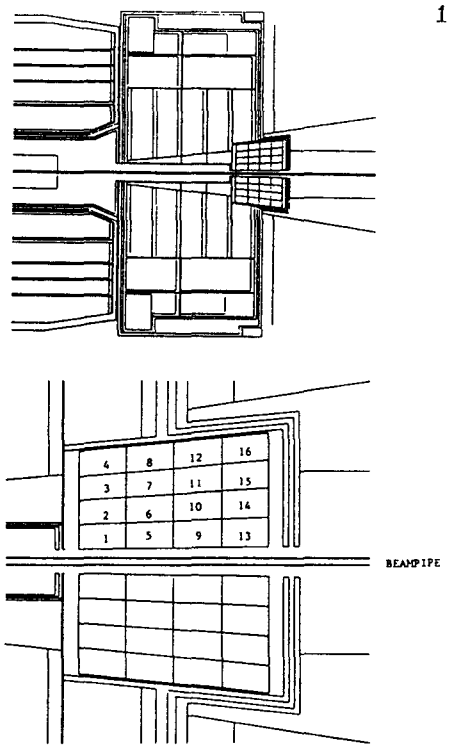

Figure 1: A) Overall position of the Forward Calorimeter. B) Expanded view of the 16 FCAL segments.

	4.91-5.1674m	5.1674-5.4248m	5.4248-5.6822m	5.6822-5.9396m
.7721°-2.329°	29151	9197	3197	2680
2.329°-3.886°	81569	29977	11280	7278
3.886°-5.443°	327871	135803	49483	27098
5.443°-~7°	1661758	759587	346474	223088

Table 3: Total number of spallation nuclei per cm³-s produced by the LAHET code system within the 16 FCAL regions. A typical isotopic distribution is found in figure 4.

	4.91-5.1674m	5.1674-5.4248m	5.4248-5.6822m	5.6822-5.9396m
.7721°-2.329°	1.806×10^7	0.847×10^7	0.311×10^7	0.288×10^7
2.329°-3.886°	5.962×10^7	3.455×10^7	1.344×10^7	0.795×10^7
3.886°-5.443°	20.999×10^7	13.623×10^7	5.806×10^7	2.783×10^7
5.443°-~7°	58.246×10^7	41.429×10^7	20.646×10^7	10.521×10^7

Table 4: MCNP Volume flux in neutrons/cm²-s in the 16 FCAL regions. Statistical errors on these figures run from 3-6%.

elements	(#/b/cm)
^{1}H	0.000090389
^{3}H	0.000000011
^{12}C	0.00019681
^{13}C	0.00000219
^{14}N	0.000018029
^{15}N	0.000000069
^{16}O	0.00003611
^{17}O	0.00000001
^{18}O	0.000000069
^{36}Ar	0.00000455
^{38}Ar	0.00000085
^{40}Ar	0.001344599
^{58}Fe	0.004143989
^{60}Fe	0.00158427
^{61}Fe	0.000068585
^{62}Fe	0.000217912
^{64}Fe	0.000055236
^{63}Cu	0.001777669
^{65}Cu	0.00079233
^{180}W	0.000063119
^{182}W	0.0138338
^{183}W	0.007511279
^{184}W	0.0161482
^{186}W	0.015043599

Table 1: Composition of the Forward Calorimeter.

	4.91-5.1674m	5.1674-5.4248m	5.4248-5.6822m	5.6822-5.9396m
.7721°-2.329°	131626.	138688.	145846.	153098.
2.329°-3.886°	91689.	101294.	111377.	121939.
3.886°-5.443°	00784.	07162.	73836.	81338.
5.443°-~7°	30240.	33408.	38734.	40217.

Table 2: Volume in cm^3 in each of the 16 regions of the FCAL. The top row indicates the range in Z, the first column, the range in θ.

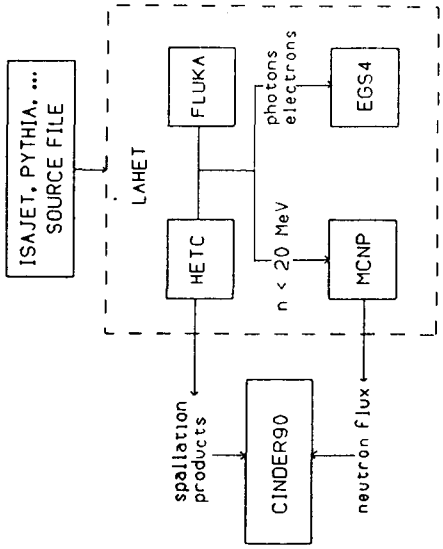

Figure 3: Flowchart of the various simulation codes.

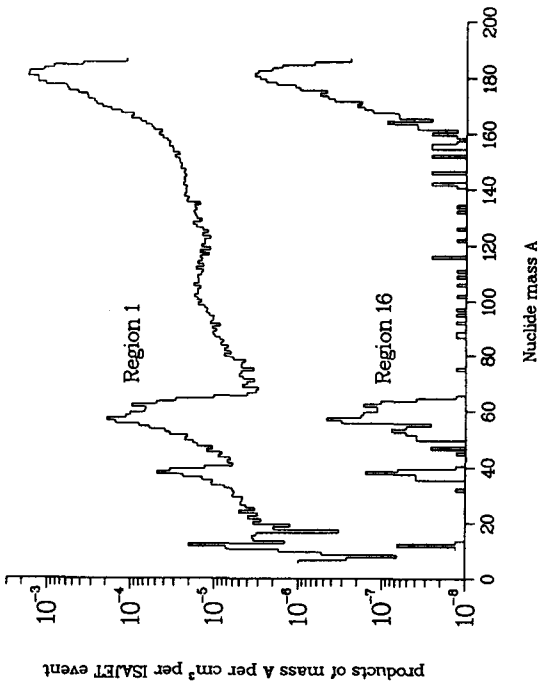

Fig. 4 Distribution of high-energy spallation and fission products in regions 1 and 16 of the GEM detector forward calorimeter.

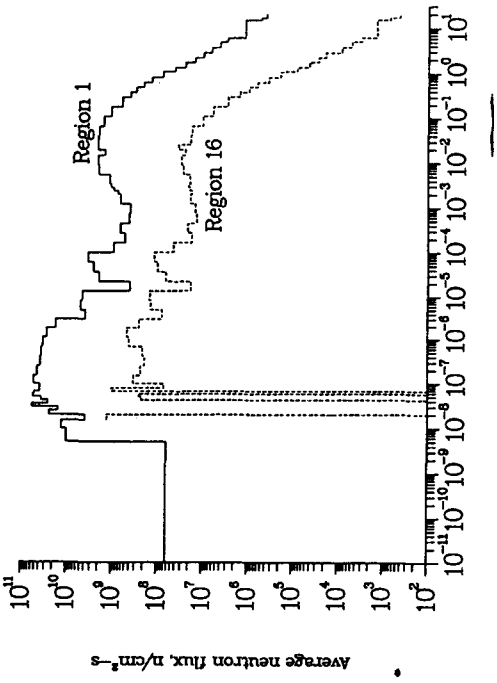

Fig 5 Average neutron flux in regions 1 16 of GEM forward calorimeter from tandem ISAJET-SUPERHET-MCNP calculations.

1598

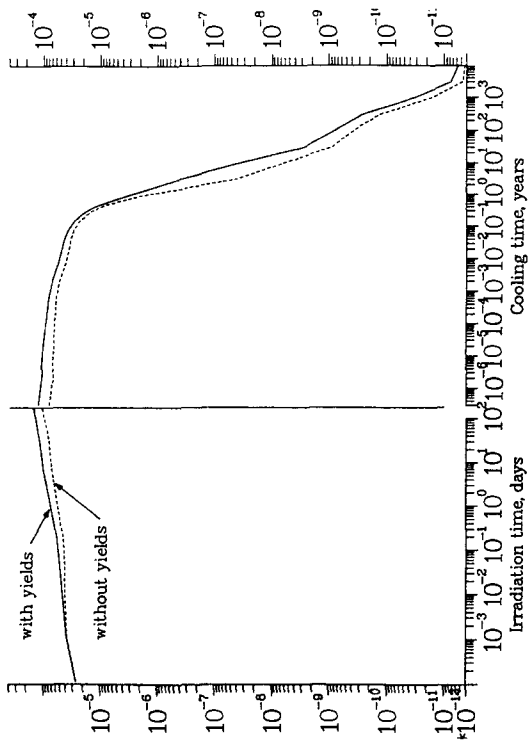

Comparison of Region 1 activity density calculated with and without high-energy spallation and fission yields.

1599

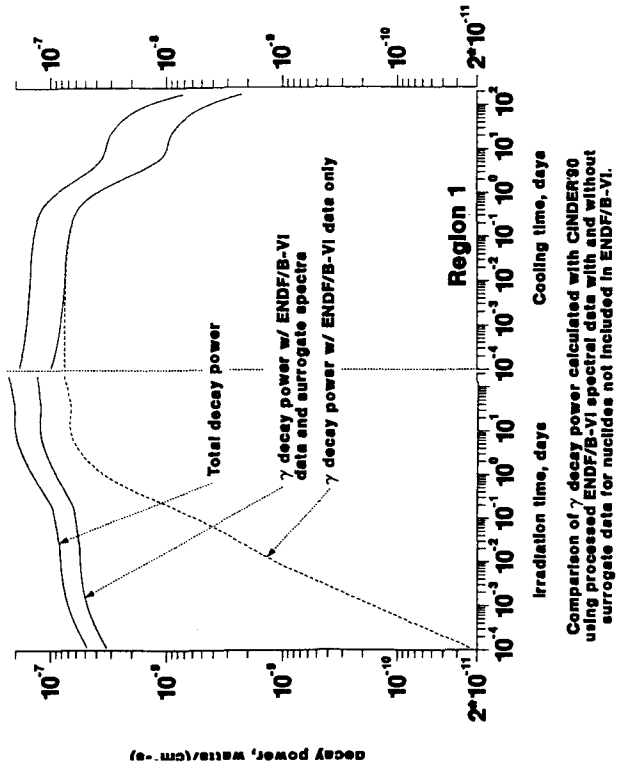

Comparison of γ decay power calculated with CINDER'90 using processed ENDF/B-VI spectral data with and without surrogate data for nuclides not included in ENDF/B-VI.

1600

Point–kernel shielding method calculations were made with the major radionuclide sources at 1 day cooling. Infinite–slab calculations for the Region 1 inventories and composition show that the dose–equivalent rate at 10 cm from the slab face is about 270 mRem/h. Also, γ sources deeper than about 2 cm contribute little to dose–equivalent rate at long cooling times.

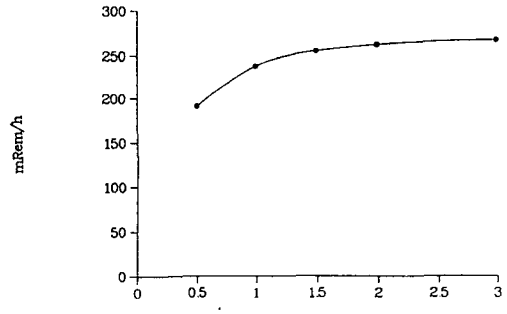

Dose–equivalent rate (mRem/h) 10 cm from slab face for region 1 inventory at 1 day cooling

1601

SDC

Activation Studies

(to be done)

Direction from A. Palounek & H. Ziock

Simulation by Dick Prael, Laurie Waters,...

Activation by Bill Wilson & Tal England

Present Status of SDCSIM (Calorimeter Part)

Makoto Asai
Hiroshima Institute of Technology

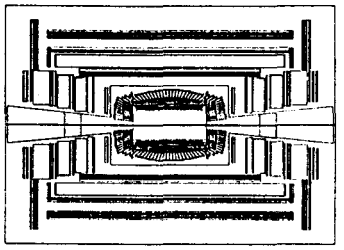

Calorimeter Packages:

- *CL -- Barrel and endcap Tile/Fiber calorimeter with Shower-Max calorimeter*
- *CI -- Forward calorimeter*
- *CF -- EM / Hadron shower shape and punchthrough parametrization*
- *CP -- Detailed (tile level) description*

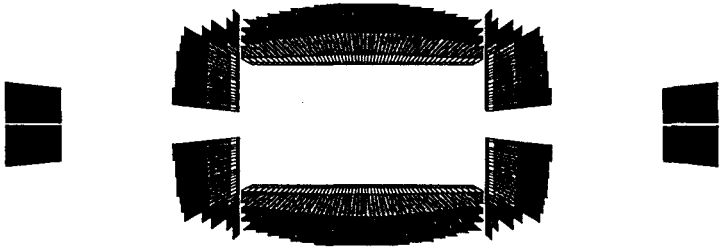

Contact person(s) for each package

CL -- Barrel and endcap Tile/Fiber calorimeter with Shower-Max calorimeter
Makoto Asai

CI -- Forward calorimeter
Mike Wendling, Myungyun Pang, Makoto Asai

CF -- EM / Hadron shower shape and punchthrough parametrization
Makoto Asai

CP -- Detailed (tile level) description
Marc Turcotte, PK Job

FL -- Liquid scinti/quartz tube forward calorimeter
Peter Copeland

CC -- Clustering and jet finding (available for next release)
Weimin Wu

User parameters for CL and CI packages

`CL/SHOWER_MAX thkb thke`

- `thkb` : *Thickness of the barrel shower_max calorimeter*
- `thke` : *Thickness of the endcap shower_max calorimeter*

`CL/DEPTH depb depe`

- `depb` : *Depth in X0 for barrel shower_max calorimeter*
- `depe` : *Depth in X0 for endcap shower_max calorimeter*

`CL/IRON_PLATE thirb thire`

- `thirb` : *Thickness of iron plate at the end of calorimeter*
- `thire` : *Thickness of iron plate at the end of calorimeter*

Other geometrical parameters are described in `CLGEOM.DAT` *and* `CIGEOM.DAT`.

User parameters for CF package

```
CF/EM_PARAMETER hiecut hiect2 shcute shspoe stepx0
CF/HD_PARAMETER hihcut hihct2 shcuth shspoh steplO
```

- `hiecut hihcut` : *Threshold energy to start parametrization #1*
- `hiect2 hihct2` : *Threshold energy to start parametrization #2*
- `shcute shcuth` : *Cut-off energy of parametrized shower*
- `shspoe shspoh` : *Energy deposition at each spot*
- `stepx0 steplO` : *Step length of parametrized shower*

```
CF/SWITCHES ltrne lespot ltrnh lhspot
```

- `ltrne` : *Transverse shape for EM shower*
- `lespot` : *Number of spot propotional to EM shower energy*
- `ltrnh` : *Transverse shape for hadron shower*
- `lhspot` : *Number of spot propotional to hadron shower energy*
  (1 for True / 0 for False)

Shower parametrization

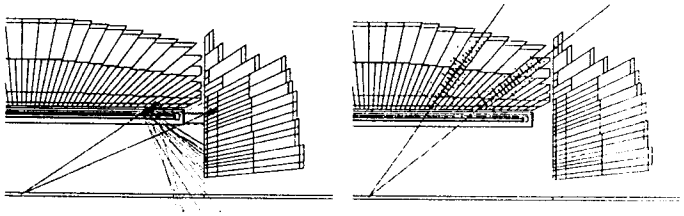

EM shower *Hadron shower*

User parameters for CF package (cont.)

```
CF/VOLUME vname [ hiecut hiect2 hihcut hihct2 ]
```

- `vname` : *Volume name to start shower parametrization*
  (Only one volume name for each tracking medium)

```
CF/THRESHOLD pthr
```

- `pthr` : *Threshold energy to skip punchthrough parametrization*

Parameters of CF package should be written in `CFPARA.CTL` *and defined with a keyword* `"CFPARA"`.

Punchthrough parametrization and EM debris

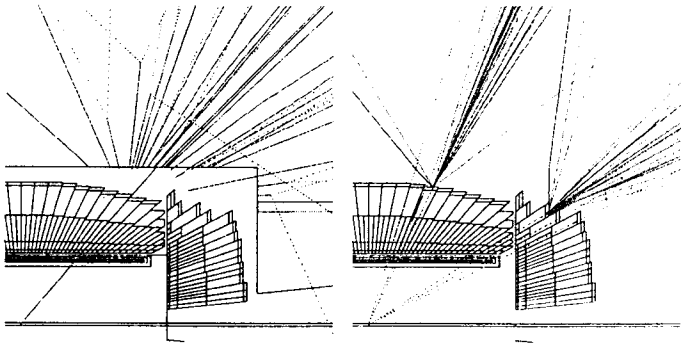

Punchthrough *EM debris*

Near future developments

> *CP and CC package will be ready for the next version release*

> *Fine tuning of shower shape parametrizations*
Tune to GEANT/GHEISHA results with CP package
Tune to CALOR89 results with CP package
Tune to results of the beam test
Optimize user parameter sets for
- *Quick and dirty study*
- *Fine and detailed study*

> *More*
Let's discuss...

Detailed module structures (CP package)

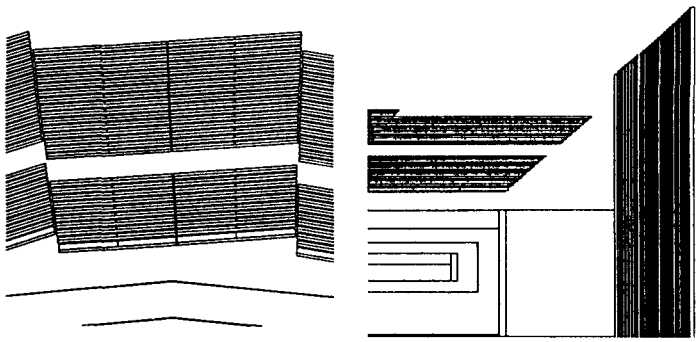

EM modules

Output banks of CL and CI package

`/RECO/HCAL/CALE`	`'10I/1I3F'`
Header part	*10 integer words*
Each hit	*1 integer + 3 floating*
	(channel no., energy deposition, eta, phi)
`/RECO/HCAL/CASM`	`'10I/1I1F'`
Header part	*10 integer words*
Each hit	*1 integer + 1 floating*
	(channel no., energy deposition)

For more detail, see `data_banks.doc` *and* `shell_zebra.doc`

Contact persons for calorimeter data structures
John Marraffino, Andy Beretvas, Makoto Asai

[6] Magnet/Calorimeter/Integration Joint

Tracking Utilities Update	J. Piles	- 1614
Calorimeter Support System	L. Bartoszek	- 1622

Tracking Utilities Update

Jonathan A. Piles
(SSCL)

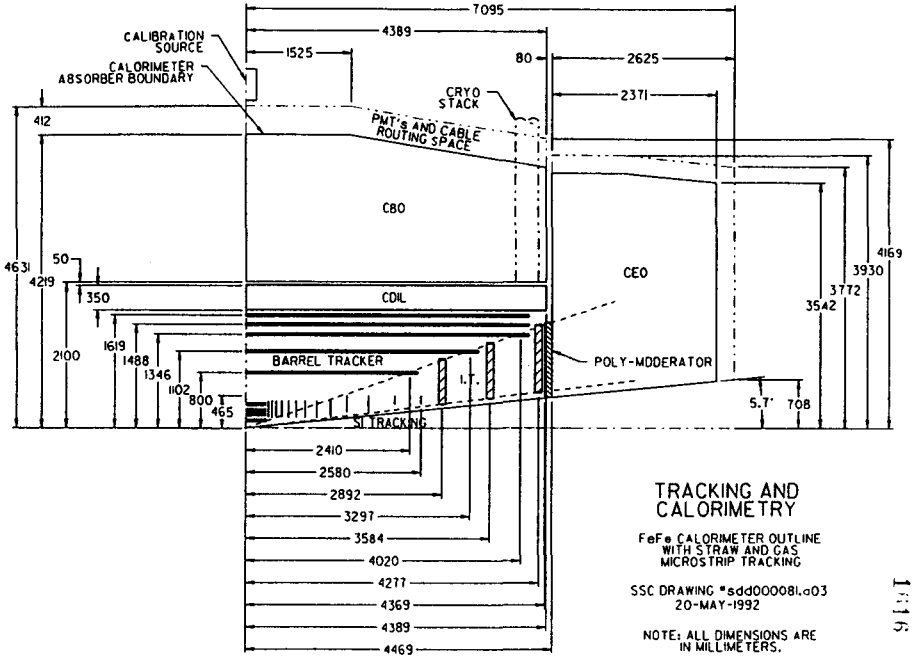

TRACKING AND CALORIMETRY

FeFe CALORIMETER OUTLINE WITH STRAW AND GAS MICROSTRIP TRACKING

SSC DRAWING #sdd000081.a03
20-MAY-1992

NOTE: ALL DIMENSIONS ARE IN MILLIMETERS.

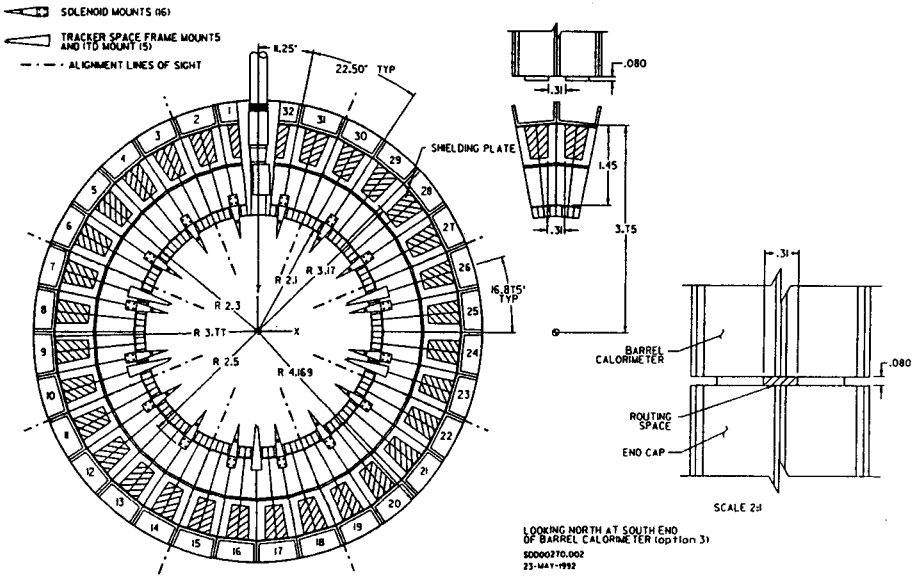

LOOKING NORTH AT SOUTH END OF BARREL CALORIMETER (option 3)
SD000270.002
23-MAY-1992

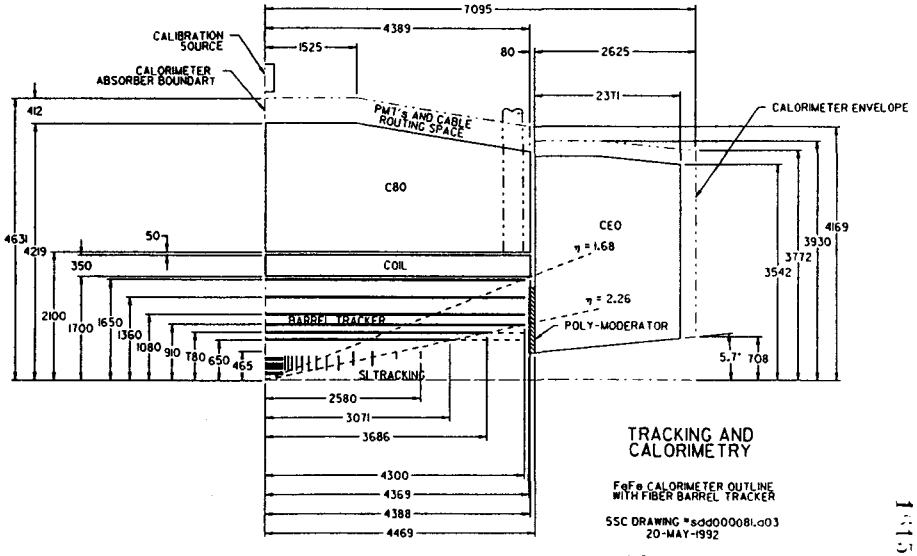

TRACKING AND CALORIMETRY

FeFe CALORIMETER OUTLINE WITH FIBER BARREL TRACKER

SSC DRAWING #sdd000081.a03
20-MAY-1992

NOTE: ALL DIMENSIONS ARE IN MILLIMETERS

1618

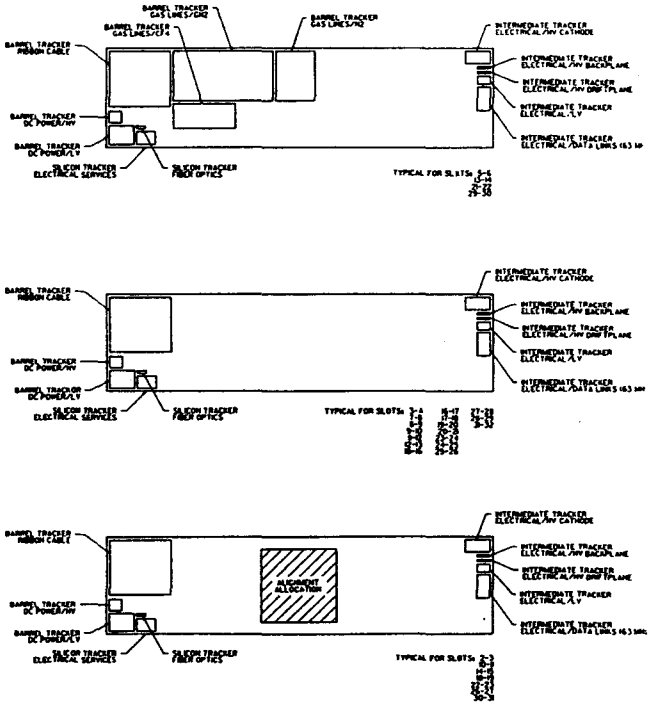

1619

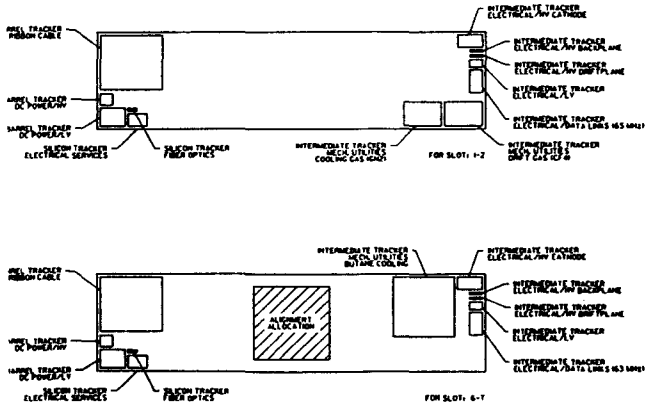

1620

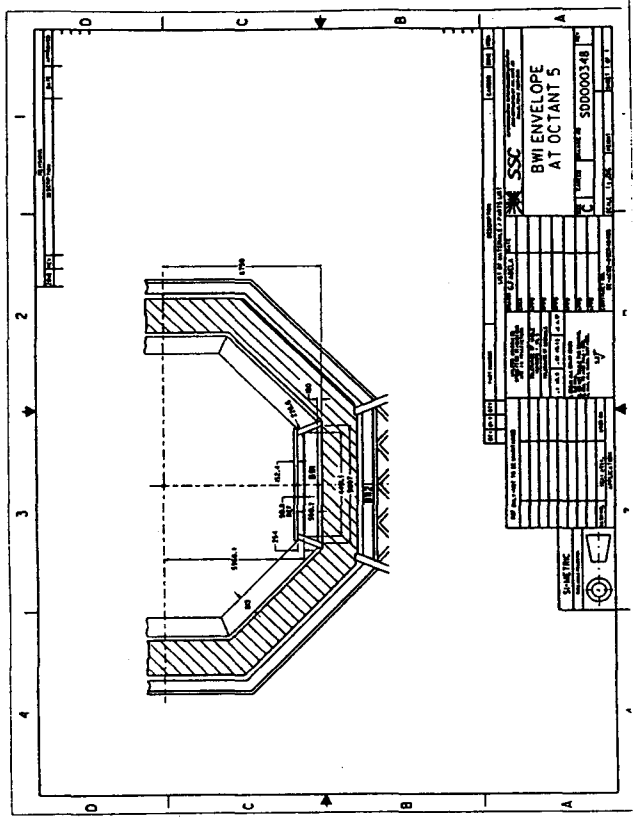

1621

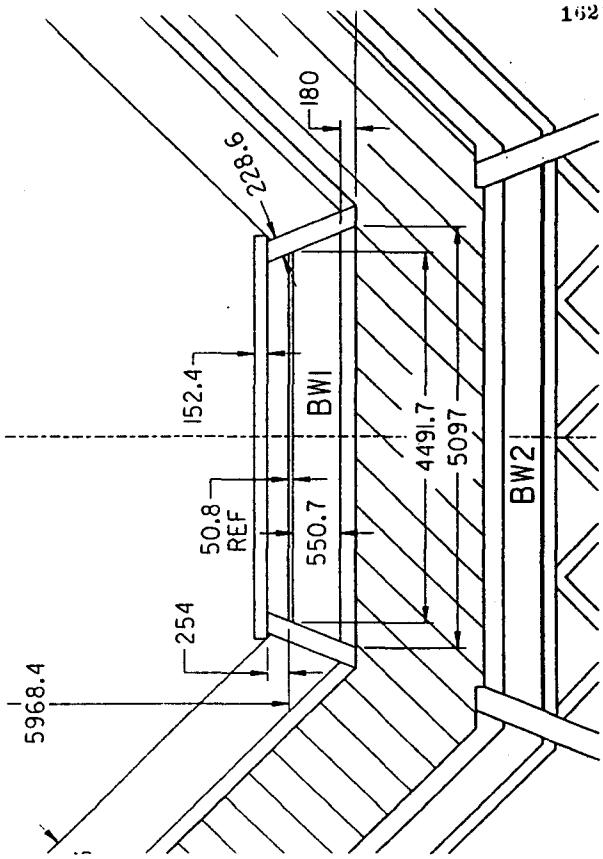

Calorimeter Support System

Larry M. Bartoszek
(Fermilab)

1622

1623

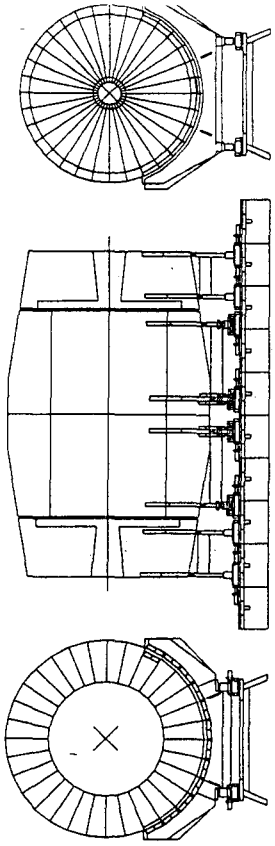

1624

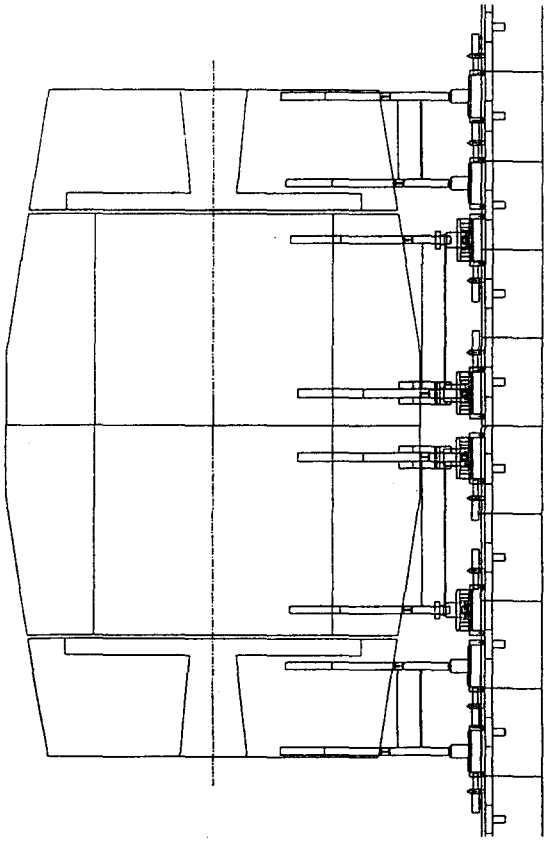

1625

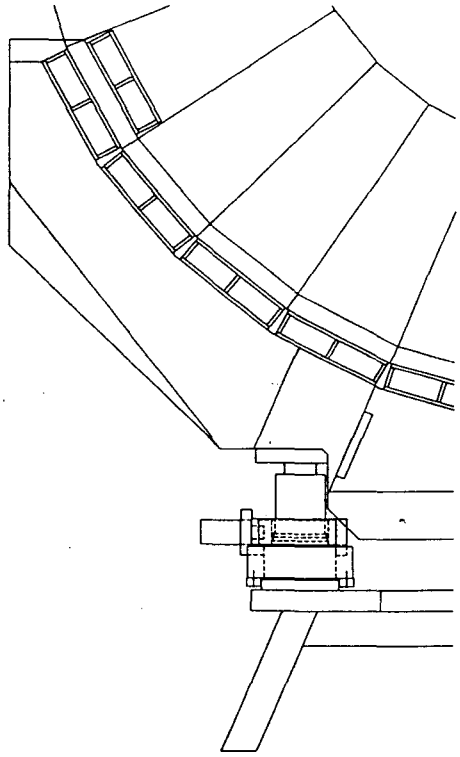

1626

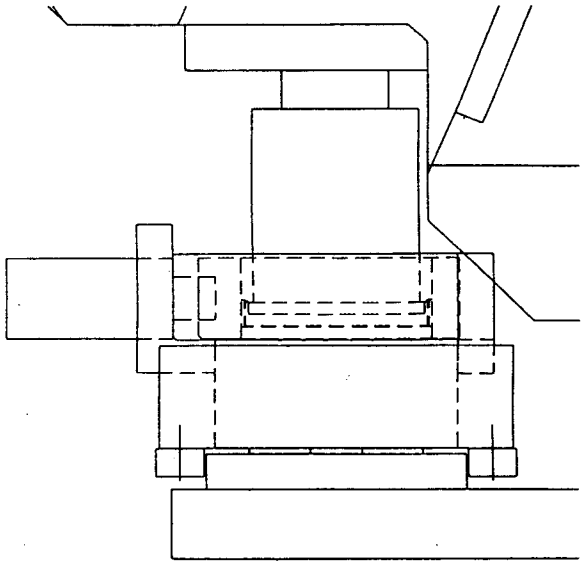

1627

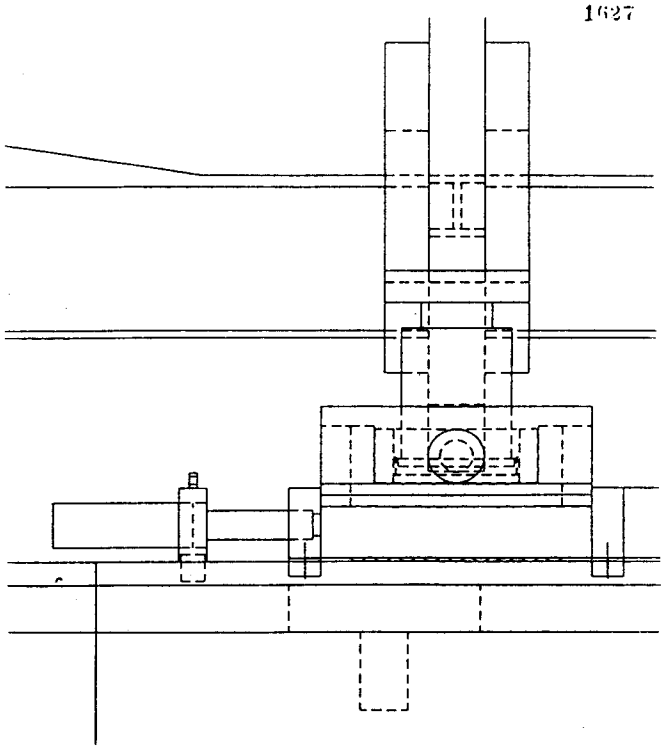

[7] Muon System

<Tube>

Mechanical Consequences of Tube Layer Ordering	C. Daly	- 1629
Cost Estimate of Barrel Muon Tubes	S. Mori	- 1650
Drift Tube Simulation Study	K. Norik	- 1652

<Intermediate System>

SDC Intermediate Muon System	D. Carlsmith	- 1669

<Forward System>

Forward System	A. Skuja	- 1679

<Labor Estimate>

Labor Estimate	C. Grinnell	- 1687

<Trigger>

RPC Solution for the SDC Muon Trigger Counters	S. Amendolia	- 1693
SDC Trigger Rates	W. Smith	- 1698

<Phi Cracks>

Physics Impact of Phi Cracks in the SDC Barrel Muon System	S. Errede / J. Wiss	- 1714
Study of Loss due to Missed Coverage in the Barrel Muon Detector	M. Daoudi / U. Nauenberg	- 1726

<Sparsification>

Sparsification Study I	S. Willis	- 1734
Sparsification Study II	Y. Asano	- 1741
Impact of Sparsification on Muon Trigger/Reconstruction Efficiency ...	N. Kanematsu	- 1752

<Background Study>

A Background computations for SDC Set-up at 40 TeV	Zholobov G. V.	- 1771
Neutron Rates in the SDC Forward Muon System - Design Optimization	A. Kulik	- 1813

Mechanical Consequences of Tube Layer Ordering

Colin H. Daly
Department of Mechanical Engineering
University of Washington

BW1 – Tube Layout Possibilities – Order by Increasing Radius

- 4 theta – 4 phi
- 4 phi – 4 theta
- 2 theta – 4 phi – 2 theta
- 2 phi – 4 theta – 2 phi
- 2 theta – 2 phi – 2 theta – 2 phi
- 2 phi – 2 theta – 2 phi – 2 theta

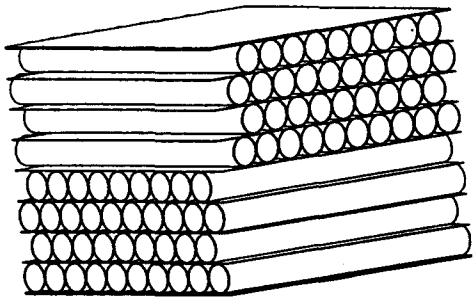

4θ, 4ϕ (or 4ϕ, 4θ) tube layout

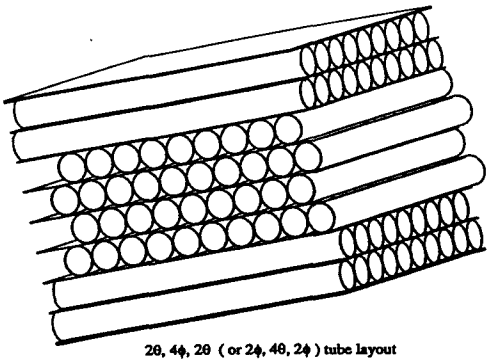

2θ, 4ϕ, 2θ (or 2ϕ, 4θ, 2ϕ) tube layout

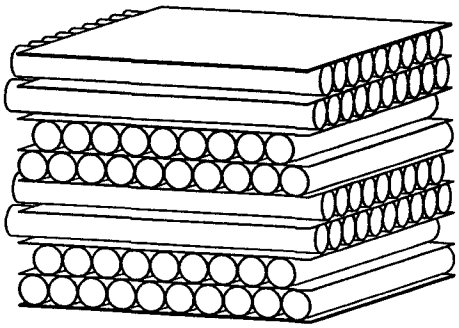

2θ, 2ϕ, 2θ, 2ϕ (or 2ϕ, 2θ, 2ϕ, 2θ) tube layout

Module Deflection Analysis (FEA)

- Need properties in 2 orthogonal directions
- Take 2 dimensional slice in each direction
- Beam models used to get properties in each direction
- FEA model of whole BW1 module
- 3-point supports - consider different locations

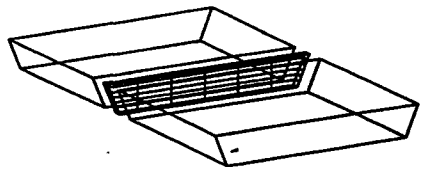

Figure 1: 2-Dimensional Slice Taken from the BW1 Module.

Beam FEA Model

- Beam cross section as module
- bar elements for ribs in each direction
- end rail - $w(x) = 4/3EI + w(x) = 2/GA$
- run for 2 different lengths - solve for E and GA
- repeat for other direction
- repeat X, Y, GXZ, GYZ, thickness and density for shell
- repeat for each rib order layout

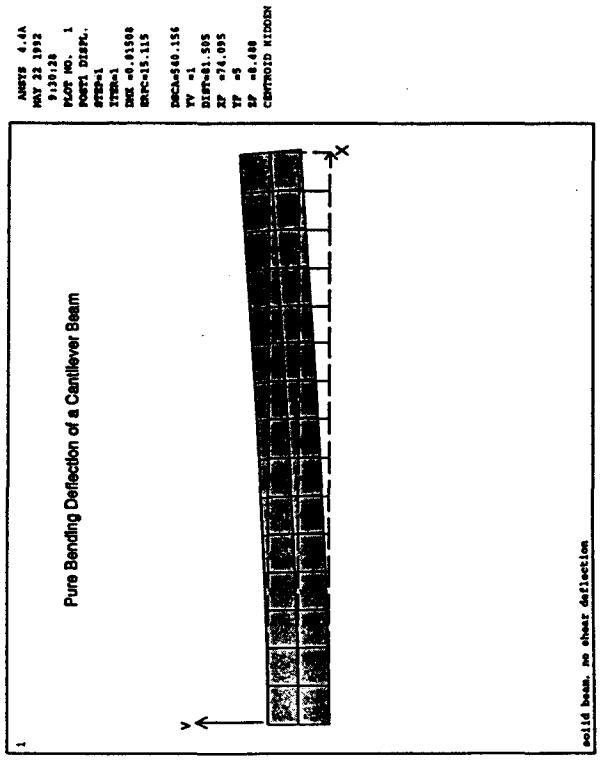

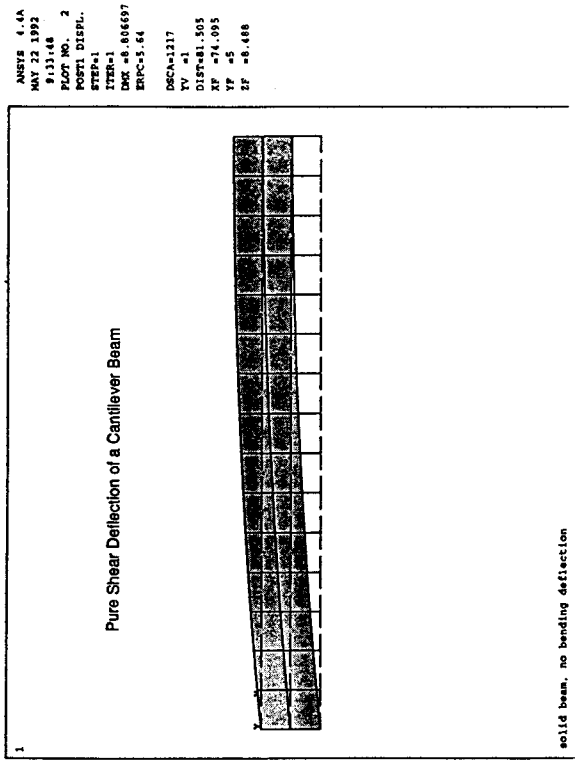

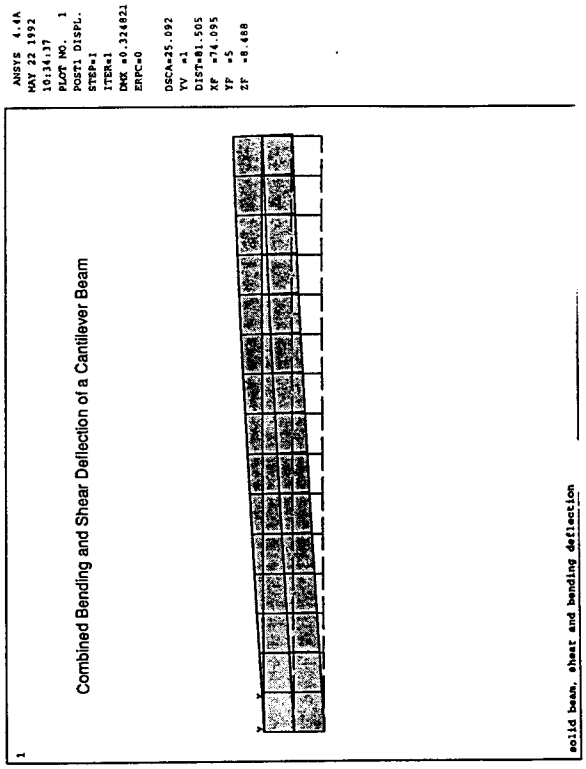

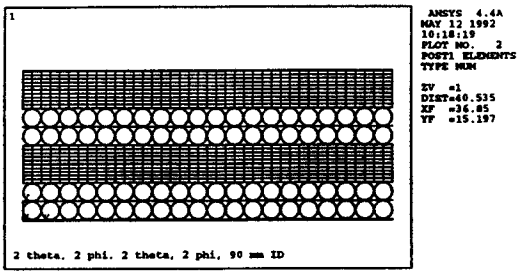

Figure 2: Cantilever Beam Model of a Cross-Section of a 2θ, 2φ, 2θ, 2φ Tube Layout.

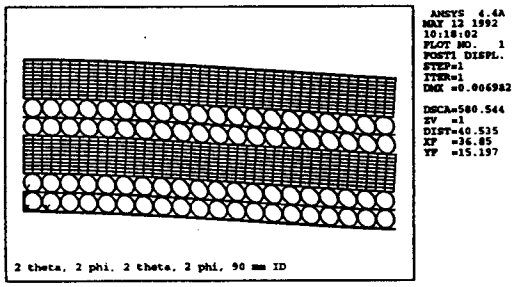

Figure 3: Deflection of a 20-tube Length of Cantilever Beam Model.

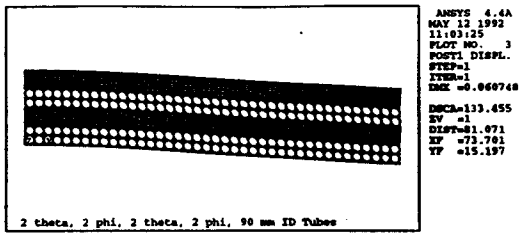

Figure 4: Deflection of a 40-tube Length of Cantilever Beam Model.

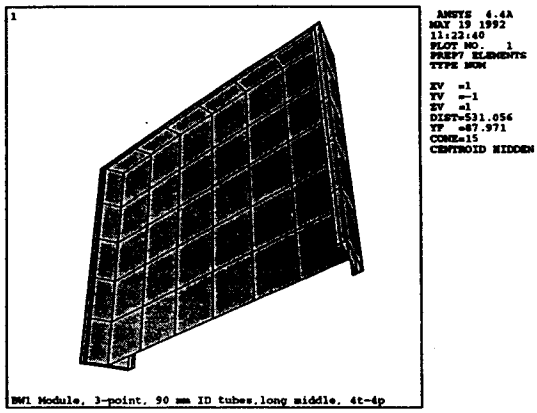

Figure 5: Finite Element Model of one half of a BW1 Module.

FEA model of BW1 module

- peripheral structure modelled in detail
- tubes/plate layers modelled as equivalent shell
- 3 point support - only 1/4 is modelled 1/2 of module
- different support locations

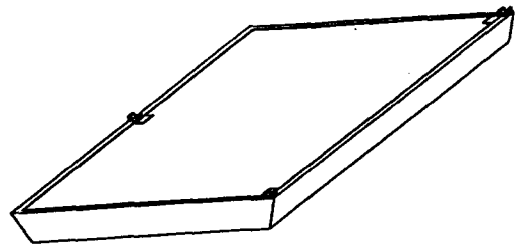

(a): BW1 Module Showing 2 Supports at Corners and 1 on the Opposite Edge.

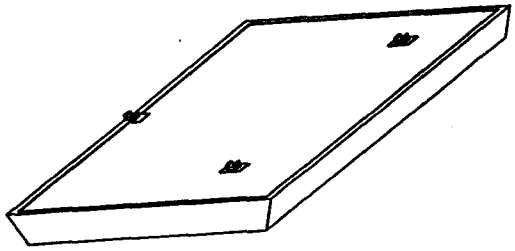

(b): BW1 Module Showing 2 Supports Moved in from Corners and 1 on the Opposite Edge

Figure 7: Different Configurations for BW1 Module Supports.

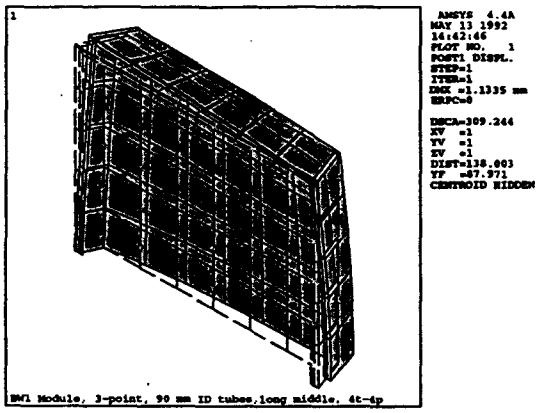

Figure 6: BW1 Module Deflection Analysis with Supports at the Corners. Module has 40 and 44 Tubes and is the Long, Middle BW1 Module. The Maximum Deflection (DMX) is 1.1335 mm.

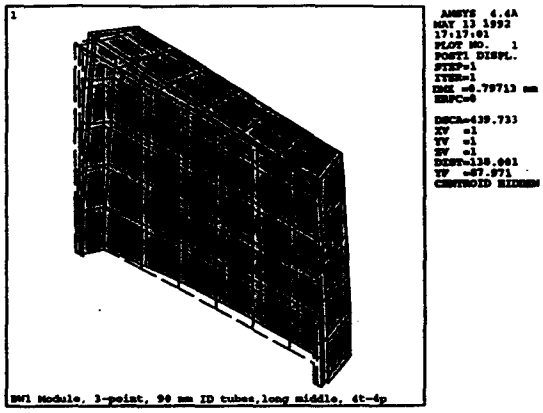

Figure 8: BW1 Module Deflection Analysis with Supports Moved in from the Corners. Module has 40 and 44 Tubes and is the Long, Middle BW1 Module. Maximum Deflection (DMX) is 0.79713 mm

Results for BW1

Deflections for Supports Moved in From Corners

Effect of Tube Order Layout in BW1 Modules

Tube Layout	Maximum Deflection (mm)
4 Theta, 4 Phi	0.797
4 Phi, 4 Theta	0.797
2 Theta, 4 Phi, 2 Theta	0.963
2 Phi, 4 Theta, 2 Phi	0.968
2 Theta, 2 Phi, 2 Theta, 2 Phi	1.066
2 Phi, 2 Theta, 2 Phi, 2 Theta	1.066

Results for BW1

Deflections for Supports At Corners

Effect of Tube Order Layout in BW1 Modules

Tube Layout	Maximum Deflection (mm)
4 Theta, 4 Phi	1.134
4 Phi, 4 Theta	1.134
2 Theta, 4 Phi, 2 Theta	1.446
2 Phi, 4 Theta, 2 Phi	1.446
2 Theta, 2 Phi, 2 Theta, 2 Phi	1.495
2 Phi, 2 Theta, 2 Phi, 2 Theta	1.495

BW3 tube order possibilities

- 4 theta, 4 phi, 2 stereo (close to theta)
- 4 phi, 1 stereo (phi), 1 stereo (theta), 4 theta
- Same modelling procedure
- No significant difference

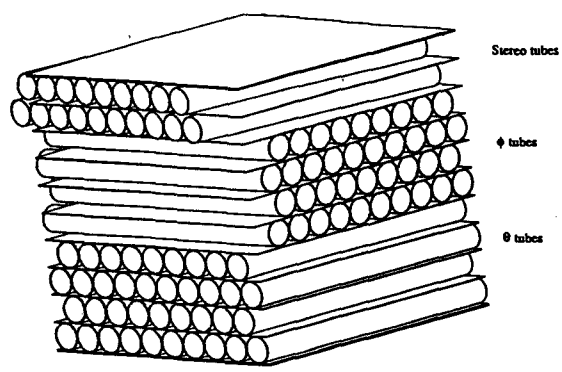

BW3 – 4θ, 4ϕ, 2 stereo (near θ) tube layout

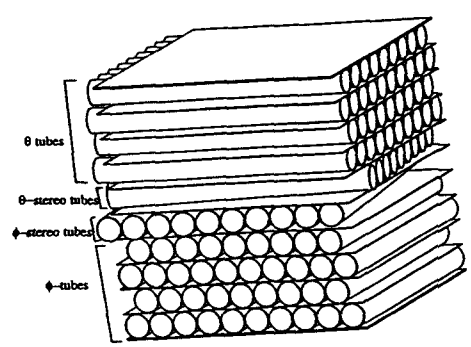

BW3 – 4ϕ, 1 ϕ–srereo, 1 θ–stereo, 4θ tube layout

Conclusions

1. Must support in front-range for BW modulation
2. Further improvement in electronics
3. U.S. lags other nations significantly here physics
4. BW deliberations are greatest in end phase
5. Need to add in the thermal detections
6. Also BW tube front for hemispheric

May 1992
S. Mori

Cost estimate of barrel muon tubes

Furukawa Electric Co., Ltd.
(Furukawa Aluminum)

9cm Φ, 1.8mm wall thickness
9m long
10,000 tubes

- Tube:
  - Raw material: ¥A*/kg
  - 6063-T3 alloy ~ ¥ 2.4 A/kg
  - Fabrication cost ~ ¥ 3.3 A/kg
    (with yellow alodyne)
  - subtotal ¥ 6.7A/kg
- End cap (aluminum section)
  - Material ¥ 679 /cap
  - Fabrication cost ¥ 1,226 /cap
  - subtotal ~ ¥ 1,900/cap

Furukawa Aluminum Co., Ltd.
VENUS
~950 modules
(8 cells/module)

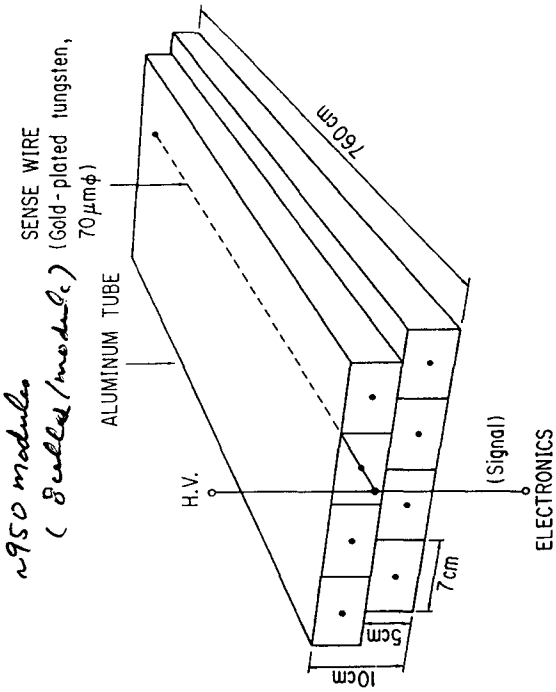

* A = ¥170 ~ 450/kg

Yerevan Physics Institute
Alikhanyan Brothers St.2,
Yerevan 375036,Armenia
Telefax: (8852)-35-00-30
e-mail:Khalatyan@M9.IHEP.SU

Drift tube simulation study

Khalatyan Norik

Yerevan Physics Institute
May 18, 1992

1. Introduction

This draft is devoted to the study of muon drift tubes using a CERN drift chamber simulation package 'GARFIELD'. The main goals are the following:

- *drift field uniformity*
- *capability for resolving multihits*

The cylindrical cells with field shaping wires have been studied. Drift field uniformity and the width of the collection region for different aspect ratios, arrangements of electrodes and voltage settings are investigated and optimized.

Due to limitations of the drift chamber simulation package used here, electrodes and tube's wall for cycle cells are simulated by rows of wires.

2. Cell parameters

The typical parameters of the cells are the following:

- *Tube's inner diameter - 72.5 mm*
- *Distance between electrodes - 52 mm*
- *Electrode's thickness - 0.6 mm*
- *Electrode's width - 32 mm*
- *Sense wire diameter - 50 μm*

- *Tube's wall thickness - 1.5 mm*

The simulation set-up of simple drift tube is shown in fig.1 with drift-lines and isochrons for various potentials. Fig.1a,b are for 3.5 kV at electrodes, 4.5 kV at sense wire and 2.0 kV at electrodes, 3.6 kV at sense wire respectivly. The width of the drift field is about 10 - 20 mm.

3. Gas

The mixture of Ar-90% - CO2-10% was used as a working gas. The drift velocity and longitudinal diffusion of electrons for a chosen gas are shown in fig.2ab as a function of E/p respectivly.

4. x(t)-correlation

In fig.3 x(t)-correlation is shown for a drift tube with one sense wire.

5. Signal simulation

For the study of two track separation inside a drift tube the signals were simulated at different positions of tracks and both signals were added. The distance between two tracks was chosen 10 mm. The clusters and electron drift-lines are shown in fig.4ab. The dashed lines represent the track. The signal simulation with the longitudinal diffusion of the electrons along the drift-lines and ion-tail are shown in fig.4. A good two track separation can be seen inside a drift tube. Time resolution is about 200 ns.

6. Space resolution

Assuming that the registering electronics has the threshold 1 electron, the space resolution was estimated using the first electron arrival time distribution at various x-positions. In fig.5 the typical arrival time distributions of 1-electron at x=2.5 cm and x=3.0 cm are shown. The space resolution versus distance is shown in fig.6 . The space resolution for one track is about 150 - 400 μm.

7. Three wires cell

The additional wires were used to achieve the field uniformity. The distance between field shaping wires and sense wire was varied. In fig.7 the drift tube set-up with drift lines (fig.7a) and x(t)-correlations (fig.7b-d) are shown for 3-wires cell. The distance between sense wires is 10mm. The signal simulations of two tracks at distance 10mm are shown in fig.8. A good two-track resolution can be seen for each wire separatly. To reduce the cost of cell and simplify the chamber operation we can use the sense wires at ground potential. In fig.9 the I-beam type cells without and with field shaping wires are shown. Of cource we may construct I-beam type cell inside cylindrical tube. This is illustrated as an example only.

8. Five wires cell

Using 5-wires cell we can reach a good capability of resolving multihits inside a single cell. The information from the each sense wire may be used separatly. The sense wires are at the following positions of y-coordinates: 0.0cm, 1.0cm, -1.0cm, 1.75cm, -1.75cm. In fig.10 the drift tube set-up with drift lines (fig.10a) and x(t)-correlations (fig.10b-f) are shown for 5-wires cell. The clusters, electron drift lines and tracks at positions 1cm and 1.5cm are shown in fig.11. The signal simulations of two tracks at distance 5mm are shown in fig.12. We see a good two-track resolution for each wire separatly. The time resolution is about 100ns. As described in previous section we can use I-beam type cell at ground potential. It is shown in fig.13 for 5-wires cell.

9. Multiwire influence on isochrons

The influence of 3-wire cell on isochrons was studied with distance 2mm between wires. In fig.14 the I-beam type cells without and with field shaping wires are shown. In this figure better time characteristics can be seen for 3-wire cell.

10. Conclusions

The one track resolution has been estimated using 1 electron arrival time distribution and it was found to be about 100-400μm versus distance from sense wire.

The drift uniformity has been achieved using additional field shaping wires (3-wire and 5-wire cells).

Multiwire cells allow to achieve good capability for resolving multihits.

The ground potential at sense wires in I-beam type cells may be used.

Good time characteristics are achieved using additional potential wires.

11. References

1. T.Zhao, Tracking Muons at SSC, SDC note 91-00003, January 15, 1991
2. Veenhof R., GARFIELD, a Drift Chamber Simulation Manual, March,25,1991
3. Peisert A. and Sauli F, Drift and Diffusion of Electrons in Gases: a compilation, CERN 84-08

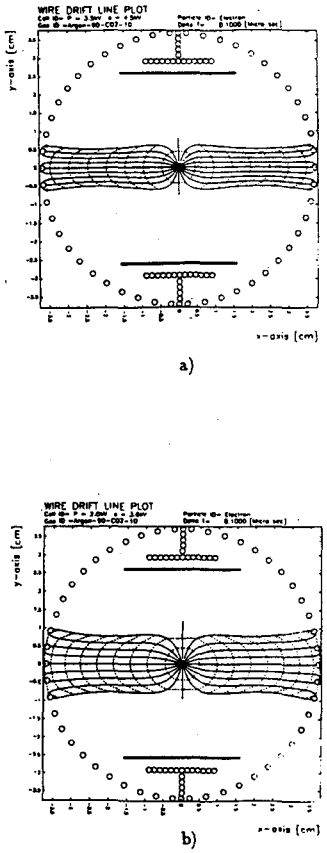

Figure 1.

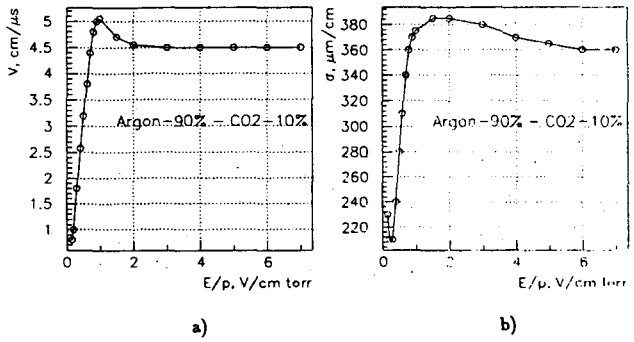

Figure 2.

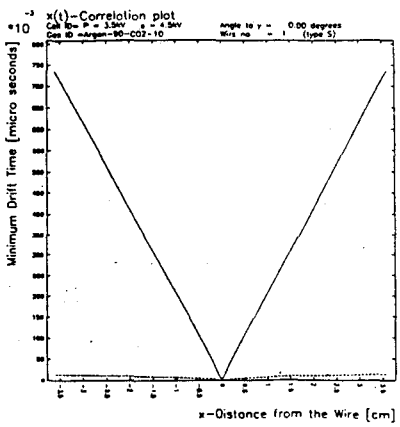

Figure 3.

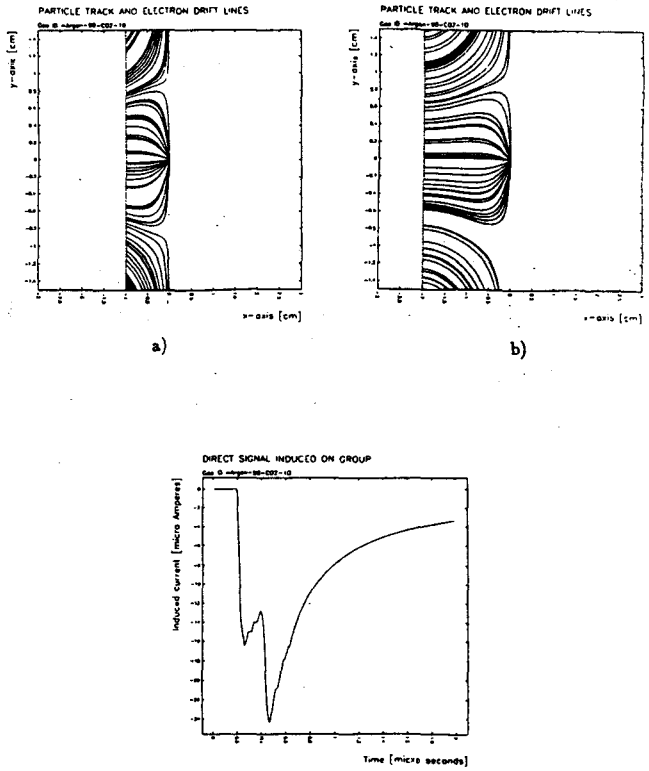

Figure 4.

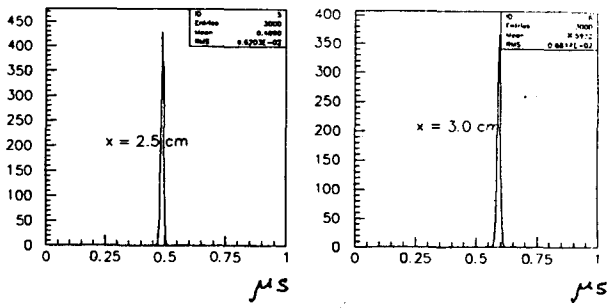

Figure 5.

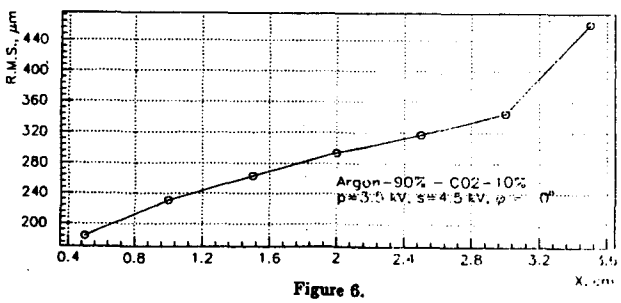

Figure 6.

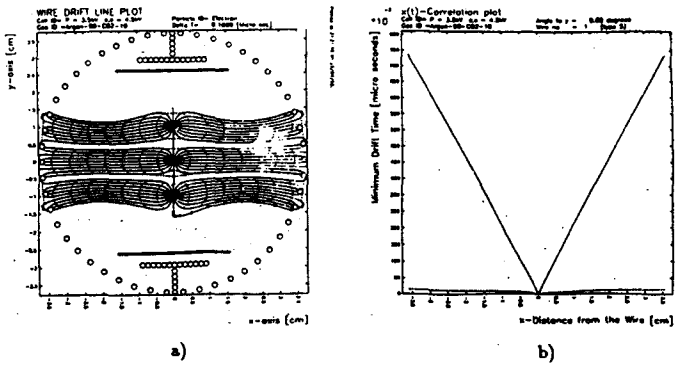

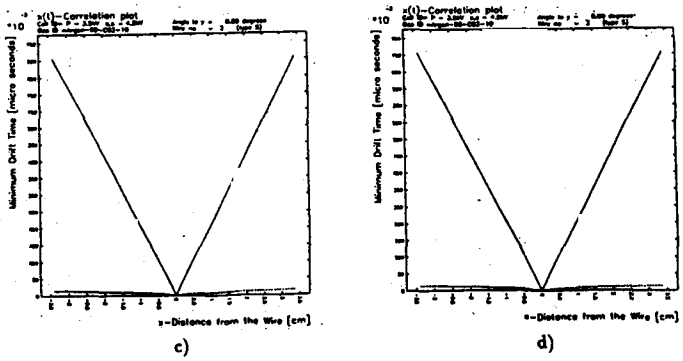

Figure 7.

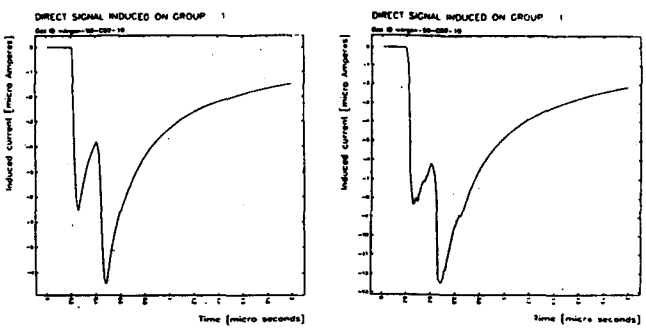

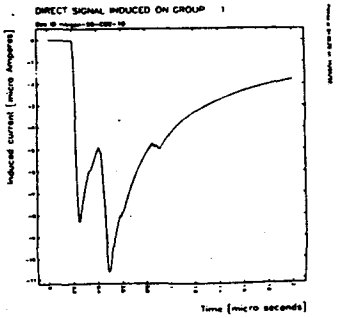

Figure 8.

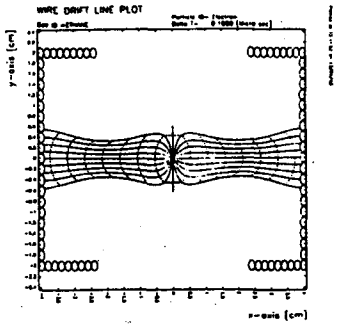

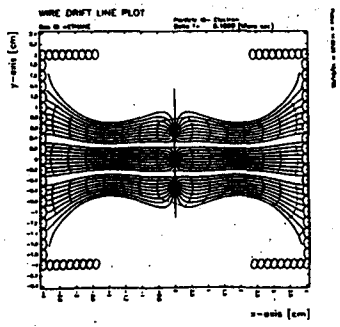

Figure 9.

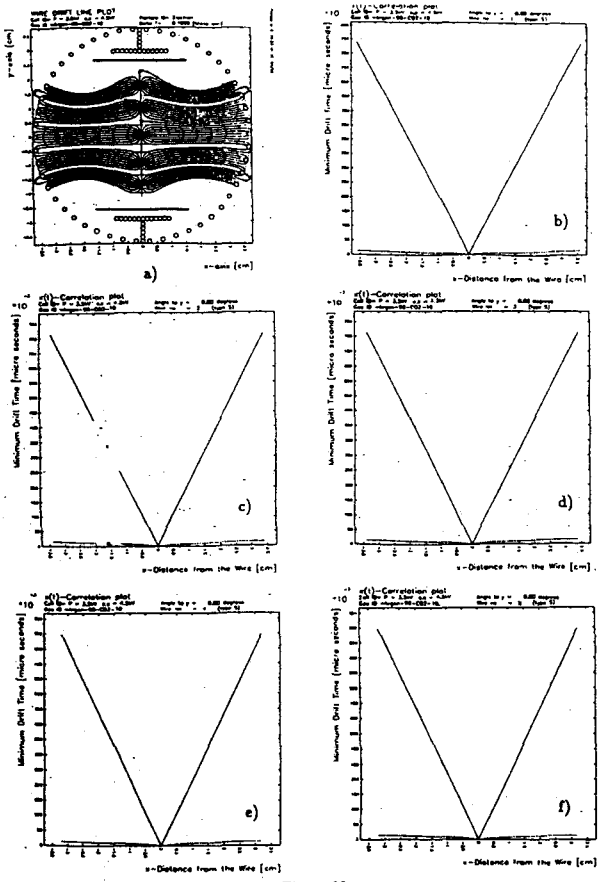

Figure 10.

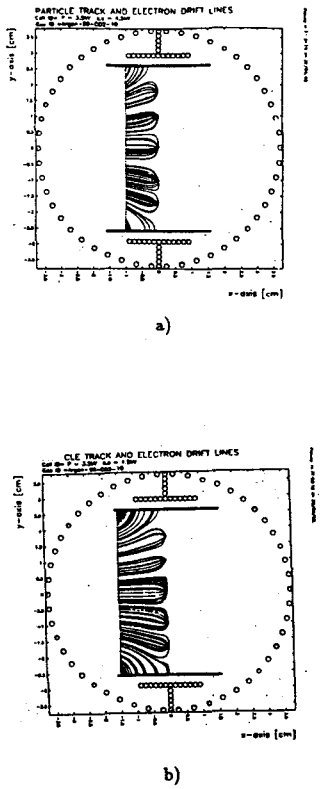

Figure 11.

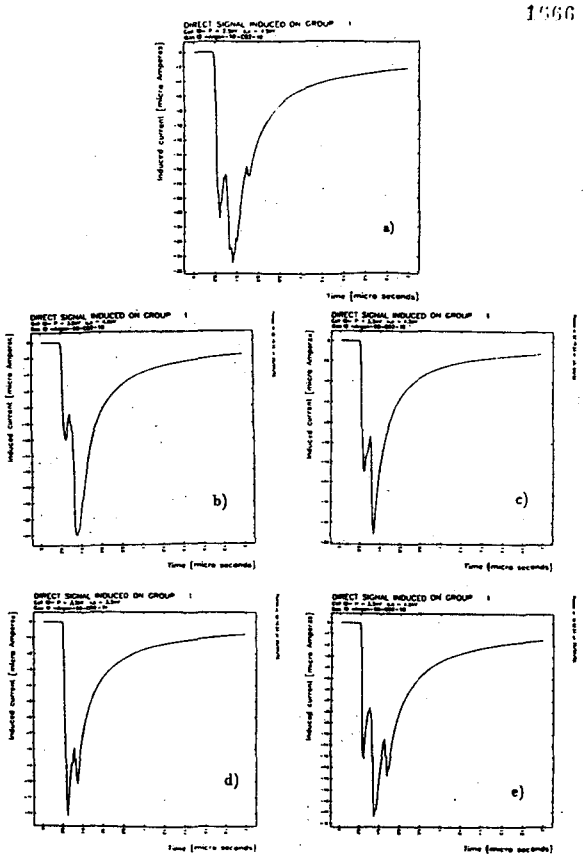

Figure 12.

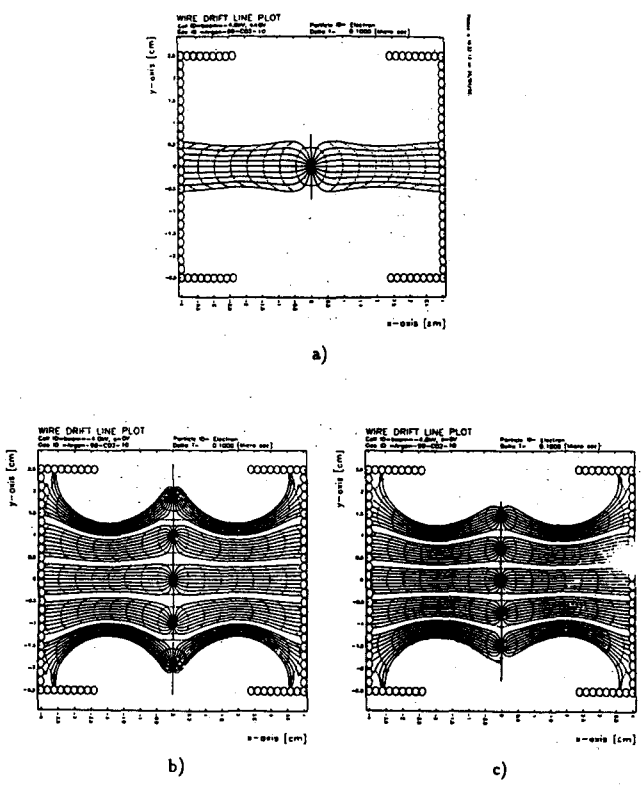

Figure 13.

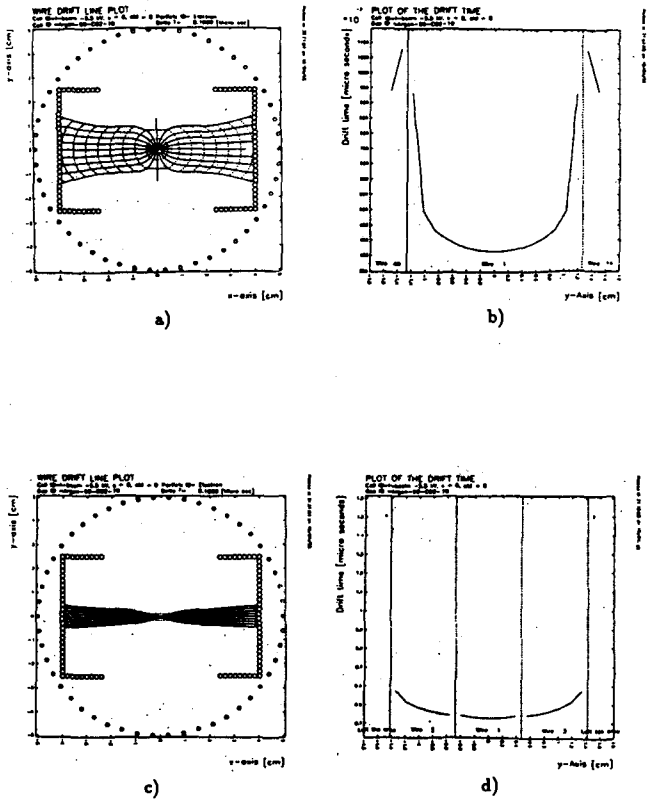
WIRE DRIFT LINE PLOT
x-axis [cm]
y-axis [cm]
a)
PLOT OF THE DRIFT TIME
Drift time [micro seconds]
y-Axis [cm]
b)
WIRE DRIFT LINE PLOT
x-axis [cm]
y-axis [cm]
c)
PLOT OF THE DRIFT TIME
Drift time [micro seconds]
y-Axis [cm]
d)

Figure 14.

SDC Intermediate Muon System

May 1992, KEK
D. Carlsmith

- configuration – integration issues
- special layout ; mechanical issues
- plans for design ; prototype

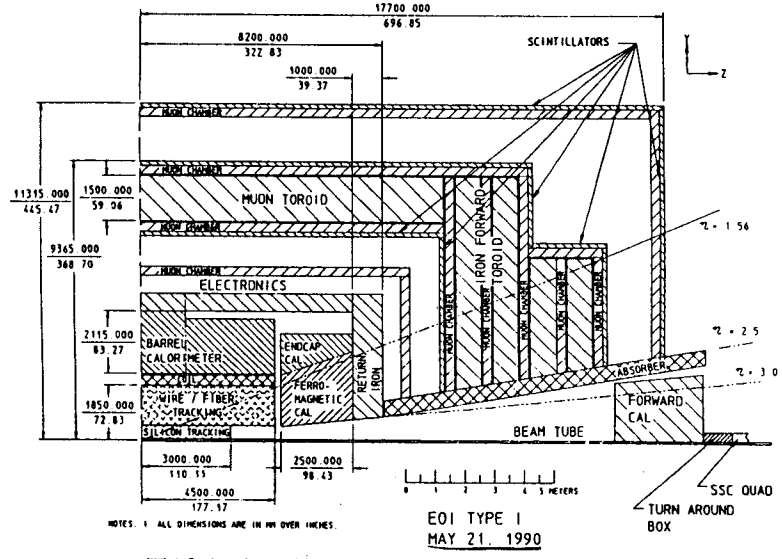

FIG. 4. Quadrant plan view of the short-coil solenoidal detector with iron-laced endcap calorimeters (Type-I). This drawing also shows an iron toroid for the intermediate-angle muon system, an alternative to the air-core toroids shown in Figs. 3 and 5.

TDR

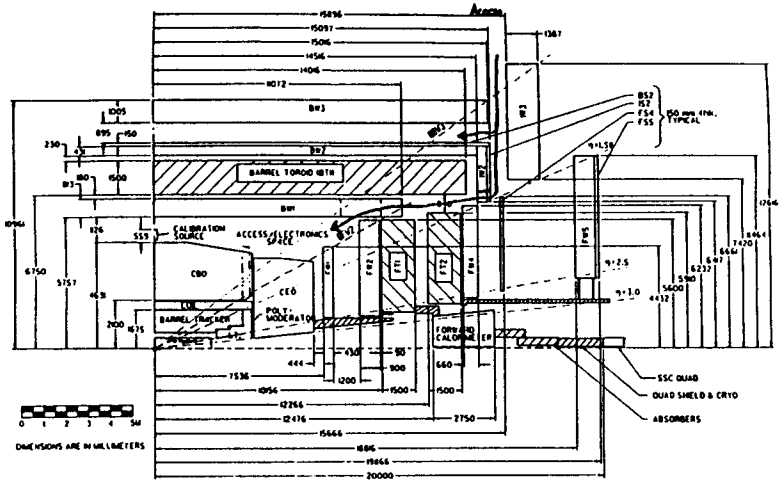

History: FW5 closer in + Ĉ ⇒ access from side

FIG. 2-7. Layout of the muon system.

Question: what holds up IW's ?

Interesting answer!

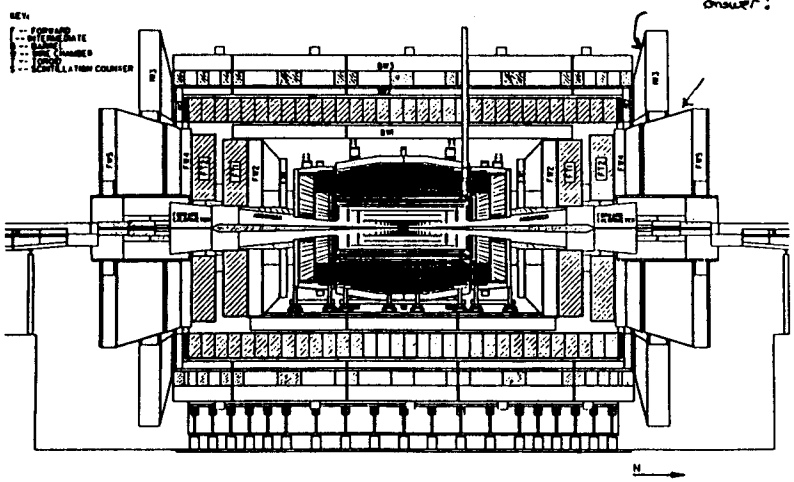

FIG. 2-2. Elevation view of the preliminary baseline detector configuration.

1673

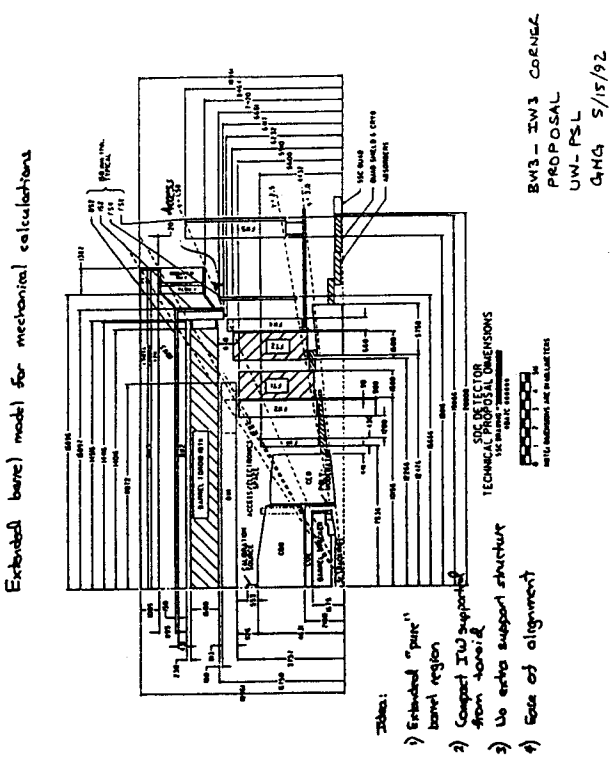

1674

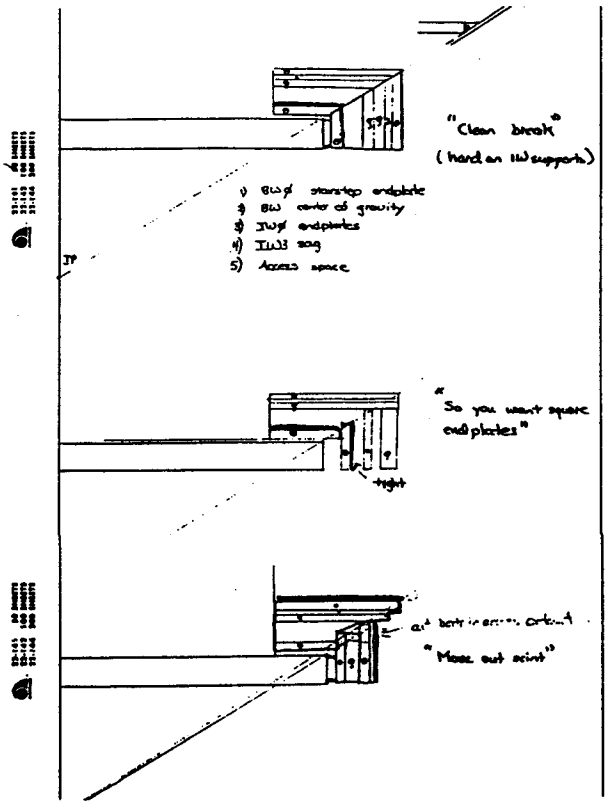

1675

Results to date:

- toroid end is crowded but there is room for mounts
- preliminary FEA ⇒ can make rigid IW2 / IW3 tower cantilevered on quasi kinematic support — FF
- the barrel can hang out — C.D.
- there are many variants of the configuration with possibly improved coverage <u>especially if scint ⇒ outside</u>

1676

Fabrication Issues.

IW2

Straightforward
Build off-site

IW3
- Many different φ tube lengths
  ⇒ special setup time ; inventory confirmation
  Tube committee take note!
- Bass end φ endplates half moons at different angles
  ⇒ special machining requirements
- φ module assembly

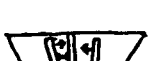

or

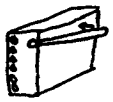

Do we need pin end "lesson" support?
Do we need glued spacers?

- 4θ + 2S + 8φ = 14 layers
  Can we hold the tolerances

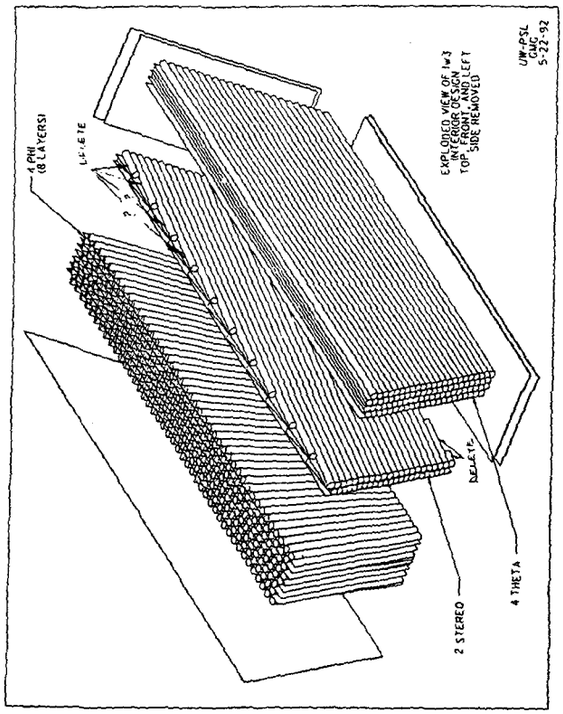

Agenda for this meeting

- blessing to procede with extended barrel/compact IW design
- select model (s) for further analysis
  - extend barrel a bit more to maximize "pure" barrel region
  - move scint outside so assembly? (review access; upgrade path)
  - violate Cherenkov upgrade space! (violated by scint support)
- Schedule

			Person weeks
92-93	Design stage task list	Physicist	24
		System Eng.	11
		M.E.	186
		E.E.	27
		Drafting	71
93-94	Construct prototypes in parallel with barrel		

1679

Forward System

Andris Skuja
(University of Maryland)

1680

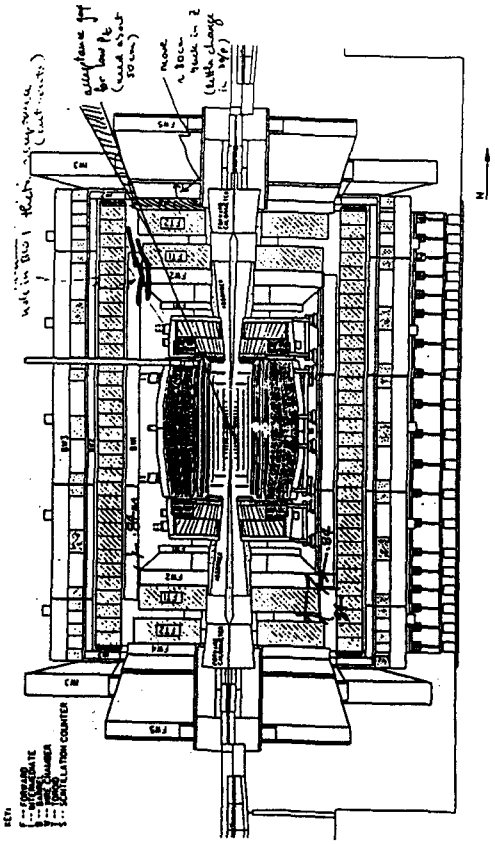

1681

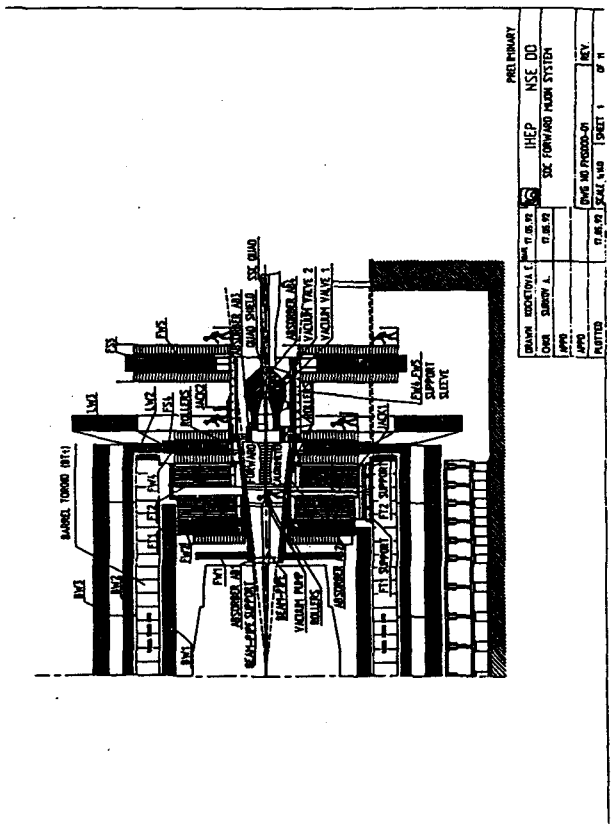

1682

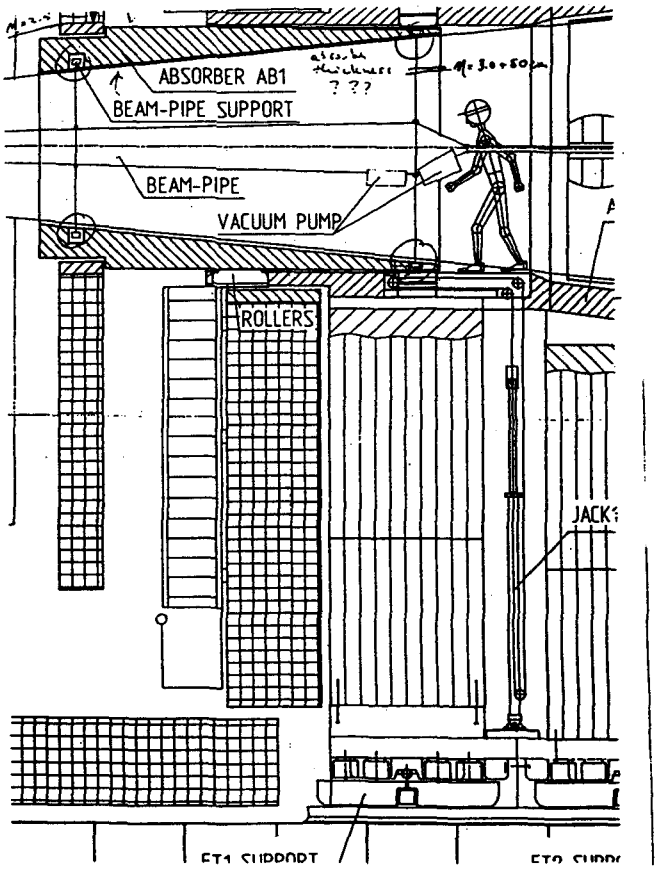

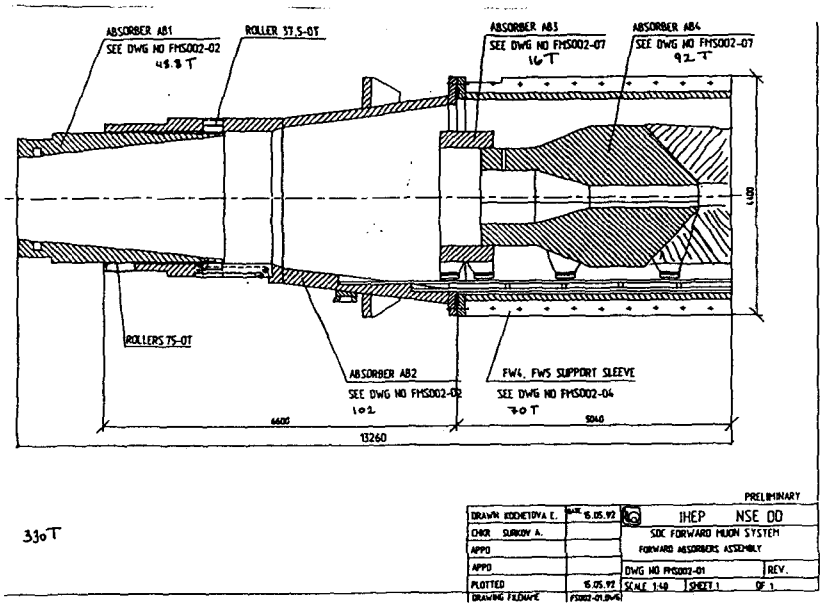

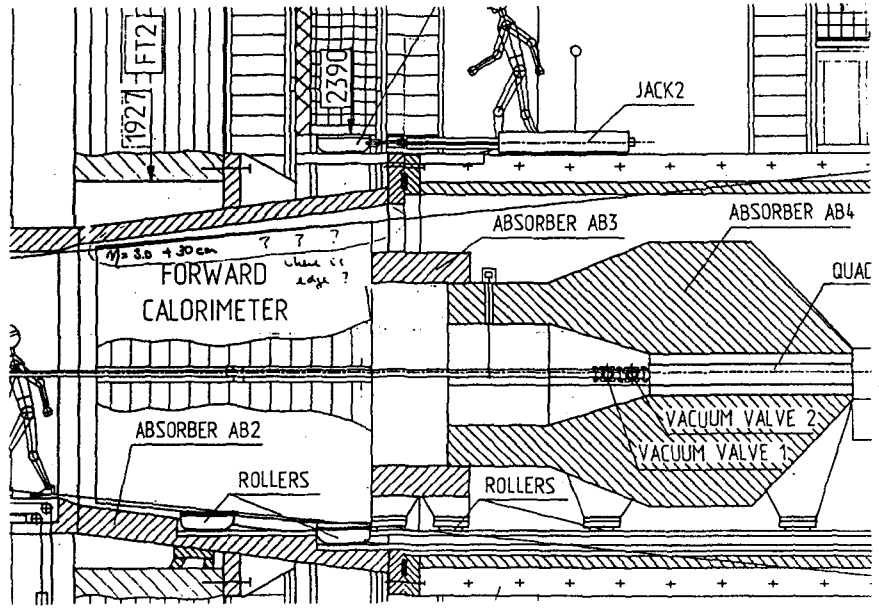

Acceptance gap for low Pt at 26°
($P_t \gtrsim 10$ GeV)

We may have to extend FWS by ~ 50 cm
FW4 by ~ 20 cm

A detailed proposal will be made at the August SDC meeting.

SSCL has estimated of opening shaft to 11m x 18m ≈ $220K

This would allow assembly of FWS on surface

(according to Frank Dawson)

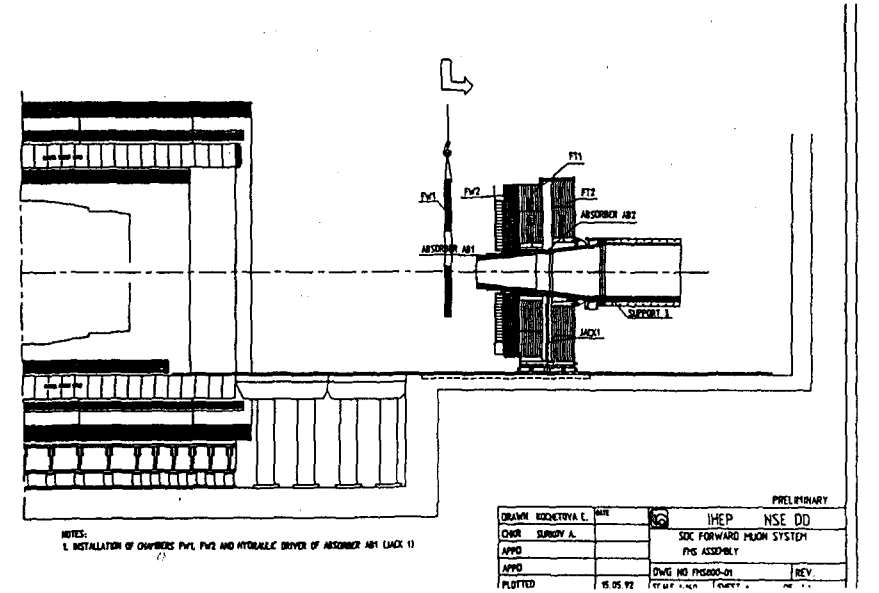

Labor Estimate

Charles M. Grinnel
(SSCL)

Configuration Definitions

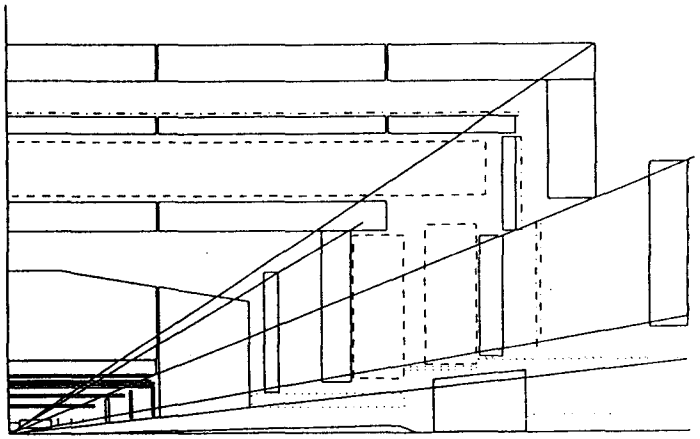

ROUGH ESTIMATE OF FY93 DESIGN BUDGET

WBS	DESCRIPTION	# OF QUARTERS FISCAL YEAR	TOTAL # OF QUARTERS DESIGN	% OF TOTAL DESIGN BUDGET	TOTAL DESIGN* BUDGET (m/d)	FY93 DESIGN BUDGET (m/d)	FY93 DESIGN BUDGET (m/y)
3.2.1	Drift Tubes	4	5	80 %	11,973	9,578	38
3.2.2	Support Structure	4	7	57 %	1,475	843	3
3.2.3	Alignment	4	11	36 %	1,757	639	3
3.2.4	Handling Fixtures	4	5	80 %	718	574	2
3.2.5	Local Utilities	4	8	50 %	237	119	0
3.2.6	Scintillator	4	5	80 %	1,323	1,058	4
3.2.7	Supermodule	4	9	44 %	7,737	3,439	14
3.2.8	Gas System	4	0	n.a.	2,682	n.a.	n.a.
3.2.9	Transportation	4	0	n.a.	168	n.a.	n.a.
3.2.10	Spares	4	0	n.a.	7	n.a.	n.a.
3.2.11	Prototypes	4	0	n.a.	1,223	n.a.	n.a.
					29,300	18,250	65

GRP	DESCRIPTION	# OF QUARTERS FISCAL YEAR	TOTAL # OF QUARTERS DESIGN	% OF TOTAL DESIGN BUDGET	TOTAL DESIGN* BUDGET (m/d)	FY93 DESIGN BUDGET (m/d)	FY93 DESIGN BUDGET (m/y)
A	Barrel System Design	4	5	90 %	12,937	10,350	41
B	Intermediate System Design	4	9	44 %	3,144	1,397	6
C	Forward System Design	4	11	36 %	8,581	2,388	10
D	Alignment System Design	4	11	36 %	1,759	640	3
E	Trigger System Design	4	5	80 %	1,324	1,059	4
F	Services	4	0	n.a.	2,682	n.a.	n.a.
G	Support Systems Design	4	11	36 %	886	322	1
H	Coordination	4	11	36 %	7	3	0
					29,300	16,156	65

* Includes all EN, EA, DR and AD mandays, excluding TE
Note: At this time (92May21) the # of Quarters is an estimate to achieve equality with chart above.

Top Level (Design) Labor Estimate Comparision

1. Top Level	Source	EN M/W	EA M/W	DR M/W	MP tot M/W
A. Barrel System Design	Colin	83	27	40	120
B. Intermediate System Design	Fashid	200	100	75	375
C. Forward System Design	Frank	0	0	0	0
D. Alignment System Design	Dave	0	0	0	0
E. Trigger System Design	Rudy	0	0	0	0
F. Services	Dick	107	53	19	179
G. Support Systems Design	Jim G.	48	24	14	86
H. Coordination	Charlie	66	33	16	117
Manpower Subtotals:		474	237	162	873
		54 %	27 %	19 %	100 %

	Unit	EN	EA	DR	AD	MP tot
A. Barrel System Design	M/D	6,519	3,259	1,085	2,074	12,937
	M/W	1,304	652	217	415	2,587
B. Intermediate System Design	M/D	1,581	791	262	510	3,144
	M/W	316	158	52	102	629
C. Forward System Design	M/D	2,313	1,656	552	1,040	6,561
	M/W	663	331	110	208	1,312
D. Alignment System Design	M/D	861	431	144	321	1,757
	M/W	172	86	29	64	351
E. Trigger System Design	M/D	666	333	112	212	1,324
	M/W	133	67	22	43	265
F. Services	M/D	1,363	682	227	410	2,682
	M/W	273	136	45	82	536
G. Support Systems Design	M/D	443	222	74	147	886
	M/W	89	44	15	29	177
H. Coordination	M/D	0	0	0	7	7
	M/W	0	0	0	1	1
Manpower Subtotals:	M/D	14,746	7,374	2,456	4,722	29,298
	M/W	2,949	1,475	491	944	5,860
		50 %	25 %	8 %	16 %	100 %

Barrel System Design Labor Estimate Comparision

A. Barrel System Design	Source	EN M/W	EA M/W	DR M/W	MP tot M/W
A. Tube Design (see barrel)	Collin	8	6	0	0
B. Function/Test (QA/QC) (see barrel)	Collin	0	9	9	0
C. Module Design	Collin	17	9	32	58
D. Tower Design	Collin	36	19	9	63
Subtotal C + D		53	42	38	162
E. Services (onboard)	Collin	0	9	0	0
no equivalent					
no equivalent					
no equivalent					
Manpower Subtotals:		53	37	41	121
		44 %	22 %	34 %	100 %

WBS	Description	Unit	EN	EA	DR	AD	MP tot
3.2.1.1	Drift Tubes	M/D	3,992	1,491	497	897	5,837
		M/W	996	299	99	173	1,167
	no equivalent						
3.2.7.1	Module	M/D	2,540	1,270	423	892	3,125
		M/W	508	254	85	179	1,025
3.2.2.1	Support Str	M/D	513	256	85	182	1,016
		M/W	103	51	17	32	203
	Subtotal 3.2.2.2+3.2.7.2	M/D	3,053	1,526	508	1,064	4,141
		M/W	611	305	102	211	1,228
3.2.5.1*	Local Utilities	M/D	54	27	9	18	108
		M/W	11	5	2	4	22
3.2.11**	Prototype	M/D	356	178	59	106	699
		M/W	71	36	12	21	140
3.2.1.4	Tooling	M/D	38	19	6	11	74
		M/W	8	4	1	2	15
3.2.1.5	Shipping Crate	M/D	36	18	6	18	78
		M/W	7	4	1	4	16
		M/D	6,618	3,259	1,086	2,074	12,037
		M/W	1,304	652	217	415	2,587
			50 %	25 %	9 %	16 %	100 %

*split between barrel and intermediate (66/34)
** split between barrel, intermediate and forward (per % of EN total)

5/20/92--8:54 PM page 1 filename: A. Barrel.1

1691

Intermediate System Design Labor Estimate Comparision

B. Intermediate System Design	Source	EN M/W	EA M/W	DR M/W	MP tot M/W
A. Tube Design (see barrel)	Fanshid	37	19	12	68
B. Function/Test (QA/QC) (see barrel)	Fanshid	17	8	2	27
C. Module Design	Fanshid	46	23	25	94
D. Tower Design	Fanshid	37	18	13	68
Subtotal C + D		83	41	38	162
E. Services (onboard)	Fanshid	48	24	17	89
F. Installation	Fanshid	15	8	7	30
Manpower Subtotals:		200	108	76	376
		53 %	27 %	20 %	100 %

WBS	Description	Unit	EN	EA	DR	AD	MP tot
3.2.1.2	Drift Tubes	M/D	890	445	148	259	1,742
		M/W	178	89	30	52	348
	no equivalent						
3.2.7.2	Module	M/D	494	247	82	192	1,015
		M/W	99	49	16	38	203
3.3.2.2	Support Str	M/D	86	43	14	24	166
		M/W	17	8	3	5	33
	Subtotal 3.2.2.2+3.2.7.2	M/D	579	290	96	216	1,181
		M/W	116	58	19	43	236
3.2.5.1*	Local Utilities	M/D	26	13	4	9	52
		M/W	5	3	1	2	10
	no equivalent						
3.2.11**	Prototype	M/D	86	43	14	26	169
		M/W	17	9	3	5	34
		M/D	1,581	791	262	510	3,144
		M/W	316	158	52	102	629
			50 %	25 %	9 %	16 %	100 %

*split between barrel and intermediate (66/34)
** split between barrel, intermediate and forward (per % of EN total)

5/20/92--8:54 PM page 1 filename: B. Intermediate.1

1692

RPC Splution for the SDC Muon Trigger Counter

Salvator R. Amendolia
(University of Pisa)

SDC MUON GROUP
KEK, May 28, 1992

PRELIMINARY BASIC ISSUES ON THE RPC SOLUTION FOR THE SDC MUON TRIGGER COUNTERS

Presented by S.R. Amendolia on behalf of the SDC Italian Group.
Information comes from References on RPC's and from unreferenced test results from Italian colleagues.

RPC = RESISTIVE PLATE COUNTERS
(evolution of the Pestov counters)

REFERENCES

BASIC: "Development of RPC", R. Santonico et al., NIM 187 (1981) 377-380

PROGRESS: "Progress in RPC", R. Cardarelli et al., NIM A263 (1988) 20-25
"Performance of RPC at beam flux up to 140 Hz/cm²", M. Bertino et al., NIM A283 (1989) 654-657

READOUT: "RPC readout system", L. Antoniazzi et al., NIM A307 (1991) 312-315

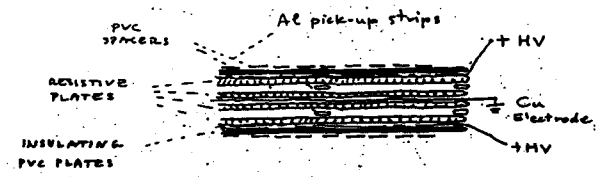

SKETCH OF DOUBLE LAYER RPC

RESOLUTIONS

TIME: 0.5 nsec on a single pad
8-10 nsec integrated on a 2x1 m² detector

SPACE: depends on pad size.
Successfully tested sizes are 6x6, 6x12, 12x12 cm². Above 12x12, pad capacitance degrades signal quality.

DEAD ZONE: due to the discharge originating the signal.
Simple "parallel plate capacitor" formula yield, in accordance with data, a dead zone of 5 mm² for a typical total induced charge of 200 pC at HV = 8000 V.

RECOVERY TIME: due to electrode relaxation time
$\Delta T \simeq \rho\varepsilon \sim 10$ msec

COUNTERS' SIZE

Tests made with 1x2 m² modules.
No counter indications in principle to build 2x2 m² modules, and to join 16 to make a 8x8 m² detector. Has to be tested.

GAS MIXTURE

Tested with Argon : Buthane = 2.5 : 1 + few % Freon

HV

Typically 8-9 kV for the tested modules

EFFICIENCY

$\varepsilon = 97\%$ on single plane, measured with cosmics.

2/3 of missing 3% due to spacers ⇒ 2 planes per module, ORed, staggered not to overlap spacers, give $\varepsilon = 99\%$ at low rate.

Single plane ε linearly drops with rate, down to $\varepsilon \sim 87\%$ for incoming flux of 90 Hz/cm² (max rate at SDC) ⇒ ORing 2 staggered planes gives $\varepsilon \gtrsim 98\%$.

A further 2% drop in ε is due to correlation of the dead times of two facing pads.

NOISE

With HV = 8 kV, dark currents are 20 μA for 6x6 cm² pads, and 80 μA for 12x12 cm² ones.

With a threshold = 60 mV, stochastic noise for a 2-plane module (1x2 m²) is 0.4 Hz/cm² at HV = 8.2 kV and 1.0 Hz/cm² at HV = 9 kV

ELECTRONICS

Under advanced development.
Single Card includes:

- 16 channels (16 single pads) front-end electronics
- Card test feature
- Remote Control of threshold and signal amplitude
- Trigger logic (to be downloaded on Xilinx PLA)
- 16 shaped output signals for eventual readout into data stream

AVAILABILITY

Industry in Italy provides assembled modules

Electronics Industry in Italy develops (and will provide) front-end and Trigger card

COST

Detector : ~ 800 $ / module / m^2
(2 RPC planes per module, plus frame)

Electronics : not quoted yet
(note ; no amplifiers needed, cost/channel estimated to be sensibly lower than for scintillators' PM + associated electronics. To be verified)

SDC TRIGGER RATES

W. Temple, W. H. Smith, S. Dasu, J. Lackey, T. Gorski
University of Wisconsin

SDC TRIGGER LEVELS

Level 1:
Identify Physics Objects:
- Electrons
- Photons
- Muons
- Taus
- Jets
- Neutrinos
- *Combinations of Above*

Level 2:
Refine Identification of Physics Objects:
- Sharper P_T Cuts
- Electrons From Conversions
- Muons from Decay/Punchthrough
- Refine Energy Sums/Clusters
- Displaced Vertices

Level 3:
Full Physics Analysis/Decisions:
- Specialized Algorithms
- Heirarchy of Decisions
- DST-type cuts on Physics

SDC TRIGGER PRINCIPLES

Philosophy:
- Local:
  - Signatures of e's, γ's, μ's, jets
  - in $\eta \times \phi$ regions
  - (ex: ν's)
- Measurably Efficient:
  - Overlapping Programmable Triggers
  - Prescaled Lower Thresholds
  - Prescaled Triggers w/ less conditions
- Efficient Use of DAQ Bandwidth:
  - Efficient Lepton and Jet Identification
  - Consistency with Offline Cuts

Benchmarks for Trigger Performance:
- e's, μ's from inclusive W's, Z's:
  - 50% efficiency (cut on lepton P_T)
- Jets, γ's at high P_T:
  - 1-2 decade overlap with lower $\sqrt{s}$ data
- Missing E_T:
  - Good efficiency for channels such as:
    - $H \rightarrow 2\ell 2\nu$
    - SUSY particles
- Low P_T multileptons:
  - B Physics

LEVEL 1

Electrons & Photons:
Find (.1 x .1) Cal Towers with E_{em} > Thr
Require E_{hac}/E_{em} < .10 - .15
Option: Pattern of surrounding quiet towers (isolation)
γ's: Match w/Shower Max in $.2\eta \times .2\phi$
e's: Find Outer Track Segments w/P_T > 10 GeV/c
- Match Track Segments w/Shower Max in ϕ in 1/64
- Assign $\Delta\eta$ = 0.2 from Shower Max to Track
- Match Track w/Cal on $\Delta\eta$=0.2, $\Delta\phi$=0.2

Muons:
Muon Tracks from Scint + θ-layers w/P_T > 10 GeV/c
Option: Find Central Tracker Sgmts w/P_T > 10 GeV/c
- Match w/Muon ϕ-layer Track Sgmts in 1/64
- Use Momentum cut on Central Tracker P_T cut
- (Use Scint to associate ϕ and θ tracks)
- Match Track w/Quiet Cal on $\Delta\eta$=0.2, $\Delta\phi$=0.2

Jets:
1.6 x 1.6 grids of overlapping towers > E_{thr}

Neutrinos:
Sum Missing E_T over .1 x .1 Towers > E_{thr}

LEVEL 1 TRIGGER STUDIES: CALORIMETER

Rate:

Level 1 Rate Target = 30 KHz
15 KHz each for Cal. and Muon Triggers

Calorimeter:

Total rate is sum of:

- single e's
- single γ's
- pairs: ee, eγ, γγ
- jets
- $\not{E}_T$

☞ Target Rate of 3 KHz for single object triggers

Procedure:

Background Rates:

- QCD 2-jet events: 20 - 400 GeV P_T
- mixed with minimum bias events
- run through hardware simulation

Find threshold for e, γ, jet, $\not{E}_T \Rightarrow$ 3 KHz
Examine threshold vs. trigger conditions
Examine efficiency vs. E_T

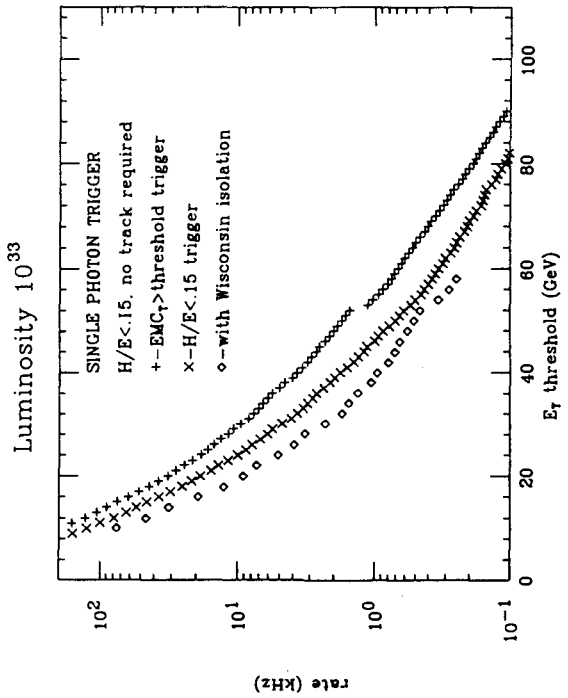

Figure 6

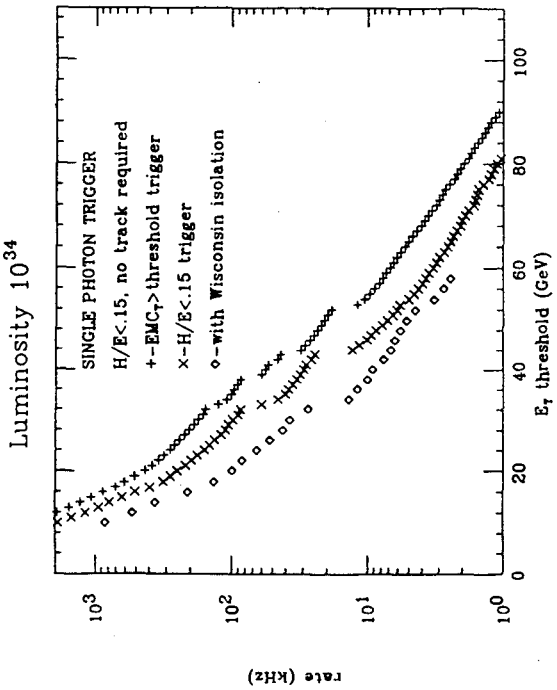

Figure 8

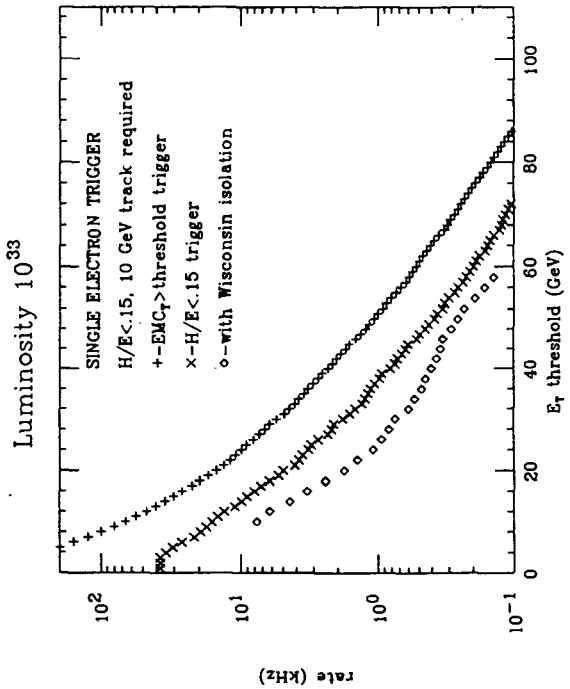

Figure 9

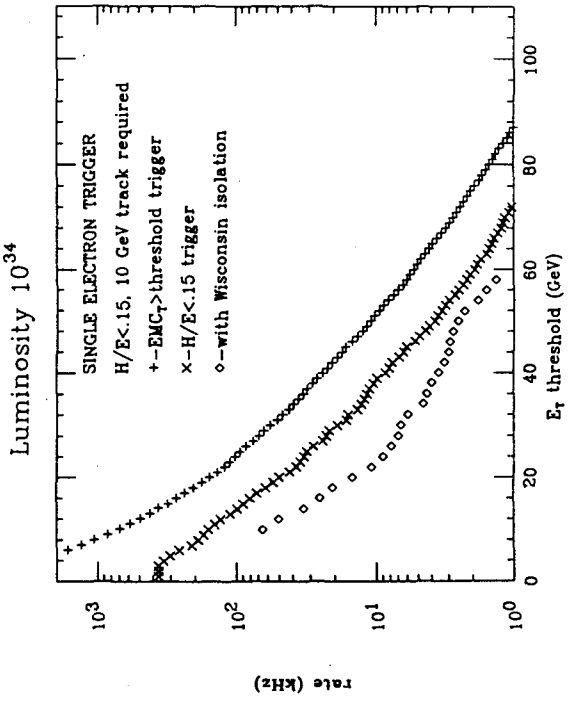

Figure 9

LEVEL 1 TRIGGER STUDIES: MUONS

Rate:

For Muon System, total rate is sum of:

- single μ's
- pairs: $\mu\mu, \mu e, \mu\gamma$
- energy: μ & jet, μ & $\not{E}_T$

☞ Target Rate of 5 KHz for single muon triggers

Procedure:

Determine Prompt and Decay Rates
Simulate Muon Trigger Circuit ($\delta T \rightarrow P_T$ cut)
Determine Threshold Response of Muon Trigger
Fold These together to calculate Trigger Rate

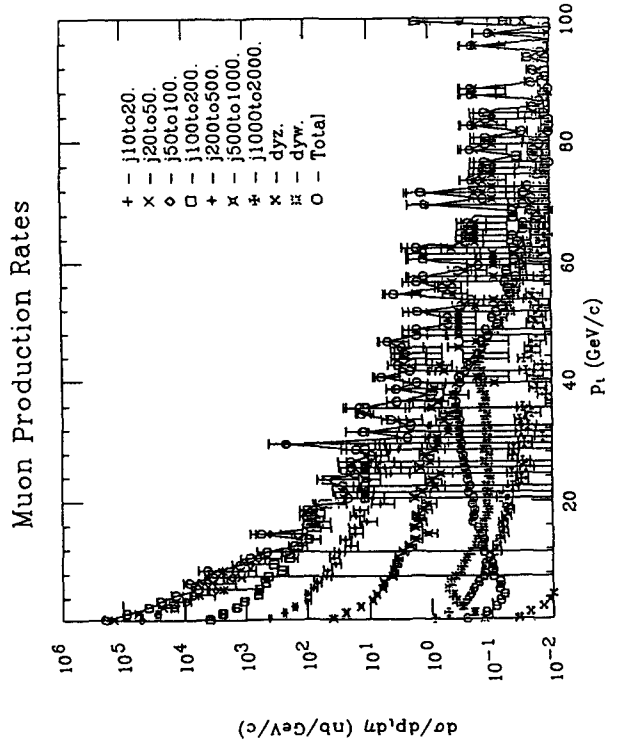

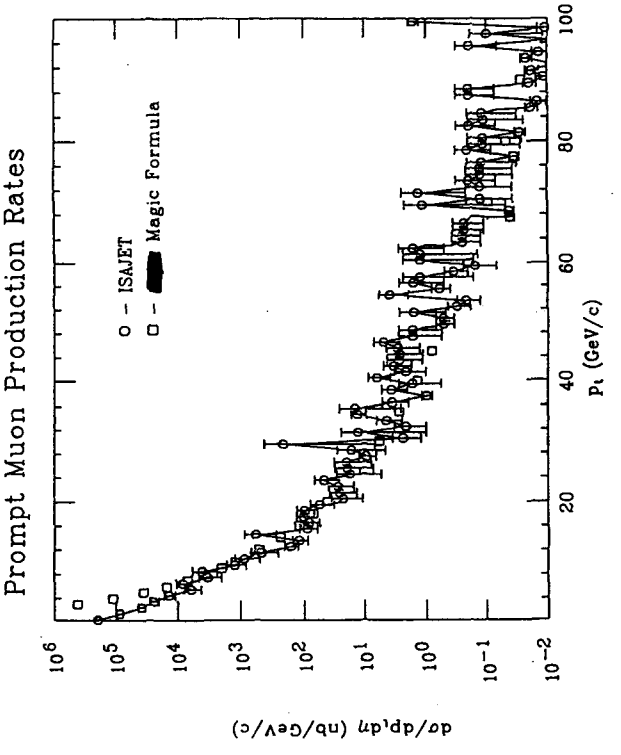

1710

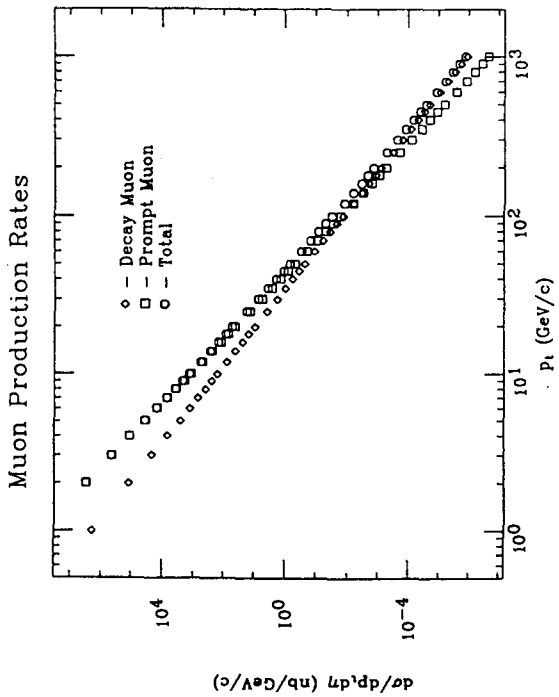

1711

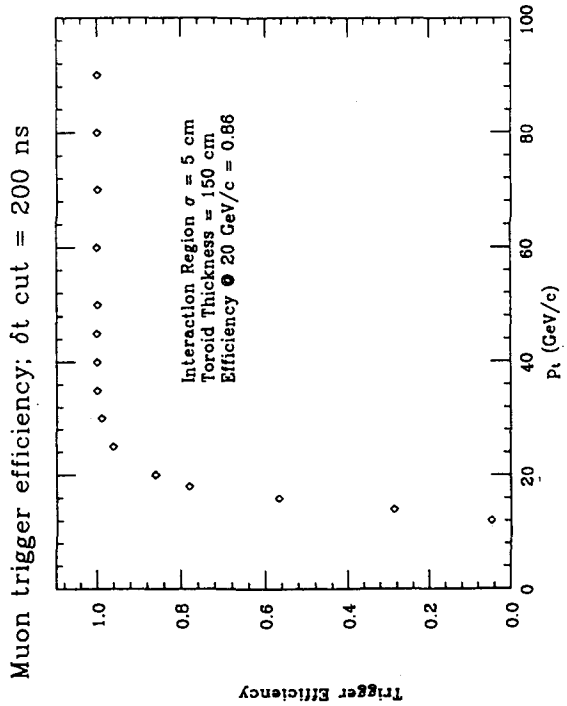

1712

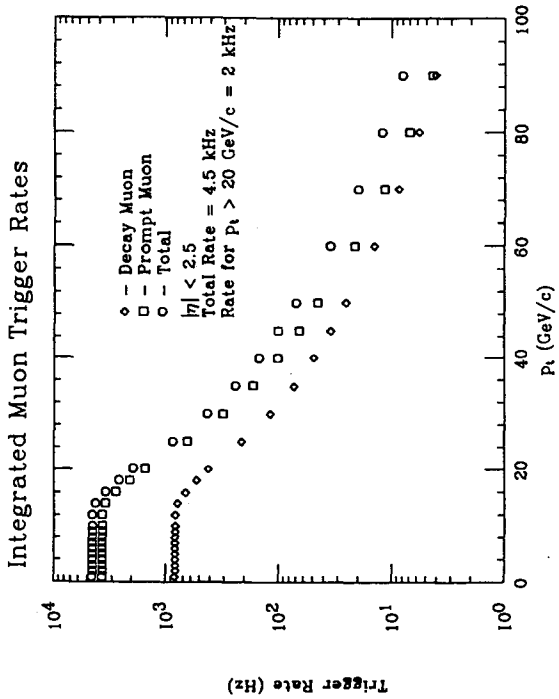

1713

Representative level 1 trigger E_t thresholds.

Trigger	Threshold
Electron	20 GeV
Photon	30 GeV
Two electrons	10 GeV
Two photons	20 GeV
Missing E_t	80 GeV
Single Tower Hadron (.1 × .1)	60 GeV
Jet (1.6 × 1.6 sum)	140 GeV
Muon	20 GeV

Steve Errede
Jim Wiss
Univ. Illinois
April 6, 1992
SDC-92-238

Physics Impact of Phi Cracks in the SDC Barrel Muon System

Abstract

This note summarizes studies of the physics impact/ramifications associated with phi cracks at the octant boundaries in the SDC barrel muon system for the 93 mm o.d. θ and ϕ tubes.

Detailed Monte Carlo simulations of various physics processes have been carried out, simulating the phi cracks associated with the SDC barrel muon system, for BW1-BW3 superlayers. The geometrical information associated with the phi cracks in the BW superlayers was kindly provided by Colin Daly of the University of Washington, and are shown in figs 1 & 2.

The input data to the SDC muon Monte Carlo simulation program consisted of a.) a random isotropic distribution of $P_T = 50\ GeV/c$ mono-chromatic muons, b.) muons from $W \to \mu\ \nu_\mu$ decay from ISAJET, c.) muons from $Z^0 \to \mu^+\mu^-$ decay from ISAJET, d.) muons from $Z'/DY \to \mu^+\mu^-$ decay from ISAJET, for muon pair masses of $M_{pair} = 200, 500\ GeV/c^2$, e.) muons from $ZZ \to 4\mu$ decay from ISAJET, f.) muons from $H \to ZZ \to 4\mu$ decay from ISAJET, for $M_H = 400\ GeV/c^2$ and $M_H = 800\ GeV/c^2$. The SDC muon Monte Carlo simulation program then transported the muons through the various B-field regions of the SDC detector (solenoid and barrel toroid), and included MCS, dE/dX loss in the barrel calorimeters, BW superlayers, the barrel muon toroid, as well as the detailed geometrical aspects of the SDC muon system.

Table I summarizes the % acceptance loss as calculated (analytically) for infinite momentum tracks, associated with the ϕ and θ views for each of the BW superlayers, and the fiducial acceptance, ϵ for muons passing completely through all three BW muon superlayers. Table II summarizes the % acceptance loss for $P_T = 50\ GeV/c$ mono-chromatic muons associated with the ϕ and θ views for each of the BW superlayers, and the fiducial acceptance, ϵ for muons passing completely through all three BW muon superlayers. Table III summarizes the % acceptance loss and overall acceptance for muons from $W \to \mu\ \nu_\mu$ production and decay. Table IVa summarizes the % acceptance loss and fiducial acceptance for muons from $Z^0 \to \mu^+\mu^-$ production and decay. Table IVb summarizes the % acceptance loss and fiducial acceptance for one and for both muons from $Z^0 \to \mu^+\mu^-$ production and decay. Table Va summarizes the % acceptance loss and fiducial acceptance for muons from $Z'/DY \to \mu^+\mu^-$ production and decay. Table Vb summarizes the % acceptance loss and fiducial acceptance for one and for both muons from $Z'/DY \to \mu^+\mu^-$ production and decay. The muon pair mass is $M_{pair} = 200\ GeV/c^2$. Table VIa summarizes the % acceptance loss and fiducial acceptance for muons from $Z'/DY \to \mu^+\mu^-$ production and decay. Table VIb summarizes the % acceptance loss and fiducial acceptance for one and for both muons from $Z'/DY \to \mu^+\mu^-$ production and decay. The muon pair mass is $M_{pair} = 500\ GeV/c^2$. Table VIIa summarizes the % acceptance loss and fiducial acceptance for muons from $ZZ \to 4\mu$ production and decay. Table VIIb summarizes the % acceptance loss and fiducial acceptance for 1-4 muons from $ZZ \to 4\mu$ production and decay. Table VIIIa summarizes the % acceptance loss and fiducial acceptance for muons from $H \to ZZ \to 4\mu$ production and decay. Table VIIIb summarizes the % acceptance loss and fiducial acceptance for 1-4 muons from $H \to ZZ \to 4\mu$ production and decay. The Higgs mass is $M_H = 400\ GeV/c^2$. Table IXa summarizes the % acceptance loss and fiducial acceptance for muons from $H \to ZZ \to 4\mu$ production and decay. Table IXb summarizes the % acceptance loss and fiducial acceptance for 1-4 muons from $H \to ZZ \to 4\mu$ production and decay. The Higgs mass is $M_H = 800\ GeV/c^2$.

Conclusions

These studies indicate that for the present design of the SDC barrel muon BW superlayers, there are $\sim 5\%$ acceptance losses associated with single muons, i.e. the single muon fiducial acceptance is $\sim 95\%$. This result is relevant for e.g. mapping out the inclusive single muon P_T spectrum, and for e.g. $W \to \mu\ \nu_\mu$ physics and e.g. $t - \bar{t} \to 1\mu + X$ physics. The losses in the $\phi-$tubes are highly correlated with the $\theta-$tube losses due to the dead space regions at the octant boundaries of the SDC barrel muon system. For processes such as $Z^0 \to \mu^+\mu^-$, there are $\sim 10\%$ losses associated with losing one, or both muons. The Z "golden" di-muon fiducial acceptance is $\sim 90\%$. Note that the Z results are approximately that obtained from squaring the % losses for e.g. muons from W decay. We also remind the reader that these losses not only impact physics results at the offline data-analysis level, but also at the trigger level. Muons from W will come in on the single-muon trigger, whereas muons from Z can come in on both the single muon and di-muon triggers. However, we do not trigger on muons not passing through the muon chambers. Similarly, for $ZZ \to 4\mu$, there are $\sim 20\%$ losses associated with losing one or more muons. The ZZ "golden" 4-muon fiducial acceptance is $\sim 80\%$. For $H \to ZZ \to 4\mu$, for $M_H = 400\ GeV/c^2$, there are again $\sim 20\%$ losses associated with losing one or more muons. The Higgs "golden" 4-muon fiducial acceptance is $\sim 80\%$. Note that to the statistical accuracy of the MC input data, no more than 2 muons per event are lost in ϕ and/or θ cracks. For $H \to ZZ \to 4\mu$, for $M_H = 800\ GeV/c^2$, there are again $\sim 20\%$ losses associated with losing one, or more muons. The Higgs "golden" 4-muon fiducial acceptance is $\sim 80\%$. A very small percentage of 3-muons are lost in ϕ and/or θ cracks in the sub-sample of C+C + C+C Higgs-to-4 muons events. Note that one expects to observe some (Higgs) mass dependence on these muon crack-acceptance results due to the kinematical correlations associated with the $H \to ZZ \to 4\mu$ production/decay process. Here again, to good approximation, the 4-muon losses are obtained by simply squaring the 2-muon losses.

We also remind the reader of the fact that the overall acceptance due to losses in the BW muon superlayers from ϕ (and other) cracks is a multiplicative factor on the geometrical/kinematical acceptance for muons from a particular physics process, even being produced in the central region of the detector in the first place. These geometrical/kinematical acceptances have been studied and discussed in previous SDC notes, see e.g. SDC-92-220 for futher details.

At the offline data-analysis level, following very closely upon the type of analyses that we routinely do on CDF for e.g. $Z^0 \to \mu^+\mu^-$ physics, the muons that do not pass through the acceptance of the BW muon superlayers can easily be recovered, as long as their momenta is well-measured in the CTD, and placing an additional requirement that their be the characteristic minimum-ionizing energy deposition signature in the calorimeter. On CDF, this "CMIO" requirement is sufficient to obtain an extremely clean dimuon sample from Z and/or high-mass Drell-Yan muon pairs. The efficiency for the "CMIO" minimum ionizing signature for high-P_T muons e.g. from $Z^0 \to \mu^+\mu^-$ on CDF has been measured to be $\epsilon_{cmio} = 98.7\%\ +0.3\%\ -0.4\%$ (CDF note 1301). We have no backgrounds, e.g. from QCD in such event samples. Cosmic ray dimuons in the mass region of interest can be potentially worrisome. They are only troublesome for dimuon pairs produced with $X_f = 0.0$ .AND. $P_T(pair) = 0.0$. In addition, if there is precise timing information, e.g. from the BW muon scintillators and/or from the barrel calorimeter, as well as precision track impact parameter information e.g. from the inner tracker silicon micro-strips, the cosmic ray backgrounds in dimuon samples can be (very) highly suppressed.

For the tetra-muon physics processes, at the offline data-analysis level, the muons lost in ϕ and/or θ cracks can be recovered as "CMIO" muons with very high efficiency. The efficiency for triggering on e.g. 2 out of 4 muons with a di-muon trigger is also high ($\epsilon_T > 90\%$), so these events should at least make it to tape with reasonably high probability.

It is also useful to compare the present design for the SDC barrel muon system with e.g. the CDF central muon system, which has cracks every 15 degrees in ϕ and in the 90 degree "blue-sky" region in θ. The CDF single muon acceptance in the central region is $\sim 75\%$. We have suffered no serious detrimental effects from the $\sim 25\%$ acceptance losses due to ϕ and θ, etc. cracks in the central region of the CDF detector in carrying out e.g. W and Z physics, searching for the Top quark (in the muon channel) at $\sqrt{s} = 1.8\ TeV\ \bar{p}-p$ collisions. To make up for these losses, one can compensate simply by running a little bit longer, increasing the integrated luminosity of the overall data sample, since the number of true signal events for a particular physics process is given by:

$$N_{true} = N_{obs} - N_{bkgnd} = \sigma * BR * \int \mathcal{L} \cdot dt * A * \epsilon$$

Where A is the overall acceptance and ϵ is the overall efficiency for a given physics process.

Thus, for 99.999% of all muon physics, the acceptance losses associated with the ϕ cracks in the BW barrel muon chambers at the octant boundaries present no significant compromise to the physics processes anticipated at the SSC. The only situation where one might wish for "perfect" coverage is for the special case of "Zoo" events, where one would like to know absolutely everything about a particular event, e.g. a lepto-quark candidate, including the nature of e.g. high-P_T tracks disappearing into regions of poor (or no) detector acceptance. Usually these events obey at least one of Murphy's laws for high energy physics, "seeking" out such regions of the detector with uncanny accuracy!

Table I

Single Muon Acceptance - Analytic

	ϕ View	θ View
BW1 Loss	4.59%	5.67%
BW2 Loss	3.63%	3.85%
BW3 Loss	2.67%	3.29%
ϵ	95.41%	94.33%

Table II

50 GeV Mono-Chromatic Muons

	ϕ View	θ View
BW1 Loss	4.1% ± 0.7%	5.3% ± 0.8%
BW2 Loss	3.7% ± 0.6%	3.7% ± 0.6%
BW3 Loss	2.5% ± 0.5%	3.4% ± 0.8%
ϵ	95.9% ± 0.7%	94.7% ± 0.8%

Table III

$W \rightarrow \mu\ \nu_\mu$ Acceptance

	ϕ View	θ View
BW1 Loss	4.5% ± 0.6%	5.6% ± 0.7%
BW2 Loss	3.6% ± 0.6%	3.8% ± 0.6%
BW3 Loss	2.7% ± 0.5%	3.1% ± 0.5%
ϵ	95.5% ± 0.8%	94.4% ± 0.7%

Table IV

$Z^0 \rightarrow \mu^+\mu^-$ Acceptance
C+C muons only

	ϕ View	θ View
BW1 Loss	4.1% ± 0.3%	5.2% ± 0.3%
BW2 Loss	3.3% ± 0.3%	3.5% ± 0.3%
BW3 Loss	2.3% ± 0.2%	2.9% ± 0.3%
ϵ	95.9% ± 0.3%	94.8% ± 0.3%

	ϕ View	θ View
1μ Loss	6.8% ± 0.9%	8.2% ± 0.9%
2μ Loss	0.8% ± 0.3%	1.1% ± 0.4%
ϵ_0	92.4% ± 0.9%	90.7% ± 1.0%
ϵ_1	93.2% ± 0.9%	91.8% ± 0.9%
ϵ_2	99.2% ± 0.3%	98.8% ± 0.4%

Table V

$Z'/DY \rightarrow \mu^+\mu^-$ Acceptance
C+C muons only
$M_{pair} = 200\ GeV/c^2$

	ϕ View	θ View
BW1 Loss	4.2% ± 0.3%	5.6% ± 0.3%
BW2 Loss	3.2% ± 0.3%	3.6% ± 0.3%
BW3 Loss	2.2% ± 0.2%	2.8% ± 0.2%
ϵ	95.8% ± 0.3%	94.4% ± 0.3%

	ϕ View	θ View
1μ Loss	6.1% ± 0.8%	7.4% ± 0.9%
2μ Loss	1.1% ± 0.4%	1.8% ± 0.5%
ϵ_0	92.8% ± 0.9%	90.8% ± 0.9%
ϵ_1	93.9% ± 0.8%	92.6% ± 0.9%
ϵ_2	98.9% ± 0.4%	98.2% ± 0.5%

Table VI

$Z'/DY \rightarrow \mu^+\mu^-$ Acceptance
C+C muons only
$M_{pair} = 500$ GeV/c^2

	ϕ View	θ View
BW1 Loss	4.2% ± 0.3%	5.3% ± 0.3%
BW2 Loss	3.3% ± 0.2%	3.6% ± 0.2%
BW3 Loss	2.2% ± 0.2%	2.9% ± 0.2%
ϵ	95.8% ± 0.3%	94.7% ± 0.3%

	ϕ View	θ View
1μ Loss	6.0% ± 0.7%	7.0% ± 0.7%
2μ Loss	1.5% ± 0.4%	2.3% ± 0.4%
ϵ_0	92.5% ± 0.7%	90.7% ± 0.8%
ϵ_1	94.0% ± 0.7%	93.0% ± 0.7%
ϵ_2	98.5% ± 0.4%	97.7% ± 0.4%

Table VII

$ZZ \rightarrow 4\mu$ Acceptance
C+C + C+C muons only

	ϕ View	θ View
BW1 Loss	4.4% ± 0.2%	5.6% ± 0.2%
BW2 Loss	3.6% ± 0.2%	3.7% ± 0.2%
BW3 Loss	2.6% ± 0.2%	3.2% ± 0.2%
ϵ	95.6% ± 0.2%	94.4% ± 0.2%

	ϕ View	θ View
1μ Loss	18.2% ± 1.9%	21.7% ± 2.1%
2μ Loss	1.3% ± 0.7%	1.6% ± 0.7%
3μ Loss	0.2% ± 0.3%	0.2% ± 0.3%
4μ Loss	0.0% ± 0.2%	0.0% ± 0.2%
ϵ_0	80.3% ± 2.0%	76.5% ± 2.1%
ϵ_1	81.8% ± 1.8%	78.3% ± 2.1%
ϵ_2	98.7% ± 0.7%	98.4% ± 0.7%
ϵ_3	99.8% ± 0.3%	99.8% ± 0.3%
ϵ_4	100.0% ± 0.2%	100.0% ± 0.2%

Table VIII

$H \rightarrow ZZ \rightarrow 4\mu$ Acceptance
C+C + C+C muons only
$M_H = 400$ GeV/c^2

	ϕ View	θ View
BW1 Loss	4.6% ± 0.2%	5.8% ± 0.2%
BW2 Loss	3.7% ± 0.2%	3.8% ± 0.2%
BW3 Loss	2.7% ± 0.1%	3.4% ± 0.2%
ϵ	95.4% ± 0.2%	94.2% ± 0.2%

	ϕ View	θ View
1μ Loss	16.2% ± 1.3%	20.3% ± 1.4%
2μ Loss	0.9% ± 0.4%	1.6% ± 0.5%
3μ Loss	0.0% ± 0.2%	0.0% ± 0.2%
4μ Loss	0.0% ± 0.2%	0.0% ± 0.2%
ϵ_0	82.9% ± 1.3%	78.1% ± 1.4%
ϵ_1	83.8% ± 1.3%	79.7% ± 1.4%
ϵ_2	99.1% ± 0.4%	98.4% ± 0.5%
ϵ_3	100.0% ± 0.2%	100.0% ± 0.2%
ϵ_4	100.0% ± 0.2%	100.0% ± 0.2%

Table IX

$H \rightarrow ZZ \rightarrow 4\mu$ Acceptance
C+C + C+C muons only
$M_H = 800$ GeV/c^2

	ϕ View	θ View
BW1 Loss	4.4% ± 0.2%	5.6% ± 0.2%
BW2 Loss	3.5% ± 0.1%	3.7% ± 0.1%
BW3 Loss	2.8% ± 0.1%	3.1% ± 0.1%
ϵ	95.6% ± 0.2%	94.4% ± 0.2%

	ϕ View	θ View
1μ Loss	16.2% ± 0.9%	19.8% ± 1.8%
2μ Loss	1.2% ± 0.3%	1.7% ± 0.3%
3μ Loss	0.1% ± 0.2%	0.1% ± 0.2%
4μ Loss	0.0% ± 0.2%	0.0% ± 0.2%
ϵ_0	82.5% ± 0.9%	78.4% ± 1.0%
ϵ_1	83.8% ± 0.9%	80.8% ± 1.8%
ϵ_2	98.8% ± 0.3%	98.3% ± 0.3%
ϵ_3	99.9% ± 0.2%	99.8% ± 0.2%
ϵ_4	100.0% ± 0.2%	100.0% ± 0.2%

11 May 1992

Study of Loss due to Missed Coverage in the Barrel Muon Detector*

Mourad Daoudi, Uriel Nauenberg, Victor Slonim
University of Colorado

* Research supported by the Department of Energy Contract DE-AC02-86ER40253 and the Texas National Research Laboratory Commission Grants RCFY9102, RCFY9103, and RCFY9205.

Using the process $H^0 \to Z^0 Z^0 \to 2\mu^+ 2\mu^-$ we have studied the loss in detection efficiency due to cracks in the barrel muon octants. We have used two Pythia generated data samples, 5000 events each, and with a Higgs mass of 400 and 700 GeV respectively. The angular coverage in *phi* for each individual muon chamber was taken into account. To first order a track was considered lost in a crack if it missed any single muon chamber; a further investigation of exactly which chambers were missed was done afterwards. This study was performed within the SDC simulation program SDCSIM. In order to speed up the computations only the lead-scintillator calorimeter (AN) and the muon detector (MU) were made active in the simulation; in addition an 18 kG solenoidal magnetic field was used in the central tracking volume.

The type of chamber considered for each barrel muon module is described in the following table. The angular coverage of each octant in *phi* (provided by Colin H. Daly of the University of Washington) for each chamber is included; the chambers

Module	Chambers	ϕ Coverage	Octant 5
BW1	4 *theta*	42°27′	36°13′
	4 *phi*	42°56′	36°52′
BW2	4 *theta*	43°16′	38°42′
BW3	4 *theta*	43°31′	39°41′
	4 *phi*	43°48′	40°13′
	2 *stereo*	43°38′	39°41′

TABLE 1: *Angular coverage in ϕ of the barrel muons chambers.*

in the bottom octant (#5) have a slightly smaller coverage due to space allocated to the support structure.

The number of muons detected (accepted) in the barrel muon system for both a 400 GeV and a 700 GeV Higgs is given in table 2.

# Barrel	400 GeV	700 GeV
0	13.7 %	9.4 %
1	16.4	11.1
2	24.0	29.3
3	23.6	18.6
4	22.2	31.0

TABLE 2: *Muon acceptance in barrel muon system for a Higgs → 4μ with a mass of 400 and 700 GeV.*

The number of muons that were lost in the cracks for each set of chambers is given in the following two tables for the 400 GeV Higgs and 700 GeV Higgs respectively. Overall 83.8 % (82.6 %) of the events from the 400 GeV (700 GeV) Higgs did not have any track missing; while 16.2 % (17.4 %) of the events had one or two missing muons. The number of events with three muons lost is negligibly small (5 events for the 400 GeV Higgs and just one event for the 700 GeV Higgs).

# Lost	All	BW1		BW2	BW3		
		theta	*phi*	*theta*	*theta*	*phi*	*stereo*
0	83.8 %	83.9	86.6	89.3	91.6	93.2	92.4
1	14.6	14.5	12.3	9.9	7.9	6.6	7.3
2	1.5	1.5	1.0	0.7	0.4	0.2	0.2

TABLE 3a: *Number of muons lost in the barrel cracks for a 400 GeV Higgs.*

In these two tables the individual fractions for each muon chamber overlap with one another. Notice that BW2 and BW3 provide a slightly better coverage

than BW1, this is consistent with the values listed in table 1. The breakdown of the numbers given in the second column (under "All") of tables 3a and 3b as a function of the number of muons detected in the barrel is shown in tables 4a and 4b.

# Lost	All	BW1		BW2	BW3		
		theta	*phi*	*theta*	*theta*	*phi*	*stereo*
0	82.6 %	82.7	86.1	89.1	91.6	93.1	92.4
1	16.3	16.2	13.1	10.4	8.0	6.7	7.3
2	1.1	1.1	0.8	0.5	0.3	0.2	0.3

TABLE 3b: *Number of muons lost in the barrel cracks for a 700 GeV Higgs.*

→ Detected ↓ Lost	1	2	3	4
0	767	1016	945	778
1	53	183	214	278
2		4	20	51
3				5

→ Detected ↓ Lost	1	2	3	4
0	510	1261	756	1120
1	46	196	169	391
2		8	6	39
3				1

TABLE 4: *Number of muons lost in cracks as a function of the number of muons detected in the barrel, a) for 400 GeV Higgs, b) for a 700 GeV Higgs.*

From these two tables we can deduce the fraction of events with at least one track missing as a function of the number of muons detected. This is shown in table 5. Thus for the case where all four muons are detected in the barrel about 30 % (28 %) of the events have at least one muon missing for a 400 GeV (700 GeV) Higgs.

# Barrel	400 GeV	700 GeV
1	6.5 %	8.3 %
2	15.5	13.9
3	19.8	18.8
4	29.7	27.7

TABLE 5: *Fraction of events with at least one track lost as a function of the number of muons detected.*

As mentioned above the meaning of "lost" refers to a track that missed any one muon chamber. Below we show in more detail where exactly the muon was lost.

Chambers missed	All		1 Lost		2 Lost	
	Trks	%	*Trks*	%	*Trks*	%
BW1 *theta*	160	17.9	130	17.8	28	18.6
BW1 *theta* + *phi*	152	17.0	125	17.1	24	16.0
BW1 *theta* + *phi* + BW2 *theta*	140	15.7	112	15.3	25	16.6
BW1 *theta* + *phi* + BW2 *theta* + BW3 *theta*	46	5.1	33	4.5	12	8.0
BW1 *theta* + *phi* + BW2 *theta* + BW3 *theta* + *stereo*	40	4.5	34	4.6	6	4.0
BW1 *theta* + *phi* + BW2 *theta* + BW3 *theta* + *phi* + *stereo*	341	38.2	282	38.7	54	36.0
SUM	879	98.4	716	98.2	149	99.3

TABLE 6a: *Number of muons lost in various (combinations of) muon chambers for a 400 GeV Higgs.*

For the 400 GeV Higgs, of the 893 tracks that were lost (from rows 3, 4, and 5 of table 4a) 341 tracks (38.2 %) missed all muon chambers, 312 tracks (34.9 %) were lost in all layers of BW1 (but produced hits in BW2 and BW3), 46 tracks (5.1 %) missed both BW1 and BW2, and 40 tracks (4.4 %) registered hits in the Phi layers of BW3 only. This is summarized in the following table where negligible fractions (< 1%) were omitted (this is reflected by the last row in the table which indicates the sum in each column). In addition, these numbers are given separately for the case where only one muon was missing and the case where two muons in the event were lost in the cracks.

Chambers missed	All		1 Lost		2 Lost	
	Trks	%	*Trks*	%	*Trks*	%
BW1 *theta*	184	20.2	161	20.0	22	21.1
BW1 *theta* + *phi*	164	18.0	148	18.4	16	15.4
BW1 *theta* + *phi* + BW2 *theta*	133	14.6	121	15.0	11	10.6
BW1 *theta* + *phi* + BW2 *theta* + BW3 *theta*	37	4.0	31	3.9	6	5.8
BW1 *theta* + *phi* + BW2 *theta* + BW3 *theta* + *stereo*	39	4.3	34	4.2	5	4.8
BW1 *theta* + *phi* + BW2 *theta* + BW3 *theta* + *phi* + *stereo*	343	37.6	299	37.2	43	41.3
SUM	899	98.7	794	98.7	103	99.0

TABLE 6b: *Number of muons lost in various (combinations of) muon chambers for a 700 GeV Higgs.*

In the case of the 700 GeV Higgs (table 6b), the fraction of tracks lost is similar to the 400 GeV case, except for the fraction of tracks missing BW1 which appears somewhat higher (38.2 % up from 34.9 %).
Note that within statistical fluctuations the losses in any chamber(s) are identical

whether one or two tracks were missing. If we consider the case mentioned above where 30 % of the 400 GeV Higgs events with all four muons detected in the barrel had at least one muon missing, we find from table 6a that only 38.2 % of those events had missed all muon chambers. In other words 11.3 % of the total number of events had at least one muon that did not register any hit in any muon chamber (for the 700 GeV case this number is 10.4 %). This reasoning can be applied to any other set of requirements needed to define a fully detected track in the muon system. A more meaningful interpretation of the losses can then be made of the figures presented in this analysis.

Octant	BW1		BW2	BW3		
	theta	*phi*	*theta*	*theta*	*phi*	*stereo*
# 5	44.7	42.6	47.1	46.2	47.8	46.3
Other	18.4	19.1	17.6	17.9	17.4	17.9

TABLE 7a: *Loss (fraction of tracks lost in %) in octant #5 compared to the average in the other seven octants. The fraction in any given octant is the sum of the relative losses in the two adjacent gaps to it. This table is for a 400 GeV Higgs.*

Octant	BW1		BW2	BW3		
	theta	*phi*	*theta*	*theta*	*phi*	*stereo*
# 5	42.0	43.2	43.5	44.6	46.6	44.6
Other	19.3	18.9	18.8	18.5	17.8	18.4

TABLE 7b: *Same as table 7a, for a 700 GeV Higgs.*

Finally we have made a comparison of the loss in octant #5 (which has a slightly reduced coverage) to the loss in the other seven octants. We find, as indicated by tables 7a and 7b, that the loss in the bottom octant of the detector is about two and a half times greater for all muon chambers. On average 20 to 25 % of the total loss is caused solely by the widening of the gaps around octant 5 to

accomodate the support frame.

In conclusion, we have performed a detailed study of the loss due to missed coverage in the barrel muon detector for a physics process involving exclusively muons in the final state. We have not made any a priori requirement as to which and how many chambers should be hit by a track in order to identify it as a muon. No information from a detector other than the muon system was used in this analysis. For the interesting case where all four muons from the Higgs are detected in the barrel, we estimate a loss of at least 10 %.

SPARSIFICATION STUDY
(WORK IN PROGRESS)

V. SIROTENKO
S. WILLIS

GENERATED 5000 MUONS AT TWO ENERGIES:
50 GeV
500 GeV
WITH AND WITHOUT ELECTROMAGNETIC BACKGROUND

LOOKED AT:
NUMBER OF HITS PER TRACK
NUMBER OF CLEAN* HITS PER TRACK
* A CLEAN HIT IS ONE WHICH IS NOT PRECEDED BY A SECOND HIT CLOSER THAN 5 mm BUT FARTHER THAN 0.5 mm
TIME DIFFERENCE DISTRIBUTION IN PROJECTIVE TRIGGER PAIRS
(NEEDS REFINEMENT)

No sparsification

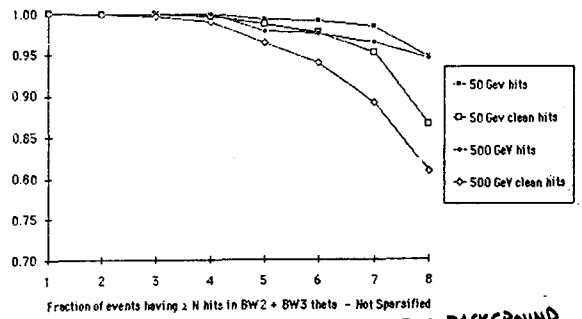

"CLEAN" HITS HAVE NO CONFUSING E.M. BACKGROUND

Page 1

Sparsification effects

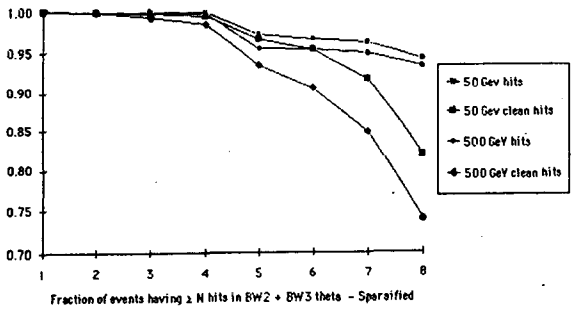

Page 1

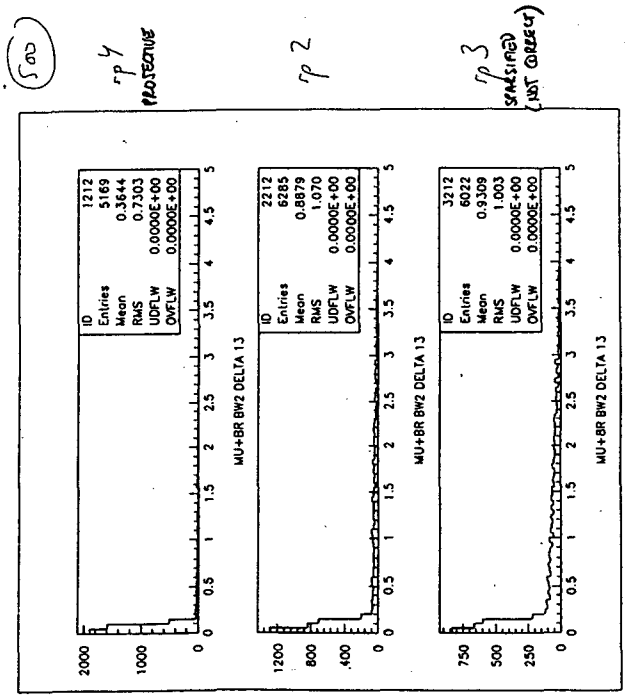

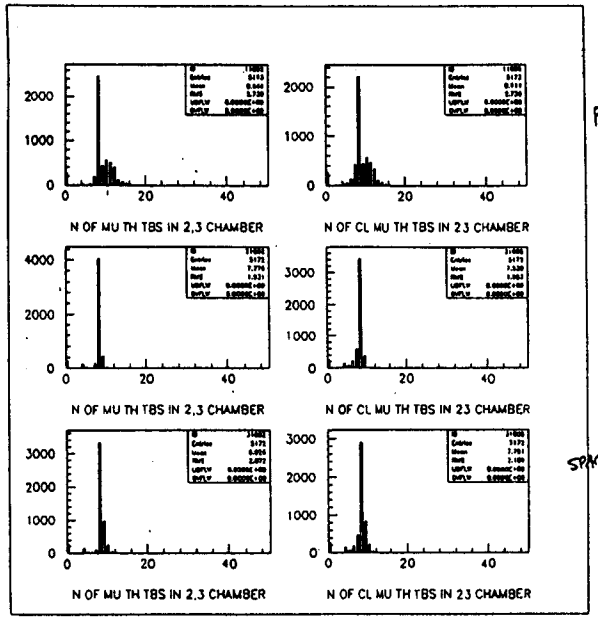

50 GeV

PROJECTIVE

SPARSIFIED

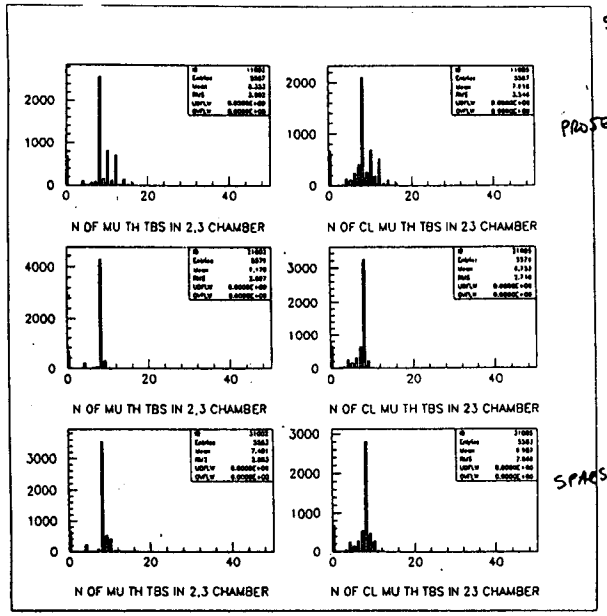

500 GeV

PROJECTIVE

SPARSIFIED

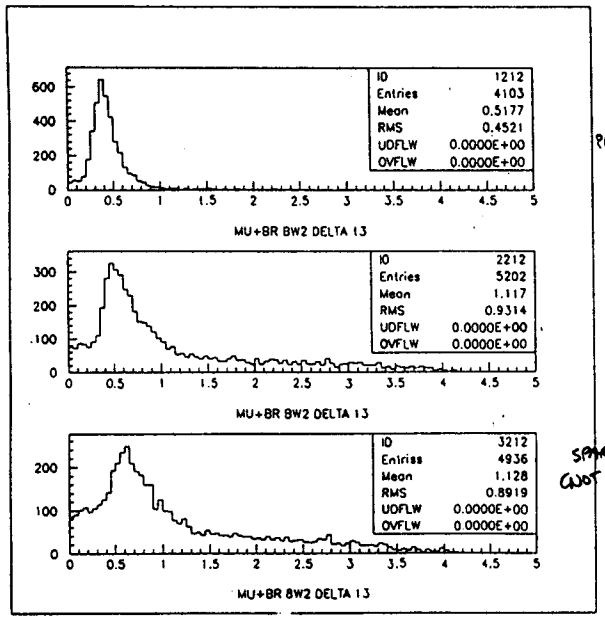

50

rp 4 PROJECTIVE

rp 2

SPARSIFIED (NOT CORRECT) rp 3

1711

Sparsification Study II

Yuzo Asano
(University of Tsukuba)

1712

Sparsified configuration
(9-10 m from the center, Θ=40-43 degree)

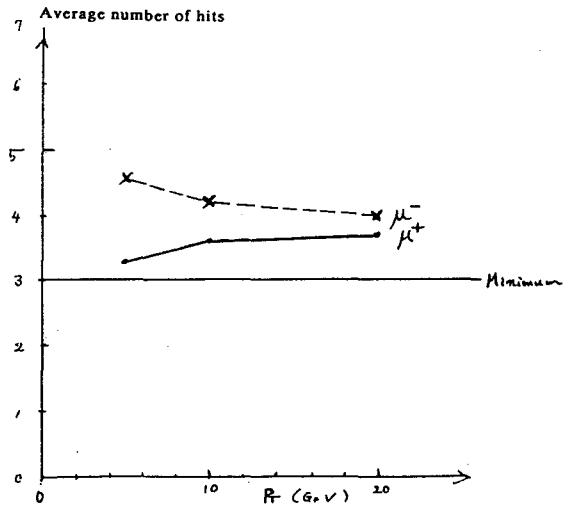

1713

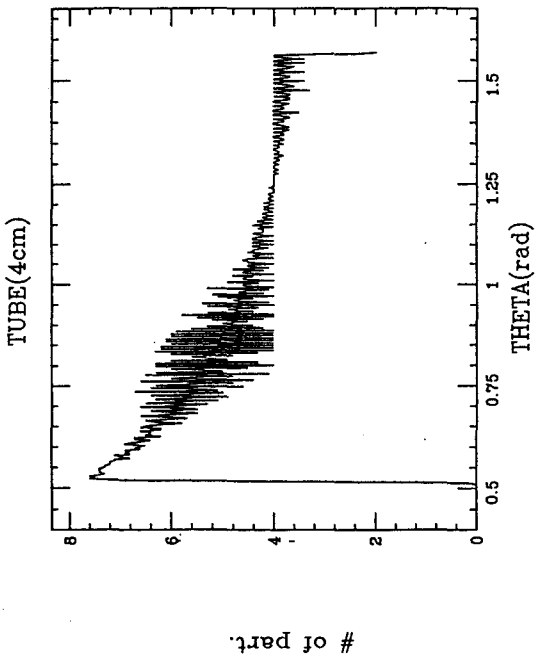

1714

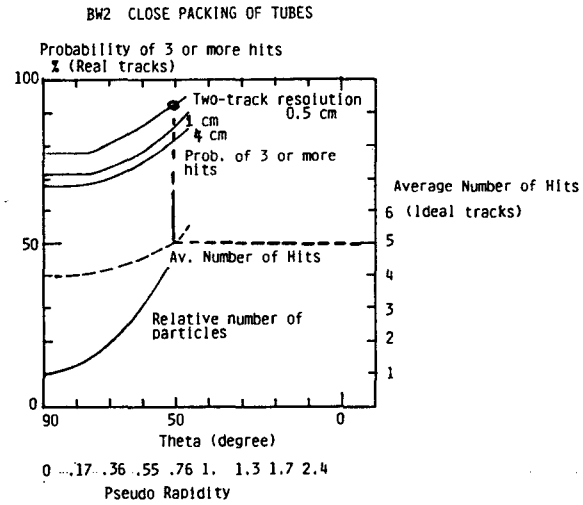

1715

Non-sparsified configuration
(9-10 m from the center, Θ=40-43 degree)

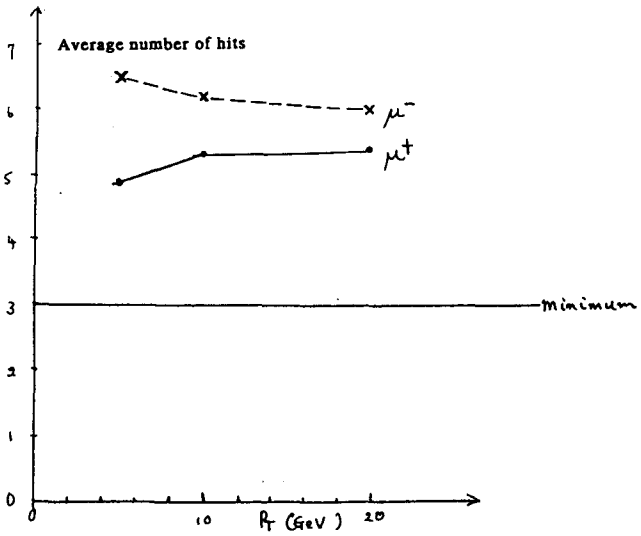

1716

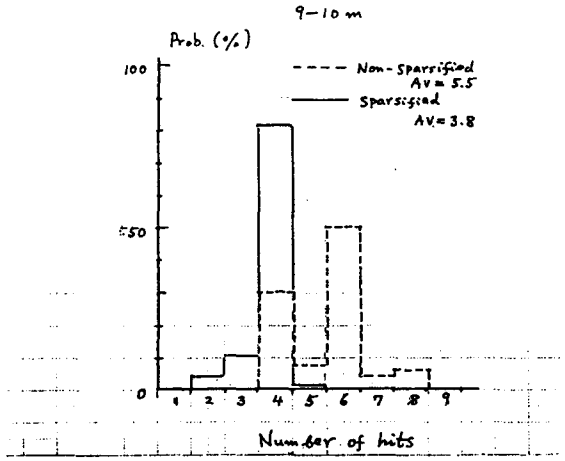

1717

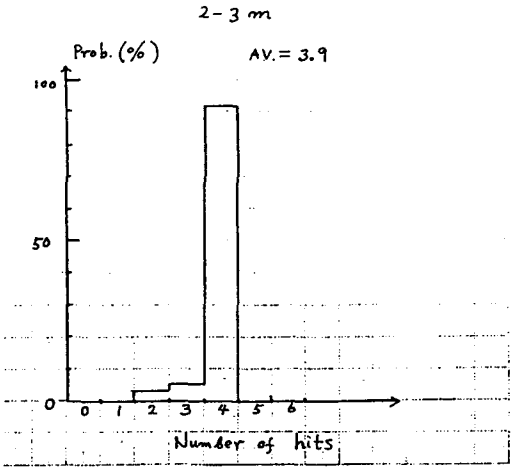

1718

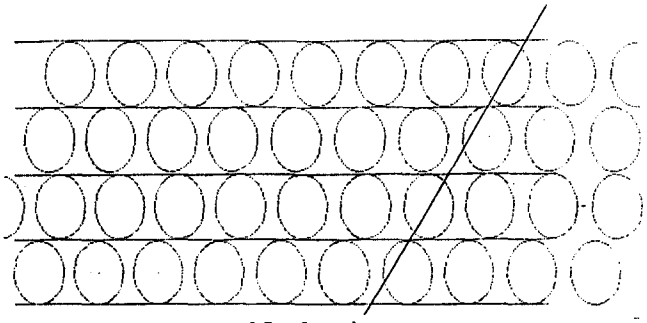

6-7 m from the center
(Θ = 51-55 degree)

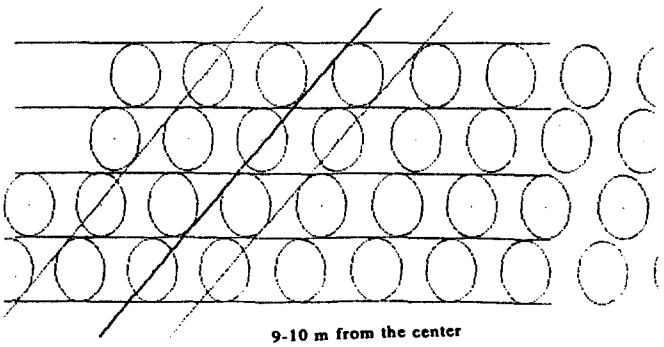

9-10 m from the center
(Θ = 40-43 degree)

Run 43

```
How many events ?? 1000
Give hit mult. to display and max. number ? 2,10
Give Pt in GeV, with the sign of muon? 5
 0  0  12  154  743  84  7  0  0  0 Av. = 3.92 Type task switch?
```

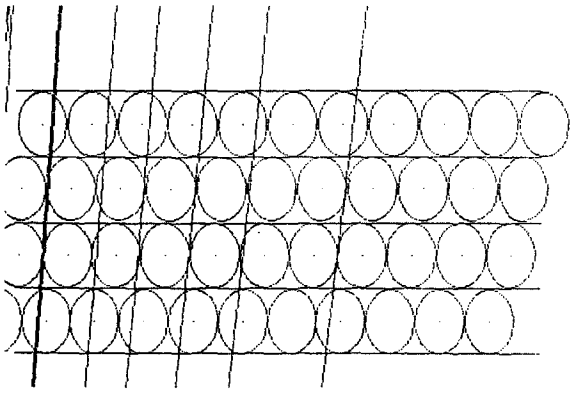

$P_T = 5$ GeV μ^+ tracks

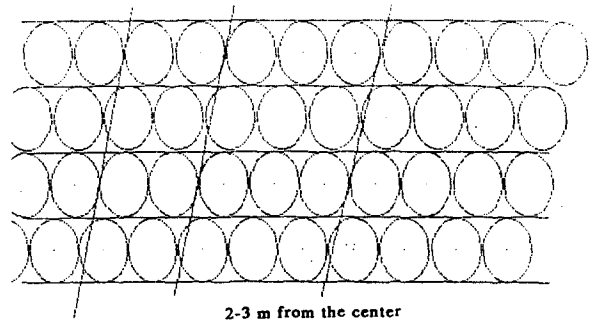

2-3 m from the center
(θ = 71-77 degree)

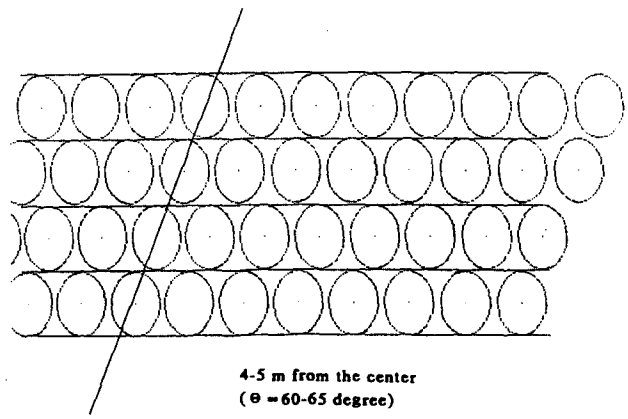

4-5 m from the center
(θ = 60-65 degree)

Tube Sparsification

Sparsified Configuration

1st layer
a track is tangential to 2 adj. tubes on the layer 1.

3rd layer = Projection to 1st layer
2nd layer = 4 cm from 1st layer
4th layer = Projection to 2nd layer

Number of tubes / station
= 7,744

(Closed pack : # of tubes = 9,920)

Reduction of 2176 tube = 22% of closed pack

Average number of hits / station ~ 3.8 tubes throughout
(only geometrical) $P_T = \infty$

But for μ^+, it becomes ~ 3.3 at $P_T = 5$ GeV

We have a large charge dependence of tracking capability for low P_T muons.
One of the charge states has unacceptably low efficiency.

Impact of Sparsification on Muon Trigger / Reconstruction Efficiency with GEANT Simulation

~~KEK~~ Nobuyuki Kanematsu
Osaka University

Contents

1. Introduction
2. Trigger Efficiency
3. Reconstruction Eff.
4. Summary

Introduction

μon interations

- multiple scattering
- energy loss
- δ - rays
- bremsstrahlung
- direct pair production

} at high energy

⋮

To know trigger efficiency, we need simulation.

GEANT simulates all of them.

Three cases were tested.

① $\theta = 90°$
② 45° with sparsification
③ 45° without sparsification

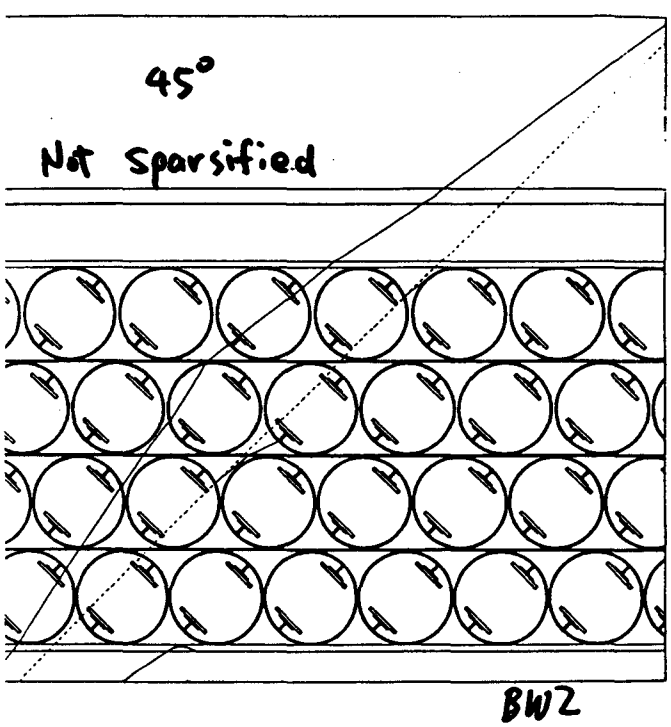

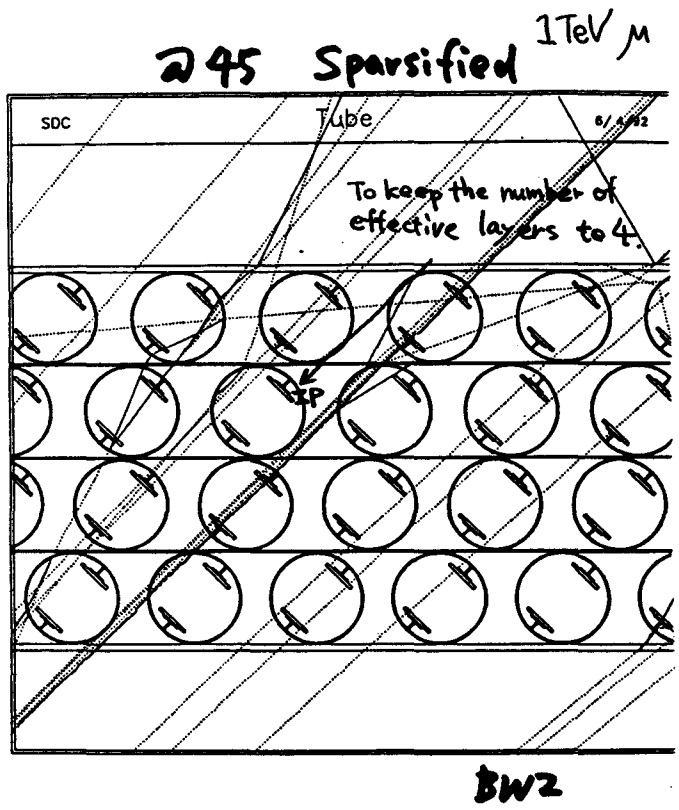

1756

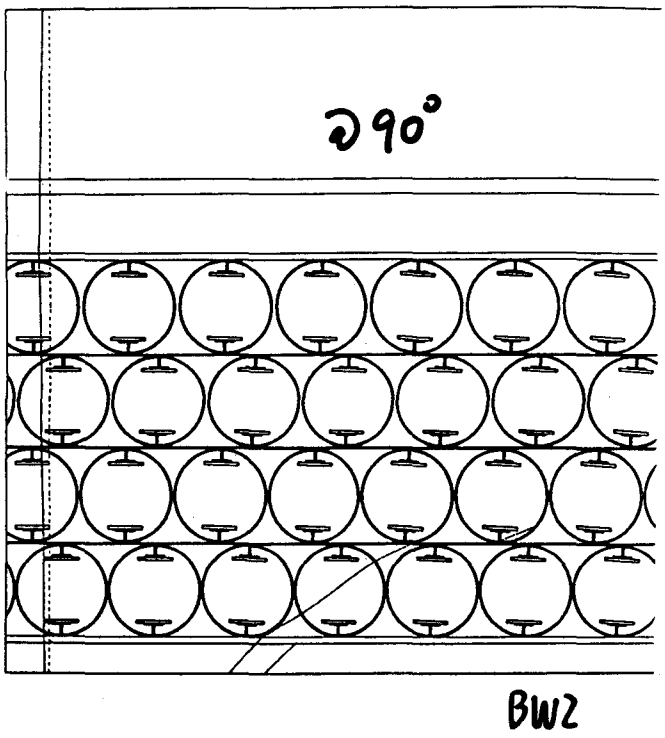

1757

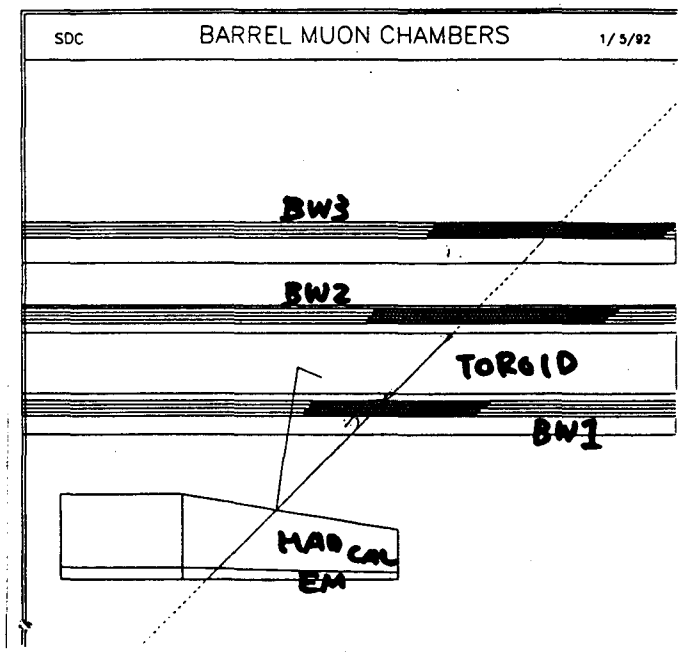

1758

Compilation of $x \to t$.

hit points in the simulation x_i

⇓

$t_i = \frac{|x_i - x_{wire}|}{v_d}$ $v_d = 5\,cm/\mu s$.

with smearing

$\sigma_x \sim 200\,\mu m$ ($\sigma_t = 4\,ns$)

⇓

Digitizing every 2ns.

⇓

Applying dead time.

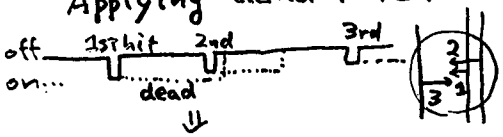

⇓

⇓

row of t's for each wire.

simulated signals

1759

Trigger (ΔT method)

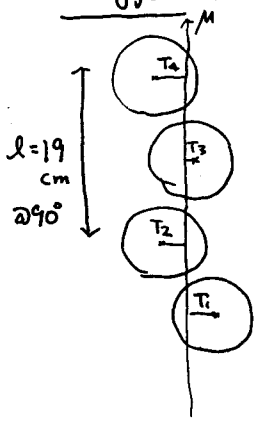

$|T_1 - T_3| < \Delta T_{cut}$

or

$|T_2 - T_4| < \Delta T_{cut}$

$\Delta T_{cut} = \frac{1}{v_d} \frac{l}{\sin\theta} \Delta\theta_{cut}$

$= \frac{1}{v_d} \frac{l}{\sin\theta} \frac{0.7}{P_{t\,thr}}$ (BW2)

↓

20 GeV/c

Level 1 trigger

~ BW2 × BW3

1760

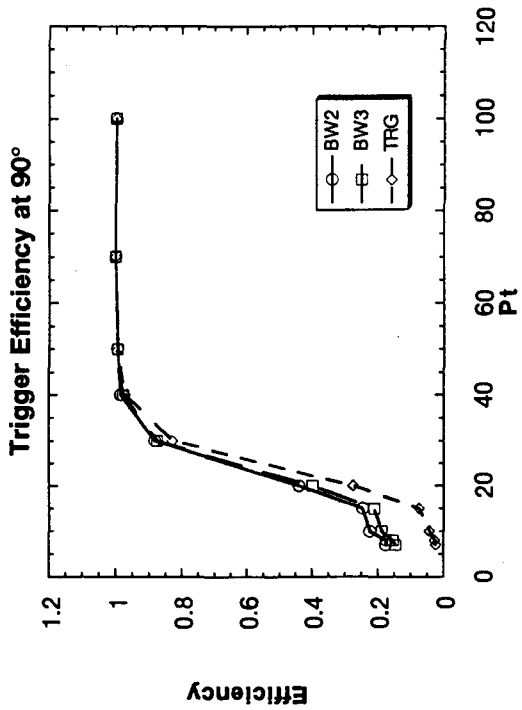

1761

low Pt fake

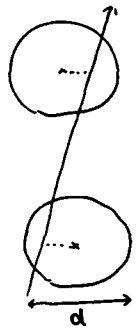

Probability

$p = \frac{v_d \Delta T_{cut}}{d}$

~7% (BW2 90°)

~10% (BW2 45° Spars)

~14% (BW2 45° Not Spars.)

Fake Probability.

2 pairs in a super layer

$p \to 2p$

BW2 × BW3

$0.8\,(2p)^2$ ~ 1.6% (BW2 90°)

↑ 3.2% (BW2 45° sp)

factor $\frac{R_{BW2}}{R_{BW3}}$ for ΔT_{cut} 6.4% (BW2 45° Non sp)

1762

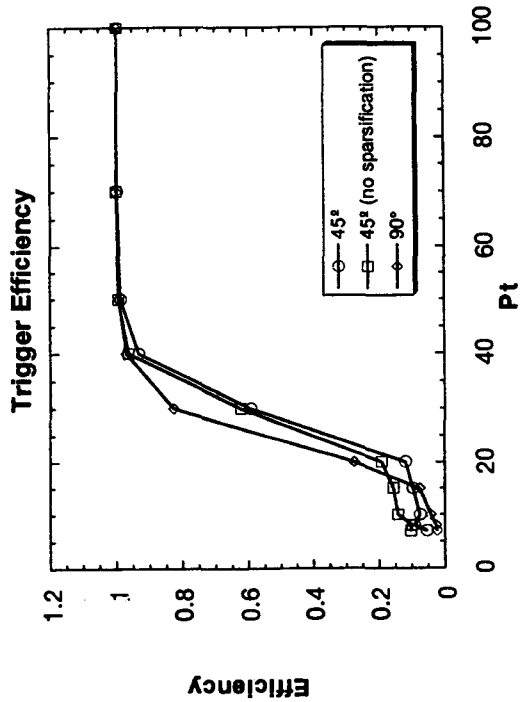

1763

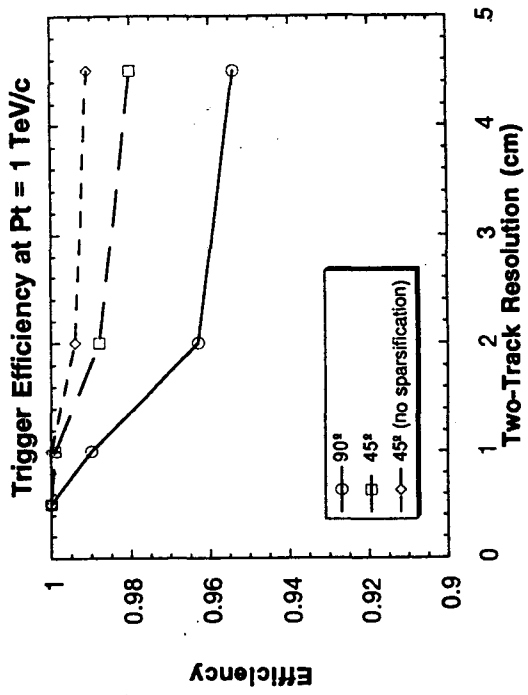

Reconstruction Efficiencies

1. $t \to x$

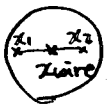

$t \to$

$x_1 = -v_d t + x_{wire}$

$x_2 = v_d t + x_{wire}$.

2. Define a road.

± 1mm road (2mm width) along the μ track given by MC.

3. Count the number of hits on the road in a super layer.

4. Assuming that 3 out of 4 hits in a super layer is enough, we get reconstruction eff.

or

6 out of 8 (BW2/BW3)

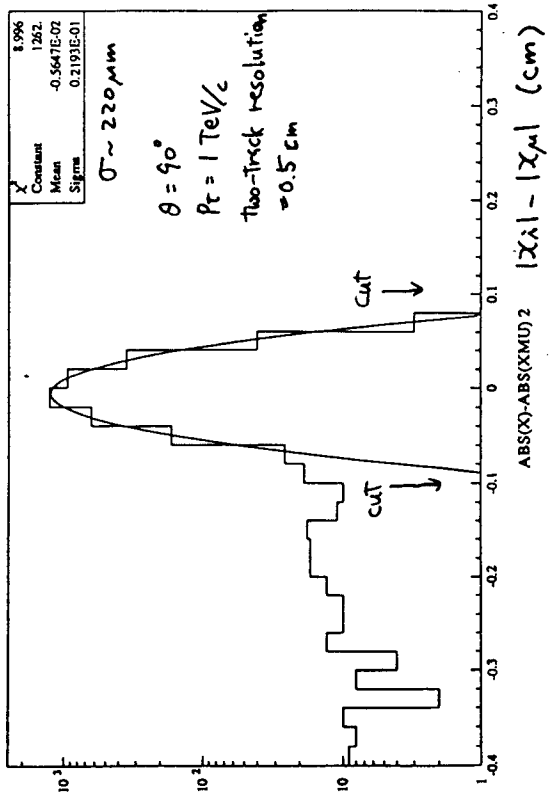

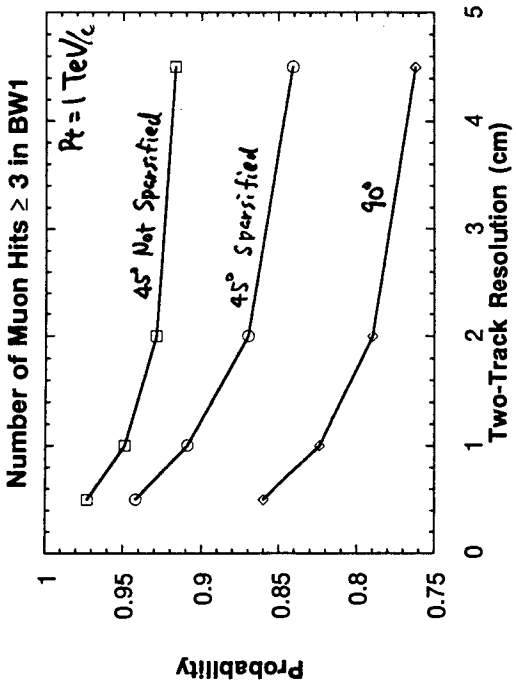

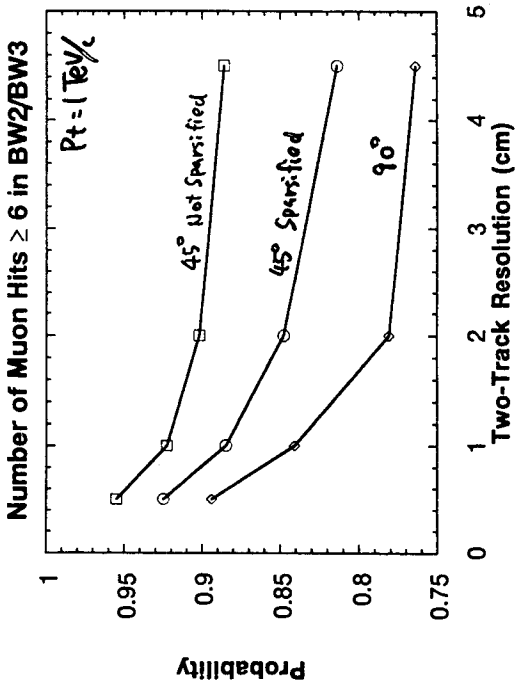

1768

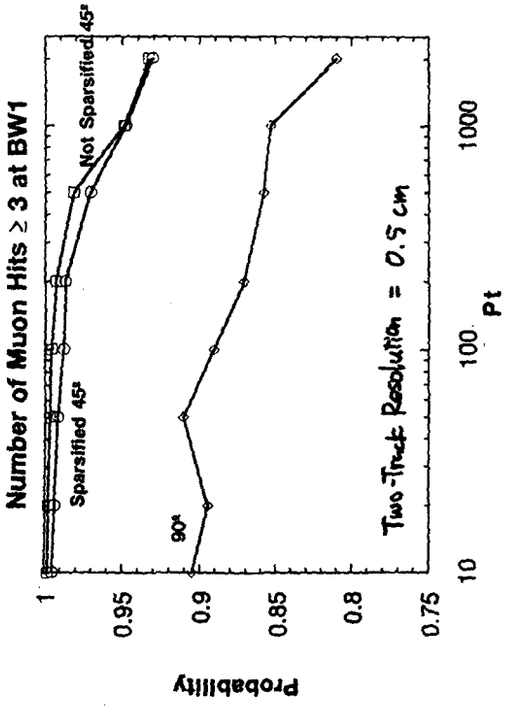

1769

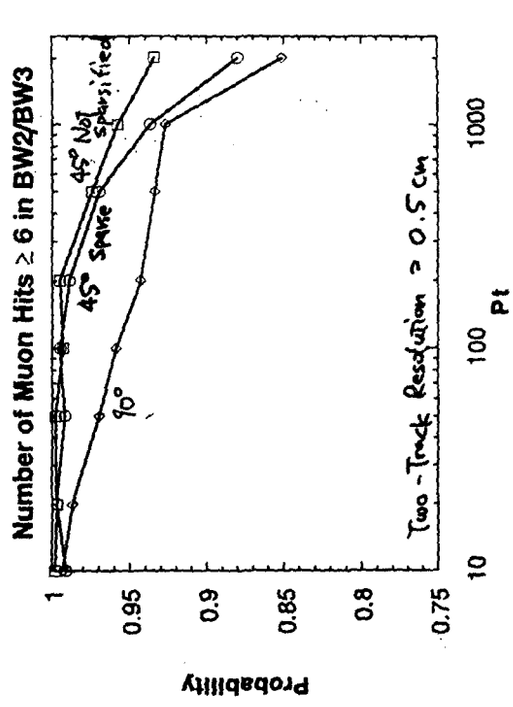

1770

Summary

- Level 1 trigger is efficient up to ~ TeV
- Low Pt fake amounts ≲ 10% for Pt thr = 20 GeV/c
- Reconstruction efficiency will become worse at high energy
- Sparsification will enhance this by ~5% at 2 TeV (BW2/BW3)

Zholobov G.V.

A background computations for SDC set-up at 40 TeV.

IHEP, Protvino, 19/05/1992 Meeting report

I would like to present some results of the Monte Carlo calculated background for SDC experimental setup. Calculations were made by use simulation code, based on GEANT3 and ISAJET program systems. I can't discuss details of simulation code. Only mention, that standard QCD twojet events were generated by ISAJET with jets $5<p_T<150$ GeV/c. GEANT3 kinetic energy cuts were taken equal to 1 MeV.

The side-view of setup is shown in fig.1. The elements shown are: vacuum Pipe, Barrel Calorimeter (CB0), Endcup Caloribeter (CE0), Forward Calorimeter (FCAL), Barrel Toroid (BT1), Forward Toroids (FT1, FT2); drift tube chambers: endcup - FW1, FW2, FW3, FW4, FW5; intermediate - IW2, IW3; central - BW1, BW2, BW3. Scintillator hodoscopes: FS4, FS5, IS2, IS3, BS2, BS3. The quadrupole shield (Collimator) and its absorbers (ABS1, ABS2). Endcup shields (SH1, SH2, SH3) and Cerencov counter FCC.

Due to central computer power limitation it was supposed that Toroids and Calorimeters are absolete absorbers, so that the main background sources are iron Shields and Absorbers, as well as drift chambers and scintillators. Only hadronic part of the shower was allowed to develope in iron shields and absorbers.

1° Vacuum pipe parameters:
Material - Aluminium,
consists of two conic sections,
R_{1min} = 2,6 cm,
R_{1max} = 25 cm,
R_{2min} = 5 cm,
wall thickness varies for tecnical reasons like:
$PIP_T(R) = R/R_{1min} \times 0,1$ cm.

2° Collimator:

R_{min} = 10 cm, R_{max} = 76 cm.

3° ABS1:
R_{min} = 47,5 cm, R_{max} = 80 cm.

4° ABS2:
R_{min} = 15 cm, R_{max} = 47,5 cm,
ABS1_T = ABS2_T = 32,5 cm.

5° Endcup shields:
SH1_T = SH2_T = 40 cm,
SH3_T = 15 cm.

All other dimensions are according to the 9/18/91 D.Shuman deiector dimensions drawing.

Drift tube chambers were considered as homogeneus mixtures of Al(5%) + $ArCO_2$(95%), ρ=0,54 g/cm^3.

The background particle hits into sensitive elements of SDC (exept calorimeters) for a typical 40 TeV event are displayed in fig.2. The listed below results are based on statistic of 408 events.

1. Background sources.

Z_{vert} vs R_{vert} - coordinates of vertices for particles entering sensitive detectors/scintillators are displayed on series of pictures (figs.3+7).

For BW1 background particles mainly come from endcup shields SH1 and SH3, Collimator and its absorbers (ABS1, ABS2), FW1, FW2, FW5 and FS5; IW2, IW3 and IS2, IS3; central part of vacuum pipe, and self.

For BW2, BW3 background particles mainly come from SH3, COLL and ABS1, ABS2; FW4, FS4 and FW5, FS5; IW2, IW3 and IS2, IS3; BW2, BW3 and BS2, BS3.

For FW1 background comes from SH1, FW2 and FW1.

For FW2 the same as for FW1.

For FW3 - from SH2.

For FW4 - from SH3; COLL and ABS1, ABS2; FS4, FW5, FS5, intermediate drift chambers and scintillators.

For FW5 - from SH3; COLL and ABS1, ABS2; FS4, FS5, FW4, FW5, IW2, IW3, IS2, IS3.

For IW2 - from SH3; COLL and ABS1, ABS2; IS2, IW3, IS3, FW5, FS5; FW4, FS4; BW2, BW3; BS2, BS3.

For IW3, FCC - same as for IW2.

For BS2, BS3 - from SH3; COLL, ABS1, ABS2; FW4, FS4; FW5, FS5; IS2, IW2; IS3, IW3; BS2, BW2, BS3, BW3.

For FS4, FS5, IS2 and IS3 - same as for IW2.

Summarizing, it should be stressed that the most pronounced background source is SH3.

2. Secondary interactions vertices inside the main background sources.

a). Vacuum pipe (fig.8).

The two sharp IP symmetric bumps are located at the flanges of the pipe sections. The first small IP symmetric bumps are situated at the tube to cone transitions, and second are due to the rigid rings. The fourth picture - perpendicular to the beam plane projection for x- and y-coordinates.

b). SH1 (fig.9).

The interactions are mainly located at the beam side.

c). SH2 (fig.10).

The main background flux comes from IP side.

d). SH3 (fig.11).

Background flux comes from the collimator side.

e). ABS1 (fig.12).

Background comes from the collimator side. Due to the ABS2 shadow effect there is no sharp degradation with radius.

f). ABS2 (fig.13).

Background comes from the collimator. Sharp increase with Z. A considerable decrease in radius.

g). COLL (fig.14).

Z- and R-distributions look very similar to longitudinal and transverse hadronic shower profiles. Strong degradation in Z (for Z>1850 cm) and R.

3. Interacting particle types and their energy spectra.

The background particle decomposition was booked according their GEANT3 codes, the first of which are:

I	2	3	4	5	6	7	8	9	10	11	12	13	14
γ	e+	e-	ν	μ+	μ-	π0	π+	π-	K0L	K+	K-	n	p

To cover kinetic energy range from 100 KeV upto 10 TeV the following function of E_{kin} was booked:

$y = \log_{10}(E_{kin}/10^{-4})$, then $E_{kin} = 10^{y-4}$ GeV.

a). Pipe (fig.15a,b).

The main particle types are γ, e^+ and e^- - i.e. mainly electromagnetic showers are produced in the pipe walls. Kinetic energy of the pipe products covers a range from 0 upto some hundreds GeV. A mean kinetic energy equals 100 MeV (y≈3). The main bump is due to electromagnetic interactions. Some

particles with E_{kin} below threshold (1 MeV) are seen, they will be stopped by the program at the first tracking step.

b). SH1 (fig.15c,d).

The main interacting particles are neutrons from intrinsic hadron shower. γ, e^+, e^-, μ^+, μ^- are mainly incoming particles. Kinetic energy spectrum spreads upto 10 GeV (y≈5) and has two bumps. The main bump (MeV's) is due to nuclear interactions, the second one in a hundreds MeV region (y≈3+4) corresponds to hadronic interactions. A mean kinetic energy equals to ~10 MeV (y≈2).

The same for SH2 (fig.16a,b).

c). SH3, ABS1, ABS2, COLL (figs.16+18).

Itneracting and produced neutrons are completely dominant. The kinetic energy spectrum is almost completely located below 10 MeV. Neutrons come from intranuclear and internuclear cascades and from nuclear evaporation. Note, that when moving from COLL to ABS2, ABS1 and SH3 kinetic energy becomes softer (from ~8 MeV for COLL upto ~3 MeV for SH3).

4. Endcup trigger hodoscopes FS4 and FS5.

One assumes the counter width to scale as $W=W_0 \sin\theta^{1.35}$ for a constant p_T threshold, W_0≈81 cm. The two layers of scintillators (FS4 and FS5) are aligned such that a ray, extending from the IP through the center of a counter in the first layer, strikes the division between two counters in the second layer. There are 30 counters in FS4 and 31 conters in FS5, matching these conditions.

Z-coordinate distributions of produced in FS4 (fig.19a) and FS5 (fig.20a) particles are flat. Radial distribution for FS4 (fig.19b) has a bell form. For FS5 (fig.20b) it has a bump at the low radius end, and decreases with R. The unnatural form of FS4 radial distribution can be explaned by relatively smaller amount of dense material on the path from Collimator to FS4, pass by ABS1.

From the particle types distributions (fig.21a for FS4 and fig.22a for FS5) it is seen that hodoscopes are mainly hitted by neutrons. Approximately equal amounts of γ's, protons and neutrons are produced inside scintillators (figs.21c and 22c), and all protons and about 13% neutrons are absorbed. The numbers of entering and leaving FS4 (figs.21a, 19d) and FS5 (figs.22a, 20d) particles are approximately equal. About 99% particles have E_{kin}<10 MeV (figs.21b and 22b).

The sharp increase of charged particle counters rates for FS4 (fig.23a) is due to:

a) increase of the counters width,
b) bell form of R-distribution,
c) the fact that only half of FS4 hodoscope overlaps FS5 hodoscope counters.

For FS5 (fig.23b) - natural form. As the result number of triggers quickly increases for higher R counters (fig.23c).

Background particles have a large time delays (fig.24). From the distributions for FS4 and FS5 mean time delay values are 650 ns for FS4 and 490 ns for FS5. Time delay is >>10 ns (time interval between IP events for σ_{tot}=100 mb, $L=10^{33} cm^{-2}s^{-1}$). So that we have continuous in time neutron background. The trigger rate can be calculated using formula:

$$\Omega_B = 2\tau \cdot n_4 \cdot n_5 \quad s^{-1}, \quad \text{where}$$

τ=5 ns - hodoscope time resolution,
n_4 and n_5 - charged particle intensities in FS4 and FS5.

Taking into account the number of simulated events N_{ev}=408, σ_{tot} and L given above, and approximately $N_4^c=N_5^c$=800 counters in each trigger layer (including two ends and asimuthal segmentation), one obtaines:

$$n_4 = \frac{N_4}{4{,}08\ N_4^c} \times 10^6 \quad s^{-1},$$

$$n_5 = \frac{N_5}{4{,}08\ N_5^c} \times 10^6 \quad s^{-1},$$

where N_4 and N_5 are the total numbers of charged particles, which have intersected FS4 and FS5 (during the time of 408 events production, equal to ~4 μs).

From Monte Carlo N_4=10270, N_5=43293. Then

$$\Omega_B \simeq 4{,}2 \times 10^5\ s^{-1}.$$

Taking into account usual event frequency

$$\Omega_E = 1/10ns = 10^8\ s^{-1},$$

for relative trigger rate one obtains

$$R = \Omega_B/\Omega_E = 4{,}2 \times 10^{-3} \quad \text{per counter.}$$

Each trigger counter frequency is independent (due to a large time delay). Then for 800 counters:

$$R = 4{,}2 \times 8 \times 10^{-1} \simeq 3 \quad \text{triggers per event !}$$

This makes endcup trigger hodoscope useless at the given background conditions.

5. Cerencov Counter FCC.

From the space coordinate distributions (fig.25) one can see that background particles come in mainly from Collimator side and leave FCC at the opposite side. Some amount of background particles comes from FS4, FW4 side. FCC is mainly traversed by neutrons and (an order smaller) γ's (fig.26a,b). A few (~0,1%) particles produce interactions (fig.26c). Produced particles are γ, e^+, e^-, n, p. Mean particle time delay equals 556 ns (fig.26d). For FCC the most interesting are distributions of γ-factors and θ - angles between incoming particle momentum and space vector, directed from IP to the particle.

According to Valery Kubarovsky private communication fast muons, coming from IP, are completely located in the region γ>40, θ<3°. From γ, θ, γ vs θ distributions of charged particles (fig.27) one can see, that traversing FCC background particles are located at small γ<20 and occupay the whole θ region from 0° upto 180°. Numbers of charged particles traversing from left to right and vice versa are approximately equal (fig.27b). Neutrons are located in the near to zero γ-region (fig.28d). No particles are found in the region γ>40, θ<3° at the given statistic level. Assuming less strong restrictions, one can obtain an upper limit for background FCC trigger rate.

There are three incoming particles, having γ>40 and θ<20°. This leads to

$$R < 3/408 = 4{,}7 \times 10^{-3} \quad \text{triggers per event.}$$

For more precise estimate more statistic is needed. FCC trigger seems to be operative at the present background level with a greate security.

There are two rescue pathes:
1) to substitute scintillator trigger by FCC,
2) to reduce background.

The first point was just discussed. Below we consider the second point.

6. How to reduce background.

In the first chapter it was stressed, that the most pronounced background source is SH3. The main background particles are neutrons with kinetic energy below 10 MeV. To remove neutron background hydrogen riched material is needed. The first step is use polyethylene SH3. The work is now in progress. Some preliminary results, based on statistic of 202 events, can be discussed.

In Z_{vert} vs R_{vert} distributions series (figs.29÷33) the SH3 pronounce remains.

Comparing with the iron SH3 results, one can conclude, that particle decomposition in sensitive detectors, except slow γ's in scintillators, retains the same (cf. figs.34a,b,c and 35a,b,c for FW5 and figs.36a,c and 22a,c for FS5), but energy spectra become harder (figs.34d,36b and 35d,22b). Background particle flux through FS5 (figs.36 and 22) is reduced by a factor ~5. The charged particle trigger counters rates (fig.37a,b) become ~10 times smaller (cf. fig.23a,b), and conventional numbers of triggers per counter (figs.37c and 23c) decrease by a factor ~100.

Particle time delyas (fig.38) halve (cf. fig.24) due to slow neutron absorbtion by polyethylene. Total numbers of charged particles, which have intersected FS4 and FS5 during the time of 202 events production, are N_4=401 and N_5=2420. Using the described in Chapter 4 procedure relative trigger rate becomes

$$R \simeq 3 \times 10^{-2} \quad \text{triggers per event.}$$

Conclusion is: polyethylene SH3 reduces trigger rate by factor ~100. The next step will be use polyethylene together with an iron.

CONTENTS

1. Background sources. 2
2. Secondary interactions vertices inside the main background sources. 3
3. Interacting particle types and their energy spectra. . .3
4. Endcup trigger hodoscopes FS4 and FS5. 4
5. Cerencov Counter FCC. 6
6. How to reduce background. 7

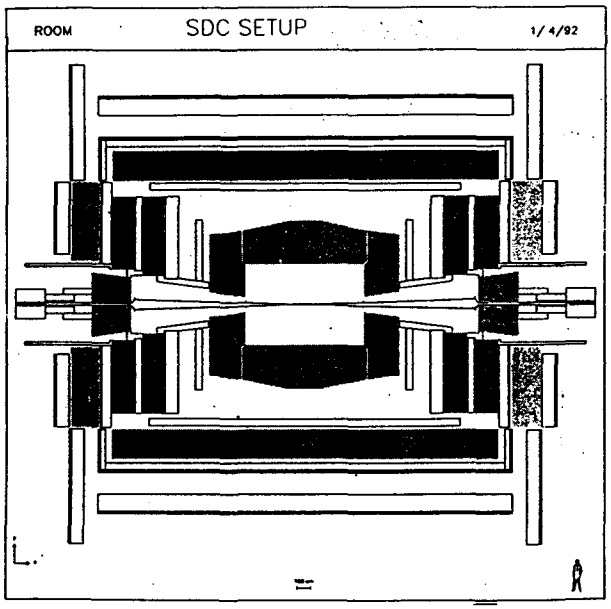

fig.1

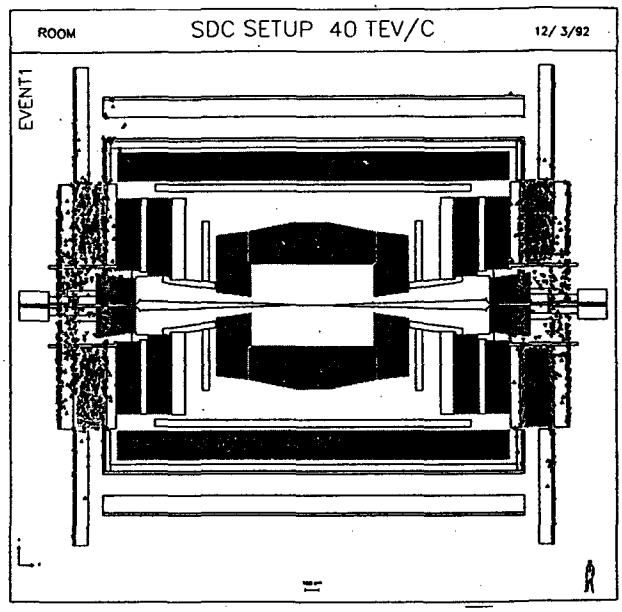

fig.2

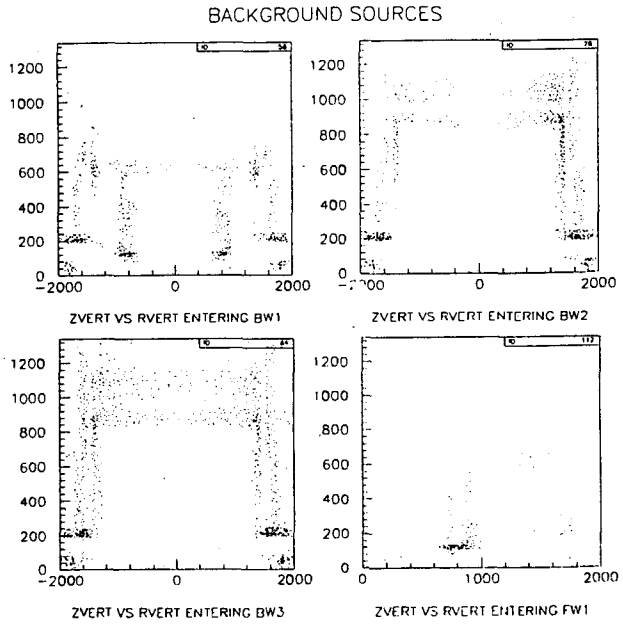

fig.3

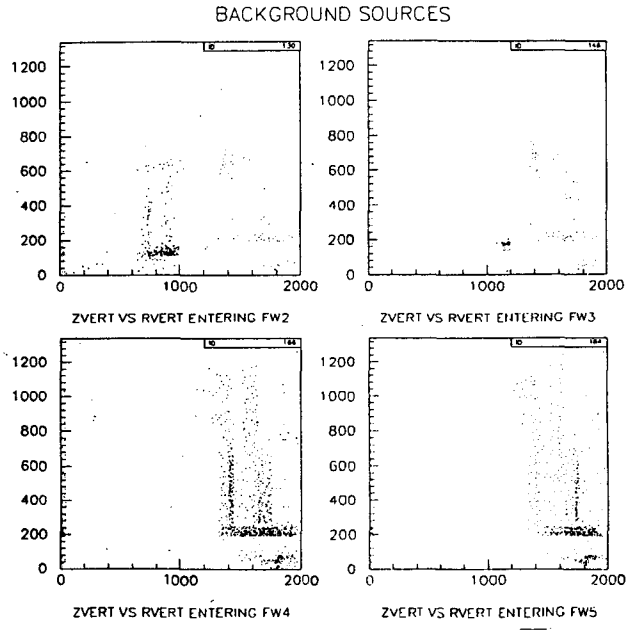

fig.4

1783

BACKGROUND SOURCES

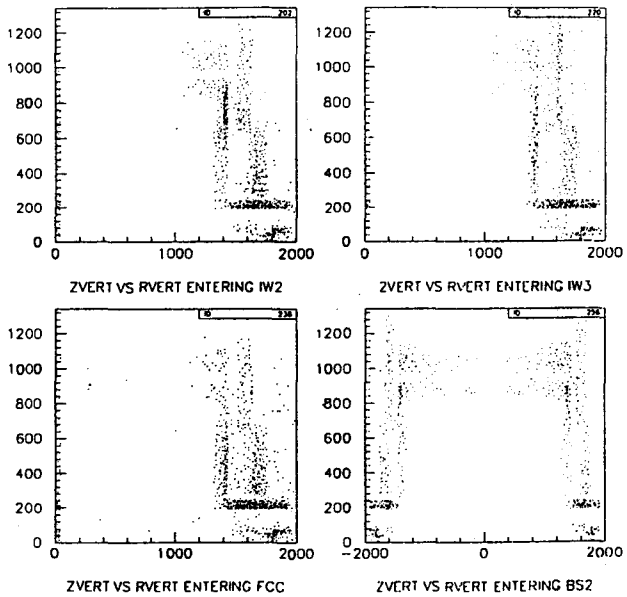

fig.5

1781

BACKGROUND SOURCES

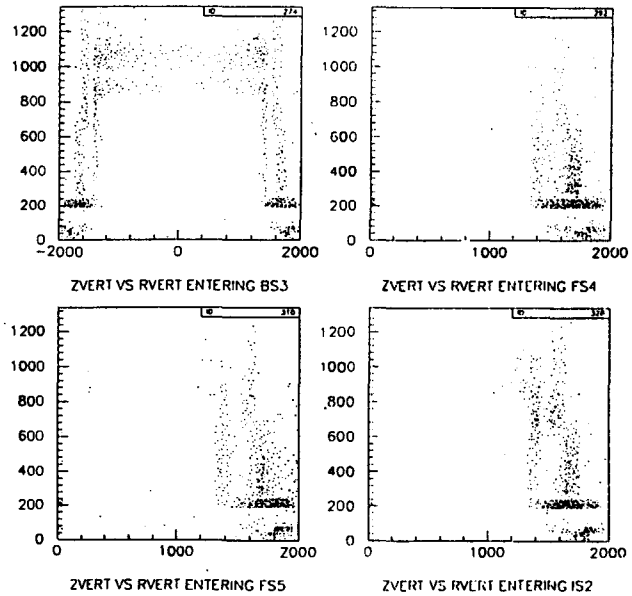

fig.6

1785

TRIGGER HODOSCOPE FS5

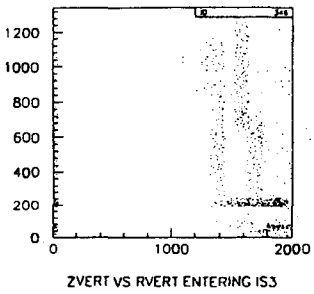

fig.7

1786

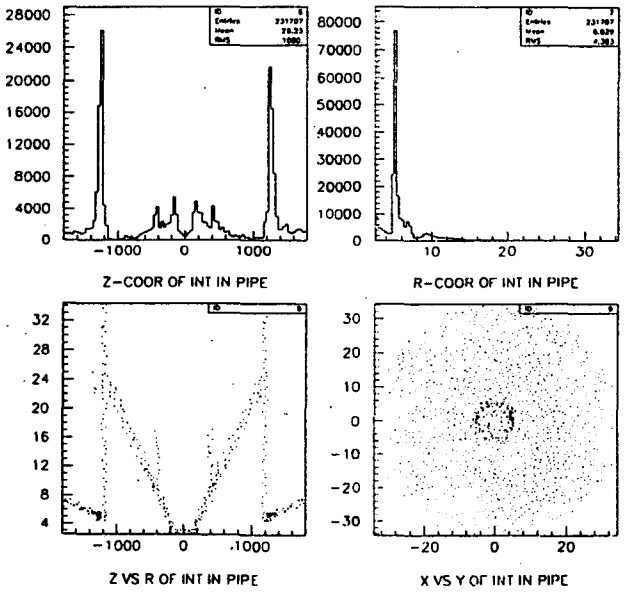

fig.8

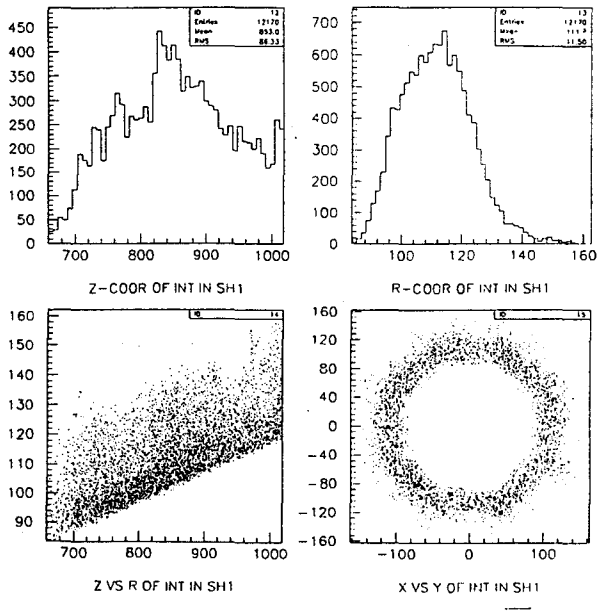

fig. 9

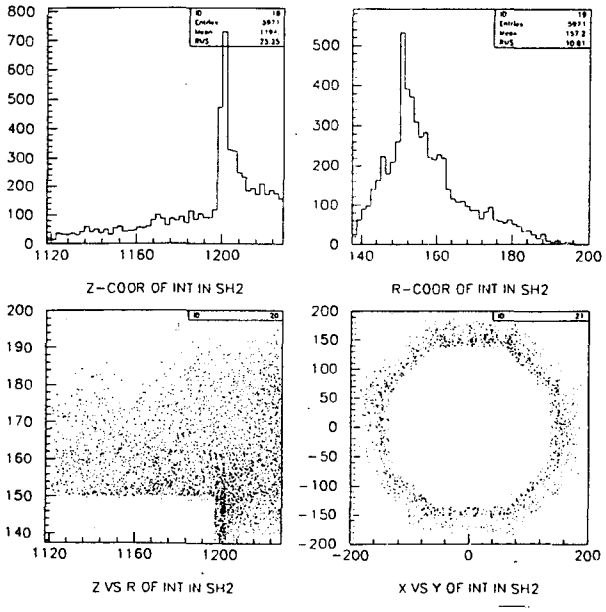

fig. 10

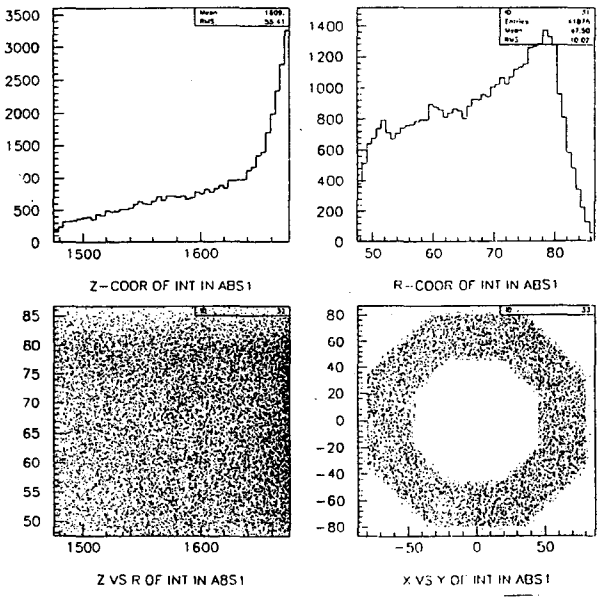

fig. 12

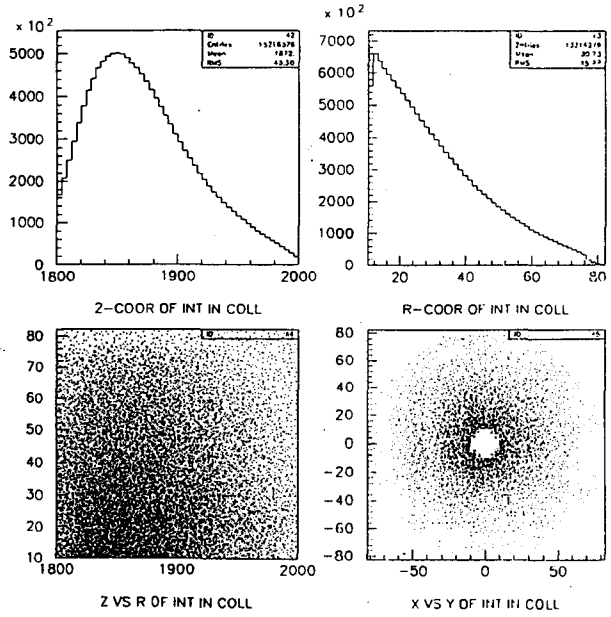

fig. 11

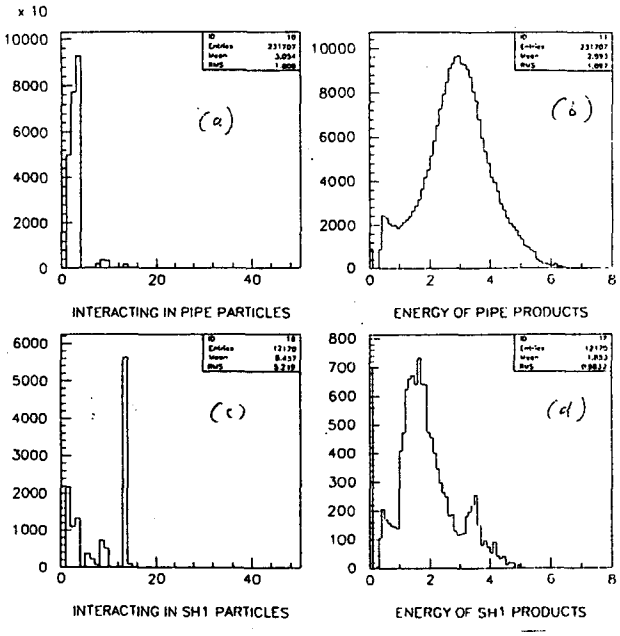

fig. 15

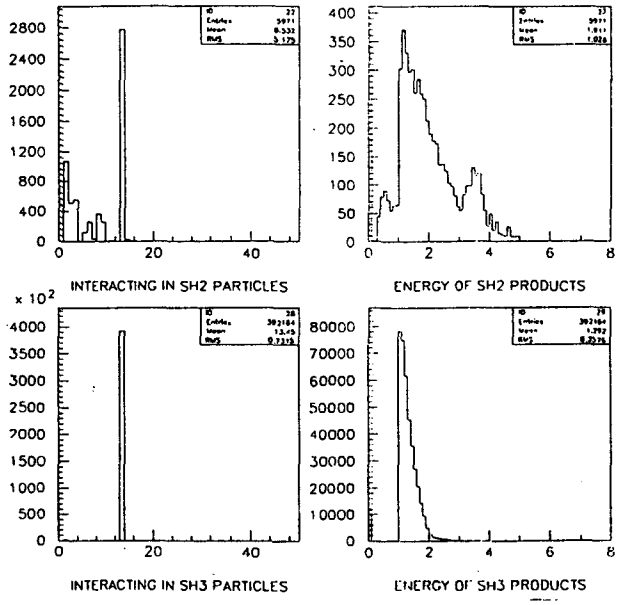

fig. 16

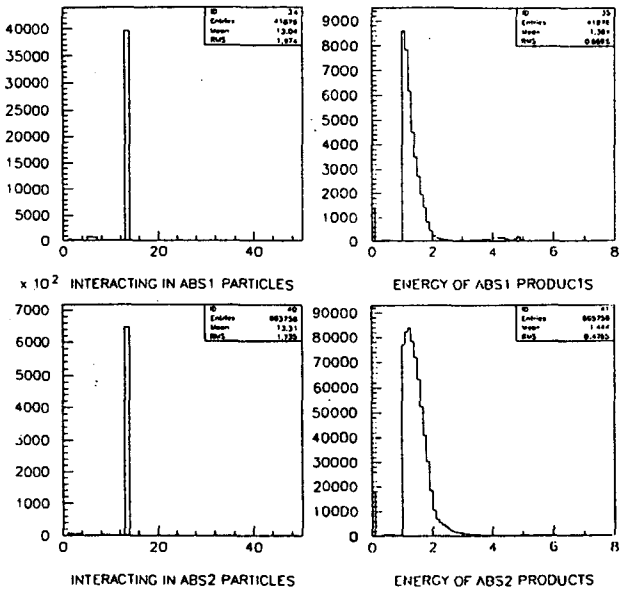

fig. 17

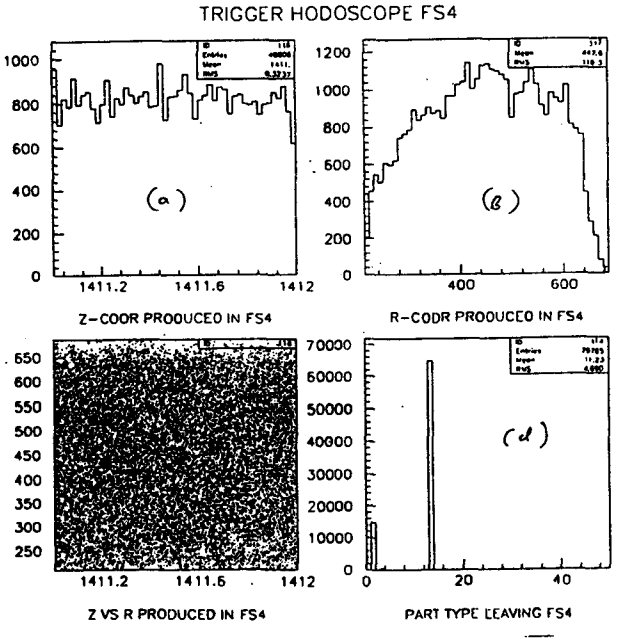

fig. 19

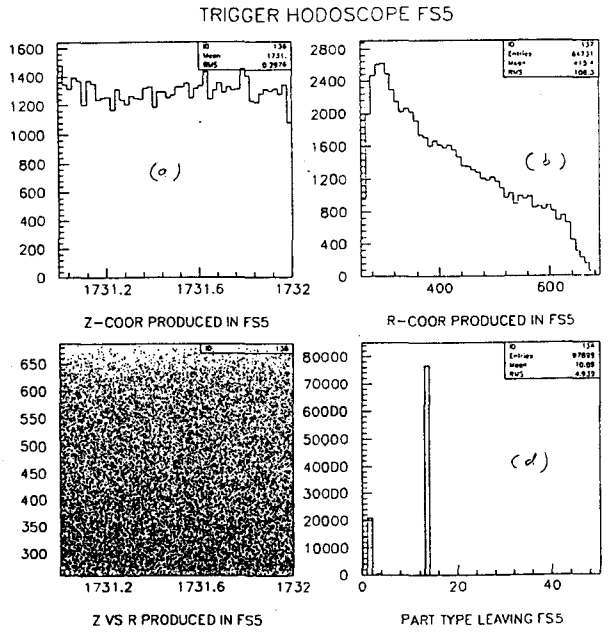

fig.20

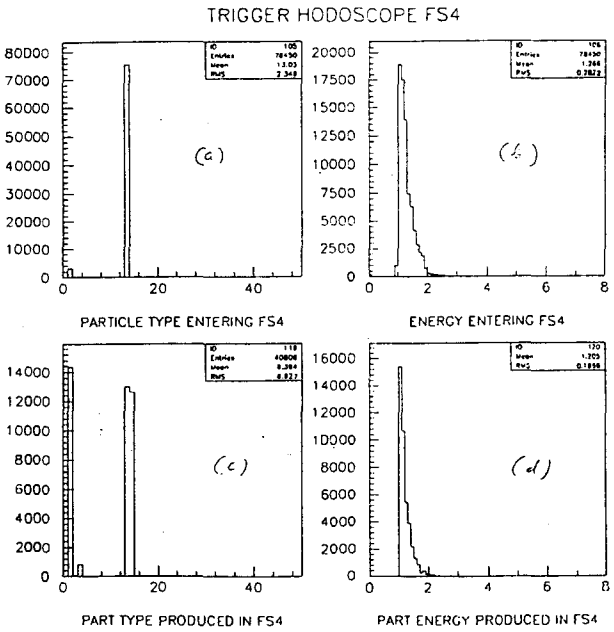

fig.21

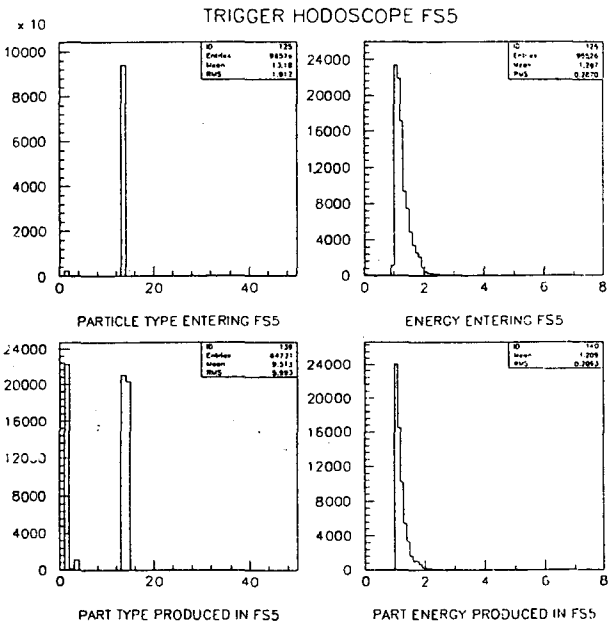

fig.22

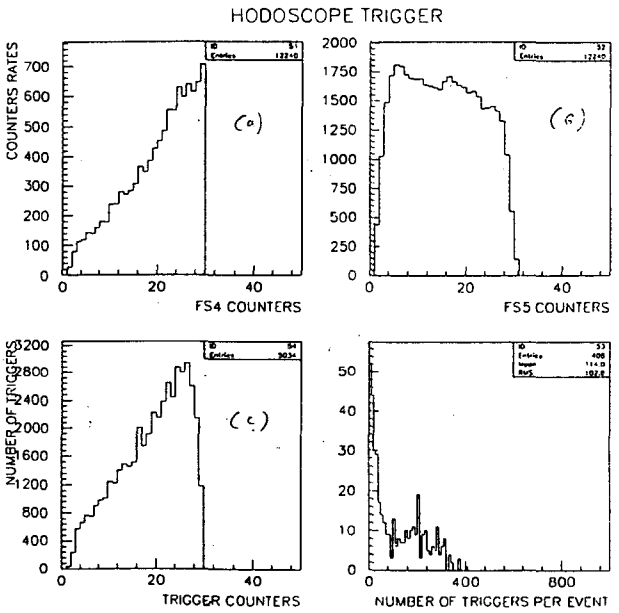

fig.23

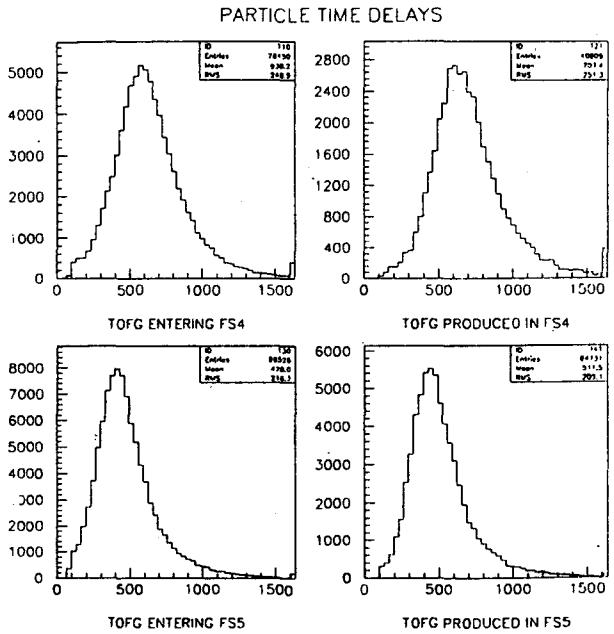

fig. 24

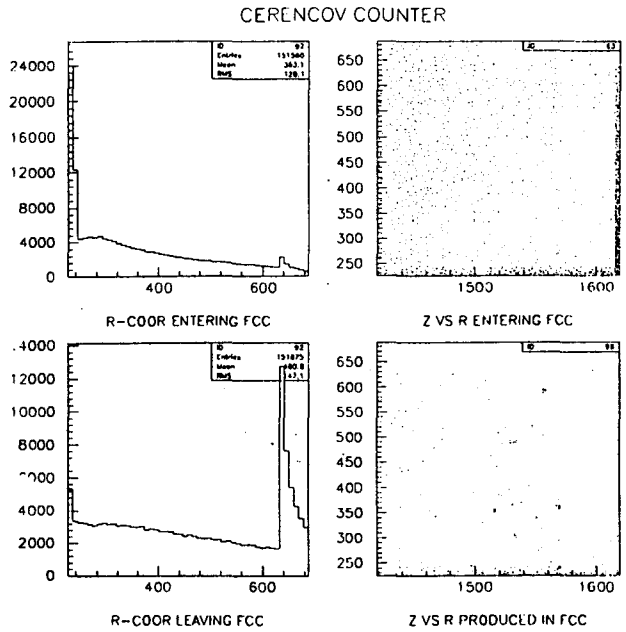

fig. 25

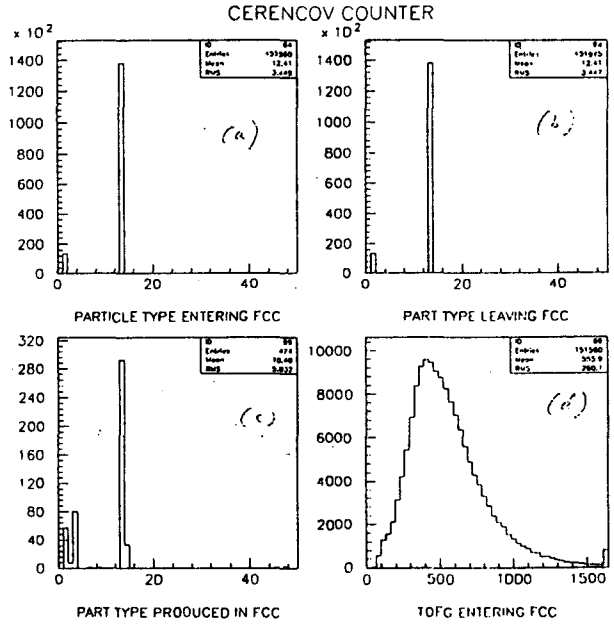

fig. 26

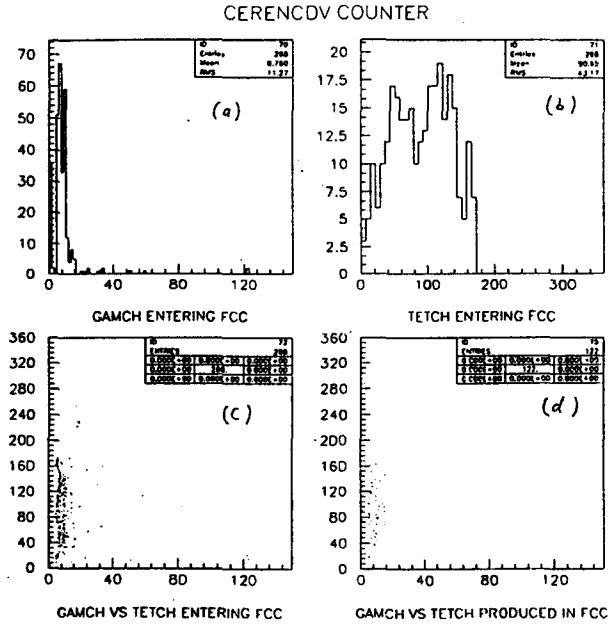

fig. 27

1803

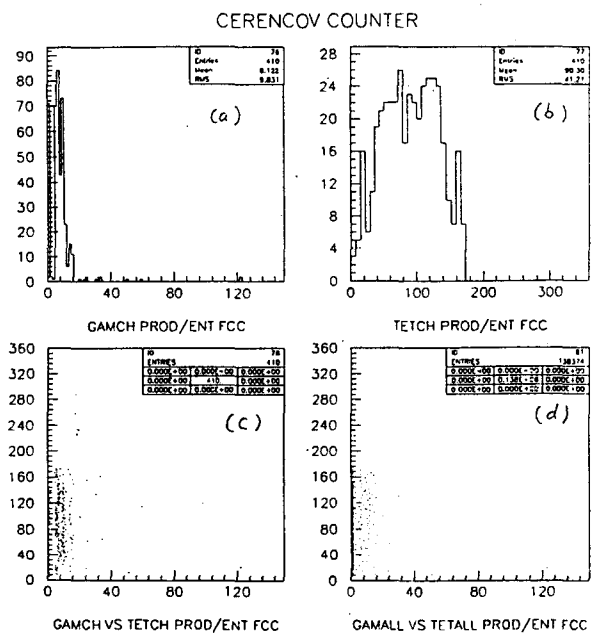

fig. 28

1804

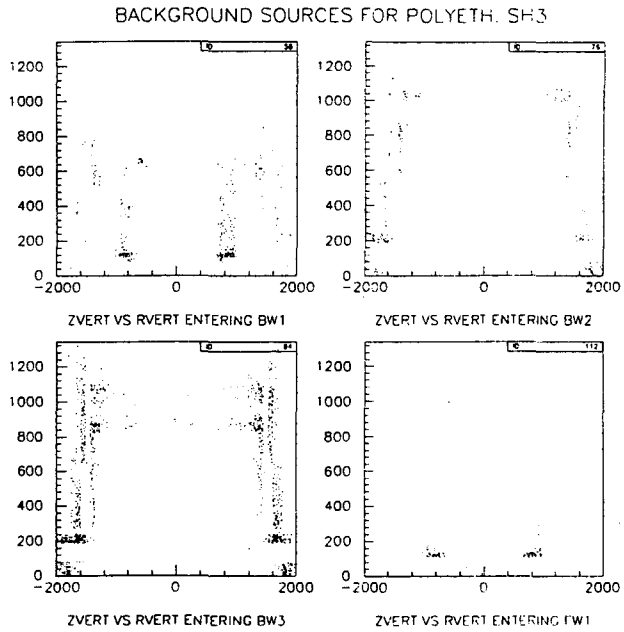

fig. 29

1805

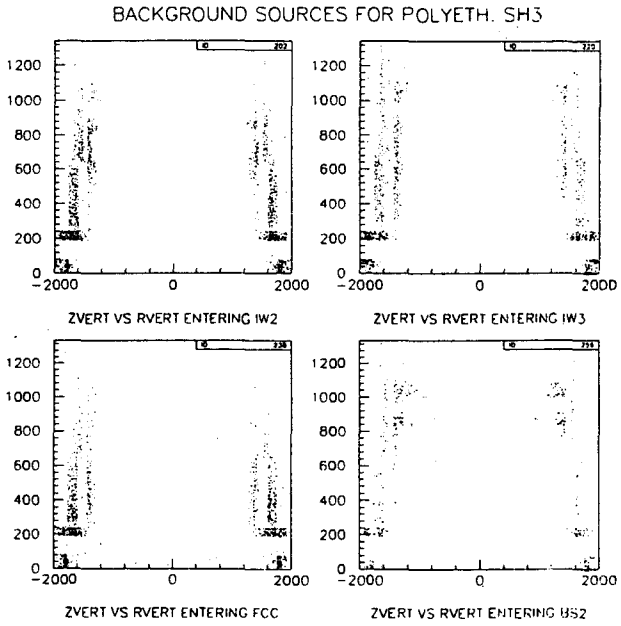

fig. 30

1806

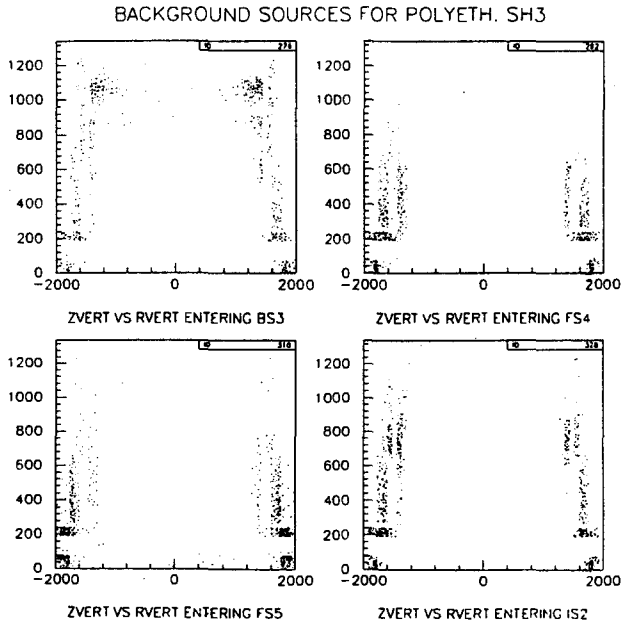

fig. 31

BACKGROUND SOURCES FOR POLYETH. SH3

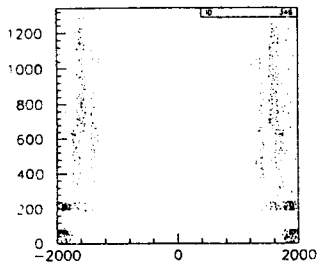

ZVERT VS RVERT ENTERING IS3

fig. 32

CHAMBER FW5 (POLYETH SH3)

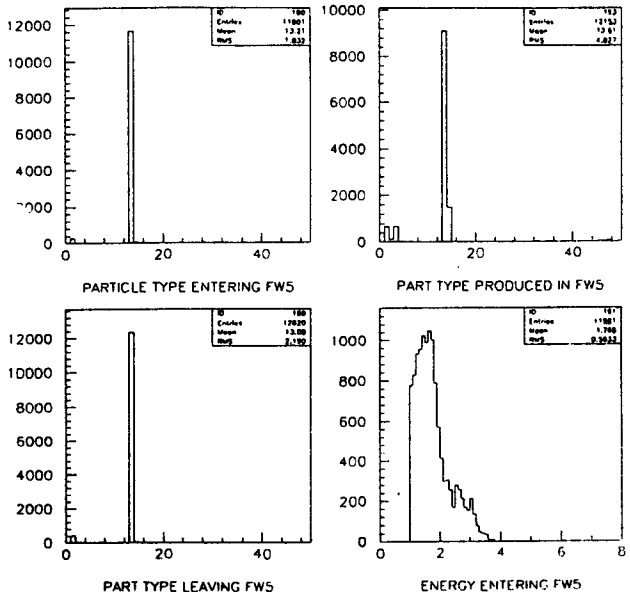

fig. 33

CHAMBER FW5 (Fe SH3)

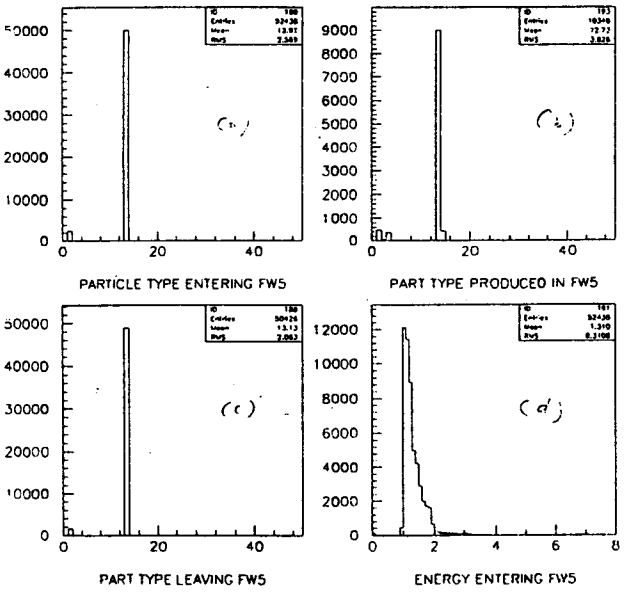

fig. 35

FS5 FOR POLYETH SH3

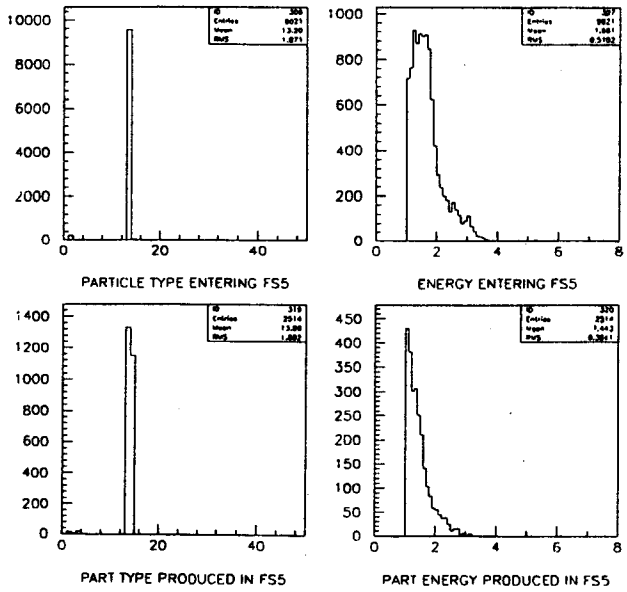

fig. 36

HODOSCOPE TRIGGER FOR POLYETH. SH3

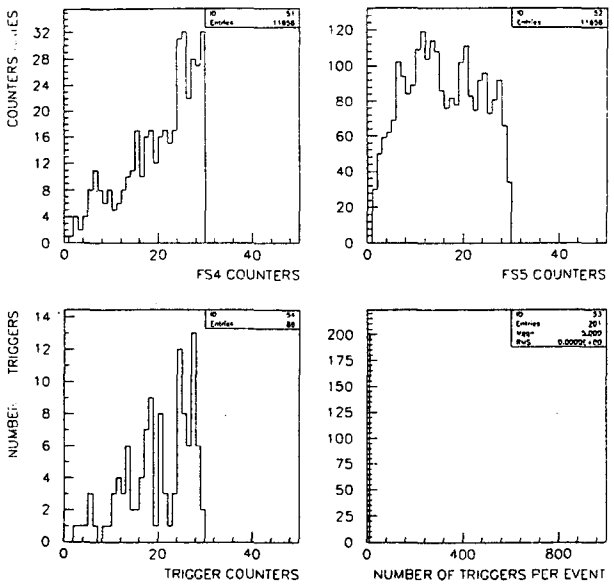

PARTICLE TIME DELAYS FOR POLYETH. SH3

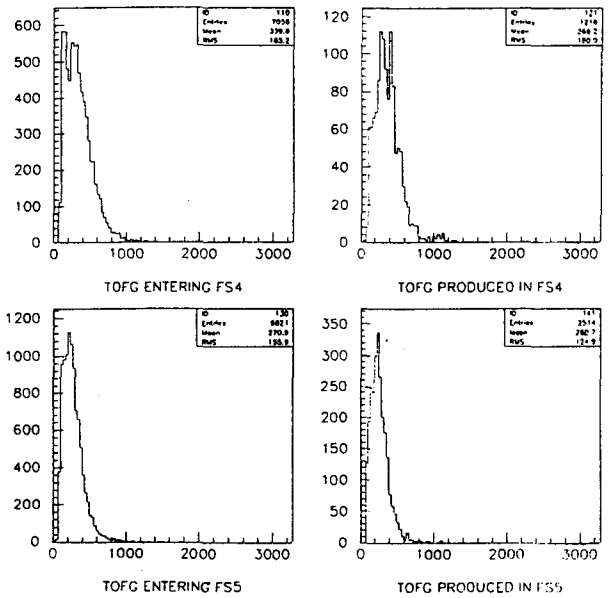

Alexei Kulik, KEK/IHEP

presented to the SDC
collaboration meeting,
May 26-29, 1992, KEK, Japan

Neutron Rates in the SDC Forward Muon System. Design Optimization.

Abstract

The simulation of the neutron rates due to beam-beam interaction down to 100 keV with the GEANT.3.14 code is presented. The geometry used differs from that of TDR by much thicker shields, especially in the rear area. The transversal leakage from the Forward calorimeter is found to be the major source of neutrons in the $\mu FW_4, \mu FW_5$ area. If FCal is placed by 1 meter closer to IP, then this effect is 4 times smaller, while the rate in $\mu FW_1, \mu FW_2$ is doubled. After this optimization the rates are: 1 neutron/event in $\mu FW_1, \mu FW_2$, 0.15 n/event in $\mu FW_4, \mu FW_5$ and $3 \cdot 10^{-3}$ n/event in μBW_2. For TDR geometry the rates of $\mu FW_4, \mu FW_5, \mu BW_2$ should be much higher.

The option to put the SSC S-Quad at 35 meters is also investigated. The backsplash is 20 times less than for 20 meters position and the same shield thickness.

As far as the 35 m option needs much longer shield, the optimization of the shields shape is done.

The data also presented on the contribution to the 1st level trigger and on the rejection power of the Čerenkovs.

1 Introduction

The SDC Forward muon system is shielded from its inside to reduce the influence of the beam-line and of the backsplash from the FCal and S-Quad Collimator. The charged particles are almost completely absorbed in this shielding thus neutrons become the major problem.

The efficiency of the neutron detection is not studied well, this depends on geometry, detection thresholds, etc... However there is an indication that this is not small. The GEANT/GHEISHA simulation shows the production of 0.2 protons per incident neutron in 1 cm thick trigger scintillation counters and about the same number of electrones; about 5 electrones/neutron are produced in the drift tubes' walls. It is rather difficult to estimate the effect in the last case because one should take into account the probability for the low-energy electrone to come out into the gas volume, also the energy cutoff for ionisation is very low. So in this study only the neutron rates are presented, the detection efficiency being another task.

The TDR shieldings are too thin to my mind, especially in the rear area where the neutron backspalsh from the S-Quad collimator is huge. So I tried much

thicker ones to be closer to the optimal design. As far as the rate dependence on the shield's thickness is known, the shields may be scaled to the desirable rate. The example of such an exercise is given in Sect.4. Another important change in the geometry deals with the FCal radius: it was increased as much as possible to reduce the transversal shower leakage which appears to be very big.

Only the beam-beam interaction is assumed to be the source of radiation. This seems to be the major effect. In any case this calculation keeps a very important feature which is common for the most of the other sources: the radiation has its origin at the beam-line area.

2 Low Energy Neutrons

The energy cutoff for the neutrons is a kind of problem. First: the neutron spectrum peaks towards low energies; second: even very slow neutrons may be essential for the detectors and third: such dense materials as an Iron are well known to be transparent for the neutrons in a MeV range. The stability of the result versus the neutron energy cutoff was studied and found to be reasonably good under some conditions.

Hydrogen-rich materials are well known to be very good to slow down the neutrons in a MeV range. So the Polyethylene shields were introduced in the geometry. GEANT3.14 code (including GHEISHA-8) was used. A good agreement of punchthrough simulations

with experimental data was demonstrated for this code (H.Fesefeldt et al., Nucl. Instr. & Meth. A292 (1990) 279).

Fig.1 illustrates how effective an Iron and a Polyethylene are for soft and hard neutrons. Note a very fast absorbtion of soft neutrons by the Polyethylene.

The base-line geometry is shown in Fig.2. Pay attention to the Polyethylene shieldings, huge Iron shielding in the rear area and to the "fat" FCal.

Fig.3a÷c show the dependence of the rates in the rear area on the neutron energy cutoff. The difference is within a factor of 1.5÷2 in the range of 100keV÷10MeV. The neutron flux coming to the 30 cm thick rear Polyethylene shielding is shown in Fig.3d. The conclusion is: the soft neutrons are almost perfectly absorbed hy the 30 cm of Polyethylene.

Fig.4 shows what happens if the Polyethylene is not thick enough. Two curves in each of 4 pictures correspond to 12 cm of Polyethylene in the forward shielding and 20 cm, the stability in the last case being much better.

The conclusion: **neutron flux calculations are reasonably stable versus energy cutoff for Polyethylene thickness more than 20 ÷ 30 cm.**

The Polyethylene is much easier for mechanical construction than the Iron. It is because of its low weight and (I hope) low price. So all the studies below address mainly to an Iron shielding as the most important issue. The forward shielding was assumed to be 30 cm thick

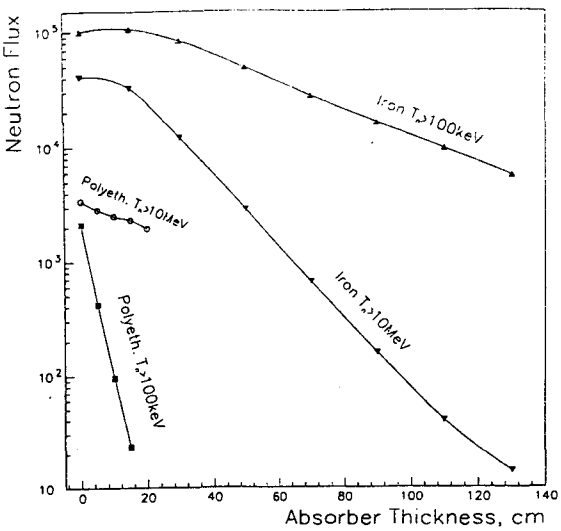

Fig.1 The absorbtion capability of Iron and Ployethylene for hard (> 10 MeV) and soft (> 100 keV) neutrons.

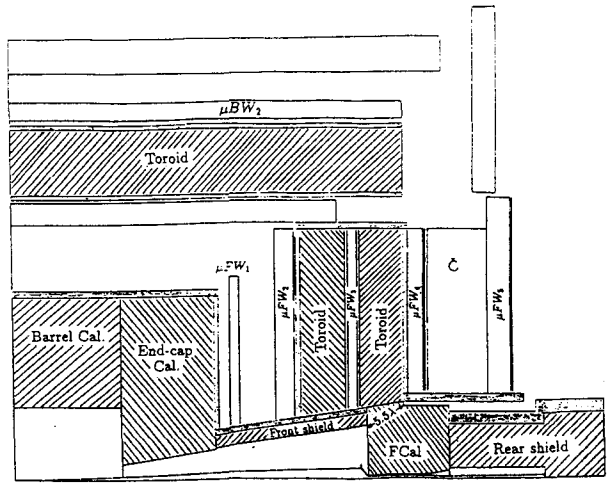

Fig.2 The base-line setup. The heavy absorbers (Iron and calorimeters) are shown in hatched and the Ployethylene shields are shown in green.

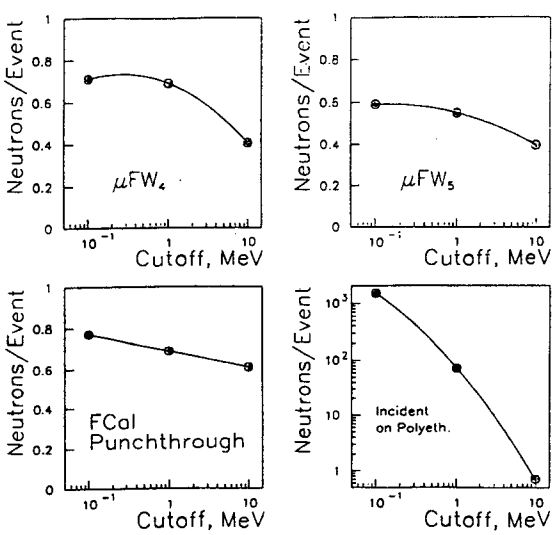

Fig.3 The stability of the neutron punchthrough calculations versus neutron energy cutoff in the rear area. The stability is reasonably good due to the very high absorbtion of low-energy neutrons in the Ployethylene.

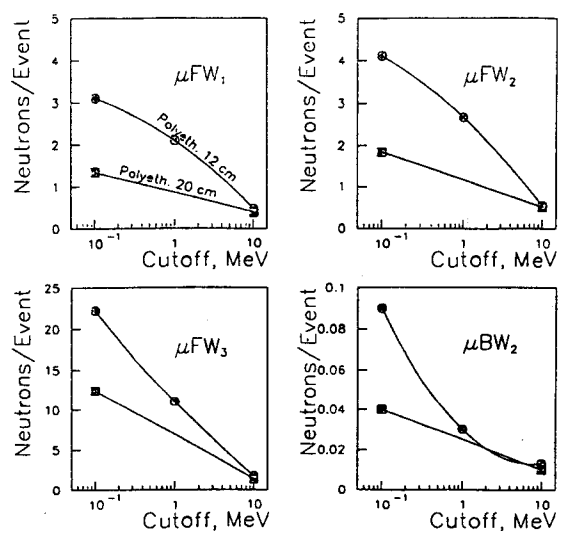

Fig.4 The stability of the neutron punchthrough calculations versus neutron energy cutoff in the front and barrel areas. Two curves correspond to 12 cm and 20 cm of Ployethylene.

Iron followed by 20 cm of Polyethylene. The neutron energy cutoff was set to 10MeV (saving a factor of $4 \div 5$ in speed), the cutoff for charged was kept at 100keV.

3 FCal Neutron Punchthrough

It comes out that FCal is not "fat" enough (in radius) to absorb all the showers' tails. It was increased as much as possible but nevertheless the FCal neutron punchthrough is the dominant effect for the $\mu FW_4, \mu FW_5$ stations. Fig.5 shows the entry point (Z,R) of neutrons to the Muon system. One can easily see that the FCal punchthrough dominates over the S-Quad backsplash. This is not so strange if you keep in your mind that the shortest way across the FCal is only 5.5λ (see Fig.2) and this way is almost in forward direction for the hadrons produced in IP.

What are the possibilities tn reduce this effect?

- **There is no room** for increasing the radius more. Even the drawing in Fig.2 is unrealistic because it hasn't a room for mechanical supports.
- **More dense calorimeter.** It depends on the choise of technology. In my study the FCal is made of a mixture of an Iron with a plastic scintillator with $\lambda \approx 25$cm. In any case it is difficult to imagine any big calorimeter with the average absorbtion length of λ <20cm. The passive "coat' made of Copper ($\lambda \approx 15$cm) of Uranium ($\lambda \approx 12$cm) may be effective.

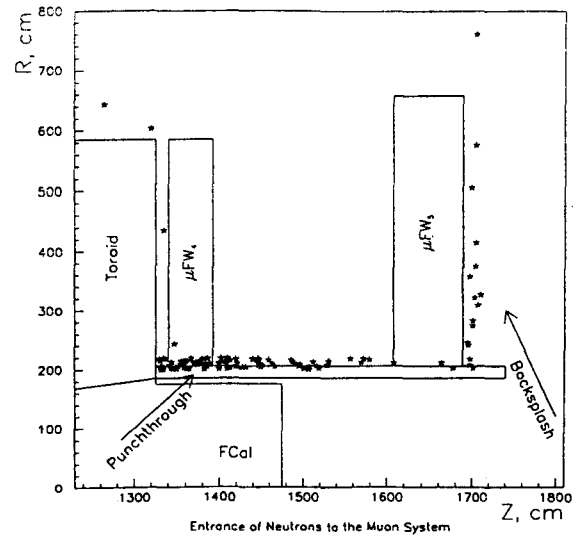

Fig.5 Entry point of neutron to the Muon system. The FCal punchthrough dominates over the S-Quad collimator backsplash.

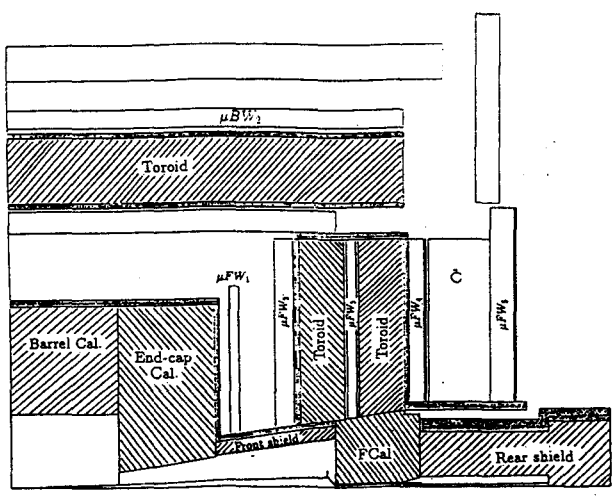

Fig.6 The new proposed position for the FCal: the second Forward toroid works as an outer "coat" for the FCal thus reducing the spray of neutrons.

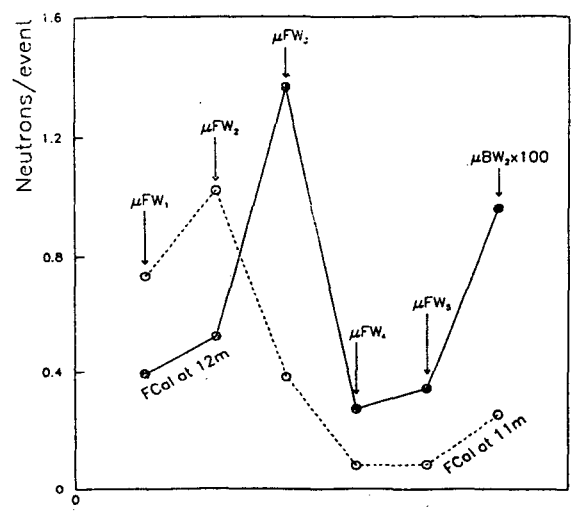

Fig.7 Total neutron rates for initial (12 m) and proposed (11 m) FCal positions. The data are normalized to one event in the IP.

- The Iron Toroid as a "coat" for the FCal. Imagine the FCal to be pushed by 1 meter closer to IP (see Fig.6). In this case the Iron of the Forward toroid prevents the transversal leakage of the showers. This option looks as the most simple one and it was studied.

Fig.7 shows the neutron rates in various areas for Z=11 meters position (dashed line) compared to Z=12 meters position (solid line):

- Rear area ($\mu FW_4, \mu FW_5$): goes down 4 times (a bit surprized of the effect to be so small). Anyway note that this means a gain of $4^2 \approx 15$ for the 2-fold accidental coincidence in the 1st level trigger.
- Front area ($\mu FW_1, \mu FW_2$): increased twice. This is because the Forward toroid is not as good to absorb the FCal backsplash as at Z=12 meters.
- μFW_3 becomes much bettter because the gap between two toroids is closed now by the FCal.
- The rate in the barrel station μBW_2 shows its behaviour similar to that of the rear area. Additional study showed that neutrons come to μBW_2 predominantly from the rear area.

4 S-Quad at 35 meters

The neutron backsplash was studied for 35 meters S-Quad position. The starting point was the 20m geome-

try (see Fig.2). The rear shield is made of 2 Iron cylinders of 1.25 meters and 1.5 meters outer radius followed by 30 cm thick Polyethylene. Then the rear shield was just "expanded" in Z from Z=20 m to Z=35 m. The total backsplash rate falls down by 20 times. Such a low rate is out of practical use because it is far below the FCal punchthrough level.

As far as the rear shield becomes very long ($\approx$ 20 meters) some effort was done to save the weight by optimizing its shape. The first step was to design the "Equi-Shape": the contribution of each piece of its surface to the total neutron rate should not depend on its Z-position. The inputs were:

- The distribution of neutrons along the shield which was calculated before.
- The solid angle for viewing $\mu FW_4, \mu FW_5$ from any particular point of the shield's surface.
- As it was shown before, the neutron flux in Iron "dies" like e^{-t/t_0}, where t stands for the absorber thickness and $t_0 \approx 14$ cm. This is valid for relatively hard neutrons ($T_n > 10$MeV), the soft fraction being assumed to be absorbed by the Polyethylene (see Sect.2).

Fig.8 shows the behaviour on Z of the solid angle and solid angle times neutrons density ("Flux"); the vertical scale is arbitrary. The solid line shows the outer profile of the calculated "Equi-Shape", the inner profile being a plain tube nf 25 cm radius. Its polycone approximation

is shown in a dashed line. The overall normalization of the thickness was chosen as to get the integral of the backsplash at about 1/3 of the FCal punchthrough in Z=11 m option. The resulting geometry is shown in Fig.9.

Then the new simulation was done with this rear shield, the results being rather close to predictions. Fig.10 demonstrates the quality of the "Equi-shape": the origins of the neutrons which come in to the Muon system are about uniform in Z. The integral of the backsplash comes to 1/2 of the FCal punchthrough instead of predicted 1/3.

Perhaps the "Equi-shape" is not the best one for optimizing rate v.s. weight, it may be further improved. Anyway the "Equi-shape" is a good first approximation to the optimal shape, let's see what do we have with it.

The uniform increment of the "Equi-shape" by each 14 cm comes to e times less backsplash. Given this scaling rule, the dependence of the rate on weight was obtained (see Fig.11). Also shown is the dependence for 20 m S-Quad position, it assumes the same scaling rule $e^{-t/14cm}$. Here we may also hope for some improvement of the shape although there is no much room for such an improvement because of the limited length. The levels of FCal punchthrough for Z=12 m and Z=11 m are also shown.

There is a clear possibility for 35 m option to build a major part of the rear shield of concrete (much cheaper) but it was not calculated till now.

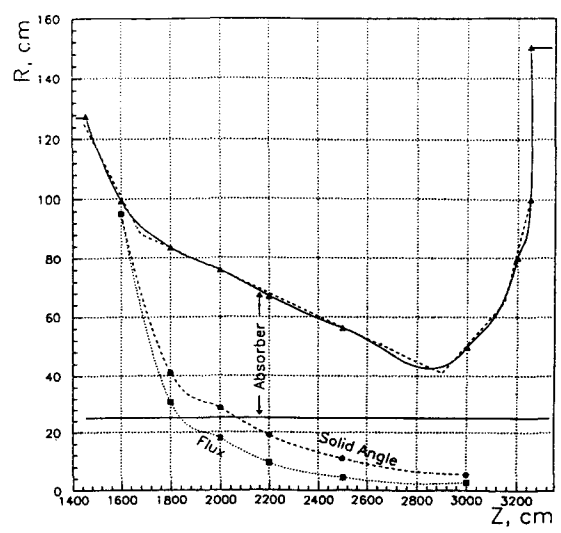

Fig.8 The calculation of the "Equi-shape" of the rear absorber. The claim for this shape is that its contribution to the Muon system rate should be uniform in Z. Also plotted are the solid angle at which μFW_4, μFW_5 are viwed from the surface of the rear shield and "Flux" which is the above solid angle times the number of neutrons. The vertical scale for the solid angle and "Flux" is arbitrary.

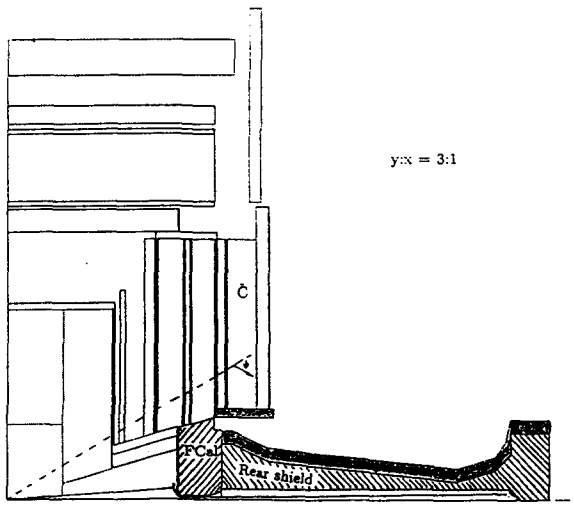

Fig.9 The SSC Quad at 35 meters with the Reer shield of the "Equi-shape".

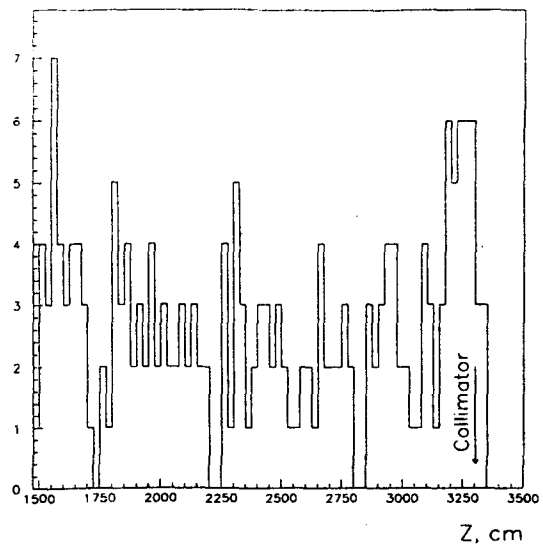

Fig.10 The distribution of the origins of the neutrons coming to the Muon system for the Rear shield of the shape shown in Figs.8,9.

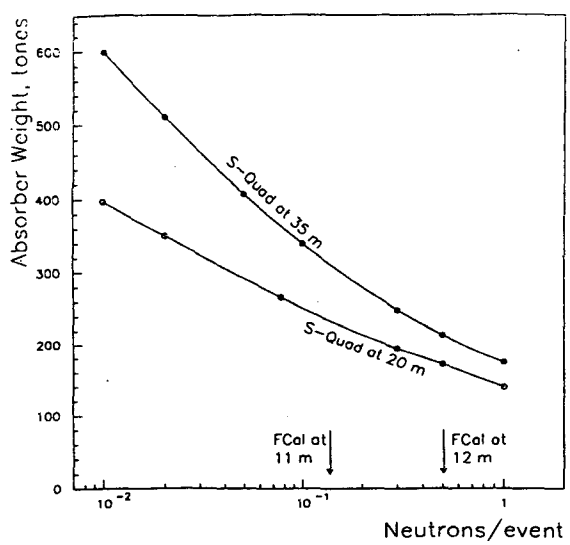

Fig.11 The optimized Rear shield weight versus the neutron rate for the SSC Quad positions of Z=35 m and Z=20 m. The reasonable scale of the desirable rate is set by the FCal punchthrough rate which is shown with arrows for the two FCal positions: Z=11 m and Z=12 m. The scaling rule of exp(-t/14 cm) is assumed for hard (above 10 MeV) neutrons while the soft component is assumed to be perfectly absorbed with the Polyethylene.

5 The Rate Distributions

Fig.12 shows the radial distribution of the neutron flux over the various muon stations (the integrals are shown in Fig.7). The contribution of the FCal punchthrough is shown separately for the μFW_5 with the hatched histogram. The vertical scale is normalized to one event and to the "ring" of 20 cm width. There are clear peaks at minimum radii because neutrons come from the beam-line area. These peaks are not so prominent for μFW_1 and μFW_3, this may be explained by the geometrical reasons.

Fig.13 shows the distribution over Z in the barrel station μBW_2. Although the statistics is rather poor, one can see a concentration towards the end of the chamber. It was revealed in additional study that 3 of these neutrons came from the rear area while 1 (the leftmost) came through the Barrel toroid.

6 Contribution to the 1st Level Trigger

Ony very rough estimation is available to the moment. It is based on the rates of charged particles produced in the scintillator counters (see Fig.14). Each of two scintillator planes has about 50 counters in radius × 8 octants × 2 arms = 800 counters. This comes to about 4 kHz/counter rate for each of the planes at the nominal luminosity of $L = 10^{33}\,\mathrm{cm}^{-2}\mathrm{s}^{-1}$. Assuming the time resolution of τ=5 ns, the rate of accidental 2-fold coincidences comes to $(4\ kHz)^2 \times 2\tau \times 800$ channels ≈

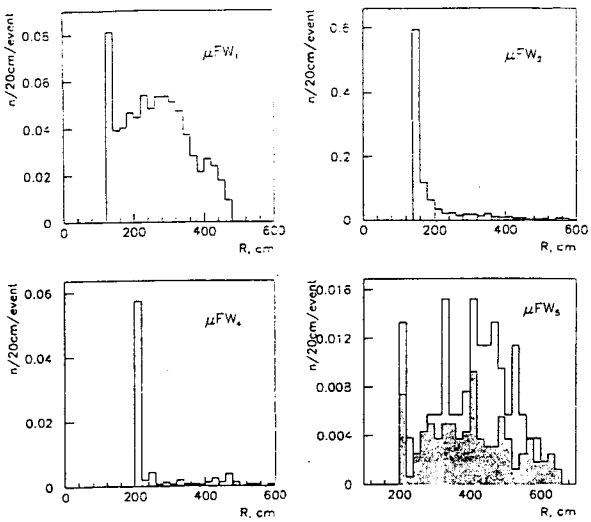

Fig.12 The radial distributions of the neutrons normalized to one event and to the "ring" of 20 cm width.

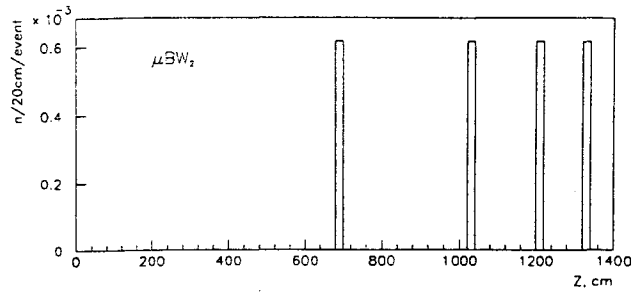

Fig.13 The distribution of neutrons along the Barrel chamber μBW_2.

120 Hz.

Althoug the above value is very low, still it is very uncertain. More certain value depends on the following issues:

- **Detection threshold.** It is preliminary estimated to be about 600 keV for the protons at far end of the scintillator bar and about 100 keV if close to PM. These values are few times lower for electrones. So rather detailed model of the counter system is required.
- **Cracks.** Is it practically possible to have such a tight packing of the detectors as it was assumed in this calculation? How many space should be left for mechanical supports, vacuum pumping, etc..? How big the cracks in the shields are?
- **Rear shield.** Will such a thick rear shield be accepted or not?
- **FCal material.** The model used contains a good fraction of plastic which should be important for absorbtion of low-energy neutrons. If the future technological choice for the FCal will not allow for the significant fraction of Hydrogen, then the neutron punchthrough rate may be much higher.
- ???

As of now it is not so easy to clarify all of the above questions. In this view the direction-selective gas Čerenkov

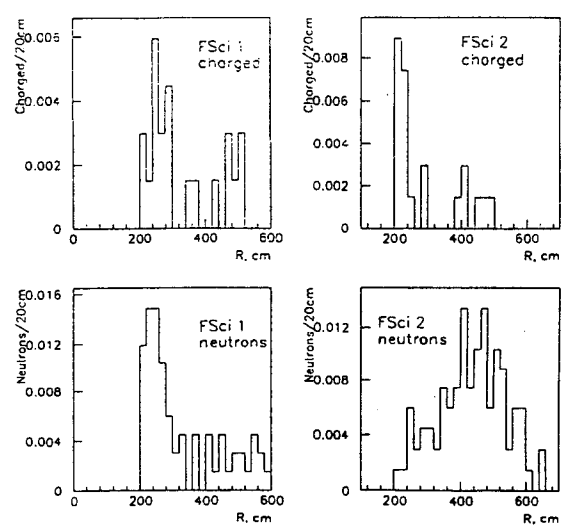

Fig.14 The radial distributions of the charged particles (above) and neutrons (below) in the Forward trigger scintillator counters. The normalization follows that of Fig.12.

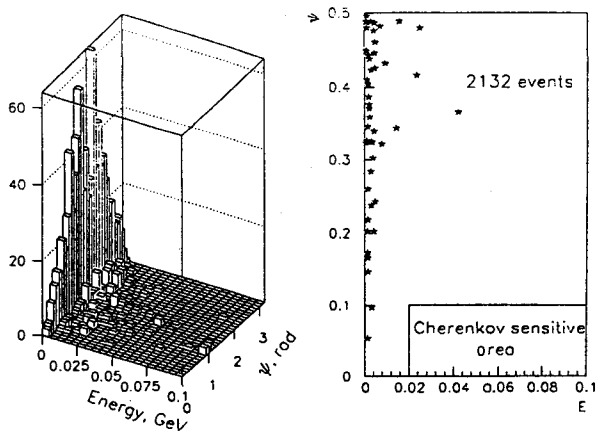

Fig.15 The biplot of the mis-angle ψ v.s. energy for charged particles in the Čerenkov area. The threshold for the electrones is 0.02 GeV and the Čerenkov direction selectivity is about 0.1 radians. The definition of the mis-angle ψ is explained in Fig.9.

counters look very attractive. Fig.15 shows the distribution of the charged particles (predominantly electrones) in energy and mis-angle ψ in Čerenkov . The definition of the mis-angle is shown in Fig.9: it is the angle between the actual momentum of the particle and the direction to the IP. The Čerenkov counter proposed by the IHEP group has two selective features: 1 - threshold of 20 MeV for the electrones in the air and 2 - it is sensitive only for small mis-angles: $\psi < 100$ mrad or so. The zoom of the Čerenkov sensitive area is shown on the right, it has no hits for more than 2000 generated events. More definite estimation of the Čerenkov rejection power depends on the details of its design but anyway Fig.15 shows the rejection power to he very high.

7 Conclusion

1. The punchthrough simulation is reasonably stable versus neutron energy cutoff for 20÷30 cm of Polyethylene following the Iron shielding.
2. The TDR shields are very thin in the rear area, they should be increaced.
3. For thick enough rear shields the neutron punchthrough of the FCal becomes the dominant source of the rate in the rear area ($\mu FW_4, \mu FW_5$) which contributes to the 1st level trigger. The rate may be 4 times reduced by moving the FCal by 1 meter closer to

IP. I propose this option. The closed SDC geometry allows to design a very clean rear muon area as compared to GEM and this feature may be essential for both the trigger and the pattern recognition issues. It would be a pity to lose this advantage.

4. The S-Quad position at Z=35 meters requires about 1.3 times more iron than at Z=20 meters but the possibility of concrete shield in the first case is still opened.
5. The contribution to the 1st level trigger seems to be low for the perfect "naive" geometry but the effects of mechanical supports, cracks, etc... are not clear now. So the direction-selective gas Čerenkovs still look attractive.
6. The front shield Polyethylene should not be thinner than 20 cm.
7. Neutron rate in the front area ($\mu FW_1, \mu FW_2$) is dominated by the Front shield punchthrough and comes to 1 neutron/event. Neutron rate in the rear area ($\mu FW_4, \mu FW_5$) is dominated by the FCal punchthrough and comes to 0.1 neutron/event for optimized FCal position. The behaviour of the rate in the barrel region (μBW_2) is similar to that of the rear area. The total rate is $3 \cdot 10^{-3}$ neutron/event for optimized FCal position.

8 Plans

- The above calculations should be redone in more realistic geometry allowing a space for the mechanical supports and pumping equipement.
- The tolerances to possible cracks and offsets should he established.
- Further optimization of the rear shield shape/material.
- As the neutron distribution along the forward shield increases towards its far end (see Fig.16 a) then the front shield shape like that shown in Fig.16 b seems to be better.

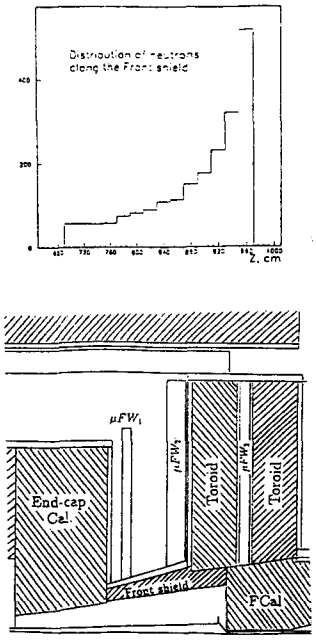

Fig.16 The distribution of neutrons along the Front shield (above) and the proposed shape of the Front shield (below).

[8] Muon/Electronics Joint

<Overview>

Muon Electronics Overview and Development Plan	S. Terada	- 1843

<Readout>

ASD Development	Y. Asano	- 1848
New TMC Design for Muon with TOSHIBA Gate Array	Y. Arai	- 1863
Status of TMC Modules	M. Ikeno	- 1871

<Trigger>

Muon Detector Trigger	J. Chapman	- 1883
Muon Trigger Electronics	H. Sakamoto	- 1898
Level-1 Muon Trigger Using Xilinx FPGA	T. Zhao	- 1924

SDC Collaboration Meeting at
KEK, May 26-29, 1992
S. Terada; KEK

Muon Electronics
Overview and Development plan

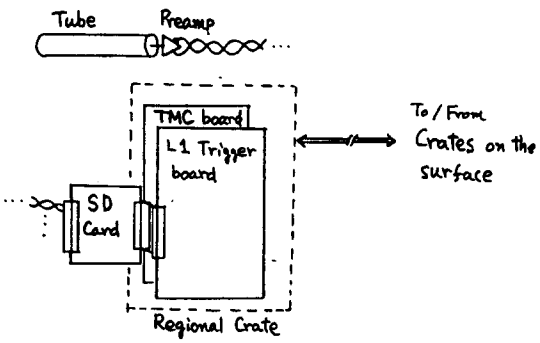

Development of Amp. Shaper Discri. (ASD)

Short term:

-For BNL Beam Test (June. 1992) ; ~4 ch.

a) Hybrid ASD used for the VENUS forward chamber

b) Penn. straw ASD chip

-For Minitower Chamber at KEK Beam Test (Feb. 1993); ~32 ch.

a) Penn. straw ASD chip?

Long term:

- For the Supertower prototype (May 1993); ~1,000 ch.

a) Muon ASD chip based on the straw ASD chip?

b) New preamp chip + New SD chip?

- For the Final Muon system (April 1994?); 100,000 ch.

a) Muon ASD chip based on the straw ASD chip?

b) New preamp chip + New SD chip?

Development of the TMC Board

-For the Minitower Chamber at KEK Beam Test (Feb. 1993); ~32 ch.

CAMAC-TMC module; 32 ch./board . 1μs Storage

- For the Supertower prototype (May 1993); ~500 ch.

VME (9U)-TMC module; 64ch./board, 1μs Storage

Development of the L1 Chamber Trigger Board

-For the Minitower Chamber at KEK Beam Test (Feb. 1993); ~32 ch.

First Prototype; 16 ch./board use FPGA's

- For the Supertower prototype (May 1993); ~500 ch.

Prototypes; 64 ch./board use FPGA's

and/or Michigan wire trigger chips?

Minitower Project at KEK Test Beam

Purpose:

a) Provide test bench for the development of a chamber trigger electronics.

b) Provide a mini-station for testing an overall read-out scheme.

Chamber Setup: Two sets of 4 x 4 tube arrays (32 ch.) simulating BW2θ and BW3θ

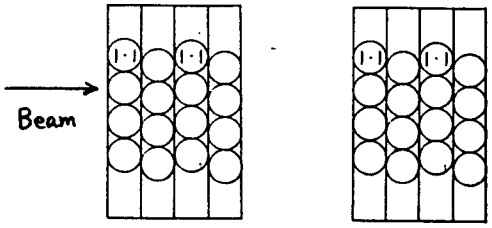

Test Beam at KEK PS:

a)T1 beam line; pion 0.5 ~ 2 GeV/c, 5 x 10^4 ppp at 1 GeV/c

b)π2 beam line; pion 1 ~ 4 GeV/c, 2 x 10^5 ppp at 3 GeV/c

Schedule: Beam Test at ~~Jan.~~ Feb. 1993

Preparation:

-Tube chambers; 32 tubes of ~ 60 cm in length

Aluminum extrusion -> Japanese vender

Endcaps and Shaping electrode -> SSCL/Washington

–Preamp. Shaper Discri.; Penn straw ASD chip?

-CAMAC-TMC module; 32ch./module , 1μs storage

-Prototype L1-trigger board. 16ch./VME (9U) board

-Portable DAQ system based on VME;

VME 9U/6U Crate

WS interface

CAMAC interface

Interrupt module

Trigger processor board

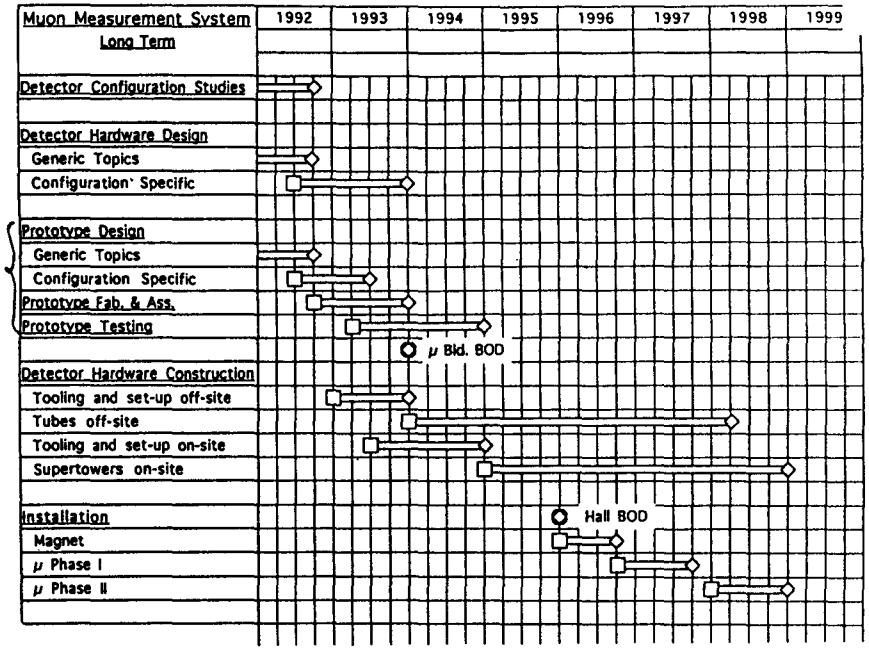
Muon Measurement System
Long Term
1992
1993
1994
1995
1996
1997
1998
1999
Detector Configuration Studies
Detector Hardware Design
Generic Topics
Configuration Specific
Prototype Design
Generic Topics
Configuration Specific
Prototype Fab. & Ass.
Prototype Testing
μ Bld. BOD
Detector Hardware Construction
Tooling and set-up off-site
Tubes off-site
Tooling and set-up on-site
Supertowers on-site
Installation
Hall BOD
Magnet
μ Phase I
μ Phase II

ASD Development

Yuzo Asano
(University of Tsukuba)

JSD Working Group on Muon Chamber ASD

M. Abe — Graduate student, Univ. of Tsukuba
Y. Asano — Institute of Applied Physics, Univ. of Tsukuba
K. Mitsuhashi — Graduate student, Univ. of Tsukuba
H. Ikeda — KEK

$R_L = 375$
$R_R = 2k$

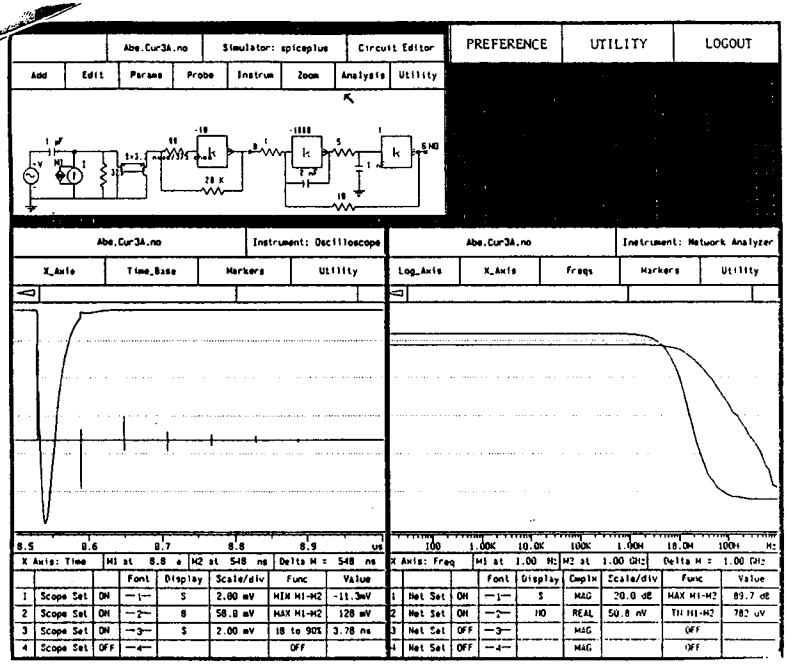

$R_L = 200$
$R_R = 2k\Omega$

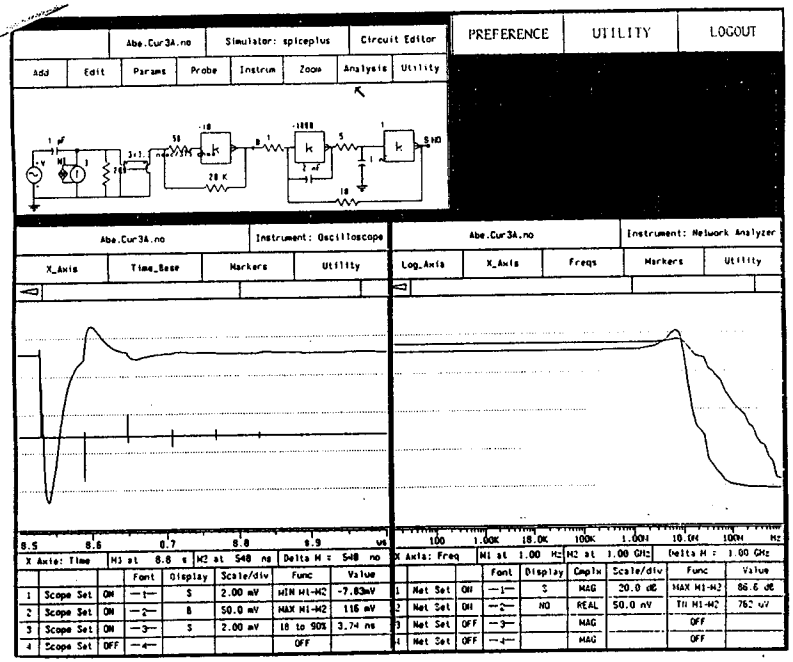

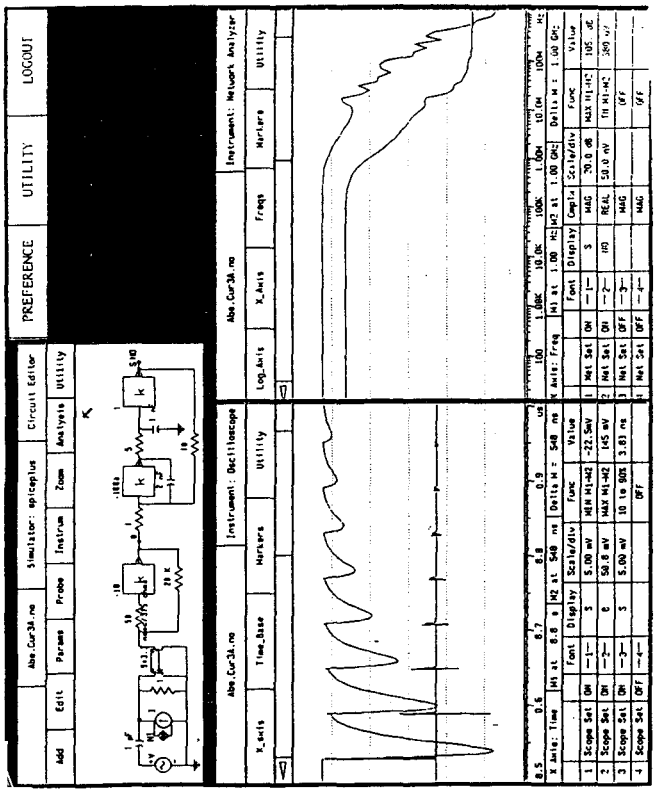

Check of simulator

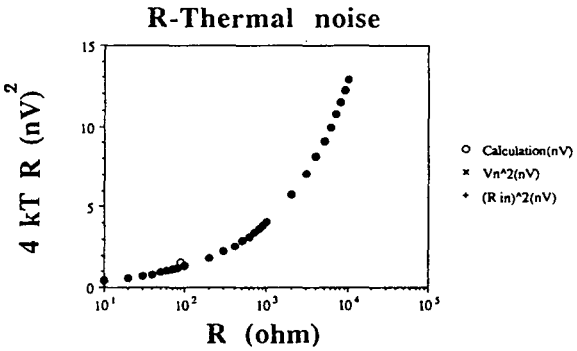

How to treat detector Capacitance

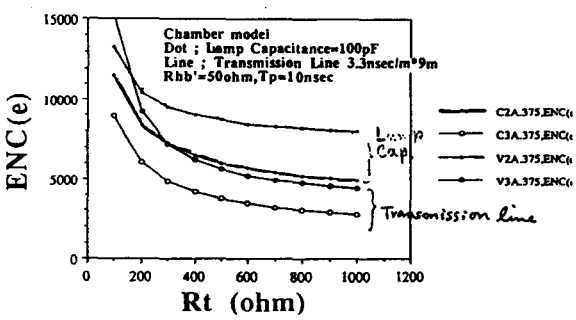

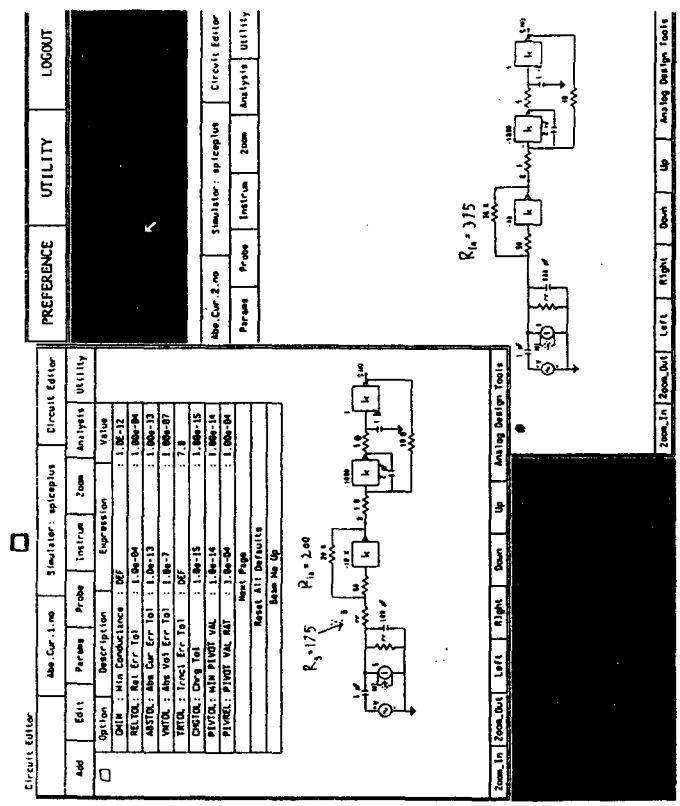

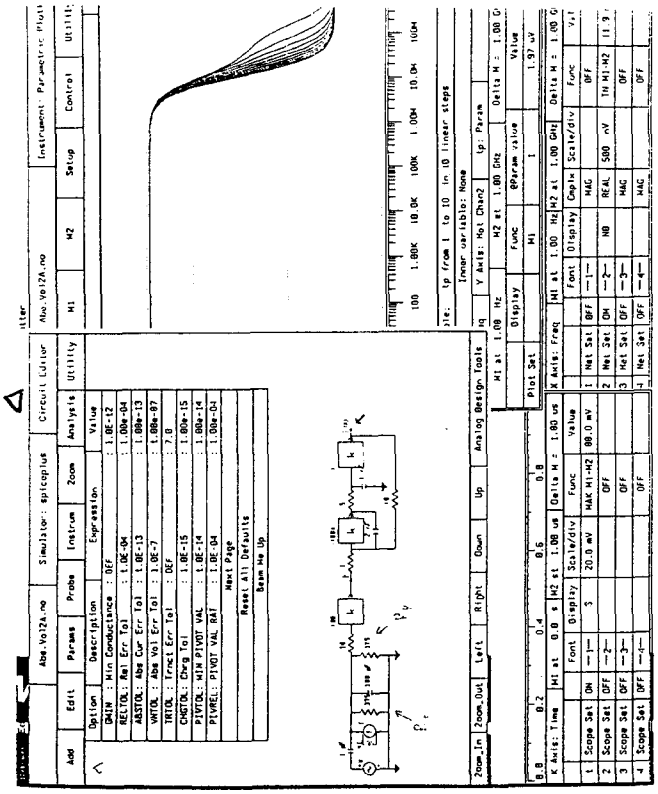

Dependence on termination resistor

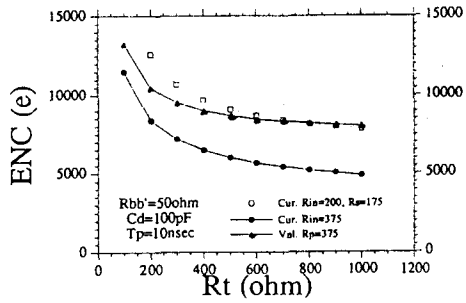

Dependence on Peaking time

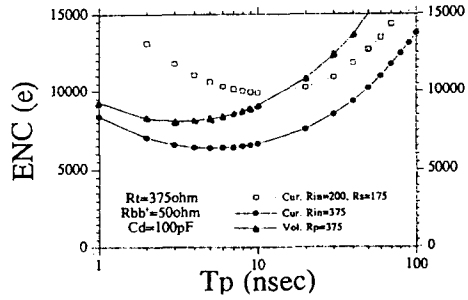

Dependence on detector Capacitance

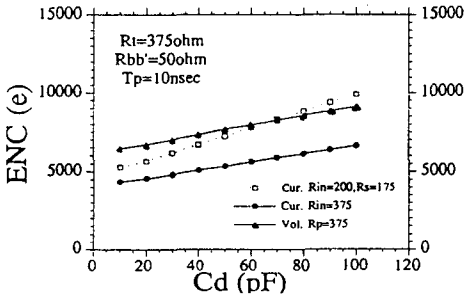

Dependence on Base resistance

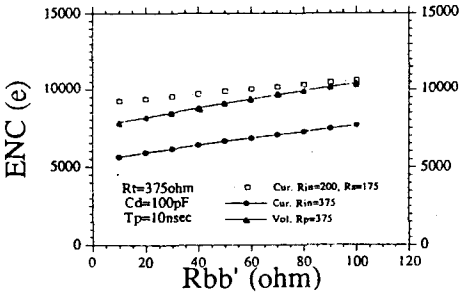

Comparison Between Current & Voltage Amp.

with a large C_D

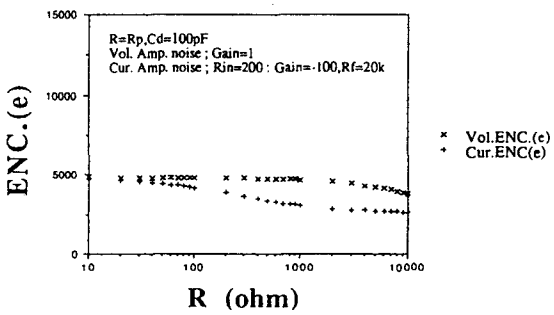

- Volatage amp. has a little larger magnitude of noises, but impedance matching would be easier.

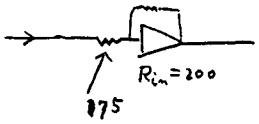

- matching with an external resistor makes the noise level comparable to vol.a

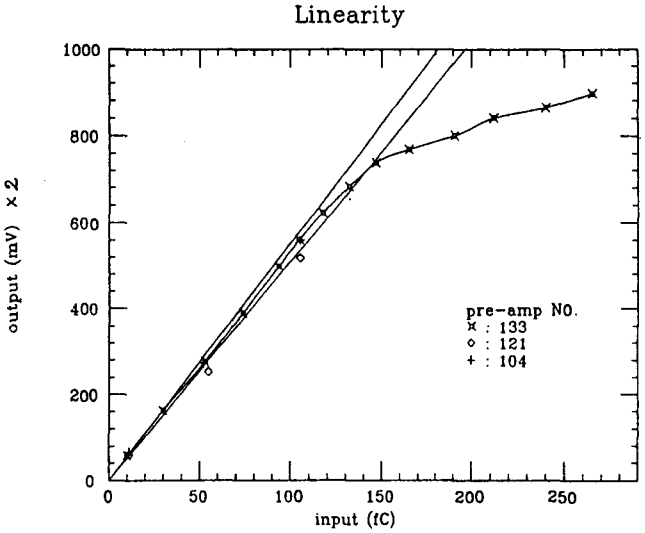

VENUS FC Pre-amp.

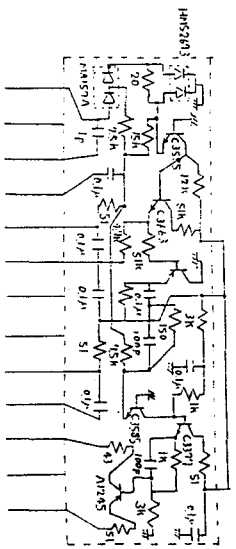

VENUS FC pre-amp.

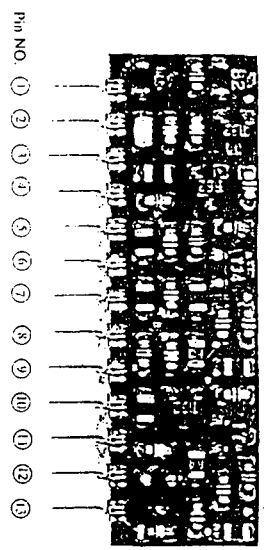

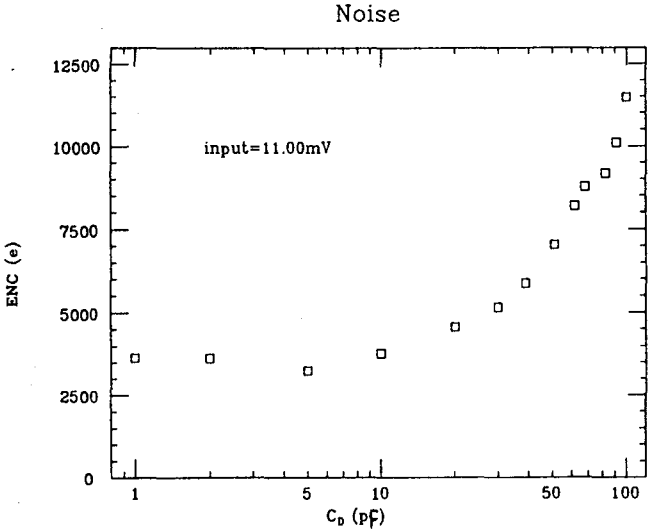

noise $\lesssim 10^4$ e required if $\leq$ 1ns time res for input charge 10^5 e.

VENUS FC pre-amp.

measurement

TC140G Series Gate Array

- 1.0 μm HC^{2}MOS Single Poly, Double Metal.
- 2.3 k ~ 172 k Gates (14 Sizes).
- Delay = 0.4 ns (2 input NAND, FO=2, L=2 mm).
- Sea-of-Gate Technology.
- Macro Cell/Function, Mega Cell/Function
  (RAM, ROM, ALU, Multiplier ...).

Toshiba Mega Cell Library

*RAM-I : Dual Port Memory
- 15.5 k Gates needed for 32 b x 128 w (4k bits) Memory.
  (4 k x 4 ch = 62 k gates)
- Address Access Time :
  Read = 7.1 ns (5V) [~12 ns (3V)]
  Write = 11.8 ns (5V) [~20 ns (3V)]

*FIFO :
- 2 k Gates needed for 8 b x 32 w FIFO.
- Cycle Time :
  Read = 12.8 ns (5V) [~21.6 ns (3V)]
  Write = 21.8 ns (5V) [~36.8 ns (3V)]
  (we may need circuit modification.)

New TMC Design with Toshiba Gate Array

SDC Collab. Meet. @KEK
1992.5.27 Y. Arai

- Toshiba Gate Array (TC140G), Library
- Toshiba CAD Software (VLCAD)
- New Cell Design (Differential Input Buffer)
- ~~Pentius Channel~~
- 9U Board TMC

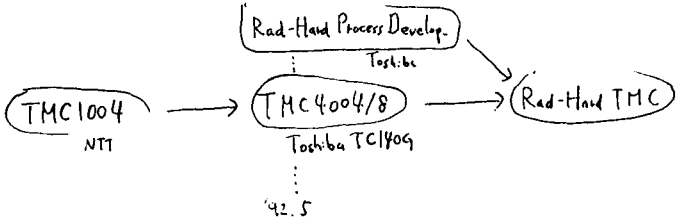

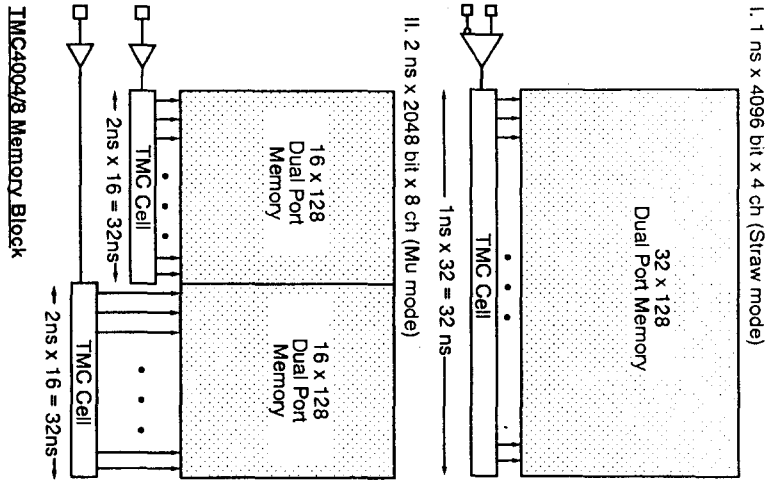

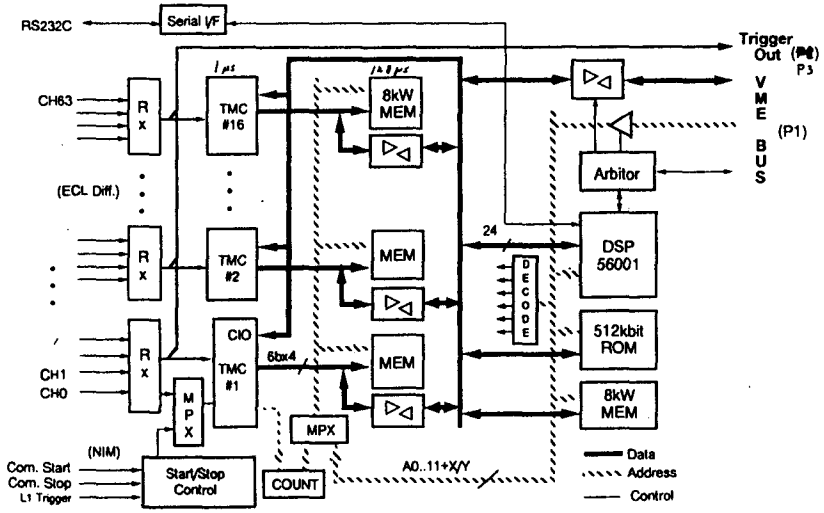

64ch TMC-VME Module (SDC Std. Board)

Toshiba CAD Softwares

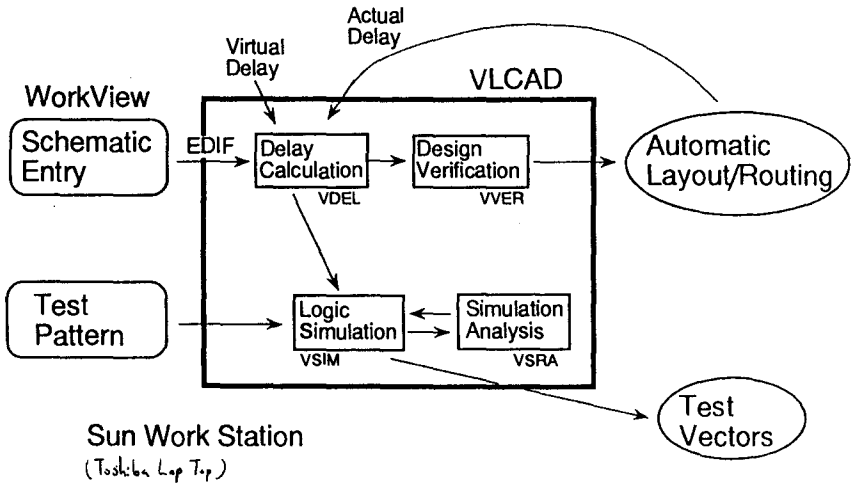

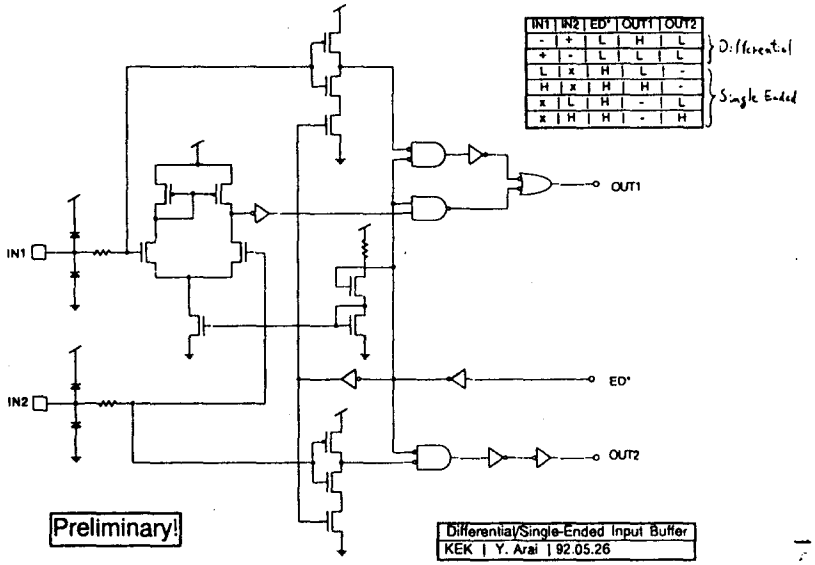

Plan

- Test Chip ... Input Buffers, TMC Cells, Feedback, ...
  (End of July)
- TMC4004/8
  (End of this year)
- TMC-VME(90) Board
  (End of this year)

STATUS OF TMC MODULES

Masahiro IKENO , KEK

1. CAMAC 32-channel TMC module

   10 modules were produced/ready for any users

2. CAMAC 32-channel Intelligent TMC module

   Circuit design completed to CAD input level and halted.
   (To start VME TMC module design)

3. VME TMC module

   Designing stage

TMC1004 32-Channel Multi-Hit TDC Module

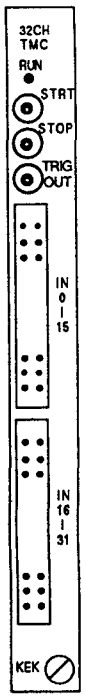

- 32 channels in single-width module
- 1ns / bit least count, σ = 0.52 ns time resolution
- 1024 bits / channel (or 2kbit / 2 ch, or 4kbit/ 4ch)
- Common stop or Common start operation
- No clear/dizitization time needed
- Rising edge detection and 6 bit encoded data output for each 32 ns data, or raw data dump for full data
- Very stable for temperature, voltage variation
- Q stop block transfer readout for encoded data
- ECL differential input for signal
- NIM level start / stop signal input
- NIM level trigger output for test purpose

Specifications

Signal Inputs :	32 Channel. ECL-differential. Input Impedance 100 Ω. Two 40-pin Flat Cable Connector. Input signal is stretched to about 32 ns internally if the width is less than 32 ns.
START Input :	One, common to all channels, 50 Ω impedance; Lemo-type connector; NIM level. Used in common Start mode.
STOP Input :	One, common to all channels, 50 Ω impedance; Lemo-type connector; NIM level. Used in common Stop mode.
TRIGGER Output :	Lemo-type connector; NIM level. Generate synchronous output pulse with internal clock when started. Used for test purpose.
Least Time Count :	1 ns/bit
Time Range :	1.024 μs (4 ch), 2.048 μs (2 ch) or 4.096 μs (1 ch)
Double Hit Resolution :	32 ns
Timing Measurement Error :	σ = 0.52 ns (including digitization error)
Integral Linearity Error :	< 1.5 bit
Differential Linearity :	< 0.2 ns
Variation of Slope : (time-to-digital conversion factor)	< 0.1 % (2.6 - 3.4 V) < 0.1 % (15 - 55 °C) < 0.1 % (chip to chip)
Channel to Channel Discontinuity:	< 0.5 bit
Data Readout :	Fast readout is done through encoded data readout (6 bit/ch) by F(0). The row which is read out is pointed by the Read Poimer (CSR1). For debugging and other purpose which requires entire data, Serial I/O mode through CSR0 can be used. This mode read out entire data of the TMC chip, but takes much longer readout time.
Data:	The proper CAMAC address and F(1) gates the 4 channel data of a TMC chip onto the R(1) to R(24). A(0) through A(7) are used for chip number.

	R24	R18	R12	R6	R1
Chip 0 : A(0)	Ch 3	Ch 2	Ch 1	Ch 0	
Chip 1 : A(1)	Ch 7	Ch 6	Ch 5	Ch 4	
	:	:	:	:	
Chip 7 : A(7)	Ch 31	Ch 30	Ch 29	Ch 28	

CAMAC Commands :	Z or C : All registers are simultaneously cleared by the CAMAC "Clear" or "Initialize" command. Requires "S2".

	X : An X=1 (Command Accepted) response is generated when a valid F, N, and A command is generated.
CAMAC Function Code :	F(0) : Read Data; requires N and A. A(0) through A(7) are used for chip address. F(1) : Read CSR0 register; requires N and A. A(0) through A(7) are used for chip address. F(4) : Read CSR1 (Read Pointer) register; requires N and A. A(0) through A(7) are used for chip address. F(6) : Read CSR2 (Write Pointer) register; requires N and A. A(0) through A(7) are used for chip address. F(9) : Reset. Reset all CSR registers and internal circuit. F(17) : Write CSR0 register; requires N and A. A(0) through A(7) are used for chip address. F(20) : Write CSR1 (Read Pointer) register; requires N and A. A(0) through A(7) are used for chip address. F(22) : Write CSR2 (Write Pointer) register; requires N and A. A(0) through A(7) are used for chip address. F(25) : Start signal recording. Used in common start mode. Functions as same as the START input, but F(25) starts signal recording with synchronous to the internal clock.
Packaging :	CAMAC 1 width module.
Power Requirement :	+6 V at 1.2 A, -6V at 0.5 A.

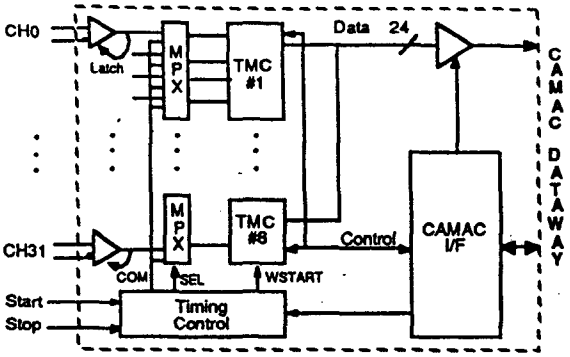

Block diagram of the TMC CAMAC module.

[Data Format]

23	18 17	12 11	6 5	0
CH3 data	CH2 data	CH1 data	CH0 data	

CAMAC Function Code

F(0) • A(0-7) : Read Data
F(1) • A(0-7) : Read CSR0
F(4) • A(0-7) : Read CSR1
F(6) • A(0-7) : Read CSR2
F(17) • A(0-7) : Write CSR0
F(20) • A(0-7) : Write CSR1
F(22) • A(0-7) : Write CSR2
F(9) : Reset
F(25) : Start

32-Ch Intelligent TMC Module

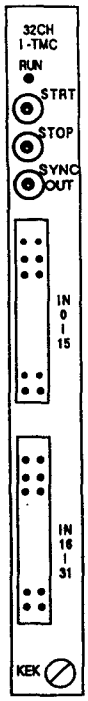

- 32 channels in single-width CAMAC module
- 1ns / bit least count, sigma = 0.52 ns time resolution
- 129 usec Full Scale
- Common stop or Common start operation
- Fast DSP56001 for Data Formatting
- Serial/Parallel I/F to DSP
- Rising/Falling edge detection and 6 bit encoded data output for each 32 ns data, or raw data dump for full data
- Very stable for temperature, voltage variation
- Q stop block transfer readout
- ECL differential input for signal
- NIM level start / stop signal input
- NIM level trigger output for test purpose

Specifications

Signal Inputs :	32 Channel. ECL-differential. Input Impedance 100 Ω. Two 40-pin Flat Cable Connector. Input signal is stretched to about 32 ns internally if the width is less than 32 ns.
START Input :	One, common to all channels, 50 Ω impedance; Lemo-type connector; NIM level. Used in common Start mode.
STOP Input :	One, common to all channels, 50 Ω impedance; Lemo-type connector; NIM level. Used in common Stop mode.
SYNC Output :	Lemo-type connector; NIM level. Generate synchronous output pulse with internal clock when started. Used for test purpose.
Least Time Count :	1 ns/bit
Maximum Time Range :	128 (ext. mem)+ 1 (TMC chip) μsec
Double Hit Resolution :	32 ns
Timing Measurement Error :	σ = 0.52 ns (including digitization error)
Integral Linearity Error :	< 1.5 bit
Differential Linearity :	< 0.2 ns
Variation of Slope : (time-to-digital conversion factor)	< 0.1 % (2.6 - 3.4 V) < 0.1 % (15 - 55 °C) < 0.1 % (chip to chip)
Channel to Channel Discontinuity:	< 0.5 bit
Data Readout :	
Data :	

CAMAC Commands :	Z or C : All registers are simultaneously cleared by the CAMAC "Clear" or "Initialize" command. Requires "S2". X : An X=1 (Command Accepted) response is generated when a valid F, N, and A command is generated.
CAMAC Function Code :	F(0)>A(0) : Read RAM Data; requires N. F(0)>A(1-8) : Read Data; requires N and A. A(1) through A(8) are used for chip address. F(1)>A(0) : Read RAM addr. register; requires N. F(1)>A(1-8) : Read CSR0 register; requires N and A. A(1) through A(8) are used for chip address. F(4)>A(0) : Read Module CSR register; requires N. F(4)>A(1-8) : Read CSR1 (Read Pointer) register; requires N and A. A(1) through A(8) are used for chip address. F(6)>A(1-8) : Read CSR2 (Write Pointer) register; requires N and A. A(1) through A(8) are used for chip address. F(9)>A(0) : Reset All. Reset all registers and internal circuit. F(9)>A(1-8) : Reset TMC. Reset all TMC registers. require N and one of A(1) through A(8) address. F(17)>A(0) : Write RAM addr. register; requires N. F(17)>A(1-8) : Write CSR0 register; requires N and A. A(1) through A(8) are used for chip address. F(20)>A(0) : Write Module CSR register; requires N. F(20)>A(1-8) : Write CSR1 (Read Pointer) register; requires N and A. A(1) through A(8) are used for chip address. F(22)>A(1-8) : Write CSR2 (Write Pointer) register; requires N and A. A(1) through A(8) are used for chip address. F(25) : Start signal recording. Used in common start mode. Functions as same as the START input.
Packaging :	CAMAC 1 width module.
Power Requirement :	+6 V at ? A, -6V at ? A.

General Description

CAMAC Module Circuit Description

Figure 1 shows the block diagram of the 32-channel Intelligent TMC CAMAC module. The module contains 8 TMC chips and a DSP56001.

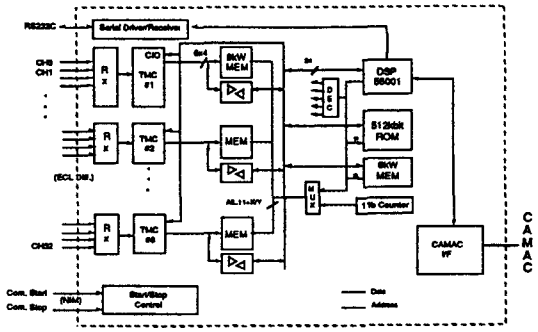

Fig.1 Block Diagram of the 32-channel Intelligent TMC CAMAC module

VME TMC MODULE

9U Single-width module

32-channel or 64-channel

129usec Full Scale

Common stop or Common start operation

DSP56001 for Data Formatting

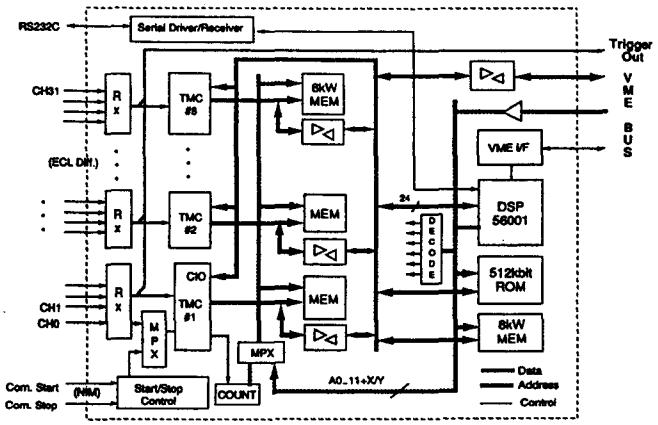

TMC-VME Module

SCHEDULE

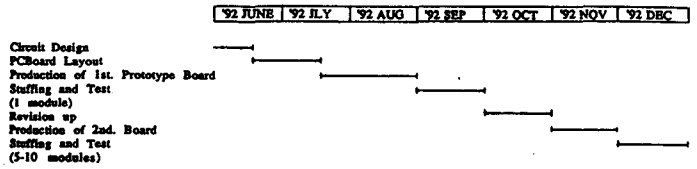

1883

Muon Detector Trigger

John W. Chapman
(University of Michigan)

1884

Muon Detector Trigger

Requirements

Design - Scintillators + Projective Wires

- Scintillators - timing to crossing
- Wires - Programable P_t thresholds

Simulation studies

Circuit development

- Scintillator circuit
- Wire circuit

Test results

Future tasks

- Supertower prototype
- Full simulation of detector/trigger
- Integrated storage,trigger,DAQ

1885

Muon P_t Distribution

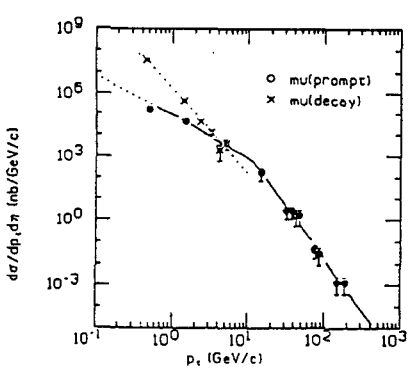

1886

Muon Rates

Rates in Barrel and Intermediate System
(Standard luminosity; $-1.5 < \eta < 1.5$)

Muons from pion and kaon decay	42 kHz
Muons from charm and bottom decay	45 kHz
Cosmic-ray muons	20kHz
Punch-thru, neutrons	<100 kHz
Total rate per scintillator	<100 Hz
Total rate above 20GeV	6 kHz

Rates in Forward System
(Standard luminosity; $1.5 < |\eta| < 2.5$)

Muons from pion and kaon decay	400 kHz
Muons from charm and bottom decay	100 kHz
Neutrons	≈MHz
Total rate per scintillator (est)	1-10 kHz

1887

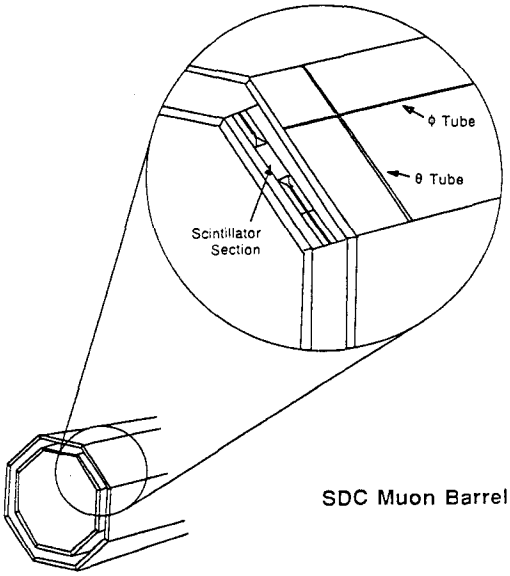

SDC Muon Barrel

1888

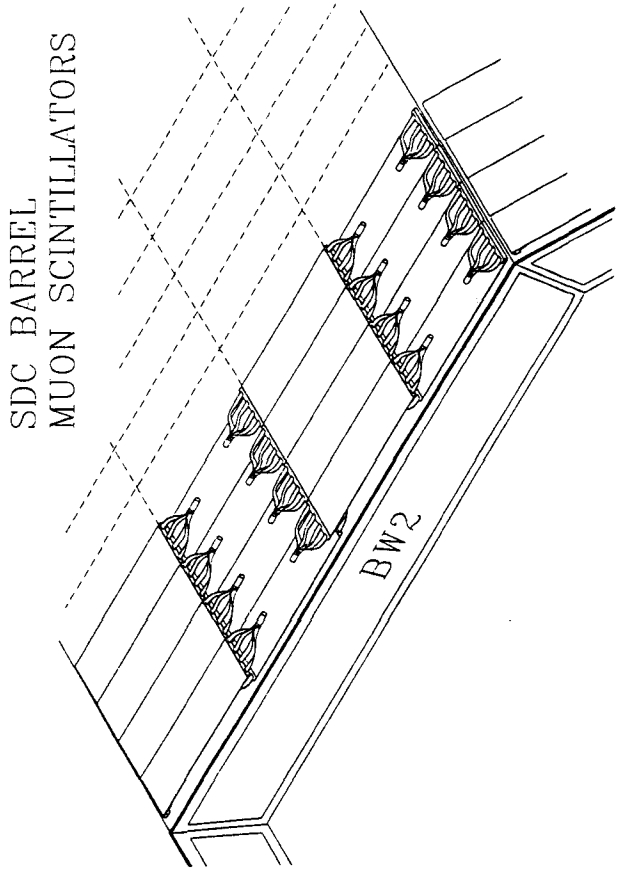

1889

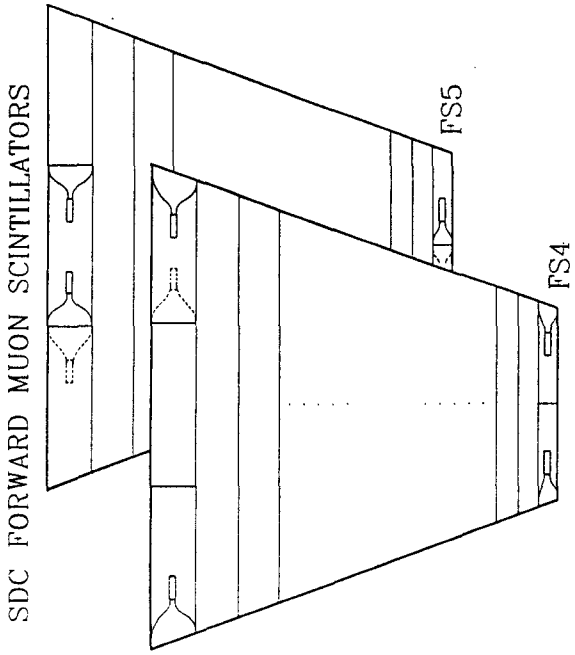

1890

Simplified Muon Trigger

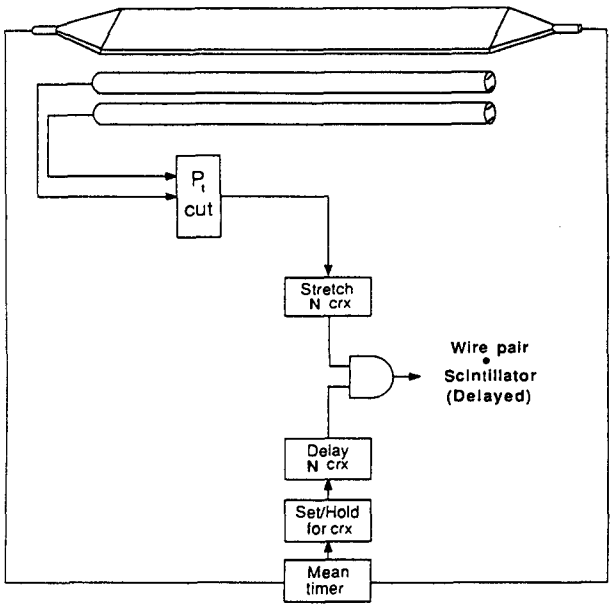

1891

Crossing Determination

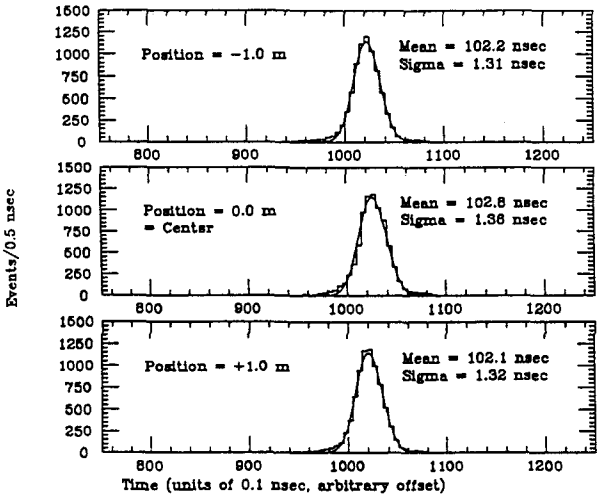

1892

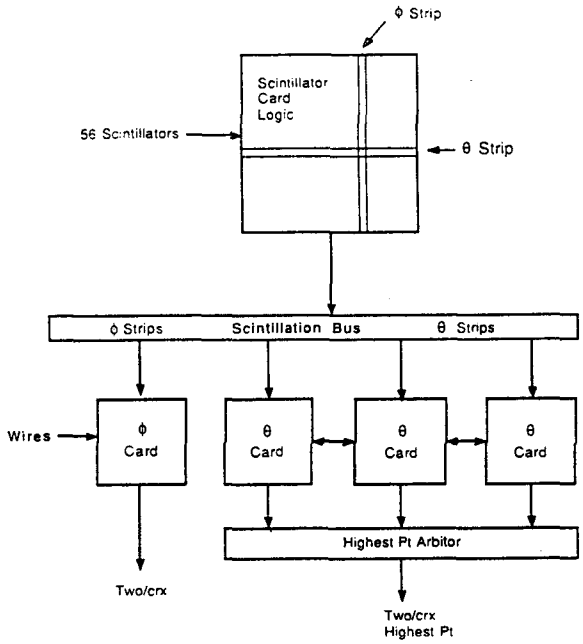

Muon Level 1 Trigger

1893

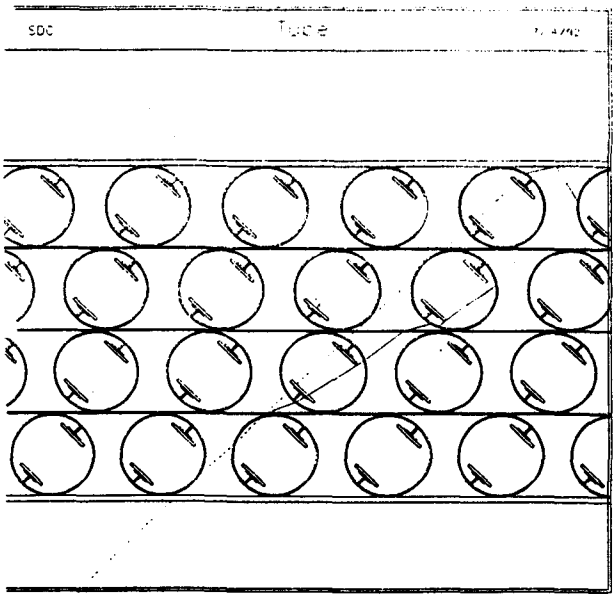

1894

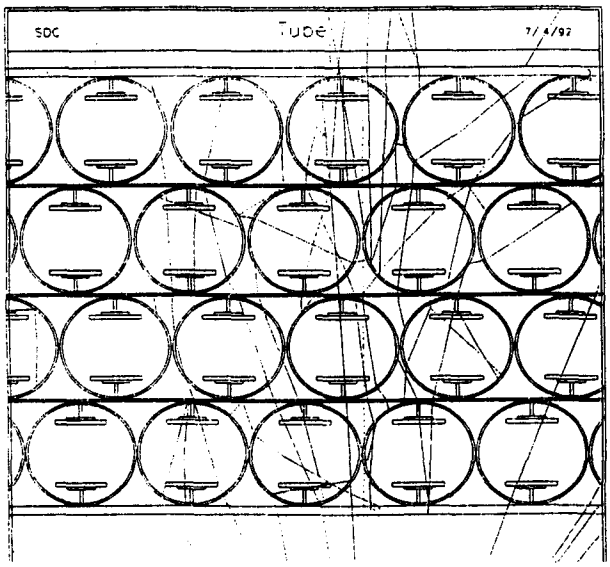

1895

Central Muon Trigger
Example P_t Thresholds

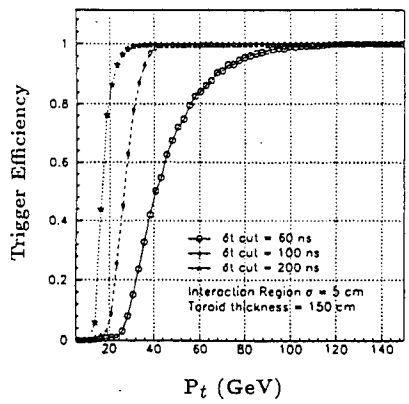

1896

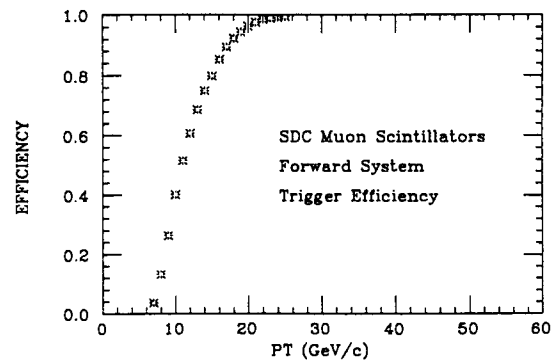

1897

SDC μ Trigger

Data Items

- 3 P_t thresholds
- 14θ 16ϕ scintillator strips
- θ wire pairs (≈300 max)
- ϕ wire pairs (≈150 max)
- Scintillator patches (224 max)

Data Sizes

- 2-bits P_t ← Level 1
- 4-bits θ scintillator
- 4-bits ϕ scintillator
- 8-bits ϕ wire pair
- 9-bits θ wire pair
- 8-bit scintillator patch address ← Level 2

Muon Trigger Electronics

KEK Hiroshi Sakamoto

Strategy for muon local trigger

Level 1

Finds a track segment in each superlayer
Counts the number of track segments

Level 2

Refines track segment information by TMC data
Connects segments among superlayers

Implementation (Prototyping)

Level 1

Time resolution of 16ns.
Field Programmable Gate Array

Level 2

TMC interface
Trigger processor array

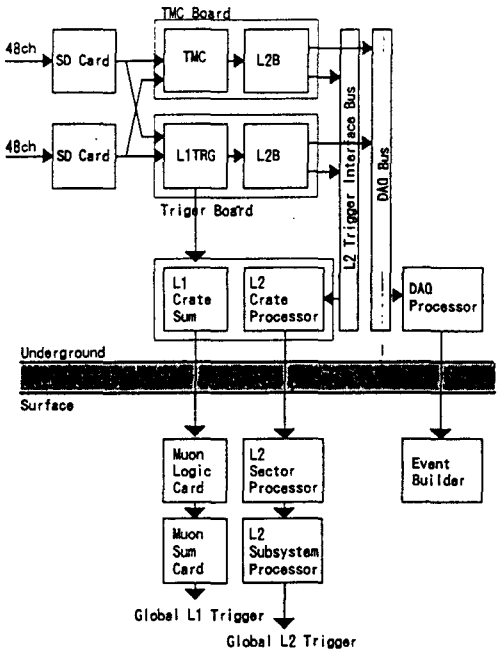

Muon Trigger System Architecture

MUTRG.DRW

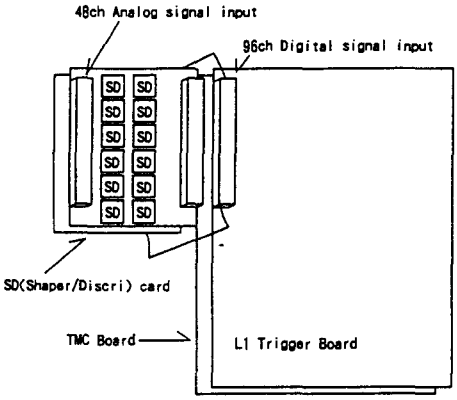

An SD card covers 48 channels from preamp.
TMC board and L1TRG board occupy adjacent 2 slots and share 96 digital inputs supplied by 2 SD cards behind the backplane.

Connection of muon input signals

SD2L1BRD.DRW

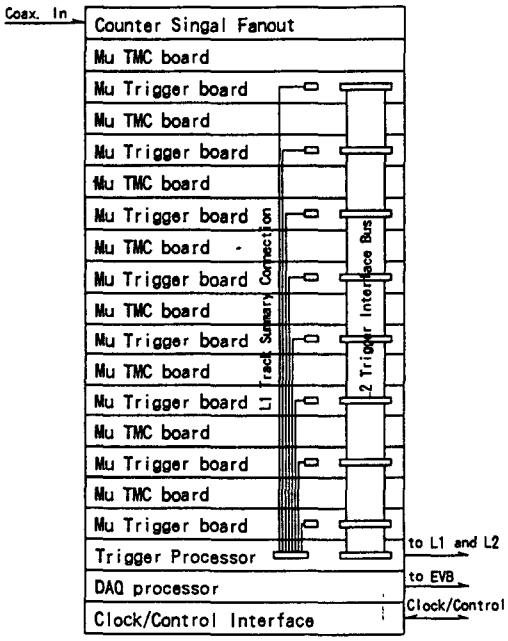

Muon read-out crate concept

MUCRATE.DRW

1902

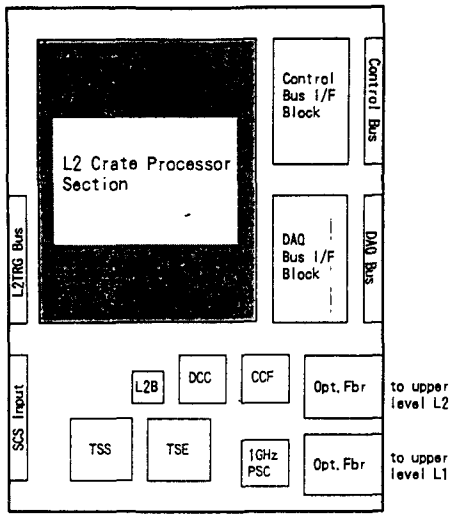

CCF: Clock and Control Fanout
DCC: Data Collection Chip
L2B: Level 2 Buffer
SCS: Track Segment Count Set
TSE: Track Segment Encoder
TSS: Track Segment Summation Circuit

Muon Crate Trigger Processor Board

1903

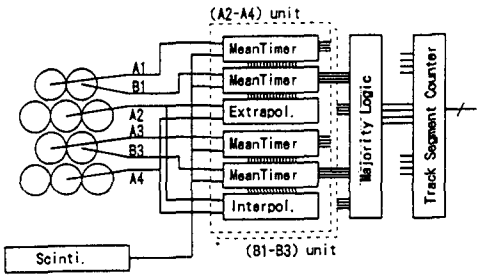

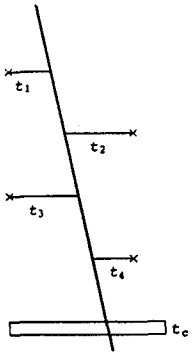

Equations

$$\frac{t_1 + t_3}{2} + t_2 = t_c + t_d$$

$$\frac{t_2 + t_4}{2} + t_3 = t_c + t_d$$

$$\frac{3t_3 - t_1}{2} + t_4 = t_c + t_d$$

$$\frac{3t_2 - t_4}{2} + t_1 = t_c + t_d$$

t_d Drift time between two anode planes.

Muon L1 Trigger Concept

TUBEL1.DRW

1901

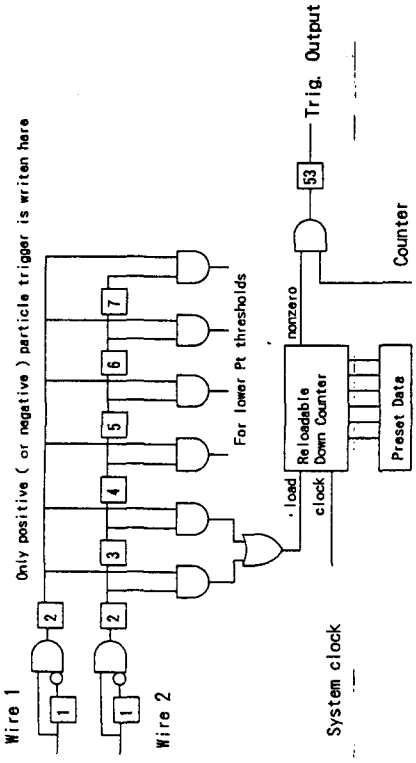

L1 Delta-T Logic

DELTA_T.DRW

1905

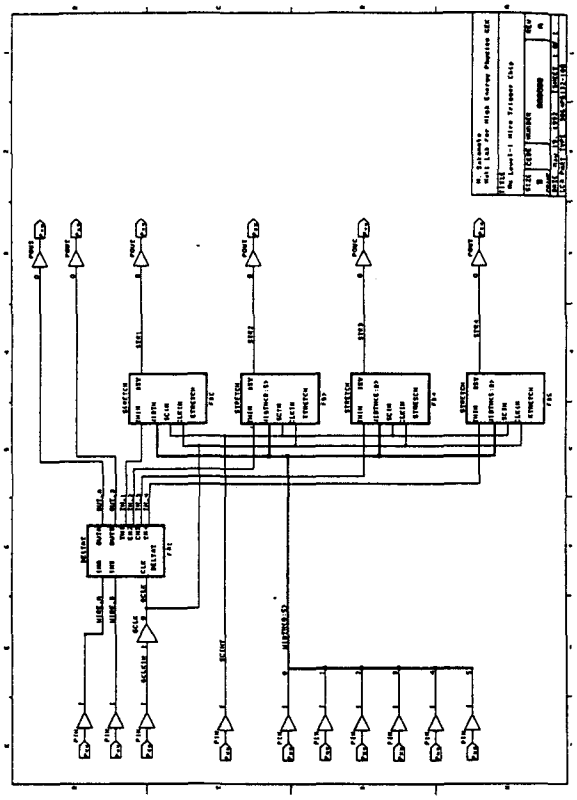

1906

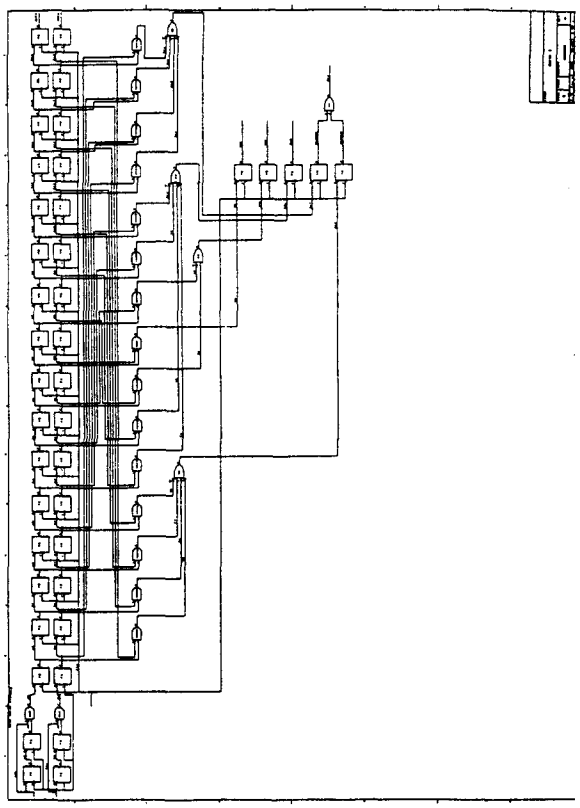

1907

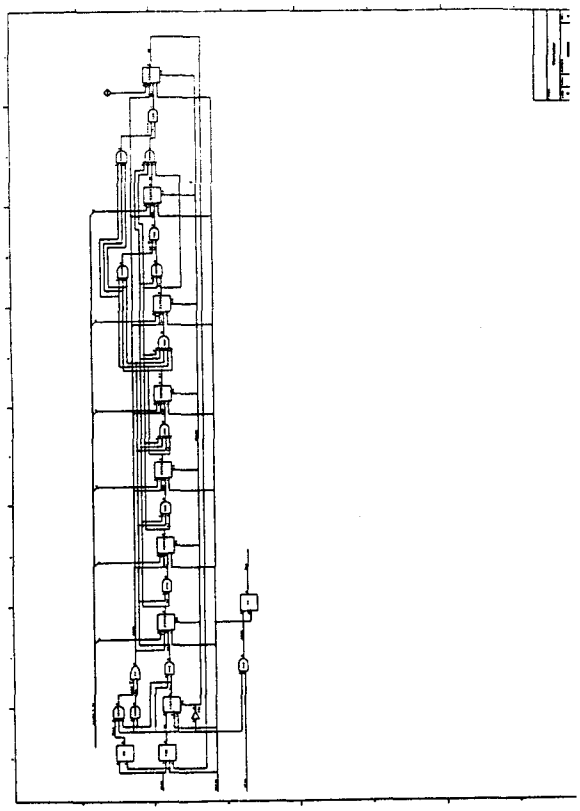

1908

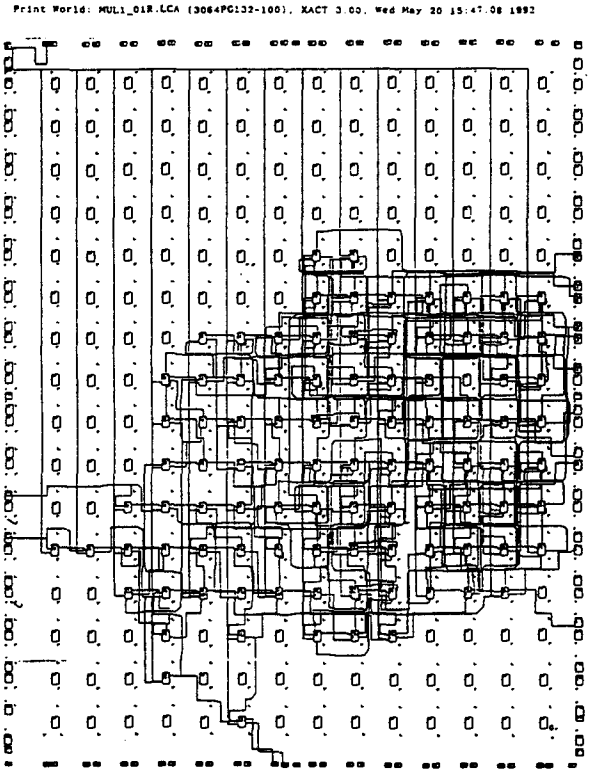

1909

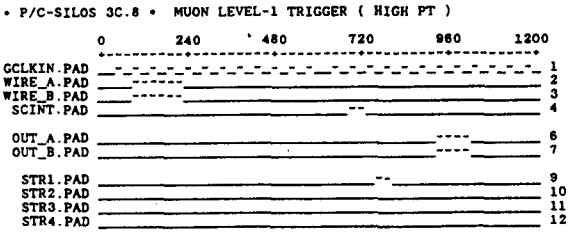

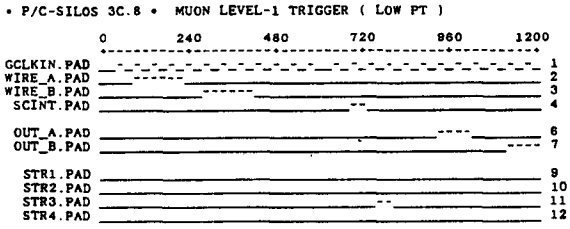

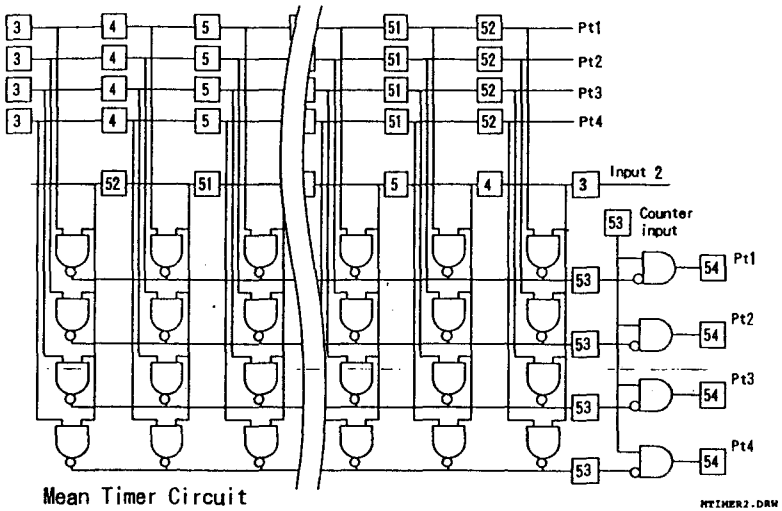

Mean Timer Circuit

MTIMER2.DRW

1912

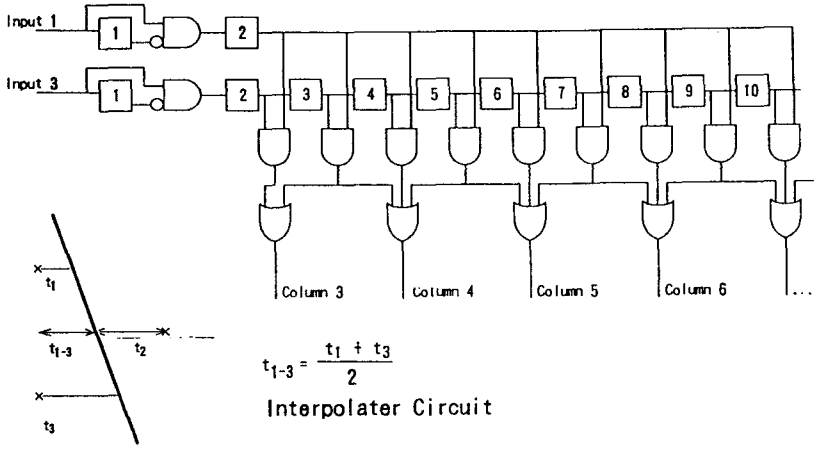

$$t_{1-3} = \frac{t_1 + t_3}{2}$$

Interpolater Circuit

L1ITP.DRW

1910

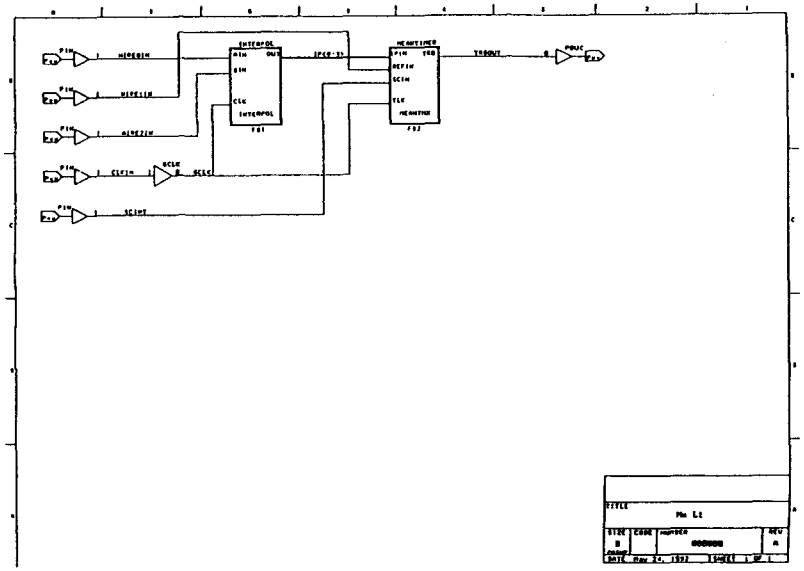

1913

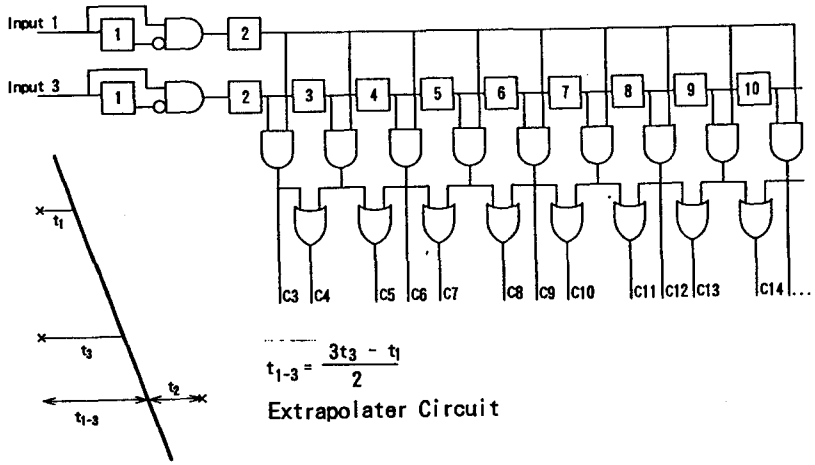

$$t_{1-3} = \frac{3t_3 - t_1}{2}$$

Extrapolater Circuit

L1EXT.DRW

1911

1914

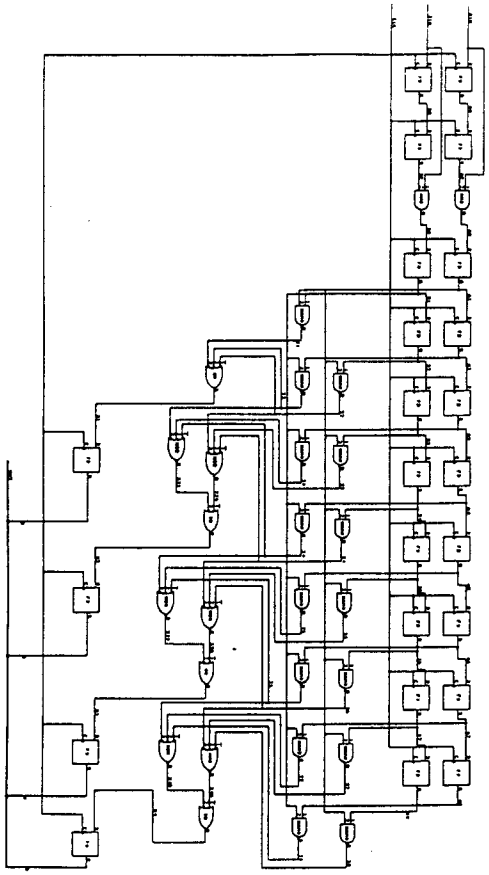

1915

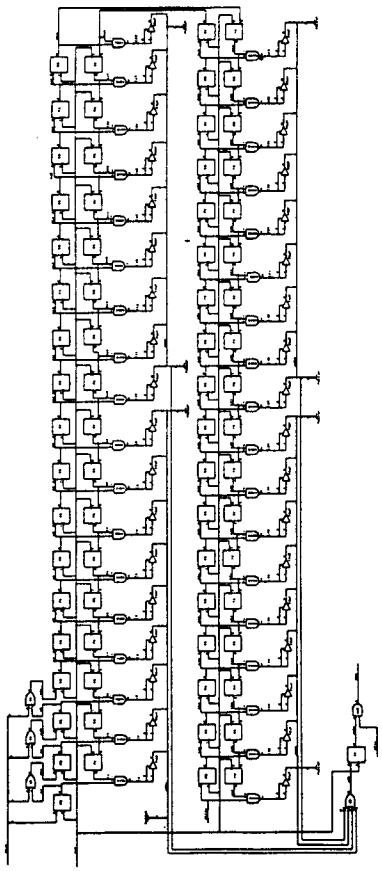

1916

```
• P/C-SILOS 3C.8 •  MU L1 INTERPOLATER/MEANTIMER CIRCUIT ( 36 STEPS )

              0        1000      2000      3000      4000      5000
              +---------+---------+---------+---------+---------+
   CLKIN.PAD  _################################################# 1
   SCINT.PAD  ______________________________________-____________ 2
 WIRE0IN.PAD  _--_____________________________________________ 3
 WIRE1IN.PAD  ____________________________________--____________ 4
 WIRE2IN.PAD  _--_____________________________________________ 5

  TRGOUT.PAD  ______________________________________#____________ 7

• P/C-SILOS 3C.8 •  MU L1 INTERPOLATER/MEANTIMER CIRCUIT ( 38 STEPS )

              0        1000      2000      3000      4000      5000
              +---------+---------+---------+---------+---------+
   CLKIN.PAD  _################################################# 1
   SCINT.PAD  ______________________________________-____________ 2
 WIRE0IN.PAD  _--_____________________________________________ 3
 WIRE1IN.PAD  ____________________________________--____________ 4
 WIRE2IN.PAD  _--_____________________________________________ 5

  TRGOUT.PAD  ______________________________________-____________ 7

• P/C-SILOS 3C.8 •  MU L1 INTERPOLATER/MEANTIMER CIRCUIT ( 36 STEPS )

              0        1000      2000      3000      4000      5000
              +---------+---------+---------+---------+---------+
   CLKIN.PAD  _################################################# 1
   SCINT.PAD  ______________________________________-____________ 2
 WIRE0IN.PAD  _--_____________________________________________ 3
 WIRE1IN.PAD  ____________________________________--____________ 4
 WIRE2IN.PAD  _--_____________________________________________ 5

  TRGOUT.PAD  ______________________________________________ 7

• P/C-SILOS 3C.8 •  MU L1 INTERPOLATER/MEANTIMER CIRCUIT ( 36 STEPS )

              0        1000      2000      3000      4000      5000
              +---------+---------+---------+---------+---------+
   CLKIN.PAD  _################################################# 1
   SCINT.PAD  ______________________________________-____________ 2
 WIRE0IN.PAD  ____________--__________________________________ 3
 WIRE1IN.PAD  ____________________________--__________________ 4
 WIRE2IN.PAD  ____________--__________________________________ 5

  TRGOUT.PAD  ______________________________________-____________ 7
```

1917

XC4000 Logic Cell Array Family

PRELIMINAR'

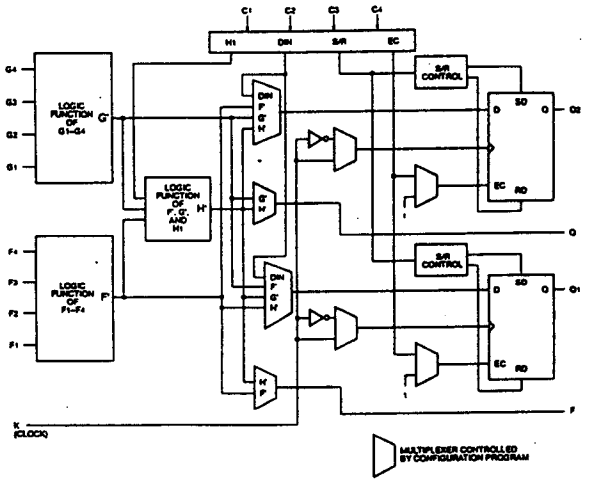

Figure 1. Simplified Block Diagram of XC4000 Configurable Logic Block

Function	XC3000 Family	XC4000 Family
8/9 bit Parity Generate/Check	14 ns / 2 CLB	5 ns / 1 CLB
24-bit Input Decode	20 ns / 5 CLBs	10 ns/ 0 CLBs
32:32 Bit Identity Comparator	16 ns/ 16 CLBs	12 ns/ 8 CLBs
16:1 Multiplexer	28 ns/ 7 CLBs	20 ns/ 5 CLBs
16-bit Synchronous Counter	35 ns/ 14 CLBs	20 ns/ 8 CLBs
16-bit Loadable Counter	60 ns/ 18 CLBs	20 ns/ 8 CLBs

Table 3. Density and Performance for Several Common Circuit Functions

Parameter	XC4000	XC3000	XC2000
Max number of flip-flops	2280	928	174
Max number of user I/O	240	144	74
Max number of RAM bits	28,800	0	0
Function generators per CLB	3	2	2
Number of logic inputs per CLB	9	5	4
Number of logic outputs per CLB	4	2	2
Number of low-skew global nets	8	2	2
Dedicated decoders	yes	no	no
Fast carry logic	yes	no	no
Internal 3-state drivers	yes	yes	no
Output slew-rate control	yes	yes	no
Power-down option	no	yes	yes
Crystal oscillator circuit	no	yes	yes

Table 2. Three Generations of Xilinx Field-Programmable Gate Array Families

Field Programmable Gate Array

	Crosspoint	Xilinx	Actel
Product	CP20K	XC4000	ACT2
Release	92/2	Available - 92/?	Available
Max. gates	20k	20k	8k
Technology	0.75 μ	0.9 μ	1.2 μ
Architecture	TPT,RLT	IOB,CLB	Logic Module
Toggle Freq.	200MHz		120MHz
System Clock	50MHz	60-70MHz	50MHz
I/O Pads	91-270	64-240	140
Input Level	CMOS,TTL	CMOS,TTL	CMOS,TTL
Pullup	yes	yes	no
Schmitt Trig.	yes	no	no
Output Option			
3state	yes	yes	yes
Through Rate	yes	yes	no
Open drain	yes	no	no
Open source	yes	no	no
Driving Curr.	4/8/12mA	12mA	8mA
MGA compat.	yes	no	no
Programming	Anti-fuse 150 Ω one time	Memory cell rewritable	Anti-fuse 500 Ω one time
JTAG I/F	yes	yes	no

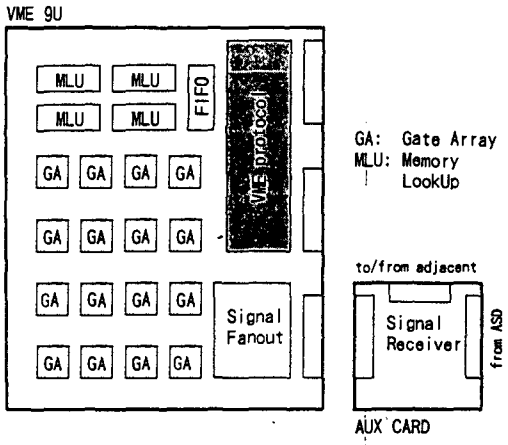

L1 TRIGGER PROTOTYPE BOARD concentual view

PROTL1.DRW

Summary

Level 1

Design study using slower but rewritable FPGA

Delta-T (Pt) detector/stretcher/coincidence
Interpolater/extrapolater/mean-timer/coincidence
Track segment counter on board/in crate

Interface to Level 2 buffer
Threshold control function
Diagnostics/monitoring function

Transport to high speed (one time write) FPGA

Level 2

Prototype L2 function

Muon TMC - L2 interface (Buffer/Trigger)
Prototype crate processor board

Evaluation of L2 performance

Algorithm for crate L2 processor
Algorithm for muon subsystem L2 processor array

1921 1

Summary and Plan

Level-1 muon Trigger

using Xilinx FPGA

T. Zhao

U. Washington

1925 2

- Tubes arranged as equally spaced layers
- But drift in θ-direction

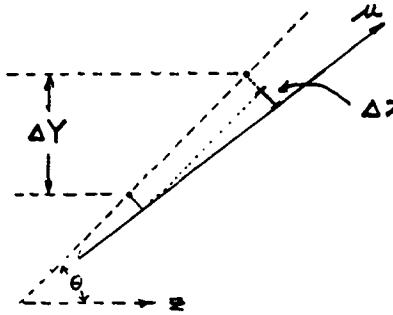

$$\Delta x = \Delta\theta \frac{\Delta Y}{\sin\theta} = \frac{\Delta Y}{2 P_t} \cdot \frac{1}{\sin\theta}$$

Δx (cm) \ θ / P_t (GeV)	90°	75°	60°	45°	30°
10	1. (200ns)	1.04	1.15	1.41	2. (400ns)
50	0.2	0.21	0.23	0.28	0.4

1926

5

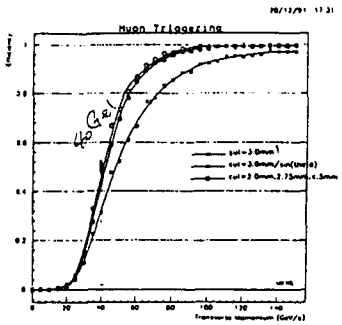

Figure 5.5. Three different cuts for round tubes.

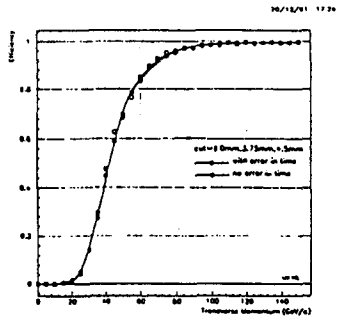

Figure 5.6. ±8 ns error of trigger electronics start and stop time makes no difference.

1927

4

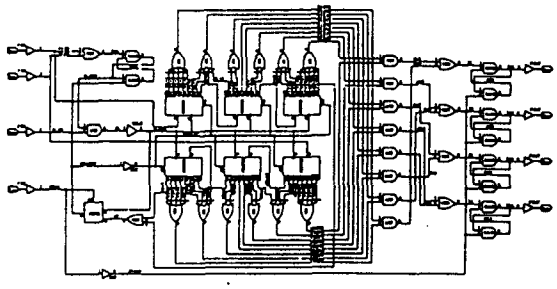

Figure 5.12. Logic diagram of circuit 2.

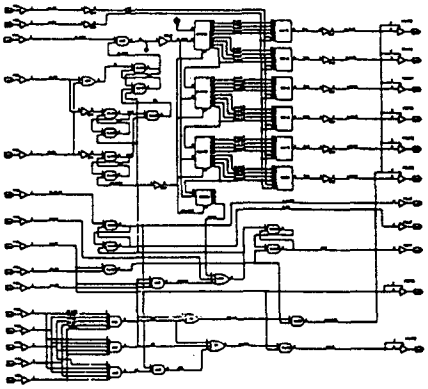

Figure 5.13. Logic diagram of the CAMAC trigger module.

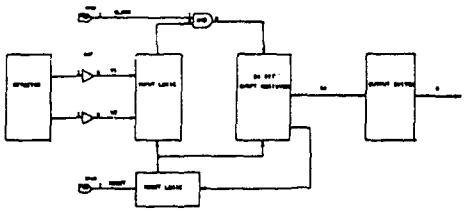

Figure 5.10. Block diagram of trigger circuits.

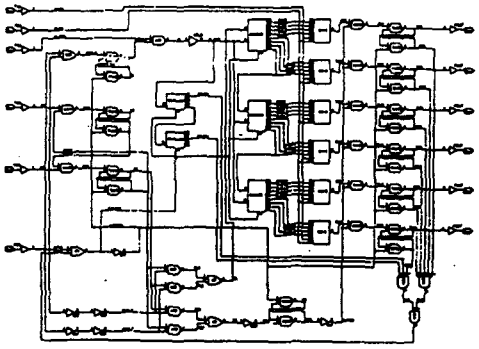

Figure 5.11. Logic diagram of circuit 1.

Δt circuits. 6

Prototype Board (CAMAC)

XC3020-100
XC3030-100 }

Clock speed : 90 MHz.

Time resolution at 60 MHz

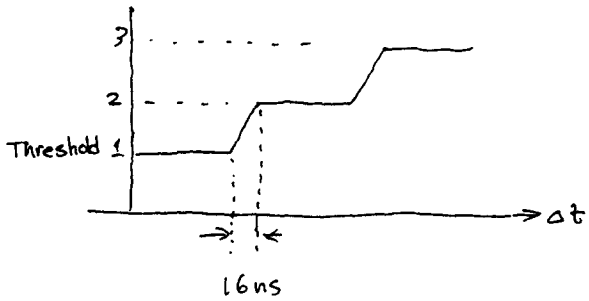

Low cost Xilinx Chips

40 pin plastic package
70 MHz

XC3020 ~$5.60 per chip

XC3030 ~$7.90 per chip

2 channels circuits can be fit in a XC-3030 chip

[9] Muon/Integration Joint

SDC Intermediate Muon System Status F. Feyzi - 1932

SDC Intermediate Muon System Status

Farshid Feyzi
(University of Wisconsin)

SDC Intermediate Muon System Status
Presented at KEK
May 26-29, 1992

University of Wisconsin-Madison
Physical Sciences Laboratory &
Department of Physics

1. Introduction

   . Design criteria is to extend the Barrel Region into the Intermediate Region by preserving coverage and trigger schemes.

   . Closed IW3/BW3 corner minimizes dead zones without overlaps.

   . IW3 order in increasing Z (reverse of barrel for better coverage):

      - 4 theta (projective)

      - 2 stereo (100 mr)
        options:
        a) no stereo, radial phi gives 22% effective stereo coverage
        b) 2s at 100 mr plus short tubes to cover triangles left
        c) s1,s2 (+/-100 mr like FW) covers 80%, plus short tubes can cover 90-% (preferred option)
        d) stheta, sphi (like proposed for barrel) it is complex

      - 4 phi (phi is radial and makes 8 physical layers)

   . IW3's are all identical and much smaller than TDR

   . IW2's are all identical except in access octants

2. Tube layout

   . Drawings and algorithm for projective theta in IW2 and IW3 with no sparsification

   . Drawings and algorithm for radial phi wires

   . Drawings and algorithm for s1,s2 and dead zone (option c above)

   . Tube counts and lengths for above

3. Supermodule/Supertower design and analysis

   . Supermodules are built from tube and plate structure, like Barrel

   . Supertower built from supermodules and outer plates

   . Preliminary FEA of assembly shows that IW3 moves as a rigid object by approximately 2.5 mm. (less deflection is possible)

   • IW2 deflection 0.5 mm

4. Scintillators need work

   . Layout
   . Support
   . Access

5. Support and alignment

   . 4-point "kinematic" supports on the barrel toroid

   . Reaction loads on the toroid have been calculated

   . Scheme for getting at impossible areas is under study

   . Positioning of mounts on the toroid to be done when barrel rails are positioned.

   . Use support struts that are in the same space as the barrel rails (180 mm inside and 230 mm outside, max). This will maximize cable tray on Barrel Toroid face.

   . Impact on all utilities for muon system, i.e. coil cooling coil power, muon gas, muon power is under study.

   . Alignment is assumed to be per TDR, but much needs more work.

6. Cost and schedule

   . Presented design tasks and durations at SSCL on 28 April.

   . Cost is assumed to be per WBS, but needs more work.

   . Schedule needs work. We propose:

      - Start of first IW supertower to follow soon after, or during, first barrel supertower, i.e. start 3rd quarter 1993, or sooner.

      - Two (or three) IW supertowers are to be ready for installation when phase I muon starts, i.e. 3rd quarter 1996.

      - All IW's installed by end of phase II, i.e. end of 1998.

7. Production plan, similar to barrel (unique aspects are under study)

   . Tube production facility layout

   . Supermodule production facility plan

   . Tooling for tubes

   . Jigging for supermodules

   . labor requirements

   . QC/QA

8. Electronics, high voltage, gas

   . Crates and distribution boxes to be located on IW3

   . Cables and tubing for IW2 to be routed through corner of IW3

   . Supertowers go into the underground hall complete with everything internal so all they need is power, gas and signal hookup.

9. Supertower assembly and installation plan

   . Constraints on other things during installation

   . Space requirements to assemble IW2, IW3 and support structure into a supertower

   . Supertowers are big (3m x 4m x 8.5m). Assembly ~~should~~ must be done on or near SDC site.

   . Installation tool

   . Storage stands

   . Storage space

file psl::d8:[farshid.sdc.text]intermkek.tx1

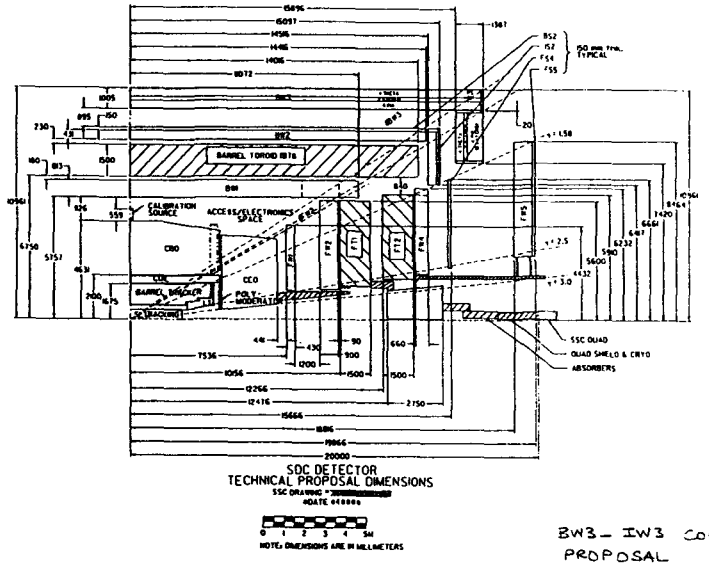

BW3 – IW3 CORNER
PROPOSAL
UW-PSL
GMG 5/15/92

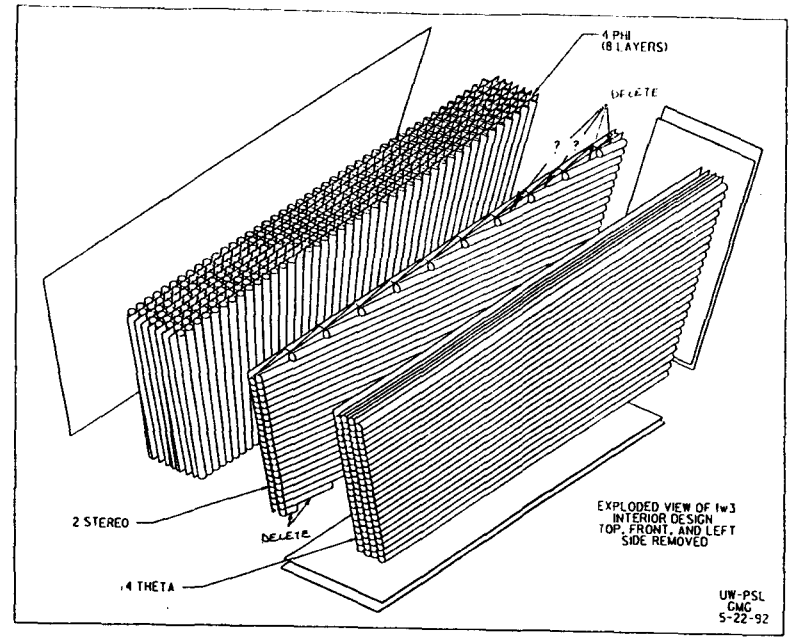

IW2 – IW3 θ TUBE LAYOUT Y-Z VIEW
(NOT TO SCALE)

• CONSTANTS:
$C = 47.05625$ mm
$S_1 = 94.1$ mm
$a = 95.7$ mm
$f = 40$ mm
$d = 93.6$ mm

• TUBE END Z LOCATIONS:
$z_1 = z_A + c$
$z_2 = z_1 + a$
$z_3 = z_1 + 2a$
$z_4 = z_1 + 3a$

• TUBE SPACING:
$S_2 = (z_2/z_1)S_1$
$S_3 = (z_3/z_1)S_1$
$S_4 = (z_4/z_1)S_1$

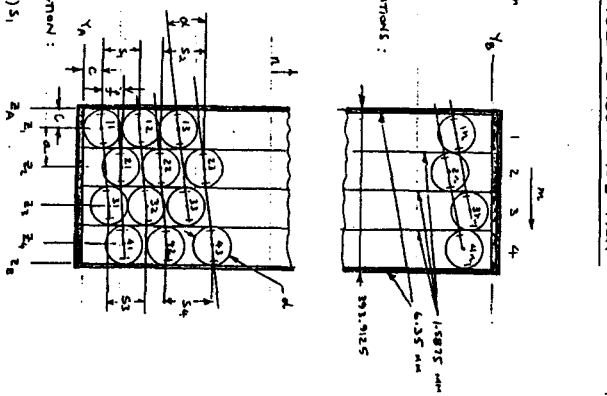

• TUBE END Y LOCATION:
$Y_{1n} = Y_A + C + (n-1)S_1$
$Y_{2n} = Y_A + C + f + (n-1)S_2$
$Y_{3n} = Y_A + C\frac{z_3}{z_1} + (n-1)S_3$
$Y_{4n} = Y_A + (C+f)\frac{z_4}{z_2} + (n-1)S_4$

IW2 – IW3 θ TUBE LAYOUT X-Y VIEW
(NOT TO SCALE)

• CONSTANTS:
$g = 14$ mm
$e_b = 100/\cos 22.5°$
$e_c =$

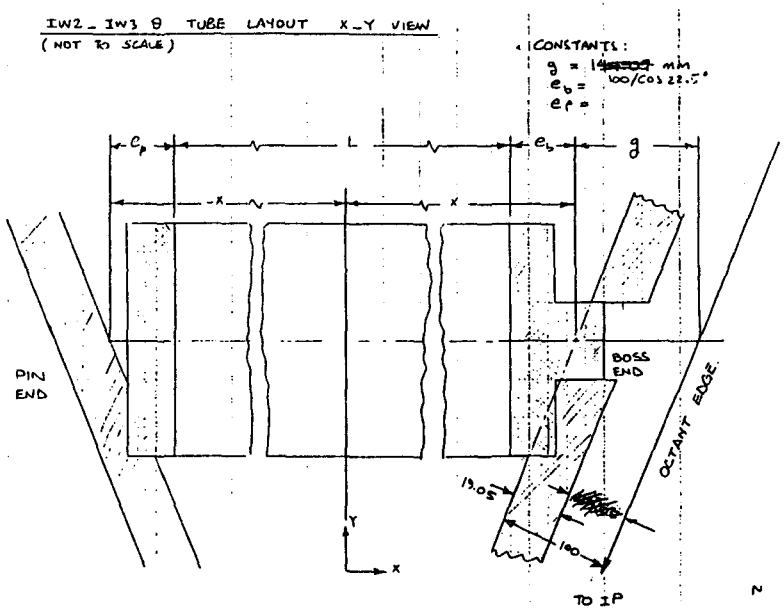

3

- TUBE COUNTS:

$$n_1 = \text{TRUNC}\left[\frac{Y_B - Y_A - 2C}{S_1}\right] + 1$$

$$n_2 = \text{TRUNC}\left[\frac{Y_B - Y_A - (2C + f)}{S_2}\right] +$$

$$n_3 = \text{TRUNC}\left[\frac{Y_A - Y_B - \left(C\frac{z_1}{z_3} + C\right)}{S_3}\right] + 1$$

$$n_4 = \text{TRUNC}\left[\frac{Y_B - Y_A - \left((C+f)\frac{z_4}{z_2} + C\right)}{S_4}\right] +$$

- TUBE ORIENTATION:

$$\alpha_{1n} = \alpha_{3n} = \tan^{-1}\frac{Y_{1n}}{z_1} = \tan^{-1}\frac{Y_{3n}}{z_3}$$

$$\alpha_{2n} = \alpha_{4n} = \tan^{-1}\frac{Y_{2n}}{z_2} = \tan^{-1}\frac{Y_{4n}}{z_4}$$

- TUBE END X LOCATIONS:

$$x_{mn} = \pm Y_{mn}\tan(22.5^\circ) - g$$

- TUBE LENGTHS:

$$L_{mn} = 2|x_{mn}| - (e_b + e_p)$$

4

IW3 Φ TUBE LAYOUT (NOT TO SCALE)

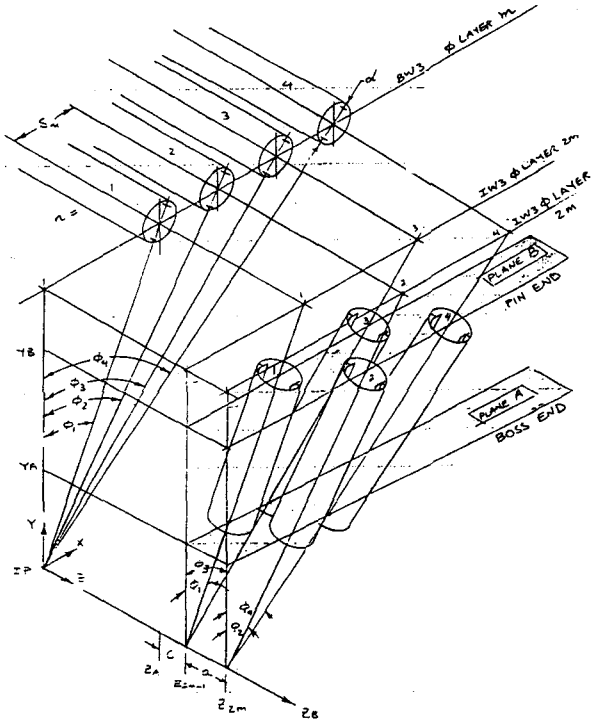

5

IW3 Φ TUBE LAYOUT

CONSTANTS:
SAME AS θ TUBES

INPUT:
(DERIVED FROM BARREL Φ LAYOUT)

Φ_n FOR $m = 1, 2, 3, 4$ AND ALL n

- TUBE END Z LOCATIONS:
  FOR $m = 1, 2, 3, 4$

$$z_{2m-1} = z_A + C + (2m-2)a$$

$$z_{2m} = z_A + C + (2m-1)a$$

TUBE END Y LOCATIONS:

Y_A
Y_B

- TUBE END X LOCATIONS:
  FOR $m = 1, 2, 3, 4$

$$x_{An} = Y_A \tan\Phi_n$$

$$x_{Bn} = Y_B \tan\Phi_n$$

- LAYER ASSIGNMENT:
  FOR $m = 1, 2, 3, 4$

IF n ODD, LAYER $= 2m-1$
IF n EVEN, LAYER $= 2m$

6

- TUBE LENGTHS:

$$L_{mn} = \left[(Y_B - Y_A)^2 + (x_{Bn} - x_{An})^2\right]^{1/2} - (e_b + e_p)$$

- TUBE ORIENTATION:

CONSTANT

- CONDITION OF INTERFERENCE:

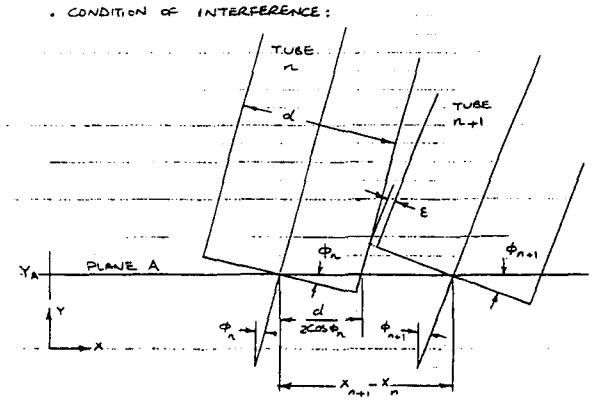

MUST ALWAYS SATISFY:

$$\varepsilon = \left[(x_{n+1} - x_n)_A - \frac{d}{2\cos\Phi_n}\right]\cos\Phi_{n+1} - \frac{d}{2} \geq 0.5 \text{ mm}$$

($\varepsilon \simeq 30$ mm AT TDR DIMENSIONS)

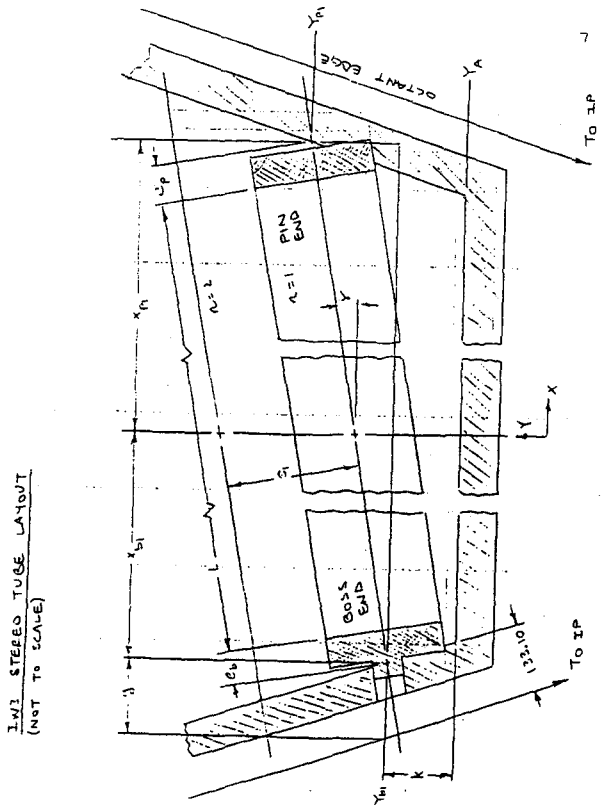

IW3 STEREO TUBE LAYOUT
(NOT TO SCALE)

7

IW3 STEREO TUBE LAYOUT

8

- CONSTANTS:
  SAME AS θ TUBES.
  $K = 50$ mm
  $\gamma \simeq 100$ mr $(5.73°)$

- TUBE END X AND Y LOCATIONS

$$Y_{bn} = Y_A + K + (n-1)\, S_1 \cos\gamma$$

$$X_{bn} = -Y_{bn} \tan(22.5°) - g$$

$$X_{pn} = X_{bn} + (Y_{pn} - Y_{bn}) \tan(22.5°)$$
$$Y_{pn} - Y_{bn} = (X_{bn} + X_{pn}) \tan\gamma$$
} SOLVE FOR X_{pn} AND X_{bn}

- TUBE LENGTHS:

$$L_n = \left[(X_p - X_b)^2 + (Y_p - Y_b)^2\right]^{1/2}_n - (e_b + e_p)$$

- TUBE END Z LOCATIONS

  SIMILAR TO θ TUBES

θ TUBE LAYOUT (NOT TO SCALE)
(ALL DIM'S IN MM)

5/7/92
FF

PRESENT:

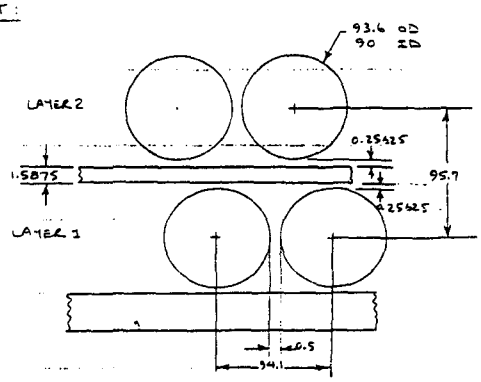

PROPOSED CHANGE:

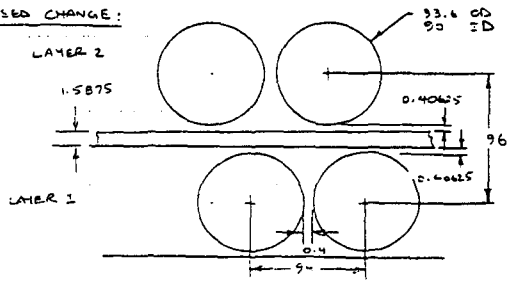

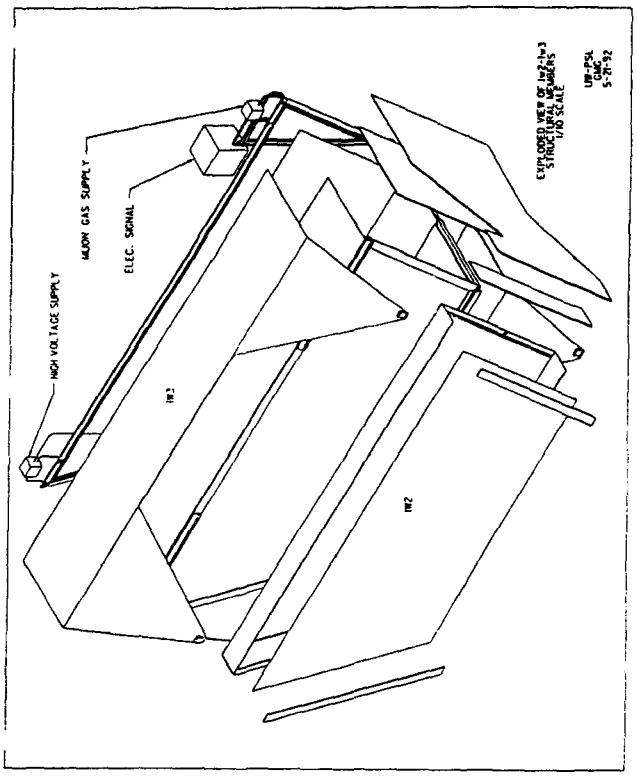

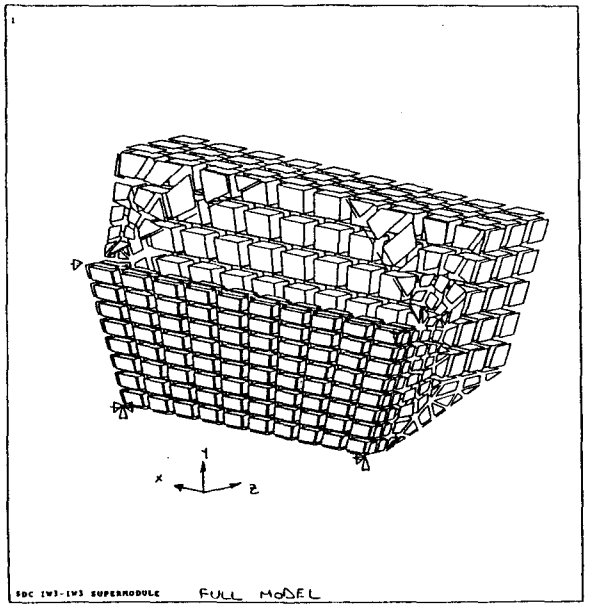

TOTAL MASS = 9313 KG

CENTEROID LOCATION

$X_c = 0$

$Y_c = 1.701$ M

$Z_c = 2.144$ M

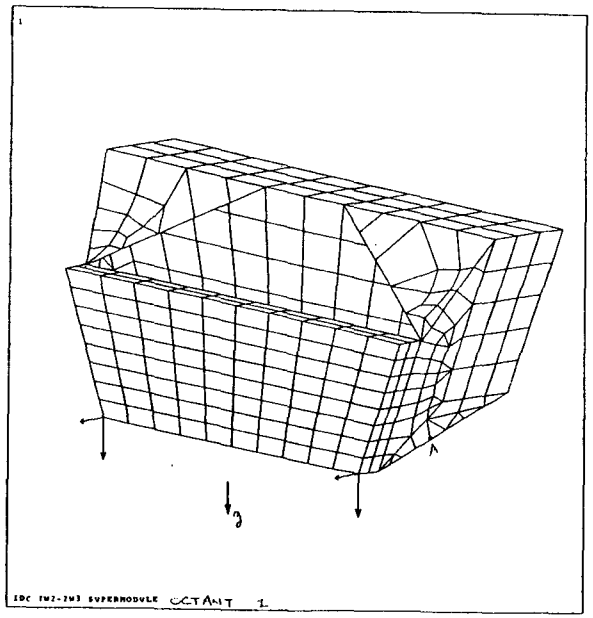

BENDING OF SIDE PLATE AT LOCATION MARKED A

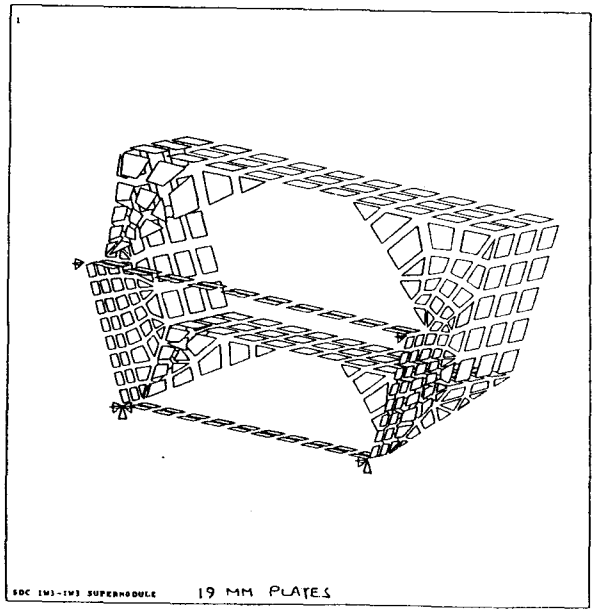

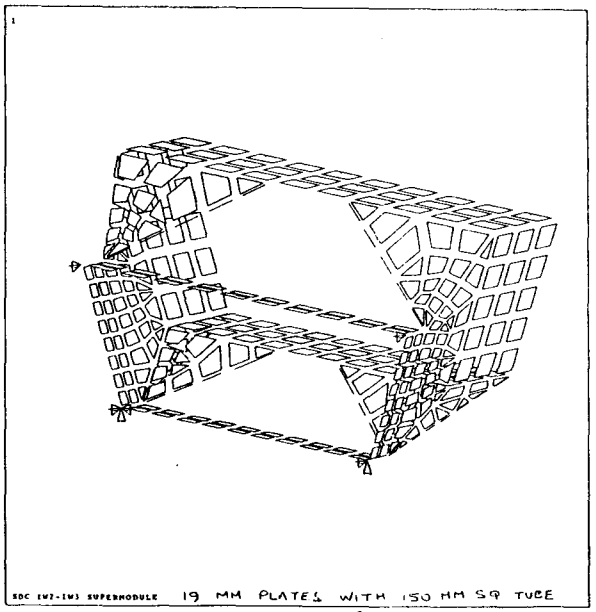

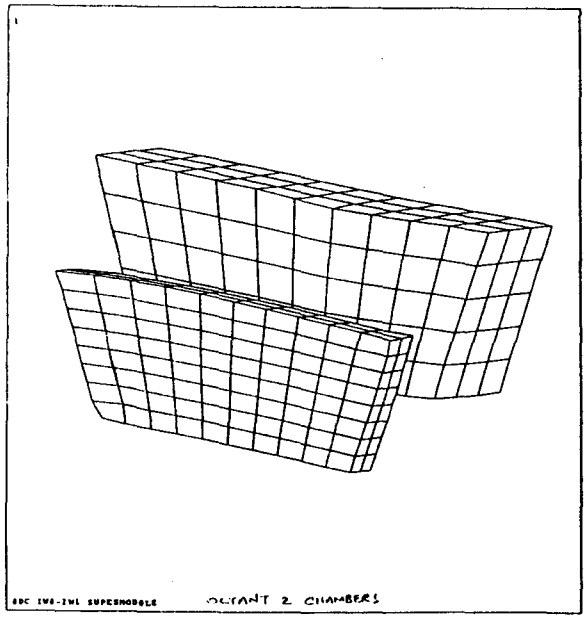

ANSYS 4.4A
MAY 21 1992
11:45:44
PLOT NO. 4
POST1 DESPL.
STEP=2
ITER=1
DMX =0.002071 m
ERPC=0

DSCA=266.715
SU =-1
TV =0.1
SV =-1
DIST=4.284
TF =1.426
SF =1.884
PRECISE HIDDEN

1951

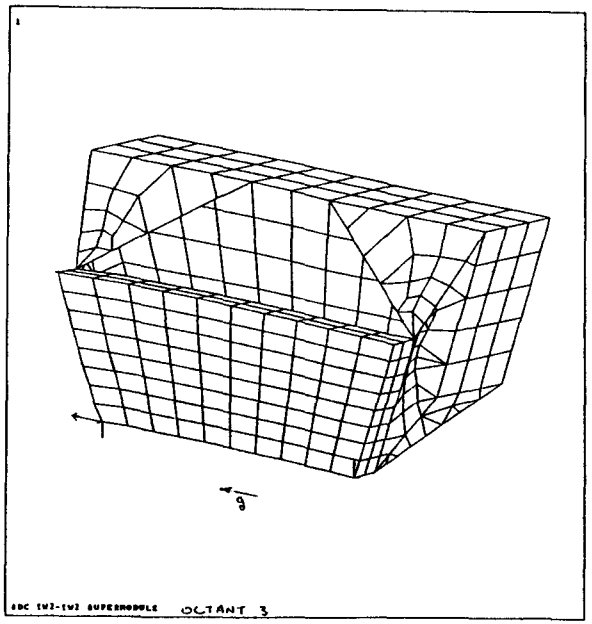

ANSYS 4.4A
MAY 21 1992
11:46:20
PLOT NO. 5
POST1 DISPL.
STEP=2
ITER=1
DMX =0.002215 m
ERPC=0
FORC

DSCA=181.629
SU =-1
TV =0.1
SV =-1
DIST=4.284
TF =1.426
SF =1.884
PRECISE HIDDEN

1952

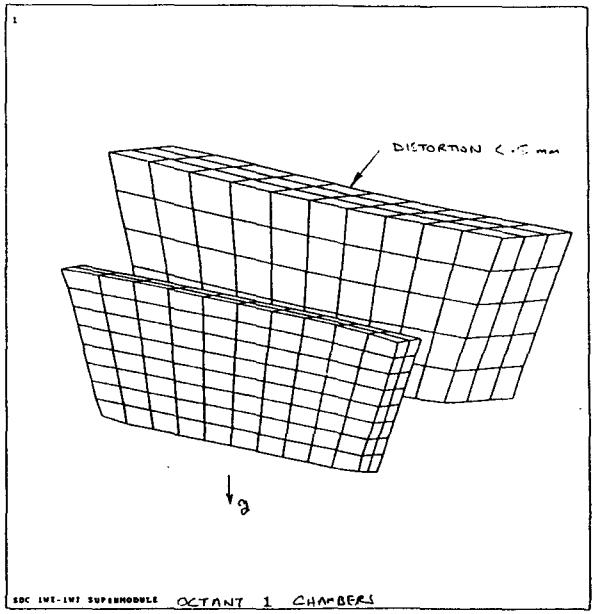

ANSYS 4.4A
MAY 21 1992
11:45:21
PLOT NO. 2
POST1 DISPL.
STEP=1
ITER=1
DMX =0.002497 m RIGID BODY MOTION OF SMS
ERPC=0

DSCA=371.557
SU =-1
TV =0.3
SV =-1
DIST=4.284
TF =1.426
SF =1.884
PRECISE HIDDEN

1953

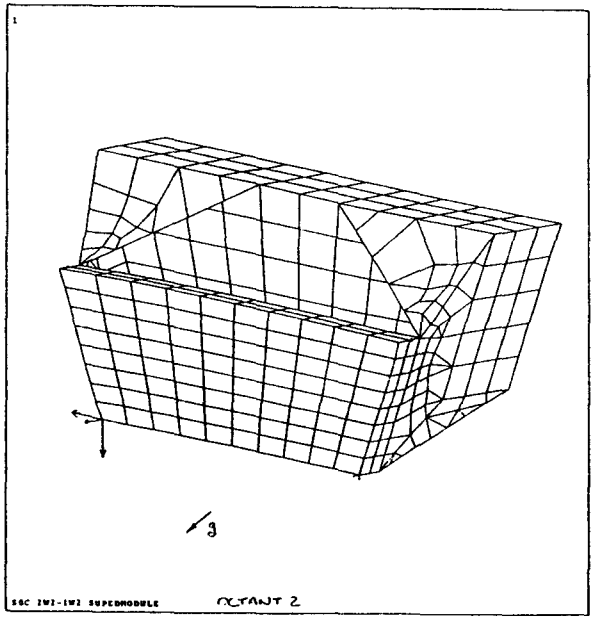

ANSYS 4.4A
MAY 21 1992
11:45:06
PLOT NO. 2
POST1 DISPL.
STEP=2
ITER=1
DMX =0.004847 m
ERPC=0
FORC

DSCA=48.191
SU =-1
TV =0.3
SV =-1
DIST=4.284
TF =1.426
SF =1.884
PRECISE HIDDEN

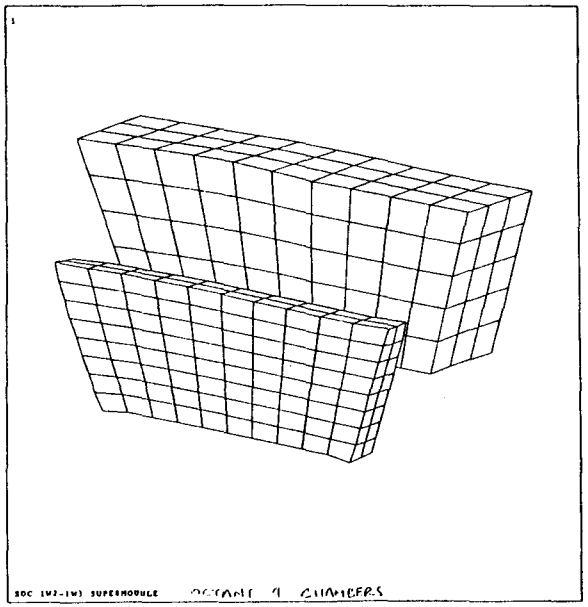

ANSYS 5.4A
MAY 21 1992
11:48:21
PLOT NO. 8
POST1 DISPL.
STEP=4
ITER=2
DMX =0.002214 m
ERPC=0

DSCA=192.246
XV =-1
YV =0.2
ZV =-1
DIST=4.288
YF =1.436
ZF =1.884
PRECISE HIDDEN

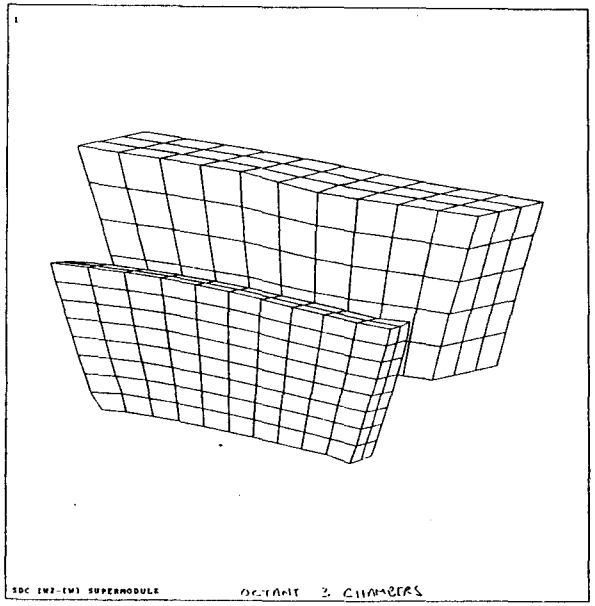

ANSYS 4.4A
MAY 21 1992
11:47:45
PLOT NO. 4
POST1 DISPL.
STEP=3
ITER=1
DMX =0.001862 m
ERPC=0

DSCA=237.734
XV =-1
YV =0.3
ZV =-1
DIST=4.284
YF =1.416
ZF =1.884
PRECISE HIDDEN

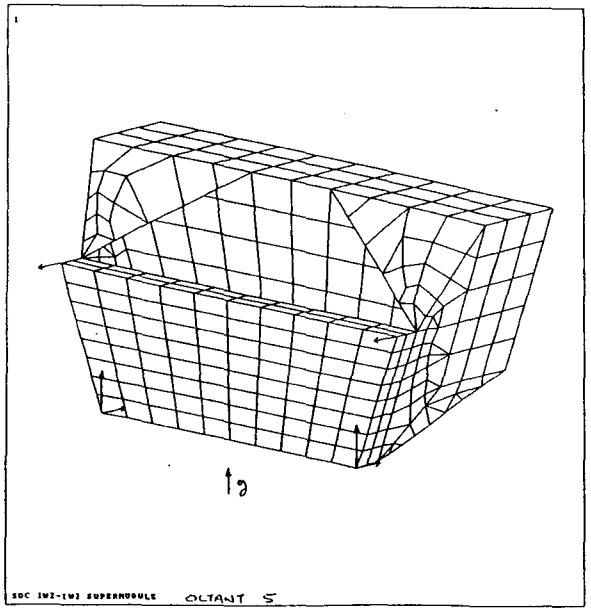

ANSYS 6.4A
MAY 21 1992
11:48:54
PLOT NO. 9
POST1 DISPL.
STEP=5
ITER=1
DMX =0.006424 m
ERPC=0
FORC

DSCA=68.629
XV =-1
YV =0.1
ZV =-1
DIST=4.284
YF =1.436
ZF =1.881
PRECISE HIDDEN

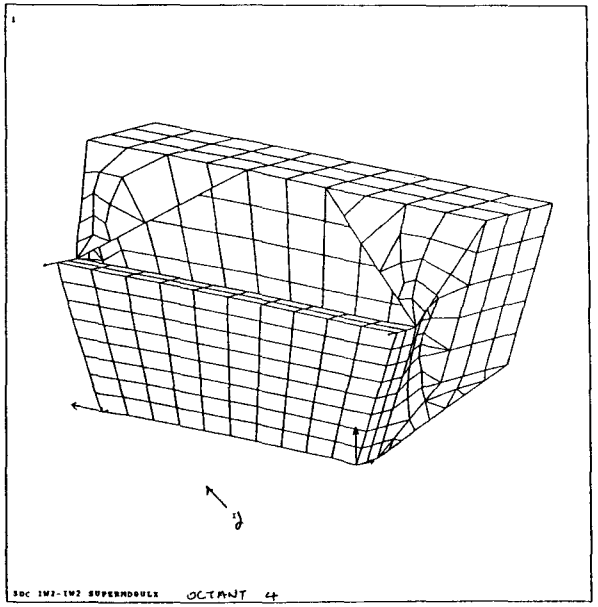

ANSYS 4.4A
MAY 21 1992
11:47:52
PLOT NO. 7
POST1 DISPL.
STEP=4
ITER=1
DMX =0.004862 m
ERPC=0
FORC

DSCA=88.101
XV =-1
YV =0.3
ZV =-1
DIST=4.284
YF =1.436
ZF =1.884
PRECISE HIDDEN

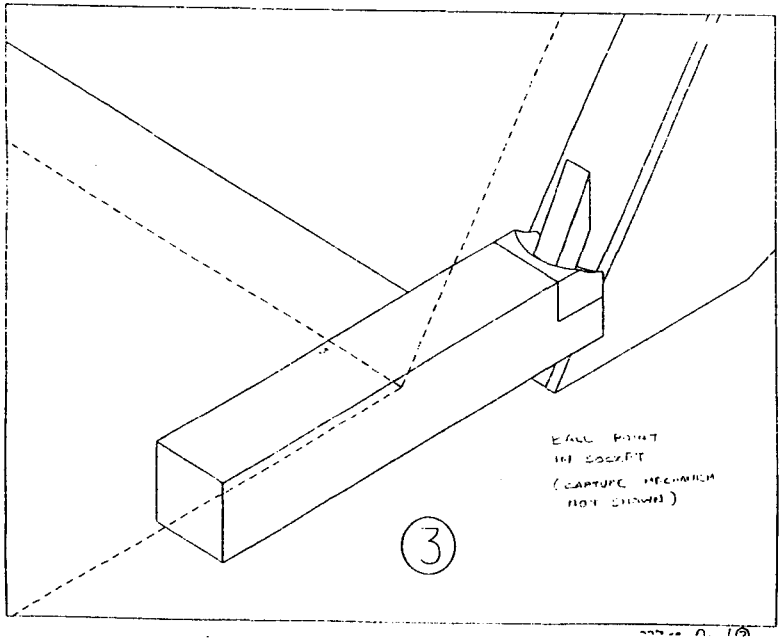

1952

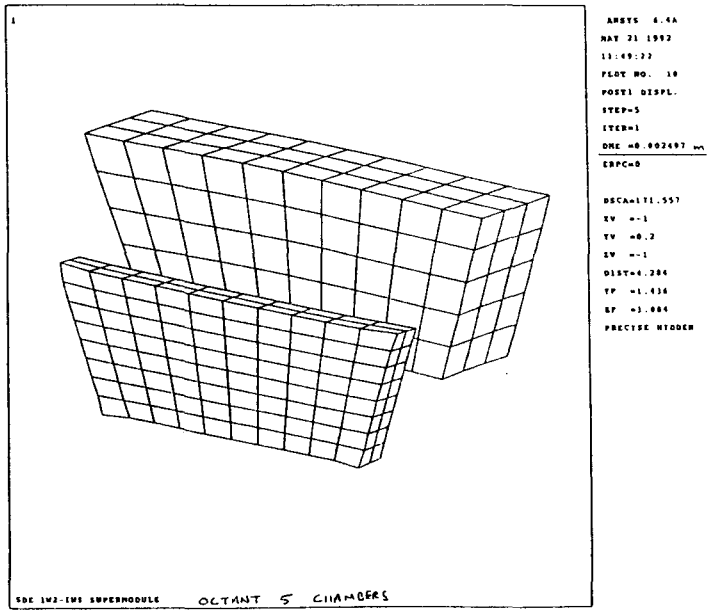

1950

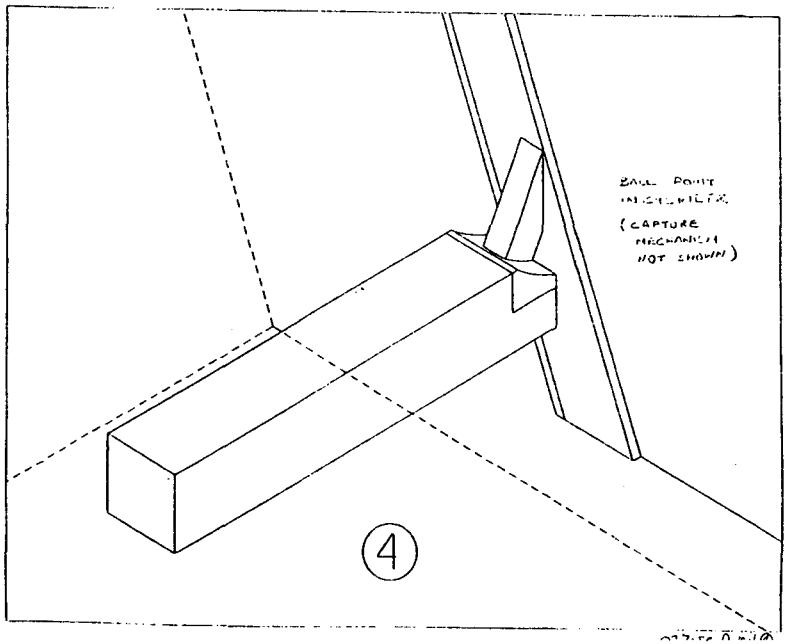

1953

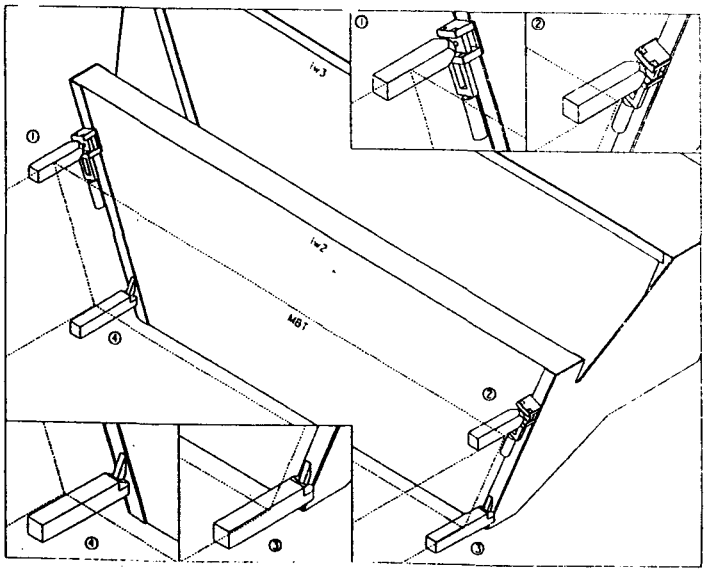

027-3e Model 027-m
5-19-92

1951

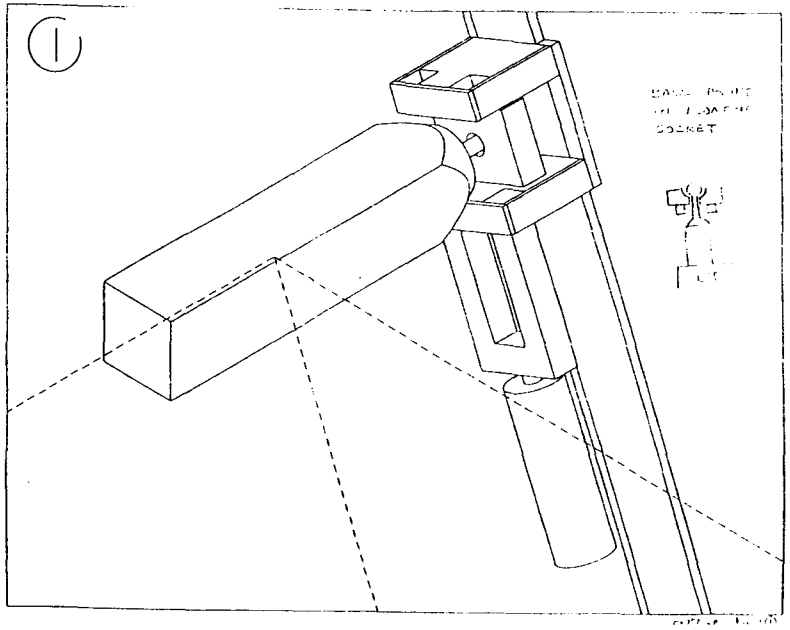
1
BALL POINT
IN FLOATING
SOCKET

1951

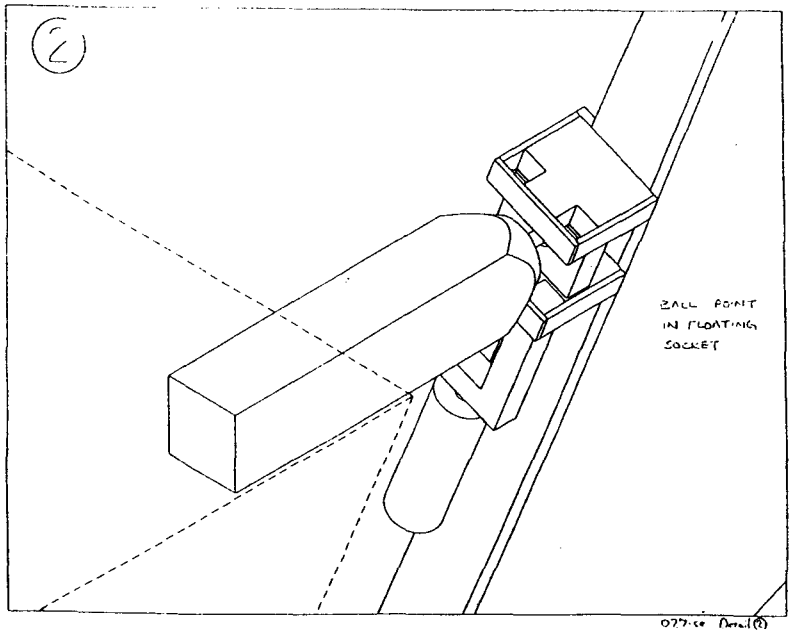
2
BALL POINT
IN FLOATING
SOCKET

1965

[10] Electronics

< Organization >

Organization Plan	A. Lankford	- 1967

< Trigger >

SDC Trigger Rates	W. Smith	- 1973
Trigger Activities in Japan	H. Sakamoto	- 1997
SDC Trigger Emulation Module	W. Smith	- 2012
Distributed Processing for Straw Tube Trigger Simulation	K. Kondoh	- 2027

< Bus Swich >

R & D of MOBY - Multi-pass Organization on Bus Yard	E. Kanatani	- 2045
High Speed Switch System	O. Sasaki	-2055

< Data Acquisition >

Interests and Resources for DAQ Subsystem in Japan	H. Fujii	- 2078
Event Builder Subsystem	M. Nomachi	- 2085
Development of the SPARC-VME-CAMAC Data Acquisition System (Potable DAQ)	Y. Takeuchi	- 2089
Potable DAQ Standard Crate	M. Nomachi	- 2109
Readout Control for High Luminosity Accelerators	R. Belusevic	- 2113

Organization Plan

Andrew J. Lankford
(University of California Irvine)

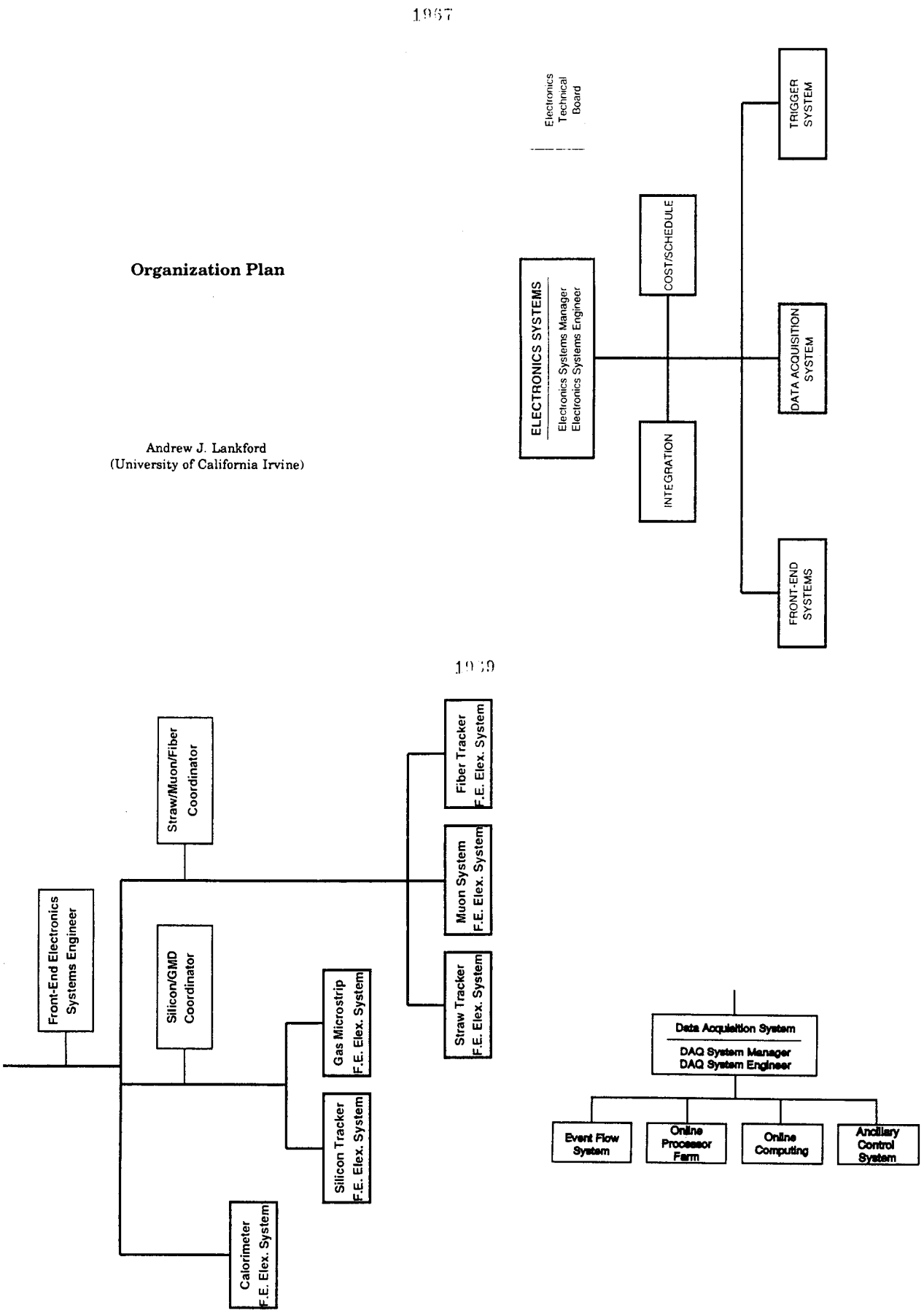

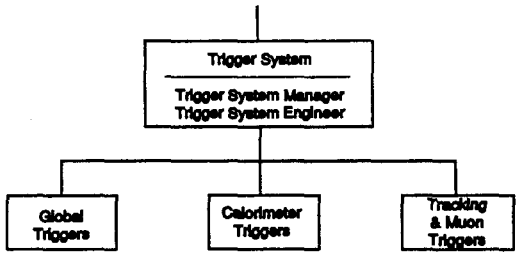
Trigger System
Trigger System Manager
Trigger System Engineer
Global Triggers
Calorimeter Triggers
Tracking & Muon Triggers

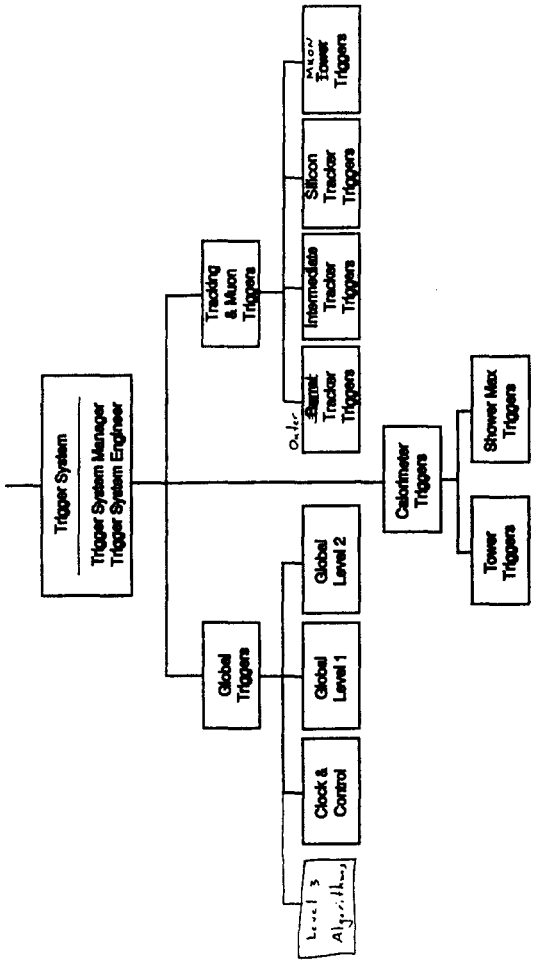
Trigger System
Trigger System Manager
Trigger System Engineer
Tracking & Muon Triggers
Global Triggers
Silicon Tracker Triggers
Intermediate Tracker Triggers
Tracker Triggers
Global Level 2
Global Level 1
Clock & Control
Calorimeter Triggers
Shower Max Triggers
Tower Triggers

SDC TRIGGER RATES

W. Temple, W. H. Smith, S. Dasu, J. Lackey, T. Gorski
University of Wisconsin

SDC TRIGGER LEVELS

Level 1:
Identify Physics Objects:
- Electrons
- Photons
- Muons
- Taus
- Jets
- Neutrinos
- *Combinations of Above*

Level 2:
Refine Identification of Physics Objects:
- Sharper P_T Cuts
- Electrons From Conversions
- Muons from Decay/Punchthrough
- Refine Energy Sums/Clusters
- Displaced Vertices

Level 3:
Full Physics Analysis/Decisions:
- Specialized Algorithms
- Heirarchy of Decisions
- DST-type cuts on Physics

SDC TRIGGER PRINCIPLES

Philosophy:
- Local:
  - Signatures of e's, γ's, μ's, jets in $\eta \times \phi$ regions
  - (ex: ν's)
- Measurably Efficient:
  - Overlapping Programmable Triggers
  - Prescaled Lower Thresholds
  - Prescaled Triggers w/ less conditions
- Efficient Use of DAQ Bandwidth:
  - Efficient Lepton and Jet Identification
  - Consistency with Offline Cuts

Benchmarks for Trigger Performance:
- e's, μ's from inclusive W's, Z's:
  - 50% efficiency (cut on lepton P_T)
- Jets, γ's at high P_T:
  - 1-2 decade overlap with lower $\sqrt{s}$ data
- Missing E_T:
  - Good efficiency for channels such as:
    - $H \rightarrow 2\ell 2\nu$
    - SUSY particles
- Low P_T multileptons:
  - B Physics

LEVEL 1

Electrons & Photons:
Find (.1 x .1) Cal Towers with E_{em} > Thr
Require E_{hac}/E_{em} < .10 - .15
Option: Pattern of surrounding quiet towers (isolation)
γ's: Match w/Shower Max in $.2\eta \times .2\phi$
e's: Find Outer Track Segments w/P_T > 10 GeV/c
- Match Track Segments w/Shower Max in ϕ in 1/64
- Assign $\Delta\eta = 0.2$ from Shower Max to Track
- Match Track w/Cal on $\Delta\eta$=0.2, $\Delta\phi$=0.2

Muons:
Muon Tracks from Scint + θ-layers w/P_T > 10 GeV/c
Option: Find Central Tracker Sgmts w/P_T > 10 GeV/c
- Match w/Muon ϕ-layer Track Sgmts in 1/64
- Use Momentum cut on Central Tracker P_T cut
- (Use Scint to associate ϕ and θ tracks)
- Match Track w/Quiet Cal on $\Delta\eta$=0.2, $\Delta\phi$=0.2

Jets:
1.6 x 1.6 grids of overlapping towers > E_{thr}

Neutrinos:
Sum Missing E_T over .1 x .1 Towers > E_{thr}

LEVEL 1 TRIGGER STUDIES: CALORIMETER

Rate:

Level 1 Rate Target = 30 KHz
15 KHz each for Cal. and Muon Triggers

Calorimeter:

Total rate is sum of:
- single e's
- single γ's
- pairs: ee, eγ, γγ
- jets
- $\not{E}_T$

☞ Target Rate of 3 KHz for single object triggers

Procedure:

Background Rates:
- QCD 2-jet events: 20 - 400 GeV P_T
- mixed with minimum bias events
- run through hardware simulation

Find threshold for e, γ, jet, $\not{E}_T \Rightarrow$ 3 KHz
Examine threshold vs. trigger conditions
Examine efficiency vs. E_T

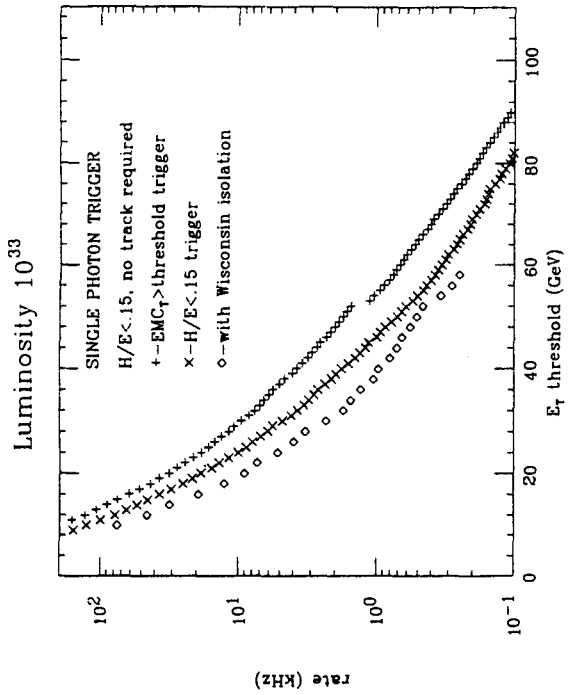

Figure 8

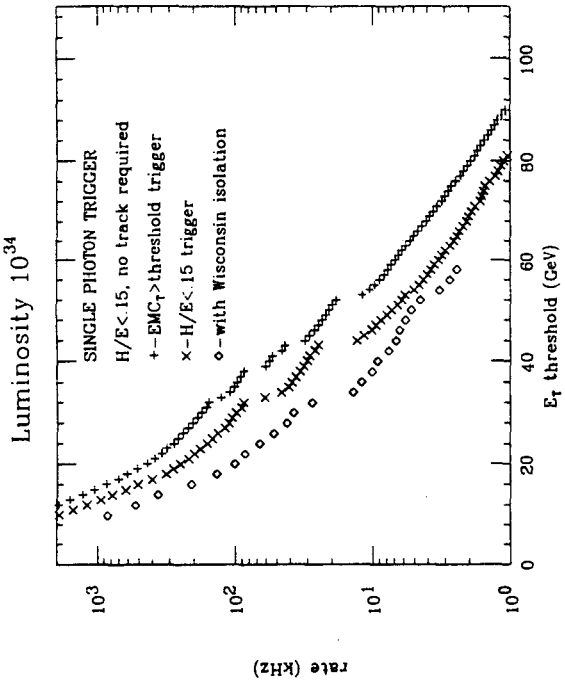

Figure 8

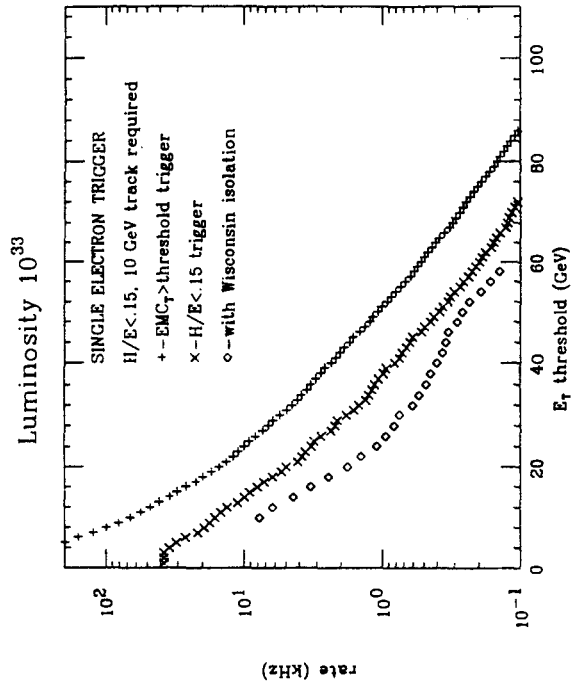

Figure 9

Background rate vs. Z Rate

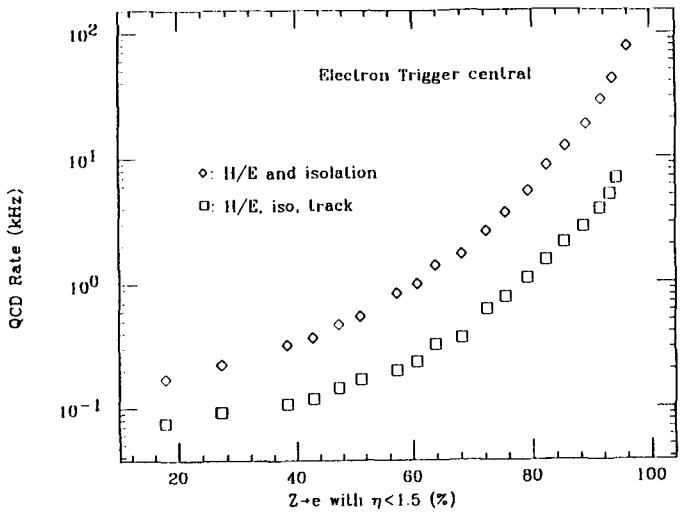

Figure 9

1983

JET TRIGGER RATES LUMINOSITY 10^{33}

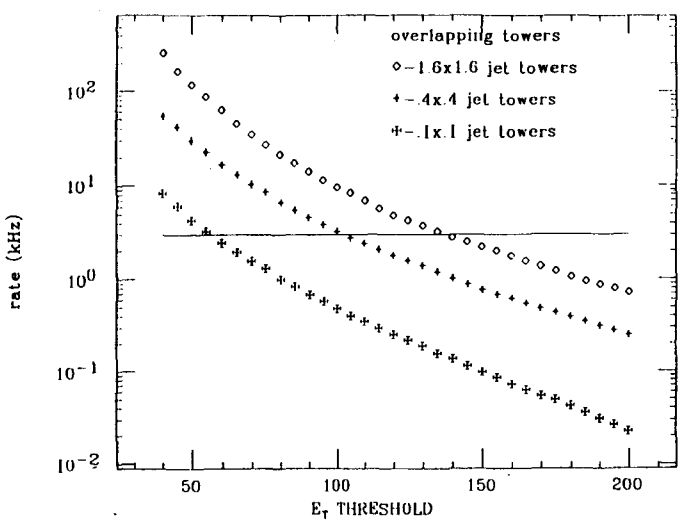

Figure 1

1981

Luminosity 10^{34}

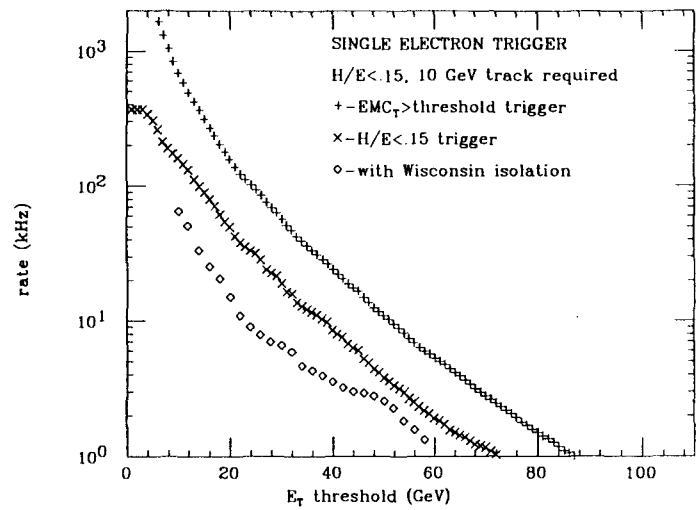

Figure 9

1981

Background rate vs. W Rate

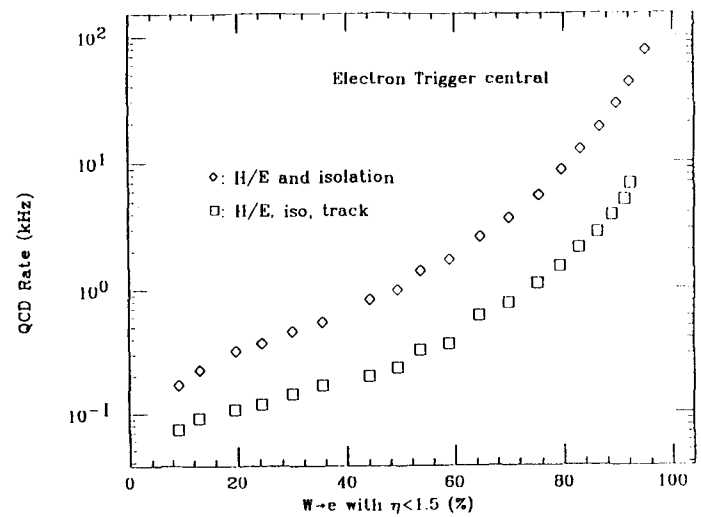

Figure 8

1982

Jet Trigger Efficiency– Luminosity 10^{33}

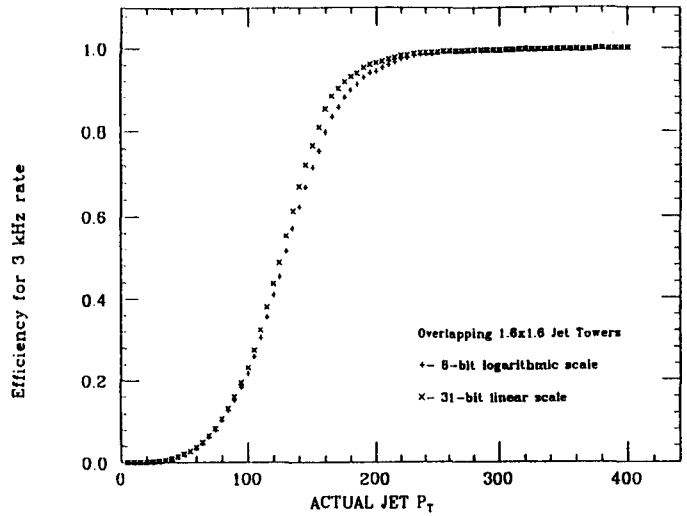

Figure 76

Jet Trigger Efficiency– Luminosity 10^{33}

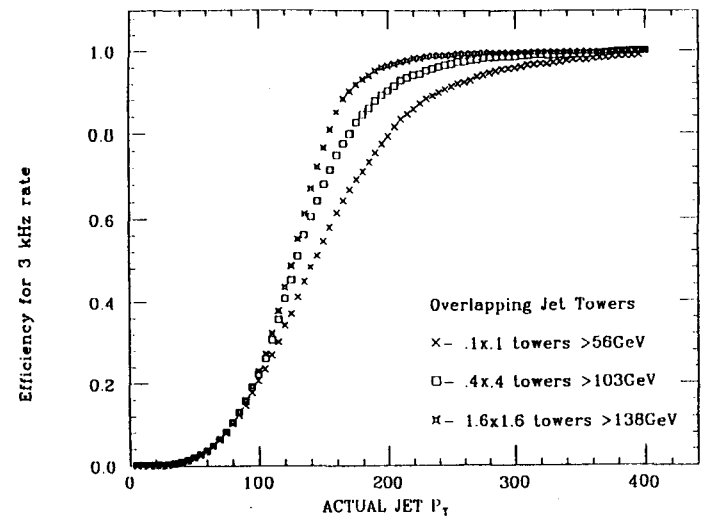

Figure 3

Type of jet trigger	3 kHz at 10^{33}	10 kHz at 10^{34}
.1 × .1	287	387
.4 × .4 non-overlapping	243[3]	336[2]
1.6 × 1.6 non-overlapping	211	281[3]
.4 × .4 overlapping	229	313[2]
1.6 × 1.6 overlapping	190	253[3]
1.6 × 1.6 overlap/8-bit scale	205	268[3]
all have low energy cutoff at .1 GeV except as noted [2] – low energy cutoff at .2 GeV [3] – low energy cutoff at .5 GeV		

Jet p_T at which 95% efficiency is achieved (GeV)

Jet Trigger Efficiency– Luminosity 10^{33}

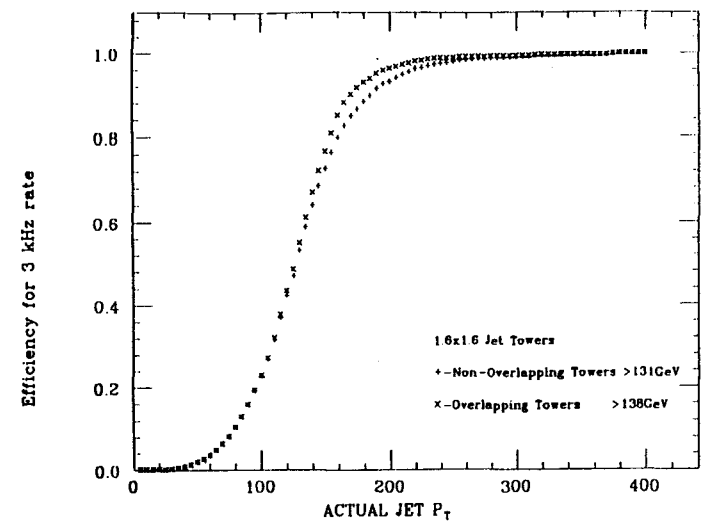

Figure 17

1989

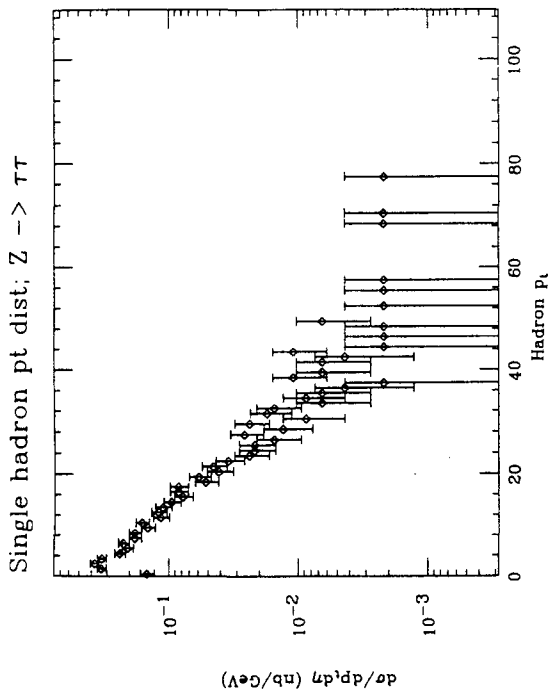

1990

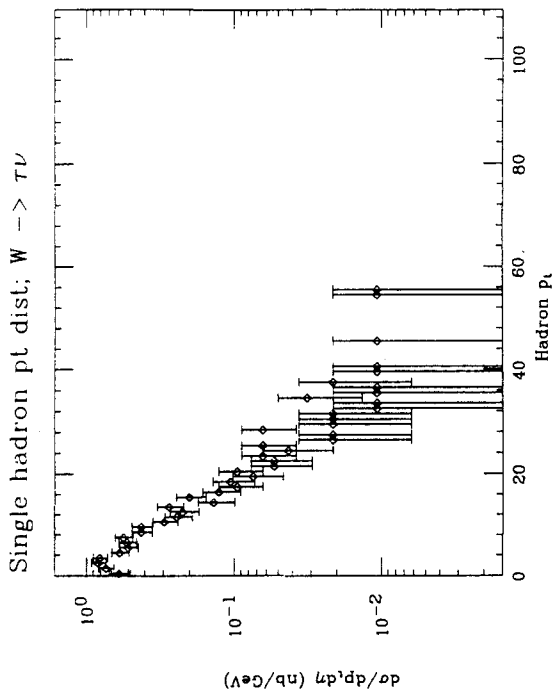

1991

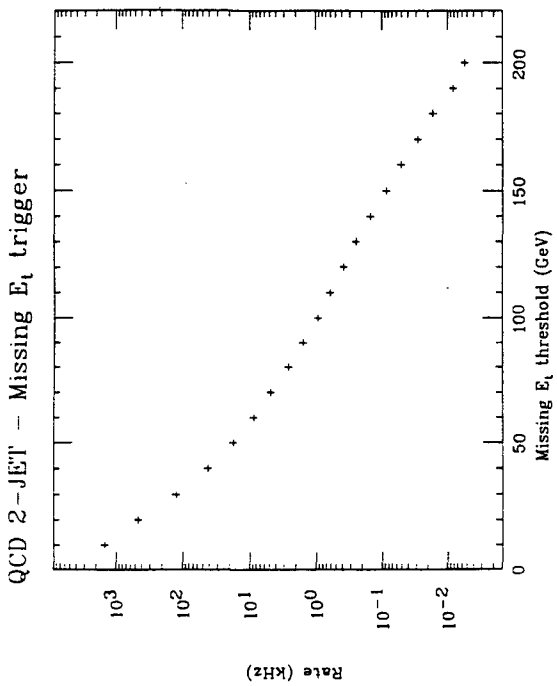

Figure 12

1992

LEVEL 1 TRIGGER STUDIES: MUONS

Rate:

For Muon System, total rate is sum of:

- single μ's
- pairs: $\mu\mu, \mu e, \mu\gamma$
- energy: μ & jet, μ & $\not{E}_T$

☞ Target Rate of 5 KHz for single muon triggers

Procedure:

Determine Prompt and Decay Rates
Simulate Muon Trigger Circuit ($\delta T \rightarrow P_T$ cut)
Determine Threshold Response of Muon Trigger
Fold These together to calculate Trigger Rate

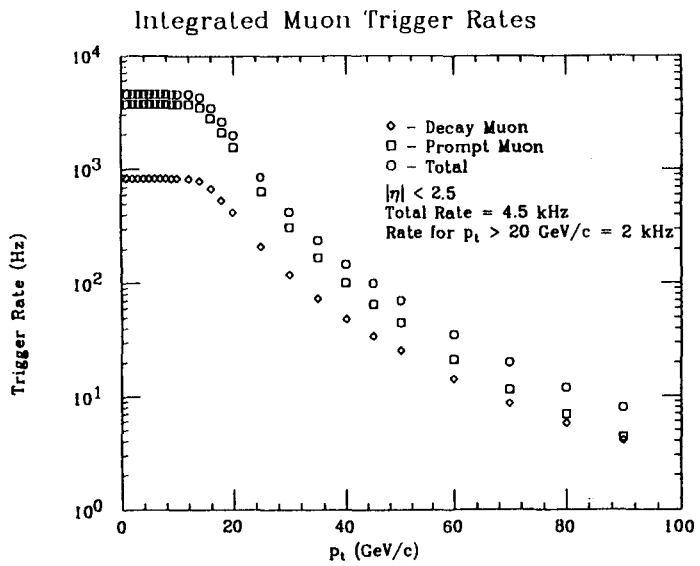

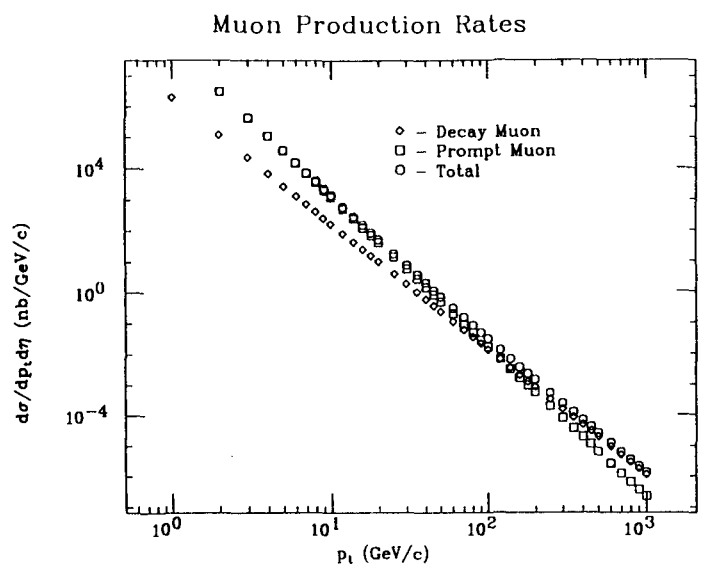

Representative level 1 trigger E_t thresholds.

Trigger	Threshold
Electron	20 GeV
Photon	30 GeV
Two electrons	10 GeV
Two photons	20 GeV
Missing E_t	80 GeV
Single Tower Hadron (.1 × .1)	60 GeV
Jet (1.6 × 1.6 sum)	140 GeV
Muon	20 GeV

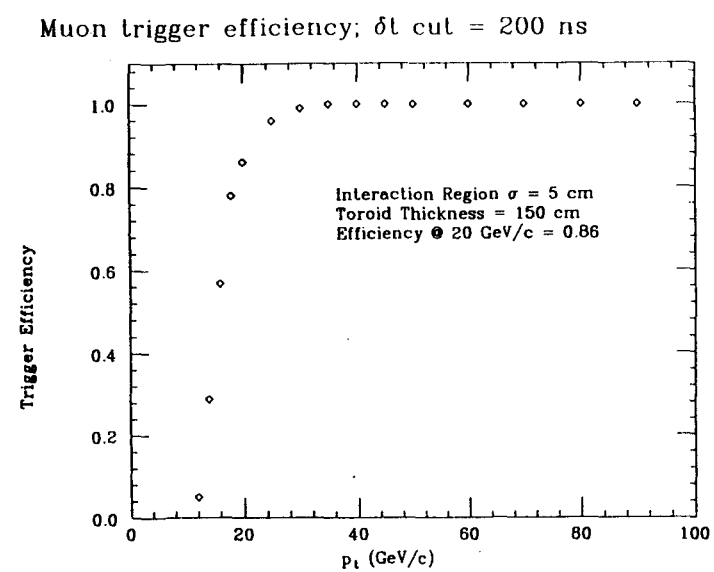

Trigger Activities in Japan

KEK Hiroshi Sakamoto

Level 1

Muon trigger prototype
mini-tower
Pipeline trigger implementation
Field Programmable Gate Array

Level 2

Muon trigger prototype
TMC-L2 interface
Architecture R&D
Scalable Bus Switch

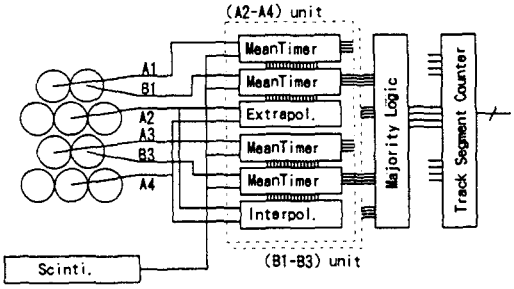

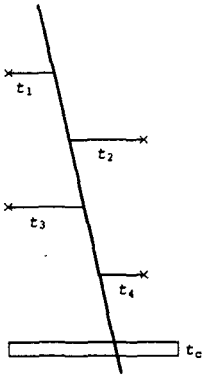

Equations

$$\frac{t_1 + t_3}{2} + t_2 = t_c + t_d$$

$$\frac{t_2 + t_4}{2} + t_3 = t_c + t_d$$

$$\frac{3\,t_3 - t_1}{2} + t_4 = t_c + t_d$$

$$\frac{3\,t_2 - t_4}{2} + t_1 = t_c + t_d$$

t_d Drift time between two anode planes.

Muon L1 Trigger Concept

TUBEL1.DRW

1999

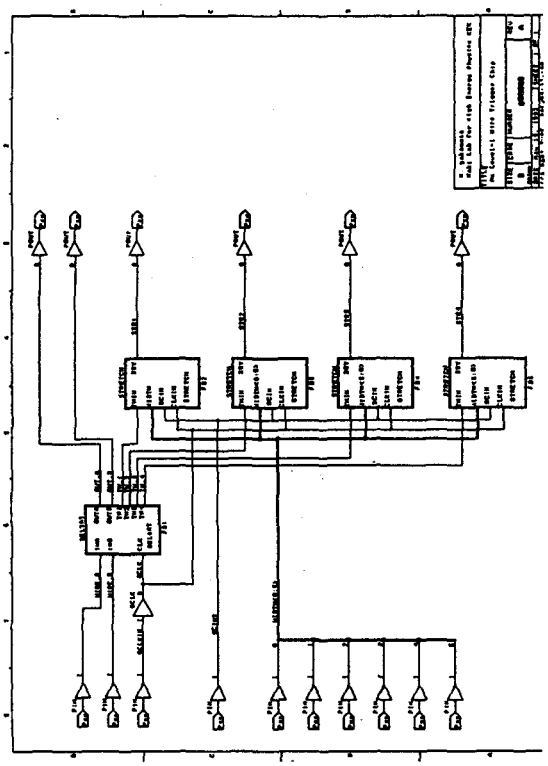

2000

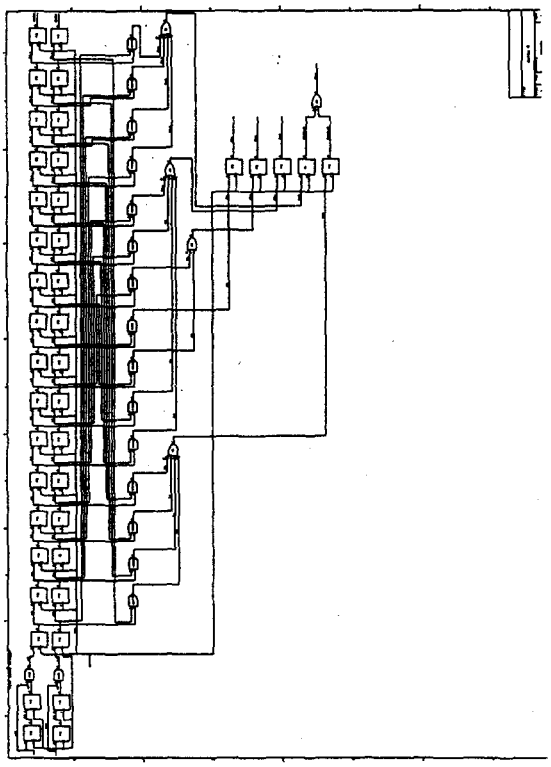

2001

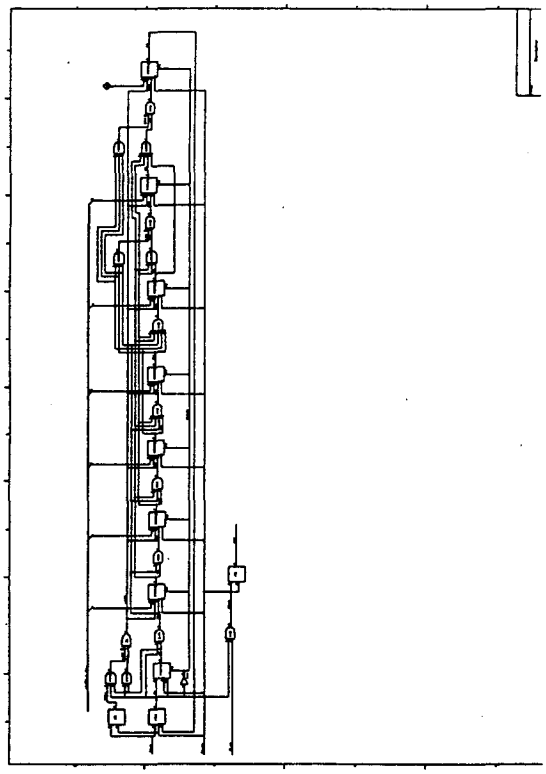

2002

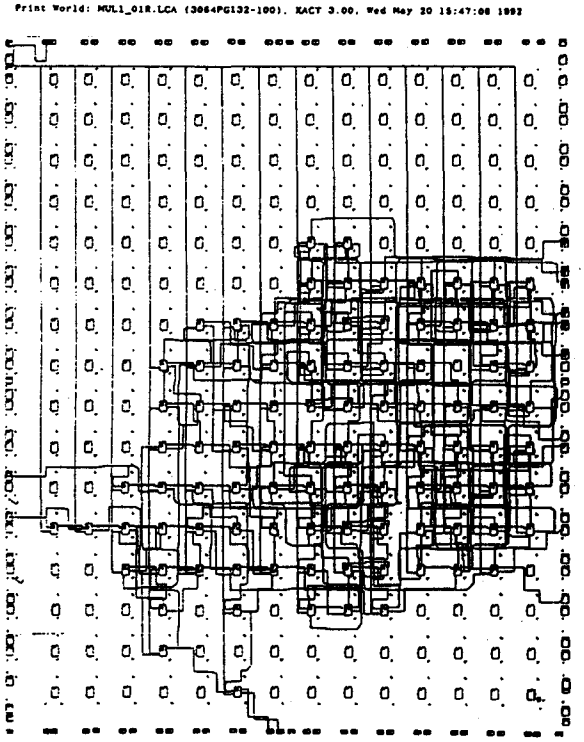

2003

XC4000 Logic Cell Array Family

PRELIMINARY

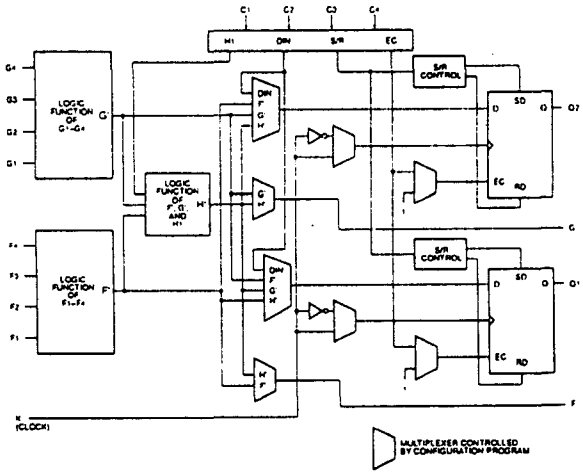

Figure 1. Simplified Block Diagram of XC4000 Configurable Logic Block

Function	XC3000 Family	XC4000 Family
8/9 bit Parity Generate/Check	14 ns / 2 CLB	5 ns / 1 CLB
24-bit Input Decode	20 ns / 5 CLBs	10 ns/ 0 CLBs
32:32 Bit Identity Comparator	16 ns/ 16 CLBs	12 ns/ 8 CLBs
16:1 Multiplexer	28 ns/ 7 CLBs	20 ns/ 5 CLBs
16-bit Synchronous Counter	35 ns/ 14 CLBs	20 ns/ 8 CLBs
16-bit Loadable Counter	60 ns/ 18 CLBs	20 ns/ 8 CLBs

Table 3. Density and Performance for Several Common Circuit Functions

2004

Parameter	XC4000	XC3000	XC2000
Max number of flip-flops	2280	928	174
Max number of user I/O	240	144	74
Max number of RAM bits	28,800	0	0
Function generators per CLB	3	2	2
Number of logic inputs per CLB	9	5	4
Number of logic outputs per CLB	4	2	2
Number of low-skew global nets	8	2	2
Dedicated decoders	yes	no	no
Fast carry logic	yes	no	no
Internal 3-state drivers	yes	yes	no
Output slew-rate control	yes	yes	no
Power-down option	no	yes	yes
Crystal oscillator circuit	no	yes	yes

Table 2. Three Generations of Xilinx Field-Programmable Gate Array Families

2005

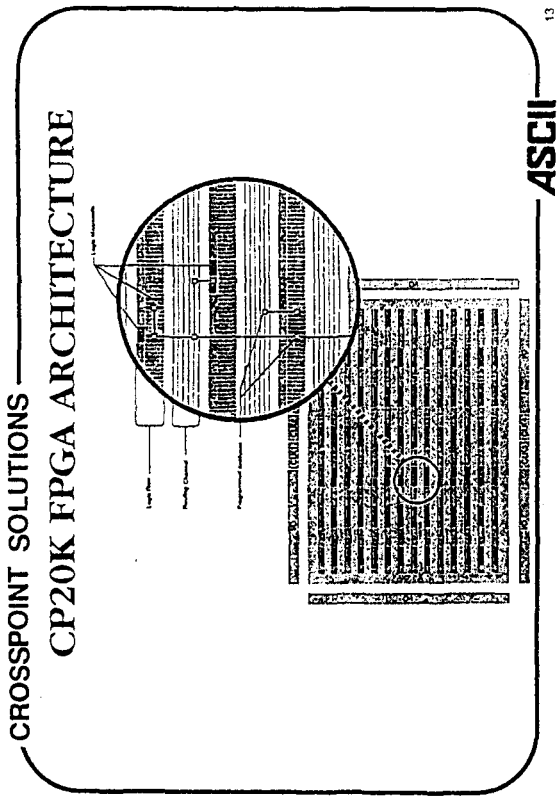

2006

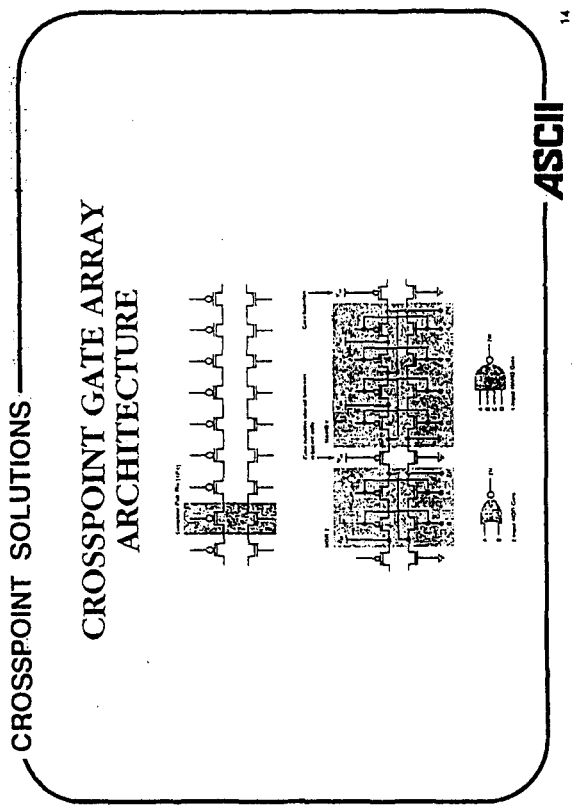

2007

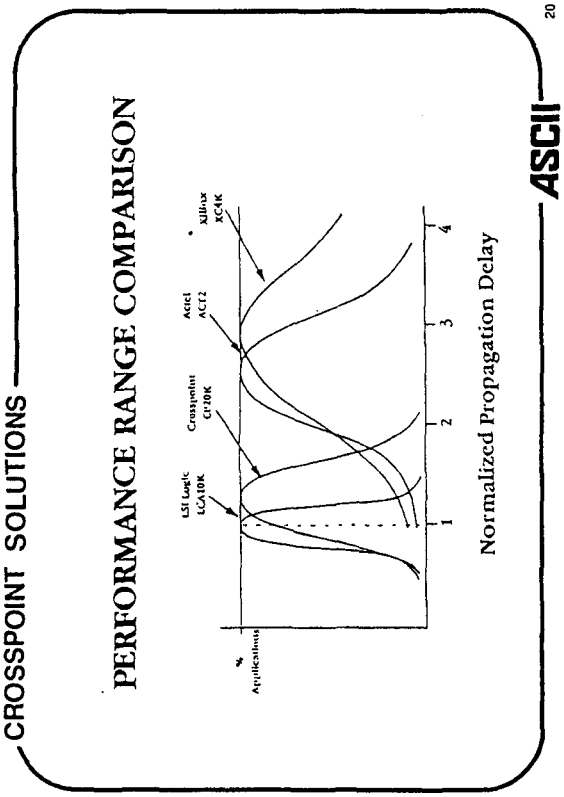

2008

Field Programmable Gate Array

	Crosspoint	Xilinx	Actel
Product	CP20K	XC4000	ACT2
Release	92/2	Available – 92/?	Available
Max. gates	20k	20k	8k
Technology	0.75 μ	0.9 μ	1.2 μ
Architecture	TPT,RLT	IOB,CLB	Logic Module
Toggle Freq.	200MHz		120MHz
System Clock	50MHz	60–70MHz	50MHz
I/O Pads	91–270	64–240	140
Input Level	CMOS,TTL	CMOS,TTL	CMOS,TTL
Pullup	yes	yes	no
Schmitt Trig.	yes	no	no
Output Option			
3state	yes	yes	yes
Through Rate	yes	yes	no
Open drain	yes	no	no
Open source	yes	no	no
Driving Curr.	4/8/12mA	12mA	8mA
MGA compat.	yes	no	no
Programming	Anti-fuse 150 Ω one time	Memory cell rewritable	Anti-fuse 500 Ω one time
JTAG I/F	yes	yes	no

2009

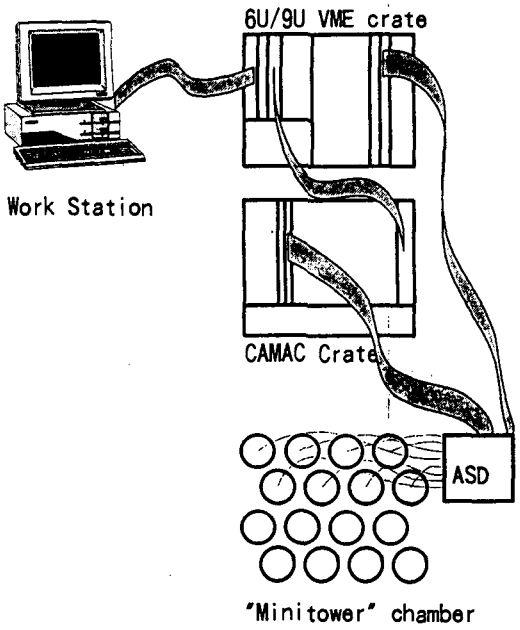

MINITOWER CHAMBER TRIGGER TEST BENCH

TESTBENCH.DRW

2010

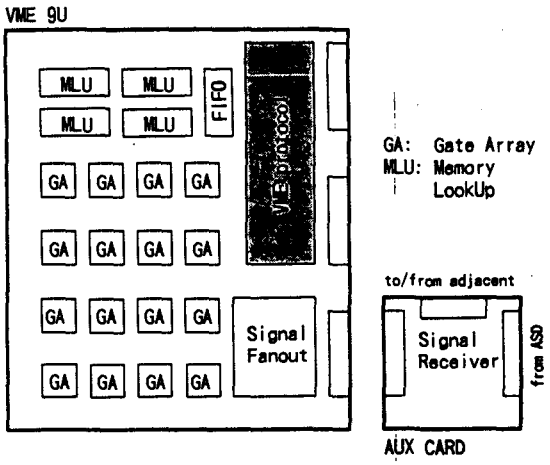

L1 TRIGGER PROTOTYPE BOARD conceptual view

PROTL1.DRW

2011

L2 Sector processor concept

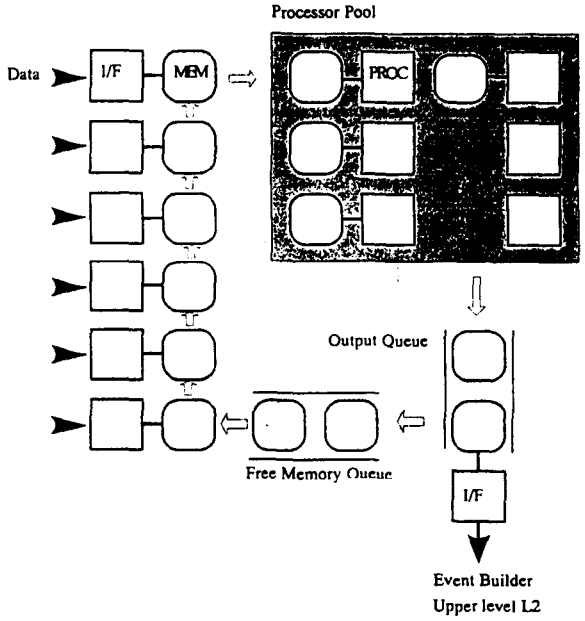

SDC TRIGGER EMULATION MODULE

(TEM)

T. Gorski, W.H. Smith, S. Dasu, J. Lackey
University of Wisconsin

TEM FUNCTION

- Emulates the Clock & Control Function of Global Trigger System.
- Used in test bench debugging of front end electronics & DAQ systems.
- Used in test beam experiments to provide interface to accelerator clock, external trigger, DAQ processor (incl. gating logic).
- Provides for a smooth transition to integration of subsystem into final trigger system.
- Output Signals:
  - Level 1 Accept/Reject
  - Level 2 Accept
  - Level 2 Reject
  - Level 1 Synch
  - Level 1 Reset
  - Bunch Crossing 0
  - Test Trigger (Empty Bunch Crossing)
  - Clock (60 MHz internal or external)

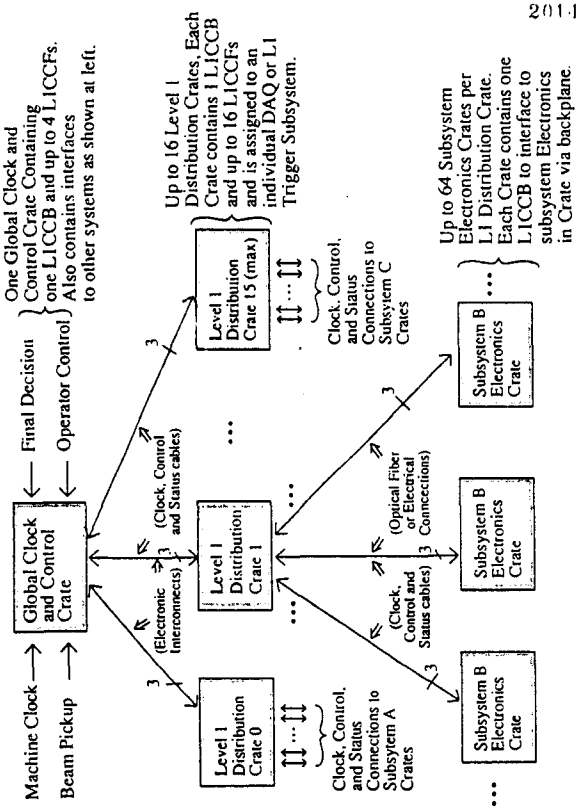

Level 1 Clock and Control Distribution
Hardware Configuration for Pipeline Length Calculations

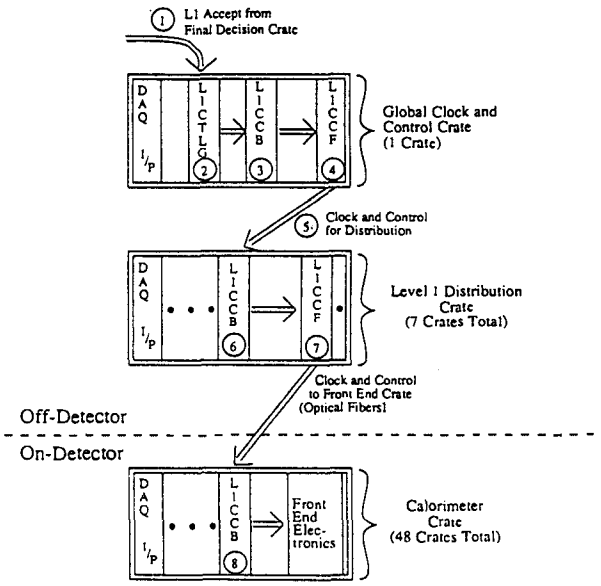

Figure 6

2016

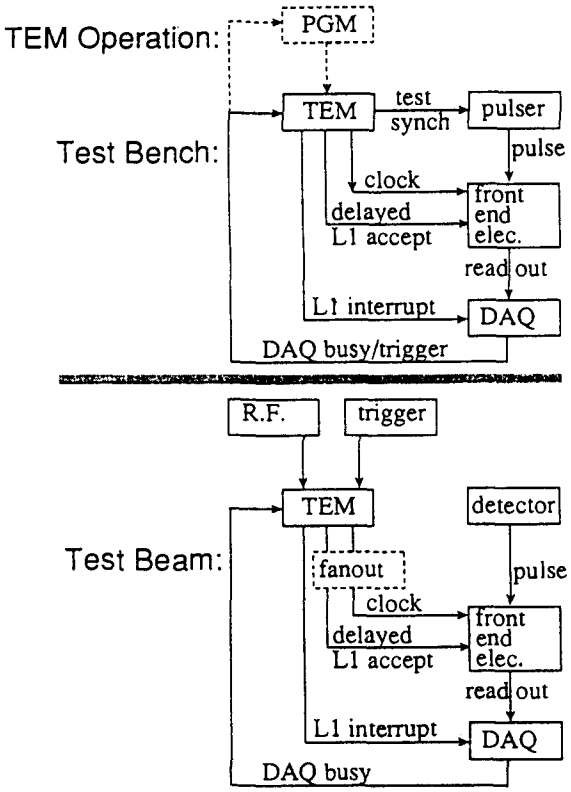

2017

TEM OPERATION

- DAQ can fill output pattern in FIFO and play back at 60 MHZ for 8 µsec.
- Pattern can be brought in through input connector and delayed up to 8 µsec by FIFO (time is programmable).
- Pattern has one bit used for stopping clocks and one bit for test trigger.
- L1 Accept is gated on DAQ busy, TEM can raise busy and wait for DAQ to clear or issue L1 Accepts until DAQ raises busy.
- TEM counts L1 Accepts requested, L1 Accepts issued, and DAQ deadtime.
- TEM issues interrupt to DAQ if deadtime exceeds preset value.
- TEM can be reset by DAQ or front panel reset button, counters reset by external signal.
- TEM Packaged as a 6U VME module with A24:D16 Slave operation.

2018

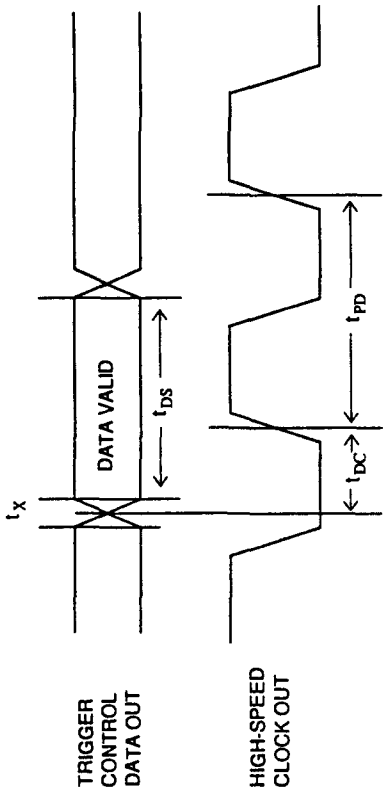

2019

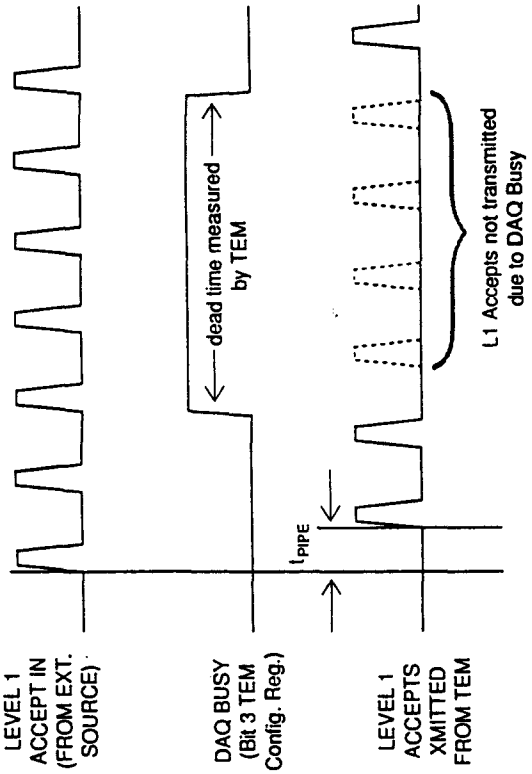

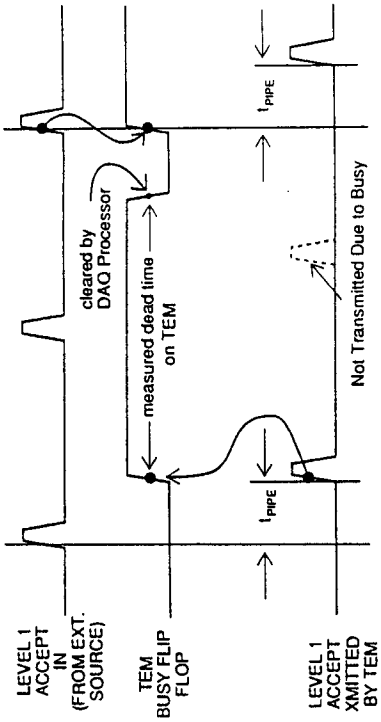

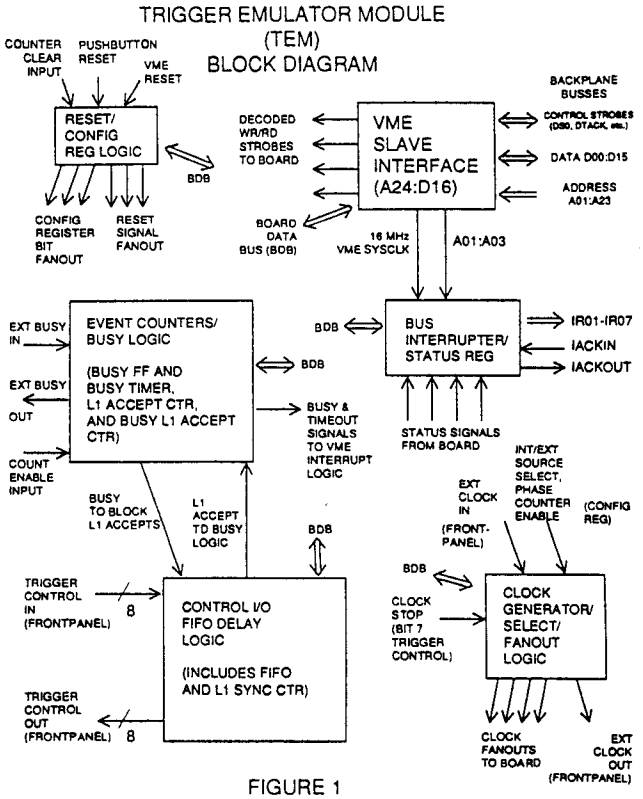

FIGURE 1

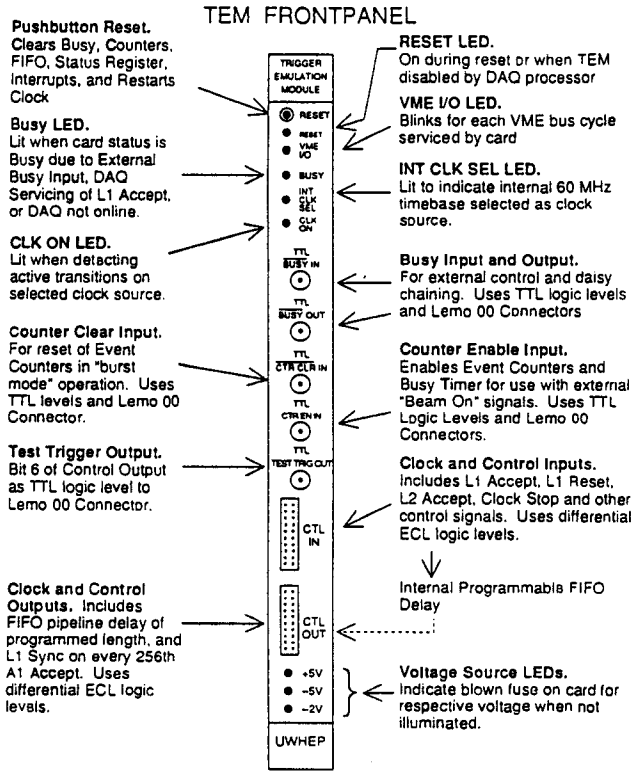

FIGURE 2

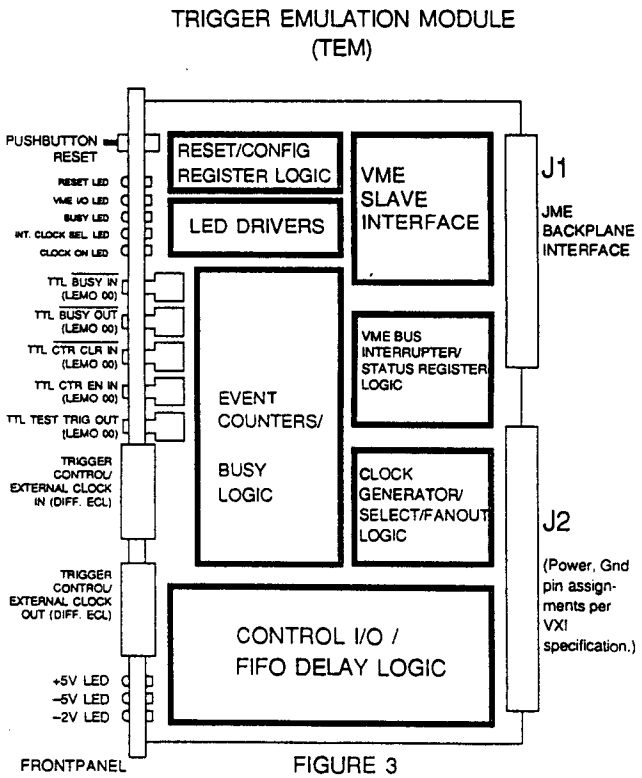

FIGURE 3

Bit Number	Definition
0	Level 1 Accept
1	Level 2 Accept
2	Level 2 Reject
3	Level 1 Sync
4	Level 1 Reset
5	Bunch Crossing 0/Spare
6	Empty Bunch/Test Trigger
7	Clock Stop

Table 1: Trigger Control Word Bit Definitions

Bit Number	Definition
0	Busy Input 0 = External Busy Input inactive 1 = External Busy Input active
1	Board Busy 0 = Board Not Busy, L1 Accepts Transmitted 1 = Board Busy, L1 Accepts Blocked
2	Busy Flip Flop Status 0 = Flip Flop not set 1 = Flip Flop set by Level 1 Accept. Board Busy = true
3	Clock Stop Status 0 = Clock Running Enabled 1 = Clock Stopped
4–7	Spare
8	Level 1 Accept Transmitted (Maskable Interrupt Source) 0 = No Level 1 Accept Transmitted since last Clear 1 = Level 1 Accept Transmitted
9	Level 2 Accept Transmitted (Maskable Interrupt Source) 0 = No Level 2 Accept Transmitted since last Clear 1 = Level 2 Accept Transmitted
10	Level 2 Reject Transmitted (Maskable Interrupt Source) 0 = No Level 2 Reject Transmitted since last Clear 1 = Level 2 Reject Transmitted
11	Level 1 Reset Transmitted (Maskable Interrupt Source) 0 = No Level 1 Reset Transmitted since last Clear 1 = Level 1 Reset Transmitted
12	Busy Timeout (Maskable Interrupt Source) 0 = Busy Timer has not Expired 1 = Busy Timer has Expired
13	Counter Overflow (Maskable Interrupt Source) 0 = Level 1 Accept Event Counter within range 1 = Level 1 Accept Event Counter overflow
14–15	Spare

Table 2: Preliminary Status Register Bit Definitions

t Number	Definition
0	DAQ Processor Online 0 = offline, DAQ Processor not ready, assert BUSY 1 = online
1	L1 Accept Counter Enables 0 = disable counting 1 = enable counting
2	High-Speed Clock Source Select 0 = 60 MHz on-board oscillator 1 = External Clock In
3	Busy Timer Enable 0 = disable Busy Timer 1 = enable Busy Timer
4	Busy Flip Flop Enable 0 = disable Busy Flip Flop 1 = enable Busy Flip Flop, automatically setting Busy status on Level 1 Accept
5–7	Spare
8	L1 Accept Interrupt Mask 0 = disable VME Interrupt on Level 1 Accept 1 = enable VME Interrupt on Level 1 Accept
9	L2 Accept Interrupt Mask 0 = disable VME Interrupt on Level 2 Accept 1 = enable VME Interrupt on Level 2 Accept
10	L2 Reject Interrupt Mask 0 = disable VME Interrupt on Level 2 Reject 1 = enable VME Interrupt on Level 2 Reject
11	L1 Reset Interrupt Mask 0 = disable VME Interrupt on Level 1 Reset 1 = enable VME Interrupt on Level 1 Reset
12	Busy Timeout Interrupt Mask 0 = disable VME Interrupt on Busy Timeout 1 = enable VME Interrupt on Busy Timeout
13	Counter Overflow Interrupt Mask 0 = disable VME Interrupt on L1 Accept Counter overflow 1 = enable VME Interrupt on L1 Accept Counter overflow
14–15	Spare

Table 3: Preliminary Configuration Register Bit Definitions

Distributed proccessing

for

STRAW tube trigger simulation

(jsd farm at KEK)

TOKYO
METROPORITAN
UNIVERSITY

K.KONDOH

Contents

1. Motivation
2. The structure of "jsd farm"
3. Definition of "SPEED" and "SPEED UP CURVE"
4. SPEED UP CURVE for PYTHIA
   4.1. Only 1 NFS server disk
   4.2. 11 local disk
5. SPEED UP CURVE for SDCSHELL
   (using one NFS server disk)
6. Introduction of workstations at TMU
   (TokyoMetropolitanUniversity)
7. Summary

1. Motivation

Prof. Chapman requested us to carry out the Monte Carlo simulation for STRAW chambers as much as possible using distributed workstations(DEC5000s) available at KEK(**11** sets) and TMU(**44** sets) .

We intend to do urgently this job.

We measured the basic performance of the distributed processing using the "jsd farm" at KEK.

2. The structure of jsd farm

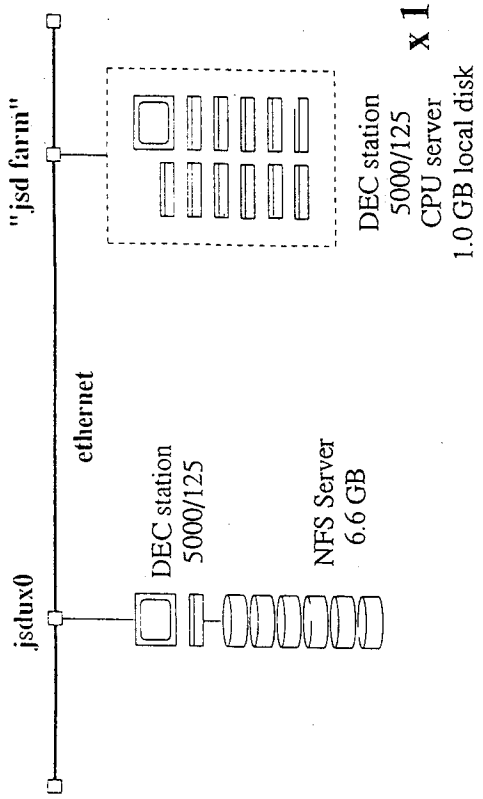

(Fig. 1)

3. SPEED & SPEED UP CURVE

$$\text{SPEED} = \frac{(\text{Elapsed Time for 1CPU})}{(\text{Whole Elapsed Time})} * (\#\text{CPU})$$

SPEED UP CURVE :

The variation of the speed when the number of CPU servers is increased.

4. SPEED UP CURVE for PYTHIA

We checked the efficiency of "jsd farm" system as a function of the rate of job output and CPU time.

4.1.

Using <u>only 1</u> NFS server disk

Because of the limitations of network traffic and NFS server, we can't get 100% efficiency.

SPEED UP CURVE

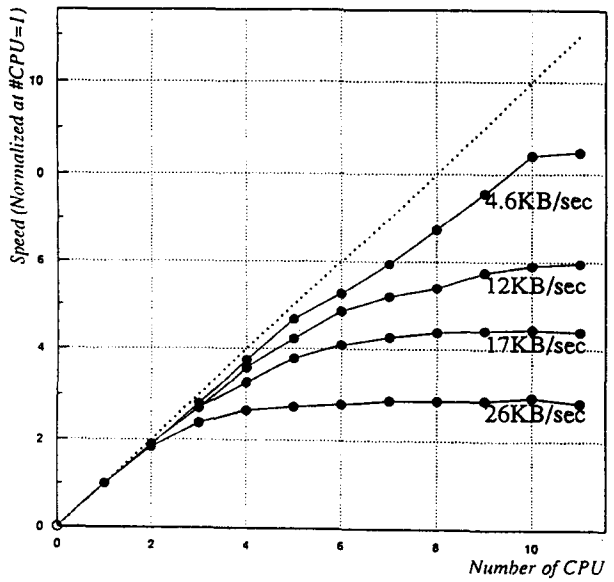

(Fig.2)

4.2.

Using each 11 local disk

Each DEC station has 1.0GB local disk. When we use local disks not NFS server disk, we can expect the better efficiency.

The data need not run through the ethernet nor NFS server.

SPEED UP CURVE

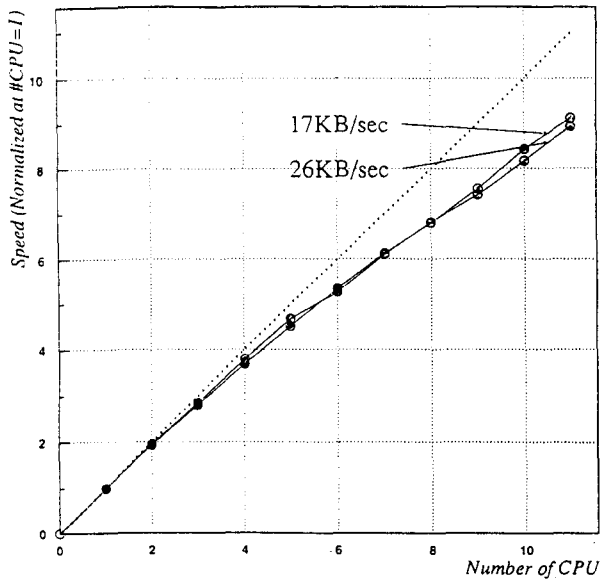

(Fig.3)

5. SPEED UP CURVE for SDCSHELL

In case of SDCSHELL, the rate of job output and CPU time is small because the CPU time per event is longer.

The efficiency for distributed processing becomes higher.

SPEED UP CURVE

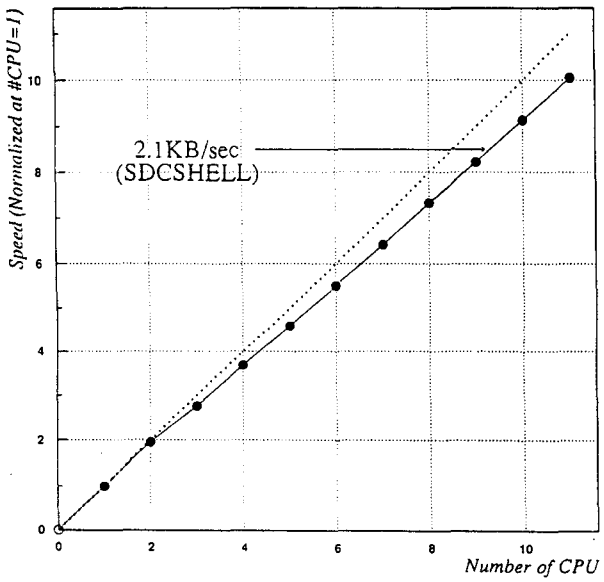

(Fig.4)

6. Introduction of Workstations at TMU

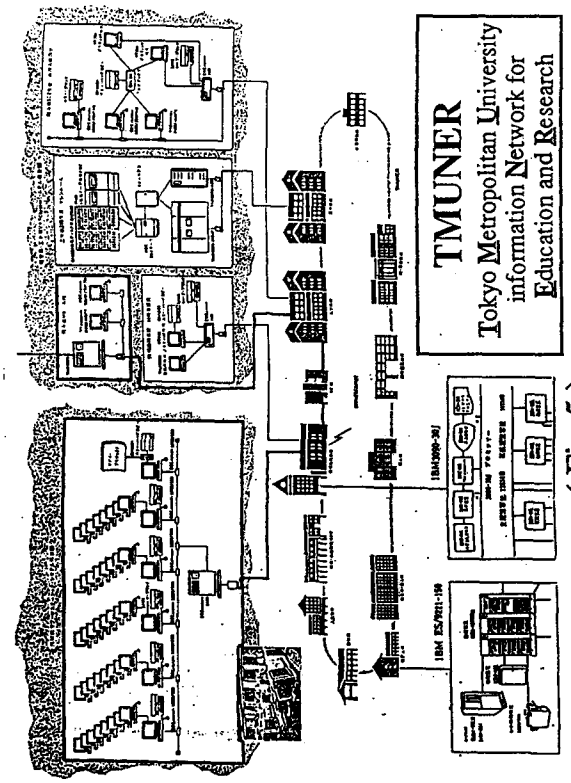

(Fig.5)

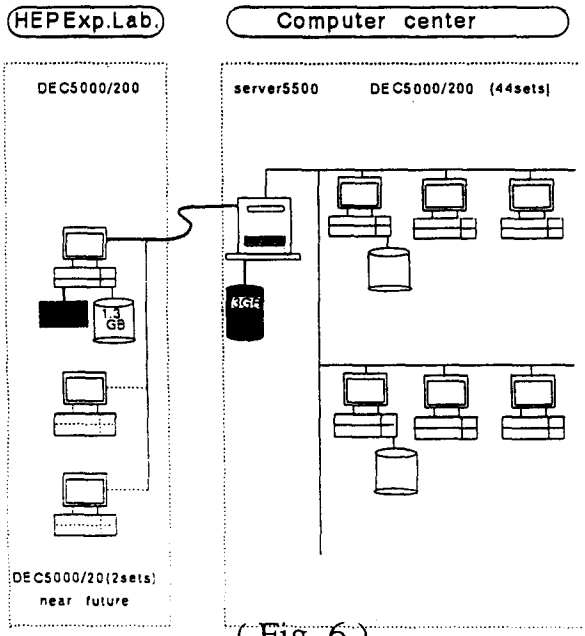

(Fig. 6)

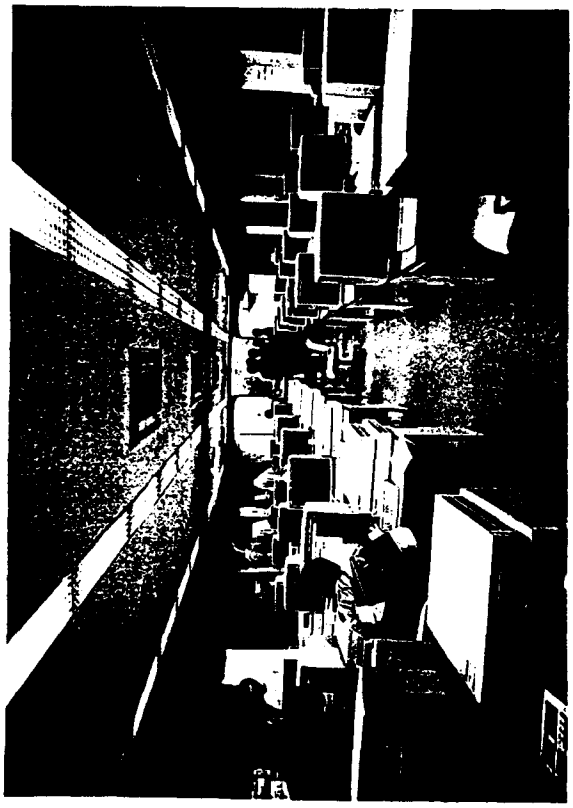

7. Summary

• We measured the performance of distributed processing with 11 DEC stations at KEK.

• We found that our distributed processing is effective for the program like SDCSHELL (the rate of job output and CPU time is small).

• We are now trying to do the SDCSHELL calculations at TMU.

• We are ready to install STRAW tube trigger simulation to "jsd farm".

8. APPENDIX

Promissing example for ZEUS detector simulation

Conditions

70 sec / event
70 KB / event
1.0 KB /sec
500 events / 1CPU
Using 20 CPUs
10 hours / 10,000 events

Efficiency for distributed processing for this job is

97 %

R & D of MOBY
- Multi-pass Organization on Bus Yard

E. Kanatani
(Okayama University)

R&D OF MOBY

– Multi-pass Organization on Bus Yard –

< Contents >

1. Implementation
   (1) main feature
   (2) operating architecture
   (3) special components
2. Properties
   (1) address and data size
   (2) timing characteristics
3. Schedule

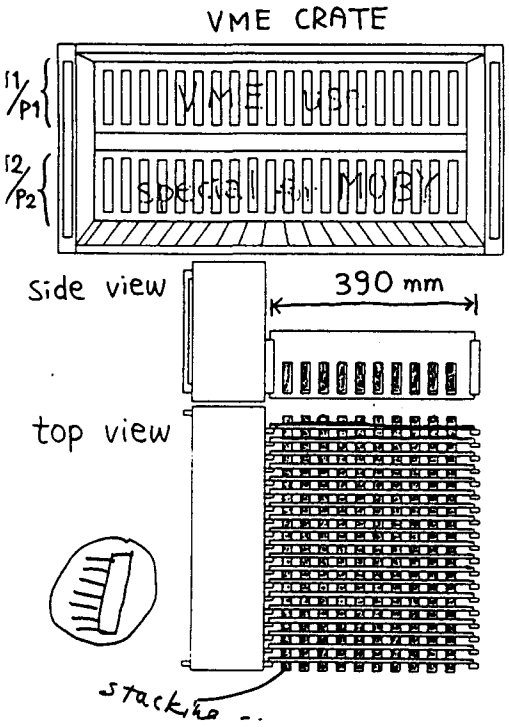

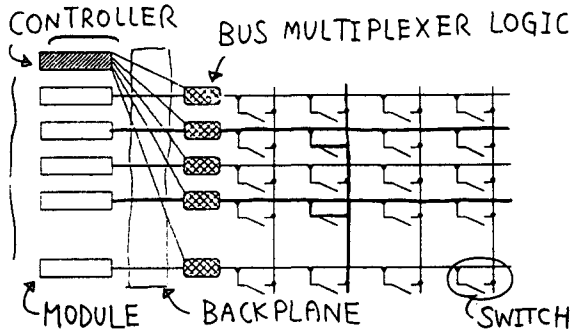

(1) BUS MULTIPLEXER (= MUX)
It switches over 10 rows of bus, assigns it to a module in the same slot.

(2) CONTROLLER
It controls each MUX individually in SOFTWARE.

(3) J2/P2 BACKPLANE
Where CON and MUX communicate.

2049

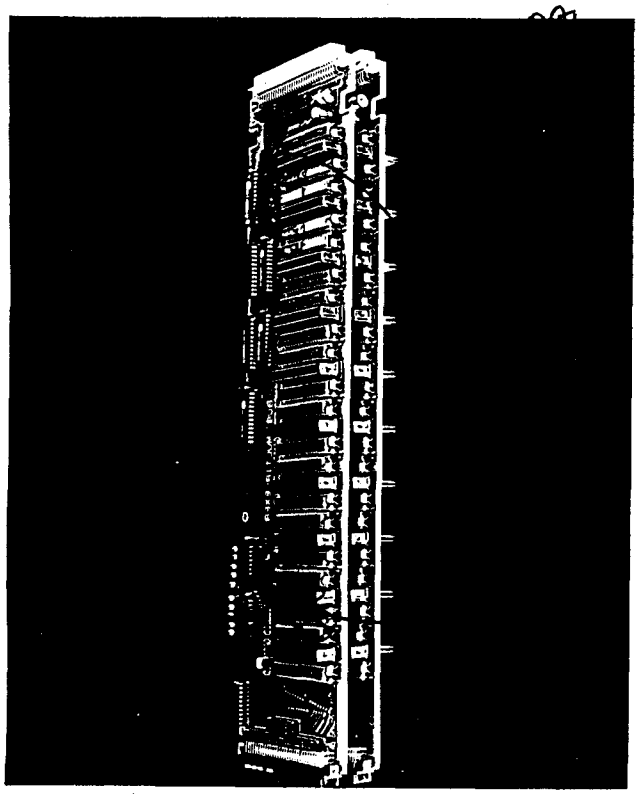

2050

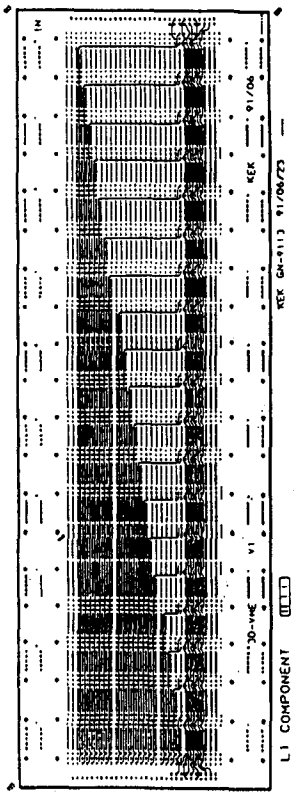

2051

< PROPERTIES >

address size : 16 x 2 (=32) bit

data size : 16 bit

In MOBY, address is transfered every in a packet of 16 bit address

⇩

extended version

address : (32 x 2) = 64 bit

2052

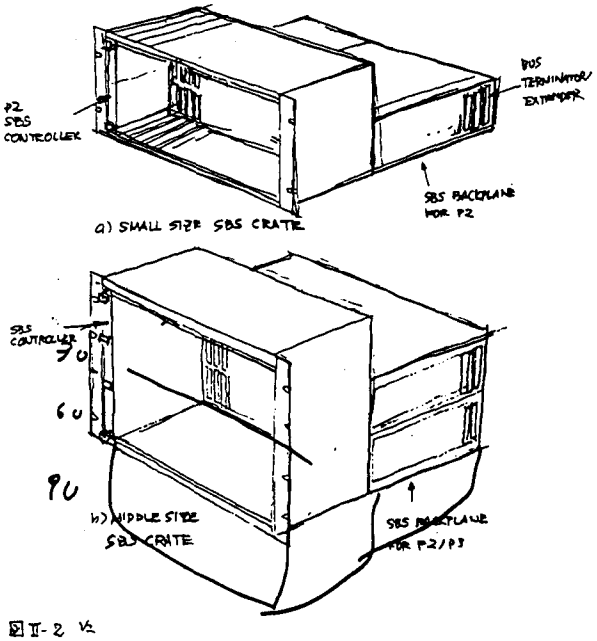

図 II-2 V2

timing characteristics

- switching ~160ns
- random transfer
  ~400~250ns → 3~4MH
- propergation delay
  ~ 25~30ns

< Schedule >

Test with 20 pieces of CPU board will be carried out around next month.

- Block Transfer
- Software environment

High Speed Switch System

Osamu Sasaki
(KEK)

Fujitsu ECL Gate Masterslice E128H

It is an ECL semi-custom integrated circuit that has 128 gates equivalent density. Compared with a conventional ECL gate array, it has the following features:

Implementation of customer specified funtions
Specialized in handling high speed signals (up to 3 Gbs), rather than circuit complexity
Fast rise/fall time and small jitter for clear output eye pattern
Power and speed trade-off

Internal Gate Propergation Delay
75 ps (typical, single-ended)
55 ps (typical, differential)
Output Rise/Fall Time : 95 ps / 75 ps (typical)
Flip-Flop Toggle Freq. : 4 GHz (typical)

Developement Cost	5M yen ($38K)
Minimum lot	200 pieces

25K yen ($190) each at the first lot

1.4 E128H Circuit Structure

1.4.1 Chip Layout

The E128H chip structure is shown in the figure below. It contains:

* 16 (4x4) Internal Cells to implement customer specific logic functions
* 8 Output Buffers which generate clear output signals
* 4 Delay Gates for signal timing adjustment
* 4 Bias Voltage Generator circuits
* Input Signal Sharpener for sharpening input signals from the test equipment

The Internal Cells are arranged in a 4 x 4 matrix with wiring channel area surrounding each of the Internal Cells.

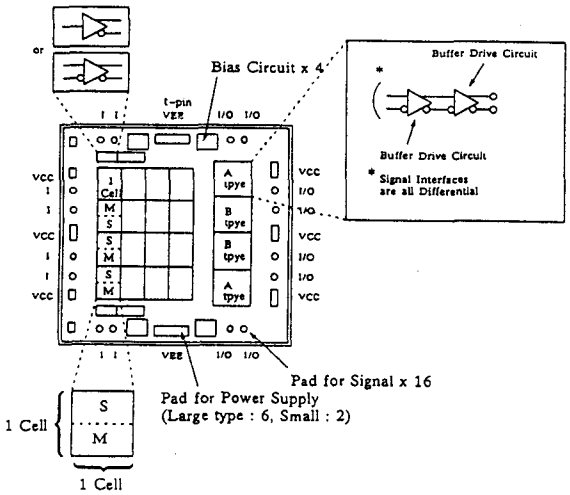

1.4.2 Internal Cell

The E128H contains 16 Internal Cells. Each Internal Cell consists of two sections called "M-part" and "S-part", and a cell bias circuit. To implement a logic function, the series gate circuit technology is used so that a logic function is realized with the minimum amount of components.
The figure below shows representative logic macros which can be implemented in an Internal Cell.

There is a family of logic functional macros predefined for customer's logic designs. These macros are specified in the "MACRO SPECIFICATION" (document#GAT10318Δ).

The cell bias circuit is locally used to supply bias voltage within the Internal Cell. It is not used only when the Internal Cell is left unused at all.

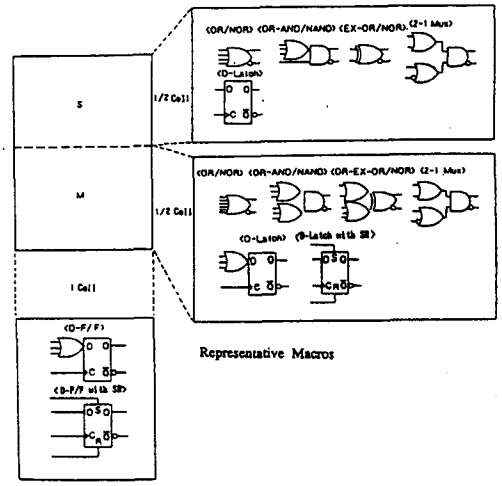

(ICS) and emitter follower current (IEF). These selections are done by selecting macro types during logic designs by customers. With these selections, a designer can implement optimal power and speed combinations in the circuit.

As tabulated below, the Internal Cell has the fixed ICS and allows three options for IEF. IEF values are programmed in a logic macro by programming emitter follower termination resistor values.
The Output Buffer has three options for ICS.

ICS and IEF Options

	ICS	IEF
Internal Cell	1.0 mA	0.5 mA 1.0 mA 2.0 mA
Output Buffer	4 mA 8 mA 16 mA	External 50 Ω to VT (-2V)

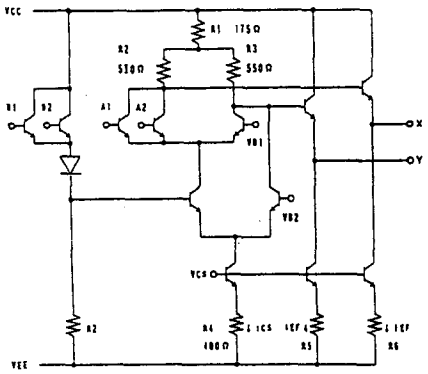

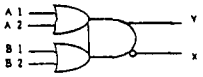

$Y = (A1 + A2) \cdot (B1 + B2)$

$X = \overline{(A1 + A2) \cdot (B1 + B2)}$

The package for the E128H is the 24-pin circular flat package. This package is intended for an efficient conductive cooling, achieving a low junction-to-case thermal resistance.

* Dimensions : Shown below (Case NO. FPT-24C-A03)
* Thermal Resistance : 6 °C/W (Junction to Case)

Note : The bottom (heat-spreader) of the package is connected to VEE.

Each of input and output pins are design as a transmission line having a characteristics impedance of 50 Ω, which minimize signal distortions in the package.
The S11 and S12 characteristics are shown below.

S11 Characteristics

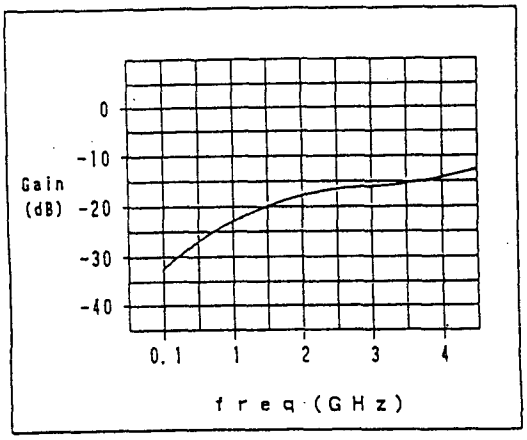

MB1850

4 X 4 Barrel Shifter / Dual 2 X 2 Barrel Shifter

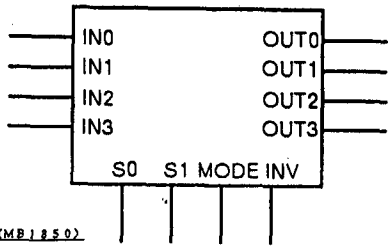

真理値表 (MB1850)

MODE	S0	S1	INV			OUT0	OUT1	OUT2	OUT3
0	0	0	0			IN0	IN1	IN2	IN3
0	1	0	0			IN1	IN2	IN3	IN0
0	0	1	0			IN2	IN3	IN0	IN1
0	1	1	0			IN3	IN0	IN1	IN2
0	0	0	1			TN0	TN1	TN2	TN3
0	1	0	1			TN1	TN2	TN3	TN0
0	0	1	1			TN2	TN3	TN0	TN1
0	1	1	1			TN3	TN0	TN1	TN2
1	0	0	0			IN0	IN1	IN2	IN3
1	1	0	0			IN1	IN0	IN2	IN3
1	0	1	0			IN0	IN1	IN3	IN2
1	1	1	0			IN1	IN0	IN3	IN2
1	0	0	1			TN0	TN1	TN2	TN3
1	1	0	1			TN1	TN0	TN2	TN3
1	0	1	1			TN0	TN1	TN3	TN2
1	1	1	1			TN1	TN0	TN3	TN2

0 ··· VIL 1 ··· VIH

4 X 4 MODE=0

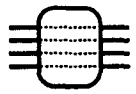

S0=0, S1=0

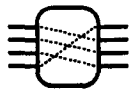

S0=1, S1=0

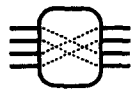

S0=0, S1=1

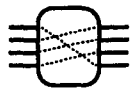

S0=1, S1=1

Dual 2 X 2 MODE=1

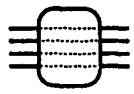

S0=0, S1=0

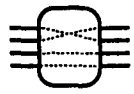

S0=1, S1=0

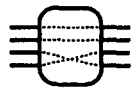

S0=0, S1=1

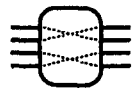

S0=1, S1=1

I. 機能概要

1. 機能（MB1850）

4 X 4 Barrel Shifter / Dual 2 x 2 Barrel Shifter

2. 論理図（MB185D）

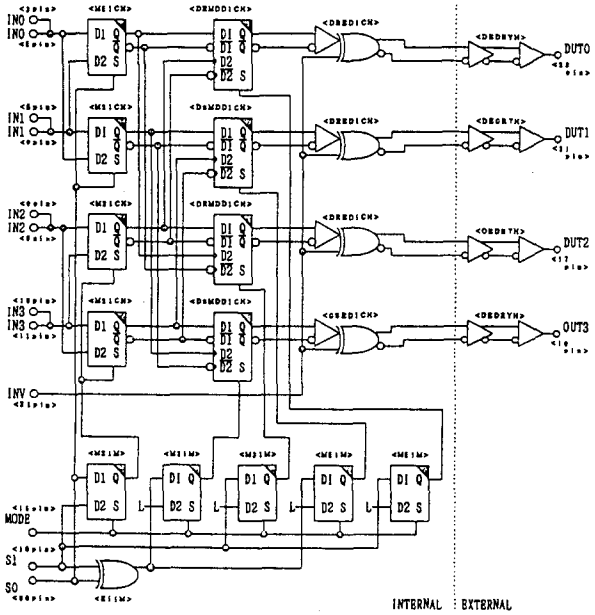

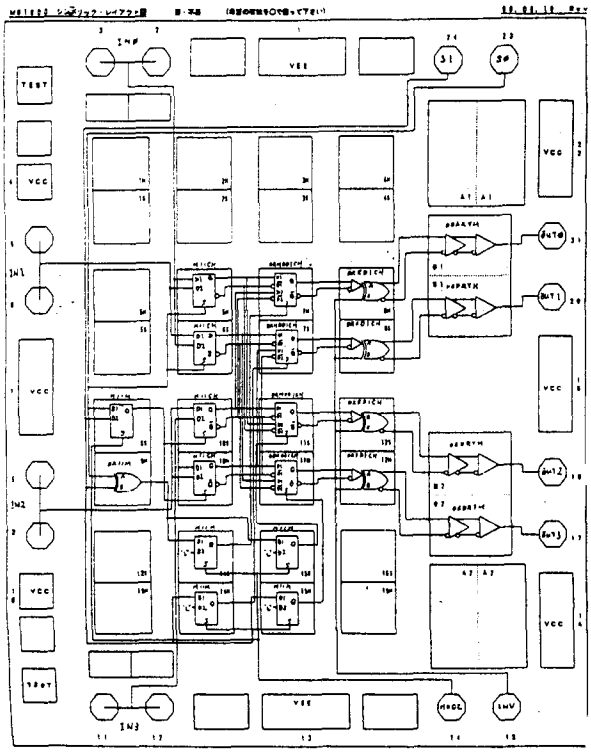

Feed Through Input

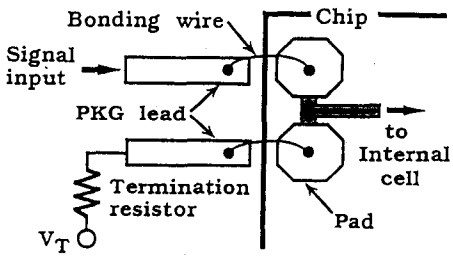

Application Examples

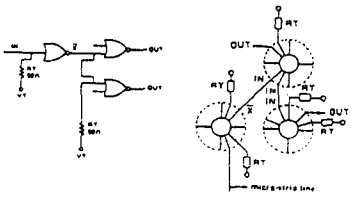

5. 交流特性 —（1）

(VCC(4, 7, 10, 16, 19, 22 ピン)=+2.00V , VBB(1, 13 ピン)=-3.20V)

項目	伝播経路	記号	温度 (Tc)	MIN	TYP	MAX	単位	条件
伝播遅延時間 (50%-50%)	INn ⇒ DUTn	tpLH	25℃	—	396	545	pS	出力=50Ω to GND MODE, S0, S1, INV入力ピン VIN=VIL
		tpHL	25℃	—	401	560	pS	

注）数値は、ターゲット値を示します。

入力パルス条件 ：VIH=+1.10V, VIL=+0.30V
tr/tf≦200pS
PRR=500MHz (INn)
INn, OUTn ：IN0～3, OUT0～3

交流特性 —（2）

(VCC(4, 7, 10, 16, 19, 22 ピン)=+2.00V , VBB(1, 13 ピン)=-3.20V)

項目	記号	出力ゲート (ピン NO.)	温度 (Tc)	MIN	TYP	MAX	単位	条件
出力立上り時間 (20%-80%)	tr	15, 17, 21, 23	25℃	—	145	225	pS	出力=50Ω to GND
出力立下り時間 (20%-80%)	tf	15, 17, 21, 23	25℃	—	85	150	pS	出力=50Ω to GND

注）数値は、ターゲット値を示します。

入力パルス条件 ：VIH=+1.10V, VIL=+0.30V
tr/tf≦200pS
PRR=500MHz (INn)
INn, OUTn ：IN0～3, OUT0～3

8 X 8 Barrel Shifter

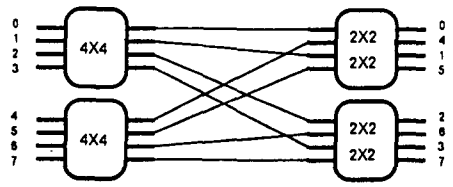

16 X 16 Barrel Shifter

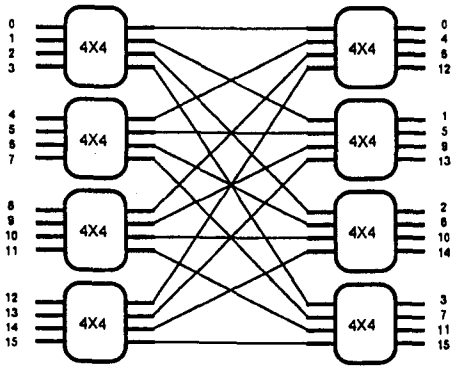

An "n X n" Barrel Shifter can be built by using the MB1850's, where "n" is a binary number such as 8, 16 32,128 etc.

VME Barrel Shifter Module

CRATE customized
- VME 6U
- 21 slots
  - 5 slots normal J1, J2 connector
  - 16 slots normal J1 connector
    J2(DIN41612) is used for power supplies to modules.

GND
- -5.2V ECL
- -2.0V ECL termination
- 5.2V "positive" ECL and TTL-ECL converter
- 5.2-2.0 V (3.2V) "positive" ECL termination

MODULE 6U high double width VME

TYPE 3 types
- Dual 4X4 / Quad 2X2 for "negative" ECL
- Dual 4X4 / Quad 2X2 for "positive" ECL
- Single 8X8 for "negative" ECL

VME ADDRESS SPACE
- short access (A01-A15)
- module address A03-A15
  - Broadcast
    when A03-A06 = "F", A07-A15 equals to a module address and a write cycle.

DATA 16-bit (D00-D15)

Barrel Shifter Control Data

One MB1850 is controlled by four signals, S0, S1, MODE and INV.

S0, S1	select a configuration
MODE	select a mode, 4X4 or dual 2X2
INV	select inverted or non-inverted outputs

16-bit data is provided for MB1850's from a ROM or a REGISTER in the VME Barrel Shifter Module.

1st MB1850	3rd MB1850
0th-bit S0	8th-bit S0
1st-bit S1	9th-bit S1
2nd-bit MODE	10th-bit MODE
3rd-bit INV	11th-bit INV

2nd MB1850	4th MB1850
4th-bit S0	12th-bit S0
5th-bit S1	13th-bit S1
6th-bit MODE	14th-bit MODE
7th-bit INV	15th-bit INV

CONTROL

ROM mode

The barrel shifter IC's are controlled by 16-bit data that is stored in the ROM (16 X 64k) beforehand. The address counter for the ROM is controlled via VME instructions or NIM signals (STEP, RESET) through a front panel.

STEP	ROM address increment
RESET	ROM address reset

REGISTER mode

The barrel shifter IC's are controlled by 16-bit data that are stuck on the REGISTER via a VME instruction.

READ

A=0 (A01=0, A02=0) read barrel shifter control data

A=1 (A01=1, A02=0) read ROM address counter

A=2 (A01=0, A02=1) read allowed maximum value of address counter

A=3 (A01=1, A02=1) read control status word

WRITE

A=0 (A01=0, A02=0) write barrel shifter control data to REGISTER

A=1 (A01=1, A02=0) preset ROM address counter

A=2 (A01=0, A02=1) write control status word (8th- and 9th-bit only)

A=3 (A01=1, A02=1) write control status word

CONTROL STATUS WORD

0th-bit select source of barrel shifter control data from ROM (L) or REGISTER (H)

1st-bit mask (H) external STEP UP (from front panel) or not (L)

2nd-bitmask (L) external RESET (address counter for ROM, from front panel) or not (L)

3rd-bit auto set up ON (L) or OFF (H)

8th-bit soft STEP UP (H) the address counter (write only)

9th-bit soft SET UP (H) (write only)

default = L ## Other bits are not used.

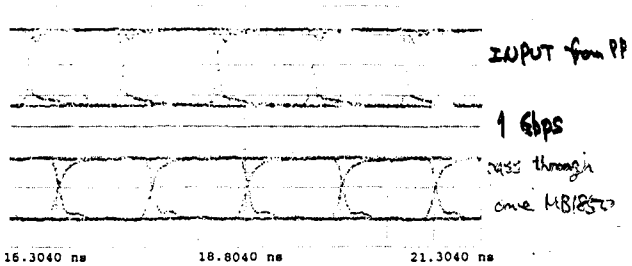

Ch. 3 = 40.00 mVolts/div Offset = -129.0 mVolts
Ch. 4 = 40.00 mVolts/div Offset = -126.7 mVolts
Timebase = 500 ps/div Delay = 16.3040 ns

Trigger on External at Pos. Edge at -6.000 mVolts

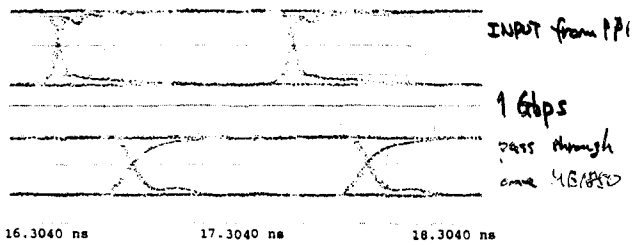

Ch. 3 = 40.00 mVolts/div Offset = -129.0 mVolts
Ch. 4 = 40.00 mVolts/div Offset = -126.7 mVolts
Timebase = 200 ps/div Delay = 16.3040 ns

Trigger on External at Pos. Edge at -6.000 mVolts

triggered by divided clock of PPG

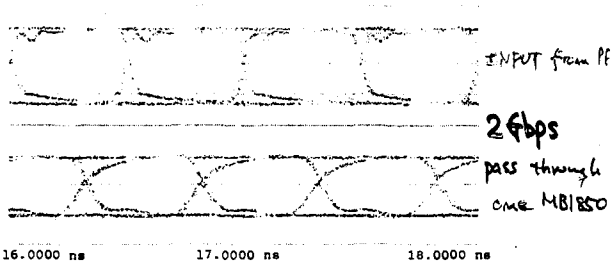

Ch. 3 = 40.00 mVolts/div Offset = -129.0 mVolts
Ch. 4 = 40.00 mVolts/div Offset = -126.7 mVolts
Timebase = 200 ps/div Delay = 16.0000 ns

Trigger on External at Pos. Edge at -6.000 mVolts

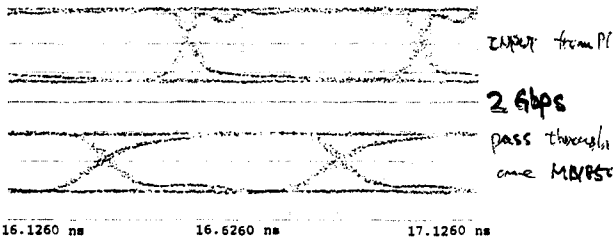

Ch. 3 = 40.00 mVolts/div Offset = -129.0 mVolts
Ch. 4 = 40.00 mVolts/div Offset = -126.7 mVolts
Timebase = 100 ps/div Delay = 16.1260 ns

Trigger on External at Pos. Edge at -6.000 mVolts

triggered by divided clock of PPG

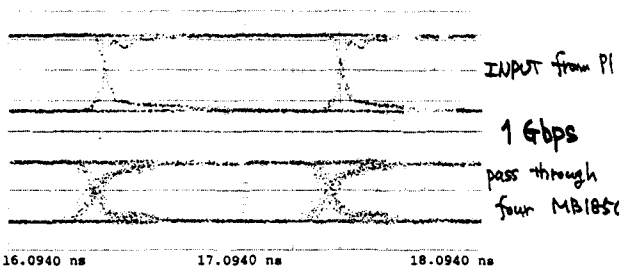

Ch. 3 = 40.00 mVolts/div Offset = -129.0 mVolts
Ch. 4 = 40.00 mVolts/div Offset = -126.7 mVolts
Timebase = 200 ps/div Delay = 16.0940 ns

Trigger on External at Pos. Edge at -6.000 mVolts

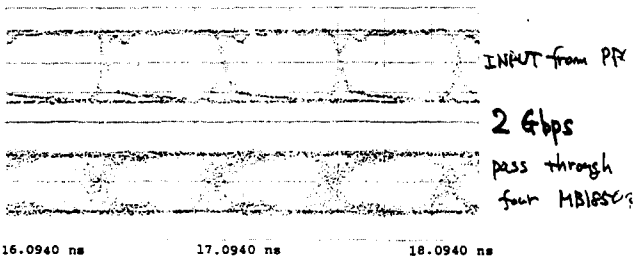

Ch. 3 = 40.00 mVolts/div Offset = -129.0 mVolts
Ch. 4 = 40.00 mVolts/div Offset = -126.7 mVolts
Timebase = 200 ps/div Delay = 16.0940 ns

Trigger on External at Pos. Edge at -6.000 mVolts

triggered by divided clock of PPG

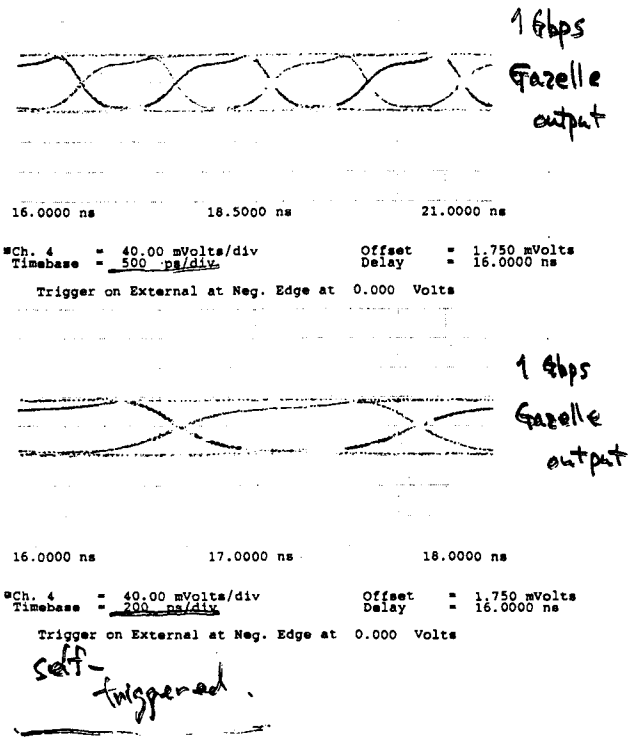

TEST

when signals pass through one MB1850

We could handle high speed signals up to 3Gbps.

when pass through four MB1850's

up to 2Gbps ?

TEST with HOT ROD Coax Interface Card of Gazelle

The Gazelle could transmit and receive data at rates of up to 1Gbps through the Barrel Shifter System with no failure, where signals pass through up to 7 MB1850's.

Barrel Shifter System for SDC

CRATE SDC standard 9U VME crate

what is the standard?

BASE MODULE

9U high double width VME

Quad 4X4 / Octal 2X2 Barrel Shifer Module
Single 16X16 Barrel Shifter Module

An "n X n" Barrel Shifter System can be built by using the base modules, where "n" is a binary number such as 32, 64, 128 etc. For example, 256X256 barrel shifter can be built using thirty two 16X16 base modules . (requires 256 MB 1850's) In this case, each signal path contains four MB1850's. 512X512 can be built using sixty four 16X16 and thirty two Octal 2X2 Barrel shifter base modules.

Optical to Electrical Converter Module

upto 1Gbps

Electrical to Optical Converter Module

Is it necessary?

required cable length?

signal attenuation in a coaxial cable

Interests and Resources for DAQ subsystem in Japan

H.Fujii (KEK)

28-May-1992

Budget for DAQ subsystem
(JFY'92)

1. Auxiliary modules for Barrel shifter	2000 K yen
2. CPU modules for system control	0 K yen
3. Data generator (CPU) modules	1500 K yen
4.Data receiver (CPU) modules	1500 K yen
5. Switch modules for FNAL	4000 K yen

Other Related Systems

1. Optmodulator readout system (Ohsuka)	500 K yen
2. Multi-wavelength opttransfer system (Ujiie)	0 K yen
3. First level pipeline trigger (Sakamoto)	5000 K yen
4. Bus-switch & trigger system for muon test (Sakamoto)	4000 K yen

Data link transceiver & Event Builder
(M.Nomachi, O.Sasaki, T.Ohsuka and H.Fujii)

Main components
1. Optical data link transceiver
2. Opt-ECL converter
3. Barrel shifter

In JFY'91
We have built

1. Optical data link transceiver (120Mbps = 8MB/s incl. overhead)	8 modules
2. 4x4 barrel shifter	2 modules
3. Opt-ECL converter	2 modules

In JFY'92
We will add

1. Data generator (CPU) modules	1 module
2. Data receiver (CPU)modules (Online farm simulation)	1 module
3. Auxiliay modules for barrel shifter	

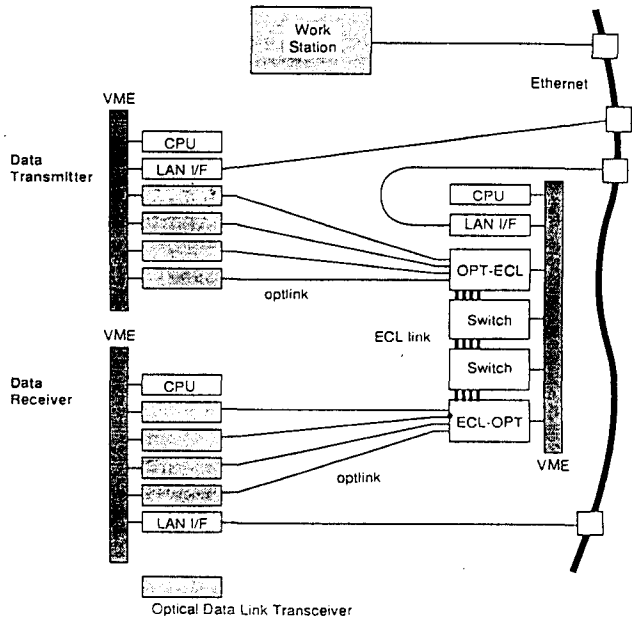

Fig 1

Push Type Optical Data Transceiver

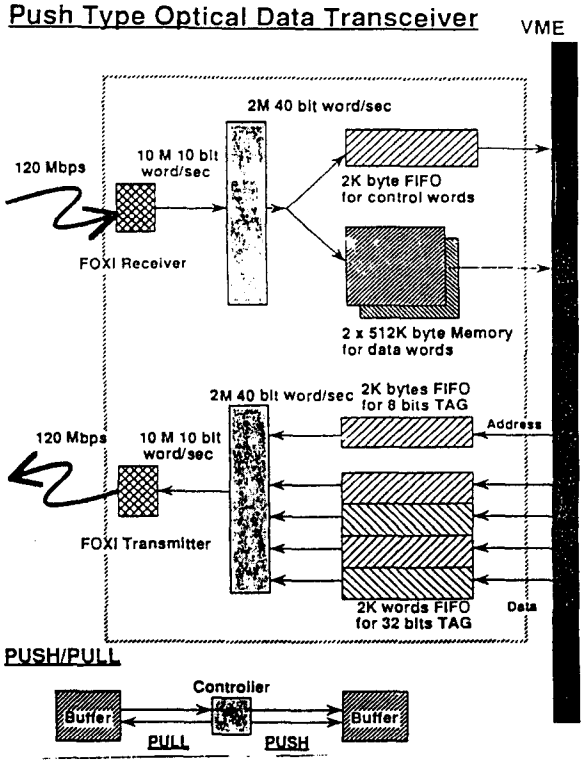

Portable DAQ software

According to the discussions on May 7th and 8th at the SSCL, we will develop the following software packages (KEK + Japanese Universities)

1. Histgramming
2. Display
3. Buffer manager
4. DECstation VME interface

DAQ for test experiments at KEK

1. Muon chambers
2. Si detectors (?)

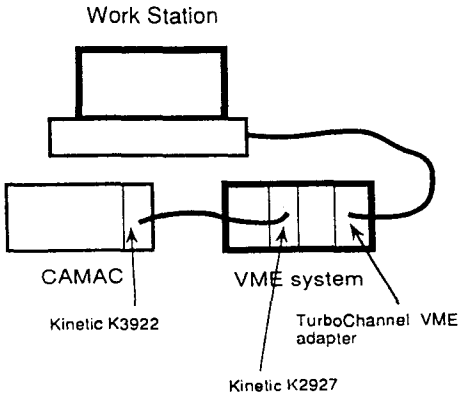

DECStation 5000

TurboChannel VME adapter
Kinetic K2917 VME-CAMAC interface
Kinetic K3922 CAMAC-CC

Event Builder Subsystem

Masa Nomachi

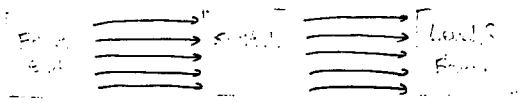

High Speed Network

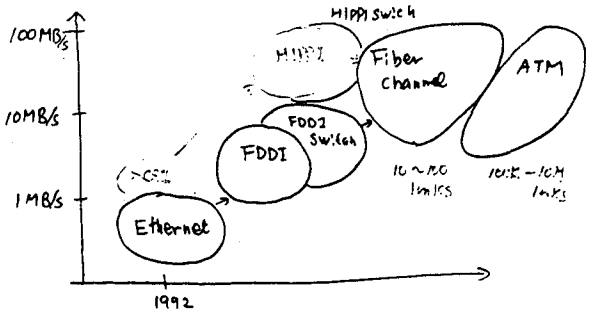

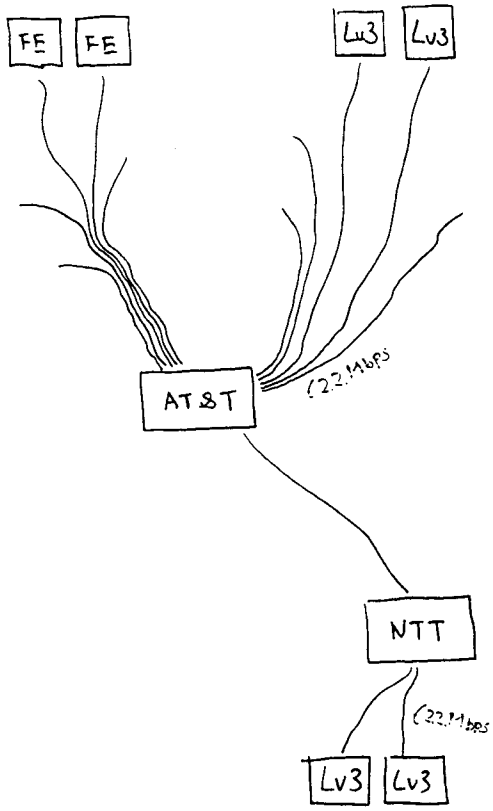

How to make a large Switch

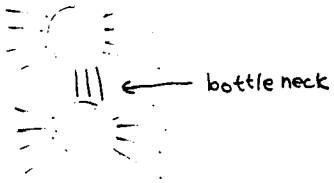

Cross bar	Barrel Shifter
Any combination ⇒ Network	Limitted connection ⇒ only for Event Builder
$N!$ combinations	N combination
$O(n(\log n)^2)$	$O(n(\log n))$
Commercial	Non Commercial

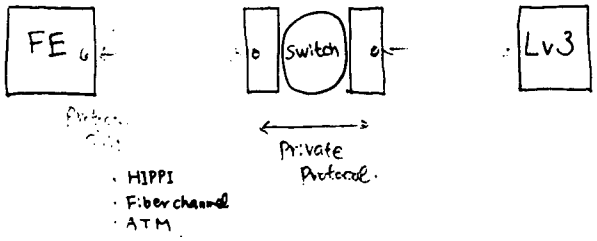

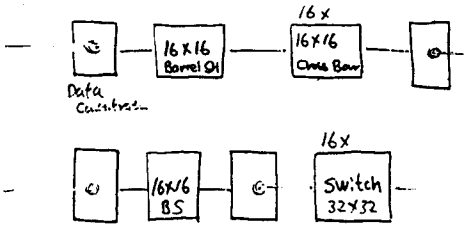

25-MAY-19
SDC
at KEK

Development of The SPARC-VME-CAMAC Data Acquisition System

(Portable DAQ)

Yasuo TAKEUCHI

Department of Physics,
Tokyo Institute of Technology (T.I.T.)

CONTENTS

Motivation to develop
SPARC-VME-CAMAC system
CAMAC device driver
Data acquisition programs (TDAQ)
Test of TDAQ
Summary & Conclusion

MOTIVATION

1. KAMIOKANDE / SUPER-KAMIOKANDE (SK) experiment
   (Imaging water Cerenkov detector)

◎ Requirements of the SK DAQ system

Fast data acquisition
Easy to maintenance
Analysis on the spot
....

- UNIX data acquisition (DAQ) !
- Simple UNIX DAQ system will be scaled up to large DAQ system.

2. General purpose DAQ system

inexpensive
small
easy to maintenance
...
(for lab. of Univ.

☞ In the first stage,
we constructed simple RISC/UNIX DAQ
we checked real-time property of RISC/UNIX

Why do we use RISC/UNIX ?

Good network, file system, handling ....

Fast CPU ⇒ Data acquisition and analysis carried out in UNIX

Not expensive

Good portability
⇒ analyze the data at the place where the data was taken

RISC/UNIX will be (is ?) standard.

1 problem

But, UNIX is not real-time operating system!

➥ We used "**device driver**" to solve this problem.

Ensuring real-timeness

UNIX dose not assure real-time response!

How can we get real-time response in UNIX ?

1. Use RISC CPU

Complex ISC ⋮ Reduced Instruction Set Computer

Fast (20-50MIPS)
cf. CISC(1-20MIPS)

e.g. SPARC CPU (RISC) 28.5 MIPS
VAX CPU (CISC) ~1 MIPS

2. Develop device driver (in kernel)

Device drivers enable us .....

- highest priority
- interrupt handling
- direct access to hardware
- using DMA

Important to DAQ

2093

UNIX Device Driver

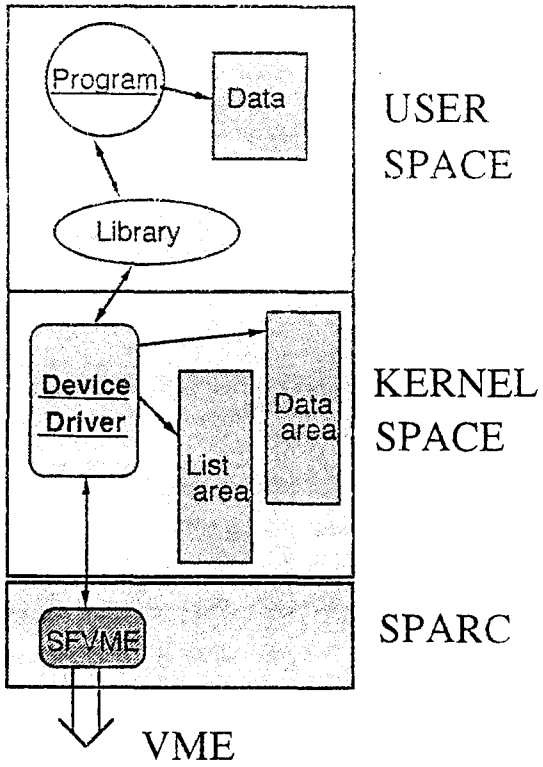

2094

SPARC-VME-CAMAC

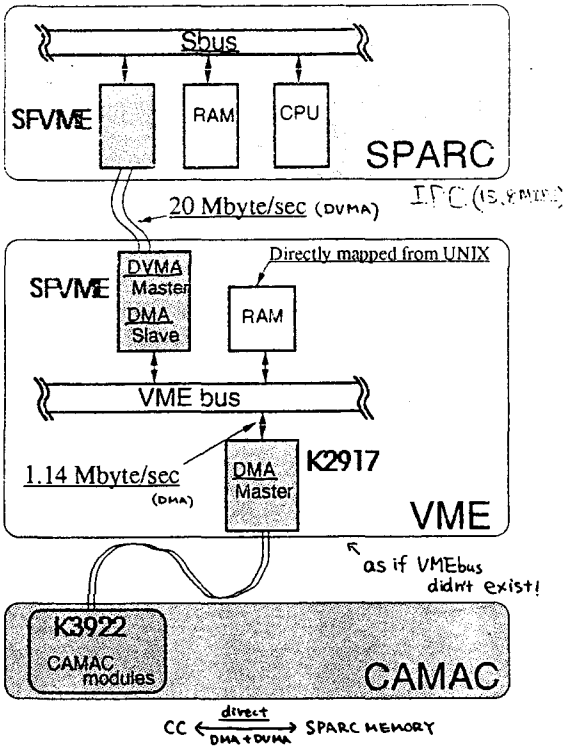

2095

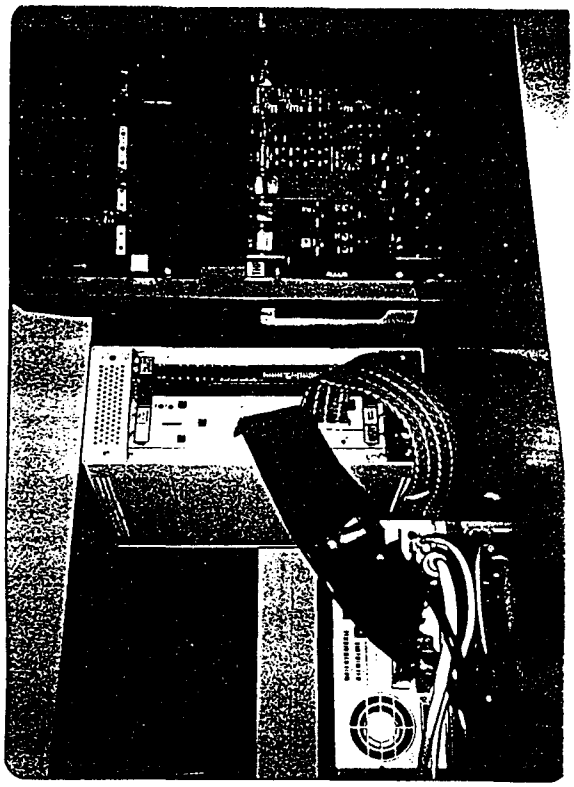

2096

CAMAC Device Driver/Library

- FORTRAN 77 and C callable
- Equip list processing in the device driver (UNIX kernel space)
- Compatible with those on VAX / VMS developed by KEK online group
- Easy to modify (all C)
- To some degree, they enable us real-time access to CAMAC.

Performance of CAMAC library

① LAM interrupt latency

referred from KEK

	IPC	μVAX II
function call	228	1000
list processing	182	160-190

measured

Compar-able

(μsec)

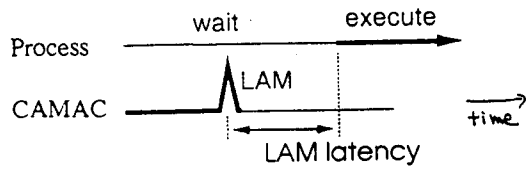

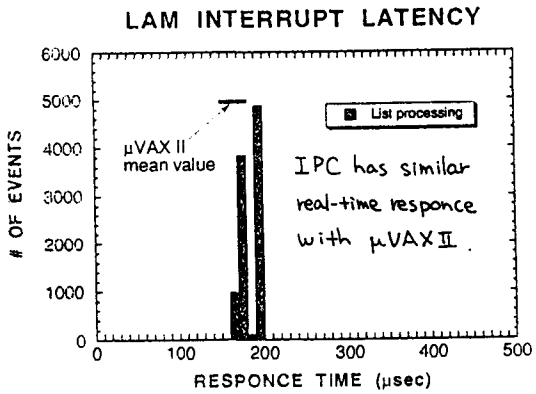

CAMAC actions

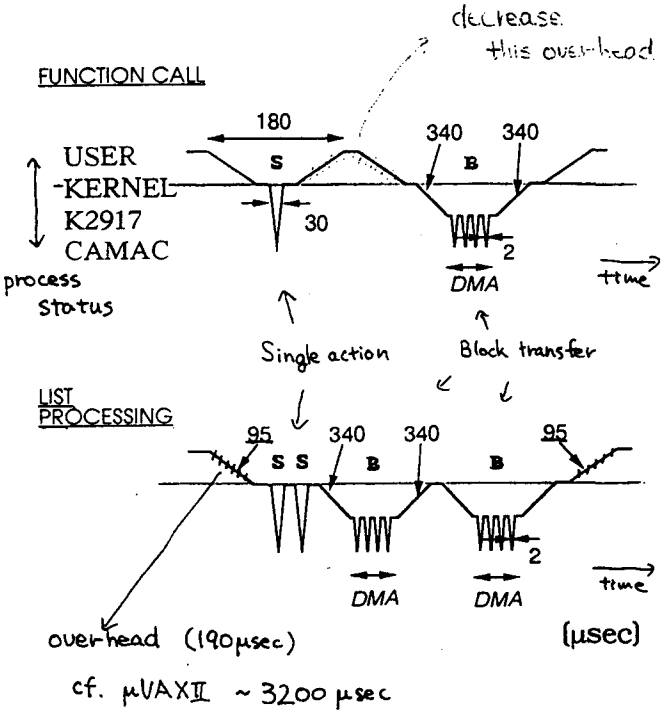

② CAMAC single action

		IPC	μVAX II
function call from FORTRAN,C	16bit R	180	1100
	W	180	1100
	NDT	171	1100
list processing in device driver (kernel mode)	16bit R	29	32
	W	29	31
	NDT	21	26

6times faster

compar-able

NDT: No Data Transfer

(μsec)

③ CAMAC block transfer

	IPC	μVAX II
16bit R	2.88	2.5
DB	2.09	1.7
Overhead (function)	1000	2000
Overhead (list proc.)	750	400

(μsec/word)

slightly slower

(μsec)

DB: Double Buffer mode (K3922) Read

2101

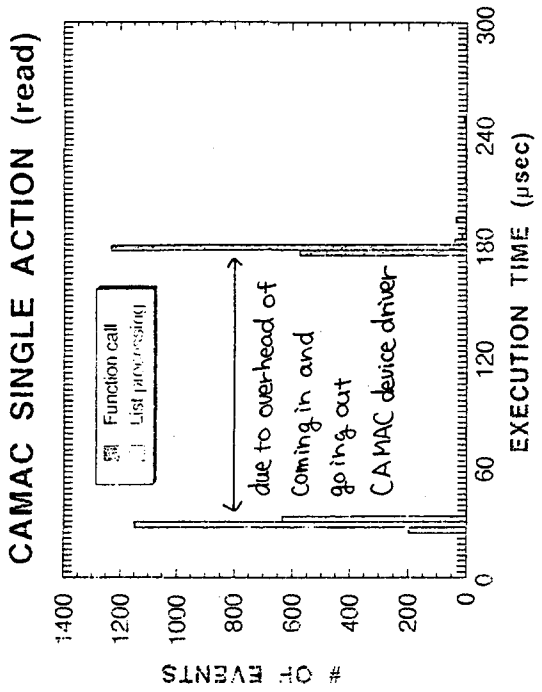

2102

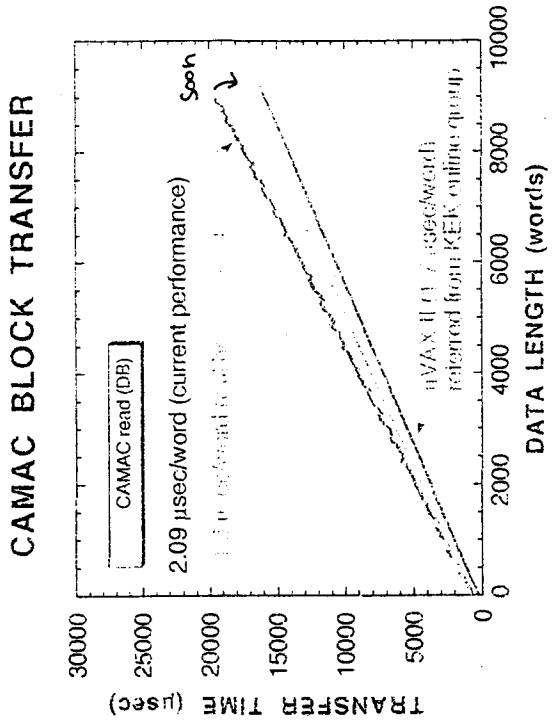

2103

DAQ programs on SPARC

TITech Data Acquisition programs (TDAQ)

- Simple Buffer Manager
- Data Collector
- Data Recorder
- DAQ System Manager
- Control Panel (user interface with XView)

2104

TITech Data Acquisition system

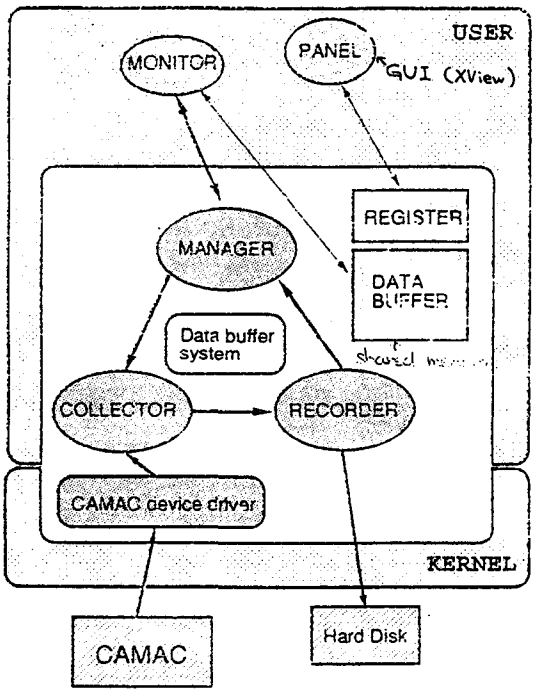

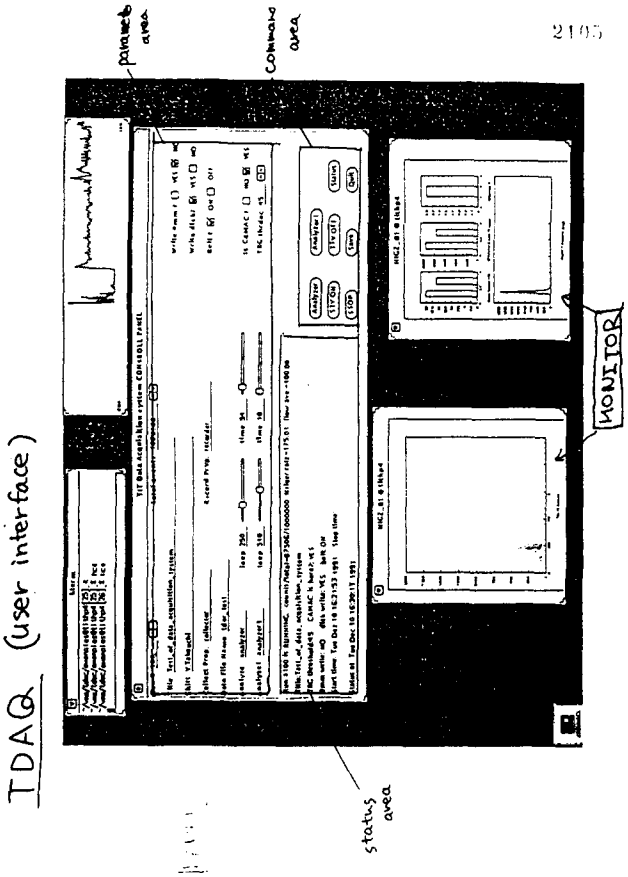

Bench test of the TDAQ system

(performance test UNIX DAQ system)

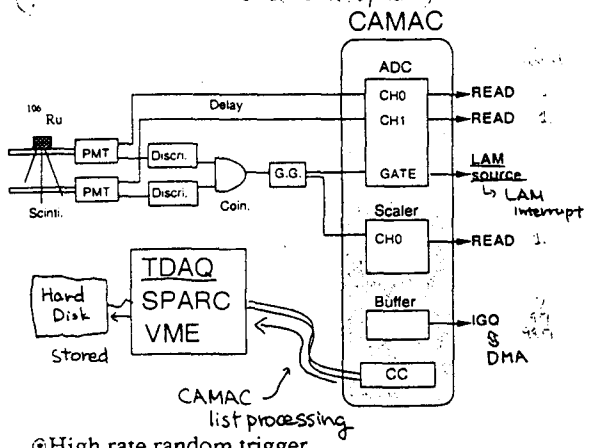

◎High rate random trigger

only take (calc.)

Data size		Max. acquisition rate	
10	words/event	360 Hz	(1.4k)
100		300	(0.7k)
1000		120	(0.3k)

will be improved.
(not well optimized!)

Beam test experiment at KEK

(KEK, T.I.T., Nara W. U.)

(An example. TDAQ was already used!)

- A beam test of CsI crystals for KEK B-Factory
- Use KEK PS $\pi 2$ beam line
- Trigger rate: 20 Hz
- Data size: 100 bytes/trigger
- Data taken during 2 weeks in Jan. 1992
- Data acquisition and analysis was done about same time
- There was no serious problem!

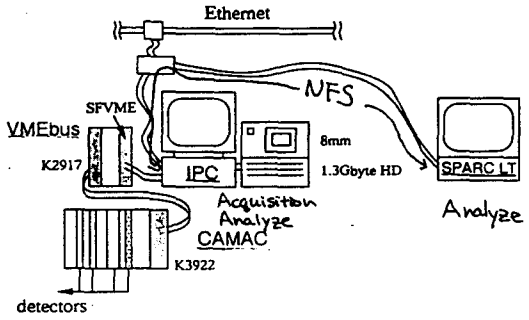

Summary & Conclusion

◎ An inexpensive (about $20000), small (≈ IBM PC) and high performance (≥ μVAX II) RISC / UNIX data acquisition system was constructed.

◎ We made come true equivalent real-time response with μVAX II on IPC by means of the CAMAC device driver about 180 μsec.

◎ Overall, the performance of the CAMAC library on SPARC IPC was better than that on μVAX II / VMS.

◎ TDAQ is already used (or tested) at T.I.T., KEK, Kamioka, SSCL ....

◎ We are still improving TDAQsystem.
(e.g. new DAQ computer,
K2917's list processing,
new device driver)

2109

Potable DAQ Standard Crate

M. Nomachi
(KEK)

2110

Portable DAQ standard crate

VME + UNIX Work Station

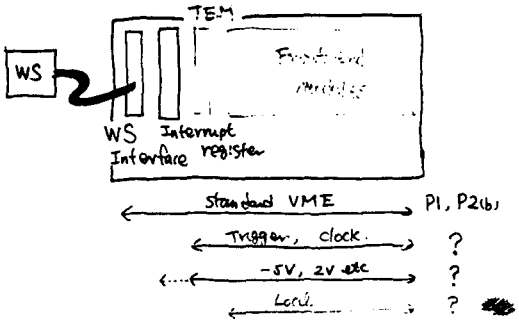

Where ?

- Front
- P2 a,c — for VSB
- P3 (only for 9U) — 6U is standard.
- Internal DC-DC converter.

Use standard Backplane (J1+J2) !

2111

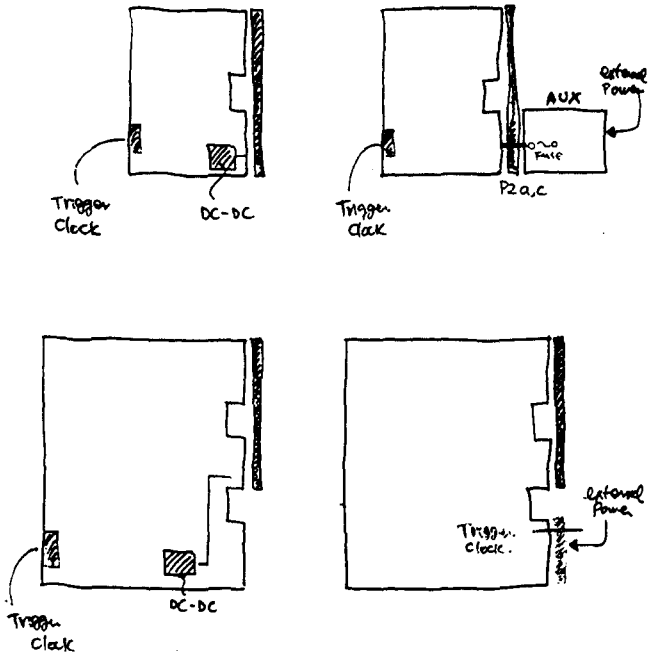

2112

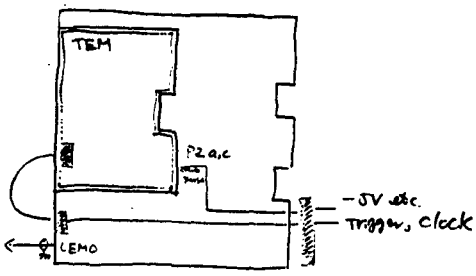

, w/ on special P3 back plane.

- Standard module
  - TRIG, clock → Front.
  - Power → 9U, internal.
    6U P2, a,c (VX1)
- Front end module
  - TRIG, Clock → 6U Front, 9U P3
  - Power → P2a,c, P3

↓

Standard

1993 !

Nuclear Instruments and Methods in Physics Research A307 (1991) 110–115
North-Holland

Readout control for high luminosity accelerators (*)

R. Belusevic† and G. Nixon
Department of Physics and Astronomy, University College London, London WC1E 6BT, UK

Received 15 April 1991

† Now at KEK

(*) Talk given at the ECFA conf. in Aachen (Oct. 1990)

Simplified design implemented in ZEUS DAQ

Requirements:

- Transfer speed ~100 Mbytes/s
- Processing power to match the above rates
- Concurrency with respect to data transfer & processing
- Flexibility (indep. of detector & crate type)
- Simplicity of hardware & operating software
- Data compaction & trigger (pre)processing before readout

Possible solutions:

- Reduce interfacing logic & eliminate bus arbitration:
  a) single controller/μ capable of multitasking & parallel processing
  b) Dual ported memories (DPMs) throughout the system
- Reduce real-time overheads
- Provide easy & uninterrupted access to data for emb. μs
- Form a pipeline of reduced data on readout cards
- Use fast (~Gbit/s) intercrate serial links

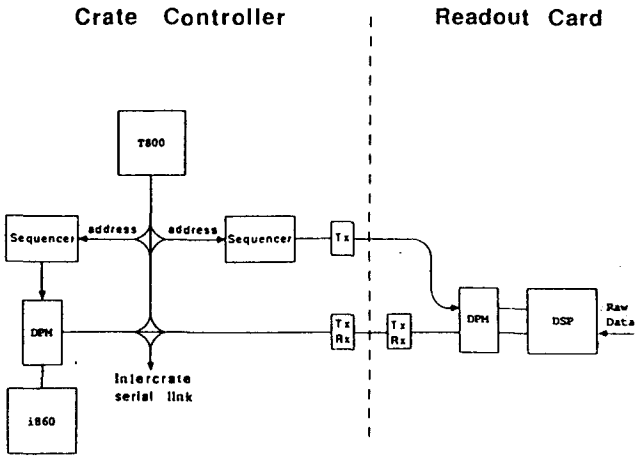

Block diagram showing system's main components and data flow within a crate.

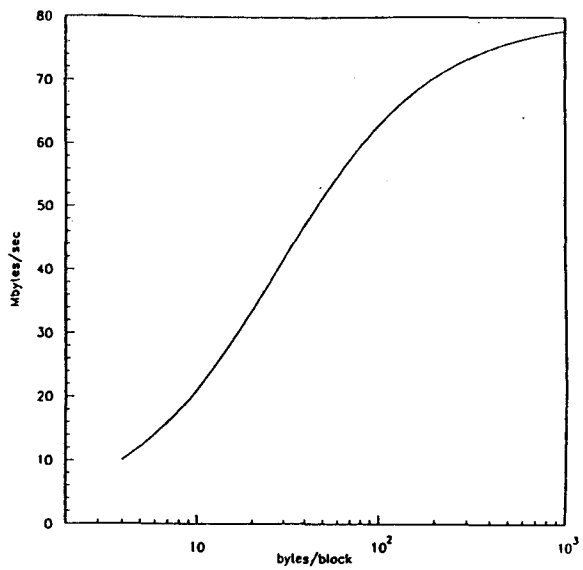

Data transfer speed as a function of block size.

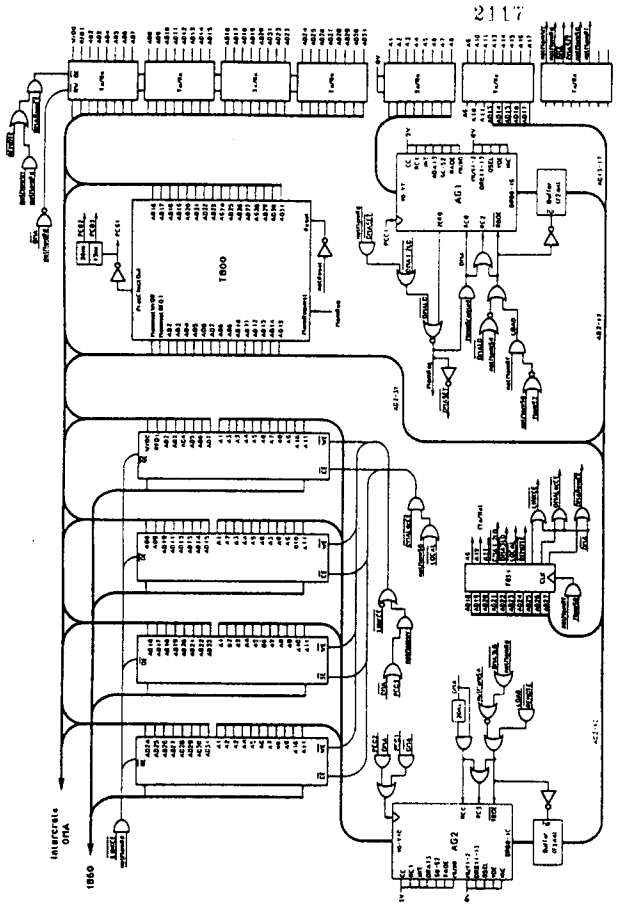

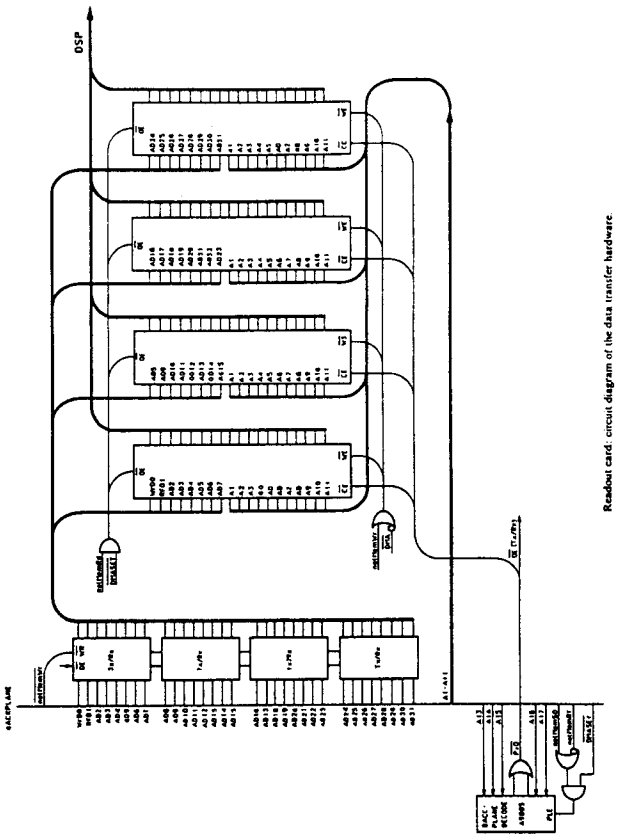

Readout card: circuit diagram of the data transfer hardware.

HOT ROD

1 Gbit/sec DATA COMMUNICATIONS

- Convenient 2-Chip Implementation
  - One transmitter device, one receiver device
- 1 Gbit/sec Maximum Data Rate
  - 3 more selectable rates (500, 250, 125 Mbit/sec)
- TTL-Level 40-Bit Data Bus
  - Fully compatible with 32-bit μP systems
  - 25 MHz parallel data rate
- Fiber Optic or Coaxial Media
  - Flexibility from meters to kilometers

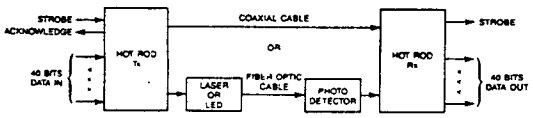

[11] Computing

<Overview>

Strategy and Plan for SDC Computing	L. Price	-2121

<Task Force>

Core Software Task Force	S. Frederiksen	-2132
SDC Core Task Communications Services	G. Kubena	-2147
Data Modelling Package Task Force Requirements	B. Scipioni	-2170
Status of Software Development Task Force	A. White	-2182

<Distibuted Computing System>

JSD Farm: Distibuted Computing Facility at KEK	Y. Morita	-2218
Distibuted Computing System at Tokyo Metropolitan University	S. Kitamura	-2230
Harnessing Modern Virtual-Memory Systems for Distibuted Computing of SSC	H. Yoshida	-2245
Evolution of Computers to Massive Parallel Processors	K. Hasegawa	-2274
Development of Simple Distibuted Batch Processing System	M. Kawaguchi	-2294

<SDCSIM>

SDCSIM	S. Kunori	-2307
Japanese Activities for SDCSIM	M. Asai	-2326

STRATEGY AND PLAN FOR SDC COMPUTING

KEK Collaboration Meeting

L. E. Price
May 27, 1992

OFFLINE COMPUTING SCHEDULE

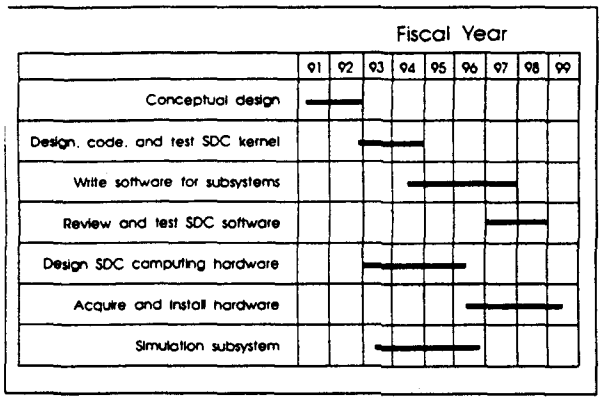

Planned Computing Organization

Computing Manager

At SSC Laboratory

Area Coordinators

Core software

Detector software

Networking and Communications

Production system

Analysis server system

Simulation system

Regional centers

Calibration

Detector software coordinators

Tracking

Calorimetry

Muon

Trigger

Committees

Computing Technical Committee
- Plan SDC computing system
- Assess progress
- Advise manager

Software Committee
- Core software coordinator
- Tracking software coordinator
- Calorimeter software coordinator
- Muon software coordinator

Production Software Review Board
- Certifies software for use in production reconstruction

Computing review committee
- High level review by experts inside and outside of SDC

Physics Research Computing Group

HARDWARE COSTS AT SSCL

Table 10-7
SDC computing costs.

Cost Element	FY92 M$
Production storage system:	
Tertiary storage system	3.70
Communications link to online	0.25
Production computing farm (10^5 SSCUPS)	6.00
Production disk system(s)	1.50
Software	2.00
Data distribution system	1.00
Express line system	1.00
Simulation system (10^5 SSCUPS)	6.00
Local analysis system	2.20
External Networking	0.25
Total	23.90

Scaling assumptions:
Cost of cpu ÷ 1.4 /year
Cost of storage ÷ 1.2 /year

EFFORT AT SSCL

Table 10-8
SSCL manpower required for SDC computing.

Task	FTE-yr.
SDC Computing Support group 4(1992) - 10(1999)	25
Hardware	
Requirement analysis	3
System design	6
System modeling	2
Procurement	2
Installation	5
Testing	5
Software	
Core system (production and analysis)	
Requirements analysis	5
Design	10
Coding	5
Testing	5
Reviews	2
Documentation	3
Physics/Detector Systems	20
(additional 80 FTE-yr provided by the SDC)	
Simulation software	10
(additional 40 FTE-yr provided by the SDC)	
	118

NEAR TERM TASKS

Decisions

What software does SDC need soon?

- Define core software--existing TF
- Data model and structures--existing TF
- Software development process--existing TF
- Simulation software to use in near term

Support test beam efforts; '93? '94?

Detailed plan for evolution of simulation software (Task force?)

NEAR TERM TASKS

Development Of Core Software

In common with GEM?

Planned contribution to HEPLIB?

Detailed definition of core software task

- Define, design, code, test
- Skills, # FTE, duration at each stage

NEAR TERM TASKS

Organization

Computing project manager (at SSCL)

Need volunteers/applicants!

Start now to hire relevant people

Define relationship to PR computing group and GEM

Identify software people from subsystems and integrate

Start meetings to define software boundaries and procedures

NEAR TERM TASKS

Cost and Schedule

Accident that we have not been asked to provide a detailed cost and schedule comparable to hardware subsystems

Detailed cost: task force?

Detailed schedule: task force?

} 1 T.F.

Including simulation

...and test beam if part of our task.

NEAR TERM TASKS

Who will do the work?

I think that a detailed cost and schedule will show that not all the work can be done by the envisioned group at SSCL

Therefore we have to do part of the work

Once we have detailed tasks, we will need to come to the computing group and match people with tasks.

That makes the schedule and task list even more urgent.

Core Software Task Force

Soren G. Frederiksen
(SSCL)

CORE SOFTWARE TASK FORCE

- Members
  - Soren G. Frederiksen (Chairman)
  - Bernard Traversat
  - Ute Nixdorf
  - Jean Huang
  - Shuichi Kunori
  - Glen Kubena
  - Chris Day
  - Brad Hubbard
  - David Adams
  - Youhei Morita
  - Katsuya Amako

1

- Charter
  - To write up a requirements document for the Core Software.
  - Document due in September-October 1992.
- Meetings
  - Have had them about every 2 weeks
  - Have had 4 meetings so far
- Architecture Model
  - Based on "Toaster Model"
  - Not "cast in stone" but mainly used for discussion
  - Very popular and "standard" model

Continuation of CORE SOFTWARE TASK FORCE

2

Toaster Model

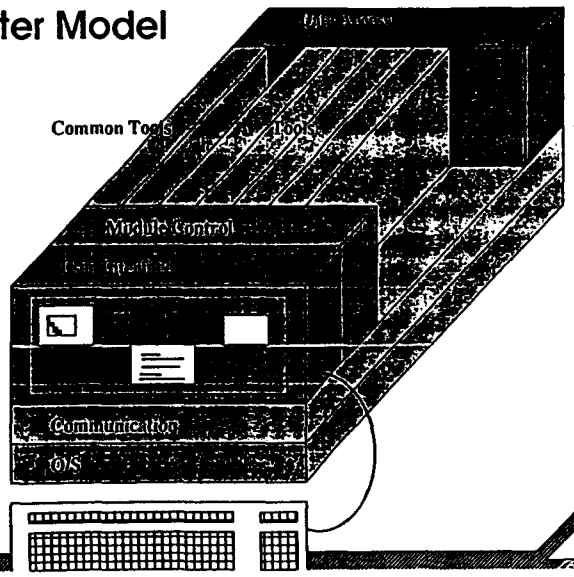

3

- Toaster Components
  - Data Access Service
    - Defined by Data Modeling Task Force (Brian Scipioni)
  - Communication Service
  - Module Control Service
  - Graphical User Interface
    - To be determined, probably commercial
  - Common Tools
  - Toast/Module
    - Written by users/collaboration members
    - stand-alone packages

4

2136

- Glossary (MY DEFINITIONS)
  - Module=Toast
    - Stand-alone process with well defined inputs and outputs
  - Tool
    - A small sub-portion of a module. Is dependent on a module
  - Common Tools
    - Collection of tools used by 2 or more modules
  - Utility Modules
    - Collection of Modules used for general purposes
    - Maintained by central group at SSCL
  - Services
    - Basic components of Toaster

5

2137

- Example
  - Study of M.C. (Pythia) simulation
  - Use a "Utility Module" which does event generation
    - Pythia generator is a "Tool" inside this module
  - User will write his/her own "Module"
  - Load "Module" along with "Services"
    - Data Access
    - Module Control
    - Communication
    - G.U.I.
  - Run "Toaster"

Continuation of

6

2138

Requirements

- Module Control
  - Initiates and activates modules along 1 or more ordered path
  - No direct communication between modules
  - all communication is via the communication service using:
    - Module Control Protocol
    - Interface Control Protocol
    - Data Flow Control Protocol
  - Possible to have mutiple copies of modules running
  - Has meta-data structure which keeps track of event flow
  - Multiple input data streams

7

2139

- Logical event flow is independent of physical mass storage choice
- Able to filter or tag events based on filter module's decision
- Identical module control interface for sequential access and random access data flow
- Dynamic module linking
- Same architecture for parallel and sequential process.
- Error handling
- Must run efficiently
- Able to exit to O/S
- Multiple modes of run control:
  - Message driven

- Data driven
- Interactive
- Able to support looping
- Has conditional response.
- Logical multilevel modules support
- Dynamic user intervention

■ Communication

- Provides two way communication between components
- Supports distributed heterogeneous environment
- View of communication services is via an application programming interface.
- Object Request Broker (ORB) provides comm. serv.

- supports one (or more?) of the following:
  - Messages
  - O/S Process invocation
  - Remote procedure calls
- Clients (toast) see objects only through the perspective of a language and has no knowledge of the implementation
- Object implementation is the methods and data associated with the object.
- Objects must register with the ORB
- An interface repository is used to keep the interface definitions
- Capabilities required of Communication services
  - Placement management tools
  - interface definition tools

- GUI tool
- Communication tool output
- Location independence and location brokering
- Dynamic binding
- Presentation services
- Error handling/reporting
- Security
- Concurrency
- Initiator/responder roles decoupled from client/server roles
- Looks like standard call
- Easy to use IDL
- Hide underlying services

■ Common Tools

- A "toolbox" of utility routines
- NOT a stand-alone program, but a library

CONCLUSION

- Core Software Task Force still on track.
- Already have preliminary requirements
- Plan/hope to print summary on a monthly basis
- **NEED input from rest of collaboration**
  - Send comments/questions to members of task force
  - or **soren@truth.ssc.gov**
    SSCVX1::SOREN
    soren@sscvx1.bitnet
- Requirements document due Sept./Oct. 1992

14

2116

- User written pacakges are in general not a common tool.
- Libraries used by "Services" are not Common Tools.
- Accessible from Fortran, Fortran90, C and C++.
- Usable on any POSIX compliant machine
- Fully documented
- Maintained by central group at SSCL
- Authorization needed to entitle a routine in common tools.
- Well defined set of inputs and outputs
- common tool cannot be run as a module
- Must be self contained and not depend on other tools

Continuation of Requirements 12

2114

- required common tools:
  - Mathematical routines
  - High level graphics routines
  - Random number generators
  - 3D geometry handling routines
  - Sorting programs
  - Histogramming routines.
- UTILITY TOOLS???
  - MINUIT like package
  - track finding package
  - cluster finding package
  - PAW-like package???

Continuation of Requirements 13

2115

SDC Core Task

Communications Services

May 22, 1992

Chris Day, Bernard Traversat
Glenn Kubena, Ken Liao

Contents

General Definition of Communications Services 1

Communications Services Architectural Concepts 3

Concrete Near Term Options 4

Capabilities Required of Communications Services 5

Appendix 7

General Definition of Communications Services

- Provides two way communications between components (e.g. toast) of the Core Architecture (toaster model)
- Supports distributed heterogeneous environment
- Client's view of communication service is via an application programming interface, supported by an interface definition language, which hides implementation details of the underlying communication services. (The communication service itself might be replaced transparently to the client's knowledge)
- Supports one (or more?) of the following communications mechanisms
  - Messages : Operations on messages include, for example, create, delete, update, send, receive, acknowledge, reply and ignore. There may also be registration and de-registration operations if a multicast delivery service is used. It is with this operation that a tool or service indicates what kind of messages it is or is not interested in (e.g. all messages referring to my objects).

  - OS Process Invocation (e.g. exec, fork, invoke and spawn)
  - Remote procedure calls

Communications Services Architectural Concepts

- Strategic (Long term; tends to be more abstract)
  - Common Object Request Broker Architecture (CORBA)
    - Object Request Broker (ORB) provides communication services
    - Client (e.g. toast) see Objects only through the perspective of a language mapping (interface definition language). Client has no knowledge of the implementation of the Object, where it is, or which ORB is used to access it.
    - Object implementation is the methods and data associated with the object. Various implementations include separate servers, libraries, a program per method, an encapsulated application, an object oriented data base, etc.
    - Objects must register with the ORB
    - An interface repository is used to keep the interface definitions

Concrete Near Term Options

- OSF DCE RPC
  - Like a normal call
  - Includes an IDL
  - Data translation across heterogeneous systems
  - Server location transparency (server registration with naming service, client binding service)
  - Concurrency via threads
- Workbench/Softbench BMS
  - Tool registers with BMS indicating which events it wants to be posted with
  - Client sends message to tool via BMS without knowledge of the tool's location or detailed function
  - Tools are encapsulated via C++ or EDL
- Other

Capabilities Required of Communications Services

- Communications Tools
  - Placement Mgmt. Tools
  - Interface Definition Tools
  - GUI Tool
  - Comm. Tool Output
- Communications System
  - Location independence and location brokering
  - Dynamic binding
  - Presentation services (i.e. data conversion, etc.)
  - Error handling/reporting
  - Security (peer-to-peer authentication and authorization)
  - Concurrency, both client and server
  - Asynchronous access if desired
  - Initiator/responder roles decoupled from client/server roles

- Communications APIs
  - Look like standard call
  - Easy to use IDL
  - Hide underlying service

Appendix

- Acronym List
  - BMS - Broadcast Message Services
  - CORBA - Common Object Request Broker
  - ORB - Object Request Broker
  - DCE - Distributed Computing Environment
  - EDL - Encapsulation Definition Language
  - IDL - Interface Definition Language
  - OSF - Open Software Foundation
  - RPC - Remote Procedure Call
  -
  -
  -
- Glossary
- References

IBM SDC Prototyping Plan

Currently Not Funded or Approved

May 22, 1992

IBM Team
Tony Elam, Bob Ennis
Glenn Kubena, Ken Liao
Larry Roberts, Dennis Stoker
Jim West

Point of Contact: Glenn Kubena
IBM Federal Sector Company
Houston, Texas
(713) 282-7635
KUBENA@HOUVMSCC.VNET.IBM.COM

Contents

IBM SDC Prototype Plan Genesis 1
Prototype Goals / Expected Benefits 2
Focus 3
Step 1 - Populate the Data Base 4
Step 2 - Set up the analysis environment 7
Step 3 - Use and evaluate 9
Future Options 11
Attachment on FORTRAN 90 12

IBM SDC Prototype Plan Genesis

This plan represents the results of a meeting on 5/7/92 between Chris Day, Andrea Palounek and IBMers Ken Liao, Larry Roberts, Bob Ennis and Glenn Kubena on the subject of IBM SDC prototyping activities. This plan includes Andrea's and Chris' recommendations on how joint SDC/IBM prototyping activities could help prove and evaluate concepts being developed under the Core, Data and Process task force activities.

This plan will be updated pending review comments from Andrea, Chris and other interested parties.

Please note that this activity is currently not funded or approved.

Prototype Goals / Expected Benefits

- Try out NIST toaster concepts and get real timely feedback on what works and does not work (Complement Core Detailed Design beginning FY 93)
- Get some hands-on experience with encapsulator tools, C++, OODBMS, GUI tools, ...
- Understand real feasibility/problems of encapsulating FORTRAN codes within the Core "toaster"
- Understand FORTRAN 90 pros/cons
- Understand real feasibility/problems of accessing data objects; begin to evaluate performance aspects of data object access
- Try out different data models and see what works
- Begin to prototype a really useful user interface
- Complement, not duplicate HPCCI prototype

Focus

- Goal is not to simulate the detector; rather focus on coming up with a good toaster
- Commercial hardware and software being used is not being pushed as the final or perfect solution –> Simply need to try out concepts and get some real feedback on pros/cons
- Depends heavily on physicists' participation in design, development and evaluation

Step 1 - Populate the Data Base

- Approach : Encapsulate physics event generator in a version of the toaster model. Capture event output and convert to object model instantiation and store on OODBMS for later retrieval and analysis. Use an Object Oriented analysis tool to design candidate data base schema and produce data dictionary

- Software Used
  - ISAJET Physics Event Generator
    - Rationale : Well understood; physicists have lots of experience with it; easily available; provides history of what happens after collision
  - Workbench (Encapsulator and Broadcast Message Services)
    - Rationale : Provides prototype of communications services and an encapsulator tool

  - C++ Compiler and optional C++ Development Environment (ProCASE or Centerline)
    - Rationale : Needed to develop the "bridge" code which reads ISAJET output files and writes to Objectivity OODBMS. Also, the "encapsulation" code for executing ISAJET under workbench can be written in C++.
      - Note : The "bridge" code identified above could be a prototype for a future data importation tool (e.g. from SDC SIM to OODBMS schema). This bridge code would also allow experimentation with different OODBMS data base schema.
  - Objectivity OODBMS
    - Rationale : Prototypes an object oriented physics data base using a commerical OODBMS. Has an online schema and data browser which can be evaluated.

- Paradigm Plus Schema Designer
  - Rationale : Prototypes an object oriented model(s) of the physics event data base using Rumbaugh notation and produces Objectivity Data Definition Language
- AIX Composer (User Interface Management Software), LPEXX editor
  - Rationale : Prototypes a GUI which edits ISAJET input files and executes ISAJET (e.g. generate a certain number of events from ISAJET). Gives hands on experience on ease of use or difficulity of use of encapsulated Physics code.
- Option to look at VISAJET which is an X-Windows based GUI for running ISAJET (Available from Fermi Lab, Paul LaBrun)

Step 2 - Set up the analysis environment

- Approach : Set up an environment where physicists can develop and execute analysis code which accesses the data base and produces graphical output. Set up a "point and click" user interface for analysis execution.
- Software Used
  - Workbench (Encapsulator and Broadcast Message Services)
    - Rationale : Provides prototype of communications services and an encapsulator tool
  - C++ Compiler and optional C++ Development Environment (ProCASE or Centerline), FORTRAN and FORTRAN LPEXX editor and/or FORTRAN 90 (see attachment)
    - Rationale : Fortran and/or C++ needed to develop the analysis code. A C++ bridge to Objectivity would be needed to access the data objects. The encapuslation code would be C++.

- Objectivity OODBMS
  - Rationale : Prototypes an object oriented physics data base using a commerical OODBMS. Physicists may also develop "user filters"
- AIX Composer (User Interface Management Software)
  - Rationale : Prototypes a GUI which executes point and click analysis, Can be used to customize GUI (widgets, ...)
- Hippoplotamus Histogramming Package (tbd) and/or some commercial statistical plotting package
  - Hippoplotamus conversion from Objective C to C++ under this prototyping activity would be beneficial since it would make it more portable to entire collaboration. (But, conversion effort may not be trivial)

Step 3 - Use and evaluate

- Approach : Provide copy at SSCL, in Houston lab and at "trail blazer" institutions (LBL?, Rice?, LANL?, Argonne?,Fermi?,KEK?..) for evaluation and feedback.
- Software Used
  - Workbench (Encapsulator and Broadcast Message Services) Or equivalent Softbench on HP
  - C++ Compiler and optional C++ Development Environment (ProCASE or Centerline), FORTRAN and FORTRAN LPEXX editor and/or FORTRAN 90
  - Objectivity OODBMS
  - Hippoplotamus Histogramming Package (tbd) and/or some commercial statistical plotting package
- Try to get special pricing or evaluation copies of commercial software

- Houston lab might concentrate on performance measurements and Physicists might concentrate more on User Interface and functionality (i.e. "Can I do my job this way"?)

Future Options

- Evaluate applicability, feasibility and performance impacts of schema evolution (changing the schema while maintaining backwards compatibility)
- Integrate prototype into IEEE Mass Store Reference model and evaluate scalability
- Prototype a truly distributed data base to address the concerns of data synchronization, data integrity, data duplication, ...

Attachment on FORTRAN 90

FORTRAN 90 Note: We learned the following through our IBM grapevine. FORTRAN 90 has been approved as an international standard by ISO but not yet in the US by ANSII (being worked by the X3J3 group). There are three FORTRAN 90 compilers available for the RS6000. These are really interpretors that produce C or FORTRAN 77 code. The three are NAG from England which produces C code, PARASOFT which produces FORTRAN 77 code and VAST (in beta test) from Pacific Sieria which produces FORTRAN 77 code. We will be receiving pricing and other details from our IBM expert in Toronto, Janice Shepherd. Janice also has a presentation on FORTRAN 90 capabilities which she is mailing. She is also available to make the presentation at the SSCL if requested and funded.

Data Modelling Package Task Force Requirements

Brian L. Scipioni
(SSCL)

Data Modelling Package Task Force Requirements

by

Chris Day, Bob Ennis, Irwin Gaines, Jean Huang, Ed May,
Ute Nixdorf, Larry Price, Forest Rouse, Brian Scipioni,
Yoshi Takaiwa, Saul Youssef

Audiences

- The developers of the Data Modelling Package
- The core-developer
- The user-developer
- The more general collaboration audience.

Requirements Catagories

- **Implementation Independent Requirements**
  What the tool must do regardless of how it is implemented
- **Global Constraints**
  Implementation specific requirements which are of global importance and are, therefore, not considered reviewable as design options
- **Desirables**
  These should be incorporated resource permitting.

Event-based Requirements

- **Analysis-time**

  Those data modelling activities which involve the logical definitions and associations among the data as is done in Entity Relationship modelling, for example.

- **Coding-time**

  Those data modelling activities which occur in direct support of, and during the time of, the physicist writing code.

- **Run-time**

  Those features of the data modelling package which execute while the physics application is running.

2.1 Implementation Independent Requirements

2.1.1 Analysis-time

2.1.1.1 User defined data types.
2.1.1.2 Plain data structures.
2.1.1.3 There should be user-defined lifetimes for types of data.
2.1.1.4 Certain classes should be built-in.
2.1.1.5 Event type and cross-event type are built-in types.
2.1.1.6 Data modelling operations on objects or collections of objects (classes).
2.1.1.7 Schema available to application at analysis-time
2.1.1.8 Edit or browse classes and dictionary interactively.
2.1.1.9 Schema evolution history/versioning accessible from repository.
2.1.1.10 Report generation capability for meta-data, e.g., schema, data dictionary from the browser.
2.1.1.11 Standard data modelling methodology.
2.1.1.12 The tool must support an object-oriented approach.
2.1.1.13 Cardinality between objects must be defined in relationships.

2.1.1.14 Error reporting during analysis.
2.1.1.15 Must have a Graphical User Interface (GUI) as well as text interface.
2.1.1.16 Same look and feel from the browser as from the rest of the tool. Must have the ability for multi-user presentations.
2.1.1.17 The modelling tool must have a generic levelling capability.
2.1.1.18 Direct manipulation of graphical objects.

2.1.2 Coding-time

2.1.2.1 Simple access to complex data types.
2.1.2.2 Must be able to refer to objects or types via relationships (pointers).
2.1.2.3 Access to data by name (not pointers) at coding-time.
2.1.2.4 Generate machine independent code for objects, templates, include files.
2.1.2.5 Package must include a make-like facility.
2.1.2.6 Accessible from 6 line FORTRAN program.
2.1.2.7 Full functionality from FORTRAN 90, C, and C++.
2.1.2.8 Error reporting during coding.

2.3 Desirables

2.3.1 Analysis-time

2.3.1.1 Reverse engineering capability for existing code.

2.3.1.2 Ability to import data model representations from existing C++ classes or Zebra banks, YBOS, flat files, etc.

2.3.1.3 Optimization tool for data model structuring.

2.3.2 Run-time

2.3.2.1 Migrate data from one DBMS to another.

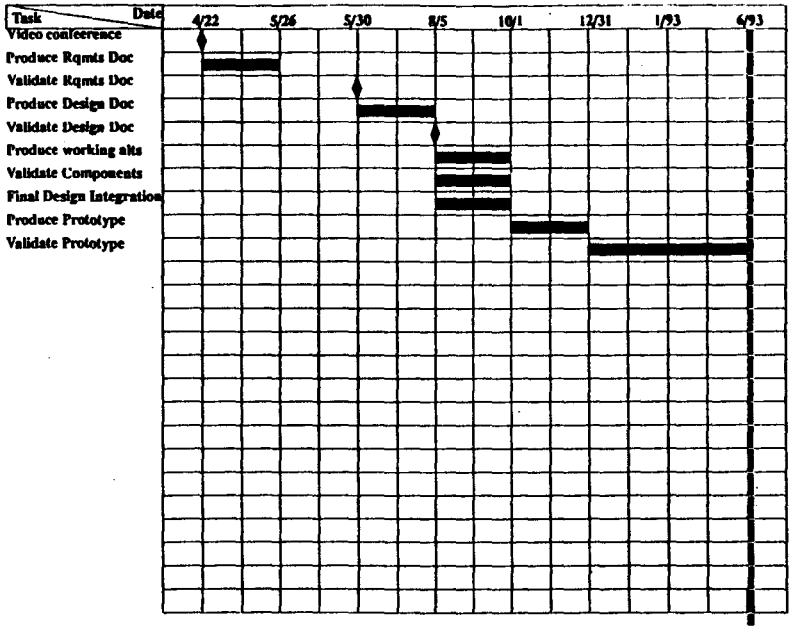

2.1.3 Run-time

2.1.3.1 Schema must be available to application at run time.

2.1.3.2 Error reporting during run-time.

2.1.3.3 Interactive data query language.

2.1.3.4 Report generation capability for physics data.

2.1.3.5 Interactive as well as programmatic interface to tool.

2.1.3.6 No significant performance penalty for using the tool, regardless of the amount of data.

2.1.3.7 The Data Repository should keep database of data access patterns to support future design and optimization efforts.

2.1.3.8 Data access method independent of media.

2.1.3.9 Data interface to OO-DBMS or R-DBMS.

2.1.3.10 Application and machine independent data structures.

2.2 Global Constraints

2.2.1 Inexpensive for individual users to acquire commercial components.

2.2.2 Machine independent tool.

2.2.3 UNIX based.

2.2.4 Tool must be compatible with the architecture of the Core Software Development task force.

Status of Software Development Task Force

Andrew P. White
(University of Texas at Arlington)

SDC Software Process Document Outline Draft

Version 4

May 22, 1992

Larry W. Roberts

IBM Federal Systems Company
3700 Bay Area Boulevard
Houston, Texas 77058

IBM

Assumptions

1. This document addresses processes for development and control of **software** specific to SDC Offline Computing. However, commonality and possible use to meet SDC Online Computing needs are not precluded.
2. The software processes described here depend on the existence of a SDC offline "global" system and network facilities (i.e., a SDC offline "global" system will be architected and implemented, in addition to the dispersed, heterogeneous environments of SDC users, within which the software processes will fit).
3. The software processes will be established so that automated support can be utilized to the maximum extent practical.

Definitions NEW!

SDC Offline Global System
SDC offline hardware, software and services architected and provided to meet the needs of the SDC Collaboration as a whole.

SDC Offline Global Software
Software comprising part of the SDC Offline Global System developed (or acquired), *integrated and maintained* by a SDC Central Group. Included are the following classes of software (as described in this document):

NEW

- "Core" services
- "Core" software, including graphical user interface
- Data management software
- SDC Physics Application Developer's Toolkit

NOTE DEF^N.

Common Physics Software
Software developed by physicists outside the SDC Central Group which undergoes a technical "certification" process to be incorporated into the SDC baseline. Included are the following classes of software (as described in this document):

- "Core" common tools/utilities
- Common physics applications/tools
- Production reconstruction
- Level 3 trigger

Contents

Classes of SDC Software 1

Organization 12

Global Software Development Process 14

Common Physics Software Certification 21

Common Tools / Utilities Process 24

Common Physics Applications Process 25

Production Reconstruction Process 26

Level 3 Trigger Process 27

User Application Software Process 28

Systems Administration 29

Schedule 30

Classes of SDC Software

1. * Core Services (~~Irwin's System Services Class~~) * NEW NAME
   - Components
     a. Operating system (ASSUMED PROVIDED)
     b. System management services
     c. Network operating system/management
     d. Code management
     e. Metrics collector
   - Mostly commercial
   - Integration/maintenance by small SDC central group - rigorously controlled

2. Core Software
   a. Communication Services
      - Components
        1) Distributed message service
        2) Distributed remote procedure call
        3) Communications application program interface (API)
      - Commercial plus newly developed
      - Development/Integration/maintenance by small SDC central group - rigorously controlled
   b. Module Control (~~Part of Irwin's Physics Analysis Framework Class~~)
      - Components
        1) Process definition
        2) Process enactment
        3) Module execution shell
      - Commercial and/or newly developed
      - Development/integration/maintenance by small SDC central group - rigorously controlled

   c. Common Tools / ~~Utilities (Irwin's Utilities Class)~~
      - Components
        1) Plotting package(s)
        2) Event display package
        3) Electron identification package, etc. (10 - 15 packages)
      - New (plus reuse) development
      - Each package externally developed by small, dispersed groups
      - "Certification" process to incorporate
      - Integration by small SDC central group - controlled
      - Maintenance by combined small SDC central group plus developer groups - controlled

d. Graphical User Interface (~~Part of Irwin's Physics~~ Analysis Framework Class)

- Components
  1) UI builder
  2) Presentation service
  3) GUI application program interface (API)
- Commercial plus newly developed
- Development/integration/maintenance by small SDC central group - rigorously controlled

3. Data Management Software
   - Components
     a. Data modeling
        1) Graphical user interface
        2) Data base schema definition output
     b. Data repository
        1) Data base schema definitions
        2) File/object catalog
        3) Efficient data query/extraction
        4) Schema evolution
     c. Data repository API
        1) Complex data structure support
        2) FORTRAN and C(++) support
   - Commercial plus newly developed
   - Development/integration/maintenance by small SDC central group - rigorously controlled

4. SDC Physics Application Developer's Toolkit
   - Components
     a. Editor(s), compiler(s), debugger(s)
     b. Process enactment / code management clients (option)
     c. User's and Style Guides
     d. Data access, etc., standards
     e. Checklist(s)
   - Commercial plus HEP community "standard" tools
   - Development/integration/maintenance by small SDC central group - rigorously controlled

5. Production Reconstruction (Irwin~~'s Production Reconstruction Class)~~
   - New (plus reuse) development
     - Use SDC Application Developer's Toolkit
   - Combination of pieces developed separately, external to SDC central group
   - Integrated and robustness verified by (external) technical "czar"
   - "Certification" process to incorporate
   - "Formal" (version, baseline, change) control
   - Low change frequency

6. Level 3 Trigger (~~Irwin's Level 3 Class)~~
   - New (plus reuse) development
     - Use SDC Application Developer's Toolkit
   - Combination of pieces developed separately, external to SDC central group
   - "Certification" process to incorporate
   - Relatively high change frequency
   - Flexible control
     - "SWAT team" change / maintenance
     - Audit trail

7. Common Physics Applications (~~Part of Irwin's Utilities Class?~~)
   - Components
     - Widely used physics applications, routines (HEPlib, etc.)
     - Common and widely used tools
   - Externally developed and used
   - Being made available "as is" in applications repository
   - "Certification" process to incorporate

8. User Applications (~~Irwin's User Modules Class~~)
   - Components
     - Custom written applications by physicists using SDC Application Developer's Toolkit (e.g., standard data access, etc.)
     - Custom written applications by physicists (roll your own)
   - User (organization) controls software development, baseline, maintenance
   - SDC global system needs to ensure user applications cannot "damage" data base, module control framework

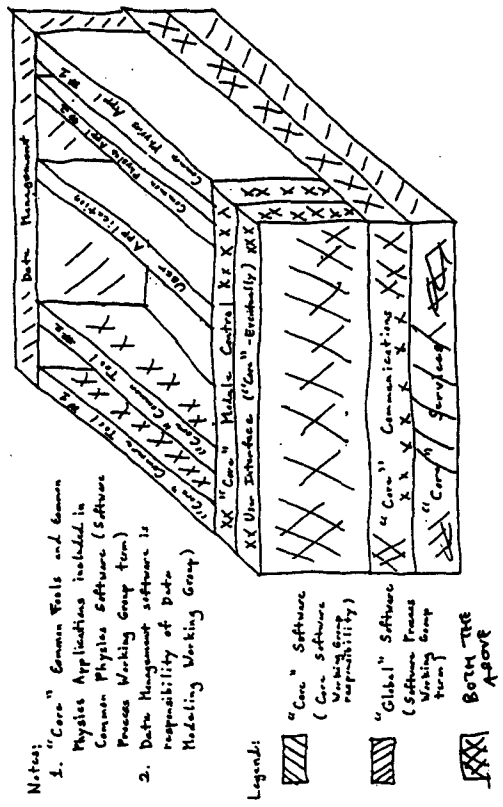

Toaster Model of SDC Offline Software for Physics Analysis

Organization

1. Process Owner - SDC Computing Group
   - Working Owner - SDC Central Group
2. Responsibilities
   a. Developing "global" (core, data management, toolkit) software
   b. Performing systems administration of global system
   c. Certifying common physics software
      - "Core" common tools/utilities
      - Level 3 trigger
      - Production reconstruction
      - Common physics applications/tools
   d. Providing SDC Application Developer's Toolkit (standard data access, etc.)
   e. Managing applications repository
   f. Making global / Level 3 / production reconstruction build deliveries/installations

   g. Performing maintenance
      - Maintaining "global" software
      - Negotiating maintenance arrangements on common physics software
      - Coordinating Level 3 "SWAT team"
   h. Managing global and common physics software baselines (configuration/code management)
3. Lines of Authority (to SDC Collaboration)
4. Management Controls
   a. Software Review Board (SRB)
      - Approves/disapproves changes to baselines
   b. Certification Board (same as SRB?)
      - Certifies changes/additions to common physics software meet certification requirements
      - Audits Level 3 "SWAT team" changes
   c. Products
   d. Support tools/systems

Global Software Development Process

- Applies to global software, except "core" common tools/utilities
- Formal, rigorous process, yet flexible enough to meet changing needs and make improvements
- Iterative waterfall or spiral lifecycle
- Take advantage of latest software technology
- Utilized by SDC Central Group

- Initial development
  - Phases
    - Planning
      - Establish risks/dependencies
      - Develop schedule
      - Produce development plan
    - Requirements (analysis)
      - Rapid prototyping of GUI
    - Design
      - Make or buy (acquire)
    - Code
      - New software
      - Software modifications
    - Integration
    - Verification/Test
    - Build Delivery/Installation
      - Includes SDC Application Developer's Toolkit (first deliverable)

- Inspections (within development team)

Type	When
Requirements / Design	During requirements and design phases
Code	During coding phase
Test case	Prior to verification / test phase

- Reviews (SDC Computing Group -> SDC Collaboration)

Type	When
Requirements / Design	End of design phase
System Verification Complete (Acceptance)	End of verification / test phase

- Configuration Management (under SRB)
  - Manage source, etc., libraries (library management)
  - Establish baselines (configuration identification)
    - Source/object/builds
    - Test cases
    - Documentation

- Maintenance
  - Problem report handling (see following scenario)
  - Change request (CR) handling (see following scenario)
  - Configuration Management (under SRB)
    - Control baselines (configuration control)
      - Assess/disposition problem reports
      - Assess/disposition change requests
      - Schedule fixes/changes
    - Manage source, etc., libraries (library management)

- Problem Report Scenario
  1. User or help desk submits problem report describing problem encountered and circumstances
  2. Software Review Board or designated authority prioritizes problem report and assigns maintainer to investigate
  3. Maintainer provides workaround if applicable
  4. Software Review Board dispositions problem report based on results of investigation
     - If fix not necessary, problem report is returned to submitter with explanation (possible documentation update)
     - If fix necessary, it is scheduled for incorporation
  5. Fix is developed, verified and released
     - Includes updated documentation
  6. Problem report is closed

- Change Request Scenario
  1. User/developer submits Change Request (CR) describing desired change
  2. Software Review Board assigns maintainer to assess CR based on:
     - Resource impact to incorporate change
     - User community impact
  3. Software Review Board dispositions/prioritizes CR
     - If rejected, CR is returned to user/developer with rationale
     - If approved, CR is scheduled for incorporation
  4. Change is developed, verified and released
     - May be packaged with other CRs into a new "version" or "release"
     - Includes updated documentation
  5. CR is closed

- Rationale for formal global software process
  - Importance of software to entire SDC
  - Multiple developers
  - Early detection of errors and resulting savings
  - Easier maintenance
  - Can be partially automated

Common Physics Software Certification

- Assumptions
  - Common physics software developed outside formal process of SDC Central Group
    - "Core" common tools/utilities
    - Common physics applications/tools
    - Production reconstruction
    - Level 3 trigger
  - Software undergoes technical "certification" process to be incorporated into SDC baseline

- Certification - software meets requirements / standards for:
  - "Robustness" for use by SDC
    - "Regression" tests run and analyzed by: (1) SDC Central Group, or (2) developer / submitter and reviewed by SDC Central Group
  - Documentation
    - Requirements/design specification
    - User's guide
  - Maintenance arrangement
- Maintenance
  - If conducted in accordance with maintenance arrangement, no recertification
  - Upgrades developed externally processed as new Change Requests (CRs) requiring recertification

- Certification Scenario
  1. Developer/submitter submits Change Request (CR) to incorporate application into SDC Common Physics Software baseline.
  2. SDC Certification Board assesses/prioritizes CR.
  3. Developer/submitter furnishes documentation, evidence that application meets certification requirements, and negotiated maintenance arrangement
  4. Certification Board "certifies" application, recommends disposition of CR to Software Review Board
  5. Software Review Board dispositions CR
  6. If approved, application is incorporated into SDC baseline / applications repository
     - Application is cataloged and made available for SDC use

Common Tools / Utilities Process

- Certification / integration / build process
- Certification
  - Less stringent standards than those for production reconstruction and Level 3 trigger - but more than those for common physics applications need style guide
  - Testing burden on developer/submitter
- Integration by SDC Central Group with developer/submitter support
  - Integrate into module control framework
- Build/release of upgraded module control framework to SDC users by SDC Central Group

Common Physics Applications Process

- Certification and integration process
- Certification
  - Less stringent standards than those for production reconstruction, Level 3 trigger, and "core" standard application packages/utilities
  - Testing burden on developer/submitter
- Integration by SDC Central Group with developer/submitter support if available
  - Catalog common physics applications in repository and make available for use

Production Reconstruction Process

- Certification / integration / build process
- Rigorous process
  - Certification
  - Testing
  - Change control / maintenance
- Certification
  - Stringent standards
  - Testing burden shared between SDC Central Group and developer/submitter
- Integration / build by SDC Central Group
  - Pre-defined test suite

Level 3 Trigger Process

- Initial certification / integration / build process - rigorous
- "SWAT team" approach to change / maintenance
  - Expedited process
    - Decisions made out-of-board, etc.
  - Scope size, complexity of changes/fixes
  - Leave audit trail
  - Based on advanced preparation
- SWAT team advanced preparation
  - Collaboration experts in respective areas identified, on-call
  - Good documentation
  - Analysis tools
  - Test suite
- SWAT team staffed by SDC Central Group and collaboration experts

User Application Software Process

- Assumptions
  - User applications developed external to SDC formal (core) process
  - User applications developed outside scope of SDC certification process
  - Development, test, maintenance, configuration (code) control and documentation is solely responsibility of user (organization)
  - Safeguards against "damage" to SDC data base, module control framework built into data base manager, network management, etc.
- For user applications planning to use SDC application toolkit:
  1. SDC Central Group provides SDC Application Developer's Toolkit to user
  2. SDC Central Group provides problem support on toolkit
- If it is desired to add user application to SDC common physics software baseline:
  - User application must undergo certification process

Systems Administration

- Integrating global software components
- Building and installing global software (central and regional centers)
- Cataloging and library management of common physics applications
- Systems management
- Network management
- System tuning for performance
- Global software maintenance
- Negotiating and overseeing maintenance arrangements for common physics software
- User problem support
  - Informal
    - Help desk
  - Formal
    - Incoming problem report tracking

Schedule

- List of schedule dependencies (or portray on schedule)
- High level schedule

Larry Roberts, IBM
4/10/92

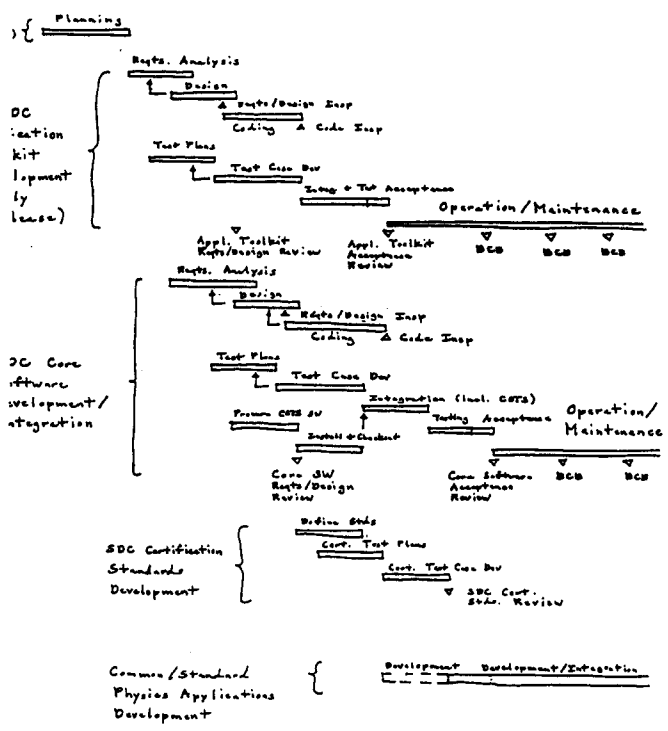

NOT DRAWN TO SCALE

May 26, 1992
Y. Morita
KEK Computing Center

JSD Farm:
Distributed Computing Facility at KEK

Youhei Morita
(KEK)

JSD Farm:

Distributed Computing Facility at KEK

Introduction

Distributed computing using shell-script

Efficiencies

Introduction

JSD Farm:

- **Cheap and quick solution for local MC computing needs**

  System Management ~ 0.3 FTE
  Library Management ~ 0.2 FTE x 3
  (SDCSHELL, CERNLIB, Pythia...)

- **DECstation 5000/125 x 12**

sdux0	File Server
sdfm0-1	Login Platform
sdfm2-s	CPU Farm

Distributed Computing using Shell-script

User-friendly mechanism for job submission and control

```
% submit <ctl-file> <nodename>
% rps [ -a ] <nodename>
% jobmon <nodename>
% chprio <nodename> <priority>
% rkill <nodename>
```

"Job Parallelism"
-> cheap solution to CPU-bound MC jobs

Application-dependent script
(SDCSHELL, Pythia, ...)

No totalitarian job control
-> control and responsibility on user-side

Helps users to learn UNIX features

- **Homogeneous System Configuration**

  NIS for integrated User ID
  /etc/hosts.equiv for rlogin / rsh
  NFS for common file system
  /jsdsys
  /jsdhome/<user>
  /data1/<user>
  /data2/<user>
  /scratch/<user>
  /keklib/cern
  /sdcshell
  .....

- **'Trusted' System**

  System is used by JSD members only
  -> no dedicated resource management

  No dynamic load balancing
  (considering NQS/Exec though)

  No access restrictions to each CPU

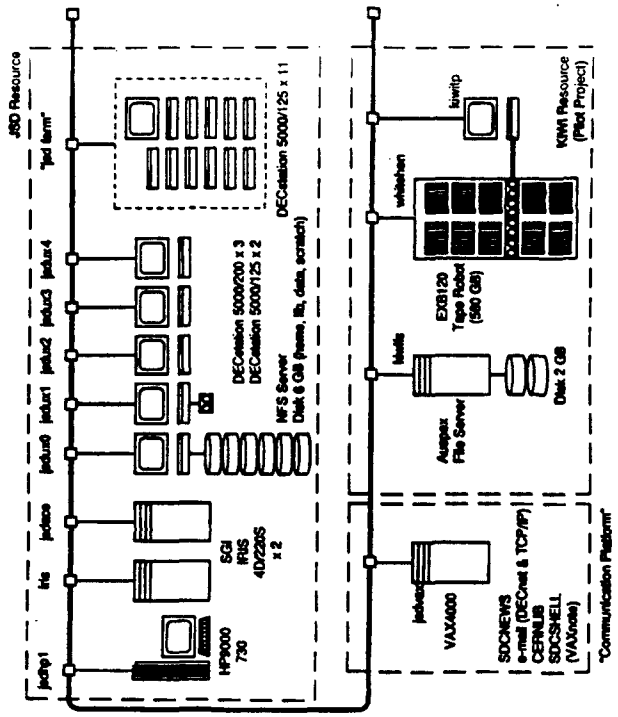

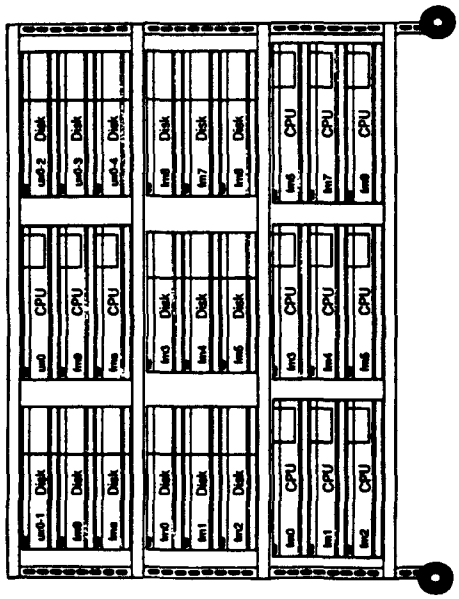

Efficiencies

MC programs: Standalone Pythia
SDCSIM / SDCSHELL

Case 1: Write MC output data to NFS server
Case 2: Write MC output data to local disk

For the case of NFS server, efficiency of "Job Parallelism" largely depends on the rate of job output and CPU time.

Job output rate / CPU < 10 KB/sec

For the case of local disk, efficiency is much higher. (But hard to optimize the usage of scattered disk resource.)

Effective distributed MC computing is to take a balance between two trade-off's:

- **Performance bottleneck on NFS server**
- **Utilization of scattered local resource**

-> User education covers the shortage of the system management manpower!

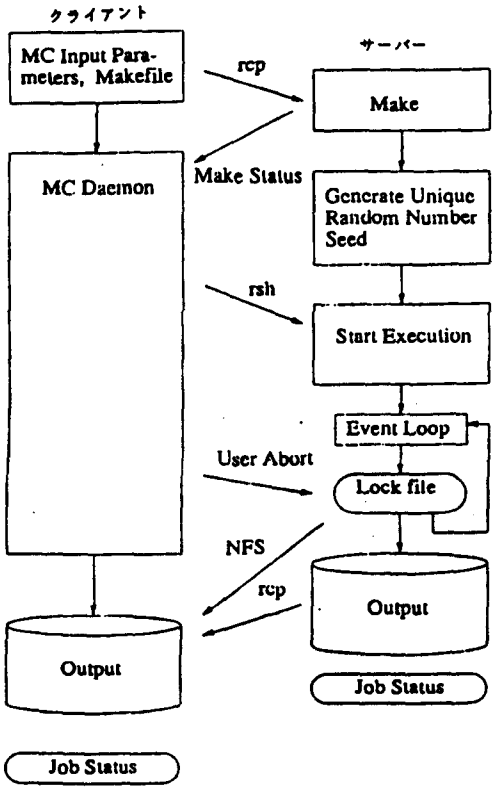
クライアント
サーバー
MC Input Parameters, Makefile
rcp
Make
Make Status
MC Daemon
Generate Unique Random Number Seed
rsh
Start Execution
Event Loop
User Abort
Lock file
NFS
rcp
Output
Output
Job Status
Job Status

図2

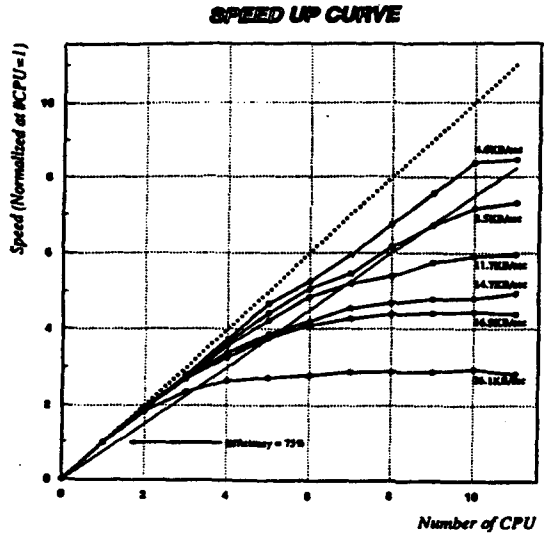
SPEED UP CURVE
Speed (Normalized at #CPU=1)
Number of CPU

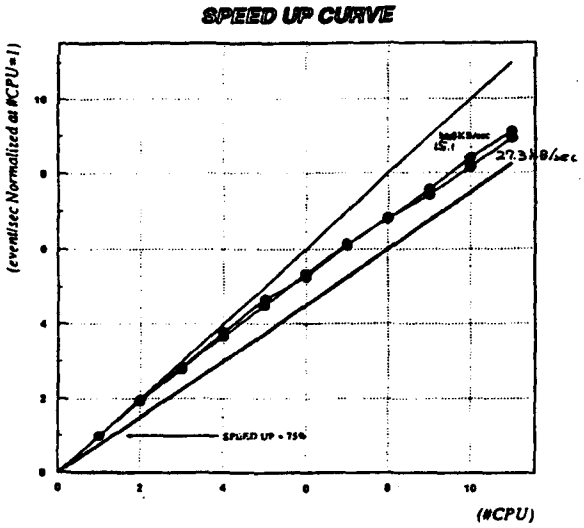
SPEED UP CURVE
(eventlsec Normalized at #CPU=1)
(#CPU)

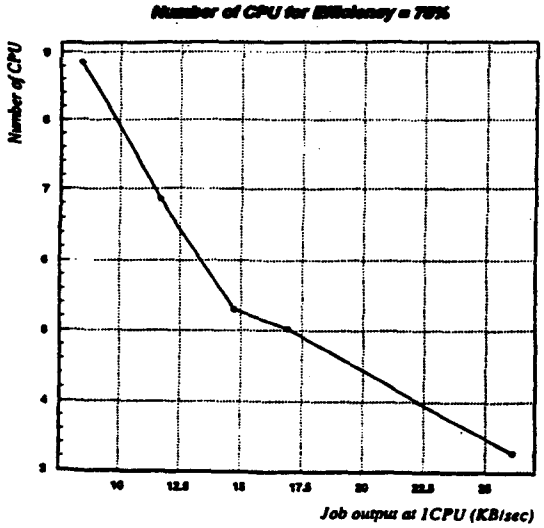
Number of CPU for Efficiency = 75%
Number of CPU
Job output at 1CPU (KBlsec)

KEK SDC (26th May 1992)

Distributed computing system at Tokyo Metropolitan University

S.Kitamura

Tokyo Metropolitan University

1. Network and Computers
2. Activity of DEC5000's

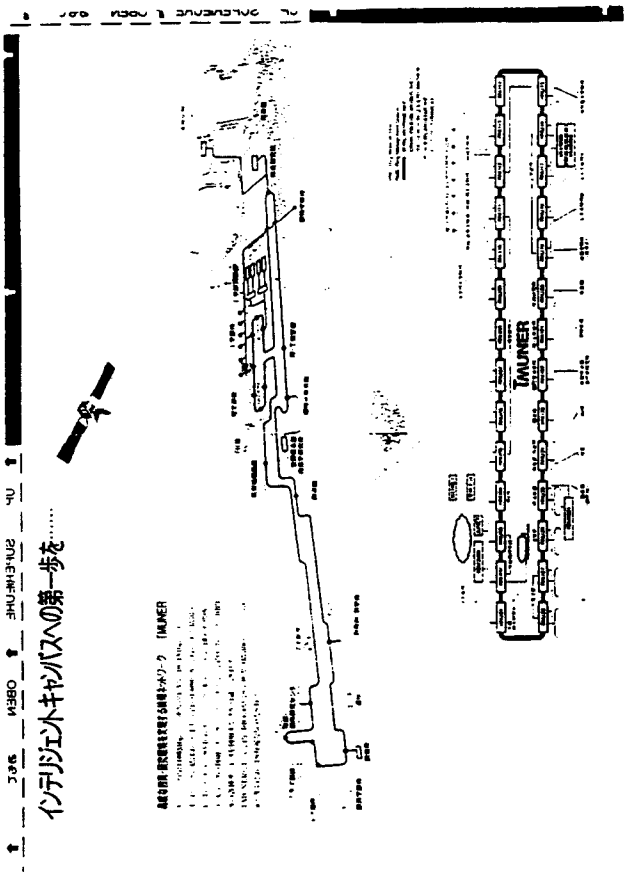

Block diagram of the network

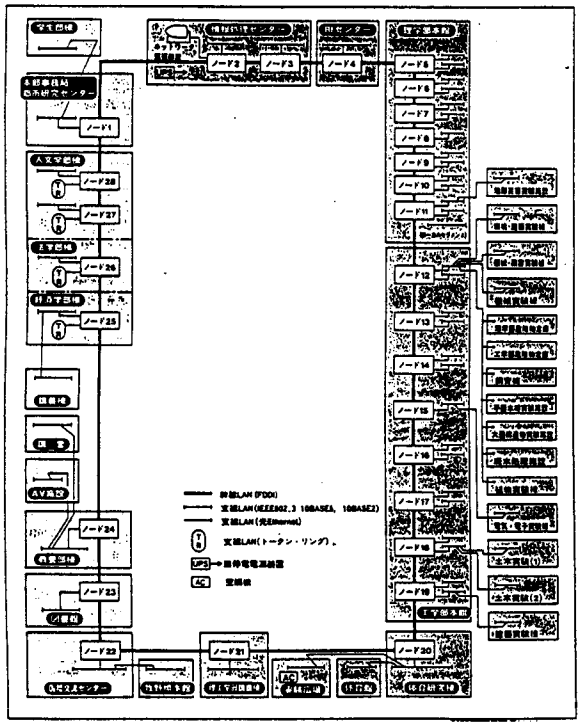

From FDDI backbone to each office

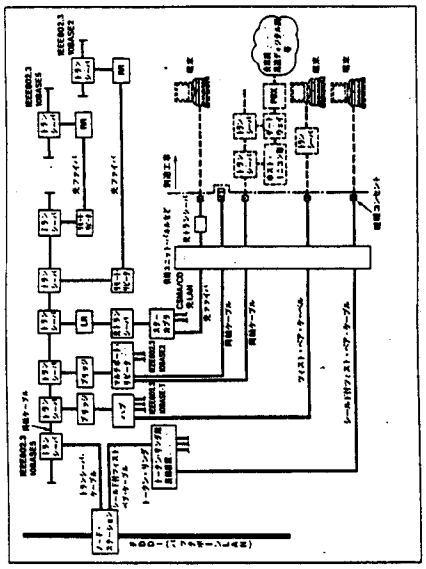

2234

Summary of network and computers

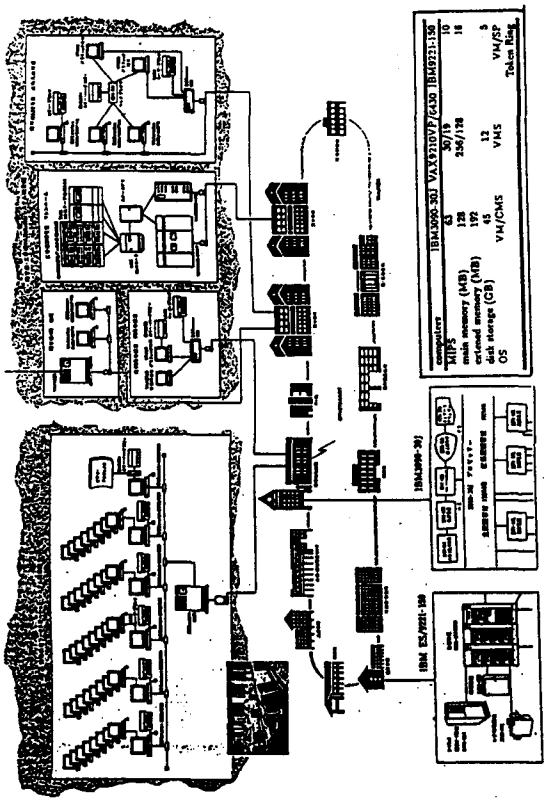

2235

2236 7

Distributed DEC5000 workstations

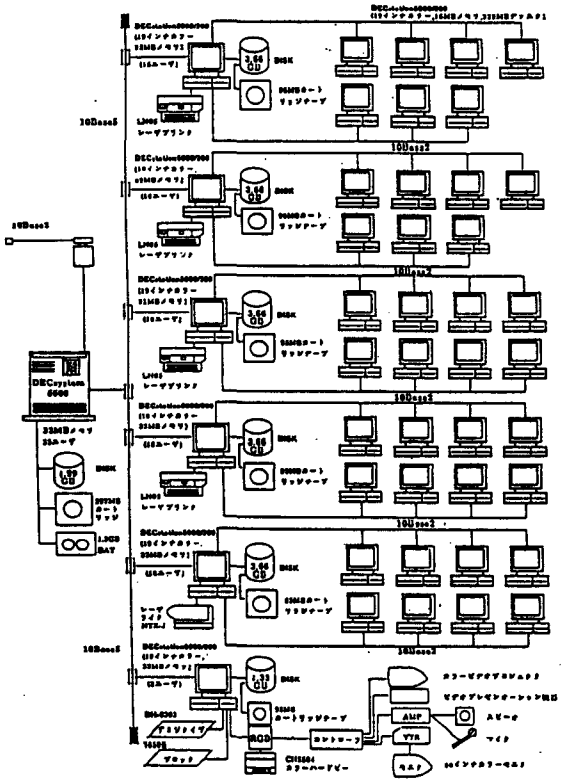

2237 8

Data transfer

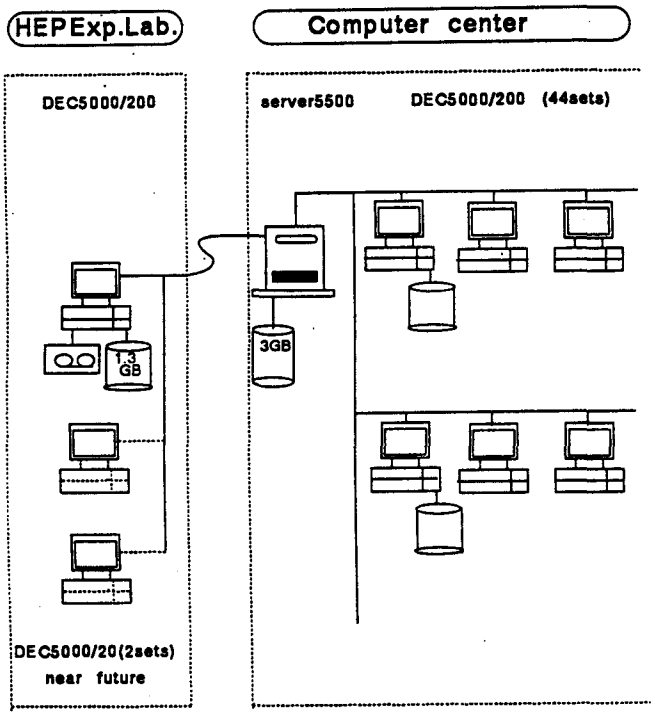

2238 9

Simple job to run in parallel

Hit-lost Monte Carlo method to evaluate a volume of sphere.

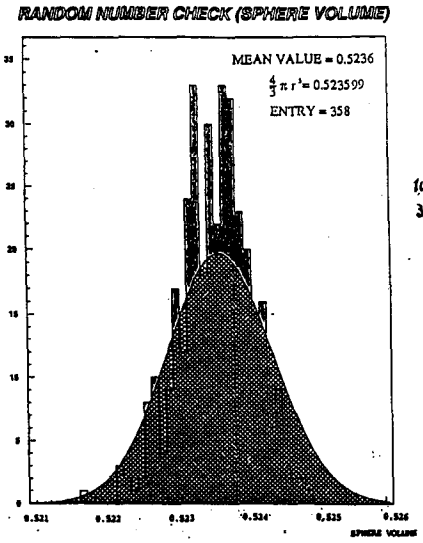

1,000,000 points
358 times
rsh command

2239 10

How they work in parallel

(submitted at night)

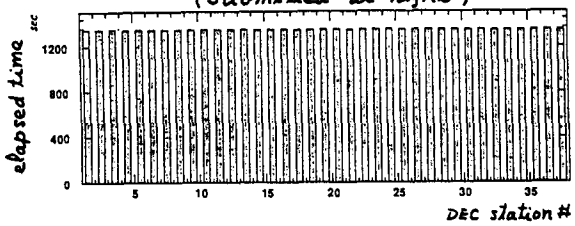

(submitted in daytime)

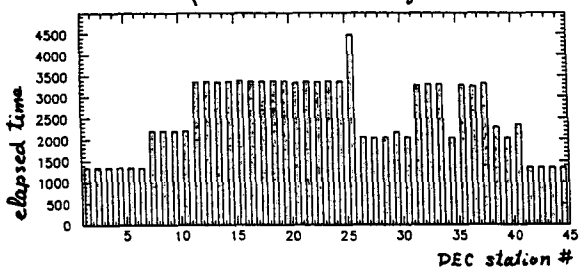

2210 11

Volumes of n-dimensional sphere

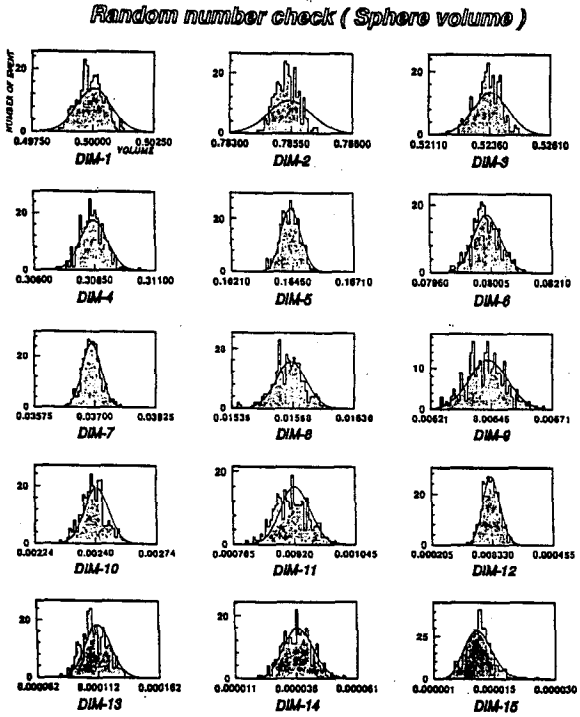

2211 12

Simulation using PYTHIA

Higgs particle production at SSC energy

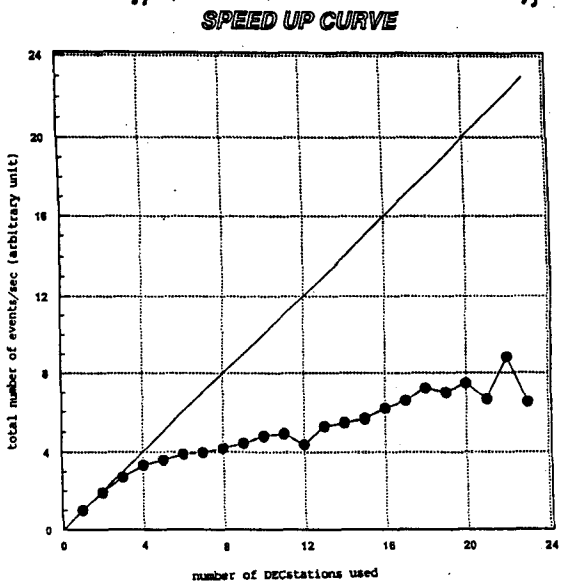

(~1.2 sec/event
~25 kB/event)

Client-server model for simulation

Y. Morita (SDC-91-0033)

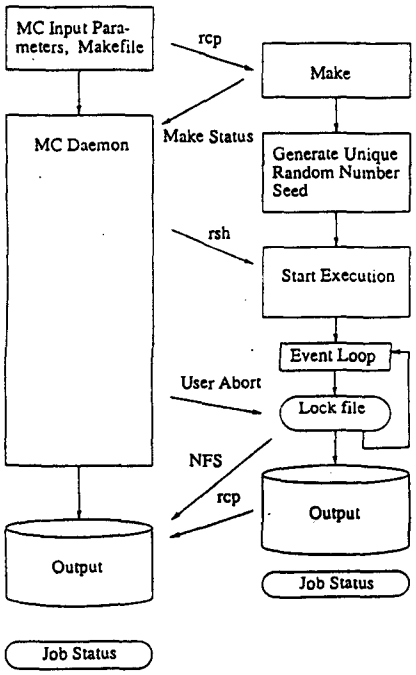

Example: Simulation of ZEUS detector (HERA, DESY)

10,000 events/night using 20 workstations.

70 sec/event, 70 KB/event ⇒ 1 KB/sec

In this case, we found that the network traffic problem is negligibly small.

SPEED UP CURVE

S. Funaki et al

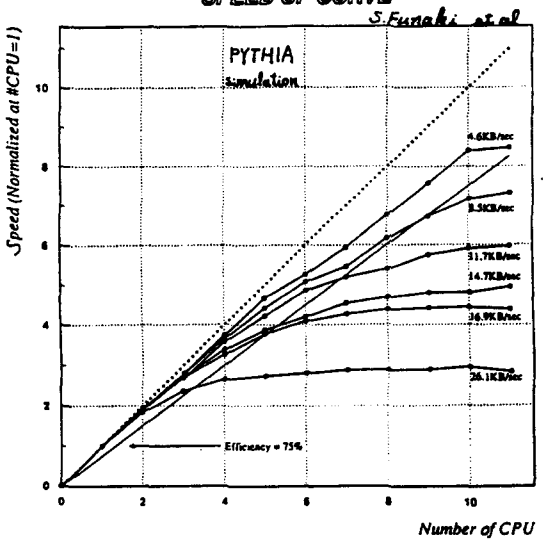

Summary

1. We have utilized a set of 44 DEC5000 workstations for Monte Carlo simulations running jobs in parallel.

2. In case of CPU intensive jobs, their performance was highly efficient in total. In case of I/O required jobs for one of the disk strages, limitations due to network traffic lowered their performance.

3. We are now producing simulated events of the HERA-ZEUS detector with high efficiency.

4. The straw chamber group intends to simulate events using these workstations for trigger study.

5. The latest version of SDCSHELL has been installed.

Harnessing Modern Virtual-Memory Systems for Distributed Computing of SSC

Hajime YOSHIDA
Naruto University of Education

SDC Collaboration Meeting
May 26 – 29, 1992
KEK

1 Scope of the Talk

Distributed Operating System for SSC programming.

1. Distributed Monte Carlo event generation
2. Distributed event analysis
3. Requirements
4. Why not UNIX?
5. Mapped files
6. Why Mach?
7. Model revisited.
8. Conclusion

2 Models of Distributed Computing for SSC

2.1 Distributed Monte Carlo Event Generation

Morita et al. : Pythia and SDCSHELL

2.1.1 Nature of Computing

- M.C. data are generated by the independent hosts and written in a NFS file.
- No data sharing is required.
- Little communication among processes running on independent computers.
- Bottleneck is writing data with NFS.
- RAID can improve **local** I/O capability.

Distributed Monte Carlo Generation

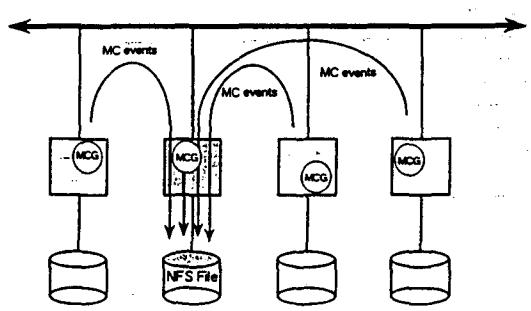

Distributed Event Analysis and Display

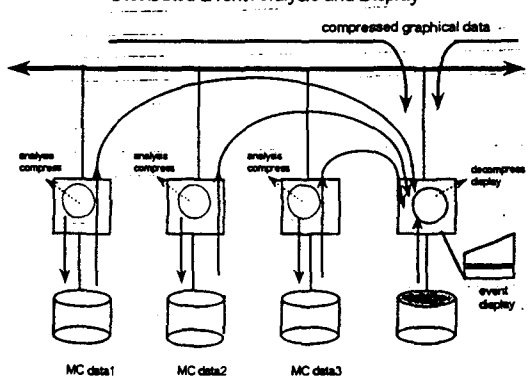

2.1.2 Performance Consideration

With extremely simplified model

- saturation of NFS network I/O capability,
- parallel computation
- sequential NFS write operation

the speed-up factor α with n hosts is written as;

$$\alpha = \frac{n(1+x)}{1+nx}$$

, where $x = \frac{NFSwritetime}{CPUtime}$.

In case of Pythia event generation,
NFS write speed $\sim$ 80 KB/s. (With NFS accelerator currently available, $\sim$ 400 KB/s is attained.)

Conclusion:

Assuming a 100,000 × VAX system, which may be composed of $\sim$ 1000 RISC workstations connected via fast LANs,

- Faster Network; FDDI(10 × Ethernet) and more,
- Better implementation of standard protocol suite. (For example, TCP/IP running on 10 MIPS CPU can handle upto 500 MBS.)
- Since CPU speed will be $\sim$ ×10 improved, the factor x will remain unchanged.
- Need of machine-level distribution of a file.

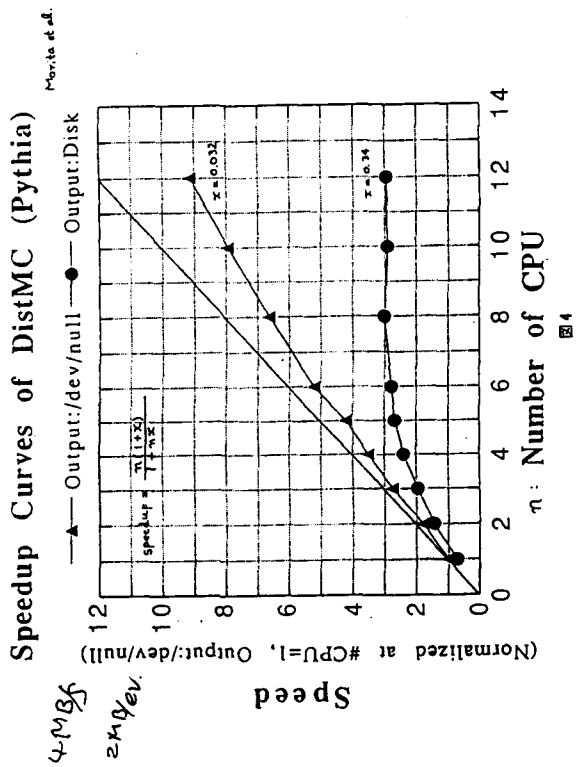

図4

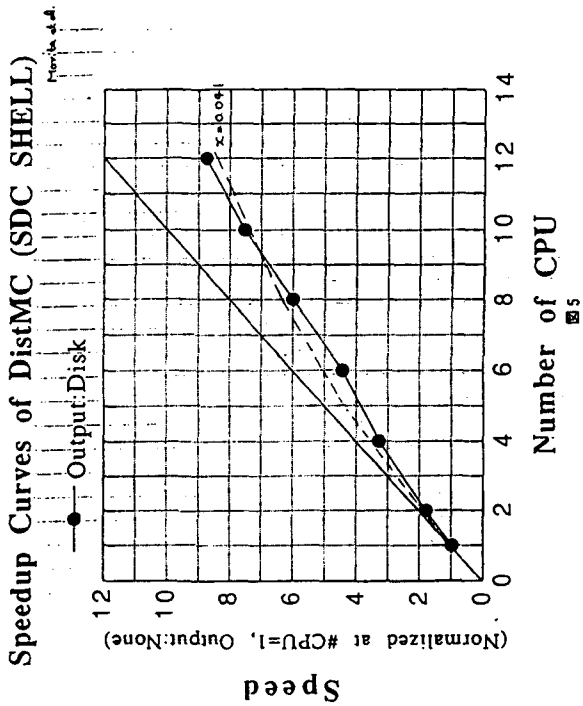

図5

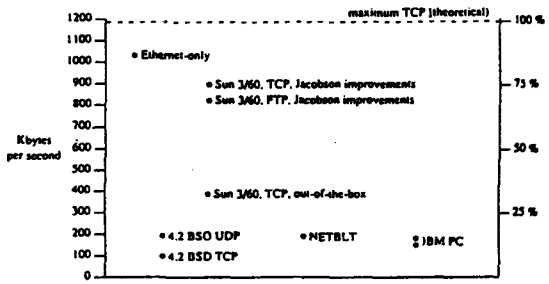

Figure 17.7 Network performance on a 10 Mbit/sec Ethernet.

What do we learn from all these numbers? First, network performance differs greatly from one implementation to the next. Also, as shown by Jacobson's results, it is possible to obtain network throughput within 75% of the theoretical maximum, for an Ethernet using current hardware. Chesson [1987] provides insight about some potential problems when the raw network speed increases the next order of magnitude, from the 10 megabit/sec Ethernet to the 100 megabit/sec FDDI.

Another set of interesting numbers is from Borman [1989]. Using two Cray computers and HYPERchannel interfaces he obtained TCP transfer rates of 1500 Kbytes/sec. This value is just above the top of the graph in Figure 17.7. But, his measurements between two Cray computers connected with an HSX high-speed channel show a TCP transfer rate of 23,750 Kbytes/sec. This value is 20 times the maximum theoretical value shown in Figure 17.7.

Clark et al. [1989] perform a detailed analysis of TCP and IP. Their analysis was to determine the amount of overhead imposed by the transport protocol—TCP, which requires IP. To do this they took the existing BSD implementation of TCP, optimized the source code and determined the number of machine instructions required to send and receive packets. They then determined that for a 10 MIPS processor and a packet size of 4000 bytes the throughput could be 530 Mbits/sec. Since the next generation of LANs will operate around 100 Mbits/sec, they claim it is not necessary to redesign the transport protocols to handle these higher speeds, it is just necessary to implement them properly. Additionally, their analysis of an existing system, the BSD TCP on a Sun 3/60, shows that the normal overhead imposed by the operating system and the overhead involved in moving the data between the user process and TCP, exceeds the overhead imposed by the transport protocol.

Stevens Unix Network Programming

2.2 Distributed Event Analysis

1. Read an event. Efficient file I/O is required.
2. Share the data of the event among collaborating processes.
3. Processes treat data, communicationg and synchronizing themselves.
4. File or record locking mechanism is required.
5. Store the value-added results in the secondary memory.
6. Display the event.

Compared with distributed M. C. generation,

- mean raw data size is almost same,
- mean analysis time is much smaller that that of event generation, and
- display information is additional.

So, network bottleneck will be more serious.

2.3 Distribution of Data and Processes

Schemes of distribution:

- Data are stored in the secondary memories; HDD/MT etc..
- Data of an event may be distributed among network-wide secondary memories;
  - on event-by-event basis
  - on Sub-Detector basis
  - other formats?
- Multiple processes collaborate to treat data.
  - A process handles a whole event.
  - A process handles a sub-detector data,
  - Other formats?
- Processes vs processors;
  - Processes are running on a single computer, (mono-processor or tightly-coupled multiprocessor)
  - Processes are running on distributed computers on network(s). (loosely-coupled computers)

Similarity to distributed transactions ⇒ need of new system of data and memory management.

2.4 Requirements

- Need of machine-scalable file system ⇒ System-side ToDo. f.e. NAS2,3, IEEE, ...
  - Bottleneck of NFS-like file system is prohibitive.
  - Maintaining logically single file which is distributed on a network, or network-wide disk striping.
- Efficient file I/O (including disk I/O and Network) which minimize *open-seek-read/write-close* operations, to avoid moving/copying data as far as possible. ⇒ System-side, modern virtual-memory system, mapped files.
- Sharing data among independent processes without copying original data. ⇒ System-side, VM
- Efficient facility for Inter/Remote Process Communication. ⇒ System-side, Message-based IPC and VM.
- Needs of data compression for event display. ⇒ User-side.
  - Raw data should not be transferred to the user event display. (Not a bitmap image of a face but a wink)
  - Compress the data locally and move compressed data across the network.

3 Why not UNIX, can it be our platform for coming 20 years?

An extract from *The Design and Implementation of 4.3BSD UNIX* by Leffler et al. (designers and implementers);

..... *"4.3BSD is not perfect. In particular, the virtual-memory system needs to be completely replaced. The new virtual-memory system needs to provide algorithms that are better suited to the large memories and slow disks currently available, and needs to be less VAX architecture independent."* .....

.... *A requirement for 4.2BSD was that it support large sparce address space, mapped files and shared memory. An interface was specified, called mmap(),* ..... *Ultimately, 4.2BSD was shipped without the mmap() interface because of the pressures to make other features, such as networking available.*

Further development of the mmap() interface continued during the work on 4.3BSD. Over 40 companies and research groups participated ..... *Several of the companies have implemented the revised interface.*

Once again, time pressures prevented 4.3BSD from providing an implementation of the interface. Although the latter could have been built into the existing 4.3BSD virtual memory system, the developers decided not to do so because that implementation was nearly 10 years old. Furthermore, the original virtual memory design was based on the assumption that computer memories were small and expensive, whereas disks were locally connected, fast, large and inexpensive. Thus, the virtual memory system was designed to be frugal with its use of memory at the expense of generating extra disk traffic. ....

Attempting to improve the old implementation incrementally seemed doomed to failure. A completely new design, on the other hand, could take advantage of large memories, conserve disk transfers, and have the potential to run on multiprocessors. At the time of 4.3BSD release, few of the implementations of virtual memory had been completed. ..... *The hope is that the correct choices will become clear, and that a new virtual memory system can be crafted for the next Berkekey UNIX system from the work of the new implementation.* .....

4 Mapped Files

After more than 10 years since its conception, mapped file is a part of the functions of modern virtual-memory systems, and is currently realized on many UNIX systems.

4.1 Why Mapped File?

Again, after S. J. Leffler et al.

The biggest incentive for memory mapping is the need for

- *accessing big files and for*
- *passing large quantities of data between processes.*

The `mmap()` *interface will provide a way for both of these tasks to be done* **without copying.**

- Some 4BSD (including SUN OS) and System V UNIX implement *mmap*() system call by rewriting its virtual-memory system.
- Mach implements advanced virtual-memory system and provides a set of functional system calls *vm_xxxx*(). Mach's mapped file is implemented as its UNIX interface.
- 4.4BSD adopts Mach's virtual memory system.
- Mapped file is and will be the standard of UI and OSF UNIX.

4.2 Memory Mapped Files in UNIX and Mach

4.2.1 Unix File Paradigm

open-seek-read/write-close

A user *opens* a file and *seeks* it to get random access of the file's data and uses *kernel buffers* and user's *process buffer* by themselves. (or C standard library functions for stream buffered I/O).

4.2.2 Mapped File

- *mmap* system call of System V / SUN OS.
  `paddr = mmap(s_addr, numbytes, prot, flags, fd, offset);`
- *map_fd* UNIX domain system call of Mach.
  `map_fd(fd, offset, addr, find_space, numbytes);`

1. Data file of any size is mapped into the user's logical address space.
2. Once mapped, file access is done by indexing or pointer operations like arrays in memory.
3. No seek operation, no extra copies, no buffering associated with read()/write() system calls are required, thus efficient handling of data is possible.
4. Distinction of sequential and random access no more concerns us. Structured data (record) are accessed as if they are in memory.

This allows us to implement more elegant algorithm to treat structured data.

5. The file system behaves as a pager. Whether data portion currently accessed is in memory or not is transparent to user programs.
6. Independent processes can share a data file by mapping it into their respective address spaces. No copying is necessary.
7. well-suited for API and shared libraries.

UNIX File Access

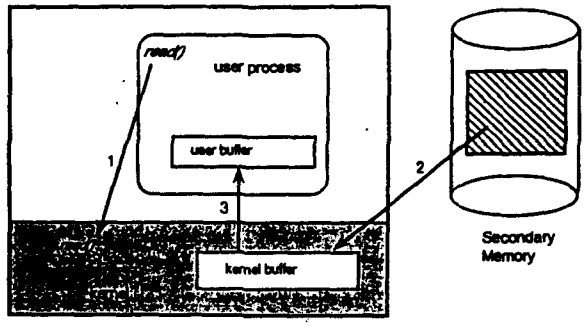

Memory Mapped File

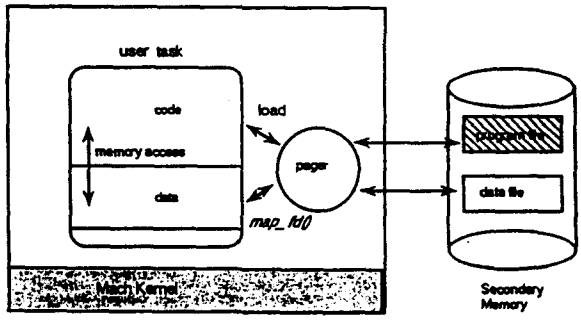

Virtual Address Spaces

2261

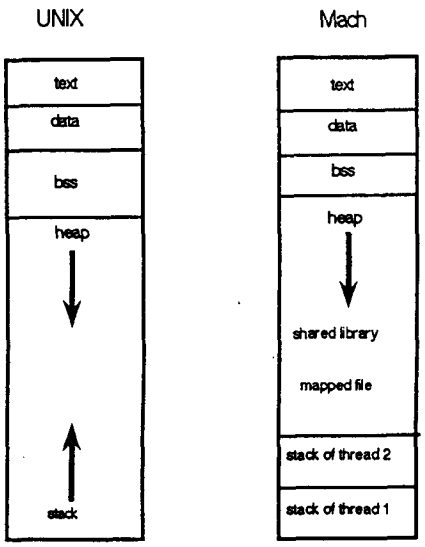

Sharing Data with Mapped File

2262

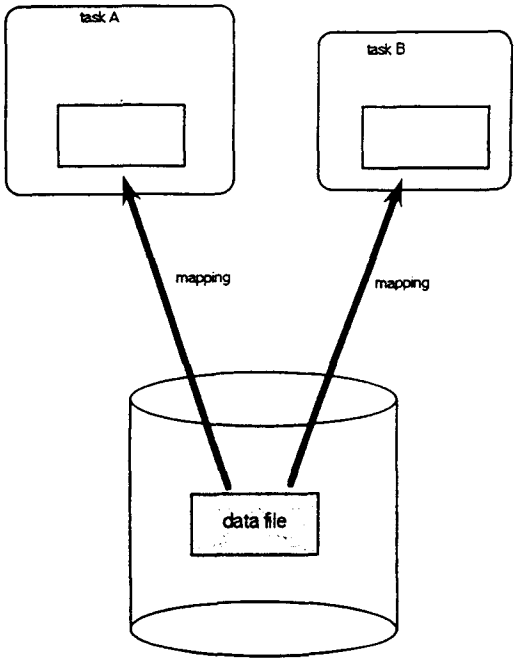

File size is only limited by that of the logical address space.

Locking and exclusive access is user's responsability

2263

5 Why Mach?

5.1 Distributed Operating Systems

- Mach ⇒ OSF/1
- Chorus ⇒ USL
- V-System, Sprite, Clouds, Amoeba, LOCUS etc.

5.2 Recent Progress of Mach

- Mach before 2.5 → NeXT
- Mach 2.5 → Luna
- Mach 2.6 → OSF/1 DEC's ALPHA, HP
- Mach 3.0 → kernelized kernel

Be careful! Mach is always in development stage.

2264

OSF/1 is Path to UNIX Technology of the 90's

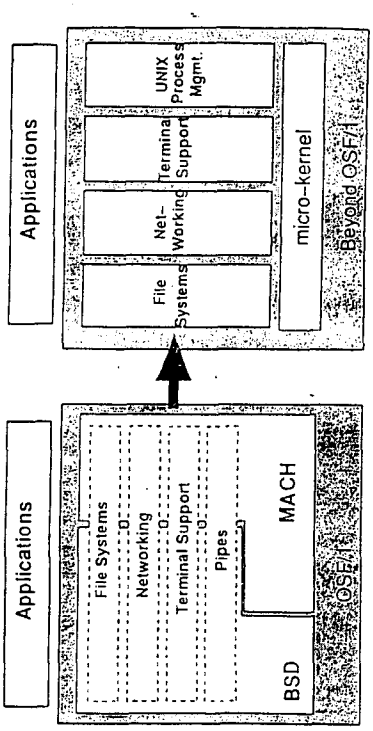

Operating System Features Comparison

Vendor Operating System Version Number Availability	DEC DEC OSF/1 1.0 Now	Sun Solaris 1.0 Now	HP HP-UX 8.0 Now	IBM AIX 3.1 Now	USL Sys V 4 Now
Operating System					
Kernel Base	OSF/1	BSD	Sys V	AIX	SVR4
Disk Mirroring	Yes	Optional	Optional	Yes	Add-on*
Multi-Disk Volumes	Yes	Optional	No	Yes	Add-on*
On-Line Partition Growth	Yes	Optional	No	No	Add-on*
Kernel Threads	Yes	No	No	No	SVR4 MP
Memory Mapped Files	Yes	Yes	No	Yes	Yes
Realtime Extensions	Yes	No	Yes	Yes	Yes
Shared Libraries	Yes	Yes	Yes	Yes	Yes
External Pagers	Yes	No	No	No	No
Streams	Yes	Yes	No	No	Yes
Sockets	Yes	Yes	Yes	Yes	Yes
OSF/1 Kernel Commitment	First	No	Yes	Yes	APIs
Standards					
OSF/Motif	Yes	No	Yes	Yes	No
OSF/AES	Yes	No	Soon	Soon	Soon
X/Open XPG3 Base Branding	Yes	No	Yes	Yes	Yes
POSIX 1003.1	Yes	Yes	Yes	Yes	Yes
Software Development					
Integrated CASE Tools	Yes	Yes	Yes	No	No
ANSI C Compiler	Yes	Yes	Yes	Yes	Yes
C++ Support	Summer	Optional	Optional	3rd Party	Optional
CDA Support	Yes	No	No	No	No
OSF/DCE Support	Starter Kit	No	Soon	Soon	Soon

USL delivers an add-on as a feature which may be layered on top of existing functionality and released without completely re-releasing the entire operating system.

AIX is a trademark of International Business Machines Corporation.
IBM is a registered trademark of International Business Machines Corporation.
Sun and Solaris are trademark of Sun Microsystems, Inc.
HP-UX is a registered trademark of Hewlett-Packard Company.
OSF/1 and OSF/Motif are trademarks of the Open Software Foundation, Inc.
X/Open is a trademark of the X/Open Company, formed in the UK and other countries.
SVR4 is a trademark of the services of Electrical and Electronic Engineers (IEEE).
UNIX is a registered trademark of UNIX System Laboratories, Inc.
DEC and CDA are trademarks of Digital Equipment Corporation

digital

5.3 Mach's Charercteristics

Mach supports;

- Large address space,
- Parallel and distributed processing,
- Advanced virtual memory system, and
- 4.3BSD system calls.

Virtual-memory is the key technology of Mach.

Its virtual-memory provides much more advanced functionalities than mapped files.

- Tasks and Threads — separation of resources from execution
- Port and Message — targetted to distributed systems
- Message based IPC — integrated with VM, highly efficient implementation of IPC is provided.
- Virtual Memory — efficient and versatile system
- Full implementation of 4BSD.

Time To Fork vs. Process Size

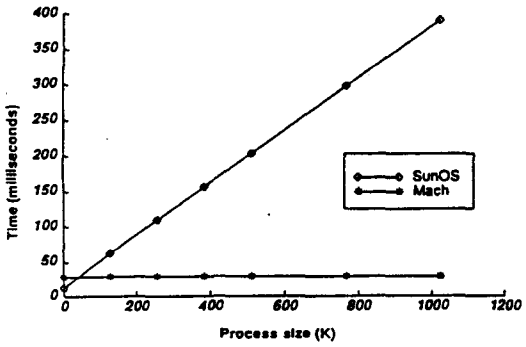

Figure 6.1: Time to fork on a Sun 3/260, no pages touched in child

Time To Fork vs. Amount of Data Touched in Child

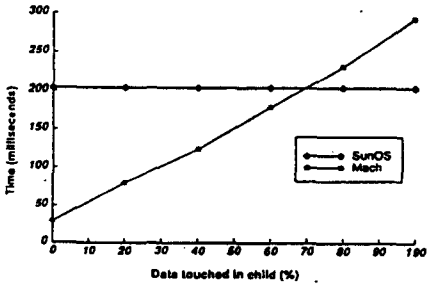

Figure 6.2: Time to fork versus amount of data written in child on a Sun 3/260 (process size is 512K)

Architecture-Independent Virtual Memory Management — R. Tevanian Jr. CMU-CS-88-106

Mach's IPC Task A send a message to task B via port p.

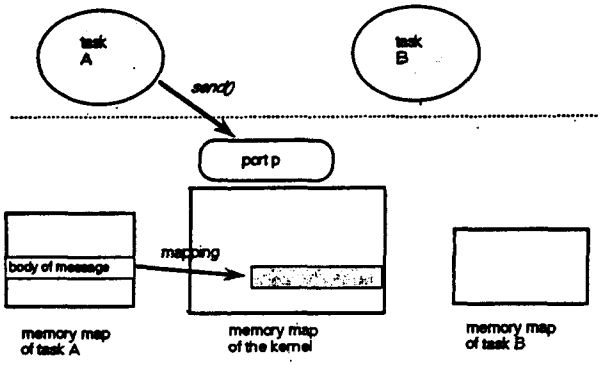

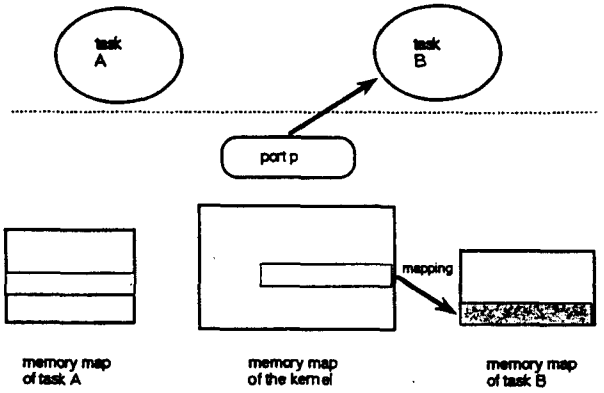

5.4 Mach's Virtual-Memory System

- Machine independent; requirement to the hardware is a memory system managed on page basis.
- Separation of the paging system from the virtual-memory system:
  - Virtual-memory system manages the relation between the virtual spaces of tasks and the real memory.
  - Paging system guarantees the consistency between regions of the secondary memories and the real memory.
- Paging program is out of the kernel and is a user program (external pagers). Thus, user can create new pagers for his own applications:

  Examples of network pagers;
  - his own strategy for paging (for example V=R etc.).
  - Network Virtual Memory
  - Distributed Shared Memory
- Physical memory (its abstraction is the *Resident Page Table.*) is used as a cache of *Virtual Memory Objects* which is an abstraction of the secondary storage.
- Memory objects are managed by the virtual-memory system of the Mach kernel.

- An *Address Map* corresponds to a task (of Mach) or a process (of UNIX). An entry of the doubly-linked *Address Map* list reflect a mapping from addresses to a memory object.
- A paging object may be implemented by any object that can handle requests to read and write data (i.e. port).
- Parallel and distributed processings are supported by providing efficient data sharing between tasks.

6 The Model Revisited & Conclusion

6.1 With Mapped files

Within a host;

- implementing a working model of collaborating processes
- writing general I/O libraries handling MC data files without using read/write system call (or standard C libraries)

6.2 With Mach's VM

- Network-wide pager
- netwok-wide file system
- implementing a working model of network collaborating processes

External Pager and Network Pager

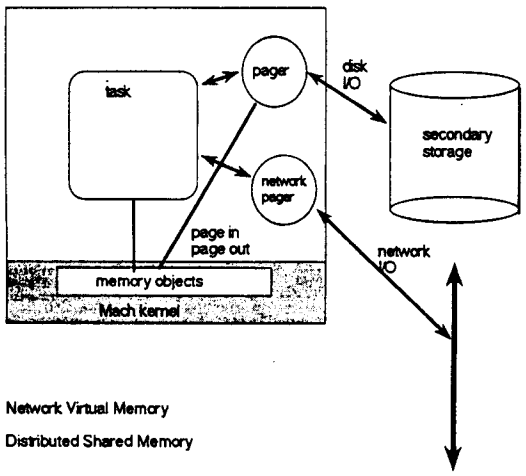

Network Virtual Memory

Distributed Shared Memory

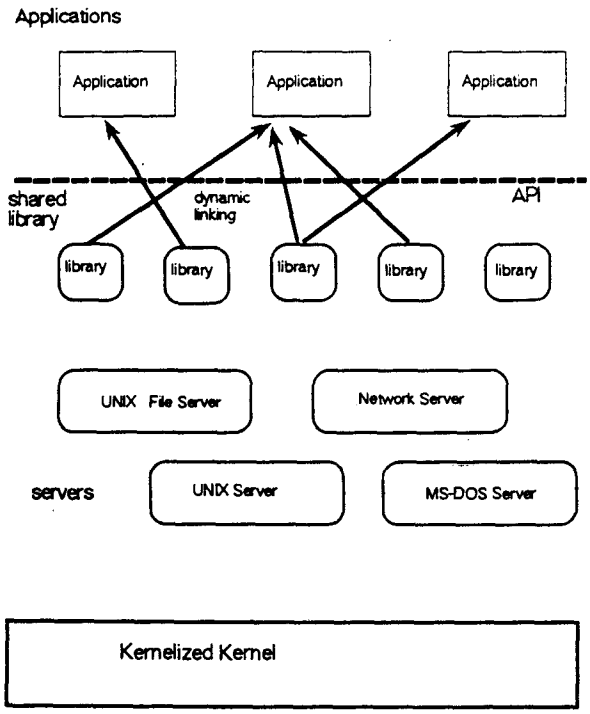
Applications
Application
Application
Application
shared library
dynamic linking
API
library
library
library
library
library
UNIX File Server
Network Server
servers
UNIX Server
MS-DOS Server
Kernelized Kernel

Evolution of Computers to Massively Parallel Processors

Katsuo Hasegawa
Tohoku University

SDC Collaboration Meeting
May 26, 1992, KEK

Contents

1. Introduction
2. History of computing
3. Shower simulation
4. Parallelism
5. Supercomputer approach
6. Some examples of solutions
7. MPP enviroment at KEK
8. Summary

"Speedup of Shower Simulation Using Super Parallel Processors"

Katsuo Hasegawa
Physics(*), Tohoku University

Abstract: The algorithm of the electromagnetic shower simulation code developed by the author many years ago is shown and its concepts are discussed. New ideas to speed up the shower simulation using new computer technologies like massive parallel machines are presented.

§1. Introduction

We are aware of the fact the modern computers have been evolving and we have also been changing our intelligence how to deal with them. This can be said like that we are obliged to seek for something new. We might have a feeling of fear when we think there might be some experts somewhero, because we have to learn almost everything that has been made by other people. Computers, circuits, languages, etc. It is the same thought we are pressurized with uneasiness to consider first we get to catch up before we take a lead in mastering UNIX, new computer languages, etc. We would be frustrated if the speed of computation is slow. This must have been the most basic motivation to speed up computers, and we still believe there can be some faster machines. Then we would think of what we must do on them. Therefore, we must be wise enough in choosing good themes. This would lead to balance the weights of application versus architecture. Parallel processing is undoubtedly the state-of-the-art computing trend. In this article the author intends to show an example in simulating the electromagnetic shower and explain how to reach the thoughts.

§2. History of Computing

In the past and even at present the history of computing has been the one of improvement to speed up, to be smaller, to be more economical, to be easier to use, etc. These imprnvements have been motivated by complaints or dissatisfaction as well as a lnt of effort of many manufacturers. Nowadays, however, we need a generalized concept for "simulation". This means somewhat paradoxically that you can consume the computer time as much as you like. We must find nut good reasons to take some amount of computing time. But to the author, the term of "speedup" stimulates his curiosity beyond the ones of "for what purposes". In general, this tendency might be seen especially in high energy physics; Event generation, Detector simulation, Tracking, and shower simulation, etc. Some parts of computing would be quite fitting to the vector machine in a pipeline algorithm, while the others might efficiently fit to parallel machine in some parallel processing

algorithms. It might be too bold to say we look for good computers in order to find out good themes. But it is interesting to try to make a history of computers from a viewpoint of computing power. Figure 1 is one of a trial.

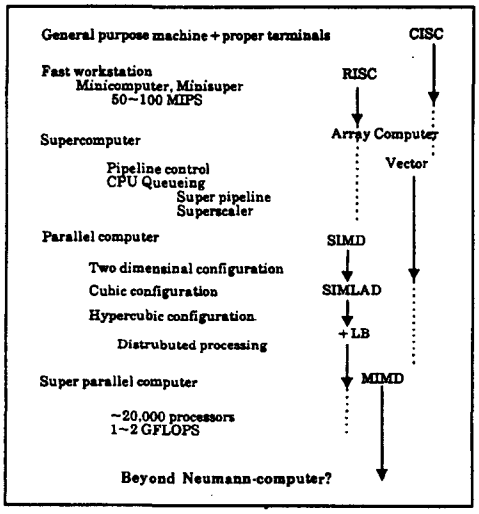

Fig. 1. Computer history viewed by computing power.

§3. Shower simulation

The author had written an unpublished article about the electromagnetic shower simulation in 1977 when the group was doing a couple of bubble chamber experiments with Tantalum plates in the Brookhaven National Laboratory 80-inch chamber and the KEK 1m chamber[1]. At that time many people had started the similer analyses and developed separately the program codes like EGS at SLAC, Stanford, and GHEISHA at CERN, Geneve, etc. Such developments have been done to contribute to high energy physics

especially for calorimetry and electron identification in the counter experiments, while in the bubble chamber experiments, this simulation was used to evaluate the detection efficiencies of gamma rays, π^0's, electrons and positrons. Electromagnetic process can be simplified in some matter at some depth in the following way. If the known material is exposed to incoming γ or $e^{\pm}$ of known momentum, then using the radiation length of the matter and dividing the matter into very small intervals along the incoming particle path, we can figure out the probability of a few elementary processes of electromagnetic interactions like Compton scattering, Bremmsstrahlung, pair production, energy loss through multiple scattering, etc. The conceptional diagram is shown in Fig. 2.

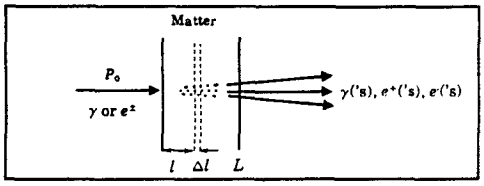

Fig. 2. Conceptional diagram of electromagnetic interaction.

In Fig. 2 the interval Δl does not have to be infenitesimal and has to be optimized to the level of possible occurrences of elementary processes. And these formula must be well parametrized for all of them, because a simple algorithm can be lead to infinity by $1/k$ factor where k is the energy of outgoing lepton. The first step is simple for there is only one particle incoming. However, the second step can have either one or two particles, and as it goes deeper inside the number of particles can be fairy large depending on the incident energy. As it goes higher, many hadronic processes open and this makes everything too far beyond possible calculations. Therefore hadronic processes were neglected and not included. The simulation program was separated to two parts, one is to compute the integrated probabilities with discrete energy interval, while the other is to simulate the shower using the probabilities after reading the table. For any value of energy, the code is made to compute probabilty functions by interpolating among the related and necessary numbers in the table. The random number generation function for pair production is shown in Fig. 3. The detail of the program is not described here and one of the results of comparison of the output with the correspondent in Fig. 4. The good agreement can be seen.

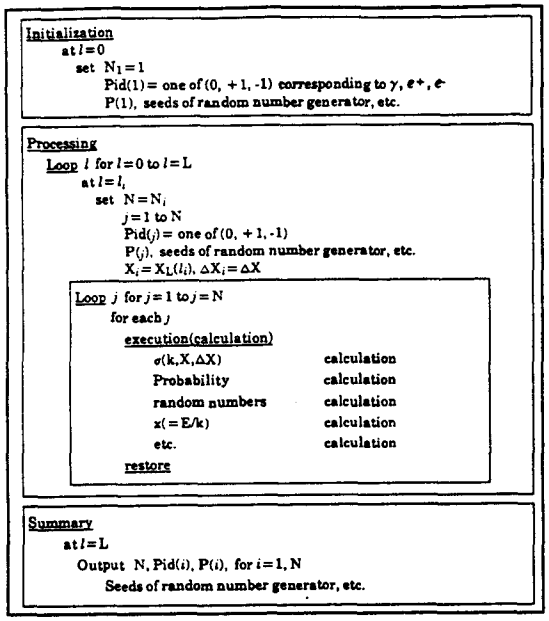

Fig. 5. Logical loop structure of shower simulation.

SIMD, SIMD, or SIMD+LB, or even MIMD, probably, an investigation leads te the author to remind that even parallelism can be found, still there remains problems how to establish good communications among huge number of co-processors occupying with some dimension in space. We could easily imagine how effectively our brains are working with many neural circuit modules cooperating.

Fig. 3 Random number generation function for pair production.

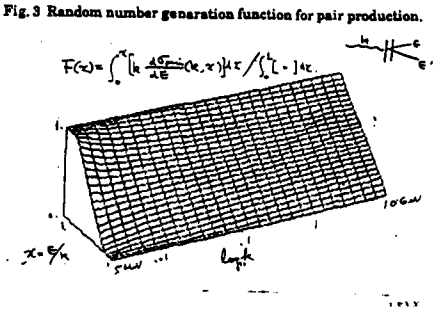

Fig. 4(a) Electron multiplicity obtained from measurement.

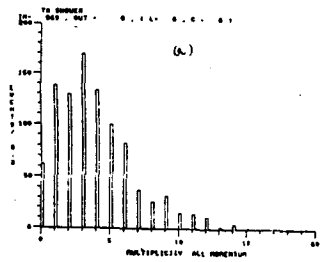

Fig. 4(b) Electron multiplicity obtained from simulation.

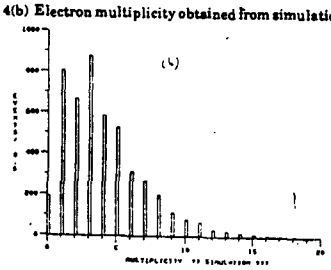


```
Vector X[1000],                 /* local data */
       INDEX,                   /* local pointer into X array */
       ITERS;                   /* number of iterations for that data point*/

forall processors
    INDEX <- 1;                 /* all processors start at the first */
    ITERS <- 0;

while (some-processors-busy)    /* termination for entire program */
    forall processors with INDEX <= 1000
        perform computation on X[INDEX];
        ITERS <- ITERS + 1;
        /* for those processors whose elements converged  */
        /* or reached the maximum allowed, proceed to the */
        /* next datum. */
        forall processors that have converged
          or (ITERS > MAXITERATIONS) then
            INDEX <- INDEX + 1; /* proceed to next datum */
            ITERS <- 0;         /* reset iteration count */
```

Figure 3: Mandelbrot code with reload.

```
DONE <- false;
COUNT <- 0;
while not(DONE)
    forall processors with INDEX <= 1000
        perform computation on X[INDEX];
        ITERS <- ITERS + 1;
        forall converged or (ITERS > MAXITERATIONS) then
            set processor converged;
        if (COUNT mod IL = 0) then       /* if new load interval */
            forall converged processors /* for those processors     */
                INDEX <- INDEX + 1;     /* that are done computing  */
                ITERS <- 0;             /* advance to the next point*/
    COUNT <- COUNT + 1;
    if (COUNT mod IG = 0)
        if (global_convergence) DONE = true;
```

Figure 4: Mandelbrot code with periodic reload.

§6. Summary

Referring a code of shower simulation program, the author tried to find out any method to speed up on the contemporaly parallel computers. There exist some different features among various machines, and it turned out that the manufacturers also want to know the needs and demands of users trying to improve their performance. In such an environment, users have also to be aware of daily progress and be ready to modify the algorithms used in their codes in order to catch up and to contribute to make the computers evolving themselves.

Reference

1. K.Hasegawa, Shower Simulation, unpublished, Sep 1977.
2. S.Tomboulian and M.Papas, The Third Symposium on the Frontiers of Massively Parallel Computation; College Park, MD; Oct 8-10, 1990.

Iteration Counts for Solving 512 x 512 Mandelbrot with 4K PEs								
real	imaginary	minimum iters	SIMLAD	%impr	%eff	SIMLAD +LB	%impr	%eff
(-2.0,0.5)	(-1.25,1.25)	15740	64373	-1	24	25949	59	61
(-1.251,-1.25)	(0.024,0.025)	7157	42774	33	17	11995	81	60
(-0.6,-0.5)	(-0.6,-0.5)	22401	64333	-1	35	33080	48	68
(0.28,0.27)	(0.0,0.01)	41864	64511	-1	65	52574	18	80
(-1.26,-1.24)	(0.01,0.03)	53190	64488	-1	82	61114	5	87
(0.2732,0.2741)	(-0.0084,-0.0055)	8388	33759	47	25	13123	79	64

Table 1: Mandelbrot iteration counts for $I_L = 24$ and $I_G = 1$.

Timing for Solving 512 x 512 Mandelbrot with 4K PEs							
real	imaginary	SIMLAD	%impr	%eff	SIMLAD +LB	%impr	%eff
(-2.0,0.5)	(-1.25,1.25)	20.54	-7	23	8.39	56	57
(-1.251,-1.25)	(0.024,0.025)	13.68	29	16	3.85	80	56
(-0.6,-0.5)	(-8.6,-0.5)	20.38	-6	33	10.86	45	63
(0.26,0.27)	(0.0,0.01)	20.66	-7	61	16.93	12	74
(-1.26,-1.24)	(0.01,0.03)	20.74	-8	77	19.68	-2	81
(0.2732,0.2741)	(-0.0084,-0.0055)	10.85	44	23	4.22	78	60

Table 2: Mandelbrot timings for $I_L = 24$ and $I_G = 1$.

Traditional Supercomputer Approaches

- Expensive to buy and maintain
- Poor price/performance ratios
- Architectural limitations
  - Maximum peformance limited by physics
  - Peak performance vs. real performance
  - Limited memory
  - Reliability: shared memory, few CPUs
  - Little scalability

Traditional Hardware Approaches

Increasing the Number of Processors Causes Bottlenecks

- Tightly coupled → Memory bottleneck

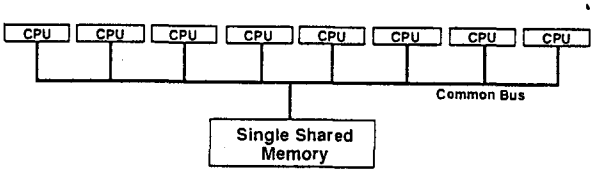

Fixed Memory Bus Bandwidth Limits Performance

- Loosely coupled → Interconnect bottleneck

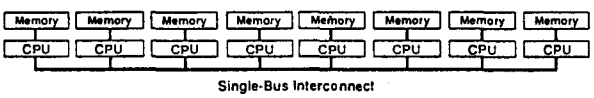

Fixed Interconnect Bandwidth Limits Performance

Approaches to Parallel Processing

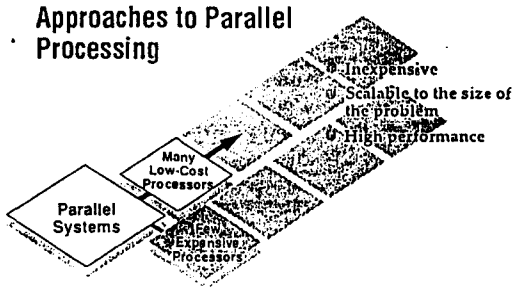

Approaches to Parallel Processing

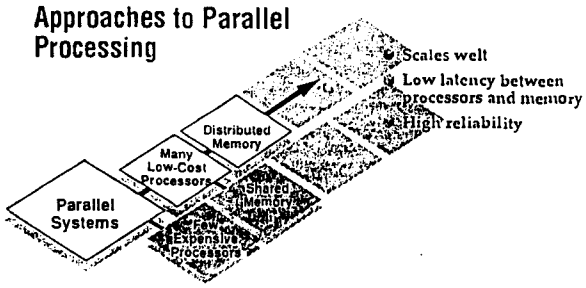

Approaches to Parallel Processing

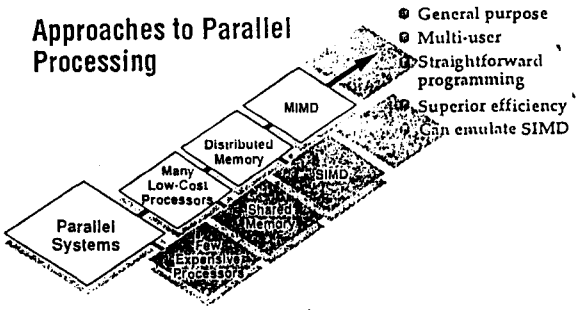

- General purpose
- Multi-user
- Straightforward programming
- Superior efficiency
- Can emulate SIMD

Approaches to Parallel Processing

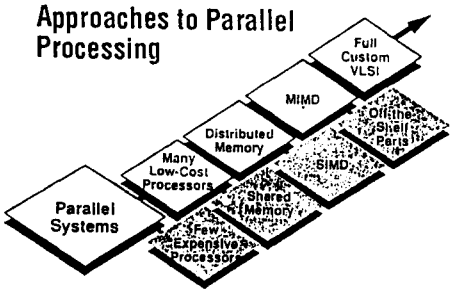

- Low cost
- Few parts per node
- High reliability
- Maximum scalability

The Solution:

Scalable Parallel Processing

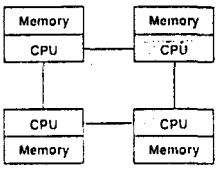

Parallel processing eliminates both bottlenecks

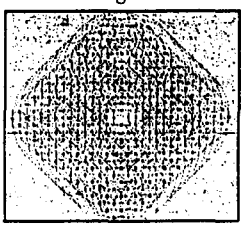

256 processors

Memory, CPU, and I/O scales linearly to meet customer needs

nCUBE Architecture

Summary

	Architectural Range	*Model 80.*
Processors	8-8192	8192
Main Memory	8-256,000 Mbytes	65,536 Mbytes
Processor/Memory Bandwidth	640 Gbytes/sec	640 Gbytes/sec
Scalar MFLOPS	26-27,000	27,000
MIPS	60-60,000	60,000
I/O Bandwidth	36 Gbytes/sec.	16 Gbytes/sec.
Disk Storage Capacity (Gbytes)	4096 Gbytes	1792 Gbytes

Approaches to Parallel Processing

The Hypercube Architecture

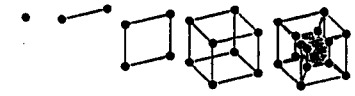

Where n represents the order of the hypercube

- Approximates a complete connection of the processors
- Each node can communicate quickly with every other node in the system
  - Accomplished in the nCUBE system by direct "cut-through" hardware routing

Benefits of the Hypercube Architecture

The Hypercube can Emulate All Other Topologies

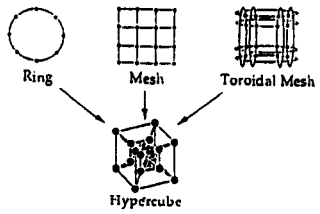

Benefits of the Hypercube Architecture

- Unmatched price/performance
  - No unique nodes
  - No bottlenecks
- Multi-user, multi-application environment
- Densest interconnect topology
- Highest interprocessor communications bandwidth
- Most scalable topology

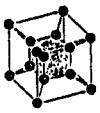

1992年2月27日
"分散型ネットワークの研究"
KEK
川端 / 石川 正
(内容)

$e^+e^- \rightarrow \nu_e\bar{\nu}_e\gamma$

を使ったベンチマーク

machine	cpu (sec)	ファコム比
FACOM M780/30	191.90	1.00
HITAC S820/80	7.08	27.1
HITAC M880/210	119.04	1.61
HP 9000/720	314.40	1/1.64
IBM RS6000/530	321.48	1/1.68
SGI P.Iris	1087.47	1/5.67
INTEL i860	1305.58	1/6.80
SUN SPARC	2617.37	1/13.6

INTEL 6.8 ノードで1ファコム.

AP1000 13.6 ノードで1ファコム.

1. KEKの並列計算機

	INTEL iPSC/860	nCUBE nCUBE2	Fujitsu AP1000
ノード	16	16	16
最大性能	1280 MFLOPS	53.2 MFLOPS	48 MFLOPS
各ノードのメモリ	16 MB	4 MB	16 MB
ネットワーク	Hyper-cube	Hyper-cube	2-D torus
所外最大利用可能ノード	64	–	512

すべてMIMDマシーン (Multiple Instruction Multiple Data). ノード間のデータ通信は，ライブラリーによっておこなう.

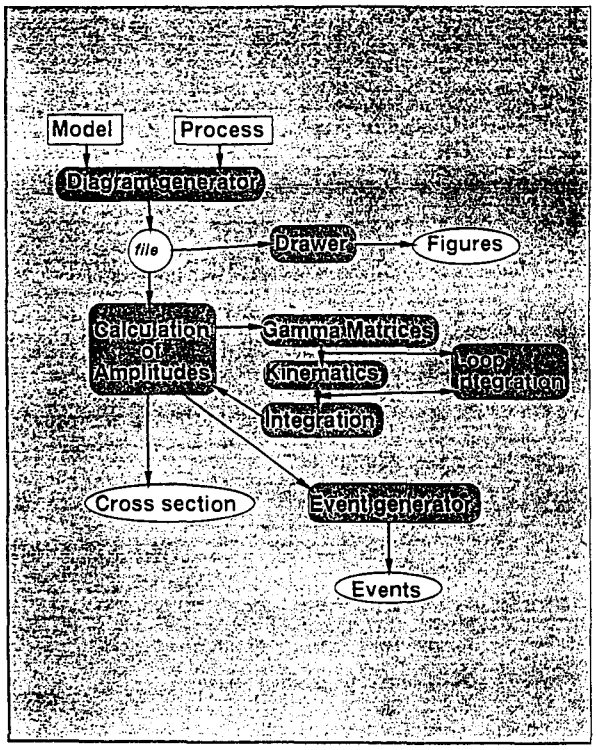

$e^+e^- \to W^+W^-\gamma\gamma$

INTEL iPSC/860

Node 数	cpu (sec)	Speed-up	Efficiency (%)
1	116313.10		
2	58240.56	2.0	99.86
4	29184.59	4.0	99.64
8	14653.84	7.9	99.22
16	7377.60	15.8	98.54
32	3767.30	30.9	96.48
64	1922.70	60.5	94.52

$T_P = 109.63 + 116355.47/P$

並列度 = 99.91%

AP1000

node 数	cpu (sec)	Speed-up	Efficiency (%)
1	340081.8		
4	85408.0	4.0	99.6
16	21570.8	15.8	98.5
32	11104.3	30.6	95.7
64	5674.6	59.9	93.6
128	2854.0	119.2	93.1
256	1443.7	235.6	92.0

$T_P = 110.80 + 346392.33/P$

並列度 = 99.97%

Summary

1. Computers of various architectures were reviewed.
2. The motivation of the survey and research was introduced.
3. Some examples of the programming were shown.
4. Another aspects of computing related to communication were presented.

Fukui University

Development of Simple Distributed Batch Processing System

Minato KAWAGUTI
Department of Information Science
Fukui University

SDC Collaboration Meeting KEK May 26, 1992

1 Objective of the Development

1. Realization of Handy Batch Processing
2. Experimentation on a Scalable Batch System

2 Design Goals

1. Automation of Control and Management
2. Minimal Disturbance to the Remote Hosts
3. Reduced Load to the Network
4. Freedom from Conceivable Constraints (license, etc.)
5. Realization of User-Designable Remote Processing

3 Assumptions

1. UNIX + TCP/IP
2. Uses Berkeley's Remote Copy ("rcp")
3. Between Secure Hosts
4. Mainly for Batch-Type Jobs

4 Implementation Details

1. C + lex + bison (yacc)
2. Client-Server Scheme
3. Server as a Daemon
4. Status of Remote Hosts Monitored Intensively
5. Jobs Executed Based on a 'Prescription'
6. Remote Hosts Classified into Groups
7. Best Suited Host Selected Automatically
8. Files Transferred Semi-automatically
9. Normal Termination of Each Job Confirmed
10. Intermediate Files Deleted Automatically unless Otherwise Specified

5 Monitoring of the Remote Hosts

1. CPU type
2. OS Version
3. `/usr/spool/rwho/whod.*` — load averages (1, 5, 15 min)
4. vmstat — Operational Status of CPU
5. iostat — I/O Activities
6. df — Available Disk Volume
7. netstat — Network Collisions

6 Comparisons

1. ONC (Open Network Computing)
   (a) SunRPC: based on UDP/IP
      i. high-level programming
         A. limited to UDP/IP
         B. synchronized with remote job termination
         C. XDR filtering mandatory
      ii. program in low-level mode
         A. TCP/IP may be used
         B. flexible
   (b) public domain software
2. NCS (Network Computing System)
   (a) NCS/RPC: based on UDP/IP
   (b) Network Data Representation (filtered by receiver)
   (c) proprietary software
3. Ours
   (a) our own RPC: based on TCP/IP
   (b) hand-made from scratch

7 UDP/IP versus TCP/IP

1. UDP/IP — User Datagram Protocol
   (a) connectionless
   (b) small overhead
   (c) unreliable
   (d) packet oriented
   (e) unsuitable for large volume data transfer
2. TCP/IP — Transmission Control Protocol
   (a) maintains connection
   (b) reliable
   (c) large initial overhead
   (d) stream oriented

8 'Remote Function Call (RFC)' [Our own RPC]

1. Hand-made
2. Akin to 'Remote Procedure Call'
3. Client-Server Scheme
4. Executes a "Function" at Remote Host
5. Utilizes `exec()` System Call
6. Client Does Not Wait for Completion of Execution (Asynchronous)
7. Remote Host Keeps Temporarily the Return Values
8. Return Values Sent Back on Demand from the Client
9. Communication Between Sockets through TCP/IP

9 Generation of the Server and the Client

1. Home-Made Compiler ('rfcgen') Generates Client-Server Source Code Pair
2. Same Server Source Program Shipped to All Remote Hosts
3. Each Remote Hosts Compiles It with Its cc Compiler

10 'Datastation'

1. Return Values of Executed 'Functions' Kept Temporarily
2. Responds to Enquiry from the Client
3. [hostname + uptime stamp + process ID] Distinguishes a Client
4. 'Tag' Given by Client Identifies the Executed 'Function'
5. Simultaneous Service to Multiple Clients (Users)

11 'Remote Job System (rjob)' ← Our own remote batch (intepreter + ...)

1. Uses 'Remote Function Call'
2. User Writes a 'Prescription'
3. 'rjob' Interprets It
4. Files Transferred Through 'rcp'
5. Records Kept in a Log File

12 Prescription for 'rjob'

1. 'Declarations'
2. 'Instructions'

13 'Declarations'

1. Specify a Log File
2. 'Classify' the Remote Hosts into Groups
3. Definition of 'Macros'

14 'Instructions'

1. Labels
2. Host Class
3. Priority
4. Files To Be Sent
5. Files To Be Received
6. Shell-Level Commands
7. Files To Be Kept There

15 Unique Features

1. Entirely Hand-Made
2. Good Portability
3. User-Specified Files Transfer
4. No Need for 'root Privilege'
5. No Need for a Help from System Administrator
6. Hopefully Minimal Network Load

16 Conclusions

1. Prototype Version
2. Relatively Small Program Size [illegible] lines
3. Needs Some More Work for Real-World Use
   (a) Robustness
   (b) Convenience

Sample Program – I

"presentation"

```
/* file: rjbison */
/* generates a simple compiler by lex and bison */

logfile = "logbis";

typify {
    type( 1) = {
        maggie
    };
    type( 2) = {
        maggie, iimps1, iisun1
    };
    type( 3) = {
        iconvex1
    };
};

var {
    ret = "/var/home/ug/nakamura/rmtjob5/client/exp";
};
```

grouping of remote hosts

local

host group

```
lexbison [1] {
    send    "{ret}/exbison/*.[ly]"
    recv    "{ret}/bres/*"

    comm    "lex rjob.l"
            "bison -d rjob.y"
```

files to be transferred

commands

Sample Program – II

```
/* file: test;   compiles by LaTeX remotely /
logfile = "logtex";
typify {
    type( 1) = {
        maggie
    };
    type( 2) = {
        iimps1, iisun1, maggie
    };
    type( 3) = {
        iconvex1
    };
};
var {
    home = "/var/home/ug/nakamura";
    base = "/var/home/ug/nakamura/texfile";
    ret = "/var/home/ug/nakamura/rmtjob5/client/exp";
};

/* jobs */
nemesis_tex [1] {
    send    "{base}/nemesis.tex"
    recv    "{ret}/nemesis.*"

    comm    "nlatex nemesis.tex"
}

nemesis_lips3 [1] {
    send    "{ret}/nemesis.dvi"
    comm    "lips3dvi  nemesis.dvi"
```

date =

independent

date =?

Sample Program – III

```
/* file: tstsh;  executes shell commands remotely */

logfile = "loglog";

typify {
    type(1) = {
        iimps1
    };
    type(2) = {
        maggie
    };
    type( 3) = {
        iconvex1
    };
};

var {
    home = "/var/home/ug/nakamura";
    base = "rmtjob5/client/exp";
};

/* jobs */
rwhoa  [2] {
    comm
        "rwho -a" (  ,"{home}/{base}/tf1",  )
}

wcgrep [2] {
    comm
        "wc -l" ( "{home}/{base}/tf1",
                  "{home}/{base}/tf3",  )

        "grep maggie"
```

stdin stdout stderr

Server Start-up

```
Script started on Mon Feb 24 22:04:01 1992
iimps1[nakamura 101]% rsh maggie ps x.
  PID TT STAT  TIME COMMAND
 7503 ?  S     0:00 csh -c ps x
 7508 ?  R     0:00 ps x
iimps1[nakamura 102]% rsh maggie dtst4
iimps1[nakamura 103]% rsh maggie serv_rj5
iimps1[nakamura 104]% rsh maggie ps x
  PID TT STAT  TIME COMMAND
 7530 ?  S     0:00 /var/home/ug/nakamura/rjprog/datastation4
/var/home/ug/naka
 7538 ?  S     0:00 /var/home/ug/nakamura/rj5/serv_rjob5 /var/
home/ug/nakamura/
 7540 ?  S     0:00 csh -c ps x
 7545 ?  R     0:00 ps x
iimps1[nakamura 105]% exit
iimps1[nakamura 106]%
script done on Mon Feb 24 22:05:20 1992
```

datastation

server

Execution of rjob Interpreter

```
Script started on Mon Feb 24 22:19:27 1992
iimps1[nakamura 101]% ls
bres/           rfc_dtst_ports  test
exbison/        rjbison         typescript
iimps1[nakamura 102]% rjob5 rjbison
iimps1[nakamura 103]% cat logbis

<< Job "lexbison" started at maggie.  Mon Feb 24 22:19:42 19
92

>> Job "lexbison" was completed at maggie.  Mon Feb 24 22:19
:55 1992

complete.Mon Feb 24 22:19:56 1992
iimps1[nakamura 104]% rjob5 test
^Ciimps1[nakamura 105]% cat logtex
<< Job "nemesis_tex" started at maggie.  Mon Feb 24 22:21:11
1992

job(nemesis_tex):errer at maggie..receive a bad-terminating-
status of aimed-program(/usr/local/bin/virtex       \&jlplai
n  nemesis.tex)

terminated.
make a file: remaining_job.rjob
iimps1[nakamura 106]% exit
iimps1[nakamura 107]%
script done on Mon Feb 24 22:23:51 1992
```

S D C S I M

S.Kunori

28-May-1992

What is SDCSIM ?

```
SHELL   framework (event loop, i/o)
  |
  |--SE  interface to event generator
  |
  |--SG  interface to Geant simulation
  |
  |--SR  interface to reconstruction
  |
  |--US  interface to user analysis
```

outline of talk

- o available packages
- o SHELL system
- o status of program
- o conclusion

AVAILABLE PACKAGES:

Utilities Library

RA random number generator
UT general utility

Interface Packages

SE event generator
  herwig, isajet, pythia
  prtgun (sigle partilce generator)

SG geant detector simulation.
  - tracking simulation
  ST (silicon), SF (fiber)
  WR (wire), WF (hybrid),
  PX (pixel)
  PM (microstip), KM (knife edge)
  FT (fast tracking simulator)
  - calorimeter simulation
  AN (scintilator) - LOI design
  CL (barrel+endcap with show max)
  CP (barrel+endcap- tile level)
  CI (forward)
  CF (shower+punchthrough parametrization)
  - muon simulation
  MU
  - special purpose
  RT (ray tracing I)
  RL (ray tracing II)
  SO (user hooks)
  SW (track swim)

SR event reconstruction.
  TF (combined track reconstruction)
  - subpackages of TF.
    TS (Silicon coordinate/ segment/track reconstruction)
    AH (Wire/fiber hybrid segment reconstruction)
    AR (Straw segment reconstruction)
    AT (Combined detector track reconstruction)
    RW (Wire segment/ combined track reconstruction)
    TR (Fiber coordinate /combined track reconstruction)
    PX (Pixel coordinate /segment reconstruction)

  CC (clustering and jet finding)

  MR (muon track finding)
  MA (muon track fit)

SA event analysis.

  (none)

US empty user analysis package

Choices for the system

Language: F77
with almost no extension.
(plan to relax, this summer)

no direct call for OPEN/CLOSE
(use interface routine)

Data structure: Zebra with user interface
(SZ package)

Control files: KUIP (Kit for User Interface package from CERN)

Code management: PATCHY
with minimum fanctionalities.
correction is done deck by deck

Organisation of program packages:
divide to small packages and assign two letters to each package as package name and first two letters of suroutine common block name.

Distribution: No automatic distribution

The SDC SHELL library on SSCVX1

```
SDCSHELL
  |
  |--MAIL      mailing distribution lists.
  |
  |--INIT      definition file for logicals.
  |
  |--NEW
  |   :
  |   :     (same as below)
  |
  |--V03
  |   :
  |   :     (same as below)
  |
  |--V04     -- released on 27-Feb-1992 --
      |
      |--SRC     all files for distribution.
      |
      |--MGR     command files (make)
      |--BIN     executables
      |--CRA     cradles
      |--DAT     data/constant files
      |--DBG     sources for debugger
      |--DOC     documentations
      |--LIB     object libraries
      |--PAM     pam (.car) files
```

Passive distribution: Each machine needs to copy files in SRC and split to other subdir.

Status of Simulation/Reconstruction

EVENT GENERATION:

- HERWIG, ISAJET, PYTHIA sigle particle
- mixture of above for multiple interactions

TRACKING: (detector simulation)

- codes for major options - done
- generate raw data bank (digitization plus hits)

TRACKING: (reconstruction)

- local track finding/fitting have been written for most of options. (segment finding and fitting)
- global track finding/fitting code (first version) has been written.
- vertex finding- not yet

CALORIMETER: (detector simulation)

- barrel+end geometry (no tile) (19-Dec-91, by L.Bartosek) shower max detector — CL by Asai
- barrel+end geometry (tile) — CP by Turcotte & Job
- forward geometry — CI by Pang & Wendling & Asai
- forward liq.scinti/quartz tube — FL by Copeland
- fast shower simlater with hadron punchthrough (for CL and CI) — CF by Asai & Bakken

  CF uses R.McNeil's routine for the punchthrough.
- output bank = CALE (energy in phi-eta-depth)

CALORIMETER: (reconstruction)

- clustering/jet finding — CC by Wu

MUON: (detector simulation) — MU by Kunori & Sirotenko & Slonim

- geometry with forward absorber + projective beam pipe (in SG)
- output banks= PTRJ (track trajectry)
  MUHI (hits in muon detector)
  MUXI (hits at outer surface of central tracker)
  MUDI (digitisation)

MUON: (reconstruction)

- local track finding/fitting L1 trigger (forward only) — MR by Kunori
- global track fitting — MA by Slonim

MAGNETIC FIELD:

- uniform solenoidal field w/o return flux
- full solenoidal field map with return flux (by B.Wands for Dec-91 calorimeter design)
- uniform toroidal field

2315

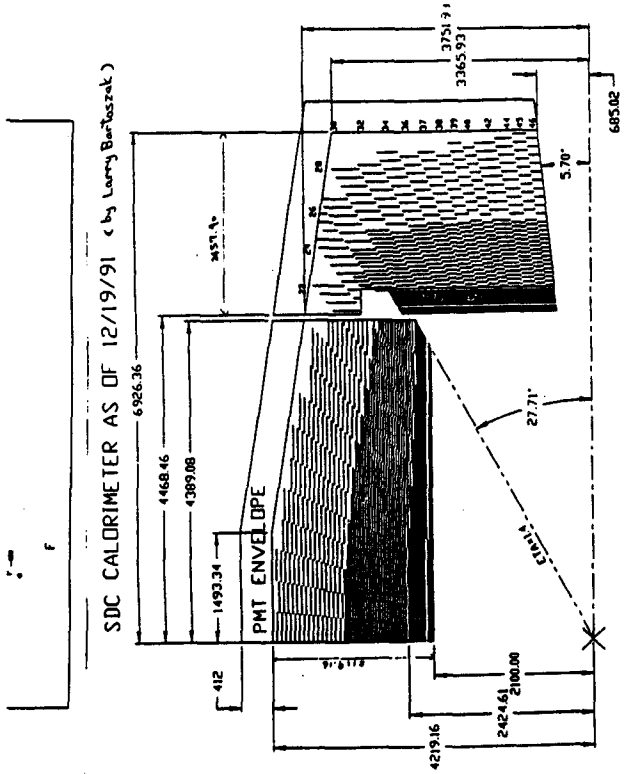

2316

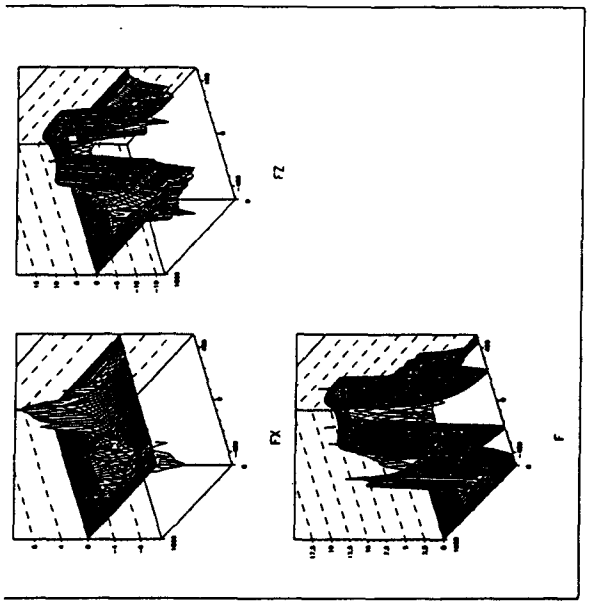

2317

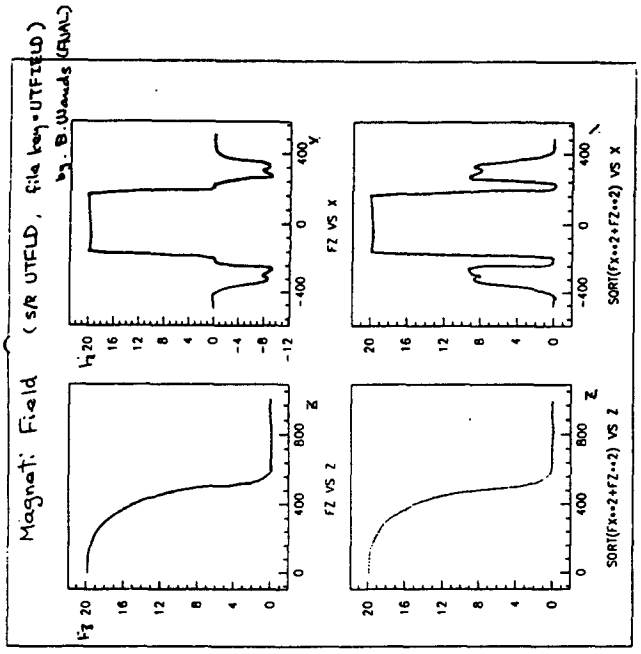

2318

Conclusion
---

1. SDCSIM is now simulating most of detectors.

2. Now main efforts are on event reconstruction and trigger simulation.

3. Big improvement is expected for calorimeter and muon code in Version 5. (July-92)

4. We need to improve many areas in the program.
   - o documentation (update by 1-July-92)
   - o interactive operation
   - o event display
   - o performance (speed, size)
   - o trigger simulation (organisation)
   - o very fast simulation

5. Next release (Version 5) in July-92
   --- submit new code,docs by 01-july-92

Future

- The SDC computing group will soon start designing NEW SHELL.

  I predict that current SDCSIM will be supported by the NEW SHELL system and evolved over many years.

Future SDC Simulation Program

(detector simulation)

23-Apr-1992

S.Kunori

Outline

Functional requirements
Classes of simulation programs
Output from simulation programs
Development procedure
Current status
Plan

Functionl Requirements

r1. verify detector design.

r2. help to develop/test the event reconstruction program. [low stat.]

r3. help to develop/test the L3 trigger program. [med.stat.]

r4. help to develop/test algorithms in the data analysis program. [med.stat.]

r5. give estimations of statistical and systematic uncertainties in pysics results. [med.stat] [high stat. 100hz]

===> The output from the simulation program will be processed through the entire L3-Reconstruction-Analysis chain and also a part of the chain.

+ (additional)

r6. help to develop/test the online offline computing system.

Classes of Simulation programs

1. FULL = very detailed
   - o slow speed
   - o large event size
   - o based on all known basic physics processes
   - o capable to predict some unknown behaviors of detectors

   --> simulate RAW data (=input to the reconstruction program) and data at itermediate stage in the reconstruction program.

2. HYBRID = hybrid of FULL and FAST
   - o medium speed
   - o medium event size
   - o simulate critical detectors well

   --> simulate some of RAW data

3. FAST = fully parametrized
   - o fast speed
   - o small event size
   - o detector response is fully parametrized.
   - o basic event reconstruction is parametrized.

   --> simulate input data to the Data Analysis program

Output from the Simulation programs

FULL/HYBRID/FAST shuold output events in the same data format.

```
          +----------+                 FULL
          | detector |                   |
          |----------|                   |
          |   RAW    |                <==|
          +----------+                   |
               |                         |
+-------------------------------+        |
|    reconstruction program     |        |
|-------------------------------|        |
| HIT-COORD    ENERGY    FILTER |   <-|
| SEGEMENTS              TRIGGER |   <-|
| TRACKS                        |   <-|
| VERTICES                      |   <-|   FAST
|                               |     |
|(PARTICLES)   CLUSTER          |   <-| <==|
|                               |     |    |
| ELEC PHOT MUON  JET  MISSING  |   <-| <==|
|                               |     |    |
|        W  Z  T  B ...         |   <-| <==|
+-------------------------------+        |    |
               |                         |    |
  +----------------------------+         |    |
  | analysis program (physicist) |       |    |
  |----------------------------|         |    |
  |     Higgs     New-Quarks   |     <-| <-|
  |     SUSY      New-Force    |     <-| <-|
  |       :                    |
  +----------------------------+
```

Development Procedure

Who will develop? = each detector group.

1. Define the data structure (banks) in the offline chain, RAW-RECO-ANALYSIS.
   - understand the detector
   - understand the reconstruction program, ESPECIALLY HOW TO TEST IT.

2. Define the data structure for the detector parameters.
   - Common for the simulation program and reconstruction program.

3. Develop the FULL simulation program.
   - choose a framework for FULL simulation.
     IS GEANT GOOD ENOUGH?
     precision: 10 microns vs 10 meters?
     efficiency: can be better?
     support: totally rely on CERN?
   - conceptual design for FULL/HYBRID/FAST.
     (the framework may be shared.)

4. Develop the HYBRID program
   - parametrize detector responses for HYBRID and FAST program.
     (use data from FULL and test beam)

5. Develop the FAST program
   - Parametrize detector response for the FAST program. (use data from FULL, HYBRID and test beam)

6. Tune all programs using data from the SDC detector. (Year 2000!)

Current Status

1. SDCSIM

   - Geant based.
     - almost_FULL + HYBRID
     - almost completed to simulate 'RAW', but need more work.
   - corresponding reconstruction programs
     - TRACKING
       Advanced.
       Track has been reconstructed.
       Vertex finding is not yet.
     - CALORIMETER
       None, but there is a plan to add a clustering program.
     - MUON
       Global track fitting exists.
       Trigger simulater for the forward muon chamber system exists.
       Track finding for the forward muon in progress.
       None for barrel.

2. Other simulation programs.

   - SSCSIM (Fermilab)
   - Trigger simulator (Triger group, UC,UW)
   - Stand alone Geant
     Forward Calorimeter (ISU)
     Muon (KEK, others)
   - other fast simulators
     :

NO COMMON DATA FORMAT TO COMMUNICATE BETWEEN DIFFERENT PROGRAMS.

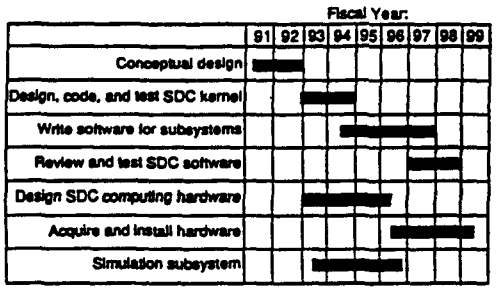

FIG. 10-8. Bar chart of schedule for major SDC computing activitie

Japanese activities for SDCSIM

Makoto Asai
Hiroshima Institute of Technology

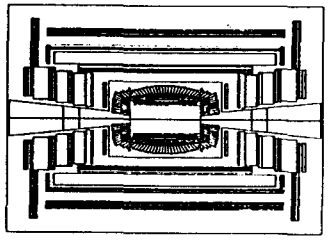

Contributions to the current version of SDCSIM

SDCSIM frame
- *RA (Random number control) -- Y.Takaiwa (co-auther)*

Event generator section
- *SE (Event generator frame) -- Y.Takaiwa (co-auther)*

Detector simulator section
- *CL (Tile/fiber calorimeter) -- M.Asai*
- *CI (Forward calorimeter) -- M.Asai (co-auther)*
- *CF (Shower shape and punchthrough parametrization) -- M.Asai*
- *RT (Ray-tracing utilities) -- M.Asai*

Reconstruction section
- *SW (Track swimming routine) -- M.Asai*

Calorimeter Packages:

- *CL -- Barrel and endcap Tile/Fiber calorimeter with Shower-Max calorimeter*
- *CI -- Forward calorimeter*
- *CF -- EM / Hadron shower shape and punchthrough parametrization*

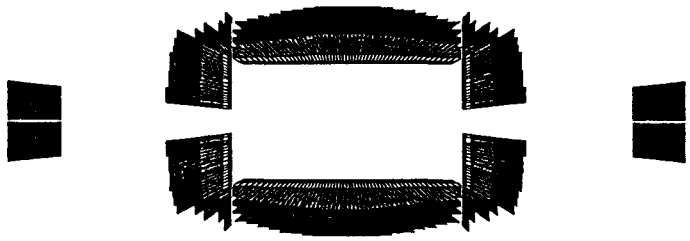

Shower parametrization

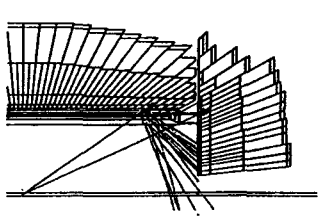

EM shower

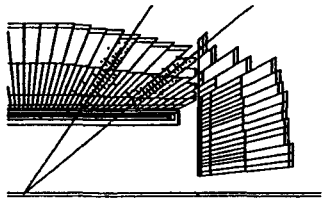

Hadron shower

Near future developments

> *Fine tuning of shower shape parametrizations*
Tune to GEANT/GHEISHA results
Tune to results of the beam test
Optimize user parameter sets for
- *Quick and dirty study*
- *Fine and detailed study*

> *Reconstruction package of barrel and intermediate muon tracker*
Track finding
Swimming back to the central tracker
Connection with tracks found in the central tracker
Trigger simulator for first and/or second level

> *More*
Let's discuss...

Punchthrough parametrization and EM debris

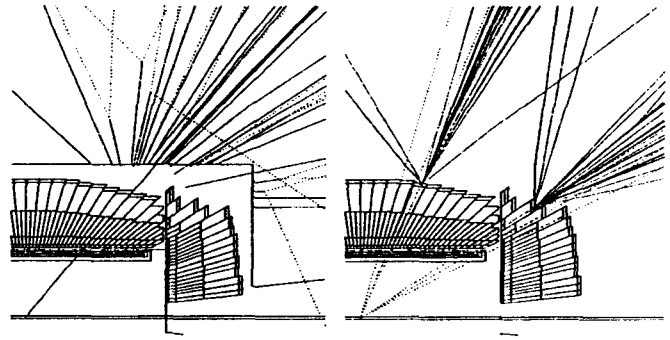

Punchthrough *EM debris*

SDCSIM on Japanese nodes

Machine fravours:
DEC station, SGI, SUN, and VAX

Sites:
KEK, Tohoku univ., Tsukuba univ.,
Tokyo metropolitan univ., Kyoto univ.,
Wakayama medical college, Hiroshima univ.,
Hiroshima inst. tech.,
and others...

Used to study for:
Silicon micro-strip detector
Straw tube tracker
Material effects of solenoid magnet
Tile/fiber calorimeter
Muon chambers *and others...*

Appendix

- List of Participants
- Photographs

Name	Institution
Salvator R. Amendolia	University of Pisa
Larry M. Bartoszek	Fermilab
James R. Bensinger	SSCL
Richard V. Berg	University of Pennsylvania
Myron Campbell	University of Michigan
Duncan Carlsmith	University of Wisconsin
John W. Chapman	University of Michigan
Priscilla B. Cushman	Yale University
Colin H. Daly	University of Washington
Richard J. Davisson	University of Washington
Tom Dombeck	SSCL
L. S. Durkin	Ohio State University
John E. Elias	Fermilab
Steven M. Errede	University of Illinois
Gary J. Feldman	Harverd University
Farshid Feyzi	University of Wisconsin - Madison, PSL
Peter H. Fisher	Johns Hopkins University
William T. Ford	University of Colorado
G. William Foster	Fermilab
Soren G. Frederiksen	SSCL
Alan Fry	SSCL
Toru Fukui	SSCL
Murdoch Gilchriese	LBL
Nikos D. Giokaris	Rockffeller University
Alfred T. Goshaw	Duke University
Daniel P. Green	Fermilab
Alexander A. Grillo	Santa Cruz Institute for Particle Physics (SCIPP)
Charles M. Grinnell	SSCL
Laszlo J. Gutay	Purdue University
Vasken Hagopian	Florida state University
Harald Johnstad	SSCL
Kyu Seok Kang	Kangnung University
Do-won Kim	Kangnung University
Thomas B.W. Kirk	Argonne National Laboratory
David S. Koltick	Purdue University
Glenn T. Kubena	IBM (Houston)

Name	Institution
Alexei V. Kulik	IHEP (Protvino) / KEK
Shuichi Kunori	University of Maryland
Andrew J. Lankford	University of California Irvine
T. Y. Ling	Ohio State University
Henry J. Lubatti	SSCL
Vera G. Luth	SSCL
William Miller	Los Alamos National Laboratory
Thomas Muller	UCLA
Ureil Nauenberg	University of Colorado
Mitchell Newcomer	University of Pennsylvania
Harold O. Ogren	Indiana University
Seog Oh	Duke University
Sung Keun Park	Korea University
Yeong Mouk Park	Gyung Sung University
Jonathan A. Piles	SSCL
Lawrence E. Price	Argonne National Laboratory
David R. Rust	Indiana University
Hartmut F.-W. Sadrozinski	Santa Cruz Institute for Particle Physics (SCIPP)
Brian L. Scipioni	SSCL
Abe Seiden	Santa Cruz Institute for Particle Physics (SCIPP)
Pekka K. Sinervo	University of Toronto
Andris Skuja	University of Maryland
Wesley H. Smith	University of Wisconsin
Helmuth Spieler	LBL
Roger L. Swensrud	Westinghouse Science & Technology Center
Paul Taras	Universite de Montreal
Rudolf Thun	University of Michigan
Tim S. Thurston	SSCL
George H. Trilling	LBL
David Underwood	Argonne National Laboratory
Robert C. Walker	University of Rochester
Qingfang Wang	Rockefeller University
Alan J. Weinstein	California Institute of Technology
Brian Keith Wheeler	Fermilab
Andrew P. White	University of Texas at Arlington
Hugh Williams	University of Pennsylvania

Name	Institution
Suzanne E. Willis	Northern Illinois University
William B. Wilson	Los Alamos National Laboratory
Tianchi Zhao	University of Washington
Hans J. Ziock	Los Alamos National Laboratory

Name	Institution
Fumio Abe	KEK
Kohya Abe	Tohoku University
Katsuya Amako	KEK
Yasuo Arai	KEK
Makoto Asai	Hiroshima Institute of Technology
Yuzo Asano	University of Tsukuba
Masami Chiba	Tokyo Metroporitan University
Tsuneo Emura	Tokyo University of Agriculture and Technology
Hirofumi Fujii	KEK
Yoshiaki Fujii	KEK
Ryosuke Hamatsu	Tokyo Metropolitan University
Kazuhiko Hara	University of Tsukuba
Katsuo Hasegawa	Tohoku University
Tatsushige Hirose	Tokyo Metroporitan University
Masahiro Ikeno	KEK
Hiroyuki Iwasaki	KEK
Yohsei Iwata	Hiroshima University
Seiji Kabe	KEK
Nobuyuki Kanematsu	Osaka University
Minato Kawaguti	Fukui University
Ryusaburo Kikuchi	Kyoto University
Shinhong Kim	University of Tsukuba
Shoichi Kitamura	Tokyo Metropolitan University
Shigeharu Kobayashi	Saga University
Kouji Kondo	Tokyo Metropolitan University
Kunitaka Kondo	University of Tsukuba
Takahiko Kondo	KEK
Taro Masumaru	Tokyo Metropolitan University
Kozo Miyake	Kyoto University
Hitoshi Miyata	Niigata University
Shigeki Mori	University of Tsukuba
Youhei Morita	KEK
Akira Murakami	Saga University
Yorikiyo Nagashima	Osaka University
Itsuo Nakano	University of Tsukuba
Masaharu Nomachi	KEK

Name	Institution
Shigeru Odaka	KEK
Tokio K. Ohska	KEK
Takashi Ohsugi	Hiroshima University
Hiroshi Sakamoto	KEK
Osamu Sasaki	KEK
Masaomi Shioden	Ibaraki College of Technology
Fumio Sudo	Tokyo University of Agriculture and Technology
Kasuke Takahashi	KEK
Yoshinobu Takaiwa	KEK
Yasuo Takeuchi	Tokyo Institute of Technology
Koji Takikawa	University of Tsukuba
Norio Tamura	Okayama University
Susumu Terada	KEK
Yoshiki Teramoto	Osaka City University
Norihiko Ujiie	KEK
Yoshinobu Unno	KEK
Yasushi Watanabe	Tokyo Institute of Technology
Yoshiyuki Watase	KEK
Akira Yamamoto	KEK
Kazuo Yamauchi	Tokyo Metropolitan University
Yoshiji Yasu	KEK
Kiyoshi Yasuoka	University of Tsukuba
Hajime Yoshida	Naruto Kyoiku University
Haruo Yuta	Tohoku University

Name	Company
Kenichi Fukatsu	Kawasaki Heavy Industries
Toshikazu Hakamata	Hamamatsu Photonics
Yutaka Hirata	TOSHIBA
H. Kakui	Ishikawajima-Harima Heavy Industries
Hiroyuki Kikuchi	NTT Electronics Technology Corporation
Susumu Mine	TOSHIBA
Yuichi Mizukawa	Kuraray Corporation
Hiroshi Mukai	TOSHIBA
Kozo Nakao	Kuraray Corporation
Kiyogiku Nishikawa	Matsusada Precision Devices Inc
Kenichi Nishimura	Matsusada Precision Devices Inc
Osamu Shinji	Kuraray Corporation
Seiji Suzuki	Hamamatsu Photonics
K. Takagi	Hamamatsu Photonics
Junichi Takeuchi	Hamamatsu Photonics
Yuji Yoshizawa	Hamamatsu Photonics

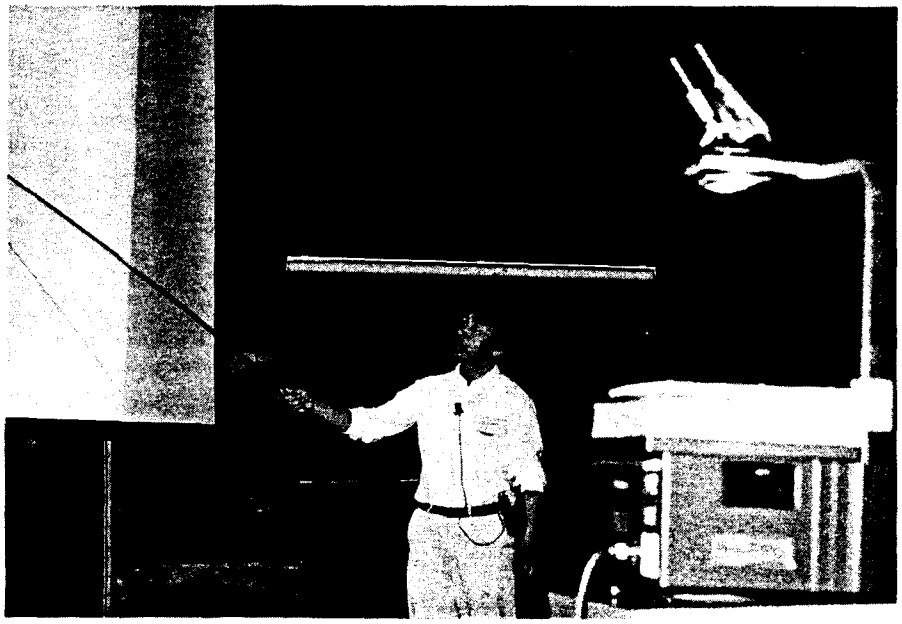

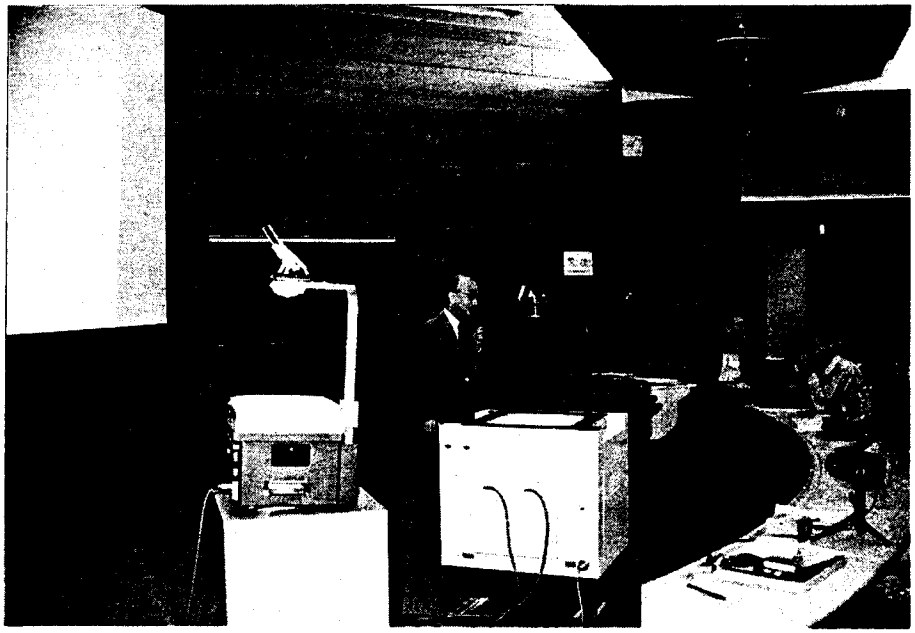

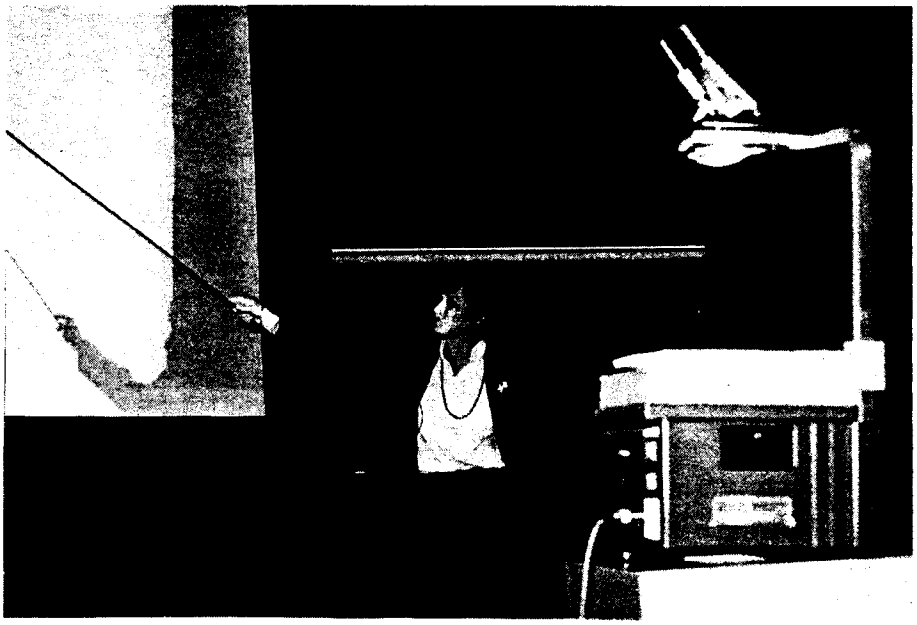

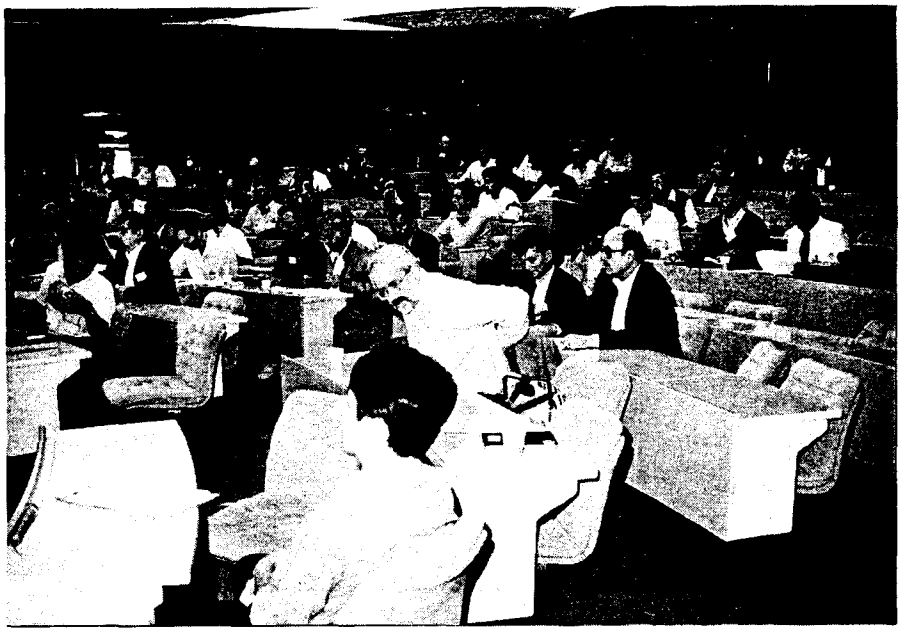

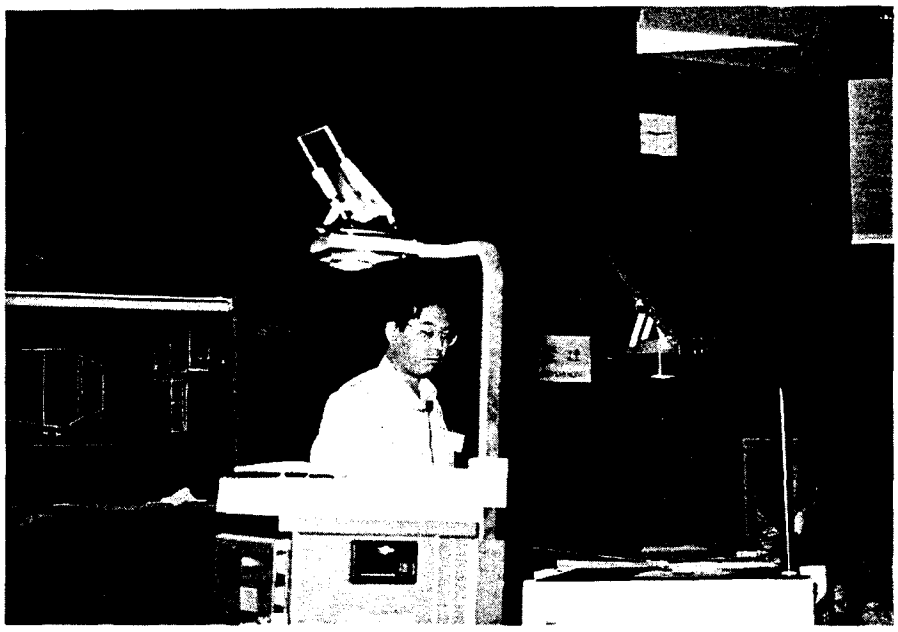

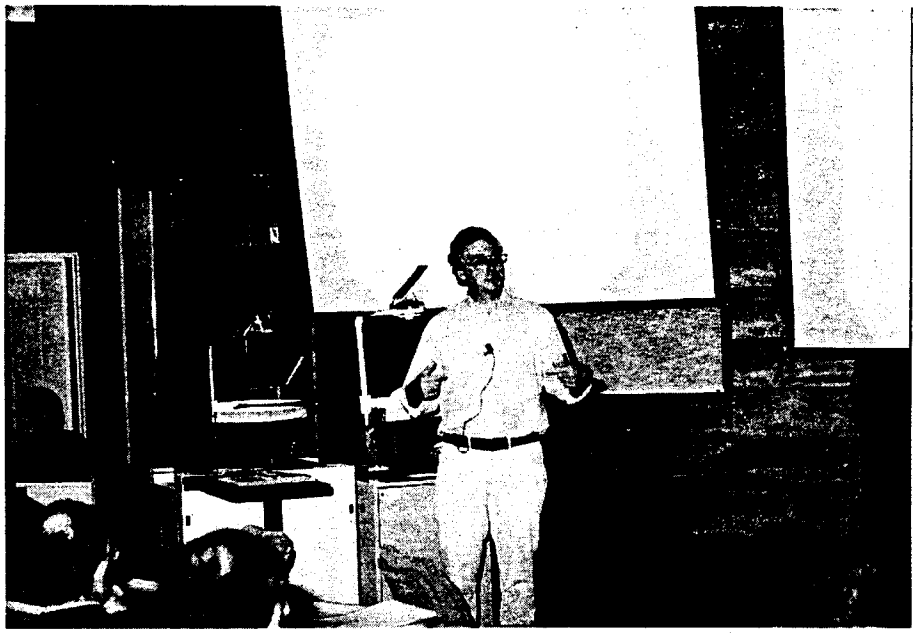

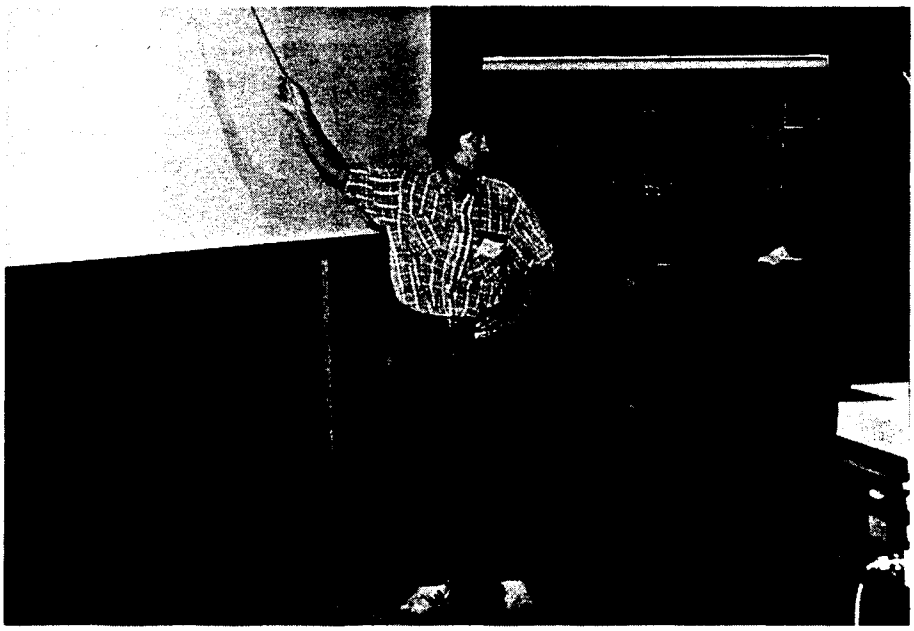

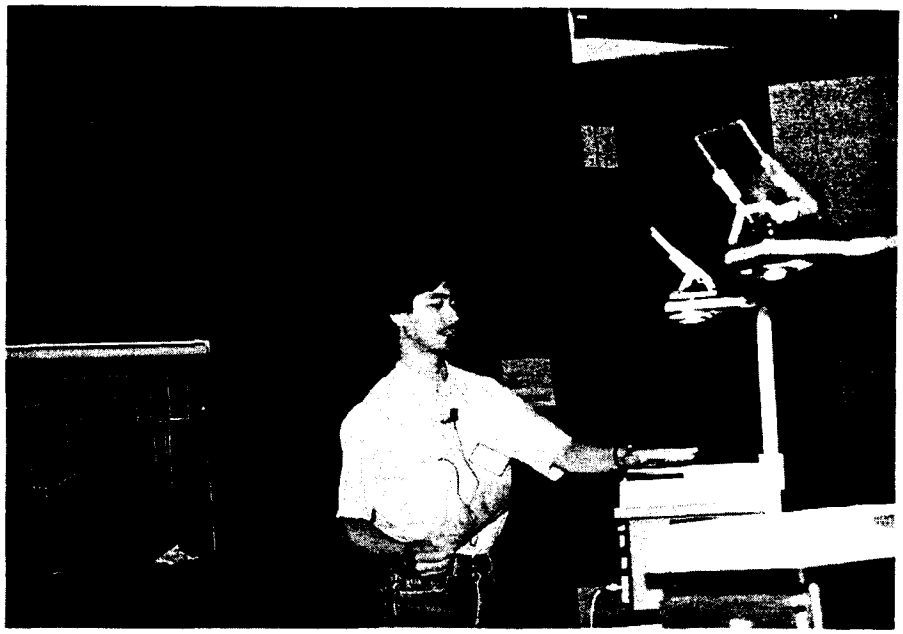

Registration